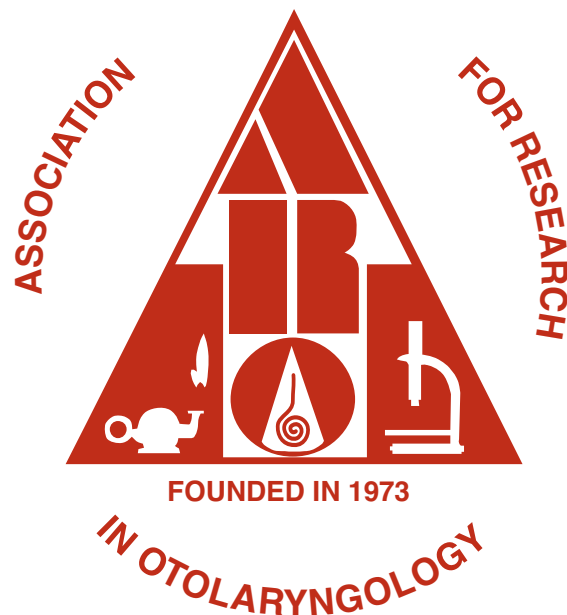


**ABSTRACTS OF THE TWENTY-SEVENTH ANNUAL
MIDWINTER RESEARCH MEETING**

**ASSOCIATION FOR RESEARCH
IN OTOLARYNGOLOGY**



FEBRUARY 21-26, 2004

**Adams Mark Hotel
Daytona Beach, Florida**

**ABSTRACTS OF THE TWENTY-SEVENTH ANNUAL
MIDWINTER RESEARCH MEETING
OF THE**

Association for
Research in
Otolaryngology

February 21-26, 2004

Daytona **B**each, **F**lorida, **U**SA

Peter A. Santi, Ph.D.

Editor

Association for Research in Otolaryngology
19 Mantua Road, Mt. Royal, NJ 08061 USA

ISSN-0742-3152

The *Abstracts of the Association for Research in Otolaryngology* is published annually and consists of abstracts presented at the Annual MidWinter Research Meeting. A limited number of copies of this and previous books of abstracts (1978-2003) is available.

Please address your order or inquiry to:

Association for Research in Otolaryngology
19 Mantua Road
Mt. Royal, NJ 08061 USA

General Inquiry

Phone (856) 423-0041 Fax (856) 423-3420
E-Mail: headquarters@aro.org

Meetings

Phone: (856) 423-7222 Ext. 350
E-Mail: meetings@aro.org

This book was prepared from abstracts that were entered electronically by the authors. Authors submitted abstracts over the World Wide Web using Mira Digital Publishing's PaperCutter™ Online Abstract Management System. Any mistakes in spelling and grammar in the abstracts are the responsibility of the authors. The Program Committee performed the difficult task of reviewing and organizing the abstracts into sessions. The Program Committee Chair, Dr. Robert Shannon, the President, Dr. Edwin M. Monsell, and Past-President, Dr. Donata Oertel constructed the final program. Mira electronically scheduled the abstracts and prepared Adobe Acrobat pdf files of the Program and Abstract Books. These abstracts and previous years' abstracts are available at: <http://www.aro.org>.

Citation of these abstracts in publications should be as follows:

Authors, year, title, Assoc. Res. Otolaryngol. Abs.: page number.

For Example:

Rehm, Horgan, Kenna, 2004, Patient's and Family's Understanding of Genetic Test Results for Hearing Loss: Ignorance is Bliss?, Assoc. Res. Otolaryngol. Abs.: 1059.



2004 ARO Midwinter Meeting

General Chair

Edwin M. Monsell MD, PhD (2003-2004)

Program Organizing Committee

Robert V. Shannon, PhD, Chair (2001-2005)

Robin L. Davis, PhD (2002-2005)

Michael P. Gorga, PhD (2002-2005)

Anna Lysakowski, PhD (2002-2005)

John Middlebrooks, PhD (2003-2006)

Lloyd B. Minor, MD (2002-2005)

Kevin Ohlemiller, PhD (2003-2006)

Alan Palmer, PhD (2003-2006)

Christine Petit, MD, PhD (2001-2004)

Neil Segil, PhD (2001-2004)

Russell L. Snyder, PhD (2001-2004)

Mark Warchol, PhD (2001-2004)

Elizabeth Keithley, PhD, *Facility Liaison, ex officio*

Peter Santi, PhD, ARO Editor, *Council Liaison, ex officio*

Donata Oertel, PhD, *Council Liaison*

Program Publications

Peter Santi, PhD, Editor

Diversity & Minority Affairs Committee

Ann M. Thompson, PhD, Chair (2002-2005)

Henry J. Adler, PhD (2003-2006)

Ricardo Cristobal, MD PhD (2002-2005)

Xiaohong Deng, MS (2003-2006)

Jagmeet Kanwal, PhD (2003-2006)

Vishakha W. Rawool, PhD (2003-2006)

Duane Simmons, PhD (2003-2006)

Steven Rauch, MD, *Council Liaison* (2003-2004)

Graduate Student/Postdoctoral Travel Awards

Douglas Cotanche, PhD, Chair (2002-2005)

Matthew Kelly, PhD (2002-2005)

Laura Hurley (2003-2006)

Jennifer Stone, PhD (2002-2005)

Physician Research Training

Hilary A. Brody, MD, PhD, Chair (2002-2005)

Carol A. Bauer, MD (2001-2004)

Holly H. Birdsall, MD, PhD (2001-2004)

Marc Coltrera, MD (2003-2006)

Diane Durham, PhD (2003-2006)

Bruce J. Gantz, MD (2002-2005)

Larry Lustig, MD (2003-2006)

Michael J. McKenna, MD (2001-2004)

Alan G. Micco, (2001-2004)

J. Gail Neely, MD (2002-2005)

Debara Tucci, MD (2003-2006)

James F. Battey, MD, PhD, NIDCD Dir., *ex officio*

Maureen Hannley, PhD, Exec VP Rsch., *ex officio*

Phillip Wackym, MD, *Council Liaison* (2003-2004)

Award of Merit Committee

Peter Dallos, PhD, Chair (2003-2006)

Jonathan Ashmore, PhD (2001-2004)

Laurel Carney, PhD (2001-2004)

Ellen Covey, PhD (2002-2005)

Lloyd Minor, MD (2003-2006)

Adrian Perachio, PhD (2001-2004)

David Lim, MD, *Council Liaison* (2002-2004)

Presidential Welcome

We are all looking forward to a great Mid-Winter Meeting February 21-26, 2004 here in Daytona. Please be sure to thank our exhibitors, who support our meeting and help us keep our costs down.

I am happy to report that our beloved ARO is financially sound and thriving. Several initiatives are underway to keep us moving in the right directions.

Advisors tell us that organizations like ours should have a reserve fund equal to 1½ times our annual budget. Over recent years we have built up our reserves to about equal to our annual budget, so we are slowly approaching our goal of financial security.

Unfortunately, our expenses, which are mostly related to the Mid-Winter Meeting, have been rising for several years. Charges by hotels nationwide have risen for meeting rooms, food service, and audio-visual services.

JARO has been a wonderful editorial success under the editorship of Eric Young. Last February the Council voted to dip into our reserves to purchase additional pages from Springer Verlag to reduce the publication delay that is the downside of our success. JARO Committee CoChairs Art Popper and Jerry Popelka asked a subcommittee to make recommendations about page charges. Bob Ruben, Charlie Liberman, and Paul Manis completed this work. The Council is currently weighing our options. Many journals the size of JARO have page charges; we are trying to avoid them.

Our mantra in selecting the meeting site has always been “something cheap on the beach!” Unfortunately the increasing price of venues suitable for a meeting the size and needs of the Mid-Winter Meeting may force a difficult choice for a location after our contract expires. We can fix some of the simple things at the Adams Mark, such as the lighting and space for posters. In the meantime we need your continued support and understanding. Please continue to stay at the Adams Mark Hotel. If registration falls below contract levels, ARO has to pay the difference. We are hoping that the recent sale of the hotel to the Pyramid group will result in management improvements.

The sources of ARO’s strength remain what they always have been: our science, our collegiality, the interaction of scientists and clinicians, our committee members, and a dedicated core of hard-working leaders. All of our Council members and committee chairs are doing an outstanding job. We should all give special thanks to Betsy Keithley, Secretary-Treasurer; Peter Santi, Editor; and Bob Shannon, Program Committee Chair. Past Presidents Donata Oertel and Judy Dubno have been wonderful mentors and contributors, too. Darla Dobson is doing a great job in her new role of Executive Director and Lisa Astorga, our Meetings Manager has been a very effective advocate for ARO. Please thank all our Council members and chairs for their service any time you get a chance.

Now, let’s have a wonderful celebration of science!

Ed Monsell
President





Donata Oertel, PhD
2004 Award of Merit Recipient

Donata Oertel, PhD

2004 Award of Merit Recipient

Fireflies, paramecia, and barnacles marked the early and varied beginnings of a distinguished career in neuronal sensory science and developed electrophysiological recording skills that would be a basis for later undertakings.

A major career change was taken upon joining Bill Rhode's lab in the Department of Neurophysiology at Wisconsin where she was introduced to the wonders of the auditory system. Together with Phil Smith they provided some of the first intracellular recordings of physiologically characterized and morphologically identified cells in the cochlear nucleus of cat. This was also a period when *in vitro* recording was being developed in other parts of the central nervous system and Donata saw an opportunity to add a new dimension to the study of the auditory system. A mouse brain slice preparation of the cochlear nucleus was soon developed that would become her laboratory's trademark.

While initially characterizing chopper and bushy cells in the anteroventral cochlear nucleus (AVCN), together with students and postdocs, she soon began revealing studies of cell types of the dorsal cochlear nucleus (DCN) as well as the pathways connecting the two subdivisions. These studies brought to light several original ideas regarding the fundamental auditory response properties of different cell types *in vivo* and how these responses might be strongly influenced by their intrinsic membrane characteristics and their interconnections. This is perhaps one of Donata's most outstanding scientific traits, the ability to extrapolate basic *in vitro* intracellular observations to their potential physiological role in encoding auditory cues. Her genuine enthusiasm for such unique ideas have always led to considerable discussion and debate among students and colleagues and been instrumental in moving the field forward.

Her initial observation about the fundamental differences between bushy cell and chopper physiology was first met with considerable skepticism but has now led to studies of intrinsic membrane features and their potential role in cell function at all levels of the auditory central nervous system. Together with Wickesberg, Donata revealed the details of the 2-way interconnection between AVCN and DCN and suggested that the inhibition of AVCN cells by DCN could be correlated with echo suppression. Recent studies with Fugino and Gardner demonstrated plasticity of only a certain class of synapses on principal cells in the DCN. The characterization of octopus cells in the posteroventral cochlear nucleus provided landmark observations that helped to explain their curious onset response and exquisite phase locking *in vivo*. Together with Robertson and Golding, she showed that the extraordinarily low membrane resistance of this cell type meant that each synaptic input produced only a small rapidly decaying post-synaptic potential and thus required the arrival of a large number of nearly simultaneous inputs to fire the cell. Later studies with Ferragamo characterized the ionic currents important for the function of these cells and showed their relevance to the high rate of change of membrane potential required to activate action potentials.

Beyond numerous contributions to cochlear nucleus physiology and the training of graduate students and postdocs, she has been extraordinarily giving in all aspects of her professional career. Editorial activities too numerous to mention, a leadership role in the ARO, professional reviews, course development and teaching combined with service at the local and national levels, former chair of Neurophysiology and President of ARO all characterize her love of science and her benevolent nature.

Thanks to Donata Oertel and her colleagues, much is now known about the cochlear nucleus as the first central auditory center and its role in the functional sorting of the auditory information that is delivered to the rest of the central auditory system. All those who have known and worked with her can truly say that she is an exceptional and dedicated scientist.

PRESIDENTIAL CITATION: JOSEPH ELMER HAWKINS, Jr.

A familiar and distinguished figure at the ARO meetings, Joseph Elmer Hawkins is for all of us an example of the true scholar. During his 65-year scientific career (his first publication appeared in 1939 and his most recent was published in 2004) he has shaped the field of otologic research. His research defies categorization and he has made outstanding contributions in the many subjects that he touched upon. Some of us may consider him best-known for his work on ototoxicity, particularly on aminoglycoside antibiotics. Others may recall his years at Harvard together with Hallowell Davis and Bob Galambos, where he participated in the first experiments on the traumatic effects of noise on human ears – his own ears included. Together with S.S. Stevens, he published seminal papers in the psychoacoustics of auditory masking and on auditory evoked potentials. And he refined our view of the inner ear in numerous studies on microdissections that included some of the finest characterizations of human pathology.

While the breadth of his research and its depth are impressive enough, Joe Hawkins's scholarship was never limited to the laboratory. He is a student of many cultures and languages, lecturing in three, conversing in six, and reading eleven. Members of ARO will also appreciate him as the historian whose posters have entertained and educated us – one of which we will see at this meeting.

Joe Hawkins hails from Texas and graduated from Baylor University. He went on to Oxford, England, as a Rhodes scholar, and to Harvard, where he obtained his Ph.D. in 1941. Following academic appointments in Sweden and the U.S. and a stint in the pharmaceutical industry, he joined the faculty of the University of Michigan in 1963 and became Emeritus Professor in 1984. As Emeritus, he has continued his pursuits of science and scholarship, teaching at his alma mater Baylor and continuing to mentor students, fellows and colleagues alike at Michigan. To this day he has maintained an almost daily presence at the Kresge Hearing Research Institute, researching and writing his historical sketches. Among his many honors is the Award of Merit of the Association of Research in Otolaryngology, which he received in 1985. He would probably feel even more honored if we would all pronounce “cochlea” with a short “o” as he has taught us for so many years.

A scholar and humanist, an educator and cherished colleague, Joseph Elmer Hawkins will be 90 years old on March 4th, 2004.

(Jochen Schacht)

Association for Research in Otolaryngology

Executive Offices

19 Mantua Road, Mt. Royal, NJ 08061 USA

Phone: (856) 423-0041 Fax: (856) 423-3420 E-Mail: headquarters@aro.org

Meetings Phone: (856) 423-7222 x 350 Meetings E-mail: meetings@aro.org

ARO Council Members 2003-2004

President: Edwin M. Monsell, MD, PhD
Professor, Wayne State University
Department of Otolaryngology & HNS
4201 St. Antoine 5E-UHC
Detroit, MI 48201

Secretary/Treasurer: Elizabeth Keithley, PhD
Professor, Univ of California San Diego
9500 Gilman Drive, 0666
LaJolla, CA 92093

President-Elect: William E. Brownell, PhD
Professor, Baylor College of Medicine
Dept. of Otolaryngology & Comm Sci
Houston, TX 77030

Editor: Peter Santi, PhD
University of Minnesota
Department of Otolaryngology
Lions Research Bldg, Room 121
2001 Sixth St. SE
Minneapolis, MN 55455

Past President: Donata Oertel, PhD
University of Wisconsin Medical School
Department of Physiology
1300 University Avenue
Madison, WI 53706

Historian: David J. Lim, MD
House Ear Institute
2100 W. Third St., Fifth Floor
Los Angeles, CA 90057

Council Members at Large

Phillip A. Wackym, MD
Professor and Chairman
Medical College of Wisconsin
Dept. of Otolaryngology & Comm. Sciences
9200 West Wisconsin Avenue
Milwaukee, WI 53226

Nina Kraus, PhD
Northwestern University
2299 N. Campus Drive
Searle Bldg.
Evanston, IL 60208-3550

Steven Rauch, MD
Massachusetts Eye & Ear Infirmary
Eaton Peabody Laboratory
243 Charles Street
Boston, MA 02114

Past Presidents

1973-74 David L. Hilding, MD
1974-75 Jack Vernon, PhD
1975-76 Robert A. Butler, PhD
1976-77 David J. Lim, MD
1977-78 Vicente Honrubia, MD
1978-80 F. Owen Black, MD
1980-81 Barbara Bohne, PhD
1981-82 Robert H. Mathog, MD
1982-83 Josef M. Miller, PhD
1983-84 Maxwell Abramson, MD
1984-85 William C. Stebbins, PhD
1985-86 Robert J. Ruben, MD
1986-87 Donald W. Nielsen, PhD
1987-88 George A. Gates, MD
1988-89 William A. Yost, PhD
1989-90 Joseph B. Nadol, Jr., MD
1990-91 Ilsa R. Schwartz, PhD
1991-92 Jeffrey P. Harris, MD, PhD
1992-93 Peter Dallos, PhD
1993-94 Robert A. Dobie, MD
1994-95 Allen F. Ryan, PhD
1995-96 Bruce J. Gantz, MD
1996-97 M. Charles Liberman, PhD
1997-98 Leonard P. Rybak, MD, PhD
1998-99 Edwin W. Rubel, PhD
2000-01 Richard A. Chole, MD, PhD
2001-02 Judy R. Dubno, PhD
2002-03 Richard T. Miyamoto, MD
2003-04 Donata Oertel, PhD

Award of Merit Recipients

1978 Harold Schuknecht, MD
1979 Merle Lawrence, PhD
1980 Juergen Tonndorf, MD
1981 Catherine Smith, PhD
1982 Hallowell Davis, MD
1983 Ernest Glen Wever, PhD
1984 Teruzo Konishi, MD
1985 Joseph Hawkins, PhD
1986 Raphael Lorente de Nó, MD
1987 Jerzy E. Rose, MD
1988 Josef Zwislocki, PhD
1989 Åke Flöck, PhD
1990 Robert Kimura, PhD
1991 William D. Neff, PhD
1992 Jan Wersäll, PhD
1993 David Lim, MD
1994 Peter Dallos, PhD
1995 Kirsten Osen, MD
1996 Ruediger Thalmann, MD & Isolde Thalmann, PhD
1997 Jay Goldberg, PhD
1998 Robert Galambos, MD, PhD
1999 Murray B. Sachs, PhD
2000 David M. Green, PhD
2001 William S. Rhode, PhD
2002 A. James Hudspeth, MD, PhD
2003 David T. Kemp, PhD
2004 Donata Oertel, PhD

Table of Contents

	Abstract Number
Short Course	Embryonic Stem Cells: From Cell Culture to Clinic
Presidential Symposium	
A:	Ototoxicity 1-6
Symposium	
B:	Contemporary Experimental Approaches to the Study of Gustation and Olfaction 7-13
Symposium	
C:	Vestibular Development and Adaptation During Spaceflight 14-19
Poster	
D1:	Clinical Otolaryngology: Otology 20-39
D2:	Clinical Otolaryngology: Head & Neck 40-46
D3:	Clinical Audiology 47-61
D4:	Vestibular: Clinical 62-83
D5:	Cochlear Implants: Clinical Issues 84-96
D6:	Otoacoustic Emissions 1: Mostly DPOAEs 97-115
D7:	Speech 116-122
D8:	Psychophysics: Loudness Plus 123-130
D9:	Auditory Midbrain and Cortex: Learning and Plasticity 131-140
D10:	Auditory Midbrain and Cortex: Binaural and Spatial Hearing 141-150
D11:	Auditory Midbrain and Cortex: Spectral Processing and CNS Prosthesis 151-160
D12:	Auditory Brainstem: Comparative 161-166
D13:	Sound Localization Development and Plasticity 167-171
D14:	Inner Ear Inflammation 172-177
D15:	Ototoxic Injury: Prevention & Treatment 178-191
D16:	Inner Ear: Cochlear Fluids 192-203
D17:	Hair Cells: Stereocilia and Transduction 204-212
D18:	Development 1 213-230
D19:	Genetics: Human Deafness, Mapping, New Genes 1 231-242
Special Event	
E1:	NIDCD Research and Training Workshop for New Investigators 243-243
Special Event	
E2:	Animal Rights and the ARO: The Prospective of Targeted Members 244-244
Symposium	
F:	Cell Adhesion: Lessons for the Development and Physiology of Hair cells 245-252
Podium	
G:	Bilateral Cochlear Implants and AES 253-263
Symposium	
H:	Neurotrophin Induced Neuro-protection 264-269
Podium	
I:	Vestibular 270-278
Poster	
J1:	Middle Ear 1: Disease Processes 279-301
J2:	Animal Psychophysics 302-315
J3:	Ascending Auditory Pathways: Midbrain and Cortex 316-326
J4:	Auditory Midbrain and Cortex: Temporal Processing 327-336
J5:	Tinnitus and CNS Consequences of Deafness 337-346
J6:	Auditory Brainstem Evoked Potentials 347-356
J7:	Auditory Brainstem: Anatomical Projections, Ascending and Descending 357-366
J8:	Auditory Brainstem Development and Aging 367-372
J9:	Vestibular: Central 373-378
J10:	Noise Injury: Mechanisms 379-396
J11:	Inner Ear Ischemic Injury Mechanisms 397-399
J12:	Ototoxic Injury: Mechanisms 1 400-413
J13:	Inner Ear Morphology 414-428
J14:	Inner Ear Genetic Screening 429-432
J15:	Outer Hair Cells and Motility 433-452
J16:	Hair Cells: Membranes and Ion Channels 453-467
J17:	Development 2 468-490
J18:	Genetics: Mouse Models 1 491-504
Symposium	
K:	Virally-Mediated Gene Transfer: from Virology to Practice 505-509
Workshop	
L:	The Influence of Evan Relkin on Auditory Science: From the Middle Ear to the CNS and Back Again 510-516

	Abstract Number
Podium	
M:	Molecular Physiology of the Inner Ear: Genetic and Functional Genomic Approaches.....517-521
Podium	
N:	Cochlear Injury: Prevention and Treatment.....522-531
Poster	
O1:	Otoacoustic Emissions 2: SFOAEs, SOAEs, MOC532-545
O2:	Psychophysics: Miscellaneous546-556
O3:	Cochlear Implants: Miscellaneous557-570
O4:	Auditory Cortex: Functional Organization571-580
O5:	Auditory Cortical Mechanisms581-590
O6:	CNS Synaptic and Membrane Mechanisms591-600
O7:	Sound Localization: VIII Nerve to IC.....601-608
O8:	Sound Localization: Masking, Lesions, Precedence and Reverberation609-619
O9:	Sound Localization Psychophysics620-625
O10:	Vestibular: Periphery 1626-642
O11:	Aging: Animal Studies643-662
O12:	Aging: Human Studies663-670
O13:	Ototoxic Injury: Mechanisms 2.....671-683
O14:	Noise Injury: Prevention & Treatment684-691
O15:	Inner Ear: Ion channels and Receptors692-702
O16:	Hair Cells: Synaptic Mechanisms703-718
O17:	Development 4.....719-740
O18:	Regeneration 1741-758
O19:	Genetics: Mouse Models 2.....759-767
Presidential Lecture	
P:	Presidential Lecture and Award Ceremony768-768
Symposium	
Q:	Neurobiological Perspectives on the Inferior Colliculus: Generalized Systems and Species Specializations769-774
Podium	
R:	Development 3.....775-789
Podium	
S:	Hair Cells: Stereocilia, Transduction, and Motility.....790-804
Podium	
T:	Speech Pattern Processing and Psychophysical Learning.....805-814
Poster	
U1:	Middle Ear 2: Models, Normative Data, Reflexes815-833
U2:	Psychophysics: Modulation.....834-842
U3:	Cochlear Implants: Physiology and Temporal Processing.....843-852
U4:	Auditory Midbrain and Cortex: Coding of Periodicity and Frequency Modulation.....853-862
U5:	Auditory Midbrain and Cortex: Evoked Potentials and Imaging863-872
U6:	Auditory Midbrain and Cortex: Speech and Communication Sounds873-881
U7:	Auditory Brainstem Pathology and Lesions882-896
U8:	Auditory Brainstem Receptors and Channels.....897-911
U9:	Auditory Brainstem: Analysis of Complex Signals912-925
U10:	Vestibular: Periphery 2.....926-941
U11:	Auditory Nerve942-960
U12:	Mouse Models of Human Deafness961-968
U13:	Inner Ear: Functional Analysis.....969-984
U14:	Inner Ear: Homeostatic Mechanisms985-1000
U15:	Inner Ear Mechanics.....1001-1024
U16:	Hair Cells: Molecular Structure and Gene Expression1025-1029
U17:	Regeneration 21030-1040
U18:	Genetics: Gene Expression.....1041-1050
U19:	Genetics: Human Deafness, Mapping, New Genes 2.....1051-1059

1 Ototoxicity

Brian Blakley

Department of Otolaryngology, University of Manitoba, 820 Sherbrook Street, Room GB421, Winnipeg, Manitoba, Canada

Ototoxicity is of great concern for clinicians and basic scientists interested in the ear so it is a fitting and important topic for this meeting. This presentation is an overview of this broad topic.

Recognition that therapeutic agents could affect the ear probably first started in 1954 after streptomycin was introduced. Since that time several families of drugs have been introduced that may adversely affect hearing, balance or both. The most prominent of these include the aminoglycosides and platinum-containing chemotherapeutic agents.

Aminoglycosides are still used in healthcare because they are effective and inexpensive. The aminoglycosides are primarily used in treating infections that may be caused by gram-negative bacteria such as *Pseudomonas* sp. Until recently there were no oral antibiotics that effectively treat these infections. Ironically *Pseudomonas* is usually the cause of infection in external otitis and chronic otitis media. Although new antibiotics may have similar efficacy there are still strains of bacteria that are much more sensitive to aminoglycosides. In some countries and situations, these two benefits are thought to outweigh the risks of ototoxicity.

Cisplatin is probably the single most effective chemotherapy agent for certain types of cancer. While it remains in common use, chemotherapy is unlikely to cure these cancers so there is controversy regarding the risk: benefit ratio of this drug.

There are similarities and differences in ototoxicity. Most ototoxic agents affect the basal region of the cochlea initially, progressing from outer hair cells then to inner hair cells. High frequency hearing is affected first and low frequencies and speech recognition is affected later. This similarity may reflect a similar biochemical mechanism of action. On the other hand it appears that some aminoglycosides affect the cochlea and others preferentially affect vestibular hair cells. While neural plasticity provides great capacity for vestibular compensation this is less impressive for cochlear dysfunction.

Topical otic drops have recently become important considerations in ototoxicity. While aminoglycoside drops have been the mainstay of topical treatment for many years their use has been recently questioned, particularly for gentamicin. Unfortunately the organisms that usually cause infections such as chronic otitis media and external otitis are resistant to most antibiotics.

2 Oxidative Damage and Antioxidant Therapeutics in Age-Associated Diseases

Robert A. Floyd

Free Radical Biology and Aging Research Program, Oklahoma Medical Research Foundation, 825 NE 13th, Oklahoma City, OK, United States

Oxygen metabolism leads to formation of a small amount of reactive oxygen species (ROS) as byproducts. Recent advances demonstrate that ROS in addition to causing oxidative damage, especially when they are present at high levels, are also involved in critical signaling processes important in stress-adaptive responses. Aging is associated with increased diseases (including enhanced hearing

loss) and also with increased oxidative damage caused by ROS. Thus the oxidative damage linkage to age-associated diseases implicates effectiveness of anti-oxidant based therapeutics. Many epidemiology studies demonstrating decreased incidences of age-associated diseases with enhanced consumption of food containing antioxidant components supports this concept. In contrast however, follow-up studies where specific dietary antioxidants have been given as supplements have not in general been effective. These seemingly contradictory observations have been rationalized as due to the absence of other unknown dietary components not present in a balanced proportion in the supplemented diet. The results highlight the complexity of ROS involvement in disease processes and the lack of understanding of specific antioxidant action in biological systems and in disease processes specifically. Our heightened awareness of these problems have come from results of studies conducted on the protective actions of spin-trapping nitrones in several models of age-associated diseases. These and other studies will be reviewed and discussed in light of the surprises encountered and the complexities we uncovered.

3 Abstract Unavailable

4 Cisplatin Ototoxicity: Pharmacology and Chemoprotection

Leonard P. Rybak

Division of Otolaryngology and Department of Pharmacology, Southern Illinois University School of Medicine, P.O. Box 19653, Springfield, IL, United States

Animal experiments have demonstrated that following cisplatin administration, the primary targets of ototoxicity are the outer hair cells of the basal turn. Damage to the cells in the stria vascularis and spiral ganglion neurons can also occur. Cisplatin exposure appears to result in free radical formation. The mechanisms underlying the generation of free radicals are under active investigation. Potential sources include DNA damage and/or enzymes present within cochlear tissues, such as NADPH oxidase, inducible nitric oxide synthase (iNOS) and xanthine oxidase. This, in turn, may result in generation of free radicals, such as superoxide and hydroxyl free radicals, which can deplete antioxidant defense systems in the cochlea and produce lipid peroxides, including the highly toxic 4-hydroxy-nonenal. This can activate the biochemical cascade of apoptosis. Chemoprotective strategies have included the administration of free radical scavengers or antioxidants, cisplatin-binding agents, iron chelators, adenosine receptor agonists, inhibitors of iNOS, caspase inhibitors and the inhibitor of p53, pifithrin-alpha. These protective molecules have been administered systemically, on the round window membrane or by perilymphatic perfusion. The advantages and drawbacks of these various approaches to chemoprotection of the cochlea will be discussed.

(Supported by NIH Grant #R01-DC 02396)

5 Abstract Unavailable

6 Clinical Use of Aminoglycosides in Meniere's disease

Stephen P. Cass

Department of Otolaryngology, University of Colorado, East Ninth Avenue B205, Denver, CO, United States

Meniere's disease refers to a pattern of symptoms including fluctuating hearing loss, aural fullness, tinnitus and recurring attacking of severe, incapacitating vertigo. While endolymphatic hydrops has been identified as a pathological correlate, the underlying pathological mechanisms remain unknown and no curative treatment for the disorder currently exists.

Mild symptoms associated with Meniere's disease are typically treated conservatively with salt restricted diets, diuretics, and various other oral medications used to provide symptomatic relief. In about 10% of patients, the symptoms are severe and disabling. In these patients, ablation of vestibular function in the ear affected by Meniere's disease is currently the most effective way to stop persistent, recurring attacks of incapacitating vertigo.

A number of methods are available to ablate vestibular function including surgical labyrinthectomy, vestibular nerve section, and intratympanic gentamicin therapy. Intratympanic gentamicin therapy refers to a minimally invasive procedure involving instillation of an ototoxic agent, such as gentamicin, in the middle ear space to cause unilateral ablation of peripheral vestibular function. The most common ablative treatment of disabling vertigo associated with Meniere's disease is now the use of intratympanic gentamicin.

Schuknecht can be credited with introducing the idea of delivering a therapeutic drug to the inner by injecting the drug into the middle ear. In 1957, Schuknecht published his experience with injecting streptomycin into the middle ear to control recurrent episodes of vertigo in 8 patients with Meniere's disease. He concluded that intratympanic streptomycin could effectively ablate labyrinthine function.

Since that time the clinical use of aminoglycosides in Meniere's disease has evolved and grown exponentially. There is now substantial data that supports its effectiveness. Clinical data on intratympanic gentamicin therapy will be reviewed and discussed with an emphasis on questions that remain unanswered and challenges that lie ahead.

7 Genomic Distribution of Odorant and Taste Receptor Genes

Barbara J. Trask

Human Biology Division, Fred Hutchinson Cancer Research Center, 1100 Fairview Ave N., C3-168, Seattle, WA, United States

Roughly 0.5% of genes in mammalian genomes encode the receptors that mediate chemosensation. In this talk, I will review the work of many groups on the genomic organization of these genes. The olfactory receptor (OR) family is the largest gene family in mammals, with well over 1000 functional members expressed in the main olfactory epithelium of mice. The human family consists of over 900 genes, but only about a third of these genes appears to be capable of encoding a functional receptor. The OR genes are organized in clusters distributed on ~50 locations in the mouse

genome and ~100 locations in the human genome. The genes encoding the smaller families of V1R and V2R pheromone receptors, which are expressed in the vomeronasal organ, also reside in clusters in multiple chromosome locations in mice. The largest cluster has no counterpart in the human genome, and only one potentially functional human V1R or V2R gene has been identified. By a regulatory regime that is still not understood, each sensory neuron expresses only a single allele of single gene, chosen apparently randomly from among the many, widely distributed options in the genome. The enormous diversity of volatile odorants is thus recognized through the expression of large repertoires of receptors in sensory epithelia. In contrast, structurally diverse taste stimuli, such as amino acids, sugars, and bitter-tasting compounds, activate much smaller repertoires of receptors. These receptors are encoded by two unrelated gene families and expressed in sensory epithelial cells on the surface of the tongue. The three members of TAS1R family together mediate sweet and umami taste and reside on human chromosome 1. At least 30 TAS2R receptors, located in three genomic clusters, respond to bitter tastes. Odorant receptor genes occupy some of the most dynamic regions of mammalian genomes. These gene clusters arose by a series of local and inter-chromosomal duplications that involved segments of DNA much larger than the genes themselves. The clusters were subsequently modified by deletion, mutation, and gene conversion-like events. Much change has been recent: over half of OR genes in the mouse and human genomes appears to have arisen since the species diverged, and inter-individual variation is observed for some human OR genes in their number and chromosomal location (in addition to sequence polymorphisms). The high homology among recently duplicated OR clusters in the human genome predisposes these regions to ectopic recombination that can result in chromosome abnormalities associated with clinical disorders.

8 Abstract Unavailable

9 Mechanisms Underlying Odor Perception in Mammals

Buck Linda

Division of Basic Sciences, Howard Hughes Medical Institute, 1100 Fairview Avenue North A3-020, Seattle, WA, United States

The mammalian olfactory system can detect and discriminate an immense variety of volatile chemicals. It also detects pheromones that stimulate instinctive behaviors. How do mammals distinguish such a large variety of chemicals? And how are those chemicals translated by the brain into diverse perceptions and behaviors? In initial studies, we identified a multigene family encoding ~1000 different odorant receptors (ORs) in the nose. We later found an unrelated family of ~140 candidate pheromone receptors in the vomeronasal organ, another olfactory structure. We found that odor identities are encoded in a combinatorial fashion, with partially overlapping combinations of ORs detecting, and thereby encoding, different odorants. We also found that the combinatorial OR inputs undergo a series of transformations as odor signals travel from the nose to the olfactory bulb and then to the olfactory cortex. Our studies showed that neurons expressing the same OR are randomly distributed in 4 zones in the nose, but their axons converge at two specific spots in the bulb, creating a stereotyped sensory map in which inputs from different ORs are segregated. In

the olfactory cortex, we again found a stereotyped map of OR inputs. However, in sharp contrast to the arrangement in the bulb, different OR inputs appear to overlap in a complex pattern in the cortex. Moreover, single cortical neurons may receive combinatorial input from different ORs, allowing an integration of OR inputs important to the generation of odor perceptions. Our studies further indicate that signals derived from the same ORs are processed in parallel in olfactory cortical subareas thought to have different functions, but that certain subareas may receive signals from a selected subset of ORs.

10 Insights into taste transduction and perception from molecular, biochemical and transgenic studies

Robert F. Margolskee

Physiology & Biophysics, Howard Hughes Medical Institute at Mount Sinai School of Medicine, 1425 Madison Ave, New York, NY, United States

We have identified several taste cell signaling elements involved in transducing responses to sweet, bitter and *umami* (glutamate) compounds. These include: 1) α -gustducin, the α -subunit of a transducin-like G protein; 2) G β 3 and G γ 13, gustducin's $\beta\gamma$ -subunits; 3) α -transducin; 4) PDE1A, a phosphodiesterase; 5) Trpm5, a store activated calcium/cation channel; 6) T1r3, a G protein coupled receptor (GPCR).

We have used in vitro and in vivo assays to characterize the roles of these proteins in taste signaling. Bitter-responsive T2r/Trb taste receptors couple selectively to gustducin. α -gustducin activates PDE1A to degrade cNMPs, while $\beta\gamma$ -gustducin activates phospholipase C β 2 to generate inositol trisphosphate and diacyl glycerol. The subsequent steps in the G $\beta\gamma$ -phospholipase-IP $_3$ pathway are apparently activation of IP $_3$ type III receptors (IP $_3$ R3) and release of Ca $^{++}$ from internal stores followed by neurotransmitter release. Ca $^{++}$ influx in response to release from internal stores may be mediated by the transient receptor potential channel, Trpm5. In sum, bitter taste transduction utilizes heterotrimeric gustducin to mediate two responses: a decrease in cNMPs via its α -subunit and a rise in IP $_3$ via its $\beta\gamma$ moiety.

Knockout mice lacking α -gustducin display markedly reduced behavioral and nerve responses to bitter, sweet and umami compounds, implicating gustducin in the transduction of these tastes. Trpm5 knockout mice show similar deficits in their responses to bitter, sweet and umami. Studies with single and double knockout mice lacking α -gustducin and/or α -transducin show that α -transducin is involved in umami, but not in bitter or sweet. T1r3 knockout mice show no preference for artificial sweeteners, and have diminished, but not abolished, responses to sugars and umami compounds indicating that T1r3-independent sweet- and umami-responsive receptors and/or pathways exist in taste cells.

11 Regulation of Odorant Receptor Expression

Randall Reed¹, Joseph Lewcock²

¹*Department of Molecular Biology and Genetics, Johns Hopkins University, 725 N Wolfe St, Baltimore, MD, United States,*

²*Molecular Biology and Genetics, Johns Hopkins University, 725 N Wolfe Street, Baltimore, MD, United States*

The expression of a single odorant receptor (OR) from a repertoire

of more than 1000 genes contributes to odor coding and axonal targeting. The genes encoding these receptors each possess a simple genomic structure and small DNA segments surrounding the transcription initiation sites are sufficient to direct expression of reporters in a pattern that mimics the endogenous genes. One remarkable aspect of this gene regulation is that each olfactory neuron expresses OR protein from only one allele of this large, dispersed gene family. The mechanisms responsible for this regulation remain largely unknown. We have used targeted transgenesis to define a new role for OR protein as an essential regulator in the establishment of mono-allelic OR expression. An OR-promoter driven reporter expresses in a receptor like pattern, but unlike a native OR, is co-expressed with an additional OR allele. Expression of a functional OR from the identical promoter eliminates expression of other OR alleles. The presence of an untranslatable OR coding sequence in the mRNA is insufficient to exclude expression of a second OR. Together, these data identify the OR protein as a critical element in a feedback pathway that regulates odorant receptor selection. Current efforts in the laboratory are focused on elucidating the nature of the feedback signal and the mechanisms that lead to selective receptor expression.

12 Axon Targeting in Taste: Development of Sensory Ganglia and Target Gustatory Organs

Charlotte Mistretta

School of Dentistry, University of Michigan, 1011 N University Avenue, Ann Arbor, MI, United States

To develop gustatory circuits, neurons in sensory ganglia must establish connections with peripheral taste organs and central brainstem nuclei. Our recent focus is on factors that regulate: development of a specific set of taste organs in embryonic rat tongue, the fungiform papillae; and, functional differentiation of ganglia innervating these papillae, the geniculate and trigeminal. Fungiform papillae arise as nerve-free organs in a distinctive pattern, become densely innervated, and acquire taste buds and somatosensory receptors to transmit complex sensation from the tongue via ganglion neurons. The geniculate ganglion innervates apical papilla epithelium and eventually the taste buds, whereas the trigeminal ganglion innervates lateral papilla, and inter-papilla, epithelium. Thus, these ganglia must develop connections with contiguous but functionally distinct tongue tissue.

To study taste organ formation, we developed embryonic tongue cultures that retain morphological and molecular information from in vivo tongue and papillae. We have shown distinct roles for secreted factors, including sonic hedgehog, in separable processes of tongue and papilla formation and patterning. To understand differentiation of the innervating neurons from geniculate and trigeminal ganglia, we culture entire embryonic ganglia. Based on whole cell electrophysiological recordings, exposure to specific neurotrophins in vitro differentially affects excitability and discharge properties in ganglion neurons, before and during papilla formation. Furthermore, using sensitivity to tetrodotoxin to distinguish activity of sodium channels, it is clear that channel profiles in geniculate and trigeminal ganglia are selectively regulated by neurotrophins. Because these channels affect discharge patterns of lingual sensory neurons, regulation of ganglion electrophysiology by specific neurotrophins can direct differentiation of circuits for

tongue sensation.

(Supported by NIH, NIDCD Grant DC 000456)

13 Olfaction Targeted

Peter Mombaerts

Division of Basic Sciences, Fred Hutchinson Cancer Center, 1100 Fairview Ave North A3-020, Seattle, WA, United States

The olfactory system provides sensory information about the chemical composition of the external world. Olfactory chemoreception initiates in mammals at the level of sensory neurons that are located in the main olfactory epithelium and the epithelium of the vomeronasal organ (VNO). The former mediates mainly the detection of volatile odorants. The VNO mediates mainly the detection of nonvolatile odorants, many of which are pheromones. These are chemical signals that provide information about gender, dominance and reproductive status between individuals of the same species.

The dichotomy between the main and vomeronasal (or accessory) olfactory systems is further reflected at the level of the molecules that serve as receptors, or putative receptors, for their respective sensory stimuli. In the main olfactory system, odorant receptor (OR) genes encode seven-transmembrane proteins and are members of a multigene family that may comprise as many as 1000 genes in mouse and human. In the accessory olfactory system, two families of genes encoding seven-transmembrane proteins have been proposed to encode pheromone receptors. The first family of vomeronasal receptor (VR) genes is expressed selectively in neurons of the apical zone of the epithelium of the VNO. The second family of VR genes is expressed in neurons of the basal layer. There are no conserved motifs between the two families of VRs, and VRs have no sequence homology with ORs.

These chemosensory receptors are encoded by some of the most complex gene repertoires in the mammalian genome. Mining the Celera and public databases, we composed a first near-complete draft of the mouse V1R repertoire, cataloguing 137 intact genes in 12 distinct families. Our exploration of the human V1R repertoire resulted in the discovery of the five human V1R genes with an intact open reading frame.

Axons of neurons expressing a given V1R or V2R converge onto numerous glomeruli in the accessory olfactory bulb. Interestingly, dendrites of second-order neurons (mitral cells) frequently project to glomeruli of the same type. Thus, the initial divergent pattern of projections is rendered convergent in the accessory olfactory bulb.

14 Development Of Vestibular Otolith Receptors And Afferents During Spaceflight.

J David Dickman^{1,2}, Anna Lysakowski³, David Huss¹, Steve Price³

¹Otolaryngology, Washington University, 660 S Euclid, Box 8115, St. Louis, MO, United States, ²Anatomy and Neurobiology, Washington University, 660 S Euclid, Box 8115, St. Louis, MO, United States, ³Anatomy and Cell Biology, University of Illinois at Chicago, 808 S Wood St, Chicago, IL, United States

Development of the utricle and saccule vestibular otolith organs was examined in embryonic quails raised from fertilization in either control 1g, microgravity (0g), or hypergravity conditions .

Control 1g, 0g, and 2g fertilized eggs were arrested from development by cooling, placed into an incubator (ADF - SHOT, Inc), and either flown on shuttle Endeavor (0g, 1g in space centrifuge, STS-108) in space or into a ground lab centrifuge (2g) for 12 days. Upon gravity condition attainment, the ADF temperature was raised to 60° C, with a constant 65% relative humidity. Four 0g quail embryos and six 1g embryos were recovered alive at E12 upon shuttle landing. Twelve 2g animals and ten additional control 1g embryos were raised in ground ADF incubator conditions. The utricle and saccule otolith organs were harvested from all E12 embryos for study. The 0g embryos had smaller mean body weights (2.4 gms) as compared to either 1g controls (3.5 gms) or 2g (3.4gms) embryos. The ratios of otoconial stone weight/body weight increased by 40% in 0g and 75% in 2g embryos as compared to both flight and ground 1g controls. In addition, the mean saccular epithelium area was smallest in 0g embryos, middle sized in 1g embryos and largest in 2g embryos. Examination of the hair cell stereocilia polarizations showed that normal organizational arrangements were present for all gravity conditions. Number of hair cells and type are currently being assessed. Neural tracing (HRP) experiments were performed on all E12 embryos. Results showed that 0g embryo afferents had small axonal diameters, fewer branches and less synaptic contacts. 1g embryo afferents had larger axons, were more branched with numerous arborizations, and had more terminals. Embryos from 2g conditions had the largest diameter axons, most numerous terminal branches and terminals. Quantitative reconstructions of afferents from all animals is under study.

Supported in part by funds from NASA NCC2-1159.

15 Ultrastructural Analysis of Quail Vestibular Otolith Receptors in Microgravity

Anna Lysakowski¹, Steven D. Price¹, David Huss², J. David Dickman²

¹Anatomy and Cell Biology, Univ. of Illinois at Chicago, 808 S. Wood St., Chicago, IL, United States, ²Dept. of Otolaryngology, Washington University, 660 Euclid Ave., St. Louis, MO, United States

Development of the utricle and saccule vestibular otolith organs was examined in embryonic quails raised from fertilization in either normal 1g or microgravity (0g), or during 2g centrifugation on Earth. Fertilized eggs (single breeding colony, Univ. Wisconsin) were arrested from development by cooling, placed into an incubator (ADF - SHOT, Inc), and flown on STS108 for 12 days in space. Upon orbital insertion (2 hrs), the ADF temperature was raised to 99°F, with a constant 66% humidity. Four 0g quail embryos and six 1g embryos were recovered alive at E12 upon shuttle landing. Ten additional control embryos were raised in a normal ground ADF. The otolith organs were harvested for study from all E12 embryos. The 0g embryos had smaller mean body weights (2.4 gms) as compared to the 1g controls (3.5 gms). Hair cell number was not affected. In addition, mean saccular area was smaller in 0g as compared to 1g embryos. Electron microscopic observations reveal that striolar type I hair cells, in particular, have more synaptic ribbons per hair cell under both the 0g and 2g conditions. Our 0g hair cells showed more signs of cellular damage. These results suggest that gravity serves as a dependent variable for vestibular system development.

Supported by NASA NCC2-1159 and NASA NAG2-1589.

16 Hypersensitivity And Readaptation Of Utricular Nerve Afferents To Earth's 1g Following Exposure To Microgravity

R. Boyle¹, S. M. Highstein², A. F. Mensinger³

¹BioVIS Center, NASA, Mail Stop 239-11 Ames Research Center, Moffett Field, CA, United States, ²Department of Otolaryngology, Washington University, 4566 Scott Avenue Box 8115, St. Louis, MO, United States, ³Department of Otolaryngology, Washington University, 1049 University Drive, Duluth, MN, United States

The utricular organ is comprised of a hair cell neuroepithelium, a gel layer and a weight-lending otolith mass. Tilts and inertial accelerations of the head displace the hair bundles relative to the otolith mass, initiate the transduction process that transform the vector sum of the imposing accelerations into a neural code. Within the central pathways the otolith code is combined with canal signals and other sensory modalities to form a central representation of the body in space. Thus an abnormal otolith component of the gravito-inertial vector should have profound effects upon orientation and equilibrium, and might underlie the initial disorientation to microgravity and later readaptation syndromes after return to Earth's 1g. We studied the neural readaptation to Earth's 1g using electrophysiological techniques. The discharge and response characteristics of utricular afferents in toadfish were measured upon return from a 9-day (STS-95) and 15-day (STS-90) exposure to microgravity aboard two NASA shuttle orbital flights. Six recording sessions were made sequentially 10-117 hrs postflight. The most striking result is the occurrence of hypersensitive afferents, having nearly saturating response to such minor displacements of < 0.5 mm at 0.006g within the first day postflight; on average response sensitivity was elevated 3-fold during the first day postflight. Readaptation appeared over the course of about a day: afferent responses of 30 day postflight and control fish were similar. The microgravity exposure apparently resulted in a temporary up-regulation of the response sensitivity. Hypersensitivity recorded in the first hours postflight is in line with the data in rats by Ross indicating an increase in synaptic bodies due to microgravity exposure. The time course of return to normal afferent sensitivity parallels the decrease in disorientation in astronauts following return from space. (Supported by NASA, NIH and NASDA)

17 Rats in Space: Ultrastructural Studies of Cerebellar Cortex

Gay R. Holstein¹, Victor L. Friedrich Jr.², Giorgio P. Martinelli³

¹Neurology, Mount Sinai School of Medicine, Box 1140; One Gustave Levy Place, New York, NY, United States, ²Fishberg Center for Neurobiology, Mount Sinai School of Medicine, One Gustave Levy Place, New York, NY, United States, ³Neurology, Mount Sinai School of Medicine, One Gustave Levy Place, New York, NY, United States

During initial exposure to spaceflight, astronauts may experience postural illusions, motor abnormalities, and symptoms similar to motion sickness. These abnormalities usually resolve within several days, but may recur immediately after return to Earth. The neural mechanisms underlying these abnormalities are unknown. Toward that end, our laboratory has conducted studies of cerebellar cortex from adult rats flown on STS-90. We have examined tissue

from three time points during and following the 17-day mission, and compared tissue from flight animals with that of controls housed in flight-type cages maintained on Earth. For all subjects, the brainstem was removed and immersion-fixed for 18 days in a buffered aldehyde solution. Vibratome sections of the entire cerebellum were collected serially and processed for ultrastructural analysis. Thin sections from equivalent parasagittal nodular zones in flight and control samples were cut and analyzed.

In the flight rats sacrificed after 24 hours in microgravity, nodular Purkinje cells contained large cisternal stacks organized into lamellar bodies. Degeneration and synapse retraction were also present in Purkinje cell dendrites of these animals. In contrast, cerebellar cortical tissue from rats sacrificed on orbit after 14 days in microgravity did not show these structural alterations. The Purkinje cells appeared normal and healthy, with the usual complement of organelles including normal single cisterns. However, the cerebellar cortex of flight rats sacrificed 24 hr after the shuttle mission appeared similar to the samples from animals sacrificed 24 hr after shuttle launch. Lamellar bodies were frequent and extensive, and synapse retraction was observed. These data indicate that structural reorganization occurs in the cerebellar cortex during periods of change in the gravitational environment, and suggest a structural neurologic basis for the behavioral responses to altered gravity.

Supported by the NIH National Institute for Deafness and Other Communication Disorders (NIDCD grant DC02451) and by NASA (contracts NAG 2-946 and NCC2-1173).

18 Lost in Space: The neurophysiology of spatial orientation in microgravity

James J Knierim^{1,2}, Bruce L McNaughton², Gina R Poe²

¹Neurobiology & Anatomy, University of Texas-Houston Medical School, P.O. Box 20708, Houston, TX, United States, ²ARL Div. of Neural Systems, Memory, and Aging, University of Arizona, Life Sciences North Bldg., Room 384, Tucson, AZ, United States

Purpose. Place cells of the rat hippocampus combine self-motion and landmark information to fire in a spatially selective manner. Place cells are tightly coupled to head direction cells, which integrate the horizontal component of head angular velocity and are insensitive to pitch or roll. The hypothesis that 3-dimensional navigation in space flight can lead to mismatches between head direction signals and external landmarks, and thus result in abnormal spatial tuning of place cells, was tested on NASA's Neurolab Space Shuttle mission.

Methods. Rats were implanted with multiple electrodes and trained to run laps on a rectangular track on the ground. In flight, ensembles of 20-40 CA1 cells were recorded as rats navigated a new track that spanned 3 orthogonal surfaces.

Results. Place cell firing was abnormal in 2 of 3 rats tested on flight-day 4. The cells of one rat showed no spatial tuning at all. In a second rat, some cells displayed normal spatial tuning, but other cells displayed an abnormal radial symmetry in their spatial firing patterns. On flight-day 9, however, both rats had normal, highly selective place cells that discriminated among corresponding locations on the 3 orthogonal surfaces of the track.

Conclusions. Hippocampal cells can form unique, reliable representations of 3 orthogonal surfaces in microgravity, but they

appear to require either a period of adaptation to microgravity or more experience with the environment than is typically required in normal gravity. It remains to be determined whether the hippocampus in microgravity can fully represent all 6 spatial coordinates (3 spatial and 3 directional), or whether the system adapts by representing up-down relative to the body axis, as is often subjectively reported by humans, and thus developing independent 2-dimensional representations for each surface.

Supported by NASA, NIH, and ONR

19 Spaceflight influences on neurovestibular reactions

Laurence R. Young

MIT, Room 37-219, Cambridge, MA, United States

Exposure to extended periods of weightlessness in orbital flight has profound effects on the neurovestibular system and influences head and eye movements, postural control, and spatial orientation. The associated space motion sickness is among the earliest of the signs of adaptation to this new environment. We review the prominent neurovestibular phenomena associated with going into space and returning to earth and relate the issues to vestibular compensation and rehabilitation. Results from the Spacelab SLS-2 mission as well as the more recent Neurolab mission are included. A significant reduction in postflight ocular counterrolling and changes in ocular counterrolling left/right asymmetries after 2 weeks in space found in SLS-2, was brought into question in Neurolab.

20 Opening Plugged Tympanostomy Tubes: Effect of Inner Diameter and Shaft Length

Ajay J Mehta¹, Gary R Stevens², Patrick Joseph Antonelli¹

¹Otolaryngology, University of Florida, Box 100264, Gainesville, FL, United States, ²Biostatistics, University of Florida, Box 100264, Gainesville, FL, United States

Objective: To determine if tympanostomy tube (TT) inner diameter or shaft length impacts the rate of mucoid plug clearance.

Design: Ex vivo model.

Methods: Silicone TTs with different inner diameters (ID) and shaft length (SL) pairings (1.14 mm ID x 12 mm SL vs. 1.14 mm ID x 1 mm SL; 1.14 mm ID x 4.8 mm SL vs. 1.32 mm ID x 4.8 mm SL) were plugged with middle ear mucus (n = 15 / group) and placed in a model ear chamber. Ofloxacin otic solution was instilled into the chamber to cover the plugged TT and the time to clearance of each plug was recorded.

Results: TTs with larger IDs (p = 0.019) and greater SLs (p = 0.033) cleared plugs more rapidly. However, the difference in the percentage of tubes that unplugged was not significant (p = 0.151).

Conclusions: Rate of ex vivo TT plug clearance may be altered by changing TT inner diameter and shaft length.

21 Simple guideline for exploratory tympanotomy to identify idiopathic perilymph fistula

Satoshi Seki, Hideo Shinoda, Sugata Takahashi

Otolaryngology, Niigata University Faculty of medicine, Asahimachi 1, Niigata, Japan

The only way of confirming idiopathic perilymph fistula (IPF) is to perform exploratory tympanotomy (ET) and directly find perilymph leakage. We compared the observations in IPF cases confirmed by ET with those in strongly suspected IPF cases who had clear incidents but ET were not performed, and reported that persistent nystagmus without vertigo is the useful observation for IPF and rest is important to treat IPF without closure operation.

There are a lot of situations in which we waver the existence of IPF and many unnecessary situations for ET because of the improvement of hearing loss and vertigo. Sixteen IPF cases including some recurrence cases were investigated to set the simple guideline for ET, analyzed several observations in IPF such as the effect of rest on hearing, nystagmus on electronystagmography (ENG), pure tone audiogram (PTA), change of hearing level and so on.

In 38 % of IPF cases, hearing improvements at rest (in the morning, after 30 to 60 min rest or by observance at rest on the bed) were shown. 88 % of them presented some abnormal findings as persistent positional or spontaneous nystagmus without vertigo (mean 3 months) or with vertigo, fistula symptom and positional nystagmus with head in the affected ear down on ENG. On PTA 88 % of them had hearing loss at 8000Hz and 68 % of them did fluctuation of hearing at low-mid frequencies. If frequencies of hearing fluctuation were not limited at low-mid frequencies, in 94 % hearing fluctuations were seen or hearing loss worsened progressively.

We conclude that fluctuating or progressive hearing loss is requisite finding to perform ET, and if at least one of observations among hearing improvement at rest, persistent nystagmus with or without vertigo and fistula symptom is presented we should undergo ET to verify the leakage of perilymph fistula.

22 Internal evaluation of the cochlea using of a cochlear endoscope and laser-Doppler flowmetry

Michihiko Sone¹, Tsutomu Nakashima¹, Shinji Naganawa², Taku Hattori³

¹Otorhinolaryngology, Nagoya University Graduate School of Medicine, 65 Tsurumai-cho, Showa-ku, Nagoya, Japan,

²Radiology, Nagoya University Graduate School of medicine, 65 Tsurumai-cho, Showa-ku, Nagoya, Japan, ³Otorhinolaryngology, Nagoya University Graduate School of Medicine, 65 Tsurumai-cho, Showa-ku, Nagoya, Japan

Determining the etiology of profound hearing loss is hindered by the inaccessibility of the inner ear in vivo. In the ears of patients receiving cochlear implants, we have attempted to evaluate the cochlea from the inside by examining the scala tympani with a flexible endoscope and measuring cochlear blood flow by laser-Doppler flowmetry. Preoperative CT and MRI examinations provide information on the patency of the cochlea. Surgical procedures for cochlear implantation can be performed without

difficulty in most patients with profound sensorineural hearing loss, except for cases with structural anomalies or ossification. Performing cochlear implantation under conventional microscopy means that the electrode insertion after cochleotomy is a partially blind procedure. In addition to the internal evaluation of the cochlea, the flexible cochlear endoscope aids in safe and reliable electrode insertion. The cochlear endoscope should be small in diameter and soft enough to pass along the curved cochlea. We used fibers made from multiple-components instead of conventional quartz fibers and would have been able to observe the ascending segment of the cochlea through the fiberscope. We also evaluated the cochlear blood flow with the tip of the probe in the scala tympani. Reduction of the cochlear blood flow was identified in patients with cochlear ossification after meningitis and in patients with idiopathic progressive sensorineural hearing loss. Fibrous or bony occlusion of the perilymphatic space has been suggested to be related to disturbances of the cochlear blood flow. We would also discuss our observations of the inside of the cochlea, using a virtual endoscopy.

23 Incus observations after long-term use of the Vibrant Soundbridge system

Ingo Todt, Alexander Blödwow, Dietmar Basta, Arne Ernst
Department of Otolaryngology, Unfallklinik Berlin, Warenastr. 7, Berlin, Germany

Aim: To evaluate FMT (floating mass transducer)- related incus changes after long-term use of the Vibrant Soundbridge system .

Method: In a retrospective case report of explantation of the Vibrant Soundbridge system we present to our knowledge the first observations of long term changes of the incus.

Results: After 4 years of FMT fixation related changes of the long process of the incus were of minor degree. Macroscopic observation of the incus show no necrosis but light erosions on the area of the clamp. Microscopic observations of the incus show decent histological changes.

Conclusion: With the knowledge of stapes revision surgery observations the long process of the incus is known to be one of the most sensitive regions of the middle ear. On the pattern of minor changes of the long forceps of the incus after 4 years of FMT-fixation no general conclusions except that of a possible region of complications can be made.

24 Realistic simulation of otosurgical approaches by a new computer based haptic 3D-model

Rudolf Leuwer¹, Andreas Petersik², Bernhard Pflesser², Ulf Tiede², Karl-Heinz Höhne²

¹ENT-Department, Hamburg University Medical School, Martinistr. 52, Hamburg, Germany, ²Institute of Mathematics and Computer Science in Medicine, Hamburg University Medical School, Martinistr. 52, Hamburg, Germany

Introduction: Both, the profound knowledge of temporal bone anatomy and surgical skills are prerequisites for any otologic surgeon. Hence, otosurgical training crucially depends on the availability of a temporal bone lab. Aim of the present project was to create a system for realistic computer simulation of laterobasal

surgical approaches.

Methods: For the new system a volumetric high resolution temporal bone model was created, derived from human CT-data. This model was completed by a method for high resolution, multi-point collision detection. Thus, the information of collisions between the model and the virtual surgical drill as well as its resulting forces are calculated and presented to the surgeon via a haptic device. Simultaneously the current 3D visual model is modified according to the surgical cut off.

Results: The multi-volume visualization technique allows real-time visualization of interactively generated cut surfaces and at the same time highly detailed haptic feedback of the manipulation. The virtual "hardness" of the "bone" can be varied as well as the diameter of the drill head. The arrangement of the screen and the haptic device simulates the real situation in a temporal bone lab. The spatial perception is enhanced by stereoscopic viewing with shutter-glasses.

Conclusion: The system presented here, both facilitates the understanding of the complex surgical anatomy of the temporal bone and renders the haptic sensation of the bone preparation. Thus it is a promising new tool for the otosurgical training.

25 Congenital MCMV Infection In The Auditory System of SCID Mice

Nigel Keith Woolf^{1,2}, Dawn V Jaquish¹, Anurdha Desai¹, Fred J Koehn¹

¹Surgery, UCSD Medical School, 9500 Gilman Drive, La Jolla, CA, United States, ²Surgery, VA Medical Center at San Diego, 3350 La Jolla Village Drive, San Diego, CA, United States

SCID (severe combined immunodeficient) mice, unlike immunocompetent mice, were found to be highly susceptible to congenital MCMV (murine cytomegalovirus) infection. Following intrauterine transplacental injection into the amniotic compartment at embryonic (E) age E11 with 68 PFU of a recombinant Smith strain MCMV which expresses an EGFP reporter gene (rMCMV kindly provided by Drs. Stanley Henry and John Hamilton: Henry et al. *J Virol Meth* 89:61, 2000), 75% of the injected litters had at least one rMCMV infected embryo. Forty-four percent (12/27) of the surviving injected embryos at E18 were congenitally infected: 75% of the infected embryos had rMCMV immunolocalized in their brains and 58% rMCMV immunolocalized in their cochleas. Within the cochleas, rMCMV was primarily confined to spiral ganglion cells, central projections of the VIIIth nerve trunk within the modiolus, and resorbing mesenchymal cells within scala tympani and scala vestibuli. Congenital infection, identified by immunolocalization of rMCMV in the brain and/or cochlea, correlated with significant changes in cerebral mRNA expression patterns of multiple pro-inflammatory cytokines, chemokines, and their receptors. However, congenital rMCMV infection-induced modulation of cerebral pro-inflammatory cytokines and chemokines at E18 did not correlate with inflammatory cell infiltration into the CNS or cochlea. These results suggest that, once the virus has circumvented the placental barrier, the severe T- and B-cell immunodeficiencies in SCID mice significantly facilitates permissiveness for congenital MCMV infection, with a distinct viral tropism for the brain and cochlea.

26 The Patulous Eustachian Tube — New Diagnostic Procedures and Therapeutic Options

Sören Wenzel¹, Hartwig Seedorf², Thomas Kucinski³,
Hannes Maier¹, Rudolf Leuwer¹

¹ENT-Department, University of Hamburg Medical School,
Martinistr. 52, Hamburg, Germany, ²Dental Prosthetics,
University of Hamburg Medical School, Martinistr. 52, Hamburg,
Germany, ³Neuroradiology, University of Hamburg Medical
School, Martinistr. 52, Hamburg, Germany

Objectives: Clinical presentation of the patulous eustachian tube is complex and etiology as well as pathomorphism still unclear. Therefore no definitive and causal treatment is available and success often poor or only temporarily. It was the aim to examine the clinical role of the masticatory muscles and Ostmann's fatty tissue in abnormal patency of the tube to determine therapeutical consequences.

Methods: In a study of 16 consecutive patients with patulous eustachian tube syndrome individual clinical problems, causal pathomorphism, and the therapy were investigated. Patients were examined by an ENT specialist, a radiologist, and a specialized dentist. The criteria were the anamnesis, MRI findings of the paratubal structures, and orthodontology results.

Results: All patients had normal audiograms, autophony and aural fullness in one or both ears. In 9 cases symptoms were temporarily relieved in head-down position. 3 patients experienced excessive weight loss and 4 had a temporomandibular disorder. 6 patients showed a reduced Ostmann's fatty tissue and 7 patients had an atrophy of the medial pterygoid muscle in MRI.

Conclusions: The clinical picture of patulous Eustachian tube is caused by different pathoanatomical findings of the tubal environment. The multidimensional pathogenesis requires additional diagnostics (MRI, orthodontology) to initiate causal and sufficient treatment. The atrophy of the medial pterygoid muscle is a new decisive aspect of the mechanisms of abnormal patency of the eustachian tube. This knowledge must influence the consecutive surgical or orthodontologic therapy.

27 Induction of Inducible Nitric Oxide Synthase and Apoptosis by LPS and TNF- α in Nasal Microvascular Endothelial Cells

Shoji Arai, Narinobu Harada, Akihiko Nakamura, Shingo Kakimoto, Hiromi Ikeda, Nobuo Kubo, Toshio Yamashita
*Otolaryngology, Kansai Medical University, Fumizonochi 10-15,
Moriguchi, Japan*

Disorder of endothelial barrier leads to an abnormal leakage of blood components, resulting in tissue edema and dysfunction. This microvascular leakage also plays an important role in airway inflammation and may contribute to the pathogenesis of airway disease such as asthma. It has been suggested that endogenous nitric oxide (NO) plays an important role in the regulation of airway microvascular leakage (Mehta et al., *Am J Physiol.* 275: L961-968, 1998). Inflammatory mediators such as cytokines and growth factors liberated by leakage also have the potential effects to endothelium dysfunction. However little is known about the role of microvascular leakage in nasal disease such as allergic rhinitis and sinusitis.

In the present study, we investigated whether LPS and TNF- α can induce expression of inducible nitric oxide synthase (iNOS) and apoptosis in cultured nasal microvascular endothelial cells (MVECs). Under normal condition, weak expression of iNOS in MVECs was observed compared with the control staining without iNOS antibody which showed no fluorescence staining signal. iNOS expression under normal condition was suppressed by 1400W, an inhibitor of iNOS. These results suggest that iNOS may be expressed in MVECs under normal condition. Stimulation of LPS and TNF- α for 24 hours increased expression of iNOS in MVECs, respectively. Co-administration of LPS and TNF- α for 24 hours induced intense expression of iNOS in MVECs compared with the expression by each substance alone. 1400W suppressed iNOS expression by co-administration of LPS and TNF- α , dose-dependently. To confirm apoptotic cell death, nuclear morphology was examined by the DNA-binding dye Hoechst 33342. Co-administration of LPS and TNF- α induced apoptosis in MVECs using Hoechst 33342. The present study suggests that LPS and TNF- α can induce expression of iNOS and apoptosis in MVECs. Our results also suggest that microvascular leakage may play an important role in nasal inflammation and edema.

28 Matrix Metallo-Proteinases in Cholesteatoma: a Non-invasive Assay Correlates with Clinical Invasiveness

Eric E. Smouha¹, Lorne M. Golub², Hsi-Ming Lee², Timo Sorsa³, Stanley Zucker⁴

¹Otolaryngology, SUNY Stony Brook, HSC T 19 090, SUNY, Stony Brook, NY, United States, ²Oral Biology and Pathology, SUNY Stony Brook, School of Dental Medicine, Stony Brook, NY, United States, ³Periodontology and Medicinal Chemistry, University of Helsinki, PL63 Haartmaninkatu 8, Helsinki, Finland, ⁴Medical Oncology, SUNY Stony Brook, VA Medical Center, Northport, NY, United States

Hypothesis: Collagenase activity, as measured by a non-invasive method, correlates with tissue levels of matrix metallo-proteinase (MMP) enzymes in cholesteatoma biopsies, and can serve as a surrogate marker for disease activity.

Background: Cholesteatoma is an inflammatory ear disease characterized by invasiveness and bone destruction, features which are mediated by collagenases. Prior studies have shown that MMP enzymes are responsible for collagenase activity in cholesteatoma.

Methods: In patients undergoing surgery for cholesteatoma, a micro-aliquot of tympanic membrane fluid (TMF) was eluted on filter paper, and a tissue biopsy was also taken. TMF-collagenase activity was measured by incubating extracts from these samples with an MMP-susceptible octapeptide substrate. In extracts from the tissue biopsies, collagenase activity was similarly measured, and levels of MMP-9 and MMP-2 were determined by zymography, and MMP-8, MMP-13, and MMP-1 were measured by western blot. TMF-collagenase and tissue MMP levels were also correlated with a clinical scale of disease activity. These results were compared with samples obtained from control patients with non-cholesteatoma chronic ear disease.

Results: TMF-collagenase activity, when stratified into levels of zero, low (<50%), or high (>50%) activity, correlated well with tissue collagenase activity and with clinical scores of disease severity

and bone destruction. TMF-collagenase activity reflected the levels of MMP-8, 1, 13, 2, and 9 in the underlying tissue.

Conclusions: Collagenase activity can be measured by a non-invasive method that reflects the enzyme activity in cholesteatoma tissue. TMF-collagenase activity correlates with tissue levels of MMP-8, 1, 13, 2, and 9, and with clinical scores of disease severity. TMF-collagenase activity is therefore a valuable biomarker for disease activity, and may be useful for evaluating therapeutic interventions.

29 Middle Ear Therapy with L-NAME for Meningogenic Labyrinthitis Ossificans

Fan Si, Sorin L. Ilie, Hilary A. Brodie, Steven P. Tinling

Department of Otolaryngology, University of California, Davis, Rm 209 1515 Newton Ct., Davis, CA, United States

Middle Ear Therapy with L-NAME for Meningogenic Labyrinthitis Ossificans

One of the suspected mechanisms for the damage associated with pneumococcal meningitis is the stimulation in the production of nitric oxide (NO), a free radical which damages tissue. This study attempts to limit the development of NO in pneumococcal meningitis by instilling N^o-nitro-L-arginine methyl ester (L-NAME), a NO synthase inhibitor, into the middle ear.

Pneumococcal meningitis was induced in four groups of gerbils by intrathecal injection of *Streptococcus Pneumoniae* type 3 followed by a one-week course of penicillin. The animals in group 1, 2, and 3 received a middle-ear injection of L-NAME (200mM, 400mM and 200mM concentrations) on days 0, 0 and 2 respectively. Group-4 served as the infected control. ABR was measured pre-operatively and 90-day post induction of meningitis. The animals' temporal bones were analyzed histologically at the conclusion of the study.

Penetration of L-NAME into the cochlea was assessed by measuring the L-NAME activity in the perilymph, which was determined using a commercial kit (Calbiochem-Novabiochem, UK) that uses the conversion of arginine to citrulline as a measure of NOS activity. Instillation of L-NAME into the middle ear was demonstrated to permeate the round window into the inner ear in a dose-dependent manner.

The average deterioration in pure tone thresholds following the induction of meningitis in group 1, 2, 3 and 4 at 5 kHz and 30 kHz were (54db, 58db), (32.5db, 48db), (20.5db, 48.5db) and (67db, 75.5db), respectively. The mean proportional area of cochlear lumen filled with fibrosis or neo-ossification was greatest in group-4 animals, followed by group 1, next to group 2 and 3.

These results suggest nitric oxide plays a significant role in the cochlear damage following the induction of meningitis. L-NAME, injected into the middle ear, diffuses into the cochlea and reduces post-meningitic hearing loss and labyrinthitis ossificans by inhibition of nitric oxide formation.

Supported by a research grant from the DRF.

30 Internal temperature of the cochlea correlates best with temporalis muscle temperature: application to testing for otoprotective effect of mild hypothermia on surgical trauma induced hearing loss

Adrien A Eshraghi^{1,2}, Marek Polak¹, Omar Nehme¹, Jiahe He¹, Ophelia F Alonso³, Fred F Telischi¹, Dalton W Dietrich³, Thomas J Balkany¹, Thomas R Van De Water¹

¹Otolaryngology, University of Miami, PO box 016960, Miami, FL, United States, ²Surgery, VA Medical Center, 1201 NW16th street, Miami, FL, United States, ³Neurological Surgery, University of Miami, PO box 016960, Miami, FL, United States

Hypothermia has been shown to provide a protective effect in laboratory animal models of stroke, brain trauma and myocardial ischemia. Hypothermia has also been shown to lessen the deleterious effect of acoustic trauma and ischemia on auditory function. Because of the increasing trend of implantation of patients with residual hearing, the application of mild hypothermia during surgery to protect hearing is our ultimate goal. Rectal temperature has been used to define the degree of hypothermia in sound trauma and cochlear ischemia experiments, while in some brain trauma experiments the temporalis muscle temperature has been demonstrated to best reflect the internal temperature of brain tissue. Using whole body cooling, we measured changes of temperature with rectal, cochlear, temporalis muscle and brain probes in anesthetized laboratory rats. Data obtained from these four different sites in 6 adult laboratory rats were evaluated. Statistical analysis showed that the highest correlation was between the temperature of cochlea and the temperature of temporal muscle. Regression analysis showed that cochlear temperature could be predicted with temperature of temporal muscle with correlation coefficient (r) of 0.969 (p < 0.001, F = 1264.8). Furthermore, correlation coefficient between temperature of cochlea and temperature of rectum was 0.959 (p < 0.001, F = 930.1) and correlation coefficient between temperature of cochlea and temperature of brain was 0.914 (p < 0.001, F = 414.6). Correlation between temperature of temporal muscle and temperature of brain was 0.946 (p < 0.001, F = 701.3). ANOVA single factor test showed no significant effect of place of the temperature measurement ((= 0.05, p = 0.755, F = 0.39).

Future experiments will utilize a temporalis muscle temperature probe during a state of mild hypothermia to determine if this lowering of the body temperature can protect against hearing loss caused by surgery related trauma.

31 The therapeutic effect of the formulas selected with method of liver spleen kidney and stasis theory of TCM on the new sensorineural deafness

Weijun Xuan¹, Yuyou Huang^{1,2}, Xiaofan He², Yinyin Lan²

¹Department of Otolaryngology, Traditional Chinese Medical University of Guangxi, Hearing Research Center, Nanning, China, People's Republic of, ²Department of Otolaryngology, Traditional Chinese Medical University of Guangxi, Hearing Research Center, Nanning, China, People's Republic of

Objective: To observe the therapeutic effect of the traditional Chinese medical formulas selected with method of liver spleen

kidney and stasis theory of TCM on the new sensorineural deafness, and inquire into the mechanism of TCM and modern pharmacological action. Method: Under the conduct of the liver spleen kidney and stasis theory of TCM, clinical experience, modern pharmacology, etiology and pathology, the formulas consists of the traditional Chinese medicines witch have the action of the soothing the liver, strengthening the spleen, tonifying the kidney, and promoting blood circulation. Selected 50 cases with complaint of sudden deafness witch case history were during one month. They were randomized to divide into the treating group of 25 cases with integrated the Chinese traditional medical formulas and western medicine, and the controlling group of 25 cases with western medicine. Another 20 cases with complaint of various sensorineural deafness, witch case history was above one but less than three months, were treated by the Chinese traditional medical formulas. Result: The total effective rate or cure and obvious effective rate was significantly higher in treating group than in controlling group ($p < 0.05$). Another treating group treated by Only the Chinese traditional medical formulas also obtain definite therapeutic effect. Conclusion: It suggests, based on the study, that formulas with method of liver spleen kidney and stasis theory of TCM against the new sensorineural deafness possess the distinguishing features with wide pharmacological basis, directing at various causes of disease and pathologic change, obviously promoting therapeutic effect.

32 Ethnicity and Phenotypic Presentation of a Pediatric Non-Sensorineural Hearing Loss Population to a Multidisciplinary Hearing Loss Clinic

Jose G. Gurrola II¹, James Coticchia²

¹*School of Medicine, Case Western Reserve University, 10900 Euclid Ave, Cleveland, OH, United States*, ²*Dept of Otolaryngology Head and Neck Surgery, Wayne State University, 4201 S. Antoine, 5E-UHC, Detroit, MI, United States*

This report describes the ethnicity and phenotypic presentation of children with nonsyndromic sensorineural hearing loss (SNHL) to a multidisciplinary hearing loss clinic. Patients range from ages 1 to 16 with 29 females and 34 males. Each patient received a comprehensive evaluation consisting of examination of prenatal/antenatal risk factors, history of present illness, family history, physical exam, metabolic testing, high-resolution temporal bone imaging, physicoacoustic audiograms, tympanograms and DPOAEs. Genetic evaluations were performed for each patient along with testing for Connexin 26 and A1555G mitochondrial mutations. While none of the patients tested positive for the A1555G mutation, 5 were homozygous positive for Connexin 26 35delG mutations. Overall, 54% percent of the patients presenting were Caucasian, 25% were African-American (AA), 11% were Hispanic and 10% were of unknown ethnicity. Of the patients testing positive for the Connexin 26 mutation, 3 were Caucasian, one Hispanic and one patient unknown. Seven of the 63 patients presented with inner ear anomalies: 5 Caucasian and 2 AA. None of the patients testing positive for Connexin 26 mutations presented with inner ear anomalies. In regard to family history, 47% of Caucasians, 40% of AA, 57% of Hispanics, and 67% of the unknown group presented with a family history of hearing loss. Hearing loss presentations demonstrated 76% of Caucasians, 75%

of AA, 71% of Hispanics and 100% of the unknown group had bilateral hearing loss. In each ethnic group, greater than 78% of the patients presented with hearing loss of greater than two years. This loss tended to be stable in the majority of cases. The difference in ethnicity may be a factor in the genetic mutations identified and is consistent with other reports indicating a low incidence of Connexin 26 mutations in AA, other factors such as inner ear anomalies and positive family history were not distinctly different among the different ethnic groups.

33 Antibiotic and Steroid Prophylaxis for Hearing Loss Secondary to Semicircular Canal Transection in Pseudomonas Otitis Media

James C. Lee¹, Rahim A Remtulla², Mei Zhang³, Patrick J. Antonelli¹

¹*Otolaryngology, University of Florida, Box 100264, Gainesville, FL, United States*, ²*Drexel University, University of Florida, Box 100264, Gainesville, FL, United States*, ³*Communicative Disorders, University of Florida, Room 225, Griffin Floyd, Gainesville, FL, United States*

Objectives: Accidental violation of the semicircular canals (SC) in the presence of otitis media (OM) is commonly associated with permanent sensorineural hearing loss (HL). The purpose of this experiment was to determine if prophylactic administration of antibiotics or corticosteroids can attenuate the severity of HL in a guinea pig model.

Study Design: Prospective and controlled animal model.

Methods: OM was induced in pigmented guinea pigs by bilateral, transtympanic injection of *Pseudomonas aeruginosa* (PA). 2–4 days later, one horizontal SC was randomly transected. In the first series of guinea pigs, enrofloxacin was initiated either immediately before or after surgery. In the second series, all guinea pigs received prophylactic enrofloxacin and half received prophylactic dexamethasone. Hearing was tested before and after surgery.

Results: Cultures were positive for PA in 47 of 47 ears. SC transection was associated with significant HL. HL was significantly greater in animals given antibiotics after transection (16 vs 32 dB for clicks, 0.0220). Addition of prophylactic steroids did not further reduce HL (7 vs. 14 dB for clicks, $p = 0.6919$).

Conclusion: HL due to SC transection in the presence of PA may be attenuated with prophylactic antibiotic therapy in a guinea pig OM model.

34 Medications Used By Tinnitus Patients and their Impact on Treatment

Margaret M Jastreboff¹, Douglas E Mattox¹, Lisa Payne², Pawel J Jastreboff¹

¹*Otolaryngology, Emory University School of Medicine, 1365-A Clifton Road, NE, Atlanta, GA, United States*, ²*Otolaryngology, Emory Clinic, 1365-A Clifton Road, NE, Atlanta, GA, United States*

Many drugs have been tried to alleviate tinnitus, or to reduce anxiety, depression, sleep deprivation - the most common problems induced by tinnitus. There is no drug which has been proven to be effective for tinnitus treatment without profound side effects. Medications utilized by tinnitus patients frequently complicate

their condition and treatments. Since tinnitus is frequently not the only health problem, many patients use medications for other conditions as well.

Patients' medications were reviewed and divided into groups on the basis of their chemical category (e.g., benzodiazepines), mechanisms of action (e.g., calcium channel blockers) or typical application (e.g., antidepressants). Patients were treated with Tinnitus Retraining Therapy (TRT). As TRT is aimed at inducing plastic changes in the brain, drugs interfering with brain activity were analyzed separately. Tinnitus severity and the progress of the treatment were assessed by Tinnitus Handicap Inventory (THI) during initial and follow-up visits.

Results from over 300 patients were analyzed and revealed that close to 75% were on at least one form of medication, most commonly on drugs affecting brain activity. Approximately 30% of the patients were on antidepressants or anxiety medications. Benzodiazepines were most frequently used. Patients on psychotropic medications tend to have higher initial THI scores and exhibit smaller improvement when treated with TRT.

35 Antibiotic and Steroid Prophylaxis for Hearing Loss Secondary to Semicircular Canal Transection in *Pseudomonas* Otitis Media

James Lee¹, Rahim Remtulla¹, Patrick Antonelli¹, Mei Zhang²

¹Otolaryngology, University of Florida, 1600 Archer Rd, Gainesville, Florida, United States, ²Communicative Disorders, University of Florida, 1600 Archer Rd, Gainesville, Florida, United States

ABSTRACT

Objectives: Accidental violation of the semicircular canals (SC) in the presence of otitis media (OM) is commonly associated with permanent sensorineural hearing loss (HL). The purpose of this experiment was to determine if prophylactic administration of antibiotics or corticosteroids can attenuate the severity of HL in a guinea pig model.

Study Design: Prospective and controlled animal model.

Methods: OM was induced in pigmented guinea pigs by bilateral, transtympanic injection of *Pseudomonas aeruginosa* (PA). 2–4 days later, one horizontal SC was randomly transected. In the first series of guinea pigs, enrofloxacin was initiated either immediately before or after surgery. In the second series, all guinea pigs received prophylactic enrofloxacin and half received prophylactic dexamethasone. Hearing was tested before and after surgery.

Results: Cultures were positive for PA in 47 of 47 ears. SC transection was associated with significant HL. HL was significantly greater in animals given antibiotics after transection (16 vs 32 dB for clicks, 0.0220). Addition of prophylactic steroids did not further reduce HL (7 vs. 14 dB for clicks, $p = 0.6919$).

Conclusion: HL due to SC transection in the presence of PA may be attenuated with prophylactic antibiotic therapy in a guinea pig OM model.

36 Combination of Low Dose Mineralocorticoid and Glucocorticoid Effective in Control of Hearing Loss in Autoimmune Mice

Dennis R. Trune, Beth Kempton, Sarah K. Parrish
Oregon Hearing Research Center, Oregon Health & Science University, 3181 SW Sam Jackson Park Rd, Portland, Oregon, United States

The standard therapy for sudden hearing loss or autoimmune hearing loss is the glucocorticoid prednisone. However, the severe side effects of systemic glucocorticoids often prevent long term management of hearing loss. Alternative steroid treatments that minimize or eliminate these systemic effects would have significant benefit in the control of such hearing disorders. Toward this end, this laboratory has been studying the impact of steroid treatments on the control of hearing loss in the MRL/MpJ-Fas^{lpr} autoimmune mouse model. Previous studies in these mice have shown that hearing loss progresses with systemic immune complex formation, inner ear pathology is limited to the stria vascularis, and treatment with the mineralocorticoid aldosterone is as effective as prednisolone in reversing hearing loss (Trune & Kempton, *Hear. Res.* 155:9-20, 2001). The present study was conducted to determine if the two steroids in combination would be more effective than their equivalent doses alone. If reduced levels of each are required when combined, it may lead to better control of hearing disorders with less severe side effects.

MRL/MpJ-Fas^{lpr} mice normally develop hearing loss at 3-4 months of age, so mice were tested for baseline ABR thresholds at 3 months and then treated with steroids in their drinking water for two months. Mice were given aldosterone (3 or 5 $\mu\text{g}/\text{kg}$) or prednisolone (1 or 3 mg/kg) to determine the lowest effective dose of each. Other mice were given the two steroids in combination doses of Pred 0.5 mg -Aldo 1.5 μg ; Pred 1 mg -Aldo 3 μg ; or Pred 1.5 mg -Aldo 5 μg . The various groups were tested monthly to determine the relative impact of the different steroid treatments had in controlling hearing loss. Analyses showed that hearing loss was not prevented by prednisolone at 1 mg/kg or by aldosterone at 3 $\mu\text{g}/\text{kg}$ when given alone. However, the two steroids at these particular doses in combination did effectively control hearing loss. These results suggest that combination drug therapy may lead to equally effective treatments for hearing loss using lower doses. The ability to manage hearing loss while minimizing systemic levels may be beneficial in reducing the detrimental side effects often experienced with glucocorticoid therapy.

(Supported by NIH-NIDCD R01 DC 05593)

37 Comparison of the Natural Mineralocorticoid Aldosterone and a Synthetic Analog Fludrocortisone Acetate in Control of Hearing Loss in Autoimmune Mice

Dennis R. Trune, Beth Kempton, Sarah K. Parrish

Oregon Hearing Research Center, Oregon Health & Science University, 3181 SW Sam Jackson Park Rd, Portland, Oregon, United States

Effective management of autoimmune hearing loss is achieved with the glucocorticoid prednisone, although the underlying cochlear mechanisms are unknown. Studies of MRL/MpJ-Fas^{lpr} autoimmune mice have shown that inner ear pathology is limited to the stria vascularis and treatment with the mineralocorticoid aldosterone is as effective as prednisolone in reversing hearing loss (Trune & Kempton, *Hear. Res.* 155:9-20, 2001). The implication is that stria ion transport is compromised in systemic autoimmune diseases and the mineralocorticoid actions of the glucocorticoid prednisone may be involved in control of autoimmune hearing loss.

The long term use of the natural mineralocorticoid aldosterone is compromised by normal feedback adjustments to decrease aldosterone production or modify its effects through aldosterone escape. The synthetic mineralocorticoid fludrocortisone acetate (Florinef® Acetate) is used clinically to enhance sodium reabsorption, but its role in hearing control has not been evaluated. Therefore, MRL/MpJ-Fas^{lpr} autoimmune mice were treated with fludrocortisone or aldosterone to evaluate their respective abilities to control progression of autoimmune hearing loss.

Baseline ABR thresholds were determined at 3 months of age, prior to autoimmune disease and hearing loss onset. Mice were then treated with either fludrocortisone (10 µg/kg) or aldosterone (15 µg/kg) in their drinking water. Untreated autoimmune mice received tap water. At the end of the first month of treatment, aldosterone treated mice had significantly better thresholds than the other two groups. At the end of two months, the fludrocortisone mice had significantly better thresholds than either of the other two groups. These findings imply aldosterone may be effective in short term treatment, but the body's feedback mechanisms to control its production may limit its effects long term. On the other hand, the therapeutic analog fludrocortisone may provide better long term management without suppression of natural mineralocorticoid production. The potential clinical application of fludrocortisone to control stria-related hearing disorders is a provocative implication of these findings, particularly in light of the side effects of glucocorticoid treatment.

(Supported by NIH-NIDCD R01 DC 05593)

38 The effects of type1 diabetes mellitus on the cochlear structure and vasculature in human temporal bones

Hisaki Fukushima^{1,2}, Sebahattin Cureoglu¹, Patricia A Schachern¹, Michael M Paparella³, Naomi Fukushima¹, Tamotsu Harada²

¹Otolaryngology, University of Minnesota, 420 Delaware Street, Minneapolis, MN, United States, ²Otolaryngology, Kawasaki Medical School, 577, Kurashiki, Japan, ³Otolaryngology, Minnesota Ear Head and Neck Clinic, 701 25th Ave.S. Suite 200, Minneapolis, MN, United States

The typical hearing loss attributed to diabetes is a gradually progressive, bilateral, sensorineural hearing loss. The microangiopathy associated with diabetes has been proposed to affect inner ear vasculature causing degeneration of inner ear structures and finally hearing loss. However, some authors also believe acoustic neuropathy is the pathogenic mechanism responsible for hearing loss in the patients with diabetes. To examine the effects of diabetes on the cochlea, we conducted a study of temporal bones from patients with insulin-dependent diabetes. In the present study, 24 temporal bones from 12 patients with type1 diabetes mellitus and 18 temporal bones from nine normal cases were studied. The thickness of the wall of the capillaries under the basilar membrane was quantified by using imaging techniques. Cochlear hair cells and spiral ganglion cells were counted. In addition, the areas of the stria vascularis and spiral ligament were quantified.

The capillary walls in the diabetics (mean 2.37±0.64µm) were thicker than the normal controls (mean 1.47±0.34µm) (p<0.05). Loss of the outer hair cells was significant in the lower basal turn of the cochlea in diabetics. Atrophy of stria vascularis in the upper turns of the cochlea in diabetic group was significantly higher than normal group (p<0.05). The number of spiral ganglion cells and the area of spiral ligament were normal.

This study suggests that diabetic hearing loss results from microangiopathic involvement of inner ear vessels and subsequently stria vascularis atrophy and hair cell loss.

39 Tinnitus and hearing loss following administration of ototoxic drugs in humans: Results of a large prospective study

Dawn Konrad-Martin^{1,2}, David S. Phillips¹, James A. Henry¹, Wendy J. Helt¹, Jane S. Gordon¹, Kelly M. Deal¹, Stephen A. Fausti¹

¹Nat'l. Cntr. for Rehab. Auditory Research (NCRAR), Portland VA Medical Center, 3710 SW US Veterans Hospital RD, Portland, OR, United States, ²Department of Otolaryngology, Head & Neck Surgery, Oregon Health and Science University, 3181 SW Sam Jackson Park RD, Portland, OR, United States

This prospective study describes ototoxicity-induced tinnitus and the relationship between drug-induced changes in hearing and tinnitus status. The study was part of a Veteran's Affairs Rehab R&D project to develop methods for early detection and monitoring of ototoxicity-induced hearing loss. Subjects were 488 patients receiving cisplatin or carboplatin (CDDP group), aminoglycoside antibiotics (AMG group), or non-ototoxic drugs (Control group); 962 ears met inclusion criteria. Behavioral hearing thresholds were

measured through 16,000 Hz and were compared to results of ear-specific tinnitus surveys. Audiometric and survey data were obtained prior to, during, and following drug treatment. Baseline tinnitus rates were high across groups (40% for the CDDP group, 39% for the AMG group, and 34% for Controls), possibly because subjects were mostly older, noise-exposed veterans with some pre-existing hearing loss. Ears free from tinnitus at baseline were used to evaluate ototoxicity-induced tinnitus onset. Few control subjects, 7 out of 67, or 10%, developed tinnitus in at least one ear over the study period. Incidence in terms of ears was 7% (9/125). Tinnitus developed in a significantly greater proportion of CDDP subjects (61/158 or 40%) and ears (100/289 or 35%), and AMG subjects (18/76 or 24%) and ears (28/139 or 20%) compared to Controls. Thus, the estimated risk for developing tinnitus is 3.7 times greater ($38.6/10.4=3.7$) for CDDP patients, and 2.3 times greater ($23.7/10.4=2.3$) for AMG patients, compared to hospitalized patients receiving non-ototoxic drugs. Hearing changes occurred in a significantly greater proportion of CDDP subjects compared to AMG subjects (52% of CDDP ears, 21% of AMG ears). Within each drug-treatment group, tinnitus onset and hearing change occurred with similar frequency, but within an individual did not always co-occur. The temporal relationship between loss of hearing and tinnitus onset following ototoxic-drug treatment will be discussed. (Work supported by the VA Rehab. R&D Service, C3213R and E3239V).

40 Pediatric Laryngeal Paralysis — A New Proposed Surgical Therapy

Brian Rotenberg¹, Vito Forte¹, Sam Daniel²

¹Otolaryngology, Hospital for Sick Children, 555 University Ave., Toronto, Ontario, Canada, ²Hospital for Sick Children, Montreal Childrens Hospital, 555 University Ave., Toronto, Ontario, Canada

ABSTRACT

Objectives:

The cricothyroid muscle (CTM) has a separate innervation from that of intrinsic laryngeal muscles, and therefore its action may contribute to airflow resistance in children with a laryngeal paralysis (LP) secondary to recurrent laryngeal nerve (RLN) palsy. We proposed removal of the CTM as a means of indirectly widening the paralysed neonatal glottis.

Methods:

A prospective study was conducted using a piglet animal model to simulate LP and evaluate the proposed treatment's outcome. LP was induced via bilateral RLN sectioning in 11 piglets. The CTMs were then removed. Animals acted as their own controls. Outcome measures consisted of serial inspiratory and expiratory airflow resistance measurements taken 1) with no intervention (as a baseline control), 2) after RLN sectioning and 3) after CTM removal. Several animals were awakened to assess their clinical responses to the interventions. The paired Student t-test was used for statistical analysis.

Results:

Inspiratory airflow resistance was significantly increased by RLN sectioning ($p=0.0062$) and then significantly decreased after subsequent CTM removal ($p=0.0005$). Clinical responses to the interventions mirrored the measured findings.

Conclusions:

Removal of the CTM significantly decreases inspiratory airway resistance in piglets with induced LP. This proposed surgical therapy for pediatric bilateral LP warrants further investigation.

41 The application of double-photic way supporting laryngoscope combined rigid nasendoscope to vocal operation

Qiulai Hou¹, Jianjun Wang², Luhua Dong², Huajie Mao³, Xuehua Ye⁴

¹Department of Otolaryngology, Lin Hai Otorhinolaryngology Institute, 110 Huan Chen Bei Road, Linhai, China, People's Republic of, ²Department of Otolaryngology, Lin Hai Otorhinolaryngology Institute, 110 Huan Cheng Bei Road, Linhai, China, People's Republic of, ³Department of Otolaryngology, Lin Hai Otorhinolaryngology Institute, 110 Huan Cheng Bei Road, Linhai, Zhejiang, ⁴Department of Otolaryngology, Lin Hai Otorhinolaryngology Institute, 110 Huan Cheng Road, Linhai, China, People's Republic of

To explain the effect of the application of self-designing double-photic way supporting laryngoscope in vocal operation. We surgically excised 41 patients (20 cases of vocal polypi, 8 cases of vocal nodules, 6 cases of Reinke spatic edema, 4 cases of vocal epidermoid cyst, 2 cases of villous tumor, 1 case of vocal squamous cell carcinoma) by taking self-designing double-photic way supporting laryngoscope combined rigid nasendoscope and optical imaging system, and subjectively and objectively estimated before and after operation by using laryngoscope and acoustic value. We detected the vocal cord and edge were orderly and smooth, and the vocal movements were symmetrical, and the vocal closure was well with the examination of laryngoscope and optical imaging system., EGG-jitter, EGG-shimmer, EGG-NNE, Contact Quotient Perturbation(CQP) and Contact Index Perturbation (CIP were significantly difference before and after vocal operation($P<0.01$). Max. phonation time ratio markedly prolongs ($P<0.05$) after operation. This technique has wide field of vision, strong resolving power to normal and pathological tissue, veracity of operation, handy and flexible operation, multi-purpose and focus free. It deserve to be extended.

42 Optical imaging of intrinsic signals in rat olfactory bulb for odor stimulation

Toru Miyazawa¹, Tokio Sugai², Koichi Tomoda¹, Norihiko Onoda²

¹Otolaryngology, Kanazawa medical university, 1-1daigaku uchi-nadamachi kahokugun, Ishikawa, Japan, ²physiology, Kanazawa medical university, 1-1daigaku uchinadamachi kahokugun, Ishikawa, Japan

The odor signals received by sensory neurons in the olfactory epithelium are transmitted to glomeruli of the olfactory bulb (OB) through their axons. Recently, the technique of intrinsic signal imaging in rat or mouse OB was applied to map the glomerular activities of various odorants. In this study, we adapted this technique to visualize how odor concentration and structure are represented spatially in the rat OB. Further, we used enantiomer pairs to study whether the spatial pattern of glomerular activity provided a basis for enantiomer discrimination.

After anesthesia, a skull overlying the dorsal surface of the OB was thinned until vessels were visible. Intrinsic signal images of reflected light (646 nm) from the dorsal surface of the OB were collected using a CCD camera. Each trial consisted of a pair of records with and without odor stimulation at 2 min intervals. This trial was repeated 6-8 times. Then, averaged differential images with and without stimulation were calculated and significant ($p < 0.05$) regions were statistically defined as active regions.

After odor stimulation, some active regions appeared as discrete roughly circular zones with a diameter of around 100-200 mm. When the focus was adjusted to different depths (0 - 600 mm), the peak of intrinsic signal was at 100-200 mm. Together with histological findings, it was confirmed that these active regions represent activated glomeruli. One or more glomeruli were activated for particular odorants, and spatial patterns of these glomerular activities were different among odorants. Further, these activities disappeared by occlusion of nasal cavity, indicating that these activities are primarily induced by odorant. Further, increasing concentration increased the number of additional glomerular activations. Finally, results using enantiomers indicated that the activity patterns were similar within an enantiomer pair, but individual glomeruli were differentially activated.

43 Acoustical and aerodynamical analysis in esophageal and prosthetic tracheoesophageal speech

Francisco Vázquez de la Iglesia¹, Secundino Fernandez Gonzalez², Noelia Sánchez Ferrándiz³, Noelia Sánchez Ferrándiz³, Rafael García-Tapia Urrutia⁴

¹Otolaryngology, Clínica Universitaria de Navarra, Avenida de Pio XII s/n, Pamplona, Spain, ²Otolaryngology, Clínica Universitaria de Navarra, Avenida de Pio XII s/n, Pamplona, Spain,

³Otolaryngology, Clínica Universitaria de Navarra, Avenida de Pio XII s/n, Pamplona, Spain, ⁴Otolaryngology, Clínica Universitaria de Navarra, Avenida Pio XII s/n, Pamplona, Spain

Introduction

The purpose of this study is to describe objective voice and aerodynamic features in laryngectomy patients with esophageal and prosthetic tracheoesophageal speech.

We wanted to determine correlations among aerodynamic and acoustic variables, like airflow rate, neoglottic pressure, laryngeal resistance and efficiency of voice production.

Material and methods:

Our subjects were comprised of 18 laryngectomized patients (all male). Mean age of speakers was 64.1 years. sixteen used esophageal voice (EV) and two Bloom-Singer voice prosthesis (VP).

The patients were asked to produce sustained /a/, /i/ vowels (Spanish) as well as /pa/, the tree items were recorded in upright and sitting position. All measurements were made using Voice Plus Alamed Corporation software.

Following acoustic and aerodynamic measurements were made: fundamental frequency (Fo), jitter, shimmer, intensity, harmonic-noise ratio (HNR), intraoral pressure, mean subneoglottic flow and laryngeal resistance. We have used the SPSS software to analyze variables.

Results:

There is a relationship among aerodynamic findings and efficiency of voice production in the sample.

The upright position determines accurately aerodynamic profile overcoat VP patients. Subneoglottic pressure is the most reliable variable among acoustic parameters, rising in pressure determines drops in jitter and HNR, and Fo values tend to equalize normal values.

Discussion:

In most studies, mean Fo of male laryngectomized speakers was found to vary from 88Hz to 112 Hz.

We also found that VP speakers and EV speakers had similar acoustic parameters, but the pulmonary inlet of VP achieve a maximum phonation time and better speaking rate, although no statistical differences were found. The neoglottic physiology may be understood by objective aerodynamic measurements, thus a more reliable parameters (flow, pressure) are the "key" in the development of an acceptable voice, overcoat pressure variable.

Conclusion:

Voice rehabilitation should be the main purpose for head and neck surgeons and speech therapist. The method we had follow, should be of interest in the goal of understanding the neoglottic segment and giving our patients the best way to improve their communication skills upon objective methodology.

44 New Clinical Method for Sublingual and/or Minor Salivary Gland Function

Hikaru Uchida¹, Toru Miyazawa¹, Chiyonori Ino², Susumu Sugai³, Koichi Tomoda¹

¹Otolaryngology, Kanazawa medical university, 1-1 Daigaku, Uchinada, Kahokugun, Ishikawa, Japan, ²Otolaryngology, Kansai medical university, 10-15Fumizono-cho, Moriguchi, Osaka, Japan, ³Hematology and immunology, Kanazawa medical university, 1-1 Daigaku, Uchinada, Kahokugun, Ishikawa, Japan

Objective: We introduce the new method to evaluate of sublingual and/or minor salivary gland function using a test paper applied iodine-starch reaction.

Methods: A test paper(1~1cm) was placed on the mucosal surface of the lower lip for 30 seconds for examination of the minor salivary gland function, and on the sublingual fold for 15 seconds in the sublingual gland function. Then, we counted the number of the blue stained spots occurring as a reaction of iodine and starch on the test paper, and compared among normal control group, oral dryness group and Sjogren's syndrome group. In addition, the histopathological findings, the results of the Gum test and the number of spots were analyzed in Sjogren's syndrome group.

Results: In controls, age induced changes of the average number of spots was no significant differences statistically in both salivary glands. The average number of spots in the patients with oral dryness was less than that in normal control individuals, and in the patient with Sjogren's syndrome was the lowest number in this study. In Sjogren's syndrome group, the number of the spots of minor salivary gland was not correlated with Gum test but that was correlated with histopathological findings.

45 Magnitude and variability of oral pressure and esophageal pressure in esophageal speech.

Secudino Fernández, Francisco Vazquez de la Iglesia, Noelia Sanchez, Rafael Garcia-Tapia

Otolaryngology/HNS, University of Navarra, Apdo. 4209, Pamplona, Spain

Aerodynamic aspects of esophageal voice production in laryngectomees have been studied to clarify and compare the physiology of injection in the oropharynx and in the esophagus.

Simultaneous measurements of sub, suprapseudoglottic and esophageal pressure were carried out during air injection, air deglutition and during phonation. Transpseudoglottic flow and sound pressure were measured too.

Relationships between the variables were computed by means of regression analysis and Pearson's product-moment-correlations.

Results:

Speakers with lower esophageal pressure during injection have higher suprapseudoglottic pressure and higher mean airflow rate during phonation.

There is a positive correlation between esophageal pressure and oral or suprapseudoglottic pressure during phonation.

Conclusion

The efficiency of injection is improved by esophageal pressure lower values; this fact and its increment during phonation are very important factors in the esophageal voice production and its intelligibility

46 Development and Characterization of a Transgene Expressing Selectively Replicating Oncolytic Virus for Head and Neck Squamous Cell Cancer

Adam M. Zanation¹, William Wood², Wendell G. Yarbrough³

¹*Department of Otolaryngology/Head and Neck Surgery, University of North Carolina Chapel Hill, 101 Manning Drive, Chapel Hill, NC, United States*, ²*School of Medicine, University of North Carolina Chapel Hill, 101 Manning Drive, Chapel Hill, NC, United States*, ³*Department of Otolaryngology/Head and Neck Surgery, Vanderbilt, Vanderbilt Hospital, Nashville, TN, United States*

The ONYX-015 virus is an E1B mutated adenovirus that has been shown to be selectively replicating and oncolytic in p53 mutant cancers. This virus has had promising usage in Phase One and Two trials with Head and Neck Cancer. Up to this point, the virus has attacked cancer through its replication and lytic cycle only. No one has described applying a transgene to this viral vector. ARF (alternate reading frame) protein is a tumor suppressor gene located at the INK4a gene locus and it controls the p53 apoptotic pathway. ARF is likely the most frequently mutated single gene in Head and Neck Cancer, up to 80% of cancer cases. We had utilized the technique of DNA recombination and PCR based assays to develop an ONYX-015-ARF virus. The virus was subsequently purified through plaque assays. PCR based testing revealed the virus isolated to be pure, to contain the E1B mutation and to contain the

ARF gene. We have demonstrated that the transgene is expressed in infected cells. That the virus replicates and appears to have cytopathic effects on HNSCC cell lines in a manner that depends on p53 status. The addition of the ARF transgene could broaden the oncolytic effects of the ONYX-015 virus for future clinical trials. The use of a replicating virus for gene delivery also solves the problem of 100% cell infection rates that are needed in delivery of gene therapy with prior non replicating viral vectors.

47 Progressive Low-Frequency Hearing Loss During Early Adulthood in Fischer 344 Rats

Jiri Popelar¹, Daniel Groh^{1,2}, Jana Mazelova¹, Josef Syka¹

¹*Auditory Neuroscience, Institute of Experimental Medicine AS CR, Videnska 1083, Prague, Czech Republic*, ²*ENT Clinic, Charles University, 2nd Medical Faculty, V Uvalu 84, Prague, Czech Republic*

Fischer 344 (F344) rats are often used as an animal model for the study of the mechanisms underlying age-related hearing loss (presbycusis). Whereas the anatomical, neurochemical and neurophysiological changes in the auditory system have been previously documented in old and very old F344 rats, the hearing function of young and adult F344 rats is known to a lesser extent. The aim of this study was to monitor hearing function in young (1-month-old) and adult (6-month- and 12-month-old) F344 rats using distortion product otoacoustic emission (DPOAE) and auditory brainstem response (ABR) recordings. The results were compared with control group of Long Evans (LE) rats of the same age. In young, 1-month-old F344 rats, significantly higher ABR thresholds (mainly at low frequencies of 1 - 2 kHz) were found in comparison with the LE strain, and DPOAEs were absent at frequencies below 2-2.5 kHz. Whereas ABR thresholds did not change significantly during the first year of life of F344 rats, the low-frequency deficit in DPOAEs progressed, and DP-grams in adult rats were shifted towards higher frequencies in comparison with young animals. The amplitudes of click-evoked ABRs in 1-month-old F344 and LE rats were similar, but in 12-month-old F344 rats the ABR amplitudes were significantly smaller than in LE rats of the corresponding age. Other parameters of ABRs (wave I latency, duration of the response) were almost identical in both rat strains at any age. The results demonstrate a significant progressive low-frequency deficit in young F344 rats, which is probably related to the many genetic mutations present in this rat strain. The low-frequency hearing loss thus precedes the later occurring classical age-related high-frequency hearing loss.

48 High Doses of Amifostine Ameliorate Cisplatin-Induced Ototoxicity But Cause Neurotoxicity In Hamsters As Evidenced by Auditory Brainstem Responses

Michael W. Church¹, Brian W. Blakley², Don L. Burgio³, Anil K. Gupta³

¹*Ob/Gyn & Otolaryngology, Wayne State University, 275 East Hancock, Detroit, MI, United States*, ²*Otolaryngology, Univ. Manitoba, 820 Sherbrook Str., Winnipeg, MB, Canada*, ³*Otolaryngology, Wayne State Univ., 5E UHC, Detroit, MI, United States*

Chemoprotective agents help reduce the toxic side effects (e.g.,

ototoxicity, nephrotoxicity, hematotoxicity, neurotoxicity) of chemotherapy drugs such as cisplatin. The conventional belief is that the chemoprotective agent WR-2721 (Amifostine) does not protect against cisplatin-induced ototoxicity. There is no knowledge, however, about the efficacy of high doses of WR-2721 (WR) in protecting against cisplatin-induced ototoxicity. Thus, the dose-dependent effects of WR in possibly ameliorating cisplatin-induced ototoxicity were investigated. Hamsters were given a series of 5 cisplatin injections (3 mg/kg/injection once every other day, i.p.) either alone or in combination with 18, 40, 80 or 400 mg/kg/injection of the rescue agent WR (n = 5 or 10/group). Other groups received either 80 mg/kg/injection WR alone (n = 5) or were untreated (n = 14). Ototoxicity was assessed by auditory brainstem responses (ABR). WR provided dose-dependent rescue from cisplatin's ototoxicity with no protection at the low dose of 18 mg/kg, moderate protection at 40 mg/kg, and nearly complete protection at 80 and 400 mg/kg. However, WR doses of 40mg/kg or higher caused neurotoxicity as evidenced by prolongations in the ABR's interpeak latencies. Thus, high doses of WR provided the beneficial effect of protecting against cisplatin-induced ototoxicity, but had the harmful side effect of neurotoxicity. Previous failures to find chemoprotection from cisplatin-induced ototoxicity were likely due to the use of WR doses that were too small. It is suggested that human clinical trials search for a WR dose that is high enough to ameliorate cisplatin-induced ototoxicity but low enough to avoid permanent neurotoxic consequences. (Supported by NIH grants R01 DA05536, T32-DC00029 and the Karmanos Cancer Institute).

49 A Large-Scale Study of Auditory Function in Diabetic Veterans

Nancy Vaughan, **Daniel McDermott**, Stephen Fausti
National Center for Rehabilitative Auditory Research, Portland VA Medical Center, 3710 SW US Veterans Hospital Rd., Portland, OR, United States

The National Center for Rehabilitative Auditory Research has accumulated audiometric data on 694 diabetic and non-diabetic veterans. This is the largest and most comprehensive study to date to investigate the effects of diabetes on hearing function. A battery of clinical audiometric tests was chosen to evaluate the effects of diabetes on auditory function from the cochlea through the auditory centers in the midbrain. The analyses to date show that cochlear sensitivity as measured by pure tone thresholds is not significantly different between the diabetic and non-diabetic groups.

Cochlear function as measured by otoacoustic emission (OAE) amplitudes across a wide frequency range revealed that otoacoustic emission amplitudes decreased as a function of increasing frequency in both groups. Although there was a tendency for DPOAE amplitudes to be greater in the diabetic group, there was a significant difference between the groups only at two frequencies: 2220 and 2494 Hz. The differences were small, on the order of 2 dB or less.

In contrast to the cochlear test results, the auditory brainstem response (ABR) results revealed prolonged conduction times in the central auditory neural pathways. Both absolute (III and V) and interpeak (I-V, I-III) latencies were prolonged in the ABR results in diabetic patients compared to non-diabetic controls. The I-V interpeak latency delay is consistent with a prolonged central con-

duction time. The I-III interval prolongation suggests that the delay is located primarily in the lower auditory brainstem pathway.

These results indicate that cochlear test results (OAE and hearing thresholds) do not reflect significant changes associated with diabetes. Auditory changes associated with diabetes occur primarily beyond the cochlea and affect central auditory processing in the form of neural conduction time delays.

These findings are discussed in relation to diabetic complications, metabolic control, insulin status, and duration of disease. The question is whether additional levels of neural processing are affected by diabetes which could put diabetic patients at risk for speech understanding difficulties associated with auditory and cognitive processing deficits. Future areas of investigation are outlined.

50 Enhancement of dynamic ranges and stimulus feature discrimination in the electrical stimulation

Dukhwan Lim, Chongsun Kim, Sun O Chang
Department of Otolaryngology, Seoul National University, 28 Yungundong Chongnogu, Seoul, Korea, Republic of

The aim of this study was to evaluate roles of dynamic ranges and performances of stimulus feature discrimination in the auditory nervous system. The subject group included cochlear implantees with various etiologies of hearing loss. Intra-operative electrically-evoked stapedial reflex thresholds, compound action potentials, and brain-stem responses were compared with auditory feature discrimination scores as prospective performance indicators. Results showed that some performances improved notably in limited frequency ranges over stimulation periods although initial stimulation levels were varied widely. The improvement was gradually saturated and the outcome was related in part with increased stimulus levels, especially with enhanced upper ends of the dynamic ranges. Extreme levels of electrically-evoked responses indicated lower initial behavioral performances in stimulus feature discrimination. It was necessary to include interaction patterns of channels in modeling the process although no preferred orders of presentation were noted in this analysis. In conclusion, quantitative level dependent assessment was indicative of discrimination performances under specific conditions. This data may be helpful in analyzing and modeling the effects of electrophysiological dynamic ranges on stimulus feature discrimination.

51 Rationale for High Frequency Tinnitus Masking

Martin Louis Lenhardt
Biomedical Engineering & Otolaryngology, Virginia Commonwealth University, 1112 E Clay St Box 980168 MCV, Richmond, Virginia, United States

Rationale for High Frequency Tinnitus Masking

High audio frequency and low ultrasonic masking has been effective for some tinnitus patients. Most tinnitus patients report a pitch match in the 4-8 kHz range in the presence of some high frequency hearing loss. Typical high frequency stimulation is limited by the mechanics of the middle ear, therefore bone or fluid conduction are the modalities of choice. Specialized high frequency

actuators can deliver stimulation in the 10-30 kHz range and the stimulation may be tonal, narrow band noise or more complex and pulsative in composition using various modulation schemes.

Imaging studies have led to the theory that the brain reorganizes its primary auditory frequency map in cases of severe disabling tinnitus. The frequency map increases dramatically for the tinnitus frequency (producing activation over a larger area of the cortex than normal) which can lead to greater perceptual salience of the tinnitus sound. Similar changes may also occur in the insula based on preliminary imaging data. Compression of the tinnitus modified frequency map might be accomplished by applying sound *above* the tinnitus frequency. Low frequency ultrasound, demodulated as high audio stimulation, or direct high audio stimulation are good candidates for tinnitus treatment.

52 Optimizing the stimuli to evoke the AMFR in neonates

Raquel Riquelme¹, Natacha Teissier², Blagoje Filipovic¹, Klaus Hartung³, Gerald Leonard⁴, Shigeyuki kuwada¹

¹Neuroscience, University of Connecticut, Health Center, 263 Farmington avn, Farmington, ct, United States, ²ENT, University of Paris, 32 alee ventanant, Paris, France, ³Research, Bose Corporation, Framingham Technology Park, Framingham, MA, United States, ⁴SURGERY, University of Connecticut, Health Center, DOW-S1A130, Farmington, ct, United States

Optimizing the stimuli to evoke the AMFR in neonates

The amplitude modulation following response (AMFR, a.k.a ASSR) is a promising tool for assessing hearing on a frequency-by-frequency basis. The purpose here is to report procedures that serve to enhance the detection of this scalp potential in neonates. Scalp recordings were made between the forehead and linked mastoids in full term and premature babies (n = 150) that were usually asleep. Stimuli were delivered via insert earphones. The presence of the AMFR was based on the magnitude squared coherence algorithm. Using tonal carriers (500 and 2000 Hz) we assessed the effect of envelope shape on the AMFR. Specifically, we compared a sinusoidal envelope with a half-wave rectified version of this envelope. The rectified envelope evoked a larger response that was detected faster than those to the sinusoidal envelope. Then, using the rectified envelope, we found that the time to detect the AMFR was similar for a broad range of modulation frequencies (~40 to 90 Hz). Next we examined the effect of using a noise bandwidth as a carrier. As bandwidth increased the detection of the AMFR became faster. Moreover, responses at 40 dB SPL were routinely obtained. We conclude that the AMFR may be a preferred alternative to the click evoked auditory brainstem response (ABR) since its frequency specificity can be controlled.

Supported by the Donaghue Foundation and Hartford Hospital

53 Frequency-Specific Threshold Prediction using the Auditory Steady-State Response (ASSR) and the Toneburst Auditory Brainstem Response (ABR): A Within-Subject Comparison

Tiffany A. Johnson^{1,2}, Carolyn J. Brown^{2,3}

¹Hearing Research, Boys Town National Research Hospital, 555 N. 30th Street, Omaha, NE, United States, ²Speech Pathology and Audiology, The University of Iowa, 119 SHC, Iowa City, IA, United States, ³Otolaryngology/Head and Neck Surgery, The University of Iowa, 200 Hawkins Drive, Iowa City, IA, United States

Both the toneburst ABR and the ASSR can be used to measure evoked-potential thresholds as a function of frequency. Because the spectra of the stimuli used to evoke the ABR and the ASSR differ, the accuracy with which behavioral thresholds can be predicted from ABR thresholds and ASSR thresholds also may differ, particularly in individuals with steeply sloping hearing losses. This study compared the predictive accuracy of toneburst ABR thresholds measured with two stimulation protocols (Blackman-gated tonebursts, linear-gated tonebursts plus notched noise) to the accuracy of ASSR thresholds measured with two stimulation protocols (100% AM, 100% AM plus 25% FM). Evoked-potential thresholds were recorded in 10 individuals with sloping hearing losses and were compared to results from two control groups: 14 individuals with normal hearing, 10 individuals with flat losses. In the group data, there was no difference in the agreement between behavioral and ABR thresholds using either the Blackman-gated toneburst protocol or the linear-gated toneburst plus notched noise protocol. There was also no difference in the accuracy with which behavioral thresholds were predicted from the ASSR thresholds evoked with either the 100% AM protocol or the 100% AM plus 25% FM protocol. Finally, there was no difference in the relative accuracy of the ASSR thresholds as compared to the ABR thresholds. However, for the four individuals with the most steeply sloping hearing losses, ASSR thresholds better predicted behavioral thresholds, compared to the toneburst ABR. Among these individuals, the toneburst ABR underestimated behavioral thresholds in regions of hearing loss. This suggests that the spread of energy associated with short-duration, rapid-onset tonebursts resulted in excitation of regions of less hearing loss, distant from the nominal frequency.

Work supported by the National Organization for Hearing Research. Preparation of the poster was supported by NIH (T32 DC00013).

54 Different Manifestations of Auditory Neuropathy

Paul R. Kileny, Bruce M Edwards, Terry A Zwolan

Otolaryngology, University of Michigan, 1500 E Medical Center Drive, Ann Arbor, Michigan, United States

Patients with auditory neuropathy (AN) present with significant sensorineural hearing loss, poor speech perception and in some cases impaired temporal processing. The diagnosis is based on discrepancies between different objective measures: cochlear microphonics are present, the auditory brainstem response and the cochlear nerve action potential are absent, and otoacoustic emis-

sions indicating unimpaired outer hair cell function are present. There have been several reports on children with a diagnosis of AN who have benefited from cochlear implantation. There have also been reports of hearing recovery in patients with a diagnosis of AN. This presentation demonstrates two distinctly different manifestations. The first, "classic" manifestation involves patients with the typical diagnostic criteria for AN considered to be cochlear implant candidates. Prior to implantation the electric auditory brainstem response (EABR) was elicited with transtympanic, pulsatile electrical promontory stimulation. In all cases an EABR characterized by waves III and V was obtained. Post implantation they demonstrate improved auditory detection skills and some speech recognition. A different manifestation of AN is illustrated by the case of a now one year old patient with hyperbilirubinemia requiring two exchange transfusions, who passed an initial newborn ABR hearing screening. A follow up ABR obtained at two months of age along with parental report indicated the presence of a severe to profound bilateral hearing loss. An inspection of the ABR traces obtained with constant polarity clicks, revealed the presence of appropriate polarity cochlear microphonics but little else. He was managed with amplification and was evaluated for cochlear implant candidacy. However, repeated follow up testing revealed normal hearing in the soundfield, confirmed by the emergence of wave V of the ABR with a threshold of 25 dB for clicks.

55 Words in noise versus words in babble in normals and neurological patients.

Nanthini Kunaratnam^{1,2}, Doris Eva Bamiou³, Stuart Rosen⁴, Mazal Cohen², Linda M Luxon^{2,3}

¹Department of Otolaryngology, Tan Tock Seng Hospital, 48.Kingsmead Road, Singapore, Singapore, ²Academic Unit of Audiological Medicine, Institute of Child Health, 30. Guilford Street, London, United Kingdom, ³Department of Neuro-otology, National Hospital for Neurology and Neurosurgery, Queens Square, London, United Kingdom, ⁴Department of Phonetics And Linguistics, University College of London, Room G27, Wolfson House, 4.Stephenson Way, London, London, United States

ABSTRACT

Speech in noise and in multitalker babble are both tests used to characterize the functional deficits in listeners with peripheral hearing loss, auditory neuropathy and central auditory nervous system disorders. These tests may help identify hearing difficulties present in noise that are not evident in standard audiometric evaluations conducted in the quiet. However, the comparative efficacy of these tests in pathologies of the brain has not been well described. The objective of this study is to evaluate the identification of monosyllabic words in speech-shaped noise versus babble as a tool in the clinical evaluation of word recognition in the UK population. We tested 27 normal UK born subjects age range 20 – 60 years and 8 patients with neurological lesions. Speech reception thresholds were estimated using an adaptive technique. Both the normal and the neurological groups had worse performance levels for the words in babble test as opposed to words in noise. The neurological group showed a higher degree of performance deterioration for words in babble than in noise compared to the normal group. Words in babble may thus be a promising tool in the functional assessment of auditory dysfunction.

56 Neonatal ABRs Suggest Cochlear and Retrocochlear Hearing Disorders in Apert Syndrome

M. W. Church¹, F. E. Eldis², N. J. Kazzi³, D. O. Robinson⁴

¹Ob/Gyn, Wayne State Univ., 275 E. Hancock, Detroit, MI, United States, ²Comm. Dis. Clin., Children's Hosp., 3901 Beaubien, Detroit, MI, United States, ³Peds., WSU, Hutzel Hosp., Detroit, MI, United States, ⁴Audiol., WSU, 567 Manoogian, Detroit, MI, United States

Apert syndrome is a form of craniosynostosis characterized by premature fusion of the cranial sutures, craniofacial dysostosis, hypertelorism, ptosis, high arched palate, midface hypoplasia, syndactyly of hands & feet, joint & internal organ anomalies, & mental retardation. Some forms of craniosynostosis (e.g., Pfeiffer and Crouzon syndromes) are associated with conductive, sensorineural and mixed hearing losses. Apert syndrome, however, has only been associated with conductive hearing losses. Sensorineural and central hearing disorders and auditory brainstem responses (ABRs) in Apert syndrome have not been described. A literature review suggests that this is due to a lack of inquiry. Thus, we gathered ABRs from an Apert syndrome infant. The infant was full-term (38 wk) with head circumference and body weight below the 10th percentile. "Diagnostic" ABRs were collected at 8 days postpartum. The ABRs had significant prolongations of Wave I latencies and the Wave I-III inter-peak latencies (IPLs). The infant also failed neonatal otoacoustic emission (OAE) testing. Follow-up evaluations with tympanometry and OAEs at 1 month suggested normal middle ear function but a possible sensorineural hearing loss. Further evaluation is pending. The delayed Wave I latencies and abnormal OAEs with normal middle ear function suggest a cochlear (sensory) disorder. The prolongations of the Wave I-III IPL suggest a retrocochlear (neural) disorder somewhere between the distal portion of the auditory nerve (Wave I) and the cochlear nucleus (Wave III) inclusively. In sum, these results suggest that Apert syndrome may be associated with cochlear and retrocochlear hearing disorders. These findings have implications for the evaluation and management of such patients.

57 Central Auditory Processing Disorder (CAPD) in School Age Children: Diagnosis & Implications

Stuart Rosen¹, Mazal Cohen², Iyngaram Vanniasegaram³

¹Phonetics & Linguistics, UCL, 4 Stephenson Way, London, United Kingdom, ²Academic Unit of Audiological Medicine, Institute of Child Health, 30 Guilford Street, London, United Kingdom, ³Department of Audiological Medicine, St George's Hospital, 117 Suttons Lane, Hornchurch, Essex, United Kingdom

There is currently much concern about the role of central auditory processing disorders (CAPD) in the cognitive development of children, particularly regarding language competence. In order to clarify this, we applied a battery of auditory tests to 32 children who were referred for an auditory evaluation because of listening/hearing problems but who were all within normal limits for standard audiometric assessments (suspected CAPD - sCAPD). Their performance was compared to a group of 33 age-matched controls. Neither backward nor simultaneous masking distinguished the two

groups, but two simple discrimination tasks did. One was a verbal task using consonant cluster minimal pairs of real words, and the other a non-verbal task using two short tone pairs differing in fundamental frequency at varying interstimulus intervals. Together, these two tasks detected impaired listening skills in 56% of the sCAPD children but only 6% of the controls. Thus, a significant proportion of sCAPD children appear to have genuine auditory problems, although almost all appear to have no detectable deficit. A subgroup of the children was then tested on a variety of measures of cognitive skills. The sCAPD group scored consistently lower than the controls on both verbal (vocabulary and grammar) and nonverbal skills. Strikingly, sCAPD children with relatively good auditory performance did not differ on these measures of cognitive ability from sCAPD children with poor auditory performance (but note that no measure of reading ability was available). Therefore, although CAPD in children can be diagnosed to at least some extent, the presence or absence of CAPD appears to have little impact on the development of the verbal and nonverbal skills tested here.

58 Diagnosing Auditory Processing Difficulties (APD): The Auditory Processing Inventory for Children (APIC)

Justin Cowan, Adrian C Davis, Sally E Hind, David R Moore

Institute of Hearing Research, Medical Research Council, University Park, Nottingham, United Kingdom

Children with APD are recognised by teachers, parents and health-care professionals and yet the prevalence, incidence, typical presenting signs, inter-relationships with other conditions, and impact on the individual and family remain to be ascertained. This project explores presenting symptoms of APD in childhood and delineates the characteristics of APD among children through the development of a self-report APD questionnaire and behavioural test battery for ages 5-14 years. The APIC consists of 37 behavioural scenarios describing situations in which APDs are thought to be manifest. Items are rated on a 4-point scale by the child or parent. The theoretical rationale of the APIC is based on operational definition models and includes subscales for spatial localisation, auditory discrimination, pattern recognition, temporal processing, and performance decrements with competing acoustic signals or degraded signals. The APIC subscales have been found to have satisfactory internal reliability and normative data are reported. The validation of the APIC involved an index group from the above study, selected on the basis of performance on the questionnaire. They underwent testing of peripheral hearing (pure-tone audiometry, tympanometry and acoustic reflexes), auditory processing (binaural, spectral and temporal), auditory attention (selective and sustained), general cognitive ability (verbal and non-verbal), and language functioning (phonological and linguistic). The APIC and a behavioural test battery for APD is a considerable advance in the assessment and management of children with APD. Future work will involve the development of an optimised screening questionnaire for use in a population study.

59 Auditory effects of SSRIs in clinically depressed female subjects

Kamakshi V Gopal

Speech and Hearing Sciences, Univ. of North Texas, 907 W. Sycamore Dr., Denton, TX, United States

Abstract

The purpose of the study was to identify the role of serotonin in the auditory system. Since direct manipulation of serotonin in the brain is difficult, the effects of selective serotonin reuptake inhibitors (SSRI) known to enhance serotonergic transmission in the brain were analyzed in clinically depressed individuals.

A total of twenty-five adult female subjects participated in the study. The experimental group consisted of 14 clinically depressed female subjects, and the control group consisted of 11 non-depressed females. A battery of tests was administered to the experimental group twice, once while the individuals were not on SSRI medication, and once while they were on SSRI medication.

The control group was also administered the same test battery twice within a span of 4 months. A repeated measures ANOVA was used to identify significant differences between the groups.

No significant differences were found for the control group between the two rounds on any test measure. The experimental group, however, showed significantly larger transient otoacoustic emissions in both ears, poorer SCAN-A composite scores, and larger amplitude growth functions for ABR peak V and ALR peak N1P2, during the unmedicated round compared to the medicated round.

Based on the results obtained, we conclude that the increased serotonin levels (due to reduced reuptake of serotonin) brought about by SSRI medication may be contributing to the significant changes seen in auditory measures in the experimental group.

60 Speech Intelligibility in Patients with Multiple Sclerosis

David Joseph Lilly, Michele M. Hutter, Stephen A. Fausti, Dennis Bourdette, M. Samantha Lewis

VA National Center for Rehabilitative Auditory Research, VA Medical Center, 3710 S.W. VA Hospital Road, Portland, OR, United States

Multiple sclerosis (MS) is an immune-mediated disease of the central nervous system that affects over 350,000 Americans. The prevalence of peripheral hearing loss in MS is less than 10%. Still, when patients with multiple sclerosis are asked specifically about difficulties with hearing, 40% to 60% report problems with the comprehension of speech when there is a background of noise. The primary focus of this study was to address objectively the most common auditory complaint from patients with MS: "I cannot understand speech in a setting where other people are talking."

The patient group comprised 10 patients with a clinical diagnosis of "definite" or "primary-progressive" MS and a control group of 10 subjects without MS. Each MS patient and each matched control was seen for three experimental sessions. During the first session, we evaluated monaural auditory function. During the second session we evaluated otoacoustic emissions, masking-level differences and performance on the Staggered-Spondaic-Word (SSW)

Test. During the third session we measured speech intelligibility binaurally in the sound field for the IEEE sentences in a babble surround of 16 speakers talking simultaneously. The target sentences always were presented at 65 dBA Leq. The babble was varied systematically over a range of 20 signal-to-noise ratios. During this session, we also used a noninvasive tympanic-membrane wick electrode to generate electrocochleographic data.

Our findings suggest that patients with MS have significantly more difficulty understanding speech in a background of multitalker babble than control subjects when both groups are matched with respect to age, to sex and to audiometric configuration. This finding holds even when the MS patients have little difficulty with speech intelligibility in quiet. The MS patients also produce abnormal results on those auditory and neurophysiologic tests that require precise timing of neural events or synchronous impulse firing in groups of neurons.

61 Direct Imaging and Parameterization of the External Auditory Canal

David A Fabry

Audiology, Phonak Hearing Systems, 4520 Weaver Parkway, Warrenville, IL, United States

This paper will discuss the results of a preliminary study that used CT/MRI to directly image the external auditory canal for purposes of making an earmold or hearing aid shell. Both ears of a single subject were imaged, using spiral CT and MRI methods, with 1) open ear canals with the patient's jaw open and jaw closed, and also 2) with the ears occluded with silicone material used for "conventional" ear impression process. Subsequently, the conventional earmold impressions were scanned, using a laser imaging technique, and compared to the three-dimensional accuracy of the CT/MRI images in software. Additionally, hearing aid shells were manufactured and compared for all three methods (CT/MRI/scanned ear impression). Results indicated that CT assessed the bony structures more accurately, while MRI provided improved resolution of soft tissue. Results will be discussed using three-dimensional overlays of different imaging techniques. Conclusions will address technical obstacles to eliminating the use of traditional earmold impressions, and opportunities for use of imaging techniques, particularly for pediatric applications.

62 The effects of exercise intervention with and without head motion in normals after visual modification

Kim Robin Gottshall^{1,2}, Robert J. Moore¹, Michael E. Hoffer¹, Helen S. Cohen³

¹Otolaryngology, Naval Medical Center San Diego, 34800 Bob Wilson Drive, San Diego, CA, United States, ²Otolaryngology, Department of Defense Spatial Orientation Center, 34800 Bob Wilson Drive, San Diego, CA, United States, ³Otolaryngology, Baylor, One Baylor Plaza, Houston, TX, United States

Vestibular physical therapy has become an increasingly popular and useful clinical entity in treating individuals with balance disorders. Despite the recognized benefits of therapy, objective outcomes based studies demonstrating the degree of difference produced by exercise therapy are lacking. We have been working with a visual distortion model in which temporary balance disorders

are created in normal individuals so that we could study the effects of rehabilitation in a controlled situation. We have previously described that variable task vestibular physical therapy improved adaptation in these artificially spatially distorted individuals when compared to a non-rehabilitation group. In this study we examine the active head motion component of the variable task therapy for its rehabilitation effect. We compared a group of artificially spatially disoriented individuals performing whole body exercises without volitional head motion to a second group that performed whole body exercises with volitional head motion. We describe the results in these two groups and demonstrate that the volitional head motion was the key factor in improving adaptation to active dynamic tasks moving through space. This study provides further objective evidence of the beneficial effects of vestibular physical therapy and begins to illuminate the components of the therapy that may be the most effective.

63 Horizontal Canal Benign Positional Vertigo Vestibular Test Findings

Judith White¹, Kathleen D Coale²

¹Otolaryngology, Cleveland Clinic Foundation, 9500 Euclid Ave. A71, Cleveland, Ohio, United States, ²Physical Therapy, Lahey Clinic, 41 Mall Rd., Burlington, MA, United States

The vestibular test data of a case series of sixteen patients with idiopathic horizontal semicircular canal benign positional vertigo (HSC-BPV) are described. Basic infrared video nystagmography, sinusoidal vertical axis rotation, positional testing, computerized dynamic posturography (CDP), Dynamic Gait Index (DGI) and modified Clinical Test of Sensory Integration and Balance (CTSIB) data are reviewed. Geotropic and ageotropic HSC-BPV are compared and contrasted.

Dix-Hallpike position testing is less sensitive than supine head turns in detecting HSC-BPV, and may fail to pick up HSC-BPV entirely. Horizontal canal function is specifically tested with calorics and sinusoidal vertical axis rotation. In this series, caloric testing abnormalities occurred in geotropic HSC-BPV patients. Canalith material in the horizontal canal may affect free endolymph flow in response to caloric stimulation. Postural control was assessed with the DGI and modified CTSIB, and abnormalities were noted in the ageotropic HSC-BPV group, including walking with horizontal head turns and sharpened Romberg with eyes closed. None of the patients in the geotropic HSC-BPV group had postural control abnormalities. CDP was normal in both geotropic and ageotropic HSC-BPV groups.

HSC-BPV is a rare subtype of benign positional vertigo, but appropriate assessment can improve patient identification.

64 Effects of Vestibular Loss on Orthostatic Responses to Tilts in the Pitch Plane

Scott J Wood¹, Jorge M Serrador², F Owen Black³, Angus H Rupert¹, Todd T Schlegel⁴

¹*Spatial Orientation, Naval Aerospace Medical Research Laboratory, 51 Hovey Road, Pensacola, FL, United States*, ²*HRC Research and Training Institute, Harvard Medical School, 1200 Centre Street, Boston, MA, United States*, ³*Neurotology Research, Legacy Health System, 1225 NE 2nd Ave, Portland, OR, United States*, ⁴*Human Adaptation and Countermeasures Office, NASA Johnson Space Center, Nasa Rd 1, Houston, TX, United States*

The purpose of this study was to determine the extent to which vestibular loss might impair orthostatic responses to passive tilts in the pitch plane in human subjects. Data were obtained from six subjects having chronic bilateral vestibular loss and six healthy individuals matched for age, gender, and body mass index. Vestibular loss was assessed with a comprehensive battery including dynamic posturography, vestibulo-ocular and optokinetic reflexes, vestibular evoked myogenic potentials, and ocular counterrolling. Head up tilt tests were conducted using a motorized two-axis table that allowed subjects to be tilted in the pitch plane from either a supine or prone body orientation at a slow rate (8 deg/s). The sessions consisted of three tilts, each consisting of 20 min rest in a horizontal position, tilt to 80 deg upright for 10 min, and then return to the horizontal position for 5 min. The tilts were performed in darkness (supine and prone) or in light (supine only). Background music was used to mask auditory orientation cues. Autonomic measurements included beat-to-beat recordings of blood pressure (Finapres), heart rate (ECG), cerebral blood flow velocity in the middle cerebral artery (transcranial Doppler), end tidal CO₂, respiratory rate and volume (Respritrace), and stroke volume (impedance cardiography). For both patients and control subjects, cerebral blood flow appeared to exhibit the most rapid adjustment following transient changes in posture. Outside of a greater cerebral hypoperfusion in patients during the later stages of tilt, responses did not differ dramatically between the vestibular loss and control subjects, or between tilts performed in light and dark room conditions. Thus, with the exception of cerebrovascular regulation, we conclude that orthostatic responses during slow postural tilts are not substantially impaired in humans following chronic loss of vestibular function, a result that might reflect compensation by nonvisual graviceptor inputs (e.g., somatosensory) or other circulatory reflex mechanisms.

Sponsors: NIH (DC 5547), NASA (NCC9-129), Legacy Health System, Navy

65 Pathophysiology of Migraine-Related Dizziness

Joseph M. Furman¹, Dawn A. Marcus², Patrick J. Sparto³, Mark S. Redfern⁴, J. Richard Jennings⁵

¹*Otolaryngology, University of Pittsburgh, 200 Lothrop Street, Pittsburgh, PA, United States*, ²*Anesthesiology, University of Pittsburgh, 2404 Bellwood Court, Pittsburgh, PA, United States*, ³*Physical Therapy, University of Pittsburgh, 200 Lothrop Street, Pittsburgh, PA, United States*, ⁴*Bioengineering, University of Pittsburgh, 200 Lothrop Street, Pittsburgh, PA, United States*, ⁵*Psychiatry, University of Pittsburgh, 3811 O'Hara Street, Pittsburgh, PA, United States*

The pathophysiological basis for migraine-related dizziness is unknown but may relate to both central and peripheral vestibular abnormalities. The present study was undertaken to explore several potential abnormalities in migraine-related dizziness by assessing vestibulo-ocular function, vestibulo-spinal function, visual-postural responses, spatial orientation, and attention-balance interference in well-defined patients. Subjects included headache-free controls (C), subjects who met the International Headache Society (IHS) criteria for migraine but who had no symptoms suggestive of a vestibular system abnormality (M-V), and subjects who met both IHS criteria for migraine and the Neuhauser criteria for migraine-related vestibulopathy (M+V). Subjects with recognized neurotologic syndromes such as Meniere's disease were excluded from all groups. For each experimental paradigm, five subjects from each group were tested. Abnormalities in M+V subjects included: decreased VOR gain, increased sway on both Equitest platform posturography and in response to optic flow in an immersive virtual environment, slowed reaction time on dual tasks of interference between attentional processes and the VOR, and excessive visual dependence of subjective visual vertical.

Taken together, these results suggest that patients with migraine-related dizziness manifest abnormalities in vestibular function and are more visually dependent than persons with migraine without vertigo or headache-free controls. The basis for these group differences is uncertain but may relate to serotonergic mechanisms in the central vestibular system.

This study was supported by the National Headache Foundation, Merck & Company, the Eye and Ear Foundation, and the Raymond & Elizabeth Bloch Charitable and Educational Foundation.

66 The Role of Central and Peripheral Optic Flow in the Control of Upright Posture Within a Mixed-Frequency Visual Environment

Jeffrey G Jasko¹, Patrick J Sparto^{2,3}, Mark S Redfern^{1,3}, Patrick J Loughlin^{1,4}

¹BioEngineering, University of Pittsburgh, 750 Benedum Hall, Pittsburgh, PA, United States, ²Physical Therapy, University of Pittsburgh, 6035 Forbes Tower, Pittsburgh, PA, United States, ³Otolaryngology, University of Pittsburgh, EEI 153, Pittsburgh, PA, United States, ⁴Electrical Engineering, University of Pittsburgh, 348 Benedum Hall, Pittsburgh, PA, United States

The goal of this study was to investigate the influence of optic flow on upright posture when patterns in the central and peripheral fields of view (FOVs) move simultaneously but at different sinusoidal frequencies.

Twenty healthy subjects (9 male, 11 female; ages 21-30) participated in the experiment. They were surrounded by an image encompassing 180° x 70° (horiz. x vert.) FOV. The central stimulus was a pattern of alternating black-and-white concentric rings, and the peripheral stimulus consisted of black-and-white checkers. There were two visual combinations: in one, the central optic flow stimulus moved at 0.1 Hz while the peripheral optic flow moved at 0.25 Hz; in the other, the frequencies were reversed. The peak-to-peak amplitude of all stimuli was 16 cm. In addition, there were 2 support surface conditions: fixed and sway-referenced. Head position was recorded during the 90-second trials. A statistical test determined whether there was a significant response at either stimulus frequency. Subjects who had significant responses during fl of the trials were considered "responders". Root-mean-square (RMS) sway of the responders' data was calculated at both stimulus frequencies using a bandpass filter, and then normalized to their quiet-stance sway. Within each visual/platform condition, the normalized sway at the peripheral frequency was compared to the normalized sway at the central frequency using paired t-tests.

There were more significant responses to the peripheral optic flow stimulus (58/80) than there were to the central optic flow (16/80). Thirteen subjects were classified as responders. In 3 of the 4 visual/platform conditions, the normalized RMS sway at the peripheral frequency was significantly greater than the normalized sway at the central frequency. This suggests that the postural system is more sensitive to optic flow in the peripheral FOV, regardless of frequency.

Supported by NIH P30-DC05205, K25-AG01049

67 Effectiveness of Treatments for Benign Paroxysmal Positional Vertigo of the Posterior Semicircular Canal

Helen S Cohen¹, Kay T Kimball²

¹Otorhinolaryngology, Baylor College of Medicine, One Baylor Plaza, Houston, TX, United States, ²(co-owner), Statistical Design and Analysis, 106 Blue Jay Drive, Austin, TX, United States

Benign paroxysmal positional vertigo (BPPV) is the most common vestibular disorder. Non-medical, non-surgical treatments for this disorder have become popular recently. Despite approximately 25

years of reports describing active repositioning exercises, passive repositioning maneuvers and habituation exercises no single study has previously compared the most commonly used standard treatments to a sham maneuver. In this study we compared a modified version of Epley's canalith repositioning maneuver, Semont's liberatory maneuver, Brandt & Daroff's repositioning exercise, and our version of vertigo habituation exercises to a sham repositioning maneuver.

Adults with unilateral BPPV were subjects, randomized to the five groups. Subjects were either treated with a repositioning maneuver in the laboratory or instructed in exercises and given written instructions to do the exercises at home for one week. They were pre- and post-tested on vertigo intensity and frequency, computerized dynamic posturography, Dix-Hallpike responses and independence in activities of daily living. Post-tests were given 1 week after treatment and approximately 3 months and 6 months later. Data analyses used multilevel analyses. Semont and Epley maneuvers were the most effective, significantly better than the sham maneuver on most measures. Exercise groups were intermediate between repositioning maneuvers and the sham maneuver and not significantly different than any treatments. These data suggest that the passive repositioning maneuvers are the most effective treatments. Supported by NIH grant DC03602.

68 Vestibular function in patients with Meniere's disease at the end of the treatment with intratympanic gentamicin

Nicolas Perez¹, Julio Rama¹, Eduardo Martin²

¹Otorhinolaryngology, Clinica Universitaria de Navarra, Pio XII-36, Pamplona, Spain, ²Otorhinolaryngology, Hospital Casa de Salud, Dr. Candela 10, Valencia, Spain

Objective: This study aimed to analyze vestibular function at the end of the treatment with intratympanic injections of gentamicin in patients with unilateral Meniere's Disease (MD) who are refractory to medical treatment. Bedside vestibular examination will be compared to laboratory vestibular function tests results. **Study Design.** Prospective. **Setting.** Tertiary medical center **Patients.** 33 Patients with unilateral Meniere's Disease according to AAO-HNS guidelines (1995), who had been unresponsive to medical therapy for at least one year. **Intervention.** Intratympanic injections of a prepared gentamicin concentration of 27 mg/ml were performed at weekly intervals until the development of symptoms and/or signs indicative of vestibular hypofunction in the treated ear. **Main Outcome Measure.** Two different rotatory chair tests provided data of vestibular function: phase, gain and symmetry of the vestibulo-ocular reflex after sinusoidal harmonic acceleration (SHA) test with peak chair velocity of 50°s⁻¹ and, time constant of the VOR after impulse rotation 100°s⁻¹. **Results.** Time constant of the VOR after ipsilesional impulse rotations and gain of VOR after sinusoidal low frequency and velocity stimulation are significantly reduced according to the number of signs that were added in the bedside examination but not to the number of injections. In this regard hearing loss was more frequently found in patients receiving 2 or more injections.

69 Postural stability after vestibular schwannoma surgery as evaluated by visual feedback posturography

Meeli Hirvonen, Heikki Aalto, Timo P Hirvonen
*Otolaryngology, Helsinki University Central Hospital,
Haartmaninkatu 4 E, Helsinki, Finland*

Even up to two-thirds of the patients report persistent symptoms of dysequilibrium months to years after the vestibular schwannoma (VS) surgery. The follow-up of vestibular-ocular function only using traditional vestibular tests seems insufficient with regard to the functional status of the patient. The aim was to evaluate changes in postural control of VS patients prior to and after the surgery in challenged stance condition using visual feedback posturography (VFP).

In the VFP the subject uses integrally sensory input from visual, proprioceptive, and vestibular sense organs for postural control by moving her center of gravity marker on a computer screen to chosen targets by leaning her body on the platform. The accuracy, velocity, and side difference of the movements are measured. Twenty-eight patients (mean 45, range 26-67 years) with VS were recorded repeatedly three times: a day prior to, a month, and 3 months after the VS surgery.

The accuracy of the postural control was reduced both prior to and after the operation. The ability to stay inside distant targets worsened after the operation, but it recovered partly in the third test session. The sway velocity of the postural control movements to the targets remained unchanged. The overall performance during the VFP was abnormal in less than half of the patients in first (12/28), second (13/28), and third (8/20) test sessions. Side difference in postural control was encountered in only one patient prior to the surgery, and in three patients a month postoperatively.

The postural control was at best prior to the surgery, which indicates that adaptive mechanisms in postural control compensate well the slow progressive deficit caused by the VS. Postural control worsens after the operation, after which a partial recovery is seen.

70 Balance sensory organization in cochlear implanted children with congenital profoundly hearing loss

Hamlet Suarez, Alejo Suarez

Lab. of Audiology and Vestibular Pathophysiology, School of Medicine, C. de Guayaquil 1332, Montevideo, Uruguay

The postural parameters (COP distribution area and Sway velocity) of two groups of cochlear implanted children (Below and above 5 y/o) were tested using the "Test of Equilibrium Under Sensory Altered Conditions" using a force platform. This test was performed with and without the cochlear implant connected. Postural responses were studied by means of the time-frequency scalogram using wavelets and the sway frequency content was measured in arbitrary units of energy density. We evaluated: 1) Which sensory information (Visual-Vestibular-Somatosensory) is most relevant in the development of postural control. 2) How the auditory information is involved to improve the postural control strategies.

Compared with the control group the somatosensory information

is more relevant in the group of implanted children and the auditory information didn't change the postural control parameters in the different test conditions.

71 Effects of Constricted Visual Field on Human Postural Control

Claire Gianna-Poulin¹, Valerie Stallings², F. Owen Black², George Cioffi³

¹Neurological Sciences Institute, OHSU, 1225 NE 2nd Avenue, Portland, OR, United States, ²Neurology Research, Legacy Clinical Research & Technology Center, 1225 NE 2nd Ave, Portland, OR, United States, ³Ophthalmology Research, Legacy Clinical Research & Technology Center, 1225 NE 2nd Ave, Portland, OR

Claire Gianna-Poulin, Valerie Stallings, F. Owen Black, & George Cioffi

The contribution of vision to postural control was studied in 16 subjects with constricted central or peripheral visual fields. Five had glaucoma in both eyes, seven had glaucoma in one eye, three had macular degeneration in both eyes and one had macular degeneration in one eye. Ophthalmologic examination included static visual acuity and Goldmann and/or Humphrey visual field tests. Vestibular examination included caloric, earth-vertical rotational tests and vestibular-autorotation tests. Vestibulo-ocular reflexes in response to earth-vertical axis rotation were normal in fourteen of the sixteen patients. Two subjects had a slightly decreased time constant in response to pseudorandom rotational stimuli, with one of these two patients showing decreased gains for both single sine and pseudorandom stimuli. Postural control was examined using sensory organization (SOT), motor control and automatic response adaptation tests (EquiTest system). Patients with binocular visual field impairments were tested with both eyes viewing while patients with monocular visual impairment were tested with both eyes viewing and with only the study eye viewing. All subjects had normal equilibrium scores for SOT1, 2 and 3 (earth-fixed support surface) conditions. Our analysis focused on the comparison of postural stability during SOT trials which use a sway-referenced support surface (SOT4 – earth-fixed visual surround, SOT5 – eyes closed, SOT6 – sway-referenced visual surround). In subjects with visual field impairments, the contribution of visual inputs to postural control appears to depend on: 1) the size of the remaining peripheral visual field 2) the status of the covered eye. In the case of monocular testing, subjects demonstrated less reliance on visual inputs when the covered eye had better vision than when the covered eye had the more impaired vision than the study eye. These findings suggest that: 1) peripheral vision is predominant for visual contributions to postural control when a visual background with normal contrast is used and 2) adaptation to a visual field impairment will increase the weighting of visual inputs during sensorimotor postural control challenges. Supported by NIH (NIDCD) DC 00205.

72 Head Position Dependency of induced Nystagmus to Ice Water Irrigation in peripheral vestibulopathy

Byung Yoon Choi¹, Ja -Won Koo², Seung Ha Oh¹, Sun O Chang¹, Chong -Sun Kim¹

¹Otolaryngology, Seoul National University Hospital, Chong Ro Gu yongon dong, Seoul, Korea, Republic of, ²Otolaryngology, Seoul National University Bundang Hospital, Bun Dang Gu Koo Mi Dong, Sung Nam, Korea, Republic of

Determination of head position dependency using ice water test is necessary to distinguish paresis from paralysis of peripheral vestibulopathy. According to Coats and Smith, caloric response is composed of head position-dependent convection component (Cc) and head position-non dependent direct thermal component (Tc). If LSC function appropriately, the direction of caloric nystagmus of ice water test depends upon the head position but the amplitude is not symmetrical due to position-non dependent component. We investigated head position dependency of induced nystagmus for the candidates of ice water caloric test and estimated the portion of the direct thermal effect to ice water on eye movement according to the horizontal canal plugging model of Paige. From Jan.2003 through September 2003, 21 patients, who showed no induced nystagmus during warm irrigation, were included in this study. Following forty milliliter of ice water irrigation in supine & prone position, the maximum slow phase eye velocity (SPEV) and direction of nystagmus were assessed using video nystagmography system. Seven cases showed head-position dependency and were interpreted as having functional LSC. In 6 of 7 cases, the amplitude of nystagmus in supine position was larger than that in prone. Fourteen cases did not show head position dependency suggesting the absence of end organ function. In this group, calculated Tc by Paige's formula was 3.25°/sec and corrected mean Tc was 1.11°/sec, considering the effect of SN. Head position dependency to ice water irrigation can provide a valuable information when vestibular ablative procedures are considered.

73 Comparison between nose-up and nose-down sinusoidal off-vertical axis rotation and earth vertical axis rotation

Izumi Koizuka, Miki Azuma, Shoji Watanabe, Kazuteru Suzuki

Otolaryngology, St. Marianna University School of Medicine, 2-16-1 Sugao, Miyamae-ku, Kawasaki, Japan

The contributions of semicircular canal versus otolith organ signals to the vestibulo-ocular reflex (VOR) were investigated by providing canal-only (earth vertical axis rotation: EVAR) and canal plus otolith 30-degree nose-up and nose-down conditions (off-vertical axis rotation: OVAR). Horizontal and vertical eye movements were recorded in eight healthy adults, ranging in age from 28 to 40 (mean 29.5), using an infrared video recording system (SensoMotoroc Instrument. GmbH, Berlin). Stimuli were carried out, sinusoidally, at 0.2 Hz, 0.4 Hz and 0.8 Hz in frequency and 60 deg/sec in maximum angular head velocity in both EVAR and OVAR. All subjects showed significant gain reduction in OVAR at 0.8Hz both in nose-up and nose-down conditions ($p < 0.05$). Percent gain change was approximately -24%.

It is well known that the duration of post-rotatory nystagmus is shortened by head tilt, a phenomenon that has been attributed to rapid discharge of the velocity storage mechanism. We have investigated the relative importance of the various sensory signals associated with post-rotatory head tilt using both EVAR and OVAR. We concluded that the tilt suppression of post-rotatory nystagmus is primarily a function of otolith influence on the velocity storage system.

In the present study, we concluded that the gain reduction in OVAR at 0.8Hz both in nose-up and nose-down conditions may be contributed by compatible mechanism of the tilt suppression of post-rotatory nystagmus.

74 Correlation of VEMP and Vestibular Test Battery Results in Meniere's Disease

Steven D. Rauch^{1,2}, M. Beatriz Silveira¹, John J. Guinan^{2,3}, Guangwei Zhou⁴, Sharon G. Kujawa^{2,4}, Conrad Wall, III¹, Barabara S. Herrmann^{2,4}

¹Otolaryngology, Mass. Eye and Ear Infirmary, 243 Charles St., Boston, MA, United States, ²Otology and Laryngology, Harvard Medical School, 243 Charles St., Boston, MA, United States, ³Eaton-Peabody Laboratory, Mass. Eye and Ear Infirmary, 243 Charles St., Boston, MA, United States, ⁴Audiology, Mass. Eye and Ear Infirmary, 243 Charles St., Boston, MA, United States

Toneburst-evoked VEMP demonstrates a significant difference in threshold and tuning between normal and Meniere's disease (MD) ears. VEMP threshold and tuning may be abnormal in the unaffected ears of patients with unilateral MD. VEMP does not correlate with ipsilateral audiometric thresholds. Correlation of VEMP and standard vestibular function tests in MD has not been previously reported. We explored the relationship of VEMP to other vestibular function tests in MD and tested the hypothesis that the side with poorer VEMP thresholds will be correlated with the side-of-disease. Twenty adult subjects with unilateral MD underwent otologic and audiometric evaluation, conventional vestibular test battery and VEMP testing. Side-of-disease was assigned clinically based on symptoms, otologic exam, and audiometry. This assignment was compared to vestibular test battery and VEMP results. Vestibular test results were analyzed by the multivariate method of Dimitri et al. (2002) to determine side-of-disease. VEMP interaural threshold difference was calculated for each of 4 stimuli (250, 500, 1000Hz, click), with the higher threshold considered pathologic and symmetric thresholds scored as "indeterminate." Multivariate statistical analysis of vestibular testing agreed with clinical assignment of side-of-disease in 14/20 of cases. In 5/6 cases where the vestibular test battery assignment was incorrect, the VEMP correctly localized the side-of-disease. However, the VEMP also made incorrect assignment in 6-8/20 cases. We conclude that VEMP is highly correlated with side-of-disease in unilateral MD, even though occult bilateral changes may diminish interaural asymmetry. The capacity for the VEMP to identify the side-of-disease is approximately equal to the best available multivariate statistical treatments of a vestibular test battery. VEMP is a robust measure of inner ear dysfunction providing information complementary to that of audiometry and conventional vestibular function testing in MD patients.

(Research supported by NIH-NIDCD RO1DC04425)

75 The subjective horizontal: A new test of otolith function

John HJ Allum¹, Achim G Beule², Rudolph R Probst¹

¹Dept of ORL, University Hospital, Petersgraben 4, Basel, Switzerland, ²Dept of ORL, University Hospital, Walther-Rathenau-Str.43-45, Greifswald, Germany

The purpose of this study was to determine if the subjective notion of horizontal was affected in subjects with an unilateral neurectomy of the vestibular nerve due to a cerebellar pontine angle tumor removal (UVN) and therefore if this test of the horizontal perception could be dependent on otolith function. Subjects (12 UVN mean age 54 +/-15 years; 20, age matched normals; and 12 young normals, 26 +/-4 years of age) stood on a platform that was tilted slowly 5 deg at 1 deg/s in any one of 8 combinations of roll and pitch (2 forwards, 6 backwards). Subjects were required to use a hand-held joystick controller and return the platform back to horizontal without looking at their feet. Once the subject indicated that the platform surface was horizontal, the roll and pitch angular deviation from horizontal was noted. Each tilt position was repeated twice in random order. One series was completed with eyes open and the other with eyes closed. Normal subjects showed average deviations in pitch and roll with eyes open and closed of about 0.5 deg with elderly subjects showing larger mean pitch deviations of 0.8 deg when the platform tipped backwards and into roll. UVN subjects showed consistent mean deviations of 2 deg on average that were significantly different from age-matched normals for tilts towards the lesion side with eyes open, and more significant under eyes closed conditions. In contrast to normals, UVN subjects needed to grasp the handrails when tilted towards the lesion side. The results indicate that testing the subjective horizontal would provide a simple functional test of otolith function which is lesion-side specific. The elderly have a reduced sense of this percept compared to young normals.

76 Quadraphonic auditory feedback of trunk sway for improving balance control during stance and gait tasks

John HJ Allum, Lars Nijhuis, Judith Hegeman, Flurin Honegger

Dept of ORL, University Hospital, Petersgraben 4, Basel, Switzerland

In an attempt to improve balance control during stance and gait tests we provided acute unilateral peripheral vestibular loss subjects (UVL), compensated bilateral vestibular loss subjects (BVL) and healthy age-matched subjects auditory feedback (AF) of their trunk angular motion. Roll and pitch angular trunk displacements were recorded with angular velocity transducers mounted just above the waist. Either angular position information or angular velocity information was feedback to the subject using 4 loudspeakers placed left, right, front and back of the 4 by 4 m test environment. When angular or velocity position thresholds were exceeded a tone emitted from the speaker at 30 dB HL towards which the subject moved. The volume increased to a maximum level of 70 dB HL with increasing angular deviation. Stance tasks involved standing on 2 legs with eyes open and closed. Gait tasks consisted of tandem gait, normal walking with eyes open and closed or walking with the head pitching, get up from a stool and

walking and walking up and down stairs. Stance and tandem gait tasks were repeated with a foam support-surface. Amplitudes of trunk sway reduced most with AF for stance and tasks with eyes closed (tandem walking tasks). The reduction was most significant for UVL, then BVL and least for normal subjects. Feedback of trunk angular position rather than angular velocity caused a significant 50% reduction of pitch sway for stance tasks and angular velocity feedback caused a 50% reduction in roll sway for tandem gait tasks. These results indicate that vestibular loss and normal subjects can incorporate the prosthetic sensory information into their balance commands, however position information appears more useful during stance trials and angular velocity during gait trials. Future work will involve determining the effect of combining angular position and velocity AF information and the effect of AF on compensation processes for acute UVL.

77 Utricular versus horizontal semicircular canal function in healthy subjects and vertigo patients - a comparison

Floris L Wuyts^{1,2}, Mieke Hoppenbrouwers², Griet Pauwels², Paul H Van de Heyning²

¹Biomedical Physics, University of Antwerp, Groenenborgerlaan 171, Antwerp, Belgium, ²Otolaryngology, University Hospital of Antwerp, Wilrijkstraat 10, Edegem, Belgium

Goal: We tested the utricular function and the horizontal semicircular canal function, side by side, in 53 subjects, of whom 35 vertigo patients and 18 healthy subjects.

The utricular function was unilaterally tested by means of the unilateral centrifugation test. Two parameters of interest are the utricular sensitivity (i.e. the slope of the linear regression between the ocular counter rolling and the gravito-inertial acceleration tilt of the head centre) and the utricular preponderance (i.e. the intercept of this linear regression). The caloric test was performed to evaluate the horizontal semicircular canal function. The responsiveness of the horizontal semicircular canals (i.e. the sum of the maximum slow-component velocity of each of the four irrigations) and the canal preponderance were assessed. By assessing these functions in the same subjects, a better knowledge can be obtained of the inter-relationship of utricle and semi-circular canals in both healthy subjects as in patients with specific vestibular lesions.

Results: The correlation between the responsiveness of the horizontal semicircular canals and the utricular sensitivity is significant for the right eye ($r^2 = 0.20$, $p = .001$) as well as for the left eye ($r^2 = 0.31$, $p < .001$). The correlation between the canal preponderance and the utricular preponderance is significant for the right eye ($r^2 = 0.10$, $p = .024$) as well as for the left eye ($r^2 = 0.08$, $p = .036$).

Conclusions: Weak but significant correlations are found between the responsiveness of the horizontal semicircular canals and the utricular sensitivity, and between the canal and the utricular preponderance. Several causes underlie the relative poor correlation, i.e. the canal and utricular functions are certainly not identically affected in the different diseases and the intra individual variation adds to this poor correlation. The extrapolation of the findings of e.g. the caloric test to the entire labyrinth proves to be quite inaccurate.

78 Novel Approach to Vestibular Rehabilitation Utilizing Upper Cervical Spine Physiotherapy Techniques

John G. Oas¹, Frank Gargano², Neil Cherian³

¹Neurology & Otolaryngology, Cleveland Clinic Lerner College of Medicine of CWRU, 9500 Euclid AVE; Desk A71, Cleveland, OH, United States, ²Physical Therapy, Rehabilitex, Inc., 30455 Solon RD, Solon, OH, United States, ³Neurology, Cleveland Clinic Foundation, 9500 Euclid AVE; Desk T33, Cleveland, OH, United States

Background: Vestibular rehabilitation physical therapy is based on principles of sensorimotor reintegration as a means to facilitate central adaptation to peripheral vestibular losses, yet the precise nature of how this occurs remains undetermined. The cervico-ocular and vestibulo-collic reflexes are physiologically and biomechanically linked to the upper cervical spine through afferent and efferent pathways respectively. Changes in these reflexes can occur as a result of either biomechanical derangements or peripheral vestibular losses. We sought to identify the contribution of upper cervical spine biomechanics in vestibular rehabilitation by studying the outcome of neck physiotherapy done before traditional vestibular rehabilitation physical therapy was performed.

Methods: 14 patients were carefully chosen to receive neck physiotherapy in advance of vestibular rehabilitation physical therapy on the basis of intent to treat election clinically. The Dizziness Handicap Inventory (DHI) was used to measure the intensity of vestibular symptoms before and after treatment. Quantitative measurements of cervical range of movement (CROM) were assessed to quantify the biomechanical status of the cervical spine before and after treatment. physiotherapy techniques of soft tissue stretching and painless segmental mobilization were combined with strengthening exercises to increase active range of motion. No sensorimotor integration techniques were allowed during the study. A two-tailed t-test statistical analysis was used to assess treatment effects on CROM and DHI. ANOVA statistical analysis between CROM and DHI was also performed.

Results: CROM measurements increased ($P < 0.01$) and DHI decreased ($P < 0.001$) significantly as a result of neck physiotherapy. There were no significant correlations between CROM variables and DHI changes.

Conclusions: Neck physiotherapy techniques alone provide a significant reduction in vestibular symptoms as a result of improved spatial bandwidth of cervical afferent input to the vestibular nuclei and central vestibular pathways. Limitations in upper cervical mobility could impair traditional techniques of vestibular rehabilitation physical therapy if ignored.

79 Mediolateral Stability of Vestibulopathic & Healthy Individuals During Paced & Non-Paced Gait

Kathleen Sienko¹, Conrad Wall², Lars Oddsson³

¹HST/MEEI, MIT/HMS, 243 Charles Street, Boston, Massachusetts, United States, ²Otology & Laryngology, MEEI/HMS, 243 Charles Street, Boston, Massachusetts, United States, ³NeuroMuscular Research Center, Boston University, 19 Deerfield Street, Boston, Massachusetts, United States

Gait instability is characteristic of vestibulopathic patients, astronauts/cosmonauts returning from long-duration space flight, and the elderly. Advanced diagnostic testing regimens with enhanced sensitivity for accurate identification of patients with vestibular dysfunction are currently under development. One prospective diagnostic technique involves the analysis of locomotor recovery from controlled perturbations during gait. Eleven healthy and eight vestibulopathic subjects with unilateral vestibular loss (100% Reduced Vestibular Response asymmetry from the caloric test) resulting from surgery for vestibular schwannoma were selected for this investigation. The vestibulopathic subjects employed in this investigation comprised a special subset of patients. Despite their known vestibulopathy, all subjects scored within the normal range on the computerized dynamic posturography Sensory Organization Tests. The previously reported perturbation protocol consisted of 24 trials of paced walking along a 15 m walkway, during which randomly interspersed surface perturbations were delivered with the right foot in stance in two possible directions at two possible magnitudes in half of the trials. The vestibulopathic group had significantly greater changes in their moment arm responses compared to controls and required a greater number of steps to return to normal pre-perturbation gait. The aim of the present study is to complete the characterization of the mediolateral stability of vestibulopathic and healthy individuals by examining the previously unanalyzed non-perturbed free and paced gait trials. We have compared the healthy and vestibulopathic groups by examining basic parameters of M/L stability during the non-perturbed free and paced gait trials to determine whether or not one can distinguish between the two populations without applying a surface perturbation. Additionally, this study compares the results of the perturbed trials with non-perturbed trials and explores the prospective use of perturbed versus non-perturbed gait as a clinical diagnostic indicator of impaired sensorimotor function resulting from vestibular dysfunction and/or long duration space flight.

80 The compact stabilometer without force-plate

Toshihiko Oba¹, Kazuoki Otsuki¹, Masao Toji¹, Junichi Otsuki¹, Soichiro Matsushita², Kaoru Ogawa³

¹Otolaryngology, Tokyo Saiseikai Central Hospital, 1-4-17 Mita, Minato-ku, Japan, ²Computational Science & Engineering, Faculty of Engineering, Toyo Univ., 2100 Kujirai, Kawagoe, Japan, ³Otolaryngology, School of medicine, Keio University, 35 Shinanomachi, Shinjuku, Japan

Abstract

In diagnosis for sense of equilibratory by conventional stabilometer, the distribution of the weight resting on the sole of a foot is

measured when a user gets on horizontal surface of the platform. We made the compact balance monitor (A wearable sense of balance monitoring system towards daily health care. The 7th IEEE International Symposium on Wearable Computers in press) and arranged it for diagnosing the vertigo. This device was equipped with the accelerometer in spite of the heavy force-plate (10-kilograms). We made the special software system worked in Windows-Xp system. We studied the body sway of healthy people suffering from vertigo induced by caloric test and tested this system for the new stabilometer. We used this system for people who suffering from vestibular disorder.

Methods

Subjects were 8 healthy men who were asked to maintain an upright standing position for 60 seconds with eyes closed with this device around the time when the caloric test applied to the right ear with cold water. Parameters were checked around the time when the test. Subjects who suffering from vestibular disorders (BPPV, etc.) were asked to maintain an upright standing position on the platform.

Results

Everyone had left-beating nystagmus and their sway patterns were left-to-right type after the test. The device analyzed other parameters based on the locus chart. The significant difference of these machines between pre- and post- caloric test was found at parameters. Similar trace was found in this system and the conventional stabilometer among people suffering from vestibular disorder.

Discussion

The nystagmus derived from the disturbance of the vestibulo-ocular system and the increasing the body sway derived from the disturbance of the vestibulo-spinal system are appeared after caloric test in the conventional stabilometer. The increasing the body-sway was appeared after the test in this system. The synchronized trace pattern was found in these systems among people suffering from vestibular disorder. From the result of this study, this system might be useful to diagnose the disorder of the sense of equilibratory as the new stabilometer.

81 Sensory Re-Weighting In Human Postural Control During Moving-Scene Perturbations

Arash Mahboobin¹, Patrick Loughlin², Mark Redfern³, Patrick Sparto³

¹Dept. of Electrical Engineering, University of Pittsburgh, 348 Benedum Hall, Pittsburgh, PA, United States, ²Depts. of Electrical Engineering, and BioEngineering, University of Pittsburgh, 348 Benedum Hall, Pittsburgh, PA, United States, ³Depts. of Bioengineering, and Otolaryngology, University of Pittsburgh, 750 Benedum Hall, Pittsburgh, PA, United States

Recent studies suggest that a "sensory re-weighting" postural control strategy is utilized depending upon environmental conditions and the reliability of sensory orientation and movement information (e.g., Peterka 2002, Peterka and Loughlin 2003). The aim of this study was to further investigate this hypothesis by evoking anterior-posterior (AP) body sway using visual stimuli during sway-referencing of the support surface.

Five healthy adults participated in this study. Subjects stood on a

posture platform while looking at a visual scene that encompassed the full horizontal field of view. A sequence of scene movements was presented to the subjects consisting of 30 s of quiet stance (stationary scene), 2 s of visual push (scene moved with constant velocity 30 cm towards subjects over 2 s) followed by 10 s of no scene movement, then 2 s of visual pull (scene moved back to initial position over 2 s) and another 10 s of no scene movement. The scene then moved randomly (scene position driven by 0.05-0.5 Hz white Gaussian noise, 8 cm RMS power) towards and away from the subject for 60 s, immediately after which subjects experienced another set of push/pull sequences. This was followed by 30 s of quiet stance and then a third, final set of visual push/pull perturbations. Three trials were taken. Peak power of stimulus-response data (squared velocity of AP-COP) was computed over a 6 s interval after each push and pull. We hypothesized that the persistent visual perturbation (random moving scene) while standing on a sway-referenced platform would cause a sensory re-weighting resulting in a reduced push/pull response compared to the initial push/pull response prior to random scene movement. Results showed a significantly smaller response ($p < 0.05$) in the second push/pull sequence compared to the first push/pull sequence. There was no significant difference between the first and third push/pull sequences. A trial effect was also found, with greater responses in the first trial compared to subsequent trials. These results suggest that sensory re-weighting occurs during persistent visual perturbation, and that habituation to moving scene perturbations can occur with repeated exposure. [Supported by NIH DC04435 and DC05205]

82 Postural Instability and Vestibular Dysfunction in Friedreich's Ataxia

John H. Anderson¹, Peka Christova¹, Christopher M. Gomez²

¹Otolaryngology, University of Minnesota, 516 Delaware St. S.E., Minneapolis, MN, United States, ²Neurology, University of Minnesota, 516 Delaware St. S.E., Minneapolis, MN, United States

Since the discovery of the X25 gene for Friedreich's ataxia (FA) (Campuzano et al, Science, 271:1423-1427, 1996), several reports have documented the considerable phenotypic variability within and among different families. It is clear also that there can be a considerable variation in the age of onset and the rate of progression of the disease process. However, since the early clinical descriptions (cf., Harding, Adv Neurol, 61:1-14, 1993) of the symptoms and movement abnormalities in FA, there have been relatively few reports quantifying eye movement (Furman et al., Arch Neurol, 40:343-346, 1983; Spieker et al., J Neurol, 242:517-521, 1995) and postural abnormalities (cf., Hallett, Adv Neurol, 87:155-163, 2001) in FA. Although those studies have documented a reduced gain for the vestibulo-ocular reflex (VOR) and increased sway with posturography recordings, correlations between quantitative physiological parameters and the clinical state of the disease or the progression of the disease over time have not been studied in detail. The present study addresses this. Four FA patients were tested. The VOR was recorded in the dark and during visual suppression and posturography was done with the Equitest protocol. The results showed that the VOR gain and visual suppression of the VOR were reduced, and the magnitude of this

depended on the clinical severity of the disease. The pattern of sway scores reflected the presence of both a somatosensory and vestibulo-spinal deficit and the scores were correlated with disease severity. Furthermore, such a correlation was evident in another motor task, pointing a finger at a target on a touch screen in front of the patient. Further testing of these and other patients over extended time periods should help to define quantifiable parameters that could be used to track the progression of FA and the effectiveness of treatment modalities.

83 Functional Deficits are Correlated with Decreased Reliance on Vestibular Information in People with Chronic Unilateral Vestibular Loss

Kennyn Statler, Diane Wrisley, Robert Peterka, Fay Horak
Neurological Sciences Institute, Oregon Health & Sciences University, 505 NW 185th Ave, Portland, OR, United States

Subjects with chronic unilateral vestibular loss (UVLs) often complain of functional deficits in dynamic situations. We hypothesized that UVLs with fewer functional deficits would demonstrate normal reliance on vestibular information for balance control whereas those with more functional deficits would rely more heavily on proprioceptive information.

Complete UVLs were matched with healthy control subjects by age and gender. Subjects were exposed to lateral, pseudorandom support surface (SS) rotations of 1, 2, 4, and 8 deg with their eyes closed. Relative weighting of vestibular and proprioceptive inputs was determined from a curve fit based on a feedback model of postural control to experimental transfer function data obtained from spectral analysis of SS rotation and COM response. The degree of functional vestibular compensation was determined using the Dizziness Handicap Inventory (DHI), the Activities-specific Balance Confidence Scale (ABC), and the Vestibular Activities of Daily Living (ADL) Scale.

Both controls and UVLs showed increasing reliance on vestibular and decreasing reliance on proprioceptive information as SS rotation amplitudes increased. However, UVLs were approximately 50% less reliant on vestibular information than controls and differences were greater for the larger SS rotations, suggesting a change in vestibular gain. Subjects with poorer levels of vestibular compensation (as evidenced by higher scores on the DHI, lower scores on the ABC, and lower scores on the ADL scale) demonstrated decreased reliance on vestibular inputs.

The results indicate that UVLs with fewer functional deficits most resemble normal controls. But even these UVLs showed decreased reliance on vestibular information compared to controls.

Supported by NIH grants DC 1849 and DC 5870.

84 Mixed stimulation modes in cochlear implant processing: A psychophysical report on intensity discrimination

Bomjun Kwon¹, Chris van den Honert¹, Jay Gantz²

¹*Research, Cochlear Americas, 400 Inverness Parkway, Englewood, CO, United States,* ²*Mechanical Engineering, Franklin W. Olin College of Engineering, Olin Way, Needham, MA, United States*

A stimulation mode (whether monopolar(MP) or bipolar(BP)) in a cochlear implant is usually determined at the time of mapping and is fixed throughout the use of the device. In an attempt to increase the number of informational channels in speech processing, we conceived of an idea to utilize multiple stimulation modes within one map; we are investigating the feasibility of a novel speech processing coding strategy based on such a scheme. This is the first psychophysical report on the use of multiple or mixed modes of stimulation.

In this study, the intensity discrimination of a MP stimulus was measured in the presence of a masker. Both MP and BP modes were used for the masker. During the pilot study, we found that the mere existence of masker at a constant level did not necessarily impair an implant recipient's ability to discriminate between intensity levels. Therefore, a random intensity fluctuation was added to the masker to degrade the recipient's performance. The two maskers (MP or BP) were loudness balanced to make a fair comparison. The masker was stimulated at adjacent electrodes with respect to the target stimulation. Two sites of stimulation were chosen for the target: electrode 19 and 11. Several different levels, from a soft to medium, were chosen for the target. So far, results from 3 patients have shown that the jnd with a BP masker is significantly lower than the jnd with a MP masker. This indicates that subjects are better at the suprathreshold task if the target and masker are stimulated in different modes, possibly due to a facilitation in the segregation of stimuli. Furthermore, patient's anecdotal reports that the sound percepts of BP and MP stimulation are categorically different suggests that an ingenious distribution of different stimulation modes to encode a speech signal may enable us to represent highly sophisticated perceptual speech cues that are not conveyed through traditional speech coding strategies.

85 Effects of High-Rate Pulse Trains on Intensity Discrimination by Cochlear Implant Users

Ted A. Meyer, Jay T. Rubinstein, Haiming Chen, Felix Y. Chau

Department of Otolaryngology-HNS, University of Iowa, 200 Hawkins Dr. 2nd Fl. PFP, Iowa City, IA, United States

It has previously been demonstrated that the addition of a high-rate "conditioning" or "desynchronizing" pulse train produces spontaneous-like activity in a computational model of the deafened auditory nerve [Rubinstein et. al., *Hear Res*, 1999]. Animal studies support these predictions. We have recently demonstrated gains in dynamic range [Hong et al., *Otol & Neurotol*, 2003] and improved frequency discrimination [Meyer et al., *Otol & Neurotol*, submitted] on individual electrodes by users of the Clarion C-II cochlear implant. In the present study, we examined the effects of a 5000-

pps biphasic conditioning pulse train on intensity discrimination across the dynamic range of a single electrode pair. Using a 3-interval forced-choice adaptive staircase, the chosen electrode pair was stimulated with three 202-Hz, 500-ms sinusoid bursts. The two reference stimuli were presented at a constant intensity, while the test signal was of greater intensity than the references. The procedures were carried out with and without the conditioning pulse train. Preliminary results from two subjects in whom the conditioning pulse train increased the dynamic range show similar intensity discrimination capabilities with or without the conditioner along the upper portion of the dynamic range. Furthermore, at the lower end of the dynamic range, the conditioner allows the listeners to make fine intensity judgments at levels well below their thresholds measured without the conditioner. Implications will be discussed.

(Supported by NIH/NIDCD program project DC00242, Advanced Bionics Corporation)

86 Effects of High-Rate Pulse Trains on Intensity Discrimination

Christina Runge-Samuels, Jill B Firszt, Wolfgang Gaggl, Phillip A Wackym

Otolaryngology and Communication Sciences, Medical College of Wisconsin, 9200 W. Wisconsin Ave., Milwaukee, WI, United States

Research has shown that high-rate (5 kHz) constant-amplitude pulse trains may increase the dynamic range of hearing for cochlear implant users. Hong et al. (2003) showed with sinusoidal stimuli that high-rate pulses increased dynamic range by an average of 6.7 dB, primarily by lowering threshold. The usefulness of the wider dynamic range and the effects of high-rate pulses on implant performance are of interest. To address these issues, intensity discrimination of sinusoidal signals was measured on electrode 14 using a 3AFC adaptive procedure in users of the Clarion CII device. Three consecutive monopolar 1000 Hz sinusoids were presented, two of a 'standard' intensity (I) and one of a higher intensity (I+ Δ I). The subjects selected the louder sound. The increment of Δ I was adjusted until a correct-response probability of 79.4% was reached [Levitt, JASA 1971]. Discrimination was measured at 4-5 supra-threshold standard intensities. The testing was performed with and without monopolar 5 kHz biphasic pulses presented simultaneously on electrodes 13 and 15. Discrimination performance was characterized by Weber fractions in dB (10 log Δ I/I) and plotted as a function of standard intensity. The y-intercept of the functions' regressions were defined as an index of overall sensitivity to intensity change [see Nelson et al. JASA 1996]. The effects of high-rate pulses on threshold and dynamic range were variable across subjects. In general, discrimination performance increased as standard intensity increased, as has been previously reported [Shannon et al. Hear Res 1983]. Within subjects, some intensity levels showed improved performance with high-rate pulses. However, within and across subjects there was a tendency for a decrease in overall sensitivity to intensity change in the presence of high-rate pulses.

Supported by intramural funds from the Department of Otolaryngology and Communication Sciences, Medical College of Wisconsin and Advanced Bionics Corporation

87 Effect of combining different carriers across bands on speech intelligibility in cochlear implant simulation

Nathaniel A. Whitmal, III, Sarah F. Poissant, Richard L. Freyman, Karen S. Helfer

Communication Disorders, University of Massachusetts, Rm. 6 Arnold House, Amherst, MA, United States

Listeners with normal hearing are able to extract substantial speech information from the temporal envelopes of a limited number of frequency channels, providing useful insights into mechanisms of speech recognition in general, as well as cochlear implant processing and listening. The channels are usually driven by narrowband noise or sinusoidal carriers at the center frequency of the channel. Published data show that speech recognition is relatively unaffected by carrier type (Dorman et al., JASA 102:2403-2411, 1997), although noise and tonal carriers produce entirely different sound qualities. The current study asks whether speech intelligibility is compromised when different types of carriers are used in different bands. Recordings of sentences were processed by a 6-band version of the cochlear implant simulation described by Qin and Oxenham (JASA 114:446-454, 2003), which in the current implementation allowed either a selected subset of bands or all bands to be presented. In "consistent-carrier" conditions, either tones or noise were used as carriers in all selected bands. In "mixed-carrier" conditions, tonal carriers were used in a subset of bands, while noise carriers were used in a complementary subset. Preliminary results indicated that speech recognition by normal-hearing subjects listening in quiet did not decline in mixed-carrier relative to consistent-carrier conditions. However, when competing speech processed identically to the target speech was introduced, in some conditions the stimuli appeared to segregate into a tonal stream and a noise stream rather than into separate voices. This poster will report on the extent to which this unexpected segregation is detrimental to intelligibility. Possible implications for hybrid strategies in cochlear implantation will be discussed.

Work supported by NIDCD DC01625.

88 Matching Frequencies to Electrodes in Cochlear Implants: Initial Evaluation of a New Method

Adam R. Kaiser¹, Mario A. Svirsky²

¹*Otolaryngology, Indiana U. School of Med., 702 Barnhill Dr., Indianapolis, IN, United States*, ²*Otolaryngology, Indiana U. School of Med.; Dept. of Elect. Eng., Purdue Sch. of Eng., 699 West Drive RR-044, Indianapolis, IN, United States*

Cochlear implants (CI's) are sensory aids that allow listeners with profound hearing loss to perceive sound through electrical stimulation of auditory neurons. The acoustic input signal is filtered into several frequency bands. The amount of energy in each frequency band is monotonic with the amplitude of the electrical stimulation delivered to the corresponding intracochlear electrode. A frequency-to-electrode map is the function that determines the correspondence between each analysis filter and the intracochlear location of the electrode to be stimulated. Although CI's mimic the tonotopicity of a normal cochlea (i.e., higher frequency bands are associated with electrodes closer to the base of the cochlea), there

can be a frequency mismatch. This means that the characteristic frequency of stimulated neurons can be quite different from the acoustic frequency of the input. Several studies indicate that this frequency mismatch may be detrimental to speech perception. The mismatch depends in part on electrode location and cochlear size, but it can be minimized by an appropriate choice of the frequency-to-electrode map.

The purpose of this study was to develop a new adjustment technique to facilitate the selection of the frequency-to-electrode map. The technique relies on real-time adjustment of the frequency-to-electrode map while subjects listen to pre-recorded running speech. In a pilot test of the new technique, four subjects with normal hearing listened to a cochlear implant simulation that included a known amount of frequency mismatch. Their speech perception was tested before and after adjusting their simulated frequency-to-electrode map. In all cases, the selected frequency-to-electrode map tended to reduce the initial frequency mismatch. Speech perception was better after the adjustment, and this effect was more pronounced with larger pre-adjustment mismatches. Support NIH-NIDCD DC03937

89 Noise Has a Greater Effect on Speech Recognition for Prelinguistically Deafened Cochlear Implant Recipients Compared to Those with Postlingual Deafness

Jill B. Firszt, Wolfgang Gaggl, Christina L. Runge-Samuels, Phillip A. Wackym

Otolaryngology and Communication Sciences, Medical College of Wisconsin, 9200 W. Wisconsin Avenue, Milwaukee, WI, United States

Although adults with prelinguistic onset of profound hearing loss have received cochlear implants, there are few published reports on performance measures of speech perception for this population. In the present study, subjects were adults who had either prelinguistic onset of deafness (prior to age 2 years) or postlinguistic onset of profound hearing loss (after age 4 years). All subjects had complete electrode insertions of their cochlear implant devices, were implanted as adults (after age 20 years), and had open-set speech recognition. Scores for the subjects in each of the two groups were matched on the Hearing in Noise Test (HINT), a test of sentence recognition, when tested in quiet at 60 dB SPL. All subjects were evaluated in the presence of speech spectrum noise at a +8 signal-to-noise ratio. The difference in performance in the quiet and noise conditions was calculated for each subject. A comparison of the score differences showed a significantly larger decrease ($p < 0.05$) for those with prelinguistic hearing loss compared to those with later postlinguistic onset. These study findings suggest an association between prelinguistic hearing loss and impairment in the perception of speech in the presence of noise. Prelingual profound hearing loss results in central reorganization of the auditory pathways including neural processes involved with listening in background noise. Given this, it is possible that long periods of sensory deprivation and limited access to sound in early childhood impacts the ability to resolve the acoustic properties of speech in the presence of highly competitive environments, such as when listening in noise.

Supported by Deafness Research Foundation, NIH/NIDCD K23DC05410

90 Predicting cochlear implant outcome in highly variable group of congenital deaf children: importance of central processing

Hyo Jeong Lee¹, Seung-Ha Oh¹, Kim Chong Sun¹, Kang EunJoo², Lee Dong Soo²

¹*Otolaryngology, Seoul National University, College of Medicine, 28 Yongon-dong, Chongro-gu, Seoul, Korea, Republic of,*

²*Nuclear Medicine, Seoul National University, College of Medicine, 28 Yongon-dong, Chongro-gu, Seoul, Korea, Republic of*

Several demographic characteristics were approved as major predictive factors of speech perception capacity after cochlear implantation in congenital deaf children. But the published literature has consistently reported large individual differences among users. Authors investigate cerebral cortical metabolism of children with most variable outcome. To define the highly variable group, speech perception ability of 29 prelingually deafened children who can be followed more than 4 years were analyzed. Authors noted prelingually deafened children with 5 to 7 years old age at implantation showed the most variable outcome based on the speech perception capacity. Preoperative 18-fluorodeoxyglucose positron emission tomography (FDG-PET) imaging were taken in 11 children (7 boys and 4 girls) aged from 5 to 7 1/2 years old at implantation, who had been followed at least 2 years after implantation. They were divided into good group and poor group according to the speech perception capacity measured using K-CID obtained at 2 years after implantation. Preoperative cerebral cortical metabolism was compared between groups. The good group showed higher metabolism in both frontal areas, particularly left dorsolateral prefrontal gyrus and left inferior parietal area. These areas were well known to be involved with verbal working memory. On the other hand, the higher metabolic areas of poor group are congregated into the posteroventral part of the brain; right inferior occipital and both fusiform gyri, which concern visual input processing and visual knowledge. These results suggest that children who had more capacity for verbal working memory preoperatively, can perform better. However, children who were more dependent to visual input derive only minimal benefit. Our study with FDG-PET might provide possible way to predict outcome of cochlear implantation more precisely.

91 Simulation of a 'Hole' in Hearing: Perceptual Adaptation by Normally Hearing Listeners to Spectrally-Warped Speech

Matthew Smith, Andrew Faulkner

Department of Phonetics & Linguistics, University College London, 4 Stephenson Way, London, United Kingdom

In this simulation study, the effect of dropping the channels of information that would normally be represented in a spectral "hole" region was compared with conditions that retained this information by presenting it to channels on either side of the hole. Such a reassignment partially preserves the information that would be lost; however, it also entails a warping of the place-code of the spectral envelope, which may in itself lead to poorer performance. Subjects were given training (3 hours of connected discourse tracking) in two "preservation" conditions, A and B, in order to

compare performance against a baseline “dropped” condition. A 10mm hole (420Hz - 2.2kHz) was created in the tonotopic representation of the speech signal (frequency range 130Hz - 4.5kHz). In condition A speech was divided into 12 contiguous frequency bands and synthesized as the sum of 6 noise carrier bands, with those bands that would normally be represented in the hole region being evenly split and rerouted to channels immediately adjacent to both sides of the hole - envelopes from these bands were summed and averaged with the envelope of the relevant hole-adjacent band. In condition B speech was divided into 6 contiguous bands and synthesized as the sum of 6 noise carrier bands with the same centre and cut-off frequencies as for A (three channels apical to the hole and three basal). In the “dropped” condition centre frequencies of the 12 analysis and carrier bands were matched but those carrier bands that would normally have been represented in the hole region were effectively switched off, again leaving three channels apical and basal to the hole.

Performance in condition B, in which spectral warping was spread over the entire frequency range, was significantly and consistently better than in A, where information was warped over a relatively short range to hole-adjacent channels. Significantly, performance in the “preservation” conditions improved considerably with training (e.g. condition B sentence scores rose from 32% to 70% keywords correct). Post-training scores were also much higher than baseline scores in the “dropped” condition (mean = 17% for sentences). This suggests that rerouting spectral information around a hole is better than simply dropping it, even though differences may not be apparent in acute studies.

92 Analysis of Programming Levels as a Possible Outcome Predictor: A Cross-Device Study of Pediatric and Adult Cochlear Implant Users

Edward Holman Overstreet¹, Sudhir R. Belagaje², Karen Iler Kirk³, Kelly Lormore⁴, Teresa Zwolan⁵

¹Research and Development, Advanced Bionics Corporation, 25129 Rye Canyon Loop, Santa Clarita, California, United States,

²School of Medicine, Indiana University, Indiana University, Indianapolis, IN, United States, ³School of Medicine, Department of Otolaryngology-Head and Neck Surgery, Indiana University,

Riley Research Wing 044, 699 West Drive, Indianapolis, IN, United States, ⁴Audiology, Indiana University, Riley Research Wing 044, 699 West Drive, Indianapolis, IN, United States,

⁵University of Michigan Cochlear Implant Program, University of Michigan, 475 Market Place, Building 1, Suite A, Ann Arbor, MI, United States

Even with modern cochlear implants there still remains large variability in outcomes within cochlear implant recipients. If better performance predictors could be identified, patients might be more successfully tracked into appropriate therapy and insight might be gained into how to better optimize programming parameters in poorer performers. It has long been theorized that reduced neural survival contributes to poor performance in cochlear implant recipients, yet useful clinical guidelines for assessing and comparing patient program level requirements have not been described. These level requirements may reflect a component of neural integrity. In fact, several studies have shown that neural thresholds from the cochlea, a probable indicator of neural survival, tend to

occur within the patient's electrical dynamic range tracking with program levels. This study examined patient program levels and their relationship to outcome measures in pediatric and adult participants (N>100) implanted with either Clarion CI/CII, Nucleus 24/24Contour, or MEDEL Tempo+ devices. Only participants using a newer coding strategy (HiResolution, MPS, CIS, ACE, or SPEAK) in mono-polar mode were included. Adult inclusion criteria were: post-linguistically deafened, normal cochlear anatomy, and open-set word and sentence recognition testing at 3-6 months of device use. Pediatric inclusion criteria were: age at onset of deafness < 36 months, normal cochlear anatomy, age at implantation < 60 months, and no known cognitive impairments that may influence performance. In pediatric subjects, age-appropriate speech perception measures obtained between 24-36 months after initial stimulation were used to assess outcome. In order make comparisons across devices and programs of different pulse durations, all program levels were converted into units of charge. Preliminary analyses support the hypothesis that there exists a normative charge-need range that is consistent across devices and that where a patient falls in the charge-need continuum may impact outcome.

93 Correlation between later outcome of cochlea implantation and cerebral activity in children with early onset deaf

Kang EunJoo¹, Seung-Ha Oh², Lee Dong Soo¹, Hyo Jeong Lee², Kim Chong Sun²

¹Nuclear Medicine, Seoul National University, College of Medicine, 28 Yongon-dong, Chongro-gu, Seoul, Korea, Republic of, ²Otolaryngology, Seoul National University, College of Medicine, 28 Yongon-dong, Chongro-gu, Seoul, Korea, Republic of

Degree to which auditory speech perception takes place following regaining of auditory sensation after cochlear implantation (CI) differs greatly especially in the children patients with early deaf onset who have never learned auditory language. Age of these deaf children at the CI is also known as one of critical factors to determine the outcome of the CI. Here, we studied a group of early onset deaf children (n=8, age 2.1 ~ 13.2 yr.) in order to understand neural substrates underlying development of auditory language following CI.

A group of deaf children (n=8) underwent F18-FDG PET scan both before the CI surgery (pre-CI PET) and after the CI surgery (post-CI PET). Performance of auditory speech perception was also measured with the Korean version of CID (Central Institute of Deaf) test given in both occasions. Using SPM99, correlations of the amount of FDG-uptake with the CID scores or with age were examined in both PET images obtained from the same patient group.

The deaf children who showed better CI outcome had had greater glucose metabolism in the dorsal part of brain, especially right hemisphere and hypometabolism in the medial and inferior prefrontal as well as bilateral temporal regions when they were deaf. However, these differences in the brain regions with hyper/hypo glucose metabolism among these patients were greatly reduced after the CI, yet the pattern remained same. Brain regions showing increased brain activity with increased developmental age also dif-

fer between the time when they were profound deaf and the time when they gained the auditory sensation. Age-associated metabolism recovery was found in the auditory region of superior temporal gyrus.

Age (duration of deaf) affected the regional glucose metabolism in the deaf patients. However, the individual differences in regional brain activity determine the degree of the auditory language development following the CI in the children with early onset deaf.

94 FMRI Evaluation of a Novel Cochlear Implant Rehabilitation Strategy Reveals Correlation of Cortical Activity with Speech Perception Performance is Dependent on Stimuli Used for Training

Thomas M Talavage^{1,2}, Mario A Svirsky³, Eri Haneda¹, Heidi Neuburger³

¹*School of Electrical and Computer Engineering, Purdue University, 465 Northwestern Avenue, West Lafayette, IN, United States*, ²*Department of Biomedical Engineering, Purdue University, 465 Northwestern Avenue, West Lafayette, IN, United States*, ³*Department of Otolaryngology-Head and Neck Surgery, Indiana University School of Medicine, 699 West Drive, RR-044, Indianapolis, IN, United States*

An important reason for the enormous variation in individual performance of post-lingually deaf cochlear implant (CI) users to perceive speech is proposed to be related to alterations made to the speech signal by the CI. Sub-optimal neural encoding of external acoustic stimuli may contribute to the difficulty many CI users have in understanding spoken language. The signal delivered to the auditory nerve by a CI is both spectrally impoverished and shifted upward in frequency with respect to the cochlear stimulation experienced by a normal-hearing (NH) subject. To improve adaptation, we propose a novel rehabilitation procedure in which the upward shift is introduced gradually. Initial absence of a shift is expected to provide speech signals to the CI user that are more consistent with those encountered prior to hearing loss, accelerating adaptation. Six NH subjects were trained and tested (15 sessions) on speech stimuli processed using an acoustic CI simulator emulating frequency shifts up to 6.5mm. The Standard group was presented only stimuli altered to simulate a 6.5mm shift. The Experimental group was presented stimuli having simulated shifts that varied by session, increasing from 0mm to 6.5mm over ten sessions. Three fMRI sessions were conducted on each subject. Three types of speech stimuli were used in these sessions: unfiltered words (NS), words processed to simulate a 3.25mm shift (HS); and words processed to simulate a 6.5mm shift (FS). Behavioral testing results support our hypothesis that the subjects in the Experimental group approach asymptotic performance more rapidly. Cortical responses detected with fMRI in Broca's area and Wernicke's areas exhibit correlation with speech perception performance, but only when subjects were presented stimuli having shifts on which they were trained (FS for Standard; HS and FS for Experimental). These results suggest that the gradual introduction of the shift may accelerate neural adaptation to CI stimulation.

95 Functional Imaging of Cerebral Plasticity After Cochlear Implantation

Charles J. Limb^{1,2}, Eric B. Ortigoza¹, John K. Niparko², Allen R. Braun¹

¹*National Institute on Deafness and Other Communication Disorders, National Institutes of Health, 9000 Rockville Pike, Bethesda, MD, United States*, ²*Otolaryngology-Head and Neck Surgery, Johns Hopkins University School of Medicine, 601 N. Caroline St., Baltimore, MD, United States*

Auditory performance after cochlear implantation varies among individuals. Many patients show improvement over time with continued implant-mediated listening experience. This improvement occurs even though the physical and functional characteristics of the implant remain constant. Other patients demonstrate no such improvement. Using functional neuroimaging methods, we sought to identify changes in cerebral activity that might underlie changes in performance.

H₂¹⁵O positron-emission tomography (PET) scanning was employed longitudinally to study neural activity following cochlear implantation. Postlingually deafened human subjects ($n=4$) with right-sided cochlear implants were studied from 1-2 weeks to 24 months post-activation. Subject performance was assessed using hearing-in-noise test (HINT) scores. Fifteen intravenous injections of H₂¹⁵O were administered per scanning session, with five injections each for resting state and two tasks. While in the scanner, subjects performed both a lexical decision task (identifying real vs. nonsense words) and a pitch perception task (identifying pitches as higher or lower).

Data were analyzed using Statistical Parametric Mapping 99. Contrast analyses ([task-rest] for each session or [task-task] over time) were performed to identify regions of activity. For the subject with the best performance (mean HINT scores >95%), there was a significant increase over time in cortical activity, particularly in the superior and middle temporal gyri ($p<0.001$). These changes were seen for both lexical decision and pitch discrimination tasks. In subjects with poor performance (mean HINT scores <15%), there was less activity in the auditory cortex for both lexical and pitch discrimination tasks, and less increase in activity over time compared to good performers ($p<0.001$).

These data reveal that increased activity in the superior and middle temporal gyri correlates with improved performance after cochlear implantation. In addition, a lack of increased activity in these cortical areas over time may partially explain poor outcomes. These data contribute to a novel method of examining the effects of cochlear implantation on the brain, and to evaluate why certain users fail to gain benefit after implantation.

96 Acoustic Correlates of the Variation in the Number of Channels Needed to Identify the Sources of Familiar Environmental Sounds

Valeriy Shafiro

Dept. of Speech and Hearing Sciences, City University of New York, 365 Fifth Ave, New York, NY, United States

Identifying sources of many nonspeech environmental sounds is a perceptual task that is routinely performed by all normal-hearing listeners. Information about sound sources has practical signifi-

cance for the listener, and can be used by the listener to alter his/her behavior depending on the identity and behavior of sound-producing objects in the immediate environment. However, when the spectrum of environmental sounds is impoverished, as may be the case for users of auditory prostheses, listeners' ability to identify sound sources suffers.

Interestingly, individual environmental sounds are not equally affected by equal declines in spectral resolution. Previous research (Shafiro, 2003. Unpublished dissertation) has demonstrated that noisy, temporally patterned sounds (e.g., heartbeat, helicopter, thunder) generally require fewer frequency channels to be identified than sounds with a higher degree of "pitchness" (e.g., doorbell, glass breaking, church bell). This research reports on a follow-up investigation of acoustic parameters that may be associated with the differences among environmental sounds in terms of the number of frequency channels required for source identification. It describes an exploratory set of acoustic measures that may be used to distinguish environmental sounds that need only few (i.e., 2 or 4) channels from sounds that need a large number of channels (i.e., 16 or more) to be accurately identified. Measures of both spectral and temporal characteristics of the selected sounds will be considered, and implications for determining the optimal number of channels for environmental sound perception with a cochlear implant will be discussed.

97 Evaluation of Distortion Products Produced by the Human Auditory System

Shaum P. Bhagat¹, Craig A. Champlin²

¹Communication Sciences and Disorders, Louisiana State University, 163 Music and Dramatic Arts Bldg, Baton Rouge, Louisiana, United States, ²Communication Sciences and Disorders, The University of Texas at Austin, CMA 7.214, Austin, Texas, United States

During the simultaneous presentation of two primary tones to the ear ($f_1, f_2; f_2 > f_1$), intermodulation distortion products can be measured acoustically in the ear canal and electrically as scalp-recorded auditory evoked potentials. The purpose of this investigation was to elucidate the sources of nonlinearity within the human auditory system responsible for generating the quadratic difference tone ($f_2 - f_1$) and the cubic difference tone ($2f_1 - f_2$). Three experiments were conducted. During the first experiment, measurements of distortion-product otoacoustic emissions and auditory evoked potentials were obtained from 24 normal-hearing adults (12 male) in conditions with and without presentation of a contralateral noise. The effects of primary-tone duration and mode of presentation of the primaries (monotic vs. dichotic) on measurements of auditory evoked potentials were examined in the second and third experiments. The results from the first experiment indicated that overall, both acoustical and electrical distortion products were suppressed during presentation of a contralateral noise. However, greater suppression occurred at the electrical cubic difference tone compared to the electrical quadratic difference tone. The second experiment revealed that growth in electrical distortion-product amplitude accompanied increases in primary-tone duration. The results of the third experiment demonstrated that electrical distortion products were more prevalent when the primaries were presented monotically. The findings from the first experiment of the investigation supported the conjecture that a cochlear nonlinearity produced

acoustical and electrical cubic difference tones. Evidence from the second and third experiments concerning the origin of electrical distortion products was inconclusive, and contributions from both cochlear and neural nonlinear sources could not be ruled out.

98 Input-Output Functions from single Source Distortion Product Otoacoustic Emissions

Manfred Mauermann, Birger Kollmeier

Medizinische Physik, Universität Oldenburg, Carl-von-Ossietzky Str. 9-11, Oldenburg, Germany

Input-output (I/O) functions from $2f_1 - f_2$ distortion product otoacoustic emissions (DPOAE) could be a powerful diagnostic tool for cochlear hearing loss, e.g. to predict individual pure tone thresholds, or to estimate recruitment in subjects with cochlear hearing loss.

It is widely accepted that DPOAE in humans with f_2/f_1 around 1.2 can be interpreted as the vector sum of two components from different cochlear sources, an initial distortion component with its source close to the characteristic place of f_2 and a second component generated around $2f_1 - f_2$. However, most studies on DPOAE I/O functions do not take into account possible effects of the second DPOAE source. On the other hand, studies on DPOAE source separation mostly investigated one fixed set of primary levels.

Therefore the current study investigates the influence of the second component on DPOAE I/O functions ($L_2 = 20-80$ dB SPL, $L_1 = 39\text{dB} + 0.4 \cdot L_2$, $f_2 = 1.5-4.5$ kHz, $f_2/f_1 = 1.2$) and looks for the separability of the DPOAE components at different primary levels. "Standard" two source DPOAE I/O functions are compared with I/O functions from the initial distortion component only. The two DPOAE components are separated by using (a) the method of latency windowing and (b) the method of selective suppression (see e.g. Khaluri et al., 2001; JASA, 109: 622-637). The comparison of these two methods allows to optimize the separation parameters e.g. to find adequate suppressor levels for the selective suppression paradigm at different primary levels.

The results from six normal hearing and one hearing impaired subject show:

- (I) The relative contribution of the second DPOAE source increases with decreasing stimulus levels.
- (II) The variability of DPOAE I/O functions of adjacent frequencies is strongly reduced for I/O functions from the initial distortion component only.
- (III) Suppressor levels of about 60 dB SPL give adequate suppression of the second source for the investigated primary levels (30-70 dB SPL).

99 DPOAE Suppression Tuning Curves: Effect of Suppression Criterion

Tiffany A. Johnson¹, Michael P. Gorga^{1,2}, Stephen T. Neely¹, Darcia M. Dierking², Brenda M. Hoover²

¹Hearing Research, Boys Town National Research Hospital, 555 N. 30th Street, Omaha, NE, United States, ²Audiology, Boys Town National Research Hospital, 555 N. 30th Street, Omaha, NE, United States

DPOAE suppression tuning curves (STCs) typically are constructed using either 3 or 6 dB of suppression as the criterion

amount of suppression. If the slopes of the suppression versus suppressor level functions are constant across frequency, then the DPOAE STC will be the same regardless of criteria. However, the slopes of these functions differ across frequency; therefore, the shape of the STC, to some extent, should depend on the criterion used to construct it. We present DPOAE STCs constructed using suppression criteria ranging from 3 dB of suppression ("threshold" of suppression) to complete suppression ("threshold" of response). The effect of suppression criterion was examined across a range of primary levels when $f_2 = 4$ kHz in both normal-hearing and hearing-impaired human ears. Normal and impaired ears produced roughly similar Q values (Q_{10} and Q_{ERB}) when the suppression criterion was 3 or 6 dB, although some variability was evident in relation to L_2 . At low probe levels ($L_2 = 20$ or 30 dB SPL), however, the Q values for subjects with normal hearing increased to a greater extent as the criterion amount of suppression for constructing the STC increased. In contrast, tip-to-tail differences decreased as probe level increased, but were relatively unaffected by the criteria, with normal-hearing subjects producing larger tip-to-tail differences regardless of how the STCs were constructed. It is unclear which STC criterion is most appropriate for comparison to other measures of tuning. However, for comparison with tuning curves based on "threshold" measurements, such as psychophysical tuning curves, DPOAE STCs defined by the completely suppressed response might represent the most appropriate approach.

Work supported by NIH (R01 DC02251 and T32 DC00013).

100 Fast DPOAE I/O measurements covering L_1 - L_2 stimulus level space

Stephen T. Neely, Darcia M. Dierking, Brenda M. Hoover, Michael P. Gorga

Hearing Research, Boys Town National Research Hospital, 555 North 30 Street, Omaha, NE, United States

Fast DPOAE I/O measurements covering L_1 - L_2 stimulus level space

In order to more completely characterize the distortion product otoacoustic emission (DPOAE) at a particular frequency, it is of interest to know the DPOAE level for all possible combinations of stimulus tone levels L_1 and L_2 . The time required by traditional methods to measure DPOAE levels for many primary-level combinations can be reduced by using a fast DPOAE I/O procedure, in which primary levels are varied continuously within a single stimulus waveform. If L_1 and L_2 are modulated sinusoidally (on a dB scale), then they follow a Lissajous path (LP) in L_1 - L_2 space. Measurements have been obtained using such stimuli in four human ears at 1 and 4 kHz. DPOAE levels obtained by LP method are consistent with levels measured by traditional methods, but have the advantage of showing the DPOAE level surface over a substantial area of the L_1 - L_2 space. The topology of this surface varies with frequency and across subjects in ways that might bring into question previously held assumptions about underlying response properties. The LP method may be a useful way to obtain optimal DPOAE levels or to evaluate middle-ear forward and reverse transmission.

Work supported by NIH (R01 DC02251).

101 An extensive f_1, f_2 area map study of DPOAE in the frog.

Sebastian W.F. Meenderink¹, Peter M. Narins², Pim van Dijk¹

¹ENT, University Hospital Maastricht, PO BOX 5800, Maastricht, Netherlands, ²Physiological Science, University of California, Los Angeles, 621 Young Drive South, Los Angeles, California, United States

Mammalian DPOAEs are currently thought to be the mixture of at least two components. Not only do these components arise at different tonotopic locations in the cochlea, their generation mechanisms are also different. As a consequence of these two different generation mechanisms the components have different phase characteristics. Which component dominates in the DPOAE measured in the ear canal depends on stimulus parameters, especially the ratio f_2/f_1 . Although experimental techniques are available to study either one of these components exclusively, it has been shown recently that systematic exploration of f_1, f_2 area maps also show the presence of two components.

The frog inner ear lacks a cochlea. Instead there are two papillae specialized in detecting airborne sound. The amphibian papilla (AP) is a structure comparable with the cochlea in the sense that it exhibits tonotopic organization. The basilar papilla (BP) is a relatively simple organ consisting of a low number of hair cells, all tuned to the same frequency. Both papillae lack a basilar membrane, and the presence of a traveling wave is still not resolved. Although these differences, especially in the BP, exclude two sites of DPOAE generation, two DPOAE components generated by different mechanisms can not be ruled out *a priori*.

We explored the f_1, f_2 area map to see whether DPOAEs from the frog ear are also a mixture of two components generated by two different mechanisms. The results indicate that one component is dominant in both the AP and the BP. The phase characteristics of this component are similar to the reflection component in the cochlea. Although the results do not exclude the presence of a 2nd component, preliminary model studies indicate that a single nonlinearity is sufficient to account for the observed DPOAE behavior.

102 Using sweeping tones to evaluate DPOAE fine structure.

Glenis R Long¹, Carrick L Talmadge², Jungmee Lee¹

¹Speech and Hearing Sciences, Graduate Center CUNY, 365 Fifth Ave, New York, NY, United States, ²National Center for Physical Acoustics, University of Mississippi, Coliseum Drive, University, MS, United States

The level of DPOAEs of normal hearing individuals can vary by as much as 30 dB with small frequency changes (a phenomenon known as DPOAE fine structure), due to the interaction of components from two different regions of the cochlea (the nonlinear generator region and the reflection component from the DP region). An efficient procedure to separate these two components would improve the clinical and research utility of DPOAE. In this study, two procedures for evaluating DPOAE fine structure are compared: DPOAE generated by discrete tones vs sweep tones. The sweep DPOAE data is analyzed with a least squares fit filter that is similar to a heterodyne filter. Sweep rates of greater than 8 s per

octave permit rapid evaluation of the cochlear fine structure. A higher sweep rate of 2s per octave provides DPOAE without fine structure, because the longer latency reflection component falls outside the range of the filter. Consequently, depending on sweep rate, DPOAE obtained with sweeping tones can be used either to get more rapid estimates of DPOAE fine structure or to obtain estimates of DPOAE from the generator region uncontaminated by energy from the reflection region

103 Modification of DPOAE fine structure by contralateral stimulation.

Glenis R Long¹, Carrick L Talmadge², Jungmee Lee¹

¹Speech and Hearing Sciences, Graduate Center CUNY, 365 Fifth Ave, New York, NY, United States, ²National Center for Physical Acoustics, University of Mississippi, Coliseum Drive, University, MS, United States

If distortion product otoacoustic emissions (DPOAE) are evaluated with high enough frequency resolution, they show pseudo-periodic variations ("fine structure") in level and phase with frequency. This fine structure is generated by the interaction of two components, whose phases vary at different rates with frequency. One of these components is from the generator region (slow phase variation with frequency) and the other from near the tonotopic frequency of the DPOAE (rapid phase change with frequency), and corresponds to the region of the cochlear associated with reflection of the distortion product frequency. Efferent stimulation has the greatest effect on the basilar membrane response of low-level stimulation; consequently we expect contralateral stimulation to have a major effect on the reflection-site component. Depending on the relative levels of the two components, contralateral stimulation produces either a reduction of the fine structure (generator component larger) or an enhancement of the fine structure (reflection component larger). Changes in the phases of the two components typically lead to a downward frequency shift of the DPOAE fine structure.

104 Analysis of DPOAE fine structure in 35 normal hearing humans

Karen Reuter, Dorte Hammershoi

Department of Acoustics, Aalborg University, Fredrik Bajers Vej 7, B5, Aalborg Øst, Denmark

Distortion product otoacoustic emission (DPOAE) is the response of the inner ear to two pure-tone stimuli and is the result of the non-linear interaction of the tones in the cochlea. When DPOAEs are measured with high frequency resolution, a DPOAE fine structure can be revealed, which is characterized by consistent patterns of amplitude maxima and minima. In the literature the disappearance of DPOAE fine structure is suggested to be a sensitive measure for the detection of hearing impairment. The origin of the DPOAE fine structure is not fully understood, and in the literature there exist some disagreements about the bandwidth of the fine structure, the dependency of the fine structure on DPOAE measurement parameters and the correlation between fine structure prevalence and hearing threshold.

In this study the prevalence and characteristics of the DPOAE fine structure in young normal-hearing humans were investigated. The DPOAE fine structure of 35 test subjects was measured with

$L1/L2 = 65/45$ dB, $f1/f2 = 1.22$, covering a frequency range of $f2$ from 1-6 kHz. The results show that a fine structure is not prevalent for all subjects within the full measured frequency range. The pattern of the fine structure is analyzed according to prevalence, bandwidth of the periodicity and depth of the notches.

One further experiment is planned in which the DPOAE fine structure is measured before and after a tonal over-exposure. The purpose is to investigate whether the DPOAE fine structure disappears when the hearing is mildly overexposed, as e.g. indicated by a temporary threshold shift. If available, the results of this study will be presented.

105 Comparison of DPOAE-Derived Phase-Gradient Estimate of Cochlear Delay with Two Time Domain OAE Measures

Rachel M Roberts, Robert H Withnell

Speech and Hearing Sciences, Indiana University, 200 South Jordan Avenue, Bloomington, Indiana, United States

Cochlear delay measured with otoacoustic emissions (OAEs) has typically been derived from the phase-gradient estimate of group delay. For stimulus frequency OAEs, such a measure can provide a valid estimate of cochlear delay, with some qualifications (Shera & Guinan, 2003; Goodman et. al., 2003). Cochlear delay has also been inferred from the distortion product otoacoustic emission (DPOAE) phase-gradient by varying one or other of the stimulus frequencies and obtaining the phase derivative with respect to the varying frequency. DPOAE phase-gradient estimates of delay have shown a frequency-dependence concordant with cochlear tonotopic organization (Kimberley et. al., 1993) but it has been argued based on theoretical grounds that these estimates do not provide an accurate measure of cochlear delay (Shera et. al., 2000; Tubis et. al., 2000). Here we compare delays derived using the DPOAE phase-gradient estimate to those measured directly in the time domain using amplitude modulated tone burst (AMTB) OAEs and DPOAEs. DPOAE phase was measured with $f2/f1$ between 1.17 and 1.23 (fixed $f2$, $f2 = 4.5, 9$ or 18 kHz) for the $2f1-f2$ nonlinear distortion component generated in the $f2$ region. The $2f1-f2$ component arising from its characteristic place was suppressed using a tone near in frequency to $2f1-f2$, with the suppressor tone cancelled from the ear canal recording using asynchronous averaging and electrical cancellation using a phase-shifter prior to digitization. AMTB OAEs were evoked using a nonlinear extraction paradigm in the region of 4.5, 9 and 18 kHz with a 23 Hz modulation rate. DPOAE time domain recordings were obtained using a pulsed tone paradigm with the DPOAE extracted using an LSF technique. With comparison of the three estimates of cochlear delay we consider the question "what is the physical meaning of DPOAE derived phase-gradient estimates of delay?"

106 Double modulation pattern of DPOAEs due to low-frequency biasing

Lin Bian, Mark E. Chertoff

Hearing and Speech, University of Kansas Medical Center, 3901 Rainbow Blvd., Kansas City, KS, United States

A time-domain method has been developed to obtain a cochlear transducer function (f_{tr}) using low-frequency modulated distortion product otoacoustic emissions (DPOAEs). This method is based

on the principle that the magnitude of the cubic difference tone (CDT, $2f_1-f_2$) is proportional to the absolute value of the third derivative of a sigmoid-shaped f_{tr} at low primary levels (Bian *et al.*, 2002, JASA, 112:198). The CDT magnitude obtained with this time-domain method as a function of bias level demonstrate a double modulation pattern consisting of two typical shapes of the absolute value of the third derivative of the f_{tr} , each contains a center-lobe and two side-lobes. In ten gerbils, DPOAEs were biased by a 25 Hz tone at 20 Pa (120 dB SPL) with the primary level levels ranging from 50 –70 dB SPL ($f_1=3968$, $f_2=5120$ Hz). The CDT magnitudes were obtained with a 512-point FFT window moving along three cycles of the bias tone. The center of the CDT-bias function shifted towards positive sound pressures when the bias level was rising, and towards negative pressures while decreasing in bias level. The double modulation pattern was characterized with various indices. Separation due to loading or unloading of the cochlear transducer by the bias tone was consistent among all the primary levels. Other indices showed level-dependent characteristics that were shared between the loading/unloading processes. Magnitudes of the center- and side-lobes increased with primary levels, but showed different growth patterns. The width of the center-lobe widened with increasing in primary level. The low-frequency modulation of CDT was more effective at lower primary levels. The separation of the center-peaks of the CDT-bias functions depending on the phase of the bias tone indicates that the cochlear transduction is hysteretic and level-dependent. Indices of the CDT double modulation pattern can be used to directly access cochlear f_{tr} and its hysteresis.

Supported by NIH/NIDCD grants: R03 DC006165 and R01 DC02117

107 Evidence for Postnatal Maturation of Human Cochlear Function?

Carolina Abdala¹, Leslie Visser-Dumont¹, Ellen Ma²

¹Children's Auditory Research, House Ear Institute, 2100 W. Third St., Los Angeles, CA, United States, ²Neonatology, University of Southern California, School of Medicine, 1240 North Mission Rd., Los Angeles, CA, United States

DPOAE suppression tuning and suppression growth have been studied in prematurely born and term-born neonates to investigate maturation of human cochlear function. Several studies have found that DPOAE suppression tuning curves (STC) in neonates are narrower, steeper on the low-frequency flank and suppression growth is excessively compressive for low-frequency side suppressor tones. Recent data from our laboratory confirm that both prematurely born neonates that have reached "term-like" age (40 post-conceptual weeks), as well as term-born neonates, continue to show these immaturities in DPOAE suppression, in particular at $f_2 = 1500$ and 6000 Hz. This suggests that subtle immaturities in cochlear function may persist into the early postnatal period. In the present study, DPOAE suppression data were collected in 10 term-born neonates, 9 three-month-old infants and 10 normal-hearing adults subjects at $f_2 = 6000$ Hz, using moderate level pure tones (65-55 dB SPL) and a 1.21 f_2/f_1 ratio. Results indicate that three-month-old infants show DPOAE suppression tuning and growth similar to newborns and both infant groups show data that differs significantly from adult data. The three-month-old infants continue to show narrower tuning with a sharper low-frequency flank

and atypically shallow suppression growth for the lowest frequency suppressor tones. Although not adult-like, data collected from the older infants is moving in an adult-like direction and beginning to approximate adult values. Future research is needed to investigate the source of this postnatal immaturity in DPOAE suppression to determine if it is of cochlear origin or related to other aspects of auditory system maturation (i.e. maturation of the medial efferent system or conductive pathways).

108 Transient SFOAE and DPOAE in normal and impaired ears: Effects of stimulus level on latency and self-suppression

Dawn Konrad-Martin¹, Jeffrey L. Simmons², Douglas H. Keefe²

¹Natl. Cntr. for Rehab. Auditory Research (NCRAR), Portland VA Medical Center, 3710 SW US Veterans Hospital RD, Portland, OR, United States, ²Center for Hearing Research, Boys Town National Research Hospital, 555 N 30th Street, Omaha, NE, United States

Transient-evoked stimulus-frequency (SF) and distortion-product (DP) otoacoustic emissions (OAE) were measured in 12 hearing-impaired and 20 normal-hearing subjects using tone pip (pp) pairs, gated tone (gg) pairs, and, for DPOAE, continuous and gated tone (cg) pairs. Stimulus conditions and individual-ear responses were described previously (Konrad-Martin and Keefe, J. Acoust. Soc. Am., in press). Temporal envelopes of stimulus and OAE waveforms were obtained by narrow-band filtering at the stimulus or DP frequency. Mean SFOAE latencies in normal ears at 2.7 and 4.0 kHz decreased with increasing stimulus level (over a 30-dB range) by 60% and 50%, respectively, and were significantly larger than latencies in impaired ears. At probe levels of 40 dB SPL in normal ears, the present results for time-domain SFOAE latencies (5.6 ms at 2.7 kHz, 4.9 ms at 4.0 kHz) agree with frequency-domain SFOAE group delays (5.9 ms at 2.7 kHz, 4.6 ms at 4.0 kHz) (Shera *et al.*, Proc. Natl. Acad. Sci., 2002). With the assumption that cochlear transmission is minimum phase, auditory filter bandwidths were calculated from recorded SFOAE latencies as a function of probe level and hearing status. Transient-evoked SFOAE appear to provide a rapid, non-invasive measure of cochlear tuning. DPOAE latencies (for pp, gg, cg stimulus pairs) varied less as a function of level than SFOAE latencies, 25% over a 30-dB range, although DPOAE latencies tended to be shorter in impaired relative to normal ears at equal SPL. The ppSFOAE SPL within the main spectral lobe of the pip stimulus was higher for normal ears in the higher-frequency half of the pip than in the lower-frequency half. This frequency asymmetry may be due to an asymmetry in two-tone suppression within the main spectral lobe of the tone pip. Such suppression effects may influence cochlear encoding of complex sounds in speech and music. (Work supported by the NIH, RO1 DC03784, and the VA Rehab. R&D Service, E3239V.)

109 Predicting severity of cochlear hair cell damage in adult chickens using distortion product otoacoustic emission input-output functions

Jeffery Lichtenhan^{1,2}, Mark Chertoff¹, Susan Smittkamp^{1,2}, Dianne Durham², Douglas Girod²

¹Department of Hearing and Speech, University of Kansas Medical Center, 3901 Rainbow Blvd., Kansas City, Ks, United States, ²Department of Otolaryngology, Head and Neck Surgery, University of Kansas Medical Center, 3901 Rainbow Blvd., Kansas City, Ks, United States

Distortion product otoacoustic emissions (DPOAEs) have been used as a quantitative tool for assessing mammalian outer hair cell presence and function. For example, Hofstetter et al. (Hearing Research 112: 199-215, 1997) showed a negative correlation between DPOAE amplitude and outer hair cell loss. Here we attempt to extend the utility of DPOAEs by using area and shape of the input-output (I/O) function to predict severity of anatomical hair cell damage in chicken. Using DPOAEs in this fashion will aid in monitoring damage and regeneration of avian hair cells as well as understanding the generator(s) of DPOAEs in chicken.

Commercially raised adult chickens were used as subjects (n=67) because they present with a wide range of cochlear hair cell damage despite their ability to regenerate hair cells (Durham et al., Hearing Research 166: 82-95, 2002). DPOAE I/O functions were recorded at 2f₁-f₂ with f₁ frequencies = 0.5, 1, 2, 3, and 4 kHz, f₂/f₁=1.2, L1=L2, and L1=20-80dB SPL. Cochleae were removed and sensory epithelia were prepared for scanning electron microscopy (SEM). SEM montages were evaluated by two judges who examined f₁ to f₂ epithelial regions and categorized animals into a normal, mild, severe, or a total damage group according to the status of the hair cells in the given region. The area under the DPOAE I/O functions and above the system's distortion or noise floor was calculated. A single-factor ANOVA revealed that the area of the normal and mild damage groups differed from the severe and total damage groups. A two-factor (group and signal level), repeated (signal level) measures ANOVA with polynomial trend analysis showed that the I/O function shape differed between several damage groups. Thus, area and shape of I/O functions can be used to index severity of cochlear hair cell damage and may reflect anatomic/physiologic status of cochlear hair cells.

Supported by NIH grant DC004982

110 Suppression DP-grams in Normal and Noise-Exposed Rabbits.

C. A. Porter, G. K. Martin, B. B. Stagner, B. L. Lonsbury-Martin

Otolaryngology (B-205), University of Colorado Health Sciences Center, 4200 East Ninth Ave, Denver, Colorado, United States

DPOAE suppression protocols usually provide limited information regarding suppression as a function of multiple test frequencies thus making it difficult to relate suppression to the amount or pattern of cochlear dysfunction. The present study used a novel procedure to compare traditional (control) and suppression DP-grams (SDP-grams) in awake rabbits before and after noise exposure. With this approach, changes in suppression parameters were cal-

culated as a function of f₂ and related to patterns of DPOAE loss following a closed sound-field exposure to a 2-h, 110-dB SPL, 2-kHz octave-band noise in one ear of each anesthetized rabbit. Control and SDP-grams re-measured at 1, 2 and 3 wk post exposure were compared to baseline measures. Control DP-grams were obtained (f₂/f₁=1.25) at 4 primary-tone levels (70/70, 65/65, 60/55, 55/45 dB SPL) with f₂ ranging from 1.4-20.6 kHz in 5th-oct steps. These DP-gram levels were then repeated in the presence of a suppressor tone (ST) presented at one of 5 frequencies with respect to f₂ (-30 Hz, -1/2 and -1 oct) and f₁ (+1/2 and +1 oct). For each of the 5 ST frequencies, ST was increased in 2-dB steps from 35-85 dB SPL resulting in 25 SDP-grams. The corresponding control DP-gram was then subtracted from each SDP-gram to obtain the amount of suppression as a function of f₂. These difference values were used to generate contour plots to reveal regions of iso-suppression as a function of ST level and f₂ frequency. From these plots, suppression thresholds were extracted and growth slopes calculated (Gorga et al 2003). In normal ears the amount of suppression as function of f₂ was quite variable as evidenced by numerous irregularities in the contour plots. Following noise exposure, suppression thresholds remained unchanged, while suppression growth decreased on the low-frequency side of the maximum DPOAE loss and showed tendencies to increase in regions of relatively normal DPOAEs. (NIDCD DC000613, DC003114).

111 Acute Effects of Cochlear Insult on CAP, DPOAE and EEOAE

Karin Halsey¹, Kristen Haubenreich², Karl Grosh², David F. Dolan¹

¹KHRI, University of Michigan, 1301 E. Ann St., Ann Arbor, Michigan, United States, ²Mechanical Engineering, University of Michigan, 3124 G.G. Brown, Ann Arbor, Michigan, United States

In this study the acute effect of loud sound on the cochlear action potential (CAP), distortion product otoacoustic emission (DPOAE), electrically evoked otoacoustic emission (EEOAE) are determined.

Pigmented guinea pigs were anesthetized, given a tracheostomy, and placed in a head holder. External pinna, tragus, and ear canal were removed, and the bulla was exposed. An electrode (Ag) was placed on the round window, and a return electrode (AgCl) placed in the neck. Animals were either exposed to high frequency (25 kHz) or low frequency (1 kHz) tones at varying intensities. Responses were recorded prior to and at regular intervals after exposure. The CAP was measured using TDT system II/III, SigGen and BioSig software. The DPOAE was measured using TDT system II/III, MatLab code written in house, and EEOAE sweeps were obtained with a lock-in amplifier (SRS SR830) and MatLab code written in house.

The CAP and DPOAE show qualitatively similar frequency specific changes due to the effects of loud sound. Low frequency exposures were found to produce either broad frequency effects or a more low-frequency only specific effect. High frequency exposures produced localized high frequency losses.

Amplitude of the EEOAE was not a good indicator of damage from low or high frequency exposures. However, the fine structure (scalloped amplitude fluctuations on the order of 10 dB over a few hundred Hz) showed a frequency specific change that correlated to

the frequency of sound stimulation.

Time delay spectrum (TDS) of the EEOAE in high frequency exposed animals showed a decrease in early portion of the long delay component (LDC). Low frequency exposures producing low-frequency threshold shifts produce minimal changes in the LDC. Low frequency exposures producing broad threshold shifts altered the LDC.

The work was supported by NIH Grant RO1 DC04194

112 Longitudinal Tracking of the Effects of Cochlear Insult on CAP, DPOAE and EEOAE

Karin Halsey¹, Kristen Haubenreich², David F. Dolan¹, **Karl Grosh²**

¹KHRI, University of Michigan, 1301 E. Ann St., Ann Arbor, Michigan, United States, ²Mechanical Engineering, University of Michigan, 3124 G.G. Brown, Ann Arbor, Michigan, United States

In this study the effect of loud sound and ototoxic drugs on the cochlear action potential (CAP), distortion product otoacoustic emission (DPOAE) and electrically evoked otoacoustic emission (EEOAE) were determined.

Pigmented guinea pigs were anesthetized (xylazine, ketamine, and acepromazine), and chronically implanted with a round window (RW) and ground electrodes (platinum iridium). After recovery, animals were exposed to noise (1/3 octave band noise, varying intensities to produce temporary (TTS) and permanent (PTS) threshold shifts, with physiology recorded prior to and at regular intervals after noise exposure or drug-induced deafening. Physiology included CAP (TDT system II/III), DPOAE (TDT system II/III, MatLab code written in house), and EEOAE sweeps (SRS 830 lock-in amplifier, MatLab code written in house). For kanamycin-ethacrynic acid deafening, animals were administered subcutaneous kanamycin (450 mg/kg), then anesthetized for intravenous administration of 50 mg/kg ethacrynic acid two hours later.

We found that the CAP and DPOAE show qualitatively similar changes due to the effects of loud sound. EEOAE also showed a frequency specific change in fine structure that was consistent across animals. When the remaining outer hair cells (OHCs) were eliminated with kanamycin and ethacrynic acid, the residual CAP and DPOAE were eliminated. EEOAE fine structure was likewise eliminated and its overall level was depressed (but not eliminated) in the animals studied at the submission of this abstract. The long delay component of the time delay spectrum (TDS) for the EEOAE was significantly reduced relative to the short delay component, indicating loss of OHCs. The residual EEOAE amplitude may indicate failure to completely eliminate all OHCs, or indicate the possibility of non-OHC mediated response to RW electrical stimulation.

We will also show data comparing these responses in animals with TTS and PTS.

The work was supported by NIH Grant RO1 DC04194

113 Comparison of behavioral and DPOAE upper frequency limits and DPOAE fine structure in normal-hearing and hearing-impaired subjects

Kathleen T Dunckley, Kelly M Deal, Elizabeth Leigh-Paffenroth, Dawn L Konrad-Martin, David J Lilly, Stephen A Fausti

NCRAR, Portland VA Medical Center, 3710 SW US Veterans Hospital Rd, Portland, OR, United States

Certain therapeutic drug treatments can damage the cochlea (ototoxicity). Ototoxicity affects the higher-frequency regions of the cochlea before affecting lower-frequency regions. A behavioral "sensitive range for ototoxicity" (SRO) has been identified near the upper-frequency limit of hearing as a time-efficient and sensitive probe for ototoxic change (Fausti et al., 1999, Fausti, et al. 2003). Behavioral testing, however, is not appropriate for many sick patients who are unable to respond reliably. Therefore, an objective measure of hearing status is an important component of an ototoxicity-monitoring program. This study is part of a VA RR&D National Center for Rehabilitative Auditory Research project to develop methods for early detection and monitoring of ototoxicity-induced hearing loss. The purpose of this study is to determine the relations between 3 measures: behavioral SRO, the highest frequency able to elicit a distortion-product otoacoustic emission (DPOAE), and the frequency regions where fine structure is present. Ten normal-hearing subjects and ten subjects with cochlear hearing loss were tested twice within a month. The behavioral SRO is the highest frequency with a threshold less than or equal to 100 dB SPL and the six lower adjacent frequencies. Behavioral hearing thresholds were measured from 0.5-20 kHz, in 1/6-octave steps within the SRO. DPOAEs were elicited in fi-octave steps at f2 from 0.7-14 kHz and in 1/48-octave-steps in the octave with the highest DPOAE response. F2/f1 was 1.22, and L1=L2 at 65 dB SPL. These data will establish how characteristics of high-frequency DPOAEs, including fine structure, relate to behavioral thresholds in normal-hearing and hearing-impaired subjects. Potential applications for monitoring DPOAE fine structure in patients receiving ototoxic medications will be discussed. (Work supported by Veteran's Affairs Medical Research 06-300).

114 Occupational exposure to styrene is associated with the damage of the cochlea

Mariola Sliwinska-Kowalska¹, Ewa Zamyslowska-Szmytko², Piotr Kotylo², Marta Fiszer², Marek Bak², Wieslaw Szymczak³

¹Department of Physical Hazards, Nofer Institute of Occupational Medicine, St. Teresa St 8, Lodz, Poland, ²Center of Audiology and Phoniatrics, Nofer Institute of Occupational Medicine, St. Teresa St 8, Lodz, Poland, ³Department of Epidemiology, Nofer Institute of Occupational Medicine, St. Teresa St 8, Lodz, Poland

It has been shown that occupational exposure to styrene is associated with increased probability of developing hearing loss (1,2). However, the site of the lesion of the auditory organ remains unknown. The function of hearing of 107 male workers from glass fiber reinforced industry exposed to styrene was assessed bilaterally by means of pure-tone audiometry (PTA), otoacoustic emis-

sion (transient-evoked otoacoustic emission – TEOAE and distortion-product otoacoustic emission – DPOAE), auditory brainstem responses (ABR) and cognitive event related potentials P-300. The results were referred to the group of 119 male workers exposed only to noise (above 85 dB-A) and 71 white-collar workers exposed neither to noise nor solvents. Age was accounted for as a confounding variable in all statistical models used in the study.

PTA showed significantly poorer hearing thresholds in styrene-exposed and noise-exposed groups as compared to controls, while TEOAE level was slightly higher in both exposed populations. Although there was no impairment in TEOAE, DPOAE showed significantly lower levels of emission at high frequencies (4, 5 and 6 kHz) in styrene-exposed as well as in noise-exposed workers, with poorer values in the latter group. The ABR results showed shorter inter-wave I-V interval in styrene-exposed group that would indicate cochlear effect of exposure and exclude any retro-cochlear damage. P-300 test results did not differ significantly between styrene-exposed and control group, denying auditory cortex deficit.

The study suggests that occupational exposure to styrene is associated with the damage of the cochlea at high frequency region. DPOAE may be considered as an important diagnostic tool that could be useful in hearing preservation programs.

1. Morata TC, Johnson AC, Nylen P, et al. Audiometric findings in workers exposed to low levels of styrene and noise. *J Occup Environ Med* 2002; 44(9): 806-814.

2. Sliwiska-Kowalska M, Zamyslowska-Szmytko E, Szymczak W, et al. Ototoxic effects of occupational exposure to styrene and co-exposure to styrene and noise. *J Occup Environ Med* 2003; 45(1): 15-24.

Acknowledgment

The study was supported by the project of the 5th EC program "NoiseChem" (Contract No QLRT-2000-00293).

115 Which specificity can be expected in OAE newborn hearing screening

Anne Mueller, Rudolf Leuwer, Regina Hagemann, Hannes Maier

ENT, University of Hamburg Medical School, Martinistr. 52, Hamburg, Germany

The recording of otoacoustic emissions (OAE) provides a quick and easy to handle tool for inner ear diagnostics in newborn hearing screening. Today most systems detect a sufficient percentage of hearing impairments. In contrast the specificity is known to be less satisfying, which determines the rate of necessary follow-up-diagnostics causing additional costs. This study was performed to evaluate the sensitivity and specificity of DPOAE and TEOAE in relation to individual hearing loss.

TEOAE and DPOAE were recorded with the A Baers/ A OAE™ Bio-logic device in mixed population of patients (n=1190, average age =26 y). Screening results at each frequency were compared against pure tone audiograms as gold-standard. The sensitivity and specificity of the OAE results was determined as a function of the decision-threshold between normal and impaired hearing from the audiograms.

Assuming a generally accepted decision threshold of >35 dB for

hearing impairment the automatic DPOAE had an acceptable sensitivity of 94.7% and a moderate specificity of 86.3%. In contrast the TEOAE showed a higher sensitivity of 99.2% but a striking poor average specificity of 52.1%. The specificity was better at low frequencies (DPOAE: 91.9%, 2kHz, TEOAE: 53.1%, 1.5kHz) than at high frequencies (DPOAE: 79.6 %, 6kHz, TEOAE: 39.8%, 4kHz). Comparison with a younger patient group (< 4y, n = 61) showed no indication for a pronounced age dependence of our result.

The good sensitivity of automatic DPOAE and TEOAE screening with the A Baers/A OAE™ demonstrates that this technique is well suited to detect hearing loss not only in infants. In contrast, its bad specificity will cause frequent additional hearing tests and increase costs. Namely for universal newborn hearing screening the high amount of false positive results needs to be improved.

116 Effects of Age and Hearing on Recognition of Time-expanded Speech

Sandra Gordon-Salant¹, Peter J. Fitzgibbons², Sarah Friedman¹

¹Hearing and Speech Sciences, University of Maryland, LeFrak Hall, College Park, MD, United States, ²Audiology and Speech, Gallaudet University, 800 Florida Ave, NE, Washington, DC, United States

These experiments measured the influence of stimulus temporal alterations on speech recognition by younger and older listeners with and without hearing loss. The hypotheses were: 1) the benefits of time expansion occur for speech spoken at a rapid rate but not for speech spoken at a normal rate; 2) selective time expansion of consonants produces greater score increments than other forms of selective time expansion; and 3) older listeners benefit significantly from time expansion of speech. Listeners were young and elderly adults with normal hearing or sensorineural hearing loss. Two syntactic forms of the SPIN sentences were presented in quiet in various speech-rate conditions: natural rate, uniform time expansion (200%), uniform time compression (50%), or selective time expansion (200%) for consonants, vowels, or pauses applied to both normal-rate and uniform time-compressed speech. Listeners showed excellent and stable performance for normal-rate speech, regardless of time expansion method. Decrements in performance were observed for uniform time compression of speech, but performance improved considerably with selective time expansion applied to the time-compressed materials. Selective time expansion of consonants appeared to produce the largest benefit. Hearing-impaired listeners performed more poorly than normal-hearing listeners in all conditions. Age-related deficits were observed primarily in the time-compressed speech conditions. The findings support the hypothesis that older listeners and listeners with hearing impairment can derive considerable advantage for selective time expansion of consonants applied to rapid speech, without a corresponding decrement when applied to normal-rate baseline speech conditions.

This research was supported by a grant from the National Institute on Aging.

117 Binaural Advantage for Speech for Younger and Older Adults with Normal Hearing

Judy R. Dubno, Amy R. Horwitz, Jayne B. Ahlstrom

Department of Otolaryngology-Head and Neck Surgery, Medical University of South Carolina, 135 Rutledge Avenue, Charleston, SC, United States

Speech recognition improves when speech and noise are separated in space, relative to conditions wherein speech and noise both emanate from the front (0° azimuth). This occurs in part because the ear away from the noise enjoys an improved signal-to-noise ratio (SNR) in the high frequencies (head shadow). With the noise at the listener's side (90°), level and time differences at the two ears enable speech and noise to be processed separately. Results of a previous study suggested an age-related difference in the use of these interaural cues. The current study measured the spatial-separation advantage attributed to binaural interactions *other than* simple head-shadow effects in younger and older adults with normal hearing. The first experiment compared benefit of spatial separation for binaural and monaural listening. In binaural listening, thresholds for HINT sentences were measured with two loudspeaker configurations: (1) sentences and HINT-shaped noise at 0° and (2) sentences at 0° and HINT-shaped noise at 90°. In monaural listening, the conditions were the same except that the ear closer to the noise in the 90° condition was plugged. With the noise source at 90°, the only difference between binaural and monaural listening was the contribution of a second ear with an unfavorable SNR. If speech recognition improved in binaural listening, the advantage of interaural difference cues provided by a second ear outweighed that ear's poorer SNR. In the second experiment, HINT sentences were at 0° while different samples of HINT-shaped noise were at +90° and -90°. In this arrangement, the SNR was equal at the two ears, but because speech and noise emanated from different locations, difference cues were available at the two ears to provide a binaural advantage. Age-related differences in binaural advantage will be assessed, along with another measure of binaural processing, the masking-level difference for tones and speech.

Supported by NIH/NIDCD

118 Contralateral Interference from Speech-Like Maskers in a Dichotic Cocktail Party Listening Task

Douglas S. Brungart, Brian D. Simpson

Human Effectiveness Directorate, Air Force Research Laboratory, 2610 Seventh Street, WPAFB, OH, United States

Recent results in our laboratory have shown that listeners who are attending to the quieter of two speech signals in one ear (the target ear) are highly susceptible to interference from normal or time-reversed speech signals presented in the unattended ear. However, speech-shaped noise signals presented in the unattended ear have little or no impact on performance in the two-talker target-ear listening task. In the current study, we further investigated the differences between speech and non-speech contralateral interferers with three signals that have parametrically adjustable speech-like properties: 1) a signal based on a cochlear implant simulation composed of up to 15 logarithmically-spaced fixed-frequency amplitude-modulated sinewaves; 2) a Shannon-speech signal com-

posed of 1,2,3, 5, 10 or 15 fixed-frequency bands of envelope-modulated noise; and 3) a so-called "sinewave speech" signal composed of up to four sinewaves tracking the first four formants of a speech signal. In each case, we first used the Coordinate Response Measure (CRM) to evaluate speech intelligibility as a function of the number of bands in the speech-like stimulus. Then we used the CRM to evaluate two-talker listening performance in the target ear while systematically varying the number of bands in the speech-like masker in the unattended ear. In all three cases, we found a systematic decrease in performance in the two-talker listening task as the number of bands in the contralateral speech-like masker increased. However, the contralateral interference caused by the speech-like masking signals was not highly correlated with their intelligibility, suggesting that intelligibility may not be a good predictor of the amount of informational masking a speech-like interferer will produce.

119 Frequency-weighting functions for temporal envelope information used to identify consonants in quiet and in noise.

Frederic Apoux, Sid P. Bacon

Speech and Hearing Science, Arizona State University, PO Box 870102, Tempe, AZ, United States

Previous studies have shown that normal-hearing (NH) listeners employ similar frequency-weighting strategies to one another in a given speech-reception task, although differences across studies suggest that those strategies may differ depending upon the listening condition. The present study was concerned primarily with frequency-weighting functions for temporal envelope information and secondarily with how those functions might change with the addition of background noise. To force listeners to use primarily temporal envelope cues, a four-channel noise-band speech processor was implemented. To create a hole in the spectrum, speech stimuli were synthesized with only 3 of the 4 bands. Six NH listeners identified consonants in consonant-vowel and vowel-consonant disyllables presented in quiet and in noise at signal-to-noise ratios leading to a 1/3 decrease in recognition scores from the quiet condition. Results indicated that the 4 bands contributed equally to consonant identification in quiet. In noise, however, listeners placed relatively more weight upon the highest frequency band, while the 3 remaining bands received a similar weight. A pilot experiment indicated that the differences between quiet and noise were not due to listeners using information in the transition bands in quiet. Overall, individual differences were very small. Thus, these data confirm that NH listeners use remarkably similar strategies to identify speech, although that strategy may vary as a function of the background. Finally, these results also show that frequency-weighting functions obtained with spectrally degraded speech diverge substantially from previously obtained weights with uncorrupted speech, suggesting that hearing-impaired listeners with severely reduced frequency selectivity could use strategies that differ from those used by NH listeners. [Work supported by NIDCD.]

120 Application of Independent Component Analysis to hearing aid to enhance the speech discrimination

Jong Ho Won¹, Sang Min Lee¹, Sung Hwa Hong², Jihwan Woo¹, Baek-Hwan Cho¹, In-Young Kim¹, Sun. I. Kim¹

¹Biomedical engineering, College of Medicine, Hanyang University, Sungdong P.O.Box 55, Seoul, 133-605, KOREA, Seoul, Korea, Republic of, ²Department of Otorhinolaryngology-Head and Neck Surgery, Sungkyunkwan University School of Medicine, 50 Irwon-dong Gangnam-gu, Seoul, KOREA 135-710, Seoul, Korea, Republic of

The goal of a hearing aid is to modify the acoustic signals to produce the best sound for hearing impaired. However, hearing aid users commonly complain of difficulty in understanding speech in the presence of background noise. If a hearing aid give a voice signal clearly in the background noise by a speech discrimination method, it would be helpful for hearing impaired. This paper describes a new method to discriminate between a speech and a noise by Independent Component Analysis (ICA). We carried out experiments using speech signal and noise signal such as babble noise, car noise and factory noise with a BTE hearing aid with dual microphone. One microphone was headed anterior direction and other posterior. The speech source signals consist of either one or two syllables that audiologist usually used for speech audiometry and noise signals were selected from the Noisex-92 database. A front speaker that delivers target speech was located in ahead of the hearing and a rear speaker that delivers noise was located behind the hearing aid. We obtained two sound signals from each microphone that were mixed a target speech with noise and then we applied ICA using MATLAB. We compared the proposed method with the spectral subtraction method to evaluate the performance. The correlation coefficients were calculated between original speech signal and discriminated signal for both methods. The result showed that the correlation coefficient of the proposed method was higher than that of spectral subtraction method. Therefore our conclusion is application of ICA to hearing aid could improve speech discrimination in the loud noise environment.

Supported by grant of the Korea Health 21 R&D Project, Ministry of Health & Welfare, Republic of Korea. (02-PJ3-PG6-Ev10-0001)

121 Audiovisual Speech: Bimodal Interaction in the Human Brainstem

Gabriella AE Musacchia¹, Mikko Sams², Trent Nicol¹, Nina Kraus¹

¹Communication Sciences, Northwestern University, 2640 N. Campus Dr, Evanston, IL, United States, ²Cognitive Technology, University of Helsinki, Finland, P.O.Box 9203, FIN-02015 HUT, Finland

Seeing lip movements while hearing speech produces an enhanced perception of the message. Conventional theories posit that subcortical structures process unimodal information and sensory-specific or supramodal cortical structures combine those representations into an audiovisual (AV) percept. In this study, event-related potentials from the human brainstem were generated

by congruent AV (acoustic and visual match), acoustic alone (AA) and conflicting AV (acoustic and visual mismatch) stimuli. Evidence for AV interaction was seen in response timing and magnitude differences across conditions. The timing of the congruent AV response to the stimulus onset (10.07ms poststimulus) was later than both the AA (8.97ms) and the conflicting AV (9.79ms) responses. Congruent AV root-mean-square amplitude over 10-30ms was smaller than AA and conflicting AV conditions. Point-to-point t-tests revealed both conflicting and congruent AV responses were different than their predicted sum of AA and visual alone stimuli. Taken together, this indicates that the sum of the unimodal acoustic and visual encoding mechanisms are different from those encoding bimodal information. In addition, we concluded that the context of the visual information affected the subcortical response. Our discovery of audiovisual interaction in the human brainstem sheds new light on neural mechanisms of bimodal integration and suggests that subcortical structures may have a role in priming the system for audiovisual speech processing.

Supported by NIH RO1DC01510

122 Contribution of bone conduction pathway to voice perception

David Basinger¹, Hannes Maier², Rudolf Leuwer², Bernd Waldmann¹

¹., Otologics LLC, 5445 Airport Blvd, Boulder, CO, United States,

²Otolaryngology, University Hospital Hamburg-Eppendorf, Martinistr. 52, Hamburg, Germany

A speaker's own voice enters his inner ear via at least two pathways: (1) via air conduction, and (2) via bone conduction through the skull. The relative contribution of bone conduction can be inferred from psychoacoustic masking experiments (Pörschmann 2000, *Acustica*). In our study, skull vibration during vocalization and during external stimulation are measured directly by laser Doppler vibrometry (LDV).

Subjects were asked to sing a single note, while sound pressure level behind the ear and the vibration of their forehead was recorded by LDV. In a second experiment, subjects were stimulated with a bone vibrator placed on the mastoid and the vibration of the forehead and upper teeth was measured. Additionally, the vibration on the bone screw was measured in BAH users. Sound and vibration were recorded for offline frequency analysis.

Vibration during vocalization. The difference between sound pressure level (dB SPL) and vibration acceleration (dB re 1g) ranges from 130-140 dB (<800 Hz) down to 105 dB (1500 Hz) and back up to 120 dB (>2000 Hz). Below 500 Hz and above 2000 Hz little variability (<10 dB) between all voices was found. In the mid frequencies 500-2000 Hz, the range is 20 dB, and female voices tend to produce 10-20 dB less vibration than male voices.

Bone vibrator stimulation. Forehead vibration was -100 to -110 dB re 1g for 0 dB HL stimulus, with little variability between subjects (< 6 dB). Vibration of upper front teeth was even higher below 1000 Hz.

Vibration levels during vocalization were converted to sensation levels, using the bone vibrator data. Resulting sensation levels of the bone conduction are 0-35 dB attenuated re to air conduction.

Conclusion. During normal listening conditions, bone conducted

signal arrives before the air conduction, so the “natural” sound of one’s own voice consists of the air conduction part, preceded by a bone conduction part attenuated by 0-35 dB.

123 LOUDNESS FUNCTIONS OF COCHLEAR IMPLANT LISTENERS: A POSSIBLE DEVELOPMENTAL INFLUENCE

Robert L Smith^{1,2}, Nicole M. Sanpetrino¹, Jozef J. Zwislocki¹

¹*Institute for Sensory Research, Syracuse University, 621 Skytop Road, Syracuse, New York, United States*, ²*Department of Bioengineering and Neuroscience, Syracuse University, Link Hall, Syracuse, New York, United States*

Studies in a number of sensory systems have revealed that sensation magnitude, including loudness, is generally related to stimulus intensity by a power law. In contrast, a variety of functions have been reported relating loudness to stimulating current in cochlear implant (CI) listeners. All show an expansive growth relative to acoustic loudness versus sound intensity, but they differ in quantitative form. CI loudness functions from different laboratories include exponentials, power laws, higher-order polynomials and combinations thereof. Furthermore, the methods used to obtain the functions generally involved constraints that may have biased their shapes, particularly related to assigning a fixed number to a maximum acceptable level (MAL).

In contrast, the present study attempts to minimize bias by using the method of absolute magnitude balance (AMB; e.g. J.J. Zwislocki, *Percept. & Psychophysics* 33, 460 [1983]) and cross modality matching (CMM). Using these methods loudness functions were obtained for subjects with Nucleus 22 and 24 devices and various bipolar electrode pairs. Subjects were first asked to match numbers to line lengths, and then vice versa, without any limitations on the numbers they used and without any explicit reference to upper or lower bounds on numbers. This provided practice for the subject and also allowed evaluation of the subject’s internal relationship between the sensory magnitude of numbers and that of line length, generally close to a linear relationship. Listeners were then instructed to match loudness of CI stimulation and numbers by using their internal, natural scale to evaluate loudness. A second analogous experiment was performed using CMM between loudness and line length. Consistent loudness functions were found using both methods.

AMB and CMM results to date suggest that different adult CI listeners can exhibit different forms of loudness function, dependent in part on their acoustic experience and development. For 4 listeners with considerable acoustic experience prior to implantation, loudness grew according to an expansive nonlinearity resembling many previous results. However, for 3 subjects with little or no useful acoustic experience prior to implantation, loudness grew approximately in direct proportion to stimulating current. These results suggest that the shape of the loudness function is molded in part by the nature and processing of auditory input prior to implantation.

124 Reaction Time to Narrowband and Broadband Noise: Loudness vs. Sensation Level

Eva Wagner^{1,2}, Mary Florentine^{1,2}, Søren Buus^{1,3}, Joe McCormack³

¹*Institute of Hearing, Speech & Language, Northeastern University, 360 Huntington Ave, Boston, MA, United States*, ²*SLPA Dept. (106A FR), Northeastern University, 360 Huntington Ave, Boston, MA, United States*, ³*ECE Dept. (440 DA), Northeastern University, 360 Huntington Ave, Boston, MA, United States*

Reaction time (RT) decreases as sound pressure level (SPL) increases. Since loudness also changes with SPL, many studies have used RT as an indirect measure of loudness. However, sensation level (SL) also increases with SPL. Therefore, it is unclear to what extent RT is governed by loudness and to what extent it is governed by SL. To separate the effects of loudness and SL, RT was measured to stimuli for which loudness and SL depend on SPL in distinctly different ways. The present study consists of two experiments employing the same six normal-hearing listeners. The stimuli were two noise bands with bandwidths of 125 Hz and 1500 Hz, geometrically centered on 1000 Hz. In Experiment 1, RTs to the noises at equal SLs were measured from near threshold to near 100 dB SPL. In Experiment 2, loudness matches between the noises were obtained over a similarly wide range of levels. Many previous studies have shown that at equal SLs the broadband noise is louder than the narrowband noise, as a result of spectral loudness summation. The size of the difference depends markedly on level, with the greatest difference at moderate levels for normal-hearing listeners. Therefore, if loudness governs RT, any difference in RT to the narrowband noise and to the broadband noise should be greatest at moderate levels. Overall, the RT difference should vary with SPL in the same way as the loudness of each of the noises. Accordingly, the amount of loudness summation derived from equal-RT contours should agree with loudness matches between the two noises. Apart from one discrepant listener, the agreement is very good; differences in RT reflect measured differences in the loudness of the two noises. The present results indicate that for most listeners, loudness rather than SL governs RT.

(Supported by NIH/NIDCD Grant No. R01 DC 02241).

125 The perception of loudness near threshold in hearing-impaired ears: recruitment or softness imperception?

Brian Moore

Dept. of Experimental Psychology, University of Cambridge, Downing Street, Cambridge, United Kingdom

Loudness recruitment occurs commonly in cases of cochlear hearing loss. It is usually characterised as an abnormally rapid growth in loudness level once the sound level exceeds the (elevated) absolute threshold. However, Buus and Florentine (2002) have suggested that recruitment is caused primarily by an abnormally large loudness at absolute threshold; above threshold, loudness is assumed to grow at a normal rate, or a rate only a little greater than normal. Thus, in an ear with recruitment, the sound is assumed to be markedly louder than normal even when it is barely audible.

This has been called “softness imperception”. To evaluate this idea, subjects were tested who had a hearing loss that varied with frequency. Loudness-matching functions were obtained between tones at two frequencies, one, *fn*, where the absolute threshold was nearly normal and one, *fl*, where there was a moderate hearing loss. Absolute thresholds were measured for each frequency using an adaptive three-alternative forced-choice task, and measurements were repeated at the start of each test session to check for changes in absolute threshold across sessions. Loudness matches were obtained between a tone at one frequency that was fixed in level and a tone at the other frequency that was variable in level. The frequency of the fixed tone could be either *fn* or *fl*. The tones were presented in regular alternation and the level of the variable tone could be adjusted using buttons on a response box. Loudness matching was possible for sensation levels (SLs) as low as 2 dB. When the fixed tone had frequency *fl* and was presented at a very low SL, it was matched by a tone at *fn* with approximately the same SL (e.g., 2 dB SL matched 2 dB SL). This relationship held for SLs up to 4-6 dB. The results imply that the tone at *fl* sounded very soft when it was at a very low SL, which is not consistent with the concept of softness imperception.

126 Loudness Reduction and its Relation to Enhancement

Deborah Ann Fantini, Christopher John Plack

Psychology, University of Essex, Wivenhoe Park, Colchester, United Kingdom

Loudness enhancement, a perceived elevation in loudness, of a standard tone may occur when the tone is preceded or followed by a more intense “inducer” tone. The opposite effect also occurs: a perceived reduction in loudness occurs when a standard tone is preceded or followed by a weaker tone [Zwicker and Sokolich (1974) P&P 16, 87-90]. The present experiments were conducted to determine whether loudness reduction operates similarly to loudness enhancement. In two experiments, the standard and inducer were 1-kHz pure tones. The standard tone was 10-ms in duration and 80 dB SPL. The inducer was 40 dB SPL and either 10 or 200 ms in duration. The loudness of the standard was measured with either a preceding, following, or flanking (preceding and following) inducer. An equal-loudness match with no inducer was also obtained to provide a control. In experiment one, the frequency of the 10-ms comparison was 1 kHz, the same as that of the standard. In experiment two, the comparison frequency was 4 kHz. Experiment one showed a 10-dB reduction in perceived loudness with either following or preceding 10-ms inducers, and twice that with flanking inducers, consistent with the idea of a long time constant over which loudness may be averaged. The amount of reduction decreased by about half with the 200-ms inducers. Consistent with loudness enhancement results, loudness reduction appeared to be greater with short-duration stimuli. Experiment two yielded a similar pattern of results with a 4-kHz comparison. Unlike previous results with loudness enhancement, the magnitude of reduction was much less than when a 1-kHz comparison was used, consistent with the loudness recalibration hypothesis of Scharf et al. [(2002) JASA 112, 807-810]. [Supported by Wellcome Trust Grant 058474.]

127 Loudness Level and Loudness as Functions of Tone Duration and Intensity

Nicole M. Sanpetrino¹, Jozef J. Zwislocki²

¹*Bioengineering and Neuroscience, Institute for Sensory Research, Syracuse University, 621 Skytop Rd, Syracuse, NY, United States,* ²*Bioengineering and Neuroscience, Institute for Sensory Research, Syracuse University, 621 Skytop Rd., Syracuse, NY, United States*

The main purpose of this study was to determine the loudness growth of a 1-kHz tone with its duration while minimizing the possible confusion by the observers between the loudness- and duration- variables. Such a confusion may easily arise when a short tone burst is compared to a tone burst of longer duration. Two experiments were performed. In the first, loudness was determined as a function of SPL referred to the detection threshold for 500-msec tone bursts with burst duration serving as a discrete parameter ranging from 20 to 500 msec. The method of cross-modality matching (CMM) between loudness and line-length was employed. In the second experiment loudness was determined by absolute magnitude estimation (AME) as a function of SL referred to the detection threshold at each duration. The two experiments were performed on two overlapping groups of 4 observers each. They had clinically normal hearing at the test frequency. Both experiments produced approximately coinciding loudness functions, independent of tone duration, when the corresponding SLs served as the independent variables. When the inferred loudness magnitudes were expressed as functions of SL referred to the longest tone duration, the loudness functions were shifted along the SL axis according to respective detection thresholds so that temporal summation appeared to have the same effect on the loudness level as on the threshold. However, because of the compression effect inherent in the loudness functions, loudness itself, as measured by line-length matching or numerical estimates, increased much less, except at very low SLs.

128 The Linearity of Temporal Summation

Christopher J. Plack¹, Andrew J. Oxenham², Vit Drga¹

¹*Department of Psychology, University of Essex, Wivenhoe Park, Colchester, United Kingdom,* ²*Research Laboratory of Electronics, Massachusetts Institute of Technology, Bldg. 36-763, Cambridge, MA, United States*

A recent model of non-simultaneous masking includes a non-linearity, representing the compressive response of the basilar membrane, followed by a *linear* leaky integrator. The present experiment used two non-overlapping forward maskers to test the linearity of the integration stage. The signal was a 4-ms, 4-kHz pure tone presented 10 ms after a 200-ms wideband noise masker (M1; bandwidth: 2800-5600 Hz), and/or 4 ms after a 6-ms narrowband noise masker (M2; bandwidth: 3400-4800 Hz). In the first stage of the experiment, the signal was presented at 40 dB SL and the level of M1 found that just masked the signal. This level was used for the remainder of the experiment. In the second stage, the masked threshold of M2 was measured in the presence of M1. In the final stage of the experiment, the level of M2 was varied between -12 dB and +12 dB of its threshold in the presence of M1. Signal thresholds were measured in the presence of M1 alone, M2 alone, and M1 and M2 combined. These three thresholds can be used to esti-

mate the compression exponent for the peripheral non-linearity. Overall, the estimated exponent was not found to vary substantially with the level of M2, suggesting that the two maskers combined in an additive way (i.e., there was little evidence of a suppressive or inhibitory interaction between the maskers). Furthermore, adding M2 to M1 produced a substantial increase in masking, even when M2 was 12 dB below its own masked threshold. This has implications for explanations of forward masking based on adaptation or neural inhibition. [Supported by EPSRC Grant GR/N07219.]

129 Detection of high-frequency spectral notches as a function of level

Ana Alves-Pinto, Enrique A. Lopez-Poveda

Institute of Neuroscience of Castilla y Leon, University of Salamanca, Avda. Alfonso X "El Sabio" s/n, Salamanca, Spain

In experiment I, the threshold depth for detecting a spectral notch centered at 8 kHz in an otherwise flat-spectrum noise was measured as a function of the noise spectrum level. Threshold depths increased gradually with spectrum level. This result is explained in terms of the broadening of cochlear filters with level and of the narrow dynamic range of most auditory nerve (AN) fibers. Experiment II investigated the extent that notch detection is affected by stimulus duration. On average, threshold depths were larger for shorter (25-ms) than for longer (220-ms) stimuli, particularly at higher sensation levels. This suggests that the adapted AN response is important for encoding spectral information, despite the fact that spectral features may be more clearly encoded at the onset, where AN fibers have a wider dynamic range. In experiment III, the steady spectral notch was replaced by a dynamic one whose center frequency changed abruptly after 110 ms from 7 to 9 kHz. Depths in this condition improved at high levels. Therefore, transient spectral information is more easily detected at high levels, which relates to the wide dynamic range of AN fibers for sudden increases in level. [Work supported by FIS PI020343, G03/203, and MCYT].

130 Monaural Intensity Discrimination Under Dichotic Conditions

Daniel E. Shub^{1,2}, H. Steven Colburn^{1,2}

¹*Speech and Hearing Bioscience and Technology, Harvard-Massachusetts Institute of Technology, 44 Cummington St., Boston, Ma, United States*, ²*Hearing Research Center, Boston University, 44 Cummington St., Boston, Ma, United States*

In this study, subjects completed a monaural intensity discrimination task at the ipsilateral ear under a variety of conditions that are defined by the "distractor" stimulus at the contralateral ear (including no stimulus). The goal is to test the hypothesis that normal-hearing listeners can access information from the two ears independently. Since all the information for the task is carried at the ipsilateral ear, a processor with access to each ear could ignore the contralateral ear. The monaural target, a narrowband noise centered at 500 Hz with a 50-Hz bandwidth and 250-ms duration, was presented in the ipsilateral ear. The interaural relations of the target and distractor (time, level and coherence, corresponding to the ITD, ILD and IC respectively) were varied across conditions. Subject performance was measured with a 4-interval (2-cue, 2-AFC) adaptive paradigm. In the most complicated condition the

IC was held fixed at unity and the ITD and the ILD were roved (1200 μ s and 30 dB respectively) on an interval-by-interval basis.

The addition of a fixed distractor did not significantly affect performance (compared to the monotonic condition). Similarly, only small effects were measured when the IC was fixed at unity and either the ITD or the ILD was roved. This lack of a measured affect of the distractor is consistent with the hypothesis that binaural loudness and laterality both carry useful information in these conditions. In conditions in which both the laterality and binaural loudness are compromised (for example due to simultaneous roving of both the ITD and ILD), the distractor severely degrades monaural intensity discrimination performance (increases in threshold from ~1 dB to over 5 dB). This change in performance, due to the presence of the distractor, is inconsistent with models of monaural intensity discrimination in which only the ipsilateral ear is considered.

[Supported by NIH grants 5-T32-DC00038-11 and R01 DC 00100].

131 Plasticity of Inferior Collicular Neurons in the Big Brown Bat

Yongkui Zhang, Nobuo Suga

Department of Biology, Washington University, One Brookings Dr., St. Louis, MO, United States

Focal electric stimulation of the auditory cortex (AC) or auditory fear conditioning evoke best frequency (BF) shifts of cortical and collicular neurons. The collicular BF shift is produced by corticofugal feedback and depends on the relationship in BF between recorded and stimulated neurons. It is, however, not yet known whether collicular neurons show BF shifts without corticofugal feedback. In our present research with the big brown bat, we stimulated neurons in the central nucleus of the inferior colliculus with short trains of electric pulses (0.2 ms long, 100 nA) and studied BF shifts of nearby collicular neurons. The BF shift-BF difference curve of collicular neurons is basically the same for collicular and cortical stimulation. The collicular BF shift evoked by collicular stimulation lasted about 1.5 hrs, although that evoked by cortical electric stimulation (or conditioning) lasts up to 3.5 hrs. The collicular BF shift evoked by collicular electric stimulation is abolished when the auditory cortex is inactivated during the stimulation. Therefore, corticofugal feedback is necessary for the plastic change of collicular neurons. There appears to be no intrinsic collicular mechanism for this plasticity based on the neural interaction between neurons in the ascending auditory system. (Supported by NIDCD DC00175)

132 Development of Reorganization of the Auditory Cortex Caused by Fear Conditioning: Effect of Atropine

Weiqing Ji, Nubuo Suga

Department of Biology, Washington University, One Brookings Dr., St. Louis, MO, United States

Reorganization of the frequency map in the central auditory system is based on shifts in the best frequencies (BFs), together with the frequency-response curves of auditory neurons. In the big brown bat, conditioning with acoustic stimulation followed by electric leg-stimulation causes BF shifts of collicular and cortical

neurons. The collicular BF shift develops quickly and is short-term, whereas the cortical BF shift develops slowly and is long-term. The acetylcholine level in the auditory cortex must be high during conditioning to develop the long-term cortical BF shift. We studied the effect of atropine (an antagonist of muscarinic acetylcholine receptors) applied to the auditory cortex on the development of the long-term cortical BF shift in the awake bat caused by a 30-min-long conditioning session. We found: (1) the cortical BF shift starts to develop ~15 min after the onset of the conditioning, gradually increases over 60 min, and reach a plateau, (2) the cortical BF shift changes from short-term to long-term ~45 min after the onset of the conditioning, (3) the cortical BF shift can plateau at different frequencies between the BF of a given neuron in the control condition and the frequency of the conditioning tone, (4) the maximum BF shift is determined ~70 min after the onset of the conditioning, and (5) acetylcholine plays an important role in the development of the cortical BF shift. Its role ends ~180 min after the onset of the conditioning. (Supported by NIDCD DC-00175).

133 Center-Surround Reorganization of Frequency Map of Auditory Cortex in Big Brown Bat

Xiaofeng Ma, Nubuo Suga

Department of Biology, Washington University, One Brookings Dr., St. Louis, MO, United States

Focal electric stimulation of the auditory cortex (AC) evokes two types of shifts of best frequencies (BFs): centripetal BF shifts (shifts toward the BF of electrically stimulated cortical neurons) and centrifugal BF shifts (shifts away from the stimulated cortical BF). Centripetal and centrifugal BF shifts respectively result in the expanded and compressed reorganization of the frequency map in the AC and subcortical auditory nuclei. In the AC of Mongolian gerbil, a large area for centripetal BF shifts evoked by focal cortical electric stimulation is surrounded by a zone for small centrifugal BF shifts. Such center-surround reorganization thus far has been found only in the Mongolian gerbil. Our present research demonstrates that center-surround organization also occurs in the AC of the big brown bat. Two different species of mammals apparently share the same mechanism for cortical reorganization. In the mustached bat, electric stimulation of cortical DSCF neurons evokes the centrifugal BF shifts in a large area of the AC and inferior colliculus. Bicuculline (an antagonist of inhibitory GABA-A receptors) applied to the stimulation site changes centrifugal BF shifts to centripetal BF shifts. That is, inhibition in the AC is responsible for evoking centrifugal BF shifts. Our present research indicates that in the big brown bat, small centrifugal BF shifts at the surround is also due to inhibition because they changed to centripetal BF shifts by bicuculline. The centrifugal BF shifts in a highly specialized AC of the mustached bat and non- or less-specialized AC of the big brown bat both are based on the same mechanism. (supported by NIDCD DC00175)

134 Role of corticofugal adjustment in experience-dependent plasticity in the inferior colliculus of the mouse

Yunfeng Zhang, Hakes J. Jacqueline, Jun Yan

Physiology and Biophysics, University of Calgary, 3330 Hospital Drive NW, Calgary, Alberta, Canada

A main feature of experience-dependent auditory plasticity is frequency specificity. However, the underlying neural mechanism remains unclear. Cholinergic basal forebrain has shown to be an important neural substrate for the experience-dependent plasticity in the auditory cortex. Since it does not carry any auditory information, neural mechanism responsible for the frequency specificity may need to be found in the central auditory system. Recent studies have demonstrated that corticofugal adjustment mediates profound frequency-specific plasticity in the central auditory system. To examine the involvement of corticofugal adjustment in experience-dependent neural plasticity in the central auditory system, we evoked plasticity in the central nucleus of the mouse inferior colliculus by electrical stimulation of the basal forebrain paired with a tone (hereafter, tone-NB pairing). We previously demonstrated that tone-NB pairing could induce systematical shift in the best frequency (BF) of cortical neurons toward the frequency of the paired tone. We show here that tone-NB pairing evoked similar plastic changes in the inferior colliculus. Tone-NB pairing did not change the collicular BFs when the collicular BFs were identical to the frequency of the paired tone. On the other hand, tone-NB pairing shifted collicular BFs toward the frequency of the paired tone. The shift in collicular BFs after tone-NB pairing was linearly correlated to the difference between collicular BFs and the frequencies of the paired tone. Compared with cortical plasticity, the shifting range of collicular BFs was smaller. Since the cholinergic projections from the basal forebrain does not innervate collicular neurons, the tone-NB pairing evoked collicular plasticity should be derived from the tone-NB pairing evoked cortical plasticity through the corticofugal projections. Our data show that cortical application of atropine, the muscarinic acetylcholine receptor antagonist completely abolished the collicular plasticity evoked by tone-NB pairing. Therefore, our findings suggest that corticofugal adjustment is an important neural mechanism for the experience-dependent neural plasticity in the central auditory system.

This study is supported by the Alberta Heritage Foundation for Medical Research and the Canadian Institutes of Health Research.

135 The role of salient behavioral cues in dynamic receptive field plasticity

Jonathan Fritz, Mounya Elhilali, Shihab Shamma

Institute for Systems Research, University of Maryland, A.V. Williams, College Park, MD, United States

How do single neurons in the auditory cortex adapt to the presence of salient cues in auditory tasks? We studied task-related dynamic cortical change while the animal was engaged in: (1) spectral tasks such as tone detection or discrimination, in (2) temporal tasks such as gap detection or tone duration discrimination, and also in (3) spectrotemporal tasks such as FM detection and FM directional

discrimination. By measuring the spectrotemporal receptive field (STRF) of single neurons in A1, we could quantitatively describe the STRF changes in shape, which resulted as the animal went from passive to active behavioral conditions. We trained five ferrets, using aversive conditioning, to detect variable tonal targets against a background of rippled noise stimuli. They quickly learned a variety of other tasks, all of which were variations on a basic task paradigm, in which the animal learned to discriminate between a set of similar reference stimuli and distinct target stimuli. Performance on each task required attention to a salient cue. We studied adaptive responses by comparing STRFs in the awake, but non-behaving ferret vs. STRFs measured while the ferret performed various auditory tasks. The STRFs were derived using standard reverse correlation techniques. Neuronal responses to the same ripple stimuli were then measured in the context of an active detection or discrimination task. We recorded single units in A1 of trained ferrets and our current data (Nature Neuroscience 2003) indicates that >60% of neuronal STRFs changed during behavior in a consistent pattern. Our working hypothesis is that these STRF changes serve to adaptively enhance task performance. For example we would predict that in the (1) spectral detection task, at the tonal target frequency, excitatory responses in the STRF would be enhanced and inhibitory responses reduced; (2) spectral discrimination task, responses would change differentially at the reference frequency compared to the target frequency; (3) temporal detection task, STRF excitatory regions would be temporally sharpened, and STRF latency would decrease; (4) spectrotemporal tasks, changes would occur along both the spectral and temporal dimensions. We shall illustrate these effects at the single-unit and population levels and critically examine these predictions.

136 Contributions of Experience and Acetylcholine to Environmental Plasticity in Auditory Cortex

Cherie R. Percaccio, Autumn L. Pruette, Shilpa T. Mistry, Eric J. Kildebeck, Ye Ting H. Chen, Michael P. Kilgard

School of Brain and Behavioral Sciences, The University of Texas at Dallas, 2601 North Floyd Road, Richardson, TX, United States

We have previously demonstrated that cortical responses of rats housed in an enriched environment are twice the amplitude of responses from standard housed rats (Percaccio et. al. ARO 2002). The current experiments were designed to investigate the contributions of exercise, social stimulation, passive sound exposure, and cholinergic modulation on the auditory evoked potential plasticity observed in the earlier study. Responses to noise bursts and tones were recorded 1-2 times a week for a period of months. To investigate the influence of acetylcholine on enrichment-induced plasticity, animals were injected with a highly specific cholinergic immunotoxin (or an inactive control), and housed in the enriched environment. Otherwise, animals were housed in environments designed to isolate particular components of enrichment. Preliminary results indicate that neither social nor exercise enrichment alone are significantly different from animals housed in a standard environment. These groups are significantly different from auditory exposure alone and animals housed in an enriched environment, which are not different from each other. Rats with cholinergic lesions are not significantly different from animals with an intact nucleus basalis regardless of environment. In all

groups, environmental plasticity was more readily observable using tones that do not completely saturate auditory cortex responses. These results indicate that acetylcholine is not necessary for environmental plasticity, and auditory exposure alone is sufficient to cause substantial experience dependent plasticity.

137 Progressive Decay of Cortical Map Reorganization Induced by Basal Forebrain Activation in Rat A1

Rafael A. Carrasco, Amanda Puckett, Pritesh K. Pandya, Alyssa McMenemy, Joanna Gibbons, Raluca Moucha, Roshini Jain, Michael P. Kilgard

School of Behavioral and Brain Sciences, University of Texas at Dallas, PO Box 830688, GR 41, Richardson, TX, United States

One of the ongoing goals of our research effort has been to determine the rules that govern remodeling of tonotopic maps in primary auditory cortex (A1) of young adult rats. It has previously been documented that massive and progressive reorganization of A1 can occur with daily episodic activation of neuromodulatory inputs paired with tonal stimuli (Kilgard & Merzenich, 1998). In previous studies, the magnitude of representational reorganization in A1 was determined twenty-four to forty-eight hours after the last conditioning session. An open question is how long these experimental manipulations on cortical representation endure. Therefore, the major goal of this study was to determine the duration and decay of cortical map reorganization after the cessation of one month of daily conditioning.

To determine the progressive decay of A1 map reorganization, a 19 kHz tone was repeatedly paired with electrical activation of the basal forebrain ~350 times a day for one month in sixteen animals. Cortical representation of tones was determined by conducting acute mapping experiments at 5, 10, or 20 days after the termination of the basal forebrain-tone pairing procedure. In addition to confirming robust map reorganization twenty-four hours after the last conditioning session, our preliminary results reveal a noticeable change in map structure over time. Specifically, it appears that cortical remodeling induced by our pairing protocol endures for at least ten days. At twenty days, we observe a restoration of the normal tonotopic map structure that more closely resembles naïve control animals. Thus, we conclude that the magnitude of representational changes caused by our conditioning protocol decrements as a function of time.

Supported in part by R03-DC04534-02 (MPK), the McDonnell Foundation, and the Callier Excellence in Education Fund

138 Auditory Learning Involving Complex Sounds Increases the Spectrotemporal Complexity of Cortical Receptive Fields

Jennifer F. Linden¹, Itzel Orduna^{2,3}, Maneesh Sahani¹, Eduardo Mercado III^{2,3}, Michael M. Merzenich¹

¹Keck Center for Integrative Neuroscience, University of California, San Francisco, 513 Parnassus Avenue, Box 0732, San Francisco, California, United States, ²Center for Molecular and Behavioral Neuroscience, Rutgers University, 197 University Avenue, Newark, New Jersey, United States, ³Psychology, University at Buffalo, SUNY, 350 Park Hall, Buffalo, New York, United States

To examine how primary auditory cortex is affected by learning involving complex sounds, we trained rats and mice to discriminate sequences of frequency sweeps, and then analyzed spectrotemporal receptive fields (STRFs) in both naive and trained animals. Extracellular recordings were obtained in anesthetized animals during presentations of the spectrally rich, temporally dynamic random chord stimuli used for reverse-correlation, and also during presentations of the spectrotemporally complex stimuli used for behavioral training. STRFs were then derived from responses to the dynamic random chord stimuli, and used to predict neuronal responses to the behavioral training stimuli. We found that STRFs from trained animals were more spectrotemporally inseparable than STRFs from naive animals; that is, STRFs from trained animals revealed greater interaction between spectral and temporal response properties. Moreover, STRFs from trained animals predicted neuronal responses to the behavioral training stimuli more accurately than did STRFs from naive animals. These results suggest that auditory learning involving complex sounds increases the spectrotemporal complexity of receptive fields in primary auditory cortex, so as to facilitate the processing of behaviorally relevant acoustic features. Supported by NIH DC00399, UCSF REAC Grant, NIH NS10414, NSF PECASE Grant, and NSF Doctoral Dissertation Grant.

139 Nitric Oxide-containing Neurons within the Cortex and Amygdala in the Brain of the Mustached Bat, *Pteronotus parnellii*.

Palle D. Prasada Rao, Jagmeet S. Kanwal

Physiology and Biophysics, Georgetown University, 3900 Reservoir Rd, NW, Washington, D.C., United States

In mustached bats, a highly vocal species, social communication calls can mediate short-term changes within cortical neurons as well as the animal's physiology and behavior. Nitric oxide (NO) mediates response potentiation in the auditory cortex and is well suited to process dynamic stimuli such as complex sounds. As a first step towards establishing the role of NO in call processing, we examined the distribution of the enzymes, neuronal nitric oxide synthase (NOS) and nicotinamide adenine dinucleotide phosphate-diaphorase (NADPHd), as markers of NO in the brain of mustached bats. Both procedures (immunocytochemical for NOS and histochemical for NADPHd) established the presence of NO within neurons in the auditory, frontal and cingulate cortex and amygdala. The auditory cortex exhibited a dense network of fibers. In layers I and II NO neurons were small ($12.4 \pm 1.6 \mu\text{m}$). All

labeled neurons were of the nonpyramidal and multipolar type. In layers V and VI, NO neurons were large ($24.9 \pm 4.6 \mu\text{m}$ in diameter) with relatively long dendrites ($142.3 \pm 38.8 \mu\text{m}$). In the frontal cortex, many small neurons were labeled in layer I and large neurons with long dendrites ($98.9 \pm 36.1 \mu\text{m}$) were generally present in deeper layers. The fiber network in the frontal cortex was less dense than that in the auditory cortex. The lateral nucleus of the amygdala showed many large neurons; also a moderate fiber network was present throughout the amygdala. Since oxytocin (OT) is known to play an important role in social vocal behaviors, we also performed a double-label (immunocytochemical for OT and histochemical for NOS) procedure. This revealed the presence of process-soma contacts between many NADPHd- and OT-containing neurons. On the basis of these data, we propose that NO neurons may play an important role in auditory and possibly call processing both independently and in concert with OT neurons.

Supported by NIH/NIDCD research grant DC02054 to J.K.

140 Effects of continuous low-level stimulation after an acoustic trauma upon ABR thresholds and cortical tonotopic maps.

Arnaud Jean Norena^{1,2}, Jos Jan Eggermont³

¹Neurosciences, University of Calgary, 2500, University Drive, NW, Calgary, Alberta, Canada, ²Neurosciences, CNRS, 50 Avenue Tony Garnier, Lyon, France, ³Neurosciences, University of Calgary, 2500, University Dr, NW, Calgary, Alberta, Canada

It is well known that cochlear damages are followed by dramatic central changes – i.e. tonotopic reorganization. Namely, neurons with a characteristic frequency (CF) within the hearing loss region become sensitive to the frequency band adjacent to the hearing loss. A decrease in the afferent inputs due to the hearing loss has been hypothesized to cause this reorganization. If this statement is correct, it is then theoretically possible to prevent such reorganization in compensating the decrease in the afferent inputs. This topic may be of clinical interest in preventing the potential detrimental effect of central reorganization on perception (tinnitus...). The present study addressed this issue. In order to induce a hearing loss, cats were exposed for 4 hours to a narrow band of noise (centered at 5 kHz) at about 120 dB SPL. Thereafter, cats were immediately stimulated with a high-pass filtered multi-tone stimulus and over a period of few weeks – until the cats were used for multi-unit activity recordings in primary auditory cortex. Surprisingly, the findings suggest that the stimulation limits the occurrence of a hearing loss (measured by ABRs) to the frequency region between the trauma frequency and one octave above the trauma frequency. In addition, we did not observe any tonotopic reorganization.

141 Neural modeling of the spectral processing pathway from dorsal cochlear nucleus to inferior colliculus

Zhi Lu, Jeremiah Kimball, Oleg Lomakin, Kevin A Davis
Biomedical Engineering, University of Rochester, 601 Elmwood Ave., Box 603, Rochester, NY, United States

The filtering properties of the cat's pinna add prominent spectral notches to free-field sounds that are a principal cue to the localization of sound source elevation. Physiological and behavioral evidence suggests that the dorsal cochlear nucleus (DCN) initiates a

functional pathway that is specialized to process this directional feature. Type O units in the central nucleus of the inferior colliculus (ICC) are a primary target of ascending DCN projections and thus may represent a mid brain specialization for the processing of spectral cues for sound localization. When tested with a notched noise stimulus whose center frequency is changed each trial to move across the receptive field of the unit, DCN type IV units show a tuned inhibition for a notch centered at their best frequency (BF). In contrast, type O units show a tuned excitation for a spectral notch whose rising edge is located just below BF. These differences suggest that interactions within the ICC alter the spectral integration properties of type O units. To elucidate the response properties of these unknown inputs, a simple computational model of type O units was created that included three input populations: type IV units (as modeled by Hancock and Voigt 1999); excitatory; and inhibitory units. Simulations were carried out for a range of model configurations (e.g. with or without local excitatory inputs) and non-DCN unit sensitivities to narrow and wideband stimuli, and results were in terms of model type O unit rate versus center frequency curves for notched noise. The results suggest that the spectral integration properties of type O units can be accounted for qualitatively by a model in which DCN influences are transformed in the ICC by a convergence of wideband excitatory and frequency-tuned inhibitory inputs. Supported by NIDCD grant R01 DC 05161-03.

142 Comparison of Temporal Features in Responses to Broadband Noise in Auditory Nerve and Binaural Cells in the Inferior Colliculus

Philip X Joris, Bram Van de Sande, Dries H Louage, Marcel van der Heijden

Lab. of Auditory Neurophysiology, K.U.Leuven, Campus GHB O&N, B-3000 Leuven, Belgium

Low-frequency cells in the inferior colliculus (IC) show sensitivity to interaural time differences (ITDs) of broadband noise. This sensitivity can be studied by measuring the noise-delay function, i.e. the dependence of spike rate on ITD, which typically has a damped oscillatory shape. Several features of this shape are well-predicted by the so-called composite curve, which is generated by linear addition of responses to tonal binaural beats (Yin et al., *J. Neurophysiol.*, 1986). The feature of interest here is the degree of damping, which tends to be stronger in composite curves. This was hypothesized by Yin et al. to be a manifestation of the cochlear mechanism that also causes two-tone suppression.

To test this hypothesis we recorded cat auditory nerve responses to broadband noise and to iso-level tones. The tones were presented sequentially and linearly spaced in frequency so as to bracket the response area of the fiber. From the tonal responses we constructed shuffled autocorrelograms (Joris, *J. Neurosci.*, 2003), which we added for all frequencies to obtain a monaural composite curve. This curve was compared with the shuffled autocorrelogram of the responses to broadband noise.

Without exception, composite curves were more damped than autocorrelograms to broadband noise of the same nerve fiber. We surmise that the main reason for this difference is the limited dynamic range of tonal phase-locking, rather than two-tone sup-

pression.

Although the average trend is thus in the same direction for auditory nerve and IC, i.e. more damping to tones than to noise, the relationship between the two sets of responses is much more variable in the IC than in the nerve. A mechanism that differentially affects damping to tones and noise must therefore exist between the level of the nerve and the IC.

Supported by the Fund for Scientific Research - Flanders (G.0083.02) and Research Fund K.U.Leuven (OT/10/42). MvdH was supported by a K.U.Leuven fellowship (F/00/92).

143 The effect of binaural stimulation on frequency resolution in the rat inferior colliculus (IC) determined by sound-induced Fos protein expression.

Yue Yang, Richard L Saint Marie, Douglas L Oliver

Neuroscience, University of Connecticut Health Center, 263 Farmington Avenue, Farmington, CT, United States

Separate groups of neurons activated by different sound stimuli may provide a substrate for parallel processing of acoustic information. Consequently, two widely separated tones activate two separate groups of neurons, while two closely located tones may activate the same group of neurons within the tonotopic organization of the auditory system. However, it is not known whether binaural stimulation facilitates the separation of neurons processing different frequencies of sound. In this study, we compared the responses of neurons in the IC to monaural and binaural tones. Sinusoidally amplitude-modulated (SAM) tones (14Hz modulation) with their carrier frequencies (between 8 and 22.6KHz) separated at 0.25, 0.5 or 1 octave were alternately presented (1.0 s every 1.3 s) in the free field for 2 hr to both unilaterally tympanectomized and normal bilaterally hearing rats. Animals were unanesthetized during sound exposure and previously sound isolated. The sound source was directly above the animal's head. Sound levels were 30 dB, 40 dB, or as high as 80 dB SPL. Immunocytochemical localization of Fos was used to measure neuronal activity. When two stimuli were separated by 1 or 0.5 octave apart, two distinct bands of immunoreactive neurons were detected in the central nucleus of IC in both monaural and binaural hearing animals. When the stimuli were 0.25 octave apart, frequency histograms of immunoreactive neurons merged into a single band with two peaks separated by 65µm. In paired monaural/binaural cases, binaural stimulation produced band peaks 50-170% higher than monaural stimulation, but bandwidths only 18-40% wider than comparable monaural stimulation. These data demonstrate the facilitatory effects of binaural stimulation on neuronal responses in the IC. At the same time, they suggest that binaural stimulation does not improve frequency resolution based on the activation of separate neural populations.

Supported by NIH grant DC00189

144 The Time Dependence of Binaural Interaction in the Rat's Central Nucleus of the Inferior Colliculus

Huiming Zhang, Jack B. Kelly

Psychology Department, Carleton University, 1125 Colonel By Drive, Ottawa, Ontario, Canada

Neural responses to dichotic tone bursts in the central nucleus of the inferior colliculus (ICC) are strongly affected by interaural level differences. In the rat, most contralaterally excited ICC neurons are inhibited by ipsilateral stimulation and reduce their firing rate as the ipsilateral sound pressure level is increased. Other neurons show binaural facilitation or complex patterns of binaural interaction. In the present study, we examined whether the pattern (i.e., inhibitory or excitatory) and/or the extent of binaural interaction in the rat's ICC were the same or different during early and late parts of the response to a 100 ms dichotic tone burst. Typically we compared the responses during and after the first 20 ms of the tone burst. Although most neurons had similar binaural interaction patterns for the early and late parts of the response, many neurons showed differences in the extent of interaction. Some neurons showed binaural inhibition or facilitation during only one part of the response (i.e., early or late, but not both). Also, in some cases, binaural inhibition was found during one part of the response, but binaural facilitation during the other. Our results suggest that binaural interaction in the ICC can depend on the time course of a binaural level stimulus. The time-dependence of binaural interaction in the ICC may have implications for the representation of sound location when interaural level differences are used as cues.

Research supported by NSERC of Canada.

145 Auditory pathways in a subject with callosal agenesis: A whole-scalp neuromagnetic study

Ken-ichi Kaneko^{1,2}, Maryse Lassonde³, Franco Lepore³, Riitta Hari²

¹*Department of Otolaryngology, Fukui Red Cross Hospital, 2-4-1Tsukimi, Fukui, Japan,* ²*Low Temperature Laboratory, Helsinki University of Technology, Otakaari3A, Espoo, Finland,*

³*Department of Psychology, University of Montreal, 90 ave. Vincent-d'Indy, Montreal, Quebec, Canada*

The auditory cortices of both hemispheres receive input from both ears. However, it is not clear whether the ipsilateral input reaches the human auditory cortex directly via direct pathways or whether the ipsilateral auditory responses are transmitted via corpus callosum from the contralateral hemisphere. To address this question we examined whole-scalp magnetoencephalographic (MEG) cortical responses of a subject with callosal agenesis and total lack of anterior commissure. Monaural 1-kHz tones, amplitude-modulated at 39.1 Hz and 41.1 Hz, elicited steady-state fields (SSFs) in both hemispheres, thereby indicating existence of ipsilateral pathways to the auditory cortex. Frequency-tagging of MEG signals was used to investigate binaural interaction by amplitude-modulating binaurally presented continuous 1-kHz tones at 39.1 Hz in the right ear and at 41.1 Hz in the left. Similarly as in the control group of 18 subjects, the acallosal subject showed in both hemispheres smaller responses to binaural than monaural stimulation, and

stronger suppression of responses to ipsilateral than contralateral input during binaural stimulation. The long-latency responses to monaural left-ear 50-ms tones peaked at 105 ms in the right and at 111 ms in the left hemisphere, and to monaural right-ear tones 102 ms in the right and 108 ms in the left hemisphere, with similar patterns to left-ear and right-ear stimuli. These findings suggest that the binaural interaction reflected at the level of the auditory cortices does not require callosal connections.

146 Signal detection in the auditory midbrain: Neural correlates and mechanisms of spatial release from masking

Courtney C. Lane^{1,2}, Bertrand Delgutte^{1,2}, H. Steven Colburn³

¹*Eaton-Peabody Lab., MEEI, 243 Charles St, Boston, MA, United States,* ²*Speech and Hearing Bioscience and Technology, MIT/Harvard, 243 Charles St, Boston, MA, United States,* ³*Hearing Research Center, Boston University, 44 Cummington Street, Boston, MA, United States*

Spatial release from masking (SRM) is the improvement in detection obtained when a signal is separated in space from a masker. Previous studies suggest that, at low frequencies, listeners use interaural time differences (ITDs) to improve signal detection when signals and maskers are spatially separated in azimuth. To determine how individual neurons respond to spatially separated signals and maskers, we recorded from low-frequency, ITD-sensitive neurons in the inferior colliculus (IC) of anesthetized cats and developed a computational model of the neuron responses.

The stimulus was a 40-Hz broadband chirp train in continuous broadband noise; stimulus azimuth was simulated using head-related transfer functions. For several signal and noise azimuths, we measured the individual unit responses and thresholds, defined as the signal-to-noise ratio (SNR) for which the signal can be detected for 75% of the stimulus presentations. We also developed a computational model of the neuron responses, which incorporated both interaural cross-correlation and amplitude-modulation sensitivity. The sensitivity to amplitude modulation was required to predict large discharge rate differences in response to the signal compared to the noise.

To relate these neurophysiological and modeling results to human behavioral thresholds, we defined population thresholds based on the most sensitive neurons in the population. The neural population thresholds were similar to human behavioral thresholds in both magnitude and dependence on signal and masker azimuth, indicating that low-frequency, ITD-sensitive neurons in the IC may play a role in low-frequency spatial release from masking in humans. Both interaural correlation and modulation sensitivity were required for the model population thresholds to predict human behavioral thresholds. The need for modulation sensitivity to predict both individual neuron responses and human behavioral thresholds suggests that binaural and temporal processing are interacting in binaural signal detection. This interaction is significant because most natural sounds, including speech, have pronounced envelope fluctuations that previous models of binaural detection have not utilized.

Supported by NIH grants DC02258, DC00119 and DC00038.

147 Auditory Cortex Lesions Affect Spatial Release From Masking

Henry E. Heffner¹, Ian A. Harrington²

¹Psychology, University of Toledo, 2801 W. Bancroft, Toledo, OH, United States, ²Kresge Hearing Research Institute, University of Michigan, 1301 E. Ann St., Ann Arbor, MI, United States

The obvious advantage of being able to determine the location of sound in space is that it enables an animal to locate sound-making objects. However, another advantage is that it helps to detect a signal in a noisy environment when the signal is spatially separate from the masking noise, a phenomenon referred to as “spatial release from masking.” Because ablation of auditory cortex in primates abolishes the ability to localize sound, it seems reasonable that it would also reduce, if not eliminate, the improvement in detectability that normally occurs when a signal is moved away from a masking sound.

Six Japanese macaques (*Macaca fuscata*) were used in this experiment. Two of the animals were normal, two had lesions of the left superior temporal gyrus, and two had lesions of the right superior temporal gyrus. Prior testing had demonstrated that the operated animals were unable to localize sound throughout the contralesional hemifield (beyond about 15-20° of midline); their localization ability in the ipsilesional field, on the other hand, was normal.

The monkeys were tested for their ability to detect a 1-kHz tone with and without the presence of a narrow band noise masker (0.5 - 2 kHz) in a free-field situation. The animals were tested separately in the left and right hemifields with the masker located 30° from midline and the signal located either 30° or 90° from midline. The masking level difference was calculated as the difference in the amount of masking for the signal located at 30° vs 90° from midline.

The masking level difference for the normal monkeys did not differ between the two hemifields. However, the monkeys with unilateral lesions showed a consistent and substantial difference between hemifields, with little or no release from masking in the contralesional hemifield when the signal was moved away from the masker. These results suggest that the cortical mechanism for sound localization is also involved in spatial release from masking.

148 Evaluation of a Limited-Channel Model for Spatial Coding in Auditory Cortex

G. Christopher Stecker, Ian A. Harrington, Ewan A. Macpherson, John C. Middlebrooks

Kresge Hearing Research Institute, University of Michigan, 1301 East Ann St, Ann Arbor, MI, United States

The majority of neurons in the auditory cortex exhibit broad spatial tuning and respond best to sound sources in the contralateral hemifield. For most neurons, the point of maximum response corresponds to locations near the acoustic axis of the contralateral pinna or to other locations producing large interaural differences. Relatively few neurons exhibit sharp spatial tuning or maximum responses for near-midline azimuths, despite the fact that spatial acuity is highest in that region. These observations (which appear to hold throughout the auditory cortex) are troubling for models of spatial representation in the auditory cortex that employ either local “labeled lines” or coarse population codes with quasi-uni-

form spatial sampling; in both cases, distributions of preferred location are expected to sample space evenly or perhaps with higher density in high-acuity regions. Here, we examine an alternative model in which space is coded by the joint activity of a small number (e.g., two) of spatial “channels” (McAlpine et al., 2001, Nat. Neurosci. 4:396). In this model, the responses of most neurons are expected to favor either contralateral or ipsilateral locations, and to change abruptly across the interaural midline. The model fits well with general observations of spatial tuning in the cortex, and with the processing of interaural cues by neurons in the superior olivary complex, inferior colliculus, and cortex. Our current results argue in favor of the limited-channel model. For the majority of neurons recorded in cortical fields A1, PAF, and DZ of the anesthetized cat, spatial tuning is sharpest across the midline regardless of preferred location. Moreover, spatial information encoded in neural spike patterns provides for best discrimination across the midline. In fact, we found a significant number of cortical neurons capable of discriminating across-midline azimuth differences of 20° or less, despite apparently broad tuning when assessed through more traditional means. [Supported by NIDCD and NSF-DBI]

149 Behavioral Dissociation of “What” and “Where” Processing in Non-Primary Auditory Cortex of the Cat

Stephen G. Lomber, Shveta Malhotra

School of Behavioral and Brain Sciences, The University of Texas at Dallas, 2601 N. Floyd Road, GR41, Richardson, Texas, United States

In non-primary auditory cortex, anatomical and electrophysiological investigations suggest the existence of “what” and “where” processing systems similar to those described in extrastriate visual cortex of humans, monkeys, and cats. In this study, we examined the possible dissociation of these functions in the behaving cat. We specifically sought to test the hypothesis that the anterior auditory field (AAF) is critical for auditory pattern processing and that the posterior auditory field (PAF) is essential for auditory spatial localization. Three cats were trained to perform three tasks: 1) An auditory pattern discrimination. The animals were required to learn and discriminate temporally-matched Morse code-type pattern sequences. 2) An auditory spatial localization task. The animals had to localize a 100 msec broad-band stimulus (20dB SPL above background), presented at 15 deg intervals, in a standard orienting arena. 3) An auditory detection task that required the animals to indicate the presence or absence of a broad-band noise burst. Following training, each cat was bilaterally implanted with cryoloops placed over both AAF and PAF cortices that permitted the localized and reversible deactivation of each cortical locus. This experimental design permitted double dissociations to be performed within the same animal. Bilateral deactivation of AAF cortex resulted in deficits on the temporal pattern discrimination task and did not alter performance on the spatial localization task. Bilateral deactivation of PAF cortex resulted in deficits on the spatial localization task and did not alter performance on the temporal pattern discrimination task. Deactivation of neither AAF, nor PAF, cortices resulted in deficits on the detection task. Therefore, we were able to doubly dissociate “what” and “where” processing regions and provide the first behavioral demonstration of the exist-

tence of these separate processing systems in non-primary auditory cortex. Sponsored by NIDCD.

150 MEG Responses to Huggins Pitch - Time Course and Hemispheric Differences

Maria Chait¹, Jonathan Z. Simon², David Poeppel³

¹Neuroscience and Cognitive Science Program, University of Maryland, 1401 Marie Mount Hall, College Park, MD, United States, ²Departments of Biology and Electrical and Computer Engineering, University of Maryland, 2209 AV Williams Building, College Park, MD, United States, ³Departments of Biology and Linguistics, University of Maryland, 1401 Marie Mount Hall, College Park, MD, United States

Huggins dichotic pitch (HP) is generated by presenting a random noise signal to one ear, and the same noise with a phase shift over a narrow frequency band to the other ear. The percept is that of a faint tonal object (corresponding to the center frequency of the phase-shifted band) embedded in noise. Here we compare the cortical auditory evoked responses to HP with those of tones embedded in noise. These perceptually similar but physically very different stimuli are interesting tools for the study of pitch processing in auditory cortex.

The signals were 1500 ms long, consisting of 1000 ms interaurally correlated white noise followed by either HP (with a center frequency of 200, 400, 600 or 1000 Hz) or a tone of those frequencies embedded in matched noise (TN). All stimuli had similar power spectral densities and matched perceived tone loudness.

Auditory cortical responses were recorded using a 160 channel whole head MEG system (KIT, Kanazawa, Japan) while subjects (N=20) were performing a tone detection task. Waveform analysis reveals that all participants had comparable response trajectories. In particular, each participant showed a clear onset response at ~150ms post HP/TN onset (modulated by perceived tone and lateralized to the left) with a characteristic M100 spatial distribution. These response properties are similar for both HP and TN stimuli but are significantly earlier (~30 ms difference in peak latency) for HP trials. In a follow-up experiment the stimuli were altered so that the initial 1000 ms were replaced by an

interaurally uncorrelated white noise. This modification resulted in a reversal of relative peak latency such that TN stimuli elicited a response ~30 ms earlier than the HP stimuli. These data speak to brainstem models of binaural interaction and indicate that the difference may originate in activity patterns as early as the MSO. The significance of these findings to models of cortical expansion of latency disparities is discussed.

151 Bias in the measurement of frequency response curves

Nachum Ulanovsky^{1,2}, Liora Las^{1,2}, Israel Nelken^{1,2}

¹Physiology, Hebrew University, Hadassah Medical School, Jerusalem, Israel, ²Interdisciplinary Center for Neural Computation, Hebrew University, Givat-Ram, Jerusalem, Israel

Several functional roles have been suggested for neuronal adaptation, including gain control, change detection and optimization of information transmission. We have previously shown that neurons in primary auditory cortex (A1) respond more strongly to a sound when it appears rarely in a sequence than to the same sound when

common, as a result of stimulus-specific adaptation - suggesting a role for adaptation in novelty detection. Here we propose a new role for adaptation: the tagging of eccentric stimuli.

Adaptation can alter neuronal tuning curves, but it is widely assumed that adaptation-induced bias is minimized when stimuli are randomized, equi-probable and have the same amplitude. We therefore checked the effect of adaptation on measurement of tuning curves. We recorded activity of neurons in A1 of halothane-anesthetized cats, in response to randomly presented tones with 10 repetitions of 20 frequencies, covering a range of 1 octave.

We found that adaptation was stronger for frequencies at the center of the frequency range, than for eccentric frequencies at the edges. This occurred since the trials that preceded 'central' frequencies had a smaller parametric difference from those frequencies (average difference of 1/4 octave) than the trials that preceded eccentric frequencies (average difference of 1/2 octave). Since adaptation is stronger for similar consecutive stimuli, this resulted in stronger adaptation to 'central' frequencies, and in enhanced responses to eccentric stimuli.

This finding has both methodological and theoretical consequences. Methodologically, measuring response curves using unbiased stimuli (randomized and equi-probable), nevertheless results in a bias in the shape of the response curves, with selective suppression at 'central' stimuli. Theoretically, the enhancement of responses to eccentric stimuli may facilitate the detection of stimuli that differ parametrically from all other stimuli in a soundscape - which may be important behaviorally.

152 Pressure vs. decibel modulation in spectrotemporal representations: How nonlinear are auditory cortical stimuli?

David Klein¹, Didier Depireux², Jonathan Simon¹, Shihab Shamma¹

¹Institute for Systems Research, University of Maryland, A.V. Williams, College Park, MD, United States, ²Anatomy and Neurobiology, University of Maryland, 685 W. Baltimore Str, Baltimore, MD, United States

Used to characterize the responses of central auditory neurons, the spectrotemporal receptive field (STRF) is the best linear approximation to the stimulus-response relationship, where the stimulus is a spectrotemporal representation of the acoustic waveform, i.e. the temporal modulation of stimulus amplitude in an array of discrete frequency bands. Several studies have examined the sufficiency of the STRF description - the degree to which this stimulus-response relationship is linear - in various species and auditory loci. Comparisons between these studies, especially in quantification of the linearity, are impeded by different definitions of stimulus amplitude. Sound pressure level, intensity (pressure squared) and their logarithms (decibels or dB) have been used in different studies, each nonlinearly related to the other. In order to study how these choices affect the apparent linearity of the responses of single neurons in primary auditory cortex (A1), we recorded responses to two different sets of dynamic broadband stimuli suitable for measuring the STRF by reverse correlation. In their respective spectrotemporal representations, the two sets look identical; however, one representation specifies linear pressure modulation, while the other specifies dB modulation. We find that while

the STRF measurements are very similar between the two conditions, the sufficiency of the STRF description is starkly different; the responses are much more nonlinear with respect to dB modulation. Additionally, the strength of the nonlinearity depends on the structure of the STRF and the stimulus. We find that the nonlinearity is consistent with an (expansive) exponentiation of the stimulus representation, required to transform dB back into pressure. We discuss the implications of these results for investigating various neural nonlinearities with these and other commonly used stimuli, in cortex and in other auditory loci.

153 Spectro-Temporal Feature Selectivity, Mutual Information, and Spiking Reliability

Monty Armando Escabi^{1,2}, Reza Nassiri², Heather L. Read³

¹*Electrical Engineering, University of Connecticut, 371 Fairfield Rd, Storrs, CT, United States*, ²*Biomedical Engineering, University of Connecticut, 371 Fairfield Rd, Storrs, CT, United States*, ³*Psychology, University of Connecticut, Bousfield Psychology Building, Storrs, CT, United States*

Sensory coding of sound patterns in environmental stimuli relies on a precise representation of spectro-temporal features of the sound waveform. Do auditory neurons “linearly encode” such spectro-temporal information or are they better suited for “detecting” spectro-temporal features in complex sounds. We examine this issue by studying the fidelity of the encoding on a single spike-feature basis. Neuronal recordings from the central nucleus of the inferior colliculus of cats shows that a subset of neurons reliably signal the occurrence of a highly stereotyped spectro-temporal stimulus feature. By comparison, other neurons respond to a wide assortment of stimulus patterns. Information theoretic analysis reveals a direct relationship between information per spike and the measured feature selectivity. In contrast, a tradeoff is shown between the encoded information per spike (or feature selectivity) and the response spike rate. Neurons with the highest encoding reliability respond with exceptionally low spike rates (down to 0.05 spikes/sec), but do so with great fidelity. At the opposite extreme neurons can exhibit substantially high spike rates (up to ~ 100 Hz) but with low reliability. The results suggest that stimulus-specificity can be classified along a continuum from low spectrotemporal specificity, as for linear filtering, to high selectivity expressed by a precise stimulus-response relationship and sparse spiking. These neural subpopulations, exhibiting a tradeoff in stimulus-response specificity and response throughput, may serve complementary roles in the coding of complex environmental stimuli.

154 Responses of Local Neural Populations in the Inferior Colliculus

Chandran Seshagiri¹, Bertrand Delgutte²

¹*Speech and Hearing Biosciences and Technology, Harvard-MIT Division of Health, Sciences, and Technology, 243 Charles St., Boston, MA, United States*, ²*Eaton-Peabody Laboratory, Massachusetts Eye and Ear Infirmary, 243 Charles St., Boston, MA, United States*

The cellular anatomy of the central nucleus of the inferior colliculus (ICC) reveals a laminar organization of cells and incoming fibers. Physiological investigation shows that individual cells

within a lamina exhibit similar characteristic frequencies. Anatomical studies suggest that local regions within a lamina may receive similar inputs from auditory brainstem nuclei and create a functional group. This organization suggests that local groups of cells may exhibit similar response characteristics.

To study the individual responses of local groups of cells, we recorded multiple units in the inferior colliculus of anesthetized cats using ‘tetrodes.’ Tetrodes sample the extracellular space in four spatially distinct locations and allow us to reconstruct the single-unit contributions from the multi-unit recording. While the spatial arrangement of the tetrode improves classification of spike waveforms by unit, the cross-channel correlation in the noise can also be exploited to improve detection of neural events. Using tetrodes and our detection and classification strategies, we have been able to reconstruct single-unit spike trains for up to five units from a single recording location.

In response to pure tones, units of a local cluster exhibit similar best frequencies as expected. Also, we find that of approximately twenty six simultaneously recorded pairs, all pairs exhibit a threshold within 10dB of each other, and approximately two-thirds of the pairs have thresholds within 5dB. However, we observe differences in temporal discharge patterns to pure tones and broadband noise. Also, we have looked for temporal correlation between the discharge patterns of simultaneously recorded pairs of units, and we find that neighboring ICC units show no significant correlation in response to pure tones, although stimulus-induced correlation has been seen when the tone is embedded in broadband noise.

Supported by NIH Grants DC02258 and DC00038.

155 Neural Correlates of Auditory Stream Segregation in Humans Using fMRI

E. Courtenay Wilson¹, Jennifer Melcher², Christophe Micheyl³, Andrew Oxenham³

¹*Speech and Hearing Bioscience and Technology, MIT, 77 Massachusetts Ave, 36-713, Cambridge, MA, United States*,

²*Eaton-Peabody Laboratory, Massachusetts Eye and Ear Infirmary, 243 Charles Street, Boston, MA, United States*,

³*Research Laboratory of Electronics, MIT, 77 Massachusetts Ave, 36-713, Cambridge, MA, United States*

The aim of this study was to look for neural correlates of auditory stream segregation in humans using blood oxygenation level dependent (BOLD) functional magnetic resonance imaging (fMRI). Previous research has demonstrated differences in temporal fMRI activation patterns in auditory cortex that depend on stimulus presentation rate. Specifically, neural response patterns change from a phasic response to the onset and offset of a sequence at fast rates, to a sustained response throughout the sequence at slow rates. We hypothesized that these differences may depend on the perceptual organization of the elements within the sequence. For instance, when a sequence elicits the perception of two streams, the perceived rate of each stream is half the global physical rate. The stimuli consisted of alternating-frequency 100-ms tone bursts (ABAB) presented over a duration of 32 s. The A and B tones were either identical or were separated in frequency by 20 semitones. These frequency differences were selected based on the results of preliminary psychophysical tests, which we performed to ensure that they would elicit clear “one stream” and

“two stream” percepts, respectively. The BOLD fMRI neural activity patterns in response to these stimuli were analyzed using a general linear model and physiological basis functions that capture key features of the temporal response pattern. Preliminary results showed that the neural response pattern changed from a more phasic onset and offset response to a more sustained response as frequency difference increased from 0 to 20 semitones. These results are consistent with the hypothesis that temporal neural response patterns in the auditory cortex may depend not on the physical stimulus repetition rate, but on the perceived repetition rate, following auditory streaming. [Supported by Hertz Foundation Fellowship, NIDCD grant R01 DC 05216, Tinnitus Research Consortium #00-03-030]

156 Discrimination of tones in noise by rats

Lung-Hao Tai^{1,2}, Marta Moita¹, Anthony Zador¹

¹Zador Lab, Cold Spring Harbor laboratory, 1 Bungtown Road, Cold Spring Harbor, New York, United States, ²Neurobiology and Behavior, State University of New York, Stony Brook, SUNY at Stony Brook, Stony Brook, New York, United States

How do animals discriminate tones in background noise? As a first step to probing the cortical mechanisms whereby animals make decisions based on auditory stimuli, we trained Long-Evans rats to discriminate pure tones imbedded in a white noise background in a two alternative forced choice paradigm, adapted from a similar olfactory task (Uchida and Mainen, 2003). Subjects triggered the auditory stimulus by means of a nose poke to a center nosecone, and were rewarded (~50µl water) if they responded with a second nosepoke into the appropriate nosecone (right, 1kHz or left, 15kHz). Training was fast (2-3 weeks), and performance on the easiest discriminations could exceed 95%. Typical reaction times were short (several hundred milliseconds). Performance deteriorated in a systematic way with decreased signal to noise ratio and with decreased tone duration. This paradigm offers an ideal model system for studying the neural correlates of two competing perceptions whose representations are likely to be in distinct areas of any tonotopically organized region of auditory cortex.

Uchida, N. and Mainen, Z. (2003) Speed and accuracy of olfactory discrimination in the rat. *Nature Neuroscience*. In press.

157 Relation between intrinsic connections and isofrequency contours in the inferior colliculus of the big brown bat, *Eptesicus fuscus*.

Kimberly Miller, John H. Casseday, Ellen Covey

Psychology, University of Washington, Box 351525, Seattle, WA, United States

Information processing in the inferior colliculus (IC) depends on interactions between ascending pathways and intrinsic circuitry. To determine how local projections of neurons in the IC are related to tonotopic organization, we conducted experiments in which we placed a small iontophoretic injection of biodegradable amine (BDA) at a physiologically characterized location in the IC. We then used electrophysiological recording to delineate the extent of the isofrequency contour that contained the injection site and marked the boundaries of the isofrequency contour by small deposits of Chicago sky blue. We analyzed patterns of anterograde and retro-

grade transport relative to the physiologically determined isofrequency contour to determine whether BDA-labeled cell bodies and fibers were confined to the isofrequency contour itself or whether they extended outside of it. In all of the cases that we examined, the majority of labeled cell bodies were located ventrolateral to the BDA injection, within the isofrequency contour, and labeled fibers were located dorsomedial to the injection, also within the isofrequency contour. Label extended throughout most of the rostrocaudal extent of the IC as well as in the dorsomedial and ventrolateral directions. Some labeled cell bodies were located outside the isofrequency contour. These were mainly large multipolar neurons. The above evidence suggests that, although there is some communication between isofrequency contours, the bulk of intrinsic projections within the IC are consistently confined within their specific isofrequency contour. Within a given isofrequency contour, there is a consistent organization in which intrinsic connections ascend from the ventrolateral portion to more dorsomedial points along the contour.

Supported by NIH Grants DC-00607 and DC-00287.

158 Effects of Electrical Stimulation of the Inferior Colliculus on Tonotopic Projections to the Auditory Cortex in Light of a Midbrain Auditory Prosthesis

Hubert H Lim^{1,2}, David J Anderson^{1,2}

¹Dept. of Biomedical Engineering, Univ. of Michigan, 2200 Bonisteel Blvd., Ann Arbor, MI, United States, ²Kresge Hearing Research Institute, Univ. of Michigan, 1301 East Ann St., Ann Arbor, MI, United States

We are interested in investigating the feasibility for hearing restoration via electrical stimulation of the inferior colliculus central nucleus (ICC), which has a well-defined tonotopic structure that is easily accessible in humans [Lenarz et al., *Abst. CIAP*, 2003]. In a previous conference paper [Lim & Anderson, 2003] we showed that frequency-specific stimulation at low threshold levels is achievable via electrical stimulation of the ICC in guinea pigs. In those experiments we positioned two 16-channel electrodes, one along the tonotopic axis of the ICC and one along the tonotopic gradient of the primary auditory cortex (A1). The best frequency (BF) for each site was determined in response to acoustic pure tones to ensure both electrodes were aligned along similar frequency ranges. We then stimulated each ICC site with single monopolar pulses and recorded the corresponding activity in A1. As an extension to that study and in light of a midbrain auditory prosthesis (MAP), we performed similar experiments to further characterize the effects of ICC stimulation on the transfer of frequency-specific information to A1 and to compare these results with those obtained for cochlear stimulation to assess potential perceptual effects. Consistent with previous results, we observe frequency-specific stimulation in ICC where A1 neurons with similar BFs to those of the stimulated ICC neurons tend to exhibit the lowest stimulation thresholds, shortest latencies, and greatest activity across all the recorded A1 sites and stimulation levels used for a given ICC site. Compared to results obtained for cochlear stimulation [Bierer & Middlebrooks, 2002], ICC stimulation provides more localized spread of activation in A1, lower stimulation thresholds, and greater dynamic ranges. These findings suggest that a frequency-place coding scheme may be utilized for a MAP

with lower stimulation thresholds and better level and frequency discrimination than cochlear implants. However, we also observe that placement of our electrodes along the isofrequency dimensions of both ICC and A1 can alter the strength and pattern of activity recorded in A1 indicating that ICC stimulation may be too specific and that a three-dimensional array that effectively spans the entire ICC may be necessary.

Supported by NIH/NIDCD T32 DC00011 and NIH/NIBIB P41 EB2030

159 Relating spatiotemporal patterns in the ongoing cortical activity to the interpretation of intracortical microstimulation

Matthias Deliano, Frank W. Ohl, Henning Scheich

ALS, Leibniz Institute for Neurobiology, Brennekestr. 6, Magdeburg, Germany

In the development of neuroprosthetic devices, electrical microstimulation in the depth of sensory neocortex might provide a promising alternative to peripheral nerve stimulation [1]. The lack of success in the development of sensory cortex prostheses may be based on a too naive transfer of unidirectional stimulation procedures operative in peripheral neuroprostheses. We have recently shown that cortical activity underlying cognitive aspects of information processing does occur in form of transient spatial patterns of activity distribution emerging from the ongoing cortical activity without apparent relationship to the times of stimulus occurrence [2]. These aspects of information processing pertain to the perceptual sorting of stimuli into meaningful categories and will hence be elemental to the correct interpretation of a stimulus delivered by a sensory cortical prosthesis. Here we applied intracortical microstimulation to the auditory cortex of the Mongolian gerbil via a simple unidirectionally operating cortical implant [3]. In parallel we recorded an epidural multichannel electrocorticogram. Animals were trained in a GO/(NO-GO)-paradigm to discriminate stimulation sites in the low and high frequency region of the tonotopic map of the primary auditory cortex. We analyzed patterns of ongoing cortical activity in relation to electrical microstimulation and its behavioral interpretation. With our work we want to take first steps in the construction of a novel type of interactive cortex prosthesis, which controls its operation interactively with the recorded brain state to ensure optimized communication between prosthesis and the nervous system.

[1] Brindley, G.S. & Lewin, W.S. (1968) *J. Physiol.* 196: 479-493.

[2] Ohl, F.W. et al. (2001) *Nature* 412: 733-736.

[3] Scheich, H. and Breindl, A. (2002) *Audiol. Neurootol.* 7: 191-194.

160 Auditory Midbrain Implant – Design and Evaluation

Minoo Lenarz¹, Guenter Reuter¹, Jim Patrick², Thomas Lenarz¹

¹*Dept. of Otolaryngology, Medical University of Hannover, Carl-Neuberg-Str. 1, Hannover, Germany,* ²*Chief Scientist, Cochlear Ltd., 14 Mars Road, Lane Cove, Australia*

The performance of auditory brainstem implantation using surface

electrodes on the cochlear nucleus have proven to be an effective method of auditory rehabilitation in patients with bilateral neural deafness. However, the overall performance is considerably poorer than the average performance of multi-channel cochlear implant recipients, which can be related to the ABI's poor access to the tonotopic organisation of the cochlear nucleus.

The aim of our research is to develop a penetrating microelectrode for specific stimulation of the isofrequency layers of the central nucleus of the inferior colliculus (IC).

A penetrating stylet-type electrode with 20 electrode rings was developed, each having a width of 200 microns. The 6 mm array with a sharp tip is rigid enough for insertion. Right after removal of the stylet, the electrode becomes pliable and adjusts to the motions of the surrounding brain structures. To date, cadaver experiments and acute animal experiments in cats have been performed.

5 human heads were used to develop the surgical approach and investigate the insertion properties. A medially extended suboccipital/retrosigmoid craniotomy was performed. The IC can be easily exposed via a subtentorial approach and a slight retraction of the cerebellum. The electrode can be inserted under direct vision from dorsal-lateral to anterior-medial and meets the isofrequency layers of the central nucleus (light microscopy).

Following parietal craniotomy, the occipital cortex of cats was elevated. After exposure of the IC the electrode was inserted in dorsal-lateral to anterior-medial direction. The electrode was used to perform near-field recordings after frequency-specific acoustic stimulation. A clear frequency gradient was observed along the array. Stimulating with the array, cortical far-field responses were recorded using tone bursts between 1 and 16 kHz. Histological examinations revealed a sharp insertion canal without collateral damage.

The auditory midbrain implant at the IC may present an alternative to penetrating ABIs at the cochlear nucleus.

161 72 Sharpening of directional responses by auditory cells in the brainstem of the toadfish, *Opsanus tau*

Richard R. Fay, Peggy L. Walton

Parmly Hearing Institute, Loyola University Chicago, 6430 N. Kenmore, Chicago, IL 60626

We have been investigating how the the auditory system of a fish encodes directional information that could be used to compute the location of a sound source. We simulate the particle motion component of underwater sound using a shaker table to produce sinusoidal motion along linear pathways at 30 deg intervals in horizontal and midsagittal planes. Here we compare directional responses from the descending octaval nucleus (DON) in the medulla and the torus semicircularis (TS) of the midbrain. Extracellular recordings were made from 90 units in the left DON (which receives ipsilateral primary afferent input) and 107 units in the left TS (which receives input from the left and right DON). Recording electrodes were glass pipettes with tip diameters of 5-10 microns (3M KCl, 4% neurobiotin to mark locations). We compared the sharpening of the directional response by calculating the average of spike rates at the stimulus angles adjacent to the best direction (+ and - 30 deg) and dividing that average by the spike

rate at the best direction to obtain the sharpening ratio (SR). Primary afferents, which do not show sharpening, have a cosinusoidal response with a SR about 0.87. In the DON, 63% of the cells had directional sharpening in azimuth (with SR < 0.8) and 18% were highly sharpened (with SR < 0.5); 68% had sharpening in elevation, with 30% highly sharpened. In the TS, 84% of the cells had directional sharpening in azimuth, with 54% highly sharpened; 87% had sharpening in elevation, with 42% highly sharpened. We conclude that sharpening first occurs in the DON and some additional sharpening occurs in the ascending pathway to the midbrain, particularly in azimuth. Sharpening is likely caused by inhibitory inputs from directional afferents that differ in directional orientation from those causing excitation. (Funded by the NIH and the Parmlly Hearing Institute)

162 Organization of the Medullary Octavolateral Nuclei in a Teleost Fish.

Seth Tomchik, Zhongmin Lu

Biology, University of Miami, 1301 Memorial Dr., Coral Gables, FL, United States

Octavolateral nuclei in the teleost medulla process ascending information from the otolith organs, semicircular canals, and the lateral line system. Most medullary octavolateral nuclei and the Mauthner cell receive projections from multiple octavolateral organs, but it is not known how these projections overlap spatially within each nucleus. The organization of the first order octavolateral nuclei in the hindbrain of the sleeper goby (*Dormitator latifrons*) was studied by tracing the central projections of multiple octavolateral nerves with different 10,000 MW fluorescent dextrans. Three dimensional reconstructions of the octavolateral nuclei were made, and spatial convergence of octavolateral input was analyzed in each nucleus. The anterior octaval nucleus and descending octaval nucleus receive projections mainly from the otolith organs, and the projections are spatially separate within each nucleus. Lateral line projections terminate in the medial and caudal nuclei, and are relatively separate from the other octavolateral projections. The magnocellular nucleus and Mauthner cell receive highly convergent projections from all otolith organs and semicircular canals. The tangential nucleus and ventral descending octaval nucleus receive overlapping projections from the utricle and horizontal canal. These data indicate that the terminal fields from octavolateral afferents overlap more in some hindbrain nuclei than others. The degree of overlap may have functional significance. Auditory and lateral line nuclei appear to receive relatively segregated input from each octavolateral organ, while the vestibular nuclei and the Mauthner cell receive highly convergent input. (This work was supported by University of Miami start-up funds and NIH/NIDCD grants R29DC003275 and R01DC003275)

163 Temporal Responses in the Dorsal Medullary Nucleus of the South African Clawed Frog

Taffeta Marie Elliott¹, Jakob Christensen-Dalsgaard², Darcy B. Kelley³

¹Neurobiology and Biology, Columbia University, 1212 Amsterdam Av, Fairchild 911, MC2430, New York, NY, United States, ²Biology Institute, University of Southern Denmark, Campusvej 55, Odense, Denmark, ³Neurobiology and Biology, Columbia University, 1212 Amsterdam Av, Fairchild 911, MC2432, New York, NY, United States

Male and female aquatic South African clawed frogs, *Xenopus laevis*, call in different behavioral contexts. Calls are made up of trains of clicks that differ in rate. As a preliminary step towards understanding how the auditory system processes temporal patterns such as click rate, we investigate how calls are represented in the dorsal medullary nucleus (DMN), a homologue of the cochlear nucleus. We record *in vivo* in frogs stimulated with both pure tones and recorded calls. To circumvent problems of underwater sound stimulation, we directly vibrate the cartilagenous tympanic disk. DMN cells show no preference for click rate but synchronize to click envelopes. Initial analysis reveals that temporal discharge patterns include phasic burst patterns in addition to onset responses and primary-like firing patterns. Results will inform future recordings from higher nuclei, where we expect to find selection for click rate.

164 Prolonged maturation of cochlear function in the barn owl after hatching

Christine Koepl¹, Regina Nickel²

¹Zoologie, Technische Universitaet Muenchen, Lichtenbergstr. 4, Garching, Germany, ²Institute of Laryngology and Otology, University College of London, 330-332 Gray's Inn Road, London, United Kingdom

The barn owl (*Tyto alba*) is a well known model for neural mechanisms of sound localization. Owls are altricial birds and maturation of auditory brainstem and midbrain centres is known to occur gradually over weeks and months, partly under the guidance of the visual system. It is unknown at present what the timecourse of maturation of the basilar papilla (or cochlea), is and how it may be contributing to more central maturation processes.

Evoked potentials in response to tone-pip stimuli at frequencies between 500 Hz and 10 kHz were recorded at the round-window membrane of anaesthetised barn owls aged between 6 and 97 days posthatch. Hair-cell responses (cochlear microphonic, CM) were observed at all frequencies from the earliest age tested. However, thresholds were high initially and did not reach stable, adult-like values until P30-P40. Neural responses (compound action potential, CAP) were initially only seen in response to 1-3 kHz at high levels (80-110 dB SPL). Higher-frequency responses then appeared gradually and thresholds improved gradually with increasing age. Around P40, CAP thresholds up to 6 kHz were adult-like. The highest-frequency thresholds (7-10 kHz) remained at the upper end of the adult range and appeared to take another month to reach mature sensitivity. CAP amplitudes took longest to mature and did not reach adult-like values at any frequency until 3 months of age.

These data show that hearing in barn owls develops entirely posthatching. Adult neural sensitivity across the full adult hearing range was achieved around fledging time (about 9 weeks). The even later maturation of CAP amplitudes is most interesting, since it indicates a prolonged immaturity in the temporal synchrony of spiking. This could be a limiting factor for the development of temporal processing circuits in the brainstem.

165 Possible Contribution of The Contralateral Superior Olivary Nucleus Input to Avian Nucleus Magnocellularis Response Properties

R. Michael Burger¹, Eric Bauer², Edwin W Rubel²

¹Otolaryngology-HNS, University of Washington, Box 357923 U. Washington, Seattle, WA, United States, ²Otolaryngology-HNS, University of Washington, Box 357923, Seattle, WA, United States

Nucleus Magnocellularis (NM) and n. Angularis (NA) are the targets of the avian auditory nerve and comprise the avian cochlear nucleus. NM neurons are known to respond to acoustic stimuli with precise phase-locked discharges. NM in turn provides bilateral input to n. Laminaris (NL) where interaural time disparities are computed from its phase-locked inputs. A fourth nucleus, the superior olive (SON) completes and ipsilateral inhibitory feedback loop. NM, NA and NL receive inhibitory GABAergic input from the SON, while the ipsilateral NA and NL provide the primary excitatory input to SON. An interesting additional feature of SON circuitry is that both SONs are reciprocally coupled, presumably by inhibitory inputs. Conceptual and computational models derived from available anatomy and in vitro physiology suggest that each SON functions to regulate NM activity differentially on either side of the brain. We used an acoustic paradigm to test the possible binaural role of the SON in NM response properties. In P5-P10 day old chicks we determined the best frequency of NM neurons on one side of the brain to ipsilateral acoustic stimuli and then added contralateral stimuli that varied in frequency and intensity. Preliminary results demonstrate that contralateral stimulation (BF) results in an increase in firing rate that is consistent with a release from inhibition. Pharmacological block of GABA receptors with multibarrel recording pipettes in NM confirm a GABAergic suppression of spikes under normal conditions at BF. Interestingly, contralateral stimulation off BF causes spike suppression during ipsilateral tone presentation at BF. It appears that NM neurons receive frequency specific facilitation and lateral inhibition that are derived from the contralateral ear. Grant Support: DC00395, DC00466, DC00018

166 Hearing in the Ruby-throated Hummingbird (*Archilochus colubris*: Trochilidae)

Bernard Lohr, Robert J. Dooling

Department of Psychology, University of Maryland, Bldg. 144, Campus Drive, College Park, Maryland, United States

While there are numerous physiological and behavioral studies of auditory sensitivity in small birds, there have been no studies of hearing in hummingbirds to date. Hummingbirds are especially interesting because they are one of the three groups of birds

(Passeriformes, Psittaciformes, and Apodiformes: Trochilidae) in which it has been shown that vocal learning occurs. The present study examined auditory sensitivity in the ruby-throated hummingbird (*Archilochus colubris*) using the auditory brainstem response (ABR), measured subdermally, as a means of estimating hearing thresholds. Subjects were presented with both rectangular-pulse clicks and tone burst stimuli. Clicks were 0.1 ms in duration and were presented in ascending order from 50 -110 dB SPL. Tone bursts were 5 ms in duration with a 1 ms rise/fall, and were presented in ascending order from 45 -105 dB SPL at frequencies ranging from 500 - 23,000 Hz. Thresholds were computed from latency-intensity and amplitude-intensity functions at all frequencies. Results suggest that ruby-throated hummingbirds are most sensitive between 2,000 - 3,000 Hz, and that sensitivity falls off rapidly outside this range when compared with the hearing of other small birds. [Work supported by NIH].

167 The development of the acoustical cues to sound location in cats

Daniel J Tollin

Department of Physiology, University of Wisconsin, 1300 University Ave, Madison, WI, United States

There are three acoustical cues to sound location: Interaural differences in time (ITDs) and level (ILDs) and monaural spectral shape cues. In adult cats, these cues vary with location, their ultimate magnitude depending on the physical dimensions of head and pinnae. During development, the increasing interaural distance associated with a growing head and pinnae are expected to result in cues that will change continuously until maturation is complete. While there have been many physiological studies on the development of the neural mechanisms of sound localization in cats, there have been no detailed studies on the development of the three cues to location themselves in this species. Here we report measurements of both the physical dimensions of the head and pinnae as well as acoustical measurements of the cues to localization of cats aged 4 weeks to adulthood. The localization cues were computed from measurements of Directional Transfer Functions (DTFs). At 4 weeks, ILD depends little on azimuth for frequencies < 5 kHz; and for sources varying in elevation along the median plane, a prominent spectral "notch" is located at higher frequencies than in the older cats. As the cats develop, the spectral cues shift to lower frequencies and the frequencies at which ILDs become substantial (> 10 dB) also shift lower so that in adults, ILDs are prominent for frequencies down to 2-3 kHz. The magnitude of the ITD cue also increased with age. As expected, the changes in ILDs, ITDs and the spectral features are correlated with the increasing size of the head and pinnae. These data give insights into the development of the physiological mechanisms of sound localization. Supported by NIH grant DC05122

168 Developmental Changes in the Precedence Effect: Effect of Stimulus Type and Delay.

Smita S Agrawal, Ruth Y Litovsky, GongQiang Yu

Waisman Center, University of Wisconsin-Madison, 1500 Highland Avenue, Madison, WI, United States

When two similar sounds are presented from different locations with a brief delay, only one sound is heard whose perceived loca-

tion is dominated by the first source. This auditory phenomenon is known as the Precedence Effect (PE). Although the lagging source is not localized as an independent event, under some conditions, adults are able to extract its directional cues. The PE is thought to not only facilitate accurate localization of sound sources but also aid speech intelligibility by suppressing the perception of echoes in reverberant environments. Developmental studies suggest that this ability changes during the early years of life. Significant improvements are seen in both echo thresholds and spatial tasks like the Minimum Audible Angle (MAA). Litovsky [J. Acoust. Soc. Am., 102(3), 1739-45, 1997] found that while single-source MAAs were similar to those of adults by 5 yrs, in the presence of a single reflection MAAs increased significantly. The age at which adult performance is reached is not known. In an attempt to obtain a more comprehensive picture of the development of the PE, the present study measures MAA thresholds using a number of delays (1, 5, 10 and 30 ms), with clicks and speech (a more realistic stimulus), at a number of ages. We hypothesize that speech MAA thresholds will be higher than those with clicks, especially at smaller delays. Subjects were normal hearing children of ages 3:6 to 5:5 yrs, 5:6 to 7:5 yrs and 7:6 to 9:5 yrs, with 10 children in each age group (n=30). Ten adults served as controls. On each subject, MAA thresholds were measured in the horizontal plane, for single-source (control) and 8 PE conditions (2 stimuli x 4 delays). Preliminary results indicate significant improvements in MAA with an increase in age in the PE condition and worse MAA thresholds with speech than clicks. This reiterates the significance of acoustical treatment of classrooms, especially for younger children.

169 Monaural And Binaural Contributions To Developmental Adaptation To Altered Localization-Cue Values

Robert AA Campbell, David R Moore, Andrew J King

Laboratory of Physiology, University of Oxford, Parks Rd, Oxford, United Kingdom

Previous studies have demonstrated that altered sensory inputs can induce compensatory changes in auditory spatial processing. Here we have investigated the role of monaural and binaural mechanisms in the capacity of ferrets to learn during infancy to use abnormal spatial cue values to localize sound. A 12-speaker azimuth localization task was used to measure the accuracy of approach-to-target and head-orienting responses to broadband noise bursts of different durations (2000-40 ms). Adult ferrets were tested that had been raised from hearing onset with one of three acoustic-cue manipulations: 1. Unilateral earplug. 2. Unilateral cochlear ablation. 3. Unilateral earplug plus removal of the pinna and concha of the contralateral ear. In contrast to the effects of acute monaural occlusion, animals raised and tested with a unilateral earplug performed almost as well as normally-reared controls, indicating substantial adaptation to the altered spatial cues. Subsequent removal and reinsertion of the earplug resulted in little change in the rate or pattern of errors. This raises the possibility that the basis for the adaptation may involve learning to utilize monaural spectral cues and to ignore the abnormal binaural cues. However, monaural cues alone are not sufficient for adaptation as the ferrets reared with a unilateral cochlear ablation performed very poorly. Nevertheless, these cues may be involved in

guiding adaptation to the earplug, as removal of the pinna and concha of the unplugged ear led to larger localization errors than in the animals raised with a unilateral earplug alone. These results suggest that infant-plugged animals are cross-referencing between monaural and binaural localization cues as they adapt to the earplug.

170 Development of communication calls in the big brown bat, *Eptesicus fuscus*

M Carter, C M Rafano, E Covey, J H Casseday

Psychology, University of Washington, Box 351525, Seattle, WA, United States

Big brown bat pups start vocalizing at birth. To study the development of vocalization, we recorded calls of infants born in captivity from postnatal day one until about 6 weeks after birth. Just after birth, all of the vocalizations appeared to be mother-infant communication calls. Until about 4 days of age, there was one type of vocalization that consisted of downward frequency sweeps with 5-7 harmonics. The fundamental had a center frequency of 12 kHz, a bandwidth of 7 kHz, a duration of 35-40 ms and an interpulse interval of 160 ms. At about 4 postnatal days, the call appeared to differentiate into two different types. The original call began to occur primarily when the pup was reunited with its mother after isolation (reunite call). The other type of call emerged when the pup was isolated from its mother (isolation call). The differences between the original call and the isolation call increased as the pup matured. By three weeks of age the center frequency of the fundamental had increased to 28 kHz, the bandwidth had increased to 25 kHz, the number of harmonics had decreased to 3-4, the interpulse interval had decreased to 110 ms, and the duration of the fundamental had decreased to 8-12 ms. The harmonic structure of the reunite call was unique for each individual and stayed relatively consistent from postnatal day 4 throughout the 6 weeks of data collection. The constancy of the pup's reunite call suggests that it could serve as a means by which a mother can identify her own offspring in a colony with many pups. At postnatal day 6-7, pups also started to emit vocalizations that resembled echolocation calls in that they had two harmonics, a fundamental centered at 42 kHz, a bandwidth of about 30 kHz, and a duration of 5 ms. The early echolocation calls are similar to the late stage isolation calls, suggesting that echolocation calls are derived from isolation calls.

Supported by NIH Grants DC-00287 and DC-00607.

171 Plasticity in the Auditory Brainstem of Adult Mongolian Gerbils induced by Acoustic Noise

Ida Kollmar, Benedikt Grothe

Auditory Processing, Max Planck Institute of Neurobiology, Am Klopferspitz 18a, D-82152 Martinsried, Germany

Neuronal plasticity is an important mechanism for learning and adaptation to environmental changes. Plasticity in the auditory system of mammals, however, has almost exclusively been investigated with invasive techniques. In the present study we investigate the plasticity of sound localization mechanism using a non-invasive approach. In mammals, interaural time differences (ITDs), a major cue for sound localization, are encoded in the medial superior olive (MSO) by a complex temporal interaction of binaural

excitatory and inhibitory inputs. The MSO projects directly to the dorsal nucleus of the lateral lemniscus (DNLL). During a critical period during development ITD tuning of DNLL neurons becomes tuned to the physiological range. Omnidirectional white noise influences this development (Seidl and Grothe 2003 submitted). Here, we investigated the influences of noise in adult animals with presumably normal ITD tuning.

We compared ITD-sensitivity of 119 DNLL neurons from three groups of adult gerbils. All animals were raised in a normal acoustic environment. A control group was never exposed to noise, a second group was exposed to noise for 14 days as adults and then tested within 7 days after exposure, and a third group was exposed to the noise but recovered for at least 14 days after exposure.

Exposure to omnidirectional noise significantly, but reversibly altered the ITD coding in adult animals by shifting the average best ITD (in cycles) to longer interaural delays (contralateral stimulus leading). Additionally, the modulation depth in the physiological relevant range increased. These effects, however, were not visible anymore, when animals were allowed to recover for more than 14 days.

These experiments show a quantifiable, reversible plasticity in sound localization mechanisms, which can be used as a model-system to investigate adult plasticity in the auditory brainstem, without invasive treatment.

172 The Recombinant Tissue Plasminogen Activator (rtPA) Enhances IL-8 And Matrix Metalloproteinase 1 Activities

Brandon D Hill¹, Usha Nair¹, Siva Kanangat¹, Renzo Mora², Marco Barbieri², Mohammad Habiby Kermany¹, Tai June Yoo¹

¹Allergy/Immunology, University of Tennessee, 956 Court Ave., B318, Memphis, TN, United States, ²Dept. of Otorhinolaryngology, University of Genoa, e-Cliniche, L.go Rosanno Benzi, 10, Genoa, Italy

Introduction: The rtPA has been used extensively for cardiovascular disease to lyse preformed clots. However the dosage used (100mg) for the treatment of the myocardial infarction results cerebrovascular accidents in 9% of patients treated.

The tPA therapy with much lower dosage (3 mg bid) dose for 2 weeks duration was found to be effective in restoring hearing in certain hearing loss patients. (R. Mora et al *Annals Oto Rhino Laryn*, in press). The specific aim of this study is to examine the effect of tPA on inflammatory cascades. Methods: We have added Actlyse (rtPA) in graded concentration to 80% confluent monolayers of A549 (human lung epithelial cells – obtained from ATCC) in a 24 well plate. They were then incubated at 37 °C (5% CO₂). The cells were harvested after 24 hours. Total RNA was isolated and reversed transcribed using oligo dT and AMV Reverse Transcriptase. The CDNAs for house keeping gene GAPDH, Chemokines, MMP-1 (matrix collagen degrading enzymes) were amplified IL-1a, IL-6, cxc chemokine IL-8 (a potent angiogenic factor and neutrophil chemattractant). Results: We observed a significant increase in steady state mRNA level of IL-8 and mmp-1 in tPA treated human lung epithelial cell line, in a concentration dependent manner. Conclusion: These results indicate that the pathophysiologic effects of tPA are mediated through regulating inflammatory cascade.

173 Serum Levels of Pro-Inflammatory Cytokines and Hearing Loss in the MRL-Fas^{lpr} mouse

D. Michael Patterson, William N. Snyder, Michael J. Ruckenstein, Michael Anne Gratton

Otorhinolaryngology-HNS, University of Pennsylvania, 3400 Spruce St, Philadelphia, PA, United States

The MRL-Fas^{lpr} (Lupus) mouse has been used to model autoimmune sensorineural hearing loss. This mouse displays elevated auditory brainstem response thresholds, decreased endocochlear potentials, and degeneration of the stria vascularis in the absence of immune complex deposition or any inflammatory infiltrate within the inner ear. Dysregulation of the local cytokine milieu has been implicated in the disease process of other organ systems in this model. We propose that systemic cytokine dysregulation alters the local cytokine environment of the inner ear, causing the observed pathology in the MRL-Fas^{lpr} mouse. Our aim is to determine whether a relationship exists between the systemic dysregulation of cytokines and onset of hearing loss.

MRL-Fas^{lpr} and MRL/MpJ mice were bred inhouse. Auditory sensitivity was determined and serum samples were obtained at 3, 6, 10, 15 and 20 weeks of age. The auditory brainstem response thresholds were obtained using tone burst stimuli at 2, 4, 8, 16, 24, and 32 kHz. Whole blood was collected at the same time via the retro-orbital sinus, allowed to clot at room temperature for 2h, centrifuged at 2800 r.p.m. for 15 min. The supernatant sera was frozen at -20° C. Commercially available ELISA kits were used to determine the serum levels of pro-inflammatory cytokines.

Onset of elevated thresholds at 2 and 4 kHz was found to be associated with increased serum content of IL-1β. Previous work from our laboratory has demonstrated that IL-1 receptor 1 is located on endothelial cells as well as basal cells and type I, II and V fibrocytes of the lateral wall. Combined, these data suggest that sensorineural hearing loss in the MRL-Fas^{lpr} mouse may be mediated by the action of elevated circulating cytokines on the endothelial cells of the lateral wall.

Supported by Deafness Research Foundation to DMP and National Organization of Hearing Research to MAG

174 Fas ligand, Apoptosis and Inner Ear Immunity

Xiaobo Wang^{1,2}, Peter B Billings^{1,2}, Allen F Ryan^{1,2}, Elizabeth M Keithley^{1,2}

¹Head and Neck Surgery, University of California, San Diego, 3350 La Jolla Village Drive, San Diego, CA, United States,

²Otolaryngology/Head and Neck Surgery, Veterans Affairs Medical Center, 3350 La Jolla Village Drive, San Diego, CA, United States

Apoptosis of leukocytes is a normal phase of an immune response. It has been hypothesized that the anterior chamber of the eye, an immuno-privileged site, achieves this state, in part, by constitutive Fas-ligand expression inducing apoptosis of Fas-expressing - infiltrating inflammatory cells. Based on the observation that Fas ligand expression increases during cochlear inflammation, we hypothesized that injection of Fas ligand into the cochlea during an experimentally induced immune response might ameliorate the response

and thereby protect the cochlea from damage and hearing loss.

Guinea pigs were sensitized to KLH by subcutaneous injection of KLH with adjuvant. The basal turn scala tympani of both cochleas was challenged with KLH (60 mg/ml, 5-10 μ l). An osmotic minipump (Alzet #2001, 1 μ l/hour) with 5 μ g/ml recombinant human soluble Fas-ligand in gp albumin was surgically implanted into the right cochlea of six animals. Control cochleas (n=2) received vehicle alone. ABR thresholds were measured before the initial surgery and prior to sacrifice by cardiac perfusion with saline and 4% paraformaldehyde 7 days later. Inflammation was rated with a scale of 1-5 in H&E stained, paraffin sections.

KLH injected cochleas showed the characteristic presence of leukocytes in scala tympani. Cochleas that received KLH and Fas-ligand also were inflamed. The median inflammation rating was 4, while the KLH alone cochleas had a median rating of 2. The KLH plus Fas-ligand cochleas had a median hearing loss of 67 dB, while the KLH-alone cochleas had a median hearing loss of 20 dB (non-parametric rank sum tests for both measures, $p > 0.05$ not significant). TUNEL assay revealed apoptosis among leukocytes in both groups.

It is concluded that the presence of Fas-ligand in the perilymph of inflamed cochleas did not reduce either the amount of inflammation or hearing loss in response to antigen.

Support: NIDCD grants DC04268, DC00139 and the Medical Research Service, Dept. of Veterans Affairs

175 Antibodies against the cochlin intervening domain recognize all three isoforms and demonstrate co-expression of cochlin with CTL2

Thankam S Nair¹, Sushma Yarlagadda², Charla Harvey³, Kelley Kozma⁴, Pavan Kommareddi⁵, Thomas E Carey⁵

¹Oto, KHRI, 1301 E Ann St #6020, Ann Arbor, MI, United States,

²Otolaryngology, Kresge Hearing Institute, 1301 E Ann, Ann Arbor, MI, United States, ³Otolaryngology, Kresge Hearing Research Institute, 1301 E Ann, Ann Arbor, MI, United States,

⁴Otolaryngology, Kresge Hearing Research Institute, 1301 E Ann, Ann Arbor, MI, United States, ⁵Otolaryngology, Kresge Research Institute, 1301 E Ann, Ann Arbor, MI, United States

The KHRI-3 antibody binds to a guinea pig inner ear supporting cell antigen and causes hearing loss. Autoimmune patient sera also contain antibodies that bind to guinea pig inner ear supporting cells with the distinctive "wine glass" pattern observed with KHRI-3 and these antibodies bind to the 68-72 kDa protein immunoprecipitated by KHRI-3. To better understand the mechanism of antibody induced hearing loss, we affinity purified the KHRI-3 antigen which we identified as CTL2, a transmembrane protein member of the choline transporter-like protein family. We discovered and sequenced a 64 kDa protein that co-precipitates with CTL2. This protein is the guinea pig homologue of cochlin, the product of COCH-5B2 gene. Cochlin mutations cause an autosomal dominant non-syndromic hereditary hearing disorder (DFNA9). There are 3 Cochlin isoforms of 63, 44 and 41 kDa. The 63 kDa form incorporates an LCCL domain and two von Willebrand factor A (vWFA) domains in tandem. The 41 and 44 kDa isoforms lack the LCCL domain, and may be due to alternative splicing or post-translational modifications. We postulate that cochlin and CTL2 interact in a functional complex. To study this

relationship and examine co-expression in tissue we raised antisera and monoclonal antibodies against the cochlin intervening domain between the two vWFA domains. These antibodies recognize all three isoforms on western blots. The anti-cochlin antibodies bind to the phalangeal process of outer pillars and Deiter's cells in the organ of Corti with a punctate pattern very similar to KHRI-3 antibody. This is the first demonstration of cochlin expression in the organ of Corti. These antibodies can serve as important tools for studying function, co-precipitation, co-localization of cochlin with CTL-2, and should help to determine their role in inner ear autoimmune disease.

(Supported by the Ruth and Lynn Townsend Family Fund, R01 DC03686 and the NIH Rheumatic Core Diseases Center ?1 P30 AR048310)

176 Cloning and subcloning of CTL2 for functional characterization

Pavan K Kommareddi¹, Thankam S Nair², Takeharu Kanazawa³, Thomas E Carey²

¹Otolaryngology, KHRI, 1301 E Ann St #6020, Ann Arbor, MI, United States,

²OTO, KHRI, 1301 E Ann St #6020, Ann Arbor, MI, United States, ³OTO, CCGC, 1301 E Ann St #6020, Ann Arbor, MI, United States

CTL2 protein was identified as the target antigen of the KHRI-3 mouse monoclonal antibody. KHRI-3 binds to inner ear supporting cells of the organ of Corti and causes hearing loss in guinea pigs. Antibodies in sera from patients suspected of having autoimmune sensorineural hearing loss bind to the guinea pig organ of Corti with a staining pattern similar to that of KHRI-3 suggesting CTL2 as a possible target of autoantibodies. Immunoprecipitation of CTL2 with KHRI-3 co-precipitates other proteins including cochlin, HSP-70, actin and cytokeratins. To better understand the function of CTL2, a panel of human cell lines were screened for CTL2 expression, and mRNA from these cells was used to clone the human full-length cDNA. We amplified and cloned the human CTL2 2121 bp open reading frame from the UM-SCC-11A cell line plus the Kozak consensus sequence into pGEM-T vector. The cloned sequence was verified by sequencing through the University of Michigan sequencing core and comparing to the human genomic and cDNA CTL2 sequence using the NCBI database. The cloned CTL2 has been subcloned into PhrGFP-C vector using restriction enzymes SacII and blunted to make a CTL2-GFP fusion vector for studying cellular and subcellular localization of CTL2 in vertebrate cells. Stably transfected human cells will be used to examine the function of CTL2. We have made five different subclones in pTriEx 4-Neo multi expression vector using XhoI, SmaI and NcoI restriction enzymes to express protein with and without N- and C- terminal His tags in bacteria, insect and vertebrate cells. The His tags will be used for purification of proteins and then removed from the protein by digesting with enterokinase. We plan to use the purified protein for crystallization and structural studies as well as for the screening of sera from patients with sudden hearing loss. We plan to use the clone to make a recombinant bait protein which will be incorporated into the yeast two-hybrid system to elucidate the domains that regulate protein-protein interactions of CTL2 in the inner ear.

Fellowship: NIH T32 DC00011

Research Supported By: Townsend Family Fund, R01 DC03686.

177 Elucidating the Role of Bone Morphogenetic Proteins in Meningogenic Labyrinthitis Ossificans

Sarah S Connell¹, Hilary A Brodie¹, Steven P Tinling²

¹Otolaryngology, University of California Davis, 2521 Stockton Blvd Ste 7200, Sacramento, CA, United States, ²Otolaryngology, University of California Davis, 1515 Newton Court Rm 209, Davis, CA, United States

Background: The interplay between Bone Morphogenetic Proteins (BMPs) and their antagonists governs developmental and cellular processes as diverse as the formation of joints in the skeletal system and neurogenesis in the adult brain. To date the role of BMPs and their antagonist Noggin in bone forming diseases of the labyrinth have remained unknown.

Hypothesis: BMPs regulate new bone formation in the labyrinth under pathologic conditions. Inhibition of BMPs with Noggin coated agarose beads implanted in round window niche provides a location specific reduction of new bone formation in the basal turn of the cochlea.

Methods: Twenty-eight gerbils underwent placement of agarose beads into bilateral round window niches and intrathecal injection of *Streptococcus pneumoniae* into the cisterna magna. In each animal, one ear received Noggin coated beads and the contralateral side received control beads. Prior to infection, baseline ABRs were obtained, and post-op ABRs were performed on day 28 prior to gerbil sacrifice. One month later, the bullae were harvested, decalcified, and embedded in plastic. Mid-modiolar sections of the cochlea were mounted and stained. The proportional area of the cochlear lumen with fibrosis and neo-ossification was assessed. Three infected animals and one normal control were reserved for immunohistochemical analysis of the cochlea. They were sacrificed on post-operative day 5 and embedded in paraffin after decalcification.

Results: Using a gerbil model for meningogenic labyrinthitis ossificans, noggin delivered by microbeads did not improve hearing outcomes or reduce labyrinthitis ossificans.

Conclusion: These data suggest a local application of Noggin does not mitigate the neo-ossification associated with labyrinthitis ossificans.

178 Prosurvival and Proapoptotic Intracellular Signaling in Rat Spiral Ganglion Neurons (SGNs) In Vivo After the Loss of Hair Cells

Shaheen Ara Alam, Steven H Green

Biol. Sci. & Otolaryngol., University of Iowa, 143 Biology Building, Iowa City, Iowa, United States

Hair cells, the auditory sensory cells, are the sole presynaptic input to SGNs, which die after loss of the hair cells. We destroy hair cells by daily injection of kanamycin (400 mg/kg/day) into rats from postnatal day 8 (P8) to P16; hair cell loss is confirmed by loss of ABR. After kanamycin treatment, SGN number decreases gradually over a period of 14-15 weeks in the rat. An important question is why the death of the SGN population is gradual, what distinguishes a cell that dies soon after deafferentation from one that dies many weeks later? This could be important in developing

treatments to prevent SGN death in people using cochlear implants to replace lost hair cells. We have therefore initiated a detailed description of the status of intracellular signaling in the SGNs of kanamycin-treated rats. These are assayed at P16, immediately after deafening; at P23, just prior to the onset of detectable SGN loss; at P32, when SGN loss is significant; and at P60, midway through the cell death period. To assess prosurvival signaling, we analyzed the level of CREB, PKB and MAPK phosphorylation by immunohistochemistry and western blot. We find that these prosurvival signals do not change detectably in deafferented SGNs, consistent with SGNs having sources of trophic support in addition to hair cells. Rather, SGN death after loss of hair cells may be due more to activation of proapoptotic signaling pathways than to inactivation of trophic signaling. We observe an increase in phosphorylation of c-Jun in ganglia of deafened rats. Immunohistochemical analysis confirms that this increase occurs in the neurons. Further experiments using an in vitro model are in progress to determine how trophic signals available to SGNs suppress proapoptotic signaling.

179 Protection against Cisplatin-Induced Ototoxicity in Rats by Ginkgo biloba Extract (EGb 761)

Xinyan Huang¹, Craig A. Whitworth², Leonard P. Rybak³

¹Surgery, SIU School of Medicine, P. O. Box 19662, Springfield, IL, United States, ²Surgery, SIU School of Medicine, P. O. Box 19628, Springfield, IL, United States, ³Surgery, SIU School of Medicine, P. O. Box 19653, Springfield, IL, United States

Cisplatin is a widely used anticancer agent with several severe dose-limiting side effects including ototoxicity. It has been shown that cisplatin-induced ototoxicity corresponds with a depletion of the cochlear antioxidant system and increased lipid peroxidation. Reactive oxygen and nitrogen species play an important role in cisplatin toxicity. A standardized Ginkgo biloba Extract, EGb 761, is a potent antioxidant capable of scavenging free radicals, inhibiting nitric oxide synthesis, reducing lipid peroxidation, and protecting against apoptosis. The purpose of this study was to investigate the effect of EGb 761 on cisplatin-induced ototoxicity in rats.

Male Wistar rats were divided into 4 groups and were treated as follows, 1) vehicle control; 2) cisplatin (13 mg/kg, ip); 3) EGb 761 (200mg/kg, ip); 4) EGb 761 plus cisplatin. Auditory brainstem responses (ABR) were measured pre- and 72 hours post-treatment, and threshold shifts were determined. Endocochlear potentials (EP) were also obtained at 72 hours post-treatment.

Cisplatin treated rats showed significant ABR threshold shifts across all frequencies (click, and 2, 4, 8, 16 and 32 kHz tones) compared to other groups ($p < 0.001$). Rats treated with EGb 761 plus cisplatin did not show significant ABR threshold shifts ($p > 0.05$). Similarly, the EPs of cisplatin treated rats were decreased significantly about 50% in comparison to the other groups ($p < 0.001$). The EPs of EGb 761 plus cisplatin treated rats were similar to vehicle control group or EGb 761 only group ($p > 0.05$).

These results demonstrate Ginkgo biloba Extract EGb 761 protects against cisplatin-induced ototoxicity.

This research was supported by the National Institutes of Health NIH (NIDCD) # RO1 DC02396.

180 The combined BDNF and BMP7 transgenes induce tissue growth in the scala tympani

Toshihiko Nakaizumi¹, Ryosei Minoda², Yehoash Raphael³

¹Otolaryngology, Kanazawa Medical University, 11-8 Ougi, Kanazawa, Japan, ²Otolaryngology, The Univ. of Michigan, 1150 W. Med. Cntr. Dr., Ann Arbor, MI, United States

One of the challenges often facing the cochlear implant procedure is growth of connective tissue in the cochlear fluid spaces. This is especially critical in meningitis patients whose scalae often ossify following the infection. To better understand the implications of this tissue response for the implantation, and to develop and model for cochlear ossification, we set out to use molecules that may influence the cochlea in a similar way. The bone morphogenetic protein (BMP) family of proteins has been shown to influence growth of connective tissue and other cell types. The goal of this experiment was to determine the influence of BMP7 and BDNF on the cochlea following elimination of hair cells. BDNF was chosen due to its known effects in enhancing survival of denervated spiral ganglion cells (SGC).

Young guinea pigs were deafened with kanamycin and ethacrynic acid. Seven days later, *BDNF* and *BMP7* transgenes were delivered into the scala tympani via the round window membrane. We inoculated 5 μ l of adenoviral suspension containing a mixture of *Ad.BDNF* and *Ad.BMP7* into the left ear. Animals were sacrificed 30 days after deafening and their inner ears embedded in plastic and sectioned for morphological analysis. We determined that in *Ad.BDNF* and *Ad.BMP7* treated ears, the scala tympani was invaded by varying amounts of cellular material. In some animals the entire cross-section of scala tympani was filled with connective tissue, throughout the cochlear spiral, and in other animals only the basal turn was involved. The area of the scala tympani adjacent to the habenula perforate contained cells that appeared to have migrated from Rosenthal's canal. In control groups that received *Ad.BDNF* or *Ad.BMP7* alone, this cellular invasion was not observed. These data show an experimental model for inducing connective tissue growth in the cochlear fluid space and implicate BMP7 in regulating the invasion of the scala tympani.

Supported by the Royal National Institute for Deaf People (RNID).

181 Expression of IGF Binding Proteins in mouse vestibular sensory organs following gentamicin ototoxicity

Park Yong-Ho¹, Seung-Ha Oh¹, Shin Dong-Hoon², Kim Jaehyup², Kim Chong Sun¹, Yehoash Raphael³

¹Otolaryngology, Seoul National University, College of Medicine, 28 Yongon-dong, Chongro-gu, Seoul, Korea, Republic of,

²Anatomy, Seoul National University, College of Medicine, 28 Yongon-dong, Chongro-gu, Seoul, Korea, Republic of,

³Otolaryngology, Kresge Hearing Research Institute, The University of Michigan Medical School, 1301 East Ann Street, Ann Arbor, MI, United States

Several growth factors have been found to be associated with the regeneration and repair of damaged hair cells. Among these factors is IGF-I, which has been shown to enhance proliferation dur-

ing hair cell development and to increase hair cell regeneration in the avian basilar papilla. IGF Binding Proteins are a family of secreted proteins that specifically bind IGF-I and IGF-II. Circulating IGF/IGFBP complexes prolong the half-life of IGF and alter the biological activity of IGF. We have previously used gene array assay to investigate gene expression changes in the mouse vestibular epithelium following an ototoxic insult, and demonstrated (2001 ARO abstract #141), a change of IGFBP-2 and IGFBP-5. This study was designed to localize these IGFBPs at the cellular level with immunocytochemical techniques following ototoxic damage. 40 μ g of gentamicin was administered into the left posterior or lateral semicircular canal of mice using a syringe pump and animals were sacrificed at 4, 7, 14 or 28 days after surgery. In control ears, the expression of IGFBP-2, 4, and 5 were detected in the sensory epithelium. On the contrary, in the gentamicin treated ear, expression of IGFBP appeared to increase in the non-sensory epithelium immediately after the insult. However, four weeks after the insult, IGFBP 4 and 5 were upregulated in the neural region while IGFBP-2 dose not. These findings suggest that different IGFBPs play different roles in the response of the vestibular epithelium to ototoxic lesions.

Supported by NIH-NIDCD grant DC01634 (YR).

182 Pan-caspase inhibitor and caspase 9 inhibitor alleviate gentamicin-induced cochlea damage in guinea pigs

Takeshi Okuda, Kazuma Sugahara, Hiroaki Shimogori, Hiroshi Yamashita

Department of Otolaryngology, Yamaguchi University School of Medicine, Minamikogushi 1-1-1, Ube, Japan

On a disorder of inner ear hair cell of various drug including aminoglycoside drug, the probability that apoptosis is involvement of the cell death is reported. The efficacy of pan-caspase inhibitor and caspase 9 inhibitor for cochlear hair cells protection were evaluated in vivo. Gentamicin (12 mg/ml) was delivered via osmotic pump into the cochlear perilymphatic space of five guinea pigs at 0.5 μ l/h for 14 days. Other five animals were given z-Val-Ala-Asp(Ome)-fluoromethyl ketone (z-VAD-FMK: 250 μ M) in addition to gentamicin and other five animals were given Z-Leu-Glu(OMe)-His-Asp(OMe)-FMK (z-LEHD-FMK: 250 μ M) in addition to gentamicin. We assessed auditory brain stem response (ABR) thresholds to evaluate cochlear function and observed the sensory epithelium using fluorescent microscopy. The shift in auditory brainstem response thresholds at 4, 7, and 14 days after gentamicin administration were repressed in animals that received z-VAD-FMK or z-LEHD-FMK. Cochlear sensory hair cells survived in animals that received gentamicin with z-VAD-FMK or z-LEHD-FMK, whereas sensory hair cells in animals that received only gentamicin were damaged. These results suggest that in vivo auditory cell death induced by gentamicin involves apoptosis via caspase activation.

183 The role of edaravone , a free radical scavenger ,against the peripheral vestibular disorder induced by streptomycin.

Kuniyoshi Tanaka, Hiroaki Shimogori, Osamu Horiike, Tsuyoshi Takemoto, Hiroshi Yamashita

Department of Otolaryngology, Yamaguchi University School of Medicine, Minamikogushi 1-1-1, Ube, Japan

Attempts were made to investigate the role of edaravone, an antioxidant agent clinically used, on the peripheral vestibular disorder induced by streptomycin. A tiny hole was made adjacent to the round window in the guinea pig right ear, and 30% streptomycin was infused through this hole by osmotic pump for 24 h. Infusion rate was set at 0.5 μ l/h. Eight animals received edaravone at a dose of 3 mg/kg i.p. once a day for 7 days after treatment (systemic application group). Six animals received the same amount of saline i.p. in the same manner (control group). In another 6 animals treated with streptomycin, edaravone-soaked gelform (3 mg/ml) was put on the round window membrane before wound closure (local application group). After treatment, spontaneous nystagmus and yaw head tilt were observed. No statistical difference was observed in the spontaneous nystagmus number or yaw head tilt between the systemic application and saline groups. In the local application group, spontaneous nystagmus numbers were statistically smaller than those in the systemic application group at 6, 9, 12, 18 and 24 h after treatment. Furthermore, in the local application group, yaw head tilt was also statistically smaller than that in the systemic application group at 6 h after treatment. These data indicate that topical application of edaravone may be useful to treat peripheral vestibular disorder induced by streptomycin.

184 Three Methods of Inner Ear Trophic Factor Delivery to Recover Vestibular Function and Morphology from Gentamicin-induced Vestibular Toxicity in the Guinea Pig

Gavin E Jones, Ronald L Jackson, Jianzhong Liu, Michael Costello, Xianxi Ge, John KM Coleman, Jared F Boasen, Elizabeth A Harper, Nancy E Kuzdak, Richard Dana Kopke

Otolaryngology, DOD Spatial Orientation Center, 34800 Bob Wilson Dr, San Diego, CA, United States

We reported (ARO 2003) that inner ears infused with brain-derived neurotrophic factor (BDNF), retinoic acid, insulin-like growth factor one and transforming growth factor-alpha demonstrated a significant recovery in vestibular function and a return of calyceal-hair cell (CHC) units after gentamicin ablation, especially when all four trophic factors (TFs) were in the infusate. Importantly, the presence of BDNF in the infusate was linked to a greater recovery of CHC units compared to the other TFs. Expanding on these findings, this study compares the efficacy of three inner ear delivery methods using our TF technology (all four TFs) on vestibular function and morphology after gentamicin ablation. The goal is to develop an inner ear delivery technique that may be used clinically which is less invasive and takes advantage of the round window membrane (RWM) as a portal to the inner ear. The three methods are: (1) a middle ear application onto the RWM of a fibrin glue containing growth factors, (2) the RWM

microcatheter connected to an osmotic pump which constantly applies TFs onto the membrane and (3) a microcannula-catheter pump system which passes directly through the RWM. Balance function was assessed by sinusoidal Earth-vertical axis rotation for semicircular canal function (horizontal vestibulo-ocular reflex - HVOR gain). Otolithic function was measured by constant 30 degrees off Earth-vertical axis rotation (OVAR) to determine gain (slow phase eye velocity modulation) and bias velocity (offset of slow phase eye velocity from zero velocity). Female albino guinea pigs were instilled bilaterally with transbullar gentamicin. One-week later animals received all four TFs in carrier vehicle via one of the three delivery methods. Controls received gentamicin then one of the delivery methods with only carrier vehicle. All animals were implanted with head fixation devices and scleral search coils, and balance function was tested on a rotational rate table 12 to 13 weeks after gentamicin. Balance function was within normal ranges for delivery of TFs for the RWM microcatheter but not for the fibrin-glue method. Early data for the microcannula approach is similar to the RWM microcatheter. All control gentamicin-only groups failed to reach normal balance function levels. (Funded by the Office of Naval Research)

185 Antioxidant Protection from Styrene-Induced Hearing Loss

Donald Henderson¹, Weiping Yang^{1,2}, Bohua Hu¹

¹*Department of Communication disorders and science, State University of NY at Buffalo, 215 Parker Hall, 3435 Main St., Buffalo, NY, United States,* ²*Institute of Otolaryngology, Chinese PLA General Hospital, Fu-Xing Road, Beijing, China, People's Republic of*

There is a growing awareness that certain industrial chemicals can cause hearing loss and positively interact with noise. Styrene has been reported to be ototoxic causing a mild to moderate hearing loss with degenerated OHCs in the middle turn of the cochlea. Given that noise and ototoxic drugs produce similar effects that can be partially prevented with antioxidant therapy, then it is reasonable to ask whether the effects of styrene can also be prevented with antioxidants. Twenty Long-Evans rats (450-550 grams) had their hearing estimated with brainstem-evoked potentials recorded in lightly anesthetized animals with a needle electrode. The 20 rats were divided into three groups: olive oil, styrene (400 mg/kg in 0.2 mL olive oil), styrene and L-NAC (325 mg/kg IP). Treatment was given for 5 days a week for 3 weeks and then hearing was remeasured and the cochleas were harvested and analyzed. The styrene treated rats developed an average of 19 dB threshold shift (N = 8), while the L-NAC/styrene group had an average of 2 dB threshold shift (N = 9). The cochleograms showed a broad loss for the styrene exposure of approximately 60 % of OHC missing while the L-NAC/styrene had approximately 20% missing hair cell loss. The results will be discussed in terms of the mechanism of styrene-induced pathology and how L-NAC may prevent it.

Supported by NIDCD P01-DC03600-1A1

186 Co-transfection of cochlear cultures with recombinant adenoviruses expressing calpastatin and NT-3 gene protects spiral ganglions from delayed neuron death

Ping Wang¹, Dalian Ding¹, Te-Chung Lee², Baodong Du³, Richard J. Salvi¹

¹Center for Hearing and Deafness, State University of New York at Buffalo, 3435 Main Street, Buffalo, NY, United States,

²Biochemistry, University of Buffalo, 3435 Main Street, Buffalo, New York, United States, ³Otolaryngology, University of Jilin, 1 Xinmin Street, Changchun, China, People's Republic of

Previous experimental studies suggest that two factors play important roles in delayed spiral ganglion neuron (SGN) death. One is the loss of neurotrophic factors and the other is activation of calcium activated proteases, or calpains. NT-3, a neurotrophic factor present in hair cells, appears to play an important role in SGN survival. Calpastatin, a calpain inhibitor, suppress calpains and protect neurons from injury-induced death. The purpose of this project was to determine if co-transfection of NT-3 gene and calpastatin could protect SGN from delayed neuron death arising from aminoglycoside-induced hair cell loss. We constructed two adenoviral vector, pAd/calpastatin and pAd/NT-3, using pAdeasy-1 system. Cochlear organotypic cultures were pre-transfected with Ad/calpastatin (1X10⁹VP/ml), Ad/NT-3 (1X10⁹VP/ml), or combination for 3 h. A model of delayed SGN death was developed by treating cochlear cultures with 2 mM gentamicin. SGN were immunolabeled with a primary antibody against the 200 kD neurofilament protein and TRITC-labeled secondary antibody. Gentamicin treatment resulted in destruction in of all hair cells after 24 h. Most SGN were present 1-day post-gentamicin treatment but most SGN had degenerated by 7 days post-treatment. A quantitative analysis showed that only 12.3% of SGN were present when cochlear were treated with gentamicin alone. SGN survival increased to 20.8% in the Ad/calpastatin / gentamicin group, 42.2% in the Ad/NT-3 / gentamicin group and 64.4% in the group treated with the combination of the two viral vectors. These results indicate that SGN survival from gentamicin treatment can be significantly enhanced by co-transfecting the cochlea with the combination of NT-3 and calpastatin.

187 DASPEI may block aminoglycoside-induced hair cell loss in the lateral line of zebrafish

Kelly N. Owens^{1,2}, Remy Pujol^{2,3}, Jameel Itani^{2,4}, Lisa Cunningham^{1,2}, Edwin W Rubel^{1,2}, David W. Raible^{2,4}

¹Otolaryngology-HNS, University of Washington, Box 357923, Seattle, WA, United States, ²Virginia Merrill Bloedel Hearing Research Center, University of Washington, Box 357923, Seattle, WA, United States, ³INSERM Unit 583, University of Montpellier 1, 71, Rue De Navacelles, Montpellier, France, ⁴Biological Structure, University of Washington, Box 357420, Seattle, WA, United States

Wildtype zebrafish larvae treated with neomycin for 1 hour followed by a 3 hour recovery exhibit loss of lateral line hair cells in a dose-dependent manner when monitored with the potentiometric vital dye DASPEI (Harris et al. 2003). We have examined the process of hair cell loss with a variety of protocols to study initial

neomycin-induced events. First, exposure and recovery time were shortened (30 min. neomycin exposure and 1 hour recovery with DASPEI staining in the final 15 min.). The short protocol resulted in a dose-dependent loss of hair cells akin to the original protocol, indicating that response to neomycin is quite rapid in this system. Second, animals were exposed to neomycin for 15 or 30 min., stained with DASPEI for 15 min. and immediately examined (no recovery). Even at relatively low concentrations of neomycin, we observed a reduction in DASPEI staining and some hair cells with ultrastructural changes, suggesting early apoptotic-like events. Animals treated with higher doses of neomycin for 15 or 30 min. with no recovery period exhibited an attenuated response, indicating that either neomycin action was not yet complete or that presence of DASPEI immediately following the neomycin exposure perturbed the action of neomycin. The third protocol is identical to the short protocol, except preceded by DASPEI staining for 15 min., and a 20 min. recovery and examination period. Neomycin exposure preceded by DASPEI pretreatment resulted in only partial reduction of DASPEI staining of hair cells. Similar levels of DASPEI staining are observed regardless of neomycin dose (using 0 – 200 μ M neomycin), indicating hair cells are present. This contrasts with the dose-dependent reduction in DASPEI staining observed with the short protocol alone (which differs only in the treatment prior to neomycin exposure) and suggests that DASPEI pretreatment can interfere with neomycin ototoxicity. Supported by NIDCD DC 05987, DC00018, DC04661 and Bloedel Traveling Scholars Program

188 Glutathione monoethyl ester (GSHe) protects auditory hair cells from 4-hydroxynonenal (HNE) induced-loss in organ of Corti explants

Jose W Ruiz, Jose Guzman, Thomas J Balkany, Thomas R Van De Water

Department of Otolaryngology, University of Miami, PO Box 016960 (D-48), Miami, FL, United States

Apoptosis of auditory hair cells (HC) is induced by insults such as sound trauma, hypoxia/ischemia, aminoglycosides, and chemotherapeutic agents that generate oxidative stress. These insults lead to production of reactive oxygen species (ROS) and free radicals, which interact with membrane phospholipids to produce a toxic aldehyde, 4-hydroxynonenal (HNE). Glutathione monoethyl ester (GSHe) can protect both auditory neurons and HC's from cisplatin-induced damage. Ebselen (EBS) mimics glutathione peroxidase and is reported in animal studies to be partially protective against acoustic trauma, gentamicin, and cisplatin induced ototoxicities.

The present study investigated the effectiveness of EBS and GSHe to protect organ of Corti explants from HNE. Four day-old rat organ of Corti explants were excised and placed on 0.4 μ m Millipore inserts with either control medium or medium containing either 15 μ M EBS or 10mM GSHe. The explants were incubated for 24 hrs and then 100, 200, or 400 μ M concentrations of HNE were added and explants were cultured for an additional 48 hrs. Parallel untreated control explants were cultured and after day 3 all organ of Corti explants were fixed in 4% paraformaldehyde then labeled with F-actin binding agent, FITC-phalloidin. Phalloidin labeled HCs were counted from basal, middle, and api-

cal segments of the explants. Control cultures showed almost no loss of HCs, while HNE exposed cultures all had large areas of significant HC destruction. GSHe provided a significant level of protection to HCs from HNE-induced loss in our in vitro model of stress induced HC loss.

Because HNE has been suggested to be a major toxic factor in many disease processes with oxidative stress, the current results suggest that GSHe will be an effective anti-apoptotic therapy for the treatment of the cochlea to prevent HC loss following an oxidative stress generating insult. Supported by a grant from Med El to TJB and TRV.

189 Transplantation of Mouse Embryonic Neural Stem Cells into the Cochlea of the Gerbil

Hainan Lang¹, Bradley A Schulte^{1,2}, Ling Wei², Michelle Hedrick², Richard A Schmiedt¹

¹Dept. of Otolaryngology-Head and Neck Surgery, Medical University of SC, 135 Rutledge Avenue, Charleston, SC, United States, ²Dept. of Pathology and Laboratory Medicine, Medical University of SC, 165 Ashley Avenue, Suite 309, Charleston, SC, United States

Transplantation of embryonic stem (ES) cells offers a potential strategy for repairing neural tissue (Wei et al, Stroke 34: 297, 2003). Here we examined the feasibility of ES cell transplantation in the ear. ES cells were differentiated using the 4-/4+ protocol in vitro. To identify ES cells after transplantation, the cells were marked with green fluorescent protein and pre-labeled with BrdU and Hoechst. The ES cells were transferred into either normal ears or ears deafened by prior exposure to ouabain which results in profound auditory neuropathy (Schmiedt et al., JARO 03: 223-233). A volume of 2-3 µl with a cell density of 3-4 x 10⁷ cells/ml was injected through the round window membrane. Three of four normal ears showed ES cell survival in the scala tympani, scala vestibuli and vestibular labyrinth. ES cell survival had no effect on distortion product otoacoustic emissions (DPOAEs), auditory-nerve compound action potential (CAP) thresholds or endocochlear potentials (EP) at 7-10 days after transplantation. In one normal ear along the basal turn, ES cells were found under the tectorial membrane adjacent to the limbus in the inner sulcus and again were associated with no functional loss. In another cochlea, stem cells were present in the spiral ligament of the basal turn and had migrated superiorly to the region just lateral to the spiral prominence and outer sulcus. In this ear there was a 20-30 dB loss in CAP thresholds at 16-20 kHz, a 20-30 mV decline in the EP and a decrease in DPOAEs at 16-20 kHz possibly owing to injection trauma. ES cells were never seen in the scala media. In fact, there was a dramatic loss of DPOAEs, CAP thresholds and EP after scala media penetration with the injection pipette. The ouabain-treated gerbils are currently under investigation.

Supported by NIH/NIA 14748, NIH/NIDCD 00713, NIH/NS 37373, NIH/NS 045155 and AHA-Burgher Award 0170063N.

190 The histone deacetylase inhibitor sodium butyrate ameliorates cisplatin-induced hearing loss in guinea pigs

David W Roberson^{1,2}, Marie Drottler¹, Rajiv Ratan³, M Charles Liberman⁴

¹Otolaryngology, Children's Hospital Boston, 300 Longwood Ave, Boston, MA, United States, ²Otology and Laryngology, Harvard University, 243 Charles Street, Boston, MA, United States, ³Neurology, Beth Israel Deaconess Hospital, 77 Avenue Louis Pasteur, Boston, MA, United States, ⁴Otology and Laryngology, Harvard University, 243 Charles St., Boston, MA, United States

A number of agents ameliorate cisplatin-induced hearing loss, including sodium thiosulfate, N-acetylcysteine and methionine (Doolittle et al., Clin Can Res 7:493; Fegahl et al., Laryngoscope 111:1147; Li et al., NeuroToxicology 22:163). Most are antioxidants, and systemic administration in humans might interfere with the tumoricidal effect of cisplatin. We sought to identify an agent that could be otoprotective without compromising anti-cancer effect. Histone deacetylase (HDAC) inhibitors are a unique class of anti-cancer agents that are also neuroprotective. Their anti-cancer effect is due to interference with cell cycle (Vigushin & Coombes, Anti-Cancer Drugs 13:1). Their neuroprotective effect is likely via a different mechanism (Ryu et al., PNAS 100:4281). We hypothesized that these agents might be otoprotective and, if so, would be candidate agents for otoprotection in humans receiving high dose cisplatin. Female Hartley Albino guinea pigs were treated with 1.2 gm/kg sodium butyrate IP for 12 days. Control animals received an equal volume of saline IP. On day 5, 14 mg/kg cisplatin was given IP. Outer hair cell (OHC) function was assessed with evoked distortion product otoacoustic emissions before and after treatment, and threshold shifts were averaged from 3500 to 14000 Hz. The average threshold shift in animals receiving saline "protection" was 7.1 dB and in animals receiving butyrate protection 2.8 dB (p = 0.03 by 2-way ANOVA). We conclude that sodium butyrate is effective in ameliorating cisplatin-induced OHC damage in guinea pigs, and may hold promise as an otoprotective agent in humans.

191 A novel drug delivery system into the inner ear

Tsuyoshi Endo¹, Takayuki Nakagawa¹, Tomoko Kita^{1,2}, Fukuichiro Iguchi¹, Tae-Soo Kim¹, Tetsuya Tamura¹, Yasushi Naito¹, Yasushi Tabata³, Juichi Ito¹

¹Department of Otolaryngology, Head and Neck Surgery, Kyoto university, 54 Kawahara-cho Shogoin Sakyo-ku, Kyoto, Japan, ²Horizontal Medical Research Organization, Kyoto university, 54 Kawahara-cho Shogoin Sakyo-ku, Kyoto, Japan, ³Institute for Frontier Medical Science, Kyoto university, 54 Kawahara-cho Shogoin Sakyo-ku, Kyoto, Japan

<Introduction> Recent studies have demonstrated that neurotrophic factors not only maintain survival of auditory neurons, but that these surviving neurons retain functionality. However, a sustained delivery system for application of neurotrophins is desirable compared with a single administration. The aim of this study was to develop a sustained delivery system for application of neurotrophins into the inner ear. We used a new material, the biodegradable gel, for this purpose. <Material and methods>

Guinea pigs were used as experimental animals. For confirmation of drug delivery from middle ear to inner ear, the otic bulla of guinea pigs was opened for exposure of the round window. A piece of biodegradable gel immersed with BDNF was put on the round window membrane. Control animals were received a single injection of BDNF at the same dose through the cochlear lateral wall. Three days later, the perilymph of animals was collected and concentrations of BDNF in the perilymph were assessed by an enzyme-linked immunosorbent assay (ELISA). For confirmation of BDNF gel protective effects against ototoxic treatment, we performed 2nd examination. At day 1, we gave kanamycin and Ethacrinic acid as ototoxic treatment. At day 18, A piece of biodegradable gel immersed with BDNF was put on the round window membrane. Control animals were given physiologic saline on the round window membrane. At day 21 and 25, we performed EABR. At day 25, we performed histological analysis for protection of SGs. <Results and Conclusion> The concentrations of BDNF in the perilymph collected from animals treated with a biodegradable gel were significantly higher than those collected from animals received a single injection. 2nd examination showed that there are significant difference in thresholds of EABR and density of SGNs between both groups. Present findings indicate that the biodegradable gel is a useful material for sustained delivery of nerutrophins to the inner ear.

192 A Three-Dimensional Model of Substance Distribution in the Cochlea after Round Window Application

Stefan KR Plontke¹, Alec N Salt², Raimund Wegener³, Hans-Peter Zenner¹, Norbert Siedow³

¹Dept. of Otorhinolaryngology, Tübingen Hearing Research Center (THRC), University of Tübingen, E.-Aulhorn-Str. 5, Tübingen, Germany, ²Dept. of Otolaryngology, Washington University in St. Louis, 660 South Euclid Avenue, St. Louis, MO, United States, ³Fraunhofer Institute, of Industrial Mathematics, Gottlieb-Daimler-Str. 49, Kaiserslautern, Germany

Delivering drugs to the inner ear by applying them to the round window membrane is increasingly being used to treat inner ear disorders. Computer simulations provide a valuable tool to evaluate application protocols and drug delivery systems, and to extrapolate from animal studies to the larger cochlea of the human.

A three-dimensional model of the cochlea was constructed taking geometric dimensions from the guinea pig cochlea. Drug propagation along and between compartments was described by passive diffusion. A three-dimensional model was implemented in a commercial software package for finite-element calculations (ANSYS). Typical results for 3D computations of different delivery strategies showed very different concentration time courses, peak concentrations and apical-basal concentration gradients similar to what has been shown in computer simulations using an established one-dimensional model.

In order to compare predictions from the three-dimensional and one-dimensional models, a general approach of dimensionality was developed. Testing of this general approach for a variety of examples showed a good correspondence for the two models at least for small objects and fast diffusion processes. Using this approach, a one-dimensional model corresponding to the initially

described three-dimensional model was derived.

Extensive testing of the three-dimensional model and comparison of the simulations after dimensionality reduction is now required. It is of special interest to determine the influence of cochlear characteristics such as the relatively large cross-sectional area of the basal turn and the curved nature of the cochlea on the simulations. Also, the effect of different delivery scenarios, especially brief intratympanic applications, needs to be evaluated.

This work was supported by a grants from ZEBET/BfR (Germany) to SKRP and NIDCD (DC01368) to ANS. We thank S. Pereverzyev and K. Tatman for their assistance with the simulations.

193 Microdialysis for studying pharmacokinetics in the inner ear and interpretation of results using a finite element model

Hartmut Hahn¹, Stefan KR Plontke¹, Alec N Salt², Hans-Peter Zenner¹

¹Dept. of Otorhinolaryngology, Tübingen Hearing Research Center (THRC), University of Tübingen, E.-Aulhorn-Str. 5, Tübingen, Germany, ²Dept. of Otolaryngology, Washington University in St. Louis, 660 South Euclid Avenue, St. Louis, MO, United States

Microdialysis can efficiently be applied to the recovery of drugs from inner ear fluids after topical administration to the round window membrane (RWM). The advantages of microdialysis for pharmacokinetic studies include, 1) the use of repeated measurements, 2) prevention of artifacts from perilymph volume loss through leaks, and 3) less disturbance of perilymph due to the low amount of drug recovery.

The aim of this study was to critically analyze the influence of microdialysis on the substance concentrations in small fluid spaces, to correct for artifacts due to microdialysis by the means of a finite element model and to derive the concentration time course of a clinically relevant drug, Dexamethasone, in the guinea pig cochlea after RWM application.

In vitro experiments, sodium fluorescein was continuously recovered from vessels of 1ml, 100µl, 10µl and 5.6µl, the last volume resembling scala tympani volume in the guinea pig (4.8µl). When measured in 1ml volumes (n=8) constant fluorescein levels could be observed over the total time period whereas a decrease in the concentration was detectable in 100µl (n=9), 10µl (n=13) and 5.6µl vessels (n=11). With a finite-element-computer-model (<http://oto.wustl.edu/cochlea>) these data could be simulated considering the actual microdialysis parameters of the experiment, e.g. dimensions of the reservoirs, recovery and perfusion rates and molecular weight of the dye. In vivo experiments fluorescein and/or dexamethasone were applied continuously to the RWM and recovered from scala tympani using microdialysis. The measured values were corrected using the model which allowed us to better estimate the actual concentration-time course and clearance rates from the cochlea.

The fact that microdialysis itself also contributes to the clearance of a drug from the cochlea needs to be considered when interpreting pharmacokinetic studies using microdialysis in vivo.

Supported by University of Tübingen fortune-project no: 1001-0-0 (SKRP)

194 Responses of the Endolymphatic Sac to Perilymphatic Pressure Manipulations Suggest the Presence of a One-way Valve.

Alec N. Salt¹, Helge Rask-Andersen²

¹Otolaryngology, Washington University Medical School, 660 South Euclid, St. Louis, MO, United States, ²Otolaryngology, University Hospital of Uppsala, 751 85, Uppsala, Sweden

It has not been well established what situations result in endolymph movements to or from the endolymphatic sac (ES). In a prior study, we showed with ES recordings that changes of luminal K⁺, Na⁺ and endolymphatic sac potential (ESP) could be induced by manipulations of endolymph volume in the cochlea (Salt and DeMott, 2000, *Hear. Res.* 149, 46). The direction of change was opposite for injections and withdrawals of fluid, suggesting that endolymph movements could occur in either direction. We have now studied the influence of perilymphatic manipulations on K⁺ and ESP changes in the ES of guinea pigs. Although perilymph withdrawals caused K⁺ and ESP reductions, the majority of perilymph injections did not induce measurable changes in the ES. Pressure measurements from the ES showed that transmission of labyrinthine pressures to the sac lumen was directionally sensitive, with negative pressures transmitted more effectively than positive ones. These physiologic data suggest that the endolymphatic duct is closed in most animals when pressure in the vestibule is increased. Anatomic study of the region where the endolymphatic duct enters the vestibule shows that the wall of the membranous sinus of the endolymphatic duct could collapse against the bony wall during pressure applications. This would close the entrance to the endolymphatic duct and act as a mechanical one-way valve, restricting flow of endolymph from the saccule to the ES. The endolymphatic sinus could potentially play an important role in detecting and compensating for abnormal endolymph volume states.

This study was supported by NIDCD RO1 DC01368 (AS) and the Swedish Research Council, VR Project 3908 (HR).

195 Evaluation of a Novel Method for Sampling Scala Tympani Perilymph by Collecting Fluid from the Cochlear Apex.

Alec N. Salt, Shane A. Hale

Otolaryngology, Washington University Medical School, 660 South Euclid, St. Louis, MO, United States

The collection of cochlear perilymph samples is technically difficult. A widely used method is to aspirate samples through the round window (RW) membrane. This can result in contamination of the sample with high levels of cerebrospinal fluid (CSF) due to the proximity of the sampling site to the cochlear aqueduct. To increase the proportion of perilymph in the sample, it appeared logical to take samples at a location further away from the cochlear aqueduct. We therefore developed a technique for sampling scala tympani (ST) perilymph from the apex of the cochlea.

The goal was to perforate the cochlear apex and collect all the fluid that emerged. To achieve this, a "cup" was constructed around the intact apex with silicone adhesive. When the apex was perforated, positive intracochlear pressure caused a fluid bead to form within the silicone cup. The fluid was drawn by capillary action into a cal-

ibrated glass pipette. We evaluated the method using the marker ion trimethylphenylammonium (TMPA). TMPA was applied to perilymph either by RW irrigation or by microinjection into the apical turn. The TMPA concentration of a 10 μ L sample obtained by apical sampling was compared with that measured in perilymph by a TMPA-selective electrode prior to taking the sample. Data were interpreted with a finite element model of the cochlear fluids that was used to simulate each aspect of the experiment. The results were consistent with the sample being composed of more than 97 % of the TMPA from ST perilymph, diluted with CSF. The sample concentration can be corrected for the CSF dilution based on the known ST volume, which has been estimated to be 4.7 μ L.

This method of sampling from the apex is technically straightforward and provides a greater proportion of perilymph in the sample than does sampling through the RW.

This study was supported by NIDCD RO1 DC01368.

196 Ouabain-induced vacuole formation in marginal cells in the stria vascularis is dependent on perilymphatic Na⁺

Kasumi Higashiyama, Shunji Takeuchi, Hiroshi Azuma, Taizo Takeda

Otolaryngology, Kochi Medical School, Okocho-Kohasu, Nankoku, Japan

The activity of Na⁺-K⁺-ATPase in the basolateral membrane of marginal cells in the stria vascularis is high. Ouabain, an inhibitor of Na⁺-K⁺-ATPase, causes not only a decline in the endocochlear potential (EP) but also acute vacuolar changes in the stria vascularis (Bosher, 1980, *Acta Otolaryngol* 90: 219-229, Marcus et al., 1981, *Hear Res* 4: 149-160). Our electron microscopic study revealed that ouabain-induced vacuoles were membrane-coated vesicles. Accordingly, we speculated that ion transport may underlie this vacuole formation and examined the role of perilymphatic Na⁺ for this morphological change. Guinea pigs were anesthetized and perilymphatic perfusion was performed from the scala tympani of the basal turn to the scala vestibuli of the basal turn at a flow rate of 10 μ L/min. The EP was measured from the second turn. Morphological changes in the stria vascularis of the second turn were examined by transmission electron microscopy. Perilymphatic perfusion with a control perfusate did not cause apparent changes in both the EP and the stria morphology. Perilymphatic perfusion with 1 mM ouabain dissolved in the control perfusate for 50 min caused a decline in the EP to approximately -40 mV and many vesicles of a wide range of sizes in marginal cells. In addition, bulging of marginal cells into the scala media was observed. Perilymphatic perfusion with a Na⁺-free perfusate for 30 min caused a decline in the EP by 15-30 mV. Perilymphatic perfusion with the Na⁺-free perfusate followed by additional 50-min perfusion with 1mM ouabain (dissolved in the Na⁺-free perfusate) caused a decline in the EP to approximately -30 mV but not the vacuolar changes in marginal cells. These results indicate that perilymphatic Na⁺ is responsible for this morphological change, and suggest that Na⁺ transporters may exist in the membrane of vacuoles.

197 The Effects of Leupeptin on the Inner Ear of the Chinchilla

Michael E. Hoffer^{1,2}, J. Clay Finley¹, Peter Killian¹, Kim R. Gottshall¹, Derin Wester¹, Carey D. Balaban³

¹Otolaryngology, Naval Medical Center San Diego, 34800 BobWilson Dr., San Diego, CA, United States, ²Naval Medical Center San Diego, Department of Defense Spatial Orientation Center, 34800 BobWilson Dr., San Diego, CA, United States, ³Otolaryngology, University of Pittsburgh, 203 Lothrop Street, Pittsburgh, PA, United States

Calpains are naturally occurring calcium-activated cysteine proteases. Calpain activation has been demonstrated to play an active role in a number of pathological neurodegenerative conditions and in neurological damage following anoxic or traumatic brain injury. Calpain-antagonists have been demonstrated to be neuroprotective and reduce damage that occurs after a variety of acquired traumatic or anoxic brain injuries. A number of studies have demonstrated that calpain inhibitors may protect neurons of the inner ear from toxic damage, as well. Leupeptin is a newly developed calpain inhibitor. It has been suggested that this drug may be an excellent candidate medicine to treat toxic damage of the inner ear. One of the important issues with the use of calpain inhibitors is the route of administration. Systemic administration of the medicine may produce unwanted side effects, so that local administration of the medicine may offer the safest and most efficacious route to treat inner ear damage. Our lab has been active in studying the effects of medicines on the inner ear via middle ear administration. To date we have not studied the effects of locally administered calpain inhibitors on the inner ear. In this study, we report the effects of leupeptin administration on the inner ear via a middle ear sustained release device. We describe several audiological testing paradigms allowing us to measure the sensorineural hearing loss in our Chinchilla model and to account for the conductive hearing loss induced by the presence of the sustained release device. We report the effects of the medicine on sensorineural hearing and balance function at 4 hours, 24 hours, 48 hours, 72 hours, and seven days after administration. In order to effectively utilize new classes of medicines to treat inner ear disorders, proper methods of administration and the effects of this administration on normal ears must be studied in detail. This study begins to answer some important basic and clinically relevant questions with regards to calpain inhibitors.

198 Increased Expression of Alpha Subunit of Epithelial Sodium Channel (α -ENaC) and of SGK Can Account for Therapeutic Action of Glucocorticoids in Meniere's Disease

Daniel C. Marcus, Satyanarayana R. Pondugula, Joel Sanneman, Nithyanandhini Raveendran

Anatomy & Physiology, Kansas State University, 228 Coles Hall, Manhattan, KS, United States

We have previously shown that SCCD epithelium secretes Cl⁻ under control of cAMP [Milhaud et al., *Am. J. Physiol.*, 2002] and absorbs Na⁺ under control of glucocorticoids [Pondugula et al., *ARO* 2003]. We sought to determine whether glucocorticoids up- or down-regulated expression of genes involved in Na⁺ transport in

SCCD cells by employing microarray technology. Primary cultures of SCCD cells were grown to confluence on 6.5 mm diameter permeable supports prepared as before and the amiloride-sensitive short circuit current was found to be markedly increased after exposure to 100 nM dexamethasone (DEX) for 24 hours. mRNA was extracted from monolayers exposed to DEX and from those cultured without added steroid. The quality and quantity of mRNA was assessed with an Agilent 2100 BioAnalyzer and processed for use with Affymetrix rat230A/B chip sets after 2-times amplification with an *in vitro* transcription protocol. DEX-treated cultures were found to up regulate transcript levels of the α subunit of ENaC but not β and γ subunits. This result was verified by quantitative RT-PCR using gene-specific primers for α , β and γ ENaC subunits. It is thought that α -ENaC is a limiting constituent that acts as a chaperone for the other subunits in trafficking to the apical plasma membrane [May et al., *J Am Soc Nephrol.*, 1997]. Preliminary gene array analysis also showed an up-regulation of sgk, whose corresponding protein increases the amount of ENaC retained in the plasma membrane. These results are consistent with genomic regulation by DEX of short circuit current across SCCD epithelium by increase in the level of α -ENaC in the apical membrane. Water would passively follow the active sodium extrusion from endolymph. We conclude that increased sodium absorption by SCCD cells can account for the clinical observation that glucocorticoid administration leads to reductions in episodes of vertigo in Meniere's patients [Barrs et al., *Laryngoscope*, 2001]. Supported by NIH NIDCD R01-DC00212.

199 CFTR Chloride Channels Mediate cAMP-stimulated Secretion by Semicircular Canal Duct Epithelial Cells

Satya R. Pondugula, Joel Sanneman, Julie A. Long, Nithyanandhini Raveendran, Daniel C. Marcus

Anatomy & Physiology, Kansas State University, 228 Coles Hall, Manhattan, KS, United States

Semicircular canal duct epithelial cells (SCCD) contribute to the homeostasis of vestibular endolymphatic ion composition by secretion of Cl⁻ under adrenergic control via cAMP [Milhaud PG et al., 2002]. This epithelium is also capable of absorbing Na⁺ under glucocorticoid stimulation [Pondugula et al., *ARO* 2003, 2004]. We sought to determine whether Cl⁻ secretion by SCCD epithelium was mediated by CFTR, a cAMP-regulated Cl⁻ channel. SCCD cells of neonatal rats were cultured to confluence on permeable supports and equivalent short circuit current (I_{sc}) was measured. Forskolin (FSK; 10 μ M) an activator of adenylyl cyclase and 8-Br-cAMP (500 μ M) stimulated I_{sc} as did the nonselective phosphodiesterase (PDE) inhibitor IBMX (250 μ M) and selective cAMP-specific PDE-4 inhibitor R0-20-1724 (100 μ M) inhibitor, demonstrating constitutive activity of adenylyl cyclase. Expression of PDE-4 was shown by preliminary gene array experiments. Stimulation by FSK was greater after 20 h exposure to natural and synthetic glucocorticoids. Adenylyl cyclase-stimulated I_{sc} was partially inhibited by bumetanide, a blocker of Na₂Cl₂K-cotransport. Apical addition of genistein (Gen; 30 μ M) stimulated I_{sc} after prior stimulation with sub maximal concentrations of FSK but not after full stimulation of AC. This response to genistein is often taken as evidence for mediation of Cl⁻ secretion by CFTR. Both gene microarray analysis and RT-PCR demonstrated the

presence of transcripts for CFTR in SCCD. Further, a specific inhibitor of CFTR (CFTRinh-172 [5 μ M; Ma T et al., 2002]) decreased I_{sc} significantly. These results all support the proposition that CFTR Cl channels provide at least part of the molecular basis for anion secretion across the apical cell membrane of SCCD epithelium. Preliminary gene array experiments revealed expression of other Cl channel transcripts, but none of these are known to be activated by cAMP. Supported by NIH R01-DC212.

200 Sodium Absorption by Semicircular Canal Duct (SCCD) Epithelium via ENaC is Stimulated by Glucocorticoids

Satyanarayana R. Pondugula, Joel Sanneman, Daniel C. Marcus

Anatomy & Physiology, Kansas State University, 228 Coles Hall, Manhattan, KS, United States

We sought to determine whether SCCD are capable of cation absorption in response to corticosteroids in addition to the known secretion of Cl⁻ stimulated by cAMP. SCCD cells of neonatal rats were cultured to confluence on permeable supports and used to measure equivalent short circuit current (I_{sc}) in an Ussing chamber. Further, the expression of ENaC subunits was investigated using RT-PCR. Dexamethasone (DEX), hydrocortisone (HC), corticosterone (CORT) and aldosterone (ALDO) increased I_{sc} over a 7–24 h interval. The time course is consistent with genomic regulation of I_{sc}. I_{sc} was blocked and resistance increased by apical amiloride (AMIL; IC₅₀: 0.5 μ M) and benzamil (IC₅₀: 55 nM) but not EIPA. DEX, HC, CORT and ALDO stimulated AMIL-sensitive I_{sc} with an EC₅₀ of 12, 13, 31 and 106 nM respectively. The effective concentrations of DEX are within the therapeutic plasma concentration range (0.05–0.1 μ M after I/V administration of 5 mg of DEX) and of HC & CORT are within the physiological range of plasma concentration (0.1–0.6 μ M & 0.1–1 μ M). Transcripts for α , β & γ -ENaC subunits were found in both untreated and dexamethasone-treated conditions. Observation of about 20 % of AMIL-sensitive I_{sc} when either apical Na⁺ was replaced with K⁺ or under *in vivo*-like conditions is consistent with K⁺ transport via ENaC. DEX, HC and ALDO stimulated I_{sc} was inhibited by the glucocorticoid receptor (GR) antagonist RU-486 but not by the mineralocorticoid receptor antagonist spironolactone, suggesting stimulation of I_{sc} by activation of GR. Furthermore, AMIL did not prevent stimulation of I_{sc} by forskolin. We conclude that SCCD contribute to the homeostasis of endolymph by GR-stimulated transport of Na⁺ via ENaC in addition to β_2 -adrenergic receptor-coupled Cl⁻ transport. These results can account for the therapeutic action of glucocorticoids in the treatment of vertigo associated with Meniere's Disease. Supported by NIH NIDCD R01-DC212.

201 Loss of KCNJ10 protein expression abolishes endocochlear potential and causes deafness in Pendred syndrome mouse model

Philine Wangemann¹, Erin M Itza¹, Beatrice Albrecht¹, Tao Wu¹, Sairam V Jabba¹, Rajanikanth J Maganti¹, Jun Ho Lee¹, Lorraine A Everett², Susan M Wall³, Ines E Royaux², Eric D Green², Daniel C Marcus¹

¹*Anatomy & Physiology, Kansas State University, 1600 Denison Ave, Manhattan, KS, United States.* ²*Genome Technology Branch, NHGRI, NIH, 31 Center Drive, MSC 2033, Bethesda, MD, United States.* ³*Renal Division, Emory University, School of Medicine, Atlanta, GA, United States*

Pendred syndrome, a common autosomal-recessive disorder characterized by congenital deafness and goiter, is caused by mutations of SLC26A4, which codes for pendrin. In this study we focused on the relationship between pendrin and deafness using mice that have (Slc26a4^{+/+}) or lack a complete Slc26a4 gene (Slc26a4^{-/-}). Pendrin was found in the cochlea in the apical membranes of spiral prominence cells and spindle-shaped cells of stria vascularis, in outer sulcus and root cells. Endolymph volume in Slc26a4^{-/-} mice was enlarged and tissue masses in areas normally occupied by type I and II fibrocytes were reduced. Slc26a4^{-/-} mice lacked the endocochlear potential, which is generated across the basal cell barrier by the K⁺ channel KCNJ10 expressed in intermediate cells. The basal cell barrier appeared intact, intermediate cells and KCNJ10 mRNA were present but KCNJ10 protein was absent. Endolymphatic K⁺ concentrations were normal and membrane proteins necessary for K⁺ secretion were present including the K⁺ channel KCNQ1 and KCNE1, Na⁺/2Cl⁻/K⁺ cotransporter SLC12A2 and the gap junction GJB2. These observations demonstrate that pendrin dysfunction leads to a loss of KCNJ10 protein expression and a loss of the endocochlear potential, which may be associated with, if not the cause of, deafness in Pendred syndrome.

202 The immunohistochemical analysis of pendrin in the mouse inner ear

Takahiko Yoshino¹, Eisuke Sato¹, Tsutomu Nakashima¹, Michihiko Sone¹, Atsuo Nakayama²

¹*Otolaryngology, University of Nagoya, 65, Tsurumai-cho, Showa-ku, Nagoya, Japan.* ²*pathology 1, University of Nagoya, 65, Tsurumai-cho, Showa-ku, Nagoya, Japan*

Pendred's syndrome (PS) is an autosomal recessive disorder characterized by deafness and goiter, which is caused by mutations in the Pendred's syndrome gene (PDS) (SLC26A4). PDS encodes a membrane protein named pendrin and is considered to act as an anion transporter. Expression pattern of the PDS ortholog (Pds) mRNA in the developing auditory and vestibular systems in mice was previously reported. But the localization of pendrin was not confirmed. We generated antipeptide antibodies against the human pendrin (amino acid 766-780, EELDVQDEAMRTIAS). We performed Western blot analysis about human thyroid and mouse tissue samples to confirm the detection of pendrin. Then we performed immunohistochemical analysis in the mouse inner ears. We detected pendrin in the endolymphatic duct and sac, utricle, saccule, and external sulcus, confirming the expression patterns of mRNA. The most pronounced pendrin expression was seen in the apical membrane of endolymphatic duct and sac, which are

thought to absorb the endolymphatic fluid. This suggests that pendrin plays a role of endolymph absorption. The other expressed regions are thought to secrete the endolymphatic fluid. In addition, we detected pendrin in Hensen cells and Claudius cells which are also thought to concern the regulation of endolymphatic fluid. They suggest that pendrin has an important role in this regulation as an anion transporter. In this study, we detected pendrin in spiral ganglion of cochlea. Further detailed studies of ganglion cells will be necessary. These studies provide key toward defining the role of pendrin for inner ear development and elucidating the pathogenic mechanisms underlying the deafness in PS.

203 Immunolocalization of vacuolar H⁺-ATPase a4 subunit, Pendrin and Carbonic Anhydrase 2 and AE2 in the mouse inner ear

Hongwei Dou¹, Jie Ling², Zhaohui Wang², John Greinwald¹, Manoocher Soleimani³, Fiona Karet⁴, Seth Alper⁵, Daniel Choo¹

¹Otolaryngology, center for hearing and deafness research, 3333 burnet avenue, cincinnati, ohio, United States, ²medicine, university of cincinnati, 231 albert sabin way, cincinnati, ohio, United States, ³medicine, cincinnati VA medical center, 3200 vine street, cincinnati, ohio, United States, ⁴human genetics, MRC Institute, Wellcome Trust/MRC Building, Addenbrooke's Hospital, Hills Road, Cambridge CB2 2XY, United Kingdom, ⁵medicine, harvard medical school, 330 Brookline Avenue, boston, Massachusetts, United States

The development and maintenance of a proper endolymph environment is critical to the normal functioning of the inner ear. The endolymphatic sac (ES) has long been proposed to play a role in this process by regulating the volume and composition of endolymph through its resorption and secretion capacities. The luminal fluid of the ES has a pH of 6.6 to 7. Maintaining ES luminal acidity is thought to be important for the normal function of the ES. The acid-base regulation mechanisms of the ES are unknown. In this study, we investigated the expression patterns of acid-base regulators, including vacuolar (v)H⁺-ATPase, anion Cl⁻/HCO₃⁻ exchanger, carbonic anhydrase II (CAII) and pendrin (Pds) in the ES epithelium by immunohistochemistry. We demonstrated that the proton pump and Pds located at the apical membrane in selected ES cells. Anion exchanger AE2 was expressed homogeneously at the basolateral membrane of all ES cells. We also found that proton pump- and Pds-expressing ES cells also expressed cytosolic CAII. Co-expression of proton pump, Pds and CAII in selected ES cells suggest that special ES cells are responsible for the acid-base regulation of the endolymph in the ES.

204 A Novel Pattern of Cadherin 23 Expression

Ayala Lagziel¹, Zubair M Ahmed^{1,2}, Julie M Schultz¹, Robert J Morell¹, Thomas B Friedman¹, Inna A Belyantseva¹

¹Laboratory of Molecular Genetics, National Institute on Deafness and Other Communication Disorders National Institute of Health, 5 Research Ct., Rockville, MD, United States, ²CEMB, The Punjab University, Canal Bank Rd., Lahore, Pakistan

CDH23 mutant alleles are associated with syndromic (*USH1D*) or isolated deafness (*DFNB12*) in humans (Bork et al. 2001, Bolz et

al. 2001) and in waltzer mice (Di Palma et al. 2001). We previously reported the two isoforms of *CDH23* (with and without exon 68). Presently, we are characterizing novel transcripts of *CDH23* and are refining the cellular and subcellular localization of cadherin 23 in the mouse inner ear. Consistent with previous studies, we found cadherin 23 localized to inner ear hair cell stereocilia and Reissner's membrane. Here we report a new location for cadherin 23 in the auditory and vestibular hair cell kinocilia. In waltzer mice hair cell stereocilia are disorganized and the kinocilium is misplaced. A single kinocilium accompanies a stereocilia bundle on each hair cell. The kinocilium is associated with establishment of the polarity of hair cell stereocilia bundle and is presumably involved in stereocilia regeneration. In the mouse organ of Corti (OC), kinocilia are no longer present after postnatal day 10 (P10). But in the vestibule, kinocilia persist through adulthood, as does the capacity of vestibular hair cells to regenerate. In both the OC and vestibule, as visualized by immunocytochemistry, cadherin 23 appears first in stereocilia, and later in kinocilia. Cadherin 23 stereocilia staining is lost by P30, at a time when all OC and majority of vestibular hair cells have matured. However, when cadherin 23 is no longer detected in vestibular hair cell stereocilia, it persists in kinocilia. Moreover, we detected cadherin 23 expression in hair cell kinocilia of chick basilar papilla and frog macula. In summary, the transient mode of expression of cadherin 23, and its localization in the kinocilium of different species suggest evolutionary conserved roles in hair bundle development and establishment of polarity of hair cell bundles and possibly in vestibular stereocilia regeneration.

205 PCDH15 splice variant and immunolocalization of protocadherin 15 in the inner ear

Zubair M Ahmed^{1,2}, Saima Riazuddin¹, Sheikh Riazuddin², Edward R Wilcox¹, Thomas B Friedman¹, Inna A Belyantseva¹

¹Section on Human Genetics, Laboratory of Molecular Genetics, NIDCD/NIH, 5 Research court, Rockville, Maryland, United States, ²CEMB, The Punjab University, Canal Bank Road, Lahore, Pakistan

Congenital profound deafness, retinitis pigmentosa and vestibular areflexia are the hallmarks of Usher syndrome type I (USH1). There are seven loci for USH1 and genes for five of them have been identified. Mutant alleles of *PCDH15* are responsible for USH1 linked to the *USH1F* locus (Ahmed et al. 2001) as well as nonsyndromic recessive deafness *DFNB23* (Ahmed et al. submitted). The Ames waltzer (*av*) phenotype is due to a recessive mutation of *Pcdh15* (Alagramam et al. 2001). Our next objective was a functional dissection of *PCDH15*. (1) Northern blot analyses of *PCDH15/Pcdh15* demonstrated alternate splice transcripts (3.5 kb, 5.5 kb and 8.0 kb). We characterize the 3.5 kb transcript (isoform B) using human retina cDNA. The translation start codon of isoform B is in an unreported exon downstream of all known *av* mutations. (2) Using an antibody raised against a cytoplasmic domain (exon 33-common to both isoforms), protocadherin 15 was detected in the wild type mouse inner ear along the length of hair cell stereocilia between the actin core and stereocilia membrane, but the tips of stereocilia were devoid of staining. A similar pattern of stereocilia staining was observed in vestibular hair cells

of the cristae ampullares and maculae of the utricle and saccule. The distribution and developmental pattern of protocadherin 15 in stereocilia of inner ear hair cells, taken together with the known function of protocadherins in cell adhesion, suggest that at least one of the protocadherin 15 isoforms may participate in the development and maintenance of the lateral links, the fine strands interconnecting the sides of adjacent stereocilia.

206 Identification of Myosin VI-Binding Partners in the Inner Ear

Tama Sobe¹, Irit Gottfried¹, Ronna Hertzano¹, Vanessa Walsh², Mary-Claire King², Karen B. Avraham¹

¹*Dept. of Human Genetics and Molecular Medicine, Sackler School of Medicine, Tel Aviv University, Tel Aviv, Israel,*

²*Departments of Medicine and Genome Sciences, University of Washington, 1959 NE Pacific St., Seattle, WA, United States*

Mutations in the molecular motor myosin VI are associated with human and mouse deafness. Myosin VI is involved in endocytosis and trafficking in both non-sensory and sensory cells. A number of proteins that interact with myosin VI have been identified recently, including GIPC, DAB2 and SAP97. However, nothing is known regarding the role of these proteins in the inner ear, nor have myosin VI-binding partners been found by directly screening inner ear tissue. We constructed a yeast two-hybrid library expressing inner ear proteins to search for myosin VI-interacting partners, using sensory epithelia as the starting material to enrich for proteins specific to the various cell types within the organ of Corti. We screened the library using a portion of the myosin VI tail as bait and identified several new and known myosin VI partners, including GIPC, a PDZ-domain protein that is a component of a G protein-coupled signaling complex involved in regulating vesicular trafficking. We confirmed the interaction of myosin VI with new binding partners and examined their localization in the inner ear, as well as in myosin VI-null Snell's waltzer mice. Fuller characterization of the myosin VI partners in the inner ear will provide a more complete global picture of the network of this critical motor, particularly as it relates to auditory and vestibular dysfunction. We will also identify additional proteins essential for inner ear function and perhaps associated with human deafness as well.

207 Defining Myosin-1c Interactions with Stereociliary Receptors

Kelli R. Phillips^{1,2}, Song Tong^{1,3}, Janet L. Cyr^{1,3}

¹*Sensory Neuroscience Research Center, West Virginia University School of Medicine, 1 Medical Center Drive, Morgantown, WV, United States,*

²*Dept. of Biochemistry and Molecular Pharmacology, West Virginia University School of Medicine, 1 Medical Center Drive, Morgantown, WV, United States,* ³*Dept. of Otolaryngology, West Virginia University School of Medicine, 1 Medical Center Drive, Morgantown, WV, United States*

Myosin-1c (Myo1c) is essential to mechanotransduction in vestibular hair cells where it powers the process of slow adaptation. As the adaptation motor, Myo1c must interact with other components of the transduction apparatus. To examine these interactions we employ an *in situ* binding assay in which recombinant Myo1c protein fragments are allowed to bind to intracellular hair-cell receptors. Using this assay, Myo1c fragments containing the

first two IQ domains (IQ1 and IQ2) of its neck region were shown to interact with receptors at the tips of stereocilia, the site of hair-cell transduction. This portion of Myo1c also binds calmodulin (CaM), and excess CaM has been shown to disrupt Myo1c interactions with stereociliary receptors. It is our goal to further describe these interactions.

A cross-species sequence analysis of the IQ domains of Myo1c reveals a high degree of identity in IQ2. The observed conservation is unlikely to be required only for CaM binding. Therefore, we predict that IQ2 may also bind to Myo1c receptors and that CaM blocks receptor interaction by binding to IQ2 and masking the receptor interaction site. Furthermore, we predict that CaM bound at IQ1 also plays a role in receptor binding. To explore the role of CaM in Myo1c's interactions with stereociliary receptors, we have created recombinant Myo1c protein fragments with mutations in the IQ consensus sequences of IQ1 and IQ2. The capacity of the purified fragments to interact with stereociliary receptors in the presence and absence of excess CaM has been evaluated. Myo1c fragments mutated within IQ2 bind to intracellular receptors. As predicted, this interaction is not blocked by the addition of excess CaM. These data implicate IQ2 in receptor interactions and suggest that the binding of CaM to this domain may regulate these interactions. Currently, the role of IQ1 is being explored in similar studies.

This work is supported by the American Hearing Research Foundation.

208 Understanding Myosins in Fish Hair Cells: Zebrafish are Only Part of the Story

Allison B Coffin¹, Arthur N Popper¹, Matthew Kelley²

¹*Department of Biology, University of Maryland, Biology-Psychology Bldg, College Park, MD, United States,* ²*Section on Developmental Neuroscience, National Institute on Deafness and Other Communication Disorders, 31 Center Drive, Bethesda, MD, United States*

Unconventional myosins VI and VIIa have been implicated in some forms of human hereditary deafness. Research in mice shows that a mutation in either gene causes severe hair bundle pathology. Recently, work in inner ear myosins has expanded to include the zebrafish (*Danio rerio*), an organism amenable to developmental studies and genetic manipulation. In order to fully understand the phenotype of mutant zebrafish such as *mariner* (a myosin VIIa mutant) we must first understand myosin structure and function in wild-type animals. This begins by examining gene expression and protein distribution of myosins VI and VIIa within the zebrafish inner ear. Using reverse transcription-polymerase chain reaction we showed that mRNA for both myosins is expressed in the zebrafish inner ear. We then used indirect immunofluorescence to show that within the zebrafish inner ear, myosin VI and VIIa proteins are expressed exclusively in hair cells. Confocal imaging revealed that both proteins are distributed throughout the hair bundles and in the cell body cytoplasm of hair cells in all inner ear epithelia. We then compared myosin distribution between inner ears of several fish species. If these proteins play critical roles in hair bundle structure and function, and if all fish hair cells are homogenous, we would expect to see identical protein distribution patterns in all fish ears. Surprisingly, myosin VI distribution differs between utricular hair cells of the zebrafish and other fishes such as American shad

(*Alosa sapidissima*) and lake sturgeon (*Acipenser fulvescens*). These differences highlight the structural and functional heterogeneity of fish hair cells. Furthermore, this finding suggests that a better understanding of unconventional myosin function may be achieved through comparative studies between fishes that differ in hair cell myosin distribution.

209 Structure of the stereocilia side links and morphology of auditory hair bundle in relation to noise exposure

Vladimir Tsuprun, Patricia Schachern, Sebahattin Cureoglu, Michael Paparella

Otolaryngology, University of Minnesota, 2001 Sixth Str. S.E., Minneapolis, MN, United States

The structure of the stereocilia side links and morphology of auditory hair bundle in relation to noise exposure in the chinchilla was investigated by transmission electron microscopy. The outer hair cell (OHC) stereocilia side link was suggested to consist of extracellular, membrane-bound regions and thin filaments. Two beaded filaments were folded at their distal ends and fastened in one globule in the center between stereocilia. An intracellular, submembrane layer appeared to form a bridge between the actin core and the extracellular, membrane-bound region of the side links. In normal physiological conditions, most OHC stereocilia had a regular distribution of side links, forming a 'zipper-like' lattice between stereocilium shafts. Side links of the inner hair cell (IHC) stereocilia have similar filamentous appearance, but were observed less commonly and had decreased structural organization than those of the OHC stereocilia. Different patterns of stereocilia interconnections in normal animals were found to correlate with morphological changes of stereocilia bundles in acoustic trauma. Ultrastructural analysis of OHC and IHC stereocilia showed that a large number of the side links could survive narrow-band (1-2 kHz) acoustic stimulation of 114 dB SPL for 2 hrs or 123 dB SPL for 15 min. Disarray, separation, close attachment and fusion of stereocilia were more frequently observed for IHC stereocilia and OHC stereocilia that were poorly connected or that lacked side links, consistent with an important role of the side links in maintaining bundle integrity and prevention of stereocilia fusion. Most disarrayed OHC and IHC stereocilia recovered to a normal erect state with restored orientation of the side links after 14-28 days, which correlated with partial recovery of auditory sensitivity. However, direct attachments of plasma membranes, ruptured links, fusion and blebs were seen on some stereocilia even after 28 days and appear to be permanent. Close apposition and disruption of stereociliary membranes was found to precede their fusion to one continuous membrane surrounding several stereocilia.

210 Mechano-Electrical Transduction of Outer Hair Cells Studied in a Gerbil Hemicochlea

David ZZ He, Shuping Jia

Dept. of Biomedical Sciences, Creighton University, 2500 California Plaza, Omaha, NE, United States

Mammalian cochlear hair cells respond to basilar member vibration by producing a receptor potential. The first step towards the generation of the receptor potential is the deflection of the hair bundle, and the subsequent flow of transducer currents through the

mechanosensitive transducer channels on the tip of stereocilia. Although the mechano-electrical or forward, transduction in non-mammalian and mammalian vestibular hair cells has been well studied, the forward transduction in adult cochlear outer hair cells (OHCs) has not been fully explored, primarily because of technical difficulties. We recorded OHC transducer currents, receptor potentials, and basilar membrane motion in a more in vivo-like and relatively intact preparation, the hemicochlea. Hemicochlea was prepared from 25- to 30-day-old gerbils using a standard vibratome. Transducer currents (or receptor potentials) were recorded from OHCs under whole-cell patch-clamp condition during basilar membrane vibration evoked by a vibrating glass paddle. Basilar membrane motion was simultaneously measured using a photodiode-based measurement system. Our results show that motion of the basilar membrane toward the scala vestibuli generated a large inward current. The current saturated around 200 pA for a basilar membrane motion of 300 nm at 100 Hz in the apex. The basilar membrane motion was largely linear between 50 and 300 nm although some asymmetry was observed. The current, reversing polarity between 0 and 10 mV, was blocked by streptomycin. Removal of intracellular Cl⁻ had no effect on the transducer current. Supported by NIH grants R21 DC 06039 and R01 DC 04696 from the NIDCD.

211 Impulse responses of the cupula in the fish lateral line

Branislava Curcic, Sietse van Netten

Neurobiophysics, University of Groningen, Nijenborgh 4, Groningen, Netherlands

Natural stimuli that deflect the cupula and bundles of the hair cells deviate from the narrow frequency stimuli, which are commonly used to investigate the peripheral lateral line organ. In order to investigate the time characteristics of this organ, we measured cupular responses to a pulse stimulus. This approach provides direct information on timing, speed and sensitivity of the system under *in vivo* conditions. The information obtained in this way is not necessarily the same as that acquired from measurements of cupular frequency responses, as the cupula is known to behave nonlinearly due to the mechanical gating apparatus of the hair cells (van Netten and Khanna, 1994, PNAS, 91, 1549-53).

Experiments were performed on neuromasts in the supra-orbital lateral line canal of the ruffe (*Gymnocephalus cernuus*; $n = 8$). Cupulae were stimulated with a sphere producing either a step or a sinusoidal displacement (100-300 nm) of the local fluid flow past the cupula. The motion of the cupula was measured with a laser interferometer microscope.

The cupular displacement response to fluid displacement pulses shows the behavior of a damped oscillator with a series of peaks (P1, P2...). P1 follows the fluid step without significant time delay. P2 occurs at 4.1 ± 1.7 ms after P1, in the opposite direction, with an amplitude of 40.5 ± 16.8 % of that of P1. P3 occurs at 12.7 ± 5.5 ms after P1, in the fluid step direction, with an amplitude of 16.7 ± 8.2 % of that of P1. The resonance frequency (140 ± 70 Hz), and the quality factor (1.77 ± 0.53) determined from these time responses are comparable to those found from directly measured frequency responses. A detailed comparison of frequency characteristics obtained from FFT's of the pulse responses and directly measured frequency responses also did not show signifi-

cant differences. This indicates that the gating spring non-linearities do not severely affect the responses of the system for the range of stimulus intensities that we used.

212 Internalization of plasma membrane Ca^{2+} -ATPase 2 (PMCA2) from rat cochlea hair cell stereocilia plasma membrane

M'hamed Grati, Robert J. Wenthold

Lab of Neurochemistry, NIDCD/NIH, 50 South Drive, Bethesda, MD, United States

Hair cells are polarized epithelial cells. Their non-permeable tight junctional belt separates their plasma membrane (PM) into two distinct domains: the apical PM including the membrane of the mechanosensory hair bundle, and the basolateral membrane, which includes the afferent and efferent synaptic regions. The regulation of protein delivery to both PM domains is poorly understood. To investigate apical membrane protein trafficking in hair cells, we are studying recycling of plasma membrane Ca^{2+} -ATPase-2 (PMCA2); PMCA2 is highly expressed in the cochlea and the vestibule hair cell-stereocilia. For this study, we generated two polyclonal antibodies against a peptide from the extracellular loop of the protein. PMCA2 is exclusively apically targeted into the hair bundle of the outer and inner hair cells of the cochlea with a higher abundance in the outer hair cells, forming distinct clusters uniformly distributed along the membrane of the stereocilia. After 1 hour of antibody-antigen binding in live cochlea explants in serum free medium, fixation, permeabilization and staining of the specimens, we were able to image an abundant internalization of this stereocilia membrane component in both inner and outer hair cells. The internalized protein is associated with vesicles located close to the apical PM in the pericuticular necklace predominantly to the side of the taller stereocilia, and in the infracuticular space above the nucleus in multivesicular body-like structures. Some fractions of the internalized protein were colocalized with early endosome and trans-Golgi compartment markers. Finally, in a few experiments where we extended the internalization course to 2 hours, a sub-fraction of the recycled proteins were found in the canalicular reticulum network in the apical pole. Our imaging data show no translocation of the internalized protein to the synaptic pole of the hair cells during the first two hours of internalization.

213 Control of Wnt5a signaling in the developing inner ear by Shh

Wei Liu¹, Robert Kang¹, Geming Li¹, Lijun Li¹, Eric Bergson¹, **Dorothy A. Frenz**²

¹Otolaryngology, Albert Einstein College of Medicine, 1410 Pelham Parkway South, Bronx, New York, United States,

²Otolaryngology and Anatomy & Structural Biology, Albert Einstein College of Medicine, 1410 Pelham Parkway South, Bronx, New York, United States

The mammalian inner ear is a complex sensory organ that develops in response to a series of inductive tissue interactions. The precise molecular mechanisms which control these interactions are not yet fully understood. However, increasing evidence indicates that evolutionary conserved signaling pathways involved in tissue patterning and morphogenesis participate in regulation of inner ear development. The Wnt gene family comprises a class of signaling

molecules that mediate inductive interactions between neighboring cells and that elicit a diverse range of cellular responses during embryonic development. Previous studies in our laboratory have demonstrated the expression of Wnt5a, both at the protein and gene level, in the developing mouse inner ear. This study tests the function of Wnt5a in signaling of the epithelial-mesenchymal interactions that guide inner ear development. Our findings demonstrate that blocking of endogenous Wnt5a in high density culture with Wnt5a specific antisense oligonucleotide suppresses otic epithelial-periotic mesenchymal interactions. To begin to ascertain if cooperative interactions between Wnt5a and other signaling pathways specify inner ear morphogenesis, the relationship between Wnt5a and Sonic hedgehog (Shh), a signaling molecule known to mediate inner ear development, was investigated. Supplementation of cultured periotic mesenchyme containing otic epithelium with exogenous Shh peptide (10 ng/ml) resulted in a marked increase in immunolabeling for endogenous Wnt5a. Consistent with this finding, immunostaining for Wnt5a was markedly diminished in the developing inner ear in mice with a targeted mutation of the Shh gene. Our findings support Wnt5a as a mediator of otic epithelial-periotic mesenchymal interactions in the developing inner ear, and suggest that signaling by Wnt5a may be controlled by the Shh signaling pathway.

214 Expression of Nkx6.1 and Olig Transcription Factors in the Developing Inner Ear

Paul J Chestovich, Heather L Aloor, Takako Kondo, Eri Hashino

Otolaryngology-HNS, Indiana University School of Medicine, 699 West Drive, RR132, Indianapolis, IN, United States

Nkx6.1 homeodomain transcription factor and its downstream targets, Olig bHLH transcription factors, play essential roles in cell fate specification in the spinal cord. However, little is known about the functions of these transcription factors in inner ear development. To gain insights into their novel functions, we investigated the expression of Nkx6.1, Olig1, Olig2 and Olig3 mRNAs in the developing mouse inner ear using quantitative RT-PCR. As these genes are known to be expressed in the developing spinal cord, spinal cord tissue was used as a positive control. A high level of Nkx6.1 mRNA expression was detected in the otocyst as early as E9, and the expression level remained high throughout the developmental stages tested (E9 to P20). Expression of Olig1 and Olig2 mRNAs was barely detectable, only 1.6% and 0.1% of the Nkx6.1 mRNA level, respectively in the E10 otocyst. Their expression levels remained very low throughout development. In contrast, Olig3 mRNA expression was high, approximately 25% of the Nkx6.1 mRNA level, at early developmental stages (E9-10). The expression level of Olig3, however, declined sharply after E10. The early onset of Nkx6.1 and Olig3 expression in the otocyst suggests their potential roles in early developmental events, such as neural cell fate specification and Schwann cell differentiation. Since Nkx6.1 expression is induced by Sonic hedgehog (Shh) signaling, the results also suggest that Shh-mediated neurogenesis in the otocyst is controlled, at least in part, by Nkx6.1 and/or Olig3 functions. The temporal expression of Olig3 in contrast with the continued expression of Nkx6.1 suggests the existence of another upstream effector that down-regulates Olig3. In situ hybridization experi-

ments are currently underway to determine cellular sites in the inner ear that express Nkx6.1 and Olig3 transcripts.

Supported by NIH R21DC005507 and T32DC000012

215 The Effect of Retinoic Acid on Transforming Growth Factor Beta Signal Transduction During Inner Ear Development

Sydney C. Butts¹, Wei Liu¹, Dorothy A. Frenz²

¹Otolaryngology, Albert Einstein College of Medicine, 1410 Pelham Parkway South, Bronx, New York, United States,

²Otolaryngology and Anatomy and Structural Biology, Albert Einstein College of Medicine, 1410 Pelham Parkway South, Bronx, New York, United States

all-trans Retinoic Acid (atRA) exposure during mouse embryonic development leads to malformations of the epithelial and mesenchymal derived tissues that form the inner ear. Transforming Growth Factor Beta-1 (TGFB-1) is an important mediator of the communication between these tissues and guides the inductive effects of the otic epithelium on the adjacent mesenchyme. Disruption of this signaling has been shown to lead to inner ear malformations in a mouse model. Mice exposed to atRA early in development demonstrated marked decreases in the expression of TGFB-1 compared to control animals. Phenotypically, the otocyst and peri-otic mesenchyme showed developmental arrest, with no specializations characteristic of the normal inner ear.

We propose that in addition to its effect on TGFB-1, atRA also disrupts signaling by down-regulating expression of the TGFB receptor found on target mesenchymal cells. Immunohistochemical staining was done on inner ear specimens from control mice and from mice exposed to atRA on embryonic day nine which were then sacrificed on E10.5, 12, 13 and 14. There was a marked decrease in staining for the receptor in the peri-otic mesenchyme of atRA exposed mice compared to controls.

Disruptions in TGFB signaling may also occur downstream of these events. Smad proteins are the intracellular substrates of the TGFB receptor, a homodimer that is a serine/threonine kinase. Smad2 is the primary substrate of the TGFB receptor and localizes to the nucleus after phosphorylation to act as a transcription factor. Preliminary studies have shown a decrease in Smad2 expression in atRA exposed mice. To quantify the protein levels in these animals, Western blot analysis is being used with antibodies specific for Smad2 and for the TGFB receptor protein type II. Our data suggest that there are multiple disruption points in TGFB signaling as a result of atRA exposure during inner ear development.

216 β -catenin distribution in the developing cochlea of mice.

Shinji Takebayashi¹, Takayuki Nakagawa¹, Ken Kojima¹, Tae-Soo Kim¹, Tomko Kita^{1,2}, Tsuyoshi Endo¹, Fukuichiro Iguchi¹, Norio Yamamoto¹, Yasushi Naito¹, Juichi Ito¹

¹Otolaryngology, Head and Neck surgery, Kyoto University, Sakyo-ku Shogoinkawahara-cho 54, Kyoto, Japan, ²Horizontal Medical Research Organization, Kyoto University, Sakyo-ku Shogoin, Kyoto, Japan

Introduction: Once hair cells are damaged, it is difficult to regenerate them. One reason for this is the very strictly regulated cell

cycle. If we could regulate this cell cycle, it might be possible to regenerate hair cells. In recent studies, numerous proteins regulating cell proliferation have been found. β -catenin activates cyclin D and c-myc, which participate in cell proliferation and differentiation. In addition, β -catenin plays a role in morphogenesis, since it binds to the cytoplasmic domain of E-cadherin. In this study, we evaluated the expression patterns of β -catenin in the cochlea during the development of normal mice to elucidate the function of β -catenin.

Materials and Methods: ICR mouse inner ear tissues at embryonic day 9 (E9), E10, E12, E14, E17, and postnatal day 7 (P7) were used as experimental specimens. Immunohistochemistry for β -catenin and phospho- β -catenin was performed. Ki67 was used as a proliferating cell marker. Myosin7a was used as a hair cell marker.

Results and Conclusions: β -catenin expression was observed not only throughout the cell membranes of the E10 developing otic epithelial cells but also in the nuclei of them, and phospho- β -catenin expression was detected in the soma of them. This suggests that β -catenin is overproduced and plays a role in cell proliferation of the developing otocyst.

The shift in distribution of β -catenin expression patterns during the maturation of the cochlea. β -catenin expression was mostly observed on the apical side in the E14 cochlea, and accumulated around hair cells and medial areas of greater epithelial ridge (GER) at E17. Though β -catenin expression was observed around pillar cells after birth, it gradually disappeared from the hair cells and GER. Since the distribution of expression patterns of β -catenin was changed during the maturation, β -catenin may be concerned with the maturation of the cochlea.

217 Effect of Extracellular Matrix Composition on Cell Migration from the Early Otocyst

Dawn Davies

Physiology, University of Bristol, School of Medical Sciences, University Walk, Bristol, United Kingdom

Neural precursors migrate from the antero-ventral aspect of the otocyst early in development to form the cochlear-vestibular ganglion (CVG). Previous studies have shown growth factor mediation of neuroblast migration (Hossain and Morest, 2000, *J. Neurosci. Res.* 62, 40-55); however, little is known about cell-cell and cell-substrate interactions involved in this process. I have previously shown a decrease in expression of members of the integrin family of cell adhesion molecules associated with cell migration from the otocyst (Davies and Holley, 2002, *J. Comp. Neurol.* 445, 122-132), suggesting that modulation of these receptors and/or their extracellular matrix (ECM) ligands may be involved in CVG formation.

The aim of this study was to investigate whether ECM influences cell migration from the early otocyst. At embryonic day (E)10, fibronectin (FN), laminin 1 (LM1) and collagen IV (CollIV) were expressed in the basement membrane of the developing murine otocyst, as assessed by immunohistochemistry. In addition, expression of FN extended into the surrounding mesenchyme. In areas of neuroblast migration, the basement membrane was disrupted as shown by disorganised and punctate ECM immunostaining. Cell migration from murine E10 otocyst explants plated onto

purified ECM components exhibited marked differences depending on the substrate. On FN, large numbers of migrating cells were observed emerging from the explant within 24hrs of plating. The majority of these cells had a fibroblast-like morphology although some polar cells were evident. In contrast, both LM1 and CollIV supported more modest levels of migration. Cells on these substrates were more likely to migrate as single cells and exhibited a polar morphology. This suggests that the substrate may influence migrating cell type. Future work will concentrate on the integrin receptors involved in these cell-substrate interactions.

218 The expression pattern and subcellular localization of Musashi-1 in developing mouse inner ear

Hirofumi Sakaguchi¹, Toshihiro Suzuki¹, Takeshi Yaoi², Hideyuki Okano³, Shinji Fushiki², Yasuo Hisa¹

¹Department of Otolaryngology, Kyoto Prefectural University of Medicine, 465 Kajii-cho, Kyoto, Japan, ²Department of Pathology and Applied Neurobiology, Kyoto Prefectural University of Medicine, 465 Kajii-cho, Kyoto, Japan, ³Department of Physiology, Keio University School of Medicine, Shinjuku-ku, Tokyo, Japan

Musashi1 (Msi1) is an RNA binding protein highly expressed in embryonic neural progenitor cells and adult neural stem cells. Msi1 activates Notch signal via translational repression of a Notch antagonist, m-Numb, which one of the targets of Msi1 encodes. In mammalian central nervous system, Notch signaling contributes to maintain the undifferentiated state and the renewal ability of the progenitor cells and the stem cells. In mammalian cochlea, hair cells and supporting cells originates from the same progenitor cells and Notch signaling has been shown to play a role in cell fate determination of hair cells and supporting cells. Inhibition of Notch signal prevents the differentiation of supporting cells and leads to an increase in number of hair cells. We, therefore, expected that an activator of Notch signal, Msi1, may be involving in the differentiation of hair cells and supporting cells. In this study, we examined the expression of Msi1 in the mouse developing inner ear (at embryonic days (E)10-adult) by immunohistochemistry using monoclonal antibody against Msi1. A monoclonal antibody revealed that Msi1 is expressed in Cochleo-vestibular ganglion cells and in all cells in developing sensory epithelium before hair cells appeared at E14. Selective loss of Msi-1 immunoreactivity is observed in vestibular hair cells after E14 and in cochlear hair cells after E16. The timing of this selective loss appears to correspond with the production of hair cells by terminal mitosis. On the other hand, Msi-1 expression in cochlear and vestibular supporting cells is maintained from E14 to adult except for transient decrease of the expression in Hensen's cells during E16-P0. Moreover, it is noteworthy that, during the first 2weeks after birth, Msi1 is progressively translocated from cytoplasm to nucleus in all of Msi1-positive cells. These data suggest that Msi1 could involve in maturation as well as differentiation of supporting cells in the inner ear.

219 Expression of Hes1 and Musashi1 in the Inner Ear of Developing and Adult Mice

Junko Murata¹, Ayako Murayama², Arata Horii¹, Katsumi Doi¹, Tamotsu Harada³, Hideyuki Okano², Takeshi Kubo¹

¹Department of Otolaryngology, Osaka University Medical School, 2-2 Yamadaoka, Suita, Japan, ²Department of Physiology, Keio University School of Medicine, 35 Shinanomachi, Shinjuku, Japan, ³Department of Otolaryngology, Kawasaki Medical School, 35 Matsushima, Kurashiki, Japan

Musashi1 (Msi1) is a neural RNA-binding protein expressed in neural stem/progenitor cells, astroglial progenitor cells and astrocytes in the central nervous system. Thus, Msi1 is considered one of the neural stem cell markers. It has also been demonstrated recently that Msi1 could activate CSL-dependent Notch pathway (Imai T et al., Mol. Cell. Biol., 2001). Notch lateral inhibition, which has a function in CNS development, is thought to play an important role in hair cell (HC) differentiation during embryonic period. After passing through terminal mitosis, some cells in the sensory epithelium of the cochlea begin to express Jagged2 and to activate Notch1 in the adjacent cells, which are to develop as supporting cells (SCs), at least partially through the function of Hes1. Jagged2-expressing cells will become HCs. Previously, we demonstrated that Msi1 was expressed in SCs, but not in HCs of young adult mouse inner ear by immunohistochemistry using monoclonal antibody against Msi1 (Murata J et al., ARO Abstr., 2003). In the present study, we investigated Msi1 and Hes1 expression in the sensory epithelia of developing and adult mouse inner ear. Msi1 was expressed in SCs not in HCs of the organ of Corti, both at P7 and P32. Hes1 immunostaininhg was also found only in SCs in the organ of Corti at P7, however it was found mainly in HCs at P32 stage. In utricular and saccular maculae, both Msi1 and Hes1 immunostainigs existed in SCs and only Hes1 reactive product was found in some of the HCs at P7. In these otoconial organs of P32, the staining of Msi1 disappeared, and the strong immunostaining of Hes1 was found in HCs. In the mammalian inner ear, especially in the adult cochlea, HC regeneration from SCs has been supposed to be strictly inhibited. Our result implies that Notch lateral inhibition may function for this quiescent state of the sensory epithelium by direct CSL-mediated activation of GFAP promoter, and the transcriptional activation of Hes1 is not involved.

220 Expression of platelet derived growth factors in the developing cochlea of rats

Yun Woo Lee¹, Massashi Ozeki², Steven K Juhn¹, Jizhen Lin²

¹Otolaryngology, Univ. of Minnesota, 2001 6th St. S.E., Minneapolis, Minnesota, United States, ²Otolaryngology, Univ. of Minnesota, 2001 6th St. S.E., Minneapolis, Minnesota, United States

Platelet-derived growth factor (PDGF) is involved in the control of cell proliferation, differentiation and survival in various tissues of vertebrates. However, little is known about the expression of PDGF in the developing cochlea of rodents. In this study, we examined the expression of PDGF family genes in the developing cochlear tissue of rats using microarrays and tested their role in the proliferation of progenitor hair cells using cellular and molecular

biology techniques. It was found that the genes for PDGF-A, PDGFR-a and PDGFR-b were highly expressed in the rapidly growing otocyst on embryonic day 12-14 (E12-E14) and weakly expressed thereafter. Reverse transcription polymer chain reaction (RT-PCR) demonstrated the expression of PDGF-C and confirmed the expression of PDGF-A, PDGFR-a and PDGFR-b in the developing cochlear tissue of rats and the cultured progenitor hair cells. Inhibition of PDGFs expression in the cultured progenitor hair cells with antisense oligonucleotides reduced the DNA synthesis, suggesting that the PDGFs and their receptors play a role in the proliferation of the developing cochlear hair cells.

221 Developmental Regulation of the Mouse Semicircular Canals: the Role of *Fam3c*

Valentina V. Pilipenko, Alisa Reece, Daniel I. Choo, John H. Greinwald, Jr.

Otolaryngology, Center for Hearing and Deafness Research, 3333 Burnet Ave., Cincinnati, OH, United States

The molecular mechanisms of inner ear semicircular canal development are poorly understood. In the mouse model, few genes are known to regulate the development of the semicircular canals. These include the cytokines *Bmp2*, *Bmp4*, and the *Wnt* family of genes and transcription factors in the *Dlx*, *Otx*, *Prx*, and *Nkx/Hmx* family of genes. Using *in situ* hybridization we identified a novel mouse gene, *Fam3c*, that is expressed at embryonic days 14 (E14) and E16 in areas of the developing semicircular canals. At these stages all 3 semicircular canals are formed but still have a thick outer epithelial rim that is rapidly proliferating. In addition, *Fam3c* was also expressed in the brain and nonsensory epithelium of the vestibule (E14/16) and the cochlea postnatal day 8 (P8). *Fam3c* showed an eccentric pattern of expression that overlapped with proliferating epithelium of the developing semicircular canals. At E18 and P8, no *Fam3c* mRNA signal was detected in the semicircular canals. We examined the spatial and temporal patterns of *Fam3c* expression in comparison with other genes known to be involved in the developing inner ear and specifically the semicircular canals. We found concurrent expression of *Fam3c* with *Dlx5*, which suggests a possible role for *Fam3c* in semicircular canal embryogenesis.

222 Morphological changes and apoptosis disturbance induced by retinoic acid in the mouse craniofacial embryogenesis

Toru Sasaki¹, Toshio Ishibashi², Kimitaka Kaga¹

¹*Department of Otolaryngology, University of Tokyo, 7-3-1, Hongo, Bunkyo-ku, Tokyo, Japan*, ²*Department of Otolaryngology, Social Insurance Central General Hospital, 3-22-1, Hyakunin-cho, Shinjuku-ku, Tokyo, Japan*

Retinoic acid (RA) is a derivative of vitamin A with potent teratogenicity and it causes miscellaneous malformations when administered to mammals during pregnancy. In this study, we administered RA to pregnant mice in order to observe morphological changes and the apoptosis disturbance in the craniofacial region by way of TUNEL method. ICR mice were mated overnight and the morning of vaginal plug occurrence was designated as E0 (embryonic day 0). Pregnant mice were injected single doses of 12.5mg/kg all-trans-RA dissolved in soybean oil intraperitoneally

on E7. Control pregnant mice, injected soybean oil without RA, were prepared as well. Mice were sacrificed on E9 and fetuses were obtained from the uteri and prepared for examination. The fetuses were first examined for macroscopic malformations, photographed and fixed in formaldehyde for histological preparations. The specimens were sectioned at a thickness of 5µm. TUNEL positive-cells were observed with particular attention to the otocyst, the first and second branchial arches, and surrounding mesenchyme. In RA fetuses, TUNEL positive cells were seen mainly in ventral part of both otocysts and bilateral first branchial grooves. The sites corresponding to future trigeminal ganglions presented small clusters of TUNEL positive cells. In the control fetuses, TUNEL positive cells were not seen in the otocysts. The apoptosis disturbance early in the pregnancy is possibly related to the malformations caused by RA.

223 Altered Gene Expression in the Developing Kreisler Inner Ear

daniel choo¹, alisa lynn reece¹, jaye ward¹, zhengshi lin², hongwei dou¹, john greinwald¹

¹*Otolaryngology, center for hearing and deafness research, 3333 burnet avenue, cincinnati, ohio, United States*, ²*Lab of Molecular Biology, NIDCD, 5 research court, rockville, MD, United States*

The kreisler mouse has been identified as an x-ray induced strain with hindbrain and inner ear defects resulting from mutation of the kreisler or mafB gene; a zinc finger, leucine zipper transcription factor. The inner ears are grossly malformed with semicircular canal abnormalities as well as poorly differentiated cochleas. Of particular interest to us is the failure of kreisler mice to form an endolymphatic duct and sac. Given the importance of these structures to normal inner ear fluid homeostasis as well as the significance of the endolymphatic duct and sac to pathologic conditions such as meniere's disease, we sought to examine the molecular processes involved in development of the mouse endolymphatic duct and sac. We performed *in situ* hybridization experiments on kreisler embryos using riboprobes for a battery of genes including *Gbx2*, *Dlx5*, *Wnt2b*, *Msx1*, *EphA4*, *Pax2*, *Bmp4*, *Pds*, *Trp2* and others. These data indicate that *Gbx2* and *Wnt2b* are downregulated as a result of kreisler mutation while expression of *Dlx5*, *Pax2*, *EphA4* and others are unaffected in kreisler mutants. Later in development, gene expression patterns suggest that overall patterning of the inner ear is disrupted in kreisler. In the abnormal vestibular portions of mutant embryos, *Bmp4* expression is noted in odd, scattered patches of cells suggesting that some sensory cell formation still occurs. In the dilated and uncoiled cochleas, expression of lateral wall markers such as *Trp2* and *Pds* are noted in aberrant relative positions. Our data indicate that genes such as *Gbx2* and *Wnt2b* are involved in a kreisler signaling pathway that is somehow involved in guiding endolymphatic duct and sac morphogenesis. Interestingly, other genes such as *Dlx5* (the mutant of which also fails to develop an endolymphatic duct and sac) is unaffected. We discuss the possible epistatic relationships in this signaling pathway and the potentially complex gene interactions involved in this mouse mutant.

224 Abnormal development of semicircular canal and otoconia in head tossing mice

Seung-Ha Oh¹, Chan-Ho Hwang², Yong-Ho Park¹, Ji-Young Park¹, Jun-Beom Park¹, Chang-Woo Song³, Sun-O Chang¹, Chong-Sun Kim¹

¹Otolaryngology, Seoul National University, College of Medicine, 28 Yeongon-dong, Chongno-gu, Seoul, Korea, Republic of,

²Otolaryngology, Dong-A University, College of Medicine, 3-1, Dongdaeshin-dong, Seo-gu, Busan, Korea, Republic of, ³Mutant mouse laboratory, Korea Research Institute of Chemical Technology, P.O. BOX 107, Yusong, Taejon, Korea, Republic of

Phenotypic characterization from chemical mutagenesis is a promising method for revealing gene function. In the previous study, we analyzed the ENU mutant mice that show autosomal recessive hereditary pattern and abnormal behavior, like head tossing and circling movement. The major anomalies in this mutant were an undeveloped posterior semicircular canal and abnormal shape of otolith. In present study, we intended to observe the abnormal development of inner ear using paint injection. Apoptotic changes of embryo were also examined using immunocytochemistry. Paint injection of different stage of embryo indicates that the membranous labyrinth of posterior canal stops to develop at 13 embryologic days. In order to analyze the change of otolith shape and size according to the age, we performed SEM study on both macula sacculi and macula utriculi at different ages. The shape and size of otolith are highly variable regardless of its age and we could not find a specific pattern of those. The sizes of otolith is about 4.5 ~ 160 µm in utricle and 6.5 ~ 98 µm in saccule. However the number of otolith is always fewer in utricle than in saccule. This may consist with the fact that this mutant has more severe anomaly in pars superior than pars inferior.

225 The Homeobox gene *Emx2* underlies Middle Ear and Inner Ear Defects in the Deaf Mouse Mutant Pardon

Charlotte Rebecca Rhodes¹, Nicholas Parkinson², Hsun Tsai², Debra Brooker², Siobhan Mansell², Nigel Spurr³, A Jackie Hunter³, Steve M Brown², Karen P Steel¹

¹MRC, Institute of Hearing Research, University Park, Nottingham, United Kingdom, ²MRC, Mammalian Genetics Unit, Harwell Business Centre, Didcot, United Kingdom,

³GlaxoSmithKline Pharmaceuticals, GlaxoSmithKline, New Frontiers Science Park, Harlow, United Kingdom

The dominant mouse mutation Pardon (*Pdo*) was isolated due to the lack of a Preyer reflex (ear flick) in response to sound from a large-scale ENU mutagenesis programme (Nolan *et al.*, 2000). Dissection of the middle ear revealed malformations in all three ossicles, rendering the ossicular chain incomplete. Examination of homozygote ossicles revealed the complete absence of the incus. Hair cell counts in the apical turn of the organ of Corti revealed a significant 22.7% increase of outer hair cells. Raised compound action potential thresholds in *Pdo*/+ mutants suggested a combined sensorineural/conductive hearing loss.

We identified a missense mutation in the homeobox gene *Emx2* in *Pdo* mutants. A complementation test between *Pdo* and *Emx2* knock out mice (*Emx2*^{ko}) support the hypothesis that the *Emx2*

mutation is responsible for these defects, identifying a new function for this gene in the development of specific structures in the ear.

Supported by the MRC, EC contract CT97-2715 and Defeating Deafness.

226 Ultrastructure of Inner and Outer Hair Cells of Ames Waltzer Mice During Development

Karen S. Pawlowski^{1,2}, Charles G. Wright¹, Kumar N. Alagramam³

¹Otolaryngology Head and Neck Surgery, UT Southwestern Medical Center, 5323 Harry Hines Blvd, Dallas, TX, United States,

²School of Behavioral and Brain Sciences, UT Dallas, 1966 Inwood Road, Dallas, TX, United States, ³Otolaryngology- HNS, University Hospitals of Cleveland, Case Western Reserve University, 11100 Euclid Ave., Cleveland, OH, United States

The mouse Ames waltzer (*av*) is a recessive mutation that causes deafness and vestibular dysfunction associated with degeneration of the inner ear neuroepithelia. The gene that harbors the *av* mutation is protocadherin 15 (*Pcdh15*). *Pcdh15*^{av-J} and *Pcdh15*^{av-2J} alleles of Ames waltzer bear in-frame deletion of exon(s) coding for the extracellular cadherin domains, which are predicted to be less deleterious compared to functional-null mutations associated with *Pcdh15*^{av-3J} and *Pcdh15*^{av-Tg} alleles. Alleles of Ames waltzer mice have no auditory and essentially no vestibular function at the earliest ages testable. Observations with light and scanning electron microscopy show disruption of the cuticular plate during development, followed by degeneration of the organ of Corti and subsequent spiral ganglion cell loss. It is apparent that *Pcdh15* has a role in normal development of the organ of Corti and its function is presently under study. One approach in understanding the role of *Pcdh15* in organ of Corti development is to determine the sequence of ultrastructural changes that precede cell breakdown. The earliest observable changes in the organ of Corti found thus far involve the disorganization of the cuticular plate and abnormalities of the stereocilia, as seen via scanning electron microscopy. The present study was undertaken to observe intracellular ultrastructural alterations in the inner and outer hair cells of several alleles of Ames waltzer mice during development, using transmission electron microscopy to determine what changes other than disorganization of stereocilia may be present.

Preliminary observations include evidence of fracture of stereocilia rootlets in outer hair cells and disorganization of the rootlets within the cuticular plate by 10 days post natal (P10). Basal bodies of the outer hair cell are often out of position and abnormalities in the dense cuticle of the cuticular plate can be seen by P10 and earlier.

227 Induction of semicircular canal formation by its sensory organ: the roles of BMPs and FGFs.

Weise Chang, Doris K Wu

LMB, National Institute on Deafness and Other Communication Disorders, 5 Research Court, 2B34, Rockville, MD, United States

Three primary cell fates are established during early stages of inner ear development: neurons of the VIII ganglion, sensory cells,

and cells which form the non-sensory structures. The molecular mechanisms for establishing each of these fates are largely unknown. Based on some of our earlier studies involving axial rotations of chicken otocysts, we postulated that sensory tissues might induce development of the non-sensory structures of the inner ear.

Bmp4 (Bone morphogenetic protein 4) is a member of the TGF- β gene family and plays an important role in the development of multiple tissues during embryogenesis. In the mouse inner ear, *Bmp4* is expressed in the three presumptive cristae, and this expression pattern is conserved among chicken, frogs, and zebrafish. *Bmp4* knockout mice are early embryonic lethal. To investigate the role of *Bmp4* in inner ear development, we generated *Bmp4* conditional knock out (*Bmp4-cko*) mice using *Foxg1-cre* (provided by Susan McConnell) and *Bmp4-lox* (provided by Brigid Hogan) mouse lines. The inner ears of (*Bmp4-cko*) mice from these crosses lack all three cristae and semicircular canals. While the phenotype is variable due to incomplete elimination of *Bmp4* expression in the inner ear, these results show that *Bmp4* is important for the development of cristae and semicircular canals, and provide direct evidence that sensory tissues induce the development of non-sensory tissues. These results will be discussed in light of our recent finding that FGFs in the sensory tissues are important for promoting canal development by up-regulating *Bmp2*. Our preliminary results suggest that FGFs and BMP4 might positively regulate each other in the presumptive cristae.

228 Immunoreactivity for calcium binding proteins in developing and mature sensory epithelia of the avian inner ear.

Annegret Falkner¹, Keith Denny², Jennifer Stone³

¹Oto-HNS, University of Washington, Pacific Avenue, Seattle, WA, United States, ²School of Nursing, University of Washington, Pacific Avenue, Seattle, WA, United States, ³Oto-HNS and VM Bloedel Hearing Research Center, University of Washington, Pacific Avenue, Seattle, WA, United States

Calcium binding proteins (CaBPs) are regulators of cell function that have been detected in sensory and neural tissues of the inner ear. We examined immunoreactivity (IR) for three CaBPs, calbindin (28kD), calretinin, and calmodulin, in the chick inner ear between embryonic stage 23 and post-hatch day 7. At stage 23, IR for calbindin and calretinin is seen in the presumptive anterior crista and saccular macula in a streaky pattern and in neurons in the cochleovestibular ganglion (CVG). By stage 27, intense IR for calbindin in hair cells is detected in three cristae and three maculae (sacculae, utricle, and lagena) but does not emerge in the basilar papilla (BP) until stage 29. At that time, calbindin IR is concentrated at the hair cell apical surface and light in the cytoplasm. Intense IR for calretinin is evident in posterior and anterior cristae and in the CVG by stage 25, and it emerges in the lateral crista and utricular macula by stage 27. Calretinin IR is strong throughout the hair cell cytoplasm, being heaviest near the lumen. Neural processes in the sensory epithelia are also labeled. Calmodulin IR in young hair cells is seen in posterior and anterior cristae at stage 25 and in the BP at stage 29. No expression in the CVG was noted. Throughout development, punctate IR is seen with all antibodies in various non-sensory epithelial tissues in the otocyst. In post-hatch chicks, we examined CaBP IR in the utricle and BP.

Calbindin IR is seen in calyceal nerves contacting type I hair cells in the utricle and in hair cell stereocilia in the BP. Antibodies to calretinin label type II hair cells and neural processes in the utricle and supporting cells and neural processes in the BP. Antibodies to calmodulin label the cuticular plates and stereocilia of all hair cells in the BP and utricle. Hair cell cytoplasm is also calmodulin-IR in the BP and in marginal regions of the utricular macula.

Support was provided by grants DC03696, DC04661, and NAG2-1514.

229 Mutations in otopetrin-1 affect the genesis of otoliths and localization of Starmaker in zebrafish

Teresa Nicolson¹, Christian Soellner²

¹OHRC and Vollum Institute, OHSU, 3181 SW Sam Jackson Park Road, Portland, Oregon, United States, ²Genetics, MPI fuer Entwicklungsbiologie, Spemannstr. 35, Tuebingen, Germany

Homozygous backstroke mutants completely lack otoliths, the stone-like macular structures that are necessary for balance and hearing in zebrafish. Using a candidate gene approach, we cloned the backstroke gene and found a missense mutation in otopetrin-1. Otopetrin-1 was previously shown to be responsible for vestibular defects in tilted mice. tilted mice also lack otoconia, the analogous structure necessary for balance in mammals. Otopetrin-1 encodes a large protein with 12 transmembrane domains that may function as a transporter, ion channel or receptor. The backstroke allele, tm317d, contains a mutation that leads to a deletion of two transmembrane domains (TMD 9 and 10). In zebrafish, otopetrin-1 is expressed within the developing otocyst as early as the 15 somite stage (approx. 16 hours post fertilization). At later stages, its expression is largely restricted to hair cells. otopetrin-1 is also expressed in lateral line hair cells. We tested hair cell function in lateral line hair cells with the vital dye, FM1-43; uptake of FM1-43 was normal in backstroke mutants, suggesting that hair-cell function is unaffected. In mice, Otopetrin-1 localizes to the gelatinous membranes of macular organs, potentially suggesting a direct role in otolith formation. We tested localization of a marker of otoliths, Starmaker, in backstroke mutants. Starmaker participates in otolith biogenesis by regulating crystal size and polymorph selection of calcium carbonate, the predominant mineral in otoliths. Starmaker is expressed in hair cells and supporting cells, and secreted into the lumen of the otocyst where it binds to seeding particles that form the initial core or nucleus of the otolith. In backstroke mutants (24 hpf), we found that secretion of Starmaker from hair cells into the otocyst lumen was defective; Starmaker accumulated within the hair-cell bodies. At later stages, Starmaker protein accumulated within the otolithic membrane, suggesting that secretion from supporting cells was normal. In contrast to backstroke mutants, another otolith mutant that lacks otoliths, keinstein, did not show abnormal accumulation within the neuroepithelium. However, both mutants lack Starmaker-labeled seeding particles, suggesting that this initial process of otolith biogenesis is abnormal. Further studies on the role of otopetrin-1 in seeding particle formation are underway.

230 Developmental Biology and Kinetics of the Epidermis of the Mammalian Tympanic Membrane: Review and Suggested Program for Molecular Investigation

Leslie Michaels¹, Holger Sudhoff², Rifat Hamoudi¹, Sava Soucek³, Jianning Liang⁴

¹Histopathology, University College London, Rockefeller Building, University Street, London, United Kingdom, ²Otolaryngology, University of Bochum, Bleistrasse 15, Bochum, Germany, ³Otolaryngology, St. Mary's Hospital, Praed Street, London, United Kingdom, ⁴Institute of Laryngology and Otology, University College London, Gray's Inn Road, London, United Kingdom

Auditory epithelial migration (AEM), the constant lateral movement of the eardrum epidermis to free it from keratin so as to enhance audition, is the continuance of embryonic and fetal cell proliferation leading to apoptosis instead of growth. Pathways of growth/AEM originate in two folds of the fundus of the first branchial groove: 1. Fundal extension plate (FEP) grows out from about / of the periphery of the fundus. At the annular pole of the FEP lies a heavily mitotic zone. The moderately mitotic medial epidermis of the FEP (handle of malleus and pars flaccida covering epidermis) grows towards the annular zone and that on the lateral side of the FEP grows away from the annular epidermis to form about / of the deep external canal epidermis circumference. After growth of the tympanic membrane ceases, AEM along the same pathway replaces growth and there is evidence of apoptosis of epidermal cells at junction of deep with superficial canal. 2. Meatal plate (MP) arises from the remaining fl of the periphery of the fundus and forms in the same way except that its medial epidermis is thin and poorly mitotic, forming the pars tensa covering epidermis and growth/AEM follow a radial pathway away from the pars flaccida and malleus handle-covering epidermis to the annular pole. Cells showing different phases of epidermal cell growth/AEM and apoptosis are thus located in different topographical areas.

A program of molecular analysis of this model could be carried out by cutting out portions of annulus, medial and lateral epidermis of FEP and MP derivatives in sections of human fetuses and mouse embryos at different stages of development for expression profiling, quantitative PCR techniques and raising antibodies for immunohistochemistry. The expression levels of the various cell cycle and apoptotic genes could also be used to study the regulatory mechanisms of the cell cycle during development. Such work may throw light on AEM and the origin of cholesteatoma.

231 Genomic Structure, Cochlear Expression and Mutation Screening of KCNK6, a Candidate Gene for DFNA4

Anand N. Mhatre¹, Jiang Li¹, Arthur F. Chen², C. Spencer Yost³, Richard J. H. Smith², Christoph H. Kindler⁴, Anil K. Lalwani⁵

¹Dept. of Otolaryngology, New York University School of Medicine, 550 First Ave., MSB 497B, New York, NY, United States, ²Dept. of Otolaryngology, University of Iowa, 200 Hawkins Dr., Iowa City, IA, United States, ³Dept. of Anesthesia, University of California San Francisco, 513 Parnassus Ave., San Francisco, CA, United States, ⁴Dept. of Anesthesia, University Clinics Basel, Kantonsspital, CH-4031, Basel, Switzerland, ⁵Dept. of Otolaryngology, New York University School of Medicine, 550 First Ave., NBV 5 East 5, New York, NY, United States

KCNK6 encodes a tandem pore domain potassium channel, TWIK-2, that maps to chromosome 19. Both STS and linkage maps established KCNK6 as a positional candidate gene for DFNA4, a form of autosomal dominant non-syndromic hereditary hearing loss. Identification and characterization of Kcnk6 expression within the mouse cochlea via RT-PCR established the gene as a functional candidate for DFNA4. Subsequent immunoblot analysis of the mouse cochlear homogenate yielded a distinct 35 kDa band corresponding to the calculated molecular weight of the mouse Twik-2. Immunohistochemical studies localized Twik-2 expression in the cochlea predominantly within the stria vascularis. This vascular tissue borders the cochlear duct and is a critical regulator of potassium concentration in the endolymph. Genomic structure of TWIK-2 was subsequently determined and shown to consist of three coding exons with splice acceptor and donor sites in accord with the consensus GT-AG rule. Two separate DFNA4 families were screened for KCNK6 sequence alterations. No mutations were found thus excluding TWIK-2 as the DFNA4 candidate disease gene. Nevertheless, expression of Twik-2 within the stria vascularis suggests a potential role for this protein as one of the terminal components of the potassium ion recycling pathway that contributes towards its reabsorption into the endolymph.

232 Fine Mapping and Candidate Genes Screening for the DFNA41 Locus.

Denise Yan¹, Xiao Mei Ouyang¹, zheng-Yi Chen², Li Lin Du¹, Thomas J Balkany¹, Xue Zhong Liu¹

¹Dept of Otolaryngology, University of Miami, 1601 NW 12TH Avenue, Mailman Center, RM6023, Miami, Florida, United States, ²Dept Neurology, Harvard Medical School, 50 Fruit Street, Boston, Massachusetts, United States

We previously mapped the DFNA41 locus to a 15 cM region on chromosome 12q24.32-qter in a large multigenerational Chinese family with progressive hearing impairment. Linkage data and key recombinant individuals placed the locus distal to DFNA25 in an interval defined by D12S1609 and the telomere of the q arm of the chromosome 12. The human chromosome region containing DFNA41 is syntenic to the mouse chromosome5. The Bronx walzer (bv), a mouse recessive deafness mutation mapped to this region is proximal to the DFNA41 locus. Using a positional and functional candidate gene approach, two novel genes highly expressed in the inner ear are being screened by direct sequencing.

Sequence analysis of the five and seven coding exons of Q8N3T6 and KIAA0692 respectively revealed four different sequence changes in the Q8N3T6 gene detected in a homozygous state in one affected subject. However, three of the changes that are located in the coding sequences are synonymous and one is in the intron 3, so are not considered to be responsible for the hearing loss. To further refine the candidate interval, we typed the members of the family with 6 highly informative single nucleotide polymorphisms (SNPs) retrieved from public databases that are in region of D12S343, marker for which a maximum two point lod score of 6.56 at $\theta=0.0$ was obtained. The SNPs used, each with an approximate heterozygosity of 0.5 in Asians span a distance of 40 kb. Interestingly, for 3 nearby SNPs spanning a 7kb interval, an overtransmission ($p<0.01$) of the less-frequent alleles from parents to affected offsprings was observed. Two potential candidate genes in the refined interval are currently under scrutiny.

Supported by RO1 05575

233 Identification of a New Gene for Otosclerosis, OTSC4

Zippora Brownstein¹, Moshe Frydman^{1,2}, Karen B. Avraham¹

¹*Dept. of Human Genetics and Molecular Medicine, Sackler School of Medicine, Tel Aviv University, Tel Aviv, Israel,* ²*Genetics Institute, Haim Sheba Medical Center, Tel Hashomer, Tel Hashomer, Israel*

Otosclerosis is a common bone disorder with a prevalence of 0.2%-1% among adults. The bone dysplasia leads to a progressive hearing impairment that begins as a conductive hearing loss (HL), and might develop into a mixed to sensorineural (SN) HL. The age of onset is usually 20-40 years. A combination of genetic and environmental factors is believed to be involved in the etiology of the disease. The mode of inheritance appears to be autosomal dominant, with reduced penetrance. Thus far, the chromosomal locations of three loci for otosclerosis have been reported on chromosomes 15q25-q26, 7q34-36 and 6p21.3-22.3.

Thirty members of an Israeli family with otosclerosis (Family O) are participating in our research project, twelve of whom are affected. We excluded linkage to the three loci reported, and a whole genome scan was performed at the Laboratory of DNA Analysis at the Institute of Life Sciences, Hebrew University of Jerusalem. Four hundred polymorphic markers were evaluated. Three possible regions of linkage were identified. We have recently defined the chromosomal region for linkage with a LOD score of 3.14. The interval includes several genes involved in bone homeostasis and may be good candidates for genes causing otosclerosis.

234 Identification of the DFNB17 gene

John Herman Greinwald, Yingshi Guo, Valentina Pilipenko

Otolaryngology, Cincinnati Children's Hospital, 3333 Burnet Ave, Cincinnati, Ohio, United States

Yingshi Guo¹, Valentina Pilipenko¹, Lynne H.Y. Lim¹, Hongwei Dou¹, C.R. Srikumari Srisailapathy², Arabandi Ramesh², Daniel I Choo¹, Richard J.H. Smith³, John H. Greinwald¹

¹Center for Hearing and Deafness Research, Department of

Otolaryngology, Cincinnati Children's Hospital Medical Center, Cincinnati, OH, ²Department of Genetics, University of Madras, Madras, India. ³Department of Otolaryngology, University of Iowa, Iowa City, IA.

Corresponding author:

John H. Greinwald, Jr., M.D.

Assistant Professor

Center for Hearing and Deafness Research

Head, Auditory Genetics Laboratory

Department of Otolaryngology (OSB3)

Cincinnati Children's Hospital

Cincinnati, OH 45229

chdr@chdr.org

www.chdr.org

513-636-4870 (phone)

513-636-2886 (fax)

ABSTRACT

We previously mapped the DFNB17 locus to a 3-4 cM interval on human chromosome 7q31 in a large consanguineous Indian family with congenital profound sensorineural hearing loss. To further refine this interval, 40 new highly polymorphic markers and 15 SNPs were analyzed against the pedigree. Analysis in the original DFNB17 family determined the interval to be more centromeric and larger than previously reported (9 cM or approximately 11 Mb on the physical map). A second unrelated consanguineous family with congenital deafness from the same geographic region was found to map to the interval, limiting the area of shared homozygosity-by-descent (HBD) to approximately 4 megabase (Mb) between markers D7S2453 and D7S525. Both families did not share the same alleles segregating with the hearing loss.

Nineteen known genes and over 20 other cDNAs have been identified in the refined DFNB17 interval, including the *SLC26A4* gene. We have determined the cDNA sequence and genomic structure for 3 other cochlear-expressed genes that map to the DFNB17 interval. These include genes coding for a putative high mobility group (HMG) box containing protein 1 (HBP1), another anion transport protein in the solute carrier family (SLC26A3), a novel synaptophysin-like protein (SYPL) presumed to be involved in vesicle transport in the neural system and 2 genes in the laminin family of extracellular basement membrane proteins (LAMB1 and LAMB4). Cochlear expression analysis of these genes is reported.

Analysis of coding, splice site and putative promotor regions these cochlear expressed genes revealed unique missense mutations in the Laminin 4 gene segregating with the hearing loss in each family. Further experiments are underway to determine the functional significance of these mutations.

235 A family with mixed hearing loss and facial palsy associated with Camurati-Engelmann Disease

Atsushi NAMBA¹, Jiro AKITA¹, Shirou IKEGAWA², Gen NISHIMURA³, Nobuhiko HAGA⁴, Shin-ichi USAMI⁵, Hideichi Shinkawa¹

¹Otorhinolaryngology, Hirosaki University School of Medicine, 5 zaifu-cho, Hirosaki, Japan, ²Laboratory for Bone and Joint Diseases, SNP Reserch Center, RIKEN, 4-6-1 Shiroganedai, Minatoku, Japan, ³Department of Radiology, Tokyo Metropolitan Kiyose Children's Hospital, 1-3-1 Umezono, kiyose-shi, Japan, ⁴Department of Pediatric Orthopaedics, Shizuoka Children's Hospital, 860 Urushiyama, Shizuoka-city, Japan, ⁵Department of Otorhinolaryngology, Shinshu University School of Medicine, 3-1-1 Asahi, Matsumoto, Japan

Camurati-Engelmann disease (CED) is an autosomal dominant progressive diaphyseal dysplasia with variable phenotype expression and mutations responsible for this disease have been detected in the TGF-beta1 gene (TGFB1). One of the phenotypes of CED is hyperostosis of the skull and radiographic changes the skull include thickening and sclerosis. Progressive sclerosis of the cranial nerve foramina has been implicated in cranial nerve deficits, including facial palsy, vestibular disturbances, and hearing loss.

A family of three patients with CED revealed mixed hearing loss; apparently caused by narrowing of the tympanic cavities leading to fixation or adhesion of the ossicles to the tympanic wall and in addition to narrowing of the internal auditory canal (IAC) leading to encroachment on nerves and vessels. One patient also had facial palsy caused by a narrowed IAC. Another patient with minor abnormality of the IAC had profound hearing loss after head trauma, and we performed cochlear implantation for auditory rehabilitation. We performed mutation analysis and found a novel TGFB1 mutation in this family; T->G (C223G) at nucleotide 667. We report here the clinical examination findings, results of gene analysis of TGFB1, and the results of cochlear implantation in this family.

236 A New Locus (DFNA53) for Autosomal Dominant Non-Syndromic Hearing Loss Maps to 14q11.2-q22.1 in a Large Chinese Family

Xiaomei Ouyang¹, Denise Yan¹, Susan Blanton², Xiaomei Ke³, Arty Pandya⁴, Li Lin Du¹, Thomas Balkany¹, Walter E Nance⁴, Xue Zhong Liu¹

¹Department of Otolaryngology, University of Miami, Mailman Center, Miami, FL, United States, ²Department of Pediatrics, University of Virginia, Box 800386, Charlottesville, VA, United States, ³Department of Otolaryngology, Beijing Medical University, 100034, Beijing, China, People's Republic of, ⁴Department of Human Genetics, Virginia Commonwealth University, 1101E Marshall ST, Richmond, VA, United States

Hearing impairment (HI) is the most common inherited human sensory defect. Approximately 80% of genetic hearing loss is non-syndromic and 15-25% of genetic cases exhibit an autosomal dominant pattern of transmission. So far, 50 autosomal dominant non-syndromic loci have been mapped and 18 genes have been

cloned. Here we present a Chinese six generation family in which non-syndromic hearing impairment is transmitted as an autosomal dominant trait. Onset of HI in all affected subjects occurred in the second decade of life, with subsequent gradual progression from moderate to profound loss. There were no obvious vestibular dysfunction and other associated abnormalities. A genome scan was carried out by the Center for Inherited Disease Research (CIDR) to test for 351 polymorphic markers distributed at approximately 10 cM intervals throughout the genome. Linkage data placed the DFNA53 locus to 14q11.2-q22.1 in a region of approximately 31 CM defined by markers D14S742 and D14S306. D14S1280, marker for which, a multipoint maximum LOD score of 5.35 (at theta=0) was obtained, is proximal to D14S975, marker linked to COCH gene, responsible for progressive cochleovestibular impairment (DFNA9). Direct sequencing of the COCH coding sequences in affected individuals excluded COCH as the DFNA53-causative gene. The DFNA53 candidate region is syntenic to the mouse chromosome 12. No mouse deafness mutant has yet been mapped to that interval. Fine mapping of the DFNA53 candidate interval using additional markers and candidate genes screening are in progress.

Supported by RO1 05575

237 Maternally inherited aminoglycoside-induced and non-syndromic deafness associated with the novel C1494T mutation in the mitochondrial 12S rRNA gene in a large Chinese family

Min Xin Guan, Hui Zhao

Human Genetics, Cincinnati Children's Hospital Medical Center, 3333 Burnet Avenue, Cincinnati, Ohio, United States

We report here the characterization of a large Chinese family with maternally transmitted aminoglycoside induced and non-syndromic deafness. In the absence of aminoglycosides, some matrilineal relatives in this family only exhibited late-onset/progressive deafness with a wide range of severity and age of onset. Notably, the average age of onset of deafness has changed from 55 years (generation II) to 10 years (generation IV). Clinical data reveal that the administration of aminoglycosides can induce or worsen deafness in matrilineal relatives. The age at the time of drug administration appears to be correlated with the severity of hearing loss experienced by affected individuals. Sequence analysis of mitochondrial DNA in this pedigree identified a homoplasmic C-to-T transition at position 1494 (C1494T) in the 12S rRNA gene. The C1494T mutation is expected to form a novel 1494U-1555A base-pair, which is in the same position as the C1494-1555G pair created by the deafness-linked A1555G mutation, at the highly conserved A-site of 12S rRNA. Exposure to high concentration of paromomycin or neomycin caused a variable but significant average increase in doubling time in lymphoblastoid cell lines derived from four symptomatic and two asymptomatic individuals in this family carrying the C1494T mutation, when compared to four control cell lines. Furthermore, a significant decrease in the rate of total oxygen consumption was observed in the mutant cell lines. Thus, our data strongly support the idea that the A-site of mitochondrial 12S rRNA is the primary target for aminoglycoside induced deafness. These results also strongly suggest that the

nuclear background plays a role in the aminoglycoside toxicity and the development of deafness phenotype associated with the C1494T mutation in the mitochondrial 12S rRNA gene.

238 Biochemical evidence for a combination of the deafness-linked mitochondrial tRNA^{Ser}(UCN) T7511C mutation with two other mtDNA mutations leading to a high penetrance of deafness

Min Xin Guan, **Xiao-Ming Li**

Human Genetics, Cincinnati Children's Hospital Medical Center, 3333 Burnet Avenue, Cincinnati, Ohio, United States

The T7511C mutation in the mitochondrial tRNA^{Ser}(UCN) gene has been associated with non-syndromic deafness in families from different ethnic backgrounds. Recently, this mutation has been found to co-segregate with homoplasmic ND1 T3308C and tRNA^{Ala}T5655C mutations in maternally-related members of a large African-American family with higher penetrance (84%) of deafness. Here, pathogenetic mechanism of the T7511C mutation has been investigated by analyzing six transformants, constructed by transferring mitochondria from lymphoblastoid cell lines into human mtDNA-less (ρ^0) cells. Three transformants derived from a deaf individual of this family carrying the homoplasmic T7511C mutation, exhibited a significant decrease (~75%) in the tRNA^{Ser}(UCN) level, compared with three control transformants. This amount of reduction in the tRNA^{Ser}(UCN) level is below a proposed threshold to support a normal rate of mitochondrial protein synthesis in the lymphoblastoid cell lines. This defect is likely a primary contributor to ~52% reduction in the rate of mitochondrial protein synthesis and marked defects in respiration and growth properties in galactose-containing medium. Interestingly, the T5655C mutation produces ~50% reduction in the tRNA^{Ala} level in mutant cells compared with that of controls. Strikingly, the T3308C mutation causes a significant decrease both in the amount of ND1 mRNA and co-transcribed tRNA^{Leu}(UR) in mutant cells. Thus, mitochondrial dysfunctions caused by the T5655C and T3308C mutations could modulate the phenotypic manifestation of the T7511C mutation. These findings provide the direct biochemical evidence that a combination of the T7511C mutation with two mtDNA mutations accounts for higher penetrance of deafness phenotype in this African American family.

239 Mutational screening of mitochondrial 12S rRNA and tRNA^{Ser}(UCN) genes in 164 deafness subjects

Min Xin Guan, **Rong-Hua Li**

Human Genetics, Cincinnati Children's Hospital Medical Center, 3333 Burnet Avenue, Cincinnati, Ohio, United States

Mutations in the mitochondrial DNA (mtDNA) have been associated with both syndromic and non-syndromic forms of sensorineural hearing loss. The mtDNA mutations associated with deafness often occur in the tRNA^{Ser}(UCN) and 12S rRNA genes. We report here the mutational screening of tRNA^{Ser}(UCN) and 12S rRNA genes in 164 deafness patients from ENT clinic of Cincinnati Children's Hospital Medical Center. Only one variant C7476T was identified in the tRNA^{Ser}(UCN) gene, while 25

nucleotide changes were found in 12S rRNA gene. Of these changes, 6 variants have been reported previously in certain control population, while the A1555G mutation responsible for aminoglycoside ototoxicity and non-syndromic deafness has been identified in one individual. Of other nucleotide changes, the novel T961G mutation occurred in three subjects is of particular interest as the deletion/insertion at position 961 has been found to be only associated with aminoglycoside induced deafness. The results indicated that the mutations in 12S rRNA gene are more frequent than those of tRNA^{Ser}(UCN) gene. The novel T961G mutation in 12S rRNA gene is likely a new mutation involved in non-syndromic and aminoglycoside toxicity.

240 Modifier Controls Severity of a Novel Dominant Low Frequency Myosin VIIA (MYO7A) Auditory Mutation

Valerie Ann Street¹, Jeremy C Kallman¹, Kevin L Kiemele²

¹Otolaryngology-HNS Department, University of Washington, V.M. Bloedel Hearing Research Center, Box 357923, Seattle, WA, United States, ²Otolaryngology-HNS Department, University of Washington, Box 356161, Seattle, WA, United States

Inherited deafness is a genetically heterogeneous disorder. Large families segregating monogenic hearing loss provide an opportunity to dissect this genetic complexity. In this report we describe the genetic mapping of progressive sensorineural hearing loss first affecting low frequency pure tone thresholds within a large pedigree to chromosome 11q13.5. A maximal pairwise LOD score of 7.23 was obtained with marker D11S4207. We identified a myosin VIIA (MYO7A) G2164C mutation that co-segregates with auditory dysfunction in the pedigree. The mutation results in a predicted G722R substitution at an evolutionarily conserved glycine residue in the MYO7A head domain. The clinical severity of the G2164C mutation varies between individuals in different family branches with similar medical and noise-exposure histories, indicating involvement of a genetic modifier. Single nucleotide polymorphism (SNPs) on the opposing MYO7A allele are being considered as modifiers of the G2164C mutation.

241 Mutations in the VLGR1 gene implicate G-protein signaling in the pathogenesis of Usher syndrome type II

Michael D Weston^{1,2}, Mirjam WJ Luijendijk³, Kurt D Humphrey⁴, Claes Möller⁵, William J Kimberling¹

¹Genetics, Boystown National Research Hospital, 555 north 30th street, Omaha, nebraska, United States, ²Biomedical Sciences, Creighton University, 2500 California Plaza, Omaha, nebraska, United States, ³Department of Human Genetics, University Medical Center Nijmegen, 6500 HB, Nijmegen, Netherlands, ⁴Biology, Creighton University, 2500 California Plaza, Omaha, nebraska, United States, ⁵Department of Audiology, Sahlgrenska University Hospital, S-413 45, Göteborg, Sweden

Background. Usher syndrome type II is a genetically heterogeneous autosomal recessive disorder classified phenotypically as congenital hearing loss and progressive retinitis pigmentosa. The USH2A gene encodes usherin, an extracellular matrix protein. The

identity of the USH2B and USH2C genes are unknown but genetically localize to chromosome 3p24.2-p23 and 5q14-q21, respectively. Of several USH2C candidate genes, VLGR1 was considered a likely candidate based on its protein motif structure and EST representation from both cochlear and retinal subtracted libraries.

Methods. VLGR1 mutation screening was performed by a combination of D-HPLC and direct sequencing of PCR products amplified from 10 independent USH2C patients and 156 other USH2 patients. Primer pairs were designed to amplify all 90 coding exons of VLGR1. Examination of VLGR1 mRNA isoform expression was performed on human and mouse fetal tissue by RT-PCR.

Results. Four isoform specific VLGR1 mutations were identified from three USH2C families and two sporadic cases, Q2301X, I2906FS; M2931FS and T6244X. To date, five USH2C probands and 11 affected siblings bear VLGR1 mutations, two probands have mutations identified in both alleles. All USH2C patients with VLGR1 mutations are female, a significant deviation from random expectations.

Conclusions. USH2C mutations have been identified in VLGR1, the largest cell surface receptor known. The ligand(s) for VLGR1 is unknown, but based on the potential extracellular and intracellular protein-protein interaction domains and its wide, albeit low mRNA expression profile, it is probable that VLGR1 serves diverse cellular and signaling processes. Furthermore, VLGR1, in its capacity as a putative G-coupled receptor, is a legitimate target in the search for possible therapeutics that may have a broad impact on all the types of Usher syndrome.

242 Autosomal dominant auditory neuropathy: genetic mapping of a novel locus (AUNA1)

Theresa Kim¹, Brandon Isaacson¹, Theru A. Sivakumaran¹, Arnold Starr², Bronya Keats³, **Marci Lesperance¹**

¹Otolaryngology Head Neck Surgery, University of Michigan, F6905 Mott, 1500 E. Medical Center Drive, Ann Arbor, MI, United States, ²Neurology, University of California Irvine, Neurology Department, Irvine, CA, United States, ³Genetics, Louisiana State University, 553 Bolivar Street, New Orleans, LA, United States

Auditory neuropathy may be associated with environmental causes such as neonatal hyperbilirubinemia or inherited as a syndrome accompanied by peripheral neuropathies such as Friedreich ataxia, Hereditary Sensorimotor Neuropathy or mitochondrial disorders. Nonsyndromic auditory neuropathy is most commonly a sporadic or recessive trait. The genetic heterogeneity of auditory neuropathy is suggested by the finding of OTOF mutations in 3 of 4 families with nonsyndromic autosomal recessive auditory neuropathy (Varga et al 2003). We have identified a family with delayed-onset, progressive, autosomal dominant auditory neuropathy (see companion abstract for detailed phenotype description). 51 family members comprising four generations including 32 affected members were available for genetic analysis. Linkage to the OTOF locus was excluded as were GJB2 mutations. SLINK analysis predicted an average maximum LOD score of 7.90, with 99.6% of replicates greater than 3.0. The genome scan was performed by the Center for Inherited Disease Research as an automated fluorescent microsatellite analysis using a marker set of

approximately 400 primer pairs with average spacing of 10 cM. Pairwise LOD scores assuming complete penetrance, gene frequency of 0.00001 and 0% phenocopy rate were calculated using the LINKAGE package. The maximum LOD score was 8.34 at $\theta = 0$ for an informative marker defining the AUNA1 locus. Fine mapping revealed a candidate region of 13.6 cM. A unique feature of the pedigree is a consanguineous marriage between affected first cousins. Semidominance is suggested by an earlier age of onset in the offspring of this marriage who are homozygous for the haplotype common to the affected family members. This candidate gene interval does not overlap with other known deafness loci. Identification of a gene responsible for auditory neuropathy will allow for genetic screening in sporadic cases or in families too small for genetic linkage analysis.

243 NIDCD Research and Training Workshop for NEW INVESTIGATORS

Amy Donahue, Nancy Freeman, Lynn Luethke, Daniel Sklare

NIDCD, NIH, 6120 Executive Blvd, 400-C, Rockville, MD, United States

This year's workshop will focus EXCLUSIVELY ON NEW INVESTIGATORS.

Following a brief overview of NIH funding mechanisms for new investigators, attendees will choose one of three breakout sessions:

1. NIH 101: How does NIH work?
2. Training and Career Development (Fs and Ks): What do I need to know?
3. Transitioning to Independence: Should I apply for an R03 or an R01?

The goal of the workshop is to provide information for successful transition from trainee/new investigator status to independent investigator (R01).

NIH 101 will provide practical information on how the NIH/NIDCD works (e.g., institute and study section assignments, application timelines, reviewer assignments, funding paylines, council activities, and the role of program and review staff).

Training and Career Development will describe the research training and career development mechanisms appropriate for budding and new investigators, including the individual fellowship awards (F30, F31 and F32) and the career development mechanisms for clinically trained investigators (K08 and K23). The NIH programs providing repayment of educational loans will also be covered.

Transitioning to Independence will provide guidance on the appropriate grant mechanisms for early career stages, and will focus on the NIDCD Small Grant Award (R03) and the New Investigator R01. This session will also include a discussion of how to avoid mistakes commonly observed in the review process.

The breakout sessions are intended to allow ample time for questions and answers. Handouts from all three breakout sessions will be available.

244 Animal Rights and the ARO: The Perspective of Targeted Members

JoAnn D. McGee, E. J. Walsh, P. Santi

Research, Boys Town National Research Hospital, 555 North 30th St., Omaha, Nebraska, United States

Given the core goal of abolishing biomedical research involving animals, the animal rights movement poses a challenge that is more than noteworthy for scientists and research institutions alike in the modern era. Technological innovations and novel strategies of activism are being combined with more traditional approaches to accomplish the singular goal of the movement. One clear element in the offensive formula of the animal rights movement is diversity of approach. In addition to theatrics, personal assault and a well orchestrated selection of targets, serious efforts to introduce biased supplementary materials into primary school curricula and lobby receptive congressional offices are the centerpieces of a long term program. Historically, with some notable exceptions, scientists, clinicians and institutional officials have reacted to the animal rights offensive defensively, unprepared to counter the aggression and hyperbole of the movement's leaders and spokespersons. An equally significant advantage operating to facilitate the efficacy of the AR movement centers on the relative isolation of animal use groups (e.g., farmers, fishers, scientists). The isolation of one group from another effectively diminishes the capacity of any one group to respond efficiently and forcefully to the challenge, regardless of whether this is a consequence of strategic planning or a naturally occurring phenomenon. Although always difficult to assess, members of the ARO will address the question of the movement's efficacy, level of success and recommend counter strategies that may bring balance to the debate.

245 Cell adhesion : lessons for the development and the physiology of the hair cells

Christine Petit

Unite de Genetique des deficits Sensoriels, Institut Pasteur, Paris, France

The sensory cells of the vertebrate acoustico-lateralis system transduce mechanical signals, sound, acceleration or movement of surrounding liquids. These cells, the hair cells, have several adhesive interactions, namely with acellular gels contacting some stereocilia or the kinocilium of the hair bundles, the surrounding supporting cells and afferent (and efferent) neurons. Moreover, it is becoming increasingly clear that stereocilia within the hair bundle are connected by "specific" adhesion molecules interacting with the stereocilia actin core. Finally, several lines of genetic evidence suggest a central role of adhesion molecules and associated molecular complexes in the development and the functioning of these cells. Indeed, cadherin 23 and protocadherin 15, integrin $\alpha 8 \beta 1$, claudin 14, as well as several extracellular matrix (ECM) glycoproteins likely involved in adhesion processes such as collagens, a tectorin, otogelin, otoancorin and usherin, have been implicated in deafness and balance defects in humans and/or mice, as well as, for some of them, in balance defects of zebrafish mutants.

Understanding how the various types of adhesive junctions of these cells influence their shape and their functioning, how these cells integrate the various mechanical forces exerted on their different plasma membrane domains and microdomains is challenging.

The goal of the first part of the symposium is to make the scientific community working on the ear aware of theoretical and experimental works developed on various types of adhesion processes studied in other cellular systems. This includes substrate adhesion, intercellular adhesion (at tight junctions, adherens junctions and the synapses) and the physical approaches that have been developed to measure adhesion forces. The second part of the symposium will be devoted to adhesion in the context of the hair cells. How the deciphering of the molecular bases of various inherited deafness forms combined with the study of the mouse and zebrafish mutants as well as the biochemical analysis can contribute to our understanding of hair cell adhesion processes, will be illustrated by the recent progress being made in the identification and the characterization of the molecular mechanisms underlying interstereocilia "adhesion", adhesion of the stereociliar tip to the tectorial membrane and hair cells-supporting cells junctions and hair cell synaptic junctions.

246 Focal adhesions: assembly, cytoskeletal connections, and mechanosensory function

Alexander Bershadsky

Department of Molecular Cell Biology, Weizmann Institute of Science, P.O.B. 26, Rehovot, Israel

Focal adhesions (FAs) are dynamic molecular complexes associated with integrin- family transmembrane receptors and connecting the actin cytoskeleton to the extracellular matrix. FA assembly is induced by tension either applied to these structures externally, or resulting from myosin II-driven cell contractility. Thus, FAs function as mechanosensors, "reporting" to the cell information about the local physical properties of the extracellular matrix. Rho, a principal molecular switch triggering FA formation, operates by activating Rho associated kinase (ROCK) and the formin homology protein, mDia1. ROCK is required for the activation of myosin II-driven contractility, and its function can be bypassed by externally applied force. Under these conditions, mDia1 remains necessary for FA assembly. mDia1 nucleates actin filaments, and in addition affects microtubule dynamics at both the plus and minus ends, which facilitates microtubule targeting toward FAs. Since microtubules interfere with myosin II-driven contractility, this enhanced targeting may create a negative feedback loop controlling FA growth.

247 Signaling, cell adhesion and morphogenesis in skin

Elaine Fuchs, Colin Jamora, Bradley J. Merrill, Kris Kobiela, Atsuko Kodama, Alec Vaezi, Agnes Kobiela

The central objective of my laboratory is to explore the mechanisms governing epithelial stem cells and their lineages in mammalian skin. Mesenchymal-epithelial interactions are critical in the decision of multipotent epithelial stem cells to adopt a hair follicle cell fate. In response to a mesenchymal cues, epithelial cells invaginate to form a hair placode. In response to a placode epithelial signals, mesenchymal cells condense to form a dermal papilla, that eventually becomes encased by the epithelium at the base of the follicle. Postnatally, additional mesenchymal-epithelial cross-talk is key to the hair cycle, stimulating the pathway that leads from slow cycling stem cells to rapidly proliferating matrix cells to differentiating hair cells. Our studies point to canonical Wnt sig-

naling as an important component of these decision making processes. A direct correlation is seen between Wnt signaling and four different times of skin development where cells have a fate choice. Transgenic and knockout studies by the laboratory underscore the functional significance of these signals. We have been exploring how other external cues collaborate with Wnts to orchestrate epithelial bud formation during follicle morphogenesis. In particular, our focus is how the cytoskeleton, adhesion and signaling are coordinated at the molecular level.

248 Cadherin/catenin-dependent regulation of synapse formation and stability

Masatoshi Takeichi

RIKEN Center for Developmental Biology, Chou-Ku, Japan

Neural networks are generated by the sequential contacts between neurons; and synapses are the sites for these contacts. Although synaptic functions have been extensively studied, the mechanisms for the recognition and adhesion between synaptic membranes remain mostly mysterious. The cadherin/catenin complex is the major adhesive machinery for epithelial and fibroblastic cells, and we and others found that this complex is also localized in synaptic junctions. Our recent studies revealed that, when the cadherin system is blocked in hippocampal neurons in vitro, synapse and spine morphogenesis is severely impaired. Similar perturbation of synapse formation was also observed in the *Drosophila* visual system, when DN-cadherin, a cadherin specifically expressed in the nervous system, had been mutated. Furthermore, mice in which the cadherin-11 gene is mutated show reduced anxiety and enhanced LTP. These findings suggest that the cadherin adhesion system plays a critical role in synapse formation and function.

249 Dynamics of cell adhesion and detachment

Francoise BROCHARD

Laboratoire Physico-Chimie, Institut Curie, 75231 Paris, Paris, France

We study (both experimentally and theoretically) the two mechanisms of attachment of a cell pressed against a sticky substrate (or another cell): i) spreading and ii) dewetting of the intercalated liquid film. An important feature of cell adhesion is the diffusion of the binders toward the contact zone. We used two types of binders strong (Biotine/Streptacidine) and weak (cadherines EC12).

We also briefly discuss the inverse process of cell detachment i) how is the force of detachment related to adhesion energy, ii) the dynamics of contact retraction and iii) why lipidic tubes are often formed during cell detachment.

250 From deafness genes to molecular mechanisms underlying the cohesion of the hair bundle

Aziz El-Amroui, Batiste Boëda, Avital Adato, Richard Goodyear, Guy Richardson, Christine PETIT

Unite de Genetique des deficients Sensoriels, Institut Pasteur, 75724 Paris Cedex 15, Paris, France

Based on our previous work implicating myosinVIIa, defective in Usher syndrome 1B, in an adhesion process, we hypothesized that the genes underlying the other genetic forms of Usher syndrome

type I (USH1) could also be involved in the interstereocilia “adhesion” and as such should provide entry points in this process. Our data showing that harmonin, cadherin 23 and myosinVIIa defective in USH1C, USH1D and USH1B respectively, belong to the same stereociliar transduction pathway, in conjunction with the disorganization of the hair bundle in the mouse mutants defective in the corresponding genes, support this proposal. Moreover, preliminary results integrate SANS, a cytoskeletal protein we recently identified as defective in USH1G, in this pathway. Finally, work in progress aims at testing whether the anchoring of adhesion molecules to the actin filaments, via a direct interaction with a PDZ-domain protein itself bound to an unconventional myosin, is a widespread adhesion process, and in particular whether or not it is involved at the other adhesion sites of the hair cells.

251 Cell adhesion molecules and deafness

Ulrich Mueller

The Scripps Research Institute, La Jolla, CA, United States

Our studies have provided evidence that an ECM receptor of the integrin family, the integrin $\alpha 8 \beta 1$, regulates the formation/maintenance of hair cell stereocilia. Using conventional and conditional (CRE/LOX) gene targeting approaches, we are analyzing the function of other members of the integrins family in hair cell development. Our data support a model where different integrins are targeted to distinct membrane domains in hair cells. Integrin downstream effectors that are implicated in regulating actin cytoskeletal dynamics, such as focal adhesion kinase, are likewise asymmetrically distributed in hair cells. These findings suggest that different integrins assemble distinct signaling complex in sub-cellular compartments of hair cells. We are directly testing this model by genetic means, and we are analyzing the relationship between integrins and other cell adhesion molecules, such as members of the cadherin superfamily.

252 Tight Junction and Adhesion Proteins in the Cochlea: Claudin 14, Cadherin 23 and Protocadherin 15

Ayala Lagziel¹, Zubair Ahmed¹, Tamar Ben-Yosef¹, Julie Schultz¹, Saima Riazuddin¹, Sheikh Riazuddin², Edward Wilcox¹, Robert Morell¹, Inna Belyantseva¹, Thomas Friedman¹

¹Lab of Molecular Genetics, NIDCD/NIH, 5 Research Court, Rockville, Maryland, United States, ²CEMB, National Center of Excellence in Molecular Biology, Punjab University, Lahore, Pakistan

Tight junctions (TJs) and adhesion molecules preserve the integrity of the cellular and extracellular fluid-filled environment of the inner ear. One role of TJs is the formation of charge-selective paracellular permeability barriers between extracellular compartments. Mutations of *CLDN14*, encoding TJ protein claudin 14, cause profound, congenital deafness (DFNB29) in humans (Wilcox et al. 2001). In the mouse organ of Corti (OC), claudin 14 is localized between hair cell-supporting cell and supporting cell TJs. In *Cldn14*-null mice, the OC develops normally but shows rapid death of outer hair cells during the second postnatal week followed by loss of inner hair cells, although the endocochlear potential and vestibular function are preserved (Ben-

Yosef et al. 2003). Protocadherin 15 and cadherin 23 are also necessary for maintenance of hair cell integrity and function. We have previously shown that mutant alleles of *CDH23* are associated with nonsyndromic deafness (DFNB12) and Usher syndrome type 1D (Bork et al. 2001), and mutant alleles of *PCDH15* are responsible for Usher syndrome type 1F (Ahmed et al. 2001) and nonsyndromic deafness DFNB23 (Ahmed et al. submitted). In mouse OC and vestibular hair cells, protocadherin 15 was localized along the stereocilia between the actin core and the stereocilia membrane in both developing and mature hair bundles. The tips of stereocilia were devoid of protocadherin 15 immuno-reactivity. In contrast, cadherin 23 expression is highest in developing stereocilia, concentrated toward their tips, and absent from mature hair cell bundles, consistent with previous reports (Siemens et al. 2002; Boeda et al. 2002). We also found cadherin 23 associated with hair cell kinocilia and Reissner's membrane. The distribution and developmental profile of these two cadherins, suggests that protocadherin 15 may be associated with the lateral links that connect adjacent stereocilia, and cadherin 23, as suggested by others, may form transient top-links of developing stereocilia and play a role in establishing hair bundle polarity.

253 Are Noise-Bands an Adequate Acoustic Model of Intra-Cochlear Electrical Stimulation? Analysis of the Perceptual Coding of the Noise-Band in the Human Auditory System

J. Brandon Laflen^{1,2}, Thomas M. Talavage², Mario A. Svirsky³, Stephen Foldes², Fan Lee²

¹Electrical and Computer Engineering, Rose-Hulman Institute of Technology, 5500 Wabash Avenue, Terre Haute, Indiana, United States, ²Electrical and Computer Engineering, Purdue University, 465 Northwestern Avenue, West Lafayette, Indiana, United States, ³Otolaryngology, Indiana University School of Medicine, 1120 South Drive, Indianapolis, Indiana, United States

A framework is presented that measures the effectiveness of noise-band representations for modeling intra-cochlear stimulation and that also proposes improved acoustic representations. This framework is developed around comparisons made between neural encodings in the auditory nerve; these encodings encompass the effects of auditory scenarios like sensori-neural hearing loss and peripheral assist devices (e.g., the cochlear implant, which stimulates the auditory nerve directly). Neural activation in the auditory nerve is viewed as a pattern in both space (the distance along the cochlea) and time. This pattern is generated by an appropriate forward model (e.g., the Auditory Image Model of Patterson, *et al.*) that represents a specific acoustic pathway leading to the auditory nerve for a given scenario. Thus, a neural activation pattern (NAP) completely describes an auditory input and a specific auditory scenario. Beginning with an auditory input, NAPs are first generated by models for two different scenarios. Then the NAPs are transformed by a "perceptual mapping" and the perceptual difference is computed. The "perceptual mapping" is taken from a set of functions developed within this framework to map perceivable differences to measurable distances in the transformed NAP vector space.

In this work, NAPs are generated under the normal-hearing sce-

nario from normal and noise-band auditory inputs and a model of the cochlear implant is developed to generate a cochlear implant-induced NAP for comparison. Several distinct "perceptual mapping" functions and a representative set of phoneme syllables are used in this study. Results across all functions and inputs demonstrate potential shortcomings in the noise-band representations of the cochlear implant for normal-hearing subjects. Further, the framework is used to develop an alternative acoustic representation that more adequately models the cochlear implant under a given "perceptual mapping."

254 Interactions between electrical and acoustical auditory nerve fiber responses of intracochlear implanted cats with residual hearing

Jochen Tillein¹, Maike Vollmer², Andrej Kral¹, Rainer Klinke¹, Rainer Hartmann¹

¹Institute of Physiology II, J.W.Goethe University, Theodor-Stern-Kai 7, Frankfurt, Germany, ²Dept. of Otolaryngology, University of California SF, 533 Parnassus Avenue, San Francisco, CA 94143-0526, United States

Profound deaf patients with residual low frequency hearing can clearly benefit from combined electric/acoustic stimulation (EAS) when compared to either electrical or acoustical stimulation alone. The present study investigates interactions of EAS on responses of auditory nerve fibers. Results from intracochlear stimulation will be compared to earlier results from extracochlear round window stimulation.

Adult normal hearing cats were implanted with multi-channel feline electrodes (MedEl) into the scala tympani. Combinations of acoustic tone bursts (at characteristic frequency, CF) and electric sinusoids (30-250 Hz) were presented at different relative intensities. Also, effects of phase shifts between acoustic amplitude modulated signals (AM, $f_{\text{carrier}}=CF$, $f_{\text{modulation}}=30\text{Hz}$) and electrical sinusoids (frequency matched to the acoustic modulation frequency) were investigated. Peristimulus time histograms, interval histograms and synchronization indices (SI) were calculated for EAS responses and compared to responses to each stimulus parameter alone.

Near electrical threshold, electrical responses were suppressed even at low acoustic intensities. In contrast, at higher currents acoustic responses were clearly suppressed by the electrical stimulus. Further, depending upon the phase relationship between the two kinds of stimuli, acoustic responses were suppressed and SIs for the electrical responses decreased.

Results demonstrate that EAS can lead to a complex suppression and desynchronization of neuronal responses. Especially at higher electrical intensities intracochlear stimulation results in a stronger suppression of acoustic responses when compared to extracochlear stimulation (ARO Abstr. 201, 2003). This may be due to more effective intracochlear stimulation with electrodes located closer to excitable neuronal structures and to an increase in hearing thresholds caused by the implantation.

Supported by DFG GS16-1/1 and MedEl Company, Austria

255 Interaction of Acoustic and Electric Excitation of the Auditory Nerve: Single-fiber Results

Charles A Miller^{1,2}, Paul J Abbas^{1,2}, Barbara K Robinson¹, Fuh-cherng Jeng², Kirill V Nourski¹

¹Otolaryngology, University of Iowa, 200 Hawkins Drive, Iowa City, IA, United States, ²Speech Pathology & Audiology, University of Iowa, 250 Hawkins Drive, Iowa City, IA, United States

Interactions between acoustic and electric excitation may be an issue for cochlear implant patients with residual hearing. The response of the acoustically driven cochlea can alter the auditory nerve's response to electrical stimulation (Moxon, 1971). Furthermore, we recently showed that the electrically evoked compound action potential (ECAP) is altered when hair-cell functionality is transiently inhibited by furosemide (Hu et al., 2003), even without any external acoustic stimulus.

We collected single-fiber responses to examine acoustic-electric interactions in greater detail. We examined responses to single electric pulses or 1000 pps electric pulse trains in the presence and absence of wideband acoustic noise. With the single-pulse paradigm, we found that the simultaneous presentation of acoustic noise doubled the dynamic range and increased jitter. In the pulse-train experiments, we presented a 100-200 ms burst of acoustic noise 50 ms after the onset of a longer (200-400 ms) electric train, providing baseline responses to the electric train both before and after noise presentation. The single-fiber experiments were performed on acute cat preparations implanted with an intracochlear electrode. Hearing sensitivity of the preparations (assessed by click-evoked CAP) was maintained within 10 dB of pre-implantation levels.

PST histograms indicated large effects of the acoustic noise on electric pulse train responses. Increased spike jitter and decreased vector strength were noted. Acoustic noise also caused depression of the electrically evoked spike activity that closely resembled an inverted PST histogram to acoustic noise. This adaptation-like effect was graded according to the acoustic level and duration. The effect tended to saturate at higher acoustic levels. These trends suggest that the degree of spike-rate adaptation relates to fiber activity, as opposed to an effect more closely related to the stimulus per se. Furthermore, we observed depression of spike rate after cessation of the acoustic noise. These results suggest that the observed adaptation effects are caused by both a synaptic mechanism and one that involves only the neural membrane.

Work supported by the NIH.

256 Responses of Binaural Neurons to Combined Auditory and Electrical Stimulation

Charles Stephen Ebert, Jr., Douglas C. Fitzpatrick, Robert D Cullen, Charles C Finley, Marc K Bassim, Carlton J Zdanski, Charles S Coffey, William Crocker, John Skaggs, Allen F Marshall, Stephanie E Falk

Otolaryngology, UNC Chapel Hill, CB #7070 Dept. of Otolaryngology UNC Chapel Hill, Chapel Hill, NC, United States

Unilateral cochlear implantation is successful at establishing benefits to the profoundly deaf, but it cannot provide the advantages of

binaural hearing—an ability to localize sounds and discriminate signals in noise. To achieve benefits in speech perception and sound localization, the binaural auditory system encodes two main cues: interaural time differences (ITDs) and interaural level differences (ILDs). Although some patients are currently receiving bilateral implants, there is little known about how binaural information is encoded in neural responses when the cochlea is stimulated electrically.

We established an animal model to examine the responses of binaural neurons to electrical stimulation. We placed a single channel, monopolar cochlear implant in a rabbit ear deafened with distilled water. For recording, the unanesthetized animal was stimulated via the implant ipsilaterally and via acoustic stimuli contralaterally. Leaving one ear hearing allowed us to determine neuronal responses to tones, clicks, and noise prior to electrical stimulation. Electrical stimuli consisted of single biphasic pulses and trains of pulses. Stimuli for determining binaural interactions were single pulses and clicks, and trains of pulses and clicks. Single and multi-unit recordings were made from the inferior colliculus.

Thresholds for the acoustic (click) stimulus tended to be low, often <0dB SPL. In contrast, the thresholds to the implant tended to be higher and less varied, corresponding to a limited dynamic range (~25dB). Also, the implant was able to stimulate neurons with a wide range of characteristic frequency, from <1000Hz to >20,000Hz. This result implies that the entire cochlea was stimulated. When we varied the ILD, many neurons showed ILD tuning consistent with the good ILD sensitivity seen in bilateral implant patients. Most neurons showed little if any ITD sensitivity to the fine structure, consistent with poor ITD sensitivity in implant patients. However, we found some ITD sensitivity using trains of pulses with frequencies characteristic of envelopes (e.g. 25 Hz). These results support suggestions that the residual ITD sensitivity seen in humans is due to envelopes.

257 Binaural Pitch Adjustment between Acoustical and Electrical Stimulation

Uwe Baumann, Andrea Nobbe

Department of Otolaryngology, Univ. of Munich Hospital GroBhadern, Marchioninstr. 15, Munich, Germany

Six users of the MED-EL Combi 40+ (C40+) cochlear implant device with moderate to profound hearing loss between 125 and 1000 Hz in the non-implanted ear took part in a binaural pitch adjustment experiment. The C40+ electrode array provides a deep insertion into the tympanic scala and a wide spatial separation of the stimulating electrodes. Due to the deep insertion it was expected, that electrodes located at or above the second cochlear turn would elicit the perception of very low pitch which might correspond to the perceptions at the non-implanted ear. The task of the subjects was to adjust the frequency of a sinusoid presented at the non-implanted ear by means of an adjusting knob until they perceived the same pitch that was elicited by a reference stimulus at the implanted ear. Acoustical and electrical stimuli were presented in an alternating order. Electrical stimulation was carried out with a fixed pulse rate of 800 pps at apical electrodes. For the individual subject, the number of applicable electrodes depended on the upper limit of the residual hearing in the non-implanted ear. The start frequency of the sinusoid was chosen randomly between 125 and 1000 Hz. For each reference electrode twenty adjustments were

collected. The results show adjustments corresponding to electrode position along the cochlea. With increasing distance from the apex, adjustments were set to higher frequencies. Between subjects, there was a considerable variation in the average adjustment for each of the tested reference electrodes. Although a full insertion of the electrode was confirmed by X-ray scans, frequency adjustments varied in between 150 and 380 Hz for the most apical electrode. The majority of the subjects showed no significantly different adjustments between the two most apical electrodes. The implication of these findings should be reflected in the design of the electrode and speech processing strategy.

258 Simulating Bilateral Cochlear Implant Processing in Normal Hearing Listeners

Patricia L. Moy, H. Steven Colburn

Biomedical Engineering, Boston University, 44 Cummings Street, Boston, MA, United States

Many cochlear implant (CI) recipients have reported improved speech intelligibility, but the effects of CI processing on interaural cues, such as interaural time difference (ITD) and interaural level difference (ILD), are still unclear. In this study, we adapted the Shannon et al. (1995) model to better understand the effects of CI processing on interaural cues. Sound localization and speech intelligibility performance are measured using simulated CI processing of virtual stimuli in normal hearing listeners.

Virtual stimuli are created using HINT sentences filtered by head-related transfer functions (HRTFs). The HRTFs were measured in a sound-treated room with a seven-loudspeaker array, positioned 5 feet from KEMAR in the horizontal plane. Behind-the-ear (BTE) microphones were placed on KEMAR during measurements to more accurately mimic the HRTFs of CI users.

In the simulation, the virtual signal was filtered into 8-frequency bands. The amplitude envelope was extracted and used to modulate an independent noise waveform for each band in each ear. With interaurally correlated noise, subjects were unable to lateralize the fused image of the waveform. Independent noise waveforms were chosen in order to avoid a coherent fine time structure. The separate bands of modulated noise were then added together and presented to the listener.

Normal hearing listeners' sound localization results are consistent with the ITD and ILD cues contained in the CI-processed signal with decorrelated noise as well as with the results of bilateral CI users in a study by Poon et al. (2003). Analysis of these cues showed that although the fine temporal structure of the signal was not present after the envelope was modulated with random noise, the envelope of the signal may offer some ITD cues to the listener. Our analysis will compare the interaural cues from signals in which the envelope waveform was used to modulate the decorrelated and correlated noise. [Supported by NIH DC00100].

259 Effect of experience on sound localization and speech intelligibility in noise in adults and children with bilateral cochlear implants

Ruth Y Litovsky¹, Jennifer Arcaroli², Aaron Parkinson², Patti Johnstone¹

¹*Waisman Center, University of Wisconsin, 1500 Highland Ave, room 567, Madison, WI, United States*, ²*Clinical Studies, Cochlear Americas, 400 Inverness, Denver, CO, United States*

In recent years, there have been improvements in speech processing strategies used in cochlear implants (CIs), which are particularly evident in speech understanding in quiet. However, for most CI users speech reception in a noisy or complex environment is still very poor. One possible reason for poor performance in noise is that most CI users have one device and cannot benefit from binaural information. A number of CI users have therefore received bilateral CIs, and in adults there are some indications that performance in some situations is significantly better. The extent to which experience with bilateral devices affects performance is still poorly understood. In addition, some children have recently also received bilateral CIs. This investigation focused on measurements of sound localization, speech intelligibility in noise for various spatial separations of speech and babble in 17 adults, most of whom were deafened post-lingually and implanted in a simultaneous procedure. Adults were tested on all measures at 3-months after activation of the CIs, and retested on the speech measures at 6-months. Children were tested on similar measures using computerized games. Three children were tested at 3- and 9-months post-activation, and several other children were also tested at 9-months. Several children with unilateral CIs also participated. In order to assess the extent to which bilateral CIs improve performance, testing was conducted with both CIs activated, and under unilateral conditions. Results suggest that, for the majority of adults, localization performance is significantly better under bilateral conditions compared with either ear in isolation. On the speech tests, performance is significantly better under a number of conditions with competing noise, and the bilateral benefit was especially evident at 6-months post-activation compared with 3-months. For children, there are also conditions under which bilateral CIs produce better performance than a single ear. There are some significant improvements in performance at 3-months compared with 9-months. These will be discussed in more detail. This work suggests that for bilaterally implanted CI users the benefit of having two CIs may require time after implantation during which the user learns to use both ears and to utilize binaural cues.

260 Sound direction identification with bilateral cochlear implants.

Arlene Neuman

Doctoral Program in Speech and Hearing Sciences, Graduate School, City University of New York, 365 Fifth Avenue, New York, NY, United States

The use of bilateral cochlear implants may lead to some of the advantages obtained with binaural hearing. The focus of this study is to determine the ability of persons with bilateral cochlear implants to localize speech and non-speech stimuli. Unilateral and

bilateral sound source identification performance of bilateral implantees is measured in the frontal arc of the horizontal plane using an array of nine loudspeakers arranged at 22.5° intervals. Sound identification performance is measured in the unilateral (right implant alone, left implant alone, and bilateral implants active) using speech stimuli and pink noise stimuli. Testing is carried out with subjects wearing their processors as programmed for daily use.

Data are analyzed to reveal the accuracy of sound source identification in each condition and differences between unilateral and bilateral performance. The accuracy of performance is compared to that of normal hearing listeners. Results to date indicate that in the unilateral condition the perceived sound source location is skewed towards the ear with the active implant. In the bilateral condition, sound source identification is improved, although not perfect. Variability is greater in the listeners with cochlear implants than in listeners with normal hearing.

261 Simulations of Bilateral Cochlear Implant Speech Reception in Noise

Christopher J Long, John M Deeks, Mei-Chern Leow, Robert P Carlyon

CBU, MRC, 15 Chaucer Rd., Cambridge, United Kingdom

Bilateral cochlear implants have been proposed as a means of improving speech understanding in noise via binaural advantages (e.g., better-ear and binaural-interaction effects). We investigate whether binaural-interaction cues are useable when only the envelope information is preserved - as is the case with many cochlear implant processors. In addition, we examine whether speech-cue integration across sides can aid performance.

To test the usability of binaural-interaction cues, six normal-hearing listeners heard a mixture of speech and noise that was either unprocessed or passed through a simulation of a cochlear implant speech processor. The stimuli were 16 medial consonants presented in quiet or in noise. The noise was diotic while the speech was either diotic or delayed by 600µsec on one side.

For the unprocessed stimuli, performance was significantly better (18%, $p < 0.01$) when the speech was delayed on one side compared to when both speech and noise were presented diotically, demonstrating a binaural-interaction advantage. However, no such advantage was observed for the processed stimuli.

To examine summation of speech information across ears, we interleaved the speech information such that the signals in the two ears occupied different frequency bands. Diotic speech and noise were processed with a 12-channel cochlear implant simulation. The 6 even-numbered channels were presented to the right ear and 6 odd channels were presented to the left. Subjects obtained an advantage of 12% (significant at $p < 0.01$) compared to the 6 even or odd channels alone which cannot be attributed to better-ear or binaural-interaction effects.

We conclude that speech processors that discard fine-structure information may not allow utilization of binaural-interaction cues. Instead, when performance with two ears exceeds that with the better ear alone, this may be due to summation of complementary speech information across sides.

Supported by the Leverhulme Trust and the RNID.

262 Report on results from a US multi-center study on adult bilateral cochlear implantation

AMY L BARCO¹, PATRICK SC D'HAESE², MARIAN ZERBI¹, PETER NOPP²

¹RESEARCH, MED-EL CORPORATION, 2222 E HWY 54 / STE B-180, DURHAM, NC, United States, ²RESEARCH, MED-EL GmbH, Fürstenweg 77a, A-6020 INNSBRUCK, Austria

A multi-center study within the United States was developed to evaluate bilateral cochlear implant outcomes in 30 post-linguistically deafened adults implanted with the MED-EL COMBI 40+. The objective of this poster presentation is to review the results of localization and speech understanding in noise and quiet. Pre- and post-operative vestibular function will also be discussed.

Speech perception testing in noise is completed using direct audio input with a portable CD player. Speech and noise materials are recorded onto CDs using head related transfer functions (HRTFs) as measured at the entrance to the ear canal. Direct audio input was chosen to reduce possible variability created by testing in the sound field using different loudspeakers and various room set-ups across centers. A decision tree is utilized to determine the appropriate signal-to-noise ratio for bilateral speech testing using CUNY sentences in noise (CCITT). The aim of the decision tree is to target a signal-to-noise ratio where the subject is performing near the 50% level in the best unilateral condition in an attempt to avoid ceiling effects in the favorable bilateral test conditions or floor effects in the more difficult unilateral conditions.

Localization testing is conducted in the horizontal-plane using a source identification task. The set-up includes an array of 20 loudspeakers. Testing is conducted in an anechoic chamber at Vanderbilt University. On each trial, a sound is presented from one of the 20 source positions, and the participant's task is to identify which loudspeaker emitted the sound. Data analyses include assessments of random error and response bias as well as a measure of overall error. Localization is evaluated separately for two different signals, a Gaussian noise burst and a speech sample.

263 Dichotic speech recognition by bilateral cochlear implant users

Arunvijay Mani, Philip Loizou

Electrical Engineering, Univ. of Texas-Dallas, 2601 N Floyd Road, EC 33, Richardson, TX, United States

Several studies have demonstrated that bilateral cochlear implants can provide significant benefit in terms of sound localization and speech recognition in noise. Bilateral implants also offer the possibility of providing dichotic electrical stimulation via a coordinated stimulation of the two implants. Potential benefits of dichotic electrical stimulation include a reduction in channel interaction since the stimulation will be alternated between the two ears, and also a reduction in power consumption since only a subset of electrodes within each ear need to be stimulated. In order for the bilateral implant users to receive these benefits, however, they must be able to spectrally fuse the information presented to the two ears.

The aim of this study is to investigate the ability of bilateral cochlear implant users to fuse spectral information presented dichotically. Two different methods of splitting the spectral infor-

mation were investigated. In the first method, the odd-index channels were presented to left ear and the even-index channels to the right ear. In the second method the lower frequency channels were presented to left ear and the high frequency channels to the right ear. For comparative purposes, speech was also presented monaurally. Bilateral implant users were fitted with a 12 channel CIS strategy and presented with sentences in quiet and in noise. Preliminary results indicated variability in performance among subjects. The performance of one subject with speech presented monaurally was significantly higher than with speech presented dichotically. In contrast, another subject performed the same with both dichotic conditions and the monaural condition in quiet. The outcome was different in noise for the same subject, as she performed significantly worse with the dichotic condition than with the monaural condition. Further data are currently being collected and will be presented.

Supported by NIDCD R01 DC03421

264 Neurotrophin-induced neuroprotection

Josef M Miller

Kresge Hearing Research Institute, University of Michigan, 1301 E. Ann St, Ann Arbor, MI, United States, Otolaryngology, Karolinska Institute, Karolinska Hospital, Stockholm, Sweden

It was in 1996 that the first reports appeared from several groups, showing that application of neurotrophic factors would enhance spiral ganglion cell survival following deafness. Since then, not only has the study of auditory nerve survival and cell death matured, but there is also a better general understanding of the role of neurotrophic factors in cell survival/maintenance in the peripheral and central nervous systems as well as in processes of age- and disease-related neurodegeneration. There is increased understanding of the programmed and environmental induced changes that occur in the expression of these factors, their signaling characteristics, and the mechanisms underlying their influence on nerve cell survival and death. We are also now learning how we can up-regulate endogenous factors or apply exogenous factors as interventions to protect cells from death. For the auditory system, we are also learning how peripheral processes of the auditory nerve can be induced to regenerate. It is therefore timely to review the topic of neurotrophin-induced neuroprotection and its application to the treatment of deafness.

The proposed symposium will bring a world expert on the general mechanisms of neurotrophin actions in the nervous system (Mark P. Mattson) and follow this with presentations on our new understanding of the mechanisms of nerve survival and death from in vitro studies of the auditory nerve cells (Steven Green), findings from in vitro studies of directed auditory nerve regrowth (Allen F. Ryan), and in vivo studies of the efficacy of neurotrophic factors to maintain and regrow the auditory nerve following deafness (Josef M. Miller). Finally, there will be a discussion of the implication of this work and potential for improvement of the benefits of cochlear implants for the deaf (Robert V. Shannon). This symposium will be of broad interest, with basic research and clinical importance and implications across a wide range of study areas. The following are brief summaries from each of the proposed presentations.

265 NEUROPROTECTIVE AND NEURORESTORATIVE SIGNAL TRANSDUCTION MECHANISMS.

Mark P Mattson

Laboratory of Neurosciences, National Institute on Aging, 5600 Nathan Shock Drive, Baltimore, MD, United States

The dysfunction and degeneration of neurons that occurs in various neurodegenerative disorders, including those involving cochlear hair cells and auditory neurons, share common cellular and molecular mechanisms. The mechanisms include oxidative stress, metabolic compromise and dysregulation of cellular calcium homeostasis. In addition, recent findings suggest that the deaths of auditory neurons in different models of deafness occurs by a process called apoptosis. My laboratory and other laboratories have shown that neurotrophic factors can protect neurons against insults relevant to the pathogenesis of deafness, by activating signal transduction pathways that induce the expression of genes encoding proteins that counteract neurodegenerative cascades. Such cytoprotective proteins include Bcl-2 family members, antioxidant enzymes and calcium-regulating proteins. The neurodegenerative process is believed to begin in synaptic compartments, and may involve overactivation of glutamate receptors and the triggering of apoptotic cascades. Neurotrophic factors protect synapses by suppressing apoptotic cascades and stabilizing mitochondrial function. Increased understanding of neuroprotective signaling is leading to novel approaches to preventing and treating deafness, including dietary manipulations that stimulate neurotrophic factor production. For example, dietary restriction (reduced caloric intake) induces the expression of brain-derived neurotrophic factor (BDNF) and stress resistance proteins (HSP-70 and GRP-78) in neurons and thereby protects them against oxidative, metabolic and excitotoxic injury (*Physiol. Rev.* 82: 637-672.)

266 Prevention of neuronal death by electrical activity: molecular mechanisms

Steven H Green

Dept. of Biological Sciences, University of Iowa, 143 Biology Building, Iowa City, IA, United States

Spiral ganglion neurons (SGNs) require hair cells for survival and gradually die in their absence. While this could limit the effectiveness of cochlear implants, mitigating factors are that the SGN death occurs over a period of years and that SGN death is reduced by electrical stimulation such as that provided by implants. Studies of cultured SGNs using molecular genetic techniques are revealing the molecular mechanisms and intracellular signals by which electrical activity and neurotrophic factors promote SGN survival. This allows us to understand how electrical activity synergizes with neurotrophic factors in promotion of survival and how electrical activity affects axonal growth, knowledge applicable to treatments directed toward improving SGN survival and promoting SGN axonal regrowth in implanted listeners. Five key results: (1) For SGN death in vivo after deafening, activation of proapoptotic signaling may be more significant than loss of prosurvival signaling. (2) In SGNs, electrical activity activates at least three prosurvival signaling pathways that act on distinct targets, in different cellular compartments. (3) Neurotrophic factors promote survival

by using intracellular signals that only partially overlap with those used by electrical activity. (4) Some of these pro-survival intracellular signals also affect axonal growth, in some cases inhibiting growth. (5) The effects of intracellular signals depend critically on their subcellular location. Activating or inhibiting specific signals or confining their activity to specific subcellular locations can restrict their actions to promotion of survival and/or axonal growth.

267 Regrowth Of Spiral Ganglion Neurites To A Cochlear Implant

Allen F Ryan¹, Lina M Mullen¹, Kwang Pak¹, Dominik Brors², Christoph Aletsee³, Stefan Dazert⁴

¹Otolaryngology, 0666, UCSD, 9500 Gilman Drive, La Jolla, CA, United States, ²Otolaryngology, University of Wurzburg, Josef-Schneider-Str. 11, Wurzburg, Germany, ³Otolaryngology, University of Wurzburg, Josef-Schneider-Str 11, Wurzburg, Germany, ⁴Otolaryngology, Ruhr-University Bochum, Bleich-Str 15, Bochum, Germany

Cochlear implants (CIs) have revolutionized treatment of the severely hearing impaired. However, some patients receive relatively less benefit from a CI. It is also clear that even optimal stimulation of the auditory system via a CI is not comparable to acoustic stimulation. A reason for this may be the number of information channels that can be achieved with a CI, less than about ten channels with current technology. This is presumably because spiral ganglion (SG) neurons and dendrites are located at a distance from CI electrodes, so that stimulation of small numbers of neurons is difficult. In contrast, the normal cochlea possesses thousands of channels, since each inner hair cell is separately innervated. If the dendrites of surviving SG neurons could be stimulated to grow very close to the electrodes of a CI in a highly ordered manner, and contact between neurites and electrodes maintained, it might be possible to create hundreds of information channels.

Neurites respond to numerous cues, from the substrates upon which they grow and from the fluids that surround them. These cues can influence neurite extension, neurite direction and neuronal survival. Substrate cues include molecules expressed on adjacent cell surfaces, acellular factors including matrix molecules, and physical cues such as surface shape and material. Soluble factors include growth factors and neurotransmitters.

We have studied the responses of SG neurons to a wide variety of neurite control cues. We have defined substances that promote the extension, branching, termination and fasciculation of neurites. We have also observed factors that provide positive directional cues, as well as repulsive cues that SG neurites avoid. We have also studied methods of delivering factors to SG neurons. These findings suggest strategies for using neurite control factors to establish relationships between SG neurons and the electrodes of a CI.

Supported by NIDCD grant DC00139, the VA Research Service, and NOHR

268 Neurotrophic factor and electrical stimulation promotes auditory nerve survival and regrowth following deafness

Josef M Miller^{1,2}, Richard Altshuler¹

¹Kresge Hearing Research Institute, University of Michigan, 1301 E. Ann St, Ann Arbor, MI, United States, ²Otolaryngology, Karolinska Institute, Karolinska Hospital, Stockholm, Sweden

Auditory nerve cell death occurs as a consequence of deafferentation following inner hair cell loss. While likely analogous to cell death following deafferentation elsewhere in the nervous system, the underlying molecular mechanisms are not fully understood. *In vitro* studies have suggested loss of neurotrophin support, changes in cellular oxidant state (either primary or secondary to neurotrophin deprivation), and changes in intracellular Ca²⁺ as contributing factors. We have demonstrated the significance of all these factors *in vivo*. Neurotrophic factors (NTF), including glial cell-line derived neurotrophic factor (GDNF*), brain derived neurotrophic factor (BDNF*), and fibroblast growth factor (FGF₁), enhance spiral ganglion cell (SGC) survival following deafferentation. Chronic electrical stimulation (ES) supports SGC survival, and its effectiveness is eliminated by the administration of an L-type Ca²⁺ channel blocker (verapamil), suggesting that changes in intracellular Ca²⁺ homeostasis mediate the protective effects of ES (consistent with *in vitro* studies of Green et al). Furthermore, benefits of ES and NTF extend beyond changes in survival, as they also promote SGC peripheral process regrowth. Local (intrascalar) or systemic antioxidant treatment partially prevents decreases in electrophysiological sensitivity that typically follow deafferentation as well as prevents SGC degeneration. These factors may promote cell survival and neurite growth through different or overlapping pathways. Having previously documented the importance of individual factors in isolation, we have assessed the relative efficacy of combination treatments. Our recent findings demonstrate an additive protective effect from a combination of NTF + ES on SGC survival and neurite outgrowth *in vivo*.

This work was supported by NIH Grant RO1 DC 03820; *NTFs supplied by Amgen.

269 Issues that neural regeneration could pose for the design of cochlear implants

Robert Shannon

Auditory Implants and Perception, House Ear Institute, 2100 W. Third St., Los Angeles, CA, United States

One of the factors limiting speech recognition with a cochlear Implant is the tonotopic selectivity of each electrode. Evidence shows that patients with present implant devices are not able to utilize the information from each electrode as an independent channel. Although present implants have 16-22 electrodes speech recognition performance is not different for 8, 16, and 22 electrodes. One potential reason for this limitation is the spread of activation from each electrode causing a smearing of the pattern of neural activation across electrodes. Neurotrophin induced regrowth of neurons and/or peripheral processes of spiral ganglion cells would reduce the distance between stimulating electrodes and activated neural elements, which should reduce stimulation current levels and thus reduce the overlap between electrodes. However,

such regrowth must be localized or it could actually degrade the tonotopic specificity of electrical stimulation. Lower thresholds and reduced cross-electrode interaction should increase the number of effective channels used by an implanted listener and so improve speech recognition. [Funded by NIDCD]

270 Fos Expression and Video-oculography During Cross-coupling Training in the Gerbil

Galen D Kaufman¹, Tara Ruttley², Tianxiang Weng¹

¹ENT, UTMB, 301 Univ. Blvd., Galveston, TX, United States, ²JSC, NASA, 2101 NASA Rd 1, Houston, TX, United States

The central brainstem patterns of Fos-defined neuronal activation and concurrent oculomotor behavior following combinations of stimuli with two simultaneous rotational axes were investigated in the Mongolian gerbil. Typically, an Earth vertical axis of rotation was combined with sinusoidal harmonic frequencies of roll or pitch motion. This cross-coupling produces Coriolis forces that are generally novel inputs for sensory integration. Continuous application of cross-coupling motion over an hour or more resulted in out-of-plane deviations of the normally horizontal VOR to horizontal rotation alone. VOR gain and phase shifts were evident depending on the particular stimulus combination. Animals subjected to a unilateral labyrinthectomy and then intense cross-coupling training during compensation revealed some improvement of VOR gain in the first few days compared to untrained animals recovering from unilateral lesion, but only for one direction of horizontal head movement. Fos expression generally decreased with training, except in the prepositus hypoglossus nucleus. Asymmetric expression in the inferior olivary C nucleus and the prepositus also differentiated the direction of horizontal motion occurring during cross-coupling. The ventrolateral outgrowth and beta nuclei of the inferior olive expressed Fos bilaterally during cross-coupling stimuli; patterns not seen with any other vestibular paradigm. The cross product of the maximum velocity for each axis of rotation did not correlate with the amount of Fos expression in general, but rather seemed to produce a maximum response for intermediate levels of stimulation, implying a frequency dependence. Cross-coupling in a lighted surround increased Fos expression in the vestibular nuclei. Our findings describe a specific circuitry dealing with the consequences of an artificial gravity (AG) environment.

271 Vestibular Responses of Rostral Fastigial Neurons

Aasef G. Shaikh¹, J. David Dickman², Dora E. Angelaki¹

¹Neurobiology, Washington University in St. Louis, 660 S. Euclid, St. Louis, MO, United States, ²Research, Central Institute for the Deaf, 4560 Clayton Avenue, St. Louis, MO, United States

Accurate awareness of spatial orientation, which is fundamental in maintaining posture and voluntary activities, is a result of complex multidimensional interactions of sensory signals originating from multiple sources and different coordinate systems. Signals originating from otolith, semicircular canal, and muscle proprioceptive receptors are examples of such sensory cues required by the CNS to execute reflex control of body posture and movement. The deep cerebellar nuclei are some of the known sites of signal convergence from vestibular and proprioceptive systems. Here we report

on the properties of primate rFN (rostral fastigial nucleus) neurons. Extracellular single unit activity evoked by combinations of 3D rotational and pure translational stimuli was recorded to identify the convergent properties of these neurons. Using novel, combined tilt/translation stimuli, we also investigated if rFN neurons can selectively encode pure translations. We have also examined the coordinate system of encoding translational motion by systematically varying both the direction of sled motion relative to the body and the static orientation of the head relative to the trunk. We found that all rFN VO neurons (51 out of 51) responded during translation in one or more directions. Thus, unlike neural responses in the vestibular nuclei (VN), none of rFN VO neurons could be characterized as Canal-Only neurons. The majority of rFN neurons, unlike those in the VN, also more closely encode the translational component rather than the total gravito-inertial acceleration. Finally, we encountered neurons in the rFN that encode translation in either head or body coordinates. The work was supported by F32 DC-006540, R01-DC04160 and NASA NAG 2-1493.

272 Different forms of VOR learning in mice reveal multiple adaptive mechanisms with distinct time courses

Bernd Michael Faulstich, Kimberly Ann Onori, Sascha du Lac

SNL-D, The Salk Institute, 10010 North Torrey Pines Rd., La Jolla, CA, United States

The oculomotor system maintains gaze stability during head movements via a combination of the vestibulo-ocular reflex (VOR) and optokinetic reflex (OKR). These behavioral reflexes exhibit a remarkable degree of plasticity, and previous studies have suggested the existence of multiple adaptive mechanisms that may be engaged under different stimulus conditions. In the present study we examined the time course and stimulus dependence of adaptive gain changes in the mouse oculomotor system following different adapting paradigms. Our goal was to provide a framework for models of oculomotor learning by investigating how the nature and time courses of adaptive gain changes depend on stimulus conditions. Adaptive gain changes were induced by vestibular deafferentation, plugging of the semicircular canals, and visual-vestibular mismatch training. Unilateral vestibular deafferentation induced a dramatic drop in VOR gain which recovered partially in two distinct temporal phases between 2-4 days and 2-3 weeks. Concomitantly, in response to high frequency visual stimulation, OKR gain increased then declined but was maintained above control values. Unilateral canal plugs, which impair head motion encoding but preserve spontaneous nerve activity, evoked similar changes in OKR gain and in the late phase of VOR gain recovery. 30 minutes of out-of-phase visual-vestibular mismatch training induced rapid gain increases in both the VOR and OKR. However, in-phase mismatch training evoked the expected decreases in VOR gain but increases in OKR gain. Our findings demonstrate that adaptive changes in the VOR learning involve multiple mechanisms with different time courses. Furthermore, since the gain changes of the OKR are apparently unidirectional while gain of the VOR can be adapted in either direction, models of motor learning in this system must assume different processing and plasticity mechanisms for image motion signals vs. head motion signals.

273 Influence of GABA Antagonists on Afferent Response Dynamics in the Crista Ampullaris

Stephen Morris Highstein¹, Gay R. Holstein², Curtis King³, William Nesse³, Georgio Martinelli⁴, Richard D. Rabbitt⁵

¹Otolaryngology, Washington University School of Medicine, Box 8115 4566 Scott Ave., Saint Louis, MO, United States,

²Neurology, Mt. Sinai School of Medicine, 5th Ave and 100th St., New York, NY, United States, ³Bioengineering, University of Utah, G6568, Salt Lake City, UT, United States, ⁴Surgery, Mt. Sinai School of Medicine, 1 Gustav Levy Pl., New York, NY, United States, ⁵Bioengineering, University Utah, G 6568, Salt Lake City, UT, United States

Comparison of hair cell versus afferent responses in the semicircular canals of the oyster toadfish reveals striking differences for both step and sinusoidal stimuli. Hair cell receptor current and voltage modulation closely mimicked hair bundle displacements while afferent firing rate discharge exhibited profound levels of adaptation to maintained hair bundle displacements and significant frequency-dependent responses for sinusoidal stimuli. The signal processing performed by the crista can be viewed as fractional mathematical differentiation (differential calculus) that acts upon velocity-sensitive hair cell voltage signals prior to transmitting the information to the brain. Data to date implicate hair-cell/afferent synaptic complex as the major site responsible for this signal processing. It has been recently shown that highly adapting semicircular canal afferents receive convergent synaptic inputs from both glutamatergic and GABAergic hair cells (Holstein et al. in press). We hypothesize that convergent glutamatergic and GABAergic transmission onto dendrites of single afferent neurons leads directly to the mathematical differentiation and adaptation of semicircular canal afferents. We suggest that the two-chemoanatomic types of hair cells have differential activation and kinetics to velocity inputs. This differentiation would impact the responses of afferents in 3 ways: the phase advance would be lost, the gain would flatten, A-type gain for low frequency stimulation would increase due to the loss of the fractional derivative (GABA inputs), and the LG Bode plots would appear identical since the LG units are hypothesized to have no GABA inputs. Present experiments were designed to test this hypothesis with specific attention to the GABA_B receptor. Antagonists were delivered systemically while monitoring single unit discharge modulation and summed nerve potentials in response to sinusoidal stimulation. Consistent with the hypothesis, GABA_B antagonists caused a gain change and phase retardation for sinusoidal stimuli in selected single unit and summed responses. Data support the hypothesis that convergent synaptic inputs play a role in shaping semicircular canal neural signals transmitted to the brain. (Supported by NIDCD grant DC01837)

274 Multiple Isoforms of the Ryanodine and IP₃ Receptors Are Expressed in Rat Inner Ear Ganglia and Endorgans

Peter Cameron, Dimple Modi, Steven D. Price, Anna Lysakowski

Anatomy and Cell Biology, Univ. of Illinois at Chicago, 808 S. Wood St., Chicago, IL, United States

Ryanodine receptor calcium release channels have been shown to be widely expressed in a variety of mammalian tissues. Ryanodine receptor type 1 has been shown to be the predominant isoform in skeletal muscle, while isoforms 2 and 3 are more abundant in cardiac muscle and hippocampus, respectively (McPherson and Campbell, JBC, 1993). There have been no studies, however, on their localization in the vestibular periphery and cochlea. In the present study, RT-PCR and immunocytochemistry were used to ascertain which ryanodine and IP₃ receptor mRNA isoforms were expressed within the maculae, cristae, vestibular and spiral ganglia, and cochlea.

Inner ear organs were dissected from 6 rats and total RNA was obtained. Rat skeletal and cardiac muscle and hippocampus were also obtained to use as positive controls. Intron-spanning primers specific for ryanodine receptor isoforms 1, 2 and 3 (Neylon et al., Biochem Biophys Res Comm, 1995) were generated and RT-PCR was performed on 20ng total RNA from each endorgan (with the exceptions of 10ng total RNA from cristae endorgans and 5.2 ng total RNA from cochlea endorgans). Results indicate that ryanodine receptor isoforms 1, 2 and 3 are present in maculae, cristae, and in vestibular and spiral ganglia. Ryanodine receptor isoform type 1 was shown to be present in cochlea, while isoforms 2 and 3 are yet to be tested. Results for IP₃ receptor isoforms 1 and 3 show their presence in maculae and spiral ganglia. Other inner ear samples remain to be tested.

Confocal microscopy also confirms the presence of RyR in auditory and vestibular periphery. Pan-ryanodine receptor antibody (Chemicon) staining indicates the presence of RyR in cochlear outer hair cells, extrastriolar hair cells in otolith organs, and hair cells in both central and peripheral crista. A pan-IP₃ receptor antibody (Chemicon) shows IP₃ labeling in calyces. We are using isoform-specific antibodies to determine more specific staining patterns.

Supported by NIH R01 DC2521.

275 Voltage-dependent and store-mediated Ca²⁺ sources in frog vestibular hair cells

Paola Perin^{1,2}, Laura Botta², Alessia Pascale³, Marialaura Amadio³, Paolo Valli²

¹NPP, University of Chicago, 947 E.58th street, Chicago, IL, United States, ²DSFFCM, University of Pavia, via Forlanini 6, Pavia, Italy, ³Pharmacology, University of Pavia, via Taramelli 2, Pavia, Italy

Voltage-dependent Ca²⁺ currents trigger transmitter release at the synapse between hair cells and afferent fibers. In frog vestibular hair cells, we have recently shown that an active CICR (Ca²⁺-induced Ca²⁺ release) process is triggered by the prolonged activation of voltage-dependent channels. This CICR is sensitive to both ryanodine and caffeine, is maximal in the supranuclear region of

the cell body, and is able to affect afferent transmission (Lelli et al. 2003). These data suggest that Ca^{2+} inflow through voltage-dependent Ca^{2+} channels in the membrane subsequently diffuses to ryanodine receptors, thereby activating CICR.

In the present work, we performed immunohistochemical, pharmacological and electrophysiological studies to localize the Ca^{2+} sources related to afferent transmission.

Using immunohistochemical methods, ryanodine receptors were localized in the same region as the maximal caffeine-sensitive Ca^{2+} increase. As regards voltage-dependent Ca^{2+} channels, labeling with anti-Cav1.3 antibodies was observed as a spot pattern on the hair cell surface, probably representing channel clusters. On the other hand, Cav1.2 and Cav2.2 antibodies labeled a subpopulation of nerve fibers, and Cav2.3 strongly labeled nerve terminals. Immunoreactivity for Cav2.3 disappeared after chronic deaf-ferentation, suggesting that R-type channels are located at the efferent synapse.

To test the presynaptic role of L-type channels in hair cells, we measured membrane capacitance variations following depolarizing steps. The experiments were performed on isolated hair cells from the frog crista in perforated whole-cell configuration. The average response to a 500 ms depolarization to 0 mV was 180 ± 40 fF ($n=10$), corresponding to the release of about 5000 vesicles. Consistently with a presynaptic role of L-type channels in hair cells, the L-type blocker nimodipine strongly reduced depolarization-evoked capacitance increases ($78 \pm 7\%$, $n=2$), whereas the N-type blocker ω -conotoxin GVIA and the R-type blocker SNX-382 had no significant effect ($n=2$ each). The incubation with ryanodine was also able to reduce capacitance steps, suggesting that both voltage-dependent and store Ca^{2+} sources are involved in afferent release, possibly over different time scales. The effects of nimodipine, ryanodine and caffeine on the rate and dynamics of quantal discharge are discussed

276 Cellular Mechanisms for Altered K^{+} Current Expression in Human NF2 Schwann Cells (SC) may be mediated by Differential Ca^{2+} Handling in the Diseased and Normal Cells

Weihong Feng¹, Nancy Ratner², Karen J Doyle³, Ebenezer N Yamoah¹

¹Center for Neuroscience/Otolaryngology, University of California Davis, 1515 Newton Ct, Davis, CA, United States, ²Cell Biology Neuro & Anatomy, University of Cincinnati, Cincinnati, 4086 Egbert Ave, Cincinnati, OH, United States, ³Otolaryngology, University of California Davis, 2521 Stockton Blvd., Ste. 7200, Sacramento, CA, United States

Neurofibromatosis type 2 (NF2) is an autosomal dominant disease that is characterized by vestibular schwannomas, and is associated with balance and hearing loss. The functional mechanisms of NF2 remain uncertain. A correlation between high outward K^{+} currents and increased cell proliferation rate has been described. In addition, previous studies in several cell types have demonstrated that Ca^{2+} tightly regulates the expression of ion channels. We studied in vitro the differential expression of K^{+} currents in Schwann cells (SCs) from human NF2 patients, and normal SCs. Outward K^{+} current was recorded by depolarizing voltage step from a holding potential

of -80 mV. Whereas a transient outward K^{+} current was observed in normal SCs, no detectable current was recorded in NF2 SCs. In contrast, a sustained outward K^{+} current was significantly enhanced in NF2 SCs by at least 3-fold compared to normal SCs.

Intracellular Ca^{2+} in normal and NF2 SCs were measured by confocal microscopy using Fluo-4 as a Ca^{2+} indicator dye; confocal images of fluo-4 fluorescence were taken every 1 second in single SCs. NF2 SCs showed a marked increase in spontaneous Ca^{2+} transient as compared to normal SCs in solutions containing 0.05 mmol/L Ca^{2+} . Treatment of cells with 30 μM cyclopiazonic acid, an intracellular Ca^{2+} pump blocker, resulted in the release of Ca^{2+} from intracellular stores in normal and NF2 SC; however the effect of cyclopiazonic acid on Ca^{2+} levels of NF2 SCs was modest compared to normal cells. We infer that altered Ca^{2+} homeostasis in the diseased SCs may mediate changes in the expression of different K^{+} conductances.

This was supported by grants to ENY (NIH-DC03828, DC04523).

277 Kir4.1 potassium channel subunit expression in the vestibular sensory epithelia of mice.

Dora Acuna¹, Akira Ishiyama², Gail Ishiyama³, Ivan A Lopez¹

¹Surgery, UCLA School of Medicine, 31-25 Rehabilitation Ctr 1000 Veteran Ave, Los Angeles, CA, United States, ²Surgery, UCLA School of Medicine, 31-25 rehabilitation Ctr 1000 Veteran Ave, Los Angeles, CA, United States, ³Neurology, UCLA School of medicine, 31-25 rehabilitation Ctr, 1000 Veteran Ave, Los Angeles, CA, United States

A critical role for Kir4.1 inwardly rectifying potassium (K) channel subunit has been demonstrated in inner ear development and hearing in mice with null mutation for this channel (Rozengurt et al., 2003. *Hear. Res.*, 177:71-80). In this model, vestibular type I hair cells (HCs) degenerate over the initial postnatal weeks, but type II HCs seem to be unaffected, which suggests a differential expression for this subunit in vestibular HCs. To date it is not clear if HCs express this K channel subunit. (Hibino et al 1997. *J Neurosci*, 17:4711-4721). However, the existence of potassium selective inwardly rectifying conductances appears to be expressed by mouse HCs (Rusch and Eatock, 1996, *Ann NY Acad. Sci* 781, 71-84). In the present study we determine the expression of Kir4.1 in the vestibular sensory epithelia of young wild type mice (4-6 weeks old) using an affinity purified rabbit polyclonal antibody against Kir4.1 and indirect immunohistochemistry. We found punctate immunoreactivity on type I HCs. This immunoreaction was concentrated in the basal pole of the hair cell somata. Type II HCs also express Kir4.1 immunoreactivity, but to a lesser extent. Kir4.1 expression was uniform throughout the sensory epithelia with no differences between the crista or utricle zones. Nerve calyces, terminals, supporting cells and transitional cells were non-immunoreactive. Control positive immunostaining included the detection of Kir4.1 in the stria vascularis and satellite cells surrounding the spiral ganglia neurons in the mouse cochlea. The staining in mouse vestibular HCs is in contrast with a previous report of no immunostaining in the vestibular sensory epithelia of the rat.

278 Mechanoelectrical Transduction (MET) and Basolateral Currents in Hair Cells of the Turtle Utricle

Katherine J Rennie¹, Anthony J Ricci²

¹Otolaryngology and Physiology and Biophysics, UCHSC, 4200 E Ninth Ave B205, Denver, CO, United States, ²Neuroscience Center and Kresge Hearing Labs, LSU, 2020 Gravier St, Suite D, New Orleans, LA, United States

In the turtle utricle type I vestibular hair cells are confined to a narrow band called the striola, whereas type II hair cells are found in both striolar and extrastriolar regions. Hair bundles in the striola are wider than those in the extrastriola and type I hair cells may have more stereocilia than type II hair cells (Peterson et al. *Ann NY Acad Sci.* 781:85-102, 1996, Severinsen et al. *JARO in press*). We have recorded whole cell responses of different hair cell types to mechanical displacement of hair bundles with a stiff glass probe in the wholemount turtle utricle.

Most type I hair cells showed a previously described large K⁺ current (I_{K1}) at a holding potential of -70 mV, which deactivated following hyperpolarizing steps to -100 mV and was not blocked by replacement of K⁺ in the patch electrode solution with Cs⁺. In some type I cells the activation of I_{K1} was shifted to more positive membrane potentials. In these cells, maximal hair bundle displacements in current clamp depolarized the membrane potential above -30 mV. Type II hair cells did not have large resting conductances and large receptor potential changes were observed in response to hair bundle displacements. In voltage clamp, striolar type II hair cells had rapidly activating, slowly inactivating outward currents, whereas smaller, rapidly activating, rapidly inactivating currents were present in extrastriolar type II hair cells.

Hair bundle displacement resulted in peak MET currents of 492 ± 216 pA (mean ± SD, n = 7) in type I hair cells, 149 ± 47 (n = 4) in striolar type II hair cells and 134 ± 52 pA (n = 4) in extrastriolar type II hair cells. MET currents adapted to maintained displacements with rapid and slow components as described previously for hair cells of the turtle papilla (Wu et al. *J. Neurophysiol.* 82:2171-2181, 1999). The larger MET currents we observed in type I hair cells may occur because type I hair cells in the turtle have more stereocilia and therefore more MET channels than type II hair cells.

Supported by an APS Research Career Enhancement Award (KJR) and NIDCD DC03896 (AJR).

279 Enhanced healing of chronic tympanic membrane perforations

Magnus von Unge¹, Malou Hultcrantz¹, Petri Olivius¹, Gregory Margolin¹, Joris JJ Dirckx², Anisur Palash Rahman³

¹ENT, Karolinska Institute and Hospital, Karolinska Sjukhuset, Stockholm, Sweden, ²BIMEF, RUCA, Groenenburgerlaan 171, Antwerp, Belgium, ³Center of Hearing Research, Karolinska Institute, Karolinska Sjukhuset, Stockholm, Sweden

Background. Chronic tympanic membrane perforations are relatively common sequel after recurrent otitis media and grommets. Surgery is often needed. We aim to evaluate possible enhancing effects of biological or biochemical agents in the healing process,

making surgery less needed. The healing process needs to be further studied and experimental models to be developed.

Acute perforations. Myringotomy was made with a 0.2mm wide laser beam in ten rats in order to create a standardized fresh perforation in the left ear. The right ear served as control. After 30 days the tympanic membrane stiffness was measured in vitro with moire interferometry. Histology was also made. Results: All perforations were healed and showed a similar displacement pattern as the controls. Discussion: The mechanical function obviously restores quickly as the fresh perforation heals.

Chronic perforations. Myringotomy was made on both sides with the laser beam in five rats and five mice. The right tympanic membrane was exposed daily to a solution of 1% cortisone for ten days. After one month the tympanic membranes were harvested and studied with histology. Results: All perforations were still open in all ears. Discussion: The chronic perforation rat model, described by Hellström et al, was thus adopted. The model also worked well in mice.

Human mesenchymal stem cell treatment. A chronic perforation was produced in both ears of ten rats. After one month all perforations were refreshed, i.e. the epithelial ring that runs along the perforation edge was removed. Then a droplet with human, mesenchymal stem cells was applied over the perforation on the left side, and a blank was applied on the right, control side. Results: The perforations did not heal in greater number in the stem cells treated ears. Discussion: In a previous study an obvious difference between stem cell-treated and not treated fresh perforations was obtained. In that study embryonic stem cells were utilized.

280 Dexamethasone inhibits high affinity sulfate transport in otosclerotic cell cultures

Yutaka Imauchi¹, Pascale Laine¹, Olivier Sterkers^{2,3}, Marc Lombes⁴, Evelyne Ferrary², Alexis Bozorg Grayeli^{2,3}

¹EMIO112, INSERM, Faculté Xavier Bichat, 18 Rue Henri Huchard, Paris, France, Metropolitan, ²EMI 0112, INSERM, Faculté Xavier Bichat, 18 Rue Henri Huchard, Paris, France, Metropolitan, ³Otolaryngology, Hôpital Beaujon, 100 Boulevard du Général Leclerc, Clichy, France, Metropolitan, ⁴U478, INSERM, Faculté Xavier Bichat, 18 Rue Henri Huchard, Paris, France, Metropolitan

Otosclerosis is a bone remodeling disorder associated with inflammatory lesions. Previously, we reported an increased high affinity sulfate transport activity in otosclerotic primary cell cultures. This activity was specifically inhibited by sodium fluoride, a drug with clinical efficacy. We investigated the effect of dexamethasone (Dex) on this sulfate transport activity in otosclerosis, since dexamethasone is proved to modulate the bone turn-over, and to inhibit the inflammatory process. Primary cell cultures were obtained from stapes and external auditory canal in otosclerosis (n=8) and control patients (n=8). A human osteoblast cell line (SaOS-2) was also studied. The effects of Dex (10⁻¹² to 10⁻⁶ M) and RU 486 (10⁻⁷ M), an antagonist of corticosteroids, were studied on the high affinity sulfate transport by sulfate uptake.

Dexamethasone inhibited the transport in only otosclerotic stapes (basal: 20.2 ± 2.38 versus 16.8 ± 1.95 pmol/μg of protein/5 min after 10⁻⁷ M Dex, P < 0.005, paired t-test). This effect appeared to be dose dependent, and was antagonized by RU 486. In contrast,

dexamethsone stimulated the sulfate transporter activity was in SaOS-2. In conclusion, Dex inhibited the sulfate transport specifically in otosclerotic stapes at therapeutic concentrations. This effect may lead to a new therapeutic option in otosclerosis.

281 17-beta estradiol effect on sulfate transporter (DTDST) activity in otosclerotic bone cell cultures and in SaOS-2

Yutaka Imauchi¹, Pascale Laine², Olivier Sterkers^{1,3}, Evelyne Ferrary¹, Alexis Bozorg Grayeli^{2,3}

¹EMI0112, INSERM, Faculté Xavier Bichat, 18 Rue Henri Huchard, Paris, France, Metropolitan, ²EMI 0112, INSERM, Faculté Xavier Bichat, 18 Rue Henri Huchard, Paris, France, Metropolitan, ³Otolaryngology, Hopital Beaujon, 100 Boulevard du General Leclerc, Clichy, France, Metropolitan

Diastrophic dysplasia sulfate transporter (DTDST) is involved in the regulation of the bone turn-over, and its activity in otosclerosis is abnormally high. Taking into account the role of estrogens in the progression of otosclerosis, the possible effect of estrogens on DTDST was investigated in otosclerotic bone cell cultures, and in SaOS-2, a human osteoblastic cell line.

Primary bone cell cultures of stapes, and external auditory canal (EAC) bone were obtained from 23 patients with otosclerosis, and from 10 control patients (cerebellopontine angle tumor surgery). These cultures, and SaOS-2 cells were assessed in parallel. Estrogen receptors (ER) were detected by RT-PCR. DTDST activity was assessed by sulfate uptake in basal condition, and after 24h incubation with 17-beta estradiol at concentrations ranging from 10⁻¹² to 10⁻⁶ M.

Both primary cell cultures, and SaOS-2 expressed type alpha ER, while type beta ER mRNA was predominantly expressed in SaOS-2. In primary cell cultures, no modification of DTDST activity could be observed by 17-beta estradiol at 10⁻⁸ M. In SaOS-2, DTDST activity was inhibited by 17-beta estradiol (93.5 ± 9.21 versus 83.6 ± 8.83 pmol/mg prot/5min, n=29, mean of differences=9.97, paired t-test, P < 0.01). In conclusion, DTDST activity is regulated by estrogens in SaOS-2, but not in primary cell cultures from stapes, and EAC. This difference in the regulation mechanisms may be related to the type of ER expressed.

282 Expression of gap junction protein connexin 43 and connexin 26 in human cholesteatoma

Yun-Hoon Choung¹, Keehyun Park¹, Sung-Kyun Moon¹, Sung Ook Kang¹, Alexander Markov Raynov²

¹Otolaryngology, Ajou University School of medicine, San 5, Wonchon-dong, Paldal-gu, Suwon, Korea, Republic of,

²Otorhinolaryngology, University Hospital "Tzaritza Joanna", Medical University – Sofia, 26, Danail Nikolaev Blvd., Sofia, Bulgaria

Background and Objectives: Cholesteatoma is an otologic disease having characteristics of hyperproliferation and differentiation of epithelial cells, and needs intercellular signal exchange through gap junctions as well as intercellular signal pathway. Connexin(Cx) is a gap junction protein for intercellular communication, and especially Cx 26 and Cx 43 are plenty in human epithelial cells. The objective of this study was to analyze the expression and possible roles of Cx 43 and Cx 26 in human

cholesteatoma comparing normal epithelium. **Study design;** Ten retroauricular skins, deep meatal skins, and cholesteatomas were taken during middle ear operations in Department of Otolaryngology, Ajou University Hospital for this study. **Methods;** Immunohistochemical staining and reverse transcription-polymerase chain reaction(RT-PCR) were used for detection of Cx 43 and Cx 26. The expression patterns of Cx 43 and Cx 26 were also compared with that of proliferation marker Ki67 for identification of roles of Cx in cholesteatoma. **Results;** In human cholesteatoma, Cx 43 and Cx 26 were expressed in whole suprabasal layer, especially in middle portion. But normal retroauricular skin showed weak expression of Cx 43 in upper spinosal and granular layers, but not in basal layers, and the restricted localization of Cx 26 in basal layer near hair follicles. The expression of Cx 43 and Cx 26 in deep meatal skin was weak but similar patterns to that of cholesteatoma. In RT-PCR, the expression of Cx 43 and Cx 26 were increased in cholesteatoma than in retroauricular skin. And Cx 43, and Cx 26-expressed epithelial cells in cholesteatoma were not identical to the Ki-67 expressed cells, suggesting Cx 43 and 26 may be related to differentiation rather than to proliferation. **Conclusion;** Human cholesteatoma showed upregulated expression and different localization of Cx 43 and Cx 26, gap junction protein for intercellular communication, compared with normal retroauricular skins, suggesting that perturbations of intercellular communication through gap junctions may be associated with the pathology of human cholesteatoma.

283 Effect of *Pseudomonas aeruginosa* virulence factors on Osteoclastogenesis in vitro

Lei Zhuang, Jae Jung, Mary Pashia, Eric Wang, Richard Chole

Otolaryngology, Washington University, 660 South Euclid Ave. Campus Box 8115, St Louis, MO, United States

Cholesteatoma is a well known complication of chronic otitis media. Cholesteatomas have a propensity to illicit inflammatory responses resulting in osteoclasts recruitment and activation. Bony erosion by osteoclasts can subsequently lead to hearing loss, vestibular damage, and invasion of central nervous system. Due to its chronic nature and likelihood of recurrence, in spite of proper topical and systemic antibiotics, surgical intervention has been the only effective measure to eradicate cholesteatoma and the underlying infection. Recent studies have suggested that recalcitrant bacterial infection is an important contributor to the chronicity and morbidity of middle ear infection. In support of this, we have demonstrated presence of bacterial biofilms in cholesteatomas. Bacteria form biofilms by first adhering to a surface and then elaborating an extracellular polymeric matrix. We hypothesized that chronic infection by *Pseudomonas aeruginosa* (PA) contributes to both the chronicity and bone resorption associated with cholesteatoma. In this study, we investigated the role of two PA secretory products, LPS (lipopolysaccharide) and exotoxin A, in osteoclastogenesis in vitro. Osteoclasts were generated in vitro using two different methods: isolated bone marrow monocyte and stromal cell co-cultures. Our results show that LPS dose dependently increased osteoclastogenesis in isolated bone marrow monocytes but not in stromal cell co-cultures. Exotoxin A had no effect on osteoclastogenesis except at high concentrations where this factor was toxic to the cells. Different species of bacteria and different

strains within species produce unique LPS serotypes. We have isolated from infected cholesteatomas 11 vigorous biofilm forming *Pseudomonas aeruginosa* strains, which we've named *Otopathogenic Pseudomonas aeruginosa* (OPPA). Future investigations will examine the differential ability of these LPS serotypes to induce osteoclasts.

284 Factors Affecting Formation and Progression of Gerbilline Cholesteatoma

Steven P. Tinling¹, Richard A. Chole²

¹Otolaryngology, University of California, Davis, 1515 Newton Ct., Rm. 209, Davis, CA, United States, ²Department of Otolaryngology, Washington University School of Medicine, 660 South Euclid Avenue, Campus Box 8115, Saint Louis, MO, United States

The role of keratinizing epithelium (KE) of the tympanic membrane (TM) and external ear canal (EAC) in the formation and progression of gerbilline cholesteatoma (C) was studied. The normal rate and migration pattern of terminal keratinocytes were measured by recording ink drop movement on the TM. The EAC and TM were then examined over time for gross pathologic changes associated with spontaneous C development, with samples taken for comparative histopathology. Also, the proliferation index (PI) for the KE of the TM and EAC was determined for normal ears and ears with spontaneous or induced C. The normal radial migration pattern and rate of 0.1 mm/day is similar to the human radial pattern and rate of 0.3 mm/day. This is in contrast to the guinea pig which does not form spontaneous C, has a non-radial pattern and a rate of 0.8 mm/day. In animals followed for spontaneous C development, the TM either remained normal or became thickened in association with a middle ear effusion. Ears with effusion either reverted to normal, had no accumulation of canal debris, had recurrent accumulation and clearing of debris or had continuous accumulation of debris with C formation. Only ears with continuous debris accumulation formed cholesteatomas. Histopathologic analysis showed significant thickening of KE of the TM and EAC in C associated with middle ear effusion when compared to normal. The greatest increase occurred in the pars flaccida (PF) and lateral and medial superior EAC. The PI was significantly increased by 7 times in C over normals. Our results support the hypothesis that C in the gerbil begins with keratin accumulation on the PF and superior medial EAC in conjunction with middle ear inflammation and an increase in the PI of the KE. The increased PI results in thickened KE and accumulation of desquamated keratin. This cycle fills the EAC from superior to inferior and continued production of trapped keratin results in distension of the TM and middle ear morbidity.

285 Proteomic analysis and Microarray of the cholesteatoma

Jeong Lim Kim¹, Gi Jung Im², Hak Hyun Jung²

¹Medical Science, Korea Univ.College of Medicine, Dept.of Otolaryn.Head&N.Surg.Korea University Hospital, Anamdong 5ga 126-1, Seoul, Korea, Democratic People's Republic of, ²Otolaryn.Head&N.Surg, Korea Univ.College of Medicine, Dept.of Otolaryn.Head&N.Surg.Korea University Hospital, Anamdong 5ga 126-1, Seoul, Korea, Democratic People's Republic of

Proteomic analysis and Microarray may be a power tools to identify and characterize the specific proteins and genes related to the pathogenesis of some diseases including cholesteatoma. The purpose of the present study was to identify the up-regulated proteins and to detect the expressional difference of genes in human cholesteatoma.

At first, cholesteatoma matrix and normal retroauricular skins were intraoperatively obtained from cholesteatoma patients. In a case of proteomics, we performed two-dimensional electrophoresis for separating the proteins by molecular weight and detected about six hundreds of protein spots and analyzed the 37 up-regulated spots by MALDI-TOF in cholesteatoma. As a result, two candidates proteins (PCNA, osteoclast stimulating factor-1) related to cellular proliferation and bone destruction were identified and we also detected seven proteins (P-13-kinase P55 gamma subunit, RET protooncogene tyrosine kinase receptor, adenosine kinase, etc.) related to the mechanism of signal transduction in the pathogenesis of cholesteatoma. And then up-regulation of PCNA and OSF-1 were confirmed by immunohistochemistry and RT-PCR.

In a case of Microarray, we extracted RNA of cholesteatoma matrix and normal retroauricular skins and labeled each RNA using MAGIC Labeling Kit for RNA Amplification (MacroGen). And then We hybridized labeled RNA mix on the Magic Oligo human chip 10K (MacroGen, 10115 genes) and performed Image analysis, Normalization, Data analysis. As a result, We detected the expressional difference of 482 genes. Among detected 482 genes, 291 genes are up-regulated and 191 genes are down-regulated in the cholesteatoma.

In these studies, we could know the changes of proteins and genes in cholesteatoma. In the not too distant future, We could be provided libraries of biomarkers and immunoarray screens for monitoring using the proteomics and Microarray technology.

286 Bacterial and Immune-Mediated Otitis Media in Mast-Cell Deficient Mice

Joerg Ebmeyer^{1,2}, Kwang Pak^{1,2}, Umay Ebmeyer¹, Masayuki Furukawa^{1,2}, David Broide³, Allen Ryan^{1,2}, Stephen Wasserman³

¹Department of Surgery/Otolaryngology, UCSD, 9500 Gilman Dr., La Jolla, California, United States, ²Department of Surgery/Otolaryngology, VA Medical Center, 3350 La Jolla Village Dr., La Jolla, California, United States, ³Department of Medicine, UCSD, 9500 Gilman Dr., La Jolla, California, United States

The mast cell is the most prevalent leukocyte in the normal middle ear (ME) mucosa, and is part of the innate immune defense of the ME. To evaluate the role of mast cells in otitis media, the MEs of mast-cell deficient (WBBF1/J kit W/WV) mice were inoculated

with nontypeable *Haemophilus influenzae* (NTHi), or the MEs of mice systemically immunized with chicken ovalbumin were challenged with the same allergen. After 72 hours, the MEs were isolated, fixed, decalcified, embedded in paraffin, sectioned and stained with H&E for light microscopy. Responses were compared to those observed in wild-type mice.

In wild-type mice, injection of bacteria alone or allergen alone induced responses similar in magnitude and pathology. This included mild-to-moderate hyperplasia of the mucosa and infiltration of the tympanic bulla by leukocytes. However, sensitized animals injected with both NTHi and allergen mounted a much more severe inflammatory reaction. The ME cavity was filled with leukocytes, and the hyperplastic ME mucosa showed prominent leukocytic infiltration.

The ME responses observed in mast cell deficient mice differed, however. There was as expected a reduced response to allergen alone in sensitized, mast cell-deficient animals compared to wild-type mice. The response to NTHi alone in mast cell deficient mice was not significantly different from that seen in wild type controls. However, challenge with bacteria plus allergen resulted in an inflammatory reaction comparable to that seen with bacteria alone; that is, little or no augmentation of the response to bacteria was observed in mast cell deficient mice. These results suggest that the strong interaction between the responses to bacteria and allergen in the MEs of wild-type mice was mediated by mast cells.

Supported by grant DC00129 from the NIH/NIDCD and by the German DFG (EB 260/1-1)

287 CYTOKINE EXPRESSION IN A HUMAN MIDDLE EAR EPITHELIAL CELL LINE FOLLOWING RESPIRATORY SYNCYTIAL VIRUS INFECTION

William Derek Light¹, Julian Dixon¹, Amanda Poston¹, Liqun Zhang², Raymond Pickles², Craig Alan Buchman¹

¹Otolaryngology-HNS, University of North Carolina, 4009 Thurston-Bowles Bldg, Chapel Hill, NC, United States, ²Cystic Fibrosis/Pulmonary Research and Treatment Center, University of North Carolina, 7219 Thurston-Bowles Bldg, Chapel Hill, NC, United States

Otitis media (OM) is a global health problem affecting millions of children and adults annually. Numerous studies implicate respiratory viruses as etiologic agents in the development of acute otitis media (AOM). Respiratory syncytial virus (RSV) is the most common of these (Heikkinen et al, NEJM 1999). While clinical evidence suggests that it plays an important role in AOM, the mechanism by which RSV induces AOM is unknown. The present study examines the effect of RSV infection on a human middle ear epithelial cell line in an effort to investigate the initiating events in virus-induced AOM.

A human middle ear epithelial cell line (HMEEC-1) (Chun et al, Ann Otol Rhinol Laryngol 2002) was plated on 96 well culture dishes at 75% confluence. Cultures were inoculated using a recombinant RSV which expresses green fluorescent protein (rgRSV). Tumor necrosis factor alpha (TNF- α) and UV-inactivated rgRSV (uvRSV) were used as positive and negative controls respectively. Media was collected each day and cytokine levels (IL-6, IL-8, and RANTES) were assayed using ELISA. Cells were lysed and total

RNA was extracted. Cytokine-specific mRNA was determined using quantitative, real-time polymerase chain reaction.

HMEEC-1 infected with rgRSV displayed cytopathic effects such as syncytia formation as early as 24 hours post-inoculation. Morphologic evidence of apoptosis was evident by 72 hours. Infection with rgRSV resulted in statistically significant increases in IL-8 and RANTES gene expression as early as 24 hours post-inoculation. No increases in IL-6 production were observed.

The findings of the present study document the response of human middle ear epithelial cells to RSV infection. This model appears useful for future studies regarding the initiating events in RSV-induced AOM.

Supported, in part, by a grant from the NIH (DC00187) and the Trilological Society

288 Ultrastructural preservation of biofilms formed by non-typeable *Hemophilus influenzae*

Siva Wu, Simon Webster, Kathryn A Rich, **Paul Webster**
Ahmanson EM and Advanced Imaging Center, House Ear Institute, 2100 West Third Street, Los Angeles, CA, United States

There is growing evidence to suggest that non-typeable *Hemophilus influenzae* (NTHi), an important cause of otitis media in children, is able to grow as a biofilm in the middle ear. This observation, if correct, may help explain bacterial persistence in chronic infections. Biofilms of NTHi have been observed in the middle ear of experimental animal systems but there is still controversy concerning their role in human infection. We presume that direct observation of biofilms in biopsy material may be required to link them with otitis media. There is emerging evidence to suggest that biofilms may be polyclonal populations of bacteria with genetic heterogeneity and genomic plasticity. Biofilm bacteria also appear to possess sophisticated communication and quorum sensing mechanisms. Future examination of signaling molecules and gene expression in biofilm populations will require ways to preserve the ultrastructural organization of biofilms. The need to understand the ultrastructural appearance for easy identification in biopsy material, and possible future analysis using affinity markers has led us to evaluate different specimen preparation protocols of biofilms formed by NTHi. Structural preservation for SEM examination was most successful if biofilms were rapidly frozen and dehydrated by freeze substitution before being critical point dried. Even so, damage due to the drying process was unavoidable. Rapid freezing and freeze substitution was also the best method for preserving ultrastructure and extracellular material for examination by TEM. Embedding in Lowicryl resin at low temperature was able to preserve fragile extracellular structures that were damaged during SEM specimen preparation. Immersion fixation using buffered aldehyde solutions caused the most disruption of biofilm organization both for examination by TEM and SEM.

289 ProInflammatory Cytokine production of Well-Differentiated Epithelial Cells in response to Parainfluenza virus type 3 infection

Julian W Dixon¹, William D Leight¹, Amanda N Poston¹, Scott H Randell², Raymond Pickles², Liqun Zhang², Craig Buchman¹

¹Otolaryngology/ Head and Neck Surgery, UNC school of medicine, 4009 Thurston Bowles, Chapel Hill, NC, United States,

²Cystic Fibrosis/Pulmonary Research Center, University of North Carolina at Chapel Hill, Thurston-Bowles, Chapel Hill, NC, United States

Parainfluenza virus is a common upper respiratory virus that is remarkably prevalent in the pediatric population. PIV is known to cause croup, tracheobronchitis, bronchiolitis and acute otitis media, all of which are responsible for considerable morbidity and expense. There is a paucity of in vitro studies that examine the inflammatory response of the respiratory epithelium to infection with PIV. The few studies that exist consist of experiments performed using cell lines, or animal cells. This project is unique in that it was designed to further clarify the innate immune response of human airway (nasal and tracheobronchial) and middle ear epithelial cells to PIV infection. The study utilized well-differentiated, primary cell cultures grown at an air/liquid interface (ALI) to closely simulate in vivo conditions by maintaining a basolateral surface where the media is introduced, and an apical surface that remains in contact with air. Using a green fluorescent protein-expressing PIV type 3, cultures readily became infected, reaching a maximum between 48 and 72 hrs after inoculation. Proinflammatory cytokines (IL-6, IL-8, RANTES) accumulated significantly following infection. In contrast to our previous work using respiratory syncytial virus (RSV) (Palmer et al, ARO 2003), PIV type 3 did not amplify the epithelial cells responsiveness to subsequent TNF-alpha stimulation. In conclusion, PIV readily infects human airway and middle ear epithelial cells and induces a characteristic cytokine profile and a different inflammatory response than the related paramyxovirus, RSV. These events are likely an important part of the pathophysiology of clinical PIV infections.

Supported, in part, by a grants from the National Institutes of Health (K23 DC00187,) and the Triological Society

290 Regulation of bacterial otitis media-induced mucosal hyperplasia in rat middle ear epithelium by JNK

Masayuki Furukawa^{1,2}, Jörg Ebmeyer^{1,2}, Kwang Pak^{1,2}, Darrell A. Austin³, Nicholas J.G. Webster³, Allen F. Ryan^{1,2}

¹Department of Surgery/Otolaryngology, UCSD, 9500 Gilman Drive, La Jolla, CA, United States, ²Department of Surgery/Otolaryngology, VA Medical Center, 3350 La Jolla Village Drive, La Jolla, CA, United States, ³Department of Medicine, UCSD, 9500 Gilman Drive, La Jolla, CA, United States

Otitis media (OM) is a common disease and the leading reason for prescribing antibiotics during childhood. Despite otalgia and temporary hearing loss, a single episode of acute OM (AOM) is not usually a severe problem. On the other hand, recurrent AOM and

chronic OM have been associated with numerous adverse long-term sequelae, including conductive and sensorineural hearing loss, impaired speech and language development, impaired academic achievement, and irreversible middle ear disease. Hyperplasia of the middle ear mucosa (MEM) is an important component of OM, involving substantial cell proliferation and differentiation. Hyperplasia contributes to the deleterious sequelae of OM, including the production of mucous and other components of middle ear effusions. Hyperplasia is also involved in fibrosis and other permanent damage that can occur in repeated and/or chronic OM. The regulation of the mucosal hyperplasia in the middle ear is therefore of clinical significance.

The present study investigates the participation of c-Jun NH2-terminal kinase (JNK) on middle ear mucosal hyperplasia in a model of bacterial OM in the rat. OM was induced by the inoculation of nontypeable *Haemophilus influenzae* into the tympanic bullae. The middle ear mucosae were dissected bilaterally from 2-5 rats at 7 time points. P-JNK was not detected in control specimens. An increase in phosphorylated (p)-JNK1 was detected by Western blot analysis 24h after bacterial inoculation, whereas p-JNK2 was first increased 6h after bacterial inoculation. The activation of JNK1 and JNK2 was highest from 24-72h after bacterial inoculation. The level of p-JNK1 returned to the control level by 5 days. The level of p-JNK2 decreased but remained elevated compared to control at 5-7 days. In contrast, the levels of total JNK were not significantly altered at any time point. JNK activation paralleled the observed hyperplasia of the middle ear mucosa, which was maximal from 24-72h and decreased to near normal by 7 days. Both the Rac/Cdc42 inhibitor *Clostridium difficile* toxinB and the JNK inhibitor CEP11004 reduced the in vitro outgrowth of explant cultures of bacterially-exposed rat middle ear epithelium. We conclude that activation of JNK via Rac/Cdc42 is a critical pathway for bacterially-induced mucosal hyperplasia during OM.

291 Inhibition of phosphatidylcholine-specific phospholipase C (PC-PLC) reduces mucin secretion from middle ear epithelium exposed to interleukin-1?

Joseph Edward Kerschner^{1,2}, Chris Yang¹, Amy Burrows¹

¹Otolaryngology, Medical College of Wisconsin, 9000 W. Wisconsin Avenue, Milwaukee, Wisconsin, United States,

²Pediatric Otolaryngology, Children's Hospital of Wisconsin, 9000 W. Wisconsin Avenue, Milwaukee, Wisconsin, United States

Otitis media is the most common diagnosis in pediatric patients who visit physicians for illness in the United States. Mucin production in response to otitis media causes significant sequelae including hearing loss and the need for surgical intervention. Because cytokines play an integral role in the mechanisms of otitis media, investigating the effect of specific cytokines on the regulation of mucin secretion and gene expression is vital to furthering our knowledge of the pathophysiology of otitis media.

We investigated the mucin secretion of cultured middle ear epithelium (MEE) in response to interleukin-1 β (IL-1 β) in the presence of increasing concentrations of D609, a known inhibitor of phosphatidylcholine-specific phospholipase C (PC-PLC). Primary cultures of chinchilla MEE were established and exposed to 2.5 ng/ml of IL-1 β containing 0, 2.5, 25 and 50 μ g/ml concentrations of

D609 in growth media after exposure to 5 $\mu\text{Ci/ml}$ tritiated glucosamine. The culture supernatant was then drawn off and loaded on sepharose columns after enzymatic degradation. The radioactivity of 2 ml fractions was measured by liquid scintillation. Mucin production was determined from the radioactivity of appropriate fractions in comparison to control.

Mucin production from cultured MEE cells increased in response to IL-1 β exposure. This increased mucin secretion was reversed in a dose-dependent manner with addition of D609. This study demonstrates the potential importance of phosphatidylcholine-specific phospholipase C in the signaling pathway leading to mucin secretion from MEE after exposure to IL-1 β . This investigation and future studies may lead to novel and efficacious treatments for otitis media through cytokine modulation.

292 The molecular mechanism of interleukin-8 transcription by pneumococcal cell wall envelope in middle ear epithelial cells of rat *in vitro*

Katsuyuki Tsuchiya¹, Yuki Hamajima¹, Youngki Kim², Frank G Ondrey³, Jizhen Lin¹

¹Otolaryngology, University of Minnesota, 2001 6th St. SE, Rm. 216 LRB, Minneapolis, MN, United States, ²Pediatrics, University of Minnesota, MMC 491 Mayo, 420 Delaware, Minneapolis, MN, United States, ³Otolaryngology, University of Minnesota, 2001 6th St. SE, Rm. 270 LRB, Minneapolis, MN, United States

Interleukin-8 (IL-8) persists in middle ear effusion and mediates the infiltration of acute and chronic inflammatory cells in the middle ear mucosa. The molecular mechanism of IL-8 production in middle ear mucosa, however, is poorly understood. In this study, we demonstrated that the transcription of IL-8 was up-regulated by proteoglycan-polysaccharides (PG-PS), a major cell wall component of pneumococcus that drives the proliferation of middle ear epithelial cells *in vitro* and induces mucous cell metaplasia in the middle ear mucosa *in vivo*. Incubation of middle ear epithelial cells with PG-PS significantly increased the transcription of IL-8 *in vitro* in association with the transcription of nuclear factor kappa B (NF- κ B). To determine whether the PG-PS-induced transcription of IL-8 is dependent upon NF- κ B, an IL-8 promoter construct with the NF- κ B binding site mutated (IL-8 promoter mutant) was used and luciferase assays measured. It was found that the luciferase activity of IL-8 promoter mutant was abrogated. To test whether PG-PS regulates the transcription of IL-8 through the activation protein-1 (AP1) and NF-IL6 (CAATT/enhancer binding protein, a nuclear factor for interleukin-6 expression) sites which are also known to exist in the IL-8 promoter, additional two IL-8 promoter mutants, one with the AP1 binding site mutated and the other with the NF-IL6 binding site mutated were used and luciferase activities measured. The results demonstrated that the luciferase activity was significantly reduced with the IL-8 promoter in which the NF-IL6 binding site is mutated whereas the luciferase activity was not affected with the IL-8 promoter mutant in which the AP-1 binding site is mutated. We concluded that PG-PS regulates the transcription of IL-8 via an NF- κ B and NF-IL6-dependent mechanism in middle ear epithelial cells *in vitro*.

293 Attachment and Entry of NTHi into Human Epithelial Cells: Modification of Host Endocytic pathways

Kathryn A Rich¹, Siva Wu², David J Lim³, Paul Webster²

¹Ahmanson Advanced Electron Microscopy and Imaging Center, House Ear Institute, 2100 West 3rd St, Los Angeles, CA, United States, ²Ahmanson Advanced Electron Microscopy and Imaging Center, House Ear Institute, 2100 West 3rd St, Los Angeles, CA, United States, ³Gonda Dept of Cell and Molecular Biology, House Ear Institute, 2100 West 3rd St, Los Angeles, CA, United States

Non-typeable *Haemophilus influenzae* (NTHi) is one of the major otitis media pathogens, particularly for recurrent infections and for otitis media with effusion. The ability of the bacteria to adhere to, and invade the epithelial lining has been proposed as an important step in the colonization and persistence of NTHi within the upper respiratory tract. While there have been several previous reports of NTHi being internalized by epithelial cells, the mechanisms of entry and the fate of the internalized bacteria have not been examined in detail. In the present study, we have used a combined light and electron microscopic examination of the attachment and entry of NTHi into Chang conjunctival epithelial cells. In addition to observing bacteria in the process of being internalized, NTHi were also observed inside the epithelial cells, either enclosed within a vacuole or apparently free in the cell cytoplasm. Even when enclosed within a vacuole, the NTHi did not always appear to be in typical phagosomes and the membranes enclosing the bacteria showed reduced labeling with two well-characterized markers of the endocytic pathway, mannose 6-phosphate receptor (MPR) and lysosome-associated membrane protein (LAMP)1. In addition, immunofluorescent microscopy and Western blotting demonstrated a reduction in the levels of cellular LAMP1 following exposure to NTHi. These data suggest that attachment and entry of NTHi results in modification of normal host endocytic pathways, in a manner that may favor its survival.

294 Expression of Leukotriene Signaling Pathway Associated Genes of Normal and Inflamed Middle Ear Mucosa in the Chinchilla Model of Otitis Media.

Geza Erdos^{1,2}, Joseph Donfack¹, Jay D. Hayes¹, Azad Ahmed¹, Randy M. Keefe¹, Fen Ze Hu^{1,2}, J. Christopher Post^{1,3}, Garth D. Ehrlich^{1,2}

¹Center for Genomic Sciences, Allegheny-Singer Research Institute, 320 E. North Ave., Pittsburgh, Pennsylvania, United States, ²Dept. of Microbiology and Immunology, Drexel University College of Medicine, Allegheny Campus, 320 E. North Ave., Pittsburgh, Pennsylvania, United States, ³Dept. of Otolaryngology, Drexel University College of Medicine, Allegheny Campus, 320 E. North Ave., Pittsburgh, Pennsylvania, United States

Otitis media is an inflammatory disease of middle ear (ME) characterized by immunocyte infiltration in the ME mucosa (MEM) along with the release of cytokines and powerful inflammatory mediators such as leukotrienes (LTs). LTs, the products of arachidonic acid metabolism, are present in the ME fluid. Production of LTs is an early response to inflammatory stimuli in the ME epithe-

lial tissue. The reaction to the released mediators is a sustained inflammation that might contribute to the OM associated hearing loss and ME damage. The chinchilla model of OM is extensively used, yet little is known about the OM related genes and gene expression pattern of this animal model, due to an almost complete lack of gene-sequence information (Only a handful of independent GenBank records all together).

We tested normal and inflamed chinchilla MEM for the presence of gene products involved in arachidonic acid metabolism (LTA4 hydrolase and LTC4 synthase) and for the expression of BLT1, CysLT1 and CysLT2 (receptors of LTs) genes. RT-PCR analysis of RNA isolated from MEM has shown that the CysLT1 and CysLT2 receptor genes are expressed in both tissues, however the expression of LTB4 receptor (BLT1) was detected only in the inflamed MEM. In contrast, the key enzyme of the LTB4 production (LTA4 hydrolase) was expressed in both normal and inflamed tissue. LTC4 synthase, which is responsible for the synthesis of CysLT receptor ligand, was only detected in the inflamed MEM. The cDNAs of these genes were sequenced and analyzed for phylogenetic relationships. Interestingly, the homology analysis of the genes revealed that they are a closer homologue to human genes than to their murine rodent relatives.

The results of this study will aid in understanding the gene expression patterns of the inflammatory process in the ME mucosa and will pave the way to develop better treatments that alleviate hearing loss and middle ear damage caused by prolonged MEM inflammation.

295 Differential Expression of Genes Encoding Mitochondrial Uncoupling Proteins in Mouse Middle Ear Mucosa after Bacterial Lipopolysaccharide Challenge

Ha-Sheng Li-Korotky¹, Chia-Yee Lo¹, Juliane M Banks¹, Tadashi Kitahara², William J Doyle³, Carey D Balaban²

¹Department of Pediatric Otolaryngology, Children's Hospital of Pittsburgh, 8152 Rangos Research Center, Pittsburgh, PA, United States, ²Department of Otolaryngology, University of Pittsburgh School of Medicine, Eye & Ear Institute, 203 Lothrop Street, Suite 153, Pittsburgh, PA, United States, ³Department of Otolaryngology, University of Pittsburgh School of Medicine, 8152 Rangos Research Center, Pittsburgh, PA, United States

Otitis media (OM) is one of the most frequent diseases in infants and children. Most available adjunctive therapies are neither specific nor effective because the etiology of OM is complex and the molecular pathways leading to inflammation are poorly understood. Our recent studies in gene expression profiling of the middle ear mucosa (MEM) from the murine model of acute OM using Affymetrix murine GeneChip (MOE 430A) revealed that a gene cluster encoding mitochondrial uncoupling proteins (Ucps) was differentially modified in the inflamed MEM induced by bacterial lipopolysaccharide (LPS). Results from real-time PCR demonstrated that Ucps are expressed in the normal MEM of mice with the order Ucp2>Ucp4>Ucp5>Ucp3>Ucp1. At 12 h and 48 h after ME LPS challenge, the low abundantly expressed Ucp1 gene in normal MEM was dramatically induced during the early development of OM, but other more abundantly expressed Ucps showed insignificant change or were slightly reduced. Our results also

reveal that although high-density oligonucleotide chip technology is a powerful tool for throughput screening of disease genes, it is not sensitive enough to isolate low abundantly expressed transcripts that may have very important roles in disease development and resolution. Ucps are a family of mitochondrial membrane proteins that uncouple electron transport from ATP production by transporting protons across the inner membrane. Until very recently, the Ucp1, present only in brown adipose tissue, was considered to be the only mitochondrial carrier protein that stimulated heat production by dissipating the proton gradient generated during respiration across the inner mitochondrial membrane and therefore uncoupling respiration from ATP synthesis. Our findings provide new evidence of the MEM-specific expression of Ucp1 during the pathogenesis of OM, and imply that Ucp1 is fundamentally important in cellular pathophysiological processes involving detoxification of free radicals generated by mitochondria during ME inflammation.

296 Expression and Regulation of the Pattern Recognition Receptors, Toll-like Receptors, in Murine Acute Otitis Media Induced by Lipopolysaccharide

Ha-Sheng Li-Korotky^{1,2}, Juliane M Banks¹, Chia-Yee Lo¹, William J Doyle², Alper M Cuneyt^{1,2}, J. Douglas Swarts^{1,2}

¹Department of Pediatric Otolaryngology, Children's Hospital of Pittsburgh, 8152 Rangos Research Center, Pittsburgh, PA, United States, ²Department of Otolaryngology, University of Pittsburgh School of Medicine, 8152 Rangos Research Center, Pittsburgh, PA, United States

Otitis media (OM) is one of the most common diseases in infants and children. Lipopolysaccharide (LPS), a principal endotoxin of the outer membrane of Gram-negative bacteria, is present in a high percentage of the human middle ear (ME) effusions including those that are negative for bacteria by culture. Recent studies have elucidated how LPS is recognized by monocytes and macrophages of the innate immune system via toll-like receptors (Tlrs) that are innate recognition molecules important for immune responses against pathogens. In this study, gene expression patterns of Cd14 and Tlrs in the middle ear mucosa (MEM) from the murine model of acute OM were profiled at 12 h and 48 h after ME LPS challenge using Affymetrix murine GeneChip (MOE 430A) and real-time PCR. Results demonstrated that Cd14 and Tlrs are expressed in the normal MEM of mice with the order Tlr4>Tlr3>Tlr2>Tlr1>Tlr9>Tlr5>Tlr8>Tlr7>Tlr6. Tlr2, Tlr6, Tlr1, Tlr9, and Tlr7 were dramatically induced at 12 h after ME LPS challenge. Cd14 that is expressed in the normal MEM is a most intensively induced signal during early events of OM development. Our data suggest that these innate recognition molecules act directly or indirectly on the immune response by activating ME host cells involved in inflammatory processes.

297 Expression and Regulation of Middle Ear Epithelial Ion Transporters in Lipopolysaccharide-Induced Acute Otitis Media of Nos2-Deficient Mice

Ha-Sheng Li-Korotky^{1,2}, Chia-Yee Lo¹, Juliane M Banks¹, William J Doyle², J. Douglas Swarts^{1,2}, Patricia A Hebda^{1,2}, Alper M Cunejt^{1,2}

¹Department of Pediatric Otolaryngology, Children's Hospital of Pittsburgh, 8152 Rangos Research Center, Pittsburgh, PA, United States, ²Department of Otolaryngology, University of Pittsburgh School of Medicine, 8152 Rangos Research Center, Pittsburgh, PA, United States

Otitis media (OM) is one of the most common diseases in infants and children and is characterized by middle ear mucosal (MEM) inflammation with or without ME effusion. An essential function of the MEM is to maintain an air-filled and fluid-free ME for maximum sound transmission and active trans-epithelial ion transport is a primary regulatory system for the maintenance of MEM water balance, osmotic homeostasis and mucociliary function. Nevertheless, tissue-specific expression, role and regulation of the ion transport in maintenance of normal MEM equilibrium as well as in the pathogenesis of OM are undefined. Our recent studies in gene expression profiling of the MEM from a rat model of acute OM have revealed that a gene cluster encoding Na⁺ transport proteins (pump, channel, and exchanger) was simultaneously inhibited, and a signaling intermediate, inducible nitric oxide synthase (Nos2) was consistently augmented during disease development. In this study, we used homozygous Nos2 knockout (ko) mice compared with wild-type (wt) C57BL/6J mice to identify time-dependent, disease-specific expression patterns of ion transporters and potential regulatory molecules in the MEM of LPS-induced OM. Gene expression profiling in the MEM from the murine models of acute OM was performed at 12 h and 48 h after ME LPS challenge using Affymetrix murine GeneChip (MOE 430A) and real-time PCR. Results demonstrated time-dependent differential regulation of gene clusters encoding ion and water transporters, showing that the Nos2 is an up-stream negative signal for regulating ME fluid transport and participating in the pathways leading to the MEM inflammation. The panoramic assessment of the gene expression during the early course of the MEM inflammation will help reveal the Nos2-related and other novel signaling pathways that are involved in the dysregulation of MEM function and the pathogenesis of acute OM and ME effusion.

298 Effect of corticosteroids on nitric oxide and mucin production in experimentally induced otitis media

Ernest O. John¹, Kaalan E. Johnson¹, Samantha Kaura¹, Seong Kook Park¹, Morrill T. Moorehead², Timothy T.K. Jung¹

¹Surgery, Div. of Otolaryngology - Head and Neck Surgery, Loma Linda University School of Medicine, VA hospital, Loma Linda, CA, United States, ²Pathology, Loma Linda University School of Medicine, VA hospital, Loma Linda, CA, United States

Background: It has been previously suggested that nitric oxide is involved in the pathogenesis of mucoid middle ear effusion

(MEE). A positive correlation has been observed between nitric oxide and mucin production in the MEE of humans and experimentally induced MEE in chinchilla.

Objective: The purpose of this study is to determine the effect of corticosteroids on nitric oxide and mucin production in lipopolysaccharide (LPS) induced otitis media in chinchilla.

Methods: OME was induced in adult chinchillas by injecting LPS 0.3 mg/0.3 ml into the bullae. Three groups were studied, LPS 0.3 mg (alone) and LPS 0.3 mg + 0.1% dexamethasone, and LPS 0.3 mg + 1% rimexolone. After 96 hours, the animals were euthanized, MEE fluid was collected, and the temporal bones were harvested for histopathological analysis. Samples of middle ear fluid were analyzed for mucin by periodic acid-Schiff method and NO metabolites using the Griess method.

Results: The amount of mucin and nitric oxide obtained was highest in the LPS alone group (1126 ± 220 µg, mean ± SE, 28 ± 5 µMole), compared to the LPS + dexamethasone group (709 ± 93 µg, 13 ± 2 µMole), and the LPS + rimexolone group (808 ± 82 µg, 11 ± 2 µMole). A positive correlation was observed in total amounts of nitric oxide and mucin (0.94) and to a lesser degree in concentration (0.52).

Conclusion: This study shows that corticosteroids reduce production of nitric oxide and mucin in LPS induced otitis media in chinchilla. It was also noted that the correlation between amount of nitric oxide and the amount of mucin production was greater than the correlation between concentrations.

299 Nitric Oxide Regulation of Developmental Bone Metabolism

Tetsuji Sanuki¹, Brian T Faddis², Richard A Chole²

¹Otolaryngology, Washington University in St. Louis, 660 South Euclid Ave., St. Louis, MO, United States, ²Otolaryngology, Washington University in St. Louis, 660 South Euclid Ave., St. Louis, MO, United States

Nitric Oxide (NO) is a free radical involved in the regulation of many physiological processes such as vascular relaxation, neuro-transmission, platelet aggregation and immune response. Several recent investigations have focused on the possible influence of NO on the local control of the bone cell activity as well as systemic bone metabolism in general. The endothelial isoform of nitric oxide synthase (NOS3) is widely expressed in bone on a constitutive basis, whereas inducible NOS (NOS2) is only expressed in response to inflammatory stimuli. Only recently has it been demonstrated that neuronal NOS (NOS1) is expressed by bone cells. NO synthesized by NOS3 and also NOS2 is strongly implicated in regulation of bone metabolism exerting powerful effects on cells of both the osteoblast and osteoclast lineage. However, the specific functional role of these enzymes in these cells and their effects on bone turnover are not clearly defined. In this study we show how disruption of NOS genes results in a significant impairment of bone development demonstrated by conventional static and dynamic histomorphometry performed on the femur and tibia of 4, 8, and 12 week-old NOS1, NOS2, and NOS3 knockout mice and their wild type littermates. We also performed X-ray densitometry of tail vertebrae and collected long bone physical measurements and whole body weights. Male NOS1 knockout mice showed significantly reduced bone development compared to their

wildtype littermates. However, female NOS1 mice showed no significant difference in bone development compared to their wild-type littermates. Female NOS3 knockouts however, did show reduced bone development compared to wildtype littermates. The results of these studies suggest that NOS1 and NOS3 genes play an important role in bone development and that sex hormones may influence developmental bone metabolism via a nitric oxide pathway.

300 Role of Glutamate Receptors in NOS1-Mediated Osteoclast Activity

Brian T Faddis¹, Tetsuji Sanuki²

¹Otolaryngology, Washington University in St. Louis, 660 South Euclid Ave, St. Louis, MO, United States, ²Otolaryngology, Washington University in St. Louis, 660 South Euclid Ave., St. Louis, MO, United States

One of the hallmarks of many middle ear diseases is aberrant osteoclast activity that can lead to massive bony tissue destruction. The mechanism of osteoclast activation in these diseases is not well understood. We recently demonstrated a role for the neuronal isoform of nitric oxide synthase in osteoclast development and resorption (Jung et al., *J. Cell. Biochem.*, 89:613-621, 2003). Briefly, mice with a targeted deletion of NOS1, demonstrated a reduced osteoclast response in a model of inflammatory bone resorption *in vivo*. Similarly, osteoclasts derived from the bone marrow of NOS1 knockout mice showed an abnormally large phenotype as well as reduced resorptive ability *in vitro*. Since osteoclasts cultured in the presence of glutamate receptor antagonists demonstrate a phenotype similar to our NOS1 knockout osteoclasts, we examined the possibility that these two findings represent a common pathway in osteoclast activation. This pathway may be synonymous with the well known neuronal signaling cascade of nitric oxide production via glutamate receptor activation. Immunofluorescence studies using antibodies to NMDAR1 revealed the presence of NMDA receptors on both osteoclast precursors and mature osteoclasts *in vitro*. The majority of mononuclear precursors did not show a positive label for NMDA receptors. Similar osteoclast cultures loaded with the NO indicator, diaminofluorescein (DAF), showed a robust increase in DAF fluorescence following exposure to the glutamate receptor agonist, N-methyl, D-aspartate (NMDA). Absolute gray value intensity of twelve control and twelve NMDA-exposed osteoclasts revealed a greater than 100% increase in DAF fluorescence following NMDA exposure (Control mean = 29.78; NMDA mean = 69.11; $p < 0.001$). These results support the hypothesized osteoclast signaling cascade that would allow nitric oxide production triggered by glutamate receptor activation.

301 Vestibulotomy About the Displaced Facial Nerve

Jizhou Guo¹, Shouqin Zhao¹

ENT, Beijing Tongren Hospital, Chongwenmen, Beijing, China, People's Republic of

Abstract: Objective To investigate the feasibility of vestibulotomy above the displaced facial nerve. Methods From January 2000 to January 2002, eight patients with severe congenital conductive hearing loss underwent the vestibulotomy above displaced facial

nerve and reconstruction of the ossicular chain with a total ossicular replacement prosthesis, which all for the congenital middle ear deformity and the facial nerve overhang and concealed the oval window niche or lied inferior to the oval window. In four of eight cases, the facial nerve was transposed in order to access the oval window niche. Results Hearing improved 15dB in 2 ears, 16~25dB in 3 ears and 26dB or more in 3 ears. In no case was there a postoperative facial paresis. With 4 months to 28 months follow up, the postoperative hearing gain was stable. Conclusions Vestibulotomy above displacement of the facial nerve allows a final chance of achieving serviceable hearing through surgery. The lack of facial nerve injury and the potential for hearing restoration make this procedure feasible in otherwise marginal or poor surgical candidates.

Key words: Ear disease, Deformity, Facial nerve displacement, Oval window, Vestibulotomy.

302 Auditory Feedback Control of Echolocation Call Duration and Repetition Rate

Michael Smotherman, Walter Metzner

Physiological Science, UCLA, 621 Charles Young Dr. S., Los Angeles, CA, United States

Echolocating bats rely upon auditory cues to guide adjustments in the temporal parameters of subsequent echolocation calls. Many species of bats have been observed to make rapid adjustments in call duration and repetition rate during flight, and there appear to be many similarities in the ways different species of bats adjust the timing of echolocation calls during foraging. We chose to investigate the effects of changing auditory feedback on the timing of subsequent echolocation calls in stationary horseshoe bats. Stationary horseshoe bats are already known to adjust call frequency in response to pitch-shifted auditory feedback. We sought to quantify the effect of frequency-shifted playback on the time course of subsequent call emissions. Furthermore, since it is widely presumed that echo delay is the chief factor driving changes in call repetition rate during flight, we also investigated the effects of changing echo delay on call repetition rate in stationary bats. **Results:** Surprisingly, echo frequency and echo delay were found to have equally important yet distinctly different effects on the temporal patterns of calling behavior. Positive shifts in echo frequency routinely caused bats to switch from long-duration single calls to short-duration pairs of calls (i.e. doublets.). Increasing echo delay caused a systematic increase in the inter-pulse interval (IPI) occurring between calls, but caused no accompanying change in call duration. We conclude that echo frequency and delay work synergistically to control the timing of echolocation call emission in horseshoe bats.

303 Classification of natural textures in echolocation

Jan-Eric Grunwald, Sven Schörnich, Lutz Wiegrebe

Dept. Biologie II, University of Munich, Luisenstr. 14, Muenchen, Germany

Through echolocation, a bat can not only find out about the position of an object in the dark, but also about its structure. A tree, however, is a very complex object; it has thousands of reflective surfaces which result in a chaotic acoustic image. Technically, the

acoustic image of an object is the object's impulse response, i.e., the echo recorded when the object is ensonified with an acoustic impulse. The detailed analysis of the acoustic image is the basis for the bats' extraordinary object-recognition capabilities. Previous work has shown that a measure of the degree of envelope fluctuation of the impulse response, like the Crest factor or the waveform 4th moment can be efficiently used to classify the chaotic acoustic images of natural objects and textures (Muller and Kuc, 2000). Here, a phantom-object, playback experiment is used to demonstrate that the echolocating bat *Phyllostomus discolor* can evaluate a statistical property of chaotic acoustic images, the degree of envelope fluctuation. The acoustic images of the phantom objects consisted of up to 4,000 stochastically distributed reflections. It is shown that bats spontaneously classify acoustic images according to their degree of envelope fluctuation, quantified as the 4th moment of the acoustic-image waveform. This perceptual dimension, related to echo roughness, enables the bats to evaluate complex natural textures, such as foliage types, in a meaningful manner.

References

Muller, R. and Kuc, R. (2000), "Foliage echoes: a probe into the ecological acoustics of bat echolocation," *J. Acoust. Soc. Am.* 108, 836-845.

304 Context Driven "Prosodic" Variation in a Social Call Emitted by Mustached Bats, *Pteronotus parnellii*

Matthew J Clement, Jagmeet S Kanwal

Physiology and Biophysics, Georgetown University, 3900 Reservoir Rd, NW, Washington, DC, United States

Mustached bats use at least 33 calls for social communication. The acoustic parameters defining the multidimensional boundaries of each call are somewhat variable. This variation may signal the sex, identity, and/or the emotional state of the caller. To examine the possibility of "prosodic" variation in the long Quasi Constant Frequency (QCFI) call, we observed the behavioral context in which the same individuals emit this call. Using an infrared-sensitive Sony camcorder (TRV310) and a condenser microphone, we recorded the vocal and social behavior of 15 bats (5 females) housed in a semi-natural environment. Simultaneously, sounds were digitized at a sampling rate of 250 kHz and recorded directly to a computer's hard drive. Males emitted the QCFI syllable as a train in three different behavioral contexts: as a call to a female (QCFI-F), as a call to another male (QCFI-M) and as a general call to conspecifics (QCFI-G). QCFI-F calls were associated with genital inspection by the caller 70% of the time (QCFI-M: 5%; QCFI-G: 0%). QCFI-M calls were associated with nose touching and/or face licking between males (88%). Often, these calls consisted of spontaneously triggered bouts that extended for several minutes. QCFI-G calls were emitted in response to a physical attack by conspecifics. The fundamental frequency, depth of frequency modulation and syllable number per train varied significantly ($p < 0.0001$) with the context in which it was emitted (QCFI-F: 6.13 ± 0.02 kHz, $4.6 \pm 0.1\%$ and 5.2 ± 0.5 syllables, respectively; QCFI-M: 6.95 ± 0.04 kHz, $8.0 \pm 0.4\%$ and 2.9 ± 0.2 syllables, respectively; QCFI-G: 7.28 ± 0.03 kHz, $10.3 \pm 0.3\%$, 14.0 ± 4.6 syllables, respectively). These data demonstrate prosodic variation in QCFI emitted in

three different contexts with a likely difference in its perceived meaning. We propose that QCFI-F functions as a greeting call, QCFI-M as an affiliative call, and QCFI-G as an appeasement call. Supported by NIH/NIDCD research grants DC02054 to J.K. and DC04733 to C. Portfors.

305 Testosterone Implants Alter the Frequency Range of Zebra Finch Songs

Jeffrey Cynx¹, N. Jay Bean², Ian Jay Rossman³

¹*Psychology, Vassar College, Mail Drop 408, Poughkeepsie, NY, United States,* ²*Psychology, Vassar College, 124 Raymond Avenue, Poughkeepsie, NY, United States,* ³*Biopsychology, Vassar College, 124 Raymond Avenue, Poughkeepsie, NY, United States*

An increase in testosterone levels in songbirds could increase the mass of the muscles that control the production of song, which in turn would cause a change in song quality. Many species of songbirds are sensitive to small changes in frequency range; therefore increased testosterone levels could not only change production, but also other birds' responses to song. To investigate whether changes in testosterone alter the frequency range of zebra finch song, we assigned male zebra finches to two groups, one of which received testosterone implants and the other empty silastic capsule implants. We then recorded song up to 52 weeks after the surgery and measured any frequency changes in either group. After 5 weeks statistically significant decreases were found in the fundamental frequency of the selected harmonic stacks in the songs of the testosterone-treated birds. No changes were found in the fundamental frequencies of the control group. The frequency change remained after the effects of the testosterone implants ended. These data show that high levels of testosterone affect the frequency range of zebra finch songs.

306 Measures of acoustic variation in directed budgerigar vocal production.

Michael S. Osmanski, Robert J. Dooling

Department of Psychology, University of Maryland, Biology/Psychology Building, College Park, MD, United States

The contact calls of budgerigars are short (~150 msec), frequency modulated, learned vocalizations that are used to maintain social bonds and flock cohesion. Normal budgerigar vocal production, like birdsong and human speech, depends on auditory feedback. The stereotypy with which budgerigars produce contact calls in natural situations suggests a pressure to maintain precision in the acoustic structure of these calls. This study sought to determine the range of variation in contact calls produced in a controlled operant environment under situations of selective and non-selective reinforcement. Four budgerigars were trained to produce a specific contact call by matching a stored template in order to obtain a brief food reward. Each budgerigar produced 50-70 contact calls per test session and the coefficient of variation for various acoustic characteristics were determined both within and across sessions. The birds were then trained to produce higher or lower frequency vocalizations falling outside the range of variability of their initial contact calls. The coefficient of variation for the same acoustic characteristics as before were measured for the altered calls. Results indicate that budgerigars can maintain a high degree of

precision in the production of contact calls, even when induced to alter the average frequency range of those calls. [This work supported by NIH grant DC-00198 to RJD and NIDCD training grant DC-00046].

307 Temporal Resolution in Hearing-Impaired Belgian Waterslager Canaries

Amanda M. Lauer, Robert J. Dooling

Dept. of Psychology, University of Maryland, Dept. of Psychology, University of Maryland, College Park, MD, United States

Belgian Waterslager (BWS) canaries have a permanent hereditary hearing loss that is associated with hair cell abnormalities. Previous work showed that discrimination of temporal fine structure may be slightly enhanced in BWS compared to normal-hearing canaries of other strains (nonBWS). Here we further investigate temporal resolution in BWS and non-BWS canaries by measuring the minimum detectible time interval between two sounds. Thresholds for detecting brief gaps in 300 ms bursts of noise were measured at several sound levels using operant conditioning and the Method of Constant Stimuli. Average gap detection thresholds ranged from approximately 2 ms at 75 dB SPL to 11 ms at 60 dB SPL in BWS, and from 4 ms at 75 dB SPL to 5 ms at 60 dB SPL in nonBWS. At higher SPLs, gap detection thresholds for BWS were as good as or better than nonBWS; however, thresholds were much higher in BWS at the lowest SPL (60 dB). This SPL corresponds to a sensation level of only 10 dB in BWS. These results confirm that temporal resolving power is unusually good in BWS canaries at least at high sensations levels, but may be compromised at low SLs. [Supported by NIH DC01372 to RJD and DC05450 to AML]

308 A Novel Behavioral Paradigm for Assessing Tinnitus Using Schedule Induced Polydipsia Avoidance Conditioning (SIP-AC)

Edward Lobarinas, Wei Sun, Ross Cushing, Richard Salvi

Center for Hearing and Deafness, University at Buffalo, 215 Parker Hall, Buffalo, NY, United States

A novel behavioral technique to measure the onset and recovery of tinnitus was used to evaluate the effects of a series of salicylate doses in rats. Food-deprived subjects autoshaped to lick for water during intervals of intermittently delivered food pellets (FT-1) by being placed under schedule-induced polydipsia (SIP) conditions. The SIP-induced licking was then placed under the control of foot shock. Licking occurring in the presence of sound (six stimuli, 40 dB SPL) resulted in brief foot shock. However, subjects were allowed to lick during quiet and no shock was delivered. Following training, the number of licks-in-quiet (correct response) exceeded 90% of the total licks per session. Subjects were then treated with a saline vehicle and four different doses of salicylate (50, 100, 150 and 350 mg/kg, i.p.; 2 days). Task performance was evaluated before, during, and after treatment. Licks-in-sound remained below 10% with saline and all four salicylate doses indicating that the sound stimuli were audible under all treatment conditions. Licks-in-quiet remained high during the saline control and 50 mg/kg dose of salicylate. This performance was consistent with

the absence of tinnitus. However, licks-in-quiet showed a statistically significant decline with the 150 and 350 mg/kg dose, behavior consistent with the presence of tinnitus. Licks-in-quiet gradually recovered to baseline level 2-3 days following high-dose salicylate treatments, behaviors consistent with the gradual disappearance of tinnitus. The salicylate dose needed to induce tinnitus and the length of recovery are consistent with previous reports, providing support for the method. The ability to obtain sequential estimates of tinnitus-like behavior in an animal after administering a tinnitus inducing agent could aid in understanding the underlying neural mechanisms and assessing potential treatments.

309 Operant methods for mouse psychoacoustics

Karin B. Klink, Garnet Bendig, Georg M. Klump

Institute for Biology and Environmental Science, University of Oldenburg, C.v.Ossietzky Str. 9-11, Oldenburg, Germany

Laboratory mice (*Mus musculus*) are especially suited for studies of auditory physiology since they are easy to breed, multiple mutant lines are known, and the mouse genome has been sequenced. Furthermore, mice age relatively fast and can therefore provide practical models for age-related hearing deficits. We set out to compare the suitability of two different psychoacoustic operant procedures, 2-down-1-up adaptive tracking and the method of constant stimuli, for mice. Contrary to previous studies, they require no aversive conditioning and use food deprivation rather than water deprivation (e.g., Prosen et al., 2000, *J. Neurosci. Meth.* 97: 59-67). The setup and procedure were adapted following methods that proved to be suitable in studying hearing in gerbils (Kittel et al., 2002, *Hear. Res.* 164: 69-76).

The following results were obtained for the detection of tones in six subjects. The thresholds obtained with the constant-stimuli procedure were significantly lower than those obtained with the adaptive tracking procedure (Wilcoxon two sample test, $p=0.028$). The range of thresholds among the six subjects did not differ as much in the constant-stimuli procedure as in the adaptive-tracking procedure. Thus, a constant-stimuli procedure appears to be better suited for mouse psychoacoustics. Our constant stimuli sessions consisted of 110 trials. Session length, however, could be reduced without loss of accuracy. If we discarded the first 10 trials (warm-up period), and analysed the next 100, 70 or 50 trials only, the results did not differ significantly from those session with 110 trials, neither in the threshold (Friedman test, $p=0.100$) nor in the standard deviation (Friedman test, $p=0.134$, respectively). Thus, shorter sessions could be used to obtain thresholds without significant loss of accuracy.

Supported by the DFG SFB 517

310 The Effects of Speech-Simulating Maskers on Temporal Integration in Young and Old Mongolian Gerbils

Malte Christian Kittel¹, Otto Gleich¹, Georg Klump², Ingo Hamann¹, Jürgen Strutz¹

¹*ENT Department, University of Regensburg, Franz-Josef-Strauss-Allee 11, Regensburg, Germany, ²FB 7, AG Zoophysologie & Verhalten, Carl von Ossietzky University Oldenburg, Postfach 2503, Oldenburg, Germany*

The ability of the auditory system to integrate acoustic energy over

time is generally referred to as temporal integration. In this study we examine temporal integration of young and old Mongolian gerbils (*Meriones unguiculatus*) in quiet and two different masking conditions. Gerbils were trained in a GO/NOGO-paradigm to report the detection of a pure-tone stimulus of 2 kHz. Signal durations were 10, 30, 100, 300 and 1000ms. Gerbils were tested in quiet (condition 1) or in the presence of 2 types of continuous masker (condition 2 and 3, overall level 59 dB SPL) with spectral characteristics corresponding to human speech (ICRA noise; Dreschler WA et al., 2001, *Audiology* 40, 148-157). The maskers had either a temporally unmodulated envelope (condition 2) or a modulated envelope resembling temporal characteristics of multi-talker babble (condition 3). Long-term spectra of both maskers were identical. Thresholds for one signal duration were first determined in quiet, then in the unmodulated masker and finally in the modulated masker condition. Signal duration was randomly varied during testing.

Data collected at 2 kHz in quiet confirmed that gerbils show temporal integration and in addition demonstrated that old gerbils with moderate hearing loss for long signal durations show reduced temporal integration. Threshold shifts induced by the maskers were inversely correlated with the threshold in quiet resulting in large shifts in sensitive animals and smaller shifts in animals with a moderate hearing loss. Temporal integration was also observed in the masked conditions and data for both types of maskers will be presented and discussed.

Supported by DFG (Str. 275/4-3). We thank S. Kopetschek, C. Wögerbauer and S. Arndt for assistance.

311 Cross-modal binding in a poison-dart frog

Peter M. Narins¹, Daniela S. Grabul², Kiran K. Soma¹, Walter Hoedl²

¹Physiological Science, UCLA, 621 Charles E. Young Drive South, Los Angeles, CA, United States, ²Institute of Zoology, University of Vienna, Althanstrasse 14, Vienna, Austria

The mechanisms by which the brain binds together inputs from separate modalities to effect a unified percept of events is poorly understood. Male poison-dart frogs, *Epipedobates femoralis*, physically and vigorously defend their territories against conspecific calling male intruders. Using an electromechanical frog (EMF), we were able to experimentally evoke this aggressive behavior only when an auditory cue (advertisement call) was presented simultaneously with a visual cue (vocal-sac pulsations) (Narins et al., 2003, *PNAS* 100:577-580). In the present experiments, we used a modified version of the EMF to present visual and auditory cues separated by experimentally-introduced time delays to probe temporal binding in this animal. Initially, the call followed vocal-sac motion by several seconds; this delay was then randomly varied, enabling us to determine the temporal binding delay that just evoked aggressive behavior. In the second set of experiments, the acoustic and visual cues were presented simultaneously, but the call was broadcast from a loudspeaker placed at different distances away from the visual stimulus (EMF displaying vocal-sac pulsations), in order to study spatial binding. When the call was played less than or equal to 12 cm from the visual stimulus, aggressive behavior ensued. This system has potential for the study of cross-modal binding both behaviorally and neurophysiologically, a topic which has received little attention.

Supported by NIH grant DC-00222 to PMN and Austrian Science Foundation grant FWF P 15345 to WH.

312 Profile analysis in the barn owl (*Tyto alba*)

Melanie A. Zokoll, Ulrike Langemann, Georg M. Klump
Institute for Biology and Environmental Science, University of Oldenburg, C.v.Ossietzky Str. 9-11, Oldenburg, Germany

The ability to detect an increment in the sound pressure level of one component relative to the level of other components of a complex auditory signal is called profile analysis. The barn owl (*Tyto alba*) is a bird species that shows good frequency selectivity and temporal resolution. In this study, we present data from profile analysis experiments with narrow band noise stimuli comparable to those pioneered by Fantini and Moore (1994, *JASA* 95: 2180-2191).

Four barn owls were trained in a Go/NoGo paradigm to report a level increment of a narrow band of noise (center band at 2 kHz, CB). The CB was either presented alone or in the presence of four flanking bands (FB, center frequencies 1.02, 1.43, 2.8, and 3.92 kHz). The envelopes of all noise bands were either correlated or uncorrelated. They had a bandwidth of 4, 16 or 64 Hz. The stimuli had a total duration of 200 ms. In an additional experiment with stimuli composed of correlated noise bands the increment of the center band was counterbalanced by a level decrement of all four flanking bands. Signal-detection theory was applied to determine the birds' thresholds; threshold criterion was a d' of 1.8.

A change in the spectral profile due to the level increment of the CB could be detected significantly better by the owls in correlated noise bands than in uncorrelated bands. Presenting correlated FBs in addition to the CB improved the barn owls' intensity discrimination while uncorrelated noise bands interfered with the increment detection or had no effect. Both humans (Fantini & Moore 1994) and owls appear to exploit the spectral profile as long as the fluctuations in the noise bands are correlated. While humans perform best at slow envelope fluctuations (4 Hz noise bandwidth), owls predominantly profit from comparing CB and FB levels (i.e., apply profile analysis) at faster envelope fluctuations (64 Hz noise bandwidth).

Supported by the DFG, FOR 306 "Hoerobjekte"

313 Development of the acoustic startle response in zebrafish to pure tones

David G Zeddies¹, Richard R Fay²

¹CEBH, University of Maryland, Biology-Psychology Building rm 107, College Park, Maryland, United States, ²Parmlly Hearing Institute, Loyola University - Chicago, 2565 N Sheridan Road, Chicago, Illinois, United States

Zebrafish were placed in small wells that could be driven with vertical, sinusoidal displacements. A series of tones (100, 150, 200, 300, 400, 600, 800, and 1200 Hz) of 120 ms duration with 20 ms rise/fall times were calibrated and used as stimuli. Video images of the fish were obtained and analyzed to determine the levels and frequencies at which the fish responded to the tones. It was found that fish 4 days post fertilization (dpf) do not respond to the tones, whereas fish 5 dpf to adult do respond. It was also found that the bandwidth and thresholds of the responses did not change from 5 dpf to adult – i.e. 5 dpf fish responded at the same levels and wide

frequency range as older fish, indicating that the otolithic organ adaptations for high-frequency hearing are already present in larval fish. Deflating the swimbladders in adult fish eliminated their response, but swimbladder deflation in larval fish did not affect their thresholds. Losing the response in adult fish upon swimbladder deflation is consistent with the adult fish sensing sound pressure, while the persistence of the response in the absence of the swimbladder is consistent with larval fish sensing motion directly. That the adult and larval fish respond at the same levels with intact swimbladders suggests that the acoustic startle response threshold is adjusted to maintain appropriate reactions to relevant stimuli as the fish develop.

314 Asymmetry of Masking: A Psychophysical and Physiological Study in the European Starling

Mark A. Bee, Ulrike Langemann, Georg M. Klump

Institute for Biology and Environmental Science, Oldenburg University, Carl von Ossietzky Str. 9-11, Oldenburg, Germany

In human studies of simultaneous masking, thresholds for detecting a broadband noise signal masked by tones or narrowband noise are significantly lower than thresholds for detecting tonal and narrowband noise signals masked by a broadband noise [Hall JL (1997) *JASA* 101:1023-1033]. We investigated this “asymmetry of masking” in psychophysical and physiological experiments in the European starling (*Sturnus vulgaris*). Using the same threshold criterion ($d' = 1.8$), we determined the behavioral and neural masked detection thresholds in a factorial design for signals and maskers with bandwidths of 4 Hz and 256 Hz. Five starlings were trained in a GO/NO-GO procedure to detect a 500-ms signal centered in a 700-ms masker presented at an overall level of 40 dB SPL. Average thresholds for detection of a 256-Hz wide signal in a 4-Hz wide masker were approximately 22 dB and 16 dB lower than those for detection of a 4-Hz wide signal in maskers with bandwidths that were 4 Hz and 256 Hz, respectively, and 19 dB lower than that for detection of a 256-Hz wide signal in 256-Hz wide masker. This pattern of asymmetry in masking is very similar to that reported for human subjects. We determined the neural detection thresholds for the same signal+masker combinations using radiotelemetry to record multi-unit activity in field L2 (the avian equivalent of mammalian AI) from 4 awake, unrestrained birds. Maskers were presented at an overall level that was 20 dB SPL above the pure-tone threshold. The detection thresholds for sorted single units exhibited similar patterns and magnitudes of asymmetry in masking as those observed in the behavioral experiment, although the signal-to-noise ratios for neural detection thresholds were higher. Our results suggest that starlings and humans experience a similar asymmetry of masking; therefore, starlings represent an excellent model system for investigating the physiological mechanisms of asymmetry in masking.

Supported by DFG FOR-306 and NSF INT-0107304

315 Early Lead Poisoning Decreases Chicks' Responsiveness to Naturalistic, Amplitude-Modulated Sounds

Lincoln C. Gray¹, David B. Miller²

¹*Otolaryngology, University of Texas, 6431 Fannin, Houston, TX, United States*, ²*Psychology, University of Connecticut, 406 Babbidge Road, Storrs, CT, United States*

BACKGROUND: Young birds (and children) are normally more responsive to natural (i.e. mother's voice) than artificial sounds. We can test hearing in chicks because they stop peeping when they hear a sound. The maternal alarm call of the Red Jungle Fowl (domestic chicken ancestor) was recorded in the field, and is a long growl with prominent amplitude modulations (AM). This call signals the chicks to freeze, and we expect it to be more effective than noise in eliciting hatchlings' responses. We hypothesize that AM is the critical cue for enhanced responsiveness to the natural call and determine the effect of early lead poisoning (because this causes phonetic processing disorders in children). **METHODS:** Eggs were exposed at 14 days of incubation (start of auditory development) to nothing, saline, or a high (132 mg/kg) or low (88 mg/kg) dose of lead (resulting in a “safe” blood-lead level, ~10 µg/ml, per the CDC). Subjects at 0 and 4 days of age heard 4 different stimuli: the unaltered alarm call, a noise with the same spectrum, the alarm call divided by its envelope (a call with no AM), and the noise multiplied by the call's envelope (natural AM with different fine structure). **RESULTS:** Normal chicks, but not chicks exposed to lead, were more responsive to the maternal alarm call than to equally loud noise. There is a linear relationship between AM and responsiveness in normal ($p = .01$) but not leaded birds ($p = .35$). The special sensitivity to naturalistic AM is obliterated by early lead poisoning ($p < .001$). **DISCUSSION:** Early lead poisoning is a risk factor for dyslexia and phonetic processing disorders. This deficit is thought to be due to decreased sensitivity to rapidly changing speech sounds. Lead-exposed chicks are deficient in backward masking, as are dyslexic children. Here we show another similarity between leaded chickens and dyslexic children, in that both show deficient responsiveness to temporal modulations in naturalistic sounds.

316 Development Of Midbrain And Thalamic Auditory Connections As Revealed By Multicolor Carbocyanine Dye Tracing.

Bernd Fritzsche, **Bina Gurung**

Biomedical Sciences, Creighton University, 2500 California Plaza, Omaha, NE, United States

Past research has shown that central auditory connections in mice develop prior to the onset of hearing around postnatal day 7. Neither the timing nor the degree of specificity of these initial connections is known. Studies of final mitosis suggest that thalamic nuclei may form prior to cochlear nuclei. Only a single study has investigated the development of auditory nuclei projections in embryonic rats, but not the development of colliculo-thalamic and thalamo-cortical connections. We provide here for the first time experimental information about the onset and progression of projections from the inferior colliculus (IC) to the medial geniculate body (MGB) and from the MGB to the auditory cortex (AC).

Overall, the developmental progression of projections follows the developmental progression of terminal mitosis in various nuclei, suggesting a consistent use of a developmental time table at a given nucleus independent of other nuclei. Our data suggest that neurons project specifically and reciprocally from the MGB to the AC. These MGB-AC reciprocal connections can first be labeled about a day prior to the reciprocal connections of MGB and IC. The development of IC projections to MGB is prolonged and progresses from rostral to caudal areas, in line with the rostral to caudal progression of proliferation. Brainstem nucleus projections to IC progress from lateral lemniscus (LL) nuclei to superior olive (SO) to cochlear nuclei (CN) suggesting that the input from CN to IC is delayed in line with their comparative late terminal mitosis. Overall, the auditory connection development strongly suggests that most of the overall specificity of nuclear connections is set up at least two weeks prior to the onset of sound mediated cochlear responses and thus is likely governed predominantly by molecular genetic clues.

317 Arrangement of Ascending and Descending Afferent Patterns in the Developing Auditory Midbrain and Thalamus

Mark L. Gabriele, Megan E. Taylor, Christopher C. French, Jaime E. Smoot

Biology, James Madison University, MSC 7801, Harrisonburg, VA, United States

The inferior colliculus (IC) and the medial geniculate nucleus (MGN) are major relay centers in the ascending auditory pathway. In addition to conveying ascending information, these structures receive feedback connections from the auditory cortex that are thought to modulate processing within the IC and MGN. The present study examined the spatial arrangement of developing ascending and descending projection patterns within the auditory midbrain and thalamus. Carbocyanine dyes, DiI and DiD, were used to simultaneously label ascending and descending inputs to the IC and MGN in a developmental series of fixed rat tissue (postnatal days: P0, P4, P8, and P12). Banded inputs to the IC originating from the lateral superior olive (LSO) or the dorsal nucleus of the lateral lemniscus (DNLL) were labeled in concert with the descending corticocollicular projection. In a separate series of experiments, the colliculogeniculate and corticogeniculate pathways were labeled concurrently. Regions of partial overlap of ascending and descending afferent patterns within the IC and MGN were apparent during the early postnatal period (P0 – P4). Initial overlap was most evident within the dorsal aspect of the central nucleus of the IC and within the ventral division of the MGN. By the onset of hearing (P12) ascending and descending afferent patterns were spatially segregated within the IC and MGN, exhibiting few regions of sustained overlap. Descending inputs to the IC terminated most heavily within the dorsal cortex and the external nucleus, but were also apparent within the central nucleus interdigitating with the ascending banded inputs. Similarly, while descending inputs were present in all subdivisions of the MGN, they appeared to preferentially target domains not occupied by ascending terminals. These data provide further evidence in support of a compartmentalized arrangement of functional domains within the auditory midbrain and thalamus.

318 Two Types of Laminar Afferents in the Central Nucleus of the Inferior Colliculus (ICC) from the Dorsal Cochlear Nucleus (DCN) in the Cat and Rat

Manuel S Malmierca¹, Richard L Saint Marie², Douglas L Oliver², Miguel A Merchan¹

¹Institute of Neuroscience of Castilla y Leon, University of Salamanca, Faculty of Medicine, Salamanca, Spain,

²Neuroscience, University of Connecticut Health Center, 263 Farmington Ave, Farmington, CT, United States

The ICc is a laminated structure composed of oriented dendrites and similarly oriented afferent fibers. Within a single tonotopic representation there are convergent inputs from different brainstem sources. Here, we investigated the synaptic banding patterns of projections from the cochlear nuclei in the cat and rat. Injections of dextran markers were made in the DCN after physiological characterization of each injection site. Images of the termination fields in the ICc were digitized and the size and distribution of synaptic boutons within these fields were measured with semi-automated image processing methods. The mean width of a lamina was determined as the peak width at the half height of the Gaussian distribution of boutons (see Saint Marie and Oliver, this meeting). Laminae in serial sections from each case were also plotted with NeuroLucida.

Two components in the laminae were identified: (1) a major lamina composed of thick fibers and large boutons; (2) a broader lamina composed of thin fibers and smaller boutons ($< 2.5 \mu\text{m}^2$ in rat; $< 3 \mu\text{m}^2$ in cat), that included the major lamina at its core and a paralaminar plexus. The small bouton lamina was approximately 40% wider than the major lamina in the cat and 30% wider on average in the rat. These laminae varied in width among the cases, presumably due to variations in the size and/or location of the injection sites. Regardless, the mean width of the lamina composed of smaller boutons was always significantly broader than the major lamina, and often the tail of the distribution of small bouton lamina extended 100 μm beyond the larger boutons.

The presence of both thick and thin fibers within the acoustic striae following these injections and the results of retrograde transport experiments suggest that large and small fibers/boutons within these bands may originate from different neuronal types in the DCN and ventral cochlear nucleus. We conclude that large fibers and boutons, presumably from principal neurons in DCN, provide an input with a restricted spectral representation within the ICc. Smaller fibers/boutons, on the other hand, may provide the substrate for broader interactions with adjacent isofrequency laminae in the ICc.

Support provided by: NIH DC000189, Fulbright Commission, Spanish DGES (BFI-2000-1296) and JCYL-FSE (SA084/01).

319 A Semi-Automated Image Analysis Algorithm Determines Synaptic Bouton Size and Distribution in Banded Dorsal Cochlear Nucleus (DCN) Projections to Inferior Colliculus Central Nucleus (ICC)

Richard L Saint Marie, Douglas L Oliver

Neuroscience, University of Connecticut Health Center, 263 Farmington Ave, Farmington, CT, United States

The ICc receives laminated projections from a variety of auditory brainstem structures. Previous determinations of band dimensions and/or synaptic composition have typically involved either subjective evaluations and/or tedious manual plotting, or failed to distinguish boutons from axons. Here we describe an image-processing algorithm that isolates synaptic boutons from their parent axon and determines their size and position in the band. Material was from a cat with a small injection of biotinylated dextran in DCN. The injection produced terminal bands in the ICc, visualized with avidin/peroxidase binding and DAB-NiCo reaction. Images were captured from 100 μ m thick sections with a digital camera and a 25x immersion objective in a through-focus series at 2 μ m intervals. These were deconvolved with an unsharp mask and collapsed arithmetically into a single through-focus image. Further processing with spectral filters enhanced local contrast before thresholding. Boutons (terminal and en passant) were isolated from axons with a progressive series of erosions and dilations of the objects in the thresholded mask. Contiguous objects were separated automatically by a skeletonized distance map generated between each erosion and dilation and superimposed on the contiguous objects. Boutons were identified and outlined based on size and shape filters and their outlines were superimposed on the original through-focus image for editing. Inappropriately identified objects were removed manually. The midline of the band was determined by the packing density of the boutons, and the position of each bouton was determined by generating a 16-bit distance map relative to midline and assigning the center pixel of each bouton a gray-scale value equivalent to its position. Except for editing, all procedures were automated by using batch (Photoshop, Adobe) or script (ImagePro Plus, Media Cybernetics) files that allowed thousands of boutons to be characterized in a few hours. Frequency histograms were used to determine band width and revealed that larger boutons have a narrower distribution within the bands than do smaller boutons (see Malmierca et al., this meeting). Supported by: NIH DC000189.

320 Evidence for a Fast Pathway To The Auditory Thalamus

Lucy Anne Anderson, Mark N. Wallace, Alan R. Palmer

Neurophysiology, MRC Institute of Hearing Research, University Park, Nottingham, United Kingdom

The medial geniculate nucleus (MGN), consists of dorsal (dMGN), ventral (vMGN) and medial (mMGN) sub-divisions, which are identifiable using cytochrome oxidase staining. The main ascending auditory input to the MGN is from the inferior colliculus, but a direct pathway from dorsal cochlear nucleus to mMGN in the rat has been demonstrated (Malmierca et al. 2002, *J. Neurosci* 22: 10891-10897). Here, we present data from the anaes-

thetised guinea pig consistent with a short latency pathway to mMGN. Recordings were made from 350 neurons in MGN. Frequency response areas and post-stimulus time histograms to tones differed between sub-divisions, but with substantial overlap in response characteristics.

A striking difference between sub-divisions was the response to clicks and click trains. Neurons in both mMGN and vMGN responded reliably to single clicks at rate of 5 Hz. Latencies of the responses to clicks in mMGN ranged from 3 to 16 ms, (mean 7.82 ± 3.01 ms SD). This was the only sub-division of the MGN where latencies of less than 7 ms were observed. Latencies of the responses to clicks in vMGN ranged from 7 to 19 ms (mean 9.88 ± 2.43 ms). Neurons in dMGN responded less reliably to clicks and the range of response latencies was larger from 7 to more than 30 ms (mean 13.23 ± 5.08 ms). Mean response latencies from the three sub-divisions were significantly different from each other (Scheffé, ANOVA, $p < 0.001$). The shortest latency neurons in mMGN included some which were binaural.

In subsequent multi-electrode recordings, the responses to click trains were measured. While 35% of mMGN neurons showed significant locking to 640 Hz; only 12% of vMGN neurons showed significant locking beyond 160 Hz.

The finding of the shortest latencies and following to higher click rates in mMGN is consistent with a direct input from cochlear nucleus, but there is also evidence of convergence onto these neurons from other sources.

321 Laminar Organization of Tectothalamic Bands and Synaptic Nests in the Rabbit Auditory Thalamus

David S. Velenovsky¹, Michael G. Holmes¹, Donal G. Sinex², Nathaniel T. McMullen¹

¹*Cell Biology and Anatomy, University of Arizona, 1501 N. Campbell Ave, Tucson, Arizona, United States*, ²*Speech and Hearing Science, Arizona State University, P.O. Box 871908, Tempe, AZ, United States*

We have recently proposed a model of MGv organization that incorporates cellular laminae and oriented dendritic growth to form frequency-related slabs within the MGv (Cetas et al., 2003). In the present study, we used the anterograde transport of biotinylated dextrans (BDA) to label tectothalamic axons. We report that tectothalamic axons form narrow bands closely aligned with cellular laminae in the MGv. Adult NZW rabbits were anesthetized and a small craniotomy was made for insertion of electrodes into the inferior colliculus. Animals were placed in a Kopf stereotaxic device and Carbostar3 microelectrodes were remotely advanced into the IC. TDT System 3 hardware and software were used to deliver calibrated tone and noise bursts through custom transducers. When short-latency, tightly-tuned responses were identified in the ICC, 10% BDA was iontophoresed with a current generator. Animals were allowed to recover for approximately 7-9 days and then deeply anesthetized and transcardially perfused with 4% paraformaldehyde. Coronal sections (50 μ m) were cut through the MGB and IC. ICC injection sites and anterograde-labeled axons in the MGv were visualized immunocytochemically. Mapping penetrations through the vertically-oriented laminae of the rabbit ICC revealed consistent BF throughout the penetration. Focal BDA

injection sites in the ICC labeled local collaterals with extensive band-like projections that paralleled the Nissl laminae. In the MGv, tectothalamic arbors formed narrow bands oriented parallel to the Nissl laminae of the pars lateralis. These oriented bands extended in the AP axis to form afferent sheets within the MGv. Tectothalamic axons terminated as large boutons frequently arranged in a ring-like glomerular pattern termed synaptic nests by Morest. These data provide evidence for an extraordinary structural functional correlation at this level of the auditory central nervous system. (Supported by NIH DC02410, DC05108 and the DRF)

322 Response of Inferior Colliculus Neurons to Complex Signals are Shaped by projections from the Ipsilateral Dorsal Nucleus of Lateral Lemniscus

Ruili Xie¹, George Pollak²

¹Neurobiology, University of Texas at Austin, 1 University station, C0920, Austin, TX, United States, ²Neurobiology, University of Texas at Austin, 1 University Station, C0920, Austin, TX, United States

In response to complex, social communication calls, most neurons in the IC of Mexican free tailed bats display a high degree of selectivity, in that they respond only to some calls but not to other calls, even though the calls they fail to respond to have energy in their excitatory tuning curves. The selectivity is due largely to inhibition; when inhibition is blocked with bicuculline and/or strychnine, IC neurons respond to many more calls than the same neurons responded to when inhibition was intact. One source of GABAergic inhibitory input to the IC is from the ipsilateral dorsal nucleus of the lateral lemniscus (DNLL). To evaluate the impact of the projections from the DNLL on the ipsilateral IC, we reversibly inactivated DNLL with kynurenic acid (an antagonist for glutamate receptors), and recorded the responses of neurons in the ipsilateral IC to a suite of species-specific communication calls before, during and after reversibly inactivating the DNLL.

Neurons from different sectors of IC were recorded and changes in response properties were found in neurons located in the rostral IC. Many of these IC neurons originally responded to only a few of the social calls we presented, and thus were selective. When a portion of the inhibitory input to the IC was eliminated by inactivating the DNLL, the response magnitude increased markedly in many rostral IC cells. More importantly, the vigor of the responses to the social calls not only increased, but these IC cells now responded to a larger number of calls, and thus became far less selective than when the DNLL innervation was intact. Concurrent anatomical studies also showed that injections of fluorescent tracers in the rostral IC resulted in heavier retrograde labeling in the ipsilateral DNLL than injections made in other sectors of the IC. We therefore conclude that the inhibitory DNLL inputs to ipsilateral IC are functionally shaping the signal processing in the rostral IC by suppressing some excitatory inputs. One consequence of this inhibition is that it shapes the selectivity of IC neurons for complex signals, allowing those IC cells to extract certain information from only some complex signals but not others.

Supported by NIH grant DC00268.

323 The External Nucleus of Inferior Colliculus Integrates Somatosensory and Acoustic Information

Roshini Jain^{1,2}, David J Anderson^{1,2}, Susan E Shore¹

¹Otolaryngology, University of Michigan, 1301 E Ann St, Ann Arbor, MI, United States, ²Bioengineering, University of Michigan, 1301 E Ann St, Ann Arbor, MI, United States

The external nucleus of the inferior colliculus (ICE) receives ascending projections from both auditory and somatosensory nuclei (Aitkin et al., *J. Comp. Neurol.* 196: 25- 40, 1981). Specifically, the spinal trigeminal nucleus has been shown to project to ICE in rodents (Li and Mizuno, *Neurosci. Res.* 29: 135-142, 1997). We investigated the function of the trigeminal-collicular pathways in guinea pigs by electrically stimulating the trigeminal nucleus while recording unit responses from ICE. Pairing electrical stimulation with acoustic stimuli allowed us to investigate multisensory integration.

A concentric, bipolar stimulating electrode was stereotaxically placed in the ipsilateral trigeminal nucleus. Electrical stimuli (bipolar pulses 100 μ s per phase, at intervals of 200 ms) were applied alone, or 25 ms after the onset of a 100 ms broadband noise burst. Unit responses were recorded from ICE using a 16-channel, single shank electrode, allowing simultaneous recordings from multiple units. Units were sorted using principal component analysis. Electrode placements were confirmed histologically following the experiments.

Electrical stimulation of the trigeminal nucleus produced small changes from spontaneous activity of the neurons, but resulted in significant inhibition/excitation when paired with acoustic stimuli. Such multi-sensory integration has been demonstrated in superior colliculus and sensory cortices and has been shown to play a role in plasticity that occurs after sensory deprivation. Abnormal cross-modal information processing could contribute to the perception of phantom sounds/tinnitus.

Supported by NIH grant 5 R01 DC004825-03 and Tinnitus Research Consortium.

324 Ascending Inputs to the Lateral Cortex of the Inferior Colliculus (IC) in Rat and Cat

William C. Loftus¹, Manuel S. Malmierca², Deborah C. Bishop¹, Douglas L. Oliver¹

¹Dept. of Neuroscience, University of Connecticut Health Center, 263 Farmington Ave, Farmington, CT, United States, ²The Institute of Neuroscience of Castilla y Leon, University of Salamanca, 37007 Salamanca, Salamanca, Spain

The central nucleus of the IC (ICc) is distinguished from other parts by its disc-shaped cell types and laminar organization. Previous tracer studies in both rats and cats reveal that ascending inputs to the ICc are arranged in oriented, frequency specific bands of axons aligned with layers of postsynaptic neurons. Inputs from different brainstem sources have distinct termination patterns within the ICc, but comparatively little is known about the lemniscal inputs to parts of the IC outside of the central nucleus. We made focal injections of anterograde anatomical tracers in the dorsal and ventral cochlear nuclei (DCN and VCN) of rats and cats and in the lateral superior olive (LSO) of cats, and analyzed the

labeled axons and boutons in transverse sections of the IC. DCN and VCN injections were often made in the same animal, and the best frequency at the injection site was defined physiologically. For many injections in either species, labeled inputs were found lateral to the ICc in shorter bands that were oriented nearly perpendicularly to the more medial ICc bands. In the rat, these 'lateral bands' were located in the deepest layer (layer 3) of the external cortex (ICX); in the cat, they were located in or near the ventrolateral nucleus (VL). In both species, DCN injections consistently produced labeling of lateral bands that extended over the rostral-caudal extent of the IC. In the cats, VCN injections produced labeling with more prominent patches than comparable DCN injections; this difference was also found in the rat but was not as pronounced. In cats, the LSO contributed bilateral inputs to the VL and boutons from the LSO on either side were found in adjacent patches. There was an obvious tonotopic organization to the lateral bands in the rat, with higher frequency inputs located at more ventral positions in the ICX. Based on these cross-species similarities in the afferent organization of the lateral cortex of the IC, we suggest that the third layer of ICX in the rat and the VL in the cat are homologous structures. Sponsored by NIDCD grant R01 DC00189, Fulbright Commission, Spanish DGES (BFI-2000-1296) and JCYL-FSE (SA084/01).

325 Projections from inferior colliculus to the nuclei of the lateral lemniscus studied in a slice preparation.

Elisabeth Wallhäusser-Franke¹, Katrin Meuer¹, Barbara E. Nixdorf-Bergweiler², Gerald Langner¹

¹Zoology, Darmstadt University of Technology, Schnittspahnstr. 3, Darmstadt, Germany, ²Zoology, Christian Albrecht Universität, Am Botanischen Garten 9, Kiel, Germany

The inferior colliculus appears to be the first nucleus of the ascending auditory pathway, where periodicity information is represented spatially. In its central nucleus (ICC) best modulation frequencies increase systematically from medial to lateral locations (Langner et al., *Hear. Res.* 2002). Physiological evidence now suggests a periodotopic projection from the ICC to the ventral part of the lateral lemniscus complex (VNLL) (Langner et al., *ARO* 2003). An indication of a periodotopic projection would be an orderly connection pattern between these structures that cannot be explained by their tonotopic maps.

So far a back-projection from ICC to VNLL could not be established. Therefore, we studied the projection between ICC and LL in coronal slices (3000 µm) gained from adult gerbils (*Meriones unguiculatus*). Under visual control, crystals of fluororuby and fluoroemerald were inserted into ICC. After injections, slices were incubated in a submerged chamber with cold ACSF for 20 hours. Fixation in 4% PA was followed by cryosectioning to a final thickness of 60µm.

Under these conditions both tracers were transported exclusively in the anterograde direction. Numerous labeled axons were seen to traverse VNLL dorsoventrally with the majority of thick axons not showing indications of synaptic contacts. Some labeled axons were thinner and showed varicosities or they had short collateral branches in the horizontal direction with characteristics of terminal arborizations confirming a projection from ICC to VNLL.

Horizontal branches with terminal arborizations were located preferentially in dorsal and intermediate VNLL. Preliminary evidence suggest a periodotopic organization of this projection.

Supported by the VW-Stiftung

326 Ventral Medial Geniculate Nucleus Contains Functionally and Anatomically Distinct Compartments.

Heather L. Read^{1,2}, Lee M. Miller³, Monty A. Escabi⁴, Christoph E. Schreiner⁵, Jeffery A. Wine⁶

¹Psychology, University of Connecticut, 406 Babbidge Road, Storrs, CT, United States, ²Molecular and Cell Biology, University of California, 142 Life Sciences Addition, Berkeley, CA, United States, ³Psychology, University of California at Berkeley, 4127 Tolman Hall, Berkeley, CA, United States, ⁴Electrical and Computer Engineering, University of Connecticut, 371 Fairfield Road, Storrs, CT, United States, ⁵W.M. Keck Center for Integrative Neuroscience, University of California at San Francisco, 513 Parnassus Ave, San Francisco, CA, United States, ⁶Molecular and Cell Biology, University of California at Berkeley, 142 Life Sciences Addition, Berkeley, CA, United States

Input to auditory cortex from the ventral division of the medial geniculate body (MGBv) is regarded as homogeneous in its spectral selectivities including cochleotopy. Features such as binaural properties vary topographically within MGBv. In this study we quantify density and areal pattern of MGBv neurons that project to the central narrowbandwidth (NB) region of AI. Previously, we described functional compartmentalization in AI according to intensity dependent bandwidth. Retrograde tracers were injected into the physiologically defined central NB AI region in 4 animals. Labeled MGBv neurons were plotted at 60x. The density and pattern of MGB label was analyzed with two-dimensional histograms and autocorrelation functions. In all cases, 80% of labeled neuron cell bodies were in the MGBv, and < 20% were in the medial division (MGBm). In one case, two injections in the central NB domain of AI were separated by ~1 octave. Two contiguous contours were found within the ventral subregion of MGBv. In three-dimensional reconstructions their separation changed significantly (bootstrap analysis) across the dorso-ventral and rostral-caudal axes, indicating multiple cochleotopies. Most neurons projecting to the central NB compartment arose from neurons in caudal-dorsal MGBv that had highly magnified (<<1 octave) cochleotopy. A weaker projection arose from caudal-ventral MGBv neurons with 1 octave resolution cochleotopy. Five percent of MGBv neurons were double labeled, indicating a thalamocortical divergence of up to 1 octave from the caudal-ventral cochleotopic MGBv subdomain. These findings suggest that unique thalamocortical spectral receptive field convergence patterns arise from different MGBv subdomains.

Supported by USPHS grants R01 DC2260 and R01 DC02319.

327 Contribution of Auditory Cortex to the Detection of Sinusoidal Amplitude Modulated Noise by the Rat

James E. Cooke, Jack B. Kelly

Psychology Department, Carleton University, 1125 Colonel By Drive, Ottawa, Ontario, Canada

Bilateral destruction of auditory cortex in the rat results in little or no lasting change in auditory sensitivity or performance on several simple auditory discrimination tasks. Only minor deficits have been found in the rat's ability to localize sounds in space although severe deficits have been reported for other mammals (including cat, ferret and monkey) after bilateral or unilateral auditory cortical lesions. The purpose of the present study was to examine the effects of cortical lesions in rats on auditory discriminations involving temporal processing of sounds. Sinusoidal amplitude modulated (AM) sounds were used to test temporal processing ability before and after bilateral ablation of auditory cortex. Eight rats were trained to respond to amplitude modulation of a white noise carrier using a conditioned avoidance procedure (withdrawal from a water spout to avoid a shock). The method of descending limits was used to determine threshold for detecting depth of modulation at three different modulation frequencies: 10, 100, 1000 Hz. Following cortical lesions the rats were allowed at least two weeks recovery time to avoid transient deficits and were tested again using the same avoidance procedures. Results showed significant elevations in threshold for detection of AM at 100 and 1000 Hz, but no significant change at 10 Hz following bilateral lesions of auditory cortex. There was a strong positive correlation between the size of the lesion and the severity of the deficit at modulation frequencies of 100 and 1000 Hz. The results show that there are lasting deficits in the ability of rats to detect the presence of sinusoidal AM following bilateral cortical lesions and that the deficits are most evident at higher modulation frequencies.

This research was supported by NSERC of Canada.

328 Decreased neural temporal resolution in cat auditory cortex with noise induced hearing loss.

Masahiko Tomita¹, Arnaud Norena¹, Jos Jan Eggermont²

¹Physiology and Biophysics, University of Calgary, 2500 University Drive N.W., Calgary, Alberta, Canada, ²Physiology and Biophysics, Psychology, University of Calgary, 2500 University Drive N.W., Calgary, Alberta, Canada

Hearing loss associated with an impairment of speech recognition is linked to a decrease in neural temporal resolution. In order to assess central auditory system changes in temporal resolution after a hearing loss, we investigated the effect of a noise induced hearing loss on the representation of a voice onset time (VOT) and gap duration in primary auditory cortex (AI) of the ketamine-anesthetized cat. A /ba-/pa/ continuum (VOT varied in 5 ms steps from 0-70 ms) and gaps of duration equal to the VOT, and embedded in noise, were presented. Multiple single-unit activity was recorded before and several hours after an acute acoustic trauma induced by a 1-h exposure to a pure tone at 115-120 dB SPL using multi-electrode arrays. We also obtained data from AI several weeks after 1-4 hrs exposure to 115-120 dB SPL tones or noise. We specifically

analyzed the maximum firing rate (FR_{max}) in the PSTH for the vowel or trailing noise burst, as a function of VOT and gap duration. The changes in FR_{max} for /ba-/pa/ continuum as a function of VOT matched the sigmoid psychometric function for categorical perception of /ba-/pa/. A few hours after the acoustic trauma the sigmoid fitting functions were shallower and shifted toward higher values of VOT. Several weeks after an acoustic trauma the sigmoid fitting functions were also shallower than for the normal hearing group. The less steep fitting function indicate an increased ambiguity between /ba/ and /pa/. This result is consistent with the hypothesis stating that the degradation of speech perception in hearing-loss subjects may be related to a loss of temporal resolution.

329 The Impact of a High Frequency Cochlear Lesion on Gap Thresholds and Modulation Transfer Functions from the IC of Guinea Pigs

Jian Wang¹, Michele Bowden¹, Kai Wang²

¹School of Human Communication Disorders, Dalhousie University, 5599 Fenwick St. G100, Halifax, Nova Scotia, Canada,

²ENT Department, West China Hospital of Sichuan University, 37 Guo Xue Xiang St, Chengdu, China, People's Republic of

Gap detection thresholds and modulation transfer functions (MTF) are two common measurements that are thought to reflect the temporal resolution of the auditory system. These can be evaluated either psychologically or physiologically. In this study, evoked potentials from electrodes implanted into the inferior colliculus of guinea pigs were recorded in response to a gap between noise bursts and amplitude modulated continuous tones. For gap detection, "low-band" and "high-band" gaps were generated using either low-pass or high-pass filtering of Gaussian noise with a cut-off frequency of 12 kHz. Two carrier frequencies, 8 kHz and 16 kHz, were selected for the steady-state AM stimulus to evoke the envelope following responses. Permanent threshold shifts of 40-60 dB were established beyond 12 kHz by acoustic overstimulation. The high-frequency lesions was found to produce significant increases in gap thresholds for gaps formed with noise bursts of low-band in which hearing was virtually normal. Meanwhile, the cutoff frequency of the MTFs, which showed a low-pass pattern, was significantly reduced for the 8 kHz carrier, which was in the region of normal hearing. These results suggest that high-frequency hearing loss has a great impact on the temporal resolution of low-frequency channels of the auditory system.

330 Across-channel gap detection responses in unanesthetized chinchilla IC and AC using different toneburst frequencies

Yuqing Guo¹, Robert Burkard^{1,2}

¹Center for Hearing and Deafness, University at Buffalo, 3435 Main Street, Buffalo, NY, United States, ²Communicative Disorders and Sciences, University at Buffalo, 3435 Main Street, Buffalo, NY, United States

Perceptual studies have demonstrated that there are higher gap thresholds across-channels than within-channels. This investigation evaluated the across-channel gap detection responses recorded from the inferior colliculus (IC) and auditory cortex (AC) in unanesthetized chinchillas.

In experiment 1, 8 chinchillas with right chronic IC electrodes were placed in a passive animal restraint, with an insert earphone in the left ear. In experiment 2, another group of chinchillas (n=7) with right chronic AC electrodes were stimulated with an insert earphone in the left ear. Gap stimuli were toneburst pairs with 50 ms duration and 0.5 ms risetime. The frequencies of the leader and trailer tonebursts switched between 2 kHz and 4 kHz. Gaps ranged from 0 to 64 ms.

For both experiments, onset responses to the trailer stimuli (onset 2) increased in latency and decreased in amplitude with decreasing gap; i.e., they showed forward masking. There was a stronger forward masking for the within-channel (same frequency) conditions than for the across-channel (different frequency) conditions. This difference in forward masking is substantial in IC data and small in AC data. This forward masking on the across-channel condition for the low-to-high frequency condition was larger than the high-to-low frequency condition in IC data. On the other hand, there is little change of offset responses to the leader stimuli (offset 1) with decreasing gaps. The onset 2 and offset 1 gap responses are still seen for the shortest gap condition.

Supported by NIH DC03600

331 Behavioral and Single -Unit IC Responses of CBA Mice to Partially Filled Gaps in Noise

Kathy Barsz¹, James R. Ison², Paul D. Allen², Joseph P. Walton¹

¹Otolaryngology, University of Rochester Medical Center, 601 Elmwood Ave, Rochester, NY, United States, ²Brain and Cognitive Sciences, University of Rochester, Meliora Hall - River Campus, Rochester, NY, United States

Temporal acuity in both humans and laboratory animals is typically assessed by determining the threshold for detecting brief quiet gaps in noise. In humans gap thresholds are little affected by partially filling the gap with noise until noise floors are within 6 dB of the gap markers (Forrest and Green, JASA, 1987), though the steepness of the psychometric function above the gap threshold is reduced (Green and Forrest, JASA, 1989). Here in one behavioral experiment in young CBA mice (n=23, 2 to 5 mo old) using the method of reflex audiometry we found that the asymptotic response to gaps in a 70 dB (SPL) noise surround was obtained at 4-6 ms gap durations with noise floors from 40 to 60 dB. Gap thresholds averaged 3- 4 ms in this range of floors, but increased to 15 ms for a 64 dB floor. The asymptotic response to the gaps declined as the floor increased above 50 dB. In an electrophysiological study in the inferior colliculus of young CBA mice (44 cells in total), mean spike (SEM) count to the first noise burst (NB1 = NB2 = 65 dB SPL) marking the gap declined as the surrounding noise increased from 41 dB SPL to 59 dB SPL, from 80 spikes (7.9) in Quiet to 56 (7.9) in 40 dB to 52 dB noise, to 28 spikes (4.4) in 59 dB noise. NB2 responsivity increased rapidly from a near zero level as the gap duration increased from 1ms to near asymptotic levels at 12 ms. Asymptotic mean NB2 responses approximated the level of NB1 in a quiet background, but, remarkably, were slightly but significantly higher than NB1 responses in background noise. This apparent overshoot was particularly noticeable in cells that by virtue of their near constant gap thresholds across background noise levels had been independently classified as "gap-specialized" rather than "non-spe-

cialized" cells. Work Supported By NIA Grant#AG09524 and RICHs, Rochester, NY.

332 Effect Of Component Phase On Responses Of Inferior Colliculus Neurons To Harmonic And Mistuned Complex Tones

Donal Sinex, Hongzhe Li

Speech and Hearing Science, Arizona State University, Box 870102, Tempe, AZ, United States

Mistuning one component of a harmonic complex tone produces dramatic changes in the temporal discharge patterns of inferior colliculus (IC) neurons, but has little effect on the responses of auditory nerve fibers. We have proposed a model of spectral processing in which narrowband envelope extraction followed by across-channel inhibition produces response patterns like those observed in the IC. In the original IC data, stimulus components were always added in sine phase, but the model predicts that changing component phase would have little effect on the observed discharge patterns. That prediction was tested. Eight-component harmonic complex tones were generated, with components added in sine, cosine, or random phase. The same tones were also generated with one component mistuned. Responses to harmonic tones usually exhibited no temporal pattern that could be attributed to the stimulus; this was true for all phase conditions. Tones with a mistuned component could elicit discharge patterns with distinctive patterns of low-frequency modulation. Changes in component phase changed the absolute latencies of individual response peaks but did not change the global characteristics of the discharge patterns; low-frequency modulation observed with sine-phase tones was also observed with cosine or random phase, as predicted by the model. Supported by DC00341.

333 Phase-locked Responses to Tones in the Medial Geniculate Nucleus of the Thalamus

Mark Nelson Wallace, Lucy Anne Anderson, Trevor M. Shackleton, Alan Richard Palmer

Neurophysiology, MRC Institute of Hearing Research, University Park, Nottingham, United Kingdom

We recently described phase-locked responses to pure tones in 3 areas of auditory cortex (Wallace et al. Hearing Res. 172:160-171) and now describe the location and properties of phase-locked responses in the thalamus. Pure tones (200 ms long, 2 ms rise time) were presented in a closed sound system to guinea pigs anaesthetized with a ketamine/xylazine mixture. In the ventral division of the medial geniculate nucleus (MGV) 30 single or multi-unit clusters with characteristic frequencies (CFs) of 0.1 – 1.2 kHz phase-locked to tones in the range 60 – 520 Hz. In the medial (magnocellular) division of the medial geniculate nucleus (MGM) 9 multi-units with CFs of 0.5 – 12.3 kHz phase-locked to tones in the range of 60 – 1100 Hz. Over the same stimulus frequency range we found no phase-locked responses in the dorsal division of the medial geniculate nucleus. The upper phase-locking limit of units in MGM was significantly higher than those in MGV (p = 0.001). Phase-locking responses were obtained at multiple stimulus frequencies and the best phase of the period histograms plotted against the frequency for 18 units in MGV and 7 units in MGM. All of the plots were linear and their slope corre-

sponds to the neural delay between the cochlea and thalamus. The mean phase latency for MGV (11.3 ms, range 9 – 14 ms) was significantly ($p = 0.006$) longer than for MGM (9.3 ms, range 7.5 – 11 ms). The shorter latencies in MGM are consistent with a direct input to MGM from the cochlear nucleus (Malmierca et al. *J. Neurosci.* 22:10891-10897) and may provide a shorter latency route into cortex than that via the inferior colliculus.

334 Duration Dependence of Low Frequency Inhibition among Neurons in the Inferior Colliculus of the Mustached Bat.

Don Gans, Kianoush Sheykhoslamy, Jeffrey James Wenstrup

Neurobiology, Northeastern Ohio Universities College of Medicine, 4209 State Route 44, Rootstown, Ohio, United States

In the mustached bat's inferior colliculus (IC), many neurons tuned to higher frequencies (>45 kHz) are inhibited by lower frequency sounds in the range of the first sonar harmonic (23-30 kHz). We have recently observed widespread inhibition tuned to frequencies of 10-22 kHz, frequencies associated with social vocalizations and environmental sounds but not with sonar. Here we examine whether inhibition tuned to these frequency ranges has different temporal properties. We recorded 76 single units in the mustached bat's IC with best frequencies above 45 kHz. For most of the population, strong inhibition occurred when the best frequency and lower frequency tones were presented simultaneously, suggesting that the latencies of the high frequency excitation and low frequency inhibition were closely matched. However, there was a clear frequency dependence in the effect of changes in the duration of the lower frequency signal. Among neurons in which inhibition was tuned to 23-30 kHz, 81% showed little change in the duration of inhibition as the duration of the low frequency signal was increased. For these neurons, low frequency inhibition thus appears to depend on a phasic low frequency input. In contrast, inhibition tuned to frequencies of 10-22 kHz was dependant on the duration of the low frequency signal. Specifically, the inhibition increased in proportion to the stimulus duration in 97% of these neurons. This inhibition appears to result from a sustained, low frequency inhibitory input. We believe these low frequency inhibitory interactions originate in different auditory brainstem nuclei, depending on their frequency tuning. While it is too early to speculate on the precise roles of the two populations of inhibitory neurons, it is intriguing that the 10-22 kHz inhibition, activated by non-sonar signals, is tonic and therefore consistent with the wide variety of stimulus durations characteristic of social and environmental sounds.

Supported by RO1 DC00937 from NIDCD.

335 Duration Sensitive Neurons in the Inferior Colliculus of the Rat

David Perez-Gonzalez¹, Manuel S. Malmierca¹, Jordan Moore¹, Ellen Covey^{1,2}

¹Cell Biology and Pathology, Auditory Neurophysiology Unit. Lab Neurob. Hearing. INCYL. Fac. Med. Univ. Salamanca, Campus Miguel de Unamuno, Salamanca, Spain, ²Department of Psychology, University of Washington, Box 351525, Seattle, Washington, United States

Biologically important sounds are characterized by features that include amplitude, frequency, and temporal pattern. Duration is an essential feature of behaviorally relevant sounds including human speech. Duration tuned neurons have been found in the auditory midbrain of frogs, bats, mice, and chinchillas. In the current study we analysed the responses of neurons in the inferior colliculus of the pigmented rat to sounds of different durations. Animals were anesthetized with urethane (1.5 mg/kg, i.p.) and acoustic stimuli were delivered using a closed field system. The stimuli were white noise and pure tones with durations ranging from 2 to 200 ms. We recorded extracellularly from 120 single units histologically localized to the IC. About half of these units showed some type of sensitivity to duration. Responses could be assigned to one of three categories: short-pass (12%), band-pass (18%) or long-pass (70%). Interestingly, 26 of the 37 neurons that belonged to the long-pass type had a cut-off duration of 5-10 ms. Our data indicate that the best durations and cut-offs in rats are longer than in bats. Most duration sensitive units were onset or sustained responders, as in mice. This is in contrast to echolocating bats, where most duration tuned neurons are band-pass and respond at stimulus offset. The varied response patterns and the differences between specialized and non-specialized animals suggest that several different mechanisms can create sensitivity to duration.

We thank Brandon Warren for technical assistance. Supported by the Spanish JCYL-UE (SA084/01, MSM) and DGES (BFI2000-1396, MSM, DPG) and by the NIH-NIDCD (DC00607, EC).

336 Effect of Reverberation on Neural Response to Amplitude Modulated Signals

Rama Ratnam¹, Nandini Iyer¹, Joziem B. M. Goense^{1,2}, Albert S. Feng^{1,3}

¹Beckman Institute, University of Illinois, 405 N. Mathews Ave, Urbana, IL, United States, ²Biophysics & Computational Biology, University of Illinois, 405 N. Mathews Ave, Urbana, IL, United States, ³Molecular & Integrative Physiology, University of Illinois, 405 N. Mathews Ave, Urbana, IL, United States

Acoustic reverberation is a common and natural feature of the auditory environment affecting sound communication. Echoes and reverberation distort the fine structure and the envelope of the sound, and they therefore compromise sound communication relying on envelope cues. The mating call of Northern leopard frogs, *Rana pipiens pipiens*, consists of a series of trills (having a trill rate of ~20 pulses/sec) interspersed with periods of low acoustic energy. We hypothesize that reverberation from foliage, tree-trunks, and surface barriers such as mud-banks and water surfaces serve to increase the attack and decay times of the trill components, thereby impairing the ability to detect and discriminate calls. We tested this hypothesis physiologically by assessing sin-

gle-unit responses of midbrain auditory neurons to synthetic mating calls with and without reverberation, and measured the unit's vector strength of time-locked discharges to the individual trill. For neurons showing strong time locking to "anechoic" synthesized trills, reverberation reduced their time locking ability. This reduction was due to the presence of spikes in the silent periods between trills and proportional to an increase in reverberation time. Onset synchronization was unchanged and remained robust. Reverberation typically maintained unit's spike rate, and in some cases it even increased unit's spike rate. These preliminary results suggest that call discrimination, but not detection, is likely compromised by echoes and reverberation; loss of discriminability is due to the smearing of temporal discharges of auditory neurons making it more difficult for neurons to extract the trill rate.

337 A Lateral-Inhibitory-Network Model of the Central Processing of Auditory Nerve Activity

Jennifer Ko, Harjeet S. Bajaj, Ian C. Bruce

Electrical and Computer Engineering, McMaster University, 1280 Main St. W., Hamilton, Ontario, Canada

Lateral inhibitory networks (LINs) of neurons are thought to be prominent in sensory systems and are known to enhance edges and peaks in their input excitation patterns. It is postulated that lateral inhibition contributes to the central, sub-cortical, auditory processes. A biologically realistic model of auditory LINs has been developed to investigate the effects of peripheral hearing impairment on central auditory activity. In particular, the effects on speech input and abnormal spontaneous input edges are presented. The former results indicate that abnormal speech input from the auditory periphery alters the spatio-temporal response pattern such that the neural representation of speech is degraded. The latter results may have implications in the revelation of the mechanisms of tinnitus, the phantom perception of sounds.

338 Decorticate rat: a model for the study of mechanisms of tinnitus in the unanesthetized brainstem

Thomas J. Imig¹, April H. Mullinex², Dianne Durham²

¹Molecular and Integrative Physiology, University of Kansas Medical Center, 3901 Rainbow Blvd, Kansas City, KS, United States, ²Otolaryngology/Head and Neck Surgery, University of Kansas Medical Center, 3901 Rainbow Blvd, Kansas City, KS, United States

Tinnitus is believed to reflect aberrant spontaneous activity (SA) in the auditory system. Unilateral noise exposure in rats (1 hour of 14 – 19 kHz bandpass noise, 104 dB SPL) has been shown by others to cause behavioral manifestations of tinnitus. One week following unilateral exposure to such noise, unanesthetized rats injected with 2DG and kept in a quiet sound chamber during uptake show aberrant patterns of 2DG labeling in the central auditory system. In inferior colliculus (IC) of control rats, the central nucleus (ICc) is densely labeled, and external nucleus (ICx) is less densely labeled. In noise exposed rats, the IC contralateral to the unexposed ear shows labeling similar to that in controls. In the IC contralateral to the exposed ear, ICc is less densely labeled than in controls, and ICx is more densely labeled. To relate patterns of 2DG labeling to

neuronal SA, one must obtain microelectrode recordings of neural discharge. A decorticate rat preparation was developed for this purpose because recordings can be obtained without anesthesia. Decortication is carried out under isoflurane anesthesia. Carotid arteries are ligated to minimize bleeding. The medial geniculate and more caudal parts of the brainstem are perfused by the vertebral-basilar system so ligation of the carotids does not affect blood flow in the auditory brainstem. The cerebral cortex is aspirated to expose the hippocampus along its entire extent from the dorsal midline to the ventrolateral temporal lobe, thus severing all connections between neocortex and the brainstem. This procedure leaves the MGB intact so that IC neurons are not axotomized. One hour after discontinuation of anesthesia, animals were injected with 2DG and maintained in quiet during uptake. Decortication had little effect on the pattern of labeling for both control and noise exposed groups. Thus, the decorticate rat is suitable for electrophysiological analysis of the effect of noise exposure on auditory brainstem SA.

339 Changes in neurotransmitter/amino acid levels in CNS after salicylate intoxication

Elmar Oestreicher¹, Michael Gruss², Katharina Braun², Claudius Fauser¹, Susanne Braun¹

¹ENT Department, Technical University of Munich, Ismaninger Str. 22, Munich, Germany, ²Institute of Biology, Otto-von-Guericke-Universität Magdeburg, Brenneckestr.6, Magdeburg, Germany

The neurophysiologic basis of tinnitus is still under discussion. Most of the data obtained with the salicylate model have demonstrated functional changes in the cochlea. In contrast, only little data exists regarding neurotransmitter changes in the auditory pathway. This knowledge may provide new insights into the action of salicylate in the CNS and may help establishing new therapeutic strategies.

The aim of this study was to identify possible neurochemical changes in gerbils treated with salicylate. We focused in particular on glutamatergic and GABAergic neurotransmission.

Using high pressure liquid chromatography (HPLC) we measured the levels of aspartate, glutamate, glutamine, taurine, alanine and GABA in different areas of the CNS 1 hour after administration of 350 mg/kg salicylate. In the auditory cortex we could observe a significant decrease of glutamine in the salicylate treated animals. In addition, we identified a significant decrease of alanine in the inferior colliculus after salicylate. In contrast, the prefrontal cortex showed a significant increase of GABA after salicylate intoxication.

These results demonstrate changes in the neurotransmitter/amino acid levels in both the glutamatergic and GABAergic system in the auditory pathway as well as the limbic system after salicylate intoxication.

340 Altered Spontaneous Activity in Inferior Colliculus Brain Slices after Noise Exposure in Mice

Dietmar Basta, Ingo Todt, Arne Ernst

Dept. of Otolaryngology at UKB, Free University of Berlin, Warener Straße 7, Berlin, Germany

The inferior colliculus (IC) in vivo is reportedly subject to a noise-induced decrease of GABA-related inhibitory synaptic transmission accompanied by an amplitude increase of auditory evoked responses, a widening of tuning curves and a higher neuronal discharge rate at suprathreshold levels. However, other in-vivo experiments which demonstrated no obvious changes of neuronal auditory thresholds or spontaneous activity in the IC after noise exposure did not confirm those findings, supposedly as the result of complex noise-induced interactions between different central auditory structures.

It was therefore the aim of the present study to investigate the effects of noise exposure on the spontaneous activity of single neurons in a slice preparation of the isolated mouse IC. Normal hearing, anesthetized mice were exposed for 3 hours to a pure-tone of 10 kHz at 115 dB SPL. After 7 days, auditory brainstem response recordings from the anesthetized animal and extracellular, single-unit recordings from spontaneously active neurons within the IC slice were performed in noise-exposed and in normally hearing control mice.

Noise-exposed animals showed a significant hearing loss compared to controls over the whole investigated frequency range between 5 and 22 kHz with a maximum of 55 dB between 10 and 15 kHz. The spontaneous activity of neurons in noise-exposed animals was significantly lower in all investigated isofrequency areas compared to controls. The average spontaneous activity of IC neurons was 1.1 ± 0.8 Imp/s ($n = 126$) for noise-exposed and 6.0 ± 5.2 Imp/s ($n=127$) for controls.

The present findings demonstrate a noise-related modulation of spontaneous activity which originate in the IC and possibly contribute to the generation of noise-induced tinnitus and hearing loss.

Supported by the Sonnenfeld Foundation, Berlin

341 Effects of intense sound exposure on amino acid concentrations in rat cochlea, cochlear nucleus and inferior colliculus

Kejian Chen, Matthew A Godfrey, Donald A Godfrey

Otolaryngology, Medical College of Ohio, 3065 Arlington Ave., Toledo, Ohio, United States

Tinnitus affects millions of people. There is evidence that exposure to intense sound is a major cause of tinnitus, but the chemical basis for this is understudied. We measured concentrations of 12 amino acids, including the 3 major neurotransmitters, glutamate, GABA, and glycine, in homogenates of the cochlea, ventral and dorsal cochlear nuclei, and inferior colliculus of exposed and control rats. Anesthetized adult rats were exposed to a 100 dB 10 kHz tone to the left ear for 15 or 30 minutes. Control rats were similarly anesthetized but not exposed to intense sound. Immediately after tone exposure or an equivalent duration of anesthesia, each rat was decapitated, and the temporal bones and brain regions were

quickly isolated and frozen in a Freon substitute chilled with liquid nitrogen. The frozen temporal bones were trimmed to the cochlea portions, which, along with the brain regions, were homogenized. Homogenates were stored at -80 °C until amino acid concentrations were measured by HPLC. Preliminary data have been obtained from 8 rats: 2 exposed and 2 controls for each exposure time. These data suggest some effects of intense sound on amino acid concentrations, the most consistent so far being bilateral increases of glutamate, aspartate, GABA, and taurine in the inferior colliculus of rats exposed for 30 min. These preliminary results suggest that continued use of this model, with different exposure conditions and durations, should be an efficient way to screen for effects of intense sound on amino acid metabolism in auditory structures.

Supported by NIH (NIDCD) grant DC03258

342 Changes in Chinchilla Inferior Colliculus Responses After Inner Hair Cell Loss

Ulrich W. Biebel, Jean W.Th. Smolders

Physiology II, J.W.Goethe - University, Theodor-Stern-Kai 7, D-60590 Frankfurt am Main, Germany

Carboplatin selectively destroys inner hair cells (IHC) in chinchillas resulting in a status similar to certain forms of neuropathy (Harrison, 1998, *Ear Hear* 19: 355-361). We investigated reorganization in the auditory system after selective IHC loss. We recorded from the central part of the inferior colliculus (ICC), because recent data indicate a gain control mechanism in the ICC (Salvi et al, 2000, *Hear Res* 147: 261-274).

Responses of single and multi units and evoked potentials (EP) were recorded in awake adult chinchillas before and after treatment with 80mg/kg carboplatin in a chronic preparation. Repeated ABR measurements were made via implanted gold electrodes. Stimuli were tone bursts or clicks. Characteristic frequencies (CF), unit thresholds, types of response areas and input-output-functions (IO) were compared before and after carboplatin treatment. Selective IHC loss was verified from DAPI stained surface preparations of the organ of Corti.

Spontaneous and driven spiking activity of the ICC dramatically decreased after the loss of IHC, but CF and ABR- / neuronal thresholds remained similar. Early click-EP amplitudes decreased significantly after IHC loss, and showed longer latencies. IO-functions from EP to clicks were often non-monotonic before treatment, but became monotonic or saturating after IHC loss. Small dynamic ranges (< 40 dB between threshold and peak of IO) were more often found after treatment. Threshold and dynamic range were correlated inversely in normal IC, but not after IHC loss.

Reduced EP amplitudes and loss of responsive neurons are easily related to reduced input from lower brainstem nuclei. It seems though, that after IHC loss the dynamic range is partially maintained. While in normal ICC non-monotonic neurons have different thresholds but peak at similar levels, after IHC loss thresholds become similar and I-O-functions peak at different levels.

Supported by the DFG (SFB 269)

343 Unilateral deafening differentially affects synaptic inhibition in the ipsilateral and contralateral inferior colliculus

Carmen Vale¹, Jose Manuel Juiz¹, David R Moore², Dan H Sanes³

¹Histology, University of Castilla-La Mancha, Almansa, Albacete, Spain, ²Institute of Hearing Research, MRC, University Park, Nottingham, United Kingdom, ³Center for Neural Science and Department of Biology, New York University, Washington Place, New York, New York, United States

Bilateral deafness leads to a profound weakening of synaptic inhibition in the inferior colliculus (IC) of gerbils (Vale and Sanes, 2000, 2003). To examine whether unilateral hearing loss produces similar functional alterations, we examined the effect of cochlear ablation (right ear) on inhibitory synaptic properties in the IC ipsilateral and contralateral to the deafened ear. Lateral lemniscus- and commissure-evoked inhibitory postsynaptic currents (IPSCs) were recorded in an IC brain slice preparation using whole-cell and gramicidin perforated-patch electrodes in the presence of kynurenic acid. Unilateral deafness led to a 28 mV depolarizing shift in the IPSC equilibrium potential of neurons contralateral to the cochlear ablation, but only a 12 mV depolarization in the ipsilateral IC. Lemniscus-evoked inhibitory synaptic conductance (IPSG) declined significantly in both lobes of the IC, whereas commissure-evoked IPSG declined only contralateral to the deaf ear. In contrast, an analysis of paired-pulse facilitation suggested that inhibitory transmitter release was relatively more affected ipsilateral to the deaf ear. Thus, unilateral deafness decreases inhibitory postsynaptic strength in the IC, but the magnitude of this change is greatest contralateral to the deafened ear.

Supported by NIH DC00540 (DHS); and CICYT-SAF00-0211, PAI-03-015 (Consejería de Ciencia y Tecnología; JCCM); BFI2003-09147-C02-02 (MCYT), (J.M. Juiz).

344 HIGH FREQUENCY HEARING LOSS MAY UNMASK NON-TONOTOPIC INPUTS TO NEURONS IN THE INFERIOR COLLICULUS

Richard A. Felix II, Christine Verdie Portfors

Biological Sciences, Washington State University, 14204 NE Salmon Creek Ave, Vancouver, WA, United States

The central nucleus of the inferior colliculus (ICC) receives convergent input from brainstem nuclei. In normal hearing animals such as CBA/CaJ mice, the ICC has a tonotopic organization such that characteristic frequencies (CFs) of neurons increase dorsoventrally. However, adult C57/BL6 mice with high frequency hearing loss do not show typical tonotopy. In these mice high CFs (above 20 kHz) are infrequent and there is an overrepresentation of low CFs. One hypothesis for this abnormal tonotopic organization is that loss of high frequency inputs allows for an unmasking of non-tonotopic inputs from low frequency brainstem areas. We addressed this hypothesis by examining excitatory frequency tuning curves of neurons in the ICC of CBA/CaJ mice. In particular, we were interested in multiple frequency tuning characteristics that would be suggestive of inputs from different frequency bands converging on single neurons in the ICC. We recorded responses from

single units to tones with frequencies that encompassed a large portion of the hearing range of the mouse. Dorsoventral electrode penetrations revealed a representation of frequencies from 5-64 kHz, with CFs increasing with depth. Thirty-seven percent of units had multiple tuning curves. The majority of multiply tuned units had ultrasonic CFs and a second peak of excitation at a lower frequency. In comparison, eighty-five percent of neurons in the ICC of adult C57/BL6 mice had CFs below 20 kHz, and only nine percent of those units had multiple tuning. Our findings suggest that neurons in the ICC may receive non-tonotopic inputs. In particular, many neurons in the ventral region of the mouse ICC receive a non-tonotopic low frequency input. In C57 mice the loss of high CFs may unmask the low frequency input thereby creating an overrepresentation of neurons tuned below 20 kHz.

Supported by NIDCD grant 04733 to CVP

345 Desynchronization in Deprived Auditory Cortex Revealed by Independent Component Analysis of Field Potentials

Peter Hubka^{1,2}, Rainer Hartmann¹, Rainer Klinke¹, Andrej Kral¹

¹Institute of Sensory Physiology & Neurophysiology, J.W.Goethe University, Theodor-Stern-Kai 7, Frankfurt, Germany, ²Institute of Pathological Physiology, Comenius University, Sasinkova 4, Bratislava, Slovakia

To study functional effects of auditory deprivation, local field potentials (LFPs) in the cortical field A1 (6 penetrations within the most activated cortical region, 13 depths each 300 μ m) of six adult congenitally deaf cats (CDCs) were compared to three hearing controls. The animals were stimulated through a cochlear implant (biphasic pulses, 200 μ s/phase, monopolar). Independent component and current source density analyses were applied to cortical LFPs, resulting in a set of "activation units" (AU) in each animal. These were typically monophasic. AUs possibly represent a set of synchronous transmembrane currents resulting from activation of a "synaptic patch". AUs in CDCs had significantly longer duration than in controls (1.24 \pm 0.43 ms vs. 0.99 \pm 0.40 ms, U-test, $p < 0.001$). The intervals between successive AUs were also significantly longer in CDC (2.05 \pm 0.90 ms vs 1.2 \pm 0.54 ms, U-test $p < < 0.001$). These results imply that in CDCs the cortical transmembrane currents are less synchronized and of a longer duration. To analyze intercolumnar ("lateral") relations the variability in layer distribution of independent components was compared. The average variances of activation unit amplitudes between adjacent penetrations within the same cortical depth were significantly smaller in deaf animals (0.50 \pm 0.34 mV/mm²) than in hearing controls (2.69 \pm 1.21 mV/mm², U-test, $p = 0.024$). Adjacent cortical columns are thus activated more uniformly in deaf cats than in hearing controls. Taken together, these data demonstrate that in CDCs the activity within cortical circuits is more diffuse, the synaptic currents are desynchronized and have a longer duration. In these respects the naive auditory cortex appears functionally immature.

Supported by SFB 269/C1 and DAAD.

346 Hearing Loss Disrupts The Intrinsic And Integrative Properties Of Auditory Cortical Neurons.

Vibhakar C Kotak, Gytis Svirskis, F A Lee, John Rinzel, Dan H Sanes

Center for Neural Science, New York University, 4 Washington Place, New York, NY, United States

Although hearing impairments have been assessed at a psychophysical level, cellular mechanisms underlying such deficits remain poorly defined. We asked whether sensorineural hearing loss (SNHL) disrupts the balance between excitation and inhibition that may restrict the ability of layer 2-5 pyramidal neurons in the primary auditory cortex (AI) to process sound cues. SNHL was surgically induced by bilateral cochlear ablation before hearing onset in P10 gerbils (*Meriones unguiculatus*). Using whole-cell recording techniques in a 500 μ m thalamocortical brain slice preparation, intrinsic and integrative properties of layers 2-5 pyramidal neurons were examined for 10 days following hearing onset (P13- 23). We previously reported preliminary data that hearing loss weakens intracortically-evoked inhibition and boosts thalamocortical excitation (Kotak et al., ARO and SFN abstrs. 2003). Here, we present evidence that the intrinsic discharge patterns and synaptic integrative properties are modified by SNHL. Firing patterns were characterized as depolarization-evoked onset, adapting, and sustained, or hyperpolarization-evoked rebound pattern. Following SNHL, the onset pattern was not observed, and the incidence of sustained and rebound firing increased. These changes were associated with a significant increase in resting membrane potential. (For layers 2/3: mean mV \pm SEM; control: -63.5 ± 0.8 vs. SNHL: 59.9 ± 0.9 ; $p < 0.001$, $DF = 101$). A similar trend was also seen in layer 5 pyramidal neurons ($N = 8$). Furthermore, hearing loss significantly increased the input resistance of layer 2/3 neurons. (Mean MOhm \pm SEM; control: 275 ± 13 vs. SNHL: 409 ± 30 ; $p < 0.001$, $DF = 93$). Pilot experiments on integration were performed by co-activating intracortical inhibition with depolarization-evoked action potentials (up to ~ 50 Hz). In control neurons, evoked IPSPs were typically able to block action potentials. In contrast, in the SNHL neurons tested, the efficacy of IPSPs to block action potentials was inconsistent. These results suggest that SNHL may bias the balance between intrinsic and synaptic function.

Supported by DC00540.

347 Gap detection response as a function of noise bandwidth in chinchilla IC

Yuqing Guo¹, Robert Burkard^{1,2}

¹*Center for Hearing and Deafness, University at Buffalo, 215 Parker Hall, 3435 Main Street, Buffalo, NY, United States,*

²*Communicative Disorders and Sciences, University at Buffalo, 3435 Main Street, Buffalo, NY, United States*

Perceptual studies have shown that gap detection thresholds in bandlimited noise decrease with increasing stimulus bandwidth. In the present study, this protocol is applied to investigate physiological responses from chinchillas pre-and post-carboplatin.

Seven adult chinchillas were chronically implanted tungsten electrodes in the right inferior colliculi (IC). After a recovery period,

the unanesthetized animals were passively restrained, with an insert earphone placed in the left ear. Noiseburst gaps ranged from .25 to 64 ms, with each noiseburst 50 ms in duration (0 ms rise-time). Broadband noise (BBN) as well as 100 Hz (2100-2200 Hz) and 1600 Hz (600-2200 Hz) bandlimited noise were used. Carboplatin caused an inner hair cell (IHC) loss, which ranged from moderate to severe, across animals, with little outer hair cell (OHC) loss. The onset response to the trailer stimulus increased in latency and decreased in amplitude with decreasing gap and decreasing noiseburst bandwidth, both pre-and post-carboplatin. The offset response to the leader stimulus increased in latency and decreased in amplitude with decreasing noiseburst bandwidth. The response latencies increased and the amplitudes decreased post-carboplatin. Gap threshold for the onset responses were elevated post-carboplatin in all stimulus conditions.

Supported by NIH DC03600

348 A Normative Study of ABR Latency-Intensity Function in Chinchilla Laniger

Derin Charles Wester, Clay Finley, Michael E. Hoffer, Peter Killian, Kimberly R. Gottshall, John Coleman

Otolaryngology, Naval Medical Center San Diego, 34800 Bob Wilson Dr., San Diego, CA, United States

In conjunction with ongoing research on the kinetics of Leupeptin absorption in the cochlea, auditory brainstem response (ABR) measures were collected from 19 adolescent female Chinchilla Laniger as part of pre-treatment baseline hearing sensitivity data. Latency-intensity functions for the absolute waves I, III and V, and the interpeak latencies for waves I-III, III-V and I-V were developed using a 50 microsecond click. The data were graphed to show normative mean values and 95% confidence intervals. Examples of chinchilla ABR waveform morphology and recording parameters are presented. All 19 animals showed reliable waveform morphology at 80, 60, 40 and 20 dB nHL stimulation levels. Fifteen animals (78%) showed identifiable waveform morphology at 10 dB nHL, while only 3 (22%) had identifiable wave peaks at 0 dB nHL. Thus, we have adopted 20 dB nHL as our clinical/research standard for normal chinchilla click-ABR hearing sensitivity.

349 The effects of selective efferent activation through the Inferior Colliculus on ipsilateral and contralateral cochlear responses

Wei Zhang, David F Dolan

Department of Otolaryngology, Kresge Hearing Research Institute, 1301 East Ann Street, Ann Arbor, MI, United States

Medial olivocochlear (MOC) neurons project to the outer hair cells in the cochlea and suppress cochlear gain. The inferior colliculus (IC) makes direct descending connections with MOC neurons in the brainstem. This study compared the effects of IC electrical stimulation on cochlear output from both ears. The cochlear whole-nerve action potential (CAP) and distortion product otoacoustic emissions (2f1-f2; DPOAE) were measured in both ears while stimulating the central nucleus of the IC (ICC).

Pigmented guinea pigs (300-400g) were used, anesthetized with ketamine, xylazine and acepromazine, paralyzed with tubocurarine and respired. DPOAE was obtained in each ear canal and the bulla were opened to obtain the CAP responses from the round

window. TDT (System 2 & 3) hardware & software were used to generate acoustic and electrical stimulation and data collection. IC stimulation was achieved with bipolar Teflon-insulated stainless steel electrode (0.2mm), set approximately 1 mm apart. Biphasic rectangular current pulses with each phase of 0.2 ms duration and 250 Hz were passed and different current levels were used to assess the effects of IC stimulation on CAP and DPOAE. The effects of cutting the commissure between the two ICs and the crossed olivocochlear bundle (COCB) at the floor of the fourth ventricle were compared to the pre-cut measures.

Electrical stimulation of ICC resulted in a decrease of the CAP and DPOAE amplitude in both ears. The effects on CAP and DPOAE occurred around the same frequency range in each ear. The effect of cutting the commissure had little or no effect on the efferent effect in each ear. Cutting the COCB at the floor of the 4th ventricle eliminates the contralateral efferent effect with small differences observed in the ipsilateral ear.

Supported by NIH Grant RO1 DC04194.

350 The Effects of a Second Two-Tone Stimulus on the Auditory Steady State Response (ASSR): Effects of Carrier and Modulation Frequency

Kathleen Szalda¹, Robert Burkard^{1,2}

¹Center for Hearing and Deafness, University at Buffalo, 3435 Main Street, Buffalo, NY, United States, ²Communicative Disorders and Sciences, University at Buffalo, 3435 Main Street, Buffalo, NY, United States

We examined the effects of a second two-tone, composed of different carrier frequencies and modulation frequencies (MFs), on the chinchilla ASSR. Eight chinchillas were anesthetized with ketamine/acepromazine while tungsten electrodes were chronically implanted into their inferior colliculus (IC). The stimuli presented through channel 1 consisted of a two-tone stimulus with a carrier frequency of 2000 Hz (F1/F2: 2000/2090 or 2000/2170) which resulted in MFs of either 90 or 170 Hz. The stimuli presented through channel 2 consisted of stimuli with carrier frequencies of either 500 or 8000 Hz (F1/F2: 500/629, 500/570, 8000/8129, 8000/8070 Hz), which resulted in MFs of 129 or 70 Hz. Recordings were made from the right IC, while the two-tone stimuli were presented to the left ear. Stimuli decreased from 80 to 30 dB pSPL in 10 dB steps.

Results showed that the largest response amplitudes occurred with frequencies of either 2000 or 8000 Hz, with 500 Hz responses being substantially smaller. In addition, response amplitude decreased with the addition of a second two-tone stimulus, regardless of either carrier or modulation frequency. Typically, this decrease was greatest for 500 Hz two-tone stimuli, followed by 8000 Hz, and with 2000 Hz being the least effected by the addition of a second two-tone. This pattern of effects was quantitatively similar for the different MF conditions.

Supported by NIH DC03600

351 Brainstem Timing in Learning Impaired Children with Excessive Auditory Backward Masking

Krista L Johnson, Trent G Nicol, Steven Zecker, Beverly A Wright, Nina Kraus

Communication Sciences and Disorders, Northwestern University, 2240 Campus Drive, Evanston, IL, United States

Accurate encoding of auditory information relies on rapid and synchronous activity among neuronal ensembles throughout the auditory pathway. Some children with learning impairments demonstrate auditory perception deficits that dovetail with abnormal neural representation of sound in both brainstem and cortical regions. The auditory brainstem response to a speech syllable consists of transient and sustained components, each attributable to distinct encoding mechanisms. The transient component occurs in the first few milliseconds post stimulus onset and encodes the onset of an acoustic stimulus, whereas the sustained (frequency-following) response, apparent in the succeeding tens of milliseconds, represents periodic neural activity at the same frequency as the stimulus. Auditory backward masking is a psychoacoustical phenomenon in which a signal can be masked by a subsequent sound. Although the underlying neural origins remain obscure, it can be used to test temporal acuity within the auditory system. Previous research has shown that children with learning impairments have significantly higher backward masking thresholds than normally-learning children. To understand the relationship between physiologic mechanisms and psychophysical timing performance, this study examined the brainstem response to the syllable /da/ with respect to backward masking thresholds elicited by non-speech stimuli. Subjects consisted of normal children (n=26) and two groups of learning impaired children; those with backward masking thresholds within (n=46) and below (n=19) the normal range. Learning impaired children with poor backward masking thresholds had significant delays in both the transient onset response and components within the sustained frequency following response. This result suggests that some learning impaired children, as predicted by poor performance on an auditory backward masking task, demonstrate a deficit in properly encoding onset and harmonic components of speech sounds. Supported by NIH R01 DC01510

352 Human frequency following responses: representation of pitch contours of Chinese tones

Ananthanarayan Krishnan, Jackson Gandour, Yisheng Xu

Audiology & Speech Sciences, Purdue University, 1353 Heavilon Hall, West Lafayette, IN, United States

Auditory nerve single-unit population studies have demonstrated that phase-locking plays a dominant role in the neural encoding of both the spectrum and voice pitch of speech sounds. Phase-locked neural activity underlying the scalp recorded human frequency-following response (FFR) has also been shown to encode certain spectral features of steady-state and time-variant speech sounds as well as pitch of several complex sounds that produce time-invariant pitch percepts. By extension, it was hypothesized that the

human FFR may preserve pitch-relevant information for speech sounds that elicit time-variant as well as steady-state pitch percepts. FFRs were elicited in response to the four lexical tones of Mandarin Chinese as well as to a complex auditory stimulus which was spectrally different but equivalent in fundamental frequency (F_0) contour to one of the Chinese tones. Autocorrelation-based pitch extraction measures revealed that the FFR does indeed preserve pitch-relevant information for all stimuli. Phase-locked inter-peak intervals closely followed F_0 . Spectrally different stimuli that were equivalent in F_0 similarly showed robust inter-peak intervals that followed F_0 . These findings are consistent with a pitch encoding scheme based on temporal distribution of phase-locked neural activity and lends further support to the predominant interval hypothesis.

353 Auditory brainstem Response: Relative role of suppression and excitatory masking

Ananthanarayan (Ravi) Krishnan, Payal Anand

Audiology & Speech Sciences, Purdue University, 1353 Heavilon Hall, West Lafayette, IN, United States

Psychoacoustic and physiologic studies have shown that both two-tone suppression and excitatory spread contributes to simultaneous masking. Further, spread of excitation dominates when the frequency of the masker and the probe are proximal and suppression dominates when masker and probe frequency are well apart. The purpose of this study was to evaluate the electrophysiological correlates of the role of suppression and excitatory spread on simultaneous masking of the scalp recorded human auditory brainstem responses (ABR). To this end ABRs were recorded under simultaneous and forward-masking conditions with on and off frequency maskers. Simultaneous masking produced greater amplitude and latency changes for the off-frequency maskers than forward-masking. On-frequency forward-masking produced greater latency and amplitude changes in the forward-masking conditions compared to simultaneous masking. Examination of the results revealed that excitatory masking was present for both simultaneous and forward-masking conditions. The difference in the latency and amplitude changes produced by simultaneous masking and forward-masking is taken to reflect the role of suppression. Taken together, the results of this study supports the notion that both excitatory spread and suppression contributes to masking.

354 Olivocochlear and middle ear muscle reflex interneurons in the cochlear nucleus

Ryuji Suzuki¹, Daniel J. Lee^{2,3}, M. Christian Brown^{2,3}

¹*Program in Speech and Hearing Biosciences and Technology, Harvard-MIT Division of HST, 77 Massachusetts Ave., Cambridge, MA, United States,* ²*Eaton-Peabody Laboratory, Massachusetts Eye and Ear Infirmary, 243 Charles St., Boston, MA, United States,* ³*Dept. of Otolaryngology, Harvard Medical School, 243 Charles St., Boston, MA, United States*

The auditory periphery receives descending input from olivocochlear neurons and middle ear muscle (MEM) motoneurons of the brainstem. These systems are thought to protect the inner ear from acoustic injury and lessen the effects of masking noise. The medial olivocochlear (MOC) neurons and stapedius motoneurons

are known to respond to acoustic stimuli, thus forming sound-evoked reflexes. Although the afferent limb of these reflexes must involve the auditory nerve, the interneurons and central pathways of these reflexes are not known.

In order to identify which neurons of the cochlear nucleus (CN) might be interneurons, we used focal electrical stimulation of different subdivisions of the CN while monitoring acoustic levels of primary tones and distortion product otoacoustic emissions (DPOAEs) in the ear canal. Reductions of DPOAE were observed (without changes in primary tone level) when the stimulating electrode was located in or immediately adjacent to the posteroventral subdivision (PVCN) of the CN, supporting the hypothesis that the PVCN contains the interneurons of the MOC reflex. Effects were observed bilaterally but were often greater on the ipsilateral than the contralateral side. There were no effects from stimulating the DCN. At other sites in the VCN, changes in primary tone levels were observed, as if the impedance of the ear canal had changed due to MEM activation. These preliminary results suggest that MEM reflexes are mediated by interneurons elsewhere in the VCN.

(Supported by the Howard Hughes Medical Institute and NIDCD grants DC01089 and 1 K08 DC06285)

355 High Rate Auditory Brainstem Responses in Rabbits Obtained by Continuous Loop Algorithm Deconvolution (CLAD)

Erdem Yavuz¹, Ozcan Ozdamar^{1,2}, Rafael E. Delgado^{1,3}, Fred F. Telischi^{1,2}

¹*Biomedical Engineering, University of Miami, P.O.Box 248294, Coral Gables, Florida, United States,* ²*Otolaryngology, University of Miami, 1666 NW 10th Avenue, Suite 306, Miami, Florida, United States,* ³*Software Development, Intelligent Hearing Systems Inc., 7326 S.W. 48th street, Miami, Florida, United States*

Auditory brainstem responses (ABR) are usually recorded using transient stimuli of rates no faster than 100-150 Hz due to overlap of responses. Faster stimulus rates generate convoluted responses that do not allow identification of individual ABR components. The introduction of maximum length sequences (MLS) technique to evoked potential acquisition enabled high rate recording only at very specific stimulus sequences with a wide range of instantaneous rates. A new method for high rate recording named as Continuous Loop Algorithm Deconvolution (CLAD) is proposed by Delgado and Ozdamar (2002). CLAD enables the deconvolution of overlapping responses obtained from nearly unlimited stimulus sequences to extract the original transient evoked potential. In this study CLAD method is used to obtain ABRs from rabbits under anesthesia recorded at 8 rates from 58.6 Hz to a maximum of 996.1 Hz. In addition two conventional ABR recordings at 9.3 and 19.3 Hz were obtained. For all recordings, a series of intensities between 32 to 102 dB SPL in 10 dB steps were used. Latencies and amplitudes of all identifiable waves were measured. Waves I, III and IV were observed to be the most stable ABR components and traced down to 42 dB SPL in most cases. Unlike other sensory systems, auditory system shows high resistance to adaptation and can respond at very high rates close to absolute refractory periods of neurons. CLAD is found to be a valuable tool in studying adap-

tation effects in the auditory system at high rates that was not previously possible.

356 Auditory Brainstem Response Thresholds and Characteristics Measured in Response to Sound Pressure Stimulation in the Aquatic Frog *Xenopus laevis*

Bharti Katbamna¹, John A. Brown¹, Anna M. Jelaso², Charles F. Ide²

¹Speech Pathology and Audiology, Western Michigan University, 1903 West Michigan Avenue, Kalamazoo, MI, United States,

²Environmental Institute, Western Michigan University, 1903 West Michigan Avenue, Kalamazoo, MI, United States

The South African clawed frog *Xenopus laevis* is fully adapted to aquatic environments and is most likely specialized for underwater hearing. However, recent studies that measured tympanic disk vibrations via laser vibrometry showed that sound pressure sensitivities of the *Xenopus* ear in air and water were equivalent. In the present study we measured auditory brainstem response (ABR) thresholds and characteristics produced in response to sound pressure stimulation in air and water, in 2-3 month old post-metamorphic frogs. ABRs evoked with frequency specific tone bursts below 1 kHz were characterized by the presence of multiple sinusoidal waves in the first half of the 20 ms time window, whereas at and above 1 kHz the initial positive (P1 and P2) and negative (N1) peaks dominated the response. The latencies of P1 and N1 potentials decreased as frequency increased from 1 kHz to 3.2 kHz and then prolonged from 3.4 kHz to 4 kHz. The P1-N1 amplitudes showed a bell-shaped distribution with maximum amplitudes in the 1.8-3.2 kHz region. ABR hearing thresholds were lowest (60-68 dB SPL re 20 μ Pa) in the 1.8-3.2 kHz region. Moreover, sample ABR measurements in water were comparable to those made in air, both in terms of ABR hearing thresholds and ABR wave latencies and amplitudes. These findings indicate that *Xenopus* hearing is optimal in the 1.8-3.2 kHz region and that sound pressure sensitivities of the *Xenopus* ear are comparable in air and water. These results are comparable to peak frequency vibration profiles of the tympanic disk reported in literature. Moreover, frequency dependent latency profiles indicate tonotopic organization within the *Xenopus* auditory endorgans.

Supported in part by the Western Michigan University Faculty Research and Creative Activities Support Fund and the EPA grant #R83023501-0.

357 Projections From Individual Cortical Cells to Multiple Targets in the Auditory Brainstem of Guinea Pigs

Diana L Coomes, Brett R Schofield

Anat. Sci. and Neurobiol., U. of Louisville, 500 S. Preston St, Louisville, KY, United States

Auditory cortex projects directly and bilaterally to the cochlear nucleus (CN) and the inferior colliculus (IC). We used multiple fluorescent retrograde tracers to determine whether individual cortical cells project to the left and right IC and/or to one IC and one CN.

Injections into the left and right IC labeled many cortical cells, with the majority labeled from the ipsilateral IC. Double-labeled

cells constituted up to 8% (avg. 3.4%; n=3) of the ipsilaterally-projecting cells, and up to 47% (avg. 27%; n=3) of the contralaterally-projecting cells.

Far fewer cells project to the CN than to the IC. Following injections into one IC and either CN, the double-labeled cells formed a small percentage (4-8%) of the IC-projecting cells. However, the double-labeled cells formed a large part of the population that projected to the CN. Up to 62% of cells labeled from the ipsilateral CN were also labeled from the ipsilateral IC (avg. 49%; n=3). Similarly, up to 48% of cells labeled from the contralateral CN were also labeled from the ipsilateral IC (avg. 40%; n=2). Finally, triple-label experiments revealed a small number of cells that project to the ipsilateral CN and the ipsilateral and contralateral IC.

The results indicate that most cortical cells that project to the CN or the IC project to only one of these targets (predominantly the ipsilateral IC). However, a number of cells project to multiple targets. In fact, a large fraction of the cortical cells that project to the contralateral IC or to either CN also project to the ipsilateral IC. We conclude that many cortical cells project to a single target, where they may exert a specific effect on cells within that target. In addition, a small population of cells have divergent projections that may allow them to have a broad influence at multiple sites within the brainstem auditory pathways.

Supported by NIH DC04391, DC05277.

358 Projections From the Auditory Cortex Contact Cochlear Nucleus Neurons That Project to the Inferior Colliculus in Guinea Pigs

Brett R Schofield, Diana L Coomes

Anat. Sci. and Neurobiol., U. of Louisville, 500 S. Preston St., Louisville, KY, United States

Previous studies showed a projection from auditory cortex to granule cells in the cochlear nuclei (CN) in rats (Weedman and Ryugo, 1996 J Comp Neurol 371: 311-324). We described a similar projection in guinea pigs, and showed additional cortical terminals outside the granule cell area (Schofield et al. 2001, ARO 24:44.). These regions contain cells that project directly to the inferior colliculus (IC) (unlike granule cells), raising the possibility that cortical axons make direct contacts with CN cells that project to the IC. For the present study, we address this question using multilabeling techniques.

Different fluorescent tracers were injected into one or both IC to label CN cells by retrograde transport. A different tracer was injected into one auditory cortex to label cortical axons by anterograde transport. After 12-15 days, the animal was perfused and the brain was processed for fluorescence microscopy. Left and right CN were examined for apparent contacts between cortical axons and retrogradely labeled CN cells. The results suggest that axons from the ipsilateral or contralateral cortex contact fusiform and giant cells in the dorsal CN and multipolar cells in the ventral CN that project directly to the IC. The contacts occur on cell bodies and dendrites. The target cells in the CN include cells that project ipsilaterally, contralaterally or bilaterally to the IC.

Cortical projections to CN granule cells presumably modify CN output through intrinsic circuitry. The present results suggest that cortical axons also contact projection cells of the CN, including

fusiform cells of the dorsal CN and multipolar cells in the ventral CN. We conclude that auditory cortex may exert both direct and indirect effects on ascending pathways from the CN. Physiological experiments will be needed to reveal the nature of these effects.

Supported by NIH DC04391, DC05277.

359 Cortical Descending Projections to Subcollicular Nuclei in Gerbils

Nobuyuki Kuwabara, Brett R Schofield

Anatomical Sciences and Neurobiology, University of Louisville School of Medicine, Health Sciences Center, Louisville, KY, United States

Projections from auditory cortex (AC) to subcollicular auditory nuclei were examined. To date, these projections have been described in detail only in rats (Feliciano et al., 1995, *Aud. Neurosci.* 1:287). Medial olivocochlear (MOC) cells have been identified as a target of cortical axons in the same species (Mulders and Robertson, 2000, *Hear Res.* 144:65). Gerbils, like rats, have good high frequency hearing, but in addition have good low-frequency hearing and correspondingly well-developed nuclei such as the medial superior olivary nucleus (MSO). In this study fluorescent dextrans were injected into the AC of gerbils to label cortical projections to the superior olivary complex (SOC) and cochlear nucleus (CN).

In the SOC, boutons were numerous on the ipsilateral side, where they were particularly abundant in the ventral nucleus of the trapezoid body, the superior paraolivary nucleus and the lateral superior olivary nucleus. Contralaterally, boutons were present in the same nuclei, albeit in smaller numbers. Cortical boutons were absent in the MSO bilaterally. By combining immunohistochemistry for choline acetyltransferase (ChAT, a marker of cholinergic cells) with tract tracing, we identified cortical axons that contact ChAT-positive cells in regions of the SOC that contain MOC cells. These results suggest that cortical axons contact MOC cells, which are cholinergic. In the CN, boutons were present bilaterally in similar distributions. Most boutons were in the granule cell areas, while a few boutons were located in other parts of the CN.

Our results suggest that cortical projections to the SOC and CN are extensive in gerbils. The results extend a report of Budinger et al. (2000, *Eur. J. Neurosci.* 12:2452). Further, the projections are similar to those in rats. The similarities extend to apparent contact of cortical axons with MOC cells in both species, suggesting similar functions in these two rodents.

Supported by NSF-IBN9987660 and NIH DC04391.

360 Ascending Pathways to the Lateral Superior Olive in the Rat: Neuronal Origins in the Cochlear Nucleus as a Function of Frequency Representation

John Doucet¹, Conor Sheehy¹, Jo Ellen Boche², W. Bruce Warr²

¹*Otolaryngology-Head and Neck Surgery, Johns Hopkins University, 720 Rutland Ave, Baltimore, MD, United States,*

²*Neuroanatomy Laboratory, Boys Town National Research Hospital, 555 North 30th St, Omaha, NE, United States*

The principal cells of the lateral superior olive (LSO) are known

primarily for their sensitivity to interaural intensity differences. One source of ascending projections to the LSO is the spherical bushy cells (SBC) in the ipsilateral ventral cochlear nucleus (VCN). Some recent findings suggest that VCN multipolar cells (MC) also project to the ipsilateral LSO (e.g. Doucet and Ryugo, *J Comp Neurol* 461:452-65, 2003). Our objectives in this study were to confirm that both SBC and MC project to the LSO and to determine the magnitude of their respective contributions to different frequency regions of the LSO. Sprague-Dawley rats were anesthetized and the LSO was unilaterally injected with biotinylated dextran amine (BDA). The animals were sacrificed after 7-10 days and the brain stems were sectioned using a freezing microtome. The sections were processed to produce a black reaction product. In some cases, the injection site was confined to a small part of the frequency axis of the LSO and retrogradely labeled neurons were observed in the ipsilateral VCN. The dendritic morphology of a few labeled neurons clearly confirmed that both SBC and MC were labeled. Surprisingly, the types of VCN neurons filled with BDA depended on the location of the injection site. Injections confined to the lateral (low frequency) limb of the LSO tended to label SBC in the rostral pole of the VCN. In contrast, injection sites confined to the medial (high frequency) limb filled neurons near the cochlear nerve root and in the posterior VCN. MC are the dominant cell type in these regions of the nucleus. Thus, it appears that MC are the primary source of input to the high frequency limb of the LSO whereas SBC project to the low frequency limb. One interpretation of these findings is that SBC may not represent the extreme high frequency end of the audible spectrum in the rat.

Support: R01 DC006268 (Doucet), R01 DC04395 (David K. Ryugo), P30 DC05211, and P50 DC00215 (Warr, Boche)

361 Ultrastructure of Synapses on Medial Olivocochlear Somata

Thane E. Benson¹, M. Christian Brown^{2,3}

¹*Eaton-Peabody Laboratory, Massachusetts Eye & Ear Infirmary, 243 Charles St., Boston, MA, United States,* ²*Eaton-Peabody Laboratory, Massachusetts Eye & Ear Infirmary, 243 Charles St, Boston, MA, United States,* ³*Department of Otolaryngology and Laryngology, Harvard Medical School, 243 Charles St., Boston, MA, United States*

Medial olivocochlear (MOC) neurons respond to sound and provide the efferent innervation of outer hair cells in the cochlea. To determine their synaptic inputs we retrogradely labeled MOC neurons using horseradish peroxidase injections into the cochlea. Labeled neurons were identified and documented with the light microscope before being prepared for serial-section electron microscopy. A region of the ventral nucleus of the trapezoid body contralateral to the injected cochlea was studied systematically. Here, labeled neurons had a fusiform shape (minor axes of 18 to 29 μm) and proximal dendrites that tended to orient parallel to the fascicles of the trapezoid body.

Thus far, using sections including its nucleus, 20 percent of one MOC soma has been studied systematically as have three proximal dendrites from that soma. This soma was mostly abutted by neuropil and myelinated axons. Only a few synaptic terminals were found (7 forming a total of 28 axo-somatic synapses). Similarly, the proximal dendrites examined received, at most, three terminals. Confirming and extending previous findings (Spangler et al.,

1986, ARO Absr. 9:37; Helfert et al., 1988 J. Neuroscience 8: 3111), terminals are of distinct types:

1) Fairly large, multisynaptic terminals with up to 6 punctate asymmetric synapses having mainly round vesicles clustered near the synapse. These terminals often received an evagination of the cell and shared puncta adherentia with it;

2) Smaller terminals packed with round vesicles having moderately asymmetrical synapses;

3) Small terminals with pleomorphic vesicles.

Several axon swellings with dense-core vesicles also abut the cell. The multisynaptic terminals could provide excitatory input to the MOC neuron, possibly from cochlear nucleus interneurons that drive the MOC response to sound.

(Supported by NIDCD RO1 DC01089)

362 Effects of sound level and duration on Fos-like immunoreactivity in the central auditory pathway

Teresa P. G. Santos^{1,2}, M. Christian Brown³

¹Speech and Hearing Biosciences and Technology, Harvard-MIT, 77 Massachusetts Ave., Cambridge, MA, United States, ²Gulbenkian Doctoral Program, Instituto Gulbenkian de Ciencia, Rua Quinta Grande 6, 2781 Oeiras, Portugal, ³Eaton-Peabody Laboratory, Massachusetts Eye & Ear Infirmary, 243 Charles St., Boston, MA, United States

Fos is an immediate early gene product that is expressed in neurons in auditory nuclei in response to auditory stimulation (Adams, 1995, J Comp Neurol 361:645-668; Brown and Liu, 1995, J Comp Neurol 357:85-97; Kandiel et al, 1999, Brain Res 839:292-7). The pattern of frequency-dependent Fos expression has been well characterized (Friauf, 1992, Eur J Neurosci. 4(9):798-812). However, the dependence on level and duration is still unclear for brainstem and completely unknown for auditory cortex.

We have examined Fos labeling in dorsal cochlear nucleus (DCN), anteroventral cochlear nucleus (AVCN), inferior colliculus (IC) and auditory cortex (AC) in CBA/CaJ mice. Animals were stimulated with free-field, 12 kHz tone bursts, 50 ms duration, 10/sec, with variable level (30-90 dB SPL) or duration (1min-2 hrs). Two hours after the onset of stimulation the animals were sacrificed and their brains processed to reveal Fos-like immunoreactivity.

Overall, we have observed that an increase of the level of stimulation causes an increase of the number of labeled neurons in DCN, AVCN, IC and AC. At the lowest levels used (30 dB SPL) a band of Fos labeling appears in the expected 12 kHz region in DCN, AVCN and IC although AVCN labeling is weaker than in the other two nuclei. As the level of the stimulus is increased first there is a broadening of the band of labeling in followed by the addition of new bands dorsally in DCN and ventrally in IC (which correspond to higher CF regions). These new bands cannot be explained by acoustic distortion in the stimulus. At low stimulus levels several narrow bands of labeling are observed in the AC, but as the stimulus level increases the cortical pattern of labeling becomes widespread. For moderate stimulus levels, as the duration of stimulation increases the number of Fos labeled cells also increases and in addition the labeling also becomes darker. Short stimuli (* 10 mins) induce bands of labeling in DCN and AC only.

(Supported by NIDCD DC01089)

363 Synaptic Organization of Inhibitory Feed-forward Projections from the Dorsal Cochlear Nucleus (DCN) to the Ventral Cochlear Nucleus (VCN) in the cat: A Quantitative Study.

Munirathinam Subramani, E.-Michael Ostapoff, Jeffrey A Dutton, Julia Gross, G Steven Kempe, D Kent Morest
Neuroscience, Uconn Health center, 263 Farmington Avenue, Farmington, CT, United States

The main ascending pathway from the cochlea undergoes synaptic interruption in VCN. A modulatory but inhibitory circuit is formed by corn cells of DCN, which project to VCN by a tuberculo-ventral tract (TVT). They may function to provide inhibitory fringes that sharpen the excitatory fields (center bands) of the main ascending pathway. Biotinylated dextran injections in the DCN anterogradely labeled TVT and its endings but also retrogradely filled cochlear nerve fibers and their terminals in the same regions of VCN. To distinguish TVT endings from cochlear nerve terminals, we used electron microscopy of the immunolabeled endings in VCN. Images of the labeled endings were digitized and filter-enhanced, using NIH ImageJ to permit accurate tracing of vesicles. The tracings were scanned and a random sampling method devised. Area and circularity of synaptic vesicles were measured with Optimus (v6.5) to give numerical definitions of terminal categories. The distribution of the largest endings (cochlear nerve endbulbs) correlated with the largest profiles containing large round vesicles. Their distribution in VCN defined a band, which maps to the same isofrequency band of the injection site. Surrounding the band was a fringe of smaller labeled endings. About 45% of labeled terminals were pleomorphic and were equally represented in the band and its fringes. About 10% of the labeled endings in both band and fringes were the large round type. Therefore, if there is an inhibitory fringe in the main projection pathway, it was not reflected in the distribution of TVT endings. Albeit flat-vesicle endings were unlabeled, they may provide an inhibitory component of another origin. However, the excitatory category of round vesicles of intermediate size was labeled in the band but not in the fringes. We hypothesize that these intermediate endings function to oppose the feed-forward inhibition from the TVT to the main projection pathway. Supported by NIH DC00127.

364 Projections to the inferior colliculus from the low-frequency area in the dorsal nucleus of the lateral lemniscus

Sylvie Baudoux, Benedikt Grothe

Auditory Processing, Max Planck Institute of Neurobiology, Am Klopferspitz 18a, D-82152 Martinsried, Germany

The inferior colliculus (IC) integrates excitatory and inhibitory inputs from almost all auditory brainstem nuclei. The major source of extrinsic inhibitory GABAergic inputs to the IC is the dorsal nucleus of the lateral lemniscus (DNLL). Each DNLL projects to the contralateral IC, but also, to a lesser degree, to the contralateral DNLL and to the ipsilateral IC. Whether all these projections are exclusively GABAergic, and whether different sub-populations of DNLL neurons provide different inputs to different targets, is cur-

rently unknown. To investigate the potentially differential DNLL projections we currently focus on DNLL neurons that are sensitive to interaural time differences (ITDs), a major cue to localize low-frequency sounds. GABAergic inhibition is thought to enhance the sensitivity of IC neurons to ITDs. But are low-frequency projections to the ITD sensitive area in the ipsi- and contralateral IC in fact GABAergic?

We therefore performed extracellular recordings from low-frequency DNLL neurons and made juxtacellular biocytin injections. This allows us to reconstruct the axonal and dendritic branches of the recorded neurons. The results indicate that low-frequency ITD-sensitive DNLL neurons project to the contralateral site. By contrast, neurons in the same region which show no ITD-sensitivity project to the ipsilateral IC.

Presently, immunohistochemical staining is being correlated with the biocytin positive neurons to investigate the distribution of inhibitory and excitatory inputs onto neurons in the IC.

365 Anatomical Characterization of Inferior Olive Projections to the Cochlear Nucleus in Rats

Xiping Zhan¹, Tan Pongstaporn¹, David K Ryugo^{1,2}

¹Department of Otolaryngology, Johns Hopkins University, 720 Rutland Avenue, Baltimore, MD, United States, ²Department of Neuroscience, Johns Hopkins University, 720 Rutland Avenue, Baltimore, MD, United States

The granule cell domain (GCD) of the cochlear nucleus is a polysensory integration center for the auditory system. We add to this idea by our discovery of a projection from the inferior olive (IO) to the GCD in the rat. In order to characterize this projection, we injected the IO with biotinylated dextran amine from either a dorsal or ventral approach and processed tissue for light and electron microscopic analyses. There was a predominantly contralateral projection from the inferior olive to the GCD. The terminal fibers branched repeatedly within the cochlear nucleus and terminated as small bouton endings. In addition, a few large endings in either the cochlear nucleus or cerebellum were observed. All swellings were characterized as large or small (mossy fibers or climbing fibers, respectively) based on their structure. Most but not all mossy fiber endings were attributed to "fibers-of-passage" contamination via leakage along the pipette path. Mossy fibers (MFs) were 3-8 μ m in diameter, had an irregular shape, targeted dendrites, and made many asymmetric synapses. Climbing fibers (CFs) were 1-4 μ m in diameter, had a regular shape, contacted dendritic shafts or the somata of resident GCD neurons, and made only a few synapses. Where CFs contained round synaptic vesicles of variable sizes, MFs contained round synaptic vesicles of relatively uniform size. One CF synapsed on a unipolar brush cell in the cerebellum. Targets in the GCD remain unidentified but are probably not granule cells. Interestingly, CFs and MFs in the GCD were similar in morphology to those of the cerebellar cortex. The olivary projections to the contralateral cochlear nucleus appear to be collaterals of CFs. The implication of these observations is that polysensory information involved in the functional activities of cerebellar climbing fibers may be relevant to acoustic processing in the cochlear nucleus.

Supported by NIH DC04395

366 Projections from the Spinal Trigeminal Nuclei to the Cochlear Nuclei in the Guinea Pig

Jianxun Zhou, Susan Shore

Kresge Hearing Research Institute, University of Michigan, 1301 E. Ann Street, Ann Arbor, MI, United States

The cochlear nucleus receives not only auditory inputs but also nonauditory inputs, including projections from the trigeminal sensory complex. However, the detailed anatomy and functional implications of the nonauditory innervations of the auditory system are not fully understood. It has been previously demonstrated in guinea pig that the trigeminal ganglion projects to the cochlear nucleus, with terminal labeling most dense in the marginal cell area and secondarily in the magnocellular area of the ventral cochlear nucleus (VCN, Shore et al., *J. Comp. Neurol.* 419:271-285, 2000). We continued this line of study by aiming to determine whether there is a direct projection from trigeminal nucleus to cochlear nucleus in guinea pig, and what the fine structure of this projection is. Retrograde tracers (fluorogold or biotinylated dextran amine, BDA) were pressure-injected into the VCN of guinea pigs under visual guidance. Retrogradely labeled cells were found in the spinal trigeminal nucleus, most densely in the pars interparalis and pars caudalis with the ipsilateral dominance. In addition, the retrograde labeling of dorsal column nuclei (cuneate and gracile) was also evident, predominantly ipsilateral to the injection site. Anterograde tracers of micro-ruby or biocytin were stereotaxically pressure-injected into the spinal trigeminal nucleus. Preliminary data of anterograde tracing experiments indicate that labeled puncta were found predominately in the granular cell region and the small cell cap area of VCN, as well as the deep layer of dorsal cochlear nucleus (DCN). The present study is consistent with our earlier observations, as well as similar studies observed in cats and rats, in which the primary target of somatosensory projections is the granule cell domain (GCD) of the cochlear nucleus (Itoh, et al., *Brain Res.* 400(1):145-50, 1987; Wright and Ryugo, *J. Comp. Neurol.* 365:159-72, 1996). The implications of this somatosensory projection to the GCD will be discussed.

Supported by NIH grant 5 R01 DC004825-03 and Tinnitus Research Consortium

367 Timing Encoding Capability by the Avcn Bushy Cells in Mice Affected by Early Onset Hearing Loss

Yong Wang¹, Paul B Manis²

¹Dept of Otolaryngology/Head Neck Surgery, Univ. of North Carolina at Chapel Hill, CB 7070 Bioinformatics Building, Chapel Hill, North Carolina, United States, ²Dept of Otolaryngology/Head Neck Surgery, Univ. of North Carolina at Chapel Hill, CB 7070 Bioinformatics Building, Chapel Hill, NC, United States

Discerning timing information imbedded in acoustic signals is essential for animal survival. Mammals routinely have the capability to detect an interaural time difference in the order of microseconds. To this end, bushy cells in the anterior ventral cochlear nucleus (AVCN) show greater phase-locking capability than auditory nerve fibers. Previous studies using DBA/2J strain mice, which exhibit an age-related high frequency hearing loss, have

shown changes in synaptic transmission at the calyx/endbulb of Held synapse between surviving spiral ganglion cells and bushy cells in AVCN. Spontaneous synaptic release at the affected synapse becomes less frequent, release events are smaller, and release probability declines. To further study the consequences of hearing loss on the bushy cell's ability to code timing information, we measured spike entrainment and jitter in high frequency (deaf in old animals) regions of the AVCN in response to a train of EPSPs produced by auditory nerve root stimulation in a slice preparation. Preliminary data show that both young (~20 days) and old (~42 days) animals are able to entrain stimuli of 100 Hz with some cells showing entrainment up to 300 Hz before significant dropout occurs. Response latency and spike timing jitter in response to subsequent EPSPs increase in both young and old animals as well. These results suggest that bushy neurons in the AVCN do not lose their precise firing capabilities during early stages of hearing loss in the auditory periphery.

Supported by: NIDCD Grants T32 DC04909 (YW) and R01 DC04551 (PBM)

368 Neonatal Deafening Results in Degradation of the Topographic Specificity (Frequency Resolution) of Spiral Ganglion Projections to the Cochlear Nucleus

Patricia A. Leake, Russell L. Snyder, Gary T. Hradek, Leila Chair

Otolaryngology-Head & Neck Surgery, University of California San Francisco, 533 Parnassus Avenue, Room U490, San Francisco, CA, United States

We have previously studied the development of spiral ganglion (SG) projections to the cochlear nucleus (CN) using the neuronal tracer Neurobiotin™ to label neurons in small sectors of the SG representing a narrow range of frequencies. Projections from the basal cochlea exhibit clear tonotopic organization before birth in normal kittens studied after C-section at 60-64 days gestation, several days before spontaneous activity emerges in the auditory nerve and many days before hearing onset. However, our data also revealed that significant refinement of SG projections occurs during early postnatal maturation. The topographic restriction of projections into frequency band laminae is less precise in all 3 CN subdivisions in perinatal kittens than in adults. Normalized for CN size, projections to AVCN, PVCN and DCN are about 53%, 36% and 32% broader, respectively, in neonates than in adult cats.

The present study examined CN projections in 7 adult cats that were deafened as neonates by administration of the ototoxic drug neomycin sulfate. Data show that the basic organization of CN projections into frequency band laminae is intact in deafened animals, despite severe auditory deprivation and reduction or abolition of AN activity from an early age. However, when normalized for the smaller size of the CN, projections in the deafened subjects are significantly broader than normal. Laminae in AVCN, PVCN and DCN are about 43%, 23% and 40% broader, respectively, in deafened animals than in controls. These findings suggest that neuronal activity (normal auditory experience) is essential for normal postnatal refinement of the SG projections to the CN. In early-deafened animals the fundamental tonotopic organization of the SG input is established and maintained into adulthood, but the

topographic specificity (inferred frequency resolution) of the primary afferent projections to the central auditory system is significantly degraded.

(Research Supported by NIDCD Grant #R01 DC000160.)

369 Expression of Pro-Caspase 3 in the Postnatal Mouse Cochlear Nucleus During and After a Critical Period of Afferent Dependent Survival

Julie A. Harris, Edwin W Rubel

Graduate Program in Neurobiology & Behavior, VM Bloedel Hearing Research Center and Dept. Oto-HNS, University of Washington, Box 357923, Seattle, WA, United States

Cochlear ablation performed during the first ten days after birth results in dramatic neuron loss in the anteroventral cochlear nucleus of mice. This susceptibility to loss of afferent input disappears by postnatal day 14 (P14). The molecular basis underlying this critical period of differential susceptibility to loss of afferent input remains largely unknown. We have identified several candidate genes using cDNA microarrays that change in expression in parallel with the timing of the end of this critical period. One of these candidates, caspase 3, is a cysteine protease that is important in the downstream execution of apoptosis. Microarray results revealed a 6-fold enrichment of caspase 3 mRNA in P7 cochlear nucleus (CN) compared to P21 CN. We validated these results for the caspase 3 protein using immunohistochemistry with a monoclonal antibody that recognizes the full-length pro-form of caspase 3. Caspase 3 expression in the CN declines markedly from P7 to P21. Interestingly, the distribution of labeled cells is also very different between these ages. There is a high amount of caspase 3 labeling in the granule cell layer, as well as in cells of the VCN and DCN during the critical period at P7. At P21 there are fewer labeled cells, and they are scattered more evenly throughout the entire extent of the CN. The labeled cells appear to be predominantly neurons, but the identification of labeled cell types by immunohistochemistry needs further verification. These results suggest that the developmental decrease in expression of caspase 3 mRNA and protein may be an important factor in closing the window of high susceptibility to loss of afferent input. If this is the case then upstream events in the cellular responses to deafferentation should be more similar between neonatal and older mice, a hypothesis currently under investigation.

Supported by NIDCD grants DC03829 and DC05361

370 Survival Strategies in the Cochlea Nucleus of BALB/c mice.

Esma Idrizbegovic¹, Agneta Viberg², Nenad Bogdanovic³, Barbara Canlon²

¹*Audiology, Karolinska Institutet, Huddinge University Hospital, Huddinge, Sweden,* ²*Physiology & Pharmacology, Karolinska Institutet, Karolinska Institutet, Stockholm, Sweden,* ³*Neurotec, Geriatric Section, Karolinska Institutet, Huddinge University Hospital, Huddinge, Sweden*

Aging BALB/c (BALB) mice (1, 24 and 30 months old), have been used to study the influence of cochlear pathology on calcium binding protein immunoreactivity (calbindin, parvalbumin and

calretinin) in the cochlear nucleus (posteroventral- and dorsal cochlear nucleus, PVCN and DCN). The BALB mice demonstrate progressive cochlear sensorineural pathology and hearing loss early in their life. A progressive loss of outer hair cells (OHC) was demonstrated throughout the cochlea at 24 months. A progressive loss of inner hair cells (IHC) and spiral ganglion cells (SGCs) were most severe in the cochlear base and less severe in the middle turn and in the apex at 24 months. The total number of calcium binding proteins did not show any significant changes in the PVCN and DCN between the 1, 24 and 30 months old mice, respectively. A correlation between loss in the auditory periphery and calcium binding protein expression in the PVCN and DCN was not found. This lack of correlation between the degeneration of the cochlea and that of calcium binding proteins in the cochlea nucleus is distinctly different than the pattern of degeneration found for aging C57BL/6J mice. The persistent survival of the calcium-binding proteins in the cochlea nucleus of aging BALB mice is suggestive of a survival mechanism against age-induced calcium overload in these neurons. Supported by RNID, The Swedish Research Council, Tysta Skolan and AMF.

371 Bilateral Cochlea Ablation Disrupts the Development of Banded DNLL Afferent Projections in the Rat Inferior Colliculus

Samuel R. Franklin, Judy K. Brunso-Bechtold, Craig K. Henkel

Dept. of Neurobiology and Anatomy, Program in Neuroscience, Wake Forest University School of Medicine, Medical Center Blvd., Winston Salem, North Carolina, United States

The central nucleus of the inferior colliculus (CNIC) is a site of convergence for ascending auditory projections. Within the CNIC, some excitatory and inhibitory afferents are organized in a laminar pattern of interdigitating bands. For example, inhibitory GABAergic projections from the dorsal nucleus of the lateral lemniscus (DNLL) decussate in the commissure of Probst and end in a banded pattern in the contralateral CNIC. Previous studies in our laboratory (Gabriele et al 2000) showed that DNLL afferents in the neonatal rodent CNIC are present at birth, but not banded. Moreover, unilateral cochlear ablation at P2 disrupted the development of bands within the CNIC. To determine if the overall spontaneous activity generated by the cochlea, rather than an imbalance of activity due to unilateral cochlea removal, is the critical factor in the disruption of band development within the CNIC, both cochleas were ablated in P2 rat pups. Pups were reared to P12, anesthetized, and sacrificed by transcardial perfusion of 4% paraformaldehyde. Glass pins coated in DiI (1, 1'-diiododecyl-3,3,3',3'-tetramethylindocarbocyanine perchlorate) were placed in the commissure of Probst in order to visualize contralateral DNLL afferent projections. In the CNIC of ablated animals, fluorescent label from DNLL afferents appeared less intense bilaterally, compared to control animals. Furthermore, in ablated animals, DNLL afferents failed to segregate into a refined pattern of bands compared with age-matched control animals. These results indicate that bilateral cochlear ablation disrupts the normal development of DNLL bands observed in the CNIC.

372 Ontogeny of glycinergic inhibition in the gerbil medial superior olive - an in vitro study

Anna K. Magnusson, Christoph Kapfer, Ursula Koch, Benedikt Grothe

Auditory Processing, Max-Planck Institute of Neurobiology, Am Klopferspitz 18a, Martinsried, Germany

The medial superior olivary (MSO) neurons are involved in the detection of interaural time differences (ITDs) of low frequency sounds. They are possibly the most precise time analyzing units in the mammalian brain as they exhibit a time resolution of only a few microseconds. Recently, it was shown in a morphological study that the binaural glycinergic innervation of the MSO undergoes an experience dependent spatial refinement after hearing onset (Nat Neurosci. 2002 5:247-53). Such compartmentalization of inhibitory inputs might be the structural substrate for the fast functional inhibition in MSO neurons, as indicated by in vivo studies.

In the present study, we investigated the development of membrane properties and temporal characteristics of glycinergic inputs to MSO neurons in acute gerbil brainstem slices (P12 – P18) using standard current- and voltage-clamp recording techniques. Inhibitory synaptic inputs were activated by stimulation of fibers from the medial nucleus of the trapezoid body.

Current-clamp recordings showed that the input resistance and membrane time constant of these neurons decrease after hearing onset (in accordance with Spirou et al. personal communication). In parallel, we observed an increase in inward and outward rectification. The glycinergic mediated inhibitory synaptic potentials (IPSPs) showed a decrease in rise time and half-width after hearing onset to a magnitude of a few milliseconds. Voltage clamp recordings displayed a decrease in the rise time and the decay time constant of the inhibitory synaptic currents (IPSCs) after hearing onset. Around P16 – P18, some neurons developed extremely fast kinetics with rise times below 0.3 ms and half-widths in the sub-millisecond range. The development of the fast kinetics of the inhibitory synaptic responses, which occur in the same time frame as the spatial refinement of the glycinergic inputs, may represent a specific adaptation for the detection of ITDs.

373 Effects of Postural Changes and Vestibular Lesions on Genioglossal Muscle Activity in Conscious Cats

Bill Yates¹, Stephen Cass², Lucy Cotter¹, Brian Jian¹, Heather Arendt¹, Christopher Olsheski¹, Katherine Wilkinson¹

¹Otolaryngology, University of Pittsburgh, 113 Eye and Ear Institute, Pittsburgh, PA, United States, ²Otolaryngology, University of Colorado Health Sciences Center, 4200 East Ninth Avenue B205, Denver, CO, United States

Previous studies in humans showed that genioglossal muscle activity is higher when individuals are supine than when they are upright, and prior experiments in anesthetized or decerebrate animals suggested that vestibular inputs might participate in triggering these alterations in muscle firing. The present study determined the effects of nose-up postural changes at a variety of

amplitudes on genioglossal activity in a conscious feline model, and compared these responses to those generated by ear-down tilts. Furthermore, we ascertained the effects of inner ear lesions on the alterations in genioglossal activity elicited by changes in body position. Both nose-up and ear-down body tilts produced modifications in muscle firing that were dependent on the amplitude of the rotation; however, the relative effects of ear-down and nose-up tilts on genioglossal activity were variable from animal to animal. Thus, this study revealed that changes in posture produce more complex alterations in genioglossus discharges than have been described in previous studies, which typically only considered the effects of one direction of movement. The response variability observed might reflect the fact that genioglossus has a complex organization and participates in a variety of tongue movements; in each animal EMG recordings presumably sampled the firing of different proportions of fibers in the various compartments and subcompartments of the muscle. Furthermore, removal of labyrinthine inputs resulted in a long-lasting alteration in genioglossal responses to postural changes, demonstrating that the vestibular system participates in regulating the muscle's activity.

Supported by NIH, NIDCD grant R01 DC03732

374 Emergence of spontaneous and evoked spike activity in developing chick vestibular nucleus neurons

Mei Shao¹, June C Hirsch¹, Christian Giaume^{1,2}, Kenna D Peusner¹

¹Anatomy, George Washington University Medical Center, 2300 I Street NW, Washington, DC, United States, ²Pharmacologie, College de France, 11 place Marcelin-Berthelot, Paris, France

The principal cells (PCs) of the chick tangential nucleus are vestibular nucleus neurons involved in the vestibular reflexes. Tonic firing of action potentials, both spontaneous and evoked, are essential for vestibular reflex function. The emergence of spike firing was studied in PCs, identified with infrared imaging and biocytin staining, using the whole-cell current-clamp mode. Recordings were obtained at resting membrane potential and while injecting 400 ms depolarizing current pulses. Experiments were performed on brain slices using KCl pipette solution in embryos (E16) and KMeSO₄ in hatchlings (H1 and H5). At E16, PCs had average resting membrane potentials of -68 ± 2 mV ($n=12$) and none displayed spontaneous spike activity. Eight neurons generated a single spike on depolarization, while 4 fired repetitively with a mean frequency of 8 ± 1.4 Hz (0.1 nA) or 23 ± 6 Hz (0.5 nA). At H1, spontaneous spike activity was present in 5 from 8 PCs, the mean firing frequency was 33 ± 13 Hz at a resting membrane potential of -57 ± 2 mV ($n=8$). On depolarization, the spontaneously firing neurons generated regular spikes at 90 ± 20 Hz (0.1 nA) or 131 ± 18 Hz (0.5 nA) ($n=5$), while 2 silent PCs fired repetitively and the remaining cell generated a single spike. At H5, all the PCs showed regular spontaneous spike activity with a mean frequency of 50 ± 15 Hz and a mean resting membrane potential of -56 ± 2 mV ($n=5$). On depolarization, the firing was regular with a mean frequency of 59 ± 23 Hz (0.1 nA) or 137 ± 23 Hz (0.5 nA). These results indicate that PC excitability is regulated during the critical period from late embryonic to young hatchling ages. This period is characterized by depolarization of the resting membrane potential and a switch from spontaneously silent neurons to

those generating a tonic firing of spontaneous and evoked action potentials on depolarization. The emergence of this firing pattern enables vestibular nucleus neurons to process signals in the vestibular reflex pathways.

375 Zonal Organization of Vestibulo-Cerebellum in the Control of Lateral Rectus and Medial Rectus Muscles in the Rat Using the Retrograde Transport of Pseudorabies Virus. I. Single Injection Paradigm

Isabelle Billig¹, Carey D. Balaban²

¹Otolaryngology, University of Pittsburgh, Lothrop street, Pittsburgh, PA, United States, ²Otolaryngology and Neurobiology, University of Pittsburgh, Lothrop street, Pittsburgh, PA, United States

Much literature has investigated the three-dimensional organization of neurons in flocculus/ventral paraflocculus (Fl/vPFL), in particular for their influence upon vestibulo-ocular reflex eye movements. Although activation of a central zone produces ipsilateral horizontal eye movement, anatomical tracing evidence in rats suggests that there may not be a simple one-to-one correspondence between Fl/vPFL zones and control of individual extraocular muscles (EOMs) or coplanar pairs of antagonistic muscles. This study used the retrograde transynaptic transport of pseudorabies virus (PRV) to identify the topographical organization of Purkinje cells in Fl/vPFL controlling each muscle. A survival time of 80- and 84-hours produced consistent labeling in Fl/vPFL after injecting PRV into the medial rectus and lateral rectus, respectively. The organization of Purkinje cells in the dorsal Fl and vPFL abided by the traditional boundaries, whereas the labeling pattern in the ventral Fl showed an interdigitated arrangement. In agreement with prior studies, labeled neurons were also present in specific vestibular nuclear regions within the medial and superior vestibular nuclei and group- γ . Data indicated that similarities and differences in the distribution of labeled neurons in vestibular nuclei were associated with features of labeled Purkinje cells in Fl/vPFL. This study provides the first evidence of overlapping distribution of neurons in vestibular nuclei and Fl/vPFL projecting to the EOM oculomotor pools; suggesting that some of them may be responsible for coordinating conjugate eye movements in the horizontal plane. This work was supported by the PLRHF (2101, I.B.); CMRF (PUH0013816, I.B.) and by grant RO3 DC005911 (I.B.) from the National Institutes of Health.

376 Nystagmus Characteristics Are Influenced by Attention Tasks

Joseph M. Furman, Carey Balaban, Timothy Schumann, Robert Schor

Otolaryngology, University of Pittsburgh, 200 Lothrop Street, Pittsburgh, PA, United States

Recent studies have suggested that the vestibulo-ocular reflex (VOR), optokinetic stimulation, and ocular pursuit interfere with performance of a simultaneous cognitive task. Our recent studies also suggest interference by cognitive tasks with both the slow and quick components of nystagmus. In this study, we examined the fine structure of optokinetic nystagmus (OKN) during various attention-requiring tasks. We hypothesized that the timing of nys-

tagmus quick components would, overall, be influenced by a subject's current cognitive demands. Subjects were young healthy individuals. OKN was induced by asking subjects to look at full-field vertical stripes moving horizontally at a constant velocity of 30 deg/sec. Eye movement was recorded with a dual (3D) scleral search coil. Concurrent attention-requiring tasks included answering simple questions, pushing a handheld button randomly, counting the number of occurrences of a target tone, and pushing a button after hearing a target tone. Eye movements were analyzed by representing eye position as rotation vectors. The duration of slow components was estimated using a nystagmus algorithm that identified quick and slow components of nystagmus. The slow component durations during each task condition were used to estimate the values of a model with three parameters: the mean and standard deviation of the slow component duration and a non-zero probability of "skipping a beat". Results indicated that the characteristics of OKN, based on the parameters of the nystagmus generation model, differed depending upon the type of attention-requiring task being performed. This study confirms that nystagmus generation and cognitive processing interfere with one another. These results have implications for patients with balance disorders and for patients with impaired cognition.

This work was supported by NIH grant AG10009.

377 Vestibular-like Responses of Parabrachial Nucleus Units to Off-Vertical-Axis-Rotation (OVAR) in the Macaque

Cyrus H. McCandless¹, Jianxun Zhou², Ja-won Koo³, Carey D. Balaban⁴

¹*Dept. Neurobiology & Center for the Neural Basis of Cognition, University of Pittsburgh School of Medicine, 203 Lothrop Street, Room 153, Pittsburgh, PA, United States,* ²*Kresgy Hearing Research Institute, University of Michigan Medical School, 1150 W. Medical Ctr. Dr., Ann Arbor, MI, United States,* ³*Department of Otolaryngology, University of Pittsburgh School of Medicine, 203 Lothrop Street, Room 153, Pittsburgh, PA, United States,* ⁴*Department of Otolaryngology, University of Pittsburgh Eye & Ear Institute, 203 Lothrop Street, Room 153, Pittsburgh, PA, United States*

Work in our laboratory has recently uncovered a novel population of brainstem neurons responsive to natural vestibular stimulation, located in the parabrachial nucleus (PBN) of the alert macaque monkey (Balaban et al., 2003). Prior work examined responses of these units to periodic rotational stimuli in horizontal and vertical planes. Here, we report that neurons of the PBN exhibit unique responses to a rotating linear acceleration vector produced by OVAR stimuli. Two major types of responses are evident: 1)cosinusoidal spatial tuning, and 2) a long-lasting bias-type response in which the direction of rotation corresponds with a persistent increase or decrease in firing rate. These two response types frequently co-occur in the same units, and it is likely that in many of these neurons, the latter response type is artifactual of the former type. However, in some units, a bias-type response appears to be independent of any underlying, periodic response to rotation. In either case, the magnitudes of the observed biases relative to the direction of rotation are far larger than reported for previously known vestibuloresponsive neurons. Units of the PBN may represent a novel and important new class of neurons which are capable

of persistently signaling the direction of prolonged, constant-velocity off-vertical-axis rotation. We believe that these neurons may relay integrative self-motion information to higher brain areas, particularly portions of the extended amygdala. If confirmed in our ongoing studies, these findings would have profound implications for the interpretation of behavioral and psychophysical findings in humans and non-human primates.

378 Novel Interpretation of Optokinetic Afternystagmus

Neil Cherian¹, John G Oas²

¹*Neurology, Cleveland Clinic Foundation, 9500 Euclid Ave, Cleveland, OH, United States,* ²*Neurology and Otolaryngology, Cleveland Clinic Foundation, 9500 Euclid Ave, Cleveland, OH, United States*

Optokinetic nystagmus (OKN), which is elicited by a moving visual scene across the field of vision, can be used at the bedside to demonstrate focal parieto-occipital disease and to evaluate factitious blindness. Optokinetic afternystagmus (OKAN) is noted immediately after the removal of the visual stimulus. OKAN is often a normal finding and lasts only 10-40 milliseconds. Due to usual methods of OKN generation and analysis, OKAN is often not measured. We have observed unique patterns of OKAN in our laboratory which may help to provide further insight into peripheral and central vestibular dysfunction and possibly even states of adaptation.

Our laboratory uses a rotating drum stimulus which produces a complex pattern of dots on a curved wall. The stimulus is presented initially with dots moving to the right for 30-45 seconds, followed by a stimulus-free period of 30-45 seconds in order to observe OKAN. This is then repeated in the leftward direction. Eye movement data is captured with infrared videonystagmography and analyzed using commercial vestibular laboratory software (Micromedical Technologies).

Upon review of the vestibular tests from September 2000 to March 2002, the common patterns of OKAN included: unilaterally positive, bilaterally positive (symmetric, asymmetric) and no OKAN bilaterally (time constant < 0.5 sec). Unilateral vestibular losses at times manifested an OKAN prolongation contralateral to the side of loss. The symmetric, bilaterally positive OKAN group often had a history of headache, with or without migrainous features, per clinical review. Normal vestibular testing, except for unilaterally prolonged OKAN, was quite infrequent. More commonly, a unilaterally prolonged OKAN was seen along with brief nystagmus in the same direction in other portions of positional testing. A bias of the VOR to the same direction of the OKN and/or a borderline caloric paresis (approx. 24-26%) may be seen. The clinical picture of these patients often suggested vestibular neuronitis. An asymmetric, bilaterally prolonged OKAN, when combined with the clinical picture often suggested a peripheral vestibular disturbance provoking, or unmasking, a central phenomenon such as a migraine.

In conclusion, OKAN analysis may provide insight into the further understanding of patients with vestibular disorders.

379 Noise Exposure Induced MtDNA Deletions In Rats

Weiju Han^{1,2}

¹Oregon Hearing Research Center, Oregon Health & Science University, 3181 SW Sam Jackson Park Road, Portland, Oregon, United States, ²Otolaryngology, PLA General Hospital, 28 Fu Xing Road, Bei Jing, China, People's Republic of

HAN Weijua, b, HAN Dongyia, Yang Weiyana and Jiang Sichanga.

^a Department of Otorhinolaryngology Head and Neck Surgery, General Hospital of PLA, Beijing 100853, China

^b Oregon Hearing Research Center, Oregon Health & Science University

Portland, OR 97201-3098

Corresponding author: Han Weiju (Email: hanweiju@hotmail.com)

To understand if the noise exposure can induce mtDNA deletions in rat tissues, three months old wistar rats (n=20) were exposed to 108-110dB SPL white noise for 4 hours each day continuously for 40 days. The control groups (n=20) were not exposed to the noise. The rats of two groups were tested for auditory sensitivity using the ABR technique 2 weeks following white noise exposure stops. The cochlea, cochlear nucleus, brain tissue and muscle were harvested and the total DNA was extracted. MtDNA was amplified to identify the highly conserved ND1 segment, as well as mtDNA⁴⁸³⁴ deletions. Results demonstrated a significant reduction in auditory sensitivity compared with the control group (*t* test $p < 0.01$). The incidence of rats carrying mtDNA⁴⁸³⁴ deletions in cochlea, cochlear nucleus and brain tissues in white noise exposed group were higher than that of the control group (χ^2 test $p < 0.01$). However, the incidence of rats carrying mtDNA⁴⁸³⁴ deletions in muscle tissues was no significant difference between white noise exposed group and the control group (χ^2 test $P > 0.05$). These findings indicated that white noise exposure in rats might induce mtDNA⁴⁸³⁴ deletions in auditory tissues and organs.

380 Effects of Gender, Source, and Age at Sound Exposure on Hearing in C57BL/6J Mice

Cynthia A, Prosen¹, Alyssia Rogers²

¹Psychology Department, Northern Michigan University, 306 Gries Hall, Marquette, MI, United States, ²Psychology Department, Northern Michigan University, Gries Hall, Marquette, MI, United States

The C57 mouse is a model of human presbycusis. Our previous report (Prosen et al., 2003, *Hear Res* 183:44-56) suggested that several variables contribute to the premature hearing loss experienced by C57 mice, and the current study expanded our initial exploration of factors instrumental in early-onset deafness in these mice. While human males are more susceptible to presbycusis compared to human females, the role of gender in the hearing loss of C57 mice is controversial. Similarly, subject source – laboratory vs. commercial vendor – has been linked to differentially accelerated patterns of hearing loss. Finally, the interaction between disease and noise exposure has been explored in a variety of studies, with sometimes disparate results. This study investigated the effects of these variables in young and middle-aged mice.

The auditory brainstem response (ABR) of C57BL/6J mice was

measured to click and pure tone (8, 16 and 32 kHz) stimuli. Subjects included males and females, either bred in our laboratory or obtained from the Jackson Laboratory. ABRs were measured at 2 and 7 months of age. One group of mice was sound exposed (11.2 kHz octave band of noise, 101 dB noise spectrum level, 76 minutes) at 2 months of age, while a second group was exposed at 7 months. Thresholds in all subjects were re-assessed at 8 months of age.

Data indicated that subject source had no influence on ABR thresholds. While female mice had lower thresholds at all test stimuli compared to males, the differences were not statistically significant. Age-at-exposure data were used to test the hypothesis that acoustic overstimulation is more detrimental to the young auditory nervous system that is genetically predisposed to early-onset deafness compared to mature hearing structures.

(Supported by NIDCD grant R15 DC04405).

381 The effect of nitric oxide synthase inhibitors on acoustic injury of the mouse cochlea

Hidekazu Murashita, Keiji Tabuchi, Tomofumi Hoshino, Akira Hara, Jun Kusakari

Department of Otolaryngology, Institute of Clinical Medicine, 1-1-1 Tennodai, Tsukuba, Japan

Previous studies from our laboratory have revealed that nitric oxide (NO) and nitric oxide synthase (NOS) play important roles in generation of cochlear ischemia-reperfusion injury. However, little is known about the role of NO and NOS in acoustic injury of the cochlea. In the present study, we examined the effects of NOS inhibitors on acoustic injury. Female mice were exposed to 4 kHz pure tone of 128 or 120 dB SPL for 4 hours. N-nitro-L-arginine (a non-selective NOS inhibitor, n=10) aminoguanigine (a selective inducible NOS inhibitor, n=10) or 7-nitroindazole (a selective neuronal NOS inhibitor, n=8) was given to the animals under various treatment protocols. NOS inhibitors did not have any effect on the threshold shift of auditory brainstem response from the pre-exposure level one and two weeks after the acoustic overexposure. The present finding suggest that NO and NOS may play little role in the generation mechanism of acoustic injury in the mouse cochlea.

382 Noise-Induced Changes In Gene Expression In Mouse Strains Susceptible To And Resistant To Noise Damage

Ana Elena Vazquez¹, Michael Anne Gratton²

¹Otolaryngology, University of California Davis, 1515 Newton Court, Davis, California, United States, ²Otorhinolaryngology - HNS, University of Pennsylvania, 3400 Spruce Street, Philadelphia, PA, United States

Different individuals are affected by loud noise to various degrees. Correspondingly, inbred mice strains exhibit widely different susceptibilities to noise damage. The 129Sv/Ev (129) strain was reported to exhibit exceptional resistance to noise damage (Yoshida, 2000). In contrast, the C57BL/6J is a model for noise susceptibility.

For the current work, 10-wk-old mice of 129 and C57BL/6J strains were divided into control and noise groups (12 mice in each group). The “noise” groups were exposed to a 1-h, 105-dBSPL,

10-kHz centered, octave band of noise that distinguishes the differences in susceptibility to noise damage between the 129 and the C57BL/6J strains. Although the noise protocol results in no permanent threshold shift for the 129 mice, it induces permanent cochlear dysfunction in the C57BL/6J strain. For gene expression studies the mice were sacrificed 6 h after noise exposure, and the cochlear duct was quickly microdissected. Total RNA was isolated and used to prepare biotin-labeled cRNA following the Affymetrix protocol. For gene expression profiling, the Affymetrix MGU74Av2 chip was used, containing 12,000 functionally characterized sequences plus ESTs. The data obtained was analyzed using Affymetrix Microarray Suite 5.0 and dChip software. For each sample an average of 58% of the sequences scored as expressed.

Previous studies have implicated stress-activated pathways and the induction of apoptosis in hair cell damage caused by acoustic overexposure. Although the noise exposure protocol used in these experiments had dramatically different functional outcomes for the two strains of mice, up-regulation of a subset of stress-related genes was significant in the susceptible C57BL/6J mice as well as in the resistant 129 mice. Gene expression comparisons may further reveal the underlying genes relevant to noise susceptibility in mice and humans.

Supported by NIDCD R21-DC04990 to AV

383 Recovery of the Tegmentum Vasculosum in the Noise Exposed Chick

Rohan Ramakrishna, Rachel Kurian, James C. Saunders, Michael Anne Gratton

Otorhinolaryngology-HNS, University of Pennsylvania, 3400 Spruce St, Philadelphia, PA, United States

The virtually complete recovery of auditory function following acoustic overstimulation is well established. Strikingly, the majority of recovery occurs within the first three days following noise exposure. This cannot be explained solely by hair cell recovery, as the first evidence of regenerated hair cells is not seen until 4-5 days post exposure. Moreover, the endocochlear potential returns to normal by 3-4 days post exposure. As such, we hypothesize that injury to, and subsequent recovery of the tegmentum vasculosum contributes to the re-establishment of healthy cochlear homeostasis and thus recovery of auditory function. To test this hypothesis, this study quantified the tegmental damage in noise-exposed chicks. One day-old White Leghorn chicks were exposed to a 0.9 kHz tone at 120 dB SPL for 48 h. Chicks were sacrificed immediately afterwards or allowed to recover for 6 days. Age-matched control chicks were sacrificed at the same time as the noise-exposed chicks. At time of sacrifice, basilar papillae were extracted, dehydrated in graded ethanol solutions, and then embedded in epoxy. Five 1 μ m thick sections were taken in 50 μ m increments from the basilar papilla region with maximal hair cell lesion. Digitized toluidine-blue stained images were analyzed to determine total tegmental area, dark cell area, and total number of dark cells. From this, the area occupied by dark cells (AOD) was computed and compared across groups. Age-matched controls had an AOD of 75.2% \pm 4.2 and 74.2% \pm 3.8 respectively. In contrast, the AOD immediately after noise had decreased to 39.0% \pm 6.6 while the AOD following 6 days of recovery rose to 66.1% \pm 5.8. These AODs of both post-exposure times were significantly less than the

AODs of the age-matched controls. These data indicate clear near recovery of the tegmentum following acoustic overstimulation. Thus, tegmental recovery may explain the early partial recovery of auditory threshold via re-establishment of cochlear homeostasis.

Supported by Pennsylvania Lions Hearing Research Foundation to MAG

384 Involvement of poly(ADP-ribose) synthetase in acoustic injury of the cochlea

Keiji Tabuchi, Hidekazu Murashita, Tomohuhi Hoahino, Akira Hara

Department of Otolaryngology, Institute of Clinical Medicine, 1-1-1 Tennodai, Tsukuba, Japan

We investigated effects of poly(ADP-ribose) synthetase (PARS) inhibitors on acoustic injury of the cochleae of guinea pigs and mice. In the first experiment, guinea pigs were intravenously given 3-aminobenzamide, nicotinamide or 3-aminobenzoic acid (an inactive analog of 3-aminobenzamide) immediately before the exposure to a 2 kHz pure tone of 120 dB SPL for 10 minutes. The threshold of compound action potential (CAP) and the amplitude of distortion-product otoacoustic emission (DPOAE) were measured before and 4 hours after the acoustic overexposure. In the second experiment, mice were intraperitoneally administered 3-aminobenzamide immediately before the exposure to a 4 kHz pure tone of 128 dB SPL for 4 hours. The threshold shift of auditory brainstem response (ABR) and hair cell loss were evaluated 2 weeks after the acoustic overexposure. Statistically significant decreases in the CAP threshold shifts and significant improvement in the DPOAE amplitudes were observed 4 hours after the acoustic overexposure in guinea pigs treated with 3-aminobenzamide or nicotinamide, whereas 3-aminobenzoic acid did not exert any protective effect. In addition, 3-aminobenzamide functionally and morphologically protected the cochlea 2 weeks after the acoustic overexposure in mice. These results strongly suggest that excessive activation of PARS is involved in generation of the acoustic injury.

385 Can detachment of OHCs following exposure to impulse noise cause rapid apoptosis?

Bohua Hu¹, Donald Henderson¹, Thomas M. Nicotera², Wei-Ping Yang^{1,3}

¹Department of Communication disorders and science, State University of NY at Buffalo, 215 Parker Hall, 3435 Main St., Buffalo, NY, United States, ²Molecular and Cellular Biophysics, Roswell Park Cancer Institute, Elm & Carlton Streets, Buffalo, NY, United States, ³Institute of Otolaryngology, Chinese PLA General Hospital, Fu-Xing Road, Beijing, China, People's Republic of

We have previously shown that Impulse noise can cause direct mechanical damage to the organ of Corti, leading to detachment of hair cells (HC) from supporting cells. Our most recent study has shown that impulse noise initiates an extremely rapid HC death through apoptosis. The study raises the question as to whether the rapid apoptosis resulting from exposure to intense noise is associated with loss of anchorage of HCs. The current study was designed to address this question. Chinchillas were exposed to impulse noise at the level of 155 dB pSPL. Immediately after the exposure, the animals were sacrificed. The cochleas were labeled

either with FITC-labeled phalloidin to illustrate the reticular lamina and the Deiter cell's cup or with the antibody against mitochondria to illustrate the contour of the HC base. All the specimens were double stained with propidium iodine to reveal the morphological changes of HC nuclei. After the exposure, the split of reticular lamina between the first and second or between the second and third rows of OHCs was frequently seen. However, double staining of PI revealed no spatial correlation between the site of separation and the site of apoptosis. Examination of the region of the HC bottom showed that the OHCs having apoptotic nuclei often appeared to separate from their attachment. Due to the limitations of the techniques used, it was not clear whether the separation took place between the OHC and the synapse or between the OHC and the Deiter's cup. The results of the study suggest that interruption of integrity of the reticular lamina is not a direct cause of the rapid apoptosis, but separation of OHCs at their base may play a role in the initiation of OHC apoptosis. (Supported by NIDCD P01-DC03600-1A1 and NIDCD 1R21DC04984-01)

386 Changes in Chinchilla ABR and Sensitivity to Noise After Unilateral Ablation of the Superior Cervical Ganglion

Eric Charles Bielefeld, Donald Henderson

Center for Hearing and Deafness, SUNY Buffalo, 215 Parker Hall, 3435 Main Street, Buffalo, New York, United States

The role of cochlear sympathetic fibers from the Superior Cervical Ganglion (SCG) remains unclear. Several studies have shown effects of ablation or stimulation of the SCG on cochlear potentials (Pickles, 1979; Hultcrantz, 1984; Lee and Møller, 1985). Additionally, the SCG fibers have been implicated in modulating noise-induced hearing loss (NIHL) (Borg, 1982; Hildesheimer et al., 1991, 2002; Horner et al., 2001). In the current study, we explore the effects of unilateral SCG ablation on click-evoked ABR input-output functions and threshold shift from noise exposure. The left SCG was isolated at the level of the bifurcation of the carotid artery and removed in 13 chinchillas. Click-evoked ABRs were measured while the animals were under anesthesia, before and after the SCGectomy surgery, in seven of the animals. The other six animals were implanted with inferior colliculus electrodes and exposed to a 4 kHz octave band noise for one hour at 110 dB SPL. Hearing thresholds were measured one day, three days, one week, and three weeks after the noise. TTS and PTS were calculated. Results from the pre-noise exposure click-evoked ABRs revealed that SCGectomized ears showed increased latency for all waves at all stimulus intensities, with no changes in interpeak latencies. Results from noise exposure suggest a reduced susceptibility to noise in some SCGectomized ears, but not all. (Research supported by the Center for Hearing and Deafness, University at Buffalo.)

387 Does Oxidative Stress Account for Potentiation of NIHL by Acrylonitrile?

Laurence D Fechter, Benoit Pouyatos, Caroline Gearhart

Research Service, Loma Linda VA Medical Center, 11201 Benton Street, Loma Linda, CA, United States

This research is designed to evaluate the hypothesis that chemical contaminants that disrupt intrinsic antioxidant defenses hold sig-

nificant risk for potentiating noise-induced hearing loss (NIHL). A two process model is envisaged: (a) initiation of reactive oxygen species (ROS) by moderate noise exposure and (b) promotion of oxidative stress through disrupting intrinsic antioxidant defenses. This hypothesis is tested here using acrylonitrile (ACN) one of the 50 most commonly used chemicals in the United States. ACN is used to make nylon and acrylic fibers, plastics, nitrile rubber, and as a chemical intermediary. In addition to important issues of environmental toxicity (accidental release, contamination of water and air) and occupational safety, ACN is a very interesting model compound because its metabolism is associated with significant potential for oxidative stress. ACN conjugates GSH, depleting this important antioxidant rapidly. A second pathway involves the formation of cyanide (CN) as a by-product. CN, in turn can inhibit superoxide dismutase (SOD) and produce oxidative stress through other pathways as well. Acrylonitrile administration produced significant elevation in NIHL detected as a loss in compound action potential sensitivity. The effect was particularly robust for high frequency tones and particularly when acrylonitrile and noise were given on repeated occasions. Acrylonitrile by itself did not disrupt threshold sensitivity. Administration of the spin trap agent, phenyl-N-tert butylnitron (PBN), given to rats prior to acrylonitrile and noise did block the elevation of NIHL by acrylonitrile. However, PBN was ineffective in protecting auditory function in subjects exposed to noise alone. The results suggest that oxidative stress may play a role in the promotion of NIHL by acrylonitrile. (supported in part by NIH R21 DC05503).

388 Noise-induced expressions of Hypoxia-Inducible Factor-1 in mouse inner ear according to the duration of exposure

Jong Woo Chung¹, Huny Kang², Jung-Eun Shin³, Joong Ho Ahn³

¹Otolaryngology, Asan Medical Center, University of Ulsan College of Medicine, 388-1 Pungnap-Dong, Songpa-Gu, Seoul, Korea, Republic of, ²Otolaryngology, Asan Institute of Life Science, 388-1 Pungnap-Dong, Songpa-Gu, Seoul, Korea, Republic of, ³Otolaryngology, Bundang General Jeseng Hospital, 255-2 Seohyun-Dong, Bundang-Gu, Sungnam, Korea, Republic of

HIF-1 activates transcription of genes encoding proteins that will either increase O₂ delivery (VEGF, erythropoietin) or achieve metabolic adaptation under conditions of reduced O₂ availability (glucose transporter-1, glycolytic enzymes). Noise-induced expression of HIF-1 had been reported in cochlear sensory epithelia and lateral wall tissues in guinea pig inner ear. (Matsunobu et al, 2002, ARO Abstr) HIF-1 could involve in the molecular mechanism of noise-induced cochlear damage.

In this study, we observed noise-induced expression of HIF-1 according the duration of noise exposure in mouse inner ear and aimed to investigate the role of HIF-1.

We generated 120 dB SPL broad band noise (0.2 Hz - 70 kHz) and mice were exposed to the noise for 3 hours a day. Hearing threshold was measured by ABR before and after noise exposure. Inner ear tissue was harvested after 1, 2, 3 and 5 day noise exposure and immunostaining for HIF-1 was performed.

After 1 or 2 day exposure, hearing threshold was increased with complete and incomplete recovery after 2 weeks. Expression of

HIF-1 was indefinite in cochlear sensory cells, lateral wall tissues and spiral ganglion cells. After 3 and 5 day exposure, hearing threshold was over 80 dB and there was no recovery until 4 weeks. HIF-1 was expressed in cochlea, lateral wall tissue and spirala ganglion. In 5 day exposure mouse, the HIF-1 staining was more intense.

Through these, we could suggest that HIF-1 is expressed (or activated) by irreversible tissue damage.

389 Mechanism of noise-induced hearing loss potentiation by hypoxia

Guang-Di Chen

College of Pharmacy, The University of Oklahoma Health Sciences Center, 1110 N. Stonewall Ave, Oklahoma City, Oklahoma, United States

Many people at risk of exposure to hazardous noise may also suffer from hypoxia. Noise-induced hearing loss (NIHL) potentiation by hypoxia has been observed in our previous study (Chen, 2002). However, the mechanisms through which hypoxia potentiates hearing loss are still unclear. In this report, effects of noise (10-20 kHz octave band noise at 110 dB SPL for 4 hours), hypoxia (10%O₂), and their combination on different cochlear potentials and the expression of genes coding proteins in the outer hair cell (OHC) membrane skeleton, and in the mitochondrial respiratory chain (MRC), have been determined. The physiological data showed that loss of the cochlear amplification, in which OHCs play an important role, is the main reason causing the NIHL-potentiation. The data further indicated that the loss of the cochlear amplification is not always related to the loss of the OHC receptor potential, suggesting the damage to the motor-related structure. Noise-induced up-regulation of gene expression of beta-actin, a component of the OHC membrane skeleton, was observed, possibly reflecting damage to the OHC skeleton, which affects OHC electromotility. The up-regulation of gene expression may represent the cochlear repair. Hypoxia suppressed this noise-induced gene expression and so reduced the cochlear repair. Gene expression of a MRC flavoprotein (SDHa) was also up-regulated by noise, which was potentiated by hypoxia. Damage to the cochlear amplification and the cellular power supply may underlie the NIHL-potentiation by hypoxia.

390 Proinflammatory cytokine and chemokine expression in the noise-exposed murine cochlea

Keiko Hirose¹, Jodi Keasler²

¹Otolaryngology and Neurosciences, Cleveland Clinic Foundation, 9500 Euclid Avenue A-71, Cleveland, OH, United States,

²Neurosciences, Cleveland Clinic Foundation, 9500 Euclid Avenue, Cleveland, OH, United States

Acoustic injury in the mouse has recently been reported to result in cell death in numerous sensory and non-sensory regions of the ear. Cellular injury in the non-sensory regions may be related to the activation of mononuclear phagocytes that migrate into the ear after the traumatic injury (described in Discolo, Keasler and Hirose). To study the mechanisms that result in this phagocytic cell migration, we looked for changes in gene expression of various chemoattractant molecules such as cytokines and chemokines. We harvested

cochleas from CBA-CaJ mice exposed to 2 hours of 120 dB octave band noise at various intervals after noise and processed the tissue for real time quantitative PCR. Within days after acoustic injury, we detect a substantial increase in the expression of monocyte chemoattractant protein (MCP-1) and the expression of TNF-alpha and IL-1. We describe our techniques and the time course of the response to acoustic injury with respect to the elaboration of various proinflammatory chemokines and cytokines.

391 Contribution of Acoustic Trauma to Cochlear Inflammation

Shigehisa Hashimoto¹, Arash Moradzadeh¹, Peter Billings¹, Gary S Firestein², Jeffrey P Harris¹, Elizabeth M Keithley¹

¹Otolaryngology HNS, UCSD, 9500 Gilman Dr., La Jolla, CA, United States, ²Rheumatology, Allergy, Immunology, UCSD, 9500 Gilman Dr., La Jolla, CA, United States

An immune response comprises a rapid innate response and a slow adaptive response. IL-1 β is immediately up-regulated in the fibrocytes of the spiral ligament in response to systemic lipopolysaccharide (LPS) or cochlear surgery and may be considered a component of the cochlear innate immune response. The adaptive immune response to antigen introduced non-traumatically is increased in the presence of LPS or cochlear surgery.

To examine whether acoustic trauma can induce IL-1 β expression and increase the immune response to antigen, KLH was injected intrathecally into systemically KLH-sensitized Swiss mice (n=13) with or without acoustic trauma (118 dB, 8-16 kHz noise exposure for 2 hours). Control mice received acoustic trauma with PBS injection (n=6), acoustic trauma only (n=5) and PBS injection only (n=5). Animals were sacrificed after 48 hours. Cochlear sections were stained with H&E or immunolabeled with anti-IL-1 β .

Intrathecal KLH injection results in KLH in the cochlea after 2-3 hours. KLH sensitized mice react with infiltration of inflammatory cells into scala tympani (22 +/- 18 leukocytes/section). The addition of acoustic trauma increased the number of cochlear inflammatory cells to 35 +/- 41/section (p<0.01). Acoustic trauma with or without intrathecal injection of PBS resulted in 3 +/- 2 inflammatory cells per section. PBS injection alone resulted in 0.3 +/- 0.5 inflammatory cells per section. The percentage of fibrocytes expressing IL-1 β was greater in acoustic trauma animals.

Acoustic trauma recruited leukocytes and induced fibrocyte IL-1 β expression. We hypothesize that acoustic trauma activates the cochlea and recruits inflammatory cells in a fashion similar to an innate immune response. In the presence of antigen this allows for amplification of the adaptive response to that specific antigen.

Support: NIDCD R01 DC04268 and the Medical Research Service, Dept. of Veterans Affairs

392 Inflammatory Cells in the Mouse Cochlea After Acoustic Trauma

Christopher Discolo¹, Jodi Keasler², Keiko Hirose^{1,2}

¹Otolaryngology and Communicative Disorders, Cleveland Clinic Foundation, 9500 Euclid Avenue, Desk A71, Cleveland, Ohio, United States, ²Department of Neurosciences, Cleveland Clinic Foundation, 9500 Euclid Avenue, Cleveland, Ohio, United States

Inflammatory Cells in the Mouse Cochlea After Acoustic Trauma

After acoustic trauma, the cochlea sustains dramatic cellular injury and undergoes repair over subsequent days to weeks. The role of inflammation in this repair process has not been systematically evaluated. CBA/CaJ mice were exposed to octave-band noise at 106, 112 or 120 dB SPL for 2 hours and evaluated at 1, 3, 7 and 14 days after noise. Auditory brainstem responses were used to determine thresholds. Immunohistochemistry was performed with CD45, a cell-surface marker present on all leukocytes, to identify these cells within the cochleas of control and noise exposed mice. CD45 positive cells were counted at various locations within the cochlea including the organ of Corti, spiral ligament, stria vascularis, spiral ganglion, scala tympani and scala vestibuli. All exposure groups sustained permanent threshold shift. A small population of resident monocytes were found in the control cochleas in the inferior spiral ligament that closely resemble microglia of the brain, both histologically and by immunophenotype. At all sound pressure levels, there was a significant increase in CD45 positive cells which peaked at 7 days post-exposure. After 120 dB noise, CD45 positive cells returned to baseline levels by 14 days. Immunostaining for CD3, CD68, IBA and F4/80 suggest that the majority of these cells are either macrophages or microglia. Inflammatory cells may play a critical role in the repair process after acoustic trauma by both removing cellular debris and altering the local environment through elaboration of chemical mediators. Damage to non-sensory structures may be a result of bystander injury from activation of microglia and macrophages as opposed to direct injury from acoustic injury.

393 Hair-Cell-Membrane Changes in the Cochlea Following Noise

Nicole Schmitt, Kenneth Hsu, Barbara A Bohne, Gary W Harding

Otolaryngology, Washington University School of Medicine, 660 South Euclid Ave., St. Louis, MO, United States

The morphological correlates of temporary threshold shift (TTS) remain controversial. Mulroy et al ('98) provided indirect evidence that alligator lizards with noise-induced TTS have microlesions in hair-cell plasma membranes. To test this hypothesis directly, chinchillas were exposed for 24 hrs to a 4-kHz OBN at 92 dB SPL. ABR & DPOAE testing were carried out pre- & post-exposure. Three hrs post-exposure, 3 chinchillas had EP measured & carbon particles injected into the endolymphatic space before fixation. Two chinchillas recovered for 1 or 2 wks before EP measurement, carbon injection & cochlear fixation. Two controls underwent EP measurement (74 & 89 mV), carbon injection & cochlear fixation. Cochleas were embedded in plastic, dissected as flat preparations & missing cells counted. Cytochleograms were prepared with functional data overlaid according to the chinchilla frequency-place map. Thin sections of the OC were cut in the region of maxi-

mum threshold shift (TS) for TEM. Immediately post-exposure, all animals had an ABR TS of 20-60 dB over a frequency range of 1-16 kHz & a DPOAE level shift (LS) of 10-50 dB over 2-16 kHz; EP was 21, 49 & 79 mV in the three 0-d-recovery animals. Most hair cells were present & had normal shapes by phase contrast microscopy; by TEM, OHC stereocilia were slightly disarrayed but the plasma membranes were intact. The 1-wk-recovery animal had an ABR TS of 10-20 dB for 1-16 kHz, a DPOAE LS of 12-30 dB for 3-12 kHz & an EP of 83 mV. The 2-wk-recovery animal had an ABR TS of 10-20 dB for 3-6 kHz, a DPOAE LS of 12-23 dB for 3-12 kHz & an EP of 80 mV. In the 1-wk-recovery animal, one region of the OC contained about 20% degenerating OHCs. By TEM, the apical membranes of some degenerating hair cells contained microlesions. We conclude that hair cells do not develop microlesions in noise-exposed mammalian cochleas unless the cells are degenerating.

394 Comparison of Noise-Induced DPOAE Temporary Level Shift with Detailed Histopathology

Gary W Harding, Barbara A Bohne

Otolaryngology, Washington University School of Medicine, 660 South Euclid Ave., St. Louis, MO, United States

DPOAE temporary level shift (TLS), ABR temporary threshold shift (TTS), and detailed histopathology were determined in 3 groups of chinchillas exposed to an octave band of noise (OBN) centered at 4 kHz at either 80, 86 or 92 dB SPL for 24 hours (n=3, 4, 6). DPOAEs at 39 frequencies from $f_1=0.3$ to 16 kHz ($f_2/f_1=1.23$; L_2 & $L_1=55, 65$ & 75 dB, = & \neq) and ABR thresholds at 13 frequencies from 0.5 to 20 kHz were collected pre- and post-exposure. The functional data were converted to pre- minus post-exposure shift and overlaid upon the cytochleogram of cochlear damage using the frequency-place map for the chinchilla. The magnitude and frequency-specific location of components in the $2f_1-f_2$ TLS patterns were determined and group averages for each OBN and L_1, L_2 combination were calculated. The f_2-f_1 TLS was also examined in ears with focal lesions ≥ 0.4 mm. The $2f_1-f_2$ TLS (plotted at f_1) and TTS aligned with the extent and location of damaged supporting cells. The TLS patterns had two features which were unexpected; a local minimum at about a half octave above the center of the OBN with a local maximum above and below it, and a local minimum (often with negative shift) at the apical boundary of the supporting-cell damage. The magnitudes of the TLS and TTS generally increased with increasing exposure SPL. The peaks of the TLS and TTS, as well as the local TLS pattern components moved apically as the OBN was increased. However, there was no consistent pattern-relation with L_1, L_2 combinations. In addition, neither the $2f_1-f_2$ nor f_2-f_1 TLS for any L_1, L_2 combination consistently detected focal lesions (100% OHC loss) from 0.4 to 1.2 mm in length. Often at focal lesions, the TLS went in the opposite direction from what would be expected. Thus, TLS is sensitive to and reflects a differing mechanism for noise-induced temporary hearing loss than for permanent hearing loss.

395 Hair Cell Damage and Recovery from High-Level Noise Exposures in the Amphibian Papilla of the Bullfrog.

Dwayne D Simmons^{1,2}, Miriam Burton³, Steve N Johnson³, Rebecca A Hooper¹, Richard A Baird³

¹Otolaryngology and Central Institute for the Deaf, Washington University, 660 Euclid Ave., St. Louis, MO, United States,

²Anatomy and Neurobiology, Washington University, 660 Euclid Ave., St. Louis, MO, United States, ³Research, Central Institute for the Deaf, 4560 Clayton Ave., St. Louis, MO, United States

The bullfrog amphibian papilla (AP), although lacking a basilar membrane, is a sensitive frequency analyzer that is tonotopically organized and generates distortion-products (DPs). Although aminoglycoside ototoxicity has been studied in the bullfrog inner ear, there has been no study of noise-induced damage. Our goal was to determine if (1) noise could induce hair cell damage and recovery in the AP and (2) DPs could be used to monitor the effectiveness of noise exposure and the temporal course of hair cell recovery. For this purpose, we exposed bullfrogs to 1/3- and 1-octave noise bands centered around 800 Hz for 20 hours at levels ranging from 105-155 dB SPL, measuring functional changes with DP 2f1-f2 and morphological changes with confocal microscopy 0, 3 and 9 days after noise exposure.

In control ears, we recorded the most robust DPs when the geometric mean between f1 and f2 was between 500 and 1250 Hz. The peak DP was obtained with an f2 frequency of 800 Hz with a steep low frequency growth rate and a shallower high frequency decline. Following high-level (>150 dB SPL) noise exposures, there was a 20-30 dB drop in DP levels between 500 and 1000 Hz. DPs recovered to normal levels within 3 days after noise exposure. Ears exposed to noise levels >150 dB SPL displayed significant damage, including extruding hair cells, fragmenting hair cells, and hair cells with missing hair bundles. This damage was concentrated on or near the mature hair cell margin of the caudal region. Missing hair cells were replaced by scar formations by 3 days and significant hair cell recovery was seen by 9 days after noise exposure, including numerous repairing or regenerating hair cells with immature hair bundles. Our results suggest that DPs are a sensitive predictor of hair cell damage but not of hair cell recovery. Although not well correlated with morphological recovery, DP recovery was better correlated with hair bundle number than with the number of hair cells, suggesting that DPs require intact hair bundles and are produced by active hair bundle micromechanics.

396 Leisure Noise (Toy Pistols; Rock Music) versus Broadband Noise: Short- and Long-Term Effects on the Inner Ear.

Christiane Elisabeth Michaelis, Kerstin Deingruber, Renate Scheler, Hans-Joachim Steinhoff, Wolfgang Arnold, Kerstin Lamm

ENT-Department, Technical University Munich, Ismaninger Str. 22, Munich, Germany

In the present study guinea pigs were exposed to gun shots of toy pistols (183 + 5 dB SPL p.e., 8 shots, 1/min) and rock music (106 dB mean SPL, 2 x 2,5 h). The functional and morphological influence on the cochlea was compared to the effects of broadband

noise (115 dB SPL, 2 x 2,5 h). The threshold shifts were evaluated at 1.5, 2, 3, 4, 6, 8, 12 and 16 kHz at regular time intervals until day 21 after noise exposure using ABR and DPOAE I/O functions. Furthermore hair cell loss was evaluated using a fluorescence microscope (cytococheleograms). After the acoustic trauma induced by toy pistols a permanent threshold shift of 25 - 34 dB at 3 - 6 kHz occurred. These findings were in accordance with the outer hair cell loss in the cytococheleograms. Exposure to rock music led to a permanent threshold shift of 38 - 43 dB at 8 - 16 kHz. However, hair cell counts did not differ from controls and ciliae appeared normal. Permanent threshold shifts of animals exposed to broadband noise were 23 - 32 dB at 1.5 - 8 kHz, but ciliae were damaged in the 0.4 - 1.5 kHz cochlea region while hair cell bodies appeared normal. The results lead to new aspects respecting the pathophysiology and morphology of noise-induced hearing loss.

Supported by: Deutsche Forschungsgemeinschaft DFG La 670/4-1; Dr. Helmut Legerlotz Stiftung

397 Degeneration of the fibrocytes in the spiral ligament primarily mediates hearing loss caused by acute cochlear mitochondrial dysfunction.

Yasuhide Okamoto, Noriyuki Houya, Kazusaku Kamiya, Hiroyuki Ozawa, Susumu Nakagawa, Hidenobu Tajiri, Masato Fujii, Tatsuo Matsunaga

Otolaryngology, National Tokyo Medical Center, 2-5-1 Higasigaoka, Meguro-ku, Japan

Impairment of mitochondria is thought to be one of the contributing factors in the pathogenesis of sensorineural hearing loss. To elucidate the effect of acute mitochondrial dysfunction on the cochlea, the effect of mitochondrial toxin, 3-Nitropropionic Acid (3-NP) on rat cochlea was investigated. ABR measurement and histological evaluation of the cochlea were conducted at 3h, 1d, 1w and 2w after the administration of 3-NP. Rats administered 3fÊl of 500mM 3-NP into the round window niche showed threshold shift that were beyond measurement limits at approximately 3h after the administration, and the threshold shift persisted for at least 2w. Light microscopic examination of the cochlea revealed degeneration of the spiral ligament at 3h after the administration, and that of the stria vascularis at 2w after the administration. By electron microscopy, marginal cells and intermediate cells were degenerated in stria vascularis, and type†T and type†U fibrocytes were degenerated in spiral ligament. In contrast, the organ of corti showed only mild degeneration throughout the experimental period, and spiral ganglion neurons showed only transient swelling of mitochondria. These results suggest that ABR threshold shift was primarily caused by the dysfunction of the spiral ligament. Because the spiral ligament plays essential roles in K+ ion recycling which is indispensable for normal hearing, the impairment of K+ ion homeostasis was speculated as the mechanism for the observed threshold shift. The present study revealed high vulnerability of spiral ligament to acute mitochondrial dysfunction. Because inhibition of mitochondria causes energy deficit of the cell, the pathological changes in the spiral ligament may underly the pathogenesis of acute hearing loss due to cochlear energy failure such as ischemia.

398 Immunoelectron microscopic analysis of neuronal damage caused by glutamate in the organ of Corti during ischemia

Akira Sasaki¹, Atsushi Matsubara¹, Taku Inoue¹, Keiji Tabuchi², Akiko Nakamori², Akira Hara², Hideichi Shinkawa¹

¹Department of Otorhinolaryngology, Hirosaki University School of Medicine, 5 Zaifu-cho, Hirosaki, Japan, ²Department of Otolaryngology, Institute of Clinical Medicine, University of Tsukuba, 1-1-1 Tennodai, Tsukuba, Japan

It was suggested that excessive glutamate released from intracellular stores causes neurotoxic effect in pathological states, such as during ischemia in the inner ear, as well as in the central nervous system. In the present study, we investigated the correlation between the morphological change and the cellular glutamate concentration in the organ of Corti during ischemia by means of immunoelectron microscopic analysis.

Transient local anoxia (10min, 30min) of the guinea pig inner ear was induced by pressing the left labyrinthine artery. The right sides were used as controls. Ultrathin sections of the bilateral organs of Corti were made, and glutamate and glutamine was immunostained by post-embedding immunogold procedure. The number of gold particles counted in a given area was expressed as the particle density (particles/ μm^2). The gold particle densities representing glutamate were compared between the ischemic side and the control side in hair cells and supporting cells.

The particle densities in inner and outer hair cells and supporting cells on the 30-min ischemic side were significantly lower than those of the control side. In the 10-min ischemic side, the particle densities in outer hair cells and border cells were significantly low compared to the control side. Morphological changes were also observed in afferent dendrites connecting to inner hair cells on the 30-min ischemic side.

The decrease of the cellular glutamate concentration during ischemia was thought to be due to glutamate released from intracellular stores. The morphological changes of the 30-min ischemic side may be correlated with excessive glutamate released from hair cells and supporting cells. On the other hand, glutamate release was suggested in the 10-min ischemic side, however, the morphological changes were not observed. This is consistent with the previous electrophysiological study in unilateral transient inner ear ischemic models. That study had suggested that the elevation of the compound action potential (CAP) thresholds in 10-min ischemia had been transient, however, neuronal damage of the inner ear had been irreversible in 30min of ischemic duration (Tabuchi 1998).

399 The neuronal damage and the change of cellular distribution of glutamate and glutamine in the guinea pig vestibular endorgans during ischemia

Atsushi MATSUBARA¹, Akira SASAKI¹, Keiji TABUCHI², Akiko NAKAMORI², Akira HARA², Hideichi SHINKAWA¹

¹Otorhinolaryngology, Hirosaki University School of Medicine, 5 Zaifu-cho, Hirosaki, Japan, ²Clinical Medicine, University of Tsukuba, 1-1-1 Tennodai, Tsukuba, Japan

Glutamate, an afferent neurotransmitter in the inner ear, is thought to cause neurotoxic effect through the glutamate receptors in pathological states such as ischemia, when glutamate is released excessively from intracellular stores. In the present study, we investigated the morphological ischemia-induced damage and the changes of the cellular distribution of glutamate and glutamine in the guinea pig vestibular endorgans by means of post-embedding immunoelectron microscopic analysis. Unilateral transient ischemia of the guinea pig inner ear was induced by pressing the left labyrinthine artery (10min, 30min). Although no obvious morphological change in the 10-min ischemic inner ear animals was observed in the vestibular sensory epithelia, 30-min ischemic insult caused the swelling of both bouton type endings contacting with type II cells and nerve chalice surrounding type I cells, and the enlargement of intercellular spaces between the type I hair cells and the nerve chalice. The gold particle densities (the number of particles/ μm^2) representing glutamate (visualized with 20nm gold) of the type I and type II hair cells and supporting cells on the ischemic side were lower than those on the control side, and the reduction rates of gold particle densities in 30-min ischemia were higher than those in 10-min ischemia in each cell type. It should be noted, however, that the decreased density of gold particles might be caused by cytoplasmic edema. We confirmed that this was not the case, because the gold particle densities representing glutamine (visualized with 10nm gold) on the ischemic sides were not lower than those on the control sides. Therefore, the decrease of gold particle densities representing glutamate of these cells may be due to glutamate release from these cells during ischemia. Our previous study revealed the distribution of AMPA receptors in the nerve chalice and bouton type endings (Matsubara et al. 1999). These data suggest that excessive release of glutamate from the type I and type II hair cells and the supporting cells damages the bouton type endings and the nerve chalice in 30-min ischemia.

400 Actin, but not Microtubular, Cytoskeletal Processes Mediate Closure of Supporting Cell Scar Formations.

Andrew J Hordichok, Peter S Steyger

Oregon Hearing Research Center, Oregon Health & Science University, 3181 SW Sam Jackson Park Road, Portland, Oregon, United States

Dying hair cells in vertebrate inner ear sensory organs are typically extruded from the sensory epithelium. The apices of the supporting cells surrounding the extruding hair cells converge to seal the potential breach in the sensory epithelium, thus maintaining the physical separation of the electrochemically distinct endolymph and perilymph. What are the cellular mechanisms that enable the

hair cell to be physically extruded from the epithelium and ensure epithelial closure by the surrounding supporting cells? Dynamic microtubular mechanisms have been proposed for hair cell extrusion, and dynamic actin-based mechanisms have been described for epithelial closure in MDCK cell lines (Rosenblatt et al., 2001, *Curr Biol.*, 11, 1847-57).

We tested the role of these two different mechanisms using bullfrog saccular explants incubated in gentamicin for 6 hours, and allowed to recover for an additional 18 hours. To block dynamic cytoskeletal processes, colchicine, paclitaxel (microtubule inhibitors), cytochalasin D, or latrunculin A (actin inhibitors) were added to culture media for 30 minutes prior to, during and after gentamicin treatment. After 24 hours, saccules were fixed, labeled for actin and cytokeratins, and processed for confocal microscopy.

Neither set of cytoskeletal inhibitors prevented the extrusion of saccular hair cells. Microtubule inhibitors did not prevent the expansion of supporting cell apices during hair cell extrusion. Both actin inhibitors did prevent expansion of supporting cell apices during and after hair cell extrusion, precluding supporting cell scar formation. Thus, actin-based cytoskeletal processes are involved in supporting cell scar formation. In contrast, neither actin nor microtubular processes appear to be involved in hair cell extrusion.

Funded by NIDCD 04555s and Oregon Lions Sight and Hearing Foundation.

401 Reduction of Gentamicin Uptake in Hair Cells *in vitro*

Peter S Steyger¹, Nathan Spencer^{1,2}, Andrew J Hordichok¹, Robert M Raphael², Sigrid E Myrdal¹

¹*Oregon Hearing Research Center, Oregon Health & Science University, 3181 SW Sam Jackson Park Road, Portland, Oregon, United States,* ²*Bioengineering, Rice University, MS 142, PO Box 1892, Houston, Texas, United States*

Deafness and nephrotoxicity are serious side-effects of aminoglycoside (AG) therapy. Using a cultured kidney tubule model (see companion ARO2004 abstracts), we demonstrated that uptake of fluorescently-labeled gentamicin (GTTR) into cytoplasmic and intra-nuclear compartments is saturable, mediated, at least in part, by cation channels, and regulated by TRPV1-specific agonists and antagonists. The cation blocker Ruthenium Red severely reduces GTTR uptake. Now we report utilizing similar experimental conditions to examine GTTR uptake into bullfrog saccular, and murine cochlear explants.

After live incubation with GTTR, washed, fixed and delipidated inner ear explants revealed extensive cytoplasmic and intra-nuclear GTTR labeling. In all explants tested under normal calcium concentrations, the specific, competitive, TRPV1 agonist, RTX, reduced GTTR uptake, while the specific TRPV1 antagonist, I-RTX, increased uptake. At supranormal calcium concentrations, GTTR uptake was increased in the absence of other drugs, but was decreased in the presence of RTX. The non-specific cation blocker Ruthenium Red reduced GTTR uptake, with or without additional treatments.

These data demonstrate that cellular accumulation of GTTR in inner ear explants responded to the same cation and TRPV1 regulators as did the kidney cell model. This information should provide a powerful new platform for the development of co-therapeutics that

will reduce or prevent AG cellular penetration during antibiotic treatment.

Funded by R01 04555, R21 06084, and R01 02775s.

402 TRPV1 Channel Mediates Gentamicin Entry In Cultured Kidney Cells

Sigrid E Myrdal, Peter S Steyger

Oregon Hearing Research Center, Oregon Health & Science University, 3181 SW Sam Jackson Park Road, Portland, Oregon, United States

TRP receptors are calcium permeant cation channels that transduce a variety of sensory stimuli, including pain, heat, cold, taste, light, fluid flow, osmolarity, and probably sound. Several cells responding to these stimuli also preferentially retain the aminoglycoside antibiotic (AG) gentamicin, including inner ear hair cells and kidney proximal tubule cells. AG retention by these cells can lead to permanent hearing loss and nephrotoxicity, respectively. Understanding how AGs enter cells is key to preventing cytotoxicity during AG treatment. In another poster, we show that gentamicin-conjugated Texas Red (GTTR) enters the cytoplasm and nucleus of cultured kidney cells via an endosome-independent pathway. Here, we used GTTR to investigate the mechanism of gentamicin entry.

MDCK kidney cells show cytoplasmic and nuclear GTTR uptake within 30 seconds at room temperature, precluding endosomal uptake. Examining GTTR uptake under these conditions, we tested the effects of several conditions known to regulate cation currents through TRPV1 channels. Extracellular Ca⁺⁺ altered GTTR uptake. Uptake/binding peaked at 0.16 mM Ca⁺⁺, and was reduced at higher concentrations. GTTR uptake was greatest between pH 5 and 6. Specific TRPV1 agonists, RTX and anandamide, enhanced GTTR uptake in Ca⁺⁺-free media, but reduced uptake in the presence of Ca⁺⁺, consistent with the known Ca⁺⁺-dependent desensitization of TRPV1. Paradoxically, GTTR uptake was also enhanced by competitive TRPV1 antagonists, iodo-RTX and SB366791. GTTR uptake was reduced by the non-specific cation channel blocker Ruthenium Red, and by PIP₂ in the treatment buffer. These data suggest that gentamicin can enter cells via non-selective cation channels, including TRPV1. Elucidating these uptake mechanisms could lead to therapeutic interventions in AG oto- and nephrotoxicity, and expand appreciation of TRP channel functions.

Funded by NIDCD R01 04555 and R21 06084.

403 Cytoplasmic And Nuclear Binding Of Gentamicin Does Not Require Endocytosis

Sigrid E Myrdal, Peter S Steyger

Oregon Hearing Research Center, Oregon Health & Science University, 3181 SW Sam Jackson Park Road, Portland, Oregon, United States

Understanding the uptake mechanisms of aminoglycoside antibiotics (AGs), and their sub-cellular distribution will enable identification of AG-sensitive targets, and potential uptake blockers. Using the AG gentamicin (GT) linked to the fluorophore Texas Red (GTTR), we examined the distribution of GT in kidney tubule cells, which provide a good model for inner ear cells.

As reported elsewhere, GTTR was seen in endosome-like vesicles in live or formaldehyde-fixed kidney cells. However, delipidation of fixed cells revealed GTTR labeling in the cytoplasm and nucleus, but no longer in endosomes. This novel GTTR distribution was quenched by PIP₂. GTTR cytoplasmic and nuclear binding occurred both at 37°C and on ice. At both temperatures binding was time-dependent and saturable, with increasing concentrations of unlabeled GT serially decreasing cytoplasmic and nuclear GTTR fluorescence. In cells imaged while still live, high doses of unlabeled GT did not reduce endocytotic GTTR uptake. And, no fluorescence was seen in live cells treated with GTTR on ice, showing that the endocytotic GTTR compartment is not related to cytoplasmic penetration of the drug.

These data describe a saturable, cytoplasmic and intra-nuclear gentamicin distribution that may represent the biorelevant intracellular binding sites. GTTR uptake by an endosome-independent mechanism suggests that gentamicin enters cells via ion channels or pores in the plasma membrane.

Funded by NIDCD R01 04555 and R21 06084.

404 Late Stage Apoptosis in Ejected Hair cells of the Gentamicin-Treated Avian Cochlea

Dominic A Mangiardi¹, Kate Williamson², Luke Duncan², David C Mountain¹, Douglas A Cotanche²

¹Biomedical Engineering, Boston University, 44 Cummington St, Boston, MA, United States, ²Otolaryngology, Children's Hospital of Boston, 21-27 Burlington Ave, Boston, MA, United States

Aminoglycoside-induced hair cell death in the avian cochlea occurs in a caspase-dependent manner. We have previously reported that TIAR translocation, cytochrome c release, and caspase-3 activation occur in hair cells prior to ejection from the sensory epithelium following subcutaneous injection of gentamicin (300 mg / kg) in 14 day old chicks. We now report that following ejection hair cells lose membrane integrity, exhibit packaging of nuclear contents and subsequent loss of nuclear labeling, and loss of phalloidin labeling of F-actin. These changes occurred by 96 hours after gentamicin treatment or roughly 48 hours after damaged hair cells were ejected. However, remnants of ejected hair cells were detectable as late as 168 hours with cytochrome oxidase subunit I (Cox) and myosin VI and VIIa antibody labeling (see poster by Duncan et al. for description of myosin labeling). Hair cell remnants remain in the overlying tectorial membrane while new hair cells are produced in the underlying sensory epithelium. These results contribute to a complete timeline of aminoglycoside-induced apoptotic death of avian hair cells *in vivo*.

Supported by NIH/NIDCD Grant #DC01689, the Children's Hospital Otolaryngology Foundation Research Fund and the Sarah Fuller Fund

405 Changes in Two Unconventional Myosins During Gentamicin Induced Hair Cell Death and Regeneration in the Inner Ear

Luke Duncan^{1,2}, Kate Williamson², Dom Mangiardi^{2,3}, Douglas Cotanche^{2,4}

¹Chemistry, Holy Cross College, 1 College Street, Worcester, MA, United States, ²Otolaryngology, Children's Hospital, 300 Longwood Ave, Boston, MA, United States, ³Biomedical Engineering, Boston University, 44 Cummington Street, Boston, MA, United States, ⁴Otology & Laryngology, Harvard Medical School, 243 Charles Street, Boston, MA, United States

Gentamicin is an aminoglycoside antibiotic that is cheaply produced and readily available. Unfortunately, it is also ototoxic and nephrotoxic at the effective dose regimen. The ototoxic effect of the drug causes apoptosis of the hair cells in the cochlear and vestibular system, diminishing hearing as well as balance. In mammals, this damage is irreversible; however birds have the capacity to regenerate hair cells. We have studied the changes in protein expression and distribution that accompany hair cell apoptosis in the chick cochlea induced by gentamicin treatment. Immunocytochemical labeling of chick cochlear hair cells following a single systemic gentamicin injection (300 mg/kg) revealed an unexpected response pattern for myosin VI and myosin VIIa: both of these unconventional myosins were more heavily expressed in the ejecting, dying hair cells than in normal hair cells. Expression of late stage apoptotic proteins and structural damage to hair cells were first seen 36h after gentamicin injection and ejection of dying hair cells occurred between 40-48h. The ejected hair cells remained within the overlying tectorial membrane through 168h (see abstract by Mangiardi et al). Changes in myoVI and myoVIIa expression began at 36h when labeling became more intense and extended up into stereociliary bundles. Myosin labeling of recently ejected hair cells surrounded condensing and pyknotic nuclei. At later times the pyknotic nuclei were either no longer labeled or sequestered away from the myosin label. Intense myosin labeling remained in hair cell cytoplasmic contents within the tectorial membrane long after the cells were ejected (168h). These results indicate that changes in the distribution of myoVI and myoVIIa accompany apoptosis and may play a functional role in cell death or disassembly.

Supported by NIH/NIDCD Grant #DC01689, the Children's Hospital Otolaryngology Foundation Research Fund and the Sarah Fuller Fund.

406 Actin cytoskeletal rearrangements in the cochlea induced by kanamycin

Hongyan Jiang, Su-Hua Sha, Andra Talaska, Jochen Schacht

University of Michigan, Kresge Hearing Research Institute, 1301 East Ann Street, Ann Arbor, Michigan, United States

Actin is a major component of the cytoskeleton of the organ of Corti, and redox-dependent Rho GTPase-linked pathways can control actin cytoskeletal rearrangements. Once the actin cytoskeleton is remodeled by stress stimuli, cell adhesion and permeation are altered, as well as cell functions and cell fate. Since reactive oxygen species (ROS) has been implicated as a causative

factor in aminoglycoside-induced hearing loss, investigation of the actin assembly in the organ of Corti after aminoglycoside treatment should shed further light on the cellular mechanisms involved in the loss of hair cells.

We investigated actin cytoskeleton remodelling in the mouse cochlea during kanamycin treatment. The preliminary data indicate that kanamycin decreases the level of total actin and F-actin, changes the basilar membrane structure, and alters the tight junctions between outer hair cells and supporting cells. Furthermore, beta-actin translocation into the nucleus is inhibited specifically in outer hair cells while the ADP-ribosylation factor 6 (Arf6), a GTP-binding protein, decreases only in supporting cells. These findings suggest a possible mechanism by which aminoglycoside-induced changes of the cellular redox state inhibit the activity of small GTPases that control the rearrangements of the actin cytoskeleton.

Supported by research grant DC-03685 from the National Institute on Deafness and Other Communication Disorders, NIH.

407 Aminoglycoside Ototoxicity: Formation of Free Radicals by a Ternary Gentamicin-Iron-Lipid Complex

Wojciech Lesniak^{1,2}, Vincent Pecoraro², Jochen Schacht¹

¹Kresge Hearing Research Institute, University of Michigan, 1331 E. Ann, Ann Arbor, Michigan, United States, ²Department of Chemistry, University of Michigan, 930 N. University Ave, Ann Arbor, Michigan, United States

The success of aminoglycosides as chemotherapeutic agents results from their broad spectrum of applicability which covers mostly Gram-negative bacteria, and their very low cost. However, therapy with aminoglycoside antibiotics has two predominant side effects: damage to the proximal tubules of the kidneys (nephrotoxicity) and to the sensory cells of the inner ear (ototoxicity). Nevertheless, they are currently the first choice antibiotic in developing countries and are still widely used in industrialized countries for the treatment of serious bacterial infections.

There is a large body of evidence showing that the toxicity of these drugs is related to oxidative reactions resulting from their interactions with iron ions and arachidonic acid as an electron donor. Furthermore, the degree of ototoxicity of aminoglycoside antibiotics correlates well with their binding affinity to polyphosphoinositides. To gain a more detailed understanding of the mechanism underlying aminoglycoside ototoxicity, interactions of gentamicin with phosphatidylinositol 4,5-bisphosphate (PIP₂) or arachidonic acid in the presence and absence of ferrous or ferric ions were investigated. Data from nuclear magnetic resonance and mass spectrometry suggest that, when bound to PIP₂ gentamicin in combination with iron ions, facilitates peroxidation and release of arachidonic acid which is the predominant fatty acid in the 2-position of PIP₂. The peroxidation of arachidonic acid promoted by gentamicin involves a ternary complex: one Fe²⁺ or Fe³⁺ ion chelated by one molecule of arachidonic acid (donating two oxygen atoms from the carboxyl group) and one molecule of gentamicin (contributing the 3-NH₂ group of 2-deoxystreptamine ring and the glycosidic oxygen located between the purpurosamine and 2-deoxystreptamine ring). This binding mode leaves two axial coordination sites occupied by H₂O that can be easily substituted by molecular oxygen resulting in an electron transfer reaction and

superoxide anion formation (AAFe²⁺G + O₂ ↔ [AAFe²⁺G-O₂ ↔ AAFE³⁺G-O₂·] ↔ AAFE³⁺G + O₂⁻). Superoxide anion dismutates to form H₂O₂, substrate for OH radical formation (AAFe²⁺G + H₂O₂ → AAFE³⁺G + OH· + OH·). The hydroxyl radical may then initialize the peroxidation of fatty acids leading to peroxy and alkoxy radical formation that propagate further peroxidation reactions.

This work was supported by grant DC – 03685

408 Autometallographical Amplification of Intracellular Anti-cancer Platinum Molecules

O'neil W Guthrie¹, Carey Balaban²

¹Communication Science and Disorders, University of Pittsburgh, Forbes Tower, Pittsburgh, PA, United States, ²Otolaryngology and Neurobiology, University of Pittsburgh, 203 Lothrop, Pittsburgh, PA, United States

This study utilized autometallography (Danscher et al., Neuroscience 105, 941-947, 2001) to localize platinum in tissue. Platinum molecules from the drug cisplatin were amplified by reducing silver ions to silver atoms while chelating platinum bound to intracellular ligands. This redox activity allowed for detection of platinum embedded in black silver deposits at the light microscopy level. Kidneys were harvested from a Sprague-Dawley rat that was treated with 13 mg/kg of cisplatin i.p., euthanized 24 hours later and perfused transcardially with formalin. Control kidneys were harvested from an untreated, formalin-perfused Sprague-Dawley rat. Both control and experimental tissues were post-fixed with 10% buffered formalin and cryoprotected in PBS + 30% sucrose. Free-floating sections were kept in anti-freeze solution (300 ml ethylene glycol, 500 ml PBS and 300 g sucrose) at -12° C overnight. Sections were then rinsed in Na acetate buffer before being immersed in a physical developer (AgNO₃, Na acetate trihydrate, glacial acetic acid, cetylpyridinium Cl, Triton X-100, Na tungstate and Ascorbic acid). Silver deposits were fixed in potassium thiosulfate and sections were dehydrated and cover slipped. Autometallography silver deposits were observed in the nuclei of the distal convoluted tubules of the kidney from the rat receiving systemic treatment of cisplatin. In vitro exposure of kidney tissues to 5 mM of cisplatin for 1 hour, by contrast, resulted in heavy staining of the renal cortex and less staining in the renal medulla. These findings suggest that autometallography may be a useful method for studying cisplatin uptake and distribution at the cellular level. [Supported by NIH-NIDCD (F31) DC05757-01 and the Eye & Ear Institute Foundation. The authors wish to thank Dr. Richard Salvi for providing tissue treated in vitro and Dr. Len Rybak for providing the in vivo treated materials.]

409 Effects of dihydroxybenzoate on kanamycin-distribution in kanamycin-treated mice

Tadashi Kitahara, Ha-sheng Li, Carey D Balaban

Otolaryngology, University of Pittsburgh, 203 Lothrop street Suite 153, Pittsburgh, PA, United States

Kanamycin (KM) is an aminoglycoside antibiotic, which shows toxic side effects especially on kidney and inner ear. Dihydroxybenzoate (DHB) is an antioxidant, which prevents free radicals from cell damage. In the previous paper, Wu et al. [Hear Res 158: 165-178, 2001] determined toxic doses of KM for the

mouse inner ear and protective doses of DHB. This study examined KM-distribution in KM- and/or DHB-treated mice using immunohistochemistry with anti-KM antibody.

Two mouse strains, C57BL/6 (C57) and CBA/J (CBA) mice, all at an age of 4 weeks were used. For each strain, the animals were divided into four groups as follows: saline and NaHCO₃-injected (CONT), KM and NaHCO₃-injected (KM), KM and DHB-injected (KM/DHB) and saline and DHB-injected (DHB) groups. KM sulfate was purchased from USB Corporation (OH, USA) and dissolved in physiological saline at the concentration of 35 mg kanamycin base/ml so that a dose of 700 mg of kanamycin base/kg body weight is obtained by injecting 0.02 ml/g body weight. DHB was purchased from Aldrich Chemical Corporation (WI, USA) and dissolved in 2.5% NaHCO₃ at the concentration of 15 mg/ml (pH between 7.0-8.0) so that a dose of 300 mg of DHB/kg body weight is obtained by injecting 0.02 ml/g body weight. Treatments were done twice daily for 14 days. For each group and each strain, three animals were euthanized with pentobarbital (100mg/kg, i.p.) and perfused transcardially with 0.1M PBS, followed by paraformaldehyde-lysine-periodate fixative. Anti-KM primary antibody was purchased from US Biological (MA, USA).

In the KM group, strong KM-like immunoreactivity (LIR) was detected in kidney and liver tissues in C57 and CBA. In inner ear, some of cochlear and vestibular hair cells were heavily stained and supporting cells and glial cells were moderately stained with the antibody. However, KM-LIR was hardly observed in stria vascularis, spiral or Scarpa's ganglion cells. No KM-LIR was seen in striated muscle cells or brain tissues in any strain. In the KM/DHB group, KM-LIR in kidney, liver and inner ear tissues were greatly attenuated compared with the KM group. In CONT and DHB groups, KM-LIR was absent. These findings are consistent with the concept that KM accumulation damages specifically to kidney, liver and inner ear hair cells and that DHB blocks KM accumulation and cell damage, either by inhibiting KM-uptake or by facilitating KM degradation by these cells.

(Supported by the Eye & Ear Institute Foundation).

410 Organ of Corti (OC-k3) cells as a model for oxidative stress in the cochlea

Vickram Ramkumar¹, Craig A. Whitworth², Sandeep Pingle¹, Leonard P. Rybak³

¹Pharmacology, Southern Illinois University School of Medicine, P. O. Box 19629, Springfield, IL, United States, ²Surgery, Southern Illinois University School of Medicine, P. O. Box 19628, Springfield, IL, United States, ³Surgery, Southern Illinois University School of Medicine, P. O. Box 19653, Springfield, IL, United States

We have previously shown that conditions linked to increased oxidative stress in the cochlea, such as cisplatin treatment or noise exposure, lead to increased expression of the adenosine A₁ receptor (A₁AR). The A₁AR receptors are localized to specific regions of the cochlea, such as the organ of Corti, stria vascularis and spiral ganglion cells, and their activation mediates protection of the cochlea against hearing loss induced by ototoxic drugs and noise. Detailed biochemical studies concerning the mechanism underlying these events are lacking due to the limited availability of tissue and difficulty in pharmacological manipulation *in vivo*. To avoid

these problems, we have utilized the immortalized cell line (OC-k3 cells) derived from the organ of Corti of transgenic mice in order to study regulation of the A₁AR by cisplatin. Expression of the A₁AR by OC-k3 cells was determined by radioligand binding studies and immunocytochemistry. When these cells were exposed to cisplatin (2.5 μM) for 24 h, we observed a significant increase in A₁AR expression, which correlates well with our *in vivo* findings. This increase in A₁AR expression was accompanied by an ~ 2.5 fold increase in the activity of NADPH oxidase. Examination of stress-regulated transcription by electrophoretic mobility shift assays indicate an ~ 2.5-fold increase in nuclear factor (NF)-κB but with no change in activator protein (AP)-1. The increase in (NF)-κB was attenuated when cells were treated with diphenyleneiodonium sulfate, an inhibitor of NADPH oxidase, suggesting a role of ROS in the activation of (NF)-κB in these cells. Our findings indicate that OC-k3 cells can serve as a useful model to study the mechanism(s) underlying drug ototoxicity and otoprotective agents.

We thank Dr. Federico Kalinec for providing OC-k3 cultures. This research was supported by the National Institutes of Health NIH (NIDCD) grant # RO1 DC02396.

411 The role of reactive radicals in degeneration of the auditory system of mice following cisplatin treatment

Tetsuya Tamura¹, Takayuki Nakagawa¹, Ji Eun Lee², Tae Soo Kim¹, Tsuyoshi Endo¹, Atsushi Shiga³, Fukuichiro Iguchi¹, Tomoko Kita^{1,4}, Ken Kojima¹, Juichi Ito¹

¹Department of Otolaryngology-Head and Neck Surgery, Kyoto University Graduate School of Medicine, 54 Kawahara-cho, Shogoin Sakyo-ku, Kyoto, Japan, ²Department of Otolaryngology, School of Medicine, Kyungpook National University Hospital, Samduk-dong 2-50, Jung-gu, Daegu, Korea, Republic of, ³Department of Otolaryngology, Aichi Medical University, Nagakute, Aichi, Japan, ⁴Horizontal Medical Research Organization, Kyoto University Graduate School of Medicine, Shogoin Sakyo-ku, Kyoto, Japan

[Introduction] It is suggested that reactive radical species are involved in the mechanism of cisplatin-induced hearing loss. Free radical takes various metabolism courses and changes with organizations. There are hydroxyl radical and peroxyxynitrite as a radical species with the high toxicity generated from super oxide. A hydroxyl radical is generated through hydrogen peroxide from super oxide, and, on the other hand, peroxyxynitrite is produced by the reaction of super oxide and nitric oxide. In this study, we examined the expression of two highly reactive species, hydroxyl radicals and peroxyxynitrite, on the auditory system of mice following cisplatin treatment.

[Method] Cisplatin was directly injected into left semicircular canal of the C57 B6 mice. Experimental animals were divided into 3 groups according to the doses of applied cisplatin. The temporal bone was collected after two weeks of administration. Expression of hydroxynonenal (HNE), a marker of lipid peroxidation by hydroxyl radical and nitrotyrosine (NT),

a marker for protein peroxidation by peroxyxynitrite was examined by immunohistochemistry.

[Result and consideration] The loss of outer hair cells and spiral

ganglion neurons was found in cochleae affected by cisplatin. Both HNE and NT were detected in auditory epithelia and neurons damaged by cisplatin. Interestingly, auditory hair cells were positive for HNE, but not for NT. Our findings indicate a contribution of both HNE and NT to the degeneration of the auditory system due to cisplatin, and a crucial role of the hydroxyl radical in hair cell degeneration. Hydroxyl radicals may be a key molecule for protecting auditory hair cells from cisplatin toxicity.

412 In vivo Imaging of the Lateral Line Neuromast: Characterizing Aminoglycoside Susceptibility

Felipe Santos^{1,2}, Glen MacDonald^{1,2}, Kelly N Owens^{1,2}, David W. Raible^{2,3}, Edwin W Rubel^{1,2}, Lisa L Cunningham^{1,2}

¹Otolaryngology HNS, University of Washington, Box 357923, Seattle, WA, United States, ²Bloedel Hearing Research Center, University of Washington, Box 357923, Seattle, WA, United States, ³Biological Structure, University of Washington, Box 357420, Seattle, WA, United States

Hair cells of zebrafish lateral line neuromasts die in a dose-dependent manner when exposed to the aminoglycoside antibiotic neomycin. Lateral line hair cells are present at 3 days post-fertilization (DPF 3; Raible and Kruse, 2000 *JCN* 421:189), but they are relatively insensitive to neomycin-induced death prior to DPF 5 (Murakami et al., *Hear. Res.* in press). We are examining this differential sensitivity using *in vivo* imaging techniques.

We have developed a method for labeling neuromasts and examining aminoglycoside-induced hair cell death in living zebrafish larvae. The monomeric cyanine dye Syto 21 labels both hair cells and support cells in neuromasts. ToPro-3, another monomeric cyanine dye, selectively labels hair cells. The styryl dye FM1-43 is a marker of hair cell transduction and transduction-dependent endocytosis, and it is used here as a marker of mature functional hair cells. We find that hair cells at DPF 3 are ToPro-3 positive but FM1-43 negative, suggesting a relationship between functional maturity and onset of ototoxic sensitivity. By double-labeling with ToPro-3 and FM1-43 at DPF 5, we observe aminoglycoside-induced hair cell death after just 45 minutes of exposure to high doses (200-400 μ M) of neomycin. Control neuromasts contain an average of 7.9 double-labeled hair cells (n = a total of 10 neuromasts from 5 fish). Following 1 hour of exposure to 400 μ M neomycin, we observe a 76% reduction in double-labeled hair cells. These results indicate that neomycin-induced hair cell death can occur very rapidly in the lateral line neuromasts. This preparation can be used to directly examine the relationship between the onset of mechanosensory transduction and development of sensitivity to aminoglycoside-induced hair cell death. *This work is supported by NIH DC05987; DC04661; DC00018.*

413 Hair cell degeneration in zebrafish lateral line neuromasts: A good model for understanding inner ear hair cell degeneration?

Remy Pujol^{1,2}, Kelly N. Owens³, Marc Lenoir¹, Dale Cunningham^{2,3}, Jameel Itani^{2,4}, Lisa Cunningham^{2,3}, David W. Raible^{2,4}, Edwin W Rubel^{2,3}

¹INSERM Unit 583, University Montpellier 1, 71, Rue De Navacelles, Montpellier, France, ²Virginia Merrill Bloedel Hearing Research Center, University of Washington, Box 357923, Seattle, WA, United States, ³Otolaryngology-HNS, University of Washington, Box 357923, Seattle, WA, United States, ⁴Biological Structure, University of Washington, Box 357420, Seattle, WA, United States

Hair cell loss in the mammalian cochlea in response to aminoglycoside exposure is well documented, but remains poorly understood at the molecular level, particularly with respect to genetic influences on variability. To investigate these issues, we have begun studying neomycin effects on lateral line neuromasts of larval zebrafish, *Danio rerio*, an emerging system for vertebrate genetic and developmental analysis. We have previously documented the dose-dependent relationship between lateral line hair cell loss and neomycin exposure (Harris et al. 2003). Here we directly compared early cellular events associated with aminoglycoside-induced hair cell damage in lateral line neuromasts of 5 day-old zebrafish to those in mammalian organ of Corti using TEM analysis. At low doses of neomycin (25 μ M) and short recovery times, we observed hair cells with initial signs of damage. The most pronounced indicators included swollen mitochondria, fused stereocilia and chromatin condensation in the nuclei. Swollen mitochondria were a prevalent early indication of damage in the neuromasts hair cells. Conversely, mitochondria within afferent dendrites appear quite normal. When treated with low doses of neomycin, neuromasts were frequently observed with severely damaged hair cells residing next to hair cells with no apparent sign of damage. Moderate concentrations of neomycin (50-75 μ M) in the media for only 30 minutes resulted in pronounced damage, including presence of apoptotic- and necrotic-appearing hair cells or remnants of hair cells. Despite shorter neomycin exposure these findings parallel our previous observations, and indicate neomycin-induced hair cell loss can remarkably rapidly. In addition, the early ultrastructural events observed here are strikingly similar to the first signs of ototoxicity seen in the mammalian inner ear. Our results suggest that the lateral line of zebrafish is a useful model for understanding molecular events regulating some types of hair cell degeneration. *Supported by Bloedel Traveling Scholars Program and NIDCD grants DC 05987, DC00018, and DC04661*

414 Extraordinary Saccular Diversity in a Family of Deep-Sea Fishes

Xiaohong Deng¹, Hans-Joachim Wagner², Arthur N. Popper¹

¹Dept. of Biology and Neuroscience and Cognitive Science Program, University of Maryland, 1210 Biology-Psychology Bldg, College Park, Maryland, United States, ²Anatomisches Institut, University of Tübingen, D-72074, Tübingen, Germany

A structure never before seen in any vertebrate ear was found associated with the sacculae of some fishes in the mesopelagic deep-sea family *Melamphaidae*. In addition, fishes in this family show significant inter-specific diversity in other inner ear structures.

Ears were studied using freshly dead specimens of seven species. Otoliths were removed prior to fixation and sensory epithelia were examined using SEM. The shapes of the saccular otoliths varied considerably and ranged from a highly sculpted spear shape in one species to a non-sculpted button shape in another.

Unique to several species of this group was the presence of a long, thin, stalk-like structure protruding from the ventral-posterior margin of the saccular otolith. In *Melamphaes suborbitalis* the stalk touches the bony labyrinth. Moreover, instead of the usual rigid bony labyrinth found in most fishes, the bottom part of the bony labyrinth of *M. suborbitalis* is soft and elastic. The structure of the saccular macula of *M. suborbitalis* resembles that in species having very good hearing ability, with the rostral end of the tadpole-shaped epithelium highly enlarged. However, the sensory epithelium does not contact the protruding stalk. The stalk may give support to the large otolith or provide a connection between the otolith and other structures outside the ear chamber. In contrast, the saccular otolith in another member of the family, *Scopelogadus mizolepis mizolepis*, is round and smooth and does not have the stalk-like extension. The sensory epithelium in *Scopelogadus* is like an elongated oval, with two separate nerve branches innervating the rostral-ventral and dorsal-posterior portions of the epithelium.

The study of the saccular otoliths and maculae from the family *Melamphaidae* that have such extreme difference in structure may provide evidence regarding the functional role of the shape of the otolith in hearing.

415 Reciprocal synapses from type-II afferents contacting OHCs in the adult cat.

Fabio A. Thiers^{1,2}, M. Charles Liberman^{2,3}, Barbara J. Burgess², Joseph B. Nadol Jr.^{2,3}

¹Speech and Hearing Biosciences and Technology PhD Program, Harvard/MIT Division of Health Science and Technology, 77 Massachusetts Ave. E25-519, Cambridge, MA, United States,

²Department of Otolaryngology, Massachusetts Eye and Ear Infirmary, 243 Charles St., Boston, MA, United States,

³Department of Otolaryngology and Laryngology, Harvard Medical School, 243 Charles St., Boston, MA, United States

Outer hair cells (OHCs) form synaptic contacts with type-II cochlear afferent neurons and olivocochlear efferent neurons. These afferent and efferent contacts show classic ultrastructural features of chemical synapses, including vesicle clusters within the OHC and efferent terminal, respectively, indicating the presumed

direction of synaptic transmission. Ultrastructural studies in four primate species (including humans) suggest that type II afferents engage in bidirectional communication with OHCs via reciprocal synapses (Francis & Nadol, *Hear. Res.* 64: 184, 1993).

In the present study, we investigate whether the reciprocal OHC synapse is a peculiarity of the primate cochlea. OHCs from an adult cat were studied via electron microscopy of serial sections, cut parallel to the OHC rows. The sample of 20 OHCs was from the 3rd row, at the 1.6 kHz region, where classic efferent terminals are less prevalent. As in primates, OHC terminals could be classified into two groups: 1) small, vesicle-poor and neurofilament-rich terminals (putative afferent) and 2) large, vesicle-rich, neurofilament-poor terminals (putative efferent). Putative afferent terminals formed pure efferent-like and/or reciprocal synapses in all OHCs studied: efferent contacts were defined by a sub-synaptic cistern in the OHC and a vesicle cluster within the opposing terminal. In several instances, putative afferents formed different types of synapses on neighboring OHCs. The origin of these reciprocal synapses will be clarified by evaluation of a surgically de-efferented ear.

These results suggest that bidirectional communication between OHCs and type-II cochlear afferents may be a common feature of the mammalian ear. If true, the current view that neural modulation/control of OHCs is accomplished solely by the olivocochlear system may need to be re-evaluated.

Research supported by grant from NIDCD: DC00188 (MCL).

416 Localization of Multidrug Resistance Proteins and Pgp Efflux Pump in Chinchilla inner ear

Mei Zhang¹, Dalian Ding², Richard Salvi²

¹Department of Communicative Disorders, University of Florida, 1600 SW Archer Road, Gainesville, FL, United States, ²Center for Hearing and Deafness, SUNY at Buffalo, 3435 Main Street, Buffalo, NY, United States

The toxicity of aminoglycoside antibiotics and cisplatin-like compounds are affected by the uptake and/or extrusion of these compounds among the blood, cochlear fluids and across cellular membranes. The ATP-dependent, multidrug resistance pumps, MRP1 and MRP2, and p-glycoprotein (Pgp) actively extrude xenobiotics, drugs and toxins from many tissues thereby protecting against cellular damage. To identify the location of these pumps in the chinchilla, a popular model of ototoxicity, inner ear tissues were labeled by immunofluorescence and tissues examined by confocal microscopy. In the cochlea, strong Pgp immunolabeling was evident in interdental cells, spiral ganglion neurons, efferent terminals, capillaries and fibrocytes in the spiral ligament and the inner sulcus. Moderate to light Pgp labeling was present in hair cells in the crista, maculae and inner ear. In the cochlea, MRP1 was present in interdental cells, spiral ganglion neurons, Hensen, Claudius cells and Boettcher cells, pillar cells, the stria vascularis and in the stereocilia of IHCs and OHCs. MRP1 labeled the hair cells in the maculae and cristae, but the pattern of staining was nonuniform. MRP2 immunolabeling was present in interdental cells, fibrocytes of the spiral ligament and inner sulcus, stria vascularis, cuticular plate of inner and outer hair cells, heads of the Deiter's cells and efferent terminals. In the maculae and cristae,

MRP2 was present in the cytoplasm of type I and type II hair cells. The immunolabeling patterns for MRP1 and Pgp observed in the chinchilla show both similarities as well as differences with those previously reported by Saito and colleagues for rats and guinea pigs. These results suggest that MRP1, MRP2 and Pgp are likely to play an important role in modulating the toxicity of various ototoxic drugs and may account for organ or species differences in ototoxicity.

Supported by grant NIH P01 DC03600

417 Distribution of β Tubulin Isoforms in Rat Organ of Corti in Vivo and in Vitro

Julia Vent¹, Richard F. Ludueña², Richard Hallworth¹

¹Biomedical Sciences, Creighton University, 2500 California Plaza, Omaha, NE, United States, ²Biochemistry, U.T.H.S.C.S.A., 7703 Floyd Curl Drive, San Antonio, TX, United States

Tubulin, the principal component of microtubules, exists as two polypeptides, termed α and β . Seven isoforms of β tubulin are known to exist in mammals. The β tubulin isoforms I, II, III & IV and their distribution in the rat cochlea have been examined in this study. Organotypic cultures of rat organ of Corti were grown from P0 explants and compared to whole mount sections of rat and gerbil Corti organs at different stages in development (E18 to adult). After fixation with paraformaldehyde, sections were blocked, permeabilized and immunohistochemically stained with antibodies against isoforms of β tubulin. A positive control with an anti- β tubulin antibody known to stain all β tubulin isoforms, and a negative control with primary stock, were performed. In the organ of Corti, outer hair cells contained only β_1 and β_{IV} , while inner hair cells contained only β_1 and β_{II} . Inner and outer pillar cells contained β_{II} and β_{IV} , whereas Deiters cells contained β_1 , β_{II} and β_{IV} . Only neurons stained positive for β_{III} tubulin. With maturation and development of the organ of Corti, more specialized isoforms were found in contrast to an early general staining. The rat and gerbil inner ear development of β tubulin synthesis occurs at similar stages and time frames and can therefore be utilized as models interchangeably. [Supported by NIH (DC02053 and CA 267360, Welch Foundation AQ-0726, and US Army DAMD17-98-1-8246]

418 Distribution of Spectrin Isoforms in the Organ of Corti

Heather C Jensen-Smith¹, Rebecca Van Winkle¹, Jeanine A Ursitti², Robert J Bloch³, Richard Hallworth¹

¹Biomedical Sciences, Creighton University, Criss II Room 310, Omaha, NE, United States, ²Medical Biotechnology Center, University of Maryland, 721 W Lombard St, Baltimore, MD, United States, ³Department of Physiology, University of Maryland, 655 W Baltimore St, Baltimore, MD, United States

Spectrins are large (245-280kDa) cytoskeletal proteins that are components of the membrane-associated cytoskeleton in many cell types, including epithelial cells, neurons, erythrocytes, and skeletal muscle. Spectrin heterodimers of α and β isoforms associate head to head to form tetramers or larger assemblies. Four spectrin isoforms (erythrocyte αI and βI & non-erythrocyte spectrin or fodrin αII and βII) are commonly found in the nervous system. In the cochlea, the actin-spectrin cortex of the outer hair cell (OHC) is well known. However, spectrin has also been described in other

cochlea cell types, including inner hair cells (IHCs) and pillar cells.

We have investigated the distribution of spectrin isoforms using isoform specific antibodies. We find that organ of Corti cells exhibit unique combinations of isoforms. αI was not found. αII was found in OHCs (in the cuticular plate and the cortex of the lateral wall), IHCs (also in the cuticular plate and somatic wall), pillar cells, Deiters cells, ganglion cells and spiral limbus. Label in pillar cells was close to the plasma membrane of the long process. Label in Deiters cells was found only in the membrane of the Deiters cell soma, below the OHCs. βI was found in the same structures, except that the IHC cuticular plate (but not the cortex) was weakly labeled. Label in ganglion cells was unusual in that only about 50% of the neurons were labeled. The spiral limbus was labeled in a more restricted fashion than for αII , consisting of a few cells at the lip and along the lining of the sulcus. βII was found in the same structures, but was absent from the OHC cortex. Label was found uniformly in ganglion cells. Spiral limbus label was found in interdental cells, but not in the lining of the sulcus. Our results suggest that specific combinations of spectrin isoforms are localized in different cellular compartments to support specific functional roles. [Supported by NIH (DC02053, NS17282, HL64304), the Muscular Dystrophy Association, and a Clare Booth Luce Fellowship to HCJ-S].

419 Cochlear Terminations of Single Lateral and Medial Olivocochlear Neurons in the Rat

W. Bruce Warr, Jo Ellen Boche

Neuroanatomy Laboratory, Boys Town National Research Hospital, 555 North 30th Street, Omaha, NE, United States

The efferent innervation below the inner (IHC) and outer (OHC) hair cells each represents the terminations of hundreds of olivocochlear (OC) neurons, a fact that has impeded efforts to describe the arborizations of single OC neurons. Nonetheless, single axon data can provide insights into the composition and functions of these systems. Iontophoretic delivery of biotinylated dextran amine into the superior olive of Sprague-Dawley rats occasionally labels single axons in one or both OC bundles, the peripheral terminations of which can often be fully reconstructed from surface preparations. To date we have identified the arborizations of 36 individual OC neurons, 19 lateral (LOC) and 17 medial (MOC), in a series of 47 adult male rats. Confirming previous studies, LOC axons were classified as either intrinsic or shell, based on the presence of a discrete versus diffuse arborization beneath the IHC. However, we found that intrinsic axons were of two types, those that reached the organ of Corti without branching (simple) and those that formed intraganglionic (IG) branches that eventually converged beneath the same discrete patch of IHC (converging). Regarding shell neurons, we observed them to have as many as four IG branches that innervated as much as 41% of cochlear length. The axons of MOC neurons were extremely diverse, not only in the number of their tunnel crossing fibers (TCF) (1-15), but also in the number of boutons they formed beneath the OHC (1-48) and in their basal-apical spans (1-45%). The number of TCF was correlated with the number of boutons formed, but not with their basal-apical spans. Based on the number of TCF, we recognized two types of MOC neurons: a more common sparsely-branched and a less common highly-branched group, the latter

which was strictly ipsilateral. Some functional implications of these findings will be discussed. Supported by NIH Grant NIDCD DC00215.

420 Expression of glutamate transporter GLAST and glutamine synthetase in the guinea pig cochlea

Toshihiko Kikuchi¹, Zhen-Hua Jin¹, Ryuichi Yoshida¹, Toshihiko Chiba¹, Koichi Tanaka², Toshimitsu Kobayashi¹

¹Department of Otorhinolaryngology - Head and Neck Surgery, Tohoku University Graduate School of Medicine, 1-1 Seiryomachi, Aoba-ku, Sendai, Japan, ²Laboratory of Molecular Neuroscience, School of Biomedical Science and Medical Research Institute, Tokyo Medical and Dental University, 2-3-10 Kandasurugadai, Chiyoda-ku, Japan

Immunohistochemical localization of glutamate transporter GLAST and glutamine synthetase was studied in the guinea pig cochlea. Intense GLAST-like immunoreactivity was found in the fibrocytes in the spiral ligament. GLAST-like immunostaining was also detected in the supporting cells around the inner hair cells, the inner sulcus cells, the interdental cells and satellite cells surrounding the spiral ganglion cells. Intense glutamine synthetase-like immunoreactivity was found in the fibrocytes in the spiral ligament and the basal cells of the stria vascularis and the fibrocytes in the spiral limbus. Immunostaining was also found in the satellite cells in the spiral ganglion and along the nerve fibers within the osseous spiral lamina. The limited resolution provided by the light microscope made it difficult to assign the staining to any particular cell type within the osseous spiral lamina. However, it seems likely that the glutamine synthetase-like immunostaining is restricted to the Schwann cells which form the myelin sheath of nerve fibers, as shown in the previous study (EyBalin et al. *Hear Res* 101: 93-101, 1996).

The results obtained in the present study suggest that GLAST and glutamine synthetase in these connective tissue cells in the guinea pig cochlea may function to maintain the glutamate concentration in the perilymph at a nontoxic level.

This work was supported by Grant-in-Aid for Scientific Research No. 14370546 from the Ministry of Education, Culture, Sports, Science and Technology, Japan.

421 In-vivo confocal microscopy of the guinea pig's inner ear

Igor Tomo¹, Hannes Maier², Sophie Le Calvez¹, Anders Fridberger¹, Mats Ulfendahl¹

¹ENT Dept. research lab, Karolinska Hospital, Center for hearing and communication research, Karolinska Institutet, M 1:00 Karolinska Hospital, Stockholm, Sweden, ²ENT Department, University of Hamburg, Martinistrasse 52, Hamburg, Germany

Confocal laser scanning microscopy permits detailed visualization of structures deep inside thick fluorescently labelled specimens. This makes it possible to investigate living cells inside intact tissue without prior chemical sample fixation and sectioning. Isolated guinea pig temporal bones have previously been used for confocal experiments in-vitro [Flock et al., 1999], but tissue deterioration limits their use to 3-4 hours after the death of the animal. In order to preserve the cochlea in an optimal functional and physiological

condition, we have developed an in-vivo confocal model. Using a ventral surgical approach, the inner ear is exposed in deeply anaesthetized, tracheotomized, living guinea pigs. To stain inner ear structures, scala tympani is perfused via an opening in the basal turn, delivering tissue culture medium and fluorescent vital dyes (RH 795 and calcein /AM). A small apical opening is made in the bony shell of cochlea to enable visualization using a custom-built objective lens [Maier et al., 1997]. Intravital confocal microscopy, with preserved blood and nerve supply, may offer an important tool for studying auditory physiology and the pathology of hearing loss. After acoustic over stimulation, shortening and swelling of both outer and inner hair cells as well as supporting cells was observed.

References:

Flock Å, Flock B, Fridberger A, Scarfone E, Ulfendahl M: Supporting cells contribute to control of hearing sensitivity. *J. Neurosci* 1999;19:4498-4507

Maier H, Zinn Ch, Rothe A, Tiziani H, Gummer A: Development of a narrow water immersion objective for laserinterferometric and electrophysiological applications in cell biology. *J Neurosci Methods* 1997 Nov 7;77(1):31-41.

422 Caution on using Millimetre Length instead of per cent Length for Cochleograms.

Agneta Viberg, Barbara Canlon

Physiology & Pharmacology, Karolinska Institutet, Karolinska Institutet, Stockholm, Sweden

Greenwood (1996) has shown that mechanical and physiological data from the cochlea from several species are well fitted by an exponential frequency-position function. This function assumes that the full length of the cochlea is known. If the full length of the cochlea is not known, then the per cent distance along the basilar membrane cannot be determined. This is a critical issue since quantification of hair cell loss and the plotting of these results on a cochleogram is often illustrated by using per cent distance along the basilar membrane. To analyse the variations in length and frequency distribution, whole mounts of the entire length of the cochlea (including the hook-region) were obtained from guinea pigs, rats, and mice. It was found that the total length of the cochleae could show a biological variation up to 10% (guinea pig, rat) or 3% (mouse). This variation was not due to faulty dissection of the hook-region, or any other region of the basilar membrane. The consequence of this 10% difference can result in up to a half-octave shift of the frequency place when plotted as millimetre along the basilar membrane. In order to obtain a correct frequency and place relation along the basilar membrane it is necessary to know the true length of the basilar membrane. Since the length of the cochlea has a biological variation, the number of octaves will be different for long versus short cochleae if the frequency is plotted against millimetre length. A comparison between two different formulas used to calculate the frequency-place map will be presented (Greenwood, 1996 versus Tsuji and Liberman, 1997) as well as demonstrating examples of guinea pig cochleae with selective lesions induced by acoustic trauma. Supported by RNID, The Swedish Research Council, Tysta Skolan and AMF.

423 A Physiological Place-Frequency Map of the Cochlea in the Mouse

Marcus Mueller, Karen von Huenerbein, Silivi Hoidis, Jean W. Th. Smolders

Physiology II, J.W. Goethe - University, Theodor-Stern-Kai 7, D-60590 Frankfurt am Main, Germany

Because of the existence of several transgenic mice with deficits in the auditory system, mice have become a very important model in auditory research. To provide a basis for further studies the cochlear place-frequency map in CBA/J mice was determined. Iontophoretic HRP-applications were made at several locations in the cochlear nucleus. Prior to application detailed frequency tuning curves of the auditory neurons at these locations were measured and the characteristic frequency determined. The resulting distribution of retrogradely labelled cochlear spiral ganglion cells and their processes to the inner hair cells was analysed in serial sections. By means of a three dimensional reconstruction of the basilar membrane the spatial location of the labelled fibers along the basilar membrane was measured. The response characteristics of cochlear nucleus neurons were similar to those reported earlier for the mouse and other mammals. The map was established for frequencies between 11 and 57 kHz, corresponding to positions between 80 to 13 % basilar membrane length (base = 0%, 100% = 6 mm). The slope of the cochlea map in the observed interval was about 1.5 mm/octave. This is steeper than previously described by Ehret (1975, *J.Comp.Physiol.* 103) using critical ratios. In the observed region the shape of the cochlear place-frequency map is similar to those described earlier in other mammals and similar to that determined in the mouse by sound trauma lesioning (Ou et al., 2000, *Hear. Res.* 145). However, the present physiological map is shifted by about 0.7 mm (0.5 octave) towards the apex, relative to the map obtained by sound trauma

Supported by the DFG (SFB 269)

424 Stereological Assessment of Afferent Innervation of Inner Hair Cells in C57BL/6J Mice

Alejandro Rivas¹, Peter R. Mouton², David K. Ryugo³, Howard W. Francis⁴

¹Dept. of Otolaryngology - Head and Neck Surgery, Center for Hearing Sciences, Johns Hopkins University, 1721 E Madison Street, Baltimore, MD, United States, ²Laboratory of Experimental Gerontology, National Institute on Aging, National Institutes of Health, 5600 Nathan Shock Drive, Baltimore, MD, United States, ³Dept. of Otolaryngology - Head and Neck Surgery and Neuroscience, Center for Hearing Sciences, Johns Hopkins University, School of Medicine, 720 Rutland Avenue, Baltimore, MD, United States, ⁴Dept. of Otolaryngology - Head and Neck Surgery, Division of Neurotology and Skull Base Surgery, Johns Hopkins University, School of Medicine, 601 North Caroline Street, Baltimore, MD, United States

Quantitative analysis of afferent innervation of IHCs may support the hypothesis that innervation density is related to hearing sensitivity. Due to the difficulty of serial section electron microscopy, a more efficient sampling technique was sought. We present an unbiased stereological protocol that assesses innervation density of

IHCs and terminal morphometry in C57BL/6J mice.

Six IHCs were reconstructed in 3-D using semi-serial section analysis and compared with data from the stereological method. Using the physical disector technique, we grouped disector-pairs of electron micrographs that were separated by a distance of 0.16-0.18 μm . Using systematic-random sampling, the first field of view was located at the bottom of the IHC nucleus and counts were performed towards the inferior pole of the IHC. Nerve endings (Q) were counted when present in the reference section, but absent in the lookup section of the disector-pair. Counts were repeated three times for each IHC and the average sum of counted endings (ΣQ) was calculated. The estimated total number of terminals per IHC (N_{IHC}) was determined by multiplying ΣQ by the fixed section-sampling fraction (k).

Using adjacent disector pairs (k=2), N_{IHC} was 18.67 ± 1.15 with a coefficient of variation (CV) of 0.06 at 16 kHz, and 20.67 ± 2.30 with a CV of 0.11 at 32 kHz. When sampling every other disector pair (k=4), the N_{IHC} was 17.33 ± 2.31 with CV of 0.13 and 24 ± 4 with CV of 0.17 for 16 and 32 kHz, respectively. Using 3-D reconstructions of the same cells the mean values were 19.67 ± 1.53 , and 18.00 ± 1.73 for 16 and 32 kHz, respectively.

These results suggest that unbiased stereological methods may facilitate accurate and efficient ultrastructural analyses of IHC innervation. Ongoing studies will assess the biological variability of IHC innervation among normal hearing C57BL/6J mice and changes accompanying age-related and noise-induced hearing loss.

Supported by grants: NIDCD R03DC05909, R01DC00232, K08DC00143; NOHR.

425 The Mouse Cochlea Database (MCD): High Resolution 3D Reconstructions of the Cochlea

Peter Santi¹, Andrew Blair¹, Viet Pham¹, Annabelle Schraufnagel¹, Arne Voie²

¹Otolaryngology, University of Minnesota, 2001 Sixth St. SE, Minneapolis, MN, United States, ²Bioengineering Research, Spencer Technologies, 701 16th Ave., Seattle, WA, United States

The Mouse Cochlea Database (MCD) is a collection of resources containing comprehensive bibliographic information and anatomical images of the mouse cochlea. The MCD is available at the following URL: <http://mousecochlea.ccg.umn.edu>. The purpose of this presentation is to describe the development of the 3D reconstruction resource of the MCD.

Mouse cochleas were removed from euthanized animals and fixed in paraformaldehyde, decalcified in EDTA, dehydrated in ethanol, cleared in methyl salicylate/benzyl benzoate, and infiltrated with rhodamine isothiocyanate. Digital slices through the whole, intact cochlea were imaged by Dr. Arne Voie using orthogonal-plane fluorescence optical sectioning microscopy (OPFOS; *Hearing Res.* 171:119, 2002). Anatomical structures on each image were segmented and reconstructed using the Amira™ program on a Windows PC. We have previously described Amira 3D reconstructions of the otic capsule, round and oval windows, and the membranous chambers of the mouse cochlea (*Soc. Neurosci. Abs.* #C83, 2003). The present communication extends those observations to include more detailed anatomical structures, including:

nerves, basilar and tectorial membranes, organ of Corti, tunnel of Corti, stria vascularis, and the spiral limbus. In addition to viewing the 3D relationships among the structures, certain anatomical features can be morphometrically analyzed. The 3D reconstructions are available on the MCD website, where users can select regions on the 3D reconstructions that are linked to the 2D OPFOS images, for a morphometric analysis. OPFOS images and QuickTime movies are available on the MCD website as downloadable files. As the MCD grows, additional 3D reconstructions from normal, mutant, and experimentally altered mouse cochleas will become available.

Supported by NIDCD grant R21 DC05482

426 The Lateral Wall Of The Cochlea: A Human Temporal Bone Morphometric Study

Francisco Javier Cervera-Paz¹, Manuel Jesus Manrique¹, Fred Hamilton Linthicum²

¹Otolaryngology, University of Navarra, Av. Pio XII, num. 36, Pamplona, Spain, ²Histopathology, House Ear Institute, 2100 West Third Street, Los Angeles, CA, United States

INTRODUCTION: Although violation of the inner ear remains a feared complication in otologic surgery (as it may lead to sensorineural hearing loss), hearing preservation is becoming a major issue in many techniques in which parts of the inner ear are exposed (v.g., endolymphatic sac surgery, posterior canal obliteration, or even cochlear implantation). **OBJECTIVE:** Our research is focussed in the morphometric study of the lateral wall of the cochlea to evaluate the feasibility of a new lateral approach for cochlear implantation using flat electrodes to minimize trauma, following Lenhardt's ideas. **DESIGN:** A retrospective case review of the temporal bone (TB) bank of The House Ear Institute. **MATERIAL & METHODS:** A database of approximately 1300 TB was searched for bones without conditions that may distort the otic capsule, or the spiral ligament, and had available almost all sections. We selected 36 TB sectioned in the horizontal plane, from 26 donors (12 male, 14 female), with a mean age of 66.1. All TB had been removed using the block technique, and fixed for a month in 10% buffered formalin. They had been decalcified in EDTA, embedded in celloidin, serially cut into 20-micron sections. We used sections stained with hematoxylin & eosin for the microscopic evaluation, and to measure several lengths and distances at the lateral wall of the cochlea, using optical appliances. **RESULTS:** We measured the lengths and distances in midmodiolar sections, and in sections containing the round window niche and the anterior border of the stapes footplate. These sections were selected because they may provide good data and their levels are identifiable during surgery. From the 36 TB studied, 25 were from patients with presbycusis, and displayed an atrophy of the stria vascularis and a loss of hair cells, but did not have spiral ligament pathology. The remaining 11 did not show any cochlear pathology at the lateral wall of the cochlea. We will provide detailed information about measurements performed in the poster. **CONCLUSIONS:** Knowledge of the microscopic anatomy and dimensions of the human TB is a major issue for understanding surgical relationships of the lateral wall of the cochlea.

427 Stereological estimates of total cell numbers in the developing human utricular macula

Stig Åvall Severinsen¹, Mads Sølvsten Sørensen², Jens Randel Nyengaard¹

¹Stereological and Electron Microscopy Res. Lab., Aarhus University, Ole Worms Alle 185, Århus, Denmark,

²Otolaryngology head and neck surgery, Rigshospitalet, Blegdamsvej 9, Copenhagen, Denmark

We used material from the Temporal Bone Collection of Rigshospitalet, Denmark, for estimating the total number of hair cells and supporting cells in the inner ear sensory epithelia of the utricular macula (UM) of ten children aged between 1 day and 15 years. The UM had been embedded in celloidin and cut exhaustively in 22µm thick, horizontal sections. Every tenth section was stained with HE. A modified Olympus BX-50 microscope with a motorized stage and an electronic microcator was used for counting. Good image resolution and a thin focal plane were obtained using a high numerical aperture (NA: 1.4) 60x oil immersion objective. A PC with CAST software was interfaced to a SIS Colorview 1 digital camera and the 2D unbiased counting frame was superimposed onto the live images. Vision fields were chosen by systematic, uniformly random sampling. The optical fractionator was used to estimate the total number of cells in the UM with a disector height of 10µm. Based on both orientational and morphological criteria, hair cell:supporting cell ratios were obtained on sections which had been cut perpendicular to the surface plane of the UM. The total cell number did not change during development and was approximately 71,000 (CV = 0.20). The number of hair cells increased with age in contrast to supporting cell numbers, which seemed to decrease. In children aged between 0 and 1 year (n=6) there was approximately 20,000 hair cells and 42,000 supporting cells. In children aged between 7 and 15 years (n=4) the hair cell number was approximately 32,000 and the supporting cell number was 29,000. Cells which could not be identified made up the last cells. In conclusion, the results support the idea of transdifferentiation of supporting cells into hair cells.

428 High Resolution Scanning Electron Microscopy of the Human Cochlea: A study using freshly fixed surgical specimens

Rudolf Glueckert¹, Annelies Schrott-Fischer¹, Helge Rask-Andersen², Kristian Pfaller³

¹ORL, University Innsbruck, Anichstrasse 35, Innsbruck, Austria,

²Department of Otolaryngology, University Uppsala, Karolinskastr. 7, Uppsala, Sweden, ³Institute of Anatomy and Embryology; Dept of Histology and Molecular Cell Biology, University Innsbruck, Anichstrasse 35, Innsbruck, Austria

POSTER PRESENTATION

HIGH RESOLUTION SCANNING ELECTRON MICROSCOPY OF THE HUMAN COCHLEA.

A study using freshly fixed surgical specimens

Glueckert Rudolf^{1*}, Schrott-Fischer Anneliese¹, Pfaller Kristian³, Rask-Andersen Helge²

¹Department of Otolaryngology Innsbruck University Hospital, Austria

² Department of Otolaryngology Uppsala, Sweden

³ Institute of Anatomy and Embryology; Dept of Histology and Molecular Cell Biology, University of Innsbruck, Austria

Introduction:

So far few studies have been performed on human inner ear using scanning electron microscopy (SEM). In this study we analysed the surface structure of the human cochlea using field emission SEM on freshly obtained surgical material. This technique may offer better preservation of the tissue. The inner ear structures were obtained during surgery for life-threatening petro-clival meningioma where the surgeons had decided to perform a trans-petrosal approach with re-routing of the facial nerve. Instead of sacrificing the cochlea it was dissected out and immersed immediately in buffered glutaraldehyde. The study was approved by ethical committee and the patients consent was obtained before surgery.

Material and Methods:

For Scanning Electron Microscopy (SEM). The specimens were coated with a 10-15 nm layer of gold-palladium in a BALTECH MED 020 Coating System and observed with a ZEISS DSM (digital scanning microscope) 982 Gemini Field Emission Electron Microscope.

Results and Discussion:

There was an excellent preservation of tissue following fixation. The gross structure of the cochlea taken out at surgery was generally well preserved even though the otic capsule could not be maintained in its entirety, surface relief of cell structures within the human cochlea could be analysed in detail. At the modiolar aspect of the scala vestibuli of the basal and second turn a trabecular network could be identified that has not been earlier described. The network was formed through crossing of collagen bundles or fibrils over which a thin sheet of cell layer tapering the outer surface of the scala vestibuli was anchored. The surface of the thin cell membrane showed extensive distribution of caveolae or micropinocytotic invaginations suggesting a rich fluid transport in this region. We believe that the trabecular network could represent important site for perilymph production in the human cochlea.

Supported by the Austrian Science Foundation FWF project P15948-B05 and the National Bank Foundation Österreichische Nationalbank 8745

429 Genotype-Phenotype Relationship of Connexin 26 Mutations in the Japanese Population

Tatsuo Matsunaga¹, Hiroshi Kumanomido², Masato Fujii¹, Seiji Niimi², Judy Kenyon³, Shelley Smith³, Thomas Taggart⁴, Shinichi Usami⁵

¹Otolaryngology, National Tokyo Medical Center, 2-5-1 Higashigaoka, Meguro, Tokyo, Japan, ²Otolaryngology, IUHW, 2600-1 Kitakanemaru, Otawara, Japan, ³Center for Human Molecular Genetics, University of Nebraska Medical Center, 985455 Nebraska Medical Center, Omaha, NE, United States, ⁴Hearing Research Center, SUNY at Buffalo, 215 Parker Hall, Buffalo, NY, United States, ⁵Otolaryngology, Shinshu University, 3-1-1 Asahi, Matsumoto, Japan

Mutations in Connexin 26 gene are the major cause of autosomal recessive non-syndromic hearing impairment. More than 70 different Connexin 26 mutations have been reported to be associated

with hearing loss. In order to achieve successful genetic counseling for subjects with these mutations, the genotype-phenotype relationship of Connexin 26 mutations were investigated in the Japanese population that is known to have a set of frequent mutations different from populations of European ancestry. Genotype analysis on 26 congenital deaf subjects and their parents in 19 families revealed 9 types of mutations which were considered to be pathogenic. In subjects with the heterozygous Connexin 26 mutations, del(Connexin 30:D13S1830) mutation which has been reported as the double heterozygotes with Connexin 26 mutations were investigated and this mutation was not detected in these subjects. The 235delC homozygotes were most frequent (8 subjects, 7 families) and all subjects exhibited pure tone averages (PTA) greater than or equal to 80 dB. The 235delC heterozygotes were detected in 4 subjects (3 families), and all subjects had PTA greater than or equal to 85 dB. The V37I heterozygote was detected in 1 subject whose PTA was 64 dB. Compound heterozygotes with the 235delC were detected in 10 subjects (7 families) and compound heterozygotes without 235delC were detected in 3 subjects (3 families). In these cases, subjects with the same genotype had a tendency to exhibit the similar PTA except for the subjects with 235 delC/G45E&Y136stop whose PTA ranged from 53 to 110 dB. Except for 2 subjects (235delC heterozygotes and 235delC/176-191del16) who reported some progression of hearing loss, hearing loss was stable. Audiograms were either sloping or flat type. In summary, analysis on genotype-phenotype relationship of Connexin 26 mutations appears to be useful for genetic counseling at least in part of the families with this mutation.

430 Molecular Analysis of the Temporal Bone with Laser Capture Microdissection(LCM) and TaqMan PCR

Hiroko Koda¹, Yurika Kimura², Katsumasa Takahashi³, Yukiko Iino⁴, Ken Kitamura¹

¹Otolaryngology, Tokyo Medical and Dental University, School of Medicine, 1-5-45, Yushima, Bunkyo-Ku, Japan, ²Otolaryngology, Tokyo Metropolitan Geriatric Medical Center, 35-2, Sakae-city, Itabashi-ku, Japan, ³Otolaryngology, Gunma University, 3-39-22, Showa-city, Maebashi-city, Japan, ⁴Otolaryngology, Teikyo University, 2-11-1, Kaga, Itabashi-ku, Japan

With the advent of molecular genetics, more than 90 forms of non syndromic hearing loss have been established and more than 30 deafness genes have been identified. Molecular approach to the inner ear pathology has also prospered recently.

Tissue microdissection is potentially one of the most useful techniques in molecular pathology. Laser Capture Microdissection(LCM) using UV laser allows the selective sampling of tissue from histological sections. It has been developed to procure precisely the cells of interest in a tissue specimen, in a rapid and practical manner. Together with real time PCR (TaqMan PCR), which can provide essential information to quantify the initial target copy number, it is now possible to analyze genetic alterations in a very small tissue, and further more in the cells of tissue. Using the technique of LCM and TaqMan PCR, we tried the extraction of mitochondrial DNA in the inner ear. The subject is the temporal bone of 30-year-old women who had been diagnosed MELAS. MELAS (mitochondrial myopathy, encephalopathy, lactic acidosis and stroke like syndrome) is associated with

mitochondrial DNA(mtDNA) 3243 mutation, in which sensorineural hearing loss is also a common clinical findings. We presented temporal bone histopathology before, in which characteristic findings were severe strial atrophy and severe loss of spiral ganglion cells. Loss of inner hair cells and outer hair cells was not prominent. The mutation rate of mtDNA 3243 using fluorescence bioimaging analyzer with fluorescence-labeled PCR primer was high in the present subject, which is 85% in the organ of Corti, 89% in the posterior semicircular canal and 83% in the facial canal. Using LCM and TaqMan PCR, we analyze the mutation rate of this subject more precisely.

431 Screening for *WFS1* mutations in Japanese patients with autosomal dominant low-frequency sensorineural hearing loss

Takatoshi Yashima, Yoshihiro Noguchi, Ken Kitamura
Otolaryngology, Tokyo Medical & Dental University, 1-5-45 Yushima Bunkyo-ku, Tokyo, Japan

More than 80 loci responsible for non-syndromic hearing loss have been identified so far. Most often affected is the ability to hear high frequencies, though two loci (DFNA1 and DFNA6/14) are responsible for low-frequency sensorineural hearing loss (LFSNHL). DFNA6/14 is caused by a heterozygous mutation of the Wolfram syndrome type 1 gene (*WFS1*) and is a common cause of autosomal dominant LFSNHL among populations in both Europe and the United States. In the present study, we searched for *WFS1* mutations in three unrelated Japanese patients with autosomal dominant LFSNHL. One patient carried a heterozygous G2700A mutation at codon 844 in exon 8, resulting in substitution of a threonine for an alanine (A844T). Genetic analysis of the available members of the patient's family showed that the A844T mutation segregated with LFSNHL, but was not detected in any of 140 control chromosomes. It thus appears likely that the A844T mutation is causative for hearing loss in these patients.

432 Collecting and Study of the Genetic Hearing Impairment Resource in China

Qiuju Wang¹, Weiyan Yang¹, **Dongyi Han¹**, **Yan Shen²**

¹*Otolaryngology/head and neck surgery, Otolaryngology, 28 Fuxing Road, Beijing, China, People's Republic of,* ²*Chinese National Human Genome Center, Beijing, Chinese National Human Genome Center, Beijing, #3-707 North Yongchang Road BDA, Beijing, China, People's Republic of*

Hearing loss is a common condition responsible for communication disorders affecting one in 1000 newborns. It is one of the major ailments for man. In China, auditory/speech disorders have always been a significant factor affecting people's life quality. A national poll by the China Association For the Handicapped in 1987 showed that 20.57 million people in the country were affected by auditory/speech disorders, comprising 34% of the 60 million disabled and 1.58% of the total Chinese population(1.3billion). This translates to 1.58 persons with auditory/speech disorders in every 100 general population, making auditory/speech disorders number one among all disabilities.

In our research, we first successfully established a network for collecting genetic resources of hearing impairment in China. The network covered ten provinces in the North and South of China. We

obtained the information of the deafness resources through the network and collected the resources including DNA samples, immortalized cell lines, and accompanying clinical and pedigree data according to international standards. We had collected 20 pedigrees including syndromic and nonsyndromic hereditary hearing loss. All that included one large family of hearing loss with Y-linked inheritance pattern, one family of X-linked recessive nonsyndromic hereditary hearing impairment, 10 pedigrees with autosomal dominant, 2 pedigrees with autosomal recessive nonsyndromic hereditary hearing impairment and 6 pedigree with syndromic hereditary hearing loss. All these invaluable resources provided us with the information to conduct genetic linkage studies and locate the genes for hereditary hearing impairment. By far, we have mapped a locus on 19q13.2-q13.32 in a Chinese nonsyndromic autosomal dominant progressive hearing loss family.

This work was supported by a grant from the National High Tech Development Project (2001AA221092) and by Beijing Natural Science Foundation (No.7011004) and Beijing Science and Technology Innovation Project (No. H010210160119) grants.

433 Dynamic Analysis of Outer Hair Cell Motility

Nozomu Matsumoto, Federico Kalinec

Cell and Molecular Biology, House Ear Institute, 2100 West Third Street, Los Angeles, CA, United States

Cochlear outer hair cells (OHCs) change shape in response to electrical (electromotility) as well as chemical or mechanical stimulation (slow motility). It has been recently demonstrated that OHC electromotility is necessary for the correct work of the cochlear amplifier. Full characterization of OHC electromotility, however, has been hampered by the multiplicity of methods used for the quantification of the cell's motile response. Responses measured by different techniques and under different conditions have sometimes rendered contradictory results. Here we report the computerized, continuous analysis of changes in hair cell morphology before, during and after electromotility experiments using image analysis techniques and commercially available software. Guinea pig OHCs were isolated and voltage clamped using standard whole-cell patch recording configuration. Images of these isolated OHCs were digitally recorded continuously for up to one hour at a rate of 30 frames/sec. The captured movie files were then analyzed using the "Dynamic Image Analysis System" (DIAS. Soll Technologies Inc., Iowa City, IA) software, and length, diameter, area and other parameters of the recorded cells were automatically measured. We analyzed cell's morphological changes induced by the patch procedure and by different patterns of electrical stimulation. Changes in the "baseline" of OHC length (slow motility) were measured simultaneously with the amplitude of electromotility and the mutual effects assessed. Results indicated that OHC electromotile amplitude was affected by patch procedure and slow motility. Based on these studies, we are suggesting a few experimental criteria aimed at standardizing conditions and procedures and making comparable results provided by different techniques.

434 Evidence for different anion-binding sites for the control of prestin's voltage-sensor charge movement and operating range

Volodymyr Rybalchenko, Joseph Santos-Sacchi

Otolaryngology and Neurobiology, Yale University School of Medicine, 333 Cedar St, BML 246, New Haven, CT, United States

In our previous work we found that divalent and sulfonic anions along with Cl⁻ influence the outer hair cell (OHC) transmembrane protein *prest*in, which is responsible for OHC electromotility. Anions possibly bind to intracellular residues of prestin and modulate its voltage sensitivity.

Extracellular anions enter the lateral sub-plasmalemmal space (LSpS) through a non-selective transmembrane conductance (G_{metL}), while cytoplasmic anions likely pass around a mechanical barrier presented by the OHC sub-surface cisternae. We tested the effects of increasing Cl⁻ concentrations applied extracellularly and through the patch pipette, and the effects of reference sulfonic (*Hepes*) and divalent (*maleate*) anions. We found that Cl⁻, a major prestin activator, enters LSpS with similar efficiency from outer and cytoplasmic sides. At [Cl⁻] ~ 10-30 mM on either side of the lateral membrane, Q_{max} is maximal. G_{metL} was less permeable to large anions: either reference anion had a greater effect on prestin from the intracellular side than from the extracellular side. Intracellular maleate shifts the voltage-sensitivity range of prestin to positive membrane potentials, but, compared to *Hepes*, reduces the ability of Cl⁻ to shift $V_{1/2}$ back to negative potentials. (For example, with *Hepes* in the pipette, $V_{1/2}$ is shifted from 80±4 to 40±10 mV as extracellular [Cl⁻] changes from 0 to 10 mM; with maleate in the pipette, $V_{1/2}$ is shifted from 113±4 to 76±10 mV as extracellular [Cl⁻] changes from 0 to 80 mM.) Interestingly, the usage of maleate as reference anion revealed differential effects of low Cl⁻ concentrations on the molecular mechanisms responsible for prestin's charge movement and operating voltage range. When extracellular [Cl⁻] was 0, 0.3 and 1 mM, $V_{1/2}$ remained stable (113±3, 115±3, 112±6 mV; n=5-6; mean ± se) but Q_{max} steadily increased (0.95±0.11, 1.12±0.12, 1.34±0.23), possibly indicating that Cl⁻ binding sites of different affinity control these functional parameters of prestin. (Supported by NIH NIDCD grant DC00273 to JSS)

435 Effects of tributyl-tin on chloride homeostasis and membrane capacitance in the outer hair cell

Lei Song, Joseph Santos-Sacchi

Otolaryngology and Neurobiology, Yale University, 333 Cedar St., New Haven, CT, United States

The activity of the outer hair cell (OHC) motor protein prestin is highly dependent on intracellular chloride (Cl⁻) (Oliver et al., 2001; Rybalchenko and Santos-Sacchi, 2003). Understanding membrane Cl⁻ transport processes is therefore important since it will provide a potential mechanism for modulating the cochlear amplifier. Tributyl-tin chloride (TBT) acts as a Cl⁻ ionophore; we chose to study its effects on Cl⁻ exchange across the OHC lateral membrane in order to gain insight into the function of the anion's natural pathway, G_{metL} . The whole-cell voltage clamp technique was used to evaluate OHC Cl⁻ flux via measures of nonlinear capacitance

(NLC).

Following the establishment of whole cell configuration with 1 mM Cl⁻ inside the patch pipette, the voltage at peak capacitance (V_{pkcm}) shifts to the right with a reduction in nonlinear charge transfer (Q_{max}) as a result of intracellular Cl⁻ washout. Subsequently, extracellular perfusion with graded (5-140 mM) Cl⁻ concentrations restores V_{pkcm} and Q_{max} toward original values, confirming the existence of natural pathway for membrane Cl⁻ transport (G_{metL}). However the impact of high extracellular Cl⁻ is limited in that the recovery of V_{pkcm} and Q_{max} is not complete. TBT alters the OHC's membrane Cl⁻ conductance but is without direct effect on NLC. However, since TBT facilitates the influx of Cl⁻ above that of G_{metL} , V_{pkcm} and Q_{max} are fully restored.

TBT is useful in understanding modulation of G_{metL} . For example, after exposing the OHC to 80 or 140 mM extracellular Cl⁻, the subsequent reduction of Cl⁻ to 1 mM does not bring V_{pkcm} and Q_{max} back to the values obtained prior to the increase (namely at 1 mM Cl⁻ inside and outside), suggesting that the efflux of Cl⁻ is not complete. This is confirmed since in the presence of TBT the initial values are obtained. It may be possible that changes in the conductance of G_{metL} and an intracellular Cl⁻ regulation mechanism are triggered by our manipulations of Cl⁻ concentrations.

(Supported by NIH NIDCD grant DC00273 to JSS.)

436 A closer look at the lateral membrane Cl conductance, G_{metL} .

Joseph Santos-Sacchi¹, Volodymyr Rybalchenko¹, Jun-Ping Bai¹, Lei Song¹, Dhasakumar Navaratnam²

¹Otolaryngology and Neurobiology, Yale University, 333 Cedar St, New Haven, CT, United States, ²Neurology and Neurobiology, Yale University, 333 Cedar St, New Haven, CT, United States

Recently, we identified a lateral membrane conductance, G_{metL} , that passes Cl⁻ and influences OHC prestin activity (Rybalchenko and Santos-Sacchi, *J. Physiol.* 547:873-891,2003). We had speculated that the conductance might be provided by prestin itself. Here we report that prestin is not responsible for the conductance. The following data support this conclusion. 1) The voltage dependence of G_{metL} does not follow that of prestin's nonlinear capacitance (NLC) function when the latter is shifted by either temperature or membrane tension; 2) unlike native OHCs whose NLC can be modulated by extracellular Cl⁻ levels, prestin-transfected CHO cells do not show this dependence. Thus, G_{metL} must result from the activity of another molecular species within the lateral membrane. A clue to its identity is the conductance's temperature dependence. Whereas K conductances in OHCs and Deiters' cells present a uniform Q_{10} close to 1.2 (that expected from diffusion, and indicating the absence of a lateral membrane phase change), G_{metL} shows a bimodal Q_{10} with a Q_{10} of 1.5 below 30°C and a Q_{10} of greater than 4 above that temperature. This type of behavior is reminiscent of some temperature sensitive TRP channels, where Q_{10} above threshold temperatures, ranging from 30 to 50°C, can be greater than 10. It is also interesting that TRP channels can be mechanically sensitive, as is G_{metL} . We speculate that G_{metL} may arise from a channel unique to the lateral plasma membrane.

(Supported by NIDCD grant DC00273 to JSS)

437 Effect of osmolality on lipid lateral diffusion in prestin-transfected and wildtype HEK-293 cells

J. Walter Kutz Jr., S. Kiran Chennupati, William E. Brownell

Bobby R. Alford Department of Otorhinolaryngology and Communicative Sciences, Baylor College of Medicine, One Baylor Plaza, NA 102, Houston, Texas, United States

Recent evidence has suggested that the lateral membrane protein prestin plays a role in outer hair cell (OHC) electromotility. Earlier studies showed that lipid lateral diffusion in OHCs is dependent on transmembrane potential, extracellular solution osmolality, and cell length. Because cell length changes in OHCs likely involves interactions between the cytoskeleton and plasma membrane, HEK-293 cells were transfected with prestin to determine the independent role of prestin on lipid lateral diffusion. Fluorescence recovery after photobleaching (FRAP) using a fluorescent lipid analog, Di-8-ANEPPS, was utilized to measure lipid lateral diffusion in prestin-transfected and control HEK-293 cells. There was no difference in lipid lateral diffusion between control and prestin-transfected HEK-293 cells. Both prestin-transfected and control HEK-293 cells demonstrated increased lipid lateral diffusion in hyposmotic extracellular solutions. This contrasts with earlier findings in OHCs demonstrating increased lipid lateral diffusion in hyperosmotic extracellular solutions. The difference in lipid lateral diffusion between prestin-transfected HEK-293 cells and OHCs is most likely due to the unique interactions of the plasma membrane and the specialized cytoskeleton in OHCs that is not present in HEK-293 cells.

438 Cytoskeletal Adhesion and Viscoelasticity of the Outer Hair Cells Plasma Membrane: Studies Using Optically Trapped Fluorescent Microspheres

Sergey Ermilov¹, William Brownell², Bahman Anvari¹

¹*Department of Bioengineering, Rice University, P.O. Box 1892, MS 142, Houston, Texas, United States,* ²*Department of Otorhinolaryngology and Communicative Sciences, Baylor College of Medicine, One Baylor Plaza, Houston, Texas, United States*

The plasma membrane (PM) of mammalian outer hair cells (OHCs) generates mechanical forces in response to changes in the transmembrane electrical potential, resulting in length changes that are on the order of several percent of the cell length. Mechanical properties of the OHC PM determine transfer of electromotile forces from the membrane to the rest of the cell. In this work we have used optically trapped fluorescent microspheres to study PM-cytoskeleton adhesion and visco-elastic properties of PM. In this procedure, an optically trapped fluorescent microsphere was attached to the PM on the lateral wall of OHC and subsequently pulled away to form a PM tether. Mathematical fitting of force-time or force-displacement profiles obtained by solving an inverse-problem of PM force reconstruction was used to calculate stiffness parameter of the cell wall, tether formation force and energy, steady-state tether force, and PM relaxation parameters as a function of the tether length. The experiments were carried out

under various osmotic conditions altering PM tension, and in the presence of salicylate, an anionic amphipathic drug, that is known to reduce the electromotile response.

439 Study of Chlorpromazine-induced Alterations of Outer Hair Cell Membrane Mechanics Using Optical Tweezers

David R. Murdock¹, Sergey Ermilov¹, Feng Qian¹, William E. Brownell², Bahman Anvari¹

¹*Bioengineering, Rice University, 6100 Main St., Houston, TX, United States,* ²*Otorhinolaryngology, Baylor College of Medicine, One Baylor Plaza, Houston, TX, United States*

Located within the cochlea, outer hair cells (OHCs) are specialized sensory cells that give rise to the high sensitivity and frequency resolving ability exhibited in normal mammalian hearing. In this study, we used an optical tweezers system to characterize the effects of the cationic amphipath chlorpromazine (CPZ) on the OHC lateral wall membrane, a structure that is believed to play a central role in OHC functioning. Chlorpromazine has previously been shown to alter cell membrane mechanics and is postulated to selectively partition into the inner leaflet of the plasma membrane. In our experiments, plasma membrane tethers were formed by bringing an optically-trapped polystyrene bead into contact with the plasma membrane and subsequently retracting the cell from the optically-trapped bead using a piezoelectric stage. Under one protocol, a tether was elongated to 25 μm , and maintained at that length while time-resolved tethering force relaxation to an equilibrium value (F_{eq}) and kinetic parameters were measured. The data indicate that for tethers 25 μm in length, chlorpromazine reduces F_{eq} by an average of 40 pN at a concentration of 0.1 mM. Furthermore, our findings support a general negative trend in F_{eq} at increased CPZ concentrations. Data will also be shown demonstrating the effects of multiple CPZ concentrations on single tether force relaxation parameters. Tether experiments were also conducted on human embryonic kidney (HEK) cells in order to establish a basis for comparison. The data obtained from this study demonstrate the effects of chlorpromazine on specific membrane mechanics.

440 Voltage dependent Capacitance in Wildtype Human Embryonic Kidney Cells

Brenda Farrell, Cynthia Shope, William E Brownell

Otolaryngology, Baylor College of Medicine, One Baylor Plaza NA516, Houston, TX, United States

Wildtype human embryonic kidney cells (HEK) are commonly cultured and used as a vehicle to examine the efficacy of membrane protein, prestin and its analogues. A bell-shaped curve of capacitance versus voltage is observed under voltage clamp when prestin is successfully transfected into the membranes of HEK cells. This bell-shaped curve usually exhibits a peak capacitance at a voltage of -0.04 mV and is similar to that observed when outer hair cells (OHC) are voltage clamped. We observed a small (100 fF) monotonically decreasing change in the capacitance trace when wildtype HEK cells were voltage clamped from -0.16 to 0.16 V for one (1) second in solutions containing K^+ and Ca^{2+} channel blockers, i.e., external: tetraethyl ammonium chloride (20mM), CsCl (20 mM) and CoCl_2 (2 mM); internal: CsCl (140mM). We find a monotoni-

cally increasing change in the capacitance trace when the bias is reversed (0.16 V to -0.16 V). We observed a parabolic curve which exhibits a minimum in the capacitance trace at approximately 0.05 V after coating the borosilicate glass pipette with sylgard. The capacitance-voltage parabolic plots are similar to those reported in the 1970s for model membranes (e.g. *Biophys. J* 1978; 21 1-17). We discuss the origin of the voltage dependent capacitance and the effect it may have on prestin transfected HEK cells, and its influence on forces generated by the wildtype and prestin transfected HEK cells during a voltage sweep.

441 Quinine shifts the outer hair cell nonlinear capacitance and modulates cochlear function

Jorge E Hachmeister¹, William E Brownell², John S Oghalai³

¹Bobby R. Alford Department of Otolaryngology and Communi. Sci., Baylor College of Medicine, 6501 Fannin St. NA 515, Houston, TX, United States, ²Bobby R. Alford Department of Otolaryngology and Communi. Sci., Baylor College of Medicine, 6501 Fannin St. NA 505, Houston, TX, United States, ³Bobby R. Alford Department of Otolaryngology and Communi. Sci., Baylor College of Medicine, 6501 Fannin St. NA 504, Houston, TX, United States

Quinine is a well-known drug for its use in the treatment of *Plasmodium falciparum* malaria. Its side effects on the auditory system have long been recognized and include reversible sensorineural hearing loss, tinnitus and vertigo. Sensitivity, frequency selectivity and various forms of otoacoustic emissions are reversibly reduced. Quinine has also been reported to cause ultrastructural changes, to block potassium channels, to reduce electromotility and to hyperpolarize outer hair cells (OHC). In order to characterize the effects of quinine on OHC function more directly, we examined the effects of quinine on motility-related nonlinear capacitance using the whole-cell patch-clamp technique. There was a dose dependent depolarizing shift of > 50 mV in the voltage at peak capacitance. There was no reduction in the magnitude of peak capacitance. *In vivo* perilymphatic perfusion was also performed in four guinea pigs to determine the effect of quinine on cochlear function. Quinine raised the average compound action potential threshold by 35 dB and the average DPOAE threshold by 31 dB. These results reveal quinine to have an effect similar to that of chlorpromazine (another cationic amphipath) but different than that of the anionic amphipath salicylate which reduces peak capacitance. All ionic amphipaths reduce cochlear functioning. The impact of cationic amphipaths on hearing appears to be mediated, in part, by shifting the voltage-displacement response of the outer hair cell.

Research supported by NIDCD grants DC 05131 (J.S.O) and DC02775 and DC00354 (W.E.B).

442 Investigating a novel aquaporin mRNA expression in organ of Corti

Alexander R Orem, Jing Zheng

Communication Sciences and Disorders, Northwestern University, 2240 Campus Dr, Evanston, IL, United States

The organ of Corti incorporates two distinct receptor cells: inner

hair cells (IHC) and outer hair cells (OHC). IHCs transduce vibration and are the source of essentially all auditory signals passed to the brain. OHCs, through their rapid somatic length changes, termed “electromotility,” are thought to provide feedback and amplify the auditory stimuli received by the IHCs. Both hair cells have their hair bundles exposed to the high-potassium/low-sodium endolymphatic fluid in the scala media, while their bodies are immersed in perilymphatic fluid, which has low-potassium/high-sodium content. The transformation of acoustical signals to electrical signals is mediated through ion flux from the endolymphatic fluid into hair cells. Therefore, maintaining the proper homeostasis and osmotic balance of the hair cells is crucial for accurately transforming acoustic signals. How hair cells regulate their homeostasis, such as water transport, is not clear.

A class of membrane proteins called aquaporins (AQP) can facilitate the osmotically driven passage of water molecules across the plasma membrane. Although RT-PCR and immunocytochemistry experiments did not detect expression of known AQPs in hair cells, physiological data did indicate that water transport in OHCs is mediated through aquaporin-like molecules (Belyantseva et al. 2000). We have identified a new aquaporin cDNA fragment from a gerbil OHC-IHC subtracted library. New data support the hypothesis that aquaporin is expressed in the hair cells and is possibly involved in water transport. In order to explore this hypothesis, we are investigating mRNA expression of AQP11 in the organ of Corti with RT-PCR. RNA was collected from P0 to P21 mouse organs of Corti. Semi-quantitative RT-PCR data suggest that AQP11 mRNA expression is not developmentally controlled. Additional experiments are under way to examine where the new aquaporin is expressed. [Supported by NIH Grant DC00089].

443 Prestin's phosphorylation and its voltage dependence

Levente Deak, Jing Zheng, Alexander R Orem, Guo-Guang Du, Salvador Aguiñaga, Peter Dallos

Communication Sciences and Disorders, Northwestern University, Auditory Research Laboratory, 2240 Campus Dr, Evanston, IL, United States

There has been considerable recent progress on deciphering the effects of protein phosphorylation on the electromotile response of outer hair cells (OHC). The molecular substrate of OHC electromotility, the motor protein prestin, has two cAMP/cGMP-dependent protein kinase phosphorylation sites and five potential PKC phosphorylation sites. It is not clear, however, how phosphorylation affects prestin's function. Therefore, we produced single-point mutations at putative phosphorylation sites of the molecule. The neutral amino acid alanine (A) replaced serine (S) or threonine (T) at phosphorylation sites to mimic the dephosphorylated state of prestin. The electrophysiological properties of such “dephosphorylated” prestin are studied through measurement of nonlinear capacitance (NLC) in prestin-expressing TSA cells. NLC is a signature of electromotility, commonly observed in OHCs and prestin-transfected cells. It reflects a voltage-dependent gating current caused by charge displacement in the prestin molecule. In mutants, where the serine or threonine was replaced with a neutral amino acid, the half-activating voltage (V_{pkCm}) shifted in the depolarization direction ($p < 0.01$) as compared to wild-type prestin. The mutation S238A produced a shift of ~10 mV, T560A

yielded 10-20 mV, and the double mutant S238/T560AA gave 20-30 mV shift in V_{pkCm} . It thus appears that the elimination of either phosphorylation site causes a depolarization shift. The shift appears to be cumulative with the elimination of both targeted phosphorylation sites. The data suggest the possibility that the functional activity of prestin can be modified through phosphorylation/dephosphorylation of the molecule. To further study this, we replaced S or T with negatively charged aspartic or glutamic acids (E or D) in order to mimic the phosphorylated state of prestin. Electrophysiological differences between phosphorylated and dephosphorylated prestin were analyzed. [Supported by NIH Grant DC00089]

444 Single-Channel Recordings from the Apical Surface of Outer Hair Cells with a Scanning Ion Conductance Probe

Gregory I. Frolenkov¹, Julia Gorelik², Guy P. Richardson³, Corne J. Kros³, Andrew J. Griffith¹, Yuri E. Korchev²

¹Lab. of Molecular Genetics, NIDCD/NIH, 5 Research Court, Rockville, MD, United States, ²Division of Medicine, Imperial College, Du Cane Road, W12 0NN, London, United Kingdom, ³School of Life Sciences, Univ. of Sussex, Falmer, BN1 9QG, Brighton, United Kingdom

Scanning ion conductance microscopy (SICM) can be used to scan, without touching, the surface profile of living cells with a sharp glass micropipette (50-100 nm inner diameter). SICM is an automatic feedback technique that holds the probe-sample separation constant (typically approximately 50 nm) based upon current changes that occur when the probe approaches the non-conductive surface of the cell in a conductive physiological solution. Therefore, SICM might be able to resolve cell surface structures that are not resolvable by optical microscopy, and to position the micropipette over those structures with precision on the order of tens of nanometers. After positioning, the SICM micropipette can be used for patch-clamp recording. This technique was previously used to obtain single channel recordings from submicron-sized structures such as neuronal processes (Gorelik et al., 2002, *Biophys J.* 83:3296-303) or the tips of microvilli in epithelial cells (Gu et al., 2002, *FASEB J.* 16:748-50). Here we describe our preliminary results using SICM to visualize the apical surface of cultured rat organ of Corti explants. Several successful patch-clamp recordings from the tips of individual stereocilia in the tallest row on outer hair cells have been achieved. Surprisingly, we observed channel activity in only 14% of patches at the tips of stereocilia, which was significantly less than in control recordings from the membrane over the cuticular plate at the base of the hair bundle (75%). At both of these locations, the tip of the stereocilium and the membrane overlying the cuticular plate, we usually observed fairly large-conductance channels with maximal single channel conductance ranging from 68 to 188 pS. These channels had at least two open states with different conductance levels, and reversal potentials close to zero. The goal of our presentation is to discuss the potential molecular and physiological correlates of these recordings.

445 Effect of Cytokines (TNF- α , IL-1 β , IL-1 α , IL-6, and IL-8) on Morphologic Changes of Isolated Cochlear Outer Hair Cells

Seong Kook Park^{1,2}, Earnest O. John², Kaalan E. Johnson², Christopher Fischer², Timothy T.K. Jung²

¹Otolaryngology-Head & Neck Surgery, Inje University College of Medicine, Pusanjin-ku, Pusan, Korea, Republic of, ²Surgery, Division of Otolaryngology - Head and Neck Surgery, Loma Linda University School of Medicine, VA Hospital, Loma Linda, CA, United States

Inflammatory mediators (IMs) of otitis media (OM) have been implicated in the development of sensorineural hearing loss (SNHL). Cytokines are a group of IMs that control the inflammatory and immunologic reaction of OM. Locally produced proinflammatory cytokines such as tumor necrosis factor- α (TNF- α), interleukin-1 (IL-1), IL-6, and IL-8 are considered to play an important role in the initiation and maintenance of inflammation in the pathogenesis of OM. We suspected that cytokines may induce SNHL through cytotoxic effects on the outer hair cells (OHCs). The purpose of this study is to assess the effect of TNF- α , IL-1 α , IL-1 β , IL-6, and IL-8 on morphologic changes of isolated cochlear OHCs in vitro. OHCs from cochlea of adult chinchilla were isolated and exposed to standard bathing solution (SBS) (control group), SBS with TNF- α , IL-1 α , IL-1 β , IL-6, and IL-8 (10 μ g/ml). All experiments were performed at an osmolality of 305 \pm 5 mOsm, pH 7.3, room temperature, and for up to 60 minutes. The images of OHCs were recorded using inverted microscope and analyzed on the IMAGE PRO-plus 3.0 program. Change of cell length was measured and analyzed. OHCs exposed to SBS did not show any significant changes in cell shape or length (104 \pm 0.9%, mean \pm SE). At the concentration of 10 μ g/ml of IL-1 β , no significant change was observed in cell length (100 \pm 2.5%). OHCs exposed to solution of TNF- α , IL-1 β , IL-6, and IL-8 developed shortening and ballooning of the cells. Among the cytokines tested, IL-1 β caused the greatest amount of OHCs shortening followed by TNF- α , IL-6, and IL-8. This study demonstrated that exposure to TNF- α , IL-1 β , IL-6 and IL-8 caused morphologic changes in isolated cochlear OHCs. This suggests a possible involvement of certain cytokines in the pathogenesis of sensorineural hearing loss in chronic otitis media.

446 Influence of efferent neurotransmitters upon slow and fast motility in isolated OHCs

Tamás József Batta¹, György Panyi², István Sziklai¹

¹ORL Clinic, Health Science Center, University of Debrecen, Nagyerdei Krt. 96., Debrecen, Hungary, ²Inst. Biophysics, Health Science Center, University of Debrecen, Nagyerdei Krt. 96., Debrecen, Hungary

Introduction: A force feedback within the cochlear partition is provided by the OHC electromotility, called cochlear amplifier. Its dynamic adjustment to actual requirements is regulated by several mechanisms, including the efferent innervation. The efficacy of the mechanical feedback is dependent on the global stiffness of the cells against the motor proteins work. The stiffness of cochlear outer hair cells consists of a dynamic stiffness, which is associated to the conformational changes of the prestin molecules, and a static stiffness which is processed by the cytoskeleton. **Methods:**

The stiffness of the lateral wall was measured by the glass micropipette aspiration technique using a pseudocolour image analysis method. The global stiffness was calculated from the transverse stiffness according to Ulfendahl et al. (1998, *Eur J Physiol* 436:9-15.) **Results:** We found that the stretch induced regulation of the static stiffness and the stretch induced slow cell contraction described previously are controlled by the efferent neurotransmitters. A cochleobasally biased ACh-response and cochleoapically biased GABA response was found. **Conclusion:** A steady-state loud sound stimulus generates large vibrations of the basilar membrane and concomitantly stretches the lateral wall of the OHCs which evokes greater stretch-induced cell shortening. The efferent neurotransmitters increased the stretch-induced lateral wall stiffness by about 70% and cell shortening by about 2 μ m. These changes can interfere with cochlear micromechanics and can decrease the effectivity of the electromotile force feedback. These are in agree with in situ measurements of Friedberger et al. (1998, *Neurobiol* 95:7127-7132) on the effects of acoustic overstimulation in guinea pig cochlea.

447 Expression system of prestin and characterization of CHO cells stably expressing prestin

Koji Iida¹, Kouhei Tsumoto², Izumi Kumagai², Hiroshi Wada¹

¹Department of Bioengineering and Robotics, Tohoku University, Aoba-yama 01, Sendai, Japan, ²Department of Biochemistry and Engineering, Tohoku University, Aoba-yama 07, Sendai, Japan

Mammalian hearing sensitivity relies on a mechanical amplification mechanism involving the outer hair cells (OHCs), which rapidly alter their longitudinal length in response to changes in their membrane potential. The molecular basis of this mechanism is thought to be a motor protein embedded in the lateral membrane of the OHCs. Recently, this motor protein was identified and termed prestin (Zheng, J. et al., *Nature* 405, 149-155, 2000). For further study of prestin, it is necessary to research it at the molecular level. For this reason, a method of obtaining a large amount of prestin is required. However, no large scale preparation of prestin has been reported. In this study, an attempt was therefore made to construct a mass expression system of prestin. Prestin cDNA was introduced into *Escherichia coli* (*E. coli*), insect cells and Chinese hamster ovary (CHO) cells, and the expression of prestin was examined by Western blotting. Although prestin was not expressed in *E. coli*, it was expressed in insect cells and CHO cells. In insect cells, however, the expression level was very low and expressed prestin was fragmented. By contrast, it was verified that the full-length of prestin was expressed in CHO cells. Therefore, an attempt was made to establish stable cell lines using transfected CHO cells by limiting dilution cloning. The expression and activity of prestin in generated cell lines were then confirmed by immunofluorescence and whole-cell patch-clamp measurements, respectively. Although the expression level of prestin in CHO cells was lower than that in OHCs, the generated cell lines were confirmed to stably express active prestin.

448 Cytosolic Free Calcium and Calmodulin Regulate Rapid Endocytosis in Guinea-Pig Outer Hair Cells

Toshihiko Kaneko, Csaba Harasztosi, Anthony William Gummer

Otolaryngology, Tübingen University, Elfriede-Aulhorn-Str. 5, Tübingen, Germany

FM1-43 is now a common tool to investigate endocytotic activity visually. After applying FM1-43 to isolated guinea-pig outer hair cells (OHCs), Hensen's body showed rapid and intense staining (Meyer J. et al. 2001. *Hear Res.* 161:10-22). Hensen's body is a complex of Golgi apparatus and endoplasmic reticulum, and a unique structure in OHCs. Therefore, the relationship between rapid endocytosis and Hensen's body might play important roles for OHC metabolism. But the function and/or role of rapid endocytosis and Hensen's body are not yet well understood. Calcium and calmodulin were investigated here, because in general they are known to have important roles for rapid endocytosis (Henkel AW. et al. 1996. *Curr Opin Neurobiol.* 6:350-7).

OHCs were isolated from the adult guinea-pig cochlea. FM1-43 (5 μ M) was applied locally to OHCs by pressure injection through a grass capillary. Fluorescence changes of FM1-43 were monitored using confocal laser scanning microscopy. To investigate whether rapid endocytosis is calcium and calmodulin dependent, trifluoperazine (TFP; 20 μ M) was used to inhibit calmodulin dependent phosphorylation and 1,2-bis-(O-aminophenoxy)-ethane-N,N,N',N'-tetraacetic acid (BAPTA-AM; 25 μ M) was used to chelate cytosolic free calcium rapidly. OHCs were preincubated in TFP for 15 min before measurements; experiments were made in the presence of TFP. For BAPTA-AM, preincubation was for 30 min and then it was washed out with Hanks' balanced salt solution.

Dye uptake in Hensen's body was significantly reduced in both TFP-treated and BAPTA-AM treated OHCs. This suggests that cytosolic free calcium and calmodulin are necessary for rapid endocytosis in OHCs. It has been shown in zebrafish lateral sensory hair cell that rapid endocytosis is calcium and calmodulin dependent (Seiler C. et al. 1999. *J Neurobiol.* 41:424-34). The present results are the first direct demonstration of a dependence of intracellular free calcium on rapid endocytotic activity in hair cells.

Supported by Deutscher Akademischer Austausch Dienst.

449 Nonlinear Capacitance of Outer Hair Cells in the Adult Cochlea

Anthony W. Gummer¹, Bernd W. Pritschow²

¹Otolaryngology, Tuebingen University, Elfriede-Aulhorn-Str. 5, Tuebingen, Germany, ²Otolaryngology, Tuebingen University, Elfriede-Aulhorn-Str. 5, Tuebingen, Germany

The unique, electrically induced motion of the soma of the outer hair cells (OHCs) is believed to be the basis of the extraordinary frequency selectivity and dynamic range of the mammalian cochlea. The electrical signature of this motion is a voltage-dependent membrane capacitance, with properties known for OHCs in isolation but not in situ. The aim of the present experiments was to uncover the voltage dependence of the membrane capacitance of OHCs embedded in their cellular environment

within the adult cochlea. The voltage dependence was determined, in situ for the first time, by whole-cell recordings from OHCs in a temporal bone preparation of the guinea-pig cochlea. Recordings were made in the fourth cochlear turn. Membrane capacitance exhibited similar voltage dependence to that reported for isolated OHCs: First, for membrane potentials from -110 mV to 50 mV, the dependence was a symmetric bell-shaped function deriving from a two-state Boltzmann process that describes charge movement of the voltage-sensor of the motor. The maximum voltage-sensor charge was 2.56 ± 0.41 pC, with half of the charge transferred at a membrane potential of -26.3 ± 18.2 mV; the effective valence was 0.85 ± 0.05 ($N = 13$). Second, below -110 mV and above 50 mV, evidence was found for a second voltage-dependent process, with the same Boltzmann statistics as the motor, such that this capacitance changed by a total of 2.71 ± 0.81 pF as all motors conformationally changed states. On average, the resting membrane potential (-64 ± 5 mV) appeared to be located at maximum capacitance slope, ensuring minimal harmonic distortion of the capacitive current for physiologically relevant receptor potentials. It is concluded that the voltage dependence is an intrinsic electromechanical property of the OHC, independent of the cellular environment in which it is embedded.

450 Spontaneous otoacoustic emissions: Evidence for cellular Hopf oscillators in the organ of Corti?

Christopher Shera^{1,2}

¹*Eaton-Peabody Laboratory of Auditory Physiology, Massachusetts Eye & Ear Infirmary, 243 Charles St, Boston, MA, United States,* ²*Department of Otology & Laryngology, Harvard Medical School, 25 Shattuck St, Boston, MA, United States*

Spontaneous otoacoustic emissions are commonly thought to arise through a mechanism first proposed by Gold (1948, *Proc. Roy. Soc. B*). When couched in the language of dynamical-systems theory, Gold's local-oscillator model supposes that cochlear hair cells operate near a "critical point" (e.g., a Hopf bifurcation) where spontaneous oscillation sets in. SOAEs occur when the control mechanisms needed to hold a hair cell close to the critical point break down. Because experiments have demonstrated unprovoked movements of nonmammalian hair bundles but not spontaneous OHC contractions, Gold's local-oscillator model is often invoked to argue that OHC somatic motility is unlikely to constitute the active process in mammalian hearing (e.g., Martin & Hudspeth 1999, 2001, *Proc. Nat. Acad. Sci. USA*). However, although superficially compelling, the logic of this argument is faulty because SOAEs may arise through a very different mechanism first proposed by Kemp (1979, *Arch. Otorhinolaryngol.*). In Kemp's global standing-wave model, SOAEs are continuously self-evoking stimulus-frequency emissions, a global collective phenomenon in which SOAE frequencies are determined not by local cellular properties, such as hair-bundle geometry and adaptation or transduction kinetics, but by non-local characteristics such as round-trip traveling-wave phase shifts and the impedance mismatch at the cochlear boundary with the middle ear. We present quantitative tests that distinguish between the two models. In addition to predicting the existence of multiple SOAEs with a characteristic minimum frequency spacing, the global standing-wave model accurately predicts the mean value of this spacing, its standard

deviation, and its power-law dependence on SOAE frequency. Furthermore, the model accounts for the magnitude, sign, and frequency dependence of changes in SOAE frequency that result from modulations in middle-ear stiffness. Contrary to recent claims, spontaneous emission of sound from the ear does not require the autonomous oscillation of its cellular constituents.

Supported by NIDCD/NIH grant R01 DC03687.

451 Modeling Tension and Voltage Effects on Outer Hair Cell Tether Formation

Emily Glassinger, Robert M Raphael

Bioengineering, Rice University, MS 142, Houston, TX, United States

The material properties of the outer hair cell (OHC) membrane can be characterized by pulling thin bilayer tubes, known as tethers, from the cell's surface. Although theoretical models have been developed to describe tether formation from many cell types, the applicability of these models to OHCs is limited because the OHC membrane is 1) under significant tension; 2) attached to the cytoskeleton; and 3) displays electromechanical effects. For all cells, the amount of 'excess' membrane area can influence tether behavior. We have included the effects of excess membrane area arising from thermally driven surface undulations into a thermodynamic potential for tether formation. This approach allows us to mathematically separate the effects of adhesion from the effects of membrane tension. According to our predictions, large forces (>50 pN) are required to pull even short tethers when membranes are under tension, even in the absence of significant adhesion. This suggests that the large forces required to form tethers from the OHC are due in part to the cell's turgor pressure. The magnitude of the cytoskeletal adhesion energy affects the equilibrium tether force (F) required to maintain a given tether length (L_t). These effects are pronounced at short tether lengths, with significantly more force being required to pull tethers for stronger adhesion energies. Electromechanical effects can also shift the F vs. L_t relationship. These effects are modeled by including terms into the thermodynamic potential appropriate for either active area strains (piezoelectricity) or active curvature changes (flexoelectricity). The resulting theoretical predictions suggest it is experimentally possible to distinguish between these mechanisms, thus illustrating the potential of tether formation experiments to resolve the nanoscale membrane events responsible for OHC electromotility.

452 Generalization of "area motor" model of outer hair cells

Kuni H Iwasa

NIDCD, NIH, 50 South Dr, Bethesda, Maryland, United States

A membrane motor, which induces mechanical displacements in a cell, can operate based on conformational transitions that involve changes in its membrane area (area motor) or in its stiffness (stiffness motor). Previous studies have showed that area motor model is successful in describing the motility of outer hair cells (OHC), including piezoelectric reciprocal relationship (Iwasa, Biophys J, 2001). However, recent reports (He and Dallos, PNAS, 1999; JARO, 2000) on the axial stiffness of OHC suggest that the motor may have intrinsic stiffness changes in addition to 'gating compliance' due to area changes (Iwasa, JASA, 2000). Gating compli-

ance is an increase of compliance due to the gating of mechanoreceptors (Howard and Hudspeth, Neuron, 1988) and it can take place without changes in intrinsic stiffness of individual elements that makes up the system. This effect can be very large for relatively small displacements. So far the effect of changes in intrinsic stiffness in addition to that of area has not been studied. Here we incorporate changes in intrinsic stiffness to area motor model of OHC and its one-dimensional analog, which is similar to those used for stretch sensitive channels. While such an extension is quite transparent for one-dimensional analog, it is quite complicated for the area motor model because mechanical properties of the cell membrane affect conformational changes of the motor. In some special cases of area motor model, positive cooperativity involving the motor can be predicted.

453 Distribution and effects of the beta 1 and 2 subunits of cSlo: implications for tuning

Dhasakumar Navaratnam¹, Haresha Samaranyake¹, Alberto Ortega¹, Joseph Santos-Sacchi²

¹Neurology, Yale University, 333 Cedar Street, New Haven, CT, United States, ²Surgery, Yale University, 300 Cedar Street, New Haven, CT, United States

Electrical resonance, a mechanism by which hair cells in the chick discriminate between frequencies of sound, results when the frequency of the intrinsic fluctuation in a hair cell's membrane potential coincides with the frequency of sound that hair cell best responds to (characteristic frequency), thereby allowing for a maximal release of neurotransmitter. Differences in the frequency of membrane potential oscillation in individual hair cells along the tonotopic axis are brought about primarily by the changing electrophysiological properties of the calcium gated potassium channel (Slo). A property of the Slo channel in these hair cells that relates best to the characteristic frequency is its deactivation time. Previous experiments have shown that binding to an auxiliary subunit (beta 1) from quail could explain the slower kinetics of Slo seen in low frequency cells. The exact mechanism of the faster deactivation in high frequency hair cells is not known.

We have cloned two beta subunits from the chick auditory epithelium. These two beta subunits (beta 1 and beta2) have homology to their mammalian counterparts that approximate 45% and 88% respectively. Our preliminary data confirm previous observations about the differential distribution of the beta 1 subunit in the papilla. In this study we will also present data showing the distribution of the beta 2 subunit along the tonotopic axis of the papilla and their effect on the kinetics of the Slo channel. These results have important implications on current models of the mechanisms of hair cell tuning.

Supported by NIH NIDCD grant K08 DC05352-02 to DSN and DC00273 to JSS

454 Adenoviral-Mediated Dominant-Negative Suppression of a Low-Voltage Activated Potassium Conductance in Type I Vestibular Hair Cells.

Jeffrey R. Holt, David Abraham, Gwenaëlle S.G. Géléoc
Neuroscience & Otolaryngology, University of Virginia, Lane Rd., MR4, Rm 5127, Charlottesville, VA, United States

We sought to identify the molecular substrate of the low-voltage-activated conductance, gK,L, expressed in type I hair cells of mouse and human vestibular organs. Pharmacology and immunolocalization have suggested that KCNQ subunits are expressed in type I cells, however a link between KCNQ expression and the physiologically-defined gK,L has not been established. We have taken an alternate approach: viral-mediated gene transfer into hair cells of mouse utricle organotypic cultures. We used replication incompetent (E1a/b and E3-deleted) adenoviral vectors with a bicistronic expression cassette that contained a CMV promoter followed by the gene for green fluorescent protein (GFP), an internal ribosome entry sequence and a mutant form of KCNQ4. We took advantage of the dominant-negative G285S mutation which occurs in the pore-forming region of the channel and causes the dominant, progressive hearing loss, DFNA2.

We used the whole-cell, tight-seal technique to record from P6 or older type I and type II hair cells. Infected cells were identified by expression of GFP. Boltzmann relations were fitted to conductance-voltage curves generated from tail currents evoked following families of step depolarizations. Control type II cells expressed an outward rectifier conductance, gDR, of 18 ± 7.5 nS (mean \pm S.D., $n=10$) with a Vfi of -40 ± 6.8 mV and a slope of 7.8 ± 1.7 mV. Type II cells that expressed GFP had a mean conductance of 13.4 ± 6.6 nS ($n=6$) with a Vfi of -43 ± 8.2 mV and a slope of 6.1 ± 1.6 mV indicating no significant suppression of gDR. Control type I cells expressed the large, negatively activating gK,L, with a conductance of 40 ± 17 nS ($n=11$), a Vfi of -75 ± 6.1 mV and a slope of 5.0 ± 1.2 mV. Interestingly, type I cells that expressed GFP and presumably mutant KCNQ4 revealed no evidence of gK,L but did retain a small (8.5 ± 4.8 nS, $n=15$) more positively activating conductance (-40 ± 15 mV, slope = 6.8 ± 1.9 mV) similar to gDR of type II cells. Dominant-negative suppression of gK,L with G285S KCNQ4 suggests the native channels in type I hair cells are composed of wild-type KCNQ4 and/or KCNQ3.

Supported by NIDCD grant DC05439

455 Voltage-dependent Sodium Currents in Hair Cells of Early Postnatal Rat Utricles: Regional Distribution and Molecular Identity

Julian R Wooltorton¹, Jasmine L Garcia², Ruth Anne Eatock^{1,2}

¹Neuroscience, Baylor College of Medicine, One Baylor Plaza, Houston, TX, United States, ²Otolaryngology, Baylor College of Medicine, One Baylor Plaza, Houston, TX, United States

In the rodent vestibular system, hair cells of the utricular macula sense gravitational and linear acceleration. There are two distinct regions within the macula: the striola, a zone approximately 12 cells wide centered on the line of reversal of hair bundle polarity,

and the surrounding extrastriola. In mature rodents, vestibular afferents to the two regions have distinct response properties (Goldberg et al., 1990). Voltage-dependent sodium (Na) currents in hair cells from P0-P7 rat semi-intact utricular preparations were investigated using the whole-cell patch clamp technique. To facilitate Na current recording, potassium channels were blocked by substituting Cs⁺ for K⁺ both externally and internally, and adding external 4-AP. Two populations of Na channels were distinguished by their inactivation and activation properties. One population had relatively negative voltage ranges of inactivation and activation ($V_{1/2}$ (inact) = -92.1 ± 0.5 mV, mean ± S.E.M., n = 38 cells; $V_{1/2}$ (act) = -43.1 ± 0.7 mV, n = 32), indicating that the channels would be largely inactivated at resting potentials (≈ -60 to -70 mV) and raising questions concerning their physiological importance. The second population had significantly (P < 0.001) more positive ranges of inactivation and activation ($V_{1/2}$ (inact) = -74.7 ± 0.7 mV, n = 30 cells; $V_{1/2}$ (act) = -35.0 ± 0.6 mV, n = 25). The distribution of channels varied with region: 85% of striolar hair cells had the more negatively activating Na current (28/33 cells), whereas 71% of extrastriolar hair cells had the more positively activating current (25/35 cells).

Currently, there are 9 known pore-forming Na channel α subunits. RNA was isolated from rat vestibular epithelia and ganglia of P1 and P21/22 rats and reverse-transcribed to cDNA. PCR products were obtained corresponding to the TTX-sensitive Na_v1.2, Na_v1.6 and Na_v1.7 subunits and the TTX-insensitive Na_v1.5 subunit in all tissues from both age groups. The TTX-sensitive Na_v1.4 was expressed in all tissues at P1, but not at P21/22. The TTX-resistant Na_v1.8 and Na_v1.9 subunits were not expressed in epithelia, but were present in vestibular ganglia from both age groups. Further experiments are in progress to correlate the electrophysiologically characterized Na currents with specific α subunits.

Supported by: NIH DC02058 & DC02290

456 Ca_v1.3-mediated Ca²⁺ Currents and the Maturation of Mouse Outer Hair Cells

Martina Knirsch, Marcus Michna, Stefan Muenkner, **Jutta Engel**

Institute of Physiology II and Dept. of Otolaryngology, University of Tuebingen, Gmelinstr. 5, Tuebingen, Germany

Outer hair cells (OHC) serve as electromechanical amplifiers that guarantee the unique sensitivity and frequency selectivity of the mammalian cochlea. Ca²⁺ channels seem to be essential for normal OHC development and perhaps mature function because OHCs degenerate in Ca_v1.3 (or α 1D)-deficient (Ca_v1.3^{-/-}) mice from P15 onwards (Platzer et al. 2000 Cell 102:89-97; Glueckert et al. 2003 Hear Res 178:95-105). It is unknown whether mature OHCs have functional presynapses and if type II afferent fibers innervating them are active. We recorded whole-cell Ba²⁺ currents (I_{Ba}) in neonatal and maturing OHCs in explants of the organ of Corti. Neonatal (P1-P7) outer hair cells (OHC) showed voltage-activated Ba²⁺ currents that activated at -50 mV, showed no voltage-dependent but moderate Ca²⁺-dependent inactivation and exhibited L-type pharmacology. I_{Ba} was maximal at P2 (165 ± 36 pA, n = 8) and declined with age. Reduction of I_{Ba} density to 2.5 % indicated that >97% of I_{Ba} flows through Ca_v1.3 Ca²⁺ channels in neonatal wild-type OHCs. Properties of neonatal I_{Ba} were similar but not identical to those in neonatal inner hair cells (IHC, Platzer et al. 2000), and the OHC current density was only 38 % of that in IHCs. In OHCs

aged P8-P10, I_{Ba} drastically decreased to 39 ± 13 pA (n = 8). From P11-P15, around the onset of hearing, I_{Ba} further decreased to 29 ± 8 pA (n = 9, apical and medial OHCs). At P19, apical OHCs still showed small Ba²⁺ currents ranging from 10 to 15 pA. In conclusion, I_{Ba} decreased during OHC maturation to about 10 % of its initial value. Its presence in OHCs at P19 suggests a role for presynaptic Ca²⁺ currents and afferent transmission in mature OHCs.

Supported by DFG En294/2-1,2,3

457 I-II Loop Interactions of Hair Cell Voltage-Gated Calcium Channels

Neeliyath A. Ramakrishnan¹, Dennis G. Drescher^{1,2}

¹Department of Otolaryngology, Wayne State University School of Medicine, 540 East Canfield Avenue, Detroit, MI, United States,

²Department of Biochemistry-Molecular Biology, Wayne State University School of Medicine, 540 East Canfield Avenue, Detroit, MI, United States

To identify proteins that interact intracellularly with hair-cell voltage-gated calcium channels, we performed yeast two-hybrid experiments (Matchmaker, Clontech) targeting the exon 9a-containing I-II cytoplasmic loop of subunit Cav1.3 inserted in pGBKT7 vector, as bait. For prey, a trout saccular hair-cell library was constructed in pGADT7-Rec vector in yeast strain AH109. Interacting proteins were identified in mating experiments between the AH109 library and Y187 yeast strain containing bait construct. Colonies growing on -Ade/-His/-Trp/-Leu (QDO) medium were re-tested on the same medium to confirm interaction. Further stringency was obtained by transferring the positive colonies to QDO medium containing X- α -gal and selecting blue colonies. We identified two inserts, a desmoplakin C-terminal domain C and Na/K ATPase β subunit. Interaction in AH109 was re-tested with three replicate co-transformations. The Cav1.3 I-II loop was represented by one bait construct containing hair-cell-associated exon 9a and a second lacking it. Similarly, the Cav2.2 loop was represented by one construct with an 11-aa insert (GenBank AF461707) and the other without it. We found strong interaction, in terms of number of colonies growing on QDO, for desmoplakin with the Cav1.3 I-II loop containing exon 9a. However, desmoplakin interaction was minimal or absent for the Cav1.3 I-II loop lacking exon 9a and for both of the Cav2.2 I-II loop constructs. For Na/K ATPase β subunit, there was approximately equal interaction with both of the Cav1.3 constructs, and little or no interaction with both of the Cav2.2 constructs. Negative control studies with vectors lacking inserts, or with either vector containing insert, produced no colonies. Thus, there is clear indication of interaction of desmoplakin preferentially with the Cav1.3 I-II loop containing exon 9a. Such interaction may be implicated in hair-cell protein anchoring and/or modification of channel properties.

458 PACSIN 3 is a Binding Partner of the TRPV4 Cation Channel

Sabine Mann¹, Huawei Li¹, Math Cuajungco¹, Markus Plomann², Stefan Heller¹

¹EPL - Dept. of Otolaryngology, Mass Eye & Ear Infirmary / Harvard Medical School, EPL - MEEI, 243 Charles Street, Boston, MA, United States, ²Cellular Neurobiology Unit, Centers for Biochemistry and Molecular Medicine, University of Cologne, Joseph-Stelzmann-Str 52, Cologne, Germany

TRPV4 is a cation channel that is gated by a variety of physical stimuli including mechanical forces and temperature changes. In the cochlea, TRPV4 is expressed in the organ of Corti, in marginal cells of the stria vascularis, and in auditory ganglion cells. A truncated isoform of TRPV4 lacking the amino-terminal intracellular domain displays much slower response kinetics when investigated with fluo-4-based monitoring of changes in the intracellular Ca²⁺ concentration in response to hypoosmotic stimuli. Combined with the observation that TRPV4-gating is abolished in cell-detached patches, we hypothesize that functional TRPV4 requires additional intracellular interaction partners. We set out to identify TRPV4-interacting proteins by performing yeast two-hybrid screens in a chicken two-hybrid basilar papilla cDNA library with the chicken TRPV4 amino-terminus as bait. We repeatedly isolated independent cDNA clones encoding the chicken orthologue of mammalian PACSIN 3. PACSIN 3 is the third member of the multifunctional PACSIN protein family. PACSINs have been implied in receptor regulation by recycling via endosomal and synaptic targeting. All three PACSINs are expressed in the murine cochlea and PACSIN 3 expression partially co-localizes with TRPV4 expression. Using yeast two-hybrid assays, we corroborated the interaction of rodent TRPV4 with mouse PACSIN 3 and we found that TRPV4 does not bind to PACSINs 1 and 2, neither does the related ion channel TRPV2 bind to any PACSIN isoform. We employed co-immunoprecipitation to biochemically verify the binding. Our data suggest that PACSIN 3 is a binding partner of TRPV4 in particular in the organ of Corti and in auditory ganglion cells.

459 Voltage- and Ca²⁺-gating of BK Channels in Inner Hair Cells

Henrike Thurm, Bernd Fakler, Dominik Oliver

Department of Physiology II, University of Freiburg, Hermann-Herder Str. 7, Freiburg, Germany

Potassium conductances in inner hair cells (IHCs) are carried by Ca²⁺- and voltage-dependent large conductance K⁺ channels (BK channels) and by purely voltage-gated channels (K_v and KCNQ channels). The BK current is thought to be pivotal for shaping the receptor potential due to its fast activation kinetics and large size. We examined the properties of pharmacologically isolated BK channels in IHCs from acutely isolated mouse and rat cochleae using whole-cell voltage-clamp as well as inside-out patch recordings. The latter allow for defined intracellular Ca²⁺ concentrations ([Ca²⁺]_i).

In excised inside-out patches, large BK currents of around 0.5 nA were obtained. The voltage required for half-maximal activation (V_h) was shifted to hyperpolarized potentials with increasing [Ca²⁺]_i applied to the cytoplasmic face of the patch (V_h (0 μM)=

39 mV; V_h (1 μM)= 7 mV; V_h (10 μM)= -69 mV). Accordingly, activation rates were accelerated with increased [Ca²⁺]_i. The slope of voltage dependence was independent of [Ca²⁺]_i (18 mV for an e-fold change in activation). In the whole-cell configuration, however, the activation curve was substantially steeper (8 mV) than in the patch recordings. BK currents were activated in the physiological voltage range (V_h= -44.8 mV). Activation time constants matched those obtained from patches at 10 μM Ca²⁺ over the whole voltage range tested. These findings suggested that Ca²⁺ influx through IHC Ca²⁺ channels (Ca_v1.3), which have activation characteristics similar to BK channels, might determine the gating of BK channels. However, the activation characteristics of the BK currents were unchanged by removal of extracellular Ca²⁺.

Thus, BK gating properties in the intact IHC may result from Ca²⁺ released from intracellular stores, from a Ca²⁺-independent interaction with Ca_v or from a reversible modulation of the intrinsic voltage dependence of the BK channels.

460 Subunit dependent activation of chicken BK channels by the xenoestrogen tamoxifen

Robert Keith Duncan¹, Paul Fuchs²

¹Kresge Hearing Research Institute, University of Michigan, KHR1 4038, 1301 E. Ann Street, Ann Arbor, MI, United States,

²Otolaryngology, Johns Hopkins University, 521 Traylor, 720 Rutland Ave., Baltimore, MD, United States

Large-conductance, calcium-activated potassium (BK) channels play a central role in regulating the hair cell's receptor potential by responding to depolarization induced calcium influx. In the non-mammalian vertebrate cochlea, tonotopic variations in BK channel kinetics underlie an electrical tuning mechanism, and such variations may arise from alternative splicing of the pore-forming α subunit and co-expression with accessory β subunits. Interestingly, the expression of the avian β subunit is graded along the tonotopic axis, but its role in hair cell tuning remains unproven. In mammalian BK isoforms, estrogens and xenoestrogens (e.g. tamoxifen) modulate channel activity by promoting channel opening and by reducing single channel conductance. While channel activation is dependent on β subunit co-expression, effects on unitary conductance are independent of subunit composition. In the present study, chicken BK channels were heterologously expressed in HEK293 cells. Some cells expressed a single α subunit isoform, while others were co-transfected with the chicken homolog of the mammalian β 1 subunit. Tamoxifen (1 μ M) reduced single channel conductance by 24%, and this effect was independent of β subunit co-expression. However, if the expression construct included the β subunit, tamoxifen increased channel open probability. In this case, the half-activation voltage, in 1 μ M tamoxifen, shifted to more negative voltages, by \sim 17 mV. This effect on channel gating was dose dependent, with an EC₅₀ of about 0.4 μ M. These results are extraordinarily similar to tamoxifen's effects on mammalian BK channels. The result is somewhat surprising since the avian and mammalian β subunits share less than 50% sequence identity at the amino acid level. Nevertheless, the subunit dependent activity of tamoxifen should prove to be a useful tool in probing for β subunit effects both in the mammalian and avian cochleae. Supported by NIDCD DC00276.

461 The transient potassium channel, Kv4.2, interacts with a protein containing a pentraxin domain

Dmytro Duzhyy, Margaret Harvey, Bernd Sokolowski

Otolaryngology - HNS, University of South Florida, 12901 Bruce B. Downs Blvd., Tampa, FL, United States

The transient type potassium channel, Kv4.2, is expressed in short hair cells of the chick cochlea and the cochlear ganglion. Previously, we showed that this channel is sensitive to arachidonic acid, which causes a decrease in current amplitude. We used a yeast two-hybrid screening assay to determine potential interacting partners with Kv4.2. Using the N-terminal end (2-179 amino acids) of the chicken potassium channel Kv4.2 (cKv4.2, accession number AAL56633) as bait, we screened a cDNA library made from cochlear epithelial tissue of late embryonic chicken (days 14-19), *Gallus gallus*. This screen produced a total of 68 selected clones, of which 40 represented the coding sequence for a protein containing a pentraxin (PTX) domain in its C-terminal half. Ten of these 40 clones had the longest cDNA fragment which coded a protein sequence of 420 amino acids fused to the GAL4 protein activation domain. A homology search revealed a 53% homology to mouse pentraxin 3 (accession NP_033013). To further verify interactions between these proteins, Chinese Hamster Ovary (CHO) cells were co-transfected with vectors containing cloned PPTX (protein containing PTX domain) and cKv4.2. Co-immunoprecipitation experiments, using total extracts, confirmed an interaction. An analysis of the putative primary structure using protein analysis software (TopPred2, Stockholm University) suggested that PPTX is a membrane protein with one transmembrane region. Western blot analysis of membrane fractions of CHO cells transfected with PPTX as well as immunohistochemical data confirmed these predictions. Functional studies are necessary to further verify the functional relationship of PPTX to Kv4.2.

This project was supported by grant R01 DC04295 from the NIDCD.

462 Functional Properties of Inner Ear-Specific KCNQ4 Channels and the Significance of Alternative Splicing

Weihong Feng¹, Liping Nie¹, Yi Zhang², Ana Vazquez¹, K Morris³, Kirk Beisel³, Ebenezer N Yamoah¹

¹*Center for neuroscience/Otolaryngology, University of California, Davis, 1515 Newton Ct, Davis, CA, United States,* ²*Cardiovascular Med, University of California, Davis, one shields Ave, Davis, CA, United States,* ³*Dep of Biomedical Sciences, Creighton University School of Medicine, 2500 California plaza, Omaha, NE, United States*

Inner ear KCNQ4 channels are thought to contribute towards establishing the resting potential of hair cells and controlling the flow of K⁺ in the cochlear duct. However, the functional current phenotype has not been described in detail. At least two KCNQ4 splice variants were identified and cloned and this work discussed the "wild type" (WT) KCNQ4 (homomeric KCNQ4A) and a splice variant lacking exon 9 (deletion of 54 residues in the C-terminus adjacent to the S6 domain; homomeric KCNQ4C). We determined the electrophysiological properties of the inner ear

KCNQ4 channels expressed in Chinese hamster ovarian (CHO) cells. The currents were recorded with pipette solution consisting of (in mM) 140 KCl, 1 CaCl₂, 2 MgCl₂, 3 ATP, 10 HEPES, and 10 EGTA and a bath solution without ATP and EGTA. Outward KCNQ4 WT and variant current traces were generated with depolarizing voltage steps from a holding potential of -80 mV ($f'V = 10$ mV). The WT current had slow activation kinetics, small current density and its steady state activation was shifted by ~20 mV in the positive direction compared to the variant channel current. By contrast, the variant had fast activation kinetics, large current density and the activation is shifted, leftward. The currents were sensitive to linopridine and bepridil, known blockers of the KCNQ4 channel current. The dose-response relationship was examined for the effect of linopridine on the WT current and estimated an IC₅₀ of ~11 $f'M$. The functional basis for the low levels of WT vrs variant current was done using non-stationary fluctuation analysis and the number of functional channels in CHO cells expressing the variant channel were ~2-fold larger than WT. Co-expression of the WT and variant channels resulted in the expression of current magnitudes that suggested that the two channels form heterotetramers and revealed current properties that may represent that native current phenotype. The formation of heteromultimers of the WT and variant channels may confer functional diversity in the current phenotype in different hair cells.

This was supported by grants to NIDCD DC04279.

463 An Alternative Spliced Form of The Small Conductance Ca²⁺-Activated Potassium Channel, SK2, Missing The Calmodulin Binding Domain, Is Expressed in The Cochlea.

Liping Nie¹, Weihong Feng¹, Bruce Cheung², Ebenezer Yamoah¹, Ana E Vazquez²

¹*Center for Neuroscience/Otolaryngology, University of California Davis, 1515 Newton Ct., Davis, CA, United States,*

²*Otolaryngology, University of California Davis, 1515 Newton Ct., Davis, CA, United States*

The sensory organs of hearing and balance consist of highly differentiated epithelia containing hair cells. In the mammalian cochlea, there are two distinct types of hair cells. The inner hair cells contain the machinery that transduces changes in sound pressure stimuli into afferent signals, which are transmitted to the brain. The outer hair cells, in contrast, mostly receive feedback modulation from the brainstem through cholinergic fibers that form synapses at their basal ends. This efferent control, in the mammalian cochlea, regulates frequency selectivity, enhances sensitivity in the presence of background noise and plays a role in protection from noise over-exposure.

The synapses at the base of the outer hair cells have been studied and fast inhibitory synaptic currents mediated by the small conductance Ca²⁺-activated K⁺ (SK) channels have been demonstrated. We have recently described a complete SK2 cDNA expressed in the mouse cochlea. The present findings demonstrate the cloning of an SK2 spliced variant from the cochlea using PCR methods. The KCNN2 gene encoding the SK2 channel spans 126kb in mouse chromosome 18. Comparison of the SK2 cDNA and the genomic sequences suggest that this variant originates by

alternative exon utilization. This cochlea SK2 variant differs from the SK2 channel in that it is missing the calmodulin-binding domain in the carboxyl end of the protein. A novel 19 amino acid sequence constitutes the carboxyl intracellular domain in SK2V. This amino acid sequence shows no homology to any other protein in the databases. The potential functional relevance of the expression of this SK2 variant in the cochlea is currently under investigation.

Supported by NIH grants to ENY (DC003826, DC004215) and AEV (R21-DC04990)

464 Longitudinal and radial gradients of potassium currents in the outer hair cell

Shuping Jia, David Z.Z. He

Biomedical Sciences, Creighton University Medical School, 2500 California Plaza, Omaha, NE, United States

Longitudinal and radial gradients of potassium currents in the outer hair cell

Shuping Jia, David Z.Z. He, Dept. of Biomedical Sciences, Creighton University Medical School, Omaha, NE 68175

The differences in cell's electrical properties along the longitudinal axis of the basilar papilla are known to be critical in electrical tuning in non-mammalian vertebrae where the electrical filtering properties and the expression of ionic conductances of the cells vary systematically (Art and Fettiplace, 1987; Fuchs et al., 1988). Systematic variations in electrical properties of outer hair cells (OHCs) along the cochlea in mammals have also been demonstrated (Housley and Ashmore, 1992; Mammano and Ashmore, 1996). We attempted to study the longitudinal and radial gradients of potassium currents and the development of such gradients in OHCs. Coil preparation isolated from the apical and basal turns of the cochlea from adult (30-35 DAB) and neonatal gerbils (4 to 20 DAB) was used. Whole-cell voltage-clamp recordings were made from OHCs in the coil preparation where the position of the cells along the length of the basilar membrane and within each row can be determined unambiguously. Our results show that basal turn cells have larger potassium currents than their apical turn counterparts with $I_{k,n}$ most prominent in the basal turn cells and I_k most dominant in the apical turn cells. This is consistent with a previous study (Mammano and Ashmore, 1996). In the apex, the size of potassium currents is also different among three different rows of OHCs with row 1 cells having the largest conductance. There is a significant increase of potassium conductance in the first week after birth with a peak at 8 DAB when potassium currents as large as 11 nA are recorded. The currents are reduced to approximately 1.5 nA around 3 weeks after birth. Interestingly, the radial gradient of potassium currents among three rows of OHC before 10 DAB is just the opposite of what was found in adult OHCs. Supported by NIH grant R01 DC 04696.

465 Differential Effects of Nitric Oxide on ATP-induced Ca^{2+} Signaling in Outer and Inner Hair Cells of the Guinea Pig Cochlea

Narinobu Harada, Masahiko Izumikawa, Toshihiko Kaneko, Jing Shen, Toshio Yamashita

Otolaryngology, Kansai Medical University, Fumizonochi 10-15, Moriguchi, Japan

Our recent study suggested that nitric oxide (NO) inhibited extracellular ATP-induced Ca^{2+} response by a negative-feedback mechanism in inner hair cells (IHCs) of the guinea pig cochlea (Shen et al. *Neurosci Lett*.337:135-138,2003). However little is known about effects of NO on the ATP-induced Ca^{2+} response in outer hair cells (OHCs).

In the present study, we investigated whether ATP can induce NO production and NO may affect ATP-induced Ca^{2+} signaling in OHCs using the Ca^{2+} -sensitive dye fura-2 and the NO-sensitive dye DAF-2. Extracellular ATP induced an increase in DAF-2 fluorescence, which thus indicates of NO production in OHCs. Suramin, an antagonist for P2 receptor, inhibited the ATP-induced NO production in OHCs. Furthermore, ATP-induced NO production in OHCs was significantly suppressed by the pretreatment with L-NAME, a non-specific NO synthesis inhibitor. In the absence of extracellular Ca^{2+} , ATP-induced NO production was abolished. These results suggest that the ATP-induced NO production was mainly due to a Ca^{2+} influx through the activation of P2-purinergic receptor. L-NAME inhibited the ATP-induced increase of intracellular Ca^{2+} concentrations ($[Ca^{2+}]_i$) in OHCs while L-NAME enhanced it in IHCs. SNAP, a NO donor, enhanced the ATP-induced $[Ca^{2+}]_i$ increase in OHC while SNAP inhibited it in IHCs. Our results suggest that NO enhanced the ATP-induced $[Ca^{2+}]_i$ increase in OHCs by a positive-feedback mechanism in contrast to IHCs, which showed a negative-feedback effects on the ATP-induced Ca^{2+} response.

In conclusion the present study suggests that NO has opposite effects on the ATP-induced Ca^{2+} response in OHCs and IHCs. Our results also suggest that NO may play an important role in both afferent and efferent auditory signal transduction by differential effects.

466 Nature and expression of L and non-L calcium currents by frog crista hair cells

Ivo Prigioni, Giancarlo Russo

Dept of Physiol. and Pharmac. Sci., University of Pavia, Via Forlanini 6, Pavia, Italy

Variations in the electrophysiological properties of hair cells appear to be a general feature of the vertebrate vestibular sensory organs. It is well established that type II vestibular hair cells differ in term of their ion channel expression and electrical activity. Here, we studied Ca^{2+} currents in hair cells of the frog crista ampullaris using the whole-cell variant of the patch-clamp technique. Currents were recorded in situ from hair cells in peripheral, intermediate and central regions of the sensory epithelium. Two types of Ca^{2+} currents were found: a partially inactivating current that was expressed by nearly all central cells and by about 65% of intermediate and peripheral cells, and a sustained current expressed by the remaining cell population. The mean Ca^{2+} cur-

rent amplitude was larger in intermediate cells than in central or peripheral cells. The two types of Ca²⁺ currents were composed of two components: a large, nifedipine-sensitive (NS) current and a small, nifedipine-insensitive (NI) current. The latter was resistant to SNX-482, omega-conotoxin MVIIC and omega-agatoxin IVA and to omega-conotoxin GVIA, antagonists of R, P/Q and N-type Ca²⁺ channels. The amplitude of NS and NI currents varied among peripheral cells, where the current density gradually increased from the beginning of the region toward its end. No significant variation of Ca²⁺ current density was detected in hair cells of either intermediate or central regions. These results demonstrate the presence of regional and intraregional variations in the expression of L and non-L Ca²⁺ channels in the frog crista ampullaris. Finally, immunocytochemical investigations revealed the presence of Ca²⁺ channel subunits of the alpha1D type and the unexpected expression of alpha1B-subunits. In conclusion, the presence of gradients of Ca²⁺ current density in the peripheral regions of the crista epithelium would have functional implications in differentiating transmitter release among sensory cells. This implies possible variations of the gain of the afferent neurons innervating crista hair cells.

467 Role of NO/cyclicGMP pathway on ATP-induced Ca²⁺ Response in Cochlear Inner Hair Cells of the Guinea Pig

Jing Shen, Narinobu Harada, Toshio Yamashita

Otolaryngology, Kansai Medical University, Fumizonochi 10-15, Moriguchi, Japan

Recently we demonstrated that nitric oxide (NO) inhibited the ATP-induced Ca²⁺ response by a negative-feedback mechanism in inner hair cells (IHCs) of the guinea pig cochlea (Shen et al. *Neurosci Lett.*337:135-138,2003).

Here, we investigated the role of NO/cyclicGMP pathway and neuronal nitric oxide synthase (nNOS) on the ATP-induced Ca²⁺ signaling in IHCs using fura-2 and DAF-2. In the absence of extracellular Ca²⁺, thapsigargin, Ca²⁺-ATPase inhibitor, failed to induce NO production, whereas Ca²⁺ responses were elicited. Simultaneous measurement of intracellular Ca²⁺ concentrations ([Ca²⁺]_i) and NO production showed that the ATP-induced [Ca²⁺]_i increase was preceded NO production. These results suggest that Ca²⁺ influx may be essential for the ATP-induced NO production in IHCs. L-NAME, a non-specific NOS inhibitor accelerated ATP-induced Mn²⁺ quenching in fura-2 fluorescence while SNAP, a NO donor suppressed it, suggesting that ATP-induced NO inhibits a [Ca²⁺]_i increase by a negative-feedback mechanism. The ATP-induced Ca²⁺ response was enhanced by ODQ, an inhibitor of soluble guanylate cyclase (sGC) and KT5823, an inhibitor of cyclicGMP-dependent protein kinase (PKG). 8-Br-cGMP, membrane permeable of cGMP attenuated the ATP-induced Ca²⁺ response. Moreover, the effects of L-NAME and 7-NI, a selective nNOS inhibitor did not show significant difference either in the enhancement of ATP-induced Ca²⁺ response, or in the attenuation of NO production. Immunofluorescent double staining of nNOS and eNOS using isolated IHCs revealed that nNOS punctuated in the apical region of IHCs by its intense staining compared with the homogeneous cellular distribution of eNOS.

In conclusion, the ATP-induced Ca²⁺ influx may be the principal

source for nNOS activity. Thereafter NO can be produced and conversely inhibits the ATP-induced Ca²⁺ influx via NO-cGMP-PKG pathway. Our results also suggest that nNOS and ionotropic P2X receptor may co-localize and interact with each other in the apical region of IHCs.

468 Conditional Gene Targeting in the Inner Ear by Modification of a Pax2 Bacterial Artificial Chromosome

Taka Ohyama, Andy Groves

Cell and Molecular Biology, House Ear Institute, 2100 W 3rd street, Los Angeles, CA, United States

To generate conditional inner ear knockout mice using the Cre-loxP system, we focused on the regulatory region of the Pax2 gene to isolate a specific promoter for inner ear precursor cells. Pax2 is expressed in the midbrain-hindbrain boundary, kidney, optic vesicle, spinal cord and otic vesicle during embryonic development. To analyze the regulatory region of Pax2, we isolated a BAC clone containing about 101kb of upstream sequence of the Pax2 coding region and inserted IRES-Cre-polyA into the Pax2 coding region using a BAC modification system. We established a prototype inner ear-specific Cre line with this Pax2-Cre construct.

Here, we show the analysis of this line by mating with R26R reporter mouse strains. The prototype Pax2-cre line drives functional Cre expression in the kidney, midbrain-hindbrain boundary and otic placode. Reporter positive cells are detected in the otic placode from E8.5 (7-8ss). As the inner ear develops, most of the cells derived from the otic placode are reporter-positive in this line. We have begun a preliminary analysis of beta-catenin conditional knockout mice using our prototype Pax2-Cre mice. Beta-catenin is required for the canonical Wnt signaling pathway and is also a component of adherens junctions. We found the otic placode is greatly reduced in size without beta-catenin suggesting that Wnt signaling may be involved in very early stages of otic development.

469 Distinct Functions of Sox9a and Sox9b in Otic Placode Specification

Dong Liu, Lisa Maves, Yi-Lin Yan, Monte Westerfield

Biology, University of Oregon, Institute of Neuroscience, Eugene, Oregon, United States

Cells are specified to form the otic placode in response to inductive signals from neighboring tissues like the underlying mesoderm and the adjacent hindbrain. We previously showed that Fgf3/8 dependent and independent pathways act synergistically to specify the zebrafish otic placode. The Fgf3/8 dependent pathway acts at least in part through Sox9a; the independent pathway requires Dlx3b/4b function.

A second zebrafish Sox9 gene, *sox9b* is expressed, like *sox9a*, in otic precursor cells. Loss of either Sox9a or Sox9b alone resulted in a somewhat reduced but otherwise fairly normal otic vesicle, whereas loss of both functions together blocks formation of the vesicle, suggesting that both functions are required. Over-expression of Sox9a, but not Sox9b, can induce formation of ectopic otic placodes. Upon loss of Fgf3/8, Sox9a expression is lost, however, Sox9b is still expressed. Ectopic Fgf8 induces *sox9b*, but not *sox9a*. Furthermore, Dlx3b/4b are required for expression of both

Sox9a and Sox9b. Thus, Sox9a provides an Fgf3/8-dependent instructive role in otic placode induction, whereas Sox9b augments placode induction in a partially Fgf3/8-independent, Dlx3b/4b-dependent manner. (Funds from NIH and CIHR)

470 The Characterization of a Chick Foxi1 Orthologue.

Susan Boerner, Michael Francis Teraoka Escaño, Raj K. Ladher

Laboratory for Sensory Development, RIKEN Center for Developmental Biology, 2-2-3 Minatogijima-minamimachi, chuo-ku, Kobe, Japan

The response of the future otic placode to otic inducing signals has been a subject of intense study. A combination of embryological studies in the chick and genetic studies in the mouse and fish are describing a network of inducing signals and responses. In order to synthesize these data we are beginning to investigate some of the transcription factors described in the genetic studies using more embryological approaches. Studies in the mouse and the fish have revealed the importance of a member of the forkhead family of transcription factors, foxi1, in the development of the otic placode. In the zebrafish, fox i1 has been shown to play an essential role in the induction of the otic placode. In the mouse, foxi1 plays a role in later inner ear development. We have identified a homolog of foxi1 in the chick. The expression pattern of the chick foxi1 is more like the fish than the mouse, being expressed early in the presumptive otic placode. Data is also presented discussing the function of foxi1 during the induction of the chick otic placode.

471 Gbx2 is Important for Mouse Inner Ear Development

Zhengshi Lin, Raquel Cantos, Doris K Wu

Lab of Molecular Biology, National Institute on Deafness and Other Communication Disorders, 5 Research Court, Room 2B34, Rockville, MD, United States

Gbx2 (gastrulation and brain-specific homeobox protein 2) is a transcription factor related to the Drosophila unplugged gene. Gbx2 plays a critical role in the correct patterning and development of the anterior hindbrain. In addition, Gbx2 RNA is detected in the posterior hindbrain and inner ear of mouse embryos, suggesting a role for Gbx2 in the development of these structures.

To address the role of Gbx2 in inner ear development, we analyzed the inner ears of Gbx2 knock out mice. In the inner ear, Gbx2 is initially expressed in the otic placode, and later its expression is restricted to the endolymphatic duct and sac. Paint-filled analysis of Gbx2 ^{-/-} inner ears (n=19) at 15.5/16 days post coitum revealed broad but variable phenotypes. In every ear examined the endolymphatic duct and sac were invariably missing, and the cochlear duct was enlarged and often shortened. In contrast, semi-circular canal formation was quite variable in Gbx2 mutants; about half of the inner ears examined lack anterior and posterior semicircular canals, while the lateral canal was present in all but one of the mutants. Given the restricted pattern of expression of Gbx2, the broad range of structures that were affected in mutant inner ears suggests Gbx2 plays a non-cell autonomous role in inner ear development.

Since Gbx2 is normally expressed in the posterior hindbrain, we

also examined this region in the Gbx2 mutant mice. Gene expression analyses indicated that rhombomere 5 (r5) was affected in Gbx2 ^{-/-} mutants. The expression levels of Krox 20 and EphA4 in r5 were down regulated; whereas the expression levels of Fgf3 and Kreisler were up regulated. While Hoxb1 expression in r4 appeared relatively normal, Fgf3 was ectopically expressed in this region as well as a region rostral to r4. These results suggest that Gbx2 is required for normal patterning of the caudal hindbrain. Given the important role of hindbrain signaling for inner ear development, it is possible that some of the defects observed in the inner ears of Gbx2 knockout mice may be a consequence of abnormal hindbrain signaling.

472 Ids Regulate Expression of Math1 and Hair Cell Differentiation during the Development of the Organ of Corti

Jennifer Michelle Jones^{1,2}, Mireille Montcouquiol¹, Matthew W. Kelley¹

¹NIDCD, NIH, 5 Research Ct, Rockville, MD, United States, ²Cell Biology, Georgetown University, 3900 Reservoir Rd., Washington, DC, United States

The basic Helix-Loop-Helix (bHLH) transcription factor math1 is both necessary and sufficient for hair cell differentiation in the cochlea. However the factors that regulate the temporal and spatial expression of math1 are unknown. Id proteins are good candidates for regulating the expression of math1 in the cochlea since they are known to negatively regulate many bHLH transcription factors.

In situ hybridization on alternate cochlear sections showed that prior to hair cell differentiation, id1 and math1 expression domains overlap. Once hair cells begin to differentiate, id1 expression is downregulated in cells that express math1.

To test the biological effects of ids, we overexpressed id via electroporation in the developing mouse organ of Corti at E13. Cochlear sensory progenitor cells transfected with a vector expressing EGFP alone were able to adopt any cell fate in the organ of Corti indicating that transfection and transgene expression do not bias progenitors toward a specific cell fate. To examine the role of Ids in regulating Math1 expression, explant cultures were transfected with control EGFP, math1/EGFP, or id/EGFP expression vectors. The fates of transfected cells for each condition were determined using cell type specific antibodies. When cells were transfected with control EGFP 48% developed as hair cells and 52% developed as supporting cells while 100% of cochlear progenitor cells transfected with a math1/EGFP expression vector differentiated into hair cells. In contrast, only 6% of cells transfected with id/GFP developed as hair cells and 94% developed as supporting cells.

Our data show that the over-expression of Id significantly inhibits cells from developing as hair cells. These results demonstrate that Ids play a key role in regulating Math1 expression and hair cell differentiation in the developing cochlea.

473 Id1 Stimulates the Proliferation of Progenitor Hair Cells via the NF- κ B/cyclin D1 pathway *in vitro*

Masashi Ozeki, Yuki Hamajima, Katsuyuki Tsuchiya, Eileen P Schlentz, Frank G Ondrey, Jizhen Lin

Otolaryngology, University of Minnesota, 2001 6th Street SE, Rm. 221, LRB, Minneapolis, Minnesota, United States

Dominant negative basic helix-loop-helix (dn-bHLH) transcription factors, namely, inhibitors of differentiation (Id), play an essential role in the neurogenesis of the central nervous system. However, the role of dn-bHLH in the development of cochlear sensory hair cells is not understood. In this study, we demonstrated the expression pattern of the Id genes in the developing cochlear tissue of rats and the role of Id genes in the proliferation of cultured progenitor hair cells (OC1) via a nuclear factor kappa B (NF- κ B)/cyclin D1-dependent mechanism. Two members of the Id gene family, Id1 and Id3, were highly expressed in the rapidly growing otocyst on embryonic day 12 (E12) and in the organ of Corti, spiral ganglions, and stria vascularis on postnatal day 1 (P1). Inhibition of the Id1 gene with short interfering RNA (siRNA) significantly reduced the cell proliferation of OC1 whereas enforced expression of Id1 significantly increased the cell proliferation. The latter is fully dependent upon the activity of the NF- κ B/cyclin D1 pathway. Inhibition of the NF- κ B activity with pyrrolidine dithiocarbamate (PDTC) or inhibitory kappa B alpha (I κ B $_s$) abrogated the Id1-induced cell proliferation and cyclin D1 transcription, whereas enhancement of the NF- κ B activity with p65 (subunit of NF- κ B) increased the Id1-induced cell proliferation and cyclin D1 transcription. This work demonstrates that Id1 induces the proliferation of OC1 via the NF- κ B/cyclin D1 pathway *in vitro*, and that crosstalk between Id proteins and NF- κ B may play a role in hair cell development.

474 Notch and Hes1 inhibit the proliferation of progenitor hair cells and expression of hair cell markers *in vitro*

Yuki Hamajima, Masashi Ozeki, Jizhen Lin

Otolaryngology, University of Minnesota, 2001 6th St SE, Rm. 216 LRB, Minneapolis, MN, United States

The Notch signaling pathway plays a role in the development of cellular mosaics of hair cells vs. supporting cells. The profiles of the Notch signaling pathway genes and how they are involved in this process are, however, poorly understood. In this study, we precisely dissected cochlear tissue and profiled the expression of genes involved in the Notch signaling pathway using Affymetrix microarrays and confirmed the expression of the Notch signaling pathway genes by RT-PCR. The unique expression patterns of the Notch signaling pathway genes in the ear of rats were Delta1 and 3; Jagged and Jagged 2, Notch and Notch 2, *Hes1*, 2,3 and 5. The major genes expressed were Notch, Delta1, and Hes1. Inhibition of Notch, *Hes1*, and *Hes3* gene expression in progenitor hair cells (OC1) with short interfering RNA (siRNA) and/or antisense oligos significantly increased cell numbers, DNA synthesis, and cell cycle progression compared to controls. Inhibition of the expression of *Hes1*, an important downstream molecule of the Notch signaling pathway, in OC1 upregulated the expression of Brn3.1 and

oncomodulin whereas inhibition of Notch1 up-regulated the expression of Brn3.1 but down-regulated the expression of oncomodulin, suggesting that the Notch signaling pathway genes are involved in hair cell development through the regulation of hair cell marker proteins.

475 FGF8 regulates pillar cell development in the organ of Corti

Bonnie E Jacques¹, Mark Lewandoski², Matthew W Kelley¹

¹Section on Developmental Neuroscience, NIH-NIDCD, #5 Research Ct 2B-44, Rockville, Maryland, United States, ²Laboratory of Cancer and Developmental Biology, NIH-NCI-Frederick, Bldg 539, Rm 105, Frederick, MD, United States

Pillar cells (PCs) play a vital role in hearing, however the molecular signaling pathways that regulate their development are poorly understood. Mice with a targeted-deletion of the fibroblast growth factor receptor three gene (*fgfr-3*) are characterized by a disruption in PC development and subsequent lack of formation of the tunnel of Corti. As a result, these animals exhibit profound deafness. Previous work from this laboratory has demonstrated that continuous activation of FGFR3 is required throughout PC development. The aim of the current study is to identify the endogenous ligands responsible for FGFR3 activation in the organ of Corti (OC). FGF8 and FGF17 are closely related FGFs, exhibiting high binding affinities for FGFR3. Both *fgf8* and *fgf17* are expressed in the embryonic OC, with *fgf8* being expressed specifically in inner hair cells (IHCs). To determine whether FGF8 acts as an endogenous ligand for FGFR3, we used a cre-lox strategy to generate a tissue-specific knock-out of *fgf8*. Inner ears from mice lacking *fgf8* show a dramatic reduction in the size and overall development of PCs. Similar results were obtained in explant cultures using antibodies that specifically prevent binding of FGF8 to FGF receptors. Addition of anti-FGF8 to explants at different developmental time points demonstrated that there is an ongoing requirement of FGF8 throughout PC development. In addition, exposing explants to purified FGF17 results in a dramatic increase in cells positive for PC markers and a significant decrease in the number of outer hair cells, suggesting that FGF17 may act as a second endogenous ligand for FGFR3 in the OC. These results support the hypothesis that FGF8 and/or FGF17 may act as the endogenous ligands responsible for activation of FGFR3 and the subsequent development and differentiation of PCs. The results also suggest that the positioning of PCs between inner and outer hair cells may be regulated by the limited expression of FGF8 in IHCs.

476 Math1 regulates supporting cell development in the organ of Corti

Chad Woods, Mireille Montcouquiol, Matthew Kelley
NIDCD, NIH, 5 Research Court, Rockville, MD, United States

The basic helix-loop-helix (bHLH) transcription factor Math1, a mammalian analog of *Drosophila* Atonal, has been shown to be necessary and sufficient for hair cell differentiation in the developing mammalian cochlea. However, the specific role of Math1 during the development of the cochlea remains unclear. In particular, it has been suggested that development of supporting cells is unaffected in the absence of Math1.

To examine the potential role of Math1 in development of supporting cells, the pattern of expression for math1 in the developing cochlea was examined at different developmental time points in mice expressing b-galactosidase under the control of the Math1 promoter. Results indicate that math1 is initially expressed beginning between E12.5 and E13.5. Math1 is initially diffusely expressed in a comparatively broad stripe of cells that extends along the basal-to-apical axis of the cochlear duct. As development proceeds, individual cells that express higher levels of math1 can be identified in more differentiated regions of the cochlea.

To determine whether supporting cell development is affected in the absence of math1, supporting cell phenotypes were examined in math1 mutant mice. In addition, the expression of supporting cell-specific markers, including p75ntr, S100A and TC2, was examined at E16 and E18.5. Expression of all supporting cell markers was significantly disrupted in math1 mutants.

These results suggest that math1 is transiently expressed in a large population of sensory precursors, including cells that will develop as supporting cells. Moreover, the observation that supporting cell phenotypes are disrupted in the absence of math1, demonstrates that math1 is required for the normal differentiation of supporting cells in the organ of Corti. Ongoing experiments will determine whether Math1 acts directly or indirectly on supporting cell development.

477 Towards establishing the role of Math1 in the inner ear.

Veronica Ana Matei¹, Adriano Flora², David H. Nchols³, Kirk Beisel⁴, Huda Zoghbi⁵, Bernd Fritzsche¹, Vincent Wang⁶

¹Biomedical Sciences, Creighton University, 2500 California Plaza, Omaha, NE, United States, ²Department of Pediatrics, Baylor College of Medicine, One Baylor Plaza, Houston, Texas, United States, ³Biomedical Sciences, Creighton University, 2500 California Plaza, Omaha, NE, United States, ⁴Biomedical Sciences, Creighton University, 2500 California Plaza, Omaha, NE, United States, ⁵Departments of Pediatrics, Baylor College of Medicine, One Baylor Plaza, Mail Stop 225, Houston, Texas, United States, ⁶Department of Pediatrics, Baylor College of Medicine, One Baylor Plaza, Houston, Texas, United States

Math1, an essential gene for hair cell differentiation (Bermingham et al., 1999), is also expressed in proliferative precursors in the cerebellum and spinal cord. Some data on Math1 expression in the cochlea exist, but no data on Math1 expression with respect to vestibular hair cell mitosis or sensory neuron mitosis is available. The latter is particularly important as ngn1 null mutant mice show loss of hair cells (Fritzsche et al., 2000), suggesting conservation of Ngn1-Math1 interaction as recently shown in the spinal cord (Gowan et al., 2001). Using single step BrDU labeling and confocal microscopy we show an apex to base gradient of hair cells (E11-E13.5). Few BrDU positive hair cells are found at E14.5 in the hook region and coincide with Math1 upregulation. We demonstrate this directly by doubly labeling for BrDU and Math1-beta-galactosidase. Earlier claims suggesting that Math1 is only in postmitotic cochlear hair cells (Chen et al., 2002) are confirmed for most of the cochlea. Our data on vestibular development suggest co-expression of Math1 with proliferating hair cell precursors from E12.5 onward. We also confirm earlier reports on the longi-

tudinal gradient of spiral neuron formation, progressing from the base to the apex (E10.5-E13.5). Vestibular neuron formation extends over a longer period, with no obvious correlation to the Math1 expressing sensory epithelia. Analysis of hair cell fate in Math1 null mutants shows persistence of some undifferentiated hair cell precursors until E19.5, in a pattern identical to that of Math1-beta-galactosidase heterozygotic littermates. BDNF, a neurotrophin expressed only in differentiated hair cells, shows variations along the length of the cochlea suggestive of differential regulation of expression by Math1 and other factors. Our data show a more complex and variable interaction of Math1 with proliferating and postmitotic precursors in a distinct pattern that pre-dates the latter functional differences of hair cells.

478 The Role of Cyclin-Dependent Kinase Inhibitors in the Development of the Mouse Organ of Corti

Feng Liu^{1,2}, Ping Chen¹, Yun-shain Lee¹, Neil Segil^{1,2}

¹Gonda Department of Cell and Molecular Biology, House Ear Institute, 2100 West Third St., Los Angeles, CA, United States, ²Neuroscience Program, University of Southern California, xxx, Los Angeles, CA, United States

The cell cycle is strictly regulated during organ of Corti development to produce the correct number of sensory hair cells and supporting cells required for inner ear function. The majority of sensory precursor cells withdraw from the cell cycle between E12.5 and E14.5. This occurs in a gradient of cell cycle exit starting with cells that will form the apex and ending with those that will form the base of the organ of Corti (Ruben, 1967). p27Kip1 is a cell cycle inhibitor whose absence results in persistent cell division within the organ of Corti beyond the normal period of cell cycle exit. To further define the role of p27Kip1, we studied the temporal and spatial patterns of cell cycle withdrawal of hair cell precursors in p27Kip1 homozygous mutant (p27Kip1^{-/-}) mice. We found that although the timing of the last hair cell precursor division is delayed, a gradient of cell cycle withdrawal along the cochlear duct is still observed, indicating that additional mechanisms of cell cycle exit are active in the absence of p27Kip1. To determine whether p19Ink4d, another cell cycle inhibitor present in the embryonic Organ of Corti is responsible, we studied cell cycle exit in double-mutant embryos (p27Kip1^{-/-}:p19Ink4d^{-/-}). At birth, the phenotype of the double-mutant embryos appears the same as the p27Kip1 mutant animals, indicating that p19Ink4d does not substitute for p27Kip1 during the establishment of the postmitotic sensory epithelium. Therefore, our results suggest that other factors, besides these cell cycle inhibitors, are likely to be involved in regulating cell cycle withdrawal in the developing organ of Corti.

479 Role of the F-box protein Skp2 in cell proliferation in the developing auditory system in mice

Koji Iwai¹, Takayuki Nakagawa¹, Tsuyoshi Endo¹, Tae-Soo Kim¹, Fukuichiro Iguchi¹, Norio Yamamoto¹, Shinji Takebayashi¹, Youyi Dong², Yasushi Naito¹, Juichi Ito¹

¹Otolaryngology Head and Neck Surgery, Kyoto University Graduate School of Medicine, 54 Kawahara-cho, Shogoin Sakyo-ku, Kyoto, Japan, ²Kagawa Medical University, Department of Cell Physiology, 1750-1 Ikenobe, Miki-cho, Kida-Gun, Kagawa, Japan

In order to understand the mechanisms that regulate the development of the auditory system it is necessary to understand how the cells involved proliferation and differentiation. The F-box protein, Skp2 positively regulates the G1-S transition by controlling the stability of several G1 regulators, including p27. In this study, we examine the expression of Skp2, in combination with the expression of p27.

ICR mice pups On E10 (n = 4), E12 (n = 4), E14 (n = 4) or E17 (n = 4) were harvested from pregnant females and on postnatal day 7 (P7) were prepared. Whole embryos (at E10, E12, and E14) and dissected heads (at E17 and P7) were fixed in 4% paraformaldehyde at 4°C. Anti-Skp2 rabbit polyclonal antibody, anti-Ki67 mouse monoclonal antibody, anti-p27 mouse monoclonal antibody and anti-myosin VIIa rabbit polyclonal antibody were used as primary antibody. We observed in the greater epithelial ridge (GER), primordial organ of Corti (OC) and spiral ganglion neurons (SGNs).

Co-expression of Skp2 and Ki67 was observed in the OC, GER and SGNs regions during development of the auditory system. The expression of p27, however, was detected in these regions when Skp2 and Ki67 were down-regulated. The change in these expression patterns appeared in the OC between E12 and E14, and in the GER and SGN between E17 and P7. These findings indicate that Skp2 play crucial role in regulation of cell proliferation in the developing auditory system.

480 Developmental Changes in the Expression of Retinoic Acid-Synthesizing and -Metabolizing Enzymes in the Developing Mouse Inner Ear

Raymond Romand¹, Takako Kondo², Pascal Dolle¹, Eri Hashino²

¹Institut de Biologie Moleculaire et Cellulaire, INSERM, BP 10142, Strasbourg, France, ²Otolaryngology-HNS, Indiana University School of Medicine, 699 West Drive, RR132, Indianapolis, IN, United States

Retinoic acid (RA) plays essential roles in patterning and development of the embryonic inner ear. Recent studies revealed that the precise control of RA concentrations in a local embryonic region is achieved by the balance between RA-synthesizing and -metabolizing enzymes. Enzymes involved in this control include (1) retinaldehyde dehydrogenases (Raldh1, 2, 3 and 4) that synthesize RA and (2) cytochrome p450s (Cyp26A and -B) that catabolize RA. To determine which enzymes play major roles in inner ear development and also to identify the cellular sites that synthesize or metabolize RA, we investigated expression patterns of Raldh1-4

and Cyp26 mRNAs in the mouse inner ear from E9 to P20. Our RT-PCR analysis demonstrated that expression levels and temporal patterns in expression level varied profoundly among the enzymes that we examined. Of the four Raldhs, the Raldh3 level was highest, followed by Raldh2. Raldh1 expression was very low, and detectable only at E18 or later. In contrast, Raldh4 expression was detectable only at early embryonic ages (E9-10), after which it became undetectable. Expression levels of Cyp26A and -B mRNAs were high at E9-12, after which the Cyp26A level declined sharply. Our in situ hybridization analysis indicated that expression domains of Raldhs and Cyp26s in the inner ear were largely complementary and nonoverlapping. Interestingly, strong Raldh3 signals were detected in the spiral ganglion, while Raldh3 transcripts were barely detectable in the vestibular ganglion. Expression of Cyp26s was present mainly in the otic epithelium and periotic mesenchyme regions. These results suggest that the expression of each member of the Raldh and Cyp26 families is regulated independently during inner ear development. In addition, specific and strong expression of Raldh3 in the spiral ganglion suggests novel functions of this enzyme in cochlear neuron development.

Supported by CNRS, INSERM and NIH R21DC005507

481 Cellular Growth and Rearrangement suggests a Role for Convergent Extension during the Development of the Mammalian Organ of Corti

Erynn Elizabeth McKenzie, Alison Krupin, Matthew Kelley

NIDCD, NIH, 5 Research Court, Rockville, MD, United States

The mammalian organ of Corti, one of the most highly ordered cellular patterns in any vertebrate system, is comprised of ordered rows of different cell types including inner and outer hair cells and support cells. At present, the factors that play a role in the development of this cellular pattern remain unknown, however it seems likely that physical growth of the cochlear duct could influence cellular patterning. To examine this hypothesis, we determined changes in cell size and distribution for different regions of the cochlea duct (inner sulcus, sensory epithelium, and outer sulcus) during mouse embryonic development. We show that the number of cell-cell contacts within the developing sensory epithelium decreases as the overall length of the duct increases suggesting that the spatial distribution of sensory precursors changes as the cochlea develops. To examine the nature of this change in spatial distribution the sensory precursor population was visualized at different developmental time points by labeling with an antibody against the cell cycle inhibitor p27kip1. Results indicated that while the number of p27kip1-positive cells remained constant between E14 and P0, the spatial distribution changed from comparatively short and broad early in cochlear development to comparatively long and thin at late developmental time points. These data are consistent with convergent extension, a developmentally conserved mechanism that has been shown to play a role in cellular morphogenesis in many systems. The results also suggest that convergent extension could regulate cellular patterning in the organ of Corti.

482 The Use of Ultrasound Backscatter Microscopy to Access the Developing Mouse Otocyst *in utero*

John V. Brigande¹, Donna M. Fekete²

¹Oregon Hearing Research Center, Oregon Health & Science University, 3181 SW Sam Jackson Park Rd, Portland, OR, United States, ²Biological Sciences, Purdue University, Lilly Hall, West Lafayette, IN, United States

The mouse has emerged as a powerful genetic model organism to study development and function of the inner ear. Yet relatively little is known about the lineage relationships and cell fate decisions that accompany ear development in the mouse. Because many specialized cell types are only present in the mammalian cochlea, certain lineage questions must be tackled in the mammal. Such studies require the delivery of lineage tracers to the developing ear *in utero*. We have been injecting retroviruses into the mouse otocyst at E11.5 to mark individual progenitor cells, although we now seek to target the ear at earlier stages. The challenge is that the early postimplantation mouse embryo is enshrouded in extraembryonic membranes and maternally-derived tissues that confound conventional imaging techniques. Ultrasound backscatter microscopy (UBM) is capable of transuterine imaging of the developing mouse embryo from pre-otic placode to advanced otocyst stages. At the functional core of the microscope is a miniaturized, consolidated transducer that both generates ultrasound waves at variable frequencies and captures their backscattered echoes from living tissues in real time. Transuterine UBM of E10.5 mouse embryos enabled visualization of the late otic cup/early otic vesicle as a distinct echogenic oval field bounded ventrolaterally by the anterior cardinal vein and medially by the hindbrain. UBM-guided transuterine microinjection into the E10.5 otic vesicle was achieved and will be demonstrated in digital movie format. UBM-guided transuterine microinjection of bioactive reagents into the mouse inner ear should soon be possible. Ultimately, mouse mutants that would otherwise develop with compromised inner ears could be used as test subjects for phenotypic rescue attempts by introducing bioactive reagents into the unformed otocyst.

483 Electroporation of an Episomal Expression Vector shows that Ganglion Neurons but not Glia originate from the Otic Cup

Takunori Satoh, Donna M Fekete

Biological Sciences, Purdue University, 915 W State st., West Lafayette, IN, United States

In lineage studies using retroviral vectors, we have shown that sensory cells in chicken inner ear can be clonally related to cells in the otic ganglia. However, because of the dispersed nature of alkaline phosphatase (AP) as a marker, it was difficult to exclude the possibility that some AP⁺ cells in the ganglia were not neurons but their enveloping satellite cells. Previous studies using chick-quail transplants concluded that all glial cells, and some vestibular ganglion neurons, derive from neural crest. To provide independent evidence that satellite cells are not of placodal origin, we labelled otic cup cells using plasmid encoding enhanced yellow fluorescent protein (EYFP) using conditions whereby only ectodermal cells were transfected. Because we wanted to retain plasmid out to

stages where the neurons and satellite cells were differentiated, we designed a new plasmid vector that incorporated the following: 1) Gal-4 UAS cassette to enhance expression; 2) EYFP fused with Histone 2B for nuclear localization to facilitate double-labelling with antibodies; 3) OriP/EBNA-1 viral replicon for episomal replication and segregation to each daughter cell.

Plasmid was injected into the chicken otic cup at HH stage 11.5-14, and five electric pulses of 10-20v, 1msec were delivered through a fine tungsten cathode. Ears were harvested at E9, frozen sectioned and immunostained with anti-neurofilament-160 and Alexa564-phalloidin to selectively stain neurons and glia, respectively. EYFP⁺ cells were widely distributed in the ear epithelium, ganglia and nearby epidermis. 128 EYFP⁺ nuclei in the ganglia of 9 embryos were observed with confocal microscopy. 122 were clearly neuronal, while none of the remainder had a glial phenotype. We conclude that neurons arising from the otic placode are unrelated to glia in the otic ganglia.

484 Expression of Islet1 Suggests Its Involvement in the Development of the Sensori-neural Lineage in the Inner Ear

Ling Pan¹, Lin Gan¹, Jane E Johnson², Neil Segil³, Ping Chen³

¹Center for Aging and Development, University of Rochester, 111 Road, Rochester, NY, United States, ²Center for Basic Neuroscience, University of Texas Southwestern Medical Center, 5323 Harry Hines Blvd., Dallas, TX, United States, ³Cell and Molecular Biology, house Ear Institute, 2100 W. 3rd St., Los Angeles, CA, United States

Basic helix-loop-helix (bHLH) and LIM-homeodomain (LIM-HD) transcriptional factors act cooperatively for generating cellular diversity in the nervous system. In the cochlea, the sensory hair cells and the spiral ganglion (SG) neurons that innervate the auditory sensory organ, the organ of Corti, are thought to be derived from the same lineage during development. Several bHLH genes have been shown essential for the generation of a variety of cell types in the nervous system including SG neurons and sensory hair cells in the inner ear. However, the mechanisms that specify the common progenitors and the cellular context-dependent mechanisms that confer the inner ear-specific neuronal or sensory competency/identities remain elusive. Here we show that Islet1, a LIM-HD protein, is expressed early in the otocyst in the region that gives rise to both the cochlea and SG neurons. Subsequently, the expression of Islet1 is maintained in SG neurons while transit in the sensory lineage. At embryonic day 12 (E12) in mice, the expression of Islet1 marks the entire ventral portion of the nascent cochlear epithelium encompassing the primordial organ of Corti. At E13, as the cells in the primordial organ of Corti exit the cell cycle, Islet1 is first down regulated in the region medial to the sensory primordium, followed by down-regulation in the entire cochlear epithelium at later stages. The expression of Islet1 in the developing inner ear suggests that Islet1 might be involved in the sensory-neural lineage development in the otocyst, and in specifying the SG neuron competency and identity in coordination with bHLH genes as observed in other neuronal systems.

485 LIM Homeodomain Transcription Factors in the Inner Ear

Cyrille Sage, Mingqian Huang, Zheng-Yi Chen

Neurology, Massachusetts General Hospital and Harvard Medical School, 55 Fruit St., Boston, MA, United States

Lim3 (Lhx3) and Isl-1 belong to the homeodomain transcription factor of LIM family. Studies have demonstrated that both are involved in specifying subclass identities of neurons in the spinal cord, through combinatorial expression of both genes. Lhx3 and Isl-1 are expressed in a subset of motor neurons with axons projecting ventrally for the neural tube (v-MN), whereas only Isl-1 is expressed in the motor neurons with dorsal axon projection (d-MN). Ectopic expression of Lhx3 in d-MN led to switch of the identity from d-MN to v-MN.

We studied the expression pattern of Lhx3 and Isl-1 in the developing inner ear. Isl-1 is expressed in the otocyst sensory progenitor at E11.5. Isl-1 expression is subsequently maintained in the supporting cells, and reduced in the hair cells, and the same expression pattern persists in the adult. The expression of Lhx3 starts in the vestibular hair cells at E12.5, immediately after the expression of Brn-3.1. The expression of Lhx3 is subsequently up regulated in the hair cells in the inner ear, and a similar expression pattern is present in the adult hair cells. Therefore the expression of Isl-1 and Lhx3 in the inner ear, in particular in the supporting cells and the hair cells, shares a remarkable similarity with their respective expression in the spinal cord, indicating that they may be involved in the differentiation of both cell types, through a combinatorial mechanism.

GeneChip analysis of the Brn-3.1 knockout mice showed that Lhx3 is down-regulated, whereas Isl-1 is up-regulated, in the Brn-3.1^{-/-} inner ear. Down-regulation of Lhx3 and up-regulation of Isl-1 in the Brn-3.1^{-/-} hair cells was confirmed by immunostaining using the antibodies against both transcription factors. Therefore the expression pattern in the developing inner ear, and in the Brn-3.1^{-/-} mice, placed Lhx3 downstream of Brn-3.1, likely in the Brn-3.1 pathway. The results also indicated that up-regulation of Lhx3 and down-regulation of Isl-1 may be necessary for terminal differentiation of the hair cells.

486 FGF signaling and its regulation during the development of the mouse ear

Chaoying Li¹, Xiaofen Wang¹, Daryl Scott², Suzanne L Mansour¹

¹Human Genetics, University of Utah, 15 N 2030 E RM 2100, Salt Lake City, UT, United States, ²Children's Health Research Center, University of Utah, 401 MREB, 20 North 1900 East, Salt Lake City, UT, United States

Our lab studies the roles of FGF signaling in the development of the mouse peripheral auditory system. We showed previously that Fgf3 and Fgf10 are required to initiate inner ear development and that their role is to establish patterns of gene expression in placodal ectoderm. FGF signals activate intracellular signaling pathways, primarily the ERK/MAPK cascade. Signaling through MAPKs is subject to negative feedback regulation at a variety of levels. For example, *Drosophila puc*, which encodes a dual-specificity phosphatase (DSP), is a transcriptional target of signaling through the

DJNK MAPK pathway and feeds back to dampen signaling by inactivating DJNK. We found an insertion near mouse *Dusp6*, which encodes a DSP that is specific for ERK MAPK. *Dusp6* is expressed at sites of FGF signaling and in periotic mesenchyme, which gives rise to the ossicles and otic capsule and participates in reciprocal signaling with the otic epithelium. To determine the role of *Dusp6* in ear development and to address the hypothesis that *Dusp6* functions in the ERK pathway similarly to *puc* in the DJNK pathway, we investigated *Dusp6* transcription in embryos with reduced FGF signaling and analyzed mice lacking *Dusp6*. *Dusp6* mRNA was reduced in embryos with reduced signaling through either Fgfr1 or Fgfr2. Loss of *Dusp6* caused dominant perinatal lethality with reduced penetrance. Both *Dusp6*^{+/-} and *Dusp6*^{-/-} embryos had increased levels of pERK. Affected pups were small and had craniosynostosis, reflecting activation of FGF signaling similarly to that seen in humans and mice with activating mutations in FGF receptors. In addition, the otic capsule and ossicles of small *Dusp6*^{-/-} pups were abnormal. Consistent with these observations, a small *Dusp6*^{+/-} that survived until P21 had increased ABR thresholds. Further characterization of the development of these phenotypes, progress in identifying genes redundant with *Dusp6* and in determining which FGF/ERK pathways *Dusp6* regulates will be presented.

487 Unraveling the Pathogenesis of POU4F3 Related Deafness Via the Identification of Downstream Target Genes

Ronna Hertzano^{1,2}, Mireille Montcouquiol², Sharon Rashi-Elkeles¹, Rani Elkon¹, Rechavi Gideon³, Tarik Moroy⁴, Thomas B Friedman⁵, Matthew W Kelley², Karen B Avraham¹

¹Human Genetics and Molecular Medicine, Tel Aviv University, Ramat Aviv, Tel Aviv, Israel, ²Section on Developmental Neuroscience, NIDCD, 5 RC, Rockville, MD, United States, ³Pediatric Hematology-Oncology, Sheba Medical Center, Sheba Medical Center, Tel Hashomer, Israel, ⁴Universitätsklinikum Essen, Institut für Zellbiologie, Virchowstrasse 173, Essen, Germany, ⁵Laboratory of Molecular Genetics, NIDCD, 5 RC, Rockville, MD, United States

Pou4f3 is a class IV POU domain transcription factor that plays a crucial role in the maturation and survival of the hair cells in the mouse auditory and vestibular sensory epithelia. Moreover, a mutation in *POU4F3* underlies human hereditary autosomal dominant non-syndromic hearing loss. We have previously described a global comparison analysis of embryonic inner ear mRNA expression from wild type and *Pou4f3* mutant mice. We now further validate the microarray results by a combination of real time RT-PCR, and whole mount and section *in situ* hybridization on wild type and *Pou4f3* mutant mice allowing us to identify *Gfi1*, a recently identified deafness gene, as the first bona fide downstream target of *Pou4f3*. To examine the specific role of *Gfi1* in the pathogenesis of *Pou4f3* related deafness, we performed a comparative analysis of the embryonic inner ears of both *Pou4f3* and *Gfi1* mouse mutants via a combination of immunohistochemistry and scanning electron microscopy. Our results suggest that the lack of *Gfi1* is the most likely cause of outer hair cell degeneration in the cochlea of the *Pou4f3* mutant mice. Finally, we have identified a highly conserved *Pou4f3* binding site in the *Gfi1* promoter and, by *in vitro*

transcription regulation assays, have examined the regulation of *Gfi1* expression by both wild type and mutant forms of Pou4f3.

These results represent one of the first studies using molecular and cellular biological techniques in tandem to definitively identify a transcriptional cascade in inner ear hair cells. Furthermore, the availability of mouse mutants for both Pou4f3 and *Gfi1* offers a unique opportunity to study pivotal genes in maturation and survival of the hair cells of the inner ear.

488 Detection of Cytokines in Developing and Mature Inner Ear Cells

Lynne M Bianchi¹, Zeeba Daruwalla¹, Ayo-Lynn Richards¹, Christopher Macklin¹, Susan J Allen², Kate F Barald²

¹Neuroscience, Oberlin College, 130 West Lorain St, Oberlin, OH, United States, ²Cell and Developmental Biology, University of Michigan, E. Catherine St, Ann Arbor, MI, United States

Inner ear cell lines are useful for a variety of studies, including analysis of secreted inner ear proteins. In the present study, supernatants were harvested from immortalized, embryonic inner ear cells (Barald et al., 1998) and analyzed for the presence of cytokines. Cytokines are proteins involved in a wide variety of cellular mechanisms including cell migration and proliferation. Cytokines were analyzed using Western blots and antibody arrays. Immunohistochemical analysis was then performed to determine the cellular localization of identified cytokines in the developing and mature inner ear. The identified cytokines revealed spatiotemporal differences in expression, suggesting various functions for these proteins. Further, the experiments demonstrate the usefulness of cell lines as screening tools for secreted inner ear proteins.

Supported by NIH NIDCD R15 DC05587 and NIH NIDCD R01 DC 04184

489 Developmental analysis of protein expression using proteomics in rat cochlea

Kim Young Ho¹, Jung Hak Hyun²

¹Otolaryngology, Seoul Municipal Boramae Hospital, 31-1 Boramae street, Dongjak-gu, Seoul, Korea, Republic of,

²Otolaryngology, Korea University, College of medicine, Anam-dong 5th Ave 126-1, Seongbuk-gu, Seoul, Korea, Republic of

The purpose of the present study was to compare the profiles of protein expression in rat cochlea between the first stages of development (postnatal day 5, P5 group) and adult stage (5wk group) in order to identify proteins which relate to the maturation of cochlea.

Cochleas of 5 male Sprague-Dawley rats were pooled for each stage. After the sample preparation, the isoelectric focusing (IEF) and two-dimensional polyacrylamide gel electrophoresis (2-D PAGE) were performed. Protein spots were analyzed using software package (Melanie 3.0), and the spots which show marked difference between two group were selected. To identify protein entities, peptide mass fingerprints were determined by matrix-assisted laser desorption/ionization time of flight (MALDI-TOF) mass spectrometry and database searches were performed. Twenty-seven spots (11 spots of P5 group and 16 spots of 5wk group) within the mass range 24 - 116 kDa were subjected for analysis. Thirteen proteins could be identified as increasing during maturation period. Prostaglandin-D synthase, Calretinin, Annexin V (Lipocortin V, CBP-1, Calphobindin 1), Myo-inositol-1-phos-

phate synthase A 1 (Inositol-3-phosphate synthase isoenzyme 1), Creatine kinase (B chain), Calcitonin gene-related peptide-receptor component protein (CGRP-RCP) and Neuron specific enolase (NSE, Neural enolase, Gamma enolase) that were found in adult rat cochlea (5wk group) are known to be involved to the signal transduction, post-transcriptional modification, ion channel activity, energy transduction, maturation and maintenance of nervous system during the development. This result suggests that the appearance of several sets of proteins are critical for the maturation of cochlea since the first stages of development, postnatal day 5. Further confirming experiments are necessary.

490 A Receptor-like Tyrosine Phosphatase Associated with the Apical Surface of Supporting Cells Downregulates During Postnatal Development of the Mouse Utricle

Tao Kwan, Kevin Legan, Richard Goodyear, Guy Richardson

School of Life Sciences, University of Sussex, Lewes Road, Brighton, United Kingdom

Reversible protein-tyrosine phosphorylation has important implications in the control of signal transduction, cell proliferation, and differentiation. The supporting-cell antigen (SCA) is a class III receptor-like tyrosine phosphatase (RPTP) expressed on the apical surface of supporting cells in the avian inner ear. It is down regulated in response to hair-cell loss and it has been suggested it may regulate the ability of supporting-cells to transdifferentiate or proliferate (Kruger, R et al., J Neurosci 19(12): 4815-27, 1999). It is not known whether mammalian supporting cells express a similar receptor. The most likely murine homologue of the SCA is Byp (HPTP beta-like tyrosine phosphatase, also known as Density Enhanced Phosphatase, RPTPeta, CD148, PTPRJ), a class III RPTP that has 50% identity with the SCA at the amino acid level and is up-regulated prior to the density-dependent inhibition of cell proliferation in vitro (Kuramochi, S et al., FEBS Lett 378: 7-14, 1996). A rabbit polyclonal antibody was raised to the intracellular domain of Byp and shown to react with a polypeptide of the expected mass on Western blots of lectin-purified membrane proteins from kidney and brain. Immunofluorescence staining using the polyclonal antibody to Byp shows that it is expressed on the apical surface of supporting cells in the mouse cochlea and utricle. In the cochlea, Byp is expressed on the apical surface of the entire sensory epithelium at E17 but restricted to the GER by P2. In the utricle, Byp is expressed at early postnatal stages (P2 - P16), but is down regulated by P32. RT-PCR also shows a decrease in Byp mRNA level between P2 and P32. The down-regulation of Byp correlates with the known postnatal decrease in the proliferative potential of mammalian utricular supporting cells (Corwin, JT et al., ARO Abstr 23: 272, 2000). Sponsored by the Wellcome Trust

491 The Mouse and the Ear: from pet to paradigm

Robert Ruben

Otolaryngology, Albert Einstein College of Medicine, 3400 Bainbridge Ave, Bronx, New York, United States

Unusual varieties of mice - called 'fancy mice' were enjoyed as pets in China and Japan from at least the 17th through the 20th

centuries. Among them was the “waltzing mouse,” called the Nankin mouse, described with the others in the book, *Chingan-sodategusa* published in Japan in 1787. As late as the 1850’s the waltzing mouse was thought to be the result of confinement for untold centuries in small cages (Lysenkoism?), but it is now recognized as an inner ear mutant. By the 19th century, these *waltzers* were kept as pets in Europe and North America as well as Asia. They first became subjects of scientific inquiry in Europe through W. Haacke’s article in A.E. Brehm’s 1890 *Tierleben* and as a separate communication in 1895¹. The vestibular and cochlear abnormalities of the ear of the waltzing mouse were first described by Bernard Rawitz in 1899². Abbie Lathrop brought these mice to North America as pets, raising them on her farm in Granby, Mass. where they were observed by William Castle at Harvard who brought them to the study of genetics. In this context, Robert Yerkes, then a Harvard graduate student, published his dissertation, *The Dancing Mouse: a Study in Animal behavior* in 1907, the first North American monograph detailing and correlating inner ear malformations with behavior. During the first half of the 20th century numerous investigators established the underlying genetics of many of the waltzing mouse and other unusual strains, and used these mutants to characterize the pathological anatomy and physiology of genetic deafness. Among many who have worked in this area during the first half of the 20th century are M.S. Deol, W.H. Gates, Hans Grüneberg, C.C. Little, E.M. Lord, and others. These investigators established the foundation for our current and highly fruitful use of the mouse as a model for the study of normal and abnormal cell biology of the ear.

492 High-throughput “knockouts” for Hearing Genes in Mice

Jiangang Gao, Jian Zuo

Dept. Of Developmental Neurobiology, St Jude Children’s Research Hospital, 332 N. Lauderdale St., Memphis, TN, United States

The speed with which genes important for hearing have been identified has clearly outpaced the rate at which their functions can be determined. There are many human deafness genes whose functions are unknown because of the lack of animal models. The use of transgenic and knockout mouse models is a powerful approach to the elucidation of gene function and disease mechanism. However, the methods to produce these mice are not readily available or familiar to many researchers in the hearing field. This deficiency hampers the rapid advancement of our understanding and treatment of hearing disorders. However it is now feasible to efficiently create gene-targeted mouse models for hearing in a high-throughput manner.

Based on our recent success in creating prestin, GluR?1 and other knockout mice (Lieberman et al., 2002) and ?9 AChR overexpressing mice (Zuo et al., 1999; Maison et al., 2002), we have adopted several methods for making high-throughput gene knockouts. We first obtained several existing ES cell lines with targeted mutations in three genes important for hearing and created mutant mice. Secondly, we utilized recombineering-based methods to create targeting vectors including conditional constructs for several genes important for hearing. Thirdly, we used BAC targeting vectors to transfect ES cells and screened for homologous recombination using realtime PCR and FISH. Karyotyping was performed to

confirm the normal chromosomal structure and number before blastocyst injection. Heterozygous mutant mice can be cryopreserved. Both null and conditional alleles can be obtained by crossing the heterozygous mice with well-characterized Cre lines. The resulting homozygous mutant mice can be characterized in auditory physiology and morphology. Further characterization of mutant mice will be carried out in collaboration with other laboratories.

Our effort in developing a high-throughput knockout strategy can be useful to efficiently create many mouse models for the hearing research community.

493 A Mouse Mutagenesis Screen to Identify Genes Important for hearing

Mohammad Habiby Kermany^{1,2}, Y. K. Guo³, T. J. Yoo⁴, Evgeni M. Rinchik⁵, Daniel Goldowitz⁶, Jian Zuo⁷

¹Department of Developmental Neurobiology, St. Jude Children’s Research Hospital, 332 N. Lauderdale St., Memphis, TN, United States, ²Immunology and Allegy, University of Tennessee, VA Medical Center, Memphis, TN, United States, ³Developmental Neurobiology, St. Jude Children’s Research Hospital, 332 Lauderdale St., Memphis, TN, United States, ⁴Immunology and Allegy, University of Tennessee, 956 Court Ave., Memphis, TN, United States, ⁵Life Sciences Division, Oak Ridge National Laboratory, ., Oak Ridge, TN, United States, ⁶Anatomy and Neurobiology, University of Tennessee, 855 Monroe Ave., Memphis, TN, United States, ⁷Developmental Neurobiology, St. Jude Children’s Research Hospital, 332 N. Lauderdale St., Memphis, TN, United States

Ethyl-n-nitrosourea (ENU) is a strong mutagen that introduces single base-pair changes in the genome. Mutagenesis using ENU followed by screening for abnormal neurological phenotypes in mice thus serves as a strong foundation for the genetic dissection of phenotype and genotype relationships in central nervous system as well as periphery and sensory organs. The NIH funded neuromutagenesis program in TMGC employed an ENU mutagenesis scheme in which visible or molecular markers and specific mouse strains with inverted chromosomal regions were used to easily identify mice carrying the recessive mutations. This approach offers an economy of effort and reliability in addition to pre-localizing mutations to discrete regions of the genome. Although many mutant mouse strains with auditory defects are available, identification of new genes and new alleles of “old” genes important for hearing will provide valuable resources for our understanding of hearing and deafness.

In other mutagenesis programs, startle reflex and pre-pulse inhibition were used as primary auditory screens. The rates of identifying mutants in these two assays have been low: 0.6-1.8 per 1,000 pedigrees in the two genome-wide dominant screens (GSF and Harwell, respectively). In our auditory primary screen in the TMGC neuromutagenesis program, we employed far field auditory brainstem responses (ABR) to click and pure tone stimulations at frequencies of 8, 16, and 32 kHz. In the past 16 months, we have screened a total of 172 pedigrees (553 mice). A total of 8 pedigrees (4.6%) showed hearing abnormalities of unilateral and bilateral deafness, mild to severe hearing loss, or localized hearing loss to the high frequency stimuli. Test class mice that displayed aberrant ABR results in this program are being tested further that

will explore in details functional deficits and morphological abnormalities in auditory pathway.

494 EUMORPHIA and The Sensory Systems

Emma Louise Coghill¹, Steve D.M. Brown¹, Caroline Thaug², Hamid Meziane³, Raymond Romand³, Serge Picaud⁴, Alan Hart⁵, Sally Cross⁵, Ian Jackson⁵

¹MGU & MGC, Medical Research Council, MRC Harwell, Harwell, United Kingdom, ²Department of Ophthalmic Pathology, Royal Eye Hospital Manchester, Oxford Road, Manchester, United Kingdom, ³IGBMC, IGBMC, 1 Rue Laurent Fries, Illkirch, France, ⁴Hospital St-Antoine, INSERM, 184 Rue De Faubourg, St-Antoine, France, ⁵Human Genetics Unit, Medical Research Council, Crewe Road, Edinburgh, United Kingdom

The completion of the human genome sequence highlights the need to determine the function of each of the ~35000 human genes and their role in disease. This will be greatly assisted by the development and characterisation of mouse models of human disease. Comprehensively assessing the phenotypic consequences of any change made in a gene will require systematic screens.

The initial aim of the EUMORPHIA programme is to develop and disseminate a standardized European Comprehensive First-line Phenotyping protocol (or ECFLP) for all body systems in the mouse. The sensory systems workpackage within the EUMORPHIA programme covers the study of audition, vestibular function, vision, olfaction and taste.

Two levels of first-line phenotyping have been defined; primary screens represent the routine tests making up the core of any robust first-line screen; primary extended tests are those valuable in a first-line screen, but dependent upon a variety of circumstances – such as availability of facilities, equipment, skills and resources. The tests to be included within the ECFLP have been chosen and refinement and validation using control mutant lines and specific inbred lines is underway.

Secondary screens will involve the development of new approaches in phenotyping, mutagenesis and informatics leading to improved dissemination and querying of mouse model characteristics. Within this workpackage this involves developing; OAE protocols, the use of MRI for morphological screening of the ear, aspects of a behavioural ontology, ERG and optokinetic drum protocols and a non invasive intraocular pressure technique. Progress within the sensory systems workpackage including ECFLP developments is described.

495 ABR and Hair Cell loss in wild-type muted mice

Robert Burkard^{1,2}, Da-Lian Ding¹, Yuqing Guo¹, Haiyan Jiang¹, Kathleen Szalda¹, Richard Swank³, Edward Novak³

¹Center for Hearing and Deafness, University at Buffalo, 3435 Main Street, Buffalo, NY, United States, ²Communicative Disorders and Sciences, University at Buffalo, 3435 Main Street, Buffalo, NY, United States, ³Molecular and Cellular Biophysics, Roswell Park Cancer Institute, Elm and Carlton Streets, Buffalo, NY, United States

Muted mice are a spontaneous mutation localized to chromosome 13, with a recessive pigmentary/vestibular disorder. Young adult muted mice have good hearing (by ABR) up to ~ 7 months, with

poor ABR morphology and elevated thresholds at 12 months and older. There is a normal complement of inner hair cells (IHC) and outer hair cells (OHC) at 2 months of age, with substantial IHC loss at 7 months and older. This pattern of hair cell loss was found in mice homozygotic for the muted gene (mu/mu), as well as heterozygotic mice (mu/+). We back crossed the mu/+ mice, identified those mice that were wild types, i.e., had no muted gene (+/+) as identified by PCR, and investigated their hearing and hair cell loss at 7-8 months of age. We studied five 7 month old and four 8 month old wild type (+/+) mice. One 7 month old died during ABR recording, and only their hair cell counts are used. ABR thresholds were obtained to clicks and 3, 6, 12, 24 and 36 kHz tonebursts. Mice were sacrificed, cochleae harvested, and hair cell counts made of one cochlea of each mouse. ABR thresholds for the +/+ mice were quite similar to those obtained previously to similarly aged mu/mu and mu/+ mice. The pattern of hair cell loss in the +/+ mice was similar to that seen in the mu/mu and mu/+ mice. Specifically, there was little loss of OHCs, but IHCs were missing, most prominently in the basal half of the cochlea. All 8 month old +/+ mice showed substantial IHC loss, as did two 7 month old +/+ mice. Three 7 month old +/+ mice showed minimal IHC loss. These data suggest that the muted gene does not lead to IHC loss in strain CHMU/LE, and that some other gene is leading to the adult-onset loss of IHCs. Further, the fact that only a subset of 7 month old mice had IHC loss suggests that either there is variability in when IHC loss starts in these mice, or that the onset of IHC loss is near 7 months of age.

Work supported by NIA AG05924

496 Qualitatively Different Patterns of Cochlear Noise Injury in CBA and C57BL/6 Mouse Strains

Kevin K. Ohlemiller, Jaclynn M. Lett, Patricia M. Gagnon
Otolaryngology, Washington University, 660 S. Euclid, St. Louis, MO, United States

Hirose and Liberman (JARO, 2003) showed that the endocochlear potential (EP) in CBA/CaJ mice is transiently reduced after noise exposure. At ARO 2003, we reported a negative result in C57BL/6 (C57) mice for a similar exposure (2 hr BB noise, 110 dB SPL). Young (3-4 mo) C57 and B6.CAST+*Ahl* mice show neither acute EP reduction nor lateral wall pathology, while similar-aged CBA/J and /CaJ mice show a 30-50 mV EP reduction and vacuolation of Type II fibrocytes and stria basal cells. We have extended our observations to albino C57BL/6 *c2j/c2j* mice, and have compared the correlates of permanent noise injury in CBAs and C57s.

Like C57s, albino congenics show no significant noise-related EP reduction (n=9 noise, 6 control). Thus differences between C57s and CBAs are not due to melanin. CAP thresholds at 8 wks post-noise were 25-45 dB higher at 10-20 kHz in B6.CAST+*Ahl* mice than in CBA/J mice. However, more extensive pathology was evident in the CBAs. Although the EP recovered, light microscopy revealed atrophy of the stria vascularis in 85% of sections (6 mice) and extensive loss of fibrocytes in spiral limbus (0.03±0.2 / 1,600 mm² in upper base). The incidence of stria atrophy was significantly lower in B6.CAST+*Ahl* mice (<30% of sections, 6 mice), and fibrocyte loss appeared minimal (4.8±1.4 / 1,600 mm²).

Although C57 mice—with or without *Ahl* are—more vulnerable

to noise than CBAs (Ortmann et al., ARO 2004), they sustain less injury to lateral wall and limbus for a given exposure. We posit that they carry different alleles at multiple loci that 1) render lateral wall and limbus *less* vulnerable than in CBAs, and 2) render organ of Corti *more* vulnerable than in CBAs. Preliminary analyses indicate greater incidence of supporting cell pathology (Ohlemiller, JARO 2002) in B6.CAST^{+Ahl} than in CBA/J (50% of sections vs. 17%). Because degeneration of lateral wall and limbus can have little effect on thresholds, C57 mice sustain greater noise-induced threshold elevation.

497 Inter-Strain Variation in Resistance to Acoustic Injury in Mice: Differences in Damage or Recovery?

Sharon G. Kujawa^{1,2}, M. Charles Liberman^{1,3}, Kelly M. Brinko³, Lija M. Enas², Bruce L. Tempel^{4,5}

¹Department of Otolaryngology, Harvard Medical School, 243 Charles St., Boston, MA, United States, ²Department of Audiology, Massachusetts Eye and Ear Infirmary, 243 Charles St., Boston, MA, United States, ³Eaton-Peabody Laboratory, Massachusetts Eye and Ear Infirmary, 243 Charles St., Boston, MA, United States, ⁴V.M. Bloedel Hearing Research Center, University of Washington, 1959 NE Pacific St, Seattle, WA, United States, ⁵Department of Otolaryngology-HNS, University of Washington, 1959 NE Pacific St, Seattle, WA, United States

Some strains of mice (e.g., B6) are highly vulnerable to noise-induced hearing loss (NIHL), while others (129S6, MOLF) are highly resistant, and one commonly studied strain (CB) is intermediate. In previous work, we have concentrated on the permanent threshold shifts (PTS) that can be quantified at long post-exposure times. To understand the mechanisms underlying this PTS variation, however, it is important to know whether noise vulnerability differences arise in the acute *response to* or the slow *recovery from* the noise. Thus, in the present study we compare noise-induced threshold shifts in several mouse strains at 24 hr vs. 2 wk post exposure. Groups of CB, B6, 129S6 and MOLF mice were noise exposed (8-16 kHz, 94-103 dB SPL, 2 hr). Threshold shifts were evaluated by ABR and DPOAE (5.6-45.2 kHz). Twenty-four hours following 103 dB SPL exposure, all strains showed large threshold shifts (~30-55 dB). Shifts for 129S6 and MOLF were smaller than CB and B6 at lower frequencies. Two weeks after exposure, B6 showed no threshold recovery while CB showed improvements confined to frequencies at the lower edge of the exposure band. In contrast, 129S6 and MOLF showed thresholds across frequency that had returned to near pre-exposure levels. Results suggest that PTS resistance in 129S6 and MOLF arises from enhanced recovery from acute damage. However, at some exposure levels even vulnerable animals show robust short-term shifts that recover to little or no PTS. Continuing studies will clarify the relationship between exposure level and kinetics of the post-exposure threshold shifts. This information also will guide our microarray studies of gene expression changes post exposure. Ultimate identification of the gene(s) responsible for NIHL susceptibility differences in mice will clarify mechanisms underlying noise-induced cochlear damage and will have ramifications for preventing or minimizing NIHL in humans.

NIDCD DC04983 (SGK), DC006305 (BLT)

498 Removal of the Ahl Allele from the C57BL/6 Background Does Not Improve Noise Resistance

Amanda J. Ortmann¹, Kathleen F. Faulkner¹, Patricia M. Gagnon², Kevin K. Ohlemiller²

¹Program in Speech and Hearing, Washington University, 660 S. Euclid, St. Louis, MO, United States, ²Otolaryngology, Washington University, 660 S. Euclid, St. Louis, MO, United States

C57BL/6 (C57) mice carry *Ahl*, which imparts age-related hearing loss (Johnson et al., HR 1997) and vulnerability to noise-induced hearing loss (NIHL) (Davis et al., HR 2001). Characteristics of C57s attributable to *Ahl* may be determined by examining B6.CAST^{+Ahl} (B6.CAST) mice, which are C57s in all ways except for the substitution of the *castaneus* allele at the *Ahl* locus. While previous studies indicated that B6.CAST mice are more resistant to noise than C57s (Vazquez et al., ARO 2000), these applied a single fixed exposure, and compared only young animals (2.5 mo). In a study aimed at determining the *threshold exposure* for NIHL in C57 and CBA/CaJ mice using a dose-response approach (Ohlemiller et al., HR 2000), we found little apparent influence of *Ahl* at 1-2 mo, but a pronounced influence at 5-7 mo. To determine the quantitative impact of *Ahl* on the C57 background, we have extended our methods to B6.CAST mice at 1-2 mo and 5-7 mo.

Mice (n=4-8) were exposed to broadband noise (110 dB SPL) for durations varying from .47-120 min in 2x increments. For each group, the *probability* (p) of NIHL was taken as the proportion of animals showing a criterion amount of NIHL, as determined by ABR at 3 wks post-noise. A dose-response curve was then derived by fitting a 4-parameter logistic equation to the raw data, and solving the fitted curve for the exposure duration corresponding to p=0.9. To confirm the consistency of our approach, we repeated our earlier tests of C57 mice.

Threshold exposures determined for C57s were close to those obtained previously (3.1 vs. 3.9 min at 1-2 mo; 13.4 vs. 10.7 min at 5-7 mo). At both ages, B6.CAST mice showed lower exposure thresholds (2.7 min at 1-2 mo; 7.9 min at 5-7 mo) than C57s.

When examined using threshold measures at a defined point on the NIHL dose-response curve, B6.CAST^{+Ahl} mice appear at least as vulnerable to noise as C57s, and much more vulnerable than CBA/Ca. Loci other than *Ahl* probably promote noise injury in this strain.

499 Cochlear Dysfunction in COUP-TFI Mutant Mice

Gentiana I. Wenzel¹, Fred A. Pereira², John S. Oghalai¹

¹Dept. of Otolaryngology-HNS, Baylor College of Medicine, One Baylor Plaza, NA102, Houston, TX, United States, ²Huffington Center on Aging, Baylor College of Medicine, One Baylor Plaza, N 710, Houston, TX, United States

COUP-TFI (Chicken Ovalbumin Upstream Promoter-Transcription Factor I) is an orphan member of the steroid/thyroid nuclear receptor superfamily. It is highly expressed in the developing nervous system. Null mutant COUP-TFI mice have glossopharyngeal nerve dysfunction that compromise feeding ability and

usually results in perinatal death. Surviving null mutant mice demonstrate neuronal differentiation defects, altered thalamocortical axon guidance, and apoptosis of cerebral cortical layer IV. COUP-TFI expression is also important for inner ear organogenesis. Null mutants have a shortened cochlear duct, abnormal cochlear innervation, and malformed vestibular chambers. Additionally, by P20 the organ of Corti in the basal turn has degenerated. Interestingly, the organ of Corti at the mid-modiolar region has only subtle anatomic irregularities and in particular, contains normal-appearing inner and outer hair cells. We recorded ABR and DPOAE thresholds in P16-18 null mutant COUP TFI mice and age-matched wild type controls. ABRs were evoked with a 5 msec sine wave tone pip. DPOAEs were elicited using F2=1.2*F1 and L2=L1. All measurements were performed using stimuli up to 80 dB SPL over the frequency spectrum of 1-40 kHz. Null mutant mice had no ABR and no DPOAE responses over the range of stimulation. In contrast, wild type mice had ABR thresholds of 30-50 dB, and DPOAE thresholds of 50-60 dB in the mid-to-high frequencies. In general, these responses occurred above 6.3 kHz. Both measures of hearing indicate that the COUP-TFI null mutant has profound cochlear dysfunction. Even though these mutants have cochleae with many normal anatomic features, these do not appear to have physiologic relevance.

Supported by NIH grants: DC05131 (J.S. Oghalai), DC-04585 (F. A. Pereira)

500 Characteristics of circling mouse; another candidate mouse model of DFNB6 mutation

See Youn Kwon¹, Myoung Soon Kim², Ji Hwan Woo¹, Sook Kyung Park², Young Ju Sung², Sam-Mi Yu², Won-Ho Chung², Zae Young Ryoo³, Kyoum In Cho³, Yang-Sun Cho², Hong Joon Park⁴, Sung hwa Hong²

¹Department of Biomedical engineering, College of Medicine, Hanyang University, Sungdong P.O.Box 55, Seoul, Korea, Republic of, ²Department of Otorhinolaryngology- Head and Neck Surgery, Sungkyunkwan University School of Medicine, 50 Irwon-dong Gangnam-gu, Seoul, Korea, Republic of, ³Catholic Research Institutes of Medical Science, Catholic university, 505 Banpo-dong Gangnam-gu, Seoul, Korea, Republic of, ⁴Department of Otorhinolaryngology- Head and Neck Surgery, Soree Ear Clinic, 46-16 Chungdam-dong, Gangnam-gu, Seoul, Korea, Republic of

Spontaneous mutant mice are suitable animal models for studying genetics and developmental defect of the inner ear. For example, Tmie gene defect in spinner (C57BL6 strain) seems to be a candidate gene for DFNB6. We reported a newly found spontaneous mutant mouse from the ICR strain (circling mouse) exhibiting circling and head-tossing behavior with no response to sound indicative of auditory dysfunction (ARO, 2001 & 2002). This mutation gene (cir gene) is transmitted autosomal-recessively and exists about 61cM from the centromere of chromosome 9, which is quite close to the locus for Tmie gene. We performed complementation test with these two strains, and observed morphological changes of the cochleae from spinner and circling mice on postnatal day 10 (P10), P14, P18, P22, and P35. We also measured the hearing thresholds with ABR using TDT Neurophysiology workstation. RT-PCR was done for Tmie mRNA in the brain, liver and cochlea from circling mice. It was confirmed that these animal models are

allelic. Morphologic changes of the cochleae in these strains were quite similar except tendency of earlier degeneration of the Organ of Corti in circling mice. Grossly, the inner ear developed normally by P10. However, from P14, degeneration of the organ of Corti and the spiral ganglion cells with tendency of more aggressive pathology in the base than in the apex was observed. ABR confirmed that these mice were deafened at least from P14. RT-PCR for Tmie mRNA confirmed circling mouse also has Tmie gene defect. Taken together, circling mouse is another candidate mutant mouse model for DFNB6 like spinner.

This study was supported by IN-SUNG Foundation for Medical Research (IS-2001-1)

501 A Functional Nucleotide Polymorphism in Cadherin 23 (Cdh23) is Associated with Age-Related Hearing Loss (ahl) and the Deafness Modifier mdfw

Konrad Noben-Trauth¹, Qing Yin Zheng², Kenneth R. Johnson²

¹Section on Neurogenetics, NIDCD/NIH, 5 Research Court, Rockville, MD, United States, ²The Mouse Mutant Resource, The Jackson Laboratory, 600 Main Street, Bar Harbor, ME, United States

Age related hearing loss (AHL) in mice is a genetically complex trait and parallels sensorineural presbycusis in human. Previous work by Erway and colleagues (1993) suggested the presence of two or three recessive ahl genes in C57BL/6J, BALB/c and DBA/2J. Through linkage analyses, one of these predicted polygenes, - the ahl locus - was mapped to chromosome 10. The deafness modifier mdfw accelerates hearing loss in strains that are heterozygous for a null allele for the Ca²⁺-ATPase 2 gene (Atp2b2). Using a positional cloning strategy, we identify a single nucleotide polymorphism in Cdh23 that is the main regulator of hearing thresholds in 56 inbred strains. The Cdh23<753A> variant causes in-frame skipping of exon 7. Altered adhesion function or reduced stability of cadherin 23 confers susceptibility to AHL. Homozygosity at Cdh23<753A> significantly increases susceptibility for AHL, but is not the only cause of its phenotypic manifestation. Predisposition to early-onset AHL conferred by Cdh23<753A> depends on the presence of several strain specific genetic factors, such as the mitochondrial mutation mt-Tr<9827ins8> (as in A/J), ahl2 (as in NOD/LtJ), and ahl3. A further genetic factor is the null allele of the Ca²⁺ ATPase ATP2B2, which is an important regulator of intrastereocilia Ca²⁺ levels. Haploinsufficiency at Atp2b2 and homozygosity of Cdh23<753A>, but neither alone, cause early-onset hearing loss in mdfw mice (Atp2b2<+/dfw-2J> mdfw/mdfw). General aging processes may account for variation within and among strains with late-onset hearing loss. The heterogeneity of secondary factors suggests additive or stochastic interactions with Cdh23<753A>.

502 An Eya1bor suppressor maps to mouse chromosome 4

Haoru Niu¹, Linna Makmura¹, Elizabeth M Keithley², Xiaobo Wang², Rick A Friedman¹

¹Cell and Molecular Biology, House Ear Institute, 2100 West Third St., Los Angeles, CA, United States, ²Otolaryngology, UCSD, 9500 Gilman Dr., La Jolla, CA, United States

Question Addressed: Genetic mapping and phenotypic characterization of a modifier gene of the Eya1bor mutant mouse. Methods and Measures: Phenotypic characterization, utilizing auditory evoked potentials of F2 Eya1bor homozygous mutants resulting from C3HeB/FeJ X C57BL/6J F1 heterozygous matings. Genetic mapping of the modifier locus/loci using microsatellite markers of the entire mouse genome at ~25cM intervals. Results: We have identified a modification of the originally described C3HeB/FeJ mutant phenotype in F2 Eya1bor homozygous mutants resulting from C3HeB/FeJ X C57BL/6J F1 heterozygous matings. In contrast to the C3H/HeJ mutants that display severe cochlear hypoplasia and deafness, the F2 modified mutants have varying degrees of cochlear morphogenesis and hearing. A suppressor locus has been mapped to chromosome 4 (D4Mit149). Conclusions: Mouse models have provided significant insights into many of the complex molecular mechanisms underlying mammalian inner ear development. These models, in the form of spontaneous and induced mutations, also provide powerful tools for the study of a variety of homologous forms of human syndromic and nonsyndromic hearing loss. This model described provides a system for deciphering a complex developmental pathway involved in hearing and for understanding the basis for variability in expressivity of the BOR phenotype. Clinical Significance of Study: Recently mutations in the EYA1 gene have been identified in some families with Branchio-Oto-Renal (BOR) syndrome. We have described a spontaneous mutation in the mouse orthologue, Eya1, providing a unique animal model for this human disease (Johnson et al. Hum. Mol. Genet. 84:645-653,1999). BOR syndrome displays variable penetrance and expressivity, both likely the result of genetic background effects.

503 Two New Mouse Mutants with Hearing Loss

Qing Yin Zheng, Belinda S Harris, Patricia Ward-Bailey, Heping YU, Amy Kiernan, Ken R Johnson

Genetics, The Jackson Laboratory, 600 Main Street, Bar Harbor, Maine, United States

Genetic mapping results and phenotype descriptions are presented for two new mouse mutants with hearing loss recently discovered at The Jackson Laboratory. The first mutation arose spontaneously on the BALB/cBy background. When homozygous this recessive mutation causes hearing loss and gross morphological anomalies of the inner ears. Mutant mice walk with an unbalanced gait, lean on their side, and have difficulty uprighting. They have a small body size, a variable life span, and are sterile. Two thousand F2 progeny from an intercross with CAST/Ei were used to map this mutation on central mouse chromosome 10. Allelism tests and genetic mapping have excluded all previously described deafness mutants in the genetic interval. The second mutation was induced by ethyl methanesulfonate (EMS) and is on a mixed C57BL/6J

and 129 background. This recessive mutation is named "trembler with hearing loss" (symbol *trhl*) because mutant mice have both a tremor and progressive hearing loss. Scanning Electron Microscopy analysis of mutant cochleae revealed both inner and outer hair cell degeneration. Genetic linkage crosses with CAST/Ei were used to map this mutation to mouse central chromosome 6, but is not allelic to any previously described deafness mutations.

Supported by NIDCD NIH grants: DC04376 and DC05846 to QYZ, DC62108 to KRJ.

504 T-cell Mediated Gene Therapy For Collagen Induced Ear disease CIED In Mice.

abdelwahab saeed¹, Brandon Hill¹, Yun-Kai Guo¹, Xiaoping Du¹, Mohammad Habiby Kermany¹, C. Garrison Fathman², Tai-June Yoo³

¹Allergy/Immunology, University of Tennessee, 956 Court Ave., B318, Memphis, TN, United States, ²Immunology & Rheumatology, Stanford University, 300 Pasteur Driver, Palo Alto, California, United States, ³Allergy/Immunology, University of Genoa, 956 Court Ave., B318, Memphis, TN, United States

Rationale: Objectives of this study are to see if IL-12-p40 protein is delivered to the inflammatory site of CIED, it would dampen CIED in mice. Methods: DBA1/Lac J (H2q) mice were injected with 200mg of type II collagen (CII) in CFA and received booster injection of 200mg (CII) in IFA. These mice were treated with CD4+ cells transfected with PGCY retroviral vector and IL-12-p40 gene fragment or PGCY retroviral vector only. Each animal received 106 cells. These T-cell hybridoma cells were generated from spleen cells from either CII specific or major basic protein (MBP) specific TCR transgenic mice and fused with BW 5147 TCR a-b(-) T-cell line. The gene for fluorescent protein was also transfused into CD4+ cells. These cells have homing properties to ear cartilage and joint tissues. T-cell stimulation assays, Elisa for anti-CII antibody and cytokines were analyzed and imaging of T-cell trafficking and histologic examination were done. Results: The incidence of CIED was 80% in the vector group, and 64% in the gene therapy group. Supernatant from cultures of cells transfected with IL-12-p40 produced IL-12-p40 protein. The INF-g was less in the mice with gene therapy than the control group. Conclusion: These results indicate that the local delivery of IL-12-p40 by T-cells inhibited CIED through suppression of the autoimmune response at the site of inflammation. We conclude that modifying antigen specific T-cells by transduction for local delivery of protein may prove to be a promising therapeutic strategy for the treatment of CIED.

505 Virally-mediated Gene Transfer: from virology to practice

Anne Luebke¹, Andreas Amalfitano², Nicholas Muzyczka³, Xandra Breakefield⁴, Beverly Davidson⁵, Jeffrey Holt⁶, Matthew Kelley⁷, Hinrich Staecker⁸, Anil Lalwani⁹

¹*Biomedical Engineering and Neurobiology and Anatomy, University of Rochester Medical Center, 601 Elmwood Ave., PO Box 603, Rochester, NY, United States,* ²*Pediatrics, Genetics, and Pathology, Duke University Medical Center, University Drive, Durham, NC, United States,* ³*Molecular Genetics and Neurobiology, University of Florida College of Medicine, 1600 SW Archer Road, Rm. R1-191, Gainesville, FL, United States,* ⁴*Neurology, Radiology, and Neuroscience Program, Harvard Medical School, 220 Longwood Avenue, Boston, MA, United States,* ⁵*Internal Medicine, Neurology, Physiology & Biophysics, University of Iowa, 200 Hawkins Drive, Iowa City, IA, United States,* ⁶*Neuroscience and Otolaryngology, University of Virginia, School of Medicine, Charlottesville, VA, United States,* ⁷*NIDCD, NIH, 5 Research Ct., Rockville, MD, United States,* ⁸*Otolaryngology and Surgery, University of Maryland School of Medicine, 16 South Eutaw Street, Suite 500, Baltimore, MD, United States,* ⁹*Otolaryngology, Physiology, Neuroscience, New York University School of Medicine, 550 First Avenue, New York, NY, United States*

Established and well-respected virologist researchers currently using and generating viral vectors in their own laboratories will cover the basics of each viral gene therapy delivery system (ie, Adenovirus, Adeno-associated virus (AAV), Herpes Simplex virus (HSV) and Lentivirus). Because these experts are leaders in their particular viral vector area, and are in charge of vector core laboratories at their respective institutions, they will further serve as a forum for establishing new contacts and collaborations for ARO members interested in gene transfer. Moreover, this symposium will also educate members on the advantages and disadvantages of each viral vector system, and inform ARO members of the ethical considerations required for pre-clinical trials.

Each symposium speaker will briefly cover the: (1) mode each virus uses for self-replication, (2) methods used to generate recombinant viruses or amplicons in the laboratory, (3) factors that are important for efficient viral transduction or transfection of cells (ie, promoter issues, viral receptors, etc.), (4) immune responses and potential toxicity and ethical issues, and (5) potential differences between viral serotypes. In addition, each outside expert will highlight these points with examples from their own published (and unpublished) gene transfer studies on the musculoskeletal and nervous systems. Following each outside speaker's presentation on a particular viral vector system, an ARO member will briefly highlight (<5 min) research from their laboratory and other laboratories using that particular viral vector in the inner ear.

506 Modified Adenovirus vectors offer multiple advantages for gene transfer research

Andrea Amalfitano

Division of Medical Genetics, Duke University Medical Center, Box 2618, Rm. 101B, MSRB, Durham, NC, United States

A number of different methods for introducing genes into cells have been utilized both in the basic research and the clinical realms. One viral based vector that has several positive attributes is based

upon human adenoviruses (Ad). Typically, Ad based vectors are made replication incompetent, by inserting a foreign gene of interest into the E1 region of the Ad genome, thus simultaneously deleting out the E1 genes. The resultant [E1-]Ad vector is then propagated on E1 expressing packaging cell lines (typically, human 293 cells). Our lab and others have shown however, that [E1-]Ad vectors are not truly replication incompetent, and can in fact express a number of noxious Ad derived genes that contributes to the overall toxicity profile usually associated with the use of Ad vectors. In this discussion, we will describe how additional unique modifications engineered into the [E1-]Ad genome can result in a significantly improved Ad vector, especially when considering gene transfer studies in vivo.

507 HSV amplicon vectors – big payload

Xandra Breakefield

Neuroscience Program, Harvard University, Bldg 149 13th St, Charlestown, MA, United States

HSV amplicon vectors consist of plasmid DNA packaged into herpes simplex type 1 virions. These virions efficiently deliver genes to most cell types, and capsids are transported retrogradely in neurons. When packaged helper virus-free these vectors do not perturb the electrophysiologic state of the neurons. The large transgene capacity of these vectors allows incorporation of genomic sequences up to 150 kb or concatenates of smaller amplicon units. Inclusion of elements from AAV, retrovirus or Epstein Barr virus provides a means to maintain the transgene in dividing cells via integration into the host cell genome in a region specific or random manner, or as a replicating episome, respectively. Control of transgene expression can be achieved by incorporation of all elements for tetracycline or dimerizer regulation into a single amplicon.

508 The Use of AAV Vectors for In Vivo Gene Transfer

Nicholas Muzyczka

Department of Molecular Genetics and Microbiology and The Powell Gene Therapy Center, University of Florida College of Medicine, 1600 SW Archer Road, Rm. R1-191, Gainesville, FL, United States

AAV vectors have proven to be very efficient for transducing somatic tissues in a variety of organs including liver, eye, brain and muscle. The mode of virus replication and the methods currently used for vector production will be described. Additionally, factors that are important for gene expression and transduction, and differences between different serotypes will be reviewed in the context of different target tissues. Finally, vector toxicity and immune response as well as other issues relevant to clinical applications will be discussed.

509 Lentivirus vectors for basic research and gene therapy

Beverly Davidson

Dept. of Internal Medicine, University of Iowa College of Medicine, 200 EMRB, Iowa City, IA, United States

Lentivirus vectors offer the opportunity to transduce both dividing and nondividing cells. They are easy to make in high quantities, providing researchers with tools for in vitro and in vivo studies in only three or four days. Prior studies have shown the utility of

lentiviruses in directing long term expression in brain and other tissues, resulting in protection from, or reversal of, disease, including progressive neurological diseases. A brief background of the lentivirus systems used for gene transfer will be presented, along with data demonstrating their application to in vitro and in vivo studies. Recent progress in directing lentiviruses to cell types of choice by modulation of the glycoprotein packaged with the virus, a process known as pseudotyping, will also be discussed. Finally, practical issues of how to make them, and safety concerns, will be addressed.

510 Abstract Unavailable

511 The influence of the middle ear on hearing function of developing, adult and aged animals

John J Rosowski

Eaton-Peabody Lab, Mass. Eye & Ear Infirmary, 243 Charles Street, Boston, MA, United States

Evan Relkin's graduate work concentrated on measurements of middle-ear function in the hamster. This work concentrated on two issues: (1) What was the relationship between middle-ear function and hearing? and (2) How do developmental changes in middle-ear function affect the onset of hearing function? In the 23 years since Relkin and Saunders (*Acta Otolaryngolgy*, 1980; 80: 6-14), concluded that the middle ear limited auditory function in both the developing and adult hamster, that conclusion has been tested in a handful of other vertebrate species with mixed results. Some of the work of Saunders and his coworkers demonstrated a critical middle-ear role in the timing of the development of auditory onset in chicks. More recently, the work of Overstreet and coworkers points out a large role of the inner ear in the development of hearing function and auditory frequency sensitivity in gerbils, especially at high frequencies. The published data and conclusions on this issue will be summarized and evaluated. Also, in an extension of the data on auditory development, new data on the effect of the middle ear in limiting hearing in ageing mice and humans will be illustrated and discussed. These new data suggest that while the middle-ear function changes in aged individuals, the magnitude of the change is small compared to other presbycotic changes in hearing function.

Work Supported by NIDCD

512 The role of peripheral and central noise in intensity discrimination

Fan-Gang Zeng, Bruce G. Berg, Ankoor Neil Biswas

Cognitive Sciences and Otolaryngology - Head and Neck Surgery, University of California, 364 Med Surge II, Irvine, CA, United States

A listener's ability to discriminate intensity differences is affected by both peripheral and central noise. Based on Relkin and Doucet's finding that auditory nerve fibers with different spontaneous activities have different recovery functions from prior stimulation [*Hear Res* 55:215-22 (1991)], Zeng, Turner, and Relkin showed that intensity discrimination under forward masking has a non-monotonic function with a "midlevel hump" [*Hear Res* 55:223-30 (1991)]. Their studies have spurred an extensive search

for and debate on the origin of the midlevel hump, particularly when later studies showed that an even greater midlevel hump can be observed under backward masking [Plack and Viemeister, *J Acoust Soc Am* 92:3097-101 (1992)]. Here we used a sample discrimination method to evaluate the relative contribution of peripheral and central noise to the midlevel hump under forward and backward masking. Our hypothesis was that, when the number of samples is increased, the amount of peripheral noise would decrease proportionally while that of the central noise would stay the same. We measured intensity discrimination for a number of 10-ms, 5-kHz, 70-dB SPL tones under either forward or backward masking. The masker was a 200-ms, 5-kHz tone presented at 90 dB SPL. The number of tones was increased from 1 to 2, 4, and 8 with a 10-ms gap between tones for 2 or more tones. The signal delay, defined as the interval between the offset of the masker and the offset of the last tone, was always 250 ms. Preliminary data showed that, when the number of probe tones was increased, intensity discrimination improved significantly under forward masking but much less under backward masking. This preliminary result suggests that the midlevel hump under forward and backward masking may have different origins, requiring us to carefully evaluate both peripheral and central contributions to intensity discrimination.

Supported in part by NIH RO1-DC02267 and UC Irvine Research Unit in Hearing and Speech Sciences.

513 The Structure and Function of Multipolar Cells in the Ventral Cochlear Nucleus

John Doucet

Otolaryngology-H&N Surgery, Johns Hopkins University, 720 Rutland Ave/510 Traylor, Baltimore, MD, United States

Multipolar cells (MC) are hypothesized to play an important role in the early stages of acoustic processing because their axons form a significant component of the intrinsic circuitry of the cochlear nucleus (CN) before projecting to nearly every brain stem and midbrain structure in the auditory pathway. MC are a heterogeneous lot that are probably comprised of several subclasses. However, structural and functional data collected in several labs and species support two broad classes of MC. In rats, *planar cells* have dendrites that are oriented parallel to CN isofrequency planes whereas the dendrites of *radiate cells* intersect several isofrequency planes. We have found that planar and radiate cells also differ with respect to their neurochemistry, the number of synaptic terminals on their cell body, and their axonal targets. In this talk, I will review these data and present some of our more recent findings regarding their projections to the superior olivary complex and the contralateral cochlear nucleus. Collectively, these observations are beginning to provide insight into the respective roles of planar and radiate cells in the hearing pathway.

Supported by NIH/NIDCD R01 grants DC00232 (David K. Ryugo), DC04395 (Ryugo) and DC006268 (Doucet).

514 Otoacoustic Emissions: Have We Been Barking Up the Wrong Tree?

Jonathan H. Siegel

Commun. Sci. & Disord., Northwestern University, 2240 Campus Drive, Evanston, IL, United States

Two different conceptions of otoacoustic emissions have emerged. The first, proposed by Kemp (Hearing Res. 22:95-104, 1986), postulates that otoacoustic emission exhibits two characteristic behaviors: place fixed and wave fixed. The wave-fixed mechanism envisions emissions generated over a region of the cochlea primarily near the peak of the traveling wave and associated with the activity of the nonlinear cochlear amplifier. The underlying generation pattern is determined by the spatial profile of the cochlear mechanical response. A place-fixed mechanism, postulated to explain some behaviors of emissions generated by both transient and steady-state tonal stimuli, envisions fixed reflection sites along the cochlea that result in particularly strong emission signals in the ear canal. This view has been challenged by an alternate theory that postulates two fundamentally different mechanisms of emission generation: nonlinear distortion, and a linear coherent reflection mechanism due to scattering of the forward mechanical excitation by distributed mechanical roughness near the peak of the traveling wave (Shera and Guinan, *J. Acoust. Soc. Am.* 105: 782-798, 1999).

I will report results from suppression experiments that suggest that multiple mechanisms are not necessary to account for emission behavior. Rather, it is proposed that a single distributed nonlinear generation mechanism can explain most emission phenomena. Furthermore, emission generation does not appear to be confined to near the peak of the traveling wave and appears to extend beyond the region where basilar membrane nonlinearity has been demonstrated. The degree to which otoacoustic emissions reflect the properties of the cochlear amplifier does not appear to be as strong as commonly believed. These experiments also suggest ways of extracting part of the emission that arises from the region of active and nonlinear basilar membrane response.

Supported by NIH grant DC-00419 and Northwestern University.

515 Comparison of the effects of contra- and ipsi-lateral sound stimulation as measured by DPOAEs in the rat, guinea pig and chinchilla.

Charles I Woods¹, Anita Sterns², Beth A Prieve³

¹Department of Otolaryngology, Upstate Medical University, 750 E. Adams Str., Syracuse, N.Y., United States, ²Institute for Sensory Research, Syracuse University, Skytop, Syracuse, N.Y., United States, ³Communication Sciences and Disorders, Syracuse University, Skytop, Syracuse, N.Y., United States

Comparison of the effects of contra- and ipsi-lateral sound stimulation as measured by DPOAEs in rat, guinea pig, and chinchilla.

Contra-lateral sound stimulation has been reported by many authors to alter or modulate DPOAEs. Contra-lateral stimulation has been shown to predominantly produce DPOAE suppression. When observing the temporal envelopes of DPOAEs, the onset of the envelope is also often suppressed after presentation of the primaries and this phenomenon has been labeled "onset adaptation".

Our data and others suggest that these sound evoked effects on the DPOAE are produced by the medial olivocochlear efferent pathway and by the middle ear muscle reflex. The relative contributions of these reflexes on the observed DPOAE suppression has been shown to significantly vary with species. We discuss our data in rat and chinchilla compared to that observed in guinea pig by other investigators. We also discuss anatomical correlation to the overall strength of these reflexes.

516 Inferring Olivocochlear Efferent Characteristics Using Protocols from Across-species Studies

Beth A. Prieve¹, Anita R. Sterns², Kathy Vander Werff³, Charles Woods⁴

¹Communication Sciences and Disorders, Syracuse University, 805 S. Crouse Ave, Syracuse, NY, United States, ²Institute for Sensory Research, Syracuse University, 621 Skytop Road, Syracuse, NY, United States, ³Communication Sciences and Disorders, Syracuse University, 621 Skytop Road, Syracuse, NY, United States, ⁴Otolaryngology, Upstate Medical University, 750 E. Adams St., Syracuse, NY, United States

Previous work in rats and chinchillas shows distinctive patterns of magnitude and phase changes in f1-f2 DPOAE onset adaptation and suppression by contralateral noise that are tied with the DPOAE input/output (I/O) function. Sectioning the middle ear muscles in the rats showed that large phase changes were linked with middle ear muscle reflexes. In the current study, we have explored DPOAE onset adaptation and contralateral suppression in rats and humans, using stimulus and recording conditions that are as close as possible in both species. The goals were to investigate 1) whether it could be determined in humans when middle ear muscles were contributing to DPOAE reduction, based on predictions gleaned from rat data before and after middle ear muscles were cut and 2) to compare DPOAE onset adaptation and contralateral noise suppression within human subjects. DPOAE temporal responses were collected in 7 subjects for f2 stimulus intensities 45 dB SPL to 75 dB SPL presented in 5 dB steps. The f2 stimulus frequencies were 2000 Hz and 6000 Hz. Responses were recorded with and without broadband noise presented to the opposite ear at levels from 40 to 89 dB SPL. Considerable variability in the amount of DPOAE contralateral suppression and onset adaptation was found among the 7 subjects. In some subjects, the DPOAE magnitude and phase changes exhibited a predictable pattern based on I/O function, although the pattern was different than those observed in rats. In addition, large jumps in DPOAE phase with increasing contralateral noise levels were found in some subjects, consistent with hypothesized patterns based on rat data. However, not all subjects showed significant DPOAE phase shifts in the presence of contralateral noise. All subjects showed small amounts (1 dB or less) of onset adaptation and had DPOAE suppression (generally 2 dB or less) due to contralateral noise presented at 50 dB SPL or 60 dB SPL when f2 levels were 55 dB SPL. Supported by PPG NIDCD 2P01 DC00380 and Syracuse University.

517 Espins Are Multifunctional Actin Cytoskeletal Regulatory Proteins in Mechanosensory and Chemosensory Cells

Gabriela Sekerkova¹, Lili Zheng¹, Patricia A Loomis¹, Benjarat Changyaleket¹, Donna Whitlon², Enrico Mugnaini¹, James R Bartles¹

¹Cell and Molecular Biology, Northwestern University Medical School, 303 East Chicago Avenue, Chicago, IL, United States,

²Otolaryngology-Head and Neck Surgery, Northwestern University Medical School, 303 East Chicago Avenue, Chicago, IL, United States

Espins are associated with the parallel actin bundles of hair cell stereocilia and are the target of the jerker deafness mutation. We have recently uncovered a number of new ligand-binding sites and activities of espins and discovered that espin isoforms are present in a variety of other sensory cells. In addition to binding and bundling actin filaments with high affinity, espins: (i) bind actin monomer via a WH2 consensus domain; (ii) bind profilin I, profilin IIa and the SH3 adapter protein IRSp53 via proline-rich peptides; and (iii) cause a net barbed-end elongation of treadmilling parallel actin bundles, like those found in stereocilia and microvilli. Besides hair cell stereocilia, espins are localized to the parallel actin bundle-containing processes of other sensory cells, including Merkel cells, taste cells, the sensory neurons of the vomeronasal organ, brush cells in the digestive and respiratory systems, and the solitary chemoreceptor cells of the nasal cavity. Using RT-PCR, DNA sequence analysis, transfection and western blotting, we have established that hair cells and other sensory cells contain novel espin isoforms. These isoforms, which arise through the utilization of a unique transcriptional start site and alternative splicing, differ from other espin isoforms in their interactions with actin, IRSp53 and the profilins. We have generated antibodies that distinguish between different classes of espin isoforms and have determined that hair cells and some of the other sensory cells contain multiple espin isoforms. Thus, beyond serving as actin-bundling proteins of hair cell stereocilia, our results suggest additional roles for espins as regulators of actin cytoskeletal dynamics in mechanosensory and chemosensory cells. NIH DC04314 (JRB) and DC00653 (DW).

518 Mutations in a Novel Gene are Associated with Stereocilia Defects in Inner Ear Sensory Cells of the Mouse Deafness Mutant Pirouette

David C. Kohrman^{1,2}, Hana Odeh^{1,3}, Kristina Mitchem¹, Lisa Beyer¹, Yehoash Raphael¹

¹Otolaryngology/Kresge Hearing Research Institute, University of Michigan, 1150 West Medical Center Drive, Ann Arbor, Michigan, United States, ²Human Genetics, University of Michigan, 1241 E. Catherine Street, Ann Arbor, Michigan, United States, ³Cell and Developmental Biology, University of Michigan, 1335 E. Catherine Street, Ann Arbor, Michigan, United States

The mouse mutant pirouette (*pi*) exhibits profound hearing loss and circling behavior that are inherited as autosomal recessive traits. Analysis of cochlear pathology in *pi/pi* homozygotes has previously indicated abnormally thin stereocilia during sensory

cell maturation, and the appearance of an actin-rich filament ('cytoaud') in all inner hair cells by postnatal day 10. In order to further characterize the basis for these defects in actin architecture in the mutant, we evaluated expression of the actin-binding proteins fimbrin and espin. Fimbrin was identified in the stereocilia of control and *pi/pi* mice, and in the cytoauds of *pi/pi*. Although espin was found in the stereocilia of both control and affected mice, its level was very low or absent in cytoauds. This result indicates that the actin filament cores of stereocilia and cytoauds differ in their composition of actin-binding proteins and suggests alternative mechanisms of filament assembly in the two structures.

In addition to the original spontaneous mutation at the pirouette locus, we have characterized three additional allelic strains, including a second spontaneous and two transgene insertional mutants. We have used a positional cloning strategy to obtain evidence for mutation of a novel gene in each of the four alleles. An inner ear-specific transcript of this gene encodes a protein of 290 amino acids with significant similarity to predicted proteins from a wide range of metazoans, including mammals, worms, and fruit flies. Our studies of sensory cell pathology in the inner ears of pirouette mice suggest that the gene plays a role in pathways that stabilize and/or organize parallel actin filaments during postnatal maturation of stereocilia. We have also identified a paralogous gene on mouse chromosome 18. This paralog is expressed in the inner ear, suggesting it may also play a critical role in auditory function.

(Supported by NIDCD Grants: R29-DC03049, R01-DC05401, R01-DC05053, and P30-DC05188.)

519 Mutations in Frizzled 4 and LDL-receptor-related protein 5 lead to cochlear defects similar to those observed in Norrie disease

Alain Dabdoub¹, Qiang Xu², Yanshu Wang², Phil Smallwood², Chad Woods¹, John Williams², Charlotta Lindvall-Weinreich³, Bart O Williams³, Jeremy Nathans², Matthew W Kelley¹

¹NIDCD, NIH, 5 Research Ct, Rockville, MD, United States,

²Department of Molecular Biology and Genetics, Johns Hopkins University School of Medicine, 725 N. Wolfe St., Baltimore, MD, United States, ³Laboratory of Cell Signaling and Carcinogenesis, Van Andel Institute, 333 Bostwick Ave N.E., Grand Rapids, MI, United States

Norrie disease (ND) is an inherited neurodevelopmental disorder characterized by blindness at birth, varying degrees of mental retardation, and progressive sensorineural hearing loss. The ND gene encodes a small secreted protein with a cysteine-knot domain called Norrin, with as of yet undetermined neurobiological function. A knock-out mouse model with an ND gene disruption has progressive hearing loss resulting from a defect localized to the stria vascularis, and subsequent hair cell loss.

Here we report that vascular defects and hair cell loss similar to those observed in ND mutant mice are present in the cochleae of Frizzled 4 (*fz4*) and low-density lipoprotein receptor-related protein 5 (*lrp5*) homozygote mutants. Frizzled 4 is one of the ten mammalian Wnt transmembrane receptors with a cysteine-rich binding domain, while *lrp5* is a Wnt co-receptor. *Fz4(-/-)* mice are progressively deaf, and as assayed using a lacZ knock-in reporter, *fz4* is expressed early in several cell types in the cochlea including

the stria vascularis and the hair cells. Our data show that there is a progressive enlargement followed by degeneration of vessels within the stria vascularis in the cochleae of fz4(-/-) mice proceeded by hair cell loss. In lrp5(-/-) mice we observed the same defect in the stria vascularis.

The similarities in phenotypes between ND, fz4 and lrp5 mutants strongly suggest interactions between these molecules. To test this hypothesis, we show that Norrin is a highly specific ligand for Fz4 that binds with high affinity and, in the presence of the LRP5 co-receptor, potently activates the Wnt-Frizzled signaling pathway. Our results demonstrate that Fz4 and LRP5 are necessary for the maintenance of vasculature within the stria vascularis and show a role for Frizzled signaling in maintaining the viability and integrity of the mammalian cochlea.

520 Molecular pathogenetic mechanism of maternally inherited aminoglycoside ototoxicity

Min Xin Guan

Human Genetics, Cincinnati Children's Hospital Medical Center, 3333 Burnet Avenue, Cincinnati, Ohio, United States

Mutations in the mitochondrial DNA (mtDNA) have been shown to be one of the important causes of both syndromic and non-syndromic forms of sensorineural hearing loss. In particular, the mitochondrial 12S rRNA gene is the hot spot for deafness-associated mutations, as the four mutations have been identified to be associated with aminoglycoside induced and non-syndromic deafness. The A1555G or C1494T mutations in the A-site of mitochondrial 12S rRNA account for a significant number of cases of aminoglycoside ototoxicity. These mutations make the secondary structure of the 12S rRNA similar to the corresponding region of the bacterial 16S rRNA, thus facilitating the binding and sensitivity to aminoglycosides, and causing defects in mitochondrial protein synthesis and respiration. Our biochemical data are a good agreement with clinical observation that the administration of aminoglycosides can induce or worsen deafness in matrilineal relatives. Thus, our study suggests that the A-site of mitochondrial 12S rRNA is the primary target for aminoglycoside ototoxicity. Our data also strongly suggest that the nuclear background plays a role in the aminoglycoside ototoxicity and the development of deafness phenotype associated with the mitochondrial 12S rRNA gene mutations.

521 Development of an Inner Ear cDNA Microarray

Anne B.S. Giersch^{1,2}, Anne B. O'Donovan¹, Kristen Lyall¹, Sara Hamaker¹, Bradley J. Quade^{1,2}, Cynthia C. Morton^{1,2}

¹Pathology Department, Brigham and Women's Hospital, 75 Francis Street, Boston, Massachusetts, United States, ²Pathology Department, Harvard Medical School, 25 Shattuck Street, Boston, Massachusetts, United States

In order to analyze transcriptional profiles of thousands of cochlear mRNAs simultaneously, we are developing a human and mouse inner ear cDNA microarray. Over the past several years, more than 15,000 human cochlear ESTs have been created from the Morton human fetal cochlear cDNA library and deposited in GenBank. Another 15,000 ESTs have been generated from the

mouse organ of Corti cDNA library created in the Kachar lab at NIDCD/NIH. At least one copy of each gene represented among all the human cochlear and mouse organ of Corti cDNAs will be included on the final microarrays. Also included will be cDNAs of known deafness genes, as well as appropriate controls. In total, there will be over 5,400 mouse organ of Corti expressed genes and over 4,400 human cochlear expressed genes present on the inner ear cDNA microarray. Up to 10% of these transcripts may be cochlear specific.

The human inner ear cDNA microarray has recently been completed and initial hybridization experiments using human fetal cochlea RNA vs Universal Human RNA performed. Signal correlation across slides approaches 0.9. Genes known to be highly expressed in human cochlea also show high expression levels on our array.

The mouse organ of Corti cDNA microarray is still in the production stage. Initial clone selection and amplifications are proceeding. Through a supplemental grant from the NIDCD, we are planning to make these resources available to the hearing research community on either an individual use or collaborative basis and posting results to our website for comparison of other investigators' data.

This work was supported by grants from the National Organization of Hearing Research to ABSG and the NIH/NIDCD to CCM.

522 Induction of the Hsf1-dependent stress pathway in the mouse cochlea following hyperthermia

Damon A. Fairfield, Margaret I. Lomax, Richard A. Altschuler

Kresge Hearing Research Institute, Dept. of Otolaryngology and Dept. of Cell & Developmental Biology, University of Michigan, 1301 E. Ann St., Ann Arbor, MI, United States

Cells respond to stress in a variety of ways. One of the best studied protective pathways involves induction of the heat shock proteins (Hsps). Although many Hsps are constitutively expressed in the cell, where they play a variety of functions, Hsp70 is induced in response to stress, resulting in enhanced cell survival and protection. Both noise and heat stress are known to upregulate Hsp70 in the rodent cochlea. Heat shock factor 1 (Hsf1) is the major transcription factor that regulates the stress-inducible expression of genes for Hsps and certain other stress responsive proteins. We previously demonstrated that a 41-42 °C, 15 min heat shock results in activation of Hsf1 in the rat and mouse cochlea. We now examine the expression of the downstream targets of Hsf1 in the mouse cochlea following a similar heat shock. Total RNA was isolated from the cochleae of both unstressed and heat-stressed mice 30 minutes after heat shock. We examined changes in gene expression for 11 known targets of Hsf1 following heat shock by quantitative RT-PCR analysis on an ABI Prism 7000 with TaqMan probes. Both mouse genes for inducible Hsp70 (Hsp70.1 and Hsp70.3) showed approximately 1000-fold increases following heat stress. Several other Hsp genes were upregulated between 3 to 30-fold following heat shock, including the actin regulatory protein Hsp27, the collagen binding protein Hsp47, and the molecular chaperones Hsp90 alpha (Hsp86), Hsp90 beta (Hsp84), and

Hsp110. These results suggest that several members of the Hsp1-dependent stress pathway may play a role in the cochlear stress response in the mouse. Other Hsps may also be involved but may be activated at a later time. This research was supported by NIDCD grants T32 DC00011 and P01 DC02982.

523 Activity-dependent genes, *bdnf* and *c-fos*, in the cochlear spiral ganglion neurons can be modulated differentially by salicylate and noise

Justin Tan, Lukas Ruettiger, Saida Hadjab, Ulrike Zimmermann, Iris Koepschall, Karin Rohbock, Marlies Knipper

Molecular Neurobiology, Tuebingen Hearing Research Centre, Elfriede-aulhornstrasse 5, Tuebingen, Germany

Aberrant neuronal activity and plasticity changes are thought to be the basis for a variety of neurological disorders such as epilepsy, phantom pain and phantom noise (tinnitus). The activity-dependent nature of brain-derived neurotrophic factor (*bdnf*), *c-fos* and activity-regulated cytoskeletal gene (*Arg 3.1*) single them out as candidates in mediating synaptic plasticity changes. Using *in situ* hybridisation and semi-quantitative RT-PCR, we analysed the expression pattern of these genes in the rat and mice cochlea and auditory cortices, following acute and chronic salicylate treatment, and traumatic noise exposure. We chose salicylate and noise to study gene expression patterns in the cochlea as they have previously been shown to alter nerve activity either directly or indirectly in the central auditory system. Our data suggests an altered expression of activity-dependent genes in the peripheral auditory system and auditory cortex by salicylate and noise.

Acknowledgements: This work was supported by the Deutsche Forschungsgemeinschaft Kni 316/3-2 and Fortüne 816-0-0.

524 Post-exposure treatment attenuates NIHL

Daisuke Yamashita^{1,2}, Hong Yan Jiang³, Nadine Brown³, Jochen Schacht³, Josef Miller³

¹*Otolaryngology, Keio University, 35 Shinanomachi Shinjuku-ku, Tokyo, Japan*, ²*Kresge Hearing Research Institute, University of Michigan, 1301 E. Ann Street, Ann Arbor, MI, United States*,

³*Kresge Hearing Research Institute, University of Michigan, 1301 E. Ann St, Ann Arbor, MI, United States*

Reactive oxygen species (ROS) and reactive nitrogen species (RNS) are important factors in the mechanism underlying noise-induced hearing loss (NIHL), and NIHL may be prevented by antioxidant therapy. Recently, we have demonstrated the unexpected delayed formation of free radicals 7 – 10 days following noise exposure (Yamashita et al, ARO-MWM, 2003), suggesting that post-exposure treatment, attenuating this late formation, may reduce NIHL. In the present study, we assessed the effectiveness of scavengers to reduce late ROS/RNS formation and cochlear damage from intense noise and attempted to define the effective therapeutic window for this therapy. Pigmented guinea pigs were exposed to a 4 kHz octave band noise, 120 dB SPL, for 5 h. Animals received either saline or salicylate plus Trolox as ROS and RNS scavengers, beginning 3 days prior, or immediately, 1, 3, or 5 days after noise exposure. Salicylate was given as a sq injection at 150 mg/kg/day; Trolox, ip at 100 mg/kg/day, bid. Auditory

thresholds were measured by evoked brain stem responses at 4, 8 and 16 kHz, before and ten days after noise exposure. On day 10 following exposure temporal bones were removed and processed for quantitative histological assessment of hair cell damage and markers of free radical activity. 4-HNE and nitrotyrosine (NT) were used as immunohistochemical indicators of ROS and RNS, respectively. Antioxidant treatment significantly decreased ROS and RNS formation and reduced noise-induced threshold shifts and hair cell damage. The efficacy was directly related to the time of intervention, earlier treatment being more effective. However, significant protection was observed with post-exposure treatment of up to 3 days following noise. These findings indicate that a combination of ROS and RNS scavengers can attenuate NIHL and demonstrate a window of opportunity for pharmacological rescue after intense noise trauma.

This work was supported by NIH grant DC-04058, UAW/GM funds, and the Ruth & Lynn Townsend professorship.

525 ALCAR Preserves Both The Number And Integrity Of Mitochondria In Chinchilla Hair Cells After Acoustic Overexposure

Richard D. Kopke, Xianxi Ge, Jianzhong Liu, Ronald L. Jackson, John K.M. Coleman, Michael Costello
Otolaryngology, DOD Spatial Orientation Center, 34800 Bob Wilson Dr, San Diego, CA, United States

Objectives: Previously we demonstrated that acetyl-L carnitine (ALCAR) treatment in the noise-exposed chinchilla model reduced noise-induced threshold shifts as well as inner and outer hair-cell loss (ARO 2001). Although the mechanism of hearing recovery with ALCAR has not been elucidated, we believe that ALCAR, an important compound for mitochondrial function and energetics, may have protective properties for hair cell mitochondria from noise damage. The purpose of this study was to observe the effect of ALCAR on hair cell mitochondria after acoustic overexposure. Methods: Twelve female chinchillas were divided into three groups: no noise controls and noise exposure with either saline or with ALCAR treatment. Noise exposure was octave band, 105 dB SPL, centered at 4kHz for six hours. Animals were humanely euthanized at three-weeks post-noise exposure. Cochleae were dissected, processed and imaged using transmission electron microscopy. Mitochondrial volume density was estimated using the point counting method. Average volume density was calculated for each individual cell from one of each supra- and infra- nuclear regions. Sixteen IHC and OHC were counted from each group. Results: No noise controls showed normal mitochondria, which were oval in shape with well-formed cristae and intact mitochondrial membranes. Noise-exposed saline treated animals showed that almost all of the mitochondria were damaged in cochlear hair cells. Damaged mitochondria demonstrated swelling and vacuolization. Cristae were shortened, blurred or missing with empty spaces in the matrix. Membranes were separated, peeled or ruptured. Noise-exposed ALCAR treated animals demonstrated mitochondria with much less damage. Mitochondrial volume density decreased in both IHC and OHC after noise exposure in saline treated animals compared to normal controls ($p < 0.01$) and increased with ALCAR treatment compared to noise saline ($p < 0.01$) three weeks post noise exposure. Conclusion: The findings of this study indicated that ALCAR, a mitochondrial biogene-

sis agent, preserves both the number and integrity of mitochondria in chinchilla hair cells after acoustic overexposure. (Office of Naval Research, US Army and the Naval Medical Center San Diego supported this study)

526 L-carnitine Prevents Gentamicin-induced Perinatal Hearing Loss

Gilda Kalinec¹, Raul Urrutia², Nora Esteban-Cruciani³, Federico Kalinec¹

¹Cell and Molecular Biology, House Ear Institute, 2100 West Third Street, Los Angeles, CA, United States, ²Division of Developmental Oncology and Departments of Biochemistry and Molecular Biology, Mayo Clinic, Alfred 2nd SMH, Rochester, MN, United States, ³Children's Hospital at Montefiore, Albert Einstein College of Medicine, 3415 Bainbridge Ave, Bronx, NY, United States

The evidence that infection during pregnancy is linked to premature birth has led to an increasing number of pregnant women being exposed to gentamicin and other aminoglycoside antibiotics. Thus, a number of unborn premature and full-term infants are being exposed to ototoxic agents during a period of development and maturation of the auditory organs. There is growing evidence that oxidative stress and mitochondria play important roles in aminoglycoside toxicity, although the pathways involved have not been identified. Since pregnant women readily develop deficiency in L-carnitine (LCAR), a natural micronutrient and antioxidant required for normal mitochondrial function, we wonder whether LCAR administration could help to prevent gentamicin-induced perinatal hearing loss. We have used guinea pigs as an animal model, the auditory cell line HEI-OC1 as an in vitro system, SEM and confocal microscopy, ABR, apoptosis assays and gene-profiling techniques to investigate the effects of perinatal administration of gentamicin, the mechanisms of gentamicin cell toxicity, and the potential protective role of LCAR. We found that gentamicin (100 mg/kg/day, for 7 days) administered to pregnant guinea pigs (51±2 to 57±2 days of gestation) induced significant neonatal mortality and hearing loss in mothers and newborns. Importantly, both gentamicin-induced effects were significantly diminished by LCAR supplementation (1mg/ml in drinking water, either 2 weeks prior or simultaneously with gentamicin). Studies with HEI-OC1 cells indicate that gentamicin-induced apoptosis was associated with an increase in the expression of the pro-apoptotic factor Hrk and a concomitant decrease in the expression of the anti-apoptotic factor Bcl-w. LCAR, in turn, was able to reverse the effect of gentamicin on the Bcl-w/Hrk ratio and significantly diminish apoptosis in HEI-OC1 cells. These results define a mechanism for gentamicin cell toxicity and suggest a simple clinical strategy for its prevention.

527 Chemoprotection against ototoxic effects of single and repeated cisplatin dosing in rats using oral ebselen and allopurinol.

Eric Daniel Lynch, Rende Gu, Jerry Glattfelder, Huy Tran, James LaGasse, Carol Pierce, Jonathan Kil

Research and Development, Sound Pharmaceuticals, Inc., 4010 Stone Way N Suite 120, Seattle, wa, United States

Chemotherapy patients receiving cisplatin develop several side effects including hearing loss. Ethylol, the only approved cisplatin

chemoprotectant, reduces the renal toxicity of cisplatin. Other potential chemoprotectants have been found to interfere with cisplatin tumoricidal activity, precluding their further development. In an effort to develop more effective chemoprotective agents, we assayed several chemoprotectants after single and repeated injections of cisplatin in F344 rats.

Chemoprotected rats were loaded with 8 mg/kg ebselen and 8 mg/kg allopurinol PO one hour before a single 16 mg/kg cisplatin injection IP, and further dosed with 4 mg/kg ebselen and 4 mg/kg allopurinol PO for two days. Control rats were dosed on the same schedule with cisplatin and vehicle only. ABR thresholds were measured one week prior to, and 3 days following, the last cisplatin injection using click and pure tone (8, 16, 24, and 32 kHz) stimuli. Cochleae were whole-mounted and stained with DAPI and FITC-phalloidin to assess hair cell morphology and number. Tumor burden, serum creatinine, BUN, body weights, and survival times were evaluated. In a second model, rats were loaded with either syngenic breast or ovarian tumor cells (MTLn3 1e6 SQ, NuTu-19 1e7 IP) two weeks prior to the first injection of cisplatin (6 mg/kg x 3 weekly doses). Here, rats were supported with 5 ml saline SQ starting the day after the first cisplatin injection. In both cancer models, cisplatin tumor kill was equivalent in chemoprotected and control rats. Chemoprotected rats had significantly less ABR threshold shift and hair cell loss when compared to controls. Serum creatinine, BUN, body weights, and survival times were also improved. The combined formulation of orally dosed ebselen and allopurinol successfully reduced the side effects of single and repeated cisplatin dosing without inhibiting the tumoricidal activity of cisplatin.

528 Early Gene Expression in the Organ of Corti Exposed to Gentamicin

Daniel Bodmer¹, Dominik Brors², Morana Bodmer³

¹ORL Klinik, University Hospital Zurich, Frauenklinikstr. 24, Zurich, Switzerland, ²HNO Klinik, University Hospital Würzburg, Josef-Schneiderstr. 11, Würzburg, Germany, ³HNO Klinik, University Hospital Zurich, Frauenklinikstr. 24, Zurich, Switzerland

Studies have demonstrated different pathogenetic key factors in gentamicin induced cochlear hair cell death. The productions of reactive oxygen species (ROS), as well as apoptosis related genes, play a critical role. However, a coordinated large-scale investigation of gene expression in the Organ of Corti (OC) exposed to gentamicin has not yet been conducted. We have used DNA microarray technology to compare the expression profile of OC exposed to gentamicin to the expression profile of untreated OC.

The OCs of Sprague Dawley rats were dissected and the basal turn was cultured. Half of the explants were then exposed to gentamicin, while the other half of the explants remained in culture medium alone. Gene expression was analyzed using DNA microarray technology and the dChip software package. Out of 8800 genes, 12 genes were selected on the basis of differential expression in the OC exposed to gentamicin vs. control OC.

The identity of these genes suggests that the response of the OC to the gentamicin challenge involves downregulation of specific gene families in order to alleviate the ROS and N-methyl-D-aspartate (NMDA) receptor mediated cellular stress.

529 mRNAs that encode for members of the MAPK/JNK cell death signal pathway are expressed in organ of Corti, stria vascularis/spiral ligament, and spiral ganglion tissues of laboratory rats.

Thomas R Van De Water¹, Syed Ahsan¹, Kim Baker², Cai Hong Mou¹, Jiao He¹, Adrien A Eshraghi¹, Jose Guzman¹, Hinrich Staecker², Thomas J Balkany¹

¹Otolaryngology, University of Miami School of Medicine, 1600 N.W. 10th Avenue, RMSB 3160, Miami, FL, United States,

²Surgery, Division Otolaryngology, University of Maryland School of Medicine, 16 S. Eutaw Street, Suite 500, Baltimore, MD, United States

The mitogen activated protein kinase (MAPK)/c-Jun N Terminal Kinase(JNK) pathway has been implicated as an important cell death signal cascade activated by oxidative stress-damage in a variety of tissues including the inner ear. Evidence for the activation of this signal cascade in the tissues of stress-damaged inner ears comes from both in vitro and in vivo inhibitor studies. The MAPK/JNK signal cascade consists of three classes of signal molecules: Kinase-Kinase-Kinases (e.g. MLK-3); Kinase-Kinases (e.g. MKK-7); and Kinases (e.g. JNK-1) that culminates the signal cascade by phosphorylating c-Jun (e.g. c-Jun-1) which forms an AP-1 transcription complex. To design effective otoprotective therapies it is important to know which MAPK/JNK molecules are produced in the inner ear.

The present study used RT-PCR of mRNAs isolated from undamaged cochlear duct tissues of laboratory rats to identify members of the MAPK/JNK signal cascade present in: organ of Corti; stria vascularis/spiral ligament; and spiral ganglion tissue samples. Messenger RNAs were isolated, reverse transcribed with the resultant cDNAs amplified for 35 cycles and identified on agarose gels. Oligonucleotide primer pairs were designed from published gene sequences to identify the following MAPK/JNK cell signal molecules: MKK-4; MKK-7; JNK-1, -2, -3 and two housekeeping genes: S29; and GAPDH. All of the cochlear tissue samples studied expressed transcripts for MKK-4, MKK-7, and JNK-1 while expression of JNK-3 mRNA was confined to spiral ganglion tissue.

This result demonstrates that many of the MAPK/JNK cell death pathway molecules are present within the normal cochlea and supports a role for this signaling cascade as an important initiator of oxidative stress-induced apoptosis of cochlear sensory tissues. Inhibition of the MAPK/JNK signal cascade represents an effective anti-apoptotic strategy following exposure of the cochlea to oxidative stress. Supported by a grant from Med El to TRV and TJB.

530 The effect of mild hair-cell damage and long-term hair-cell loss on the expression of the glutamate transporter GLAST in the cochlea

David N Furness, D Maxwell Lawton

Life Sciences, Keele University, Keele, Stoke-on-Trent, United Kingdom

The glutamate transporter GLAST is strongly expressed in inner phalangeal and border cells supporting the inner hair cells (IHCs)

which are thought to be glutamatergic. We have shown that GLAST expression varies with the density and activity of the afferent innervation to the IHCs and is thus regulated by factors such as the amount of glutamate released and the sensitivity of the nerve fibres. We therefore hypothesised that damage to and elimination of IHCs would alter the expression of GLAST in their supporting cells. Mild and short-term IHC damage was produced by transtympanic injection of gentamicin into the guinea-pig middle ear followed by recovery for various time periods. Long-term IHC loss was investigated using CD-1 mice up to 1 year old. Cochleae were fixed in 4% formaldehyde in phosphate buffer, dissected and immunofluorescently labelled for confocal microscopy or embedded and sectioned for post-embedding immunogold labelling using antibodies to GLAST. Mild IHC damage and short term IHC loss evoked a redistribution of GLAST in the associated supporting cells, with the GLAST labelling appearing to form patches rather than being distributed relatively evenly in the membranes. After longer term IHC and nerve-fibre loss, GLAST appeared to be down-regulated in the associated supporting cells. At the electron microscopic level, GLAST labelling appeared to diminish in relative density in the supporting-cell membranes across a transition region between where IHCs were present and where they were missing. These data suggest that if glutamate release is no longer taking place, GLAST distribution in the vicinity changes and its expression is eventually reduced.

Supported by the Wellcome Trust

531 GDNF Receptors on Non-sensory Cells May Mediate Protection of Hair Cells

Joe Adams

Otol. & Laryngol., Mass. Eye & Ear Infirmary, 243 Charles St, Boston, MA, United States

Previous work in a number of labs has shown that application of glial derived neurotrophic factor (GDNF) can promote survival of outer hair cells in ears challenged by acoustic trauma, aminoglycosides or cisplatin. These findings show that a common pathway is responsible for protection from remarkably different kinds of cochlear stress. It may safely be assumed that the survival effects of GDNF administration are mediated by members of the GDNF receptor family (GFR alpha 1-4), three of which have been reported to be expressed in the rat cochlea, based upon RT-PCR analyses (Stoeber et al., 2000). In the present study identification of cells that express GFR alpha-1(the GDNF receptor) and GFR alpha-2 (the neurturin receptor) was assessed by immunostaining mouse cochleas for the gene products. Most epithelial and non-epithelial cell classes were found to be immunopositive for both receptors, with the remarkable exceptions of outer hair cells and type II fibrocytes. The staining patterns with the two antibodies were similar, except that the antibody to the alpha-2 receptor stained root cells and interdental cells far more darkly than non-epithelial cells. The lack of staining of outer hair cells by either antibody indicates that protection of hair cells from damage via GFR-mediated processes occurs through responses that are initiated in non-sensory cells. It is not clear how such protection among cells is mediated. Another line of evidence indicating the necessity of normally functioning non-sensory cells for hair cell survival comes from recent reports of the lack of hair cell survival that occurs in animals with induced mutations of other genes that

are not expressed in hair cells, but are expressed in supporting cells (e.g., Connexin 26, Kcc4, p27). Taken together with those reports, the present results indicate that understanding mechanisms that determine hair cell survival must include understanding interrelationships of all cells that comprise the hearing organ.

532 **Using SFOAEs to Measure Tuning Characteristics of the Medial Olivocochlear (MOC) Reflex and Estimate MOC Effects on the Outer Hair Cell Nonlinearity in Human Ears**

Shawn S Goodman, Douglas H Keefe

Center for Hearing Research, Boys Town National Research Hospital, 555 North 30th Street, Omaha, NE, United States

Stimulus frequency otoacoustic emissions (SFOAEs) associated with low-level sinusoidal probes are useful in studying the medial olivocochlear (MOC) reflex because elicitors that suppress the SFOAE may also evoke the MOC reflex, whereas SFOAE probes do not evoke the reflex. Acoustic reflex (AR) effects can also be detected and avoided (Guinan et al. (2003). JARO, Epub). The frequency tuning of the ipsilateral MOC reflex in humans was examined in Exp. 1 by measuring SFOAEs (1, 2, 4 kHz) using broadband/notched noise or additional sine tones to elicit the MOC, and simultaneously monitoring for AR using a 0.28 kHz tone. While the outer hair cell (OHC) receptor potential nonlinearity has been studied using two-tone suppression at the neural, mechanical, and SFOAE levels, the use of amplitude modulation (AM) of SFOAEs is an alternative paradigm to probe this nonlinearity. In Exp. 2, the action of the MOC system was assessed by measuring AM SFOAEs before and after an MOC elicitor. For both experiments, each stimulus duration was 2 sec, in which the probe tone duration was gated on for 1350 ms (with 5 ms gating ramps) followed by a baseline recovery duration of 650 ms. The MOC elicitor was gated on 250 ms after the probe tone with a duration of 500 ms. The SFOAE suppression produced by the elicitor was measured using a residual procedure. The MOC reflex was assessed by the relative suppression of the SFOAE after the elicitor was gated off. MOC tuning was examined by varying elicitor notch width and level at various probe levels. MOC shifts in SFOAE envelope increased with probe level and decreased with notch width in some ears, and were absent in other ears. At probe levels ≥ 50 dB SPL, stimulus level-dependent noise was present, possibly obscuring two-tone suppression and MOC effects. In Exp. 2, the minima of the temporal SFOAE envelope are largely determined by the minima in the AM stimulus envelopes, which allows a simple measurement of SFOAE latency, while other details of the SFOAE envelope are determined by the form of the compressive OHC nonlinearity. *Supported by grants DC03784, DC00013, DC04662 from the NIDCD.*

533 **A Preliminary Study on Comparison of the Olivocochlear Efferent and Middle-Ear Muscle Reflexes in Frequency Selectivity Using Distortion Product Otoacoustic Emission Measurement**

Xiao-Ming Sun, Fawen Zhang

Speech Pathology & Audiology, University of South Alabama, 2000 University Commons, Mobile, AL, United States

The medial olivocochlear (MOC) and middle-ear muscle (MEM) reflexes are two peripheral control mechanisms of the auditory system, which share a similar afferent pathway. Although their efferents innervate different targets, both reflexes can be activated with sound present in the contralateral ear, mainly causing a reduction of acoustic energy to the sensory cells of the cochlea. While sharply tuned frequency selectivity of contralaterally activated MOC reflex has been confirmed in animals with neurophysiological recordings, studies in humans with otoacoustic emission measures displayed a similar picture only for 1 to 2 kHz. Frequency selectivity of the MEM reflex, with electromyographic and neurophysiological recordings in animals, was testified to be not so high as that of MOC. However, investigations on the MEM reflex in humans could only be conducted for low probe-tone frequencies, mostly 220 Hz, with the admittance test. Sun (2003, ARO) introduced the application of distortion product otoacoustic emission (DPOAE) measurement in studying the MEM reflex and its comparison to the MOC reflex in humans and indicated its potential to be a direct observation of the effects of the two reflexes on sound transmission in the middle ear and cochlea. In the present study, $2f_1-f_2$ DPOAE time course was measured at frequencies of 1 to 6 kHz in normal human ears. The contralateral ear was present with pure tones at frequencies of 0.25 to 8 kHz for two levels, 20 dB below and 10 dB above the MEM reflex threshold, which are expected to activate the MOC and MEM reflexes, respectively. The preliminary results showed that the low-level contralateral tones at the frequencies close to those of the DPOAE primary tones maximally reduced the DPOAE level, displaying evident frequency selectivity even for high-frequency DPOAEs. The high-level tones also reduced DPOAE in a frequency-selective manner with the greatest reduction at the frequencies close to or lower than the DPOAE frequency.

534 **Efferent-Mediated Adaptation of the DPOAE as a Predictor of Aminoglycoside Toxicity**

Karin Halsey, Lisa Kabara, Laura Grant, David F. Dolan
Kresge Hearing Research Institute, U. of Michigan, 1301 E. Ann St., Ann Arbor, MI, United States

Rapid efferent adaptation of the distortion product otoacoustic emission (DPOAE) predicts susceptibility to noise-induced damage, and is linked to the concentration of the efferent receptor (?). Maximum adaptation occurs at intense primary levels, rapidly switching from positive to negative orientation in a very narrow (2 dB) range of F1 and F2 levels.

Aminoglycosides are commonly used antibiotics, with the undesirable side-effect of ototoxicity. Susceptibility to hair cell damage from the aminoglycoside gentamicin can be quite variable, even

within a single strain and species of animal. Since one of gentamicin's first sites of action in the outer hair cell (OHC) is at the efferent receptor, it is possible that efferent activity could be a predictor of susceptibility to gentamicin induced damage.

Animals were anesthetized for measurement of DPOAE adaptation, permanent recording electrode implant, and baseline auditory brainstem response (ABR) at 2, 8, and 16 kHz. They were given gentamicin (160 mg/kg) daily for 14 days. During gentamicin administration, the 16 kHz ABR was screened daily with the animal awake and gently restrained. One week after the termination of dosing, the animal was anesthetized for a complete final ABR to determine threshold shifts. This dose of gentamicin produced a rapid and severe threshold shift affecting all animals. Even given the tight grouping of the onset of hearing loss in these animals, we found the number of days until hearing loss developed was related to the adaptation magnitude; animals with larger adaptation magnitude developed a hearing loss later than animals with smaller adaptation magnitude. We are currently exploring a lower gentamicin dose to strengthen the degree of this correlation.

535 The Efficacy of AM Noise for Activating the Human MOC Reflex Measured Using SFOAEs.

Bradford C Backus¹, John J Guinan²

¹Speech and Hearing Bioscience and Technology, Harvard-MIT Division of Health Science and Technology, 77 Mass. Ave., Cambridge, MA, United States, ²Eaton Peabody Lab, Mass. Eye & Ear Infirmary, Harvard Medical School, 243 Charles St, Boston, MA, United States

The medial olivocochlear (MOC) reflex is a mammalian sound-evoked reflex with an effector limb that innervates outer hair cells and reduces the mechanical response of the cochlea to sound. Determining the types of sounds that best activate the reflex will help to develop an understanding of the evolved role of the reflex as well as provide insight into the reflex's mechanisms. Of special interest are amplitude-modulated (AM) noises because they mimic the temporal envelopes of many information-carrying sounds, including speech. Prior work on the efficacy of AM noises and tones as MOC-reflex elicitors suggests that overall reflex strength varies with modulation frequency and is greatest for modulation frequencies near 100Hz. These studies, however, measured MOC-reflex strength using TEOAEs evoked by clicks or tone pips at a 50Hz presentation rate. Unfortunately, this rate may interact with and influence the efficacy of AM elicitors. In addition, prior studies did not include modulation frequencies below 50 Hz, a region where speech shows strong amplitude modulation, nor did they measure the temporal dynamics of the reflexes to determine the AC component of the reflex response. We investigate the efficacy of square-wave and sine-wave AM broad-band noises for activating the MOC reflex in individual human subjects by observing the changes these elicitors produce in SFOAEs. Our preliminary results indicate that the AC component of the MOC reflex does not follow modulation rates higher than a few Hz and is therefore unlikely to be operating on the speech envelope.

(Supported by NIDCD RO1-DC005977)

536 Level-Dependent SFOAE Variability Elicited by Equal-Frequency Primaries

Kim S. Schairer¹, Douglas Keefe¹, Walt Jesteadt¹

¹Research, Boys Town National Research Hospital, 555 North 30th Street, Omaha, NE, United States

Level-dependent variability of stimulus frequency otoacoustic emissions (SFOAE) limits detection of SFOAEs at higher stimulus levels. This variability also may be a source of "internal noise" that limits such behavioral tasks as intensity discrimination. In the current study, SFOAE stimuli were $f_1=f_2$ of 1, 2, or 4 kHz in an equal-level condition ($L_1=L_2$ of 85 to 0 dB SPL) or fixed-level condition with L_1 fixed and L_2 varied from 5 dB below L_1 down to 0 dB SPL. Fixed L_1 s were used from 40 to 80 dB SPL. This fixed-level condition is the analog to the behavioral intensity discrimination paradigm. DPOAEs were elicited with the same f_2 frequencies and L_2 range as the SFOAE equal-level condition. SFOAE variability in the equal-level condition increased as a function of L_2 , and this trend was not observed in the DPOAEs or in a test cavity. Responses in the equal-level condition averaged after discarding the first 23 vs. 92 ms after the onset of each stimulus block were similar, which suggested that the increase in variability is not due to a failure to extract stimulus artifact. SFOAE variability in each fixed-level condition was generally constant across L_2 , and it decreased as the fixed L_1 decreased. Therefore, SFOAE threshold, or the lowest L_2 at which the signal-to-noise ratio exceeded a criterion amount, decreased with decreasing fixed L_1 . Individual differences appeared to be consistent across the higher fixed- L_1 conditions within a given test frequency and ear combination. For example, a subject with higher variability than the other subjects in one fixed-level condition showed higher variability in other fixed-level conditions. Overall, the results suggest that SFOAEs elicited in fixed-level conditions may be combined with behavioral discrimination results to test for a common source of variability in the auditory system. (Work supported by NIH DC06342, DC003784, and DC04662.)

537 The relationship between TEOAEs and SFOAEs at low stimulus levels

Radha Kalluri^{1,2}, Christopher A. Shera^{1,2}

¹Eaton-Peabody Laboratory, Massachusetts Eye & Ear Infirmary, 243 Charles St, Boston, MA, United States, ²Speech and Hearing Bioscience and Technology Program, Massachusetts Institute of Technology, 77 Massachusetts Ave, Cambridge, MA, United States

Although several models of otoacoustic emissions predict that at low stimulus levels both transient-evoked and stimulus-frequency otoacoustic emissions (TEOAEs and SFOAEs) are generated by the same linear-reflection mechanism (Zweig & Shera 1995, *J. Acoust. Soc. Am.*; Talmadge et al. 1998, *J. Acoust. Soc. Am.*), a more recent model predicts that the mechanisms responsible for TEOAEs are both inherently nonlinear and fundamentally different from those responsible for SFOAEs (Nobili et al. 2003, *J. Assoc. Res. Otolaryngol.*). The goal of our experiments was to test these competing models by determining the relationship between the OAEs evoked by broad- and narrow-band stimuli. Our test was inspired by linear systems theory: If the cochlea responds linearly at low stimulus levels, its input-output response can be characterized equivalently in either the time domain using impulsive stimuli

(TEOAEs) or the frequency domain using pure tones (SFOAEs). We compare the “transfer functions” T_{TE} and T_{SF} computed from TEOAE and SFOAE measurements in normal hearing humans. T_{TE} and T_{SF} were obtained by dividing the frequency response of the corresponding OAE by that of the stimulus. Click-evoked TEOAEs were measured using a linear windowing technique at stimulus levels ranging from 35 to 80 dB SPL-peak; SFOAEs were measured using an acoustic suppression paradigm. At the lowest stimulus levels, both T_{TE} and T_{SF} become nearly independent of level, suggesting that the cochlea is operating in an approximately linear regime. As predicted by the linear-reflection models, T_{TE} and T_{SF} share a similar spectral shape, phase behavior, and dependence on stimulus level. Both transfer functions exhibit the same spectral landmarks (i.e., peaks and notches) and their phase-vs-frequency functions are almost identical. The observed agreement between T_{TE} and T_{SF} supports the hypothesis that low-level TEOAEs and SFOAEs are generated by the same linear-reflection mechanism.

Supported by NIDCD/NIH grant R01 DC03687.

538 The dual effect of “suppressor” tones on stimulus-frequency otoacoustic emissions

Christopher A. Shera¹, Arnold Tubis², Carrick L. Talmadge³, John J. Guinan, Jr.¹

¹Eaton-Peabody Laboratory, Harvard Medical School, 243 Charles St, Boston, MA, United States, ²Department of Physics, Purdue University, 1396 Physics Building, West Lafayette, IN, United States, ³National Center for Physical Acoustics, University of Mississippi, Coliseum Drive, University, MS, United States

Siegel, Temchin, and Ruggero (2003, *Assoc. Res. Otolaryngol. Abs.*, 26:679) argue that stimulus-frequency otoacoustic emissions (SFOAEs) originate from a broad region of the cochlea that extends far basal to the peak of the traveling wave. They base their conclusion on SFOAEs measured in chinchillas using a paradigm in which a more intense second tone (the “suppressor”) is assumed to eliminate probe-frequency SFOAE sources that are located between the stapes and the peak of the suppressor-tone traveling wave. Siegel et al. argue that their suppression technique allows them to map out the spatial distribution of SFOAE sources along the cochlea. We test Siegel et al.’s assumptions about the effect of the second tone by exploring their measurement paradigm in nonlinear, active cochlear models, both with and without mechanical perturbations in the organ of Corti. We show that the effect on SFOAE sources of introducing the second tone depends on the tone’s frequency relative to the probe. When the frequency of the second tone is close to the probe, the second tone acts mainly as a suppressor, reducing the effective strength of probe-frequency SFOAE sources, which are located principally about the peak of the traveling wave. However, when the frequency of the second tone is substantially higher than the probe, the second tone acts not primarily as a suppressor, but as a generator of additional SFOAE sources. The second tone creates new probe-frequency SFOAE sources by inducing mechanical perturbations and/or sources of nonlinear distortion that would not otherwise be present. Our results suggest that although near-probe suppressors can be used to estimate the total probe-frequency SFOAE, Siegel et al.’s paradigm does not generally provide a valid measure of the spatial profile of SFOAE sources within the cochlea.

Supported by NIDCD/NIH grants R01 DC03687, R29 DC03094, and R01 DC00235.

539 Similar Two-tone Suppression Patterns in SFOAEs and the Cochlear Microphonics Indicate Comparable Spatial Summation of Underlying Generators

Jonathan H. Siegel¹, Amanda J. Cerka¹, Andre N. Temchin, Mario Ruggero

Communication Sci. & Disord., Northwestern University, 2240 Campus Drive, Evanston, IL, United States

We have presented evidence that stimulus frequency otoacoustic emissions (SFOAEs) are generated over a large region of the cochlea and are subject to pronounced phase cancellation near the peak of the traveling wave envelope (Siegel et al., ARO Abst. 26: 172, 2003). It is well established that phase cancellation of the cochlear microphonic (CM), reflecting the summed receptor currents of many hair cells within the pickup region of the recording electrodes, is particularly severe when the traveling wave peaks near the recording location (Dallos, P., *The Auditory Periphery*; Academic Press, 1973; pp. 228-288.). We hypothesize that the phase distributions of both the SFOAE and CM generators, and thus the phase cancellation, are both determined by the underlying spatial phase pattern of the basilar membrane.

We tested the hypothesis by measuring the suppression of SFOAEs and round window CM in the same chinchilla cochleae using the same data collection system and stimuli. We measured the suppression of the response to a low-level (20-30 dB SPL) probe tone (f_{pr}) of fixed frequency (8 or 12 kHz) to a suppressor tone (f_{su}) of 55 dB SPL varied in frequency from just above f_{pr} to 18 kHz. On the assumption that higher f_{su} s correspond to more basal cochlear regions, estimates of the spatial profile of SFOAE and CM generators were obtained by differentiating the suppression plots of the probe response with respect to f_{su} .

Especially for the 12 kHz probe tone, the suppression patterns suggested that both the spatial extent and phase interaction between generators of SFOAEs and CM were similar. In particular, the generators of both phenomena appear to be weighted heavily toward a cochlear region extending far basal to the place of the probe tone, where there is little phase variation. Our data cast further doubt on the notion that the peak region of the basilar-membrane traveling wave dominates in generating SFOAEs (Zweig and Shera, JASA 98:2018-2047, 1995).

540 (Very) Long-term Stability of SOAEs

Edward M Burns

Speech and hearing Sciences, University of Washington, 1417 NE 42 st, Seattle, WA, United States

Spontaneous otoacoustic emissions (SOAEs) were measured longitudinally in adults and children (initial age ranges: 6 years to 41 years) for periods ranging from 4 years to 19 years. SOAEs were also measured in two females over the course of their pregnancies. The long-term longitudinal measurements show a gradual decrease in emission frequency for all emissions, in all subjects, which is approximately linear in percent shift per year, averaging about 0.25 percent per year. Changes in levels of emissions are much less consistent: although there is a general decrease in emis-

sion levels over time, particularly in older subjects, levels of individual emissions show both increases and decreases. Frequency and level shifts that correlated with birth were noted in the pregnancies but the magnitudes of these shifts were no greater than those of the monthly shifts in SOAEs in female subjects that have been reported in the literature.

541 Calcium concentration modulates spontaneous otoacoustic emission frequency

Geoffrey A Manley, Christine Köppl, Ulrike J Sienknecht
Lehrstuhl für Zoologie, Technische Universität München, Lichtenbergstrasse 4, 85747 Garching, Germany

Bundle-based active processes in hair cells may be driven by premature transduction channel closure due to the binding of calcium ions to the open channel, and this exerts a force on the bundle. The rapid twitching of hair-cell bundles is clearly a candidate driver of spontaneous otoacoustic emissions (SOAE; Hudspeth et al., 2000, PNAS 97, 11765-11772). In the Bobtail skink, SOAE are generated by an active mechanism integral to the bundle (Manley et al., 2001, PNAS 98, 2826-2831) and SOAE frequencies can be modulated by DC currents (Manley and Kirk, 2002, JARO 3, 200-208). Manley and Kirk (2001 ARO Abstract 321) showed that BAPTA in Scala media reversibly reduces SOAE frequencies. Here, we show that the frequency of SOAE peaks can be modulated up and down by changing the calcium concentration.

Glass micropipettes of large tip diameters (4-28 μ m) were introduced into Scala media of anesthetized Bobtail skinks (*Tiliqua rugosa*) while monitoring the frequencies and levels of SOAE. Electrodes were filled with a solution of 180 or 200mM KCl or with fluids of various concentrations of CaCl₂ and KCl. Solutions with no or extremely low Ca²⁺ concentrations shifted SOAE peaks to lower frequencies, solutions of >5mM CaCl₂ shifted frequency up and levels fell. This is consistent with in vitro data from sacculus hair cells (e.g., Martin and Hudspeth, 1999, PNAS 96, 14306-14311). Upward frequency shifts were limited to about 8%, however, since beyond that the amplitudes were no longer measurable.

These data suggest an important role for calcium in establishing appropriate conditions for the production of SOAE. The frequency and level shifts observed resemble those induced by DC currents (Manley and Kirk, 2002), suggesting that manipulating both hair-cell resting potential and endolymphatic calcium levels affect the same fundamental mechanism driving SOAE.

Supported by the DFG and the Raine Medical Research Foundation of W. Australia.

542 Spontaneous Otoacoustic Emissions in Tinnitus Patients

Yongbing Shi, William Hal Martin

Otolaryngology, Oregon Health & Science University, 3181 SW Sam Jackson Park Road, Portland, Oregon, United States

Otoacoustic emissions (OAEs) are believed to be the products of active cochlear mechanics. They are generally associated with relatively intact outer hair cell function. OAEs usually decrease or become undetectable when hearing loss of cochlear origin exceeds 40-50 dB HL. Subjective tinnitus is perception of sound without detectable corresponding source. It is most often seen in patients with hearing loss. It is also frequently seen in patients with head

injuries. Studies have suggested that the incidence of spontaneous otoacoustic emissions (SOAEs) is lower in patients with hearing loss and tinnitus than in normal population. There have also been reports on association between tinnitus and SOAEs of unusually high amplitudes, which can be controlled by aspirin administration. The current paper seeks to further study the relationship between SOAEs and tinnitus from a clinical point of view. Audiometric, tinnitus and SOAE data from 59 patients seen at the Oregon Health & Science University Tinnitus Clinic were reviewed. Fifty-four of these 59 patients showed sensorineural hearing loss of various degrees at the time of evaluation, mostly affecting high frequencies. SOAEs were detected in 26 ears (22%) of 19 patients (32.2%). There was no difference in SOAE incidence between male and female patients. SOAEs were recorded in four of the five patients whose pure tone thresholds were within normal limits up to 8000 Hz. SOAEs appeared to be recorded at a higher rate in patients whose tinnitus started following motor vehicle accidents or head injuries (5/10) than in other patients. Time course of tinnitus did not appear to affect SOAE detection rate. There were no correlations between SOAE frequency and matched tinnitus pitch or frequency of maximum hearing loss. Significance of these findings is discussed.

543 High Frequency Spontaneous Otoacoustic Emission and Basilar Membrane Oscillation in a Guinea Pig

Alfred L Nuttall^{1,2}, Karl Grosh³, Jiefu Zheng¹, Egbert de Boer⁴, Tianying Ren¹

¹Oregon Hearing Research Center, Oregon Health & Sciences University, 3181 SW Sam Jackson Park Road, Portland, OR, United States, ²KHRI, The University of Michigan, 1301 East Ann, Ann Arbor, MI, United States, ³Mechanical Eng., University of Michigan, 2350 Hayward St., Ann Arbor, MI, United States, ⁴Oto, Academic Medical Center, KNO Rm D2-226, Meibergdreef 9 1105 AZ Amsterdam, Netherlands

A spontaneous otoacoustic emission (SOAE) measured in the ear canal of a guinea pig had a counterpart in the spontaneous oscillation of the basilar membrane (SBMO). The ear canal level of the emission was approximately 30 dB SPL. The emission and SBMO frequency varied over time between about 14.2 kHz and 15 kHz. The best frequency at the measured location on the BM, was about 18 kHz. A pure tone above 35 dB SPL at 14 kHz could reduce the spontaneous SBMO level to the noise floor. A tone at 15 kHz increased the SBMO, and when loud enough, entrained the emission frequency. One or two octave (frequency spanning around the emission) noise stimuli also caused the SBMO to increase as the noise level increased. DC current of 100 μ A across the cochlear duct increased the SOAE and the SBMO, when the current polarity was positive (in the scala vestibuli relative to the scala tympani), and reduced them when of opposite polarity. The CAP audiogram evidenced a frequency-specific loss at 8 and 12 kHz in this animal. We conclude that a relatively high-frequency SOAE of 15 kHz originated near the 15 kHz tonotopic place and appeared at the measured BM location as a forward and/or reverse traveling wave. Electric current can modulate the level and frequency of the emission in a pattern similar to that for the mechanical tuning of the BM. Supported by NIH NIDCD R01 DC 00141, R01 DC 04084 and R01 DC 04554.

544 Elusive Entrainment

Egbert de Boer¹, Alfred L. Nuttall^{2,3}, Karl Grosh⁴

¹ORL, Academic Medical Center, Meibergdreef 9, Amsterdam, Netherlands, ²Oregon Hearing Research Center, Oregon Health & Sciences University, 3181 SW Sam Jackson Park Road, NRC04, Portland, Oregon, United States, ³KHRI, University of Michigan, 1301 East Ann Street, Ann Arbor, Michigan, United States, ⁴Dept. of Mechanical Engineering, University of Michigan, 2250 G.G. Brown Bldg, 2350 Hayward St., Ann Arbor, Michigan, United States

It is likely that spontaneous otoacoustic emissions (SOAEs) in mammalian ears arise from a complex interaction between distributed generators of acoustical power and a mechanism described as “coherent reflection” (Zweig and Shera, *J. Acoust. Soc. Am.* 98, 2018-2047, 1995). For a theoretical study it is necessary to simplify the physics of the system. Accordingly, the complex generation system has been lumped into a single oscillator embedded at a fixed location in a one-dimensional nonlinear cochlear model. Spontaneous oscillations have been observed on the basilar membrane in the basal turn of the guinea pig cochlea, and the reactions to a few types of acoustical and electrical stimuli were recorded (see the companion poster). The present study is focused on the question whether the single oscillator placed in a cochlear model shows the same properties as have been measured physiologically. First, it was established that an isolated oscillator in a cochlear model subjected to the signals as used in the physiological experiments qualitatively behaves in the same way as a single Van der Pol oscillator subjected to the same signals. Second, it was studied what is the equivalent of ‘entrainment’ in the case of stimulation by a multi-component signal and a pseudo-random noise signal. From the results it was possible to estimate the equivalent damping coefficient that governs the oscillator and the effective bandwidth of its response to extraneous signals.

545 DPOAE in Cochlear Nerve Deficiency

Sachiko Komatsubara¹, Yuki Wada¹, Hirokazu Kawano¹, Atsushi Haruta¹, Shizuo Komune¹, Takao Kodama²

¹Otorhinolaryngology, Miyazaki medical college, 5200, Kihara, Kiyotake-cho, Miyazaki-gun, Japan, ²Radiology, Miyazaki medical college, 5200, Kihara, Kiyotake-cho, Miyazaki-gun, Japan

Introduction: It is generally considered that otoacoustic emission is originated from the electromotility of outer hair cells (OHC). However it is still unclear whether efferent innervation is necessary for development of the electromotility. David Z.Z. He and Peter Dallos reported in 1997 that the ontogeny of OHC electromotility is an intrinsic process which does not require the influence of efferent innervation. In this study, the development of OHC electromotility was evaluated by DPOAE in cochlear nerve deficiency.

Materials and Methods: CT and MRI (3D-fast asymmetric spin echo: FASE) examination was carried out on patients with congenital severe sensorineural hearing loss. MRI (3D-FASE) can generally describe the routes of nerves in the internal acoustic meatus and also indicate the detail of vestibulocochlear branches in normal case. Bony canal from the fundus of internal auditory canal to the base of modiolus, which is called cochlear nerve canal, can be evaluated by CT. We compared the relationship between CT findings of narrow cochlear canal and MRI imagings of cochlear nerve

deficiency. It was determined that cochlear nerve canal with less than 1.5mm width in CT is classified as narrow cochlear nerve canal. We also examined DPOAE on patients with cochlear nerve deficiency.

Results and Conclusions: Eight patients were defined as the cochlear nerve deficiency. Five out of them underwent DPOAE. DPOAE revealed within the normal level (pass) in two patients and under the normal level (refer) in three patients. Therefore, the fact that pass of DPOAE was observed in two patients may demonstrate that OHC electromotility develop without normal efferent innervation and also indicate a clinical evidence of experimental theory in development of OHC electromotility.

546 Effects of Age and Hearing Loss on Gap Detection and the Precedence Effect: Narrow-band Stimuli

Jennifer J. Lister¹, Richard A. Roberts²

¹Communication Sciences and Disorders, University of South Florida, 4202 E. Fowler Ave. PCD 1017, Tampa, FL, United States, ²AIB Education Foundation, American Institute of Balance, 11290 Park Boulevard, Seminole, FL, United States

Older listeners with normal hearing and impaired hearing often demonstrate poorer than normal speech understanding under degraded acoustic conditions. Underlying this difficulty may be deficits in temporal resolution and the precedence effect. Temporal resolution is often studied using a gap detection paradigm in which a listener must report the perception of a silent gap between two markers. This task is similar to fusion paradigms used to measure the precedence effect. Our previous investigations have suggested a potential relationship between across-channel gap detection (as measured dichotically with fixed-frequency markers) and fusion. The purpose of the present investigation was to use additional across-channel conditions to explore this potential relationship. Fixed-frequency and frequency-disparate gap detection thresholds (GDTs) and lag burst thresholds (LBTs) were measured for three groups of listeners: (1) young with normal hearing; (2) older with normal hearing; and (3) older with sensorineural hearing loss. For measurement of GDTs, the fixed-frequency and frequency-disparate narrow-band noise markers were presented in diotic and dichotic paradigms. For measurement of LBTs, the fixed-frequency and frequency-disparate markers were presented in a traditional precedence effect paradigm. Results indicated that GDTs were significantly affected by frequency disparity and age, but LBTs were only affected by frequency disparity. Also, the pattern of results was very different for the two tasks. Specifically, largest LBTs were measured for the fixed-frequency markers whereas largest GDTs were measured for the frequency-disparate markers. Dichotic GDTs and LBTs were significantly correlated for two of the three frequency conditions. These results suggest that gap detection and fusion do not reflect the same underlying processes, but may influence each other under some conditions.

547 Cochlear nonlinearity between 500 and 8000 Hz in listeners with impaired hearing

Enrique A. Lopez-Poveda¹, Christopher J. Plack², Ray Meddis², José L. Blanco³

¹Institute for Neuroscience of Castilla y León, University of Salamanca, Avda. Alfonso X El Sabio s/n, Salamanca, Spain,

²Department of Psychology, University of Essex, Wivenhoe Park, Colchester, United Kingdom, ³Oticon University, Oticon Spain SA, Ctra. Fuencarral 24, Ed. Europa, Madrid, Spain

Cochlear nonlinearity was estimated in listeners with impaired hearing using a forward-masking method. For a fixed low-level probe, the masker level required to mask the probe was measured as a function of the masker-probe interval, to produce a temporal masking curve (TMC). TMCs were measured for probe frequencies from 500 to 8000 Hz, and for masker frequencies from 0.5 to 1.6 times the probe frequency. Unlike what happens for normal-hearing (NH) listeners (Lopez-Poveda et al. 2003, *J. Acoust. Soc. Am.* 113:951-960), TMCs for on-frequency maskers sometimes show a single slope, suggesting linear responses for tones at CF. Sometimes, however, two distinct slopes are visible, suggesting remaining compression. Both patterns are uncorrelated with absolute threshold and are consistent with selective damage to outer or inner hair cells (IHC) respectively. Remarkably, the slope of the TMCs for very low-frequency maskers is shallower for the impaired ears than for normal ones. This result implies that for NH listeners, the slope of the TMCs for very low frequency tones reflects some kind of compression, even at high CFs. It is discussed that this compression is likely occur at the IHC rather than at the basilar membrane. [Work supported by FIS PI020343, G03/203, and MCYT].

548 Peripheral Non-linearity in Listeners with Poor Speech Recognition in Noise despite Normal Hearing in Quiet

Rohima Badri, Jonathan Siegel

Communication Sciences and Disorders, Northwestern University, 2240 Campus Drive, Evanston, Illinois, United States

A large number of people complain of speech recognition problems in the presence of noise despite having normal hearing in quiet. There are evidences that suggest basilar membrane phenomena such as suppression and frequency resolution improve signal detection in noise. These phenomena may possibly be attributed to the presence of a non-linear mechanical feedback mechanism in the cochlea. Loss of this feedback mechanism leads to a more linear basilar membrane response near the peak that is reduced in amplitude and compression. In this study, we investigated whether listeners with poor speech recognition in noise show evidence of altered peripheral non-linearity. Based on the performance in Sentences-In- Noise Perception Test (Liu et al, *ARO Abst.* 26:215, 2003), listeners were assigned to two groups: one with normal speech recognition in noise and other with poor speech recognition in noise. Listeners in both groups had audiometric thresholds < 20 dB HL in both ears at all standard audiometric frequencies between 500 to 8000 Hz. Peripheral non-linearity was tested behaviorally by measuring filter shapes at 2kHz across level as described by Rosen et al. (*J Acoust Soc Am* 103(5) 2539-2550, 1998) and physiologically by studying the Distortion Product

Otoacoustic Emission (DPOAE) input-output function with f_2 fixed at 2 kHz and f_2/f_1 ratio at 1.3. In both groups, auditory filters broadened with increasing level. However, at all stimulus levels used in the present study, listeners with poor speech recognition in noise had significantly broader auditory filters with greater ERBs than the normal listeners. Moreover, in the group with reduced speech recognition in noise, compression thresholds obtained from the DPOAE measurements were significantly higher than in the normal listeners. The study suggests that a peripheral non-linear processing deficit may contribute to the poor speech recognition in noise.

Supported by Northwestern University

549 Factors influencing PTC shape for subjects with dead regions; detection of beats and combination tones

Karolina Kluk, Brian C. J. Moore

Experimental Psychology, University of Cambridge, Downing Street, Cambridge, United Kingdom

A dead region (DR) is a region of the cochlea where there are no functioning inner hair cells. A DR can be detected by measuring masked thresholds of sinusoids in threshold equalising noise (TEN); elevated thresholds at a given frequency indicate a dead region at that frequency. Another way is to measure psychophysical tuning curves (PTCs); a shifted tip of the PTC indicates a DR. We show here that the shapes of PTCs for hearing-impaired subjects can be influenced by the detection of beats and of the simple difference tone (SDT) resulting from the interaction of the signal and masker. As a result, PTCs can have tips at the signal frequency, f_s , even when f_s falls in a DR. Subjects with near-normal hearing or moderate hearing loss at low frequencies and a DR at high frequencies (diagnosed with the TEN test) were tested. PTCs for sinusoidal and narrowband noise maskers (80-, 160-, 320-Hz wide) were measured: (1) in quiet; (2) in the presence of additional low-pass noise designed to mask the simple difference tone (SDT); (3) in the presence of a pair of low-frequency tones designed to interfere with the detection of beats. In condition (1), the tip of the PTC was often at f_s , even when f_s fell in a DR, when the masker was a sinusoid or 80-Hz wide noise. This occurred much less for the wider noise bandwidths. For subjects with good low-frequency hearing, the tip at f_s was probably caused by detection of the SDT, as in condition 2, the tip of the PTC usually shifted away from f_s . For subjects with poorer low-frequency hearing, the tip at f_s was probably caused by the lack of beats when f_s equalled the masker frequency; in condition 3, the masker level was reduced for masker frequencies adjacent to the signal frequency, eliminating the tip at f_s . To minimise the influence of beats, we recommend using narrowband noise maskers with a bandwidth of 160 or 320 Hz. In cases of near-normal hearing at low frequencies, we recommend using an additional low-pass noise to mask SDTs.

550 Neuromagnetic Responses Reflect Psychoacoustic Findings in Temporal Pitch Changes

Steffen Ritter¹, Hans Günter Dosch², Hans-Joachim Specht³, André Rupp¹

¹Section of Biomagnetism, Department of Neurology, University of Heidelberg, INF 400, Heidelberg, Germany, ²Institute for Theoretical Physics, University of Heidelberg, Philosophenweg 16, Heidelberg, Germany, ³Institute of Physics, University of Heidelberg, Philosophenweg 12, Heidelberg, Germany

Regular Interval Noise (RIN) is generated by adding a delayed copy of random noise n times back to the original noise (delay-and-add). The perceived temporal pitch is proportional to the inverse of the delay (d). If gain $g=-1$ (delay-and-subtract), pitch differs significantly from the delay-and-add condition. Raatgever and Bilsen ('Auditory Physiology and Perception', Pergamon, Oxford 1992) found pitch values equal to $1/(2d)$ for delays less than about 4 to 6ms. However, pitch shifts with increasing d to ambiguous values of $1.1/d$ and $0.9/d$.

The relation of the perceived pitch and the auditory evoked fields (AEF) was studied in a combined magnetoencephalographic (MEG) and psychoacoustic study in 20 subjects. RIN segments with delay-times of 2, 4, 8, and 16ms based on 2 and 8 iterations (n) were applied with g set to +1 and -1. A spatio-temporal source model with one equivalent dipole in each hemisphere was used to analyze the neuromagnetic pitch onset response (POR). In the psychoacoustic study, a two-alternative forced choice task for paired comparisons was applied to all RIN segments. Listeners had to judge which tone was of higher pitch. For each block n was kept constant while d and g were varied. Pitch-scale values were derived using the Bradley-Terry-Luce method.

For $g=-1$ the POR exhibited significant longer latencies in the 2 and 4ms delay conditions as compared to $g=+1$. For $d=8$ or 16ms, POR latency varied within the statistical error. The linear pitch-scale values of the psychoacoustic study showed the same behaviour. Thus, the neuromagnetic POR latency mirrors the perceived pitch-shift from $1/(2d)$ to the ambiguous pitch ($1.1/d$ or $0.9/d$) for increasing delay times.

551 Nonadditivity of Energetic and Informational Masking, II: Results From a Speech Identification Task.

Gerald Kidd, Jr., Christine R. Mason, Frederick J. Gallun
Hearing Research Center and Communication Disorders, Boston University, 635 Commonwealth Avenue, Boston, MA, United States

Informational masking may be produced by masker energy located in frequency regions remote from the signal. In contrast, energetic masking occurs when masker and signal are near enough in frequency to interact directly in the auditory periphery. This study examined conditions in which the two types of maskers were combined. Previous work from our laboratory has indicated that energetic and informational maskers may interact in counterintuitive, nonadditive ways. In the previous experiment, this interaction between energetic (noise) and informational (multitone) maskers was observed in a pure-tone detection task. The combined masking effect was found to be substantially less than that of the

informational masker alone. The current study demonstrates analogous nonadditivity of masking between energetic (noise) and informational (speech) maskers in a closed-set speech identification task. The speech signals and maskers were sentences from the Coordinate Response Measure corpus (Bolia et al., JASA 107, 2000, 1065-6) that were processed to produce sets of narrow frequency bands (cf., Arbogast et al., JASA 112, 2002, 2074-85). As in the Arbogast et al. study, the narrow bands comprising the signal and masker sentences were mutually exclusive and randomized from trial to trial. The energetic masker was noise that was spectrally matched to the informational (speech) masker. Results indicated that the addition of the noise masker could improve signal identification over that achieved in the presence of the speech masker alone. In addition, identification performance improved as the level of the noise masker was increased. This result occurred regardless of whether the noise was presented in the same ear as the speech masker and signal or in the opposite ear. These results suggest that simple rules for predicting the effects of combining energetic and informational maskers are unlikely to prove successful. [Supported by NIH-NIDCD grants DC04545 and DC00100]

552 Determining the neurobiological bases of auditory perceptual grouping using neural modeling.

Fatima Tazeena Husain, Thomas Lozito, Antonio Ulloa, Barry Horwitz

Brain Imaging and Modeling Section, NIDCD, National Institutes of Health, 9000 Rockville Pike, Bldg 10, Rm 6C420, MSC 1591, Bethesda, Maryland, United States

Perceptual grouping enables the auditory system to integrate brief, disparate sounds into cohesive perceptual units. This plays a critical role in perception, for instance, allowing for the separation of attended sounds from environmental noise. The neural mechanisms underlying auditory perceptual grouping have not been studied extensively with conventional neuroimaging or electrophysiological techniques. We used a large-scale, neurobiologically realistic model of auditory processing in cortex that we developed to investigate the neural bases of several types of auditory perceptual grouping phenomena. The model was constructed based on neurophysiological and neuroanatomical data from primate and human studies. The model processes auditory objects such as tonal sweeps in a delayed match to sample short-term memory task. With this model, we can simultaneously simulate both neurophysiological and BOLD fMRI activity. We used the model to match a tonal pattern with fragmented (e.g., silent gaps inserted) versions of the same pattern. Perceptual grouping in the model broke down gradually as the degree of fragmentation increased. However, when the gaps in the fragmented stimuli were filled with simulated loud broadband noise, the stimulus was perceptually grouped as an intact stimulus. This result agrees with behavioral studies in humans and an electrophysiological study in cats. We further tested the model's ability to perform selective attention and streaming and found that the model performed poorly only on the latter. Our results are explained in the context of lateral and feed-forward connections among the modules of the model. The results implicate a particular set of cortical processing mechanisms that implement perceptual grouping. These simulation results are being used to design functional neuroimaging studies.

553 Melody Recognition of Band-Limited Noise With Synthetic Spectral Pitch

Jeremy Liu¹, Hongbin Chen¹, Larry Feth², Fan-Gang Zeng¹

¹Biomedical Engineering, University of California, Irvine, 364 Med Surge II, Irvine, CA, United States, ²Speech and Hearing Sciences, Ohio State University, 1070 Carmack Road, Columbus, OH, United States

Although cochlear implant listeners can perform relatively well in speech recognition, their ability to appreciate music is quite limited. This is largely due to the small number of independent monotonic pitches that can be encoded by electrodes in a cochlear implant. This experiment tests the use of a synthetic spectral pitch model on two toned complexes and complexes of two noise-bands. The synthetic spectral pitch is based on the IWAIF (intensity-weighted average of instantaneous frequency) model developed by Feth and his colleagues (Anantharaman, Krishnamurthy, and Feth, JASA 1993).

Twelve well-known melodies were generated using the synthetic spectral pitch model. Rhythm cues were removed and notes were presented at three frequency ranges: low (center frequency = 52-111Hz), middle (center frequency = 207-523Hz), and high (center frequency = 1656-4192Hz). To represent these melodies, we manipulated relative amplitude between two fixed-frequency tones or noise bands according to IWAIF model. Using the synthetic spectral pitch model, melodies were represented by 2, 3, 5, or 9 anchor noise-bands in a 2-octave range. The spacing of anchors is equal on the logarithmic scale: 2 octaves, 1 octave, half an octave, and a fourth of an octave respectively. The band-width of the each noise-band is equal to the anchor spacing and therefore is also equal on the logarithmic scale.

Data shows that nearly perfect performance could be achieved with an anchor spacing of a 0.25 octaves. Also, a moderate performance of 60-80% can be achieved with half octave and octave spacing. These results imply that only 40 fixed frequency noise-bands are needed to cover the range of normal hearing.

554 Perceptual learning in frequency discrimination

Ginger S. Stickney¹, Norman M. Weinberger², Fan-Gang Zeng¹

¹Otolaryngology, University of California, Irvine, 364 Med Surge II, Irvine, CA, United States, ²Neurobiology and Behavior, University of California, Irvine, 309 Qureshey Research Laboratory, Irvine, CA, United States

This study examined human perceptual learning in a frequency discrimination task. Two training frequencies were used (0.4 and 6 kHz) to investigate and compare learning behaviors that possibly depend on two separate mechanisms: a temporal neural coding mechanism for frequencies less than 5 kHz and a place coding mechanism for frequencies greater than 5 kHz. The improvement in frequency discrimination was compared for the training frequency and each of four test frequencies (.25, 1.5, 6, and 8 kHz) to measure learning generalization and specificity. Performance was tracked over five training days and compared to a single day of training, with a posttest following each. Retention was measured with a posttest two weeks following the last training day. Although

there was a large degree of variability initially, this variability decreased over training sessions. Frequency discrimination performance improved gradually, and the rate of improvement differed depending on the training frequency. With a 0.4 kHz training frequency, performance improved during the first three days of training then reached a plateau. In contrast, the 6 kHz training frequency continued to show improvement up to, and including, the fifth day of training. These results suggest that frequency discrimination via a place coding mechanism may require a much longer training period for improved discrimination. Both the pattern and the degree of frequency discrimination were maintained in the final posttest, indicating that the training-induced improvement in frequency discrimination could be retained for at least two weeks.

Supported in part by UC Irvine IRU in Hearing and Speech Sciences, NIH F32-DC-05900, and R01-DC-02267

555 Mechanisms for Processing Spectral Shape Independently of Fine Spectral Structure

Amanda R Jennings, Timothy D Griffiths

Auditory Group, The Medical School, University of Newcastle upon Tyne, Framlington Place, Newcastle upon Tyne, United Kingdom

Two experiments assessed the ability of listeners to detect changes in the spectral shape of stimuli composed of harmonic sounds and noise. This work represents an extension of profile analysis to the case where a spectral profile can be based on noise. We sought the basis for mechanisms such as the ability of listeners to recognise vowels whether they are whispered or voiced.

Experiment 1 investigated the detectability of three different spectral shape changes. Harmonic stimuli were based on a 100 Hz fundamental component with 40 harmonics. Noise stimuli had random phase spectra with amplitude spectra matched to that of the harmonic sounds. Spectral shape changes were applied to a reference stimulus, band-passed between 0.8 and 4 kHz. Using 2AFC psychophysics, subjects heard 2 pairs of stimuli and were required to detect the pair that differed in spectral shape. Pairs of harmonic (H) and noise (N) stimuli were presented in 4 conditions (HH, NN, HN, NH). Full psychometric functions were evaluated and Weibull functions were fitted to the data. Single carrier and cross carrier thresholds were similar suggesting a mechanism for spectral shape analysis that is independent of fine spectral structure. A roved-level control condition showed that this cannot be achieved by analysing the output of a single auditory filter.

Experiment 2 tested the hypothesis that the mechanism subserving detection of spectral shape change relies upon the extraction of the spectral envelope, as represented in the fibres of the auditory nerve. The harmonic stimuli had an 800 Hz fundamental component with 5 resolved harmonics. Single and cross carrier thresholds were similar despite the different auditory spectra of the harmonic sounds.

These data cannot be explained by simple comparison of the auditory spectra as represented across the fibres of the auditory nerve. We suggest an active mechanism of template analysis based on multiple looks across the auditory spectrum.

556 High-frequency ITD discrimination with 'transposed' stimuli in trained and untrained normal-hearing adults.

Daniel Rowan, Mark E Lutman

Institute of Sound and Vibration Research, University of Southampton, University Road, Southampton, United Kingdom

Following Bernstein and Trahiotis (2002, 2003), we have used 'transposed' stimuli to probe high-frequency interaural time difference (HF-ITD) sensitivity as background to the broader context of binaural sensitivity of hearing-impaired people using signal processing hearing aids or bilateral cochlear implants. We report data from two experiments using normal-hearing adults and preliminary data from a third. In the first, we replicated the finding of Bernstein and Trahiotis (2002) that, under certain conditions, comparable ITD thresholds may be found when using low-frequency pure tones and HF transposed tones in listeners who received 'substantial practice' prior to data collection. We then conducted an exploratory study with experimentally naïve listeners on ITD thresholds and the effects of training. While some listeners were readily able to detect HF-ITDs with the transposed stimuli, others were initially unable to detect HF-ITDs in excess of 1500 ms. This was despite all listeners displaying ITD sensitivity for low-frequency pure tones during initial task familiarisation. Performance for many listeners improved substantially with modest training (2400 trials), initially least sensitive listeners not reaching asymptotic performance within this time. Preliminary data from the third study designed to explore these learning effects further show that some untrained listeners can identify ITDs initially with low-frequency tones better than HF transposed tones and that performance with HF transposed tones improves more than with the low-frequency tones in these listeners. These data show that substantial learning occurs with ITD discrimination under some conditions and are important for interpreting binaural experiments in listeners who have received little training, as results may grossly underestimate optimal ability.

557 In vivo and in vitro Impedance Measurements in the Gerbil Cochlea

Gagan Kumar, Sarah Vakkalanka, Alan Micco, Claus-Peter Richter

Otolaryngology, Northwestern University, 303 E. Chicago Avenue, Chicago, Illinois, United States

Cochlear implants have become an accepted medical treatment for people with severe-to-profound hearing loss. A cochlear implant applies electrical current directly into the cochlea. The positions of the electrode contacts within the cochlea and the impedances of cochlear structures determine the path of the injected current and the consequent population of stimulated spiral ganglion cells. The present experiments determine directly impedance values for many cochlear structures.

The hemicochlea technique and the four-electrode reflection-coefficient method are used to arrive at impedance values for different structures. The hemicochlea is a cochlea cut in half along its mid modiolar plane. For measurements, the hemicochlea is immersed in artificial perilymph that selected cochlear structures are visible and accessible by the measuring probe. Impedance measurement

of a solid region falls into two distinct categories: (1) the measurement of induced potential differences as a function of the electrode array's distance from a solid region and (2) analysis of experimental data to estimate the reflection coefficient non-invasively. Measurements were performed with a custom-fabricated probe that consisted of four thin Teflon-insulated wires. Two of the electrodes were used to inject an alternating current of constant amplitude, and two of the electrodes were used to determine the voltage adjacent to the current injecting electrodes. The results of the in vitro experiments are validated by in vivo experiments using gerbils.

Resistivity, of the cochlear wall is different over scala tympani, scala media and scala vestibuli. Furthermore, the resistivity of the cochlear wall is larger compared to the modiolar wall by about a factor of two. Post-mortem, resistivity values first decrease and then seem to increase over time.

Supported by the American Hearing Research Foundation and the Department of Surgery, Evanston Northwestern Healthcare.

558 Cochlear Impedance Measurements in the Human Hemicochlea

Alan Micco, Gagan Kumar, Claus-Peter Richter

Otolaryngology, Northwestern University, 303 E. Chicago Avenue, Chicago, Illinois, United States

A cochlear implant applies electrical current into the cochlea. The positions of the electrode contacts within the cochlea and the impedances of cochlear structures determine the path of the injected current and the consequent population of stimulated spiral ganglion cells. Impedance measurements have been made in animal models. However, gerbil or guinea pig cochleae differ significantly in size from human cochleae. To account for such differences, impedance values were measured in human hemicochleae.

Human temporal were cut in half along their mid modiolar plane with a diamond wire saw. The resulting hemicochleae or cochlear slices were immersed in artificial perilymph for measurements. Impedance measurements were done using the four electrode reflection coefficient method. The impedance measurement of a solid region falls into two distinct categories: (1) the measurement of induced potential differences as a function of the electrode array's distance from a solid region and (2) analysis of experimental data to estimate the reflection coefficient non-invasively. Measurements were performed with a custom-fabricated probes that either consisted of four thin Teflon-insulated wires or four large silver wires. Two of the electrodes were used to inject an alternating current of constant amplitude, and two of the electrodes were used to determine the voltage adjacent to the current injecting electrodes.

Cochlear bone revealed a resistivity of approximately 800-1000 Ωcm . The apex of the human cochlea seemed to be electrically "capped". The resistance of the modiolar wall was smaller compared to the resistance of the cochlear wall. Current paths for currents injected via scala tympani electrodes seemed to follow along the scalae towards the round window or the facial nerve canal.

Supported by the American Hearing Research Foundation and the Department of Surgery, Evanston Northwestern Healthcare.

559 Effects of return electrode location on electrically evoked auditory brainstem responses

Steven Ho, Claus-Peter Richter

Otolaryngology, Northwestern University, 320 East Chicago Avenue, Chicago, Illinois, United States

Effects of return electrode location on electrically evoked auditory brainstem responses

Steven Ho and Claus-Peter Richter

Northwestern Medical School, Department of Otolaryngology-Head and Neck Surgery, Chicago, IL, USA

With cochlear implants, direct stimulation of auditory nerve fibers is achieved via current injection into the cochlea from a scala tympani electrode. The present hypothesis is that altering the return electrode's location increases current flow through the modiolus. It has been shown previously that the current can be increased 1.4 times across a pair of modiolar measuring electrodes when the return electrode is moved from an extra-cochlear location to the modiolar bone, and increased 2.4 times with the return electrode in the modiolus. Here, *in vivo* experiments were conducted in gerbils to verify these results and to provide evidence that a return electrode in the modiolus does not stimulate auditory nerve fibers non-specifically.

Threshold currents for electrical-evoked brainstem responses (EABR) were determined for different electrode placement. One of the electrodes was placed always in scala tympani. The second electrode, the return electrode, was placed at different locations, such as in the soft tissue at the jaw, at the apex of the cochlea, in the scala tympani, and in the modiolus.

The lowest thresholds were consistently achieved with an electrode in scala tympani and the return electrode in the modiolus. With this configuration, the threshold current was found to be 10-30 μ A, which is 2.0 times smaller compared to an extra-cochlear return electrode, and 2.3 times smaller compared to a bipolar stimulation configuration. When the current was injected between the modiolar electrode and the jaw electrode, no EABR could be evoked with currents up to 200 μ A. These results suggest that (1) the current amplitudes necessary to elicit an EABR are significantly smaller while the return electrode is placed in the modiolus, and (2) a return electrode in the modiolus is unlikely to stimulate the auditory nerve fibers non-specifically.

Supported by the American Hearing Research Foundation and the Department of Surgery, Evanston Northwestern Healthcare.

560 Postdeafening Treatment of the Cochlea by Upregulation of BDNF: Histological and Functional Effects

Yehoash Raphael, Deborah J. Colesa, Toshihiko Nakaizumi, Bryan E. Pflugst

Kresge Hearing Research Institute, University of Michigan, 1301 E. Ann St., Ann Arbor, MI, United States

Partial protection of the spiral ganglion from degeneration following deafness has been achieved in a variety of laboratories using electrical stimulation, treatment with antioxidants, and/or treatment with neurotrophins. The magnitude of the protective effects

of these treatments varies from study to study. In a previous study, we found that upregulation of BDNF or BDNF plus CNTF following systemic deafening in young guinea pigs resulted in substantial survival of spiral ganglion cells relative to cases that received no postdeafening treatment. In the studies reported here, we initiate a series of experiments to evaluate the functional effects of these postdeafening treatments at the psychophysical and electrophysiological levels. In a pilot experiment, four adult guinea pigs were divided into two groups: treated and nontreated. They were unilaterally deafened with Neomycin. Four days after deafening, genes controlling the production of BDNF and CNTF were administered by means of an adenovirus vector to the cochlea of the animals in the treatment group. Controls received a scala tympani injection of artificial perilymph. Both groups were then implanted with a two-electrode scala tympani implant and an extracochlear reference electrode. EABR thresholds were followed bi-weekly. Thresholds for bipolar stimulation were considerably lower for the treated group than for the control group. However, thresholds for monopolar stimulation, were not significantly different between the treated and control animals. Histological correlates of these results include higher spiral ganglion cell counts and a healthier appearance of spiral ganglion cells in the treated ears relative to the controls. In experiments currently in progress, we are assessing the effects of this postdeafening treatment on psychophysical detection and EABR thresholds.

Supported by the NIDCD and the RNID.

561 Quantification of Dye Distribution Inside a Cochlea Model Using Different Prototypes of Modified Cochlea Implant Electrodes

Gerrit Paasche¹, Thomas Kaiser², Thomas Lenarz¹, Timo Stoever¹

¹Dept. of Otolaryngology, Medical University of Hannover, Carl-Neuberg-Str. 1, Hannover, Germany, ²Research, Cochlear Technology Center, Cochlear Technology Center, Mechelen, Belgium

Several recent reports on animal studies show the protective effects of neurotrophic factors (NF) on spiral ganglion cells (SGC). This is of particular importance since the number of SGCs is considered to be among the factors defining the effectiveness of cochlear implants. A device for local inner ear treatment is therefore of great interest. As described previously, we modified a Contour™ electrode, as this device already contains an inbuilt lumen (for carrying the stylet prior to insertion), and tested it for the purpose of drug delivery to a plastic cochlea model.

With these prototypes we performed an *in vitro* evaluation of this system for substance distribution in a model cochlea. This model cochlea consisted of a plastic canal, representing two turns of the human cochlea. It was used to visualize the distribution of a dye (methylene blue) inside the modelled scala tympani. Three different electrode prototypes with openings at varying locations at the electrodes were used: a) release of the dye at the tip, b) release of the dye at the tip and the side of the electrode, c) release of the dye only at the side of the electrode (6 mm from the tip). A mechanical pump was used to drive the system at pump rates of 100 μ l/h and 10 μ l/h. Results showed that the dye was distributed more rapidly using the electrode with the opening at the tip than with the electrode present-

ing the outlet at the side of the array. Testing the device carrying the two delivery outlets (at tip and side) resulted in a faster dye distribution along the “active” part of the electrode array but showed a similar time course of dye concentration near the cochleostomy as the prototype with only one opening at the tip. The dye concentration changes along the whole cochlea model have been assessed using analySISÒ software (Soft Imaging System), allowing to quantify the dye distribution in a spatial and time dependent manner.

562 Ultrastructural study of auditory nerve following deafness

Annelies Schrott-Fischer¹, Mario Bitsche², Scholtz Arne², Glueckert Rudolf¹, Josef Miller³, Richard A Altschuler⁴

¹University, ENT, Anichstrasse 35, Innsbruck, Austria, ²ENT, University, Anichstrasse 35, Innsbruck, Austria, ³Research Institut, University, east Ann Street 1301, Ann Arbor, USA, United States, ⁴Research Lab., University, east Ann Street 1301, Ann Arbor, USA, United States

POSTER PRESENTATION *presenting author

Ultrastructural study of auditory nerve following deafness

Schrott-Fischer Anneliese^{1*}, Miller Joseph², Glueckert Rudolf¹, Bitsche Mario¹, Gmeiner Guenter¹, Scholtz Arne¹, Altschuler Rick²

¹Department of Otolaryngology Innsbruck University Hospital, Austria

²Kresge Hearing Research Institute, University of Michigan, Ann Arbor, USA

Introduction:

Cochlear implant benefits have been shown to depend on the survival, excitability and proximity of the auditory nerve to stimulating electrode. Presumably a greater population of proximal nerves yields a lower threshold of excitation, larger dynamic range of responsiveness, and greater selectivity of excitation across the population; and with these greater perceptual benefits. Following deaf-ferentation, there is a rapid degeneration of the peripheral process, followed by subsequent spiral ganglion cell and axonal degeneration. Pujol and Puel (1999) have shown that in the presence of a viable target, degenerated peripheral processes may regrow, and Altschuler and others (1999) have shown that provision of neurotrophic factors (NTF) and electrical stimulation (ES) in the deaf-ferented nerve may induce a regrowth. In this study we examined at the light and EM level the characteristics of peripheral processes of the auditory nerve following deafness, including time points allowing us to examine peripheral processes maintained by NTF or ES interventions, and regrown fibers follow sufficient delays (>3wks) to insure process degeneration prior to intervention.

Methods and Discussion:

Studies were performed in guinea pigs deafened by ethacrinic acid and kanamycin. NTF were applied locally via microcannula-osmotic pump to the scala tympani.

Findings on regrowth of afferent fibers using transmission electron and light microscopy are discussed with regard to cochlear implants.

Supported by NIH DC03820, General Motors & UAW, EU BioEAR

563 Can electrode insertion trauma cause a progressive loss of hearing in a rat model of cochlear implantation?

Marek Polak¹, Adrien Eshraghi^{1,2}, Jiao He¹, Thomas Balkany¹, Thomas Van De Water¹

¹Otolaryngology, University of Miami, 1666 NW 10th Ave, Miami, Florida, United States, ²Otolaryngology, Veteran's Administration Hospital, 1666 NW 10th Ave, Miami, Florida, United States

Objective measurements of hearing and auditory nerve function are necessary for evaluating the extent of damage in cochlear implant trauma studies. In the present study, hearing acuity for traumatized and contra-lateral control inner ears was assessed in a rat model of cochlear implant insertion trauma.

Five Fisher 344 strain rats were evaluated for hearing acuity before and after electrode insertion trauma. Electrode insertion trauma consisted of the insertion and withdrawal of a ball electrode through an excision site in the round window membrane into the scala tympani for a depth of 3 mm. Hearing acuity was measured before trauma and over the following seven days (i.e. 1,3,5, and 7 days post-trauma) for both experimental and control cochleae. Objective measurements of hearing function were: distortion products of otoacoustic emissions (DPOAEs) in the frequency range of 2-32 kHz and tone burst (i.e. 4 – 32 kHz) auditory evoked brain stem responses (ABRs) recorded using Intelligent Hearing Systems hardware and software.

For the experimental ear, there was a progressive increase in ABR thresholds and decrease in ABR amplitudes following electrode insertion trauma for all of the frequencies tested. The amplitude of the DPOAEs in the experimental cochlea also showed a progressive decrease following electrode insertion trauma. For the control ear, there were no significant changes in either the DPOAE amplitude or ABR thresholds following electrode insertion into the contra-lateral experimental cochlea.

These results documenting a progressive loss of hearing acuity strongly suggest that electrode insertion trauma generates oxidative stress within injured cochlear tissues which starts a chain of intercellular events that culminates in the progressive loss of hair cells by apoptosis similar to the chain of events that occurs in brain tissue following a stroke. Supported by a grant from Med El to TJB and TRV.

564 Effects of Single and Multichannel Stimulation on Spread of Activation in the Guinea Pig Inferior Colliculus Using a UCSF-type Scala Tympani Electrode

Ben H Bonham, Russell L Snyder, Steve J Rebscher

Epstein Laboratories, Dept of Otolaryngology - HNS, University of California, 533 Parnassus Ave U490E, San Francisco, CA, United States

Using cochlear implants designed specifically for the guinea pig, neural activity evoked by single- and multi-channel intracochlear electrical stimulation was examined using various stimulus waveform and electrode configurations. These included biphasic, monophasic, and pseudomonophasic pulses in monopolar, bipolar, and tripolar configurations. Neural activity across the tonotopic axis of the central nucleus of the inferior colliculus (ICC) was

recorded in response to each stimulus configuration. The neural activity was recorded using a 16-channel silicon probe* that had been fixed in place and acoustically calibrated prior to contralateral deafening and insertion of the cochlear implant. This allowed the spread of activation evoked by acoustic and electric stimuli to be compared directly. Channel interactions were identified by changes in threshold and spread of activation during simultaneous and non-simultaneous two-channel stimulation.

Activity patterns varied widely with stimulus waveform and electrode configuration. Closely spaced bipolar pairs and tripoles evoked activity patterns whose spread was comparable to that of acoustic tones. Widely spaced bipoles activated broader ICC regions, comparable to regions activated by acoustic noise bands. Monopoles activated regions so broad that their limits could not be determined. Pseudomonophasic pulses evoked more restricted patterns than biphasic pulses.

Simultaneous two-channel stimulation evoked broader activity than the union of activity evoked by the same two channels when they were stimulated individually. Non-simultaneous stimulation of two channels, offset by 1 to 10 ms, evoked activity spread comparable to the union of each channel stimulated separately.

*Recording probes were provided by the Univ of Michigan CNCT.

Supported by NIDCD RO1-DC03549, NO1-DC21006, and NO1-DC72108.

565 Effects of Long-Term Deafness and Chronic Electrical Stimulation on Temporal Processing in Cat Inferior Colliculus (IC) and Primary Auditory Cortex (AI)

Maïke Vollmer¹, Ralph E. Beitel¹, Russel L. Snyder¹, Patricia A. Leake¹, Marcia W. Raggio², Christoph E. Schreiner¹

¹Otolaryngology, University of California, 533 Parnassus Ave, San Francisco, CA, United States, ²Speech & Communication Studies, San Francisco State University, 1600 Holloway Ave, San Francisco, CA, United States

Congenitally deaf cochlear implant users implanted as adults generally have poor speech discrimination but tend to gradually improve with increasing auditory experience. To model their conditions we studied two groups of cats that were deafened neonatally and examined after prolonged periods of deafness (>2.5 years): 1) 'unstimulated' cats were implanted and studied acutely, 2) the other group received a chronic implant and several weeks of stimulation. Both groups demonstrated severe reductions in spiral ganglion cell density (1-18% of normal). Acutely deafened adult cats served as controls. To assess temporal processing in these groups we compared, e.g., best modulation frequencies (BMF), maximum following frequencies (Fmax) and first spike latencies of single neurons and multiunit clusters in the IC and AI.

In the IC, neurons in long-deafened unstimulated animals showed significantly lower mean Fmax and longer median latencies than controls. In contrast, chronic electrical stimulation in long-deafened animals resulted in a marked increase in temporal resolution (higher Fmax, shorter latencies) when compared to control animals.

In the AI, neurons in long-deafened unstimulated animals also had

the lowest mean Fmax, whereas chronic stimulation led to a significant increase in Fmax. However, Fmax of AI neurons in long-deafened stimulated animals still remained lower than those recorded in control animals. Further, there was no difference between the median latencies in the unstimulated and stimulated groups of long-deafened animals, and latencies in these cats were significantly longer than those of control animals.

These results demonstrate that, despite severe peripheral pathology, chronic electrical stimulation can partially reverse the deleterious effects of long-term neonatal deafness on temporal processing in the central auditory system, but the changes elicited are more pronounced in the IC than in the AI.

Support provided by NIH-NIDCD Contract #N01-DC-0-2108

566 Effects of Deafening and Implantation Procedures on Electrical Detection Thresholds

Bryan E. Pflugst, **Deborah J. Colesa**, **Gina Su**, Nadia Tayeh

Kresge Hearing Research Institute, University of Michigan, 1301 E. Ann St., Ann Arbor, MI, United States

In previous studies, we have noted large decreases in psychophysical detection thresholds for electrical stimulation of cochlear implants following deafening, implantation, and the onset of electrical testing. In guinea pigs, these changes occurred within the first 45 days, after which thresholds were stable over time. This result has important implications for designing experiments with cochlear implants and also provides a context for determining variables that affect detection thresholds. In this study, we examined the effects of deafening and implantation procedures on the time course of postprocedural changes in thresholds and on final-stable threshold levels. Guinea pigs (N=32) were divided into 4 groups. Group I was deafened and implanted on day 0 and electrical testing began on day 1. Group II was deafened and implanted on day 0 and electrical testing began on day 45. Group III was deafened on day 0, implanted on day 45 and electrical testing began on day 46. Group IV (not chemically deafened) was implanted on day 0 and electrical testing began on day 1. Results showed decreases in thresholds as a function of time for some subjects from all groups, but the magnitude of change was largest for Group I and smallest for Group II. Final-stable thresholds on average were highest for Group IV. These results suggest that both deafening and implantation result in temporary trauma to the auditory nerve which recovers over time and that electrical stimulation and/or learning also contribute to the observed threshold decreases. This study suggests that a useful preparation for experimental studies of cochlear implants in guinea pigs would be one that is deafened, implanted, and electrically stimulated over a 45-day period prior to the onset of data collection. This pre-experimental treatment would result in a stable experimental preparation that is more similar than acute preparations to long-term deafened and implanted patients.

Supported by NIH Grant # R01 DC03389.

567 Relationship between Across-Site Variation in T and C Levels and Speech Recognition in Cochlear Implant Users

Li Xu^{1,2}, Bryan E. Pfungst³

¹*School of Hearing, Speech & Language Sciences, Ohio University, Grover Center - W224, Athens, OH, United States,*
²*Kresge Hearing Research Institute, University of Michigan, 1301 E. Ann St., Ann Arbor, MI, United States,*
³*Kresge Hearing Research Institute, University of Michigan, 1301 E. Ann St., Ann Arbor, MI, United States*

In a previous study, we characterized the across-site variation of detection threshold levels (T levels) and the maximum comfortable loudness levels (C levels) for both monopolar and bipolar stimulation (Pfungst and Xu, 2003). The results were consistent with the idea that the across-site variation reflects variation in the functional distances between the stimulating electrodes and the sites of action-potential initiation. We believe that variation in these electrode to neuron distances are due in part to variation in the nerve survival pattern in the region of the implant, which leads to the hypothesis that large across-site variation would be associated with poor implant performance. The present study examined the functional significance of the across-site variation in relation to speech-recognition performance. Twenty-one subjects who received Nucleus CI24M (straight array) or CI24R(CS) (Contour) cochlear implants participated in the study. T and C levels were measured using the method of adjustment. Consonant, vowel, and sentence recognition were tested using the subjects' everyday speech-processing strategies. Across-site variation was quantified using the variance of the T and C levels across the entire electrode array. The results showed a moderate but significant negative correlation between speech-recognition performance and across-site variance of the T levels measured with both monopolar and bipolar electrode configurations. The correlation coefficients ranged from -0.47 to -0.70 ($p < 0.05$). These results support the hypothesis that the large across-site variation in detection thresholds reflects conditions that are detrimental to speech-recognition with cochlear implants.

This work was supported by NIDCD Grant DC03808.

568 Prediction of Maximum Comfortable Levels (MCL) using Neural Response Telemetry (NRT) in the Nucleus 24 Cochlear Implant

John King, Marek Polak, Annelie Hodges, Stacy Butts, Kathy Bricker, Rosie Simon, Natalie Washuta, Thomas Balkany

¹*Otolaryngology, University of Miami Ear Institute, 1666 NW 10th Ave, Suite 304, Miami, FL, United States*

It is generally assumed that cochlear implant programming necessitates accurate setting of programming levels, including maximum comfortable levels (MCL), of all active electrodes. In most cases, these levels can be adequately set utilizing routine clinical techniques. It has been suggested that Neural Response Telemetry (NRT) can be used to estimate behavioral levels when clinical methods are inadequate, such as in the very young child. To date, several approaches have been suggested for prediction of MCL from NRT; however, many such methods require co-application of clinical measurements along with NRT measurements to set

MCLs. Alternatively, it has been recommended that MCL be predicted by adding a fixed number of programming units to any obtained NRT thresholds.

A study was undertaken with 21 adult recipients of the Nucleus 24 device to develop reliable predictors of MCL from NRT. Multiple regression analysis was performed for each electrode to determine predictive abilities of various factors including NRT threshold (NRTT), slope of the NRT growth function (NRTSLOPE), age, length of deafness, length of cochlear implant use and electrode impedance. Results indicated that NRTT and NRTSLOPE were the only consistently significant predictive factors. Depending on the electrode, R^2 ranged from 0.116 to 0.741, with only 2 out of 22 electrodes showing non-significance at the $p = 0.001$ level when only these two factors were utilized.

During the study, it was observed that the NRT response can be influenced by the number of measurements obtained during the measurement session. Statistical analysis of the influence of this phenomenon on prediction of MCL from NRT measurements will be presented.

Overall, results indicated that NRT can be used reliably to predict MCL using the NRTT and NRTSLOPE as factors. This prediction method appears to be the most accurate means of predicting MCL from NRT when no other measures are available.

569 Bilateral Cochlear Implantation in Adults: An Overview

Patrick S.C. D'Haese¹, Amy L Barco², Heike Kühn-Inacker¹, Peter Nopp¹, Peter Schleich¹

¹*Clinical Research, MED-EL GmbH, Furstenweg 77A, A-6020 Innsbruck, Austria,*
²*Clinical Research, MED-EL North America, 2222 E HWY 54 / STE B-180, Durham, NC, United States*

Several multi-center studies are currently running within Europe and the United States looking into the potential benefits of bilateral cochlear implantation. Fields of interest are speech perception in quiet and noise, localization and subjective benefit. More than 100 patients have been evaluated within several studies. All patients were post-linguistically deafened adults implanted with the MED-EL COMBI 40+ in a single or two stage procedure. The objective of this presentation is to review the results of localization, speech understanding in noise and quiet and the subjective benefit of having two cochlear implants.

Speech perception testing in quiet and noise is completed using recorded sentence and monosyllable material. Sub-studies were performed using a fixed signal-to-noise ratio (SNR) or using an adaptive SNR.

Localization testing is conducted in the horizontal-plane using a source identification task. The set-up includes an array of 9 loudspeakers. Testing is conducted in an anechoic chamber. On each trial, a sound is presented from one of the 9 source positions, and the participant's task is to identify which loudspeaker emitted the sound. Data analyses include assessments of random error and response bias as well as a measure of overall error.

Subjective testing was done by using a custom-made questionnaire and by administering the APHAB. Data analysis is currently being performed.

570 Bilateral Cochlear Implants in Children

Patti M. Johnstone¹, Ruth Y. Litovsky¹, Aaron Parkinson², B. Robert Peters³, Jennifer Lake³, GongQiang Yu¹

¹Waisman Center, UW-Madison, 1500 Highland Ave, Madison, WI, United States, ²Clinical Studies, Cochlear Americas, 400 Inverness Parkway, Suite 400, Englewood, CO, United States, ³Cochlear Implant Program, Dallas Otolaryngology Associates, 7777 Forest Lane, Dallas, TX, United States

Binaural hearing is thought to play a crucial role in our ability to localize sounds and understand speech in noise. Children with cochlear implants (CIs) have problems in these two areas. A possible reason for their difficulties may be routine unilateral implantation that prevents benefit from binaural information. Recently, a few children with one CI, received a second CI some 3-8 years later. We have had the opportunity to measure their performance on 3 tasks designed to test binaural abilities: 1) Speech intelligibility measured in quiet and with interferers that are either coincident in space with the target (0° front) or separated (90° right/left); 2) Sound source location identification measured with 15 loudspeakers spaced 10° apart in the azimuthal plane. Subjects identified the speaker from which they thought the sound originated; 3) Using an adaptive procedure to vary angular separation between sources at right/left, minimum audible angle (MAA) was measured. Subjects indicated whether the sound was perceived to be to the left or right of midline. Testing at 2-3 months after activation of the second CI was done with either the first CI alone or with both CIs together. This paper will present those results in addition to results from follow-up tests done 9-12 months after activation of the second CI, to determine the effects of experience on binaural abilities. Results will also be compared to measures from 3 other groups of children: children with bilateral cochlear implants who were only tested 9-12 months after the activation of the second CI; children with unilateral CIs; and children with normal hearing.

571 Tetraode Recordings in the Rat Auditory Cortex during a Two Alternative Forced Choice Auditory Behavior

Gonzalo Otazu, Anthony Zador

Zadorlab, Cold Spring Harbor Laboratory, 1 Bungtown Rd, Cold Spring Harbor, NY, United States

Neural activity in the auditory cortex is complex, modulated both by the auditory stimulus and by behavioral context. In order to explore this interaction, we trained rats to perform a two alternative forced choice auditory discrimination task, (see Tai et al., this meeting). Subjects poked left or right depending on the frequency (1 or 10 KHz, respectively) of a pure tone imbedded in background noise. Task difficulty was controlled by the varying the signal to noise ratio.

We used chronic tetrodes to record single unit, multi-unit and local field potential responses from the auditory cortex of freely moving rats performing this task. Neuronal activity was modulated both by the stimulus and by the subject's behavior. While some neurons showed robust, short-latency stimulus-locked responses to the stimuli, others did not. In some cases, neurons with stimulus-locked responses were recorded simultaneously on the same tetrode as other nearby units that failed to show clear stimulus modulation, suggesting that tone-responsiveness during this task is

not a simple function of cortical (tonotopic) location. In some neurons, firing probability was correlated with the subject's left/right decision. These experiments may help elucidate the role of the auditory cortex in decision making during a demanding auditory task.

572 Chronic multi-electrode recordings in midbrain and cortex of the freely-moving ferret

Peter Marvit, Bing-Zhong Chen, Heather D Dobbins, Yadong Ji, Didier A Depireux

Anatomy and Neurobiology, University of Maryland, Baltimore, 685 W. Baltimore Str - HSF 222, Baltimore, MD, United States

Ferrets (*Mustela putorius furo*) were chronically implanted with multi-electrode microdrives (Precision Machining). These 12-electrode microdrives, previously used in hippocampal recordings in mice and rats, allow the depth of each electrode to be independently adjusted. We have successfully recorded from single cells in auditory cortex and inferior colliculus in both restrained and freely-moving awake ferrets. Recordings show good cell isolation with little or no movement artifacts. Results of these recordings will be presented. In addition, preliminary results from a behavioral set-up, compatible with the above electrode system, will be shown.

573 Investigating The Functional Organization Of Ferret Auditory Cortex Using Multi-Electrode Recording

Jennifer K Bizley, Fernando R Nodal, Andrew J King

Laboratory of Physiology, University of Oxford, Parks Rd, Oxford, United Kingdom

Ferrets are becoming increasingly popular for studies of central auditory processing. However, the anatomical and functional organization of auditory cortex, and particularly the non-primary fields, is still poorly described in this species. Auditory cortex in the ferret extends across the ectosylvian gyrus (EG). Previous anatomical and physiological studies have identified the middle ectosylvian gyrus (MEG) as the primary region, containing primary auditory cortex (A1) and the anterior auditory field (AAF). More ventral regions, on both the posterior (PEG) and anterior (AEG) banks of the EG, are thought to contain as yet uncharacterized secondary fields.

We performed a series of electrophysiological mapping studies in order to determine the tonotopic organization of the EG. A 16-channel silicon array (U Michigan) was used to record the responses of single units and small clusters to contralaterally-presented broadband noise and pure tones. Frequency response areas were constructed and analysis included assessments of the width of tuning, response latencies and temporal response characteristics.

Using these stimuli there was little to differentiate A1 and AAF. These fields share a common tonotopic gradient, and are comparable in terms of bandwidth of tuning and response latency. We observed reversals in the best-frequency gradient of neurons moving ventrally from the MEG into both the PEG and AEG. Additionally, we found areas on the PEG that, although tone-

responsive, show no clear frequency tuning or tonotopic organization. An area on the ventral AEG responded only to noise and contained some neurons that were also visually responsive. Temporal response properties of neurons also differed outside the MEG; neurons on PEG had longer first spike and peak latencies and often displayed multi-peaked post-stimulus time histograms.

574 Spatiotemporal characteristics of responses elicited by clicks from the transverse gyrus of Heschl in humans

Igor O. Volkov¹, John F. Brugge^{1,2}, Mitchell Steinschneider³, Matthew A. Howard¹

¹Neurosurgery, University of Iowa, 200 Hawkins Drive, Iowa City, Iowa, United States, ²Waisman Center, University of Wisconsin, 1500 Highland Avenue, Madison, WI, United States, ³Neurology and Neuroscience, Albert Einstein College of Medicine, 1300 Morris Avenue, Bronx, NY, United States

The locations, boundaries and functional organization of primary auditory cortex in the human are poorly understood. Evoked potentials (EPs) and unit clusters were recorded from Heschl's gyrus (HG) using multicontact depth electrodes chronically implanted along the long axis of HG in 10 epilepsy surgery patients (U. Iowa IRB approved). Electrode trajectories and recording sites were reconstructed by 3D MRI. Usually, EPs and cluster responses elicited by clicks were distributed along the mesial 2/3 of the length of HG. Maximal response waveforms were typically triphasic, with average peak latency of 9.85, 32.4 and 110.4 ms, respectively. EP amplitude decreased systematically with distance from the focus of maximal response. The anterolateral 1/3 of HG was relatively unresponsive to click stimuli. Extracellular recordings were made from 492 units extracted from neuronal clusters. Like the EP, units exhibiting the strongest response and the shortest latency to clicks were located in posteromedial HG. Most units responded to a single click with a phasic discharge followed by suppression of spike activity lasting tens to hundreds of ms followed in turn by a rebound discharge. Discharges of 20-30% of units were time locked to the individual clicks in a train at click rates as high as 100 Hz. Unit responsiveness also decreased and latency increased systematically with distance from the focus of maximal responsiveness. Most (about 70%) units recorded at more anterolateral locations exhibited suppression of spike activity that often lasted hundreds of milliseconds.

We conclude that the primary auditory cortical field extends along the medial 2/3 of Heschl's gyrus, and is bounded by a more anterolateral field with markedly different response properties to sound stimuli. (Supported by NIH Grants DC04290, DC00116, HD03352 and by the Hoover Fund)

575 Non-homogenous Modular Organization of Cat Primary Auditory Cortex

Kazuo Imaizumi, Christoph E. Schreiner

W.M. Keck Center for Integrative Neuroscience, Univ. California at San Francisco, 513 Parnassus Ave., San Francisco, CA, United States

Cat primary auditory cortex (AI) is organized tonotopically in the posterior to anterior direction. In addition, it has been shown that cat AI has a modular organization of bandwidth orthogonal to the tonotopic bands. However, these modules have been studied only

in the mid-frequency range. To consider whether auditory information is processed uniformly in AI, it is necessary to understand its functional organization across a wide frequency range. We studied the modular organization of receptive field parameters for threshold, Q10, Q40, and latency by single- and multi-unit recordings. Bandwidth modular organization was most robustly expressed in the mid-frequency range. For low and high frequencies, this modular organization was less prominent. By contrast, for low frequencies, threshold and latency values were robustly clustered as modules along iso-frequency bands. However, this organization is discontinuous across iso-frequency bands. Characteristic frequency is over-represented in the mid-frequency range from 5 to 30 kHz for which robust bandwidth modules are found. The size of these bandwidth modules in cat AI is unusually large compared to the anterior auditory field in the cat and to AI in new world monkeys. Therefore, bandwidth modules for mid-frequencies in cat AI may represent a specialization not found in other mammals. A possible explanation for these observations is that AI receives different input information in different iso-frequency bands, which may be used for different tasks.

Supported by NIH DC02260 (C.E.S.), Hearing Research Inc., Coleman Fund

576 Functional hemispheric specialization in gerbil auditory cortex

Frank W. Ohi, Wolfram Wetzel, Henning Scheich

ALS, Leibniz Institute for Neurobiology, Brenneckestr. 6, Magdeburg, Germany

Our previous research on gerbil auditory cortex (AC) has indicated a dependence of the processing of temporally continuous spectral cues on the right AC (Wetzel, et al., *Neurosci. Lett.*, 1998) and of the processing of discontinuous cues of timing and temporal order on left AC (Wetzel, et al., *Proc. Int. Conf. Audit. Ctx.*, Magdeburg, 2003) in basic agreement with conditions in human AC (Zatorre, Belin, *Cereb. Ctx.*, 2001). Here we test the hypothesis, that left and right AC lesions in the gerbil lead to predictable orthogonal confusion patterns among a set of stimuli containing both kinds of cues.

Using a go/(no-go) avoidance paradigm gerbils were trained to discriminate two compound stimuli, each one consisting of two frequency-modulated (FM) tones separated by a short silent interval. Stimulus **S1** can be described by the expression (**LR,HR**), meaning that the first FM tone (**LR**) traversed a low (**L**) frequency region in a rising (**R**) fashion, and the second FM tone traversed a high frequency region in a rising fashion. Stimulus **S2** can analogously be described by (**HF,LF**), with **F** indicating falling pitch in the FM tones. Phenomenologically, **S1** and **S2** can be discriminated on the basis of a sequence cue (temporal order of the **L** and **H** components, ignoring **R** and **F** properties) or a modulation cue (**R** or **F**, ignoring temporal order). In a first experiment, stimulus parameters were so adjusted that the additional stimuli **S3** (**LF,HF**) and **S4** (**HR,LR**) both produced 50% of the go response rate indicating balanced saliency of both possible cues. With these stimulus parameters we first trained gerbils to discriminate **S1** and **S2** and subsequently lesioned the left or right auditory cortex. Subsequent exposure to **S3** and **S4** produced the following predicted orthogonal confusion patterns in the 2 groups: lesion left: **S1=S4**, **S2=S3**; lesion right: **S1=S3**; **S2=S4**, in agreement with our hypothesis on the functional hemispheric specialization in gerbil AC.

577 Anatomical Definition of Auditory Cortex in the Gerbil

Ken Hutson¹, Christina Benson², Nell Cant³

¹Neurobiology, Duke University Medical Center, 213 Bryan Research Bldg, Durham, NC, United States, ²Neurobiology, Duke University Medical Center, 211 Bryan Research Bldg, Durham, NC, United States, ³Neurobiology, Duke University Medical Center, 215 Bryan Research Bldg, Durham, NC, United States

In our investigation of the organization of the central auditory system in gerbil, we have found cytochrome oxidase (CO) staining to be a reliable method for recognizing discrete regions of auditory midbrain and thalamus. Here we present evidence that CO staining patterns also provide a useful tool for recognizing different regions of auditory cortex. Sections through gerbil cortex processed for CO activity exhibit a densely-stained band in the lateral temporal cortex. In transverse sections, this dense region first appears rostrally at the level of the optic chiasm, and extends caudally to the level of the caudal medial geniculate body (MG). The dense band is surrounded by paler-staining regions that abut other CO-rich areas of cortex (e.g., somatosensory and visual cortex). Injections of biotinylated dextran amine (BDA) into densely vs. lightly stained parts of temporal cortex result in differential corticothalamic projections. Injections into CO-pale regions immediately dorsal or caudal to the dense band label projections primarily to the dorsal division of the MG. BDA injections into the CO-dense band label projections predominately to the ventral division of the MG (MGv). The medial to lateral location of the terminal field in MGv varies in relation to the position of the cortical injection site. Proceeding from rostral to caudal in the CO-dense band, projections to MGv begin laterally, progress to medial portions of MGv, then return to lateral portions of MGv. The sequence of the projection patterns to MGv suggest that our injections into the CO-dense band reflect a progression from low to high to low frequency cortical representation, mirroring the frequency organization of AAF and AI found in electrophysiological maps of gerbil auditory cortex (e.g., Thomas et al., *Eur. J. Neurosci.*, 1993). The presence of the CO-dense band in lateral temporal cortex provides a simple way to identify the "core" region of auditory cortex in the gerbil.

578 Effects of Bilateral Auditory Cortex Lesions on Frequency Processing and Virtual Pitch Perception

Mark Jude Tramo^{1,2}, Christine K. Koh^{1,2}, Gaurav D Shah¹, Louis D. Braida²

¹Dept. of Neurology, Harvard Med. Sch. & Mass. General Hospital, VBK-813, Boston, MA, United States, ²Research Laboratory of Electronics, M.I.T., Bldg 36, Cambridge, MA, United States

Deficits in the ability to perceive the relative pitch of pure tones, complex tones with energy at the fundamental frequency (F0), and complex tones without energy at F0 have been reported in different patient populations following bilateral and right-sided vascular and surgical lesions involving primary auditory cortex and adjacent association areas. In order to analyze the relationships among pitch processing deficits following bilateral lesions, frequency difference thresholds were measured in a 37 year old patient (Case A1+) and 9 normal controls using an adaptive procedure, a two-

interval two-alternative forced-choice task, and 5 stimulus conditions: 1) pure tones (250 Hz); 2) harmonic complex tones with energy at F0 (250 Hz) and 6 consecutive low harmonics between 4-11; 3) low-spectrum harmonic tones without energy at F0; 4) harmonic tones with energy at F0 and 6 consecutive high harmonics between 13-20; and 5) high-spectrum harmonic tones without energy at F0. Stimuli were 500 ms in duration, separated by 200 ms, and 40 dB SL at each ear. The results for normal controls followed the expected pattern, with lower thresholds in the low-spectrum and with-F0 harmonic tone conditions than in the corresponding high-spectrum and missing-F0 conditions. Difference thresholds for Case A1+ were more than 3 SE's above the mean of normal controls in all 5 stimulus conditions. In the low-spectrum missing-F0 condition, threshold elevations for Case A1+ were equal to those found in the pure tone condition; in contrast, normal thresholds were 2.5 times higher in the low-spectrum missing-F0 condition than in the pure tone condition. In addition, Case A1+, unlike normals, did not benefit from the addition of F0 to high-spectrum harmonics. This pattern of results suggests that deficits in virtual pitch perception following bilateral auditory cortex lesions may be attributable to the same pathophysiological mechanisms that impair pure tone pitch perception.

Supported by DC03382, DC006353, and DC00117

579 Maturation Of Auditory Cortex Revealed By Auditory Evoked Potentials.

Julia L Wunderlich¹, Barbara K Cone-Wesson²

¹Otolaryngology, University of Melbourne, 390 Albert Street, East Melbourne, Australia, ²Speech and Hearing Sciences, University of Arizona, P.O. Box 210071, Tucson, Arizona, United States

The aim of the present study was to use cortical auditory evoked potentials (CAEP) as an index of auditory system development. The participants in this experiment were 10 newborns (< 7 days), 19 toddlers (13-41 months), 20 children (4-6 years) and 9 adults (18-45 years). CAEPs were obtained in response to low (400 Hz) and high (3000 Hz) tones and to the speech token /bæd/, all presented at 60 dB HL, at a rate of 0.22 Hz. Latency and amplitude measures were made for CAEP components P1, N1, P2 and N2 as a function of participant age, stimulus type and electrode montage.

CAEP component latencies were relatively stable from birth to 6 years, with adults demonstrating significantly shorter latencies compared to infants and children. Components P1 and N2 decreased in amplitude, while components N1 and P2 increased in amplitude from birth to adulthood. Words evoked significantly larger CAEPs in newborns compared to responses evoked by tones, but in other age groups the effects of stimulus type on component amplitudes and latencies were less consistent. There was evidence of immature tonotopic organization of the generators of N1 when responses from infants and young children were compared to those of adults. The scalp distribution of components N1 and P2 was clearly different in newborns and toddlers compared to children and adults. In the younger groups, both N1 and P2 were uniformly distributed across the scalp but in children and adults these components showed more focal distributions, with evidence of response laterality increasing with maturity.

The results of the present study describe, for the first time, CAEPs recorded from multiple scalp electrodes, for tones and speech

stimuli, in infants and children from birth to 6 years of age. Words evoked large amplitude CAEP in newborns. Frequency-related differences in component amplitude were apparent at all ages reflecting development of tonotopic organization of the CAEP neural generators.

580 The insula and its role in auditory processing.

Doris-Eva Bamiou^{1,2}, Frank E. Musiek³, John Stevens⁴, Maria Espasandin⁵, Martin Brown⁵, Linda M Luxon^{1,2}

¹*Neuro-otology, National Hospital for Neurology and Neurosurgery, Queen Square, London, United Kingdom,*

²*Academic Unit of Audiological Medicine, Institute of Child Health, Great Ormond Street, London, United Kingdom,*

³*Communication Sciences, University of Connecticut, Unit 1085, Storrs, CT, United States,* ⁴*Neuroradiology, National Hospital for Neurology and Neurosurgery, Queen Square, London, United Kingdom,* ⁵*Stroke Unit, National Hospital for Neurology and Neurosurgery, Queen Square, London, United Kingdom*

The insula (island of Reil) is a complex structure that serves as a visceral sensory, motor, motor association, vestibular, and somatosensory area. Its role in auditory processing is poorly understood. Studies on the insula's connectivity, a few case reports but also functional imaging studies indicate that the insular cortex may play a role in auditory processing.

We assessed auditory function in patients with structural lesions of the brain that affected the insula in isolation, or in combination with other cortical and subcortical areas. Our test battery included baseline audiometric tests, the dichotic digits test, the frequency pattern test (FPT), the duration pattern test (DPT) and other tests.

We recruited 8 patients with normal audiogram or hearing loss average not exceeding 50dBHL in both ears (3 with right and 5 with left lesions). The lesion affected the insula almost in isolation in 1, the insula and non-auditory areas of the brain in 1, the lesion centered in the insula but also affected other auditory parts of the brain in 3, the lesion affected parts of the insula and other parts of the brain in 2, and the lesion abutted the insula and included other auditory parts of the brain in 1 case.

The dichotic digits test was abnormal in 5 patients (contralaterally to the site of lesion in 4, bilaterally in 1). The frequency pattern test was abnormal in 4, could not be done in 2, and was normal in 2 patients. The duration pattern test was abnormal in 7 patients (not done in 1). All the patients but 1 who had both FPT and DPT conducted, had worse DPT scores than FPT by more than 20%, regardless of the site of the lesion.

We conclude that the insula is crucial in temporal auditory processing, while further studies are needed to evaluate which parts of the insula are involved in basic auditory processing and in integration of auditory information with other associative functions.

581 Contingency-related Firing in the Auditory Cortex of Monkeys Performing an Auditory Discrimination Task

Michael Brosch, Elena Oshurkova, Armenuhi Melikyan, Elena Selezneva, Henning Scheich

ALS, Leibniz-Institut für Neurobiologie, Brenneckestr. 6, Magdeburg, Germany

The categorical distinction of rising and falling pitch direction in a sequence of tones is essential

for the perception of melodies. While this is an easy task for humans, it is highly demanding for monkeys and requires years of training with strict temporal contingencies between the auditory stimuli, behavior, and reward. The goal of the present study was to search for neuronal mechanisms in auditory cortex underlying the performance of this auditory discrimination. Using a behavioral go/nogo procedure we trained 2 long-tail monkeys to discriminate pitch contours: After illumination of a light-emitting diode monkeys could grasp a touch bar, by which they triggered a sequence of pure tones of different frequency. Upon occurrence of a falling pitch direction monkeys had to release the touch bar. Thereafter the light and the tone sequence were turned off, and a water reward and a 5-sec intertrial interval were given to the monkeys before the next trial was started. After completion of the training we surgically prepared the monkeys for daily multi-electrode recordings from the left primary auditory cortex and caudal and lateral belt areas. We found, in addition to neuronal firing in response to the tone sequences, neuronal activation of similar magnitude in relation to non-auditory events that coordinated the auditory discrimination task, i. e., to the onset of the light as well as to the grasping and to the release of the touch bar. Single units responded to auditory and to one or several non-auditory events of the behavioral paradigm. This indicates that non-auditory events are represented by auditory neurons and suggests that a neuron may serve more than one function. The representation of non-auditory events in auditory cortex may result from an expansion of already existing intermodal cortico-cortical connections during the years the monkeys have practiced the behavioral task and may facilitate the performance of audiomotor tasks in proficient subjects.

582 Critical-Band Behavior of Neural Responses in Macaque Auditory Cortex Revealed with Two-Noise Masking

Yonatan Fishman¹, Joseph Arezzo², Mitchell Steinschneider^{1,2}

¹*Neurology, Albert Einstein College of Medicine, 1410 Pelham Parkway, Bronx, NY, United States,* ²*Neuroscience, Albert Einstein College of Medicine, 1410 Pelham Parkway, Bronx, NY, United States*

An important function of the auditory nervous system is to analyze the frequency content of environmental sounds, as indicated by the maintenance of a tonotopic organization throughout the auditory pathway. This analysis depends on the frequency resolution of auditory filters, which is often determined in psychophysical studies by measuring thresholds for tone detection in the presence of noise maskers of variable frequency separation away from the target tone. Using a two-noise masking paradigm, the present study

investigates neural correlates of auditory filter resolution in primary auditory cortex (A1) of awake macaques. Neural ensemble responses (auditory evoked potentials, multiunit activity, and current source density) evoked by a pulsed 60 dB SPL pure tone "signal" fixed at the best frequency (BF) of the recorded neural population were examined as a function of the frequency spacing (ΔF) of two continuous 80 dB SPL 50-Hz wide bands of noise, symmetrically flanking the pure tone. Minimal responses were evoked by the pure tone when ΔF was less than 20% of the BF, whereas responses abruptly increased for wider ΔF s and were maximal at $\Delta F=50\%$ (the largest ΔF examined). These findings parallel results of psychoacoustic studies examining auditory frequency resolution (critical bandwidths) in both humans and monkeys, and thereby support a role for A1 in frequency analysis, auditory signal detection, and loudness perception. Moreover, these results are comparable to findings reported for single-units in anesthetized cats (Ehret and Schreiner, *J. Comp. Physiol. A*, 1997) and population responses recorded non-invasively in humans (Sams and Salmelin, *Hear. Res.*, 1994).

583 Simple Acoustic Patterns do not Predict Responses to Natural Calls in the Frontal Auditory Field of The Mustached Bat, *Pteronotus parnellii*

Andrei V. Medvedev, Jagmeet S. Kanwal

Dept. of Physiology, Georgetown University, 3900 Reservoir Rd, NW, Washington, D.C., United States

The role of the auditory field in the frontal cortex of mammals is largely unknown. We used mustached bats to study neural responses in the frontal auditory field (FAF) to basic acoustic patterns (BAP) as well as social calls presented to awake bats. Single-unit (SU) responses and evoked local field potentials (LFPs) were recorded at 50 sites in 5 bats from the same electrodes (<10 mm tip diameter) by filtering the signal at 1-4 kHz and 1-600 Hz, respectively. All units showed sharp tuning to a BFlow of ~28 kHz and a BFhigh of ~58 kHz corresponding to the first harmonic of an echolocating pulse and the second harmonic of its echo, respectively. The BAPs were generated from combinations of the two excitatory frequencies as tone-pairs, upward, downward and sinusoidal frequency modulation, and noise bands corresponding to the two BFs. Social calls consisting of 14 simple syllables (SS) and their natural variants as well as 14 natural composites (consisting of pairs of SS) were also presented at various intensities. SU responses showed a progressive increase in latency and duration corresponding to an increase in stimulus complexity from BAPs to SS and from SS to composites (peak latency: 11 ± 0.3 , 15 ± 2 and 93 ± 23 ms; duration: 11 ± 1 , 17 ± 1 and 78 ± 19 ms, respectively; $n=24$). Responses to BAPs and SSs were single peaked whereas responses to composites were multi-peaked. Peak rates were twofold higher for SS vs BAPs and composites. All SUs showed selectivity for BAPs and calls with an average preference of 3 ± 1 (number of syllables evoking a response >50% of the maximal response). LFPs also showed a similar progression of complexity in response patterns from tone-pairs to SS and composites. Our data suggest that call-specific excitatory and inhibitory circuits prepare FAF neurons to respond with temporal dynamics that match the complexity of the stimulus.

Supported by NIDCD/NIH grant number DC02054 to J.K.

584 Interlaminar differences of spike activation threshold in the auditory cortex of the rat

Marco Atzori¹, Juan Carlos Pineda^{2,3}, Jorge Flores-Hernandez⁴

¹*Physiology, BRNI, 9601 Medical Center drive, Rockville, MD, United States,* ²*Physiology, uady, av. Itzaes, Merida, Mexico,*

³*Physiology, uady, av. itzaes, Merida, Mexico,* ⁴*Physiology, BUAP, calle Florida, Puebla, Mexico*

The neural circuits of the auditory cortex are a substrate for a dual purpose of representing and storing the auditory signal on one hand, and sending its relevant features to other cortical and subcortical areas on the other hand. The ability to process and transform the signal crucially depends on achievement of the neuronal spike threshold following spatiotemporal summation of the synaptic signals. We used patch-clamp recording in a thin slice preparation to compare neuronal responses to current injection of layer II/III and layer V neurons. We found that while the two classes of neurons do not differ in passive neuronal properties, layer II/III neurons possess a lower firing threshold relative to layer V neurons (-44.8 ± 2.4 vs. -34.3 ± 4.0 mV). We speculate that a lower spiking threshold in layer II/III neurons might favor local intracolumnar activation for representation and storage of the auditory information whereas a more positive spiking threshold for layer V neurons may prevent unnecessary cortical spread of scarcely processed signal.

585 In Vivo Whole-Cell and Cell-Attached Recordings in Primary Auditory Cortex in Awake Restrained Rats

Tomas Hromadka¹, Michael DeWeese², Anthony Zador²

¹*Watson School of Biological Sciences, Cold Spring Harbor Laboratory, 1 Bungtown Road, Cold Spring Harbor, New York, United States,* ²*Zador Lab, Cold Spring Harbor Laboratory, 1 Bungtown Road, Cold Spring Harbor, New York, United States*

Much of what is known about responses in auditory cortex is based on recordings obtained in anesthetized animals. However, it has recently become increasingly clear that response properties of neurons in awake animals can differ considerably. We have therefore recorded stimulus-evoked responses from well-isolated single units in the primary auditory cortex of head-restrained rats. We used cell-attached and whole-cell recording techniques in order to minimize both of the main sources of error in spike detection: failure to detect a spike (false negatives) and contamination by spikes from nearby neurons (false positives). These techniques also differ from conventional extracellular tungsten-electrode recording in their selection bias: With cell-attached recording, neurons are selected solely on the ability of the experimenter to form a gigaohm seal, rather than on the basis of spontaneous neuronal activity or responsiveness to particular stimuli. We sampled neuronal responses across a range of cortical layers and probed the neurons with various types of stimuli, including pure tones and FM sweeps. We find that single neurons in primary auditory cortex of awake rats display a rich repertoire of responses, ranging from binary onset responses to sustained high-frequency onset or offset responses; sometimes nearby neurons responded in very different ways.

586 Responses of Auditory Cortex Neurons to Acoustical Stimuli in Awake and Anesthetized Guinea Pigs

Daniel Suta, Jiri Popelar, **Josef Syka**

Dept. Auditory Neuroscience, Institute of Experimental Medicine, ASCR, Videnska 1083, Prague, Czech Republic

Anesthesia is very frequently used in studies of the auditory cortex even though cortical activity can be significantly affected by the application of anesthetics. The effect of anesthesia is particularly critical in studies in which natural sounds, such as species-specific vocalizations, are used as stimuli because of their complex acoustic pattern and behavioral relevance. To understand the effect of anesthesia, we recorded activity of single and multiple units in the primary auditory cortex of awake guinea pigs as well as in animals anesthetized with a mixture of ketamine and xylazine. Chronically implanted electrodes were used for recording neuronal activity in awake animals; in anesthetized animals both chronically implanted electrodes as well as electrodes introduced in acute experiments were employed. In both types of experiments, acoustical stimuli were presented in free-field conditions. Neuronal responses under both conditions generally reflected the spectral and temporal features of the acoustical stimuli. The response pattern of neurons was typically of a phasic character with a dominant onset part in the peri-stimulus time histograms. The phasic character was manifested in response to purr, where only the first phrase evoked a response in a significant portion of neurons. Purr is characterized by a relatively high repetition rate of individual phrases (>10 Hz). The overwhelming majority of neurons responded to more than one vocalization call out of a set of four tested calls in awake as well as anesthetized animals. Anesthesia was found to modulate neuronal responses to all types of stimuli, but the administration of anesthesia was not generally suppressive. In some neurons anesthesia enhanced the response to one vocalization call and suppressed the response to another call.

Supported by the grant GA CR #309/01/1063.

587 Shared and Private Variability in the Auditory Cortex

Michael DeWeese, Anthony Zador

Zadorlab, Cold Spring Harbor Laboratory, 1 Bungtown Rd, Cold Spring Harbor, NY, United States

The remarkable variability of cortical sensory responses is often assumed to impose a major constraint on efficient computation. At least some of this variability is due to structured stimulus-independent activity, raising the possibility that it is not noise. Using in vivo whole-cell patch clamp methods in rat auditory cortex, we partitioned the trial-to-trial variability underlying tone-evoked sub-threshold voltage fluctuations into a private component (which includes synaptic, thermal and other sources local to the recorded cell) and a shared component arising from network interactions. We found that the private component was remarkably small, usually about 1-3 mV; in some cases it was no larger than the fluctuations expected from stochastic quantal release. The shared component was often much larger, and showed more heterogeneity across the population, ranging from about 1-10 mV.

Our observations indicate that cortical neurons may operate in the

low noise regime, and that neuronal variability arises primarily from circuit-level interactions and need not irreversibly corrupt sensory representations.

588 Nonlinearity of Cortical Receptive Fields Measured With Natural Sounds

Michael Wehr, Christian Machens, Anthony Zador

Marks, Cold Spring Harbor Laboratory, 1 Bungtown Rd., Cold Spring Harbor, NY, United States

How do cortical neurons represent the acoustic environment? This question is conventionally addressed by probing with simple stimuli such as clicks or tone pips. Such stimuli have the advantage of yielding easily interpreted answers, but have the disadvantage that they may fail to uncover complex or higher-order neuronal response properties. Here we adopt an alternative approach, probing neuronal responses with complex acoustic stimuli, including animal vocalizations. We have used in vivo whole cell methods in the rat auditory cortex to record subthreshold membrane potential fluctuations elicited by these stimuli. Most neurons responded robustly and reliably to the complex stimuli in our ensemble. Using regularization techniques, we estimate the linear component—the spectro-temporal receptive field (STRF)—of the transformation from the sound (as represented by its time-varying spectrogram) to the neuron's membrane potential. We find that the STRF has a rich dynamical structure, including excitatory regions positioned in general accord with the prediction of the simple tuning curve. However, while the STRF successfully predicts the responses to some of the natural stimuli, it surprisingly fails completely to predict the responses to others; on average, only 11% of the response power could be predicted by the STRF. Most of the neuron's response, therefore, cannot be predicted by the linear component, even though the response is deterministically related to the stimulus. Analysis of the systematic errors of the STRF model shows that this failure cannot be attributed to simple nonlinearities such as adaptation to the mean intensity, rectification, or saturation. Rather, the highly nonlinear response properties of auditory cortical neurons are mostly dynamic, i.e., are due to the time-varying properties of the neural encoder.

589 Feedforward Inhibition in Auditory Cortex (ACx) of the Mouse.

Yakov Verbny¹, Szabo Gabor², F. Edelyi², Matthew Banks¹

¹*Anesthesiology, University of Wisconsin, Madison, 1300 University Ave., Madison, WI, United States,* ²*Gene Technology and Developmental Neurobiology, Laboratory of Molecular Biology and Genetics, Szigony u. 43, Budapest, Hungary*

Introduction: GABAergic inhibition in ACx serves to sharpen onset responses and shape the receptive field properties of pyramidal cells. The capacity of inhibitory cells to regulate the firing properties of pyramidal cells depends in part on whether inhibition is activated by thalamic excitation (feedforward inhibition), by intracortical excitation (feedback) or both. We have investigated the structural basis of feedforward inhibition in the mouse ACx.

Methods: Whole cell recordings were obtained at 34°C from LI-IV interneurons in thalamocortical brain slices (Cruikshank et al., 2002) from 2-3 wk CBA/J mice (n=8 cells) or GAD65-EGFP transgenic mice (C57Bl6/CBA background; n=15 cells). Current-

clamp responses were obtained using pipettes filled with K-gluconate. Thalamic afferents were activated by stimulating mid-way between the medial geniculate and ACx, just rostral to the hippocampus. Cells were labeled with biocytin and visualized using standard techniques. Data are expressed as mean±SD.

Results: Depolarizing current pulses triggered trains of action potentials with fast kinetics ($t_{\text{half}}=0.74\pm0.25$ ms) that exhibited moderate adaptation ($\text{ISI}_{\text{first}}/\text{ISI}_{\text{last}}=0.5\pm0.3$) during 250 ms pulses. Stimulation of thalamic afferents triggered excitatory postsynaptic potentials in 71% of cells. In some cases these cells were immediately adjacent to cells that did not show synaptic responses, suggesting that distinct populations may underlie feedforward and feedback inhibition. Interneurons exhibiting thalamic responses were located in layers I-IV. EPSPs had latencies of 8.1 ± 3.8 ms, amplitudes of 3.8 ± 3.7 mV, and half widths of 11.6 ± 6.4 ms. EPSPs were rarely superthreshold.

Conclusions: Thalamic stimulation directly excites a subpopulation of GABAergic interneurons in ACx. This feedforward inhibition may subserve fast temporal regulation of pyramidal cell output in response to acoustic transients.

This work was supported by NIH (DC006013-01), the UW Department of Anesthesiology.

590 Influence of Connectivity Parameters on Spike Patterns in Interneuronal Networks in Auditory Cortex

Elliott B. Merriam, Matthew I. Banks

Anesthesiology, University of Wisconsin, 1300 University Ave, Madison, WI, United States

Introduction: Synchronous activity in cortical interneuronal networks can shape pyramidal cell responses to acoustic stimuli and also establish internally-generated spike patterns in cortical cells. To understand how temporal patterns arise in interneuronal networks, we investigated how connectivity parameters influence spike patterns in paired recordings from LI interneurons. Observed properties of chemical and electrical synapses were used to simulate connections between uncoupled cells via dynamic clamp.

Methods: Whole cell recordings were obtained from LI interneurons in brain slices from 2-3 wk CBA/J mice at 34°C. Spontaneous GABA_A IPSCs (sIPSCs) were recorded with KCl in the pipette at -60 mV in the presence of kynurenic acid. Current-clamp recordings were obtained with K-gluconate in the pipette. Dynamic clamp software was developed by J. A. White, PhD (Boston Univ.). Cells were labeled with biocytin. Data are expressed as mean±SD.

Results: GABA_A sIPSCs in LI cells had mean amplitudes= 0.95 ± 33 nS, $t_{\text{rise}}=0.3\pm0.1$ ms, and $\tau_{\text{decay}}=6.3\pm1.3$ ms ($n=5$ cells). In paired recordings from cells <50 μm apart, both chemical (3/13 pairs) and electrical synapses (13/42 pairs; $g_{\text{coupling}}=0.44\pm0.38$ nS) were observed. In uncoupled pairs, action potentials induced by constant depolarizing currents occurred at random times in the two cells, with no significant cross correlation between the two spike trains. Simulated chemical (inhibitory) and electrical synapses led to significant correlations between the spike trains, with peak ~0 ms lag for electrical synapses and ~ $\text{ISI}_{\text{mean}}/2$ for chemical synapses. Combining electrical and chemical synapses, or prolonging τ_{decay} of chemical connections, resulted in enhanced 0 lag synchrony.

Conclusion: Electrical and chemical synaptic coupling leads to co-activation in two-cell networks of LI interneurons, with the timing and degree of correlation sensitive to the properties of the connections.

Supported by NIH (DC006013-01), UW Dept. Anesthesiology.

591 The Effect of Bicuculline and Gabazine on Temporal Processing in the Auditory Cortex of the Unanaesthetized Mongolian Gerbil

Simone Kurt¹, Holger Schulze¹, John M. Crook², Henning Scheich¹

¹Auditory, Plasticity and Speech, Leibniz Institute for Neurobiology, Brennekestr. 6, Magdeburg, Germany, ²Institute of Neuroscience, School of Biology, University of Newcastle, Henry Wellcome Building for Neuroecology, Newcastle upon Tyne, United Kingdom

To study the contribution of intracortical GABAergic inhibition in temporal processing of sounds, neuronal responses to pure tones and sinusoidally amplitude modulated (AM) tones were recorded from the left primary auditory cortex (AI) of unanaesthetized Mongolian Gerbils before, during and after microiontophoretic application of the GABA_A-receptor antagonists bicuculline (BIC) and gabazine. Pure tones and AM tones of 200 to 500 ms duration and with 5 ms linear ramps were randomly presented free field at 65 dB SPL.

Before the application of one of the GABA_A-receptor antagonists, responses of most units to AM tones showed phase-locking to the AM envelope at periodicities below 30 Hz, although in some units we observed phase-locking up to 60 Hz. When GABA_A-mediated inhibition was blocked by application of either antagonist (20-40 nA; 10±2 min), we observed an increase of spontaneous activity. Furthermore, the duration of onset responses and the discharge rates to both pure tones and AM tones increased under the BIC condition, and for some units a broadening of the frequency response range to pure tones was observed. Interestingly, whereas any phase-locked discharges that were seen in the AM responses before the application of BIC were eliminated during BIC application, phase-locking was still present during the gabazine-condition. We conclude from these results that the disappearance of the phase-locked response components observed under BIC can not be explained by the BIC-induced blocking of GABA_A-mediated inhibition, but rather seems to result from secondary BIC effects, e.g. the known influence of BIC onto Ca-channels.

Supported by DFG "ZIZAS"

592 Physiological Characteristics of NMDA Receptor Subunits in Neurons of the Inferior Colliculus

Chun-Lei Ma, Jack B. Kelly, Shu Hui Wu

Psychology Department, Carleton University, 1125 Colonel By Drive, Ottawa, ON, Canada

Our previous study showed the presence of excitatory postsynaptic currents (EPSCs) in neurons of the central nucleus of the inferior colliculus (ICC) that are mediated by NMDA receptors. The NMDA receptors in ICC neurons are subject to Mg²⁺ blockade in a voltage dependent manner. Activation of NMDA receptors in ICC

neurons doesn't require membrane depolarization induced by activation of AMPA receptors and can usually be elicited while the neuron is at the resting potential. This "unique" properties of NMDA receptors may be attributed to the composition of NMDA receptor subunits. The purpose of this study was to investigate the composition of NMDA receptors in ICC neurons and to determine how different NMDA subunits, especially NR2, contribute to properties of voltage-dependence and Mg^{2+} block. Brain slices were obtained from Wistar rats (9-13 days old). NMDA EPSCs were evoked by electrical stimulation of the lateral lemniscus and isolated by blocking AMPA, $GABA_A$ and glycine receptors with specific receptor antagonists. The NMDA EPSCs evoked in different ICC neurons showed different degrees of voltage-dependence, which were correlated with sensitivity to Mg^{2+} block. NMDA EPSCs that had a maximal current at less negative membrane potential showed a higher sensitivity to Mg^{2+} block than those that had a maximal current at more negative potential. NMDA EPSCs in individual ICC neurons could be suppressed by the NR2A or NR2B antagonists, Zn^{2+} and ifenprodil. NMDA receptors containing NR2A or 2B or both had a higher sensitivity to Mg^{2+} block. After blocking components mediated by NR2A and 2B with application of Zn^{2+} and ifenprodil, there was a remaining portion which was relatively insensitive to Mg^{2+} block, indicating the presence of NR2C and/or NR2D subunits. Different degree of voltage-dependence and sensitivity to Mg^{2+} block of NMDA receptors in different ICC neurons may be attributed to different proportions of NR2A, 2B and 2C, 2D subunits.

Supported by NSERC of Canada

593 Inhibition has Little Influence on Responses of Neurons in the Nuclei of the Lateral Lemniscus but Profoundly Shapes Responses of Neurons in the Inferior Colliculus

Ruili Xie¹, George Pollak²

¹Neurobiology, University of Texas at Austin, 1 University station, C0920, Austin, TX, United States, ²Neurobiology, University of Texas at Austin, 1 University Station, C0920, Austin, TX, United States

Here we report on the response properties in two divisions of the nuclei of the lateral lemniscus (NLL), the dorsal nucleus (DNLL) and the intermediate nucleus (INLL), and compare those properties to those of neurons in the inferior colliculus (IC). The activity of single neurons was monitored in awake Mexican free-tailed bats in response to both tones and to a suite of species-specific communication calls. The neurons in NLL were homogeneous, in that almost all DNLL neurons had similar properties, which differed from INLL neurons. The majority of INLL neurons were distinguished by their broad tuning, especially for frequencies above the neuron's best frequency. IC neurons, in contrast, were far more heterogeneous. Most IC cells had narrower tuning curves than INLL or DNLL neurons, and some IC cells failed to respond to any tone burst. Responses to complex social calls were also very different in the NLL compared to the IC. NLL neurons responded to all or most of the species-specific calls we presented, so long as the calls had energy that encroached upon their tuning curves. IC neurons were much more complex and responded only to some calls but

not to other calls, even though the calls they failed to respond to had energy in their tuning curves.

The most striking difference between neurons in the NLL and those in the IC, however, was seen when inhibition was blocked with bicuculline (BIC, antagonist to $GABA_A$ receptors) and/or strychnine (STRY, antagonist to glycine receptors). When inhibition was blocked in NLL neurons, both their tuning curves and their responses to the suite of communication calls were unchanged in the majority of NLL neurons. In marked contrast, blocking inhibition in the IC almost always caused a dramatic broadening of their tuning curves and an increase in the number of communication calls to which each neuron responded. When inhibition was blocked, the responses of IC neurons to communication calls became similar to NLL neurons. These results suggest that inhibition plays only a minor role in shaping responses in NLL neurons, while inhibition plays a dominant role in shaping the responses of IC neurons.

Supported by NIH grant DC 00268.

594 Short-term changes in gain in the inferior colliculus are calcium- and serotonin-dependent

Ilona J. Miko, Dan H. Sanes

Center for Neural Science, New York University, 4 Washington Place, New York, NY, United States

Modulation of sound level or frequency is the most salient stimulus for central auditory neurons. Previous research has identified a form of acoustic conditioning with modulated sound in the inferior colliculus (IC) that can briefly enhance a sound-evoked discharge rate, and effectively shift response characteristics. In an effort to understand the cellular basis of this conditioning effect, whole cell current-clamp recordings were obtained from gerbil IC brain slices at postnatal days 13-17. A stimulating electrode was placed on the lateral lemniscus (LL), and synaptic responses were recorded in the presence of 4mM kynurenic acid. A current pulse was first injected into each neuron to elicit a single action potential. Then a 5-second tetanic stimulus (100Hz) was delivered to the LL, and the same pre-tetanus current was immediately injected to assess change. Sixty percent of neurons showed an elevation in current-evoked spike rate following afferent stimulation, which recovered to pre-tetanus levels within 30s (N=114). The postsynaptic mechanism for induction of this short-term gain was first explored with bath application of neurotransmitter blocking agents. The gain in spike rate was blocked or reduced by an antagonist to the ionotropic Serotonin receptor, 5HT3 (N=6). Blocking high voltage-activated calcium channels with Verapamil also reduced the gain effect (N=5). While metabotropic glutamatergic and cholinergic antagonists did not block the gain effect, they sometimes enhanced it. Antagonists to GABA and glycinergic ionic currents caused no change in the gain effect. These results suggest that Serotonin activates the IC neuron via the 5HT3 receptor, leading to a rise in calcium. This synergy of serotonin and calcium causes a subtle yet long lasting change in membrane excitability, which may underlie acoustic conditioning.

595 Mechanisms of linear coding in the inferior colliculus

Shobhana Sivaramakrishnan, Susanne Sterbing-D'Angelo, Raquel Riquelme, Blagoje Filipovic, William D'Angelo, Douglas Oliver, Shigeyuki Kuwada

Neuroscience, University of Connecticut Health Center, 263 Farmington Ave, Farmington, CT, United States

A major problem in coding sensory information is the ability of the network involved to accurately code for the stimulus over its entire range of magnitudes. Using both brain slices and an unanesthetized *in vivo* preparation, we examined the relative importance of input convergence, target cell dynamics and an intact sensory network in coding sound input by the inferior colliculus. We find that a linear code of sound intensity can be reliably produced only for sounds that last longer than ~20 ms, and the tendency towards linearity increases with the duration of the sound. Linear codes are established and maintained by a time- and voltage-sensitive balance between excitatory NMDA- and inhibitory GABA_A-mediated transmission. When this balance fails, depolarization block causes spike failure and non-linear coding, especially at high sound intensities. Under conditions of depolarization block, however, the auditory system attempts to preserve a linear code by using two compensatory mechanisms at the cellular level: NMDA-mediated neuronal firing that persists beyond the sound, and synaptic depression during repeated sound presentations.

Supported by NIDCD grants DC01366 and DC00189.

596 Membrane Characteristics and Synaptic Response Properties of Neurons in the Rat's External Cortex of the Inferior Colliculus Studied using *In Vitro* Brain Slice Techniques

Tarun K. Ahuja, Shu Hui Wu

Department Of Psychology, Carleton University, Institute Of Neuroscience, 1125 Colonel By Drive, Ottawa, ON, Canada

In mammals the IC can be divided into three anatomical subdivisions: the central nucleus (ICc), the dorsal cortex (ICd) and the external cortex (ICx). The ICx receives its primary inputs from the contralateral and ipsilateral ICc, auditory cerebral cortical areas and from regions of motor and other sensory systems. This wide array of primary projections from both auditory and non-auditory sources makes the ICx a unique structure within the auditory brainstem. To better understand the physiological function of the ICx, we examined intrinsic membrane properties and synaptic responses of ICx neurons in young rat's brain slice preparations.

Visual whole-cell patch clamp recordings were taken from ICx neurons (N=63) in coronal slices from rats between the ages of 7 to 11 days postnatal. The ICx neurons studied displayed various types of firing patterns in response to depolarizing and hyperpolarizing current injection, including regular, adaptation, pauser and bursting type. Of the firing patterns observed (n=51) the regular type cells seem to constitute the majority (n=36), followed by adaptation (n=10), pauser (n=3) and bursting cells (n=2). In response to hyperpolarizing current injection, many ICx neurons (n=30) illustrated a pronounced sag in the membrane potential, possibly representing a hyperpolarization activated current (I_h).

Furthermore, many neurons (n=22) displayed a Ca²⁺-dependent rebound depolarization following hyperpolarization of the membrane with negative current injection. This Ca²⁺ rebound was observed in neurons with all of the four firing patterns. When tested (n=3), all ICx neurons displayed the presence of a Ca²⁺-mediated current expressed as Ca²⁺ spikes, uncovered when both Na⁺ and K⁺ currents were blocked. To study the synaptic responses, a stimulating electrode was placed in the ICc. The resultant graded responses displayed a combination of excitatory/inhibitory potentials and pharmacological analyses were employed.

Supported by NSERC of Canada

597 Determination of Response Patterns in the Inferior Colliculus by Synaptic Inputs and Intrinsic Membrane Properties

Douglas L Oliver, Shobhana Sivaramakrishnan

Neuroscience, University of Connecticut Health Center, 263 Farmington Ave, Farmington, CT, United States

This study examines the factors that influence the input-output relationships of single neurons in the central nucleus of the inferior colliculus (ICC). We recorded from neurons in laminar brain slices of the ICC, and activated synaptic inputs by stimulating the lateral lemniscus, the main pathway for ascending excitatory and inhibitory inputs into the ICC. Responses of neurons were examined to the activation of a fixed number of synapses, to increasing synaptic recruitment, and to trains of stimuli, and postsynaptic potentials (PSPs) and firing patterns (the output) were directly compared to postsynaptic currents (PSCs; the input).

We find that although both inhibitory and excitatory synapses are activated, the net synaptic potential is excitatory and prolonged in all ICC neurons. Synaptic inputs to ICC neurons consisted of AMPA, NMDA and GABA_A components. NMDA-receptor mediated inputs, regulated by GABA_A, were necessary for sustained firing in response to synaptic activity. ICC neurons exhibited a differential ability to reflect the duration and amplitudes of their synaptic inputs. PSP durations were a steep function of PSC duration in sustained-regular cells but much shallower in rebound-adapting and rebound-transient cells. Synaptic recruitment evoked sustained firing in both regular and adapting neurons, but the spike patterns showed clear differences related to the interaction between active conductances and passive changes in membrane potential.

Our results suggest that some ICC neurons are better able than others to maintain the fidelity of their inputs. The interaction between intrinsic membrane properties and synaptic inputs may result in a differential filtering of information by different neuron types in the ICC.

Sponsored by NIDCD grant R01 DC00189.

598 GABAergic Neurons in the Cat Inferior Colliculus

David T Larue, Harkawal S Hundal, Jeffery A Winer

Molecular and Cell Biology, University of California at Berkeley, 285 Life Sciences Addition, Berkeley, CA, United States

We studied the gamma-aminobutyric acid-containing

(GABAergic) cells in the adult cat inferior colliculus (IC) in thick sections and in post-embedded material, and in glutamic acid decarboxylase-immunostained (GAD) preparations.

The proportion of GABA immunopositive neurons in IC subdivisions differed significantly: the caudal cortex had 27%, the lateral nucleus 25%, the rostral pole nucleus 22%, the central nucleus 18%, and dorsal cortex 17%. Cell counts and measurements were taken from post-embedded material.

GABA-positive neurons were larger than GABA-negative cells in all subdivisions except the caudal cortex. This distinguished the caudal cortex from the dorsal cortex and the lateral nucleus. The largest GABAergic neurons were in the rostral pole and were almost three times the size of the non-GABAergic caudal cortex cells.

Somatic staining ranged from pale to very dark; the darker cells were more often smaller, but some large darkly staining cells were also seen. Immunoreactive preterminal axons from 1-6 μm thick were found throughout the IC, with rare fibers up to 8-10 μm . The largest fibers were in the lateral nucleus and the ventral one-third of the central nucleus. Both GABA-positive and -negative somata and proximal dendrites received GABA positive puncta. Puncta in the neuropil were also numerous.

These findings are consistent with those of others in the central nucleus of the IC (Oliver et al., *J. Comp. Neurol.* 1994, 340:27-42). The small percentage difference (20% in the prior work, 18% in this study) is attributed to slight differences in architectonic boundaries. We used an unbiased, best-fit circle method to more objectively define somatic contours, for example, when a large dendrite elongates the perikaryon. These values are systematically 20-40% smaller than those published previously.

GAD stained preparations in the horizontal plane delineated the border of the lateral nucleus and caudal cortex. A layer of large GAD-positive neurons was conspicuous at the medial border with the central nucleus.

The wide range of cell sizes may underlie local differences in IC processing. These nuclear distinctions could reflect differential contributions of GABAergic neurons in each subdivision to the tectothalamic pathway.

Supported by USPHS grant R01 DC 02319-24.

599 Serotonin 1A, 1B, and 2 receptor agonists differentially affect the auditory responses of single IC neurons.

Laura M Hurley

Biology, Indiana University, 1001 E. Third St/ Jordan Hall, Bloomington, IN, United States

Serotonergic fibers are present throughout the auditory brainstem, and serotonin has been implicated in a number of auditory-related behaviors and pathologies. However, relatively little is understood about the basis for these effects at the level of single auditory neurons. Previous studies of the effects of serotonin in the inferior colliculus (IC) revealed an unexpected heterogeneity between neurons, such that serotonin could depress, facilitate, or cause frequency-dependent effects in different subsets of neurons. At least some of this variability is likely to be mediated by the multiple serotonin receptor types that have been reported in the IC. To test this hypothesis, agonists and antagonists of 5HT 1A, 1B, and

2A/2C receptors were iontophoresed onto extracellularly recorded single IC neurons in Mexican free-tailed bats. Responses to tones were measured before, during, and after iontophoresis of the drugs. Different serotonin receptor agonists had different effects. The 5HT 1A agonist 8-OH-DPAT either depressed or facilitated spike counts, usually uniformly across frequency. The 5HT 1B receptor agonist CGS12066B decreased spike counts, and in a high proportion of neurons these decreases were frequency-specific. The 5HT 2A/2C receptor agonist DOI caused either depression or facilitation in different neurons, but the selective 5HT2C agonist MK212 facilitated spike counts. The effects of the serotonin receptor antagonists were usually opposite to those of the complementary agonists. Antagonists iontophoresed alone often altered spike counts, suggesting that they block endogenous serotonergic neuromodulation. Overall, these results strongly support the hypothesis that different receptors mediate different effects of serotonin in the IC, a situation that is common in other regions of the brain and that could confer great flexibility on the ability of serotonin to modulate auditory circuitry.

600 GABA_B Receptors Modulate Synaptic Excitation in the Rat's Central and Dorsal Nuclei of the Inferior Colliculus

Shu Hui Wu, Chun-Lei Ma, Jack B. Kelly

Psychology Department, Carleton University, 1125 Colonel By Drive, Ottawa, Ontario, Canada

We have previously shown that GABAergic inhibition in the central nucleus of the inferior colliculus (ICC) can be modulated by presynaptic GABA_B receptors. In a brain slice preparation application of the GABA_B receptor agonist, baclofen, reduced inhibitory postsynaptic responses, but did not affect any intrinsic membrane properties of the postsynaptic neurons. The purpose of this study was to investigate the role of GABA_B receptors in synaptic excitation in the ICC as well as in the dorsal cortex of the inferior colliculus (ICD). Whole-cell patch clamp recordings were made from neurons of the ICC and ICD in a brain slice preparation of 9-11 day old rats. Postsynaptic currents in ICC neurons were evoked by electrical stimulation of the lemniscal inputs, and those in ICD neurons were elicited by stimulation of synaptic inputs from the ICC. Excitatory postsynaptic currents (EPSCs) were isolated pharmacologically by blocking GABA_A and glycine receptors. The internal solution in the recording electrodes contained CsF, TEA and 4-AP which blocked K⁺ channels that may be activated by postsynaptic GABA_B receptors. The modulatory effects of GABA_B receptors on EPSCs in ICC and ICD neurons were examined by bath application of the receptor agonist, baclofen, and the antagonist, CGP 35348. The evoked EPSCs in both ICC and ICD neurons were reduced by baclofen (0.2-200 μM). The suppressive effect by baclofen was dose-dependent. The maximal reduction of the EPSCs amplitude by baclofen (5-10 μM) could be up to 90.9% in some neurons. The average reduction of the EPSCs was 66.9% for ICC neurons (n=7), and 86.2% for ICD neurons (n=5). The reduction of the EPSC amplitude was partially or completely reversed by application of CGP35348 (100-200 μM). All these results suggest that presynaptic GABA_B receptors modulate not only GABAergic inhibition in the ICC, but also glutamatergic excitation in the ICC and ICD.

Supported by NSERC and Hearing Foundation of Canada

601 Directionality of auditory nerve fibers in the gray tree frog, *Hyla versicolor*

Jakob Christensen-Dalsgaard

Institute of Biology, University of Southern Denmark, Center for Sound Communication, Campusvej 55, Odense, Denmark

Behavioral investigations of directional hearing in terrestrial frogs have been concentrated on the hylid tree frogs, where females show a robust phonotactic response to the conspecific mating call. Female gray tree frogs (*H. versicolor*) locate conspecific calls with an average error angle of approximately 20 degrees. Biophysical studies have shown that the eardrum directivity around the call frequencies is largely caused by acoustical coupling of the eardrums leading to pressure-difference receiver directivity with ovoidal characteristics and ipsi-contralateral differences of up to 10 dB (Jørgensen and Gerhardt, JCP A 169: 177-183, 1991). The high-frequency directionality of auditory nerve fibers of ranid frogs is comparable in shape and magnitude to their eardrum directionality, but the low-frequency directional information is encoded by unknown, non-tympanic pathways (Feng, JASA 68:1107-1114, 1980, Jørgensen and Christensen-Dalsgaard, JCP A 180:493-502, 1997). However, the larger ranid frogs do not show very robust phonotaxis and selection pressures for directional hearing might be small in comparison to hylid tree frogs.

The present study is the first report on directional characteristics of auditory nerve fibers in gray tree frogs. The auditory nerve was exposed dorsally and the frog was stimulated by free-field sound (tone bursts, amplitude-modulated tones and noise, and sampled *H. versicolor* calls) from twelve speakers. Results from 89 fibers show an ovoidal directional characteristic at high frequencies (above 800 Hz) and either ovoidal or figure-eight characteristic at low frequencies. The fibers show maximal responses from ipsilateral-caudal angles and minimal responses from contralateral-frontal angles. The results are qualitatively similar to the earlier studies in ranid frogs, but the directionality is larger, probably reflecting specialization for directional hearing in gray tree frogs.

602 Effects of degraded sound-localization cues on neuronal spatial specificity in the owl's IC.

Hanna B Smedstad, Clifford H Keller, Terry Takeshi Takahashi

Institute of Neuroscience, University of Oregon, 224 Huestis Hall, Eugene, OR, United States

In nature, sound waves from a source of interest sum at the eardrums with those from competing sources. The frequency-specific binaural cues derived from these composite waveforms can differ, sometimes dramatically, from those of the individual sources, degrading, potentially, the ability to localize sounds. Our model system, the barn owl (*Tyto alba*), is a nocturnal predator that can hunt by passive hearing alone, guided by a topographic map of auditory space found in the external nucleus of its inferior colliculus (ICx). The neurons of the ICx, or space-specific neurons, have spatial receptive fields due to their selectivity for frequency-specific binaural cues. In an effort to understand spatial hearing in natural environments, we measured the tolerance of ICx neurons to degraded binaural cues. To degrade the cues systematically, we jittered the frequency-specific ITD and ILD values for each location in space (i.e., the head-related transfer functions – HRTFs)

and filtered broadband noise bursts with these altered HRTFs. We then assessed, by extracellular recordings, the degree to which the spatial receptive fields of the space specific neurons ($n = 30$) remained intact. Adding noise to the ITD and ILD components of the HRTF generally decreased the spatial selectivity of the neurons. Receptive fields grew wider and less well-defined as the amount of jitter increased. In addition, we noted a decrease in inhibition that further contributed to the degradation of spatial selectivity. Overall, however, the neurons were remarkably tolerant, requiring a jitter in phase of $\pm 0.5\pi$ radians or a jitter in amplitude of over 10dB to generate a statistically-significant decrease in spatial selectivity across our sample. This tolerance may underlie the cocktail party effect wherein human sound localization remains relatively unaffected by background noise and echoes.

603 The processing of sound location cues by classes of units in the inferior colliculus

Steven M. Chase, Eric D Young

Biomedical Engineering, The Johns Hopkins University School of Medicine, 720 Rutland Ave, Baltimore, MD, United States

In the auditory brainstem, there are multiple parallel streams of processing. These converge in the central nucleus of the inferior colliculus (ICC) in a manner that is not well understood. Ramachandran et al. (1999) have shown the existence of three classes of units in the ICC (type-V, type-I, and type-O) that are hypothesized to receive their dominant input from the medial superior olive, lateral superior olive, and dorsal cochlear nucleus, respectively. This suggests that sound location information based on interaural timing differences (ITDs), interaural level differences (ILDs), and spectral shapes might be differentially represented in these ICC classes. Using virtual space stimuli we independently manipulate ITDs, ILDs, and the first spectral notch (SN) position in head related transfer functions while recording single unit responses in the ICC of decerebrate cats. We then quantify the mutual information (MI) between the responses and stimuli in two ways, under the assumption of a rate code and using the spike train distance metric of Victor and Purpura (1997). With the VP method, the role of spike timing can be assessed.

Surprisingly, we find no evidence of a segregation of sound location cue information among the unit classes. Of the 12 type-O, 15 type-I, and 10 type-V units studied with ILD manipulations, there are no statistically significant class differences in the MI carried between stimuli and responses using either the rate or VP method. The major determining factor for information about ITD manipulations is the best frequency (BF) of the unit, with type-O and type-I units coding as well as type-V units of similar BF. Finally, if one assumes a rate code, low BF units have lower MI values for SN location than mid-frequency units. This trend is reversed, however, when accounting for spike timing through the VP method, i.e., spike timing carries significant information about spectral cues at low BFs.

(Supported by NIH grants DC00115 and DC05742)

604 Detection of Interaural Correlation by Neurons in the Superior Olivary Complex and Inferior Colliculus of the Unanesthetized Rabbit

Charles S Coffey, Charles S Ebert, Marc K Bassim, William D Crocker, John D Skaggs, Douglas C Fitzpatrick¹
Otolaryngology, UNC Chapel Hill, CB #7070 Dept. of Otolaryngology UNC Chapel Hill, Chapel Hill, NC, United States

Interaural time differences (ITDs) are used for sound localization and separating signal from noise. Sound localization presumably occurs by detecting ITDs within the range available from the head width. However, many neurons, particularly if tuned to the low end of the frequency range for ITD sensitivity, show little modulation of response to ITDs within the head width. The process of encoding ITD is equivalent to cross-correlation of the signals at the two ears. Thus, sound localization may be a special ability derived from a general sensitivity to interaural correlation.

To investigate neural responses to interaural correlation, we recorded from ITD sensitive neurons in the superior olivary complex (SOC) and inferior colliculus (IC) in unanesthetized rabbits. The correlation of broadband noise was varied and threshold changes in response determined through signal detection methods.

In the SOC, we identified two populations of ITD sensitive neurons. One population fulfilled the requirements of a primary binaural interaction in that the phase locking to monaural signals predicted the tuning to ITDs. The other population typically showed sharper ITD tuning with only low levels of phase-locking to monaural signals. Most neurons in both populations showed linear response changes with interaural correlation, but some showed non-linear response changes.

The IC also contained neurons with linear and non-linear responses. The threshold change in interaural correlation (from a reference of 1) was typically smaller for non-linear than for linear neurons in both the SOC and IC. In the IC, we also studied neurons tuned to ITDs in envelopes, and found response changes only to a narrow range of correlations (1 to ~0.7) consistent with the range in the signals themselves. Thus, different types of ITD sensitive neurons are sensitive to the interaural correlation, and in mammals non-linear mechanisms improve the detection of this cue beginning at the earliest level of processing.

605 Correspondence Between Tuning to ITDs in the Envelopes of SAM Tones and Noise

Douglas C Fitzpatrick, Stephanie E Falk, Allen F Marshal, John D Skaggs

Otolaryngology, UNC Chapel Hill, CB #7070 Dept. of Otolaryngology UNC Chapel Hill, Chapel Hill, NC, United States

Interaural time differences (ITDs) can be conveyed by the fine structure of low frequency sounds or by the low frequency envelopes of low or high frequency sounds. Using sinusoidally amplitude-modulated (SAM) tones, neurons show ITD tuning to a range of modulation frequencies from less than 25 Hz to more than 500 Hz. Individual neurons show band-pass or low-pass modulation transfer functions with different center or cut-off frequencies. The amplitude modulations of broadband noises are random, but as the bandwidth decreases lower frequency modulations pre-

dominate. Such filtering can occur externally in the production of sounds, or internally through the low pass filtering properties of the cochlea.

Although ITD sensitivity to the envelopes of SAM tones has been extensively studied, relatively little is known about how these neurons respond to ITDs in the envelopes of noise. We examined the tuning of neurons to ITDs in envelopes as a function of modulation frequency to SAM tones and noise bandwidth. The neurons were recorded in the cortex and inferior colliculus of unanesthetized rabbits.

As in previous studies, the modulation transfer functions for ITD tuning to envelopes in SAM tones varied across neurons. When tested with noise, there was a correspondence between the upper cut-off frequency of the modulation transfer function and the noise bandwidth over which ITD tuning could be obtained – the lower the cut-off the narrower the bandwidth that was required. Inverting the phase of the noise in one ear did not alter the ITD tuning, indicating that the envelope and not the fine structure was the basis for the tuning. These results show that neurons can extract information about ITDs from the envelopes of noise, but only if the noise is of appropriate bandwidth.

606 Estimation of Interaural Discrimination Based on Neural Stochastic Analysis

Oren Cohen, **Ram Krips**, Miriam Furst

Electrical Engineering-Systems, Tel Aviv University, Ramat Aviv, Tel Aviv, Israel

Theoretical analysis and psychophysical measurements on human ability to lateralize sounds indicated that both interaural-time-difference (ITD) and interaural-level-difference (ILD) are significant cues for localization. Different types of models have been previously suggested for estimating the Just Noticeable Difference (JND) of ITD and ILD, including ideal detection analysis (Colburn, JASA, 54, pp. 1458-1470, 1973). Existing anatomical-based models have not succeeded in estimating all the experimental JND data.

Recently Heinz et al. (JASA, 110, pp. 2065-2084, 2001) presented a method for using neural stochastic analysis for JND estimation. They have shown a very good agreement between the model estimation and psychoacoustical data on frequency and level JND.

In the present study we have used a similar neural stochastic analysis for estimating JND of ITD and ILD. The suggested model is founded upon the fine structure of the lower parts of the brainstem auditory pathway. The cochlea is modeled as a non-linear Gamma tone filter bank with level and frequency dependence synchrony. The model continues to the Cochlear Nuclei (CN) and up to the Inferior Colliculus (IC) through the trapezoid body (TB) and the superior olivary complex (SOC).

The model calculation yields the need for coincidence detection in the neural process, in different levels of the auditory pathway, particularly, in the CN and the SOC. Neural coincidence was introduced between different ipsilateral nerve fibers in the CN, and between ipsi and contra lateral nerve fibers in the SOC.

The model is consistent with experimental results as well as anatomical structure of the auditory pathway. The model estimation matches the experimental results on JND of ITD and ILD as a function of stimulus' frequency and intensity. Different types of

lesions that were introduced in the anatomical structure of the model allow predictions of abnormal lateralization performances as obtained by Multiple Sclerosis (MS) and Stroke patients.

607 Cellular basis for ITD sensitivity in the MSO

Jesse M. Thompson, Kevin C. Rowland, George A. Spirou

Sensory Neuroscience Research Center, Dept. of Otolaryngology, Dept. of Physiology, West Virginia University School of Medicine, Box 9303 HSC, Morgantown, WV, United States

Neurons integrate a delicate balance of excitatory and inhibitory inputs over a background of their intrinsic ionic conductances. However, the interactions of synaptic inputs with intrinsic cellular properties are typically studied in isolation, and therefore are difficult to relate to the neuron's appropriate functional context. We examined these cellular properties of neurons that constitute the gerbil medial superior olive (MSO) to analyze their relative contribution in sound localization.

The onset of excitatory inputs located at proximal dendrites of a model cell were delayed in 100 μ sec increments over a 0-1500 μ sec range. These composite waveforms were injected into the somata of MSO cells of gerbils, generating simulated ITD (sITD) stimuli. Phasic, but not tonic, neurons responded with a steep decline in firing rate from entrainment to zero activity over an sITD range of 100-1400 μ sec. Short duration waveforms generated steeper sITD curves than longer duration waveforms. Application of γ -dendrotoxin (γ -DTX), a blocker of certain voltage-gated potassium channels, greatly reduced sensitivity to changes in sITD. We also studied the effects of ipSPs on sITDs by systematically inducing ipSPs at different time points relative to injection of composite waveform. Leading and lagging ipSPs could restrict the range of sITDs that activate the MSO cell. In particular, leading ipSPs could shift the maximal response to non-zero sITDs, as proposed by Brand et al. (Nature, 2002). We also showed that inhibition need not lead excitation to achieve the same result. Furthermore, small changes of less than 0.5 msec in the timing of inhibition could dramatically alter the response rate to injected eSP waveforms. Therefore, the precise temporal relationship among excitatory and inhibitory inputs is a critical determinant of MSO cell activity, and places strong constraints on processes that guide neural circuit formation during early development.

608 Interaural time difference sensitivity in the lateral superior olive of a small mammal, the Mongolian gerbil

Antje Brand^{1,2}, Benedikt Grothe², Thomas Park¹

¹*Biological Sciences, University of Illinois at Chicago, 840 West Taylor St., Chicago, IL, United States*, ²*Auditory Processing, Max-Planck-Institute of Neurobiology, Am Klopferspitz 18a, Martinsried, Germany*

LSO neurons encode interaural intensity differences by comparing excitation from the ipsilateral ear, and inhibition from the contralateral ear. Recent studies in cat and rabbit suggest that LSO cells also play a role in interaural time difference (ITD) processing for the envelopes of high frequency sounds. However, it is unclear to what extent LSO neurons contribute to ITD-processing in ani-

mals with smaller inter-ear distance, like the gerbil which has a physiologically relevant range for ITDs of only $\pm 120 \mu$ s.

To address this issue, we presented sinusoidally amplitude modulated (SAM) tones at various ITDs while recording extracellularly from single LSO cells in the anaesthetized gerbil.

For stimulation of the ipsilateral, excitatory ear alone, cells synchronized their response to modulation rates up to 715 Hz (mean 378, 140 SD). Testing neurons with ITDs (N=35) showed that cells respond minimally when the binaural stimuli were in-phase (ITD=0) or nearly so, and maximally when they were out-of-phase. For out-of-phase stimuli, the duration of inhibition was such that it did not interfere with the excitation elicited by the preceding and following SAM-cycles, even at rates of 400 Hz (2.5 ms cycle duration).

Minima of ITD functions (troughs) were between -875 and +1000 μ s ITD, and most cells displayed stable troughs over different SAM frequencies, indicating a simple interaction of excitation and inhibition (although the response of some cells suggests a more complex circuitry). Only 5 out of 35 cells had troughs within the gerbil's physiologically relevant range ($\pm 120 \mu$ s), and none of the cells showed more than minor changes within that range (on average only 5 % of the dynamic range fell within the physiological range).

Hence, in gerbils, LSO cells seem poorly suited for ITD processing, either by location of the troughs or by changes along the dynamic range of the functions, suggesting that their ITD sensitivity is an epiphenomenon of their binaural input pattern.

609 Influence of Monaural Overstimulation on Binaural Performance Measured with an Intracranial Image Task

Jacek Smurzynski, Anna Feliksiak, Rudolf Probst

Otorhinolaryngology, University Hospital Basel, Petersgraben 4, CH-4031 Basel, Switzerland

The goal of the study was to evaluate reaction of the human binaural system to sudden unilateral changes in normally hearing subjects. Monaural overstimulation with a white noise signal presented at 115 dBA SPL for 5 minutes was used to induce a temporary threshold shift (TTS). Individual baseline characteristics of monaural and binaural functions were determined by: (1) an assessment of hearing thresholds for both ears of each subject using a narrow-band noise (NBN) centered at 4 kHz and (2) an intracranial image task (lateralization) performed for the same NBN signal presented binaurally with nine values of interaural level difference (ILD) varying from -12 to +12 dB in 3-dB steps. The ILDs were created symmetrically by increasing attenuation in one channel and decreasing in the other. Signals were presented at 50 dB SL, as referenced to the threshold of the poorer ear when attenuation of the two channels was equal. Auditory sensitivity and lateralization data were collected for approximately one hour post-exposure. The protocol was repeated twice per subject to investigate intrasubject variability of TTS and of the adaptation of binaural performance. The magnitude of TTS in the 4-kHz region measured immediately after the noise exposure exhibited relatively small intrasubject variability but varied substantially among subjects and it ranged from 4 to 22 dB. Lateralization results showed fast adaptation to induced interaural hearing threshold asymmetry.

Immediately after the noise stimulation, there was a post-exposure shift of the positions of intracranial images. However, within a few minutes, NBN signals with ILD=0 produced images that were lateralized close to the midline in spite of existing hearing threshold asymmetry. Thus, subjects showed fast adaptation in terms of centering the signals that were closer to equal sound pressure levels than equal sensation levels.

Supported by Swiss National Science Foundation

610 Effects of a Preceding Tone on the Interaural-Phase-Difference Representation by Single Neurons and by Neural Populations in the Inferior Colliculus

Shigeto Furukawa¹, Katuhiro Maki¹, Makio Kashino¹, Hiroshi Riquimaroux²

¹NTT Comm. Sci. Labs, NTT Corp., 3-1 Morinosato-Wakamiya, Atsugi, Japan, ²Dept. of Knowledge Eng. & Comp. Sci., Doshisha Univ., 1-3 Tatara-Miyakodani, Kyotanabe, Japan

We examined the stimulus-history sensitivities of the representation of the interaural phase difference (IPD) in the inferior colliculus (IC) by single neurons and by populations of neurons. We recorded single-unit responses from the IC of anesthetized gerbils. The stimulus was a dichotic best-frequency tone sequence with a common level (10-20 dB re. threshold), consisting of the *precedent* (200-ms) followed by the *probe* (50-ms) with a silent gap (5-100 ms) between them. The IPDs of the two tones were varied independently. The best IPDs of individual units for the probe were relatively invariant with the precedent IPD. The overall strengths of the probe-driven responses, however, tended to decrease as the precedent IPD approached the units' characteristic IPDs (the best IPD for the no-precedent-tone condition). The result implies that the IPD representation by the *unit population* is sensitive to the IPD of a preceding tone, since the precedent would reduce rather selectively the responses of units tuned near the precedent IPD. We evaluated this notion using a version of the population vector model (Georgopoulos, 1993). We defined the population representation of a probe IPD (ϕ_{rep}) as the angle of the vector average of characteristic IPDs across units, weighted by the probe-driven responses of the units for the IPD. We found that, for a given precedent IPD, the ϕ_{rep} for a probe at a *positive* IPD relative to the precedent IPD was generally biased towards a *positive* IPD, and vice versa. That is, the ϕ_{rep} tended to shift in such a way that would emphasize the contrast of IPDs between the precedent and the probe. This context-dependency of the IPD representation may play a significant role in efficient processing of time-varying stimuli.

611 Cerebral Control of Sound Localization in the Cat: Unilateral and Bilateral Reversible Deactivation of Primary and Non-Primary Auditory Cortical Areas

Shveta Malhotra, Ameer J. Hall, Stephen G. Lomber

School of Behavioral and Brain Sciences, The University of Texas at Dallas, 2601 N. Floyd Road, GR41, Richardson, Texas, United States

Earlier studies have identified that primary auditory cortex (AI) is important for sound localization in humans, monkeys and cats. Unfortunately, little is known of the contributions of non-primary

auditory cortex to sound localization. The purpose of this study was to examine the contributions of both primary and non-primary regions of auditory cortex to sound localization during both unilateral and bilateral deactivation. To accomplish this, we trained 12 cats to perform a sound localization task and used reversible cooling deactivation to permit both unilateral and bilateral deactivations in the same cat. After attending to a central visual stimulus, animals learned to orient their head to a 100ms broad-band, white-noise stimulus emitted from a central speaker or one of 12 peripheral positions (at 15 deg intervals). Following training, each cat had 1 or 2 bilateral pairs of cryoloops chronically implanted over cortex. We examined AI, the three other tonotopic fields (anterior auditory field – AAF, posterior auditory field – PAF, ventroposterior auditory field – VPAF), as well as secondary auditory cortex (AII) and the anterior ectosylvian sulcus (AES). In accord with earlier studies, unilateral deactivation of AI caused sound localization deficits in the contralateral field. Bilateral deactivation of AI resulted in bilateral sound localization deficits throughout the 180 deg field examined. Of the three other tonotopically organized fields, only deactivation of PAF caused sound localization deficits. These deficits were virtually identical to the unilateral and bilateral deactivation results during AI deactivation. Of the two non-tonotopic regions examined, only deactivation of AES resulted in sound localization deficits. Therefore, neither unilateral nor bilateral deactivation of AAF, VPAF, or AII had any effect on sound localization. In conclusion, in addition to AI, areas PAF and AES of non-primary auditory cortex are critical for accurate sound localization.

612 Individualizing directional transfer functions of gerbils towards application to physiological studies on virtual acoustic space

Katuhiro Maki, Shigeto Furukawa

NTT Comm. Sci. Labs., NTT Corp., 3-1 Morinosato-wakamiya, Atsugi, Japan

The directional transfer functions (DTFs), the directional components of head-related transfer functions of an animal, can be used to present virtual acoustic space (VAS) stimuli to the animal through earphones in physiological experiments. However, DTFs are different between individuals. It is desired that the DTFs used for VAS stimuli are as similar as possible to the actual DTFs of the experimental subject. We examined individual differences in DTFs of gerbils, and proposed a method for estimating individualized DTFs for a specific animal from a generic set of DTFs. We surgically placed a probe microphone into the ear canal, and measured the DTFs for various sound-source directions. DTFs showed spectral features, such as peaks and notches, for frequencies above 10 kHz. The *inter-subject spectral differences* (ISSD) quantified individual differences in DTFs for a given animal pair by calculating the variance of the difference spectrum for frequencies (5-45kHz) for each source location and then averaging the variances over all 433 source directions. We attempted to reduce the ISSD by both scaling the DTFs of one animal along the frequency axis and rotating one animal's DTF along the source coordinate sphere to account for the DTF differences arising due to differences of the animal size and pinna angle. The ISSD was reduced on average by 13% after the optimal frequency scaling (OFS) only, and by 31% after both the OFS and optimal spatial rotation (OSR). The OFS

and OSR were highly correlated with differences of head diameter and pinna angle, respectively, indicating that the DTFs of a target animal could be predicted with some degree of accuracy by the anatomical measures. We developed a VAS system that generated a noise filtered by the estimated DTFs. Preliminary experiments demonstrated that the inferior collicular units generally showed some virtual-spatial sensitivities.

613 Principal Component Analysis of Ear Differences in Head Related Transfer Functions

Jinyu Qian, David A Eddins

Communicative Disorders and Sciences, University at Buffalo, 122 Cary Hall, Buffalo, NY, United States

Interaural time differences (ITD) and interaural intensity differences (IID) are two important cues in sounds localization. For sounds coming from the median sagittal plane (MSP), however, ITDs and IIDs alone cannot account for the localization abilities of human listeners. In this case, spectral cues present in the head related transfer functions (HRTFs) play a critical role. HRTFs, also known as free-field to eardrum transfer functions, are position specific. Previous research has focused on the identification of the important features of HRTFs and determining how individual HRTFs are related to specific sound source locations. Principal component analysis (PCA) is a signal processing technique that provides an efficient way to represent the underlying structure in a highly variable set of data such as HRTFs. Kistler and Wightman (1992; *J. Acoust. Soc. Am.* 91, 1637-1647) analyzed a single set of HRTFs from the left and right ears of 10 subjects using the PCA technique and demonstrated a relationship between the resulting principal directions and sound source location. In the present study, a similar PCA analysis of HRTFs was used to investigate the importance of interaural spectral cues in sound localization. Specifically, HRTFs from the left and the right ears were subjected to separate PCA analyses and the results were compared to a PCA analysis of the HRTFs combined across ears. These analyses included HRTFs from 1250 locations for each of 44 subjects and were obtained from the CIPIC HRTF Database (Algazi et al., 2001; IEEE Workshop on Applications of Signal Processing to Audio and Acoustics, 21-24). These results illustrated a clear relationship between principal directions and specific sound source locations. More importantly, however, comparisons of ear-specific analyses to the combined analysis revealed significant interaural spectral information associated with specific sound source locations.

614 The Influence of Sound Source Position on Free-Field Measurements of the Precedence Effect in Cats

Micheal L. Dent, Daniel J. Tollin, Tom C.T. Yin

Department of Physiology, University of Wisconsin, 1300 University Ave., 290 MSC, Madison, WI, United States

The precedence effect (PE) allows listeners to accurately localize sounds in the presence of reflections that arrive at the ears later in time and from different locations in space than the primary sounds. Studies of the PE show that listeners presented with a sound source and a later arriving simulated reflection from a dif-

ferent location can accurately localize the primary sound for inter-stimulus delays (ISDs) of 0.5 to 5 ms, a stage of the PE known as localization dominance. At shorter ISDs, listeners perceive one sound at a phantom location between the sources, known as summing localization, and at longer ISDs, above the echo threshold, listeners perceive two sounds at the separate source locations.

For the PE to enable accurate localization of sounds in reverberant environments, it must be robust across a wide variety of signal locations. We have previously shown that cats behaviorally experience the PE when sound sources are separated by 30-40 degrees. Here we extend those experiments to include sounds separated by 20-160 degrees. Two cats were trained using operant conditioning techniques to make gaze shifts (combined eye and head movements) to the apparent location of auditory and visual targets for a food reward. Next, pairs of lead-lag stimuli were presented to either side of the cats but symmetrically around the midline, and separated by ISDs ranging from 0.1-70 ms. Since we rewarded the cats on these trials for making any gaze shift, PE trials were presented at a rate of less than 10% of all trials. Results show that cats experience the stages of the PE at all lead-lag speaker separations, although localization dominance was not as strong for the largest separation angles. These experiments show that the PE is relatively invariant across different sound locations, which is an important feature for accurate sound localization in naturally reverberant environments.

Supported by NIDCD grants DC02840, DC006124 (MLD), DC00376 (DJT), DC00116 (TCTY).

615 Effects of Spectral Content on Distance Perception in Reverberant Space

Norbert Kopco^{1,2}, Barbara Gail Shinn-Cunningham¹

¹*Hearing Research Center, Boston University, 677 Beacon St., Boston, MA, United States,* ²*Cybernetics and Artificial Intelligence, Technical University, Vysokoskolska 4, c.dv. 151, Kosice, Slovakia*

In an anechoic environment, distance perception for nearby sources degrades if there is no low-frequency spectral content in a stimulus, presumably because of the importance of low-frequency interaural level difference cues (Brungart, *J. Acoust. Soc. Am.* 106:3589-3602). However, distance perception is essentially the same for monaural and binaural stimuli simulated at nearby distances in reverberant space (Shinn-Cunningham, Santarelli, and Kopco, 1999 ARO Abstract #103). These results suggest that low-frequency stimulus content may be less critical for distance perception of nearby sources in reverberant space than in anechoic space. The current study examines the effect of spectral content on distance perception in reverberant space.

Sources were simulated using individually measured head-related-transfer functions taken in a classroom. Sources were simulated at distances from 0.15 to 1.7 m, either directly in front or to the right of the listener. Stimuli were 300-ms-long noise bursts generated by filtering and time windowing white noise. Three broadband (wideband, low-pass, and high-pass) and three narrowband (200-Hz wide stimuli centered at 400, 3000, and 5600 Hz) conditions were tested.

Although inter-subject differences in overall ability were large, the effects of stimulus spectral content were consistent. In general,

accuracy was better for broadband than for narrowband stimuli, and better for lateral than for medial sources. In addition, judgments were least accurate for high-pass stimuli.

These results suggest that low-frequency content provides important cues for source distance in reverberant environments, as it does in free-field conditions. However, distance information may be encoded by different stimulus attributes in reverberant and anechoic space.

[Work supported by AFOSR and the National Academy of Sciences]

616 Responses of a Simple MSO Population Model to Realistic Reverberant Signals

Kosuke Kawakyu^{1,2}, Barbara Gail Shinn-Cunningham¹

¹Hearing Research Center, Boston University, 677 Beacon St., Boston, MA, United States, ²Speech and Hearing, Bioscience and Technology, Massachusetts Institute of Technology, 77 Massachusetts Ave., Cambridge, MA, United States

In order to quantify how natural echoes and reverberation impact sound localization, reverberant HRTFs measured in a moderate-sized classroom were used to simulate the signals reaching a listener. The resulting left- and right-ear signals were processed through a simple computational model to estimate how a population of medial superior olive (MSO) neurons responds to sources from different locations relative to the listener and different listener locations in the room.

Left- and right-ear signals were processed through an auditory-nerve fiber (ANF) model (Heinz et al., *Acoust Res Letters Online*, 2001) to estimate the instantaneous firing rates of fibers tuned to a range of characteristic frequencies (CFs). Frequency-matched left- and right-ear ANF responses were cross-correlated (using a sliding window with length inversely proportional to the CF) to estimate the time-varying responses across a population of coincidence-detector neurons. These “raw” results show that interaural decorrelation from echoes and reverberation greatly distorts interaural time differences (ITDs). For broadband signals, ITDs vary dramatically over time, but have a mean value that matches the “true” (anechoic) ITD. In contrast, for pure tone signals, output ITDs are constant over time but “wrong” (i.e., differ from the value that would arise in anechoic space). Further, distortion was most dramatic when the listener was near a wall, when there were early and intense echoes.

For each CF and time instance, the population response was combined to generate an instantaneous estimate of source laterality. Resulting estimates degrade with source distance (as the relative strength of reverberant energy increases) and with proximity to the walls of a room. However, even in the worst conditions, final estimates of source laterality for broadband signals are relatively precise when information is combined over time and / or across CF. In contrast, steady-state tones can only be localized accurately from the cues present at the onset of the signal.

[Work supported by NIDCD and AFOSR]

617 Can Room Reverberation be Modeled as Statistical Interaural Decorrelation?

Sasha Devore^{1,2}, Sanaz Zhalehdoust Sani^{2,3}, Barbara Shinn-Cunningham^{2,4}

¹Speech and Hearing Bioscience and Technology Program, Harvard-MIT Division of Health Sciences and Tech., 677 Beacon St., Cambridge, MA, United States, ²Hearing Research Center, Boston University, 677 Beacon St., Boston, MA, United States, ³Biomedical Engineering, Boston University, 677 Beacon St., Boston, MA, United States, ⁴Cognitive and Neural Systems and Biomedical Engineering, Boston University, 677 Beacon St., Boston, MA, United States

In anechoic environments listeners are often able to use differences in the interaural cues (e.g. ITD and ILD) of spatially separated sources to improve detection and identification of auditory targets. In reverberant environments, echoes and reverberation produce instantaneous variations in interaural cues and decorrelate the signals reaching a listener's ears. It is known that the binaural masking level difference (BMLD) is smaller for a decorrelated masker than for a perfectly correlated masker. Similarly, the amount of spatial unmasking observed in real-world listening conditions decreases in the presence of reverberation. The current study examines whether the effects of realistic room reverberation on spatial unmasking can be fully characterized and modeled by knowing the interaural correlation of the masker, or whether the structure of the reverberant energy also affects spatial unmasking.

Detection thresholds were measured for both co-located and separated target (500 Hz or 2000 Hz pure-tone) and masker (white-noise). Sources were simulated in anechoic and reverberant environments using KEMAR (non-individualized) head-related transfer-functions.

Preliminary results indicate that room reverberation leads to a marked decrease of spatial unmasking. However, room reverberation can also lead to modest bilateral advantages that are subject-dependent. These idiosyncratic bilateral advantages are qualitatively different from the advantages that arise from traditional binaural processing, as they often do not depend on spatial separation of the target and masker. We hypothesize that the interaural decorrelation and temporal structure in the sum of the direct and reflected masker waveforms are critical for explaining these effects. Specifically, we suggest that the decorrelated signals at the ears provide “independent looks” at the summed target and masker, providing bilateral listening advantages that do not depend directly on ITD.

[Work supported by AFOSR and NIH]

618 Spatial echo suppression in echolocation?

Maike Schuchmann, Mathias Hübner, Lutz Wiegrebe
Biologie II, University of Munich, Luisenstr. 14, Munich, Germany

Echolocating bats can localise prey with high spatial accuracy. An ensounded prey object will not only reflect the sound in the direction of the emitting bat but also into other directions. Thus, it is highly likely that a bat will hear not only the echo coming directly from the prey object, but also higher-order echoes which produce acoustic mirror images of the prey with misleading spatial infor-

mation.

In humans and other mammals, the spatial information of echoes is suppressed: the directional information of that sound which reaches the ears first dominates the perceived position of a sound source (localization dominance).

The current experiments with bats were designed to investigate whether *Megaderma lyra* and *Phyllostomus discolor* spontaneously show localization dominance both in echolocation and in a passive hearing condition.

In the echolocation condition, only one of five tested *M. lyra* individuals and none of two *P. discolor* individuals showed significant suppression of higher-order echoes for any of the lead-lag delays tested (0 to 12.8 ms). These data indicate that while bats may be able to suppress the spatial information of higher-order echoes, this is not a mandatory auditory processing strategy and may be recruited only when the bat benefits from this suppression.

Data for localisation dominance in the passive hearing condition with click stimulation will also be presented.

619 Precedence Effect with Sound Sources in the Median Sagittal Plane

Gongqiang Yu, Ruth L Litovsky

Waisman Center, University of Wisconsin-Madison, 1500 Highland Ave, Madison, WI, United States

The precedence effect (PE) has been studied extensively in the azimuthal plane (AP), but little is known about the extent to which the PE also operates in the median sagittal plane (MSP); since binaural cues are minimal or absent in the MSP, listeners must rely on monaural spectral/level cues to localize sounds. This investigation focused on three measures of the PE in the MSP in order to better understand the extent to which mechanisms involved in spatial hearing operate similarly whether binaural or monaural cues are available. Pairs of 10 ms lead-lag Gaussian noise bursts (delays ranging from 0 to about 20 ms) were presented from different locations (-60 to 60 degrees in elevation) on a vertical arc in an anechoic chamber. Experiment 1 explored the phenomenon of fusion, whereby subjects reported whether one or two sound(s) were perceived. Experiment 2 explored the phenomenon of discrimination suppression, whereby listeners' ability to discriminate changes in the position of the lagging source was measured, with feedback on every trial. Experiment 3 repeated the fusion and discrimination suppression measures, but with a "buildup" paradigm in which a "test" lead-lag pair was preceded by 10 identical lead-lag pairs. This paradigm has traditionally only been used in the AP. Results suggest that: (1) In absence of buildup, fusion echo thresholds are 5 to 13 ms, delays that are similar to those reported in the AP. (2) Discrimination suppression without buildup suggested inter-subject variability in the extent to which the PE was operational. Some listeners showed delay-dependent performance similar to that observed in the AP, whereby %correct improves with increased delay. Other listeners performed well regardless of delay, suggesting that for those listeners the spectral/level cues are not as strongly suppressed as binaural cues, even at brief delays. (3) Buildup in the MSP occurred in some listeners under some conditions, but not as robustly as it is known to be in the AP. Together, these findings suggest that the PE in the MSP does not function identically to that which has been observed in the AP, and that

models of the PE that focus on binaural cues as the primary source of input should also incorporate monaural spectral/level cues.

620 Spatial Resolution along a Cone of Confusion

Johahn Leung, Simon Carlile

Department of Physiology, University of Sydney, Anderson-Stuart Building, F13, Sydney, Australia

A cone of confusion describes locations in space where the binaural cues are identical and is roughly symmetrically arranged around the interaural axis. Spectral cues generated by the location dependent filtering of the outer ear are used to determine the location of a sound source on the cone of confusion. We examined the variation in the just noticeable difference (JND) of the locations of sequential stimuli along cones of confusion. Furthermore, individualised head related transfer functions were analysed to explore the differences in spectral cues required for this discrimination. A 2AFC paradigm was used to quantify the JND between a reference and a test stimuli (150ms, broadband noise). Subjects were required to determine the direction of the test stimulus (higher or lower) in relation to the reference. Four locations (0°, 60°, 120° and 180° polar angles) along multiple cones of confusion were examined in an anechoic environment. While there were substantial inter-subject differences in the JNDs for each location there was a consistent pattern in the variation of the magnitude of the JNDs across the locations tested. The data indicate that subjects performed best (JND: 4° - 6° at 75% discrimination) at locations in front and close to the audio-visual horizon (0° polar angle) with a minor increase in JND (6° - 7° at 75% discrimination) for locations behind the subjects and close to the audio-visual horizon (180° polar angle). For upper location (60° and 120° polar angles), in most cases, the JNDs increased by a factor of between 2 and 5. The spectral cues underlying this variation in performance was explored by comparing the overall levels of excitation (as estimated using Glasberg and Moore, 1990 *Hear Res* 47:103-138) above and below the primary spectral notch. For some subjects the location dependent variation in this ratio correlated well with their variation in perceptual resolution on the cone of confusion. This work was supported by ARC grant A79905421.

621 Ventriloquism and anti-ventriloquism: optimal cross-modal integration accounts for audiovisual localisation

David Alais¹, David Burr²

¹Department of Physiology, University of Sydney, Eastern Avenue, Camperdown, Australia, ²Istituto di Neurofisiologia, CNR, Via Moruzzi 1, Pisa, Italy

AIM: To test whether the ventriloquist effect can be accounted for by a maximum likelihood model of optimal cross-modal integration. METHOD: Spatial localisation accuracy was first measured unimodally. Observers localised either sound-clicks or light-blobs with a Gaussian spatial profile. In bimodal conditions, both stimuli were presented together. In all conditions there were two brief stimulus presentations (slightly offset) and observers indicated which appeared more rightward. We next measured bimodal localisation accuracy for blob/click pairings. In conflict presentations, the visual and auditory stimuli were displaced either side of the

midline. In no-conflict presentations, both were left or right of midline. Observers indicated which presentation appeared more rightward. RESULTS: For visual uni-modal presentations, localisation accuracy depended on Gaussian width, being best for the smallest blobs and worst for the largest. Localisation accuracy for the auditory click (whose location was defined by ITD) was around 6°, midway between the three visual stimuli. In bimodal conditions, the blob width dictated audiovisual localisation when the blob was small (i.e., vision dominated audition in incongruent stimuli, the classic ventriloquist effect). For large blobs, the reverse held: the click dominated perceived bimodal stimulus location (“inverse ventriloquist effect”). For mid-sized blobs, both modalities contributed equally to perceived location. CONCLUSION: Both effects are very well modelled by a maximum likelihood estimation model of information combination. On this model, the bimodal estimate of location is statistically optimised through weighted combination of the unimodal estimates, with the weight for each modality given by the inverse accuracy of its estimate.

622 Binaural weighting of monaural spectral cues for sound localization

Ewan A. Macpherson, Andrew T. Sabin, John C. Middlebrooks

Kresge Hearing Research Institute, University of Michigan, 1301 E. Ann St., Ann Arbor, MI, United States

For human listeners, primary cues for localization in the vertical plane are provided by the direction-dependent filtering of the pinnae. Previous studies [e.g., Hofman and Van Opstal, 2003, *Exp. Brain. Res.*, 148:458–470] have shown that for targets away from the median plane, the spectral cue from the near ear is most influential. In this experiment, we quantified the relative influence of

the monaural spectral cues from the ears ipsilateral and contralateral to a target, and determined whether their weighting depends on the apparent lateral angle of the target or simply on the interaural energy difference. Human listeners indicated the apparent position of 100-ms, wideband, noise-burst targets either by orienting their heads or by aligning an acoustic pointer with the target sound. The targets were synthesized in virtual auditory space and

presented over headphones. The DTF filters for the two ears either corresponded to the same location or to two different locations separated vertically by 20 or 40 degrees. That is, the left and right monaural spectra could “point” to the same location or to different locations. In one condition, target locations lay 30 degrees left or right of the median plane. In a second condition, target locations lay on the median plane, but apparent lateral angle was manipulated by attenuating (by 10 dB) or delaying (by 300 μs) the signal at one ear or the other. Weighting of each ear’s spectral information was determined by a multiple regression between the elevations to which each ear’s spectrum “pointed” and the vertical component of listeners’ judgements. In both conditions, higher weight was typically given to the ear ipsilateral to the perceived lateral angle.

Because the interaural delay manipulation altered the monaural cue weighting but did not alter the interaural level difference, the weighting cannot simply be a function of the greater signal energy at the ipsilateral ear.

623 Localization of sound at near-threshold intensities

Andrew T. Sabin, Ewan A. Macpherson, John C. Middlebrooks

Kresge Hearing Research Institute, University of Michigan, 1301 E. Ann St., Ann Arbor, MI, United States

Physiological measurements of spatial selectivity of auditory neurons generally show that tuning is relatively narrow and precise at low sound levels, broadening and becoming less precise at higher levels. The apparent degradation of neuronal spatial tuning at increasing sound levels conflicts with the generally good localization performance of human subjects in psychophysical studies. In the present study, we quantified psychophysical localization performance across a wide range of sensation levels beginning at the threshold of audibility. Broadband flat-spectrum stimuli were presented at 200 locations evenly distributed in space at sensation levels ranging from 0 to 60 dB relative to the detection threshold for a front-positioned source. Listeners reported whether they had heard each target sound and if so, indicated its apparent direction by pointing their head. At near-threshold intensities, responses showed large variances for both lateral (left-right) and polar (up-down, front-back) components of localization judgments. That variance decreased as level increased up to about 20 dB SL. Near 0 dB SL, response polar angles were biased toward the horizontal meridian. That bias decreased with increasing sound level and usually disappeared around 20 dB SL. In contrast, response lateral angles showed little bias regardless of level. The acoustical cues for polar angle are given by characteristics of spectral shape, i.e., variations in sound level across frequencies. For that reason, one would expect that accurate polar-angle localization would require sizeable ranges of frequency to be audible. That expectation accords with the observation that polar-angle localization showed bias at near-threshold sound levels. Lateral-angle localization, in contrast, presumably could be accomplished by an accurate interaural difference cue at as little as one frequency. Consistent with that prediction, bias-free lateral localization was observed at the lowest audible levels.

624 Spatialisation of Talkers and the Segregation of Concurrent Speech

Simon Carlile, Senan Al-Mahaidi, Johahn Leung

Department of Physiology, University of Sydney, Anderson-Stuart Building, F13, Sydney, Australia

There is growing evidence that the perception of the differences in the spatial locations of multiple talkers aids in the segregation of concurrent speech (e.g. Freyman et al., 1999 *J. Acoust. Soc. Am.* 106:3578-3588). We have examined the variations in the speech reception threshold (SRT) for a target talker and two masking talkers under diotic, binaural and individualised virtual auditory space (VAS) listening conditions. The SRT was measured using the Coordinated Response Measure (Bolia et al. 2000, *J. Acoust. Soc. Am.* 107:1065-1066) and an adaptive procedure to adjust the level of the target talker. For each trial the target and masker talkers were randomly chosen (without replacement) from a pool of three male and three female talkers. A 100% recognition criterion was used as the threshold. With a reference of 0dB talker:maskers ratio, the SRT for the diotic condition was around 4dB for seven subjects. In

the VAS condition the target was placed directly ahead and the maskers at 30° to the left and right and resulted in a mean SRT of around 20dB. In the VAS condition the sound sources were clearly perceived in extra-personal space. However, when the stimuli were presented with the appropriate binaural cues but with no spectral cues, the perception of the sound sources were lateralised within the head and the SRT was around 14dB. This suggests that the percept of spatialisation in the VAS condition contributed around 6dB unmasking. Speech contains significant energy at frequencies above 5kHz (Jin et. al., J. Audio Eng. Soc., Munich, 2002) which is required for the accurate localisation of talkers. When spatialised speech was generated using a 5kHz low pass filter, the mean SRT was around 15dB. This suggests that the high frequency energy in speech plays an important role in the spatial segregation of multiple concurrent talkers.

This work was supported by the Australian Research Council grant A79905421

625 Biosonar Signals of CF-FM Bats, *Hipposideros terasensis*, measured by a Telemetry and High-speed Camera System.

Shizuko Hiryu¹, Koji Katsura¹, Hiroshi Riquimaroux¹, Yoshiaki Watanabe¹, Liang kong Lig²

¹Faculty of Engineering, Doshisha University, 1-3 Miyakodani, Tatara, Kyotanabe, Japan, ²Faculty of Biology, Tunghai University, 407, Taichung, Taiwan

The present study examined sonar pulse characteristics of leaf-nosed bats (*Hipposideros terasensis*, CF-FM bats). Their echolocation pulse has a harmonic structure where the fundamental frequency is about 35 kHz and the second harmonic is the strongest. We recorded emitted pulses during flight in a steel-walled flight chamber by a telemetry microphone system (telemike) mounted on the bat's head which transmitted echolocation signals to the receiver by radio wave. Simultaneously, using a dual high-speed video camera system in three dimensions, the flight speed of the bat was measured to estimate the echo Doppler shift. During flight, the change in the pulse CF2 frequency well correlated with the flight speed directed to the target wall in the chamber. We could see Doppler-shift compensation where the bat in flight changed the CF frequency of its pulse so that returning echo CF frequency would stay at the same frequency. Inter-pulse interval during flight was shortened in proportion to echo delay from the target wall. We also observed the echolocation behavior of the bat at rest toward which a pendulum (a ball with 8 cm diameter attached to a string of 1.5 m length) was swung. When the pendulum approached the bat, it clearly expanded the bandwidth of FM component of its pulse and shortened the pulse duration to increase the pulse rate. Also, we could see the bat changed inter-pulse interval depending on distance from the target ball at the end of the pendulum. These findings in pulse characteristics were appeared to be important for target identification and discrimination. [The present research was supported by a grant to RCAST at Doshisha University from MEXT of Japan, Special Research Grants for the Development of Characteristic Education from the Promotion and Mutual Aid Corporation for Private Schools Japan, the Innovative Cluster Creation Project promoted by MEXT.]

626 Bilateral Tetrodotoxin injection into inner ear makes Reversible blockage of VOR in guinea pig.

Hirota Hara, Hiroaki Shimogori, Kazuma Sugahara, Takeshi Okuda, Tsuyoshi Takemoto, Hiroshi Yamashita
Otorhinolaryngology, Yamaguchi University School of Medicine, 1-1-1 Minami Kogushi, Ube, Japan

The sodium channel blocker Tetrodotoxin (TTX) is an effective tool for blockade of action potentials. There are some reports that transtympanic TTX injection produced behavioral symptoms similar to those following bilateral peripheral vestibular ablation. But there are very few reports related to the effect of bilateral transtympanic TTX injection.

In this paper we show an animal model which may suitable to examine the mechanisms of vestibular compensation by means of continuous bilateral intracochlear administration of TTX by osmotic pump.

Seven guinea pigs were examined the VOR and behavior sequentially after intracochlear administration of 5mM TTX by osmotic pump bilaterally. VOR of TTX treated animals was came to no response around 12 to 24 hours after TTX administration had started. But 48 to 120 hours after TTX injection stopped, VOR recovered almost same level as those of pretreatment. Microscopic findings of inner ear specimen suggested almost no irreversible damage of semicircular canal and vestibular hair cells.

Behavioural symptoms also occurred between 12 and 24 hour after TTX administration. TTX treated animals could not stand up when they lay down 24 hour after TTX administration. But 72 hours after TTX injection started, the animals became to be able to stand up, nevertheless their VORs were no response. After TTX injection was finished, the time needed to stand up from supine to upright position was transitionally elonged 12 to 24 hours after, and recovered to pretreatment level at 120 hours after.

Transient blockage with bilateral intracochlear administration of TTX may be useful for studying the central vestibular response to recurrent or episodic vestibular disruption in the intact vestibular system.

627 Resting Synaptic Activity in Bouton Afferents of the Turtle Posterior Crista

Jin-Tang Xue, Joseph Christopher Holt, Jay M. Goldberg
Neurobiology, Pharmacology, and Physiology, University of Chicago, 947 E. 58th Street, MC 0926, Chicago, IL, United States

We have characterized quantal activity in post-synaptic recordings from afferents in the turtle posterior crista. Based on their afferent discharge properties and their responses to electrical activation of efferent fibers, the units are judged to be BT fibers, i.e. bouton (B) fibers located near the torus (T). Here we describe activity in the unstimulated (resting) condition. Spike discharge was blocked by TTX or QX-314. As judged by spectral methods and confirmed by the averaging of individual quanta, mEPSPs are fit by alpha functions, $(?t)^k \exp(-?t)$, peak in 1 – 1.5 ms, and have effective durations of 3 – 5 ms. Quantal size varies from 0.2 – 0.8 mV and is reduced by CNQX, but not by AP-5. Unstimulated quantal rates are typically 200 – 800/s and are reduced when external Ca²⁺ is lowered. There is an inverse correlation between quantal size and quantal

rate. We found no evidence for the synchronous release of multiple quanta: release of individual quanta is consistent with Poisson statistics and quantal-size histograms can be simulated by assuming the release of single quanta whose amplitude varies with a coefficient of variation of 0.25-0.50. Multi-quantal release has been proposed as a method of increasing the sensitivity of synaptic transmission. Such proposals have seldom considered the sensitivity of the post-synaptic terminal. BT fibers have an irregular discharge (Brichta and Goldberg 2000), implying high post-synaptic sensitivity (Goldberg 2000). The resting quantal depolarization, typically 0.5 - 1 mV, can sustain a maintained spike discharge averaging 20/s, again suggesting high post-synaptic sensitivity.

628 Stimulated Synaptic Activity in Bouton Afferents of the Turtle Posterior Crista

Joseph Christopher Holt, Jin-Tang Xue, **Jay M. Goldberg**
Neurobiology, Pharmacology, and Physiology, University of Chicago, 947 E. 58th Street, MC 0926, Chicago, IL, United States

Quantal activity in BT afferents was modulated by sinusoidal indentation of the canal duct at 0.3 Hz. For each unit, only a single indenter amplitude in the linear operating range was studied. As measured by shot-noise theory, quantal rates, which were 200 - 800/s at rest, increased 1.5 to 4-fold during peak excitation and were driven close to zero during peak inhibition. Maximal quantal rates were 500 - 3000 /s. There was an asymmetry between excitatory and inhibitory responses with the former being 2 - 4x larger than the latter. The asymmetry was seen even when inhibitory points approaching zero rate were excluded. Quantal responses led indentation by 40 - 45°, similar to the phase lead seen in spike discharge. The similarity in phase leads implies that most of the distinctive response dynamics of BT units arises presynaptically. No such phase lead was seen in our studies of voltage-sensitive ionic currents (Goldberg and Brichta 2002), which suggests that the critical events occur at an early, possibly micromechanical stage of transduction. Associated with the sinusoidal modulation in quantal rate, there are small ($\pm 10 - 30\%$) modulations in mEPSP duration, mEPSP peak time, and quantal size with duration and peak time being shorter and size being smaller during excitation. These effects lag peak excitatory rate changes by 20-30°. During sinusoidal indentation, there is a modulation in membrane potential that is almost in phase with quantal rate. The amplitude of the modulation during the excitatory half-cycle is typically 1.5 - 3 mV. Of the total potential modulation, 78% is accounted for by quantal activity, with the remaining 20% representing a non-quantal component, whose existence is confirmed by its persistence after quantal activity is blocked pharmacologically.

We can compare our maximal quantal rates with release rates estimated from capacitance measurements. Each BT afferent gives rise to 750 bouton endings (Brichta and Goldberg 2000). Taking the figure of 3000/s and assuming one release site per ending (Lysakowski 1996) gives a release rate of 60/s for individual sites, almost one order of magnitude smaller than the release rates found in capacitance studies (Parsons et al. 1994; Moser and Beutner 2000). (Supported by NIDCDS)

629 Afferent Responses to Efferent Activation in the Turtle Posterior Canal Involve Pharmacologically-distinct Nicotinic Receptors

Joseph Christopher Holt, Jin_Tang Xue, Jay M Goldberg

Neurobiology, Pharmacology, and Physiology, University of Chicago, 947 E. 58th Street, MC 0926, Chicago, IL, United States

Afferent fibers in the turtle posterior crista can be identified using their discharge properties and response dynamics to sinusoidal indentation and electrical stimulation of efferent fibers. During efferent stimulation, bouton afferents near the torus (BT) are inhibited, bouton afferents at intermediate positions (BM) show mixed inhibitory-excitatory responses, and calyx-bearing afferents (CD) are excited. Iontophoresis of QX-314, from the recording micro-electrode into the afferent, abolished afferent action potentials allowing us to record postsynaptic potentials in isolation while stimulating efferent fibers. Efferent inputs to hair cells (i.e. presynaptic) were distinguished from inputs to afferents (i.e. postsynaptic) using response latencies, modulation of quantal rate, and sensitivity to the glutamate receptor antagonists CNQX and AP5. Efferent responses in BT and BM units are comprised of a brief presynaptic excitation followed by a more prolonged presynaptic inhibition. These presynaptic effects most likely results from the activation of $\alpha 9/\alpha 10$ -containing nicotinic receptors ($\alpha 9/\alpha 10$ nAChRs) functionally coupled, by way of their calcium influx, to the activation of small-conductance, calcium-dependent potassium channels (SK). Consistent with this mechanism, (1) The voltage response to a single efferent shock in BT and BM afferents consists of a brief increase, followed by a more prolonged decrease, in quantal activity; (2) Both components were simultaneously blocked by $\alpha 9/\alpha 10$ nAChR antagonists or CNQX/AP5; and (3) The initial increase in quantal activity was enhanced and isolated using SK blockers. Following efferent stimulation, all three classes of afferents also show a postsynaptic depolarization that persists following the application of either $\alpha 9/\alpha 10$ nAChR antagonists or CNQX/AP5. This depolarizing component is nearly completely blocked by dihydro- β -erythroidine (DH β E) at concentrations that do not antagonize $\alpha 9/\alpha 10$ nAChRs. These observations, as well as other pharmacological considerations, suggest that efferent responses in these turtle posterior crista afferents are mediated by two distinct subtypes of nicotinic ACh receptors.

630 Edaravone protects AMPA-induced vestibular disorder in the guinea pig.

Hiroaki Shimogori, Kazuma Sugahara, Kuniyoshi Tanaka, Tsuyoshi Takemoto, Takeshi Okuda, Hiroshi Yamashita

Otolaryngology, Yamaguchi University School of Medicine, 1-1-1 Minamikogushi, Ube, Japan

Ischemic injury is one of the major causes of inner ear diseases. The ischemic injury induced elevation of glutamate concentration in the cochlear perilymph. Glutamate is the most likely neurotransmitter between hair cells and primary afferents in the inner ear. But excessive glutamate also has toxic effects on the inner ear. The aim of this study was to evaluate effects of edaravone, one of the free

radical scavengers clinically used, on AMPA-induced peripheral vestibular disorder like ischemic injury.

Thirty-five Hartley guinea pigs with normal Preyer's reflexes and normal tympanic membranes were used in this study. Intracochlear administration of AMPA (10 mM) was performed at 0.6 ml/hr for 5 minutes by a syringe pump (n = 24). In 9 animals out of 24, edaravone (3 mg/ml)-soaked gelform was put on the round window membrane just after AMPA administration. As a control group, a same amount of artificial perilymph was administered intracochlearly (n = 11). In the AMPA group, 13 animals out of 15 showed spontaneous nystagmus, and it disappeared within 18 hr after operation. In the edaravone group, frequency of the spontaneous nystagmus was decreased. In the control group, all animals showed no static symptom. One week after operation, in the AMPA group, a mean value of caloric response time in the lesioned side/ caloric response time in the intact side was statistically smaller than that in the control group. While, in the edaravone group, a mean value of caloric response time in the lesioned side/ caloric response time in the intact side was not differ from that in the control group.

Our results indicate the possibility that topical application of edaravone may be one of the candidates for treatment of vertigo induced by ischemia.

631 Synapsin and Synaptophysin Are Present in the Crista Ampullaris of the Toadfish, *Opsanus tau*.

Gay R. Holstein¹, Giorgio P. Martinelli¹, Scott C. Henderson², Victor L. Friedrich Jr.³, Richard D. Rabbitt⁴, Stephen M. Highstein⁵

¹Neurology, Mount Sinai Sch. Med., One Gustave Levy Place, New York, NY, United States, ²Molecular, Cell and Developmental Biology, Mount Sinai Sch. Med., One Gustave Levy Place, New York, NY, United States, ³Fishberg Center for Neurobiology, Mount Sinai Sch. Med., One Gustave Levy Place, New York, NY, United States, ⁴Bioengineering, U. Utah, 50 S. Central Campus Dr., Salt Lake City, UT, United States, ⁵Otolaryngology and Neurobiology, Washington U., 4566 Scott Ave., St. Louis, MO, United States

Synapsins are a family of neuron-specific phosphoproteins that are regulated by calcium and calmodulin binding, and in turn regulate synaptic vesicle exocytosis. Similarly, synaptophysin participates in the regulation of synaptic vesicle formation. Synapsin and synaptophysin have therefore been employed as markers for presynaptic terminals. We have recently demonstrated that a small population of GABAergic hair cells is present in the central region of the horizontal semicircular canal crista ampullaris, and that some such cells show substantial co-localization of GABA and glutamate. In the present study, the three-dimensional spatial distributions of synapsin and synaptophysin were visualized in relation to GABAergic and glutamatergic hair cells in the toadfish. Endorgans from fish perfused with mixed aldehydes were processed as whole mounts for immunofluorescence using monoclonal anti-GABA and/or anti-glutamate antibodies produced in our laboratory, monoclonal anti-synapsin (BD Biosciences; San Jose, CA), and polyclonal anti-synaptophysin (LabVision Corp; Fremont, CA). All cristae were visualized by multi-photon laser

scanning microscopy. Results demonstrate a discrete belt of synapsin and synaptophysin labeling across the entire crista at the level of the basal aspect of the hair cells. This site is occupied by the terminals of the efferent vestibular system, thus we propose that the label serves as a marker for presynaptic efferent terminals. No differences were observed in the synapsin and synaptophysin staining patterns. In addition, no differences were observed in these labeling patterns when compared with the distributions of GABA- and glutamate-immunolabeled hair cells. These results suggest that efferent boutons in the crista ampullaris express both synapsin and synaptophysin, and innervate GABAergic and glutamatergic hair cells non-preferentially.

Supported by NIDCD grant DC01837. Multi-photon microscopy was performed at MSSM-Microscopy SRE, supported in part with a HHMI-BRSP award to MSSM and NCI grant R24 CA095823.

632 Three-canal Biomechanics of the Human Vestibular Labyrinth

Suhrud M Rajguru, Marytheresa A Ifediba, Richard D Rabbitt

Department of Bioengineering, University of Utah, 50 South Central Campus Dr., Room 2480, Salt lake city, Utah, United States

A mathematical model of the morphologically correct 3D human labyrinth was developed to study the role of semicircular canal biomechanics in shaping neural signals transmitted to the brain under both physiological and pathological conditions. Results under physiological conditions predict temporal response dynamics carried out by the canals as well as the orientation of the prime directions used by the labyrinth to resolve 3D angular movements into separate signals carried by each canal nerve. The model was further extended to study the biomechanical origin of gravity-dependent semicircular canal responses observed under pathological conditions associated with Benign Paroxysmal Positional Vertigo (BPPV). For this, we included the influence of calcium carbonate debris (particles) moving within a canal lumen (canalithiasis) and/or adhered to a cupula (cupulolithiasis) on the time-dependent responses of the ampullary organs. Results for canalithiasis BPPV show the influence of the particles during the provocative Dix-Hallpike maneuver and illustrate 3D repositioning of the particles during a modified Epley treatment. Numerical results were obtained by modeling the labyrinth as a series of interconnected curved tubes each filled with endolymph. A low Reynold's number approximation of the Navier-Stokes equations was used, subject to appropriate viscous and kinematical boundary conditions arising from the interaction with the membranous labyrinth and visco-elastic cupula. The complete model consisted of a coupled set of differential equations describing endolymph fluid mechanics, the visco-elastic response of the cupula and the interaction between the endolymph and the cupula. Results have implications regarding the central representation of angular head movements and the understanding, assessment, and treatment of BPPV. [Supported by the NIDCD PO1 DC-01837 and NSF IBN-9816921].

633 Three-Dimensional Reconstruction of the Human Membranous Labyrinth

Marytheresa A Ifediba¹, Timothy E Hullar², Suhrud M Rajguru¹, Richard D Rabbitt¹

¹Department of Bioengineering, University of Utah, 50 S. Central Campus Dr., Room 2480, Salt Lake City, UT, United States,

²Department of Otolaryngology-HNS, Washington University School of Medicine, 660 South Euclid Avenue, Box 8115, St. Louis, MO, United States

Three-dimensional surface reconstructions of the human membranous and bony vestibular labyrinth were developed from serial temporal bone histological sections. The membranous labyrinth was manually traced to generate a series of stacked slices that defined closed contours bounding the endolymphatic space. The surface was subdivided into five segments: the lateral canal, anterior canal, posterior canal, common crus and utricle. A curved centerline was determined for each segment by lacing together a series of local centroids spaced at even intervals along the segment. The centerlines of selected segments were connected together to define closed contours around each canal loop. Tangent, normal, and binormal vectors were computed as functions of the centerline coordinates. The segmented surface data were fit with a series of curved elliptical tubes to define a parameterized model geometry. For this, a local subset of data points was selected by cutting a ~500 μm thick slice perpendicular to the tangent vector of the canal centerline. Each slice of data was fit with a short tube of elliptical cross-section. The curve fitting procedure was repeated as a function of the curved centerline coordinate for each canal to obtain a surface reconstruction composed of a series of parameterized curved tubes of elliptical cross-section. The reconstructed labyrinth was oriented in the temporal bone based on CT data and stereotactic coordinates. The model provides detailed labyrinth geometry including non-planar canal geometry, duct areas, duct eccentricities and ampullary dimensions. Results have been applied, in related work, to study normal physiology including directional coding by the semicircular canals as well as the pathological conditions such as canalithiasis BPPV. [Supported by NIH RO1-DC01837]

634 Opioid regulation of Ca^{2+} levels in the neurons of mammalian vestibular ganglia.

Paul Popper, Wolfgang Siebeneich, Phillip A Wackym

Otolaryngology and Communication Sciences, Medical College of Wisconsin, 9200 W. Wisconsin Ave., Milwaukee, WI, United States

Opioid regulation of Ca^{2+} levels in the neurons of mammalian vestibular ganglia. Paul Popper, Wolfgang Siebeneich and Phillip A. Wackym. Department of Otolaryngology and Communication Sciences, Medical College of Wisconsin, Milwaukee, Wisconsin, 53226.

Neurotransmitters and neuromodulators identified in the vestibular epithelia modulate the vestibular afferent discharge. Glutamate increases the resting levels of cytoplasmic Ca^{2+} in neurons and is the neurotransmitter mediating the hair cell-vestibular afferent communication. One approach towards understanding modulatory pathways in the vestibular epithelia is to study the effects of neuromodulators on glutamate-induced changes in levels of Ca^{2+} in the

vestibular afferent neurons. This study investigates the effects of mu opioid receptor (MOR) agonist on glutamate-induced increase in cytoplasmic Ca^{2+} levels in primary cultures of vestibular ganglion neurons.

Vestibular ganglia of adult rats were dissociated for 45 minutes at 37°C with agitation in Dulbecco's modified Eagle's medium (DMEM) containing 0.5 mg/ml collagenase III after which trypsin (0.5 mg/ml) was added and incubated for 10 more minutes. The trypsin digestion was terminated with soybean trypsin inhibitor. The dissociated cells were collected by centrifugation, washed once in DMEM and suspended in DMEM containing 10% heat inactivated horse serum, penicillin, streptomycin and 100ng/ml nerve growth factor. The cells were plated on poly-L-lysine and laminin coated glass coverslips for 24 hours.

Immunoreactivity for MOR was found in 30% of the cultured neurons, similar to the distribution seen in vestibular ganglion sections. The present study presents a powerful system for the analysis of modulation of hair cell-afferent interaction.

Supported by NIDCD R01DC02971 (P.A.W.) and an intramural grant from the Toohill Research Fund of the Department of Otolaryngology and Communication Sciences.

635 Nerve fiber estimates in the human crista ampullaris using unbiased stereological techniques

Ivan Lopez¹, Gail Ishiyama², Michael Frank¹, Yong Tang³, Robert Baloh², Akira Ishiyama¹

¹Head and Neck Surgery, UCLA School of Medicine, CHS 62-132 10833 Le Conte Avenue, Los Angeles, CA, United States,

²Neurology, UCLA School of Medicine, C246 RNRC 710 Westwood Box 951769, Los Angeles, CA, United States,

³Neurobiology, Mount Sinai School of Medicine, Fishberg Research Center for Neurobiology, New York, NY, United States

The objective of this study was to apply unbiased stereology using the fractionator stereological probe to estimate the number of nerve fibers innervating the semicircular canal crista ampullaris from subjects with no history of audiovestibular disease. The temporal bone was carefully microdissected under the operating microscope and the branches to the individual vestibular organs were transected close to the endorgan. The specimens were embedded in resin and one micron thick transverse sections were made. The Stereo Investigator v4.34 software (Micro Bright Field) was used to overlay the grids and counting frames on video images from the microscope. Using the software, a contour perimeter was drawn around the crista and a grid with two-dimensional unbiased counting frames was randomly placed on the image to count the number of myelinated fibers according to the equation: $N = Q/ASF$, where Q is the number of fibers counted within the contour and ASF is the area sampling fraction. ASF is calculated as: $ASF = xy/(dx dy)$, where x , y represent the dimensions of each counting frame ($x = 40$ micron, $y = 30$ micron) and dx , dy represent the scan grid distance ($dx = 50$ micron, $dy = 40$ micron) traveled between the counting frames. In a 26 year old, there was a total of 2123 nerve fibers in the horizontal crista. In an 85 year old, there were 1458, 1125 and 1650 nerve fibers in the horizontal, posterior and superior crista respectively. From two 98-year-old individuals we found 1038 and 1005 nerve fibers in the horizontal

crista. These values are within the range of previous reports using hand-counting techniques (Lee et al 1990, *Laryngoscope*, 100: 756-764). The advantage of the present study technique is the accuracy and reliability, and the ability to obtain nerve fiber counts from a single crista within four to six hours with appropriate training and equipment.

636 Quantitative study of the vestibular sensory epithelium in cochleosaccular dysplasia.

Shin Kariya¹, Andre LL Sampaio¹, Sebahattin Cureoglu¹, Patricia A Schachern¹, Michael M Paparella², Takeshi Kusunoki¹, Mehmet Faruk Oktay¹, Kazunori Nishizaki³

¹Otolaryngology, University of Minnesota, 420 Delaware Street, Minneapolis, MN, United States, ²Otolaryngology, Minnesota Ear Head and Neck Clinic, 701 25th Ave.S. Suite 200, Minneapolis, MN, United States, ³Otolaryngology, Okayama University, 5-4-16, shikata-cho, Okayama, Japan

Cochleosaccular dysplasia is the most common pathologic finding seen in children with profound congenital sensorineural hearing loss. The pathologic changes in cochleosaccular dysplasia include the membranous labyrinth of the cochlea and saccule with a normal utricle and semicircular canals. There has been no quantitative study on the peripheral vestibular system in cochleosaccular dysplasia. Thirteen temporal bones with congenital deafness from 10 individuals were selected for this study from the temporal bone collection of University of Minnesota that showed suitable pathological findings for the histopathologic criteria of cochleosaccular dysplasia. Age-matched normal control temporal bones were also selected. The vestibular hair cells including type I hair cells and type II hair cells were counted separately in the saccular macula, utricular macula, and three crista of the semicircular canals using Nomarski microscopy. The hair cell densities of type I, and type II hair cells in the macula of the saccule in cochleosaccular dysplasia were significantly decreased as compared with the data of normal subjects. In contrast, both type I and type II hair cells in the utricular macula and the cristae of the three semicircular canals in cochleosaccular dysplasia were well preserved, and no significant difference was observed between the data of cochleosaccular dysplasia and that of normal controls in the utricle and the three semicircular canals. These findings suggest that histopathological findings in the cochlea and saccule as compared to normal findings in the utricle and semicircular canals may be because the saccule and the cochlear duct constitute the phylogenetically younger pars inferior of the labyrinth.

637 Orientations of Human Vestibular Labyrinth Semicircular Canals

Charles C. Della Santina, Valeria Potyagaylo, Lloyd B. Minor, Americo A. Migliaccio, John P. Carey

Dept. of Otolaryngology-Head & Neck Surgery, Johns Hopkins, 601 N. Caroline St 6260B, Baltimore, MD, United States

Analysis of vestibulo-ocular reflex experiments requires knowledge of the relative and absolute orientations of semicircular canals (SCC). Data on canal plane orientations in humans are sparse, apart from a classic study of 10 skulls (Blanks et al 1975) that concluded that the horizontal and anterior SCCs are not mutually orthogonal ($111 \pm 7.6^\circ$).

We hypothesized that this departure from the ideal is due to sampling error, and that a larger sample would yield canal orientations closer to the mutually orthogonal ideal. We examined 3-D multiplanar images from computerized tomography of the temporal bones of 22 normal human subjects. Images were acquired with 0.5 mm slice thickness and reconstructed with an in-plane resolution of ~ 0.2 mm.

There was no significant difference in any value between the right side and a mirror image of the left, so data were pooled for the 44 labyrinths. The angle between the anterior and posterior SCC was $94.0 \pm 4.0^\circ$ (mean \pm SD). The angle between the anterior and horizontal SCC was $90.6 \pm 6.3^\circ$. The angle between the horizontal and posterior SCC was $92.0 \pm 7.2^\circ$. The angles between a vector normal to the left horizontal SCC and the positive Reid's stereotaxic X (+nasal), Y (+left) and Z (+superior) axes were $108.7 \pm 7.6^\circ$, $92.2 \pm 5.8^\circ$ and $19.9 \pm 7.1^\circ$, respectively. The angles between a vector normal to the left anterior SCC and the positive Reid's stereotaxic X, Y and Z axes were $125.9 \pm 5.3^\circ$, $38.4 \pm 5.1^\circ$ and $100.1 \pm 6.3^\circ$, respectively. The angles between a vector normal to the left posterior SCC and the positive Reid's stereotaxic X, Y and Z axes were $133.6 \pm 5.4^\circ$, $131.5 \pm 5.2^\circ$ and $105.6 \pm 6.6^\circ$, respectively. The angle between an anterior SCC and the contralateral posterior SCC was $15.3 \pm 7.2^\circ$.

Human SCCs are more nearly orthogonal than previously reported.

Supported by NIH R01DC02390, K08DC06216, K23DC00196.

638 Superior Canal Dehiscence is Not Due to Cephalic Displacement of the Labyrinth

Valeria Potyagaylo, Charles C. Della Santina, Lloyd B. Minor, John P. Carey

Otolaryngology - Head & Neck Surgery, Johns Hopkins, 720 Rutland, Rm 710, Baltimore, MD, United States

Superior semicircular canal dehiscence (SCD) can result in a clinical syndrome marked by sound- and pressure-evoked vertigo and hyperacusis to bone-conducted sound. Evidence to date suggests that SCD is a developmental anomaly: it frequently occurs bilaterally in the absence of any erosive lesions or intracranial hypertension, and the location of dehiscence at the floor of the middle cranial fossa is the last portion of the temporal bone to ossify during development. We hypothesized that abnormally cephalic displacement of the otic capsule within the temporal bone could be a mechanism for abnormally thin bone between the canal and the middle fossa floor. Alternatively, abnormally vertical orientation of the superior canal (which is not normally exactly vertical) or abnormal canal radius could cause dehiscence. To test these hypotheses, we examined multiplanar images from computed tomography of the temporal bones of 14 subjects with SCD 22 normal controls. CT images were acquired with 0.5 mm slice thickness and reconstructed with an in-plane resolution of ~ 0.2 mm. The superior semicircular canals in 21 dehiscent SSC were neither higher in the temporal bone nor more vertical in orientation than the superior canals of normal subjects. The mean \pm SD distance from Reid's horizontal plane to the topmost extent of the 21 SSC in dehiscent canals was 15.8 ± 1.8 mm, which was not significantly different from normal (15.0 ± 1.9 mm, $N=44$, $p>0.11$). The angle of the superior canal with respect to Reid's horizontal plane

in dehiscence SSC was $97 \pm 6.0^\circ$, which was not significantly different from normal ($100.1 \pm 6.3^\circ$, $p > 0.13$). While SCD may be due to a developmental anomaly, these data suggest that it is not due to cephalic displacement of the labyrinth or abnormally vertical orientation of the superior canal.

Supported by NIH NIDCD DC02390, DC06216 & DC00196.

639 Structural and ultrastructural changes in semicircular canal cristae after intratympanic gentamicin treatment in the chinchilla

Lee Ching Wu Anderson¹, Timo P. Hirvonen², Mohamed Lehar¹, Lloyd B. Minor¹, John Patrick Carey¹

¹Otolaryngology-Head and Neck Surgery, Johns Hopkins University School of Medicine, Ross 833, 720 Rutland Ave., Baltimore, MD, United States, ²Otolaryngology, Helsinki University Central Hospital, FI-00029 HUS, Helsinki, Finland

Intratympanic gentamicin treatment is frequently used to treat intractable vertigo due to Ménière's disease. While commonly referred to as "chemical labyrinthectomy," intratympanic gentamicin does not silence the spontaneous firing of vestibular afferents (ARO Abst. 513, 2002). We hypothesized that at least some vestibular hair cells and their synaptic specializations must be preserved in order to provide the synaptic input necessary to maintain firing in the vestibular afferents. Adult chinchillas received a single, unilateral intratympanic gentamicin injection (26.7 mg/ml, 30 min exposure); the contralateral ears served as controls. Animals were sacrificed and fixed 5-28 d later. Semicircular canal cristae were sectioned for light and electron microscopy. Cristae treated with intratympanic gentamicin had 25% of the control density of type I hair cells ($p = 0.04$) and 64% ($p = 0.07$) of the control density of type II hair cells. The density of supporting cells on the treated side was 89% of that of the control side, and was not significantly changed by intratympanic gentamicin treatment ($p = 1.0$). Electron microscopy demonstrated that remaining type II hair cells were contacted by bouton afferent endings. Ribbon synapses with post-synaptic densities and efferent boutons were also observed. A single intratympanic gentamicin treatment does not create a complete labyrinthectomy. Rather, some hair cells and their synaptic specializations are preserved, which provides the synaptic input to maintain spontaneous firing of vestibular nerve afferents. Preservation of spontaneous firing after intratympanic gentamicin may decrease the adaptive burden for the central vestibular nuclei in comparison to surgical labyrinthectomy. (Supported by NIH R03 DC005700, K23 DC00196, R01 DC02390)

640 Characteristics of Sound-evoked Vestibulo-ocular Reflexes In Awake and Trained Monkeys

Wu Zhou^{1,2}, Ivra Simpson¹, William Mustain¹, Youguo Xu¹

¹Otolaryngology and Communicative Sciences, University of Mississippi Medical Center, 2500 North State Street, Jackson, MS, United States, ²Neurology & Anatomy, University of Mississippi Medical Center, 2500 North State Street, Jackson, MS, United States

Acoustic activation of the vestibular system has been well documented and recording of vestibular-evoked myogenic potentials

has been widely accepted as an effective non-invasive clinical test of otolith function. Although sound-evoked eye movement has been observed in patients with Tullio phenomenon, it has not been demonstrated in normal human subjects. The goal of the present study is to establish a non-human primate model of sound-evoked eye movements, which can be used to study the neural mechanisms underlying acoustic activation of the vestibular system. We found that a click (0.1~1ms, 100~125 dB peak SPL) delivered to one ear evoked binocular horizontal eye movements away from the stimulated ear with latencies of 4.9 ± 0.3 ms in the ipsilateral eye and 5.3 ± 0.2 ms in the contralateral eye. The click also evoked binocular vertical eye movements with latencies of 10.3 ± 1.7 ms in the ipsilateral eye and 9.9 ± 1.5 ms in the contralateral eye. The evoked horizontal eye movements were disjunctive, with larger amplitudes in the ipsilateral eye. We found that the amplitudes of sound-evoked eye movements not only depended on the parameters of the click, such as intensity, polarity and duration, but also depended on the gaze eccentricity and vergence angle. Furthermore, we showed that the bilateral evoked responses could be predicted by the linear summation of the responses evoked by the unilateral stimulation of each ear. These results suggest that the sound-evoked eye movements in monkeys may be an useful model system to study the neural circuits underlying the acoustic activation of the vestibular system. The extension of this paradigm to humans may be useful in developing an alternative clinical test of otolith function.

Supported by NIH R01 DC05785 to Dr. Wu Zhou

641 Bilateral labyrinthectomy reduces linear acceleration-evoked cardiovascular responses in awake rats

Hong Zhu¹, James Randy Jordan¹, Xiaorong Li¹, Byron Pearson Windham¹, Ben Jeffcoat¹, Wu Zhou^{1,2}

¹Otolaryngology, University of Mississippi Medical Center, 2500 N State Street, Jackson, MS, United States, ²Neurology and Anatomy, University of Mississippi Medical Center, 2500 N State Street, Jackson, MS, United States

The vestibular-cardiovascular reflex is important in the regulation of blood pressure during postural changes. Our previous studies showed that linear acceleration, which selectively activates otolith system, induces characteristic cardiovascular responses in rats (Zhu et al., 2002). In the present study, in order to determine that the observed responses are of vestibular origin, we examined the effects of bilateral labyrinthectomy on the linear acceleration-evoked blood pressure changes in awake Sprague-Dawley rats. The rats were stabilized on a linear sled by a surgically implanted head holder. Blood pressure was measured via a chronically implanted abdominal aortic catheter. The linear motions were in four directions (forward, backward, leftward and rightward) and consisted of an acceleration phase of 200ms (3m/s^2) followed by a deceleration phase of 200ms (3m/s^2). In intact animals, transient linear motion produced short latency (about 400ms) bi-phasic responses in blood pressure in any of the four directions tested. The responses in blood pressure consisted of an increasing phase (about 4s) followed by a decreasing phase (about 4s). For the 4 of 4 rats receiving bilateral labyrinthectomy, which was achieved by intraotic injection of streptomycin, the linear acceleration-evoked blood pressure changes were significantly reduced ($p < 0.05$) one

day after the surgery. However, in 2 rats receiving unilateral labyrinthectomy, there were no changes in linear acceleration-evoked changes in blood pressure ($P>0.05$). These results suggest that the linear acceleration-evoked cardiovascular responses are of vestibular origin.

Supported by NIH R03 DA16440 to Dr. H. Zhu and NIH R01 DC05785 to Dr. W. Zhou

642 Vestibulo-Ocular Motor Processing Requires Cognitive Resources in Patients with Vestibular Loss

Mark S Redfern¹, Michael E Talkowski², Joseph M. Furman³, J Richard Jennings²

¹Department of Bioengineering, University of Pittsburgh, 110 EEI, Pittsburgh, PA, United States, ²Department of Psychiatry, University of Pittsburgh, 110 EEI, Pittsburgh, PA, United States, ³Department of Otolaryngology, University of Pittsburgh, 110 EEI, Pittsburgh, PA, United States

This study investigated the role of cognition in the vestibulo-ocular reflex (VOR) and ocular pursuit using a dual-task paradigm. We hypothesized that cognitive resources were involved in successful processing and integration of vestibular and ocular motor sensory information, and this requirement would be greater in patients with absent unilateral vestibular function. Sixteen patients with surgically confirmed absent unilateral peripheral vestibular function and sixteen healthy age and gender-matched controls underwent seven combinations of vestibular, visual, and visual-vestibular stimulations while performing three different information processing tasks (IPTs). Vestibular stimulation conditions were a semicircular canal and an otolith stimulus provided through seated chair rotations. Visual-only conditions involved fixation on a laser target and sinusoidal smooth pursuit while still, and visual-vestibular interaction included fixation on a head-fixed laser target during semicircular canal stimulation. The IPTs included three different auditory reaction time tasks: 1) Simple Reaction Time, 2) Disjunctive Reaction Time, and 3) Choice Reaction Time. The results of this investigation show increases in reaction times in patients and controls during all vestibular stimulation conditions and during ocular pursuit. There were also significant interactions of group and IPT as well as group and vestibular stimulation. Patients with unilateral vestibular dysfunction showed greater decrements in information processing during vestibular stimuli than controls. These results reveal interference between vestibulo-ocular processing and a concurrent reaction time task, suggesting the VOR and ocular motor system are dependent upon cognitive resources to some extent and are not fully automatic systems. The particularly large decrement in IPT performance of the patients as compared to controls during vestibular stimulation, but not visual stimulation or visual-vestibular interaction, imply that vestibular processes in patients who have clinically compensated for unilateral vestibular dysfunction require increased cognitive requirements for successful sensory processing and locomotion.

643 Middle Ear Transfer Function: Alterations in Aged Rats

Joseph F. Cannuscio, James C. Saunders, Michael Anne Gratton

Otorhinolaryngology-HNS, University of Pennsylvania, 3400 Spruce St, Philadelphia, PA, United States

While much is known about cochlear pathophysiology in presbycusis, little is known regarding the contribution of altered middle ear structure and function to presbycusis. The role of the middle-ear system in the aged ear has not been systematically investigated. The middle ear may be an important, and thus far unrecognized, factor contributing to hearing loss in the elderly.

We hypothesize that deterioration in structure of the aged tympanic membrane results in deterioration in the tympanic membrane velocity transfer function. The middle-ear velocity transfer function measured at the umbo of the tympanic membrane was compared between young and aged Brown-Norway rats. Measures of thickness and cellular organization were obtained from digitized images of tympanic membrane cross-sections.

Velocity transfer functions from tympanic membranes of aged Brown-Norway rats indicate that from 0.39 to 8.5 kHz, the sensitivity declines at a slightly faster rate than observed in the young adult rats. From 0.39 to 32.0 kHz, the aged animals have a decidedly lower response than the younger group. This is also true at the highest frequencies. The aged animals had decreased velocity responses from 1.6 to 9.6 dB across frequency. Measures of TM thickness were made near the tympanic ring, at the umbo, and at a location approximately halfway between. The data show that a decrease in TM thickness occurs in the region halfway between the umbo and tympanic ring in the aged rats. The difference in TM thickness as a function of aging is speculated to be due to altered collagen content of the tympanic membrane, which influences the ability of the tympanic membrane to replicate the acoustic signal. The data suggest that a portion of age-related hearing loss may be due to altered middle ear function. Furthermore, the reduction in the velocity transfer function may be related to diminished cellular content of the aged tympanic membrane.

Supported by NIA R03-AG021728 to MAG

644 Effect of age on the metabolic activity of the avian cochlear nucleus

Susan Elizabeth Smittkamp, Dianne Durham

Otolaryngology-Head and Neck Surgery, University of Kansas Medical Center, 3901 Rainbow Blvd., Kansas City, KS, United States

Most commercially raised broiler chickens display progressive cochlear degeneration with age [Durham et al., *Hear. Res.* 166 (2002) 82-95]. Recent work examining the combined effects of age and cochlear degeneration on the metabolic activity of the avian cochlear nucleus (CN) showed that in general down-regulation of metabolic activity occurs as a function of age and cochlear damage [Smittkamp et al., *Hear. Res.* 175 (2003) 101-111]. The relative contributions of age and cochlear degeneration to this change in CN metabolism are unknown.

Here, CN neuron metabolism is examined in 2, 5, 10, 30, 39, and 52 week-old commercially raised broiler chickens with normal

cochleae. Normal cochlear anatomy is verified using scanning electron microscopy. CN metabolic activity is assessed using cytochrome oxidase histochemistry. Optical density measurements are made in rostral and caudal CN neurons to assess activity in both a high and a low frequency region. CN neuron activity levels are compared across age groups of birds with normal cochleae to determine the effect of age on CN metabolism. Data from these normal birds are compared to CN activity levels of age-matched commercially raised birds with damaged cochleae from our previous study to determine the contribution of cochlear damage to the decreased CN metabolism observed previously. Data from these normal birds are also compared to CN activity levels of age-matched birds with normal cochleae from the previous study that were raised in a quiet environment to examine the effect of auditory environment on CN metabolism.

Results indicate that age alone does not result in down-regulation of CN metabolism. Commercially raised birds with damaged cochleae have significantly decreased CN activity levels when compared to age-matched commercially raised birds with normal cochleae. Therefore, the decrease in CN metabolism observed previously appears to have been caused by the extensive cochlear damage found in those birds. Auditory environment also affects CN metabolism. Birds with normal cochleae that were raised in a quiet environment have significantly decreased CN activity levels when compared to age-matched commercially raised birds with normal cochleae.

Supported by NIDCD R01 DC01589 and DC004982.

645 Volumes of Superior Olivary Nuclei of CBA Mice During Aging

Aaron Isaac Brescia¹, Robert D. Frisina², Kejian Chen¹, Donald Godfrey¹

¹Otolaryngology, Medical College of Ohio, 3065 Arlington Ave., Toledo, Ohio, United States, ²Otolaryngology, University of Rochester Medical Center, 601 Elmwood Ave., Rochester, New York, United States

Presbycusis has been associated with loss of neurons in human cochlear nucleus (Arnesen, 1982), and neuron loss in the anteroventral cochlear nucleus (AVCN) of aging CBA mice has been reported (Willott, Jackson, and Hunter, 1987). In the medial nucleus of the trapezoid body (MNTB), loss of neurons and synaptic terminals has been reported in aged rats (Casey and Feldman, 1982, 1988). We explored age-related changes in two nuclei of the superior olivary complex of CBA mice: the lateral superior olive (LSO) and MNTB. The LSO receives major input from the anterior part of the AVCN, whereas the MNTB receives major input from its posterior part. Both nuclei are intimately involved in sound localization. CBA mice 3, 12, and 24 months of age were euthanized and their brains frozen. Frozen sections were cut and alternate ones stained for Nissl substance. Nuclear boundaries were traced on both sides of each stained section (except damaged ones), and areas were calculated using NeuroLucida. Volumes were calculated as sum of area times distance between sections. Single-factor ANOVA was used to determine statistical significance. Volumes for the nuclei, in cubic millimeters, as mean \pm SEM, for 10 nuclei in 5 young mice, 8 in 4 middle-aged mice, and 10 in 5 old mice, respectively, are, for MNTB, 0.035 ± 0.0014 , 0.034 ± 0.0012 , and 0.029 ± 0.0015 , and for LSO, 0.048 ± 0.0032 ,

0.046 ± 0.0033 , and 0.047 ± 0.0040 . The lack of change in LSO resembles previous findings for neuron number in rats (Casey, 1990). The MNTB volume in the old mice was significantly smaller than in the young and middle-aged mice ($P < 0.01$). Further, among all the mice, there was a significant inverse correlation ($P < 0.01$) between elevation of auditory brainstem response threshold and average MNTB volume ($r = -0.70$). These results, with the previous findings for aged rats, suggest that declining MNTB function in old age may contribute to deterioration of hearing.

Supported by NIH (NIA) grants AG18972 and AG09524

646 Do Levels of HSF1 Change with Age in the Inferior Colliculus?

Ninef E. Zaya, Teresa S. Wilson, Larry F. Hughes, Robert H. Helfert

Surgery, Division of Otolaryngology, Southern Illinois University, P.O. Box 19638, Springfield, Illinois, United States

The inferior colliculus (IC) undergoes synaptic and dendritic losses due to aging. To what extent these losses are related to oxidative stress or deafferentation and how they may contribute to presbycusis are being studied. Heat shock factor 1 (Hsf1) is an upstream regulator of heat shock proteins and also induces superoxide dismutase. The objective of this study was to determine if Hsf1 is induced in the IC as a result of heat stress, and whether aging alters its expression.

Four- and 25-month-old F344 rats were exposed to either ambient temperature or thermal stress resulting in a 3 °C elevation in body temperature over a 30-minute time period. Following a one-hour post-stress survival time the rats were euthanized, and the ICs and cerebella (CB) harvested. Western blots were performed to measure Hsf1 in IC and CB homogenates. ANOVA was used to analyze the data.

It has been shown that protein bands for Hsf1 are located at 70-74 kDa. Using an anti-HSF1 monoclonal antibody we identified two bands near 50 kDa. We suspect that the bands contain Hsf1 protein, perhaps in a degraded form. In the 25-month old controls the protein levels in the IC bands were $21.46\% \pm 5.05\%$ greater than those measured in the 4-month old controls ($p = .017$). However, there were no detectable differences in IC levels between the two heat-stressed age groups ($p = .772$). Conversely, in the CB there were no detectable differences in protein levels between the ambient control groups ($p = .281$), but there was a trend toward elevated CB protein levels in the 25-month-old heat stressed group relative to the 4-month olds ($+23.69\% \pm 7.89\%$; $p = .085$). If the protein bands measured in this study are Hsf1, then these data suggest that Hsf1 is moderately elevated in the IC of aged rats under normal circumstances, and that its expression with or without stress may vary by brain region. Experiments are in progress to verify these findings.

Funded by Dept. of Surgery & Associate Dean for Research, SIU Sch. of Med.

647 Age-Related Kv 3.1b Expression in the Cochlear Nucleus and Inferior Colliculus of CBA/CaJ mice

Martha L Zettel, Robert D Frisina

Otolaryngology Division, University of Rochester Medical School, 601 Elmwood Ave, Rochester, New York, United States

Voltage gated potassium channels may be important in determining the temporal firing properties of auditory brainstem neurons. Kv3 channels of the Shaw family have relatively high thresholds, account for rapid repolarization, shorter spike duration, and high maximum discharge rate. Kv3.1b channel proteins are strongly expressed in the neurons of auditory brainstem of mice. Previous work by our group has shown a 76% decline in Kv3.1b expression in the medial nucleus of the trapezoid body (MNTB) in 15-month CBA mice (vs. 3-month mice). To determine if this decline is a system-wide age-related loss or is unique to the aging MNTB, we examined the relative optical density of Kv3.1b staining in the cochlear nucleus (CN) and inferior colliculus (IC) of 3-4 month, 15 month, 24-26 month, and 31-34 month CBA/CaJ mice (n=20) used in the previous study. Images of the CN and IC in Kv3.1b-immunostained sections were digitally captured using a Spot Insight® camera (Diagnostic Instr., Sterling Heights, MI). Relative optical density (OD) was determined using Image Pro Plus 4® (Media Cybernetics, Silver Springs, MD). Mean OD was determined and ANOVAs performed.

The central nucleus and dorsal cortex of the IC, as well as the octopus cell region of CN, exhibited moderate expression of Kv3.1b in mice of all age groups. Kv3.1b was also strongly expressed in the dorsal CN and remaining ventral CN. However, in stark contrast to the age-related decline found previously in MNTB, Kv3.1b expression did not decline with age in the IC and CN. Thus, the temporal processing deficits found in aging CBA/CaJ mice are not accompanied by changes in Kv3.1b channel protein expression in the IC and CN.

Support: NIH-NIA P01 AG09524, NIDCD P30 DC05409 & Int. Ctr. Hearing Speech Res.

648 Age-Related Changes in Response Properties of Rat A1 Layer V Neurons

Jeremy G Turner¹, Larry F Hughes², Donald M Caspary^{1,2}

¹Pharmacology, Southern Illinois University School of Medicine, 801 N. Rutledge, Springfield, IL, United States, ²Surgery, Southern Illinois University School of Medicine, 801 N. Rutledge, Springfield, IL, United States

FBN rats exhibit slow, progressive sensorineural hearing loss (presbycusis). In man, presbycusis is associated with known peripheral pathology and central auditory deficits. Central deficits may be due, in part, to factors including central plasticity secondary to the reduced peripheral input, as well as de novo aging effects. The present study examined central correlates of presbycusis by measuring response properties of A1 layer V neurons in young and old FBN rats. As layer V neurons represent a major output to other cortical and subcortical regions, describing age-related changes in their function could be an important first step toward understanding central aging effects on auditory processing. In vivo single-unit extracellular recordings were obtained from 114 aged

(30-32 months) and 105 young-adult layer V neurons (4-6 months). Age was associated with an altered distribution of receptive field types, with a reduction in the number of neurons showing classic V/U-shaped excitatory receptive fields and an increase in neurons showing more complex receptive fields. Three consecutive receptive field maps were obtained from all neurons. Sequential maps from old neurons varied significantly across runs. Age differentially affected the stimulus-driven activity of neurons relative to the receptive field type of the neuron studied; old neurons exhibited less on-stimulus firing in V/U-shaped receptive field neurons and more on-stimulus firing in Complex neurons (which are associated with inhibited firing in young controls). Finally, old neurons with Complex receptive fields were more easily excited using extracellular current pulses delivered to the soma. These findings provide support for the notion that age is associated with diminished signal-to-noise coding for A1 neurons and are consistent with other research suggesting that GABAergic neurotransmission in A1 may be compromised in old age. (supported by DC00151)

649 Altered GABA_A Receptor Binding in Aged Rat Primary Auditory Cortex

Lynne Ling¹, Larry Hughes², Donald M. Caspary^{1,2}

¹Pharmacology, SIU School of Medicine, 801 N. Rutledge, Springfield, IL, United States, ²Surgery, SIU School of Medicine, 801 N. Rutledge, Springfield, IL, United States

GABA has been shown to play a major role in processing complex acoustic signals at many levels of the auditory system. Primary auditory cortex (A1) is endowed with a rich network of GABAergic neurons and extrinsic GABA inputs throughout its layers. Previous studies demonstrate that aging alters GABA and glycinergic systems throughout the auditory neuroaxis, perhaps in response to an age-related slow peripheral degradation of the auditory input into the brain. Preliminary studies of A1 have shown significant age-related down-regulation of the alpha1 subunit and up-regulation of the alpha3 subunit. These findings suggest altered pharmacology of aged A1 due to altered GABA_A constructs. Quantitative receptor binding autoradiography was used to examine age-related layer-specific changes in the pharmacology of the GABA_A/benzodiazepine receptor. ³[H]TBOB, a picrotoxin analog, binds to the cage convulsant site in the chloride channel. Using increasing concentrations of GABA to modulate TBOB binding, a significant age-related decrease in TBOB binding was observed in layer VI of rat A1. The shift in the GABA dose response curve in layer VI of aged rats suggests a change in GABA's efficacy to alter ³[H]TBOB binding and likely reflects the altered GABA_A receptor subunit composition. ³[H]RO15-4513 is a sensitive ligand for GABA_A alpha subunits in GABA_A receptor constructs. Preliminary saturation analysis with this ligand found small age-related changes in the maximum number of binding sites across A1 layers, but significantly altered affinity in aged rat A1. These preliminary binding studies corroborate previous studies of age-related subunit changes of GABA_A receptor composition. These findings suggest that the changed GABA_A receptor in A1 could result in altered coding of acoustic information in the elderly. (Supported by DC00151)

650 Individual Differences on Measures of Hearing and Temporal Processing in the Aging CBA Mouse

Paul D Allen, Peter J Rivoli, James R Ison

Brain and Cognitive Sciences, University of Rochester, Meliora Hall, Rochester, NY, United States

A common observation in presbycusis research is the greater heterogeneity among old subjects compared with the young, even in laboratory mice with minimal genetic diversity and housed under strictly controlled conditions. One promising means of understanding the neurobiological basis of this age-related diversity is to measure levels of gene expression in individual animals with behaviorally and electrophysiologically well-defined phenotypes. The data presented here were collected in order to characterize the hearing of mice prior to their use in a companion study of age-related change in gene expression in the mouse cochlea and inferior colliculus (see D'Souza et al, ARO '04, in review). In addition to auditory brainstem response (ABR) thresholds, we performed 5 behavioral experiments that utilize the acoustic startle response and its inhibition by pre-stimuli, to assess auditory temporal processing in CBA mice from three age groups: 3-4 month old (YOUNG, N=10), 10-15 month old (MIDDLE-AGED, N= 17) and 26-34 month old (OLD, N= 19). ABR thresholds averaged from 3 to 48 kHz are elevated with age: +10 dB for MIDDLE-AGED mice and +43 dB for OLD mice compared to the YOUNG. The OLD mice were ranked in order of average ABR threshold and partitioned into 2 groups with average threshold shifts of +36 (OLD LT) and +53 dB (OLD HT) having mean ages of 28.7 and 30.0 months, this difference being marginally significant ($p < 0.1$). The temporal processing measure most different between OLD LT and OLD HT was temporal integration, assessed by the degree of summation of two 1-ms startle pulse as the SOA varied from 1 to 10 ms. The OLD LT mice show an integration window that is delayed and prolonged compared to the younger groups of mice, while the OLD HT animals were totally unresponsive to brief stimuli. Detection of 100 Hz SAM was robust for both old groups, while degraded compared to the younger mice, and auditory spatial discrimination and gap detection measures were very poor in both OLD groups, and auditory spatial discrimination was reduced in the MIDDLE-AGED group compared to the YOUNG. These data demonstrate that peripheral hearing loss has a dominant effect on some but not all measures of temporal processing, and that central age-related changes, presently of unknown origin, also contribute to hearing. *Work supported by NIH-NIA Grant #AG09524*

651 Progression of Hearing Loss in the C57 Mouse Model of Presbycusis: A Longitudinal Study

Marjorie S. Waterman¹, Xiaoxia Zhu¹, David Tuttle¹, Robert D. Frisina^{1,2}

¹Otolaryngology Div., Univ. Rochester Med. Sch., 601 Elmwood Ave., Rochester, New York, United States, ²Neurobiology & Anatomy, Univ. Rochester Med. Sch., 601 Elmwood Ave., Rochester, New York, United States

The C57 mouse strain displays a rapid sensorineural hearing loss (HL) making it useful for studying presbycusis - age-related hear-

ing loss (HL). This HL starts in high frequencies and extends to lower ones with age. Also, young adult C57s have poor medial olivocochlear (MOC) efferent function. The aim of this study was to determine the time course of early HL in C57s in more detail. So, auditory brainstem response (ABR), distortion product otoacoustic emissions (DP), and contralateral suppression (CS) of DPs were collected for young C57s (8 male, 8 female). From these data, auditory sensitivity, outer hair cells (OHC), and the MOC system were evaluated, respectively. ABR, DP, and CS data were collected bi-weekly from 6-10 weeks (w) of age. DP-grams were obtained with L1/L2 = 65/50 dB SPL, f1/f2=1.25, for the frequency range 5.6 to 44.8 kHz. DPs were recorded in quiet and with a contralaterally applied 3-30 kHz wideband noise (WB), both at 55 dB SPL. CS was present in all mice at low frequencies. CS was present at all frequencies at 6w, but by 10w CS was lost at mid and high frequencies. The DP-gram for 6w differed from that of 8 and 10w at frequencies ≥ 41 kHz; with 8 and 10w showing high-frequency DP declines. No DP change was noted between 8-10w. Lastly, ABRs showed no changes with age by 10w. In conclusion, C57 mice do have good MOC function at 6w but this function declines rapidly. The progression of age-related HL in C57 mice begins with the MOC system (due to both mid and high frequency declines). With aging, the declines extend to the OHC system (showing only high frequency declines thus far) and finally to overall auditory sensitivity (no change through 10w).

Support: NIH-NIA P01 AG09524, NIDCD P30 DC05409 & Int. Ctr. Hearing Speech Res.

652 Contralateral Suppression of Otoacoustic Emissions with a 12 kHz Tone Declines with Age in CBA/BaJ Mice

George I. Varghese¹, Xiaoxia Zhu¹, Robert D. Frisina^{1,2}

¹Otolaryngology Div., Univ. Rochester Med. Sch., 601 Elmwood Ave., Rochester, New York, United States, ²Int. Ctr. Hearing Speech Res., Rochester Inst. Technology, Shumway Commons, Rochester, New York, United States

One role of the medial olivocochlear (MOC) auditory efferent system is to suppress outer hair cell (OHC) responses of the cochlea when presented with a contralateral sound. Using distortion product otoacoustic emissions (DPOAEs), the effects of active suppression of the MOC as a function of age can be observed when contralateral stimulation of a pure tone is applied. We previously have shown that there are age-related declines of the MOC when white noise is presented to the contralateral ear. In this study, we measured age-related changes in CBA/BaJ mice by comparing DPOAE generation with and without 12 kHz contralateral stimulation. Young (n=8), middle (n=14) and old aged (n=12) CBA mice were tested. DPOAE-grams were obtained using L1=65 and L2=50 dB SPL, f1/f2=1.25, with 8 points per octave covering a frequency range of 5.6-44.8 kHz. The 12 kHz sound was presented contralaterally at 55 dB SPL. DPOAE grams and ABR levels showed age related hearing loss. Similarly, there was an overall decline in contralateral suppression in the middle-aged and old groups relative to the young group. The young group demonstrated maximal suppression at 12 kHz; the frequency of contralateral stimulation. These results indicate that there are significant age-related declines in the efficiency of the MOC suppression mechanism. Thus, the MOC may play a role in the early onset of

presbycusis. Further study of various pure tone frequencies as well as MOC functioning in other strains (C57) are under evaluation.

Support: NIH-NIA Grant P01 AG09524, NIDCD P30 DC05409 and Int. Ctr. Hearing & Speech Res., Rochester NY, USA.

653 Strength of the Auditory Efferent System in CBA and C57 Mice with Varying Contralateral Wideband Noise Sound Intensity

Scott R. Newman¹, Xiaoxia Zhu¹, Robert D. Frisina^{1,2}

¹Otolaryngology Div., Univ. Rochester Med. Sch., 601 Elmwood Ave., Rochester, New York, United States, ²Int. Ctr. Hearing Speech Res., Rochester Inst. Tech., Lomb Mem. Dr., Rochester, New York, United States

The auditory efferent system plays presumed roles in enhancing signals in noise, maintaining the cochlea for optimal acoustic signal processing, and preserving auditory function in the face of ototoxic events. Previous studies have employed distortion product otoacoustic emissions (DPOAEs) to measure age-related changes of the medial olivocochlear (MOC) efferent system in humans and mice, and have identified a decrease in DPOAE levels, as well as a decline in contralateral suppression (CS) with age. The objective of this study was to identify differences in the MOC efferent response with changes in the sound intensity of contralateral wideband noise. Study Design: Young adult CBA and C57 mice (2-4 months of age) were tested. Auditory brainstem responses were obtained prior to DPOAE testing to confirm normal hearing abilities. Methods: Mice were anesthetized with ketamine/xylazine. 2f1-f2 DPOAE-grams (5-44 kHz), L1=65 and L2=50 dB SPL, f1/f2=1.25, using 8 points per octave, were recorded while presenting a range of wide band noise intensity levels to the contralateral ear (0 to 67 dB SPL, 3-30 kHz bandwidth). Results: For CBAs, there was a tendency for CS to be more pronounced with higher levels of contralateral wide-band noise, especially for low frequencies of the mouse hearing range. In contrast, C57s demonstrated much less CS, and insignificant change with increasing contralateral wideband noise levels. These findings suggest that the young adult CBA efferent system is more responsive than the C57, and that responsiveness to increases in contralateral intensity occurs maximally at low frequencies.

Support: NIH grants NIA P01 AG09524, NIDCD P30 DC05409 and the Int. Ctr. Hearing Speech Res.

654 Sex Differences in Age-related Decline of the Auditory Efferent System in CBA Mice

Xiaoxia Zhu¹, SungHee Kim², Robert D. Frisina¹

¹Otolaryngology, Univ. Rochester Medical School, 601 Elmwood Ave., Rochester, New York, United States, ²Otolaryngology, Daegu Fatima Hospital, 302-1, Shinam 4 dong, Dong gu, Korea, Democratic People's Republic of

It has been known for some time that aged women have better auditory sensitivity than men, even when lifestyle factors are controlled for. Additional sex differences for age-related hearing loss (presbycusis) are beginning to be understood. Recently, Frisina et al. (2003, Soc. Neuroscience Abstr) reported that premenopausal CBA female mice have distortion product otoacoustic emissions

(DPOAEs) with greater amplitudes than age-matched males. The CBA is a mouse strain that maintains relatively good auditory sensitivity into senescence. The purpose of the present study was to evaluate sex differences in age-related changes of the medial olivocochlear (MOC) efferent system using contralateral suppression (CS) of DPOAEs. CBA mice were grouped by age (2-3 mon, 6-8 mon, 14-16 mon, 24-30 mon), and underwent auditory brainstem response (ABR) and DPOAE testing. CS magnitude was defined and calculated as DPOAE level with contralateral noise minus DPOAE level in quiet. DPOAEs were obtained with L1=65 and L2=50 dB SPL, f1/f2=1.25, using 8 points per octave covering a wide range of 5.6-44.8 kHz (geometric mean frequency). Wideband noise (3-30 kHz bandwidth) was applied to the contralateral ear at 55 dB SPL. We excluded recordings where DPOAE amplitude was less than 6 dB above the noise floor. There were age-related declines in ABR and DPOAE amplitudes in both male and female CBA mice. CS magnitude of young adult females (2-3 mon) was significantly greater than the young adult males. Females showed a bigger decline of CS with age than males. The present results suggest that as young adults, female CBA mice have a stronger MOC efferent system than males, which then declines faster with age relative to males.

Work supported by NIH-NIA P01 AG09524, NIDCD P30 DC05409 and the Int. Ctr. Hearing Speech Res.

655 The effects of grape skin preparation (GSP) on age-related hearing loss and DNA damage

Michael D Seidman¹, Nadir Ahmad¹, Dipa Joshi¹, Jake E Seidman¹, Francis Leong¹, Nimisha Patel¹, Jie Wang¹, Wayne Quirk²

¹Oto-HNS, Henry Ford Health System, 6777 West Maple Rd., West Bloomfield, MI, United States, ²Administration, Central Washington University, 400 E University Way, Ellensburg, WA, United States

This preliminary study was designed to determine the effects of Grape Seed Preparation (GSP) consumption in an aging rat model. Specifically, the study assessed the protective effects of GSP on auditory sensitivity and DNA damage. The World Health Organization (WHO) has provided evidence that the reason for the 42% lower rate of heart disease in Southern France is the consumption of red wine in general, and specifically, the ingestion of Resveratrol, a component of grapes. Grape seed preparation (GSP) was provided by the California Table Grape association and consists of red, green and blue-black California grapes. The sugar content of these grapes is ~ 15%. Thirty 14 month old Fisher 344 rats were used for the study. Fifteen subjects were gavaged 5/7 days with a vehicle control (15% sugar) while the other fifteen were gavaged on the same schedule as GSP treated subjects. Animals underwent baseline auditory testing using auditory brainstem responses (ABR), followed by the institution of the treatment or control. ABR's were then obtained every 6 months for 18 months. Results demonstrate a statistically significant protective effect on the expected auditory decline associated with normal aging in the GSP treated subjects. Histologic analysis confirms the physiologic data and DNA integrity will also be addressed. These findings support the idea that antioxidants, such as resveratrol, protect against disease states and normal aging processes.

656 Cochlear antioxidant defense systems in presbycusis

Su-Hua Sha, Hongyan Jiang, Gary Dootz, Jochen Schacht

University of Michigan, Kresge Hearing Research Institute, 1301 E. Ann Street, Ann Arbor, MI, United States

Presbycusis, age-related hearing loss, is a major reason for social isolation and loss of quality of life in the elderly. Fifty percent of people 75 years of age and older exhibit hearing loss of sufficient magnitude to confer difficulty in understanding conversational speech. Research on the biological mechanisms underlying general aging processes has identified a relationship between longevity and reactive oxygen species (ROS), and tissue survival is often correlated with increased resistance to oxidant stress. Increased mitochondrial deletions with age also indicate the effects of oxidant stress.

In this study, we use CBA mice that show largely normal auditory thresholds until 18 months of age, after which thresholds increase as measured by auditory brainstem response. The functional loss is paralleled by a loss of hair cells. Our data show that total antioxidants in the cochlea decrease with age and that Mn-superoxide dismutase (SOD2), one of the mitochondrial antioxidant enzymes, is also reduced, particularly in the outer hair cell region. Furthermore, redox sensitive signal transduction pathways are also affected as seen in a decreased level of phospho-Akt.

This study was supported by pilot grants to Dr. Sha from the National Institute of Aging (for aged animals) and from the Claude Pepper Older Americans Independence Center at the University of Michigan.

657 Influence of the iNOS Mutant Allele on Age-related Hearing Loss (ARHL) in Mice with Different Genetic Backgrounds

Irina Omelchenko, Alfred L. Nuttall

Oregon Hearing Research Center, Oregon Health & Sciences University, 3181 SW Sam Jackson Park Rd NRC04, Portland, OR, United States

Nitric Oxide (NO) plays important roles in cell physiology. The range of NO effects varies from participating in normal synapse function and in vasoregulation to forming the highly toxic compound peroxynitrite that may cause DNA breaks leading to cell aging and death. During a cell's lifetime, expression of inducible NO synthase (iNOS) increases (1) as well as does the intracellular amounts of reactive oxygen and nitrogen species. Targeted mutation of the *Nos2* locus resulting in iNOS null mice (iNOS^{-/-}) allows us to study the influence of iNOS activity on presbycusis. Hearing thresholds of several mouse strains of iNOS^{+/+} and iNOS^{-/-} in both mixed and inbred C57BL/6 (B6) genetic backgrounds were tested by auditory brainstem response (ABR) technique. iNOS^{-/-} mice on a mixed 129 X B6 genetic background have stable and normal ABR thresholds during at least 15 months of life. Yet, both 129 and B6 progenitor genetic strains have the *ahl* gene and these animals develop an age-dependent hearing impairment (2). The heterogeneity found among the many inbred mouse lines can result in an epistatic modification of phenotypes when the same genetic mutations are analyzed. This may explain why iNOS^{-/-} mice on a pure

B6 genetic background do not exhibit a difference in threshold changes from wildtype iNOS^{+/+} animals. It would be useful to conduct experiments on congenic 129 mice to eliminate confounds due to genetic heterogeneity, however our results suggest the absence of iNOS can prolong the onset of ARHL in the 129X B6 mixed genetic background. Supported by NIH NDCD R01 DC 00105.

References

1. Wu M.D. et al., (1997) Okajimas Folia Anat. Jpn 74(5), 155-65.
2. Zheng Q.Y et al., (1999) Hear. Res. 130, 94-107.

658 Accelerated Age-Related Hearing Loss in Mice Deficient for Nuclear-Factor Kappa B

Hainan Lang¹, Bradley A Schulte^{1,2}, Daohong Zhou², Richard A Schmiedt¹

¹Dept. of Otolaryngology-Head and Neck Surgery, Medical University of SC, 135 Rutledge Avenue, Charleston, SC, United States, ²Dept. of Pathology and Laboratory Medicine, Medical University of SC, 165 Ashley Avenue, Suite 309, Charleston, SC, United States

Nuclear-factor kappa B (NF-κB) is a transcription factor that regulates a variety of genes involved not only with immune and inflammatory responses, but also with cell survival. Recently NF-κB has been shown to act as an anti-apoptotic factor in the protection of neurons from apoptosis. Its activity also has been associated with synaptic plasticity. The role of this transcription factor in the cochlea is unclear. Mice lacking the p50 subunit of NF-κB and wild type controls were examined at 1, 3 and 8 months of age. Auditory-nerve compound action potential (CAP) thresholds increased with age in both knockout and wild type mice, but hearing loss occurred at a much greater rate in the knockouts. At one month of age, CAP thresholds in the knockouts were elevated by 6-10 dB relative to the wild type at all frequencies. At three months of age, thresholds in the knockouts were elevated above those in the wild type by 30 dB at high frequencies and by 20 dB at low frequencies. At eight months of age, most knockouts no longer responded to auditory stimuli, whereas the wild type mice retained CAP responses at most frequencies tested. Endocochlear potentials were normal in knockout and wild type mice and did not decrease significantly with age. Temporal bones collected after the functional testing were processed for plastic-embedded sectioning. Radial-sections in the knockout cochleas showed empty-appearing spaces under the inner hair cells, representing pathologic lesions of the dendrites of afferent inner-radial fibers. These pathologies were evident in the knockouts at all ages examined, but were not seen in wild type mice. These results demonstrate that NF-κB plays an important role in the regulation of afferent neural function. The findings also suggest that NF-κB may play a role in protection of neurons from excitotoxicity and age-related hearing loss.

Supported by NIH/NIA, NIH/NIDCD and NIH/NCI.

659 Possible Interaction Between KCNA1 Genotype and Aging on Auditory Spatial Discrimination in the Mouse

Paul D Allen, Peter J Rivoli, James R Ison

Brain and Cognitive Sciences, University of Rochester, Meliora Hall, Rochester, NY, United States

Low-threshold K⁺ conductances underpin temporal processing and control synchrony in neurons of the auditory brainstem. The Kv1.1 channel is strongly expressed in the MNTB, a nucleus involved in ILD processing. We have previously demonstrated that mice lacking the KCNA1 gene have deficits in auditory spatial discrimination using a novel behavioral task based on pre-pulse inhibition of startle. We have also shown that the same behavioral task reveals progressive degradation of auditory spatial discrimination from 3 to 24 months of age in the CBA mouse. In the current study we test the hypothesis that there is an interaction between genotype and age in KCNA1 *+/+* and *+/-* mice in auditory spatial discrimination, specifically that the heterozygote mice, with only one copy of the gene, will show stronger age-related declines than their wild-type littermates. Mice of three age-ranges were studied: 4-8 months *+/+* N=11, *+/-* N=9; 9-16 months *+/+* N=17, *+/-* N=16; 17-25 months *+/+* N=12, *+/-* N=17. Each mouse was restrained in a wire cage and oriented with head facing the mid-line of 2 high-frequency speakers having angular separations of 180, 90, 45, 22.5, or 7°. Continuous 50 kHz broadband noise was presented from one speaker then swapped to the other, 1 to 300 ms (ISI) prior to an overhead startle eliciting noise-burst. Prestimuli provide graded inhibition of the acoustic startle reflex (PPI), and speaker-swap PPI was used to assess detection and salience of change in sound location. Speaker-swap PPI increases with ISI to a maximum that generally scales with angular separation of the speakers. The ISI required for significant inhibition to occur, and for maximal inhibition to develop increases as the speaker angle is reduced and also with increasing animal age. 7° swap produced no significant PPI for any group. The aging effect in the current mice, which are derived from the C3H strain, while still present, is less pronounced than in the CBA mouse. However KCNA1 *+/-* mice do not appear to show worse spatial discrimination than their *+/+* littermates and, in fact the inhibitory effects of the swap may be more persistent in the *+/-* mice in old age. These data indicate that a single copy of the KCNA1 gene is sufficient for normal spatial acuity well into old age and perhaps suggest that KCNA1 may not be significantly down-regulated with age in the auditory brainstem. *Support Contributed By: NIA Grant # AG09524 and The Schmidt Program on Integrative Brain Research*

660 Neurotrophin Gene Expression: Microarray Profile of Age-Related Changes in the CBA Mouse Auditory System

Mary D'Souza¹, Martha L. Zettel¹, Xiaoxia Zhu¹, Martha Lynch-Erhardt¹, D. Robert Frisina^{1,2}, Andrew Brooks³, Robert D. Frisina^{1,2}

¹Otolaryngology Div., Univ. Rochester Med. Sch., 601 Elmwood Ave., Rochester, New York, United States, ²Int. Ctr. Hearing Speech Res., Rochester Int. Technology, Lomb Mem. Dr., Rochester, New York, United States, ³Ctr. Functional Genomics, Univ. Rochester Med. Sch., 601 Elmwood Ave., Rochester, New York, United States

This study examines functional aspects of age-related gene expression changes in the cochlea and inferior colliculus (IC) of CBA mice. To accomplish this, young adult (N=8), middle aged (N=17) and old (N=15) CBAs were functionally assessed with auditory brainstem responses (ABRs), distortion product otoacoustic emissions (DPOAEs) and contralateral suppression of DPOAEs. Enough usable RNA was obtained from each mouse, so that each microarray data set embodies RNA from the cochleae or ICs of an individual subject. In this report, neurotrophin factor 3 (NT-3) expression changes were differentially assessed by age. The Affymetrix GeneChipR array of *mus musculus* M430A with 20,000 probe sets was used. Initial observations: A) ABR thresholds and DPOAE magnitudes of the young and middle age mice were similar, but significant changes occurred in the old group, consistent with age-related hearing loss; B) Microarray data suggest a down-regulation of NT-3 and cell cycle control and telomere maintenance genes with the age, and increased expression levels of apoptotic genes. Current analyses are looking at relations between gene expression changes, Real time PCR, statistical analyses and hearing capabilities. Genes whose expression changes are correlated with hearing measures could be considered as potential markers to predict hearing loss in aging subjects.

Support: NIH-NIA P01 AG09524, NIDCD P30 DC05409 & Int. Ctr. Hearing Speech Res.

661 Age-Related Changes in Neurotransmitter Expression in the CBA Mouse Auditory System Using GeneChipR Microarrays

Martha Lynch-Erhardt¹, Mary D'Souza¹, Xiaoxia Zhu¹, Martha L. Zettel¹, D. Robert Frisina^{1,2}, Andrew Brooks³, Robert D. Frisina^{1,2}

¹Otolaryngology Div., Univ. Rochester Med. Sch., 601 Elmwood Ave., Rochester, NY, United States, ²Int. Ctr. Hearing Speech Res., Rochester Inst. Technology, Lomb. Mem. Dr., Rochester, NY, United States, ³Functional Genomics Ctr., Univ. Rochester Med. Sch., 601 Elmwood Ave., Rochester, NY, United States

Acetylcholine (ACh) and glycine are auditory inhibitory neurotransmitters. We previously demonstrated an upregulation of ACh-esterase (AChE) activity, the enzyme that degrades ACh, in the auditory brainstem of old CBAs. Here, we used microarray technology to examine functional aspects of age-related gene expression changes in the cochlea and inferior colliculus (IC) of CBA mice. To accomplish this, young adult (N=8), middle aged (N=17) and old (N=15) CBAs were functionally assessed with auditory

brainstem responses (ABRs), distortion product otoacoustic emissions (DPOAEs) and contralateral suppression of DPOAEs (CS). Enough usable RNA was obtained from each mouse, so that each microarray data set embodies RNA from the cochleae or ICs of an individual subject. The Affymetrix GeneChipR array of *mus musculus* M430A with 20,000 probe sets was used. A) ABR thresholds and DPOAE and CS magnitudes of the young and middle age mice were similar, but significant changes occurred in the old group, consistent with age-related hearing loss; B) Microarray data revealed age-related changes: gene expression of ACh, AChE and glycine neurotransmitter transporter was upregulated in old mice with hearing loss when compared to young adults with normal hearing. These findings expand our knowledge of genes known to be up- or down-regulated as a function of age in the inner ear and IC.

Support: NIH-NIA P01 AG09524, NIDCD P30 DC05409 & Int. Ctr. Hearing Speech Res.

662 Knockout mice lacking the taurine transporter (TAUT4) manifest accelerated age-related hair cell loss

Haiyan Jiang¹, Dalian Ding², Ulrich Warskulat³, Deiter Haussinger⁴, Richard J. Salvi²

¹Center for Hearing & Deafness, SUNY at Buffalo, 215 Parker Hall, 3435 Main Street, Buffalo, NY, United States, ²Center for Hearing & Deafness, SUNY at Buffalo, 215 Parker hall, 3435 Main Street, Buffalo, NY, United States, ³Clinic of Gastroenterology Hepatology and Infectiology, Heinrich Heine University, Moorenstrasse 5 40225, Duesseldorf, Germany, ⁴Dept. Gastroenterology Hepatology and Infection, Heinrich Heine University, Moorenstrasse 5, D 40225, Dusseldorf, Germany

Taurine, which is present at high levels in many tissues, including the brain and inner ear, plays an important role in cell volume regulation, antioxidant defense and stress responses. Since taurine cannot freely pass through lipid membranes and is transported into cells by Na⁺-dependent taurine transporters (TAUT) encoded by *taut* gene family of sodium- and chloride-coupled transporters. Since knockout mice deficient in the taurine transporter (*taut*^{-/-}) show severe retinal degeneration early in life and since taurine is expressed at high levels in most supporting cells in the inner ear, we reasoned that inactivation of the TAUT transporter would lead to degeneration of hair cells within the inner ear. To test this hypothesis, we harvested the cochleas from 3 month and 18 month old *taut*^{-/-} and WT mice and counted the number of outer hair cells (OHC) and inner hair cells (IHC). Both WT and *taut*^{-/-} mice displayed an age-related increase in the amount of OHC and IHC loss. The age-related hair cell loss, which showed the classic, progressed from base-to-apex and was greater for OHC than IHC. Consistent with our hypothesis, *taut*^{-/-} knockout mice exhibited an accelerated loss of OHC and IHC. At 3 and 18 months of age, hair cell lesions in the *taut*^{-/-} mice has progressed 12-20% further towards the apex of the cochlea than in WT mice. Thus, the loss of the TAUT transporter accelerates the rate of age-related hair cell loss.

Supported by NIH grant P01 DC03600-01A1

663 Aches and Pains of Old Age: Presbycusis

Joseph E. Hawkins, Jochen Schacht

University of Michigan, Kresge Hearing Research Institute, 1301 East Ann, Ann Arbor, MI, United States

In their old age, neither Homer's Nestor nor the Bible's Methuselah seems ever to have complained about hearing loss, although we may safely assume that they, too, were afflicted with presbycusis. This universal result of aging, demonstrable in animals as well as in man, did not become a matter of clinical and scientific interest until the closing years of the 19th century, when otologists Roosa in New York and Zwaardemaker in Amsterdam made primitive but systematic tests with tuning fork and Galton whistle of the upper-frequency limit of audition in patients ranging from childhood to old age. To the reduced hearing that they found in the elderly they gave the appropriate Greek name, but they could only speculate whether it was due to changes in the middle ear, labyrinth, acoustic nerve, or to reduced bone conduction. It was Schuknecht (1955) who postulated four forms of presbycusis: sensory, neural, stria (metabolic), and cochlear mechanical, but more recent work has suggested that vascular, hyperostotic, and central changes may also be involved. To complicate matters further, genetic influences contribute to the time course and the manifestations of presbycusis. The presbycusis ear and auditory system must also bear the marks of injuries received throughout life, of which those due to noise exposure are generally most prominent. Such wounds may have been inflicted by free radicals which play a prominent role not only in noise trauma but in all aging processes of our bodies. A gradual loss of cochlear hair cells, ascending from the extreme basal region, would probably represent "pure" presbycusis, corresponding to senile macular degeneration in the retina. However, given the frequency of lifetime acoustic insults, the inner ears of the aged most often show a variety of lesions rather than a clean loss of sensory cells.

664 Dissection of the "cocktail-party effect": Informational masking of formant transitions in a speech-analog target by a speech-analog simultaneous distractor

Pierre L Divenyi¹, Brian Gygi²

¹Speech and Hearing Research, VANCHCS, 150 Muir Rd., Martinez, CA, United States, ²Speech and Hearing Research, East Bay Institute for Research and Education, 150 Muir Rd., Bartinez, CA, United States

Pairs of sinusoidal complexes with different fundamental frequencies f_0 (107 and 189 Hz) but identical bandwidth (0.5-3 kHz) were bandpass filtered with triangularly modulated ($f_{mod}=5$ Hz) center frequency to obtain two waveforms with dynamically varying single-formant transitions. The target (S), enclosed a single modulation cycle starting either at a phase of $-\pi/2$ (up-down) or $\pi/2$ (down-up), whereas the distractor (N) started at a random modulation phase. Informational masking (IM), defined as the S/N ratio at which listeners were able to discriminate the target phase, was adaptively determined for several distractor levels and extents of frequency swing (10-55%). Results indicate that (1) experienced young listeners' IM thresholds are between 6 and 18 dB higher than similarly determined energetic masking (EM) thresholds, (2) IM thresholds are higher for low- f_0 target and high- f_0 distractor than vice versa, (3) contrary to EM, IM is not a linear function of dis-

tracter level, (4) this nonlinearity is greater for easy (large swing) than difficult (small swing) conditions, and (5) IM thresholds are much larger than EM thresholds for normal-hearing elderly than young listeners. Relevance of the results to speech understanding in babble noise and its decline in aging will be discussed.

[Work supported by the National Institute on Aging and by the Veterans Affairs Medical Research.]

665 The Effect of Perceived Spatial Separation on Informational Masking of Speech in Younger and Older Adults

Liang Li, Meredyth Daneman, James G. Qi, Bruce A. Schneider

Department of Psychology, University of Toronto at Mississauga, 3359 N Mississauga Road, Mississauga, Ontario, Canada

In a reverberant environment, listeners usually “fuse” the direct sound wave from a source with its reflections and perceive a single event as originating from the direction of the source. This phenomenon is called the precedence effect. Here we studied the degree to which perceived spatial separation, induced by the precedence effect, provided release from informational and noise masking of speech in younger and older adults. Listeners were asked to repeat nonsense sentences, which were spoken by a female talker and presented by both the left (-45 degree) and right (+45 degree) loudspeakers, when maskers, which were either speech-spectrum noise sounds or nonsense sentences spoken by other two female talkers, were presented by the same two loudspeakers. Delays between identical sounds presented over the two loudspeakers were used to control the perceived locations of the target (right only) and masker (left, center, and right). The results show that perceived separation of target speech from masking speech markedly improved speech recognition. However, when the masker was noise, perceived separation only marginally improved speech recognition. Hence, separating the perceived location (but not the physical location) of the masker from the target speech produced a much larger improvement in performance when the masker was informational (two people talking) than when the masker was noise. However, the size of this effect was the same for younger and older adults, suggesting that cognitive-level interference from an irrelevant source was no worse for older adults than it was for younger adults.

666 Age and high frequency hearing loss effect binaural speech understanding in noise using HINT

SungHee Kim¹, Robert D. Frisina^{2,3}, Susan T. Frisina^{2,3}, Frances M. Mapes³, Elizabeth D. Hickman³, D. Robert Frisina^{2,3}

¹Otolaryngology, Daegu Fatima Hospital, 302-1 Shinam 4 dong, Dong gu, Daegu, Korea, Republic of, ²Otolaryngology Division, Departments of Surgery, Neurobiology and Anatomy and Biomed, University of Rochester School of Medicine and Dentistry, 601 Elmwood Ave., Rochester, NY, United States, ³International Center for Hearing and Speech Research, National Technical Institute for the Deaf, 52 Lomb Memorial Drive, Rochester, NY, United States

The present study investigates the relative contributions of hearing loss and age to speech understanding. Subjects with normal hear-

ing and symmetric HFHL, were drawn from a pool of 267 paid volunteer adult subjects. The Ss (N=63) with normal hearing and high frequency hearing loss in middle- (38-57 yr) and old age (58+ yr) were evaluated, with the following Ns: (1) middle aged group with normal hearing (MNH, N=16), (2) middle-aged group with HFHL (MHFHL, N=9), (3) old group with normal hearing (ONH, N=19), (4) old group with HFHL (OHFHL, N=19). The Hearing in Noise Test (HINT) was used to measure speech intelligibility in quiet and in background noise. Speech was presented from a loudspeaker located at 0 azimuth in four conditions: without noise (HINT Q), with noise at 0 (HINT N0), 90 (HINT N90), and 270 (HINT N270) azimuths. HFHL affected speech understanding in the middle-aged group (MNH vs. MHFHL) for HINT Q and HINT N90, but not in the old group. There was an effect of age on speech understanding in middle-aged and old groups with normal hearing for HINT Q, HINT N0, and HINT N270, consistent with our previous study (Kim et al., 2003, ARO abstract). The OHFHL group showed similar speech understanding with ONH and MHFHL groups. These results suggest that high frequency hearing was more important for speech understanding in the middle-aged group vs. the old group.

Work supported by NIH-NIA P01 AG09524, NIDCD P30 DC05409 and the Int. Ctr. Hearing Speech Res.

667 Hormone Replacement Therapy Negatively Affects Hearing in Aged Women

Patricia Guimaraes¹, Susan T. Frisina¹, Francis Mapes², SungHee Kim¹, D. Robert Frisina^{1,2}, Robert D. Frisina^{1,2}

¹Otolaryngology Div., Univ. Rochester Med. Sch., 601 Elmwood Ave., Rochester, New York, United States, ²Int. Ctr. Hearing Speech Res., Rochester Inst. Technology, Shumway Commons, Rochester, New York, United States

The effects of female hormones on the human auditory system are controversial. This study retrospectively compared hearing abilities between two groups of post-menopausal women. Experimental group: subjects were treated with Estrogen and Progesterone (Hormone Replacement Therapy – HRT, N=32). Controls: no hormone replacement (Non Hormone Replacement Therapy – NHRT, N=32). The criteria for subject selection were: age (60-86 years), relatively healthy medical history, absence of diabetes, hypothyroidism, vertigo, significant noise exposure, middle ear problems and current/heavy smoking. Tests: pure tone audiometry, tympanometry, distortion product otoacoustic emissions (DPOAEs), hearing-in-noise-test (HINT) and contralateral suppression of DPOAEs. The NHRT group presented higher DPOAE amplitudes than the HRT group ($p < 0.02$ and $p < 0.001$ for right and left ears, respectively). In addition, a trend was observed for transient OAEs: the NHRT group presented higher amplitudes than the HRT group. The NHRT group showed larger contralateral suppression than the HRT group. As for HINT results, the NHRT group performed better than the HRT group ($p < 0.02$), across all background noise speaker locations. A trend was also observed for pure tone audiometry: the NHRT had lower thresholds than the HRT group for frequencies up to 8 kHz, while no difference was noticed for ultra-high frequencies. These findings suggest that the replacement of sex hormones (Estrogen + Progesterone) does not improve hearing in elderly women, and for some conditions, can produce hearing deficits.

Support: NIH grants NIA P01 AG09524, NIDCD P30 DC05409 and the Int. Ctr. Hearing Speech Res.

668 Familial Analysis of Presbycusis

Chandler Marietta¹, Susan T. Frisina¹, Francis Mapes², SungHee Kim¹, D. Robert Frisina^{1,2}, Robert D. Frisina^{1,2}

¹Otolaryngology Div., Univ. Rochester Med. Sch., 601 Elmwood Ave., Rochester, New York, United States, ²Int. Ctr. Hearing & Speech Res., Rochester Inst. Technology, Shumway Commons, Rochester, New York, United States

An epidemiological study by Gates et al. (Otolaryngol. Head Neck Surg., 1999) suggested a familial contribution to presbycusis. Here, we report a retrospective analysis of parent-child pairs (N=52) who underwent extensive auditory testing. Tests: audiometry, white noise (WN), speech reception (SRT), speech discrimination (SD), transiently-evoked (TEOAE) and distortion product (DP) otoacoustic emissions, contralateral suppression of TEOAEs (CS), Speech reception in quiet and noise (HINTQ, HINTN0, HINTN90, HINTN270). Four pure-tone averages were used: PTA1 (0.5,1,2 kHz), PTA2 (1,2,4 kHz), PTA3 (4,8,9 kHz), PTA4 (10,11,12,14 kHz). Also, two DP averages were used: DP1(1-2 kHz), DP2(3-7 kHz). Audiogram slopes (SLOPE) were calculated by regression analyses. Correlations were done using linear regression analyses. Thirty-one parent-child pairs were examined. Analyses revealed statistically significant (P <0.05) findings for PTA1-L, PTA2-L, PTA4-R, PTA4-L, WN-L, SRT-L, SD-L, TEOAE-R, TEOAE-L, DP1-L, DP2-R, and DP2-L. Although not statistically significant, positive trends were present in SRT-R, PTA1-R, PTA2-R, PTA3-R, WN-R, DP1-R, and HINTQ. The results for mother-child compared to father-child pairs were more strongly correlated. Our study suggests a genetic contribution to hearing in parents and their offspring for many peripheral measures. Heritability may be stronger maternally and for the left ear. We hope these findings will guide future larger epidemiological studies that explore the contribution of genetics to hearing.

Support: NIH grants NIA P01 AG09524, NIDCD P30 DC05409 and the Int. Ctr. Hearing Speech Res.

669 Longitudinal Study of Postural Control: Effects of Age, Gender and Disease

F. Owen Black¹, William H. Paloski², E. Jeffrey Metter³, Alan H. Feiveson², Louis Homer⁴

¹Neurology Research, Legacy Clinical Research & Technology Center, 1225 NE 2nd Ave, Portland, OR, United States,

²Neuroscience Laboratories, NASA/JSC, NA, Houston, TX, United States, ³Gerontology Research Center, NIA Clinical Research Branch, NA, Baltimore, MD, United States, ⁴Clinical Research & Biomedical Investigations, Legacy Clinical Research & Technology Center, 1225 NE 2nd Ave, Portland, OR, United States

Three studies demonstrated significant effects of age, gender and vestibular disorders on human postural control. Results of a cross-sectional study of postural stability (N=214, 7-81yrs) were compared statistically with a cross-sectional cohort from the Baltimore Longitudinal Study of Aging (BLSA) (N=190, 20-80yrs) and with a 10 year longitudinal study of a subset group from the first cross-sectional study (N=47, 17-80yrs). Age effects

were observed in all three groups during SOT conditions 5 & 6 which require accurate vestibular inputs for postural control. In the longitudinal study SOT 5 sway increased about 50% (t=3.81, 46 df, P=0.0004) and SOT 6 increased about 20% (t=2.05, 46 df, P=0.046). Fifty percent changes such as those observed in SOT 5 would be detectable with a power > 90%. In both cross-sectional groups, postural instability began in the late 5th or 6th decade and increased with age. Gender differences were detected in both the BLSA and the longitudinal study groups. The BLSA study demonstrated that the gender differences occur only in the lower 50th %ile. The age effects occurred only on SOTs 5 & 6 in all three studies, suggesting failing vestibular function with increasing age. However, the longitudinal study showed that vestibular effects occurred in all age decades (~50% of subjects/decade). This finding implies that the probability of vestibular disease in the population studied is independent of age. Findings from the BLSA cross-sectional study suggests that gender differences appear to affect only those subjects who perform below the population mean (lower 50th %ile), with women affected earlier (beginning in the late 4th decade) than men (early 7th decade). The BLSA study also demonstrated a statistically significant improvement in postural stability at a second test session one week after the initial test. These results have important implications for fall risk identification and prevention protocols.

Supported by NIH/NIDCD DC00205, NASA NAG9-1254, LHS RAC and NIH/NIA IRP and NASA DSO-605.

References:

1. Peterka RJ, Black FO. Age-related changes in human posture control: Sensory organization tests. *JVR*. 1990;1:73-85.

2. Feiveson AH, Metter EJ, Paloski WH. A statistical model for interpreting computerized dynamic posturography data. *IEEE Trans. Biomed. Eng.* 2002;49:300-309.

670 The Sound of Stress : Cortisol Reactivity to Stress in Tinnitus Sufferers

Odrée Dionne-Fournelle¹, Marie-Andrée Cormier², Sylvie Hébert^{1,3}, Sonia J Lupien⁴

¹École d'orthophonie et d'audiologie, Université de Montréal, CP 6128, succ. Centre-ville, Montréal, Québec, Canada, ²Sciences bio-médicales, Université de Montréal, CP 6128, succ. Centre-ville, Montréal, Québec, Canada, ³Centre de recherche, Institut universitaire de gériatrie de Montréal, 4565, Queen-Mary, Montréal, Québec, Canada, ⁴Douglas Hospital research center, McGill University, 6875, boul. Lasalle, Montréal, Québec, Canada

A classical teaching about tinnitus, i.e., the –illusory— perception of a sound in the ears or head, is that it is stress-related: Either tinnitus increases anxiety, or it is exacerbated during periods of emotional stress. Yet, a clear empirical link between tinnitus and stress has never been found. In this study we examined the relationship between tinnitus and stress by using an objective marker of stress, namely, cortisol. Cortisol is a stress-related hormone that is secreted both naturally according to a circadian rhythm, and punctually in stressful situations. Two groups of participants (one with tinnitus and one without tinnitus, matched in overall age, health status, and gender) performed the Trier Social Stress Test (TSST), a classic public speaking task followed by an arithmetic task known to increase cortisol secretion. Six salivary cortisol samples

were taken to examine reactivity to stress and recovery. The results show a hyporesponse of the tinnitus sufferers compared to controls, similar to the one found under conditions of trauma and prolonged stress. Although our findings cannot conclude on whether tinnitus causes or precedes this paradoxical suppression of the limbic-hypothalamic-pituitary-adrenocortical (LHPA) axis, they do suggest that the presence of tinnitus may influence physiological responsiveness to psychological stress.

671 Calpain activity in the amikacin poisoned rat cochlea

Sabine Ladrech¹, Matthieu Guitton¹, Mireille Gallego¹, Takaomi Saïdo², Marc Lenoir¹

¹*Physiopathologie et Thérapie des déficits sensoriels et moteurs., INSERM U583, 71 rue de Navacelles, Montpellier, France,*

²*Laboratory for Proteolytic Neuroscience, RIKEN Brain Science Institute, 2-1 Hirosawa, Wako-shi Saitama, Japan*

Calpain is an ubiquitous calcium-activated cysteine protease that is implicated in a range of cellular functions, including cell death. Exogenous calpain inhibitors have been shown to protect cochlea against noise trauma (Wang et al., 1999, *NeuroReport* 10, 811-816) and antibiotic ototoxicity (Ding et al., 2002, *Hearing Res.* 164,115-126). They also protect both hair cells and ganglion cells against hypoxia and neutrophin-withdrawal (Cheng et al., 1999, *Brain Res.* 850, 234-243). Our study provides spatial and temporal informations on calpain activity in the amikacin poisoned rat cochlea. As there was no available antibody against the active form of calpain, we used an antibody that recognizes the 150 kDa breakdown products of the fodrin &-subunit (FBDP), exclusively cleaved by calpain (Saïdo et al., 1994, *FASEB* 8, 814-822).

Rats were treated with a daily subcutaneous injection of 500 mg/kg amikacin from PND 9 to PND 16. The immunocytochemical experiments were conducted at different stages after the amikacin treatment, corresponding to the periods of hair cell degeneration, supporting cell remodeling and neuronal degradation.

By the end of the amikacin treatment, degenerating hair cells were labelled with the antibody against FBDP. After hair cells disappearance (PND 17-24), FBDP were present in Deiters cells engaged in a scarring process. Then, from PND 35 to PND 100, numerous ganglion neurons (60-70%) were immunoreactive for FBDP.

These results support the assumption (Sato et al., *ARO* 2003, n°78) that calpain plays important roles in sensory and neuronal cell degradation in the aminoglycoside poisoned cochlea. Additionally, calpain may be involved in Deiters cell remodeling during post-traumatic scar formation.

672 Hair Bundles in Ptpqr Null Mutant Mice Show an Increased Sensitivity to Aminoglycoside Antibiotics

Jane Elizabeth Bryant¹, Richard Goodyear¹, Kevin Legan¹, Corné Kros¹, Ron Seifert², Daniel Bowen-Pope², Guy Richardson¹

¹*Centre for the Study of Neuroscience, University of Sussex, Science Park Road, Brighton, United Kingdom,* ²*Department of Pathology, University of Washington, Box 357470, Seattle, Washington, United States*

Ptpqr was first identified as a receptor-like phosphatase that is upregulated in response to glomerular nephritis in the rat kidney, and has recently been shown to be an inositol lipid phosphatase. The available evidence suggests Ptpqr is the hair cell antigen (HCA), a component of hair-bundle shaft connectors. Recent studies using two transgenic mouse lines with deletions in the catalytic (Ptpqr-CAT-KO) and transmembrane domains (Ptpqr-TM-KO) of Ptpqr have shown that this enzyme is required for shaft connector formation and normal maturation of cochlear, but not vestibular, hair bundles. The inositol lipid phosphatase activity of Ptpqr suggests it regulates the levels of PIP₂, a putative aminoglycoside receptor, in the stereociliary membrane. Furthermore, the distribution of Ptpqr on hair bundles is inversely correlated with their known aminoglycoside sensitivity. For example, hair cells with Ptpqr distributed over the entire hair bundle, as in the extrastriolar region of the maculae, are relatively insensitive to aminoglycoside ototoxicity, whereas outer hair cells in the basal coil of the mature cochlea do not express Ptpqr, and are known to be very sensitive to aminoglycosides. These observations suggest levels of Ptpqr expression in hair cells may influence their sensitivity to aminoglycosides. We therefore examined the responses of vestibular hair cells to neomycin treatment in heterozygous and homozygous Ptpqr-KO mice.

Organotypic utricular cultures from homozygous or heterozygous Ptpqr-KO mice ranging in age from P27-P40 were grown in the presence or absence of 1 or 2 mM neomycin sulphate for 1 or 2 days, fixed and processed for SEM. Samples were viewed and evaluated by observers blind to the genotype of the specimen. The results show that extrastriolar hair bundles in homozygous Ptpqr-KO mice have a pronounced tendency to fuse in the presence of neomycin, whilst those in heterozygotes are usually splayed. These response characteristics allowed us to genotype samples with 100% accuracy. This increase in neomycin sensitivity may be due to an upregulation of PIP₂ levels in the stereociliary membranes of homozygous Ptpqr-KO mice. Alternatively, the absence of shaft connectors may promote stereociliary membrane fusion in the presence of polycations.

Sponsored by The Wellcome Trust, MRC and NIH.

673 Gene Expression Profiles Differ Following Exposure of Mammalian Organ of Corti Explants to Neomycin and Cisplatin.

Azel Zine¹, Nathalie Cueille², Christopher Robin Cederroth¹, Christophe Bonny³, Francois de Ribaupierre², Jean Luc Puel¹

¹Physiopathologie et Thérapie des déficits sensoriels et moteurs, Université Montpellier I, INSERM U.583, 71 rue de Navacelles, Montpellier, France, ²Institut de Physiologie, Université de Lausanne, Rue du Bugnon 7, Lausanne, Switzerland, ³Division of Medical Genetics, CHUV, Falaises 1, Lausanne, Switzerland

Neomycin, an aminoglycoside antibiotic, and cisplatin, a platinum-based anticancer drug, are two commonly used clinical drugs known to have severe ototoxic side effects. The ototoxicity of both neomycin and cisplatin have been linked to apoptosis of hair cells leading to irreversible damage to the organ of Corti. Although some components of the apoptotic pathway leading to the hair cell death have been identified, little is known about the detail intracellular molecular pathways that are triggered by an exposure to an aminoglycoside antibiotic versus cisplatin within the mammalian organ of Corti. With the potential for activation of multiple pathways in the response to both neomycin and cisplatin exposure, gene microarrays provide a high throughput tool to examine the simultaneous activity of thousands of genes.

As a first step toward examining changes in gene expression, we profiled gene expression in postnatal day three (P3) mouse organ of Corti explants exposed to either neomycin or cisplatin with a mouse apoptosis cDNA Atlas Expression Array from Clontech.

The experimental explants were exposed to either neomycin or cisplatin for 2 days in vitro. Parallel untreated, control explants were maintained for 2 days in serum free medium and were cultured concurrently with the experimental explants.

The microarray results showed a different pattern of gene expression as a consequence of either neomycin or cisplatin exposure, that have to be confirmed by semi-quantitative real time PCR. Preliminary results suggest that the ototoxic effects of neomycin and cisplatin on auditory hair cells in organ of Corti explants are mediated by different cell death signaling pathways. These findings significantly advance our understanding of the molecular mechanisms underlying aminoglycoside- versus cisplatin-induced hearing loss.

674 Hair cell loss from the combination of gentamicin and ethacrynic acid is initiated by caspase 9 and cytochrome c release

Dalian Ding, Haiyan Jiang, Sandra L McFadden, Richard J Salvi

Center for Hearing and Deafness, SUNY at Buffalo, 215 Parker Hall, 3435 Main Street, Buffalo, NY, United States

Concurrent administration of a large dose of gentamicin (GM; 125 mg/kg IM) and ethacrynic acid (EA; 40 mg/kg IV) results in the rapid destruction of all cochlear hair cells in chinchillas. To identify the cell death mechanisms involved in rapid hair cell death from high dose GM-EA treatment, we stained for cytochrome c, succinate dehydrogenase, mitochondrial membrane potential, caspase 3, 8 and 9 activity and compared this to hair cell pathology

and nuclear morphology using propidium iodide. In the base of the cochlea, destruction of the hair cell cuticular plate occurred approximately 12 h after GM/EA treatment. At 4-5 h following GM-EA treatment, succinate dehydrogenase activity and mitochondrial membrane potential had decreased greatly whereas cytochrome c and caspase 3 and 9 activity had increased substantially in the basal and middle of the cochlea. Little or no activation was seen in receptor-mediated caspase 8. Nuclear condensation and fragmentation, markers of apoptosis, occurred around 5 h in the basal turn, 6 h in the middle turn and 12 h in the apical turn. Thus, the rapid loss of hair cells following high-dose GM-EA treatment involves apoptotic cell death pathways that may be mediated by mitochondrial dysfunction, caspase 9 activation, and cytochrome c release.

Supported by NIH grant P01 DC03600-01A1

675 Temporal disruption of E-cadherin-dependent adherens junctions in the mouse vestibular epithelia following aminoglycoside treatment

Tae-Soo Kim¹, Takayuki Nakagawa¹, Shin-ichiro Kitajiri^{1,2}, Fukuichiro Iguchi¹, Tsuyoshi Endo¹, Shinji Takebayashi¹, Tetsuya Tamura¹, Koji Iwai¹, Tomoko Kita^{1,3}, Ken Kojima¹, Kiyohiro Fujino¹, Yasushi Naito¹, Juichi Ito¹

¹Department of Otolaryngology-Head and Neck Surgery, Graduate School of Medicine, Kyoto University, 54 Kawaharacho, Shogoin, Sakyo-ku, Kyoto, Japan, ²Department of Cell Biology, Graduate School of Medicine, Kyoto University, Shogoin, Sakyo-ku, Kyoto, Japan, ³Horizontal Medical Research Organization, Graduate School of Medicine, Kyoto University, Shogoin, Sakyo-ku, Kyoto, Japan

E-cadherin, Ca²⁺-dependent cell-cell adhesion molecule, is a major component of the adherens junctions (AJ) of the inner ear. E-cadherin plays a role not only in maintenance of cell-cell junctions, but also in regulation of cell proliferation. Loss of E-cadherin expression leads to cell proliferation, while restoration of E-cadherin represses proliferation. In this study, we examined effects of aminoglycoside treatment on AJ in the vestibular epithelia. Expression of E-cadherin in mouse utricles following the local application of neomycin was assessed by immunohistochemistry and Western blot analysis. Transmission electron microscopy (TEM) was employed for morphological evaluation of AJs in mouse utricles. In addition, to determine the mechanisms for effects of aminoglycosides on E-cadherin expression, effects of Ca²⁺ on E-cadherin expression were examined by using organ culture systems. Immunohistochemistry and Western blotting demonstrated that neomycin treatment induced temporal decrease of E-cadherin expression. TEM analysis confirmed temporal disruption of AJs following neomycin treatment. Control utricles exhibited the honey-comb pattern expression of E-cadherin in organotypic cultures as well as in vivo normal specimens, while utricles cultured with Ca²⁺-free or neomycin-containing medium exhibited diffuse expression of E-cadherin after 3 days of culture. These findings suggest possible involvement of Ca²⁺ homeostasis in temporal disruption of E-cadherin due to aminoglycosides.

676 Characterisation of recovery after cisplatin ototoxicity: endocochlear potentials and cisplatin concentrations.

Sjaak FL Klis, Francisca LC Wolters, Jan Willem Sepmeijer, Guido F Smoorenburg

Hearing Research Laboratories, University Medical Center, Heidelberglaan 100, Utrecht, Netherlands

Previous work has shown that within the first 2 weeks after an ototoxic insult caused by cisplatin treatment, pronounced recovery of acoustically evoked cochlear potentials occurs (Klis et al., 2002, *Hear. Res.* 164, 138-146). This recovery appeared to be based on recovery of the endocochlear potential (EP), because the EP decreased to typically 50 mV in animals measured directly after the insult and it was normal (~80 mV) 4 weeks after. In the present work we are further characterising the recovery process by refining the time resolution of these measurements. Albino guinea pigs, equipped with permanent round window electrodes, were treated daily with an i.p. injection of 1.5 mg/kg cisplatin until the compound action potential threshold (3 μ V criterion) shifted by 40 dB or more. Electrocochleography was continued and after 0, 2, 3 or 7 days (groups included thus far) the EP was measured. Moreover, the cisplatin concentration was determined in blood and perilymph with atomic absorption spectrometry. Preliminary results show parallel recovery in the EP and the electrocochleographic thresholds with possibly the exception of the first couple of days. This might suggest another factor than EP recovery responsible for initial recovery. Pt concentrations were around 80 μ g/l in perilymph at day 0 and dropped below the detection limit afterwards. In blood, the Pt concentration dropped gradually, but slowly from around 1300 μ g/l at day 0 to 400 μ g/l after 7 days.

677 Electrophysiological and morphological study of gentamicin ototoxicity in guinea pigs

Won-Ho Chung¹, Jihwan Woo², Sook Kyung Park¹, Myung Soon Kim¹, In Young Kim², Yang Sun Cho¹, Sung Hwa Hong¹

¹*Department of Otorhinolaryngology-Head and Neck Surgery, Sungkyunkwan University School of Medicine, Samsung Medical Center, 50 Irwon-dong Gangnam-gu, Seoul, Korea, Republic of,*

²*Department of Biomedical Engineering, College of Medicine, Hanyang University, Sungdong-gu, P.O.Box 55, Seoul, Korea, Republic of*

Gentamicin (GM), one of aminoglycosides, is commonly prescribed in a variety of medical conditions. However, this drug has been known to be vestibulotoxic and cochleotoxic in humans and animals. The purpose of this study is to evaluate the ototoxicity of the topically applied GM using the auditory brainstem response (ABR), fluorescent immunohistochemistry, light microscopy and scanning electron microscopy.

Gelfoam soaked with GM at different concentration, 0.5mg and 1mg, was applied onto the round window of the guinea pigs through the dorsal approach. At each concentration, thresholds were measured with ABR on 3 days(n=6), 7 days(n=6), and 14 days(n=6) after GM application. After measuring the thresholds, the cochleae and utricles were collected for fluorescent immuno-

histochemical and microscopic evaluation.

At 0.5mg GM concentration, the thresholds seemed to be elevated on 3 days and the guinea pig became completely deaf on 7 days after the application. At 1 mg GM concentration, the thresholds were elevated much earlier than at 0.5 mg GM concentration.

The number of hair cells in the utricle were significantly reduced in a time-dependent manner. The loss of hair cells in the crista ampullaris, especially type 1 hair cells, were much greater on 14 days after application than on 7 days.

This study showed that topical application of GM onto the round window induced cochleo- and vestibulotoxicity in guinea pigs in a time-dependent manner.

This work was supported by Korea Research Foundation Grant(KRF-2002-003-E00108).

678 Immunohistochemical Detection of Platinated DNA in the Cochlea of Cisplatin-Treated Guinea Pigs

Marjolein W.M. Van Ruijven, John C.M.J. De Groot, Ferry Hendriksen, Guido F. Smoorenburg

Department of Otorhinolaryngology, University Medical Centre Utrecht, Heidelberglaan 100, Utrecht, Netherlands

Cisplatin is a widely used cytotoxic drug which is effective in the treatment of a broad spectrum of tumors. Application of the drug, however, may result in nephrotoxicity and high-frequency sensorineural hearing loss. Although tracer studies have shown that radioactive cisplatin is present in the stria vascularis and the organ of Corti after acute administration, attempts to determine the exact cellular target of cisplatin by means of ultrastructural X-ray microanalysis have failed. As the anti-tumor effect of cisplatin is thought to be mediated by formation of cisplatin-DNA adducts, we have surmised that the molecular mechanism underlying its ototoxic effect is similar. We used the polyclonal NKI-A59 antiserum against cisplatin-DNA adducts to label platinated DNA in the cochleas and renal cortex of albino guinea pigs treated with cisplatin (2 mg/kg/day i.p. for 10 days).

In semithin (0.5 mm) frozen sections of microdissected cochlear turns, nuclear immunoreactivity for NKI-A59 was observed in the organ of Corti, the stria vascularis and the spiral ligament. Labelling in the organ of Corti was primarily present in the IHCs and OHCs. Occasionally, labelling was also seen in the supporting cells. Strial immunoreactivity for the antiserum was most prominent in the marginal cells and to a lesser extent in the intermediate and basal cells. In the spiral ligament, the fibrocytes also demonstrated significant labelling. In the renal cortex, nuclear immunoreactivity was present in the glomeruli and the proximal and distal tubules. In the corresponding non-treated cochleas and renal cortex samples, none of the nuclei demonstrated immunoreactivity. Thus, at 10 days cisplatin is present in several cochlear cell types. A time-sequence experiment has been started to determine the primary cochlear target of cisplatin.

Supported by grants from the Heinsius-Houbolt Foundation, the Netherlands. NKI-A59 was a gift from B. Floot and A. Begg (Netherlands Cancer Institute, Amsterdam).

679 The presence of supporting cells alters the degree and time course of cochlear neuronal degeneration after hair cell loss

Mitsuru Sugawara¹, Gabriel Corfas², M. Charles Liberman¹

¹*Eaton-Peabody Laboratory, Massachusetts Eye and Ear Infirmary, 243 Charles Street, Boston, MA, United States,*

²*Division of Neuroscience, Children's Hospital Boston, 300 Longwood Avenue, Boston, MA, United States*

A fraction of the cochlea's myelinated afferent innervation degenerates after cell loss in the organ of Corti. The degree of inner hair cell (IHC) loss is a key determinant; however, the survival of supporting cells in the IHC area may also affect the degree and time course. The present study quantifies the relation between hair cell / supporting cell survival and cochlear neuronal degeneration in two chronic models of sensorineural hearing loss: carboplatin-treated chinchilla ears and kanamycin-treated cat ears, with post-treatment survivals ranging from 3 mos. to > 5 yrs.

15 carboplatin-treated and 8 kanamycin-treated ears were fixed and embedded along with controls. Cochleas were sectioned or processed as whole mounts. In either case, hair cells and supporting cells (inner and outer pillars and Dieters cells) were counted throughout each cochlea. Neuronal degeneration was assessed by counting peripheral axons in cross-sections through the osseous spiral lamina re place-matched counts in control ears.

Carboplatin ears show near-total IHC loss without loss of IHC supporting cells. In contrast, in kanamycin ears, some areas show only IHC loss and others show loss of both IHCs and their supporting cells. Nerve and cell counts in these ears revealed that: 1) neuronal loss is seen only if IHCs are missing, 2) loss of supporting cells increases the severity and speed of neuronal degeneration, 3) when supporting cells remain, neuronal survival is 4X greater than IHC survival (e.g. 15% IHC survival supports 60% neuronal survival) even 5 yrs post treatment, and 4) neuronal degeneration during the first 6 months after lesion occurs more rapidly in the basal turn than in the apical turn.

Supported by NIDCD RO1 DC 04820

680 Apoptotic cell changes precede to manifestation of structural and functional damage in the cochlear hair cells of gentamicin-poisoned guinea pigs

Munetaka Ushio, Mitsuya Suzuki, Tatsuya Yamasoba, Kimitaka Kaga

Otolaryngology, University of Tokyo, 7-3-1, Hongo, Bunkyo-ku, Japan

Recent studies have provided significant advances in understanding the mechanism of protection of the auditory hair cells from ototoxic insult. To obtain optimal protection, it is important to know the time course of structural and functional changes in ototoxic agent-induced cochlear damage. In the current study, we observed the extent of hair cell damage and auditory brainstem response threshold shifts chronologically following injection of gentamicin (GM; 40mg/ml) into the middle ear of albino guinea pigs. The animals were euthanized 6, 12, 18, 24, and 48 hours following the injection (n=,U, each). ABR was measured prior to the

injection and at the euthanasia. ∞@Using surface preparation technique, the whole cochlea were stained with rhodamine-phalloidin and observed under fluorescent microscope (3 cochleae in each group). DNA fragmentation was detected with TUNEL method (3 cochleae in each group). ABR threshold shifts and hair cell damage were not manifested until 12 hours following GM injection and became evident 24hours following it. However, TUNEL positive cells already appeared until 6 hours following GM injection; approximately one-fourth of the outer hair cells were TUNEL-positive 6 hours following treatment. These results show that, when exposed to aminoglycosides, the hair cells start dying via apoptosis far before the structural and functional damage becomes evident. Since it is considered difficult to rescue TUNEL-positive cells, it is recommended to apply agents effective for protection of the cochlear hair cells before apoptotic pathway is activated.

681 Deafening Melanocytes with Cisplatin

Andreas Ekborn¹, Agneta Viberg², Goran Laurell¹, Barbara Canlon²

¹*Otolaryngology and Head & Neck Surgery, Karolinska Hospital, Karolinska Hospital, Stockholm, Sweden,* ²*Physiology & Pharmacology, Karolinska Institutet, Karolinska Institutet, Stockholm, Sweden*

The intermediate cells of the stria vascularis are melanocytes that produce melanin. Animals lacking melanocytes have no endocochlear potential (EP) and are deaf, while animals lacking melanin (albinos), have normal hearing. It is also known that various drugs have the capacity to affect the melanocytes and the synthesis of melanin. Cisplatin is known to cause hearing loss, partly through an effect on the stria vascularis including reduction of the EP. The hypothesis to be tested is if cisplatin affects the activity of the melanocytes resulting in an altered expression of melanin. This study used quantitative morphological analysis combined with measures of ABR thresholds at 30, 20, 12, 6, and 3 kHz. Pigmented guinea pigs received a bolus injection of cisplatin (8mg/kg iv) and 96 hrs post-injection hearing thresholds were recorded and thereafter the animals were sacrificed. Cochleae were prepared for cryosectioning and whole mounts to quantify the number of apoptotic cells (TUNEL), hair cell loss, or melanin density in the stria vascularis. The results show an inter-animal variation of ABR thresholds, elevated 15 to 40 dB at frequencies between 30 and 12 kHz and revealed a significant loss of outer hair cells in the more basal regions (15%), and a normal complement of inner hair cells. A few outer hair cells were positively TUNEL marked in the basal turn, however, no positive staining was noted in the stria vascularis. A statistically significant lower density of melanin in the intermediate cells in the basal and middle cochlear regions was found 96 hrs after cisplatin treatment compared to the control group. Significant correlations were found between melanin density, ABR threshold shifts and outer hair cell loss. These results shed light on the melanocytes and their role in modulating cisplatin-induced hearing loss. The findings further support the mutiple cytotoxic effect of cisplatin on the inner ear. Supported by RNID and The Swedish Research Council.

682 The Action and Correlation of HMG1 and iNOS in Cytotoxicity of Cisplatin

Geming Li¹, Wei Liu¹, Dorothy Frenz^{1,2}

¹Otolaryngology, Albert Einstein College of Medicine, 1410 Pelham Pkwy S Room 301, Bronx, NY, United States, ²Anatomy & Structural Biology, Albert Einstein College of Medicine, 1410 Pelham Pkwy S Room 301, Bronx, NY, United States

Cisplatin is a widely used anti-tumor compound that produces toxic side effects to specific sensitive cells, including the auditory hair cells and neurons (ototoxicity), and renal tubular cells (nephrotoxicity). However, some cell types, e.g. myocardial cells, are resistant to cisplatin toxicity. Although much attention has been directed at developing methods of protection against cisplatin ototoxicity, the mechanism by which cisplatin produces its cytotoxic effects is not well understood. The high mobility group (HMG) domain is a DNA binding motif found in non-histone chromosomal proteins, HMG1, HMG2 and transcription factors. This domain plays an important role in regulation of DNA transcription, repair of damaged DNA, and the mediation of cisplatin anti-tumor activity. Recent studies demonstrate that HMG proteins can regulate the expression of inducible nitric oxide synthase (iNOS). The product of iNOS, nitric oxide, a free radical, causes cytotoxicity induced by cisplatin. In this study, we investigated the relationship between HMG1 and iNOS in cisplatin induced ototoxicity and nephrotoxicity. Ten seven-week-old female Fisher344 rats were divided into two groups: Group I, untreated control and Group II, CDDP treated. Immunohistochemical analysis and western blot of CDDP treated specimens demonstrated increased expressions of HMG1 and iNOS in rat cochlea and kidney. However, this increase was not observed in myocardial tissue. Our findings suggest that levels of expression of HMG1 in cells may correlate with the degree of sensitivity of these cells to cisplatin cytotoxicity.

683 Quantification of Kanamycin Ototoxicity in the Mouse Utricle

Mette Kirkegaard¹, Jens R Nyengaard²

¹Dept. of Zoophysiology, University of Aarhus, CF Moellers alle, Build. 131, Aarhus, Denmark, ²Stereological Research and Electron Microscopy Laboratory, University of Aarhus, CF Moellers alle, Build. 185, Aarhus, Denmark

The inner ear sensory epithelia are sensitive to aminoglycosides which induces apoptosis in the mechano-receptive hair cells. In mammals, the recovery of the sensory epithelium is not complete, which is probably due to the limited amount of proliferation of supporting cells. The present study describes the degeneration and the following regeneration of hair cells after aminoglycoside treatment.

Mice were given two daily subcutaneous injections of kanamycin (600 or 900mg/kg) for 15 consecutive days and allowed to survive either 1 or 3 weeks after end of treatment. The total number of the different cell types was estimated from systematically sampled sections using a physical fractionator. The total volume of the sensory epithelium was estimated using the principle of Cavalieri.

Hair cells with apoptotic morphology were observed after treatment with kanamycin. There was a dose- and time-dependent

decrease in total cell number. Thus, 3 weeks after treatment with 900mg kanamycin/kg, the total number of cells was reduced from 5573 (0.09) (mean (CV)) to 4245 (0.03). This was mainly due to a reduction in the type I hair cells which were reduced from 2438 (0.12) in control to 1793 (0.02) after the kanamycin treatment. In conclusion, the type I hair cells are more sensitive to kanamycin treatment than the type II hair cells. Longer survival times are, however, needed in order to evaluate if there is a long term effect of kanamycin on type II hair cells.

684 Attenuation of cochlear damage from noise trauma by geranylgeranylacetone, an inducer of heat shock proteins.

Tsuyoshi Takemoto, Kazuma Sugahara, Kuniyoshi Tanaka, Takeshi Okuda, Hiroaki Shimogori, Hiroshi Yamashita

Department of Otolaryngology, Yamaguchi University School of Medicine, Minamikogushi 1-1-1, Ube, Japan

Recently we showed the induction of heat shock proteins in cochlea by local heat shock, and demonstrated that using HSF1 null mice heat shock response is necessary for preventing cochlea hair cells from acoustic trauma. Geranylgeranylacetone (GGA) is accepted as an inducer of the heat shock proteins at gastric mucosa, hepatocytes heart and spinal nerve, and that its response may function to protect those tissues. But there is no report about GGA inducing Hsps at cochlea, so the purpose of this study is to investigate whether GGA could induce Hsps at cochlea and have protective effect of cochlea hair cells. We used Hartley guinea pigs, and to evaluate cochlear function, we assessed thresholds of the auditory brain stem response (ABR). For histological assessment, we observed the sensory epithelium using surface preparation technique. The GGA was administered in perilymphatic space and we investigated the expression of HSP 90, 70, 27 in cochlea by western blot analysis. Next, to clarify the role of heat shock response, six hours after GGA treatment, animals were exposed to intense (130 dB SPL) noise for three hours. One week after the sound exposure, ABR threshold were recorded and we observed the second turn of the organ of Corti. Western blot analysis showed that the expression of Hsp 70, 27 was increased. After the noise exposure, there were fewer defects on outer hair cells of organ of Corti in GGA treated ears than those of the control. Otherwise, the threshold shifts up in the treated ears to the same level as those in the untreated ears. This result suggests that GGA protected cochlea hair cells from acoustic trauma histologically.

685 Stressing the Balance of Glucocorticoid Receptors by Acoustic Trauma

Yeasmin Tahera, Inna Meltser, Peter Johansson, Zhao Bian, Pontus Stierna, Barbara Canlon

Physiology & Pharmacology, Karolinska Institutet, Karolinska Institutet, Stockholm, Sweden, ²Otolaryngology, Karolinska Institutet, Huddinge University Hospital, Huddinge, Sweden

While the set points for regulating the HPA axis and glucocorticoid receptor balance are genetically determined, it is well known that environmental experiences cause both short- and long-term effects on this complex system. Stressful stimuli can disrupt the sensitive balance between corticosterone (major glucocorticoid

hormone released by adrenal cortex in response to stress) and glucocorticoid receptors (GR). In particular, acoustic trauma is known to modulate the HPA axis and one main target of this stress response is the cochlea. In order to better understand the interaction between stress responses and vulnerability to acoustic trauma, we hypothesized that: 1) corticosterone has a protective effect against acute acoustic trauma and, 2) systemic stress, not targeted specifically at the auditory system (for instance, restraint stress) could modify the response of the inner ear to acoustic trauma by modifying the corticosterone/GR balance. In order to address these issues mice (CBA/CBA) were subjected either to acoustic stress, restraint stress, or restraint stress following by acoustic trauma. These groups were either pretreated with metyrapone (corticosterone release blocker) and RU486 (GR antagonist) and compared with a saline injected control group. We found that restraint stress protected auditory brainstem response thresholds against acoustic trauma whereas pretreatment with metyrapone and RU486 abolished the protective effect and exacerbated hearing trauma. Alterations in corticosterone in blood and mRNA GR expression (PCR analysis) in the inner ear occurred in the acute phase of acoustic trauma. Summarizing these data we demonstrate that: 1) systemic stress can affect the mRNA of GR in the inner ear; and 2) a role of the corticosterone/inner ear mRNA glucocorticoid receptor balance in protecting against acoustic trauma.

686 N-acetylcysteine (NAC) and Acetyl-L-Carnitine (ALCAR) show Different Effects in Protecting the Cochlea from Noise in Chinchilla

Richard D Kopke¹, Eric C Bielefeld², Jianzhong Liu¹, Jiefu Zheng¹, Ronald L Jackson¹, Donald Henderson²

¹Otolaryngology, DOD Spatial Orientation Center, 34800 Bob Wilson Dr, San Diego, CA, United States, ²Hearing Research Lab, State University of New York, 215 Parker Hall, Buffalo, NY, United States

Objectives: Previously we have shown that systemic NAC administration reduces threshold shift and cochlear injury from impulse noise and that ALCAR reduces cochlear injury and hearing loss from steady state noise. In this study we compared NAC and ALCAR as systemically administered protective agents against impulse noise and assessed the dose response of NAC as a biological protectant against impulse noise. **Methods:** Eighteen female chinchilla were divided into three groups that underwent noise exposure: 1) saline control, 2) NAC, or 3) ALCAR. Animals were exposed to impulse noise at a level of 155 dB peak SPL for 150 repetitions. ALCAR or NAC were administered twice daily (BID) for two days and one-hour prior to and one-hour following noise exposure, then BID the following two days. For the control group, saline was injected at the same time points. Auditory brainstem responses were measured for assessing hearing threshold shift. Cochlear surface preparation was conducted for hair cell count and cytochrome c. An additional 24 animals underwent the same procedures with NAC doses as follows: 325 mg/kg, 200 mg/kg, 100 mg/kg, and 50 mg/kg. **Results:** Three weeks after exposure, permanent threshold shifts were significantly reduced to approximately 10-20 dB for animals treated with ALCAR or NAC, that were approximately 10-30 dB less than that of the control group ($p < 0.01$). Less hair cell loss was also observed in ALCAR and

NAC groups than in the control group. The degree and pattern of inner and outer hair cell loss and nature of the hearing recovery curves in the ALCAR group were different from that in the NAC group. ALCAR was more protective of IHCs and hearing recovery was more pronounced at later time points whereas NAC was more protective of OHCs and the recovery of threshold shifts was greater at earlier time points after injury. NAC was still quite effective at the lowest dose of 50 mg/kg. **Conclusions:** These findings indicate a strong protective effect of ALCAR and NAC against impulse noise-induced cochlear damage, and suggest the feasibility of using clinically available antioxidant compounds to protect the ear from acute acoustic injury. NAC and ALCAR appear to have different protective effects that may be additive or synergistic and this possibility is being studied. Funded by Office of Naval Research.

687 Prevention of Noise-Induced Hearing Loss with Src Inhibitors

Kelly Carney Harris¹, Donald Henderson², Bo hua Hu², Thomas Nicotera³

¹ENT, MUSC, 135 Rutledge Ave, Charleston, SC, United States, ²Center for Hearing and Deafness, University at Buffalo, 215 Parker Hall, buffalo, ny, United States, ³Molecular and Cellular Biophysics, Roswell Park Cancer Institute, 215 Parker Hall, buffalo, ny, United States

Intervention strategies to prevent noise-induced hearing loss (NIHL) have been developed that target various points in the cell death process (Hight et al., 2003 – antioxidants; Pirvola et al., 2000 – JNK inhibitor). We hypothesize that one of the early triggers of cochlear cell death are the changes that may occur in cellular adhesion points between the cells following a traumatic noise exposure. Changes in cellular adhesion are known to trigger Src-dependent cell death in a number of cell types. The current study uses three Src tyrosine kinase inhibitors as potential protective drugs for NIHL. Chinchillas were used as subjects. Their hearing was measured before and several times after the noise exposure and Src treatment. At 20 days post exposure, the animals were anesthetized and their cochleograms were performed. A 30 microliter drop of one of the Src inhibitors was placed on the round window of the anesthetized chinchilla; a drop of saline was placed on the other ear. After an hour the middle ear was closed and the subjects were exposed to noise. All three Src inhibitors provided protection from a 4 hour, 4 kHz octave band noise at 106 dB. The most effective drug, CH65, was then used with impulse noise and it provided significant protection. The results will be discussed in terms of triggers of apoptosis and strategies for protection.

[Research was supported by an NOHR grant]

688 Post-Administration of Antioxidants Ameliorates Noise-induced Hearing Loss from Continuous Loud Noise

John K. M. Coleman, Richard D. Kopke, Jianzhong Liu, Elizabeth Harper, Ronald L Jackson

DOD Spatial Orientation Center, Naval Medical Center San Diego, 348000 Bob Wilson Drive, San Diego, CA, United States

We have demonstrated significant success in decreasing noise induced hearing loss (NIHL) due to loud continuous noise expo-

sure by administering various antioxidant compounds either before (Kopke et al., 1999, 2000, 2001) or after the sound exposure (Kopke et al., 2002a, 2002b). Our most recent investigations have explored the efficacy of these compounds (N-acetyl-L-cysteine, NAC [I.P.; 325mg/kg] and acetyl-L-carnitine, ALCAR [I.P.; 100mg/kg]) to protect the cochlea from continuous loud sound at various times post exposure. Female chinchillas were injected starting 1, 4, and 12 hrs post exposure and then twice a day for 48 hrs to explore whether a window of efficacy post exposure exists. A second group of animals were injected with an equal volume of 0.9% saline given over a similar time schedule, exposed to the same noise paradigm and served as controls. The ABR thresholds were determined pre-noise, immediately following noise, 7 and 21 days post-noise (PN). Noise-exposed, saline injected animals at 21 days measured ABR thresholds of 14.2, 29.2, 37.5, and 41.2, dB SPL (at 1 hour injection start PN), and 12.0, 31.6, 44.1 and 37.9, dB SPL (at 4 hours injection start PN) above average pre-exposure baseline at 2, 4, 6, 8 kHz respectively. NAC-treated animals recovered to 11.3, 10.4, 21.3, and 19.1; 9.2, 21.3, 25.8, and 23.3; 12.5, 25.4, 37.5, and 34.5 at 1, 4, and 12 hrs (preliminary data), 2, 4, 6, and 8 kHz respectively. The ALCAR treated animals recovered to 6.5, 13, 21.5, and 16.5; 9, 19.5, 19, and 20; 14.1, 30.8, 40, and 35.8 at 1, 4, and 12 hrs (preliminary data), 2, 4, 6, and 8 kHz respectively. The data presented is suggestive of a window of opportunity to treat subjects post exposure. This is an encouraging result towards our long-term objective of developing agents for oral administration in clinical populations.

(The Office of Naval Research, U.S. Army and Department of Defense Spatial Orientation Center, Naval Medical Center San Diego support this work.)

689 FK506 reduces noise-induced hearing loss

Shujiro Minami, Daisuke Yamashita, Jochen Schacht, Josef Miller

Kresge Hearing Research Institute, University of Michigan, 1301 East Ann Street, Ann Arbor, Michigan, United States

The effectiveness of the immunosuppressor-growth factor FK506 (tacrolimus) to attenuate noise-induced cochlear damage was investigated. FK506 acts through FK506 binding proteins, immunophilins, which show neuroprotective and neuroregenerative effects in other systems. Recent studies also indicate that FK506s are abundant in the cochlea and dorsal cochlear nucleus, although their functional role is unclear. We show here that FK506 is a protective agent against noise-induced hearing loss in the guinea pig.

Guinea pigs were exposed to 120 dB SPL 1 OBN centered at 4 kHz for 5 h. They received artificial perilymph with or without FK506 into the left scala tympani via a microcannula and osmotic pump at 0.5 μ l/h continuously for 14 days beginning 4 days prior to noise. FK506 at 0.01, 0.1, 1, and 10 μ g/ml were studied. Auditory brainstem responses (ABR) were measured at 4, 8 and 16 kHz prior to surgery, 1 day before noise exposure, and on day 10 following noise exposure. Cochlear surface preparations were evaluated quantitatively for hair cell damage. A dose-dependent protective effect of FK506 on both sensory cell structure and auditory function was found with optimal protection at 1 and 10 μ g/ml. Further experiments will determine the mechanism of protection afforded by FK506.

Supported by NIH grant DC 04058, the Ruth & Lynn Townsend Professorship, UAW/GM funds.

690 Morphologic and functional changes in the inner ear hair cell following adenoviral vector gene delivery via the round window membrane treated with phenol

Mitsuya Suzuki^{1,2}, Tatsuya Yamasoba², Akinori Kashio¹

¹*Otolaryngology, Tokyo Metropolitan Police Hospital, 2-10-41, Fujimi, Chiyoda-ku, Japan,* ²*Otolaryngology, University of Tokyo, 7-3-1, Hongo, Bunkyo-ku, Japan*

Recently, it was demonstrated that adenovirus could transfect a variety of inner ear cells in the guinea pig through the round window membrane (RWM) damaged by local anesthetic solution containing phenol (LA). Although this delivery system may be able to reliably transfect the organ of Corti, marked morphologic damage may occur at the basal turn of the organ of Corti. This study investigated the optimal exposure time of LA, which is needed to deliver adenovirus-mediated gene via the RWM without damage to the organ of Corti. We assessed morphologic and functional damage to the inner ear following application of both LA and adenovirus vector to the RWM. We characterized adenovirus-infected cells using a vector that carried the gene for green fluorescent protein (GFP). The vector was administered to the RWM 5, 10, 20 or 40 min. following application of LA at the same site. Three days later, all animals were decapitated immediately after ABR tests. Hair cell damage was assessed morphologically in each animal using surface preparation technique. ABR tests in the 5, 10 or 20 min. group showed nearly normal thresholds at 4 KHz, 12 KHz and 20KHz. ABR tests in the 40 min. group showed mild to severe threshold shifts at 12 KHz and 20KHz. Surface preparation showed few scars in the organ of Corti of all cochlear turns and in the utricular macula in the 5 and 10 min. groups. A large number of scars were observed in the cochlear basal turn in all animals in the 40 min group. Epi-fluorescence image showed GFP negative in all specimens in the 5 min. group, suggesting the absent of adenovirus-infected hair cells and supporting cells in the cochlea and utricle of its group. We conclude that administration of adenovirus vector 10 min. following LA treatment may be suitable for safe and effective gene delivery to the guinea pig inner ear.

691 Apototic hair cell death after direct inoculation of adenovirus vectors to the scala media of the guinea pig

Shin-ichi Ishimoto, Tastuya Yamasoba, Kenji Kondo, Mitsuya Suzuki

Otolaryngology, university of Tokyo, 6-7-1 Hongo, Bunkyo-ku, Japan

The organ of Corti, especially the supporting cell, is an attractive target for interventions designed for production of new hair cells. Gene transfer has been used as a drug delivery system or for introduction of genes to the inner ear cells. Various approaches have been designed to deliver vectors to the organ of Corti. The scala media approach was successful to accomplish gene expressions in the organ of Corti. For example, conversion from the supporting cells to hair cells has been achieved by application of adenovirus vectors coding Math1 gene. However, damage to a variety of cells

including hair cells has been observed using this approach. In the current study, we assessed if such damage is caused by toxicity of viral vectors or it is surgically-induced

The guinea pigs were divided into two groups. The experimental animals (group I) were inoculated with 5 μ l of the adenovirus suspension. The control animals (group II) were given 5 μ l of the artificial endolymph. These animals were sacrificed 1 day, 3 days, and 5 days following the inoculation. The whole cochlea was dissected and each turn was mounted on slides with surface preparation technique. The presence of apoptotic cell death was determined using TUNEL methods. There were a lot of TUNEL-positive cells in the organ of Corti in both group I and II. The apoptotic hair cell death was predominant on day 1 in either group. There were no differences in the number of hair cells showing apoptosis between groups. These results suggest that the scala media approach has a potential to significantly damage the organ of Corti and that the damage observed following inoculation of virus vectors may be due chiefly to surgical procedure itself and not due to viral toxicity.

692 Where is the Spike Generator of the Cochlear Nerve? Expression of Voltage-Gated Sodium Channels in the Inner Ear of the Mouse.

Waheeda Amin Hossain, Matthew N Rasband, D Kent Morest

Neuroscience, University of Connecticut. Health Center, 263 Farmington Ave, Farmington, CT, United States

It is not well understood where in the cochlea, action potentials are first generated by the afferent nerve fibers. The initial part of the axon beneath the hair cells, the first heminode in the spiral lamina, or the portions of the axons projecting from the ganglion cell body have been suggested as possible sites. A voltage-gated sodium channel, Nav 1.6, has been implicated in generating action potentials at the initial segment and nodes of Ranvier in other nerve fibers. Thus, we used immunohistochemistry to locate Nav channels in the inner ear and cochlear nucleus of adult mice with well characterized, isoform-specific antibodies against Nav1.6 and Nav 1.2, as well as a Pan Nav antibody that recognizes all of the mammalian isoforms. Antibodies for contactin-associated protein (Caspr), a marker for paranodal regions of myelinated axons, were used to identify nodes of Ranvier. There was little or no Nav 1.6 staining of ganglion cell bodies. However, Nav 1.6 was clustered in ganglionic axons at nodes of Ranvier, where it was flanked by Caspr. The axonal processes from ganglion cell bodies stained in a pattern reminiscent of initial segments. Nav1.6 also appeared at the first heminode just within the foramina nervosa of the spiral lamina. In the organ of Corti, Nav1.6 localized to preterminal afferents and their endings on inner hair cells. The outer spiral fibers stained for Nav 1.6 in their preterminal and terminal parts beneath outer hair cells and extending to the outer pillars. In contrast, Nav 1.2 localized to the tunnel-crossing efferents up to their endings on outer hair cells, also on ganglion cell bodies. Pan sodium was expressed in the same sites as Nav1.6, but also in the cytoplasm of some ganglion cells. These data agree with the hypothesis that action potentials may be generated and regenerated at multiple sites along the cochlear nerve fiber. Supported by NIH grants NS29613, in DC06387 & NS044916 (MNR).

693 Immunohistochemical localization of voltage-gated sodium channel Nav1.6 in the guinea pig cochlea

Ryuichi Yoshida^{1,2}, Toshihiko Kikuchi¹, Toshihiko Chiba¹, Hiroshi Moriyama², Toshimitsu Kobayashi¹

¹Otorhinolaryngology-Head and Neck Surgery, Tohoku University School of Medicine, 1-1 Seiryomachi, Aoba-ku, Japan,

²Otorhinolaryngology, The Jikei University School of Medicine, 3-25-8 Nishishinbashi, Minato-ku, Japan

Nav1.6 is known to be expressed in the brain and the spinal cord and to mediate the influx of sodium ions in response to changes in membrane potential in excitable cells.

Immunohistochemical localization of voltage-gated sodium channel Nav1.6 (Scn8a) subunit in the guinea pig inner ear was studied in the present study. Intense Nav1.6-like immunoreactivity was present in the type II fibrocytes and suprastrial fibrocytes in the spiral ligament and in the fibrocytes in the spiral limbus. Immunostaining was also found in the stria vascularis and the spiral ganglion cells.

The results obtained in the present study suggest that Nav1.6 in the cochlear lateral wall and the spiral limbus may play an important role in cochlear ion homeostasis.

This is the first report that describes the expression pattern of voltage-gated sodium channel in the mammalian cochlea.

This work was supported by Grant-in-Aid for Scientific Research No.14370546 from the Ministry of Education, Culture, Sports, Science and Technology, Japan.

694 Differential Expression of Kcnq4 Alternatively Spliced Transcript Variants in Mouse Inner Ear: A Potential Role in Kcnq4-mediated Channelopathies

Kirk W. Beisel¹, Feng Feng¹, Kenneth A. Morris¹, Liping Nie², Ebenezer N. Yamoah²

¹Biomedical Sciences, Creighton University, 2500 California Plaza, Omaha, NE, United States, ²Center for Neuroscience, Dept Otolaryngology, University of California at Davis, 1544 Newton Court, Davis, CA, United States

Differential use of alternative splice variants of ion channels in inner ear neuronal and neurosensory epithelia has been implicated in their electrophysiological and functional properties. Database mining of UniGene, EST and RefSeq suggested a second splice variant of the hKCNQ4 gene. Initially, two full-length mKcnq4 variants were identified and differed in their utilization of exon 9. RT- and RACE-PCR were done on a panel of tissues to determine if additional Kcnq4 splice variants existed. Three variants (Kcnq4a-c) that differed in the utilization of two exons 9 (designated as exons 9a and 9b) or loss of exon 9 (9del) were identified in the inner ear. Kcnq4 genomic organization positioned exon 9b between 9a and 10. Kcnq4a (exon 9a) variant was present in all tissues examined, while Kcnq4b (exon 9b) and Kcnq4c (9del) were expressed only in excitatory tissues. However, Kcnq4b was weakly expressed in these tissues. Other Kcnq4 splice forms spanning exons 6-10 were also found in brain and heart. Amounts of these variants were assessed by quantitative PCR in adult spiral ganglion

(SG), organ of Corti and inner and outer hair cells. Qualitative and quantitative differential expression patterns of the exon 9 variants defined Kcnq4c as being the predominant form in SG and IHCs compared to Kcnq4a in OHCs. Also, the variant utilization and amounts of Kcnq4 vary along the length of the cochlea in these three cell types. *In vitro* electrophysiological studies showed the presence of the Kcnq4c confers a robust $I_{K,n}$ -like conductance and pharmacology consistent with Kcnq4 channels. Also the different kcnq4 isoforms associate to form functional channels. Although the pathogenic mechanism of DFNA2 [progressive high frequency hearing loss (PHFHL)] for the Kcnq4 auditory channelopathy is presently debatable, our data are compatible with the hypothesis that a dysfunctional signal transduction in the SG and IHCs imparts the PHFHL associated with Kcnq4-mediated channelopathies.

695 Identification, Expression and Localization of K⁺ Channel Subtypes KCNQ2 and 3 in the Mammalian Cochlea

Guihua Liang, Zhe Jin, Mats Ulfendahl, **Leif E Järleback**

Center for Hearing and Communication Research, Karolinska Institutet, M1:00, ENT Research Laboratory, Karolinska Hospital, Stockholm, Sweden

Potassium channels are key regulators of auditory function: e.g., by controlling membrane potential and thus neuronal excitability; and by performing crucial roles in potassium recycling thus providing the high endolymphatic [K⁺] required for cochlear transduction. These roles have been ascribed a variety of K⁺ channel families and subtypes. Noteworthy is KCNJ10 (Kir4.1) in intermediate cells of the stria vascularis which is responsible for generating the endocochlear potential and high [K⁺] in scala media.

KCNQ1 (KvLQT1) and KCNE1 (I_{Ks}) are alpha and beta subunits of a strial marginal cell K⁺ channel, and mutations in either result in deafness associated with Jervell and Lange-Nielsen syndrome. KCNQ4 (I_{Kn}) is found exclusively in outer hair cells, and its mutations underlie the non-syndromic autosomal dominant sensorineural hearing loss DFNA2. The KCNQ family of voltage-gated K⁺ channels obviously are important in hearing, however, the roles of the other members of this family in the cochlea are largely unknown.

We have previously reported the presence of time- and voltage-dependent sub-threshold non-inactivating M-like K⁺ currents in isolated outer hair cells from guinea pig cochlea. M-channels assembled from KCNQ2 and KCNQ3 subunits are present in neuronal tissues. KCNQ2 or 3 mutations are responsible for a type of childhood epilepsy, benign familial neonatal convulsion (BFNC). Other compositions of KCNQ subunits have also been suggested to result in M-type K⁺ currents. Using molecular and immunohistochemical approaches, we have pursued the expression and localization of KCNQ2 and 3 subunits in guinea pig and rat cochleae.

One-step RT-PCR analysis of KCNQ2/3 expression in micro-dissected cochleae revealed the expression of KCNQ2 splice variants in the modiolus and in the organ of Corti. In addition to those sub-fractions, KCNQ3 expression was also found the lateral wall. The identity of PCR products was verified by direct sequencing. The gene expression data was supported by immunolocalization of KCNQ2 and 3 subunits using primary antibodies (from Dr E.C.

Cooper, UCSF, and Alomone Labs, respectively) followed by immunoperoxidase or fluorescence methods. Positive immunolabeling was detected in spiral ganglion neurons (KCNQ2/3), in stria vascularis (KCNQ3), and at the base of outer hair cells (KCNQ2/3), appearing to be in efferent nerve endings and a base-to-apex gradient. These results lend further support for the presence of M channels with diverse functional properties in cochlear tissues.

696 ATP inhibits voltage sensitive potassium currents in isolated Hensen's cells of guinea-pig cochlea

Jianxiong Li¹, Xingqi Li¹, Wei Sun²

¹Otolaryngology Institute, Chinese PLA General Hospital, 28 Fuxing Road, Beijing, China, People's Republic of, ²Center for Hearing & Deafness, University at Buffalo, 3435 Main Street, Buffalo, NY, United States

There are increasing evidences suggest that ATP, a well known neurotransmitter and neuromodulator in central neural system, play an important role as an extracellular chemical messenger in cochlear. The effect of ATP on isolated Hensen's cells, one kind of supporting cells in the cochlea which supplied an ion transduction to the hair cells, were studied using the whole cell recording technique in this study. A reduction effect of ATP (0.1 to 10 μ M) on potassium current (IK⁺) were found from most of the recorded Hensen's cells (17 from 20). An inward current depends on IK⁺ was also induced by high concentration ATP (0.1 to 10 mM) which was reversely blocked by suramin (100 μ M), a purinergic antagonist. Our results suggest that ATP can block IK⁺ channels in low concentration and induced an inward current in high concentration carried by K⁺ through purinergic receptors.

Supported by the National Natural Science Foundation of P.R.China (No.39870797)

697 Molecular Cloning and Functional Identification of Merg1a Potassium Channel in Mouse Cochlea.

Liping Nie¹, Karen J Mu¹, Weihong Feng¹, Michael Anne Gratton², Ana E Vazquez¹, Ebenezer N Yamoah¹

¹Center for Neuroscience/Otolaryngology, University of California Davis, 1515 Newton Ct., Davis, CA, United States,

²Otorhinolaryngology-HNS, University of Pennsylvania, 3400 Spruce St., Philadelphia, PA, United States

Alterations in K⁺ homeostasis in the cochlear duct have profound effects on the transduction of auditory signals. Previous pharmacological, biochemical, and functional studies have identified candidate ion transporters, pumps, and channels that are involved in the K⁺ regulation in the cochlea. The present work is the first to demonstrate the molecular identification and cellular localization of ERG1a channel in mouse inner ear (MERG1a). A cDNA fragment containing the complete open reading frame of merg1a was amplified from cochlea by RT-PCR and cloned into pCRII-TOPO. The amino acid sequence of the putative protein shows typical characteristics of erg K⁺ channels with six transmembrane domains (S1-S6) and the pore region. The sequence comparison showed that mouse inner ear-specific MERG1a shares high homology with ERG1a proteins from other tissue types and

species.

The cellular distribution of MERG1a in the cochlea was investigated using both immunoperoxidase and immunofluorescence techniques. The highest levels of immuno-reactivity were found in the intermediate cells of stria vascularis and the spiral ganglion cells. In addition, low levels of expression were detected in hair cells, type II and V fibrocytes of the spiral ligament and fibrocytes underlying the interdental cells of the spiral limbus. To characterize the functional and pharmacological phenotype of the channel, the channel was expressed in a heterologous expression system (*Xenopus* oocytes). In *Xenopus* oocytes, MERG1a channel is K⁺ permeable, E4031- and rBeKm-1-sensitive, activates at relatively negative potentials, and shows characteristic rapid inactivation reflected as inward rectification at depolarized potentials: a typical property of ERG K⁺ channel family. The role of the *merg1a* in the cochlear duct will be discussed.

This work was supported by grants to LN (Deafness Research Foundation), ENY (NIH-DC03828, DC04523).

698 DFMO-induced Ototoxicity May be Derived from Drug-mediated Effects on the Inward Rectifier Kir4.1 Channel in the Inner Ear.

Liping Nie¹, Weihong Feng¹, Rodney C Diaz², Karen J Doyle², Michael Anne Gratton³, Ebenezer N Yamoah¹

¹Center for Neuroscience/Otolaryngology, University of California Davis, 1515 Newton Ct., Davis, CA, United States,

²Otolaryngology, University of California Davis, 1515 Newton Ct., Davis, CA, United States, ³Otorhinolaryngology-HNS, University of Pennsylvania, 3400 Spruce St., Philadelphia, PA, United States

Previous studies have demonstrated that inward rectification of Kir channels is mediated by both the block of the outward component of the current by cytoplasmic Mg²⁺ and by intrinsic polyamines. Ornithine decarboxylase (ODC), the key enzyme in polyamine synthesis is expressed in the organ of Corti and lateral wall of the cochlear duct, consistent with the distribution of polyamines in the inner ear. D, L-a-difluoromethylornithine (DFMO) is a cancer protective agent that irreversibly inhibits ODC activity and subsequently causes a decrease in the levels of polyamines in the cochlea. Because the Kir4.1 channel in the apical membrane of intermediate cells of the stria vascularis has been implicated as the major conduit through which a high throughput of K⁺ is attained to confer endocochlear potential (EP), we surmised that DFMO-induced ototoxicity may result from alterations of EP.

We cloned mouse cochlea specific-Kir4.1 and analyzed the channel properties in heterologous expression system (*Xenopus* oocytes). Analysis of the electrophysiological data showed that mouse cochlear Kir4.1 belongs to the intermediate rectifier channel sub-class, which is in accord with previous reports. In *Xenopus* oocytes, the channel controls the resting membrane potential, it is K⁺ permeable, Ba²⁺ and ATP sensitive, and shows a single-channel conductance of ~50 pS. DFMO, decrease the inward rectification of Kir4.1 and produces a surprising reduction in EP in mice (control; 95 ± 9 mV (n = 8); DFMO-treated; 48 ± 15 mV (n = 5)). These studies have identified traces of the cellular mechanisms of DFMO-induced ototoxicity. Moreover, DMFO may serve as a useful tool to understand the underlying mechanisms for the contribution of Kir channels in the generation of EP.

This was supported by grants to LN (Deafness Research Foundation), ENY (NIH-DC03828, DC04523).

699 Functional analysis of calcium-activated potassium (BK) channels in the inner ear

Markus HF Pfister^{1,2}, Marcus Müller¹, Matthias Sausbier³, Lukas Rüttiger¹, Marlies Knipper¹, Peter Ruth³

¹Otolaryngology, University of Tübingen, Elfriede Aulhornstr. 5, Tübingen, Germany, ²Otolaryngology, Stanford University, 300 Pasteur Drive, Palo Alto, CA, United States, ³Institute of Pharmacology, University of Tübingen, Auf der Morgenstelle 8, Tübingen, Germany

Large-conductance calcium-activated potassium (BK) channels are known to play a prominent role in the hair cell function of lower vertebrates where these channels determine electrical tuning and regulation of neurotransmitter release. Until recently, very little was known, by contrast, about the role of BK channels in the mammalian cochlea. In situ hybridization of Slo antisense riboprobes and immunocytochemistry by Skinner et al. and Langer et al. (*J Neurophysiol* 90: 320-332, 2003, *J Comp Neurol* 455: 198-209, 2003) demonstrated a strong expression of BK channels in IHCs and spiral ganglion and to a lesser extent in OHCs. Overall, these results revealed the importance of BK channels in mammalian cochlear neurotransmission and demonstrated that at the presynaptic level, fast BK channels are a significant component of the repolarizing current of IHCs. Due to these results a transgenic mouse model (BKca Knockout) was analysed electrophysiologically as well as histologically over a one year period revealing the functional importance of this channel for the hearing process.

Supported by fortune Program Nr. 1062-0-0, University of Tübingen, Germany

700 Dihydroxy-phenylglycine, a metabotropic glutamate receptor agonist, increases internal calcium concentration in embryonic chick cochlear ganglion neurons.

Brian P. Manning, William F. Sewell

Department of Otolaryngology and Program in Neuroscience, Massachusetts Eye and Ear Infirmary and Harvard Medical School, 243 Charles St., Boston, MA, United States

While much is known about the role of ionotropic, AMPA-type, glutamate receptors in mediation of moment-by-moment synaptic transmission between hair cells and their afferent fibers, auditory neurons also express other types of glutamate receptors, including metabotropic and N-methyl-D-aspartate (NMDA) receptors. The actions or functions of these other glutamate receptors in the inner ear are not well characterized. To study the roles of these receptors in auditory function, we have examined the pharmacology of metabotropic glutamatergic receptors in dissociated, embryonic-chick, auditory-ganglion cells using the ratiometric calcium indicator, Fura-2. The group 1 metabotropic glutamate receptor agonist, dihydroxyphenylglycine (DHPG), increased internal [Ca²⁺] in isolated ganglion cells with 4 temporal response patterns: (1) a transient increase (seconds), (2) a slowly building and decaying increase (minutes), (3) a transient increase followed by a slowly building and decaying increase and (4) cyclic increases

lasting for several minutes after application. Responses to DHPG were concentration-dependent with an EC_{50} of $<100 \mu\text{M}$. Responses to DHPG were reduced with the metabotropic receptor antagonist, methyl-4-carboxyphenylglycine (MCPG, $100 \mu\text{M}$).

701 Tissue-specific Expression of Edg Receptors in the Inner Ear

Zhijun Shen, Fenghe Liang, Bradley A. Schulte

Pathology & Lab Medicine, Medical University of South Carolina, 165 Ashley Avenue, Charleston, SC, United States

Endothelial differential gene receptors (Edg-Rs) belong to the G protein-coupled receptor family. To date, 8 Edg-Rs have been cloned and classified into two subfamilies. Edg-1, -3, -5, -6 and -8 are encoded by intronless genes and are activated by sphingosine-1-phosphate (S-1-P). In contrast, Edg-2, -4 and -7 are encoded by genes having two introns in the open reading frame and bind to lysophosphatidic acid (LPA).

Edg-Rs have been found in almost every organ studied, although their tissue and cell-specific expression patterns vary. Depending on the expression pattern, time and location, Edg-Rs have the ability to regulate many cellular activities including embryonic development, vascular maturation, angiogenesis and cancer cell metastasis.

We hypothesized that Edg-Rs are present in the inner ear and may be crucial to the regulation of important processes such as development, aging, ion homeostasis etc. The expression of Edg-Rs in the C57 mouse inner was screened using RT-PCR methods. Specific primers were designed for Edg-1, -2, -3, -5 and -8 based on mouse sequences. The cochlear lateral wall (including spiral ligament), organ of Corti (including spiral ganglion) and whole vestibular membranous labyrinth were dissected and pooled from 8 mice. Total RNA was isolated and reverse transcribed into cDNA. Positive PCR products were gel purified and ligated into a pCR2 vector for sequencing. Data were compared with sequences of mouse Edg-Rs from Genbank.

The results were as followings: Organ of Corti: Edg-2 and -5 were positive; Edg-3 and -8 were marginally positive. Lateral Wall: Edg1 was abundant; Edg-2 and -5 were marginally positive. Vestibular Organ: Edg-1 and -2 were expressed. These data demonstrated a tissue-specific expression pattern of Edg-Rs in the inner ear. Further investigation of the cellular localization and function of these Edg-Rs will clarify their role in the inner ear.

702 Evidence of a Stem Cell Population in the Murine Cochlea by Gene Chip Analysis

Mark Allen Parker^{1,2}, Deborah Corliss¹, Julia Anderson¹, Evan Y. Snyder³, Douglas A. Cotanche^{1,2}

¹Otolaryngology, Children's Hospital, 300 Longwood Ave, FE9, Boston, MA, United States, ²Otology and Laryngology, Harvard Medical School, 300 Longwood Ave, FE9, Boston, MA, United States, ³Stem Cell & Regeneration Program, Burnham Institute, 10901 North Torrey Pines Road, La Jolla, CA, United States

Recent evidence of a stem cell population located within the mammalian vestibular system led us to investigate whether the cochlea contains a potential stem cell niche as well. A post hoc comparison between published cochlear (Chen & Corey, *J Assoc Res Otolaryngol* 2002 Jun;3(2):140) and stem cell (Ramalho-Santos et al., *Science*. 2002 Oct 18;298(5593):597-600) gene chips

revealed the presence of a population of genes within the cochlea that share a stem cell expression profile. Of those genes expressed in the cochlea, 40% were common to genes enriched in hematopoietic stem cells, 43% were common to embryonic stem cell enriched genes, and 46% were common to genes enriched in neurospheres. Interestingly, 71% of the genes expressed in the C17.2 neural stem cell line were present in the cochlear gene chip. These results have two main implications. Foremost, they suggest that the cochlea may contain a population of stem cells. Secondly, these results suggest that this stem cell population is related more closely to neural rather than embryonic or hematopoietic stem cells. Supported by a NOHR Hair Cell Regeneration Initiative Grant and NIH/NIDCD Grant #F32 DC005866.

703 Tonotopic differences in synaptic release as measured by membrane capacitance changes in hair cells from the turtle auditory papilla.

Michael E Schnee¹, D M Lawton², David N Furness², Anthony Ricci¹

¹Neuroscience, LSU Medical School, 2020 Gravier St, New Orleans, LA, United States, ²MacKay Institute of Communication and Neuroscience, Keele University, Street, Staffordshire, United Kingdom

The turtle auditory papilla responds to frequencies between 30 and 700Hz (Crawford and Fettiplace, 1981). Previous experiments have demonstrated that the calcium channels are clustered into hot-spots that increase in number tonotopically (Ricci et al., 2000). From this, the working hypothesis is that the synaptic machinery remains constant while the number of release sites increases tonotopically allowing stochastic behavior of the release sites to encode higher frequencies. Electron microscopic analysis demonstrates that the number of synaptic ribbons more than doubles (2.3 ± 0.6 increase) between 0.3 and 0.6 relative positions along the papilla, a change very similar to that observed in the hair cell calcium current (2.24 increase) (Schnee and Ricci, 2003). It is predicted that the total available pool of vesicles increases as a function of the increased number of release sites. Calcium-dependent changes in capacitance were measured with a phase-lock amplifier in response to 20 second depolarizations to -20mV eliciting maximal calcium currents and saturating capacitance responses. Measurements of $5.4 \pm 1.2\text{pf}$ and $2.2 \pm 0.9\text{pf}$ for 0.6 and 0.3 positions were obtained, having a ratio 2.45 very similar to that found in both the calcium current and in the number of synaptic ribbons. A vesicle size of $23 \pm 2\text{nm}$ was measured from electron micrographs. When corrected for shrinkage ($\sim 30\%$) a capacitance per vesicle of 30aF was obtained giving a total number of released vesicles of $\sim 180,000$ and $73,000$ for 0.6 and 0.3 positions. As the total number of vesicles per ribbon at these positions are ~ 3100 and 1600 either ribbons can reload rapidly ($\sim 58\text{x}$ in 20 seconds) or the majority of release is via non ribbon contacts. The data is consistent with the hypothesis that there is an increase in the number of functional release sites corresponding to the increase in characteristic frequency.

Supported by DC03896 from NIDCD to AJR.

704 Characterization of the Calretinin Gene in *Rana pipiens*

Lingya Liao, William M. Roberts

Biology, University of Oregon, Institute of Neuroscience, Eugene, Oregon, United States

Calretinin, a calcium-binding protein, belongs to the EF-hand superfamily. It appears primarily in neurons but its function remains obscure. Calretinin concentration can reach to a millimolar level (~1.2mM) in cytoplasm of thin tall hair cells, a cell population estimated to be ~20% of total saccular hair cells in frog. Calretinin has been hypothesized to serve as a diffusibly mobile calcium buffer/transporter to regulate calcium signaling over nanometer distances at the presynaptic sites. (Edmonds et al., 2000, *Nature Neuroscience*, 3(8): 786-790).

Toward a better understanding of calretinin function, we have successfully cloned a calretinin gene from grass frog, *Rana pipiens*. We used degenerate primers, designed at the most conserved amino acid regions of both calretinin and calbindin, to amplify (RT-PCR) specific calretinin mRNA in sacculus. Based on the obtained cDNA information, we designed both 5' and 3' RACE (rapid amplification of cDNA ends) primers to determine the entire open reading frame (ORF). Finally, we obtained a full-length calretinin cDNA by 3' long-distance RACE. The complete calretinin cDNA is 3062bp in length with an 816bp ORF. The predicted protein contains six presumed calcium-binding sites. It is ~80% identical to the known calretinins and ~60% identical to calbindins. RT-PCR using gene specific primers showed that calretinin is expressed in sacculus, eye, and optic tectum, but not in cerebellum. In situ hybridization confirmed the presence of calretinin mRNA in saccular hair cells. Further investigation is currently underway to obtain more information of calretinin in frog.

705 Kinetics of Synaptic Vesicle Exocytosis and Membrane Retrieval in Frog Saccular Hair Cells

Mark Rutherford, William M. Roberts

Institute of Neuroscience, University of Oregon, 1254 University of Oregon, Eugene, OR, United States

We have measured changes in the whole-cell capacitance of hair cells in a semi-intact preparation of the sensory epithelium from the sacculus of *Rana pipiens* to investigate fast components of the synaptic vesicle cycle at ribbon-class synapses. Brief depolarizations lasting 1-10 msec evoke a rapid rise in membrane capacitance that we associate with a pool of synaptic vesicles that are already docked and primed for exocytosis. An additional sustained secretory component is considerably larger than the pool of docked vesicles that was identified in previous electron tomography experiments (Lenzi et al. 2002, *Neuron*, 36:649), suggesting rapid replenishment of the pool of releasable vesicles. The retrieval of membrane following the end of the depolarization had two or more kinetic components, including a very rapid recovery within tens of milliseconds. The rapid phase could correspond to a fast conventional endocytic pathway, or the endocytosis of large membrane infoldings. We are using non-hydrolyzable ATP and GTP analogs and electron tomography to investigate the anatomical correlates of these

exocytic and endocytic pathways. This research was supported by NIH grant R01 NS27142 to WMR.

706 Co-Localization of the Synaptic Ribbon to Glutamate Receptor Patches at the Chick Cochlear Hair Cells Afferent Fiber Synapse

Shunda R. Irons-Brown¹, J. Andrew Dziejewit¹, Thomas D. Parsons²

¹*ENT, University of Pennsylvania, 3400 Spruce St. 5 Ravdin-ORL, Philadelphia, Pennsylvania, United States,* ²*Veterinary Medicine, University of Pennsylvania, 382 West Street Road, Kennett Square, Pennsylvania, United States*

We employed immunocytochemistry and fluorescent laser scanning confocal microscopy to localize putative epitopes of the synaptic ribbon protein, Ribeye, and the glutamate receptor, GluR2, in the avian cochlea. Anti-GluR2 staining exhibited a punctate, patch-like pattern concentrated at the base of the hair cell. Three-dimensional reconstruction of serial image stacks confirmed that the apparent receptor patches lie along the hair cell's baso-lateral surface. A marked gradient in GluR2 patch staining was observed along the radial axis from the neural to abneural edge of the cochlear duct, consistent with the labeling of synaptic contacts between the hair cell and its afferent fibers. A noted co-localization of the synaptic ribbon to these receptor patches was observed when the cells were double-labeled cells with both anti-GluR2 and anti-Ribeye antibodies. Approximately 80% of the receptor patches examined in each tissue section overlapped with aggregates of Ribeye staining. At 2 days of age post-hatch, 83 +/- 5% (7 sections from 4 birds), and at 6 days, 78 +/- 9% (9 sections from 4 birds) of receptor patches were co-localized with a synaptic ribbon. Ongoing studies are focused on the development sequence of the synaptic ribbon-glutamate receptor morphological complex formation and distribution.

707 Modeling hair cell exocytosis using a hybrid deterministic-stochastic implementation

John H. Wittig¹, Thomas D. Parsons^{2,3}

¹*Bioengineering, University of Pennsylvania, 34th Str, Philadelphia, PA, United States,* ²*Clinical Studies - New Bolton Center, University of Pennsylvania, 382 West Street Road, Kennett Square, PA, United States,* ³*Otorhinolaryngology - Head & Neck Surgery, University of Pennsylvania, Spruce Street, Philadelphia, PA, United States*

We present a novel computational modeling approach to simulate the synaptic details of a bullfrog saccular hair cell. Our model focuses on a single pre-synaptic active zone, and addresses calcium influx, buffered calcium diffusion, and exocytosis. This ribbon synapse has been well characterized both anatomically (Lenzi et al., 1999, 2002) and physiologically (Roberts 1993; Parsons et al., 1994). We strive to explain how this synapse's temporal fidelity is shaped by specializations in the active zone microdomain, such as calcium buffering, and the relative location of calcium channels to synaptic vesicles. We also want to identify the anatomical substrate for physiologically identified vesicle pools that contribute to both neural adaptation and sustained discharge by the auditory nerve fiber.

Our modeling aims required the development of a hybrid deter-

ministic-stochastic implementation. Deterministic modeling is appropriate for describing continuous, macroscopic functions such as flux, population kinetics, and transport (Roberts 1994; Xu et al., 1997). Stochastic modeling, in contrast, is appropriate for describing the time evolving location or state of individual species (Gil et al., 2000). We deterministically modeled macroscopic properties of the synaptic physiology such as whole cell calcium current activation and buffered diffusion of calcium. We combined such techniques with stochastic models of the discrete, molecular-level events of channel gating, calcium binding, and vesicle fusion. We have confirmed our modeling technique with several sets of physiological data. Our present simulations identify a readily-releasable pool of vesicles, and the calcium dynamics required to match its observed exocytic responses.

708 The presynaptic protein Bassoon is required for synchronous synaptic transmission at the hair cell ribbon synapse

Darina Khimich^{1,2}, Regis Nouvian¹, Andreas Brandt¹, Michel Eybalin³, Wilko Altmann⁴, Eckart Gundelfinger⁴, Tobias Moser^{1,2}

¹Department of Otolaryngology, University of Goettingen, Robert-Kochstr. 40, Goettingen, Germany, ²Neuroscience Program, University of Goettingen, Robert-Kochstr. 40, Goettingen, Germany, ³U583, INSERM, 71, rue de Navacelles, MONTPELLIER, France, ⁴Dept. of Neurochemistry and Molecular Biology, Leibniz Institute for Neurobiology, Brennekestr. 6, Magdeburg, Germany

Hearing relies on the synchronous synaptic transfer between hair cells and auditory nerve. Here, we investigated the role of the presynaptic matrix protein bassoon in hearing. We show that bassoon is part of the ribbon-type hair cell active zones. Active zones of mature inner hair cells (IHCs) from loss-of-function bassoon mutants lacked the synaptic ribbon. Using membrane capacitance measurements we show that the readily releasable pool of vesicles, which mediates synchronous transmitter release, is strongly reduced in mature mutant hair cells. The calcium current density of mutant IHCs was approximately 40 % of control. Despite the lack of the ribbons and the reduced calcium influx mutant IHCs displayed nearly unchanged sustained exocytosis. Mutant mice showed a profound hearing impairment in compound action potential recordings. We conclude that bassoon is required for anchoring the ribbon at the active zone of IHCs. The presence of bassoon and/or the ribbon is essential for synchronous transmission at the hair cell synapse probably by organizing calcium channels and readily releasable vesicles at the active zones.

709 Functional characterization of the glutamate transporter GLAST in cochlear Phalangeal cells that surround inner hair cells and their afferent terminals

Elisabeth Glowatzki¹, Ning Cheng², Hakim Hiel¹, Paul A Fuchs¹, **Dwight E Bergles**²

¹Department of Otolaryngology Head and Neck Surgery, Johns Hopkins School of Medicine, 720 Rutland Ave Traylor 521, Baltimore, MD, United States, ²Department of Neuroscience, Johns Hopkins School of Medicine, 725 North Wolfe Str. WBSB 813, Baltimore, MD, United States

Inner phalangeal cells (IPCs) that surround inner hair cell (IHC) synapses express the glutamate transporter GLAST (EAAT1) at a high density (Furness and Lehre, 1997, Eur J Neurosci 9:1961), and mice lacking GLAST exhibit enhanced hearing loss following acoustic overstimulation (Habuka et al., 2000, J Neurosci 20:8750). To investigate the contribution of these transporters to glutamate removal at IHC afferent synapses, we made whole-cell recordings from IPCs in whole-mount apical turns from 5-10 day old rat cochleae. IPCs exhibited high resting potentials (~ -90mV), low membrane resistances (<50Mohm), and, when gap junctions were blocked with octanol, prominent voltage-gated potassium conductances. To amplify transporter-mediated responses, anions such as NO₃⁻ or SCN⁻ that are highly permeant through glutamate transporters were used in the internal solution. Pressure application of D-aspartate (500μM), a substrate of glutamate transporters, induced inward currents in IPCs (-50 to -200pA at -90mV) that were reversibly blocked by the glutamate transporter antagonist TBOA (200μM); in the absence of permeant anions, these currents were < -10pA in amplitude. The I-V relationship of D-aspartate responses was inwardly rectifying and did not reverse between -90 and +40mV, as expected for transporter-mediated currents. In contrast, D-aspartate application did not elicit transporter currents in recordings from either IHCs or their afferent fiber terminals. Transporter currents in outside-out patches from IPCs exhibited a larger steady-state current in response to D-aspartate than L-glutamate, a feature characteristic of GLAST transporters, and transporter currents were absent in IPCs from GLAST knockout mice. Together, these data suggest that GLAST transporters in IPCs are primarily responsible for clearing the glutamate released at IHC-afferent synapses. Supported by NIDCD 00276 and NINDS 44261.

710 The dynamic changes of glutamate-like immunoreactivity in cochlear inner hair cells of guinea pigs after noise exposure

Xingqi Li, Zulin Tan, Jun Liu, Lidong Zhao, Qing Sun, Jianhe Sun, Jianxiong Li

Department of Otolaryngology, PLA General Hospital, Institute of Otolaryngology, 28 Fuxing Road, Beijing, China, People's Republic of

To investigate the glutamate-like immunoreactivity (Glu-IR) changes in inner hair cells (IHCs) of guinea pigs cochlear after noise exposure. Guinea pigs were distributed into 6 groups: control group (g1), and groups of immediately (g2), 8 hours (g3), 1 day (g4), 3 days (g5) and 7 days (g6) after noise exposure. Their

right eardrums were broken and right external auditory meatus were blocked. The experimental groups were exposed to 120 dB SPL narrow band noise for 4 hours to damage the left cochlea. The first turn of the organ of Corti was dissected to make semithin sections and immunocytochemistry (SP dyeing). The average optical density (AOD) of Glu-IR in IHCs was measured. Compound action potential (CAP) was recorded from the round window. In g1, the AOD of Glu-IR in IHCs had no significant difference between bilateral cochleae (paired t test). In g2, the AOD of Glu-IR in IHCs of left cochleae increased compared with the right cochlea, while that of g3 decreased. There were no significant difference between the bilateral cochleae in g1, g4, g5 and g6. The CAP threshold of g2 and g3 were 69 dB SPL and 76 dB SPL respectively but no significant difference was noticed. The threshold of g4, g5 and g6 were 70 dB SPL, 65dB SPL and 54 dB SPL respectively and there were significant difference among these groups ($p < 0.01$). Glu-IR in IHCs after noise exposure changed dynamically. $[Ca^{2+}]$ in inner hair cells was increased after noise exposure. Ca^{2+} activated glutamate synthetase system and more glutamic acid was produced. Glutamic acid decreased in IHCs because of its over-releasing into synapsis. Glu-IR's recovery to normal level indicated the existence of the glutamate-glutamine circulation in the cochlea.

(Supported by the National Natural Science Foundation of China (No.39870797))

711 G α i Isoforms in a Saccular Hair Cell Preparation: mRNA and Protein Expression

Adam J. Folbe¹, Marian J. Drescher¹, Neeliyath A. Ramakrishnan¹, Khalid M. Khan², James S. Hatfield³, Dennis G. Drescher^{1,4}

¹Department of Otolaryngology, Wayne State University School of Medicine, 540 East Canfield Avenue, Detroit, MI, United States, ²Department of Biological & Biomedical Sciences, Aga Khan University, Stadium Road, Karachi, Pakistan, ³Electron Microscopy Laboratory, Veteran Affairs Medical Center, 4646 John R, Detroit, MI, United States, ⁴Department of Biochemistry-Molecular Biology, Wayne State University School of Medicine, 540 East Canfield Avenue, Detroit, MI, United States

Hair cells of the teleost saccule have previously been demonstrated to express mRNA for serotonin 5-HT1 receptor subtypes (Drescher et al., ARO Abstr. 26: 11, 2003) and dopamine D2 receptor (Oh et al., ARO Abstr. 21: 111, 1998). These receptors are predicted to inhibit adenylyl cyclase (AC) isoforms via coupling to G β γ . There are three G α i isoforms, with differential localizations at a subcellular level and differential coupling to receptor subtypes. Selectivity in cellular pathways modulated by neurotransmitter receptor activation has been increasingly attributed to additional specificity deriving from coupling to specific G α and AC isoforms. Here, we have examined the expression of message for G α i in a model hair cell preparation from the trout saccule with RT-PCR and degenerate/specific primers targeting evolutionarily conserved sequence for G α i isoforms. Two G α i isoform variant transcripts have been detected in the saccular hair cell layer. One cloned transcript, representing 92% of the coding region for G α i1, is 96% identical in amino acid sequence to G α i1. The second variant exhibited 91% identity in amino acid sequence to the first, with approximately equal identity to G α i1 and G α i3. The hair cell

G α i1 protein contains a 20-amino acid peptide epitope present in rat G α i1 not found in the G α i1/3 protein. The G α i1 epitope was targeted by an affinity-purified rabbit polyclonal antibody (sc-391, Santa Cruz Bio-technology) and the predicted 40.3 kDa protein for G α i1 in the hair cell layer revealed by western blot. Immunoreactivity for G α i1 was associated with the lateral membranes of saccular hair cells, with isolated patches juxtaposed to efferent contact. Expression of G α i1 by the saccular hair cell is consistent with reported selectively for G α i isoforms: G α i1 couples to serotonin 5-HT1A, one member of the 5-HT1 receptor subtypes expressed in the hair cell layer, with consequent inhibition of AC, putatively down-regulating hair cell transmitter release.

712 Adenylyl Cyclase-Mediated Signal Transduction in Saccular Hair Cells: Coupling to G α s/olf

Marian J. Drescher¹, Won J. Cho¹, Samantha Anne¹, James S. Hatfield², Dennis G. Drescher^{1,3}

¹Department of Otolaryngology, Wayne State University School of Medicine, 540 East Canfield Ave., Detroit, MI, United States, ²Electron Microscopy Laboratory, Veteran Affairs Medical Center, 4646 John R, Detroit, MI, United States, ³Department of Biochemistry-Molecular Biology, Wayne State University School of Medicine, 540 East Canfield Ave., Detroit, MI, United States

Adenylyl cyclase (AC)-mediated signal transduction is predicted to impact both mechanosensory transduction and transmitter release of hair cells. The identity of expressed AC isoforms underlying these AC transduction pathways has been investigated with RT-PCR applied to the hair cells of the trout saccule. Degenerate primers directed amplification of AC9:AC7:AC6 in relative abundance of 11:5:2, determined by cloning. Ca^{2+} /calmodulin-activated AC isoforms 1, (3) and 8 were not amplified, leaving G α s coupling, heretofore undetected in cochlear or vestibular hair cells, as a primary mechanism for AC activation. That G α s would be expressed in the type II-like saccular hair cells was previously suggested by amplification of cDNA for dopamine D1A3 receptor (Kewson et al., ARO Abstr. 26: 156, 2003). Degenerate primers targeting *Xenopus laevis* and *Drosophila melanogaster* G α s cDNA sequence amplified in RT-PCR two messages from the saccular hair cell preparation. With 5' and 3' RACE, we have obtained full coding sequence for one of these expressed messages and partial sequence for the second, the latter replicated in a full coding sequence from brain. Overall, the hair cell sequence indicates high amino acid identity to both G α s (81%) and G α olf (84%). While incorporating a 15 amino acid deletion which is evolutionarily conserved in G α olf, the hair cell sequence reflected a relatively equal division of amino acids between G α s and G α olf. The hair cell and brain sequences were characterized by a carboxy terminus present in G α s and G α olf of higher vertebrates, a targeted epitope allowing immunolocalization of G α s/olf protein to hair cell stereocilia and saccular hair cell membrane, the latter consistent with sites of efferent innervation. The expression of dopamine D1(A3) receptor, G α s/olf and AC5/6 in saccular hair cells is consistent with the specific coupling for the adenylyl cyclase signal transduction pathway mediating a dopamine D1 response in higher vertebrates.

713 Syntaxin 1 is Expressed in Trout Sacculus Hair Cells: RT-PCR and Immunocytochemical Observations

Khalid M. Khan^{1,2}, Neeliyath A. Ramakrishnan¹, Marian J. Drescher¹, James S. Hatfield³, Dennis G. Drescher^{1,4}

¹Department of Otolaryngology, Wayne State University School of Medicine, 540 East Canfield Avenue, Detroit, MI, United States,

²Department of Biological and Biomedical Sciences, Aga Khan University, Stadium Road, Karachi, Pakistan, ³Electron Microscopy Laboratory, Veterans Affairs Medical Center, 4646

John R Street, Detroit, MI, United States, ⁴Department of Biochemistry-Molecular Biology, Wayne State University School of Medicine, 540 East Canfield Avenue, Detroit, MI, United States

Syntaxin is one of several proteins that may be involved in the docking of synaptic vesicles, synaptic vesicle recycling, and non-synaptic membrane trafficking (Jahn and Sudhof, Ann. Rev. Biochem. 68: 863-911, 1999). Presence of syntaxin has been reported in rat auditory (Safieddine and Wenthold, Eur. J. Neurosci. 11: 803-812, 1999) and vestibular end organs (Demêmes et al., Neuroscience 98: 377-384, 2000). In the current study, we have examined the expression of message for syntaxin 1 in hair cells of the sacculus of the rainbow trout, *Oncorhynchus mykiss*, with RT-PCR using degenerate primers based on the sequence of zebrafish syntaxin. A PCR product of predicted size, 540 bp, yielded sequence with 94% amino acid identity to mouse, rat, and human syntaxin and 96% identity to zebrafish syntaxin. An anti-syntaxin 1 primary antibody (S1172, Sigma) recognized a protein of predicted size, 33 kDa, from trout brain extract in western blot. At the light microscopic level, immunoreactivity for anti-syntaxin 1 was observed within the sensory epithelium, in efferent fibers below the hair cells running parallel to the longitudinal axis of the sacculle. In addition, sub- and supranuclear immunostaining was observed within select hair cells and immunoreactivity was concentrated at the base of stereociliary arrays throughout. Immunogold electron microscopy further revealed that immunoreactivity was associated with the synaptic bodies and the basolateral and supranuclear regions of hair cells along with that present in the cuticular plate/stereociliary region of hair cells and efferent endings. These results suggest that syntaxin, expressed in the trout sacculle, is associated not only with the docking of synaptic vesicles, but may be involved in vesicle recycling and in recycling of membrane.

714 Distribution and Molecular Sequence Analysis of the $\alpha 10$ Acetylcholine Nicotinic Receptor Subunit from the Rainbow Trout, *Oncorhynchus mykiss*

Kamran Sadrazodi¹, Neeliyath A. Ramakrishnan¹, Steven F. Myers², Marian J. Drescher¹, Dennis G. Drescher^{1,3}

¹Department of Otolaryngology, Wayne State University School of Medicine, 540 East Canfield Avenue, Detroit, MI, United States,

²Department of Biology, University of Michigan-Flint, 303 East Kearsley, Flint, MI, United States, ³Department of Biochemistry-Molecular Biology, Wayne State University School of Medicine, 540 East Canfield Avenue, Detroit, MI, United States

In higher vertebrates, the $\alpha 10$ subunit, inactive as a homomer, is

thought to function heteromerically with $\alpha 9$ in forming the native hair-cell nicotinic receptor (Elgoyhen et al., PNAS 98:3501-6, 2001). An $\alpha 10$ -like gene was first identified in the rainbow trout in 1998 (Green, Drescher et al., ARO Abstr. 21:102). $\alpha 10$ has since been cloned from chick (Barabino et al., GenBank AJ295624, 2000), rat (Elgoyhen et al., 2001), and human (Lustig et al., Genomics 73:272-83, 2001). The current study reports the molecular characterization of the $\alpha 10$ -like subunit from trout olfactory mucosa. This $\alpha 10$ is expressed, less abundantly, in trout brain, retina, and pituitary. Most notably, trout $\alpha 10$ -like message is *not* found in the trout sacculus model hair cell, and is also undetectable in trout spleen, skeletal muscle, liver, and kidney. The teleost $\alpha 10$ -like subunit displays characteristic molecular features of a nicotinic subunit. However, like $\alpha 9$, a remarkable difference in teleosts is the greatly increased length of the cytoplasmic loop between membrane-spanning regions M3 and M4, compared to higher vertebrates, e.g., 130 amino acids longer for trout than human $\alpha 10$. The teleost $\alpha 10$ -like subunit is closely homologous with $\alpha 9$ and $\alpha 10$ of chick, rat, guinea pig, and human, but displays high amino acid identity for both $\alpha 9$ and $\alpha 10$; for example, trout $\alpha 10$ -like subunit is 71% identical to chick $\alpha 10$ and also 71% identical to chick $\alpha 9$. Recent genomic analysis of cholinergic receptor genes in *Fugu rubripes* (Jones et al., Genomics 82:441-51, 2003) indicates that the trout $\alpha 10$ -like subunit is similar to a *Fugu* $\alpha 9/\alpha 10$ -like gene termed $\alpha 9d$. Since the present trout $\alpha 10$ -like subunit sequence, although homologous to the $\alpha 10$ of higher vertebrates, is absent from the trout sacculus hair cell, it may not correspond to the $\alpha 10$ of birds and mammals, which is currently thought to form part of the hair-cell nicotinic receptor in those vertebrate classes.

715 Ryanodine-sensitive Membrane Currents Evoked by ACh in Cochlear Hair Cells

Paul Albert Fuchs, Hakim Hiel, Suchitra Parameshwaran-Iyer

Otolaryngology- Head and Neck Surgery, Johns Hopkins, 710 Rutland Avenue, Baltimore, Maryland, United States

Release of acetylcholine (ACh) from efferent nerve endings inhibits hair cells through the activation of calcium-dependent small conductance (SK) potassium channels. Since the hair cell's ACh receptor (AChR) is itself a ligand-gated cation channel, calcium entry through open AChRs is likely to activate SK channels directly (Glowatzki and Fuchs, 2000, Science 288:2366; Oliver et al., 2000, Neuron 26:595). At the same time, the presence of a near-membrane synaptic cistern implies a functioning calcium store, and ryanodine has been shown to alter the strength of inhibition (Sridhar et al., 1997, J. Neurosci. 17:428; Lioudyno et al., 2003 ARO abs. #418). In the present work, we examine the influence of ryanodine on membrane currents evoked in hair cells of chickens by application of 100 mM ACh. In hair cells isolated from the chicken basilar papilla, ACh produces a biphasic current with a small early inward component (through AChRs) followed within a few msec by a larger, longer-lasting (t decay ~ 300 ms) outward current (through SK channels). Low concentrations of ryanodine (1- 10 mM) had no consistent effect, although the ryanodine receptor agonist cADPR at 10 mM greatly prolonged SK currents. Surprisingly, during exposure to 100 mM ryanodine (a concentration that normally blocks ryanodine receptors) the outward SK component also was prolonged nearly two-fold. In hair

cells with an initially small SK component, application of ACh in the presence of 100 mM ryanodine produced a small (<50 pA) sustained (> 2 s) inward current that reversed in sign near 0 mV. This effect was more pronounced in cells whose SK current was diminished by cytoplasmic buffering with BAPTA, rather than the usual EGTA. This slow inward current evoked by ACh in the presence of ryanodine is reminiscent of those through 'store-operated' or TRP channels in other systems. This slow inward current may provide calcium to prolong SK channel activity. Supported by NIDCD DC01508.

716 Yeast Two Hybrid Screening of the Rat Cochlea with Hair Cell nAChRs

Omar Akil¹, Suchitra Parameshwaran-Iyer¹, Hakim Hiel¹, Paul A Fuchs¹, Lawrence Robert Lustig²

¹Otolaryngology, Johns Hopkins University, 521 Traylor Building, 720 Rutland Ave, Baltimore, MD, United States, ²Otolaryngology, Johns Hopkins University, JHOC 6241, 601 N. Caroline St, Baltimore, MD, United States

Efferent inhibition of cochlear outer hair cells is mediated by a nicotinic acetylcholine receptor (nAChR) thought to contain both $\alpha 9$ and $\alpha 10$ subunits (Elgoyhen et al., 1994 Cell 79:705; 2001 PNAS 98:3501). Although the $\alpha 10$ subunit does not form functional channels on its own, heteromeric $\alpha 9/\alpha 10$ AChRs express more robustly than $\alpha 9$ homomers, and are biophysically similar to native hair cell receptors. During development, the expression of $\alpha 10$, but not $\alpha 9$, is temporally correlated with the changing cholinergic sensitivity of cochlear inner hair cells (Katz et al., 2003, ARO abstract #635). These observations suggest that $\alpha 10$ serves as an accessory subunit that facilitates surface expression and/or other functional interactions. To examine this idea, we designed a yeast two hybrid screen using the intracellular (IC) loops of the nAChR subunits $\alpha 9$ and $\alpha 10$ as 'baits' against a rat cochlear cDNA library. The $\alpha 9$ IC loop yielded no positive clones when screened against the library. However, the $\alpha 10$ IC loop generated 200 isolated clones. One of these, a sphingolipid activator precursor (prosaposin), was represented multiple times and so was studied further. Co-immunoprecipitation with $\alpha 10$ confirmed the yeast two hybrid interaction. RT-PCR from whole rat cochlea and from isolated outer hair cells demonstrated the expression of prosaposin mRNA in these tissues. Immunohistochemistry with prosaposin antisera on rat cochlear sections revealed labeling of outer hair cells. The function of prosaposin in outer hair cells is presently unknown. Nonetheless, this initial screening effort suggests that the $\alpha 10$ subunit may indeed play a special role in protein/protein interactions that subserve localization or other functions of hair cell nAChRs. Further, these studies confirm the utility of the yeast two hybrid technique for identifying potential molecular interactions in the inner ear.

Supported by NIDCD K08 DC00189 and DC01508.

717 Ca^{2+} modulates nicotinic ACh receptors of inner hair cells in the neonatal rat cochlea.

María E. Gómez-Casati¹, Paul A. Fuchs², Ana B. Elgoyhen¹, Eleonora Katz¹

¹INGEBI, UBA-CONICET, Obligado 2490, Bs. As., Argentina, ²Dept. Oto/HNS, Johns Hopkins Univ., 720 Rutland Av., Baltimore, MD, United States

In the neonatal mammalian cochlea, inner hair cells (IHCs) are transiently innervated by efferent fibers of the olivocochlear (OC) system. This synapse is inhibitory and mediated by a nicotinic acetylcholine receptor (nAChR) (Glowatzki & Fuchs 2000). Electrophysiological and pharmacological data support the hypothesis that inhibition is brought about by Ca^{2+} flowing in through the $\alpha 9\alpha 10$ -containing nAChR and the subsequent activation of an apamin sensitive Ca^{2+} -dependent K^{+} (SK) channel.

The functional properties of native nAChRs were studied using whole-cell recordings of IHCs in excised apical turns of the rat organ of Corti (P8-11). To isolate nAChR currents from SK channel currents, experiments were performed with 10 μM BAPTA in the pipette solution and 1 nM apamin in the external solution. We examined the effects of Ca^{2+} on cation currents through the IHC nAChR. ACh-evoked currents were potentiated by low Ca^{2+} concentrations (up to 0.5 μM) and were blocked by higher concentrations of this cation. Concentration-response curves show that the receptor had an apparent affinity for ACh of $60.7 \pm 2.8 \mu M$ in a saline containing 0.5 μM Ca^{2+} . In the absence of Ca^{2+} , the EC_{50} for ACh increased, suggesting that potentiation by Ca^{2+} involves changes in the apparent affinity of the receptor for ACh. In addition to these effects of Ca^{2+} , ACh-evoked responses were reduced during continuous application of 1 μM ACh. At a holding potential of -90 mV, the current remaining after 20 sec was $54.2 \pm 1.5\%$ of its peak value. These biophysical characteristics of the IHC nAChR closely resemble those of the recombinant $\alpha 9\alpha 10$ nAChR (Elgoyhen et al., 2001, Weisstaub et al., 2002), reinforcing the hypothesis that the nAChR at the OC-IHC synapse is composed of both $\alpha 9$ and $\alpha 10$ subunits.

Funded by RO3TW006247(PF, ABE), HHMI (ABE) & NIDCD DC01508 (PF).

718 Cod106, a Novel Protein Expressed in Sensory Hair Cells and Central Neurons

Ellen Reisinger¹, Ulrike Zimmermann², Marlies Knipper², Jost Ludwig³, Nikolaj Klöcker¹, Bernd Fakler¹, Dominik Oliver¹

¹Physiology II, University of Freiburg, H.-Herder-Str. 7, Freiburg, Germany, ²Hearing Research Centre, University of Tübingen, Elfriede-Aulhornstr. 5, Tübingen, Germany, ³Botanisches Institut, Universität Bonn, Kirschallee 1, Bonn, Germany

The exquisite sensitivity of the mammalian cochlea is based on the function of many highly specialized cell types each equipped with a specific set of proteins. Identification of these proteins is expected to enhance the knowledge of physiological and pathophysiological mechanisms of the inner ear. Here, we describe a newly identified cDNA from the organ of Corti encoding a 106kDa protein, termed Cod106, with potential involvement in hair cell function. In situ hybridization on inner ear sections

revealed selective and strong expression of Cod106 mRNA in auditory and vestibular hair cells. An antibody directed against a synthetic 20aa peptide enabled us to detect Cod106 at the basal, synaptic pole of auditory outer hair cells (OHCs). Costaining with synaptophysin, a marker of efferent synaptic nerve terminals, indicated the presence of Cod106 close to the postsynaptic specializations of OHCs. In the vestibular organ, Cod106 immunoreactivity was found close to the lateral and basal cell membrane of hair cells. In brain sections, Cod106 mRNA was detected in neurons of numerous regions, showing particularly high abundance in hippocampal pyramidal cells and cerebellar granule cells. Extensive analysis of the Cod106 primary sequence revealed possible orthologous proteins of unknown function in human and mouse, but a complete lack of homology to characterized gene products. Structure predictions failed to clearly anticipate transmembrane regions or subcellular targeting signals. Heterologous expression experiments suggested that Cod106 is tightly attached to membranes, but is not an intrinsic membrane protein.

The cell-type specific expression and subcellular localization of Cod106 may be consistent with an involvement in synaptic processes.

719 Hearing loss in mice lacking the intracellular domain of ephrin-B2 or B3

Dominik Brors¹, Daniel Bodmer², Kwang Pak³, Christoph Aletsee¹, Stefan Dazert⁴, Mark Henkemeyer⁵, Allen F. Ryan³

¹Otorhinolaryngology, University of Wuerzburg, Josef-Schneider-Str.11, Wuerzburg, Germany, ²Otorhinolaryngology, University of Zurich, Rämistr. 100, Zurich, Switzerland, ³Otolaryngology, UCSD, 9500 Gilman Drive, San Diego, CA, United States, ⁴Otolaryngology, Ruhr-University Bochum, Bleichstrasse 15, Bochum, Germany, ⁵Center for Developmental Biology, University of Texas, 5323 Harry Hines Blvd., Dallas, TX, United States

Ephrins and Eph receptors play a major role in the development of the nervous system. At least for the B class of ephrins, these transmembrane molecules signal bidirectionally, with both ephrin and Eph molecules capable of serving as ligand and receptor. Recently, we showed that neurites of neonatal spiral ganglion (SG) neurons, which express ephrins B2 and B3, are repelled at the border of EphA4 stripe assays. Treatment with anti-ephrin B2 and B3 blocking antibodies eliminated the repulsion response observed at the border of EphA4 stripes, indicating that ephrins B2 and B3 mediate the response of SG neurites to EphA4 via reverse signaling (Brors et al. *J Comp Neurol* 462: 90-100, 2003).

In this study, we assessed the role of ephrins B2 and B3 in vivo. We recorded evoked auditory brainstem responses (ABRs) in mice lacking the intracellular domain of ephrin B2 and B3. In these mutants, forward ephrin/EphR signalling is normal, but reverse ephrin signalling is disrupted. Since ephrin-B2^{-/-} mice die soon after birth due to a maxillofacial defect, ephrin-B2^{-/+} and wild-type littermates were used. For ephrin-B3, ephrin-B3^{-/-}, ephrin-B2^{-/+} and wildtype littermates were tested. ABR to clicks and tone bursts at 4, 8, 16 and 32 kHz were recorded from 3 to 6 months.

Ephrin B2^{-/+} mice showed significant hearing loss at all frequencies compared to ephrin-B2^{+/+} mice. In ephrin-B3^{-/-} and ^{-/+} mice, responses to clicks and tone bursts at 8-32 kHz were signifi-

cantly reduced compared to wildtype mice. No age-related changes were observed for any group.

Our data illustrate that mice deficient in the intracellular domain of ephrins B2 and B3 display a significant hearing loss. Thus, reverse signalling by ephrins B2 and B3 is required for the normal development of mammalian auditory responses.

Supported by grant DC00139 from the NIH/NIDCD and by the VA Research Service (U.S.A.) and the DFG (Germany).

720 Slit/Robo proteins are expressed during critical stages of prenatal innervation within the mammalian cochlea

James Gordon Davis^{1,2}, Stephen Echterler^{1,2}

¹Pediatric Otolaryngology, Children's Hospital of Philadelphia, 3516 Civic Center Blvd., Philadelphia, PA, United States, ²Dept. of Otorhinolaryngology, Head and Neck Surgery, University of Pennsylvania School of Medicine, 3400 Civic Center Blvd., Philadelphia, PA, United States

Upon entering the developing auditory neuroepithelium, nerve fibers make two fundamental decisions: 1) whether to remain within the inner hair cell zone or to cross into the outer hair cell zone and 2) whether to construct terminal arbors that are oriented orthogonal to or in parallel with the cochlear duct. These choices are made by both developing afferent and efferent cochlear neurons, suggesting that they be mediated by 'differential reading' of a common set of axonal guidance molecules that are deployed at critical times and locations within the developing cochlea. The Slit family of chemorepellent axonal guidance molecules and their cognate receptors, the Robo family, are often employed in just such a fashion within the developing central nervous system. Therefore, we examined the developmental expression patterns of Slit/Robo proteins in the prenatal cochlea. Immunohistochemical analyses revealed that slit2 and slit3 protein expression began at E14.5 in the basal turn, at E15.5 in the middle turn, and by E16.5 in the apical turn. The temporal expression of slit2 and slit3 coincides with the onset of innervation in each cochlear turn. Within the sensory epithelium, the spatial expression of both slit proteins occurs within supporting cells that flank and separate both the inner and outer hair cell zones. This expression pattern suggested that Slit/Robo signaling may be functioning in the cochlea as it does in spinal cord to regulate the crossing of axons at the midline. Within the spinal cord, robo protein is upregulated within commissural axons after crossing the midline to prevent their recrossing. Similarly, we detected the robo1 protein in nerve fibers only after they had crossed the tunnel of Corti. Attempts to elucidate the function of individual Slit/Robo family members in the formation of cochlear innervation are underway. Supported by NIDCD grants DC 00493 (SME) and DC 04620(JGD).

721 Clustering of Nicotinic Acetylcholine Receptors in Hair Cells during Efferent Cochlear Synaptogenesis.

Dwayne D Simmons^{1,2}, Omar Akil³, Lawrence R Lustig³

¹Otolaryngology and Central Institute for the Deaf, Washington University, 660 Euclid Ave., St. Louis, MO, United States,

²Anatomy and Neurobiology, Washington University, 660 Euclid Ave., St. Louis, MO, United States, ³Otolaryngology-Head and Neck Surgery, Johns Hopkins University, 601 N. Caroline Street, Baltimore, MD, United States

The mechanisms that induce nicotinic acetylcholine receptor (nAChR) clustering at efferent olivocochlear (OC) synapses on hair cells are unknown. We present here evidence that nAChR clustering is coordinated with the timing of efferent synaptogenesis and may involve a rapsyn-mediated pathway. Clusters of nAChRs are visualized using bungarotoxin (BTX) labeling methods in intact preparations of the developing rat and mouse organ of Corti. At E18, there are no visible BTX-labeled plaques. At P0, BTX plaques are almost exclusively observed on IHCs in middle basal regions of the cochlear spiral. There is also little or no vesicular acetylcholine transporter (VAcHT) immunolabeling of efferent terminals. At P2, BTX plaques on IHCs are present in all but the extreme basal and apical regions whereas VAcHT-immunoreactive (VAcHT-ir) puncta are observed throughout basal regions. At P6, BTX plaques are found on both IHCs and OHCs. In middle regions of the rat cochlea at P10, BTX-labeled plaques on both IHCs and OHCs co-localize with VAcHT-ir terminals.

Previous studies at the neuromuscular junction (NMJ) have identified the rapsyn coiled-coiled domain as essential for nAChR clustering. To test whether this region binds to the nAChR alpha9 or alpha10 subunit, a yeast two-hybrid screen was performed. The coiled-coiled region was amplified from whole rat cochlea (c-rapsyn) or muscle (m-rapsyn) and subcloned, into a yeast two-hybrid binding domain (BD) vector, while the intracellular loops of either alpha9 or alpha10 were subcloned into the activating domain (AD) vectors. Both c-rapsyn and m-rapsyn demonstrated an interaction with alpha9, but not alpha10. This interaction between alpha9 and rapsyn was further confirmed by in-vitro co-immunoprecipitation, and by switching AD and BD vector inserts.

These data provide evidence that hair cell nAChRs cluster during efferent synaptogenesis. Initially, nAChR clusters are independent of efferent terminals and then become colocalized with efferent terminals. Further, our results raise the possibility that the mechanism of clustering nAChRs may involve a rapsyn-mediated pathway similar to the NMJ.

722 Developmental Acquisition of Mechanotransduction in Hair Cells of the Embryonic Mouse Utricle

Gwenaëlle S.G. Géléoc, Eric A. Stauffer, Jeffrey R. Holt
Neuroscience & Otolaryngology, University of Virginia, Lane Rd., MR4, Rm 5127, Charlottesville, VA, United States

To investigate the acquisition of sensory transduction in hair cells we excised utricles from mice between embryonic day 14 (E14) and E19. We screened for the acquisition of myosin Ic, tip-links and transduction channels and measured whole-cell currents

evoked by hair bundle deflections. We used RT-PCR to examine the expression of Myo1c, a component of the adaptation complex. We detected mRNA expression at embryonic day 17 (E17) but not E15. To examine the acquisition of tip-links we used scanning electron microscopy. We found no evidence of tip-links at E15. However, by E17 tip-links oriented along the bundle's morphological axis were clearly visible in 86% of the bundles examined. To assay for the acquisition of transduction channels we imaged the fluorescent dye, FM 1-43, which permeates non-selective cation channels. We observed a rapid increase in the number of fluorescent cells between E16 and E17. At E16 the mean fluorescence was 87 ± 185 arbitrary units ($n = 289$). By E17 nearly all of the cells examined had taken up FM 1-43 (mean brightness 1826 ± 677 a.u., $n = 208$). The uptake was blocked by the transduction channel blocker gentamicin. To test for acquisition of functional transduction we used a stiff probe or fluid-jet to displace the hair bundles and whole-cell, voltage-clamp to record transducer currents. We were unable to evoke mechanosensitive currents in E15 hair cells ($n = 11$). However, by E17 robust and mature transduction currents with maximal amplitudes that ranged between -83 and -278 pA (mean $= -164 \pm 76$ pA, $n = 8$) were evoked in all hair cells tested ($n = 12$). The currents had a mean operating range of 1.3 ± 0.4 μm and an open probability at rest of $9.1 \pm 6.5\%$. Recordings at 6-hour intervals between E16 and E17 revealed a rapid all-or-nothing onset of fully functional mechanosensitivity. We propose a model in which Myo-1c mediates the developmental assembly of the transduction apparatus.

Supported by NIDCD grants to GSGG (DC006183) and JRH (DC05439)

723 Transcriptional control of the potassium channel KCNQ4

Harald Winter¹, Juergen-Theodor Fraenzer¹, Thomas Weber¹, Ulrike Zimmermann¹, Karin Rohbock¹, Iris Köpschall¹, Hyun-Soon Geißler¹, Stephanie Christ², Karl Bauer², Ed Walsh³, JoAnn McGee³, Marlies Knipper¹

¹Molecular Neurobiology, Tuebingen Hearing Research Center, Elfriede-Aulhorn-Str. 5, Tuebingen, Germany,

²Neuroendocrinology, Max-Planck-Institute for Experimental Endocrinology, Feodor-Lynen-Str. 7, Hannover, Germany,

³Developmental Auditory Physiology Laboratory, Boys Town National Research Hospital, 555 North 30th Street, Omaha, NE, United States

Cochlear outer hair cells are responsible for the frequency-resolving capacity of the mammalian inner ear. Electrical stimulation during the hearing process induces rapid length changes of these cells, transduced by the novel motor protein prestin (Zheng et al., 2000, Nature 405). Recently Karkovets et al., 2000, PNAS 97 reported the expression pattern of a novel potassium channel, KCNQ4, in hair cells and neurons of the auditory and vestibular systems, the expression of which is linked to nonsyndromic dominant deafness, DFNA2. In outer hair cells this channel is presumed to be similar to the unusual potassium selective 'leak' current, termed IK,N, which is responsible for the repolarisation of the outer hair cells. We noted an alteration of the subcellular distribution of the outer hair cell motor protein prestin coincident to an alteration of the subcellular distribution of KCNQ4 prior to the onset of hearing. As the prestin expression itself as well as its sub-

cellular distribution revealed as being under control of thyroid hormone (TH) (Weber et al. and Knipper, 2002, PNAS 99), we analysed the effect of TH on KCNQ4 expression. By analysing various rat and mouse-models of hypothyroidism, we can show that the expression of KCNQ4 is also dependent on TH. Sequence analysis identified putative thyroid hormone response elements (TRE) in the upstream region of KCNQ4 gene which were tested for functionality using reporter gene assays and electromobility shift assays. The data suggest a TH-dependent mechanism of regulation of the KCNQ4 expression which is different of that observed for the motor protein prestin.

Supported by a grant from the SFB 430 B3/Kni Tuebingen and the NIH-NIDCD R01 DC04566.

724 BK expression in the cochlea

Lukas Rüttiger¹, Matthias Sausbier², Markus Müller³, Patricia Langer⁴, Alfons Rüschi⁴, Ulrike Zimmermann¹, Jutta Engel⁴, Bernhard Hirt³, Harald Winter¹, Claudia Braig¹, Markus Pfister³, Peter Ruth², **Marlies Knipper¹**

¹Molecular Neurobiology, Tuebingen Hearing Research Center, Elfriede-Aulhorn-Str. 5, Tuebingen, Germany, ²Institute for Pharmacology and Toxicology, University of Tuebingen, Auf der Morgenstelle 8, Tuebingen, Germany, ³Department of Otolaryngology, Tuebingen Hearing Research Center, Elfriede-Aulhorn-Str. 5, Tuebingen, Germany, ⁴Institute of Physiology II & Department of Otolaryngology, University of Tuebingen, Gmelinstr. 5, Tuebingen, Germany

The large Ca²⁺-activated K⁺ channels, named BK or maxi-K channels are composed of two structurally distinct subunits, α and β . In the inner ear physiological and anatomical studies point to the expression of α/β 1 assembled BK channels in inner and outer hair cells as well as in efferent neuronal connections. While BK channels in inner hair cells are presumed to decrease the membrane time constant to allow phase-locked receptor potentials up to high sound frequencies, the role of the BK channels at the outer hair cell level is still exclusive.

We used transgenic mice for BK α (Ruth & Sausbier, Inst. Pharmacology, Tübingen) and BK β 1 (Brenner; Univ. Texas, USA & Aldrich, Univ. Stanford, USA) to analyze the function of both channel subunits for development of normal hearing. We measured the hearing function using click and frequency ABR measurements as well as DPOAEs and analysed the phenotype using laser-confocal- and immunofluorescence microscopy as well as *in situ* hybridization studies. The results unravel an interesting unexpected role BK α 1 for normal hearing function.

LR and MS contributed equally to this work

This work was supported by the Deutsche Forschungsgemeinschaft DFG RU 403, SFB 430/Kni-B3.

725 The change of expression of vasopressin type 2 receptor and aquaporin 2 in the rat cochlea during development

Lee Jun Ho, Oh Seung Ha, Lee Hyo Jeong, Chang Sun O, Kim Chong Sun

Otolaryngology, Seoul National University, College of Medicine, 128 Yongon-dong, Chongro-gu, Seoul, Korea, Republic of

The role of vasopressin in cochlear physiology has been implicated. Our preliminary results demonstrating stimulatory effect of vasopressin at high concentration on the strial marginal cells (Lee et al, 2001) prompted us to hypothesize that vasopressin may play a role in the development of the cochlea. The authors examined the expression of vasopressin receptor type 2 (V2R) and aquaporin 2 (AQP2) in the developing cochlea of the rat by western blot. V2R antibody stained a major band with molecular mass of $\sqrt{62}$ kDa and minor band of $\sqrt{36}$ kDa, glycosylated and non-glycosylated forms, respectively. Maximal increases were detected in P2 and were maintained for P7, after which declines occurred that almost reached the basal levels within P14. However, there was no significant difference in the level of immunoreactive V2R protein in either P14 or P28 which was minimally expressed in. AQP2 antibody stained a major band of $\sqrt{47}$ kDa and minor bands of 29 kDa, glycosylated and non-glycosylated forms, respectively. The expression of AQP2 persisted in the cochlea until P7, although the intensity decreased during the mature period. The age-dependent decrease in AVP-V2 activity was not paralleled to actin expression as determined by Western blot. These results demonstrated that V2R and AQP2 are upregulated during development and then, downregulated in adult stage in the cochlea.

726 Lack of p75NTR enhances spiral ganglion neurite outgrowth in vitro without effects on hearing development in vivo

Stefan Hansen¹, Dominik Brors¹, Christoph Aletsee¹, Robert Mlynski¹, Stefan Volkenstein¹, Michael Sendtner², Allen F Ryan³, Stefan Dazert⁴

¹Otorhinolaryngology, University of Wuerzburg, Josef-Schneider-Str. 11, Wuerzburg, Germany, ²Clinical Neurobiology, University of Wuerzburg, Josef-Schneider-Str. 11, Wuerzburg, Germany, ³Otorhinolaryngology and Neurosciences, UCSD, Gilman Drive, La Jolla, CA, United States, ⁴Otorhinolaryngology, University of Bochum, Bleichstr. 15, Bochum, Germany

Introduction

Neurotrophins bind to two different types of receptors, the high affinity Trk receptors and the low affinity nerve growth factor receptor p75NTR. Various studies concerning both signaling pathways of p75NTR and interactions between p75NTR and Trk underline the role of p75NTR in the regulation of neuronal activities. In the present study the involvement of p75NTR in the development of the mammalian cochlea was investigated. We evaluated the onset of hearing in vivo and the in vitro outgrowth of SG neurites with and without supplementation of NT-3 in p75NTR knockout (p75NTR^{-/-}) mice.

Materials and Methods

ABR from p75NTR^{-/-} and wildtype (WT) mice were measured by freefield using clicks from postnatal day (P) 8 to 23. Additionally,

SG explants of both groups were removed from the cochlea at P4 and cultured for 72h in appropriate growth medium with and without NT-3. SG neurite outgrowth was evaluated histomorphometrically and analyzed statistically.

Results

In the time span evaluated, no significant differences in responds to clicks in the ABR of mutant mice compared to the WT mice were detected. SG neurites of p75NTR^{-/-} mice showed a significant increase in neurite length compared to the WT mice with and without NT-3 stimulation, whereas the neurite number did not differ significantly between both groups.

Conclusions

The results of this study indicate that p75NTR is involved in the signaling of SG neurite outgrowth but is not essential for the development and the function of the mammalian organ of Corti in the first three postnatal weeks.

Supported by the IZKF project E-21 and Forum Bochum

727 Developmental Changes in Spiral Ganglion Cell and Dendrite Counts in the Gerbil Cochlea

Sandra Koterski, Claus-Peter Richter

Otolaryngology, Northwestern University, 303 E. Chicago Avenue, Chicago, Illinois, United States

It has been documented that the population of spiral ganglion cells decreases by approximately 30% during the first postnatal week in Mongolian gerbils, with further loss thereafter. However, it is unclear whether the population of dendrites decreases at a similar rate. If the degeneration of the spiral ganglion cells parallels the degeneration of dendrites, then changes in the number of spiral ganglion cells should be correlated with changes in the number of nerve fibers. On the other hand, if the rates of degeneration are not correlated, then the rapid reduction in the number of spiral ganglion cells may occur because the cells are not connected to the organ of Corti and do not receive the stimulation necessary for survival.

We explored developmental changes in the density of spiral ganglion cells and dendrites passing through the habenula perforata of the gerbil cochlea. We examined cochleae from groups of Mongolian gerbils aged 0 days, 7 days, 20 days, 18 months, and 30 months. After harvesting, embedding, and sectioning each cochlea, we imaged the spiral ganglion cells and dendrites in each cochlear turn using light microscopy. Then we determined the density of spiral ganglion soma in Rosenthal's canal and the density dendrites at the habenula perforata for each age group using Scion Image software.

The data show that dendrite and spiral ganglion cell densities both decreased with age, but at a different rate. Moreover, the reduction in the number of spiral ganglion cells was greater than the reduction in the number of dendrites, especially in the middle turns of the cochlea.

Supported by the American Hearing Research Foundation

728 Serotonin transporter expression in the postnatal mouse auditory brainstem

Ann M. Thompson¹, Jean M. Lauder²

¹Dept. of Otorhinolaryngology, The University of Oklahoma HSC, PO Box 26901, Oklahoma City, OK, United States, ²Dept. of Cell and Developmental Biology, University of North Carolina at Chapel Hill, Mason Farm Road, 108 Taylor Hall, Chapel Hill, NC, United States

When the enzyme responsible for degrading 5-HT, monoamine oxidase A, is absent in mice, neurons in the cochlear nucleus (CN) and superior olivary complex (SOC) express 5-HT (Cases et al. 1998. *J. Neurosci.* 18:6914-6927). Expression of 5-HT in the auditory neurons appears to be transient, disappearing by 7 days after birth. The transient nature of the expression indicates that 5-HT plays a role in the development of these two auditory nuclei. To further investigate the role of 5-HT in auditory brainstem development, the expression of the 5-HT transporter was evaluated in the normal mouse brainstem at different postnatal ages.

Brain sections were collected from C3H/HeJ mice at birth (P0), P1, P9, P21-22, P35 and P50. The sections were processed immunohistochemically with an antibody raised against the 5-HT transporter. Specificity was determined with a pre-adsorption control.

Within CN, 5-HT transporter immunoreactivity (IR) was observed in neurons of the ventral cochlear nucleus (VCN) at P8, P13, P21 and P50. Neuronal cell types in the VCN that were IR included octopus, multipolar, and bushy cells. In the SOC, neurons within the three principal nuclei, the medial nucleus of the trapezoid body and the medial and lateral superior olives, were IR at the same ages. The intensity of the IR staining was noticeably higher in VCN neurons at P12, compared to other ages. Staining was absent in the pre-adsorption controls.

These results indicate that auditory brainstem neurons of the normal mouse express the 5-HT transporter postnatally. Immunoreactivity in neurons of the VCN and principal SOC nuclei, but not in neurons of the DCN, indicates a regional expression of the 5-HT transporter that is related to major ascending auditory pathways. The lack of IR at birth and at P1, suggests that, in the normal mouse, expression of the 5-HT transporter may be timed to certain developmental events in the auditory brainstem, such as dendritic and synaptic maturation.

729 BDNF Signal Transduction in Cultured Spiral Ganglion Neurites

Lina M. Mullen¹, Kwang Pak¹, Eduardo Chavez¹, Allen F. Ryan^{1,2}

¹Surgery, UC-San Diego and VAMC, 9500 Gilman Drive - MC0666, La Jolla, CA, United States, ²Neurosciences, UC-San Diego, 9500 Gilman Drive - MC0666, La Jolla, CA, United States

Binding of the neurotrophins NT-3 and BDNF to their tyrosine kinase receptors (trk) leads to the activation of signal transduction cascades that link the cell membrane to the nucleus. This activation can have many effects, including increases in neuronal survival and neurite outgrowth. Specific neurotrophin signaling pathways in the inner ear are well known to be required for survival of cochlear and vestibular neurons, as well as for appropriate

innervation of cochlear hair cells. We have previously studied transduction pathways involved in spiral ganglion neurite growth stimulation by NT-3 *in vitro*. The signal transduction pathways involved in BDNF effects on spiral ganglion neurons have received less attention.

We and others have noted a dramatic effect of BDNF on spiral ganglion neurite numbers, presumably due to increased neuronal survival. In the present study, inhibitors of specific transduction pathways were used to elucidate the signaling that is responsible for BDNF effects on neonatal spiral ganglion neurites in culture. When BDNF and an inhibitor of Ras were both present in the culture media, neurite number was dramatically reduced compared to BDNF alone. More modest reductions were seen with inhibitors of PI3 kinase and Rac/cdc42. Little or no effect of p38 or Mek/Erk MAPK inhibitors was noted. Our preliminary results suggest that neuronal survival associated with BDNF may not be mediated by the classical MEK/Erk MAPK pathway, but instead may involve Akt and JNK MAPK signaling.

Supported by the NOHR, by NIH/NIDCD grants DC04233, DC00139, and by the Medical Research Service of the VA.

730 Improved Survival of Spiral Ganglion Neurons in Dissociated Culture

Donna S. Whitlon, Kathleen V. Ketels

Otolaryngology-Head and Neck Surgery, Feinberg School of Medicine, Northwestern University, Searle Bldg., 303 E. Chicago Avenue Room 12-561, Chicago, IL, United States

Dissociated spiral ganglion (sg) cultures are potentially useful tools for studies of neural growth and development. However, even with BDNF, NT3 and serum, the two-day survival rate for sg neurons in these cultures is low, although certain interventions (cAMP analog, LIF, depolarizing medium) give improvement. In studies of dissociated sg from newborn mice, we noticed that inclusion of the adjacent non-neural tissue - the limbus and the spiral lamina, but not the epithelium - improved neural survival (ARO Abstracts, 2003). Ensuing experiments with new lots the dissociating enzyme were unsuccessful and, in fact, decreased total survival. We then explored the theory that the new enzyme left the neurons more sensitive to glutamate toxicity. Glutamate uptake by NMDA receptors, which can be inhibited by MK801, is associated with oxidative damage of neurons. Cochlear capsules from newborn mice were opened, the tissue was digested with dispase, the sg+adjacent non-neural tissue was collected, the tissue was dissociated. Cells were cultured with BDNF, NT3 and FBS in plates coated with poly-D-lysine/laminin. MK801 (10⁻⁶M) added directly to the culture medium had little effect. Inclusion of MK801 in the secondary dissection, dissociation and culture media increased neural survival (neurons/cochlea) from 221 (approx. 1.1% of the total cochlear neurons) to 715 (3.6%). When MK801 was also included in the dispase digestion, survival increased to 1710 (8.6%). If LIF was also included in the culture medium, survival improved to 2371 (11.9%). Similarly, inclusion of cystine, a substrate of the cystine-glutamate antiporter, in the dissection, dissociation and culture media, increased survival from 221 (1.1%) to 1208 (6.0%). These data indicate that sg neurons or cells upon which their survival depends can become sensitive to glutamate early during the process of preparing dissociated cultures and that inhibition of glutamate uptake can improve survival of neurons. (Supported by NIH Grant # DC00653).

731 Postnatal Development of the Cochlear Nucleus of the Mouse

Valentina Imbroglini, George A. Spirou, Peter H. Mathers, Albert S. Berrebi

Otolaryngology & Sensory Neuroscience Research Center, West Virginia Univ. School of Medicine, Health Sciences Center, Morgantown, WV, United States

The cochlear nuclear complex (CN) is a tonotopically organized structure that represents a gateway for all auditory information destined for the CNS. In mouse, CN development begins after the neural tube starts to close with neurogenesis of the largest CN neurons (E10-E14), and continues until after birth. While several studies have examined embryonic development of the CN, relatively little is known about its structural maturation and cellular differentiation that takes place after birth. Such information may be useful for further refinements of central auditory prostheses or other interventions directed at repairing or replacing damaged components of CN circuits. As a first step toward understanding the late stages of its development, we generated complete series of toluidine blue stained semithin sections and analyzed, by light microscopy, the cytological features of CN neurons at postnatal days 0 and 2 (P0 and P2) in the mouse. These are compared to similarly prepared tissues from adult mice.

At these ages, the two main CN subdivisions (DCN and the VCN) show a simplified structure characterized by a central core containing scattered large (16 μ m), pale stained neurons - which are surrounded by densely packed, smaller ovoid (~7 μ m), darkly stained cells. Moreover, even though the DCN and VCN are clearly recognized, the boundary between them is not as well defined as in the adult. By P2 a medium sized cell type is apparent (10-12 μ m) whose cytoplasm displays a heterogeneous appearance with prominent peri-nuclear staining.

These findings indicate that a great deal of cellular proliferation and differentiation must occur after P2 in the CN of the mouse. This suggests that the intrinsic circuitry of the CN is amenable to experimental manipulation and therapeutic intervention well into the first postnatal week of life. We are presently examining these tissues by electron microscopy to begin to understand the earliest stages of synaptic contact formation within the CN.

Supported by COBRE P20-15574 from the NCRR to ASB.

732 Synaptic Innervation Patterns On Hair Cells In Hatchling And Adult Belgian Waterslager (BWS) Canary

Brenda M. Ryals¹, Elena Sanovich², Robert J. Dooling³

¹Communication Sciences and Disorders, James Madison University, MSC 4304 701 Carrier Drive, Harrisonburg, Virginia, United States, ²Center for Comparative and Evolutionary Biology of Hearing, University of Maryland, Biology Psy Bldg 144, College Park, Maryland, United States, ³Psychology, University of Maryland, Biology Psy Bldg 144, College Park, Maryland, United States

Belgian Waterslager canaries have a genetic, progressive inner ear abnormality that is maintained in adulthood even though they continually regenerate hair cells. The neural consequences of the adult inner ear abnormality are minimal with only a small reduction in

neural fiber number (~12%) and cell size in the cochlear nuclei (Gleich et al 2001; Kubke et al 2002). Since adult BWS show an approximate 30% hair cell loss it has been suggested that the remaining hair cells may receive a higher afferent/hair cell ratio than normal.

Developmental studies indicate that BWS hair cell abnormalities first appear along the neural edge in the mid-basal region of the basilar papilla (BP), and that hair cell loss occurs first in the basal region of the BP (Ryals and Dooling 2002). Hair cell abnormalities and loss reach significance by 60-90 days post-hatch. Since afferent synaptic density is generally greatest in hair cells along the neural edge of the BP it seems likely that the neural environment of these hair cells faces unique challenges during BWS canary post-hatch development.

In the current study we use LM and TEM analysis to determine if these dynamic changes at the level of the hair cell are reflected in changes at the level of the synapse. Embedded papillae were sectioned transverse to the longitudinal axis at 20 micron sampling intervals. A series of thin sections for TEM analysis of synaptic terminals were taken at 20%, 50% and 80% of length from the basal tip. Reconstruction of neural synapses was modeled on the technique described by Fischer (1994). LM observations and TEM reconstruction will be discussed in terms of the chronological and positional development of the adult inner ear abnormality. These results will provide quantitative information about the neural contribution/consequences of this progressive, hereditary inner ear abnormality in the face of on-going hair cell death and regeneration.

(Supported by NIDCD R01DC001372 to RJD and BMR)

733 Glutamate Release in the Developing Glycinergic/GABAergic MNTB-LSO Pathway

Deda C Gillespie, Karl Kandler

Neurobiology, University of Pittsburgh, 3500 Terrace St, Pittsburgh, PA, United States

In adult animals, the inhibitory pathway from the MNTB to the LSO is tonotopically organized. This organization arises through processes that include synapse elimination and pruning of MNTB axon terminals, processes that are thought to depend on neuronal activity. Here, we present evidence that the developing MNTB-LSO pathway releases not only GABA and glycine but also glutamate.

Whole-cell recordings were made from LSO neurons in brainstem slices from rats, age postnatal day 1-12. After pharmacological blockade of GABA and glycine receptors, in Mg^{++} -free solution, electrical stimulation in the MNTB unexpectedly produced an inward current. This response was mediated by glutamate because it was abolished in most cells by the NMDA receptor antagonist APV (50 μ M), and in some cells by APV plus the AMPA receptor antagonist CNQX (5 μ M). Glutamate responses could also be elicited by focal photolysis of caged glutamate in the MNTB, indicating that glutamate was released by MNTB neurons, rather than by fibers of passage. The occurrence of these MNTB-elicited glutamate responses decreased with age; they were present in most cells from the first postnatal week but were seldom found at later stages.

Immunostaining showed intense label in the LSO for the vesicular glutamate and GABA/glycine transporters VGLUT1, VGLUT3 and VGAT. Individual MNTB cell bodies contained both VGLUT3 and VGAT label. Further, in the LSO, VGLUT3—but not VGLUT1—colocalized with VGAT in individual terminals.

Our results provide the first evidence for release of glutamate by a GABAergic or glycinergic pathway. We suggest that during the period of synaptic refinement, glutamate and GABA/glycine may be co-released at individual synapses. NMDA-receptor dependent mechanisms may thus contribute to the developmental refinement of this inhibitory projection. *Supported by NIH grants T32 NS07391 and DC04199.*

734 Developmental Expression Of The K⁺-Cl⁻ Transporter (KCC2) In The Central Auditory System Of The Rat

Carmen Vale, Elena Caminos, Juan Ramon Martinez-Galan, Jose Manuel Juiz

Histology, University of Castilla-La Mancha, Almansa, Albacete, Spain

Glycine and GABA, the dominant inhibitory neurotransmitters in the vertebrate CNS, are depolarizing in early development. The depolarizing effects of inhibitory neurotransmitters are attributable to a Cl⁻ reversal potential that is more positive than the resting membrane potential. In neurons, intracellular chloride concentration ([Cl⁻]_i) is regulated primarily by two cation-chloride transporter family members: a Na-K-2Cl cotransporter (NKCC1) which leads to cytoplasmic accumulation of chloride, and a K-Cl cotransporter (KCC2) which extrudes chloride. During early development [Cl⁻]_i is relatively high because of NKCC1 activity. As KCC2 expression increases [Cl⁻]_i drops below the electrochemical equilibrium, leading to a transition from inhibitory synapse-evoked depolarization to hyperpolarization.

As evidenced by immunohistochemistry combined with confocal microscopy, KCC2 immunoreactivity was present at postnatal day 3 (P3) in neurons of the ventral and dorsal cochlear nucleus, medial nucleus of the trapezoid body, lateral superior olive, and inferior colliculus. KCC2 staining pattern was similar from P3 through adulthood in all auditory nuclei analyzed. Western blots confirmed similar amount of protein in young and adult neurons. Double-labeling experiments showed colocalization of KCC2 and synaptophysin or MAP2 in adult neurons. Our results show that KCC2 is present in auditory neurons and its expression is not regulated during postnatal development.

Supported by CICYT-SAF00-0211; PAI-03-015 (Consejería de Ciencia y Tecnología;

BFI2003-09147-C02-02 (MCYT) to J.M. Juiz and University of Castilla-La Mancha grant (C Vale).

735 Postnatal formation of the calyx of Held

George A. Spirou, Janelle L. Grimes, Albert S. Berrebi, Peter H. Mathers

Sensory Neuroscience Research Center, Dept. of Otolaryngology, West Virginia University School of Medicine, Box 9303 HSC, Morgantown, WV, United States

We used serial section electron microscopy to study the innervation

of cells of the medial nucleus of the trapezoid body (MNTB) by calyceal axons in mice. We identified synaptic and punctum adherens contacts between the axon and MNTB cell and investigated the presence of mitochondria-associated adherens complexes (MACs). At postnatal day 0 (P0), synaptic and punctum adherens contacts occurred primarily with MNTB cell dendrites. At P2, we observed synaptic and punctum adherens contacts between long axonal segments and MNTB somata. From these data we estimated that all MNTB somata are contacted by calyceal axons at this age. These nerve terminals widened significantly at P3, and by P4, immature, cup-shaped calyces enveloped each MNTB cell body. Synapses and puncta adhaerentia were present at each age. These contacts achieved a high density at P3 and P4 such that the calyx terminal and MNTB cell body were not separated periodically by extended extracellular spaces as occur in adult animals. MACs were not observed until P3. Our results indicate a first phase of maturation whereby the contact point between calyceal axons and MNTB cells moves from the dendrite to cell body between P0 and P2. A second phase of maturation involves rapid growth of the calyx between P2 and P4. Although puncta adhaerentia may play a role in forming initial tonotopic connections, MAC formation likely represents a later stage of synaptogenesis.

Supported by a COBRE P20RR-15574 grant from the NIH/NCRR

736 Identification of Molecular Guidance Cues Necessary for the Formation of the Calyx of Held.

David M. Howell, Albert S. Berrebi, George A. Spirou, Peter H. Mathers

Sensory Neuroscience Research Center, Dept. of Otolaryngology, West Virginia University School of Medicine, PO Box 9303, Morgantown, WV, United States

During development, neurons utilize multiple molecular guidance cues to form appropriate synaptic contacts. Molecular factors have been identified for various pathways throughout the CNS; however, cues necessary for directing auditory connections are relatively unexplored. We are interested in identifying the molecular cues that direct globular bushy cell axons from the ventral cochlear nucleus (VCN) to the medial nucleus of the trapezoid body (MNTB) where they terminate in a tonotopic distribution as calyces of Held. Placement of DiI in the VCN of intact brains between embryonic day (E) 12.5 and postnatal day 3 permitted the anatomical extent of the projection to be evaluated. As early as E14.5, VCN efferents have already bypassed the presumptive ipsilateral superior olivary complex and crossed the ventral midline. Projections into the MNTB are not observed until E18.5 even though labeled axons have reached the contralateral inferior colliculus by E16.5. To identify candidate molecules directing this projection, we analyzed the expression patterns of netrin and slit family members with their respective receptors, deleted in colorectal cancer (DCC) and roundabout. Netrin-1 RNA expression was restricted to the midline of the auditory brainstem (E11.5 – E17.5). DCC RNA expression was present in the VCN (E13.5) and fibers in the ventral acoustic stria (VAS) were positive for DCC protein (E13.5 – E15.5). The expression profile of netrin-1 and DCC is consistent with these molecules functioning to attract growing VCN axons to the midline. Despite an identifiable VCN, VAS pro-

jections are absent in DCC-deficient embryos. Additionally, the cells comprising the MNTB are not readily identifiable in DCC-null pups. These results indicate that the netrin-DCC signaling system is required to establish the calyceal projection and possibly direct neuronal migration in the mouse auditory system.

Supported by a COBRE P20RR-15574 grant from the NIH/NCRR

737 Alterations in gene expression following lead exposure in the developing murine brainstem

Linda G. Jones, Corbin Schwanke, Mark Pershouse, Diana I. Lurie

Biomedical and Pharmaceutical Sciences, Center for Environmental Health Sciences, The University of Montana, Skaggs Bldg., Missoula, MT, United States

Lead exposure during development is associated with learning disabilities, auditory processing deficits and other neurological dysfunction. A recent study (N Engl J Med 348:1517, 2003) reported measurable decreases in the IQ scores of children with blood lead levels below the established limit of 10ug/dl. We have previously demonstrated morphological changes in the auditory brainstem of lead-exposed chicks that display deficits in backward masking and have since reported decreases in synaptophysin, non-phosphorylated neurofilament and GFAP in the auditory brainstem of lead-exposed mice.

To determine alterations in regulators of cytoskeletal and synaptic elements we used DNA microarray techniques to identify differences in gene expression between control and lead-exposed mice. Balb/c mice were exposed to 0 mM (Control), 0.1mM (Low), or 2 mM (High) lead acetate from gestation through postnatal day 21. RNA brainstem samples (n=4/ group) were used to probe custom microarrays containing toxicology and CNS genes. Increases ((1.5 fold) were observed between control and lead-exposed mice in several genes including the cytoskeletal protein MAP4, the (4 subunit of the nicotinic receptor, and in the tumour suppressor proteins, NF2 and APC. Significant decreases were found in a number of genes including divalent cation-regulated proteins. Of particular interest, the regulatory and catalytic subunits of the protein phosphatase 2A were decreased with lead treatment. Consistent with this finding is our observation that lead exposure results in increased phosphorylation of neurofilament; this cytoskeletal protein is dephosphorylated by PP2A. Our results demonstrate that exposure to even low levels of lead results in significant changes in gene expression with subsequent morphological modifications within the auditory brainstem. Such alterations may contribute to the behavioral deficits observed in children exposed to lead. Supported by NIH P20 RR17670.

738 Carbon Monoxide and Iron in Neuronal Development

Douglas S Webber¹, Ivan Lopez², Rose A Korsak¹, Dora Acuna², John Edmond¹

¹*Mental Retardation Research Center, David Geffen School of Medicine, UCLA, 760 Westwood Plaza Rm 68-155NPI, Los Angeles, CA, United States,* ²*Surgery Department, Division of Head and Neck, David Geffen School of Medicine, UCLA, 1000 Veteran Avenue 31-25 Rehabilitation Center, Los Angeles, CA, United States*

Iron deficiency (ID) and chronic mild carbon monoxide (CO) exposure are nutritional and environmental problems that can be experienced in common. ID affects the lives of more than 1.2 billion people worldwide and occurs in approximately 9 % of the children without anemia in the United States. Between 8 to 20 % of women of child-bearing age are ID. Iron and CO metabolism are intricately linked; both are released within cells by the action of heme oxygenases. Ambient concentrations of CO increase from the incomplete combustion of fossil fuels and from cigarette smoke; CO is ubiquitous to air in some communities. Chronic CO exposures, as mild as 12 ppm, results in a significant decrease in the number of cells expressing a basal level of c-Fos activity. Levels of c-Fos are about half in the CO exposed animals when compared to non exposed controls. Within the inferior colliculus (IC), the effect at these concentrations is specific to the central nucleus (CIC). The developmental deficits are permanent and persist into adulthood. ID rat pups exposed to 25 ppm CO have a reduced c-Fos expression in the CIC when compared to their age matched controls (no CO exposure). We expected to find that the combination of ID and chronic CO exposure at 25 ppm would result in a decrease in c-Fos greater than with CO alone. However, the very opposite appears to be the case, in that certain iron restricted conditions are neuro-protective to c-Fos expression as neurons develop. When iron is supplemented over that normally fed, it can enhance the number of c-Fos positive cells in the CIC over the same period of development. Paradoxically, a reduced nutritional iron status is protective in allowing the near normal development of a full complement of c-Fos positive cells over a 14-day period of CO exposure. We conclude that several critical components of the auditory pathway are selectively affected by mild CO exposure, while limiting iron status ameliorates the effect caused by mild CO exposure.

739 Neuronal Plasticity in The Cochlear Nucleus Following Acoustic Overstimulation in Mouse

Munirathinam Subramani¹, D Kent Morest²

¹*Neuroscience, Uconn Health center, 263 Farmington Avenue, Farmington, CT, United States,* ²*Neuroscience, Uconn Health Center, 263 Farmington Avenue, Farmington, CT, United States*

Cochlear damage due to acoustic overstimulation not only produces hair cell loss, it also causes significant degenerative and regenerative changes in different parts of the cochlear nucleus (CN) and in the synaptic nests, which are the tight aggregations of synaptic endings not wrapped by glial processes. F1 hybrid (C57/Bx6/J) adult mice were exposed to white noise at >4kHz at 115 dB SPL for 6 hrs. Sound-exposed and normal control mice

were perfused through the heart with 4% paraformaldehyde and 4% glutaraldehyde after 3.5, 7, 14, 30, 60, and 120 days' survival. The CN was prepared and processed for electron microscopy. Initial degenerative reactions were seen primarily in axons, dendrites, and synaptic endings in the anteroventral, posteroventral, and dorsal CN and in the small cell shell. Degeneration of axons and dendrites began as early as 3.5 days after exposure and increased progressively over the next 2 months. Some of the neuronal perikarya accumulated organellar debris, membrane fragments, and lysosomes. Although axonal endings in all areas reacted to acoustic overstimulation, the synaptic nests may be the most plastic. Finally, the degenerative events were followed by the appearance of new axons and synaptic endings at 120 days after exposure. These plastic changes indicate that a significant amount of recovery occurred after long-term survival. Quantization of these plastic changes and identification of the types of synaptic endings involved will provide important information on the mechanisms of noise-induced hearing loss. Supported by NIH Grant DC00127.

740 Prolonged Stimulation with Sound increases Angiogenesis at the Auditory Midbrain of the Neonatal Rats

Tzai Wen Chiu¹, Paul W.F. Poon²

¹*Basic Medical Institute, NCKU, University Road, Tainan, Taiwan,* ²*Physiology, NCKU, University Road, Tainan, Taiwan*

In the neonatal brain, there is a peak in angiogenesis that appears grossly in parallel with the developmental change in metabolic activity. Such process of vascularization could be associated with the sensory experience that shapes the development of neurons and their connections in the brain. For example, long-term increases in capillary have been reported in the visual cortex of rats that were reared in a complex environment. At the highly vascularized auditory midbrain, the count of blood vessels continues to rise for 2 weeks after the onset of hearing. Whether changes in angiogenesis may occur at the auditory midbrain following enriched sensory experience remain unclear.

We studied the changes in vascularization at the auditory midbrain after rats have been exposed to a mild sound early in life. Experimental rats were exposed to a steady tone (4 kHz, 65dB SPL, 10 hrs/day) during postnatal week 2. Control rats were raised in the same environment without tone. On postnatal day 15, rats were overdosed with urethane (2.5g/kg) and perfused with 0.9% normal saline followed by 4 % paraformaldehyde. Brains were dehydrated in alcohol and embedded in paraffin. Coronal sections (7 um) of the inferior colliculus (IC) were cut and stained with Haematoxylin/Eosin. For each IC, 5 sections taken at intervals of 245 um were analyzed under microscope with an image software (Image Pro Plus). The number of patent blood vessels in the IC was counted according to their size and profile orientation.

Comparing with controls, rats after tone exposure showed a significant increase ($p < 0.0001$) regarding the density of blood vessels in the central nucleus of IC. The greatest change appeared to be associated with capillaries with diameter around 8um.

Results suggested that during the early postnatal period, the vascular pattern at the auditory midbrain appears rather plastic. Acoustic stimulation lasting for 7 days can induce changes in angiogenesis.

This phenomenon may be related to changes in neuronal activity in the IC after similar acoustic treatment as reported earlier. The underlying mechanisms of sound-induced angiogenesis may be related to the changes in the level of VEGF or the expression of VEGF receptors.

(Supported in part by the Academic Excellence Program, Ministry of Education, Taiwan.)

741 *Math1* gene therapy generates new cochlear hair cells and improves hearing following experimental deafening in mature guinea pigs

Masahiko Izumikawa¹, Ryosei Minoda¹, Kohei Kawamoto², Karen Abrashkin¹, Kärin Halsey¹, Lisa Kabara¹, David F. Dolan¹, Yehoash Raphael¹

¹Department of Otolaryngology, The University of Michigan, Kresge Hearing Research Institute, 1150 West Medical center, Ann Arbor, Michigan, United States, ²Otolaryngology, Kansai Medical University, 1 Fumizonochō, Moriguchi, Japan

Ototoxicity which leads to hair cell loss in the mammalian cochlea causes permanent hearing loss. *Math1* is the mouse homolog of *atonal*, a *Drosophila* basic helix-loop-helix transcription factor gene. *Math1* gene transfer has been shown to generate new cochlear hair cells in normal adult guinea pigs (Kawamoto et al.) and in cochlear explants (Gao et al). In this study, we set out to determine the outcome of *Math1* gene therapy in experimentally-deafened guinea pigs. Young adult guinea pigs were deafened with kanamycin and ethacrynic acid. Four days later, we inoculated a recombinant adenovirus vector with the *Math1* gene insert (Ad-*Math1*) into the scala media of the left cochlea. Control animals were inoculated with adenovirus vectors with no gene insert (Ad-empty). Auditory brainstem responses (ABRs) were measured one and two months after the inoculation. After the last ABR measurement, animals were sacrificed and their cochlea prepared for histological assessment using whole-mounts stained for actin and Myo7a or SEM. In Ad-*Math1* inoculated ears, ABR thresholds in all measured frequencies (4k, 8k, 16k, and 24kHz) were significantly better as compared with contralateral ears (right ears) and with control animals. *Math1* inoculated ears contained ectopic new hair cells in the interdental cell, inner sulcus, and Hensen's cell areas as well as immature-looking hair cells within the organ of Corti. No new cells were observed in any of the control animals. Our results suggest that adenovirus-mediated overexpression of *Math1* in deafened guinea pigs leads to generation of new cochlear hair cells, resulting in partial recovery of hearing thresholds.

Support: GenVec and NIH/NIDCD Grant DC01634.

742 *Skp2* increases the number of new hair cells generated by *Math1* in the mature guinea pig cochlea.

Ryosei Minoda¹, Kohei Kawamoto², Masahiko Izumikawa¹, Yehoash Raphael¹

¹Kresge Hearing Research Institute, The University of Michigan Medical School, Room-9303 MSRB III 1150 W. Medical Center Drive, Ann Arbor, MI, United States, ²Otolaryngology, Kansai Medical University, 1 Fumizonochō, Moriguchi, Japan

Hair cell loss is irreversible, leading to permanent hearing impairment. To restore hearing, it is necessary to generate new hair cells to replace the ones that are lost. *Math1*, the mouse homolog of the *Drosophila* gene *atonal* is necessary for hair cell development. Over-expression of *Math1* in the adult guinea pig cochlea can generate new hair cells (Kawamoto et al., 2003); however, the number of new hair cells generated by *Math1* over-expression is small. This study was designed to determine whether a mitogenic co-treatment can increase the number of new hair cells generated by *Math1* gene therapy. For that purpose, we used a recombinant adenovirus with a *Skp2* gene insert. *Skp2* is a F-box protein which causes G1 to S transition through ubiquitination of p27Kip1. Normal adult guinea pigs were inoculated with the *Skp2* vector (Ad. *Skp2*) along with an adenovirus encoding the *Math1* gene (Ad. *Math1*) into the scala media of the 2nd turn in their left cochlea. Control groups were inoculated with Ad. *Math1*, Ad.empty or artificial endolymph. Two months later, we evaluated the surface morphology of the organ of Corti and surrounding tissues using SEM. The analysis showed that the number of ectopic hair cells in the combined Ad. *Math1* / Ad. *Skp2* group was significantly higher compared to the group inoculated with Ad. *Math1* alone. Animals inoculated with Ad.empty or artificial endolymph displayed no ectopic hair cells. In the combined Ad. *Math1* / Ad. *Skp2* group some of the ectopic hair cells existed as pairs. These findings suggest that increasing the number of non-sensory cells by a mitogenic treatment can enhance the number of new hair cells generated upon *Math1* over-expression.

Supported by GenVec and NIH/NIDCD Grant DC01634.

743 Vestibular hair cell regeneration and re-establishment of balance function induced by *math1* gene delivery

Hinrich Staecker¹, Mark Praetorius², Kim Baker³, Douglas Brough⁴

¹Otolaryngology, University of Maryland, 16 South Eutaw St., Baltimore, MD, United States, ²Otolaryngology, University of Saarland, 34, Flur St., D-66424 Homburg/Saar, Germany,

³Otolaryngology, University of Maryland, 16 South Eutaw St., Baltimore, United States Minor Outlying Islands, ⁴Molecular Virology, Genvec Inc, 65 Watkins Mill Road, Gaithersburg, MD, United States

Over expression of *math1* has been demonstrated to induce generation of hair cells in the cochlea in neonatal tissue culture models of the organ of Corti and *math1* generation of hair cells has recently been shown in vivo. We have examined an in vitro organotypic culture model as well as unilateral acute and bilateral chronic models of aminoglycoside vestibular injury. Delivery of *Math1*

using an adenovector (Ad) resulted in the generation of hair cells in adult mouse utricular and saccular cultures. Mice treated acutely or chronically with aminoglycosides showed recovery of a significant portion of the vestibular neuroepithelium after AdMath1.11D was infused into the inner ear. Interestingly there was no recovery of hair cells noted within the cochlea in these mouse models and no hair cells noted outside of the vestibular neuroepithelium. Assessment of animals 2 months after vector infusion demonstrated a recovery of swim times compared to non-vector treated controls, demonstrating recovery of vestibular function after Math1 gene delivery.

744 Hair Cell Induction in Neonate Mice Cochleas by Inhibiting Notch/RBP-J Signaling

Norio Yamamoto^{1,2}, Kenji Tanigaki², Masayuki Tsuji², Juichi Ito¹, Tasuku Honjo²

¹Department of Otolaryngology, Head and Neck surgery, Graduate school of Medicine, Kyoto University, 54 Shogoin Kawahara-cho Sakyo-ku, Kyoto, Japan, ²Department of Medical Chemistry, Graduate school of Medicine, Kyoto University, Yoshida Konoe, Kyoto, Japan

Notch signaling is involved in cell fate determination of various cell lineages. Notch interaction with its ligand induces the cleavage of its intracellular domain (IC) of Notch. Notch IC translocates to the nucleus and binds to RBP-J to transactivate transcription of target genes such as *hes1*. All four Notches in mammals bind to RBP-J to exert their transactivation activities.

Notch signaling inhibits hair cell specification in inner ear development, but its function after birth is unknown.

To conditionally inhibit Notch signaling without redundancy, we used mice carrying loxP-flanked RBP-J (*RBP-J^f*) alleles. Explant culture of organs of Corti is established from neonate (P3) mice with homozygous or heterozygous *RBP-J^f* alleles in addition to ROSA26 Cre reporter alleles. Five days after disrupting RBP-J genes with adenovirus vector expressing Cre recombinase, organs of Corti were immunohistochemically stained with anti Myosin7a antibody which is a specific hair cell marker in inner ears. Only in homozygous mice Myosin7a was ectopically positive in the region lateral to hair cells where usually Hensen's cells reside although the number of hair cells did not change. These ectopic hair cells were also positive for LacZ, indicating that these cells became Myosin7a positive due to disruption of RBP-J gene.

Overexpression of Math1 in organs of Corti of neonate rodent is also reported to induce ectopic hair cells. Math1 expression is inhibited by Hes1 and in turn Hes1 is the direct downstream of Notch/RBP-J signaling, suggesting that ectopic hair cell induction by disruption of RBP-J gene is through Math1 induction. We confirmed this by staining RBP-J deficient organs of Corti with anti Math1 antibody. Math1 was positive in the same region as ectopic hair cells arose. These results indicate that inhibition of Notch/RBP-J signaling might be a treatment to regenerate hair cells in sensorineural hearing impairment due to hair cell loss as well as overexpression of Math1.

745 Induction of supporting cell proliferation in the cochlea using Adenovirus encoded RNAi targeting p27Kip1 mRNA

Jonathan Kil, Rende Gu, James LaGasse, Christine Caputo, Eric Daniel Lynch

Research and Development, Sound Pharmaceuticals, Inc., 4010 Stone Way N Suite 120, Seattle, wa, United States

Terminal mitosis in the mouse cochlear sensory epithelium occurs on ~E14. The postmitotic state of the supporting cell population is thought to be mediated, in part, by the onset and maintenance of p27Kip1, a cyclin-dependent kinase inhibitor. The induction of supporting cell proliferation in postnatal mouse cochlea has previously been reported using antisense oligonucleotides against p27Kip1 mRNA (ARO 2001 Abst.78). In an effort to extend our previous findings, we have developed and analyzed double stranded RNA interference molecules (RNAi) in cell and organ cultures. U6 and CMV promoter plasmids encoding short inhibitory p27 RNA (siRNA) constructs were tested in HEK293 cells for their ability to degrade p27 mRNA encoded by an exogenously introduced CMV-p27-IRES-GFP expression plasmid. Control plasmids included siGFP and random sense RNAi encoding plasmid (pSPI130). In cell culture, p27 RNAi constructs pSPI128 and pSPI129 reduced p27 mRNA by 80-85% relative to the negative control pSPI130. In comparison, the siGFP control plasmid reduced GFP mRNA levels by 75-80%. These plasmids were used to make AdV5 stocks encoding p27 siRNAs. P3-P4 mouse cochlear cultures were transfected with AdV5 expressing p27 RNAi for 2-4 days. These cultures exhibited proliferating nuclei BrdU(+) in the supporting cell region. siGFP control cultures and cultures without virus showed significantly fewer BrdU(+) supporting cell nuclei. Cross section analysis confirmed the identity of BrdU (+) nuclei in the supporting cell region and included Hensen's, Deiter's, and inner phalangeal cells.

These data are the second demonstration of supporting cell proliferation in the wild-type mouse postnatal organ of Corti, and further validate p27Kip1 as a target for cellular regeneration in the cochlea.

746 Development of a Knock-In Model for Mammalian Hair Cell Regeneration

Elizabeth C. Smiley¹, John A. Germiller², Douglas E. Vetter³, Kate F. Barald⁴

¹Cell and Developmental Biology, University of Michigan, 1150 W. Medical Center Drive, Ann Arbor, MI, United States, ²Pediatric Otolaryngology, Children's Hospital of Philadelphia, 34th St. and Civic Center Blvd., Philadelphia, PA, United States, ³Dept. of Neuroscience, Tufts University School of Medicine, 136 Harrison Ave., Boston, MA, United States, ⁴Cell and Developmental Biology, University of Michigan, 1150 W. Medical Center Dr., Ann Arbor, MI, United States

We propose to test the hypothesis that mammalian hair cell (HC) regeneration is possible if mature HC or supporting cells (SC) are induced to re-express critically important early genes, including transcription factors and growth factors. Bone morphogenetic protein 4 (BMP4) is hypothesized to be among the control factors that initiate an expression cascade critical for HC development and

regeneration. We have chosen the pTetOn system (Clontech) to express genes downstream of the HC-specific promoter Brn3.1 (Erkman et al, 1996). The tetracycline analog, doxycycline (dox) turns on the gene of interest in this system. We are using an immortalized cell line derived from the E day 9 Immortomouse inner ear (clone 2D2) as a pilot system before producing transgenic mice. Proliferating, untransfected 2D2 cells express HC markers Brn3.1, alpha-10 AChR, myosin 7A, the BMP receptors BRK-1 and BRK-3, chordin, noggin, jagged-1 and -2 and notch-1. Previously we demonstrated that 2D2 cells could express green fluorescent protein under control of the Brn3.1 promoter. We also showed that 2D2 cells stably transformed with pTetOn and transiently transfected with luciferase/pTRE responded to dox stimulation. We now show that 2D2-pTetOn cells express mature, secreted, myc tagged BMP4 into the medium. In addition, we have substituted the Brn3.1 promoter in place of the CMV promoter in the pTetOn vector. 2D2 cells stably transformed with this construct and transiently transfected with luciferase/pTRE and the pTS suppressor construct also respond to dox stimulation (60 fold).

747 Mechanisms of Adenovirus Vector Gene Delivery to the Inner Ear

Douglas E Brough¹, Mark Praetorius², Chi Hsu¹, Hinrich Staecker³

¹Vector Sciences, GenVec Inc, 65 West Watkins Mill Road, Gaithersburg, MD, United States, ²Otolaryngology, University of Saarland, 12xx, Homburg, Germany, ³Otolaryngology Head and Neck Surgery, University of Maryland, Baltimore, 16 South Eutaw St, Baltimore, MD, United States

Gene delivery to the inner ear has the potential to treat hearing loss and balance disorders. A number of studies have shown that adenovirus vectors can transduce sensory and non-sensory cells within the inner ear. In addition, the expression of growth factors and regulatory genes has been shown to have biological effects. As more candidate therapeutic genes are being discovered, further understanding of the mechanisms involved in adenoviral vector transduction of the inner ear is needed. Multiply deficient and targeted adenovirus vectors have the potential to enhance safety and efficacy of a gene delivery candidate to treat hearing and balance disorders. The advantages that multiply deficient adenoviral vectors deleted of E1A, E1B, E3 and E4 for gene delivery to the inner ear have been shown and the ability of these vectors with modified capsids to specifically transduce the inner ear will be discussed.

748 Lentivirus Vector-Mediated Gene Delivery During Hair Cell Differentiation

Hideki Mutai, Stefan Heller

EPL - Dept. of Otolaryngology, Mass Eye & Ear Infirmary / Harvard Medical School, EPL - MEEI, 243 Charles Street, Boston, MA, United States

Lentivirus has several advantages over other viral vectors including a wide range of host cells, stable gene expression in the infected cells, and non-pathogenicity. We sought to evaluate the efficacy and the stability of lentivirus-derived EGFP expression during hair cell development *in vitro* after a single infection. LentiLox3.7 (LL3.7), which expresses enhanced green fluorescent protein (EGFP) gene under the control of cytomegalovirus promoter, was generated from

human embryonic kidney 293FT cells by co-transfection of the proviral plasmid and packaging vectors. The viral particles were recovered and concentrated to 10⁸ transduction units/ml by ultracentrifugation. For testing lentiviral injection efficacy, we used chicken inner ear organotypic cultures and a mouse stem cell model. Chicken otic vesicles at the stage 15-18 were dissected and infected with LL3. After three days in culture, a substantial number of EGFP positive cells were observed in the vesicles. Immunohistochemical study revealed that many of the infected cells belonged to the Pax-2-positive population, which gives rise to hair cells. In a second study, LL3.7 was infected into the embryonic stem (ES) cell line R1. ES cells expressed EGFP 2 days post-infection, indicating the successful avoidance of silencing mechanisms. Infected ES cells were subjected to stepwise guidance toward hair cell differentiation by using a method recently established in our laboratory. We monitored the stability of lentivirus-mediated EGFP expression throughout this stepwise guidance process. Our study provides fundamental data for lentivirus-technology for studies of inner ear development *in vitro* using gain-of-function and loss-of-function strategies.

749 AAV Mediated Gene Delivery in the Murine Cochlea *In Vitro*

Ida M Stone¹, Matthew W. Kelley², Diana I. Lurie¹, David J. Poulsen¹

¹Biomedical and Pharmaceutical Sciences, University of Montana, 32 Campus Drive, Missoula, MT, United States, ²Section on Developmental Neuroscience, National Institutes on Deafness and other Communication Disorders/NIH, 5 Research Court, Rockville, MD, United States

Adeno-associated virus (AAV) is generally considered to be an attractive vector for gene delivery. However, previous attempts to transduce auditory hair cells and support cells with AAV have not been successful. New AAV serotypes are now available that have not yet been tested in the auditory system. These vectors are able to target a wide range of cells, and in some cases, may use different receptors and co-receptors on the cell surface. For example, AAV2 has been shown to bind heparan sulfate while AAV5 binds sialic acid. To assess transduction of specific cell types within the cochlea, primary cochlear explants from CD₁ mice age E13 and P0-1 were transduced with various serotypes of AAV carrying the GFP marker gene. The explants were maintained in culture media containing AAV serotypes 1, 2, or 5 for 5 days. The cultures were then processed and immuno-stained with myosin VI to identify hair cells and GLAST or GFAP for identification of support cells. AAV5 transduced fibroblasts and neurons within the cochlear explants but not sensory epithelial cells. GFP expression was detected in hair cells and support cells following transduction with AAV1 and AAV2 under the ubiquitous CAG promoter. Under the GFAP promoter, genes have been shown to be specifically expressed in support cells of the cochlea. Primary cochlear explants were treated with AAV1 carrying GFP under the GFAP promoter to determine whether support cell specific transduction would occur. Under these conditions, GFP was observed specifically in support cells but not hair cells. Studies are currently underway to test whether AAV2 carrying GFP under the GFAP promoter will also transduce support cells. Thus, preliminary studies suggest that of the vectors studied, AAV serotype 1 appears to be the most efficient at transducing the sensory epithelia.

750 Morphology of auditory hair cell in guinea pig after transgene expression

Zi long Yu

Otolaryngology, Otolology, 2# Chongnei Street, Beijing, China, People's Republic of

Morphology of auditory hair cells in guinea pig cochlea after transgene expression

Abstract

It's very important that if recombinant adenoviral (Ad) vector can bring great damage to the auditory hair cells in guinea pig cochlea after transgene expression. In this study scanning electronic microscope was used to observe if there were auditory hair cells loss after Ad.LacZ(Ad, containing E.coli galactosidase) was inoculated into guinea pig cochlea through round window membrane. Seven days later all inner and outer hair cells were found to have expressed the LacZ gene, except for the sparely loss of outer hair cells at the basal turn and the second turn, there were not significant loss at the other turns, the inner hair cells were not absent at all turns. The impairment of auditory hair cells resulted from adenovirus vector are limited, and this vector can be used as one of the ideal deliver tools in gene therapy of the cochlea.

Key words Cochlea Transgene Adenovirus Ultrastructure

751 Recombinant Adeno-associated Virus Mediated Gene Transduction of the Cochlear Hair Cells

Yuhe Liu^{1,2}, Takashi Okada², Kianoush Sheykhosslami³, Kuniko Shimazaki⁴, Tatsuya Nomoto², Shinichi Muramatsu⁵, Rahim Ajalli¹, Koichi Takeuchi⁶, Hiroaki Mizukami², Akihiro Kume², Keiichi Ichimura¹, Keiyo Ozawa²

¹Department of Otolaryngology, Jichi Medical School, 3311-1 Yakushiji, Minamikawachi-machi, Kawachi-gun, Japan, ²Division of Genetic Therapeutics, Center for Molecular Medicine, Jichi Medical School, 3311-1 Yakushiji, Minamikawachi-machi, Kawachi-gun, Japan, ³Department of Otolaryngology, University of Tokyo, 7-3-1, Hongo, Bunkyo-ku, Tokyo, Japan, ⁴Department of Physiology, Jichi Medical School, 3311-1 Yakushiji, Minamikawachi-machi, Kawachi-gun, Japan, ⁵Department of Neurology, Jichi Medical School, 3311-1 Yakushiji, Minamikawachi-machi, Kawachi-gun, Japan, ⁶Department of Anatomy, Jichi Medical School, 3311-1 Yakushiji, Minamikawachi-machi, Kawachi-gun, Japan

Background: Virally mediated gene transduction into cochlear hair cells is a promising new approach for hearing impairment therapy. Adeno-associated virus (AAV) seems to be a good candidate for gene transfer into cochlear cells, because of its minimum cytotoxicity and long-term transgene expression.

Methods: Five serotypes of recombinant AAV vectors (AAV1-5) containing Chicken beta-actin promoter associated with cytomegalovirus immediate-early enhancer (CAG) driven EGFP and WPRE were directly microinjected into the scala tympani; and the cochlear function were monitored using ABR. The variability in the transgene expression pattern in the cochlear cells for AAV1-5 vectors was determined by visualizing EGFP expression.

Results: Each of these serotypes successfully targets distinct cell types within the cochlea. In contrast to other serotypes, AAV3 specifically transduced inner hair cells *in vivo*, and was superior in transduction of inner hair cells, although AAV1, AAV2 and AAV5 could infect inner hair cells.

Conclusion: Recombinant AAV3 might be an appropriate vector to transduce inner hair cells. Restricted transduction of cell types confined to inner hair cells by rAAV3 is ideal for hair cells gene replacement strategies.

752 Mechanisms During Renewal of Hair Cells Following Gentamicin Exposure in Postnatal Rat Utricular Explants

Mimmi Werner¹, Thomas Van De Water², Wei Liu³, Dorothy Frenz^{3,4}, Barbara Canlon⁵, Agneta Viberg⁶, Diana Berggren¹

¹Otolaryngology, University of Umeå, NUS, Umeå, Sweden, ²Otolaryngology, University of Miami, Ear Institute, Miami, Florida, United States, ³Otolaryngology, Albert Einstein College of Medicine, Bronx, New York, New York, United States, ⁴Anatomy & Structural Biology, Albert Einstein College of Medicine, Bronx, New York, New York, United States, ⁵Physiology & Pharmacology, Karolinska Institutet, KI, Stockholm, Sweden

Renewal of the mammalian vestibular sensory epithelia following aminoglycoside induced hair-cell damage has been described in many studies. However, there is an ongoing debate about the actual mechanisms that underlie this hair-cell renewal response. Self-repair of damaged hair cells, transdifferentiation of support cells into new replacement hair cells, as well as regenerative proliferation of supporting cells to form new hair cells have all been suggested in mammalian vestibular hair-cell recovery.

We have established an *in vitro* model of long-time culture (i.e. up to 28 days) of 4-day-old rat utricular maculae to study aminoglycoside induced vestibular hair-cell renewal. After a 48 h gentamicin (1mM) exposure loss of hair-cell stereociliary bundles was nearly complete with a decrease of the bundle density to 3-4% of their density prior to exposure. Renewal of hair-cell bundles was robust with a 15-fold increase reached on day 21 *in vitro*. In a parallel experiment the anti-mitotic drug aphidicolin was added to the medium during the recovery period after the gentamicin insult resulting in only a sparse renewal of hair-cell bundles (Hearing Research 2003,180:115-125). We are currently analyzing LM and TEM preparations corresponding to these experimental series. In another experiment BrdU was added to the medium during the recovery period following gentamicin insult. Maculae from these later experimental series were harvested on day 21 *in vitro*, freeze-sectioned and immunostained for BrdU and myosin VIIa. We observed BrdU-positive nuclei in all levels of the macular sensory epithelia, and myosin VIIa-positive hair cell-like cells in the apical part of the epithelia, but so far no double stained cells. Our results indicate a relationship between mitosis within the utricular sensory epithelium and renewal of the hair cell epithelium, but this mechanism does not seem to be regenerative proliferation.

753 Cell-Extracellular Matrix Interactions Limit Spreading and Proliferation in Postnatal Mammalian Utricle

Dawn Davies^{1,2}, Jeffrey T Corwin²

¹Physiology, University of Bristol, School of Medical Sciences, University Walk, Bristol, United Kingdom, ²Neuroscience and Otolaryngology, University of Virginia, MR4 Lane Rd, Charlottesville, VA, United States

Hair cell loss can result in permanent hearing or balance deficit due to limitations in regeneration unique to mammals. A key step in hair cell regeneration in other vertebrates is the production of precursors by cell division. The proliferative limitation in mammals develops soon after birth. Postnatal day (P)2 mammalian utricular epithelium exhibits a robust proliferative response to growth factor stimulation *in vitro*, which is dramatically reduced by P12 (Gu et al, 1997, ARO Midwinter Meeting Abstr. 390; Montcouquiol and Corwin, 2001, J. Neurosci. 21 974-982). Initiation of proliferation requires both growth factor- and adhesion-dependent signalling. In utricular epithelium, proliferation has been shown to be influenced by cell spreading, a process mediated by cell-cell and cell-extracellular matrix (ECM) adhesion (Warchol, 2002, J. Neurosci. 22 2607-2616). We have investigated spreading, proliferation and cell-ECM interactions associated with increasing age in isolated murine utricular epithelium. P6 tissue showed reduced spreading *in vitro* compared to embryonic day (E)18 tissue. Tissue area and number of proliferating cells were correlated at both stages studied, indicating that the relationship is independent of developmental stage and degree of spreading. Whilst reduced spreading was evident on all matrix tested, P6 tissue exhibited a greater reduction on laminin 1 (LM1) than on fibronectin. Furthermore, P6 tissue plated on striped matrix spread on poly-L-lysine stripes but was retarded on adjacent LM1 stripes. We observed changes in ECM and integrin expression in murine utricular epithelium *in situ* between E18 and P12. Decreased spreading on LM1 may be due to reduced $\alpha 6$ integrin expression but this is unlikely to account for the behaviour on other ECM. These results reveal age-related changes in cell-ECM interactions that influence tissue spreading and, thereby, suggest a potential mechanism for the limited proliferation observed in older tissue.

754 Expression of the GATA3 Transcription Factor in Cultures of Progenitor Cells from the Cochlea and Utricle

Mark E Warchol¹, Judy Speck²

¹Otolaryngology, Washington University School of Medicine, 660 South Euclid Ave., Campus Box 8115, St. Louis, MO, United States, ²Otolaryngology, Washington University School of Medicine, 660 South Euclid Ave., Box 8115, St. Louis, MO, United States

The transcription factor GATA3 is involved in the development of the inner ear and its innervation (M Rivolta and MC Holley, J Neurocytol 27: 637, 1998; A Karis et al., J Comp Neurol 429: 615, 2001; G Lawoko-Kerali et al., J Comp Neurol 442: 378, 2002). In the mammalian cochlea, GATA3 is expressed during the period of hair cell differentiation and is then downregulated. In contrast, GATA3 is widely expressed in the sensory epithelium of the

mature avian cochlea (Hawkins et al., Human Mol Genetics 12: 1261, 2003). In order to investigate the possible role of GATA3 in sensory regeneration, we are studying GATA3 expression in cultures of dissociated epithelial cells from the mature cochlea and utricle. Sensory epithelia were removed from chick cochleae or utricles, following treatment in thermolysin. Collected epithelia were then incubated in 0.05% trypsin and triturated 15x, dissociating the epithelia into single cells and small cell clusters. The resulting cell suspension was plated onto fibronectin or laminin-coated substrates and maintained in culture. After 7-10 days *in vitro*, immunoreactivity for N-cadherin was present at all cell-cell junctions and about 40% of the cochlear cells displayed nuclear immunoreactivity for GATA3. In contrast, very few cells in utricular cultures expressed GATA3. In some experiments, a pulsed laser microbeam was used to create ~100 μ m-wide 'wounds' in the epithelial cultures. Near-complete epithelial repair was observed after 24-48 hours, and this was accompanied by normal expression of GATA3 within the repaired regions. These results confirm the differential expression of GATA3 in the avian cochlea and utricle. It is notable that the expression pattern of GATA3 in the mature avian cochlea (which has a high capacity for sensory regeneration) differs considerably from the expression pattern of GATA3 in the mature mammalian cochlea (which cannot regenerate hair cells).

Supported by the NIH and NOHR

755 A transcription factor gene expression profile of regenerating chick cochleasensory epithelia.

Stavros Bashiardes¹, David Hawkins¹, Nancy Saccone¹, Mark Warchol², Michael Lovett¹

¹Genetics, Washington University, 4559 Scott Ave., St. Louis, Missouri, United States, ²Otolaryngology, Washington University, 4560 Clayton Avenue, St. Louis, Missouri, United States

Unlike mammals, many lower vertebrates have the ability to regenerate inner ear hair cells after acoustic trauma or ototoxic injury. We have analyzed temporal changes in gene expression during the early stages of regeneration in the chick cochlea *in vitro*. Analysis was carried out with the use of a unique custom-built oligonucleotide microarray consisting of probes to >1700 human transcription factor (TF) genes. Due to limited amounts of tissue, we have employed novel micro-cDNA techniques to allow such analyses. In our study, explanted chick cochlea sensory epithelia were damaged by neomycin treatment and allowed to recover. Samples were isolated at 0hrs, 24hrs and 48hrs post-treatment and expression profiles for these time points were analyzed. Multiple hybridizations and biological samples were analyzed, in order to produce statistically robust profiles of the pattern of TF genes expressed and of the major transcriptional changes in TFs during regeneration. Analysis of these time points revealed 124 genes that were significantly changed during the initial 48 hours of recovery. These include BAPX1, BNIP3L, NFATC1 and CBX6. We are currently employing RNAi to determine the effects of knocking down these genes in chick sensory epithelial cultures. This TF profile along with complementing functional studies should provide many useful new molecular markers for the study of hair cell development and regeneration, as well as pinpointing transcriptional pathways that are important for these processes.

756 Nestin expressing cells in nestin-EGFP transgenic rat inner ear

Sho Kanzaki^{1,2}, Masato Fujioka², Yasuhiro Inoue², Kaoru Ogawa², Hideyuki Okano³

¹Otorhinolaryngology, Tokyo Electrical Power Hospital, 9-2 Shinanomachi, Shinjuku, Japan, ²Otolaryngology, Keio University, 35 Shinanomachi, Shinjuku, Japan, ³Physiology, Keio University, 35 Shinanomachi, Shinjuku, Japan

Stem cells or progenitor cells in inner ear is very important for mammalian hair cell generation/regeneration. In stem cell biology, nestin is the intermediate filament transiently expressed in development. It is known as a marker of immature cells including neuroepithelial stem cells and is also potential marker of stem cells or progenitor sensory epithelial cells in inner ear. We can visualize the nestin expressing cells in inner ear of transgenic rat containing green fluorescent protein under the control of the nestin second intronic enhancer (E/nestin ; EGFP) at p28. There were numeral EGFP positive cells in sensory epithelial cell layer of vestibular organs while there was no expression of EGFP positive cells.

We examine EGFP cells can be expressed after hair cell damage.

One week after p28 rats were exposed to noise (band noise, 125dB, 4hrs), several EGFP expressing cells were found in the organ of Corti.

The present data indicated that endogenous progenitor cells expression was promoted after hair cell missing in mammalian cochlea.

757 Evidence of mitosis in sensory epithelium of the mature cochlea in the deafened guinea pig

Tatsuya Yamasoba, Kenji Kondo, Mitsuya Suzuki

Department of Otolaryngology, University of Tokyo, Hongo 7-3-1, Bunkyo-ku, Tokyo, Japan

It is currently accepted that mammalian auditory hair cells are produced only during the embryonic stage of life and not replaced when they die. Roberson and Rubel (1994) found no cell division within the cochlear sensory epithelia of gerbils after intense noise exposure. We failed to detect bromodeoxyuridine (BrdU)-positive cells in the organ of Corti in paraffin-embedded sections of the rat and guinea pig after deafening with kanamycin sulfate (KM) and ethacrynic acid (EA) (Yamasoba et al, 2002). In the sectioned cochlea, however, it is impossible to observe sensory epithelium throughout the cochlea. It is possible to miss cells showing mitosis. In the current study we assessed mitotic activity in the auditory sensory epithelium using surface preparation technique.

Guinea pigs were deafened by systemic application of KM followed by EA, and given BrdU for 10 days. The animals were then decapitated and the cochleae were immersed in 10 % formalin for 2 days. The cochleae were incubated with 3 % H₂O₂, immersed in 2 N HCl, and incubated overnight in a solution containing mouse monoclonal antibody to BrdU. After rinses, these specimens were incubated with a peroxidase-conjugated secondary antibody. After rinses, they were allowed to react with diaminobenzidine and mounted on glass slides. We found several BrdU-positive cells in the organ of Corti. The specimens were then postfixed, dehydrated, embedded in epoxy resin, and sectioned perpendicular to the basi-

lar membrane. These sections clearly demonstrated that BrdU-positive cells existed within the organ of Corti. TEM observations of ultrathin sections of these embedded sections, as well as the position of the BrdU-positive cells, indicate that the BrdU-positive cells were Deiters cells. These findings suggest that, although quite rare, the supporting cells in mature mammalian cochlea possess a potential of mitotic activity.

758 Bone Regeneration in the Rat Mandible with Bone Morphogenetic Protein-2: A Comparison of Two Carriers

Oneida Albania Arosarena, Wesley Logan Collins

Surgery/Otolaryngology, University of Kentucky, 800 Rose Street, Room C236, Lexington, Kentucky, United States

The reconstruction of mandibular defects is a surgical challenge in patients suffering from oral malignancies, facial trauma, and congenital deformities of the facial skeleton. While advances in osseous tissue engineering hold promise for eventual clinical application, the ideal osteogenic bone substitute has yet to be developed.

The objective of this study was to compare rat mandibular bone regeneration with recombinant human bone morphogenetic protein-2 (rhBMP-2) delivered with two carriers: a hyaluronic acid polymer, and a collagen carrier complexed with calcium hydroxyapatite and tricalcium phosphate (collagen/HA/TCP). This was a prospective, controlled study involving sixteen male retired breeder Sprague-Dawley rats. Critical size defects were created in the bilateral mandibular bodies of the rats, and each hemimandible was assigned to an experimental group. The defects were filled with the hyaluronic acid carrier, the hyaluronic acid carrier loaded with rhBMP-2, the collagen/HA/TCP carrier, or the collagen/HA/TCP carrier loaded with rhBMP-2. Animals were euthanized after 6 weeks, and stereologic methods were used to determine volume fractions and volumes of new bone, osteoid, marrow, fibrous tissue, and remaining implant in each group.

Specimens containing rhBMP-2 had significantly larger new bone and marrow volumes than control specimens. We found the hyaluronic acid carrier to be comparable to the collagen/HA/TCP carrier in terms of regenerated bone volume, and development of large marrow spaces. The specimens in the hyaluronan/BMP-2 tended to have larger volumes of new bone, osteoid, and marrow than collagen/HA/TCP/BMP-2 specimens, though these differences were not significant. These findings have important implications for the development of osteogenic bone substitutes used for the repair of craniofacial bone defects.

759 Genetic and Functional Analyses of Stapes Malformations In The *Brn4/Pou3f4* Mouse Mutant

Kyung Ahn¹, Daniel Samadi¹, James C. Saunders², E Bryan Crenshaw III¹

¹Dept. of Surgery/ENT, The Children's Hospital of Philadelphia, 34th & Civic Center Blvd, Philadelphia, PA, United States, ²Dept. of Otorhinolaryngology: Head & Neck Surgery, University of Pennsylvania Medical School, 36th & Hamilton Walk, Philadelphia, PA, United States

Mutations in the *Brn4/Pou3f4* gene cause congenital hearing loss in humans and mice. In humans, mutations in the orthologous gene, POU3F4, result in mixed conductive and sensorineural deafness. Previous analyses of the mouse mutant clearly demonstrate sensorineural deafness. However, the contribution of conductive hearing loss has not been fully clarified. The effect of the *Brn4/Pou3f4* gene mutation on the function and development of the stapes has been analyzed using two diverse analytical approaches; laser interferometry and *Cre* gene knockin of the *Brn4* locus to mark cell lineage during otic development.

Laser interferometry was used to measure velocity transfer functions at the umbo of adult wild type and knockout mice during constant sound pressure stimulation of the tympanic membrane. When the median behavior of the two groups were compared, the mid-range frequencies of the knockout animals showed a well-defined reduction in velocity of 12 dB at 10.0 kHz. The transfer functions suggest that *Brn4* knockouts have a considerable middle-ear sound conduction deficit.

To assess the contribution of cells that express the *Brn4* gene during stapes formation, the *Cre* recombinase gene has been introduced into the *Brn4* locus via a knockin strategy in ES cells. When this pedigree is intercrossed with the ROSA reporter, lacZ expression is induced by a *Cre*-mediated DNA rearrangement, which can be followed to assess the lineage of cells expressing the *Brn4* gene. In summary, these analyses demonstrate a functional consequence of the *Brn4/Pou3f4* mutation on stapes function, and clarify the contribution of *Brn4* gene to stapes formation.

760 Multi-organ abnormalities in mouse models for inherited muscular dystrophies suggest key role for the interface between the cell membrane and the extracellular matrix

De-Ann M. Pillers^{1,2}, Brent Barber¹, Jiaqing Pang¹, Sawan Hurst¹, Sean Rash¹, Richard Weleber³, William Woodward⁴, Dennis Trune⁵

¹Pediatrics, Oregon Health & Science Univ, 3181 SW Sam Jackson Pk Rd, NRC-5, Portland, OR, United States, ²Molecular & Medical Genetics, Oregon Health & Science Univ, 3181 SW Sam Jackson Pk Rd, NRC-5, Portland, OR, United States, ³Casey Eye Institute, Oregon Health & Science Univ, 3375 SW Terwilliger Blvd, Portland, OR, United States, ⁴Neurology, Oregon Health & Science Univ, 3181 SW Sam Jackson Pk Rd, Portland, OR, United States, ⁵Otolaryngology and Head and Neck Surgery, Oregon Health & Science Univ, 3181 SW Sam Jackson Pk Rd, NRC04, Portland, OR, United States

Introduction: Muscular dystrophies are, by definition, best known

for their muscle phenotypes. Lesser known are the co-existing non-muscle manifestations that the disorders also include.

Purpose: We sought to characterize the distribution of non-muscle phenotypes in mouse models of muscular dystrophy as a marker for a functional role of proteins implicated in muscular dystrophy in a variety of organ tissues.

Methods: We studied the *dy* mouse, a severely affected model for merosin-deficient congenital muscular dystrophy. This mouse has absence of expression of the protein subunit laminin- α 2, which results in aberrant expression of the trimer Laminin-2 and disrupts the interaction between cell and extracellular matrix (ECM) in myocytes. We hypothesized that clinical evidence of organ pathology would suggest a role for Laminin-2 and its interaction with the ECM in other cell lineages. Several physiologic tests were employed, analogous to clinical screening tests used in man.

Results: Mild to moderate sensorineural hearing loss was found and has been reported previously. A defect in retinal electrophysiology was identified. A hypertrophic cardiomyopathy which progresses to a dilated cardiomyopathy was detected. In heterozygous animals, an obese body habitus was found.

Conclusions: Proteins defective in muscular dystrophies enjoy a wide tissue distribution which may reflect a key-role in multiple organ functions. The association of sensorineural hearing loss with the muscular dystrophy phenotype suggests that the defect in the "muscle" protein is responsible for a common underlying pathobiology in both tissues. The protein complex spanning from the actin cytoskeleton to the extracellular matrix, via dystrophin, the dystrophin-associated proteins, and Laminin-2, is well-defined in myocytes but further studies are indicated to delineate its composition and contribution in other cell lineages, including the cochlea.

761 Inactivation approaches to understand the Gap Junctions roles in the cochlea

Marine Cohen-Salmon¹, Vincent Michel², Jean-Pierre Hardelin¹, Francisco del Castillo³, Stephan Maxeiner⁴, Martin Theis⁵, Klaus Willecke⁴, Christine Petit¹

¹Neurosciences, Institut Pasteur-Inserm, 25 rue du Dr Roux, Paris, France, ²Neurosciences, Institut Pasteur-Inserm, 25, rue du Dr Roux, Paris, France, ³Neurosciences, Institut Pasteur, 25 rue du Dr Roux, Paris, France, ⁴Molekulargenetik, Institut für Genetik, Universität Bonn, Bonn, Germany, ⁵Center for Neurobiology and Behavior, Columbia University, Howard Hughes Medical Institute, New York State Psychiatric Institute, New York, New York, United States

Intercellular communication through gap junctions is crucial for proper functioning of the inner ear. Indeed, mutations in several connexin genes have been found to cause hearing loss. In the cochlea, two distinct cellular networks assembled by gap junctions have been described, i.e., the epithelial network connecting all supporting cells of the sensory epithelium, and the connective tissue network which is composed of fibrocytes, and also includes basal, intermediate, and endothelial cells of the stria vascularis. We have developed ubiquitous and tissue-targeted gene inactivation approaches of the connexin genes expressed in the inner ear. We have shown that the ubiquitous absence of Cx30, or the absence of Cx26 in epithelial gap junction network causes post-natal degener-

ation of the organ of Corti, which begins soon after hearing onset. In addition, we have shown that Cx30 is crucial for the production of the endocochlear potential. Other strategies to target the inactivation of the connexin genes, either in the intermediate cells of the stria vascularis, in the endothelial cells, in the fibrocytes of the spiral ligament and spiral limbus, or in both networks of the inner ear, are now presented.

In the inner ear, only the cell distributions of connexin30 and connexin26 have been well documented. We took advantage of the lacZ reporter gene in Cx43 del/+ and Cx45 +/- mutant mice to study the expression of the connexin43 and connexin45 genes during the inner ear development. Our results indicate that connexin43 and connexin45 play a role in the otic capsule bone and the inner ear vascular system, respectively.

762 Conditional gene targeting of GJB2 resulted in profound deafness due to maturation failure of the organ of Corti

Katsuhisa Ikeda¹, Takayuki Kudo¹, Zhen-Hua Jin¹, Satoru Gotoh¹, Yukio Katori¹, Toshihiko Kikuchi¹, Osamu Minowa², Tetsuo Noda³

¹Otorhinolaryngology - Head & Neck Surgery, Tohoku University Graduate School of Medicine, 1-1 Seiryomachi, Aoba-ku, Sendai, Japan, ²Mouse Functional Genomic Research Group, Riken, Higashi-totuka, Yokohama, Japan, ³Cell Biology, The Cancer Institute, Kami-ikebukuro, Tokyo, Japan

Hereditary deafness affects about 1 in 2,000 children and mutations in the GJB2 gene are the major cause in various ethnic groups. GJB2 encodes connexin26, a putative channel component in cochlear gap junction. However, the pathogenesis of hearing loss caused by the GJB2 mutations remains obscure. The generation of a mouse model to study the function of connexin26 during hearing has been hampered by the fact that Gjb2 knockout mice are embryonic lethal (J Cell Biol 140:1453-1461, 1998). We reported that transgenic mice expressing a mutant connexin26 with R75W mutation showed severe to profound hearing loss with degeneration of the organ of Corti (Hum Mol Genet 12:995-1004). Another mouse model of targeted ablation of connexin26 specifically in epithelial gap junction network by using Cre recombinase under control of otogelin promoter also developed moderate to profound deafness and degradation of the organ of Corti (Cur Biol 12:1106-1111, 2002). In order to further confirm pathogenesis of Gjb2 mutation in recessive form, we generated targeted disruption of Gjb2 using Cre recombinase controlled by P0. Targeted disruption of Gjb2 caused profound deafness from birth, in which the auditory response has never reached maturation. Apparent degeneration of the organ of Corti was recognized, together with presumably secondary reduction of numbers of spiral ganglion cells. These findings confirmed a crucial role of Gjb2 in the cochlear function.

763 Heteromerically-assembled gap junctions (GJs) comprised of connexins26 and 30 are the major type of GJs in the cochlea and show larger Ca⁺⁺ permeability than their homomerically-assembled counterparts

Jian-Jun Sun, Shoab Ahmad, Ben-Gang Peng, **Xi Lin**

Cell and Molecular Biology, House Ear Institute, 2100 West Third Street, Los Angeles, Ca, United States

The importance of gap junctions (GJs) in hearing has been indicated by the finding that connexin (Cx) mutations are responsible for a large portion of human sensorineural hearing impairment. Despite remarkable progresses in the genetic linkage studies of deafness, why Cx mutations cause deafness remains unclear. Here we investigated whether and to what extent Cxs26 and 30 were co-assembled in the cochlea of mice. Quantitative PCR identified Cxs26 and 30, both belonging to the β -group, to be the most abundantly expressed Cxs in the cochlea. Coimmunostaining showed colocalization of Cxs 26 and 30 in most (>83%) of GJ plaques (n>1000) from various regions of the cochlea. Their co-assembly was confirmed by co-immunoprecipitation of proteins extracted from the cochlear tissues. We then quantitatively measured the Ca⁺⁺ permeability of GJs by the ratio imaging method. Homo- and/or hetero-meric GJs comprised of EGFP-fused Cx26 and/or 30 were reconstituted in HeLa cells. Our results demonstrated that heteromerically assembled GJs comprised of Cxs26 and 30, presumably representing the native molecular configuration of GJs in the cochlea, were at least twice as fast for Ca⁺⁺ ions to permeate as their homomerically assembled counterparts.

Our results, combined with the recent findings that some Cx mutations do not apparently affect biochemical couplings of GJs (e.g., V84L, R143W) and the demonstration that a reduction of Cx diversity used in assembling GJs in the cochlea causes deafness (Teubner et al, Human Mol. Genet., 2003, 12(1), 13-21), suggested that certain quantitative changes in ionic permeability, not necessarily a completely shut-off, of the GJ mediated intercellular communications are enough to cause deafness.

764 Interaction of DOCK4, a Rap GTPase Activator with Harmonin

Fang Li¹, Denise Yan¹, Wen Hui Hu², Xiao Mei Ouyang¹, Zheng Yi Chen³, John R. Bethea², **Xue Zhong Liu¹**

¹Department of Otolaryngology, University of Miami, Mailman Center, Miami, FL, United States, ²Department of Neurological surgery, University of Miami, The Miami Project to Cure Paralysis, Miami, FL, United States, ³Department of Neurology, Harvard Medical School, Wellman 425, Boston, MA, United States

Several genetic loci have been linked to USH1, and five of the relevant genes have been cloned. Harmonin, the protein encoded by USH1C, has been shown to bind, by means of its PDZ domains, with the products of other Usher syndrome genes, including Myosin VII a (USH1B), CDH23 (USH1D), PCDH15(USH1F) and SANS (USH1G). While the complexes formed by these, and other proteins are believed to be essential for the proper organization and maintenance of hair cell stereocilia, little is known of the key signaling pathways that are responsible for the process by

which the stereocilia bundle develops. In this study, we have used the yeast two hybrid system to identify molecular partners for USH1C used as bait to screen a human brain cDNA library. One of the proteins, which we identified as an interactor to USH1C, was DOCK4, a member of the CDM (ced-5, DOCK180, Myoblast City) gene family. We further confirmed the physical interaction of USH1C with DOCK4 by co-immunoprecipitation and western blot analysis in mammalian cells. Expression profile on Northern blot showed presence of DOCK4 transcripts in multiple tissues, with highest levels in brain and lung. Furthermore Unigene clustering and expression analyses by RT-PCR showed that DOCK4 is expressed in the inner ear as well as in the eye. Based on our current data, it appears that Dock4, a Rap GTPase activator and regulator of the formation of intercellular adherens junctions, is involved as a component of a macromolecular complex mediated by harmonin. Taken together, this points to a potentially important role for Rap signaling pathway in mechanisms that regulate hair cell development, maintenance or function.

Supported by NIDCD and FFB

765 Molecular pathway underlying the growth of the stereocilia

Benjamin Delprat¹, Aziz El-Amraoui¹, Isabelle Perfettini¹, Pierre Legrain², Christine Petit¹

¹Neuroscience, Institut Pasteur / INSERM, 25 rue du Dr roux, Paris, France, ²Hybrigenics, Hybrigenics, 3-5 impasse Reille, 75014, France

The physiological activity of the hair bundle depends on the proper cytoskeletal architecture of its stereocilia. Within the hair bundle, the stereocilia are precisely organised into ranks of different lengths so as to produce a staircase like pattern. The molecular mechanisms controlling the size of these stiff microvilli are not understood yet. Several deaf mouse mutants defective in stereocilia growth have now been reported. Among them, whirler and shaker-2 mice defective in whirlin, a novel PDZ domain containing protein and myosin XV, an unconventional myosin, respectively, display very similar hair bundle abnormalities. So, as to get insights into the role of these two proteins, we sought for their interacting partners using the yeast two hybrid system and a cDNA library derived from inner ear sensory area at postnatal day 2. A particular attention was paid to ligands whose putative function would provide explanations for the stereocilia growth abnormalities in the two mouse mutants. We here present the first insight into the molecular mechanism underlying the elongation process of the stereocilia.

766 Normal auditory function associated with a partial genomic deletion of mouse *Coch*

Tomoko Makishima¹, Clara I Rodriguez², Nahid G Robertson³, Cynthia C Morton³, Colin L Stewart², Andrew J Griffith¹

¹Laboratory of Molecular Genetics, NIDCD, NIH, 5 Research Court, Rockville, MD, United States, ²Cancer and Developmental Biology Laboratory, Division of Basic Science, National Cancer Institute, National Cancer Institute at Frederick, Frederick, MD, United States, ³Department of Pathology, Brigham and Women's Hospital and Harvard Medical School, 75 Francis Street, Boston, MA, United States

Dominant DFNA9 progressive hearing loss and vestibular dysfunction is caused by mutations of *COCH*. *COCH* encodes Cochlin, a secreted protein with three distinct domains: An N-terminal LCCL domain followed by vWF1 and vWF2 domains at the carboxy terminal end. All known DFNA9 mutations are missense substitutions in the LCCL domain. Here we have characterized the auditory phenotype associated with a genomic deletion of the entire mouse *Coch* gene downstream of the LCCL domain. This allele, *Coch-del*, was originally generated in order to test an unrelated hypothesis on the function of cochlin in another tissue. In contrast to wild-type mouse tissues, *Coch* mRNA or cochlin protein were undetectable by northern and western blot analyses, respectively, of homozygous *Coch-del* cochleae. These results indicate that *Coch-del* expresses little, if any, residual partial-length cochlin in the cochlea. Auditory brainstem responses to click and pure-tone stimuli (8-, 16-, and 32-kHz) were indistinguishable among wild-type, heterozygous or homozygous *Coch-del* mice at postnatal day 19 (click response thresholds: 39 ± 4 dB SPL, wild-type; 39 ± 4 dB SPL, *Coch-del* homozygotes) and at 3 months of age (click response thresholds: 35 ± 4 dB SPL, wild-type; 39 ± 4 dB SPL, heterozygotes; 33 ± 7 dB SPL, homozygotes). Furthermore, we observed no behaviors suggestive of vestibular dysfunction. Our data indicate that DFNA9 is not caused by *COCH* haploinsufficiency, but via a dominant negative or gain-of-function mechanism. This is consistent with the observation that there are no known nonsense, frameshift, or splice site (functional null) mutations of *COCH* that are associated with hearing loss, and all known mutations are missense substitutions in a single (LCCL) domain. Furthermore, *COCH/Coch* may not even be necessary for normal auditory function, although we cannot formally rule out the possibility that residual but undetectable levels of the wild-type LCCL domain are sufficient to preserve normal hearing. A mouse model of DFNA9 will thus require a knock-in of one of the reported missense substitutions.

767 Hearing loss and morphological alterations in the ears of three mouse models of lysosomal storage diseases

Yun-Kai Guo^{1,2}, Xudong Wu^{1,3}, Linda Mann⁴, Jian Zuo¹, Sandra D'Azzo⁴

¹Dept. of Developmental Neurobiology, St. Jude Children's Research Hospital, 332 N. Lauderdale St., Memphis, TN, United States, ²Department of Otorhinolaryngology-Head Neck Surgery, Central South University, XiangYa Second Hospital, Hunan, China, People's Republic of, ³Dept. Anatomy & Neurobiology, University of Tennessee, Health Science Center, 800 Madison Avenue, Memphis, TN, United States, ⁴Dept. of Genetics, St. Jude Children's Research Hospital, 332 N. Lauderdale St., Memphis, TN, United States

The lysosomal storage diseases sialidosis, galactosialidosis and GM1-gangliosidosis result from either single or combined deficiency of the enzymes neuraminidase (NEU1), protective protein/cathepsin A (PPCA), and b-galactosidase (b-gal). We have generated mouse models of these three disorders that are phenocopies of the corresponding human conditions. However, it remains to be determined whether the profound hearing loss observed in human patients also occurs in the mouse models. Here we investigated the distribution of Neu1, PPCA and b-gal in the inner ear: intense staining was detected in cochlear spiral ganglia, lateral wall, spiral limbus and vestibular organ, and weak staining in the organ of Corti. *Neu1*^{-/-} mice showed an elevated ABR threshold (50-55 dB SPL) already at 3 weeks of age. In contrast, in 1-month-old *PPCA*^{-/-} mice the thresholds were normal, but became elevated 40-45 dB SPL at 2 months. *b-gal*^{-/-} mice showed near normal thresholds at all ages. Unique for the *Neu1*^{-/-} mice was the presence of significant cerumen occlusion in the external canal and severe otitis media. Vacuolation was observed within ossicles and cochlear bone cells, stria vascularis cells, spiral ganglia and macrophages, spiral limbus, spiral prominence and Reissner's membrane cells, but not within the organ of Corti. Vestibular ganglia, hair cells and supporting cells in cristae and maculae also showed vacuolation. In *PPCA*^{-/-} mice of 2 months, morphological changes were similar to, but lighter than, those observed in aged-matched *Neu1*^{-/-} mice, and the vestibular organs appeared normal. *b-gal*^{-/-} mice displayed only a mildly thickened middle ear muscosa, and ossicles, as well as vacuolation of spiral ganglia. Our findings demonstrate that deficiency of either one of these lysosomal enzymes results in different degree of hearing impairment. These mouse models are useful for investigating the molecular bases of hearing loss in these disorders and the effects of therapies.

768 The Cochlear Nuclei

Donata Oertel

Department of Physiology, University of Wisconsin Medical School, 1300 University Avenue, Madison, WI, United States

The biophysical specializations of neurons in the ventral cochlear nucleus shape the responses to synaptic currents from the auditory nerve, determining how the timing information in the firing of auditory nerve fibers is encoded and conveyed. Differences in the intrinsic electrical properties between populations of neurons in the dorsal cochlear nucleus, whose integrative roles are deter-

mined more by the summation of excitatory with inhibitory synaptic inputs, are more subtle and play a less prominent role in differentiating responses to sound.

Voltage-sensitive potassium conductances determine whether neurons in the ventral cochlear nucleus fire tonically or phasically. In bushy and octopus cells of the ventral cochlear nucleus, low-threshold potassium conductances prevent firing shortly after the onset of a depolarization, causing them to respond phasically. Phasic responses to a small group of auditory nerve fibers allows bushy cells sharpen and convey the temporal fine structure of sounds over a small frequency range. The phasic responses to a large group of auditory nerve fibers enables octopus cells to signal the presence of synchronous firing over larger groups of auditory nerve fibers in broadband transients. In contrast, the absence of the low-threshold potassium conductance allows T stellate cells to fire tonically when they are depolarized. They can thus signal the presence of acoustic energy with steady firing for the duration of a sound.

Synapses are also specialized. Auditory nerve fibers convey ongoing acoustic information; their terminals convey the firing patterns of auditory nerve fibers whether the firing rate is high or low and relatively independently of the previous firing history. Their targets in the ventral cochlear nucleus and deep layer of the dorsal cochlear nucleus detect that neurotransmitter through rapid glutamate receptors. Receptors are slower in the superficial layers. While synapses from auditory nerve fibers are not affected by synaptic activity, synapses from the second major system of inputs to the cochlear nuclei, the parallel fibers, show long-term potentiation and depression as a function of the synaptic activity.

This work has been supported by a grant from the NIH DC00176.

769 Comparative Neuroanatomy of the Mammalian Inferior Colliculus

Nell B. Cant

Department of Neurobiology, Duke University Medical Center, P.O. Box 3209, Durham, NC, United States

The neuroanatomical organization of the inferior colliculus (IC) in various species will be discussed from two points of view, using examples from the available literature. First, the topographic organization that forms the basis for tonotopy will be compared in laboratory animals that hear different frequency ranges. Second, the extent of segregation or overlap of the terminal fields of specific inputs (from the cochlear nucleus, superior olivary complex, auditory cortex, etc.) in the IC will be addressed. Published evidence from a number of different common laboratory species will be surveyed and patterns of organization of different inputs will be compared and contrasted. One question we have addressed in the gerbil is whether routine tissue stains can be used to predict the extent of the terminal fields from specific sources. To the extent to which this is possible, such stains may aid in addressing correlations between structure and function across species.

770 Functional Organisation of the Mammalian IC Across Species

Adrian Rees

School of Neurology, Neurobiology and Psychiatry, University of Newcastle, The Medical School, Framlington Place, Newcastle upon Tyne, United Kingdom

Several parallel pathways originate in the cochlear nuclei and follow different courses through the brainstem to converge in the inferior colliculus (IC) in the midbrain. We still know relatively little about the functional organisation of this convergence, but this talk will review how recent experiments are beginning to show how these inputs contribute to the spectral and temporal response properties of neurons in the IC. It will describe what experiments using iontophoresis, and other methods of dissecting out the contribution of specific inputs, can tell us about the interplay between the excitation and inhibition that ultimately determines the responses of neurons in the IC.

Although the pure tone has proved an invaluable probe for the analysis of frequency- and temporal-response properties, it may provide only a partial description of a neuron's responses to the more complex sounds that animals normally encounter in the real world. Experiments using stimuli with more than one component reveal features of the frequency receptive field that are not apparent when mapped with pure-tone stimuli alone.

A important issue to be discussed in this talk is the growing evidence for species differences in the functional properties of neurons in the auditory midbrain. Such differences come as no surprise when considering animals with highly specialised hearing such as bats and owls, but evidence is emerging for differences in the functional organisation of the inferior colliculus between so called, "non-specialised" mammals such as cat, guinea pig, rat and mouse. While respecting the many features of auditory processing that such species have in common, these findings caution against trying to impose a single model of auditory processing in all its detail across species: from the evolutionary perspective it seems that every species maybe "special".

Supported by the Wellcome Trust

771 Specialized Synaptic Function in the Mammalian Inferior Colliculus

Douglas L Oliver

Neuroscience, University of Connecticut Health Center, 263 Farmington Ave, Farmington, CT, United States

It has long been recognized that the neuronal responses to sound in the inferior colliculus (IC) reflect the integration of ascending pathways from the cochlear nucleus, superior olive, and lateral lemniscus. However, the basis for this integration has remained unclear.

This presentation will focus on how the response properties of IC neurons may be shaped by the organization of the inputs from the lower auditory brainstem, the intrinsic membrane properties of IC neurons, and the synaptic inputs to these neurons. The neural network organization of ascending inputs to the IC provides a one basis for functional organization. *In vivo* experiments suggest that there are functional zones where excitatory inputs from the medial superior olive, the lateral superior olive, and the cochlear nucleus

terminate independently. In some cases, the prevalent excitatory input converges with a specific inhibitory input. We speculate that in this organization of *synaptic domains*, the functional zone will be created by a unique combination of excitatory and inhibitory inputs in restricted parts of a single frequency-band lamina.

Recently, the cell types in the IC have been redefined based on their discharge properties *in vitro* and the underlying unique expression of different potassium currents. Evidence of specialized synaptic function in the IC suggests that these intrinsic properties may be important for the normal processing of information about sound. The typical response of an IC neuron to lemniscal stimulation *in vitro* is a prolonged, NMDA-mediated postsynaptic response that allows sustained firing by the IC neuron. It is likely that sustained firing patterns in IC *in vivo* will reflect both intrinsic properties of different cell types and the synaptic inputs. These components of IC synaptic organization, the synaptic domain and the unique interactions of IC cell type with synaptic input, are key functional parameters for understanding the IC in many species.

Sponsored by NIDCD R01-DC00189.

772 Complex Sound Processing in Bats: Generalized Function and Species Specializations

Christine Verdie Portfors

Biological Sciences, Washington State University, 14204 NE Salmon Creek Ave, Vancouver, WA, United States

Many animals use spectrally and temporally complex species-specific vocalizations for acoustic behaviors such as communication and echolocation. Consequently, neurons in the auditory systems of these animals must be able to encode acoustic features in the vocalizations. Emerging evidence from the inferior colliculus (IC) in mustached bats, Mexican free-tailed bats and mice suggests that certain aspects of processing complex sounds may be similar across different species. In particular, some neurons in the IC of these different mammals show selectivity to communication sounds. In many neurons the selectivity to particular communication calls can be predicted based on the excitatory and inhibitory frequency response areas of the neuron. This suggests that at least some of the neural mechanisms involved in processing communication sounds at the level of the IC may be generalized across mammalian species. From an evolutionary perspective this seems plausible as many mammals use complex sounds to communicate and the basic organization of the IC is similar. However, certain animals show specialized neural response properties for encoding particular aspects of their species-specific vocalizations. Neurons in the IC of bats show certain temporal and spectral response specializations that serve echolocation behaviors. For example, neurons in the IC of many bat species show selectivity to one or more temporal aspects of sound such as duration, FM sweep direction or modulation rate. Further, the mustached bat has combination-sensitive neurons that are important for integrating both spectral and temporal information contained in echoes for behaviors such as target distance analysis. Thus, while certain features of complex sound processing seem to be generalized across mammalian species, other aspects of processing are highly specialized to suit the needs of the individual species.

773 The Avian IC: Is the owl special?

Terry Takeshi Takahashi

Institute of Neuroscience, University of Oregon, 224 Huestis Hall, Eugene, Oregon, United States

In birds and mammals, nearly all ascending auditory projections synapse in the IC. Given its pivotal position within the auditory pathway, the IC must organize, process, and preserve the information necessary for the vast array of auditory perceptions that give us a sense of our acoustical environment. The most intensely studied avian IC is that of the barn owl (*Tyto alba*), a nocturnal predator renowned for its ability to localize prey. Acoustically-guided predation, however, is not simply sound-localization. A hunting owl must discriminate the footsteps of a vole from the rustling of leaves and echoes from sounds arriving directly from an emitting source. Furthermore, all sources, including reflective surfaces, must be accurately localized in space so that the owl can avoid obstacles in its headlong plunge toward prey in darkness. I will first describe the capabilities of the owl's IC to image multiple sound sources on its auditory space map, track each source's amplitude modulations, exploit motion to segregate a target from background noise, and dampen responses to echoes. While such performance may at first seem to be specializations of an auditory predator, all animals must contend with acoustical clutter, and the ability to signal "what lies where" may be a feature common to the IC of all animals. Indeed, the barn owl's IC is quite similar, anatomically, to that of other birds, such as the chicken and pigeon, and it also has the distinctive hodologically-defined zones found in mammals. The IC therefore, may have evolved to handle all of the tasks of auditory stream segregation. The interspecific differences that we detect may be the specializations needed to accomplish these basic tasks for different frequency ranges and the modifications needed to establish the circuitry given their ancestral form.

774 Physiological correlates of behavior in the inferior colliculus: studies of the precedence effect

Tom C.T. Yin, Daniel J. Tollin, Michael L. Dent

Department of Physiology, University of Wisconsin, 1300 University Avenue, 273 Medical Science Building, Madison, WI, United States

Despite numerous anatomical and physiological studies of the inferior colliculus (IC), its functional role in various auditory behaviors remains obscure. To study the relationship between the physiology of the IC and behavior, we have been using the precedence effect (PE), an auditory illusion that allows us to localize sound sources accurately in natural acoustic environments despite the presence of conflicting reflections. First, we investigated whether cats experience the PE in a similar fashion as human subjects. Using standard operant conditioning, we trained cats to localize sound sources by making saccadic eye movements to the locations of an auditory target. When identical transient sounds were delivered from pairs of speakers with a variable interstimulus delay (ISD), the cat's localization behavior was similar to that of human subjects: for ISDs < 0.4 msec they exhibited *summing localization* by looking between the two speakers, for ISDs between 0.4 and about 10 ms they showed *localization dominance* by looking only at the leading speaker, and they showed an *echo*

threshold of about 10 ms by looking at both leading and lagging sources for ISDs > 10 ms. Next, we looked for neural correlates of the PE in the responses of single units in the IC of these behaving cats. As previously described in the anesthetized cat and unanesthetized, but non-behaving, rabbit, for ISDs on the order of a few milliseconds, the responses of IC cells to the lag were substantially reduced compared to the lag presented in isolation. The rate of recovery of responses to the lag with ISD was more similar to that found in the unanesthetized rabbit than to that in the anesthetized cat, suggesting that anesthesia, not species differences, account for discrepancies in the earlier studies. We have also examined the effect of varying the position of the leading sound on the degree of suppression to the lagging sound and have found greater amounts of recovery to the lag sound when the leading sound was farther away, which is also in accord with our behavioral results.

775 Neural Tube Plays a Major Role in the Specification of the Dorsal/Ventral Axis of the Chicken Inner Ear

Jinwoong Bok, Doris K Wu

National Institute on Deafness and other Communication Disorders, National Institutes of Health, 5 Research Court, Rockville, MD, United States

The vertebrate inner ear is derived from a simple otocyst that forms a highly organized three-dimensional structure. Organization of this structure is governed by interactions between the otic tissue and signals emanating from surrounding tissues. However, the sources and signaling pathways that direct these processes are largely unknown. Our study focuses on how the dorsal/ventral (D/V) axis of the inner ear is specified during development.

Previously, we showed that *Sonic hedgehog* (*Shh*) is important for the ventral patterning of the inner ear from analysis of *Shh* knockout mice (Riccomagno *et al.*, 2002). To further characterize the roles and sources of SHH for inner ear development, either the floor plate or the notochord, or both were surgically removed at embryonic day 1.5 (E1.5) in chicken, and the gross anatomy of the inner ears was examined at E7. Removal of both the notochord and floor plate resulted in a selective disruption of ventral inner ear structures, while dorsal vestibular structures were largely unaffected, suggesting that signal(s) from the midline structures is necessary for the ventral specification. Interestingly, removing either source of *Shh* showed that signal(s) emanating from either the notochord or the floor plate is sufficient for ventral patterning of the chicken inner ear.

Furthermore, to test the hypothesis that neural tube, rather than the surrounding mesenchymal or ectodermal tissues, specifies the D/V axis of the inner ear, we asked if the ventral neural tube was sufficient to confer ventral fates in dorsal otic tissues. This was accomplished by rotating the D/V axis of the neural tube between rhombomeres 4-6, thus juxtaposing ventral neural tube and dorsal otic tissue in ovo. One day after surgery, the D/V axis of the otocyst was accessed by analyzing expression of dorsal and ventral specific genes. Expression of *Gbx2*, a dorsally expressed gene was completely abolished, whereas expression of *Otx* and *NeuroD* which are normally expressed ventrally were upregulated in dorsal tissues. These results indicate that signals from the ventral neural

tube are sufficient for conferring ventral otic fates in normally dorsal otic tissues, over-riding possible dorsal signals emanating from surrounding mesenchyme or ectoderm.

776 Control of Inner Ear Formation by FGF-3 and FGF-10

Yolanda Alvarez, Maria Teresa Alonso, Victor Vendrell, Laura Zelarayan, Thomas Schimmang
ZMNH, UKE, Falkenried 94, Hamburg, Germany

Fibroblast growth factors control the formation of several organs, including the inner ear. Our previous analysis of FGF-3 in the chicken embryo suggested its involvement in formation of the otic placode and vesicle (Vendrell et al., 2000). We have now analysed the function of FGF-3 in the mouse embryo. Previous analysis of FGF-3 mouse mutants in which the neo gene had been inserted into the FGF-3 coding region had revealed defects during inner ear differentiation, including lack or loss of the endolymphatic duct and cochlear ganglia (Mansour et al., 1993). However, the mutant phenotype showed a variable penetrance and expressivity, which may be explained by parallel signalling pathways, a non-uniform genetic background and/or a leaky mutant allele. We have created a FGF-3 mutant in which all coding sequences for FGF-3 have been deleted (Alvarez et al., 2004). Surprisingly, mutant mice were viable and showed none of the inner ear defects previously reported (Mansour et al., 1993). To clarify the differences between these FGF-3 mutants we have now created a FGF-3 mutant allele, in which the FGF-3 coding region has been replaced by the neo gene.

To analyse the potential of FGFs to act as hindbrain-derived neural signals we have created several transgenic lines ectopically expressing FGFs in rhombomeres 3 and 5 (Alvarez et al., 2004). We have found that, next to FGF-3, FGF-10 acts as a potent inducer of ectopic vesicles with otic characteristics. To further study a potential role of FGF-10 for inner ear formation we have studied its endogenous expression pattern during this process (Alvarez et al., 2004). Before formation of the inner ear placode, FGF-10 expression is detected in the mesenchyme, underlying the surface ectoderm where the inner ear placode will be formed. Subsequently, FGF-10 shows a very dynamic expression in the developing hindbrain, next to the inner ear placode and vesicle. Since FGF-3 is also expressed in the hindbrain during these stages and partially overlaps with FGF-10 both factors may act as redundant signals for inner ear formation. We have thus created mouse mutants which lack FGF-3 and FGF-10 (Alvarez et al., 2004). These mutants developed severely reduced otic vesicles which showed a lack or strong reduction of otic marker genes. However, in less affected mutant embryos we could observe the formation of small vesicles expressing otic marker genes in their corresponding domains.

777 The roles of mouse fibroblast growth factors (Fgf)3 and Fgf8 in inner ear development

Tracy Wright, Suzi Mansour

Human Genetics, University of Utah, 15N 2030E Room 2100, Salt Lake City, UT, United States

Otic development initiates early in development when signals from the hindbrain and mesoderm induce a region of ectoderm to

thicken, forming the otic placode. The placode then invaginates and forms a vesicle that undergoes cellular differentiation and morphogenesis, resulting in a mature inner ear. Studies of mice, chick, and zebrafish have implicated several signalling molecules, including Fgfs-3, -8 and -10 and 19 in these processes. We have previously shown that, in mouse, neuroectodermal Fgf3 and mesenchymal Fgf10 are required for otic placode induction. In chick, FGF19 in combination with Wnt8C can induce the expression of otic markers in ectodermal explants. In zebrafish, fgf3 and fgf8 are required for otic induction and, in chick, Fgf8, which is expressed in the pharyngeal endoderm, can induce the expression of Fgf3 (Ladher et al, in preparation).

To characterise the role of Fgf8 in mouse inner ear development, we generated mice that lack Fgf3 and have half the normal dose of Fgf8. At E9.5, loss of Fgf3 leads to a small, ventrally localised otic vesicle. In embryos lacking Fgf3 and missing one copy of Fgf8 the vesicle is further reduced in size but appears to be patterned correctly. However, unlike fgf3/8 mutants in zebrafish where severe defects in hindbrain development have been identified, hindbrain patterning in these mutants appears to be normal. We have subsequently generated mice that are homozygous for a null mutation in Fgf3, carry an Fgf8 null allele and an Fgf8 hypomorphic allele. These embryos are expected to have even lower levels of Fgf8 than the Fgf3 mutants with one Fgf8 allele. Characterisation of this phenotype will be presented and we will analyse the role that Fgf8 plays in mouse otic development.

778 Epithelial-Mesenchymal Interactions based on FGF Signaling Control Inner Ear Morphogenesis

Ulla Pirvola¹, Johanna Mantela², David M. Ornitz³, Jukka Ylikoski⁴

¹*Institute of Biotechnology, University of Helsinki, Viikinkaari 9, Helsinki 00014, Finland,* ²*Institute of Biotechnology, University of Helsinki, Viikinkaari 9, Helsinki, Finland,* ³*Department of Molecular Biology and Pharmacology, Washington University Medical School, 660 S. Euclid, St. Louis, MO, United States,* ⁴*Department of ORL, University of Helsinki, Haartmanink. 4E, Helsinki, Finland*

Epithelial-mesenchymal interactions have been suggested to control inner ear development, but only little direct evidence exists concerning the molecules and cellular mechanisms behind these interactions. The importance of fibroblast growth factor (FGF)-FGF receptor (FGFR) signaling in reciprocal epithelial-mesenchymal interactions is well established in the development of organs such as the limb bud, lung and tooth. We hypothesized that these interactions might occur in the developing inner ear too. Here we show the expression of a Fgf ligand in the otocyst epithelium and its specific Fgfrs in the surrounding mesenchymal otic capsule. Mice carrying a targeted deletion of the Fgf gene show a hypoplastic otic capsule, which results from decreased mesenchymal proliferation at the prechondrogenic stage. The mutants also lack semicircular ducts. The primordial epithelial outpocketings of the semicircular ducts remain dilated and the fusion plates fail to form. Together, we provide genetic evidence of an otic epithelium-derived growth factor regulating expansion of the surrounding mesenchyme and of reciprocal epithelial-mesenchymal interactions governing otic epithelial development.

779 FGF10 Interactions in Semicircular Canal Development

Sarah Pauley¹, Bernd Fritzscht²

¹Biomedical Sciences, Creighton University, 2500 California Plaza, Omaha, NE, United States, ²Biomedical Sciences, Creighton University, 2500 California Plaza, Omaha, NE, United States

Formation of anterior and posterior semicircular canals and cristae depends on BMPs (Chang et al., 1999), Jagged 1 (Kiernan et al., 2001), and FGF10 (Pauley et al., 2003). FGF10 null mutants show complete agenesis of the posterior canal crista and the posterior canal. The posterior canal sensory neurons form initially and project rather normally by E11.5, but die off soon after. FGF10 null mutants have no posterior canal system at E18.5. These mutants also have deformations of the anterior and horizontal cristae, malformation of the anterior and horizontal canals, as well as altered position of the remaining sensory epithelia with respect to the utricle. Like FGF10, Jagged 1 mutants have no posterior ampulla and sometimes no anterior ampulla as well as parts of the canals adjacent to the ampullae. Similarly, BMP signaling interference results in dismorphogenesis of the semicircular canals. It has been proposed that BMP4 and FGF10 interact with each other to up-regulate BMP2 for canal formation. In nervous tissue, FGFs antagonize the antineural function of BMPs. Thus, in the absence of FGF10, no proneuronal signal for the formation of posterior canal hair cells might be established, resulting in altered BMP4 signaling in the cristae. Likewise, Jagged 1 mutation might alter BMP4/FGF10 expression in the sensory patch of the cristae through alteration of hair cell/supporting cell fate-selection. This interference might cause the reduction and/or loss of parts of the canal. We will provide data describing the effects of FGF10 null mutation on the expression of BMP2, BMP4, Math 1, and Bf1 (Fkhi1). We will also describe the effects of FGF10 null mutation on the expression of Jagged 1. With these data, we can begin to untangle the complex web of gene interactions involved in the morphogenesis, neuron formation, and hair cell differentiation in the vestibular end-organ.

780 Looptail and Circletail identify Vangl2 and Scrb1 as planar polarity genes in mammals

Mireille E montcouquiol¹, Nathalie A Sans², Rivka A Rachel³, Neal G Copeland³, Nancy A Jenkins³, Robert J Wenthold², Matthew W Kelley¹

¹Section on developmental neuroscience, NIDCD, 5 research court, rockville, MD, United States, ²Laboratory of Neurochemistry, NIDCD, 50 South Drive, Bethesda, MD, United States, ³Mouse Cancer Genetics Program, NCI, Building 539, Room 229, Frederick, MD, United States

The planar cell polarity (PCP) pathway, a non-canonical Wnt signaling pathway, regulates the coordinated orientation of cells or structures within the plane of an epithelium. The two most studied examples of PCP are the wing and compound eye of *Drosophila melanogaster*. In mammals, an example of PCP is the uniform orientation of the stereociliary bundles located at the luminal surface of each mechanosensory hair cell within the cochlear sensory epithelium. Here we show that a mutation in *Vangl2*, the mammalian homolog of *Drosophila* *Strabismus*/*Van Gogh*, results in

significant disruptions in the initial steps in the polarization of stereociliary bundles in mouse cochlea. Moreover, a mutation in *Scrb1*, encoding a member of the LAP protein family that has not been implicated in PCP previously, results in similar, but less severe, stereociliary polarization defects. Finally, polarization defects in animals that are heterozygous for both *Vangl2* and *Scrb1* are as dramatic as in *Vangl2* homozygotes, demonstrating genetic interactions between these genes in the regulation of PCP in mammals. These results suggest that *Vangl2* regulates the earliest steps of stereociliary bundle polarization, the direction of movement and/or anchoring of the kinocilium within each hair cell. In addition, our preliminary data support the existence of a molecular interaction between *Vangl2* and *Scrb1* during this process. These results represent the first demonstration of a role for the PCP pathway in planar polarization in mammals, as well as identifying *Scrb1* as a new planar polarity gene.

781 Rho GTPases Regulates the Stereociliary Bundle Polarity in the Mammalian Cochlea.

Nathalie Cueille¹, Vincent Roth¹, Michel Eybalin², Marc Lenoir², Francois de Ribaupierre³, Azel Zine⁴

¹Institut de Physiologie, Université de Lausanne, Rue du Bugnon 7, Lausanne, Switzerland, ²Physiopathologie et Thérapie des déficits sensoriels et moteurs, Université de Montpellier I, INSERM U.583, 71 rue de Navacelles, Montpellier, France,

³Institut de Physiologie, Université de Lausanne, Rue du Bugnon 7, Lausanne, Switzerland, ⁴Physiopathologie et Thérapie des déficits sensoriels et moteurs, Université Montpellier I, INSERM U.583, 71 rue de Navacelles, Montpellier, France

Auditory hair cells of the vertebrate inner ear are the mechanosensors that detect sound.

The defining feature of hair cells is the cellular projection located at the apical surface of the cells named stereocilia, which constitute the organelle of mechano-electrical transduction.

The prescribed spatial organization of the stereociliary bundles is very important for the normal transduction of acoustical signal. Despite the substantial progress recently made in defining the molecules that regulate hair cells differentiation, the molecular mechanisms involved in stereocilia morphogenesis, differentiation and polarization is still largely unknown.

RhoGTPases are molecular switches that control a wide variety of signal transduction pathway in different cell types. They are known principally for their pivotal role in regulating the actin cytoskeleton and their ability to influence cell polarity, but their specific functions in hair cells is still unclear.

Our preliminary expression study revealed that the three prototypes representative of Rho GTPase family (RhoA, Rac, Cdc42) are expressed within the auditory sensory epithelium with differential and overlapping patterns during the mouse cochlea morphogenesis.

We evaluated their functional implication by RNA interference technology (siRNA) in a model of organotypic cultures of the mouse cochlea. Preliminary results using RNA-mediated interference of RhoA, Rac1, and Cdc42 indicate that RhoA is essential for stereociliary bundles morphogenesis.

782 Unidirectional Extension Contributes to the Precise Patterning of the Sensory Arrays in the Cochlea

Xi Lin¹, Xiankui Li¹, Andres Collazo¹, Jane E Johnson², Neil Segil¹, Ping Chen¹

¹Cell and Molecular Biology, House Ear Institute, 2100 W. 3rd St., Los Angeles, CA, United States, ²Center for Basic Neuroscience, University of Texas Southwestern Medical Center, 5323 Harry Hines Blvd., Dallas, TX, United States

Polarized cell movements of convergent extension shape the vertebrate body plan and are essential for the establishment of germ layers, formation of body axes, and neurogenesis. The mammalian auditory organ, the organ of Corti, is suspended within the spiral-shaped tubular cochlea and consists of precisely arrayed sensory hair cells separated by supporting cells. The formation of this sensory mosaic involves synchronized cell cycle exit of precursors and subsequent differentiation of hair cells and supporting cells within the postmitotic sensory primordium. An important question is how the terminal differentiation of the organ of Corti is coupled to the patterning of the highly stereotyped sensory arrays as the organ grows in length. Collectively, it has been shown that the developing organ of Corti elongates and becomes thinner independent of cell proliferation (Ruben, 1967) or death (Chen et al., 2002), suggesting the involvement of cell rearrangement (Chen et al., 2002). Using an organ culture system, we demonstrated that the developing organ of Corti undergoes unidirectional extension critical for the precise patterning of the sensory hair cells independent of cell proliferation, similar to the growth of the sensory organ in vivo. Disruption of the unidirectional extension resulted in the formation of a disorganized sensory organ. Together, these data strongly support the idea that the polarized cell movements, likely through convergent extension, play an important role in coupling the terminal differentiation of hair cells and supporting cells with the patterning of the precise sensory arrays in the cochlea.

783 Morphologic characteristics of regenerated hair cells in chick sensory epithelial cultures: Effects of 3-dimensional growth conditions

Gi Soo Lee¹, Jialin Shang¹, Sam Han², Jennifer Stone¹

¹Oto-HNS and VM Bloedel Hearing Research Center, University of Washington, Pacific Avenue, Seattle, WA, United States,

²Neuroscience Program, University of Washington, Pacific Avenue, Seattle, WA, United States

Sensory epithelial (SE) hair cell regeneration occurs in non-mammalian vertebrates including birds, fish, reptiles and amphibia. Our lab uses a chick model system to study hair cell (HC) regeneration and differentiation in order to elucidate underlying mechanisms employed by birds. When subcultured from primary explants onto plastic or glass substrate coated with matrix proteins, some SE support cells divide and spontaneously differentiate into immature HCs as indicated by the simultaneous presence of cytoplasmic early-onset HC markers Myosin VI or TuJ1 and nuclear BrdU. However, the morphology of these young HCs is unlike that of new HCs seen in intact basilar papillae and utricles. Instead of prototypically thin, elongated cell bodies that suggest basal-to-

luminal polarity, cultured HCs appear stellate, with large cytoplasmic areas and no indication of polarity. Since SE are normally organized in distinct cellular layers with specific polarity, we attempted to mimic this 3-dimensional growth condition using Matrigel suspensions, mixed SE-stromal cultures, and co-cultures with SE cells plated on porous membranes suspended over stromal feeder layers. Preliminary results from immunolabeling techniques have revealed new HCs with thin cell bodies, processes at one or both ends, and directional orientation in all three conditions. In co-culture and mixed-culture systems, new HCs are located on top of either stromal cells or support cells, with cell bodies oriented vertically. In Matrigel, spheres of SE cells contain new HCs with elongated processes. These morphologic characteristics suggest that 3-dimensional growth promotes the development of polarity in regenerated HCs. Studies are currently underway to test for expression of later-onset HC genes to classify the morphologic types seen, and to quantify whether chosen conditions enhance the numbers of new HCs identified.

Support was provided by grants from NIDCD (DC03696, DC04661), NOHR, and UW-RRF.

784 Identification of a key regulator, the retinoblastoma gene (Rb), in hair cell development

Cyrille Sage¹, MingQian Huang¹, Kambiz Karimi², Duan-Sun Zhang³, Gabriel Gutierrez², Philip Hinds⁴, Jeff Corwin², David Corey³, Zheng-Yi Chen¹

¹Neurology, Massachusetts General Hospital and Harvard Medical School, Wellman 425, 55 Fruit St., Boston, ma, United States, ²Otolaryngology, University of Virginia School of Medicine, HSC Box 801392, MR-4 Building, Rm 5148, Charlottesville, VA, United States, ³Neurobiology, Howard Hughes Medical Institute, Harvard Medical School, 200 Longwood Ave, Boston, ma, United States, ⁴Pathology, Harvard Medical School, 200 Longwood Ave, Boston, ma, United States

To understand gene interactions regulating hair-cell development, we have used Affymetrix GeneChips to assess global gene expression profiles in the developing mouse utricle. Utricles were microdissected at E14, E15, E17, P0, P2, P6 and P12, and amplified RNA was hybridized to the mouse 6.5K chip sets. We found that, among many developmentally regulated genes, members of the retinoblastoma (Rb) gene family were closely associated with proliferation and differentiation of the utricle. While Rb is well known as a tumor suppressor gene, the family consists of three members (encoding the proteins pRb, p107 and Rb2/p130) more broadly involved in processes such as suppression of proliferation, induction of differentiation, tumorigenesis and protection against apoptosis.

Immunohistochemical labeling showed that Rb is present in the E12.5 otocyst. Later in embryonic development, Rb displayed prominent hair cell expression and moderate expression in supporting cells. Rb conditional knockout mice were generated by crossing mice with loxP sites flanking the Rb gene and mice with cre recombinase under the control of the collagen 1A1 promoter, which deletes Rb in the inner ear. Because these mice were perinatal lethal, we studied late embryonic inner ears. Rb was absent from both hair cells and supporting cells in Rb^{-/-} mice.

Labeling for actin and hair-cell markers revealed ~40% more hair cell bundles in utricles of Rb^{-/-} mice, and as many as 4 layers of hair cells, not all expressing bundles. Cochleas of E18.5 Rb^{-/-} mice had a striking increase in the number of hair cells, with as many as 3 rows of inner hair cells and 8 rows of outer hair cells. PCNA and hair-cell-marker double labeling showed that virtually all the hair cells were in cell division. Labeling for different hair cell markers showed that the newly derived hair cells were largely differentiated. In addition, cochlear supporting cells were also in cell division in the E18.5 Rb^{-/-} mice. Additional labeling suggested that supporting cells were induced to become hair cells in the Rb^{-/-} mice. We have therefore identified Rb as a key regulator in hair cell development.

785 BMP-Signalling is Required for Hair Cell Generation in the Chicken Ear

Huawei Li, Hong Liu, Carleton Eduardo Corrales, Hideki Mutai, Stefan Heller

EPL - Dept. of Otolaryngology, Mass Eye & Ear Infirmary / Harvard Medical School, EPL - MEEI, 243 Charles Street, Boston, MA, United States

Bone morphogenetic proteins (BMPs) belong to the transforming growth factor (TGF)-beta superfamily. BMP4, BMP5, and BMP7 are expressed in the early chicken and mouse ear, implicating BMPs in controlling cellular and morphogenetical development. Within the developing prospective sensory epithelia BMP4 is robustly expressed, which spurred our interest in addressing the roles of this factor during genesis of inner ear sensory epithelia. However, elucidation of the role of BMP4 in sensory epithelia development is hampered by the fact that BMP4 null mutant mice are lethal at early embryonic stages. A better understanding of the role of this factor during inner ear sensory epithelia formation therefore requires a suitable model system. Toward this goal, we made use of an organotypic culture of the otic vesicle in serum-free medium in which the BMP concentration can be controlled either by adding exogenous BMP4 or by blocking the action of BMPs with the soluble protein, Noggin. In control cultures, we are able to identify hair cells (by co-expression of HCA and myosin VIIa) at the third day in vitro. After 11-14 days, hair cells had developed F-actin-rich hair bundles that co-labeled with antibodies to HCA and espin. Noggin application to otic vesicle cultures significantly suppressed the formation of hair cells. We analyzed changes in the hair cell and neuronal cell populations in response to ectopic BMP4 and Noggin application using quantitative evaluation of cell proliferation and apoptosis. We propose that BMP(4)-signaling is required for hair cell generation during sensory epithelia development.

786 Genes regulated by GATA3 in the mouse cochlea

Marta Milo¹, Zheng-Yi Chen², M Huang², Grace Lawoko-Kerali¹, Marcelo Rivolta¹, **Matthew Holley¹**

¹Biomedical Sciences, University of Sheffield, Western Bank, Sheffield, United Kingdom, ²Department of Neurology, Harvard Medical School, Wellman 425, 50 Fruit Street, Boston, MA 02114, United States

The transcription factor GATA3 is essential for normal inner ear

development and haplo-insufficiency leads to hearing loss in both man and mouse. Studies with null mice suggest that GATA3 regulates genes associated with innervation. To identify genes regulated by GATA3 in the inner ear we studied gene expression profiles in two experiments with conditionally immortal cell lines. First, we studied synexpression groups of genes in UB/OC-1, a cell line derived from the cochlear duct at E13.5. Cells were cultured for 14 days under differentiating conditions and total RNA was analyzed daily with Affymetrix Mu11k oligonucleotide arrays. Second, we knocked down GATA3 in US/VOT-33, a cell line derived from the ventral otocyst at E10.5 and selected for expression of GATA3 and β -tubulin but not cytokeratin, a profile consistent with that of migrating spiral ganglion neurons. Antisense 21-mer phosphorothioate oligonucleotides were designed against GATA3 and complimentary sense sequence was used as a control. Cultured cells were transiently transfected using Lipofectamine/Plus Reagent for 24-72 hours under differentiating conditions. Total RNA was analyzed with the Affymetrix mouse expression set 430A. In UB/OC-1 the GATA3 expression profile increased to day 9 and then decreased to day 14. The synexpression group included 3 semaphorin genes and 3 others related to ephrin signalling. Synexpression groups are relevant in terms of haploinsufficiency because they can reflect dosage dependence within a group and participation in the same functional pathway. In US/VOT-33 over 200 genes were influenced by the decrease in GATA3 levels. One of the largest changes was a decrease in expression of Neuropilin 1, which is a receptor for semaphorins and specific isoforms of vascular endothelial growth factor. The results suggest that GATA3 regulates complementary receptors and ligands associated with neural guidance in different cell types during inner ear development.

787 Differential gene expression in the avian utricle sensory epithelium following damage by neomycin or laser ablation

R. David Hawkins¹, Stavros Bashiardes¹, Mark E. Warchol², Michael Lovett¹

¹Genetics, Washington University School of Medicine, 4559 Scott Ave, St. Louis, MO, United States, ²Otolaryngology, Washington University School of Medicine, 4560 Clayton Rd, St. Louis, MO, United States

The inability of cochlear hair cells to regenerate is a major cause of presbycusis, or age related hearing loss, which affects one-third of people over the age of 50. While the mammalian cochlea cannot regenerate hair cells, the avian inner ear has a remarkable ability for sensory regeneration. The specific networks of gene expression that are activated during regeneration are not known. In the present study, we examine gene expression in the avian ear during regeneration after two different types of tissue injury. In one set of experiments, cultured utricles were treated with neomycin for 24 hrs and then allowed to recover for 0 hrs, 24 hrs, and 48hrs. In other experiments, a laser microbeam was used to create linear 'wounds' in cultured sensory epithelia from the utricle. These specimens were then allowed to recover for 30 min, 1hr, 2hrs, and 3hrs. At each recovery time, cells were harvested for expression profiling, along with unlesioned time-matched controls. A micro-cDNA amplification method was used to generate enough target for profiling. Time point samples were profiled on custom oligonucleotide

arrays that contained approximately 1700 human transcription factors. Greater than 10 percent of these transcriptional regulators clustered into various trends of differential expression at the various recovery times. Common bursts of transcription at 24 hrs (in neomycin-treated specimens) and at 1 and 3 hrs (in laser lesioned specimens) were observed. Additionally, we observed commonalities and differences with regenerating avian cochlea sensory epithelia (see additional abstract by this group). Changes in the expression of CEBPG, HOXA13, ID1, and RORC appear to correlate with the onset of regeneration. Identification of key transcriptional regulators will provide insight into the genetic pathways necessary for hair cell regeneration in the avian ear and may also reveal the basis for the limitations on regeneration in the ears of mammals.

788 Purified Post-natal Mammalian Cochlear Supporting Cells Divide and Generate Sensory Hair Cells in Culture

Patricia M. White¹, Angelika Doetzlhofer¹, Yun-Shain Lee¹, Neil Segil^{1,2}, Andy Groves^{1,2}

¹Gonda Dept. of Cell and Molecular Biology, House Ear Institute, 2100 West Third St., Los Angeles, CA, United States, ²Dept. of Cell and Neurobiology, University of Southern California, Exposition Blvd., Los Angeles, CA, United States

Mammalian cochlear supporting cells do not re-enter the cell cycle *in vivo* when sensory hair cells are lost; nor do they regenerate functional sensory hair cells after damage. Here we purify supporting cells from mouse pups, using a transgenic line that expresses green fluorescent protein in supporting cells together with fluorescent activated cell sorting. We show that significant numbers of these purified supporting cells re-enter the cell cycle within 48 hours of being placed in cell culture, as assessed by BrdU incorporation. Moreover, some of the supporting cells that have incorporated BrdU in culture go on to express hair cell markers such as Myosin-VIIa and Myosin-VI. These results indicate that at least some post-natal mammalian cochlear supporting cells possess the ability to divide and generate sensory hair cells.

789 Time-lapse investigation of *in situ* repair in mammalian hair cell epithelia: Changes in spreading and proliferation over the first 2 postnatal weeks

Jason R Meyers, Jeffrey T Corwin

Otolaryngology, University of Virginia, MR4 Rm 5148 — Lane Road Extd, Charlottesville, VA, United States

Following loss of hair cells, avian supporting cells spread, fill the space previously occupied by the lost cells, and begin to proliferate. *In vitro* evidence is consistent with the hypothesis that spreading of avian supporting cells leads to proliferation (Warchol et al., 2002), so we tested whether inducing spreading might lead to proliferation in mammalian hair cell epithelia. We found that spreading of sensory epithelia delaminated from E18 mouse utricles was dependent on physical properties of the matrix. They spread when plated on a thin coating of Matrigel, but not on a thick coating of Matrigel. Proliferation followed the pattern of spreading: BrdU labeled nuclei were found throughout the epithelium on thin Matrigel, while few were labeled in the sensory epithelium on

thick Matrigel, though many cells labeled in the adjacent non-sensory epithelium. Time-lapse experiments examined whether spreading followed surgical wounding in E18 sensory epithelia *in situ*. Circular wounds (150 μ m) closed in 17 \pm 1.5 hours as supporting cells expanded, and the spread cells at the wound site re-entered the cell cycle. Thus, in delaminated epithelia and in wounded utricles from embryonic mice, spread supporting cells re-enter the cell cycle, while unspread cells rarely did.

Studies *in vitro* (Gu et al., 1997) have shown that rat epithelia lose proliferative responsiveness during the first two postnatal weeks. Therefore, we also examined spreading and proliferation in P15 utricles. On thin Matrigel, P15 sensory epithelia showed no spreading or proliferation. Circular wounds (150 μ m) made in P15 utricles remained open for at least 48 hours. Thus, spreading of delaminated mammalian supporting cells and their expansion into wounds *in situ* changes in the first 2 postnatal weeks. The loss of cell spreading suggests a possible explanation for the limited regeneration in the mature mammalian inner ear, and these data show that methods that induce cell spreading can promote proliferation.

790 ERM proteins are directly involved in the formation of stereocilia in a complicated redundant manner

Shin-ichiro Kitajiri^{1,2}, Kanehisa Fukumoto², Shojiro Kikuchi², Masaki Hata³, Takayuki Nakagawa¹, Tae Soo Kim¹, Hiroyuki Sasaki⁴, Juichi Ito¹, Sachiko Tsukita⁵, Shoichiro Tsukita²

¹Otolaryngology-Head and Neck Surgery, Kyoto University Graduate School of Medicine, Shogoin Kawaharatyo 54, Kyoto, Japan, ²Cell Biology, Kyoto University Graduate School of Medicine, Sakyo-ku, Kyoto, Japan, ³KAN Research Institute, Kyoto Research Park, Shimogyo-ku, Kyoto, Japan, ⁴Molecular Cell Biology, The Jikei University School of Medicine, Nishi-Shinbashi, Minato-ku, Tokyo, Japan, ⁵College of Medical Technology, Kyoto University, Sakyo-ku, Kyoto, Japan

Ezrin/radixin/moesin (ERM) proteins crosslink actin filaments to plasma membranes and are involved in the organization of the cortical cytoskeleton, especially in the formation of microvilli. As stereocilia are specifically developed microvilli, we examined whether ERM proteins are involved in their formation.

Immuno-staining of both young (6-day old) and adult wild-type mice showed that radixin was exclusively concentrated at stereocilia. Interestingly, ABR revealed that Rad^{-/-} mice exhibit profound deafness. In the cochlea of young Rad^{-/-} mice, the stereocilia developed normally, in which ezrin was concentrated instead of radixin, but as these mice grew up, these ezrin-based stereocilia were progressively degenerated. Similarly, radixin was also highly concentrated in the stereocilia in the vestibule of wild-type mice. In the vestibule of adult Rad^{-/-}, the ezrin-based stereocilia developed and were maintained normally, showing no degeneration and normal vestibulo-ocular reflex (VOR). These findings indicated that ERM proteins are directly involved in the formation of stereocilia in a complicated redundant manner, and that radixin is an indispensable gene for hearing through the maintenance of the stereocilia of cochlea hair cells.

Furthermore, we found that in the cochlea injured by neomycin,

ERM proteins completely disappeared from the cochlea stereocilia prior to their degeneration. Aminoglycosides specifically bind to phosphatidylinositol 4,5-bisphosphate (PIP₂), which binds to and activates ERM proteins, i.e. to enhance their ability to cross-link actin filaments to membrane proteins. Therefore, it was speculated that aminoglycosides are accumulated in hair cells to sequester PIP₂, resulting in a decrease in the amount of activated ERM proteins. Then, similarly to Rad^{-/-} mice, the stereocilia would be destroyed.

791 Localization of Myosin XVa in Stereocilia and Staircase Formation of the Hair Bundles

Inna A. Belyantseva, Erich T. Boger, Thomas B. Friedman

Lab. of Molecular Genetics, NIDCD/NIH, 5 Research Court, Rockville, MD, United States

Sensorineural deafness in humans (*DFNB3*) and shaker 2 (*Myo15^{sh2}*) mice (Friedman et al., 1995; Wang et al., 1998; Probst et al., 1998) are due to mutations of the gene encoding unconventional myosin XVa. In deaf *Myo15^{sh2/sh2}* mice, stereocilia are short, nearly equal in length and lack myosin XVa immunoreactivity. We also reported that myosin XVa mRNA and protein are expressed in cochlear hair cells (Liang et al. 1998; Anderson et al., 2000). Using two different anti-myosin XVa tail domain specific antibodies and high resolution fluorescence imaging, we now show that in the mouse, rat and guinea pig, endogenous myosin XVa is localized to the tips of the stereocilia of the cochlear and vestibular hair cells. Myosin XVa localization overlaps with the barbed ends of actin filaments and extends to the apical plasma membrane of the stereocilia. Using RT-PCR we detected two major isoforms of *Myo15a* (with [+N] and without [-N] exon 2) in the mouse inner ear. Gene gun mediated transfection of mouse inner ear sensory epithelia explants using [-N] *Myo15a*-GFP shows selective accumulation of myosin XVa-GFP at the tips of stereocilia, confirming the localization of native myosin XVa. At 96 hours after transfection, excessive accumulation of myosin XVa-GFP causes a bulbous appearance of the tips of stereocilia. These data also suggest that the N-terminus extension of myosin XVa encoded by exon 2 is not necessary for the targeting of myosin XVa to the tips of stereocilia. Transfection of COS7 cells also reveals myosin XVa-GFP at the dynamic actin region of the filopodia tips. In a wild type mouse, during embryonic development, myosin XVa was detected at the tips of stereocilia as early as E14.5 in vestibular and E18.5 in cochlear hair cells. This is the time when hair bundles begin to develop their characteristic staircase pattern. We propose that myosin XVa is essential for the graded elongation of cochlear and vestibular hair cell stereocilia during their functional maturation.

792 Three-Dimensional Structure of the Mechano-electrical Transduction and Adaptation Apparatus Obtained by Electron Tomography

Manfred Auer¹, Bram Koster², Ulrike Ziese², Chandrajit Bajaj³, Niels Volkmann⁴, Da Neng Wang⁵, A. J. Hudspeth¹

¹Laboratory of Sensory Neuroscience, The Rockefeller University, 1230 York Avenue, New York, NY, United States, ²Molecular Cell Biology, Utrecht University, Padualaan 8, Utrecht, Netherlands, ³Computer Sciences Dept and ICES, University of Texas at Austin, 24th and Speedway, Austin, TX, United States, ⁴Bioinformatics and Systems Biology, The Burnham Institute, North Torrey Pine Road, La Jolla, CA, United States, ⁵Skirball Institute, New York University Medical Center, 540 First Avenue, New York, NY, United States

Employing electron-microscopic tomography, we have examined the three-dimensional structure of the mechano-electrical transduction and adaptation machinery of the stereocilia in bullfrog saccular hair cells. Unlike other structural techniques, tomography can visualize macromolecular assemblies in their natural cellular context, for it does not rely on averaging the images of a large number of identical objects. Because the apparatus of mechano-electrical transduction is too rare and too fragile for biochemical isolation, electron tomography is the most appropriate structural tool to study its architecture. Conventional electron-microscopic imaging projects a three-dimensional volume onto the two-dimensional plane of an imaging device such that information about the object along the electron beam is superimposed. Tomographic imaging can retrieve this information by capturing a series of images of the same object at different tilt angles. The different views of the projected volume are combined and projected back into a volume that represents the mass density.

Through careful sample preparation, tomographic imaging, and image analysis, we have begun to determine the three-dimensional structure of the transduction apparatus at sufficient resolution to allow the fitting of atomic models to the data. We have focused our attention on the tip link connecting adjacent stereocilia, its insertion into the stereociliary membrane, and the adaptation motor that connects the tip link to the actin cytoskeleton. Based on our tomographic data, we can propose candidate proteins for the tip link and its insertion site. In the insertional plaque, we observe regularly spaced densities that are consistent in size and shape with being myosin molecules. We are currently analyzing these data using model fitting as well as skeletonization tools in order to retrieve quantitative information on the architecture of this fascinating molecular machinery.

793 Microvilli and stereocilia overgrowth in espin overexpressing cells in inner ear sensory epithelia

Agnieszka Katarzyna Rzadzinska¹, Mark Edward Schneider¹, James Richard Bartles², Bechara Kachar³

¹NIDCD, NIH, 9000 Rockville pike, Bethesda, Maryland, United States, ²Dept Cell/Molec Biol, Northwestern Univ Med Sch, 303 E Chicago Ave, Chicago, IL, United States, ³NIDCD, NIH, 9000 Rockville Pike, Bethesda, Maryland, United States

Hair cell stereocilia in the inner ear arise from microvilli through actin filaments elongation and their addition to the side of microvillus actin core. Parallel, cross-linked and uniformly polarized actin filaments support the microvilli and stereocilia. Whereas the microvillus' ~20 actin filaments are loosely cross-linked by espin, fimbrin and villin, the stereocilium's approximately 200 actin filaments are tightly cross-linked by fimbrin and espin, forming a paracrystal-like structure. Recent studies showed that supporting cells in the inner ear transfected with the transcription factor Math 1 (Kawamoto et al., 2003) or Hath 1 (Shou et al., 2003) develop stereocilia-like bundles and become innervated, however, it remains unclear what genes are upregulated by these trans-acting factors. Here we tested the hypothesis that overexpression of one potential target genes, espin, could induce microvilli growth and the subsequent stereocilia-like appearance in transfected supporting cells in the inner ear. We also analyzed here the effect of espin overexpression on hair cell stereocilia length and hair bundle organization. We expressed small espin-GFP in the inner ear hair and supporting cells and analyzed their apical surface 24 hours after transfection. We found that microvilli as well as stereocilia of transfected hair cells are substantially longer than their non-transfected neighbors. The majority of espin transfected supporting cells exhibit significantly longer microvilli than their non-transfected neighbors and in some cells even form bundles. Our studies suggest that espin expression level determine microvilli and stereocilia length.

794 Dynamic regulation of stereocilia structure and renewal

Agnieszka K Rzadzinska, Mark E Schneider, Caroline Davies, Bechara Kachar

NIDCD, NIH, 9000 Rockville Pike, Bethesda, Maryland, United States

Hair cell stereocilia are mechanosensitive organelles that detect nanometer scale displacements. Each stereocilium is supported by a rigid paracrystalline array of parallel, uniformly polarized and cross-linked actin filaments. Previously we showed that actin filaments in auditory hair cell stereocilia are turned over within 48 hours (Schneider et al. 2002). In the present study, we now used the same approach of transfecting cultured hair cells with beta actin-GFP to shed light on the mechanism of renewal. We have made several new observations consistent with an actin treadmill model for renewal: 1) beta actin-GFP incorporation occurred as a wave with a sharp leading front indicating that actin filaments are simultaneously elongated at stereocilia tips; 2) stereocilia length was maintained during renewal; 3) attenuation of beta actin-GFP expression caused an incorporation pulse with a sharp leading front and an attenuated trailing edge due to the chase by non-fluo-

rescent actin. Most importantly, we observed that the measured rate of the actin treadmill was proportional to the stereocilia length and that stereocilia lengths are dynamically modulated within the hair bundle. In addition we investigated the immunolocalization of three unconventional myosins, VI, VIIa, and XVa. Mutations in these proteins have been associated with deafness involving very short or disrupted stereocilia. We observed that myosin XVa caps each stereocilium and its expression levels are correlated with stereocilium length. We also confirmed that myosin VIIa is localized in the interface between the actin paracrystal and plasma membrane and could mediate a retrograde flow of the actin core. We propose that myosin XVa and other myosins contribute to self-renewal and dynamic maintenance of the stereocilia. This dynamic view provides new insight into the self-adjusting sensitivity of the hair cell transduction machinery as well as recovery of stereocilia from over-stimulation.

795 Characterizing the pore of the mechanotransducer channel in turtle auditory hair cells.

H. E. Farris, J. Goswami, A. J. Ricci

Neuroscience Center and Kresge Hearing Labs, LSU Health Science Center, 2020 Gravier St., New Orleans, LA, United States

Mechanically-gated (met) channels, located near the top of hair cell stereocilia play a pivotal role in auditory and vestibular signal detection. Surprisingly few data exist, however, regarding the molecular nature of this channel. Present work characterizes the met channel pore, a region whose properties are hypothesized to be intrinsically determined. The width of the channel was estimated by measuring the relative current amplitude when the external monovalent ions were replaced by simple amine compounds of increasing molecular weight. Plotting molecular weight against relative permeability (I_x/I_{Na}) resulted in an exponential relationship that supports the conclusion that the channel could be treated as a molecular sieve, where permeability was being dictated by molecular size and not for example by binding within the pore. A plot of molecular radii against relative permeability could best be fit by the equation $P_x/P_{Na} = (A*(1-a/r)^2)/a$ where A is a scaling factor, r is the radius of the pore and a is the radius of the amine (Adams et al., 1980). From this a pore diameter of $12.5 \pm 0.5 \text{ \AA}$ was obtained. Knowing the pore diameter and single channel conductance allows for an estimate of channel length. Using a single channel conductance of 300pS (Ricci, Crawford and Fettiplace, submitted) gave a pore length of 41 \AA . This measurement indicates a long pore that can have multiple ion occupancy as previously suggested by Lumpkin et al. (1997). The data demonstrate that the channel pore can be treated with classical approaches. The dimensions are large compared to known nonspecific cation channels like cng channels or nicotinic channels but smaller than other mechanically gated channels. These dimensions support recent pharmacological manipulations that suggest open channel block by charged amine compounds.

Supported by DC03896 from NIDCD to AJR and the Tinnitus Association.

796 Fast adaptation and hair bundle movements in mammalian cochlear hair cells

Helen Kennedy¹, Andrew Crawford², Robert Fettiplace¹

¹Department of Physiology, University of Wisconsin, 185 Medical Sciences Building, 1300 University Avenue, Madison, Wisconsin, United States, ²Department of Physiology, University of Cambridge, Downing Street, Cambridge, United Kingdom

The properties of the mechanotransducer channels have been extensively studied in hair cells of lower vertebrates where at least two types of calcium-dependent adaptation have been documented including a fast process on a millisecond time scale. Adaptation resets the operating range of the channel for a mechanical input and can in turn elicit a mechanical response capable of actively moving the hair bundle and amplifying the extrinsic stimulus. Although such adaptation has been seen in mammalian auditory hair cells, less is known about its attributes and mechanical consequences especially in hearing animals. We have recorded mechanotransducer currents in outer hair cells of rats between postnatal days 5 and 18 before and after the onset of hearing. Hair cells in the apical turn of the acutely isolated cochlea were whole-cell voltage clamped and hair bundles were deflected by axial motion of a glass rod driven by a piezoelectric stack actuator. Transducer currents possessed a fast calcium-sensitive adaptation resembling that in turtle hair cells. However the time constants were briefer, sometimes less than 0.1 ms at room temperature. Also like turtle hair cells, outer cells displayed fast, 10 to 50 nm, movements of the hair bundle towards its taller edge evoked by depolarizing voltage steps. Motion of free-standing hair bundles was detected by imaging on a dual photodiode mounted on a piezoelectric bar for calibration purposes. The bundle motion was abolished by dihydrostreptomycin at a concentration (0.2 mM) that also blocked the transducer channels. We conclude that fast adaptation in outer hair cells functions on a time scale appropriate for cycle-by-cycle regulation at the hair cell characteristic frequency, and we suggest it is linked to active motion of the hair bundle that may contribute to the cochlear amplifier.

Supported by NIH grant RO1-DC01362 to RF

797 Functional Maturation of Type I and Type II Hair Cells in the Embryonic Mouse Utricle

Gwenaëlle S.G. Géléoc, Jessica R. Risner, Jeffrey R. Holt

Neuroscience & Otolaryngology, University of Virginia, Lane Rd., MR4, Rm 5127, Charlottesville, VA, United States

To investigate the acquisition of voltage-dependent conductances in hair cells we excised utricles from mouse embryos between day 14 (E14) and E19. We used the whole-cell, tight-seal technique in voltage-clamp mode to record voltage-dependent currents and in current-clamp mode to record the membrane response to step and sinewave currents. Beginning as early as E14, depolarization evoked outward currents that reversed at -71 mV ($n=18$) similar to those carried by the delayed rectifier conductance of postnatal type II cells (Rüsch et al., *J. Neurosci.* 1998). The amplitude of the delayed rectifier conductance increased steadily as a function of developmental age from 3.9 ± 2.8 nS ($n=6$) at E15 to 15.2 ± 4.2 nS

($n=25$) at E18. Activation curves were fit with Boltzmann functions that had a mean $V_{1/2}$ of -23.9 ± 3.2 mV and a slope of 6.2 ± 1.8 mV ($n=53$). Interestingly, a second potassium conductance which was active at rest appeared in a subset of cells beginning as early as E18. The conductance was deactivated by steps to -124 mV and activated with subsequent depolarization, consistent with the low-voltage activated conductance, $g_{K,L}$, characteristic of postnatal type I hair cells. Boltzmann fits revealed a whole cell conductance of 30.6 ± 5.6 nS, a $V_{1/2}$ of -61.8 ± 7.8 mV and a slope of 6.1 ± 0.8 mV ($n=8$). We noted a strong correlation between type I morphological characteristics such as a constricted neck region and partial calyces and the presence of the $g_{K,L}$ -like conductance. In current-clamp we found that cells that expressed $g_{K,L}$ had a more negative resting potential -75.4 ± 5.4 mV ($n=4$) than those that did not -47.3 ± 13.8 mV ($n=11$, E18 to E19). Similarly, current injections evoked only small membrane depolarizations (<10 mV) in the cells that expressed $g_{K,L}$ whereas the cells that lacked $g_{K,L}$ responded with large depolarizations (>20 mV). These data suggest that the functional maturation of type I and type II hair cells in the mouse utricle begins a few days before birth.

Supported by NIDCD grants to GSGG (DC006183) and JRH (DC05439)

798 Simultaneous Recordings of Basilar Membrane Motion and Outer Hair Cell Mechano-Electrical Transducer Currents

David ZZ He, Shuping Jia

Dept. of Biomedical Sciences, Creighton University, 2500 California Plaza, Omaha, NE, United States

Transducer currents have been recorded from culture preparations (Kros et al., 1992), and from the excised segments of sensory epithelium (Hudspeth and Corey, 1977; Corey and Hudspeth, 1983; Kennedy et al., 2003) by deflecting the hair bundle with either a fluid jet or a glass fiber. We attempted to record transducer currents (or receptor potentials) from a relatively intact and more in vivo like preparation, the gerbil hemicochlea (Hu et al., 1996; Richter et al., 1998). The preparation has several advantages for the study of mechano-electrical transduction of adult cochlear hair cells. Such preparation permits us to record simultaneously the transducer current and the motion of the basilar membrane. Furthermore, the OHC hair bundle in the hemicochlea is deflected by the displacement of the tectorial membrane relative to the reticular lamina, the same way that the hair bundle is stimulated in vivo. Whole-cell patch-clamp technique was used to record transducer currents. The mechanical stimulus was coupled through the fluids to the basilar membrane using a glass paddle moving at 100 Hz. Basilar membrane motion was measured by a photodiode-based measurement system mounted on an upright microscope. From apical turn OHCs, we recorded a receptor current of ~ 220 pA (peak-to-peak) for a basilar membrane motion amplitude of 300 nm. The receptor potential was 5 mV peak-to-peak. When the cell was held at -140 mV, the current was about 400 pA with a receptor potential of 10 mV. The receptor current from middle turn OHCs was over 300 pA for a basilar membrane motion amplitude of less than 150 nm. Supported by NIH grants R21 DC 06039 and R01 DC 04696 from the NIDCD.

799 Assessment of Hair-Cell Transducer Function in Prestin Knockout Mice

Mary Ann Cheatham¹, Kristin Huynh¹, Roxanne Edge¹, Jiangang Gao², Jian Zuo², Peter Dallos¹

¹Communication Sciences and Disorders, Northwestern University, 2240 Campus Drive, Evanston, IL, United States,

²Developmental Neurobiology, St. Jude Children's Research Hospital, 332 N. Lauderdale St., Memphis, TN, United States

Measurement of cochlear potentials in mice lacking the outer hair cell (OHC) motor protein, prestin, indicates that both the cochlear microphonic (CM) and compound action potential are shifted in sensitivity. This result is consistent with a loss of amplifier gain, assuming that the basilar membrane-OHC-tectorial membrane complex is tightly coupled. Alternatively, it is also possible that a loss in transducer function, i.e., in forward transduction, could produce a similar effect by reducing the drive to individual motor elements. Experiments were, therefore, conducted to assess transducer function in wildtype (WT) mice and in homozygotes lacking prestin. In these experiments, cochlear potentials were recorded using a round window electrode in F4 generation mice (129/C57BL6) between 4 and 9 weeks of age. CM pseudotransducer functions were constructed by plotting peak positive and peak negative potentials as a function of peak pressure. By normalizing responses to the largest positive potential, the difference in sensitivity between WT and knockout (KO) mice was compensated. Results indicate that normalized pseudotransducer functions, measured in the youngest KO mice, were similar to functions obtained in WT controls. The transducer was also assayed by using AM1-43. This fluorescent styryl dye is taken up by hair cells through functional transducer channels via apical endocytosis. The dye was administered in vivo to pups at ~P13 or in vitro by exposing freshly dissected apical organ of Corti segments obtained from mice at ~7 weeks of age. In both cases, inner and outer hair cells were fluorescent. Taken together, the physiological and labeling experiments suggest that the hair cell transducer is functional in mice lacking prestin. These results are consistent with the idea that the reduction in the CM measured in KO mice is due to the absence of prestin and not to a change in transducer function. (Supported by NIH grants DC00089, DC04761, CA21765).

800 Structure – function studies of prestin, the OHC lateral membrane motor

Dhasakumar Navaratnam¹, Jun-Ping Bai², Haresha Samaranayake¹, Joseph Santos-Sacchi²

¹Neurology and Neurobiology, Yale University, 333 Cedar Street, New Haven, CT, United States, ²Otolaryngology and Neurobiology, Yale University, 333 Cedar Street, New Haven, CT, United States

Prestin, an integral membrane protein, has been identified as the outer hair cell motor that is thought to be responsible for the cochlea amplifier. A characteristic measure of this protein's activity is the voltage-dependent, non-linear capacitance (NLC) observed in cells expressing the protein. Using this measure (NLC) we and others had previously shown that the protein's voltage sensitivity was modulated by intracellular anions such as Cl⁻ (Oliver et al., 2001; Rybalchenko and Santos-Sacchi, 2003). We

had also shown that truncations in its extreme amino and carboxy termini resulted in a loss of NLC (Bai et al, ARO, 2003).

More detailed truncations of the N and C termini extend these previous observations and show a progressive reduction in NLC when prestin was truncated between residues 720 and 711. Similarly, initiating translation distal to amino acid 17 to 19 resulted in a progressive reduction NLC. Both these sets of mutations also variably affected V_{pkcm} . We were able to confirm adequate membrane targeting of these mutated forms of prestin by flow cytometry of live cells using antibodies to two peptides in the protein. Finally, we have also identified a sequence in prestin (GXXXP at the N terminal end of a helix) that when mutated results in a loss of NLC to voltage change in the presence of intracellular Cl⁻. This sequence is homologous to a highly conserved repetitive sequence in Cl⁻ channels that has been shown to form the Cl⁻ binding site by crystallography.

These results have several possible important implications. The progressive loss in NLC with truncations in the N and C termini suggest that prestin possibly interacts with other proteins. The variation in V_{pkcm} in the truncations of the protein suggests that the C and N termini affect the steady state energy profile of the protein. Our antibody staining results also question current models of prestin's membrane topology, and instead suggests a ten transmembrane protein with the first Tm domain starting at residue 94. Finally, since a single Cl⁻ channel requires several motifs with the sequence GXXXP to interact with Cl⁻ and since each molecule of prestin has one such motif, our results are indirect evidence for the formation of prestin multimers. (Supported by NIH NIDCD grant DC00273 to JSS and K08 DC05352-02 to DSN).

801 Isolated outer hair cells exhibit high frequency electrical resonance

Richard D Rabbitt¹, H.E. Ted Ayliffe¹, Sarah Clifford¹, William E Brownell²

¹Bioengineering, University of Utah, 20 South 2030 East, Room 506, Salt Lake City, UT, United States, ²Otorhinolaryngology and Communicative Sciences, Baylor College of Medicine, One Baylor Plaza, NA 102, Houston, TX, United States

Somatic electromotility of outer hair cells (OHCs) exhibits features of a piezoelectric material where the lateral wall enthalpy includes both electrical and mechanical terms. Piezoelectric theory indeed captures some of the salient features of electromotility in OHCs including Maxwell reciprocity. This same theory predicts the presence of ultrasonic resonances resulting from the interplay between kinetic energy of the vibrating mass and potential energy stored by mechanical elasticity and electrical polarization. We report here direct evidence of high-frequency electrical resonance in isolated OHCs consistent with the piezoelectric prediction. Data were obtained using cells isolated from the apical turn of the guinea pig cochlea. Individual cells were positioned in a custom micro-electro-mechanical system designed to apply apical-to-basal stimulating electric fields (1-100kHz, 1-16mV), and to record the voltage gradient along the length of the cell membrane. Cells isolated from the apical turn of the cochlea (~80 μ m length) exhibited an average fundamental resonance frequency of $f_n=11.2$ kHz (range: 7.8–15.7) and Q of 6.8 (range: 1.3–17.5). Higher-order ultrasonic resonances were also observed. Parameter estimation provided a piezoelectric coefficient of 2.8×10^{-15} C²/N²,

elastic plate compliance of $6.3 \times 10^{-5} \text{m}^2/\text{N}$ and a momentum thickness of $1.7 \mu\text{m}$ (fluid mass entrained by the moving membrane). Responses were not completely linear in that the admittance recorded using a secondary low-level 1MHz test stimulus was altered by the primary stimulus, particularly near resonance frequencies. Data also indicated a time delay between electrodes consistent with the hypothesis of a traveling wave moving from the apical end to the base of the cell. Data lead us to suggest three consequences regarding cochlear physiology. First, piezoelectric resonance may contribute to size-dependent tuning of individual hair cells. Second, the mass loading present in the cochlea could lower the fundamental resonance frequency relative to that reported here – perhaps to the range necessary for OHC resonance to directly contribute to the exquisite tuning of the cochlea. Third, higher-order ultrasonic resonances might be evoked by electrical stimulation of the cochlea (Supported by NIDCD DC-004928 and DC-00354).

802 Dynamic plasma membrane tethering force measurements of outer hair cells using optical tweezers under voltage-clamp conditions

Feng Qian¹, Sergey Ermilov¹, David Murdock¹, William Brownell², Bahman Anvari¹

¹Department of Bioengineering, Rice University, PO Box 1892, MS 142, Houston, TX, United States, ²The Bobby R. Alford Department of Otorhinolaryngology and Communicative Sciences, Baylor College of Medicine, One Baylor Plaza, NA102, Houston, TX, United States

The electromotility of the cochlear outer hair cells (OHCs) is essential to normal hearing. A piezoelectric-like mechanism associated with the plasma membrane and a membrane protein (prestin) converts transmembrane electrical potentials to mechanical energy. Cell membrane mechanical properties such as membrane-cytoskeleton detachment force, bilayer bending stiffness, and effective membrane viscosity have been studied by tether formation with micropipette aspiration, flow chamber, and optical tweezers. Among the tether formation methods, optical tweezers allow noninvasive manipulation of cells with high force resolution, and can continuously monitor dynamic tether force. To investigate the electromechanical properties of OHCs, we have integrated patch-clamp setup into an optical-tweezers system to pull plasma membrane tethers under whole-cell voltage-clamp condition. A trapped micron-size bead was brought in contact with the patched OHC membrane and subsequently moved away at a constant rate to form a plasma membrane tether. Bead displacement during tether elongation was monitored by a quadrant photodetector for dynamic measurements of the tether force. Additionally, while the tether length was in steady state, membrane potential was changed and the corresponding tether force response was measured. Forces were measured with gains that varied between $0.04 - 0.2 \text{pN/mV}$. We also compared the results from the OHCs with those obtained from wildtype human embryonic kidney (HEK) cells and prestin-transfected HEK cells.

This research is supported by grant DC02775 from NIDCD

803 The effect of mechanosensitive channels in the lateral wall on high- and moderate frequency receptor potentials of the outer hair cell

Alexander A. Spector¹, Aleksander S. Popel¹, Ruth Anne Eatock², William E. Brownell²

¹Biomedical Engineering, Johns Hopkins University, 720 Rutland Ave, Baltimore, MD, United States, ²Otolaryngology&Comm. Sci., Baylor College of Medicine, One Baylor Plaza, Houston, TX, United States

Cochlear outer hair cells convert transmembrane potentials into mechanical force at high frequencies (Dallos and Evans, 1995; Frank et al., 1999). However, the low-pass filtering associated with a conventional equivalent electric circuit of the cell challenges the functional significance of this ability. Typical values for the membrane resistance and capacitance result in a severe attenuation of the receptor potential with increasing frequency. In this study we have investigated the contribution of mechanosensitive channels to the outer hair cell's frequency response. Such channels have been observed in the outer hair cell lateral wall (Iwasa et al, 1991; Ding et al., 1991; Rybalchenko and Santos-Sacchi, 2003) and we have introduced the channels in an equivalent circuit both in the presence and absence of lateral wall piezoelectricity. If the channels are sensitive to the rate of the strain that results from the loading of outer hair cells *in vivo* the resulting modulation of ionic currents significantly affects the cell receptor potential. In particular, we found that the channels' effect strengthens the effect of the membrane piezoelectric properties (Spector et al., 2002, 2003; Weitzel et al., 2003). We show that even for quite conservative estimates of the parameters (density and conductance close to those reported in the outer hair cell lateral wall mechanosensitive channels, the channel speed about $100 \mu\text{s}$, the strain about 0.1%) the effect of the channels results in a 2-3 fold increase of the receptor potential. Greater effects can be achieved for channels as fast as mechanosensitive channels in the stereocilia (about $10 \mu\text{s}$). We have made the following conclusions regarding the relative effects of the electrical, piezoelectric, and mechanosensitive channel properties on the frequency dependence of the outer hair cell receptor potential. In the low frequency range, the potential is determined by the RC-properties; the effect of the channels becomes significant in the intermediate frequency range (between 5 and 15 kHz). This effect fades for high frequency where the piezoelectric properties become dominant. This research is supported by grants DC02775 and DC00354 from NIDCD (NIH).

804 Calcium-dependent contraction in hair cells of the amphibian papilla

Nasser A. Farahbakhsh¹, Peter M. Narins²

¹Physiological Science, UCLA, 621 Charles E. Young Drive, Los Angeles, CA, United States, ²Physiological Science, UCLA, 621 Charles Young Drive, Los Angeles, CA, United States

We have utilized the method of Holt *et al.* (Hear Res 152:25-42, 2001) to isolate the hair cells of both rostral and caudal segments of the amphibian papilla (AP) from the leopard frog, *Rana pipiens*. Our preliminary results suggest that increases in the concentration of the intracellular free calcium ($[\text{Ca}^{2+}]_i$), in the AP hair cells,

induce cell length shortening. These shortenings are composed of two phases: an initial iso-volumetric contraction (3-4%, in one minute or less), followed by a slower length decrease accompanied with swelling, suggesting movement of salt and water across the cell membrane in the latter case. These length changes are clearly $[Ca^{2+}]_i$ -mediated, because in the presence of the calcium ionophore, ionomycin, the rate of shortening is dependent on the extracellular Ca^{2+} concentration. These observations implicate the hair cells' $[Ca^{2+}]_i$ as a possible second messenger in the efferent-linked adaptive modulation of sensitivity and frequency selectivity in the amphibian papilla. The role of candidate efferent neurotransmitters in inducing changes in the hair cells' $[Ca^{2+}]_i$ is being investigated.

Supported by NIH grant no. DC-00222 to PMN.

805 Envelope Processing in the Auditory System: Spectral Decomposition or Temporal Periodicity Analysis?

Stephan D. Ewert, Torsten Dau

Centre for Applied Hearing Research, Technical University of Denmark, Oersted Plads, Building 352, Kgs. Lyngby, Denmark

Temporal envelope fluctuations play an important role in auditory communication and signal processing. Over the last years, the concept of bandpass modulation filters (MFs) has been shown to be a successful tool for describing a broad variety of modulation detection and masking data. Although a MF model can be treated, for simplicity, as a purely envelope-spectral model (envelope power spectrum model, EPSM) [e.g. Ewert and Dau., JASA 108 (2000)], the MF concept is not an envelope-spectral concept per se. In particular, within the perception model [Dau et al., JASA 102 (1997)], the (smoothed) temporal pattern at the output of modulation filters is used. The present study attempts to clarify if auditory envelope processing reflects a "true" spectral decomposition of arbitrary envelope waveforms, as would be expected from the MF concept. First, critical experiments are presented that allow for a distinction between a limited-resolution spectral decomposition or a temporal periodicity analysis based on autocorrelation. Modulation-detection thresholds were measured in the presence of a square-wave and sinusoidal masker that have the same temporal periodicity but different envelope-spectral content. Empirical data are in line with predictions obtained for the EPSM, taking into account the harmonics in the envelope spectrum caused by the square-wave masker. The empirical findings cannot be accounted for by an envelope autocorrelation model. Second, a possible limit of applicability for the EPSM is evaluated in modulation-masking configurations where the envelope-phase spectra of the masker differ, and in configurations that might promote the use of local temporal envelope features [Viemeister et al., ISH 13 (2003)]. Different decision variables are investigated based on either the envelope-power only or the temporal waveform at the output of the modulation filter.

806 Identifiability of Time-Reversed Environmental Sounds

Brian Gygi¹, Pierre L. Divenyi²

¹*Speech and Hearing Research, East Bay Institute for Research and Education, 150 Muir Road, Martinez, CA, United States,*

²*Speech and Hearing Research, VANCHS, 150 Muir Road, Martinez, CA, United States*

Some recent studies have suggested that humans have good comprehension of speech which is locally

time-reversed, i.e., segments within the signal are reversed, as long as the segments are <100 ms in duration (Saber & Perrot, 1999; Greenberg & Arai, 2001). The identification of seventy environmental sounds was tested in closed set format using time-reversed segments with durations varying from 20 ms to the full length of the sound. In general, environmental sounds were quite robust to this type of temporal distortion, with a small decrement in performance with increasing segment length. There were a number of sounds that were recognized nearly perfectly in all conditions; these tended to be continuous, slowly modulating sounds such as waves splashing and a train rolling. This relation was confirmed by a modest but significant correlation between the identifiability of the sounds and the peaks of their modulation spectra. In contrast, a few sounds with very quick transients, such as a typewriter and hammering, were very adversely affected by time reversal. The results suggest that one factor that distinguishes speech from environmental sounds is the critical importance the relative timing of the acoustic features within the signal.

[Work supported by the National Institute on Aging and by the Veterans Affairs Medical Research.]

807 Decoding Emotional Prosody Requires Fine Acoustic Frequency Resolution

Diana Sarko¹, Heidi Roth², Purvis Bedenbaugh¹

¹*Neuroscience, University of Florida, PO Box 100244, Gainesville, FL, United States,* ²*Neurology, University of North Carolina, Box 7025/3114 Bioinformatics Bldg, Chapel Hill, NC, United States*

Although speech can be recognized using primarily temporal cues and minimal acoustic frequency resolution, it is not known what frequency resolution is required to decode other speech information, such as speaker identity and emotional prosody – the emotional message in speech. Prosody perception depends on the "melody of speech" - fluctuations in pitch, rhythm and stress. We measured the acoustic spectral resolution required to recognize emotional prosody.

In this study, recorded sentences from a clinical emotional prosody test were presented to young adults. Participants were asked to identify the emotional prosody of the sentences spoken with one of five alternative emotional tones: happy, sad, angry, fearful or neutral. To control frequency resolution, the frequency range from 100-8100 Hz was noise vocoded in bands of equal width in Hz.

Consistent with previous findings, participants correctly identified the sentences 99% of the time with only 16 channels, corresponding to a bandwidth of 500 Hz. However, participants were unable to identify the emotional prosody at this frequency resolution. In order to score at the age appropriate norm for emotional prosody identification (95.3%, SD = 5.4%), participants needed 362 (+/-

100) bands, corresponding to a frequency resolution of 22 Hz.

We conclude that fine spectral resolution is required to recognize emotional prosody. Perceptual frequency resolution is coarser at high frequencies than at low frequencies. Only at the finest resolution tested does the spectral resolution of our test signals match or exceed perceptual auditory spectral resolution for acoustic frequencies below 450 Hz. We therefore additionally conclude that the low frequencies are most critical for prosody recognition.

808 Temporally Non-adjacent Acoustic Histories Shift Identification of Speech

Lori L. Holt¹, Andrew J. Lotto²

¹*Psychology, Carnegie Mellon University, 5000 Forbes Avenue, Pittsburgh, PA, United States,* ²*Research, Boys Town National Research Hospital, 555 North 30th Street, Omaha, NE, United States*

Auditory context effects occur when perception of acoustically identical signals varies as a function of neighboring sounds. For the most part, context effects have been investigated with temporally-adjacent context and target sounds. We report a novel effect of non-speech acoustic context upon speech categorization. An 'acoustic history' composed of 21 tones with a low-frequency mean (1800 Hz) or a high-frequency mean (2800 Hz) preceded a standard 2300-Hz tone and a subsequent speech syllable drawn from a series varying perceptually from /ga/ to /da/. The order of tones in the acoustic history varied on a trial-by-trial basis (thus particular acoustic characteristics varied whereas distribution characteristics were maintained). Results indicate a contrastive influence of the temporally non-adjacent acoustic history. Listeners reported more 'ga' syllables (the alternative with lower-frequency energy) following acoustic histories with 2800-Hz means and more /da/ responses to stimuli with 1800-Hz mean acoustic histories although the standard tone temporally adjacent to the speech tokens was constant across trials. The effect is resilient across dramatic changes in acoustic characteristics as long as the frequency distribution mean of the context stimuli remains constant; variability in the sampling of the acoustic history contributes very little to the observed effect. The context effect persists even when 1.3 sec of silence separates acoustic history and target. Moreover, it is highly dependent upon the spectra of the acoustic history; inverse spectra composed of notches carved from a band of white noise produce context effects in the opposite direction. Overall, results indicate that temporally non-adjacent acoustic histories elicit a pronounced contrastive influence upon central auditory processing of spectral information in subsequent stimuli and that this influence is robust enough to influence speech categorization.

809 Perceptual cancellation of reliable spectral characteristics

Michael Kieffe¹, Keith R. Kluender²

¹*School of Human Communication Disorders, Dalhousie University, 5599 Fenwick Street, Halifax, Nova Scotia, Canada,* ²*Department of Psychology, University of Wisconsin, 1202 West Johnson Street, Madison, Wisconsin, United States*

It is both true and efficient that sensorineural systems respond to change and little else. Perceptual systems do not record absolute level be it loudness, pitch, brightness, or color. This fact has been

demonstrated in every sensory domain. For example, the visual system is remarkable in maintaining color constancy over widely varying illumination such as sunlight and varieties of artificial light (incandescent, fluorescent, etc.) for which light spectra reflected from objects differ dramatically. Similarly, spectra of sounds to which one is listening are virtually always colored by the environment. Energy at some frequencies is reinforced by acoustic reflective properties of surfaces, while energy at other frequencies is dampened by acoustic absorbent materials and shapes of objects in the environment. Results will be reported for a series of experiments demonstrating how auditory systems compensate for reliable characteristics of spectral shape in acoustic signals. Specifically, listeners' perception of vowel sounds, characterized by both local (e.g., formants) and broad (e.g., tilt) spectral composition, changes radically depending upon reliable spectral composition of precursor signals. These experiments have been conducted using a variety of precursor signals consisting of meaningful and time-reversed vocoded sentences, as well as novel non-speech precursors consisting of multiple filter poles modulating sinusoidally across a source spectrum with specific local and broad spectral characteristics. Constancy across widely varying spectral compositions shares much in common with visual color constancy. However, auditory spectral constancy appears to be more effective than visual constancy in compensating for local spectral fluctuations. [Work supported by NIDCD DC-04072]

810 Infants' and adults' detection thresholds for frequency-modulated (FM) pure-tones in noise

Lori J. Leibold, Lynne A. Werner

Department of Speech and Hearing Sciences, University of Washington, 1417 NE 42nd Street, Seattle, Washington, United States

Compared to adult-directed speech (AD speech), infant-directed speech (ID speech) contains lengthened durations, wider frequency ranges, exaggerated intonation contours, and higher frequencies. Although infants appear to be more attentive and emotionally responsive to ID versus AD speech, the basis for this preference remains unclear. Colombo et al. [1995, Merrill-Palmer Quarterly] suggested that the acoustic properties of ID speech make it more detectable to infants in noise. The purpose of the current investigation was to determine infants' and adults' detection thresholds for pure-tones and frequency-modulated (FM) pure-tones in noise. Subjects were 4 month-old infants and 18-30 year-old adults with no risk factors for hearing loss. An observer-based testing method was used. Following training to 80%-correct criterion, detection thresholds were measured adaptively. Following Colombo et al., signals were frequency-modulated (FM) pure-tones corresponding to the frequency contour of AD speech (150-275-150 Hz) or ID speech (150-550-150 Hz). In addition, detection thresholds were determined for 275 Hz and 550 Hz pure-tones, corresponding to the upper frequency limit of each FM signal. Signals were 1-sec long and presented in a background of continuous broadband noise (LP 4000 Hz) presented at an overall level of 61 dB SPL. Infants' thresholds were higher than adults' thresholds across all signal conditions. However, thresholds changed with stimulus in the same way in the two age groups. Infants' and adults' thresholds were 3 dB lower for the FM signal

that was similar to ID speech compared to the FM signal that was similar to AD speech. Thresholds for both groups were also 3 dB lower for the 550 Hz pure-tone compared to the 275 Hz pure-tone, suggesting that thresholds for ID speech in noise are improved due to the inclusion of higher frequency components in the speech directed towards infants.

Supported by NIDCD DC000396, DC006122, DC04661.

811 Mechanisms of Perceptual Learning in Amplitude Modulation Detection

Ying-Yee Kong¹, Zhong-Lin Lu², Barbara Doshier³, Fan-Gang Zeng⁴

¹Cognitive Sciences, University of California, 364 Med Surge II, Irvine, CA, United States, ²Psychology, University of Southern California, Seeley G. Mudd 702, Los Angeles, CA, United States, ³Cognitive Sciences, University of California, Social Science, Irvine, CA, United States, ⁴Otolaryngology and Biomedical Engineering, University of California, 364 Med Surge II, Irvine, CA, United States

Unlike cognitive learning, perceptual learning is stimulus and task specific. We adapted the theoretical framework developed by Doshier and Lu (1998; 1999) in visual perceptual learning to identify mechanisms of perceptual learning in auditory amplitude modulation detection. By measuring an observer's performance in the presence of external noise at systematically manipulated levels, the perceptual template model characterizes the observer's perception in terms of equivalent internal noise, identification templates, and processing nonlinearities. Mechanisms of perceptual learning can be characterized as improvements of these system limitations, including stimulus enhancement, external noise exclusion, and/or internal (multiplicative) noise reduction. Four normal-hearing listeners were tested. The signal was an 8-Hz modulation of a 70-dB SPL sinusoidal carrier (6.5k Hz). All subjects were trained in 10 or more sessions in the modulation detection task tested in quiet and five noise spectrum levels (-10, 0, 10, 20, and 25 dB SPL). Modulation detection thresholds were obtained using two three-interval forced-choice procedures (2-down 1-up and 3-down 1-up) in each session. Each session included 60 trials per 2/1 staircase and 80 trials per 3/1 staircase for each of the 6 noise levels, yielding 840 trials per session. In addition, detection thresholds of the unmodulated carrier in the six levels of external noise were measured before and after perceptual training. Results showed that (1) training did not improve carrier detection, (2) training reduced modulation detection thresholds in quiet and near quiet conditions by about 3.7 dB, and (3) training did not change modulation detection thresholds in the high noise conditions. These findings imply that modulation detection training enhanced the stimulus (or, equivalently, reduced the internal additive noise) but did not optimize the identification templates, nor change the nonlinear processing in the system.

Supported by NIH RO1-DC02267

812 Different influences of temporal-interval discrimination training on average threshold and within-listener standard deviation

Beverly A. Wright^{1,2}, Yuxuan Zhang², Christopher C. Stewart¹

¹Communication Sciences and Disorders, Northwestern University, 2240 Campus Drive, Evanston, Illinois, United States,

²Institute for Neuroscience, Northwestern University, 2240 Campus Drive, Evanston, Illinois, United States

Listeners can improve their ability to discriminate between sounds with practice, indicating that auditory processing is malleable. To date, most investigations of auditory-discrimination learning have used improvements in average threshold to assess patterns of learning and generalization. We were interested in whether auditory discrimination training also led to improved performance consistency in individual listeners, and, if so, whether consistency learning followed the same time course and generalization pattern as average-threshold learning. To address these questions, we examined the within-listener standard deviations of temporal-interval discrimination thresholds obtained in a previous training experiment [Wright et al. (1997) *J. Neuro.* 17, 3956-3963]. Fourteen listeners practiced one hour per day for 10 days discriminating a standard stimulus (two 15-ms, 1-kHz tones, separated by 100 ms) from a signal stimulus in which the same tones were separated by a longer interval. For the trained condition, both the average threshold and the within-listener standard deviation improved significantly, and with a similar time course, during training. Neither type of improvement generalized to an untrained interval (50 ms) presented at the trained frequency (1 kHz). However, whereas the improvement on the average threshold generalized to the trained interval (100 ms) presented at an untrained frequency (4 kHz), the improvement on the standard deviation did not. We subsequently observed the same pattern of results in another group of 6 listeners trained on the same condition. Thus, training improved both the average threshold and performance consistency on temporal-interval discrimination. However, while average-threshold learning generalized across stimulus frequency, consistency learning occurred only for the trained stimulus, suggesting that the improvements on these two performance measures involve different learning processes. [Supported by NIDCD].

813 Frequency Discrimination Training Under Conditions Of High Stimulus Uncertainty

Sygal Amitay¹, David JC Hawkey², David R Moore¹

¹Institute of Hearing Research, Medical Research Council, University Park, Nottingham, United Kingdom, ²Institute of Hearing Research, Medical Research Council, University Park, Nottingham, United Kingdom

In perceptual learning of speech, large training sets produce optimal outcomes. We explored the effect of training set size and spread on training and generalisation of pure-tone frequency discrimination. One group of listeners (T-fixed) was trained using a fixed standard tone at 1 kHz. At outset, 2/3 of listeners had low frequency difference limens (DLFs) and 1/3 had intermediate/high DLFs. Over 7 blocks of training, rapid and dramatic improvement was observed in all listeners. DLFs at untrained frequencies (0.5, 2, 4 kHz) were all equivalent to the DLF at 1 kHz. A second group

(T-roving) trained on a roving frequency standard (900-1100 Hz). The same initial inter-subject variability was observed, but the DLFs did not improve as rapidly with training. When tested on 0.5, 1, 2 and 4 kHz after training, T-roving listeners with low initial DLFs did not differ from T-fixed, while those with high initial DLFs had poorer performance than their counterparts in the T-fixed group. A third group (T-wide) was trained on a wide-roving standard frequency (570, 840, 1170, 1600 and 2150 Hz). We expected that if the higher DLFs and slow training observed in the T-roving group resulted from stimulus uncertainty (a procedural aspect of the task), DLFs in the T-wide and T-roving groups should be similar. If, however, higher DLFs resulted from within-channel confusion, separating the standard frequencies into different channels would make the task easier. Again, 2/3 of the listeners had initially low DLFs and their learning was similar to the T-fixed group, while 1/3 had initially high DLFs and followed the training pattern of their counterparts in the T-roving group. Thus, the effect of the training set on the progress and outcome of training depends on both its contents and initial frequency discrimination ability.

814 Early Frequency Discrimination Learning: Identifying Procedural And Perceptual Components

David JC Hawkey¹, Sygal Amitay², David R Moore²

¹Institute of Hearing Research, Medical Research Council, University Park, Nottingham, United Kingdom, ²Institute of Hearing Research, Medical Research Council, University Park, Nottingham, United Kingdom

Perceptual learning studies generally allow subjects practice before data are gathered, dismissing early performance improvement as procedural learning. Our previous work has shown dramatic early performance improvement on a two interval, two alternative, forced choice (2I-2AFC) frequency discrimination task, though it was unclear what the relative contributions of procedural and perceptual learning were. To investigate these contributions, we trained separate groups of participants on 1 of 4 conditions: group 1 trained on 2I-2AFC frequency discrimination task (target condition), group 2 on 2I-2AFC auditory intensity discrimination (same modality and procedure, different relevant sensation), group 3 trained on AXB frequency discrimination (same relevant sensation, different procedure), and group 4 trained on 2I-2AFC visual contrast discrimination (different modality, same procedure). We then tested all groups on 2 blocks of the target condition. All groups thus received a similar amount of training overall and there was a common metric to assess the effect on both absolute performance and early performance improvement. All groups showed significant improvements in frequency discrimination. Improvement across the 2 target condition blocks was dependent on training: participants who hadn't trained on a frequency discrimination task (groups 2 and 4) showed more improvement than those who received a block of frequency discrimination training (groups 1 and 3). This difference suggested that naïve participants in groups 1 and 3 learned something during the first block that participants in groups 2 and 4 only learned when exposed to the target condition in block 2. This component of early performance improvement was specific to frequency discrimination, and may be labelled perceptual learning.

815 Application of the Taguchi Method to Middle-Ear Finite-Element Modelling

Li Qi¹, Chadia S. Mikhael¹, W. Robert J. Funnell^{1,2}

¹BioMedical Engineering, McGill University, 3775, rue University, Montreal, QC, Canada, ²Otolaryngology, McGill University, 3775, rue University, Montreal, QC, Canada

The quality of a finite-element model of the middle ear strongly depends on its geometry and on the choice of material properties.

Uncertainty in the geometry can arise, for example, from distortion in imaging, or from the image-segmentation process due to limited spatial resolution and contrast. Likewise, uncertainty in the choice of material-property parameters can arise from lack of relevant measurements, from ear-to-ear variability, etc. When parameter values are uncertain, the one-factor-at-a-time method is commonly used to investigate the effects of parameter variations; however, it does not take into account the possibility of interactions among parameters. One alternative, the full-factorial method, permits the analysis of parameter interactions but generally requires an excessive number of simulations. A more practical alternative is the Taguchi method, which was originally developed for industrial design. Via orthogonal matrices and analysis of variance (ANOVA), it determines the relative importance of each of the parameters and identifies any interactions among them. In this work we apply the Taguchi method for the first time to a finite-element model of the middle ear, and explore its usefulness.

816 Are Temporal Bones Useful Models of Human Middle-Ear Mechanics?

John J Rosowski¹, Alexander M Huber², Michael E Ravicz³, Richard L Goode⁴

¹Eaton-Peabody Laboratory, Mass. Eye & Ear Infirmary, 243 Charles St, Boston, MA, United States, ²Otorhinolaryngology, University Hospital Zurich, Frauenklinikstrasse, Nord II, Zurich, Switzerland, ³Eaton-Peabody Lab, Mass. Eye & Ear Infirmary, 243 Charlede Street, Boston, MA, United States, ⁴Otolaryngology-Head & Neck Surgery, Stanford Univ. School of Medicine, 300 Pasteur Drive, R135, Palo Alto, CA, United States

Since it is generally not possible to make invasive measurements of middle-ear mechanics in live humans, human temporal bones have long been used to investigate the physics and acoustics of sound conduction through normal, diseased and reconstructed human middle ears. While it is clear that drying, freezing, chemical fixatives and the buildup of static pressure within the middle ear of cadavers can alter middle-ear function, there is a good deal of evidence to suggest that the middle ears of temporal bones, maintained in cool and moist environments and with vented middle-ear spaces, function similarly to live middle ears. The best evidence comes from comparisons of mechanical measurements made in live ears with similar measurements in temporal bones (e.g. Goode et al. *Am J Otol* 17: 813-822; 1996). Recently, Ruggero and Temchin (*ARLO* 4: 53-58; 2002) suggested that "measurements of middle ear vibrations in human temporal bones ... are somehow flawed." We contend that the differences emphasized by Ruggero and Temchin can be explained either by methodological variations between studies, or by the normalization procedures employed by Ruggero and Temchin for comparing the

data from different studies. The data relevant to this question will be presented and the alternative viewpoints discussed.

Funded by NIDCD.

817 High-frequency Sound Transmission Through the Gerbil Middle Ear

Michael E. Ravicz¹, John J. Rosowski^{1,2}

¹Eaton-Peabody Lab., Massachusetts Eye & Ear Infirmary, 243 Charles St., Boston, MA, United States, ²Department of Otolaryngology and Laryngology, Harvard Medical School, 243 Charles St., Boston, MA, United States

The middle ear has sometimes been described simply as a resonant lumped-element system (mass-dominated at high frequencies: magnitude decreases 20 dB/decade, phase lag 0.5 periods) or as an ideally-terminated (matched) lossless transmission line (magnitude constant, smooth phase accumulation). A full understanding of middle-ear sound transmission requires consideration of the middle and inner ear together as a complete system.

Middle-ear transmission was assessed in gerbils by measuring stapes velocity (with a laser-Doppler vibrometer) in response to ear-canal sound pressure from 100 Hz to 60 kHz, a frequency range that spans the gerbil's range of hearing. Stapes velocity was measured from two viewing directions to estimate the dominant direction of stapes motion. The sound pressure distribution within the ear canal was investigated with a movable probe tube microphone. The middle-ear load was manipulated by draining the inner ear. The effect of opening the middle-ear air spaces was investigated.

Preliminary results show: (1) Stapes velocity in six ears (normalized by sound pressure near the umbo) was fairly constant in magnitude from 1–20 kHz with local variations and decreased by a factor of 1–10 by 60 kHz. Phase was near 0 periods at 1 kHz but decreased with frequency with local variations, lagging 1 period by 25 kHz and >2 periods by 60 kHz. These variations with frequency are inconsistent with either a resonant lumped-element system or a matched lossless transmission line. (2) Stapes motion was primarily piston-like below 40 kHz. (3) Sound pressure varied as much as 20 dB within the bony ear canal. (4) Reducing the middle-ear load produced local velocity maxima below 30 kHz and reduced velocity above 40 kHz. (5) Alterations to the bulla wall had little effect on stapes velocity above 20 kHz.

Supported by NIDCD.

818 Isolated Malleus-incus Complex: Three-Dimensional Measurements and Analysis

Jae Hoon Sim, Sunil Puria, Charles R. Steele

Department of Mechanical Engineering, Stanford University, Durand Bldg, Room 262, Stanford, CA, United States

It is now known that the malleus and incus motion changes with frequency in all three dimensions. To describe the complicated motion of the malleus and incus, the slippage at the incudo-malleolar joint should be considered.

We make detailed 3D measurements of the isolated malleus-incus complex (MIC) where the eardrum and the stapes footplate have been removed. Removing the eardrum decouples the complicated motions of the eardrum from the MIC while removing the stapes

footplate and inner ear gives greater access to the malleus and incus. Without an ear drum, the isolated malleus incus complex is directly driven by a tiny magnet attached to the umbo and a coil around the tympanic annulus. Velocities of several points on the isolated malleus-incus complex, which is attached to two stacked goniometers, are measured from several different angles. The 3-D velocity components of each point, and translation and rotation of the malleus and the incus, are calculated. Measurements are made while driving the umbo in the forward direction and the incus in the reverse direction. Measurements are made with the output freely moving, or while it is immobilized.

The measurements are used to estimate parameters of an anatomically based structural model of the isolated MIC. A mathematical model of the malleus-incus complex, which allows slippage at the incudo-malleolar joint, is introduced. Ligaments are modeled as pre-stretched linear springs and dashpots. Typical ligament positions and center of mass of the malleus and incus are specified. The input force and model parameters are obtained by least square error methods.

The 3-D motion of the malleus-incus complex is observed with slippage at the incudo-malleolar joint. The model is consistent with the measurements for frequencies below about 2 kHz. For modeling higher frequencies, more accurate description of ligament positions and center of mass of the malleus and incus is required. These measurements can be obtained using microCT imaging methods.

Work supported in part by a grant from the NIDCD of NIH (DC03085).

819 Scientific Visualization of the Incudostapedial Articulation in Humans and Cats: In 3D Still and Video Images

Clarinda Carrington Northrop, Stephen Robert Levine

Research, Temporal Bone Foundation, 9 Brimmer Street, Boston, MA, United States

Scientific Visualization of the Incudostapedial Articulation in Humans and Cats: In 3D Still and Video Images

How can you see the attachment of the elastic fibers of the joint capsule between the head of the stapes and the lenticular process of the incus? Is the anatomy of the incudostapedial articulation similar in the cat and the human? To answer these questions it would be helpful to visualize the articulation in 3D. It is possible to make 3D images with Computed Tomography or Magnetic Resonance Imaging, but with these methods it is not possible to distinguish characteristics of the soft tissues in the incudostapedial articulation. However, serial sections of celloidin embedded temporal bones scanned into a computer have enough resolution to be converted into detailed 3D images, thus clarifying these issues.

The materials used for this scientific visualization of the incudostapedial articulation were the temporal bones of two newborn and two adult humans, as well as two adult cats. The temporal bones were prepared in the routine manner for celloidin sections and every section through the incudostapedial articulation (approximately 40 sections in each ear) was studied. Each anatomical feature was segmented out of each section. These individual pieces were reassembled into 3D images using Maya software.

The shape of the lenticular process and its position relative to the head of the stapes, the attachment of the ligamentous fibers to the ossicles and to the stapedius tendon can be readily visualized which makes it possible to compare the human articulation with the cat.

Scientific visualization of the microscopic structures of the articulation between the lenticular process of the incus and the head of the stapes can be enhanced by using serially sectioned celloidin embedded temporal bone slides and computer graphics software.

820 The Influence of Complex Stapes Vibration Patterns on Hearing

Damien Sequeira¹, Christian Breuninger², Albrecht Eiber², Alexander Huber¹

¹Department of Otorhinolaryngology, Head and Neck Surgery, University Hospital of Zurich, Frauenklinikstrasse 24, Zurich, Switzerland, ²Institute B of Mechanics, University of Stuttgart, Pfaffenwaldring 9, Stuttgart, Germany

Recent studies into the vibration modes of the stapes in response to acoustic stimulation of the normal ear have revealed a complex movement pattern of its footplate. These complex vibrations can be expressed as one translational displacement and two rotational movements around the long and short axes of the stapes. At low frequencies the vibrations are predominantly piston-like (translational), but they become increasing rocking-like (rotational) at middle and high frequencies. Contrary to what occurs in the case of the translational component, the rotational components produce no net volume displacement of cochlear fluid at some distance from the footplate. Therefore, according to the classical theory, it is hypothesized that the rotational motion of the stapes is considered to be lost energy that is not transformed into a hearing sensation. It is the goal of an ongoing study to test this hypothesis. Until now no pure vibration modes of the stapes have been devised experimentally. Hence, it is the objective to develop a system, which would result in pure translational or pure rotational movements in anesthetized guinea pigs. A piezoelectric device capable of three-dimensional movement is used to stimulate the stapes superstructure at various frequencies and in various directions in order to induce different movement patterns. The desired stimuli of the device are generated by means of a custom-made feedback mechanism using a three-dimensional laser Doppler interferometer. The preliminary results of these experiments will be presented at the meeting.

821 Ossicular Ligaments and the Axis of Rotation

Hideko Heidi Nakajima^{1,2}, William T. Peake^{1,3}, John J. Rosowski^{1,2}, Saumil N. Merchant^{1,2}

¹Eaton-Peabody Laboratory, Massachusetts Eye and Ear Infirmary, 243 Charles Street, Boston, Massachusetts, United States,

²Department of Otology and Laryngology, Harvard Medical School, 243 Charles Street, Boston, Massachusetts, United States,

³Research Laboratory of Electronics, Massachusetts Institute of Technology, 77 Massachusetts Avenue, Boston, Massachusetts, United States

The axis of rotation for the malleus and incus for low-frequency sound has been described as extending from the anterior malleal

ligament (AML) to the posterior incudal ligament (PIL). We determined the effects of stiffening and removing the AML and PIL on acoustic response in temporal bones. These altered conditions are of interest clinically, because stiffening of the anterior malleal ligament (AML) has been reported to result in significant conductive hearing loss (Huber et al 2003, *Otol Rhinol Laryngol* 112:348-355) and some surgical procedures remove the AML or PIL.

Sound induced umbo and stapes velocities were measured in fresh human temporal bones by laser vibrometry. Stiffening of the AML was accomplished with cyanoacrylate glue or dental cement. The AML was removed with the anterior malleal process and the PIL was removed with the buttress (bony bridge between the short process of the incus and the facial recess near the fossa incudus).

For low frequencies, stiffening the AML resulted in 0-6 dB reductions in ossicular motion, which is too small an effect to be a clinically significant conductive hearing loss. Replacement of the AML with a cement bar resulted in 8 dB decrease, while a similar bar attached to the malleus head resulted in 15-30 dB decrease. This dependence on location of the bar is consistent with the principle that additional stiffness applied near the rotational axis has less effect than when applied away from the axis. Removal of the AML resulted in less than 5 dB change in ossicular mobility. Hato et al (*Otolaryngol Head Neck Surg* 2001;124:274-278) reported no effect of removing the PIL. Therefore, manipulation of either of the ligaments at the axis of rotation results in little effect on low-frequency middle-ear sound transmission. However, we found that removal of both the AML and PIL resulted in larger and more complex changes, indicating that at least one of the ligaments is required for normal mechanical response.

Funded by NIDCD

822 Frequency Dependence of the Mass Loading Effect: In vitro Laser Doppler Vibrometry measurements using the 'Floating Mass Transducer'

A. J. Needham^{1,2}, D. Jiang¹, A. Bibas¹, A. Fitzgerald O'Connor¹, G. Jeronimidis²

¹Dept. of Otolaryngology, Head and Neck Surgery, Guy's and St. Thomas Hospital, Lambeth Palace Road, London, United Kingdom, ²Dept. of Engineering, University of Reading, Whiteknight, Reading, United Kingdom

The sound transmission of the middle ear is dependent on the mass of the ossicular chain, its stiffness and frictional resistance. Previous research has shown that the mass loading effect is frequency dependent and stapes displacement is reduced more at higher frequencies due to an increase in inertia. However little has been done to investigate a detailed frequency response with a high number of samples per octave.

This article describes the middle ear frequency response before and after insertion of an active middle ear implant (AMEI) that imposes an additional mass on the ossicular chain. The implant was positioned in two locations along the long process of the incus to assess changes in the middle ear transfer function.

Laser Doppler vibrometry was used to measure stapes displacement before and during the placement of a Vibrant Soundbridge "floating mass transducer" (FMT) on the ossicular chain. Five cadaver temporal bones were used for the experiments and the

effects of mass and attachment site were compared to the unloaded response. Measurements were made at frequencies between 0.1 and 10 kHz and at acoustic input levels varying from 50 to 120 dB SPL. Each temporal bone acted as its own control.

Addition of the FMT caused a decrease in stapes displacement at high frequencies (between 2 and 8 kHz). However, in some bones it appeared that at very specific frequencies there was a significant loss of function of up to 30dB SPL usually between 1 and 4 kHz. Positioning the FMT as far as possible from the incudostapedial joint made little difference at low frequencies but had further detrimental effects on stapes displacement at higher frequencies.

In conclusion there is not a "perfect" placement position for the FMT that will be beneficial for every patient. Instead each patient's middle ear frequency response should be assessed individually before and during insertion of an AMEI. This would ensure the lowest possible mass loading effects, the best attachment site and adequate crimp tension. The loss in stapes displacement at various frequencies could be recorded and the active implant programmed to take account of each individual frequency response.

823 Effects of Middle Ear Suspensory Ligaments on Acoustic-Mechanical Transmission in Human Ear

Rong Zhu Gan¹, Bin Feng¹, Don Nakmali², Mark Wood²

¹*Aerospace & Mechanical Engineering, University of Oklahoma, 865 Asp Avenue, Norman, Oklahoma, United States,* ²*Research, Hough Ear Institute, 3400 NW 56th Street, Oklahoma City, Oklahoma, United States*

A bioengineering systems approach was taken to describe ear biomechanics for sound transmission through the external ear canal, middle ear and inner ear. The effects of middle ear ligaments on acoustic-mechanical transmission through the ear was first revealed using laser Doppler interferometry on human temporal bones and then predicted by a 3-dimensional (3-D) finite element model of human ear. Two laser interferometers were used to simultaneously measure movements of the stapes footplate and eardrum in temporal bones across the frequency range of 250-8000 Hz. After the control study with the intact ossicles, middle ear suspensory ligaments and muscle/tendons, such as superior malleal ligament, posterior incudal ligament, stapedial tendon, and tensor tympani muscle, were cut sequentially and the displacements of the stapes footplate and eardrum were measured repeatedly for each cut. A 3-D finite element (FE) model was created based on histological section images of a temporal bone, which provided accurate geometric data of the ear. The model includes the ossicular chain attached with six suspensory ligaments/muscles, external ear canal, and middle ear cavity. The model-derived eardrum (umbo) and stapes footplate vibrations as the sound pressure was applied in the canal near the umbo were compared with the results obtained from the temporal bones. Our results show that the effects of ligaments on transfer function of the ear are frequency sensitive and vary with individual ligaments. The FE model demonstrates that a bioengineering systems approach provides a better understanding of ear biomechanics. (Supported by Oklahoma Center for the Advancement of Science & Technology)

824 Sound transmission through the middle ear in-vivo in human and gerbil: Measurements of scala vestibuli and ear canal pressure.

Puja Kachroo¹, Vinaya Chakradeo², Jose Fayad³, Wei Dong⁴, Elizabeth Sue Olson⁵

¹*Medicine, Ross University School of Medicine, PO Box 266, Portsmouth, Dominica,* ²*Surgery, North Shore Long Island Jewish Health System, Long Island, Long Island, New York, United States,* ³*Otology, House Ear Clinic, 2100 West Third Street, Los Angeles, CA, United States,* ⁴*OTO/HNS, Columbia University, P & S 11-452 630 West 168th Street, New York, New York, United States,* ⁵*OTO/HNS and Biomedical Engineering, Columbia University, P & S 11-452 630 West 168th Street, New York, New York, United States*

Past measurements in gerbil showed that the middle ear transmitted sound to the inner ear with approximately a 30 dB gain and 25 ms delay, both values nearly independent of frequency from 2 kHz – at least 46 kHz (Olson, 1998). The basis for the middle ear delay is likely the tympanic membrane because upon sound stimulation its motion is wave-like (Khanna and Decraemer, 1997). The basic observations of middle ear transmission gain and delay were used as a starting point for the current set of measurements.

In gerbil, we sought to more definitively link the middle ear delay to the tympanic membrane by attempting to alter the delay by changing the tympanic membrane's physical properties, specifically its stiffness and mass. We were able to increase the transmission delay significantly by topical application of adhesive. Other manipulations had little effect on delay. The increase in delay suggests that the primary physical effect of the adhesive was either to increase the mass of the tympanic membrane or disrupt its fibrous layer and decrease its stiffness because an increase in stiffness is expected to decrease the transmission time.

In human we have measured scala vestibuli pressure in live human subjects undergoing cochlear implantation to see if the transmission delay and wide-band gain in live gerbil were also observed in live human. We did find a transmission delay but did not find wide-band gain. Over the frequency range where the comparison was possible both the magnitude and phase results were similar to temporal bone measurements (eg, Aibara et al., 2001). We have had only two human subjects to date and this study needs additional subjects before the results are conclusive.

825 Annular ligament of rat stapediostibular joint consists of a parallel array of numerous elastic fibers.

Mitsuru Ohashi¹, Shizuo Komune¹, Tatsuo Suganuma²

¹*Department of Otorhinolaryngology, Miyazaki Medical College, University of Miyazaki, 5200 Kihara, Kiyotake-cho, Japan,*

²*Department of Anatomy, Miyazaki Medical College, University of Miyazaki, 5200 Kihara, Kiyotake-cho, Japan*

Osteosclerosis refers to abnormal bone deposition about the stapediostibular joint (SVJ) consisting of annular ligament. So far, the basis for the osseous overgrowth has been completely obscure. We focused on the morphological structures of the annular ligament of rat SVJ by means of both light and transmission electron microscopy, and succeeded in demonstrating a quite peculiar ultra-

structure of the annular ligament.

Wistar male eight-week old rats were perfused with 4% buffered-paraformaldehyde solution via their left ventricles. The tympanic bullas were further fixed with the same fixative, and decalcified by 10% ethylene diamine tetraacetic acid and embedded in paraffin. For transmission electron microscopy, animals were fixed with a mixture of 2.5% buffered glutaraldehyde and 2% paraformaldehyde solution. Specimens were routinely processed and embedded in Epon.

Transverse sections of paraffin-embedded SVJs stained with a combined preparation of Weigert's resorcin-fuchsin and Van Gieson's method showed a number of strands of elastic fibers parallelly running from the frame of the vestibular window toward the rim of the stapes footplate where elastic fibers penetrated to their cartilage portions.

This structure was also confirmed with electron microscopy. The tannate-metal salt staining clearly demonstrated a peculiar array of elastic fibers. Interestingly, cross sections of an array of elastic fibers revealed that these fibers completely formed into a line. The supporting and maintenance structures for this peculiar elastic fibers array should be further investigated.

826 Magnetic Nanoparticles and Middle Ear Mechanics

Kenneth John Dormer^{1,2}, Charles S. Seeney³, Kevin Lewelling⁴

¹Physiology, Univ. Oklahoma HSC, 940 S.L. Young Blvd Rm 634, Oklahoma City, OK, United States, ²Research & Development, NanoBioMagnetics Inc., 124 N. Bryant Suite C3, Edmond, OK, United States, ³Exec. Offices, NanoBioMagnetics Inc., 124 N. Bryant Suite C3, Edmond, OK, United States, ⁴Physics, Oklahoma Christian University, c/o 124 N. Bryant Suite C3, Edmond, OK, United States

Novel applications for superparamagnetic nanoparticles may be generation of forces in living tissues by external magnetic fields. Our hypothesis was that ferrite nanoparticles implanted in epithelial tissue lining the middle ear ossicles and the tympanic membrane (ear drum) in guinea pigs could generate vibratory movements of the middle ear in response to an external magnetic field. Magnetite nanoparticles (NP, 12 nm diameter) encapsulated in silica and labeled with fluorescein isothiocyanate (FITC) were placed either on the middle ear mucosa or tympanic membrane of guinea pigs using sterile technique. Internalization of the NPs was facilitated during surgical recovery by an external magnetic field (0.25 T). Following 5-15 days the animals were anesthetized and a small electromagnetic coil, of the type used in semi-implantable hearing devices, (www.soundtecinc.com) inserted into the ear canal and activated with 8 volts, 1000 Hz sinusoidal). Movements of the ossicular chain were documented using laser Doppler interferometry, showing 2000Hz sinusoidal vibrations. Tissue was subsequently sectioned for laser confocal microscopy and presence of FITC documented in epithelial cells. We conclude that generation of forces in living tissue is possible by implanted magnetically susceptible NPs interacting with an external magnetic field. Supported by NIDCD Grant 1-R43-DC05528-01 to NanoBioMagnetics

827 Clinical evaluation of low level acoustic reflex audiometry

Boris Tolsdorff¹, Adrian Muenscher¹, Hannes Maier¹, Matthias Müller-Wehlau², Uwe Baumann³, Manfred Mauermann², Karsten Plotz⁴, Rudolf Leuwer¹

¹ENT, University of Hamburg Medical School, Martinistr. 52, Hamburg, Germany, ²Medizinische Physik, Universität Oldenburg, Carl-von-Ossietzky Str. 9-11, Oldenburg, Germany, ³ENT, Ludwig Maximilian University of Munich, Marchioninistr. 15, Munich, Germany, ⁴ENT, Evangelisches Krankenhaus Oldenburg, Steinweg 14-17, Oldenburg, Germany

Low level acoustic reflex (LLAR) measurements, as introduced by Neumann et al (*Audiol Neurootol* 1, 359-369, 1997), have the potential to determine the acoustic reflex threshold (ART) more sensitive than conventional methods. The aim of the current study was to evaluate the method in a group of hearing-impaired and normal-hearing subjects in a clinical setting.

For the LLAR two identical tone pulses are presented by an otoacoustic emission probe in short succession while recording the outer ear response with the probe microphone. Changes in impedance due to the acoustic reflex have a latency of some tens of milliseconds. Since the second tone pulse is presented after a sufficient long time after the first, it leads to a maximal difference between the pulses in the acoustic middle ear response. In comparison to Neumann et al. an improved ART criteria was used, utilizing the fact that successive presentations of the stimulus pair result in a comparable impedance change. The ART is therefore determined by means of the phase reproducibility of an appropriate frequency contained in the stimulus.

The ART was measured in patients (n=81) with normal tympanogram and no conductive hearing loss. The LLAR threshold was determined for sinusoids and third octave wide Schroeder phase tone complexes at 0.5, 1, 2, and 4 kHz with an adaptive algorithm. In addition the AR was measured at the same frequencies with a standard clinical device (Interacoustics AT22, AT235h or Grason Stadler GSI33) in steps of 5dB (75-105 dB HL) and the ART was visually and automatically determined. To allow a device independent comparability of the output levels, the different setups were calibrated within an artificial ear for insert ear phones (B&K 4157).

Significant lower ARTs were found for the LLAR with both tested types of tones than with the conventional devices.

828 Acoustic reflex facilitation using simultaneous stimulation with two tones at different frequencies

Hee-Yeon Shim¹, Yang-Sun Cho², Jae Yeon Choi², Sang Min Lee¹, Sun I. Kim¹, Won-Ho Chung², Sung Hwa Hong²

¹Biomedical engineering, College of Medicine, Hanyang University, Sungdong P.O.Box 55, Seoul, Korea, Republic of, ²Department of Otorhinolaryngology- Head and Neck Surgery, Sungkyunkwan University School of Medicine, 50 Irwon-dong Gangnam-gu, Seoul, Korea, Republic of

There are several methods for reducing the acoustic reflex threshold, which are known as sensitization or facilitation. Simultaneous stimulation with a high-frequency tone (facilitator) and a reflex-

eliciting tone (activator) is one of these methods.

This study was performed to analyze and generalize the tendency of the phenomena of acoustic reflex facilitation in the normal population. The acoustic reflex thresholds were measured when stimulated simultaneously with a facilitator of various amplitudes and frequencies. The degree of acoustic reflex facilitation and the patterns of the facilitation in the growth function curve were measured and analyzed. In addition, the acoustic reflex thresholds were measured with broad band noise to compare with the results from two tone stimulation.

Facilitation was observed more effectively with a facilitator at high frequencies with high amplitudes. The pattern of the growth function curves with a facilitator and an activator is quite different from those with a conventional acoustic reflex (single tone) or broad band noise.

With analysis of the factors affecting the facilitation, possible mechanisms of the acoustic reflex facilitation using simultaneous stimulation with two tones will be discussed.

Supported by grant of the Korea Health 21 R&D Project, Ministry of Health & Welfare, Republic of Korea. (02-PJ3-PG6-Ev10-0001)

829 The Aging Middle Ear: Acoustic Reflex Measures Using Wideband Energy Reflectance

M. Patrick Feeney^{1,2}, Chris A. Sanford³

¹Otolaryngology, Head & Neck Surgery, University of Washington, Box 357923, Seattle, Washington, United States, ²V. M. Bloedel Hearing Research Center, University of Washington, Box 357923, Seattle, Washington, United States, ³Speech & Hearing Sciences, University of Washington, Box 354875, Seattle, Washington, United States

Wideband changes in energy reflectance induced by the acoustic reflex were examined in 29 young-adult (M=22 years) and 16 elderly subjects (M=70 years). The group mean PTA (500, 1000 & 2000 Hz) was 6 dB HL for the young group and 20 dB HL for the elderly group. All subjects had normal 226 Hz tympanometry and middle-ear pressure within ± 10 daPa. The reflex activator was a broadband noise presented through an ER-3A earphone. Energy reflectance was measured using filtered clicks (250-2000 Hz) as the probe stimulus presented through an ER-10C microphone system using the method of Keefe and Simmons (2003, J. Acoust. Soc. Am.) implemented in Matlab. Reflectance measurements of the reflex were made by subtracting measurements obtained during a quiet baseline from those obtained in the presence of the contralateral activator noise. Reflex threshold was defined as the lowest activator level for which pairs of reflex-induced shifts in reflectance were significantly cross-correlated. The mean contralateral reflex threshold for the noise activator was 77.0 dB SPL for the young group and 81.5 dB SPL for the elderly group as calibrated in a Zwislocki coupler. At 4 dB above reflex threshold the maximum shift in reflectance occurred at approximately 600 Hz for both groups, but was 2.5 times larger for the young group (1.8% versus 4.5% shifts in reflectance). These results are consistent with previous studies employing low-frequency admittance measures. Contrary to a previous study reporting greater contralateral reflex magnitudes for young and elderly females for a noise

activator, the trend in the present data was for a greater reflex magnitude for males for both age groups. The age differences in acoustic reflex magnitude reported in this study occurred over a frequency range for which the elderly, on average, have reduced energy reflectance at ambient pressure, suggesting the possible contribution of middle-ear mechanics to this effect.

Work supported by NIH-NIDCD grant DC04129

830 Test-Retest Reliability of Wideband Reflectance Measures in Infants

Kathy R. Vander Werff, Beth A. Prieve

Communication Sciences and Disorders, Syracuse University, 621 Skytop Road (ISR), Syracuse, NY, United States

Wideband reflectance measures have been suggested as a useful tool in the assessment of middle-ear disorders (e.g. Feeney & Grant, 2003) and may provide information about the status of the middle ear over a wide frequency range. Since diagnosing middle-ear involvement in infants is particularly problematic given the inaccuracies of tympanometry in this population, additional measures of middle ear function are needed. However, there has not been a study that evaluated the consistency of repeated measurements of reflectance with or without removing and repositioning the probe in infants. In this study, wide-band reflectance measures were made in the ear canals of a group of infants under 9 months of age and a group of adults to assess the variability of reflectance tests across repeated measures. Reflectance measures were recorded twice, and then the probe was taken out and re-inserted for a third measurement. Within-subject test repeatability was excellent in adults and moderate in infants, with a wide range of variability in infants. The test-retest difference in reflectance varied by frequency. There was high variability below 500 Hz for infants, which likely relates to the fit of the probe in the ear canal as well as subject noise. In the frequency region where reflectance is the lowest (2-6 kHz), there were larger standard deviations in the reflectance test-retest difference in each frequency bin for repeated tests with the probe in place than when the probe was re-inserted. The same trend was true in adults, however the standard deviations were smaller and more similar whether or not the probe was re-inserted between measures. Across-subject variability was greater in infants than adults, and was generally larger than between-subject variability. In some cases, however, the variability across repeated trials within the same infant was as high as inter-subject variability. Support for this project was provided by the March of Dimes Foundation.

831 The contribution of middle ear function to infants' pure-tone sensitivity

Lynne A Werner¹, Sarah E Olsen¹, Nicole M Holmer²

¹Speech & Hearing Sciences, University of Washington, 1417 N.E. 42nd St., Seattle, WA, United States, ²Audiology, Children's Hospital and Regional Medical Center, 4800 Sand Point Way NE, Seattle, WA, United States

Infants' behavioral thresholds for pure-tone detection are higher than those of adults. This study evaluated the contribution of conductive immaturity to the age-related differences in pure-tone sensitivity. Pure-tone thresholds of normal hearing 3-month-olds, 6-month-olds and adults were measured using an observer-based

procedure. Listeners were trained to respond when they heard a tone, but not at other times. A threshold was estimated adaptively if the listener responded correctly 80% of the time when the tone was clearly audible. Middle ear conductance also was estimated in each listener's ear canal using the procedure developed by Keefe and his colleagues. Each listener was tested at a single frequency, 0.5-8 kHz at octave intervals. Stimuli were presented using Etymotic ER-1 insert phones, calibrated in the listener's ear canal at the test session. All listeners were expected to have normal hearing and passed screening tympanometry. Infant behavioral thresholds were higher than those of adults at all frequencies. For 6-month-olds, but not 3-month-olds, thresholds at 4 and 8 kHz were more adultlike than thresholds at lower frequencies. Six-month-olds' thresholds were slightly better than those of 3-month-olds at low frequencies, but significantly better at 4 and 8 kHz. Age-related changes in conductance followed a similar pattern: Differences between 3-month-olds and adults were greater at high frequencies, and greater improvement in conductance was observed at higher frequencies between 3 and 6 months. These parallels suggest that maturation of middle ear function contributes to improvements in hearing sensitivity during infancy. Finally, the correlation between conductance and behavioral threshold was about -0.5 and significant in each of the three age groups. Thus, individual differences in middle ear function can account for at least a portion of the differences in sensitivity among individuals at all ages. Work supported by NIH, DC00396, DC04661.

832 Experimental Study of an Adjustable Length Titanium Ossicular Prosthesis in a Temporal Bone model

Shouqin Zhao¹, Richard L Goode²

¹ENT, Beijing Tongren hospital, Chongwenmen, Beijing, China, People's Republic of, ²ENT, Stanford University Medical Center, 300 Pasteur Drive, R135, Palo Alto, CA, United States

ABSTRACT

Proper prosthesis tension is essential for excellent reconstructed middle ear sound transmission, and the tension produced by a rigid prosthesis appears to be directly related to its length. Experiments were performed in seven human temporal bones to study the effects of tension using an adjustable length titanium partial ossicular prosthesis (ALTO). A laser Doppler vibrometer system was used to measure stapes displacement in response to 406 pure tones between 0.1 and 10 kHz presented at 80 dB SPL at the tympanic membrane (TM). After a baseline measurement of stapes displacement in the intact ossicular chain, the incus was removed and the ALTO was placed between the stapes head and the malleus umbo. Stapes displacement was again measured for three conditions, one in which the prosthesis length was thought optimal and plus 0.2mm and plus 0.4 mm in length. We found that the slight increase in the length of the prosthesis decreased sound transmission in the middle ear below 1.0 kHz with no effect at higher frequencies (> 1.0 kHz).

Key words: laser Doppler vibrometer system, stapes displacement, prosthesis tension.

833 Head Holes Help Hearing: the Auditory Periphery of *Otocinclus*

Michael E. Smith¹, Darlene R. Ketten^{2,3}, Mardi C. Hastings¹, Arthur N. Popper¹

¹Department of Biology, University of Maryland, 1210 Biology/Psychology Building, College Park, MD, United States,

²Department of Biology, Woods Hole Oceanographic Institute, 93 Water Street MS #16, Woods Hole, MA, United States,

³Department of Otology and Laryngology, Harvard Medical School, 243 Charles St., Boston, MA, United States

Of all vertebrate taxa, perhaps the greatest diversity in ear and auditory peripheral structures is found among the fishes. Understanding such diversity can help us understand the evolution of vertebrate hearing and how different species solved problems of detection for diverse acoustic environments. In our exploration of such diversity, we are examining the structure and hearing in an exceptional fish, the suckermouth catfish of the genus *Otocinclus*. These fishes have unusual skull and swim bladder modifications thought to improve hearing. In our study, we used multiple imaging methods; e.g., SEM, MRI, and CT scans to visualize head anatomy. We also measured hearing capabilities via auditory brainstem response (ABR) to test whether the peripheral specializations may, indeed, enhance hearing.

The *Otocinclus* skull has large, complex, paired bones labelled the pterotic + supracleithrum. These bones surround each of the two lobes of the swim bladder and has numerous large fenestrae. It is hypothesized that these fenestrae allow for hearing specialization since sound waves can pass directly to the swim bladder without passing through bone. The audiogram for *Otocinclus* supports this view. *Otocinclus* hearing sensitivities are similar to that of related fishes at frequencies between 100 Hz and 1 kHz, but are more sensitive at frequencies above 1 kHz and have responses up to 10 kHz. In comparison, goldfish, a related species considered to have good hearing, detects sounds up to only 4 kHz. Our morphological data will be used to model how fenestrae in the pterotic + supracleithrum may relate to higher frequency hearing in *Otocinclus*. This species also produces broadband clicks with frequencies up to 10 kHz that may be used for communication. We are continuing to examine how these clicks are produced and their function.

834 Envelope-Phase Discrimination

Stanley Sheft, William A. Yost

Parmly Hearing Institute, Loyola University Chicago, 6525 N. Sheridan Road, Chicago, IL, United States

Modulation-filterbank models discard phase information above very low rates of amplitude modulation (AM). The first experiment evaluated this assumption by measuring thresholds for discriminating the starting phase of sinusoidal modulators of wideband-noise carriers. In the cued 2IFC procedure, the cue modulator was either fixed in sine phase or randomized on each trial. Duration and level were also either fixed or randomized, in this case across the stimulus presentations of each trial. In general, results confirmed that envelope-phase discrimination ability is a low-rate phenomenon with some listeners unable to perform the task once the modulation rate was greater than 12.5 Hz. For other listeners, however, thresholds were obtained in some conditions with AM rates of up to 40 Hz. Intersubject variability may in part

relate to the presence of two discrimination cues with one based on comparison of the ongoing pattern of envelope fluctuation and the other on intensity discrimination near stimulus onset and offset. In a synchrony-detection task, listeners can detect envelope-phase variation at rates of over 100 Hz due to the presence of a cross-spectral reference for phase. The second experiment measured modulation masking of synchrony detection. Without the masker present, thresholds were bandpass as a function of modulation rate with performance best at 20 Hz. The introduction of a masking component to the modulators elevated thresholds. The masking functions did not show tuning in the modulation domain; interference was greatest at the lowest and highest masker AM rates regardless of probe AM rate. Grouping based on the cross-spectral coherence of the masker modulator may have contributed to the greater interference obtained when probe and masker AM rates were distal. Collectively, the results from both experiments suggest that the phase limitation of modulation-filterbank models is too restrictive when applied across a variety of stimulus configurations.

835 Phase sensitivity as a test of spectral modulation channels

Aniket Saoji¹, David A. Eddins²

¹Center for Hearing and Deafness, University at Buffalo, 122 Cary Hall, Buffalo, New York, United States, ²Communicative Disorders and Sciences, University at Buffalo, 122 Cary Hall, Buffalo, New York, United States

One theory of spectral shape perception posits that the spectral envelope is processed by a physiologically-based spectral modulation filter bank. Evidence for such a mechanism comes from behavioral measures of modulation masking and selective adaptation, while physiological evidence comes from studies of the tuning characteristics of single cells. Analogous vision experiments have led to the theory of spatial vision via spatial modulation filter bank. Psychophysical support for this theory of vision comes from the phase sensitivity experiment of Graham and Nachmias (1971). An analogous auditory experiment is reported here to further test the relevance of the modulation filter bank concept to spectral envelope perception. The spectral contrast required to discriminate a complex spectral envelope from a flat spectrum was measured. Complex spectral envelopes were created by adding two spectral modulation frequencies (in cyc/oct), f and $3f$. The two components were either in phase (peak-add) or 180° out-of-phase (peak-subtract). When the two components had equal spectral contrast, the overall contrast was 1.33 times greater for the peak-add than the peak-subtract conditions. Overall contrast thresholds for the complex spectral envelopes, along with contrast thresholds for each individual component in isolation, were measured for three normal hearing subjects. The overall contrast thresholds were 1.29 times greater for the peak-add than the peak-subtract complex. At this threshold, the levels of f and $3f$ were similar for the peak-add and peak-subtract conditions. Clearly contrast thresholds were dependent on the contrast of the resolved components rather than on the overall spectral contrast of the complex patterns. The results are remarkably similar to theoretical predictions based on a spectral modulation filter bank and to those reported by Graham and Nachmias (1971) in the spatial-frequency domain of the visual system.

836 Modulation Masking Produced by 2nd-Order AM: Effects of AM Carrier Frequency and 2nd-Order AM Phase

Christian Füllgrabe¹, Brian C.J. Moore², Laurent Demany³, Stephan Ewert⁴, Stanley Sheft⁵, Christian Lorenzi¹

¹Laboratoire de Psychologie Expérimentale - CNRS UMR 8581, University Paris 5, 71 avenue Vaillant, Boulogne-Billancourt, France, ²Department of Experimental Psychology, University of Cambridge, Downing Street, Cambridge, United Kingdom, ³Laboratoire de Neurophysiologie - CNRS UMR 5543, University Bordeaux 2, 146 rue Léo Saignat, Bordeaux, France, ⁴Centre for Applied Hearing Research, Technical University of Denmark, Ørstedes Plads, Lyngby, Denmark, ⁵Parmlly Hearing Institute, Loyola University of Chicago, 6525 N. Sheridan Road, Chicago, Illinois, United States

Recent studies suggest that 2nd-order AM may be converted into a 1st-order AM component via a nonlinearity, and that such a component contributes to the perception of 2nd-order AM. However, 1st-order AM may be introduced in other ways. This study addressed this issue by investigating the ability to detect a 5-Hz, 1st-order probe modulator in the presence of a 2nd-order masker modulator, beating at the probe frequency. Detection performance was measured for different phase relationships between the probe and masker modulators, and different probe depths. In experiment 1, the audio carrier was a white noise. Masker carrier modulation frequencies, f_m , ranged from 64 to 2000 Hz. Detection performance was phase-dependent. The phase leading to poorest performance varied with f_m , inconsistent with the notion of a single, static nonlinearity. Simulation using linear auditory filters indicates that their outputs contain 1st-order AM at 5 Hz when only the masker is present. The magnitude and phase of this AM are partially consistent with the masking data. The 1st-order AM appears to arise from the effects of cochlear filtering and from intermodulation of aliased sidebands of the wideband carrier. Thus, a nonlinearity is not necessary to account for the results for a white noise carrier. In experiment 2, a 5-kHz sinusoidal carrier was used. In this case, no aliasing could occur. Also, the f_m was limited to a range (32-180 Hz) where linear filtering would not result in 1st-order AM at 5 Hz appearing at the outputs of the auditory filters. Detection performance was again dependent on phase and f_m . However, when a notched-noise audio masker centered at 5 kHz was added, maximum masking was observed for a fixed phase relationship, irrespective of f_m . The findings for the sinusoidal carrier indicate that a static nonlinearity influences performance when off-frequency listening is restricted, but other factors play a role when off-frequency listening is not restricted.

837 Tracking an Inaudible FM Sweep

Poppy A. C. Crum, Ervin R. Hafter

Psychology, University of California Berkeley, 3210 Tolman Hall #1650, Berkeley, CA, United States

The auditory system is robust in its ability to resolve occluded information in noisy environments. This is true, even in situations where the frequency content of the stimulus is dynamic (as in speech and music) and resolution of the missing content requires the auditory system to fill in information that has changed dynam-

ically between audible periods of time. We asked whether it is possible to use dynamic cues, such as the frequency velocity of the stimulus, to project how a sound is changing and, in so doing, to alter sensitivity along a predicted path.

Listeners heard 500 ms FM sweeps of varying velocity followed by noise-occluders of varying duration (50-200 ms). All stimuli were presented in a background of low-level noise. In a 2AFC task, listeners were asked to detect the presence of a short (?100 ms), threshold-level, pure-tone probe-signal immediately following the noise-occluder. For 60% of the conditions the frequency of the probe fell along the predicted path. For the remaining conditions its frequency was a percentage above or below the predicted path. Previous research with pure-tone cues showed that relative performance on the various probes plotted out a close approximation to a single auditory filter centered on the correct, i.e., cued frequency (Schlauch & Hafter, 1991). Similarly, results show that listeners can attend to an auditory filter that is centered on the expected frequency as predicted from the FM cue. Because the width of the noise occluder changes from trial to trial, listeners must be tracking the dynamic, unheard, information in the cue to predict where the sound will reappear. Data will be shown for a variety of FM sweeps and occluder widths.

838 Forward Masking of Amplitude Modulation

Magdalena Wojtczak, Neal Frank Viemeister

Psychology, University Of Minnesota, 75 East River Rd., Minneapolis, MN, United States

The results from studies on selective adaptation to amplitude modulation (AM) have been interpreted as providing support for the existence of neural channels specialized for processing of AM. These studies have used long exposure times (of the order of minutes) and relatively long durations of the test modulation (typically a few seconds). In contrast, the present study demonstrates a strong effect of prior exposure to AM after exposures shorter than 200 ms. This is analogous to forward masking (in the audio frequency domain) and appears to reflect a fundamentally different process from that underlying AM adaptation. More specifically, a 150-ms, 100%-modulated AM masker substantially impairs detection of a 50-ms burst of ensuing modulation imposed on the same carrier. Thresholds for detecting the brief signal modulation are elevated for temporal separations between the masker and signal AM up to about 200 ms but not for longer separations. Our data also show broad tuning of this AM forward-masking effect. Control conditions using cueing stimuli that mark the temporal end of the masker modulation, indicate that the forward masking effect is not due to temporal confusion. The results strongly suggest that there is sensory basis for the observed effect, possibly involving modulation-rate selective neural channels that adapt or continue being activated beyond the offset of the masker modulation. Implications of this surprising phenomenon for the processing of complex stimuli with fluctuating envelopes will be discussed. [Work supported by Grant No. DC00683 from NIDCD].

839 Combining Interferers in Modulation Discrimination Interference

Anastasios Sarampalis, Deborah A. Fantini, Christopher J. Plack

Department of Psychology, University of Essex, Wivenhoe Park, Colchester, United Kingdom

The detection or depth discrimination of amplitude and frequency modulation (AM and FM) is impaired in the presence of modulated interferers. This effect has been called modulation detection (or discrimination) interference (MDI). The amount of MDI depends on a number of factors, including the interferer modulation depth and the number of interfering components present. Typically, more interference is observed with increasing interferer depth. Higher thresholds can also be obtained when combining more than one interferer. It is not clear, however, whether the additivity works in the modulation domain, or whether it simply reflects the existence of additional energy in the interferer. The present study investigated AM and FM depth discrimination performance in the absence or presence of interference. Discrimination thresholds were initially measured in the absence or presence of a single sinusoidal interfering carrier, that was either unmodulated, AM, or FM. Psychometric functions for the discrimination of modulation depth were then measured as a function of the modulation depth of a single AM or FM interferer. Finally, two equally effective modulated interferers were combined and the d' values for the discrimination of modulation depth were measured. The results indicated that the amount of MDI increased (poorer performance) with increasing interferer depth. This was true regardless of target or interferer modulation type (AM or FM) and frequency placement of the interferer. Moreover, combining two equally effective interferers further increased the amount of MDI. The data in that case were accurately predicted by assuming that the two interferers added as two independent sources of noise. Overall the results indicated that AM and FM interferers behaved in a similar way throughout the experiment, supporting an MDI explanation in terms of a common dimension for both AM and FM targets and interferers.

840 AM Detection with a Roving-Level Modulation Masker: A Psychophysical Test of the Envelope Power Spectrum Model

Paul C Nelson, Laurel H Carney

Department of Bioengineering, Syracuse University, Institute for Sensory Research, 621 Skytop Road, Syracuse, NY, United States

Recently proposed modulation filter models make decisions based on the energy at the output of a modulation-frequency (fm) tuned filter (e.g., Dau et al., JASA 102: 2892-2919, 1997). A similar model in the audio-frequency domain fails to account for results from a roving-level tone-in-noise detection task: listeners' thresholds are essentially unaffected by the rove (Kidd et al., JASA 86: 1310-7, 1989), whereas a critical-band energy model predicts a significant increase in thresholds when the noise level is randomly varied between intervals. The current experiment investigates the same paradigm in the modulation-frequency domain. A two-interval, two-alternative forced-choice task was used first to estimate modulation detection thresholds in fixed-level noise for a given

carrier frequency, modulation noise bandwidth, and signal fm. The range of modulation masker levels to be used in the roving experiment was limited to those that increased detection thresholds but did not cause over-modulation in the signal interval. The modulation noise masker level was then roved between intervals, and the signal-to-noise ratio in the target interval was adjusted in the tracking procedure. Listeners' performance was significantly degraded relative to fixed-level conditions (in contrast to audio-frequency roving-level results). The data are at least qualitatively consistent with predictions made by an energy-based modulation filterbank model. Responses from a physiologically-motivated model based on interactions between inhibition and excitation were also considered and quantified for comparison to the psychophysical thresholds. [Supported by NIH DC01641].

841 DSAM predictions of the Basilar Membrane Response to Second-Order Amplitude Modulation

Rebecca Elizabeth Millman¹, Ray Meddis², Adrian Rees¹, Gary Green¹

¹School of Neurology, Neurobiology and Psychiatry, University of Newcastle upon Tyne, Framlington Place, Newcastle upon Tyne, United Kingdom, ²Centre for the Neural Basis of Hearing, University of Essex, Department of Psychology, Colchester, United Kingdom

Biologically significant sounds can be characterised by complex time-varying envelopes. Second-order amplitude modulation (AM) is a multi-component AM stimulus in which the depth of a sinusoidal AM (modulation frequency f_m) varies sinusoidally as a function of time. Second-order AM (modulation frequency $f_m\phi$) produces additional sidebands at $f_m \pm f_m\phi$ around the first-order components in the modulation spectrum of the stimulus.

Previous studies (e.g. Moore and Sek, 2000) suggested that a distortion product at $f_m\phi$ (in the modulation spectrum), generated via a nonlinearity, contributes to the detection of second-order AM. Moore and Sek (2000) also suggested that the magnitude of this distortion product increases with increasing depth of the modulation components. The aim of the present study was to test the specific hypothesis that a point model of the peripheral auditory system, DSAM (e.g. Lopez-Poveda and Meddis, 2001), can generate local distortion products. We measured the size of the distortion product generated by the static nonlinearity in the DSAM nonlinear basilar membrane (BM) model resulting from second-order AM waveforms of varying modulation depth.

Analysis of the DSAM nonlinear BM model output showed that the size of the distortion product at $f_m\phi$ increased with increasing first-order modulation depth in a nonlinear manner. However, the size of the distortion product was smaller than the detection threshold for second-order AM by at least a factor of three. The DSAM results suggest that, in a point model, a static BM nonlinearity does not generate a distortion product at $f_m\phi$ of sufficient magnitude to explain the psychophysical data for the detection of second-order AM. This discrepancy may result from the existence of a time-varying nonlinearity (e.g. Moore et al., 1999) or other central nonlinearities (e.g. Füllgrabe et al., 2003).

842 Models for Monaural Cross-Frequency Coincidence Detectors in Tone-in-Noise Detection Tasks

Xuedong Zhang¹, Laurel H Carney²

¹Biomedical Engineering, Hearing Research Center, Boston University, 44 Cummington St. /BME, Boston, MA, United States,

²Department of Bioengineering & Neuroscience, Institute for Sensory Research, Syracuse University, 621 Skytop Road, Syracuse, NY, United States

Psychophysical studies of detection of tones in noise suggest that subjects may use different cues available in the stimulus for different tasks. To study how these cues are encoded and extracted by the auditory system, we studied model coincidence detectors (shot-noise models with sub-threshold inputs) that receive convergent inputs from model auditory-nerve (AN) fibers. The effects of stimulus and model parameter values on the sensitivity of the cell (measured by the d-prime at a certain signal level) were explored in detail.

The best performing model cell for detection in wideband noise received inputs from AN fibers for which the phase relationship of the inputs was most affected by addition of the signal (we refer to this as a negative cell, because the response dropped when the signal was added). The best performing model cell for detection in narrowband noise received inputs from AN fibers that were not saturated by the stimulus and responded to the positive change in level of the total stimulus (we refer to this as a positive cell because the response increases when the signal was added). The sensitivity of positive and negative cells changed differently when different durations were used to measure the model responses. Including the onset response improved the sensitivity of the positive cell, since the onset response has a wider dynamic range, whereas the sustained response of the negative cell was more sensitive than the onset response. The performance of the model CD cell also depended on model parameters (e.g. the time constant and threshold of the shot-noise model) and changed non-monotonically with the parameter values. The time constant of the model cell with best sensitivity increased within a limited range as threshold increased. The parameter values that resulted in highest sensitivity were similar for both positive and negative cells.

[Supported by NIH DC01641 and ONR Amg Z883401]

843 The effects of cochlear implantation on auditory nerve synapses in congenitally deaf white cats.

Erika Kretzmer¹, Karen Montey², David K Ryugo^{1,2}

¹Neuroscience, Johns Hopkins University, Traylor 510, 720 Rutland Ave., Baltimore, MD, United States, ²Otolaryngology, Johns Hopkins University, Traylor 510, 720 Rutland Ave., Baltimore, MD, United States

Our long term goal is to understand the effects of hearing and deafness on the development of structure and function in the auditory system. Deafness in the developing animal has been shown to cause neuronal death, formation of novel circuits, and synaptic abnormalities. Certain plastic changes may underlie the failure of some cochlear implant recipients to benefit from the devices. One issue is to determine which, if any, structural effects of deafness

are prevented by implantation.

We implanted five deaf white kittens with 6-channel cochlear implants designed by Advanced Bionics. These implants use the human Clarion II processor but have a smaller electrode array. Three month old kittens were implanted and provided with 40 hours per week of electrical stimulation using a CIS processing strategy. The initial programming was accomplished in a manner similar to infants. After several weeks of experience, kittens could be called to eat using a unique sound, indicating successful implant function.

Our goal was to compare the structure of auditory nerve synapses across normal hearing cats, congenitally deaf white cats, and congenitally deaf white cats with a cochlear implant. To date, we examined endbulbs of Held on spherical bushy cells in the cochlear nucleus in one implanted cat. Bushy cells ipsilateral to the implant showed a marked reduction in synapse size. Endbulbs ipsilateral to the implant had a greater mitochondrial volume fraction, and a decrease in synaptic vesicle density near the post-synaptic density, as compared to the contralateral side. In this animal, auditory nerve synapses ipsilateral to the cochlear implant tend to resemble those in a hearing cat. We expect to present data from all 5 cats at the meeting.

Supported by NIH grants RO1 DC00232 and F31 DC005864 and a gift from Advanced Bionics.

844 Assessing development of the auditory system in normal-hearing children and children with cochlear implants by use of a stimulus train with decreasing inter-stimulus intervals.

Phillip M. Gilley¹, Anu Sharma², Michael Dorman³, N. Wendell Todd⁴, Kathryn Martin², Jolie Fainberg⁴

¹*Behavioral & Brain Sciences, University of Texas at Dallas, 1966 Inwood Rd., Dallas, TX, United States*, ²*Callier Advanced Hearing Research Center, University of Texas at Dallas, 1966 Inwood Rd., Dallas, TX, United States*, ³*Department of Speech and Hearing Science, Arizona State University, 200 E. Curry Rd., Ste. 146, Tempe, AZ, United States*, ⁴*Otology & Audiology, Children's Healthcare of Atlanta, 1405 Clifton Rd. NE, Atlanta, GA, United States*

We have examined the development of the central auditory system (CAS) in normal-hearing children and in children with cochlear implants. Our measure of CAS development was changes in the morphology of the cortical auditory evoked potential (CAEP) waveform as a function of stimulation rate. We have previously examined changes in the morphology of the NIP2 cortical auditory evoked potential (CAEP) in normal-hearing children (3-12 years) in response to a stimulus train with sequentially decreasing interstimulus intervals of 2000ms, 1000ms, 560ms and 360ms (Gilley et al., 2003). In that study we found that the NIP2 component was highly sensitive to changes in stimulation rate as a function of age. In general, at younger ages the NIP2 component was elicited only at the slowest stimulation rates. However, as age increased the NIP2 component was clearly apparent at successively faster stimulation rates. In the present study, we recorded CAEP responses in the same paradigm from children fitted with cochlear implants. Preliminary results indicate that some

implanted children show normal patterns of development with respect to CAEP morphology, while others do not. It is likely that age of implantation, duration of experience with the implant and the development of auditory processing abilities after implantation, among other factors, may influence these results. These results add to our understanding of the development of the central auditory pathways after cochlear implantation.

845 The Effects of Auditory Experience and Duration of Deafness on Temporal Processing in Cat Primary Auditory Cortex

Ralph E. Beitel¹, Maike Vollmer¹, Marcia W. Raggio², Christoph E. Schreiner¹

¹*Otolaryngology-HNS, University of California, 533 Parnassus Av, San Francisco, CA, United States*, ²*Speech & Communication Studies, San Francisco State University, 1600 Holloway Av, San Francisco, CA, United States*

Cochlear implant users typically show improvement in speech recognition over time, indicating that experience is an important factor for enhanced performance in electrical hearing. In this presentation we compare temporal processing in the primary auditory cortex (AI) obtained from acute microelectrode recordings in groups of cats characterized by 1) different durations of deafness, 2) presence or absence of passive (chronic) electrical stimulation of the cochlea and 3) whether training occurred with behaviorally relevant electrical signals.

Cats were deafened neonatally or as adults by injection of ototoxic drugs. Electrodes were implanted chronically in animals that received behavioral training and/or passive stimulation, whereas short-term (2 wk) and long-term (>2 years) deaf cats were implanted close to the time of the acute physiological experiment. For each stage of the study (chronic stimulation, behavior, physiology), stimuli were trains of biphasic unmodulated or sinusoidally modulated 0.2 ms/phase current pulses. Three variables were measured at each recording site in AI in each cat: the Best Modulation Frequency (BMF) that produced the maximum number of phase-locked spikes; the Cutoff Frequency at which the number of phase-locked spikes was just less than 50% of the number at BMF; and the period histogram Peak Latency.

The main results include: 1) Cats with extensive hearing histories have higher BMFs, higher Cutoff Frequencies and shorter Peak Latencies than long-term neonatally deafened cats and 2) Passively stimulated, neonatally deafened cats have lower BMFs and lower Cutoff Frequencies than cats with an extensive history of hearing. However, if neonatally deafened cats also receive behavioral training, their BMFs and Cutoff Frequencies are similar to those recorded in cats with an extensive history of hearing. The results highlight the deleterious effects of long-term deafness and the importance of behavioral context for temporal processing in AI.

Support provided by NIH-NIDCD Contract #N01-DC-0-2108

846 Effects of Treatment with Glial-Derived Neurotrophic Factor on Electrically Evoked Auditory Responses and Spiral Ganglion Survival in Deafened Guinea Pigs

Anette Elisabeth Fransson¹, Jun Maruyama², Göran Bredberg³, Josef Miller⁴, Mats Ulfendahl¹

¹Center for Hearing and Communication Research, Karolinska Institutet, KS, Hus M1:00, Stockholm, Sweden, ²Department of Otolaryngology, School of Medicine, Ehime, Ehime, Japan, ³Cochlear Implant Clinic, Huddinge University Hospital, Stockholm, Sweden, ⁴Kresge Hearing Research Institute, University of Michigan, 1301 E Ann Street, Ann Arbor, Michigan, United States

The function of a cochlear prosthesis depends largely on the survival and responsiveness of the spiral ganglion neurons. We have recently shown that local treatment with neurotrophic factors BDNF and CNTF significantly preserved the electrical sensitivity of the auditory nerve in the deafened guinea pig (PNAS 99:1657-1660, 2002). Using the same animal model it was shown that GDNF at a concentration of 10 µg/ml also offered effective treatment (Maruyama et al., ARO 2003). The purpose of this study was to further investigate the effects of GDNF but at lower concentrations and thus more appropriate to levels of potential human applications. Twenty-four guinea pigs were implanted with a combined electrode and cannula, which was inserted through the round window and attached to an osmotic pump (0.5µl/hour). All guinea pigs were given 10% neomycin into the cochlea during 48 hours for deafening. Thereafter, the animals received a four-week treatment of 1µg/ml or 100ng/ml GDNF, or artificial perilymph (AP). Each pump was changed after 2 wks and 2 wks later, the cannula was disconnected from the osmotic pump and sealed. After another 2 wks (total of 6 wks) the animals were sacrificed and the inner ear tissue prepared for structural analysis. Electrically-evoked auditory brainstem responses showed a significant difference between the GDNF and AP treated groups. The GDNF treated groups had lower thresholds compared to the controls throughout the experiment. No significant difference between the two GDNF groups was observed. The results demonstrate that GDNF intervention rescues auditory function in the inner ear at concentrations two orders of magnitude lower than what has been used previously, supporting its potential clinical application.

847 Cochlear Implant Forward Masking in an Animal Model

John C Middlebrooks¹, Ben H Bonham², Russell L Snyder²

¹Kresge Hearing Research, University of Michigan, 1301 E. Ann St., Ann Arbor, MI, United States, ²Otolaryngology, UCSF, 513 Parnassus Ave, San Francisco, CA, United States

Physiological studies of brain responses to cochlear-implant stimulation show that the spread of activation along the tonotopic axis depends upon several factors, including stimulus intensity and intra-cochlear electrode configuration. Spread of activation has been inferred to compromise functional independence of channels in a multi-channel implant. We employed forward masking as a functional measure of channel interaction. Anesthetized guinea

pigs were deafened acutely and implanted with a custom electrode array molded to the guinea-pig scala tympani. Electrical pulse trains were presented in monopolar (MP) and bipolar (BP) configurations. Neural spike activity was recorded from the central nucleus of the inferior colliculus, simultaneously at 16 sites along the tonotopic axis. As expected, BP stimulation produced relatively restricted spread of activation whereas MP stimulation activated neurons throughout most of the recording array. We tested masking of a 20-ms probe by a 100-ms masker; masker-probe delays ranged from 4 to 64 ms. Forward masking decayed with a time constant of roughly 30 ms. Masking decayed substantially with increasing intracochlear separation between masker and probe electrodes. That decay was greater with BP than with MP stimulation, but the difference due to configuration was much less than that predicted by spread-of-activation measures.

848 Effect of Inter-Phase Gap on Thresholds and Forward-Masked Excitation Patterns in Electric Hearing

Robert Paul Carlyon¹, Astrid van Wieringen², John Deeks¹, Christopher Joseph Long¹, Jan Wouters²

¹Cognition & Brain Sciences Unit, MRC, 15 Chaucer Rd, Cambridge, United Kingdom, ²Lab Exp. ORL, KU Leuven, Kapucijnenvoer 33, Leuven, Belgium

Most cochlear implants use biphasic pulse trains, in order to ensure that all current is charge-balanced. Physiological experiments with animals show that the short inter-phase gaps (IPGs) commonly used with humans raise thresholds, due to the second phase partially counteracting the first. Modeling studies also indicate that biphasic stimuli with short IPGs may result in a wider current spread than monophasic stimulation (Frijns et al, 1996).

Experiment 1 measured behavioral threshold for human cochlear implantees as a function of IPG, for two devices, and over a wider range than studied previously: 100-4900 µs for LAURA, and 8-2900 µs for the Nucleus CI24. Leading polarity alternated between pulses ("alternating phase"), stimulation was bipolar (BP+1 and BP+3 for the CI24), and pulse rate was 100 pps. Signal duration was 400 ms. For the CI24, the drop from 8 to 100 µs was 1-2 dB, consistent with earlier results with monopolar stimulation (McKay & Henshall, 2003). Thresholds continued to drop beyond 1900 µs for both devices, and the difference between 100 and 2900 µs for the CI24 ranged from 5 to 13 dB across subjects. The reduction in threshold over the longer range of IPGs may be mediated more centrally than the initial membrane depolarisation.

Experiment 2 compared forward masking by an alternating-polarity masker having a "long" IPG, compared to a masker with a short (≤100-µs) IPG. Alternating-phase, 1000-pps 20-ms signals were presented 5 ms after the 100-pps maskers, whose levels were chosen so as to produce equal amounts of masking when the signal was presented to the same channel as the masker. Preliminary results indicate that excitation patterns, measured by presenting the signal on different electrodes to the masker, are not consistently sharper for the long-IPG masker. We conclude that increasing IPGs beyond the range used clinically can produce substantial threshold reductions, but does not produce a consistently narrower spread of excitation.

849 Enhancement of Temporal Cues to Voice Pitch in Cochlear Implants

Tim Green, Andrew Faulkner, Stuart Rosen

Phonetics and Linguistics, University College London, Wolfson House, 4, Stephenson Way, London, United Kingdom

The limited spectral resolution of cochlear implant systems means that the lower harmonics that provide normal listeners with spectral pitch cues are unresolved. Temporal envelope cues to pitch are available in continuous-interleaved-sampling (CIS) processed speech but are of limited utility, particularly for higher fundamental frequencies (F_0 s). In a modified CIS processing scheme enhanced temporal cues to voice pitch were delivered by manipulating the more rapidly changing temporal structure that can represent periodicity, while spectral dynamics were signalled as normal by lower-rate components of the amplitude envelope. Low-rate amplitude envelopes were extracted using full-wave rectification and a 16 Hz smoothing filter. In voiced segments of the speech input, higher-rate temporal modulation was provided by 100% amplitude-modulation by a sawtooth waveform whose periodicity followed the F_0 of the input. Pulse levels were determined by the product of the low- and higher-rate modulation components.

One task was to label the direction of pitch movement of synthetic diphthong glides. Performance was better when the glide centre F_0 was 113 Hz rather than 226 Hz, illustrating the declining utility of temporal envelope cues as F_0 increases. While there was considerable individual variability, performance was better with modified processing than with standard CIS processing for both F_0 ranges. Better performance with modified processing was also found when listeners distinguished between the same sentences read as statements or questions, a contrast reflected in differences in F_0 contour. However, for some listeners, vowel identification performance was poorer with modified processing. Thus, while voice pitch perception can be enhanced by clarification of the temporal envelope, it is unclear whether this can be achieved without harming other aspects of speech perception.

850 Perception of Lexical Tone and Its Effect on Sentence Recognition in Children with Cochlear implants

Yu-ching KUO, Stuart Rosen, Andrew Faulkner

Phonetics & Linguistics, University College London, Dept. of Phonetics, 4 Stephenson Way, London, United Kingdom

Pitch variations, often referred as tones, are used to convey lexical meanings in tone languages such as Mandarin Chinese. However, current cochlear implants provide only limited information about voice fundamental frequency (f_0). Here we report on three experiments investigating the perception and use of tone in syllables and sentences in Mandarin speaking children using cochlear implants, and in normal-hearing controls using acoustic simulations. Experiment I investigated the extent to which tone recognition could be achieved by implant children, and whether another cue, amplitude variation, could be used to help tone recognition. Twenty-one good implant children, aged between 6 and 15, were asked to identify two types of syllable: natural speech signals with the original pitch and amplitude contours and processed speech signals with the original pitch contours but constant amplitude.

Group scores were well above chance, and one-third of these children achieved more than 80% correct. The amplitude cue showed different effects on different tones. Experiment II manipulated f_0 in sentences so as to examine its effect on sentence recognition. Sentences with natural f_0 contours were compared to sentences whose contours had been manipulated as slightly falling ones. No significant difference was found between these two types of sentences. It thus appears that implanted children can make some use of tonal information in highly constrained situations, but not when listening to running speech. Experiment III examined the effect of f_0 in sentences again, but in normal listeners, by using 2-, 4-, 8-, and 16-band vocoding of the same sentences used above. An f_0 controlled pulse carrier or a pulse carrier with a slightly falling pitch contour was used for voiced speech, and a noise carrier was used for voiceless speech. The natural f_0 was found to enhance sentence recognition significantly while spectral information was degraded, and the absence of f_0 affected young children much more than adults. Overall, these results show the importance of pitch information in a tone language and the limitations of current cochlear implants in providing it. Providing more pitch information in a cochlear implant will significantly improve speech perception in implanted children.

851 A case study: Music performance of a CLARION CII® implant user fitted with the HiResolution® strategy

Leonid Litvak, Lakshmi Mishra

Systems, Advanced Bionics, 12740 San Fernando Rd, Sylmar, CA, United States

As a group, cochlear implant patients do poorly with music. For example, they have difficulty identifying melodies based on pitch information alone. We had an opportunity to work with one user fitted with HiResolution strategy who is a semi-professional performer. We measured frequency discrimination thresholds with the subject listening to a standard HiResolution program, and while listening through a reduced channel program with only one, two, or three channels enabled. These thresholds were measured using a two-interval alternative forced-choice up-down procedure. We also performed melody recognition tests with melodies that were known to the subject, and were composed of tones of equal duration.

The subject's frequency discrimination threshold was approximately 5 Hz at 1000 Hz, and 10 Hz at 2100 Hz. This performance level is comparable to that achieved by normal-hearing listeners on the same test. At 2100 Hz, frequency discrimination thresholds were similar listening through the standard program, and while listening through three channels mapped nearest that frequency. Frequency discrimination threshold was near 60 Hz when listening through 2 channels. The subject could not perform the task with only one channel enabled.

The subject was also able to identify pure-tone melodies with no rhythm information with melodies played in the 4th, 5th and 6th octave. Subject's excellent performance on these tests corresponded with his ability to sing in tune and tune his own guitar. These results indicate that high-rate strategies like HiResolution can support a high level of music performance.

852 Simple front end for a model of the electrically stimulated auditory system

Mark E Robert

Auditory Implants and Perception, House Ear Institute, 2100 West Third street - Fifth floor, Los Angeles, California, United States

In addition to computational models of the normal auditory system there are a number of models for the electrically stimulated auditory nerve and inner ear. The latter vary in their complexity but share a front end that models the electrode-neuron interface and translates applied electrical signals into series of action potentials. For this reason they are useful tools for auditory implant research.

This presentation describes and presents results from a simple spike-generating front end based on modification of a commonly used phenomenological model, the integrate-and-fire (IAF) model of the nerve cell. The modification involves driving the model by extracellular rather than injected current. This extracellular current integrate-and-fire model (EC-IAF) is based on McNeal's model (1976, IEEE Trans BME 23(4):329-337) for subthreshold stimuli and includes a component for adaptation (described in Koch (1999) Biophysics of Computation. pp336-339).

For the preliminary work reported here the EC-IAF uses McNeal's parameter values and doubles the membrane conductance for adaptation conductance. The model assumes a pulsatile current waveform delivered by a monopolar electrode configuration. The presentation will show results from simulations of forward masking that agree qualitatively with results typically reported for this temporal psychophysics task.

853 Responses to two component modulation waveforms in the inferior colliculus (IC)

Sam Johnson, Gordon Wake, Gary Green, Adrian Rees

School of Neurology, Neurobiology and Psychiatry, University of Newcastle, The Medical School, Framlington Place, Newcastle, United Kingdom

Responses of neurons in the IC to amplitude-modulated stimuli are well reported, but have been limited to single component modulation. We have used tones modulated by two components to study the relationship between the modulation spectrum and the neuron's pure-tone frequency response area (FRA).

Responses of single neurons were recorded in the IC of the anaesthetised (urethane and Hypnorm) guinea pig to best-frequency tones, amplitude modulated by two sinusoidal components. The difference between these components was equal to the unit's best modulation frequency. Modulation sidebands were positioned within the excitatory, or inhibitory region of the unit's FRA, or in regions where there was no response to a pure tone. Modulation frequencies were above those to which the unit showed significant synchronisation, but \leq half the carrier frequency. Modulation was \leq 20 dB above threshold and at 50% depth. Envelope synchronisation was measured from the FFT of the response histogram.

When sidebands fell within the excitatory region of the FRA the discharge synchronised to the difference between the modulation frequencies. More pronounced synchronisation often occurred when sidebands were in inhibitory regions, but was out of phase with the response from the excitatory region. With sidebands out-

side the excitatory and inhibitory FRA, firing synchronised to the difference frequency in over half of the units.

Neurons in the IC are sensitive to interactions between modulation waveforms that fail to activate the unit when presented individually. When activated by a temporally varying stimulus, inhibitory regions of the FRA can enhance the unit's response. The presence of response modulation when components are positioned outside the pure-tone FRA suggests that neurons are capable of integrating information over a wider range of frequencies than is estimated by the FRA alone.

Acknowledgements

Wellcome Trust (AR), University of Newcastle (GW) and EPSRC (SRJ).

854 'Cocktail-Party Processing' in the Inferior Colliculus.

Gerald Langner, Claudia Simonis, Susanne Braun

Neuroacoustics, TU-Darmstadt, Schnittpahstr. 3, Darmstadt, Germany

Many acoustic signals are harmonic sounds which are generated by periodic vibrations of sound sources, like vocal cords. As a consequence over broad frequency ranges amplitude modulations arise which correspond to the fundamental of the broad band signals. In the modulation range between about 20 Hz and 1000 Hz such modulations elicit the percept of pitch. Since the cochlear frequency analysis separates different components of such signals into different frequency channels, it is essential for the auditory system to recombine these components. This task is particular difficult under noisy conditions (cocktail party effect) and requires information coming from binaural differences and amplitude modulations both characterizing a certain sound source.

In central inferior colliculus (ICC) auditory information converges on a tonotopically organized network. Temporal information about the envelope degrades in the ICC and is transformed into a rate-place code. Accordingly, units in the ICC are tuned to different modulation frequencies and are arranged in periodicity maps.

We analyzed the topographic organization in the gerbil by the 2-deoxyglucose technique. Stimuli were band limited harmonic complexes with fundamental frequencies ranging from 40 to 800 Hz. In addition synthetic vowels were presented either separately or simultaneously.

The analysis of 2-DG labels in the ICC show that periodicity is represented approximately orthogonal to tonotopic organization. On the basis of these findings we consider the periodotopic axis as the 2nd neural axis of the auditory system. In a plane perpendicular to the frequency band laminae of the ICC both parameters, frequency and periodicity (or modulation frequency) are mapped on logarithmic scales. The contribution of the ICC to 'cocktail-party processing' is demonstrated by spatial separation of activation patterns evoked by simultaneous stimulation with two vowels with different fundamental frequencies (periodicities).

Supported by Volkswagenstiftung, Germany

855 Neuronal interactions within the periodicity map in the primary auditory cortex of the Mongolian gerbil

Anke Deutscher, Henning Scheich, Holger Schulze

ALS, Leibniz Institute for Neurobiology, Brenneckestr. 6, Magdeburg, Germany

Many simultaneously present acoustic signals like in a cocktail-party situation (Cherry, *JASA* 25, 1953; von der Malsburg & Schneider, *Biol. Cybern.*, 54, 1986) challenge the auditory system. In such a situation the acoustic system has to segregate an individual sound from a mixture of concurrent sounds.

We follow the hypothesis that the periodicity of speech sounds, which is characteristic for a given speaker, is one of the main cues for the auditory system to solve this task.

A recent study demonstrated that two aspects of sound, frequency and periodicity, have different spatial representations in the primary auditory cortex field A1 of the Mongolian gerbil: A tonotopic map with a linear functional gradient is superimposed with a circular periodicity map (Schulze et al., *EJN*, 15, 2002). In such a circular periodicity map, all representations of different periodicities, i.e. different speakers' voices, have minimal and about equal distances from each other, an organization that may facilitate connections of equal strength between all representations within the field and therefore would allow for competitive signal processing ('winner-takes-all algorithm'). Here we report results from simultaneous electrophysiological recordings in representations of different periodicities of that map in search for the hypothesized inhibitory neuronal interactions.

Preliminary results demonstrate that in a situation where two AMs were presented simultaneously some units ("winners") responded to their best AM independent of additional AMs, whereas best AM responses of other units ("losers") could be inhibited by additional AMs.

Supported by the VolkswagenStiftung

856 Neuronal responses to amplitude modulated sounds in Mongolian gerbil auditory midbrain and cortex: periodicity coding or responses to distortion products?

Ines Schrottge, Henning Scheich, Holger Schulze

Auditory Plasticity and Speech, Leibniz Institute for Neurobiology, Brenneckestr. 6, Magdeburg, Germany

Neurons in the low frequency region of primary auditory cortex (AI) respond to amplitude modulated (AM) sounds with spectra completely outside their frequency response range (FRR). It has been argued that these responses reflect periodicity coding in AI (Schulze et al. 2002, *EJN*, 15, 1077-1084), but the possibility that they might be elicited by distortion products emerging from the cochlea nonlinearity has not yet been ruled out. As the most important distortion product within the units' FRR the difference tone $f_2 - f_1$ must be considered.

We carried out extracellular recordings in which an additional tone (cancellation tone, CT) was added to the AM at the frequency of the difference tone but with varied phase. If the observed responses would indeed be elicited by the difference tone within

the spectral receptive field of the unit, the additional tone should cancel this distortion product if presented (at equal intensity) in counter phase (cancellation experiment). Experiments by McAlpine (ARO Abs., 2002, 154) have shown, that it is possible to cancel the distortion product in the inferior colliculus (IC) by such a paradigm. To test if the distortion product within the cochlea had been cancelled, we carried out simultaneous recordings in AI and IC. First results indicate that whereas responses to AM with a spectrum outside the units' FRR could be cancelled by an additional CT on the level of the IC, they could not be cancelled on the level of AI.

We therefore conclude that the responses of AI units to AM with a spectrum completely outside their FRR reflect periodicity coding rather than spectral activation by cochlear distortion products. In contrast, the responses of IC units to the same AM stimuli seem – at least in some cases – to be elicited by distortion products.

857 Frequency, Periodicity, and the ICC: A Simple Model for Examining Tonotopic and Periodotopic Axes in the Inferior Colliculus

Socrates Deligeorges, David C Mountain

Biomedical Engineering, Boston University, 44 Cummington Street, Boston, MA, United States

The central nucleus of the inferior colliculus (ICC) is thought to play a central role in sound identification as well as creating psychophysical precepts such as pitch [Braun 2000]. Many of the cells in the ICC have a best frequency (BF) and best modulation frequency (BMF) to which they respond, the distribution of BFs and BMFs follows an orderly progression within the nucleus [Schreiner et al 1988] suggesting the idea of a place map for sound characteristics in the ICC with tonotopic and periodotopic axes. However, recordings from ICC cells have shown that individual units have BMFs that change with sound level; this finding casts doubt on the idea of a fixed sound characteristic map. To address this issue of ICC periodicity processing, a simple model was developed for a generic ICC cell that included the interactions between excitatory and inhibitory inputs. The single unit model was validated by comparisons to physiological data for single unit responses for several BFs and BMFs. Once the single cell model was shown to reproduce characteristics of ICC cells, particularly responses to change in amplitude, a set of ICC units were simulated. A matrix of cells was created with a BF (tonotopic) axis and a BMF (periodotopic) axis spanning a range of BFs from 0.1-20 kHz and BMFs from 10-500 Hz. Simulations were run for the entire ICC using sinusoidally amplitude modulated stimuli at various amplitudes. Although single cells had variable BMFs as stimulus amplitude increased, response intensity decreased when BMF shifted away from its low stimulus level value. However, the same periodotopic 'place' across the distribution of cells always had the maximal response due to contributions of off BF cells as intensity increased. Model results suggest that there may be a functional periodotopic axis in the ICC which may indeed play a role in creating a stable sound feature map.

858 Multiple Mechanisms Create Selectivity for FM Sweep Direction and Velocity Selectivity in Pallid Bat Inferior Colliculus Neurons

Zoltan M. Fuzessery, Dustin Richardson, Michael Coburn
Zoology and Physiology, University of Wyoming, 16th and Gibbon St., Laramie, WY, United States

The inferior colliculus of the pallid bat contains neurons that exhibit identical forms of selectivity for downward FM sweeps that use different mechanisms to achieve this selectivity. This report focuses primarily on the mechanisms that shape velocity selectivity. When these neurons are presented with FM sweeps of varying spectral bandwidths, they show bandpass selectivity for sweep duration that increases with bandwidth. When normalized for sweep velocity, these functions show an overlapping peaked tuning for sweep velocity. However, they are not necessarily selective for velocity itself. Instead, at least two inhibitory mechanisms create velocity tuning. The first is a shortpass sound duration selectivity that is apparent for tones, and created by an early inhibition generated by excitatory frequencies. The best duration for a tone can predict the velocity tuning from the time that the sweep spends within the excitatory tuning curve. The second mechanism involves a late high-frequency inhibition. The late arrival of inhibition, relative to excitation, allows the neuron to respond to rapid downward FM sweeps, but as sweep velocity decreases, the inhibition arrives before excitation, creating a highpass velocity selectivity. The timing of this inhibition is shaped by two factors. The first is the arrival time relative to excitation, tested under static conditions with tones. The second is the bandwidth of the inhibitory high-frequency domain. In a downward FM sweep, the broader the bandwidth, the sooner the sweep will encounter the inhibitory domain, and the sooner the inhibition will arrive. These results provide clear evidence that an auditory system will use different mechanisms to create a given form of response selectivity.

859 Responses of Mustached Bat Inferior Colliculus to Trapezoidal Frequency Modulation (TFM) I: Response Magnitude

William E. O'Neill^{1,2}, Wm. Owen Brimijoin²

¹*Neurobiology and Anatomy, University of Rochester School of Medicine and Dentistry, 601 Elmwood Ave., Rochester, NY, United States*, ²*Brain and Cognitive Sciences, University of Rochester, Meliora Hall, Box 270268, Rochester, NY, United States*

To investigate the encoding of repetitive frequency modulations, trapezoidal FM is advantageous in that it can be independently varied in both modulation frequency (periodicity) and modulation rate (FM per cycle). This permits separate evaluation of the contributions of periodicity and slope to responses to periodic modulation, and the degree to which inhibition and timing interact to produce selectivity.

We isolated single units in the bat IC and obtained responses to individual upward and downward linear FM sweeps (LFM) and TFM over a range of modulation (sweep) rates (MR) and frequencies (MF). For TFM, most units were high pass or bandpass for MR and low pass or bandpass for MF. The vast majority responded best to MFs between 16 and 32 Hz. This range is below that found in communication sounds containing periodic FM, but approximates the MFs in echoes reflected by flying insect prey.

Approximately half of the units responded most strongly to MRs of 1.125 kHz/ms. This MR is roughly equivalent to modulation rates found in communication sounds but it is unknown what rates are found in insect echoes.

IC units responded more vigorously to certain TFM configurations than to LFM of the same MR. However, average responses to individual FM sweeps within the TFM stimulus were typically smaller than responses to LFM of the same modulation rate, suggesting suppression evoked by periodic modulation that is not present in isolated sweeps. That MF also strongly affected response magnitude in the majority of units is evidence that these putative inhibitory processes may be delay-dependent.

Supported by NIDCD R01DC03717, P30-DC05409, NIMH T32 MH19942

860 Responses of Mustached Bat Inferior Colliculus to Trapezoidal Frequency Modulation (TFM) II: FM Directionality

Wm. Owen Brimijoin¹, William E. O'Neill^{1,2}

¹*Brain and Cognitive Sciences, University of Rochester, Meliora Hall, Box 270268, Rochester, NY, United States*, ²*Neurobiology and Anatomy, University of Rochester, 601 Elmwood Ave, Box 603, Rochester, NY, United States*

To investigate the encoding of repetitive frequency modulations, TFM is advantageous in that it can be independently varied in both modulation frequency (periodicity) and modulation rate (FM per cycle). This permits separate evaluation of the contributions of periodicity and slope to directional selectivity, and the degree to which inhibition and timing interact to produce selectivity.

We isolated single units in the bat IC and obtained responses to individual upward and downward linear FM sweeps (LFM) and TFM over a range of modulation (sweep) rates (MR) and frequencies (MF). A cycle-by-cycle analysis revealed that over half of the units were more strongly directionally selective for some configurations of TFM than to MR-matched LFM. The remaining units were equally directional to TFM and LFM. Greater directionality was not attributable to facilitation of the preferred phase of modulation or greater suppression of the non-preferred phase of modulation, but rather to cumulative suppression. That is, the periodic ongoing nature of the TFM stimulus caused a parallel downward shift in spike counts for both preferred and non-preferred phases; this shift resulted in apparent greater directionality due to the conventional method of quantifying directionality.

MR identically affected directionality to both TFM and LFM. That is, for all directional units, the MR that elicited the greatest directionality was the same for both TFM and LFM. In roughly half the units, directionality increased with MF. The effect of MF in the remaining units was less systematic.

The effect of FM directional selectivity on the coding of periodic FM is unclear at this stage. In terms of absolute response magnitude, non-directional units respond more strongly than directional units since they fire twice in every modulation cycle. MR- and MF-dependent directionality may serve to filter out responses to stimuli not relevant to behavior.

Supported by NIDCD R01DC03717, P30-DC05409, NIMH T32 MH19942

861 Interference of contralateral white noise with the processing of FM-direction in right human auditory cortex

Nicole Behne¹, Henning Scheich², André Brechmann¹

¹*Non-Invasive Brain Imaging, Leibniz Institute for Neurobiology, Brennekestr. 6, Magdeburg, Germany,* ²*Department of Auditory Learning & Speech, Leibniz Institute for Neurobiology, Brennekestr. 6, Magdeburg, Germany*

Frequency modulations (FM) are information bearing elements in human speech. Animal and human studies suggest that the directional categorization of FM (rising vs. falling) is a function of the right auditory cortex (AC). To test for hemispheric dominance we analyzed hemispheric differences in AC activation with fMRI under dichotic listening conditions.

FM with different center-frequencies were presented monaurally or binaurally. 17 subjects had to perform a directional categorization task. In a 2nd study we tested the influence of contralaterally presented white noise intended to interfere with the directional categorization of monaural FM.

In study I contralateral stimulation with FM led to strongest activation in each AC, binaural stimulation to intermediate and ipsilateral stimulation to weakest activation. In study II the activation of left AC was similar to study I. Contralateral FM with ipsilateral noise led to strongest activation and ipsilateral FM with contralateral noise to weakest activation. In right AC (contrary to study I) contralateral FM with ipsilateral noise led to weakest activation, bilateral FM to intermediate and ipsilateral FM with contralateral noise to largest activation.

The result of study I is in accordance with electrophysiological studies showing that the contralateral auditory pathway is mainly excitatory whereas the ipsilateral is in part inhibitory. The stronger effect of noise on the activation of right AC in study II can be explained assuming a right AC specialization for the processing of FM-direction. FM presented to the right ear does not reach right AC directly via the contralateral pathway. Thus, competition to the direct noise input may have led to increased activity in right AC.

862 Reduced right auditory cortex activity in schizophrenic patients during directional categorization of FM sweeps.

André Brechmann¹, Bernhard Bogerts², Henning Scheich³

¹*Non-Invasive Brain Imaging, Leibniz-Institute for Neurobiology, Brennekestr. 6, Magdeburg, Germany,* ²*Clinic for Psychiatry, Otto-von-Guericke-University Magdeburg, Leipziger Str. 44, Magdeburg, Germany,* ³*Auditory Learning & Speech, Leibniz-Institute for Neurobiology, Brennekestr. 6, Magdeburg, Germany*

Frequency modulations (FM) are information bearing elements in speech, and voice fundamental frequency changes are a key to discrimination of prosodies. Both the perception of prosodies which is deficient in schizophrenic patients and categorization of FM-direction seem to be a right hemispheric function. To reveal mechanisms of prosody processing we used FM sweeps as an acoustic model and investigated fMRI activation in auditory cortex (AC) during uninformed listening and categorization of FM-direction in schizophrenic patients.

FM sweeps varying in center frequency were presented to 14 subjects (7 schizophrenic patients). During the 1st scan subjects just had to attend to the stimuli (uninformed listening). In the 2nd scan (same session) they had to distinguish rising from falling FM. In each scan 80 functional volumes were collected in a 3 Tesla scanner using a low noise (54dB(A)) conventional gradient echo sequence within 12 min.

During categorization of FM direction healthy subjects revealed significantly stronger activation in right AC areas compared to uninformed listening. This task-dependent increase in activation was not observed in schizophrenic patients resulting in significantly less activation in right but not left AC compared to control subjects.

The involvement of the right auditory cortex of healthy subjects in FM directional categorization supports the important role of the right hemisphere in prosody processing even though linear FM is an impoverished model of pitch contour in prosodies. The lack of task-dependent activation in the patients is consistent with prosodic deficits and reduced hemispheric laterality in schizophrenia.

863 Two-tone versus toneburst stimuli to elicit the ASSR to single and paired frequency components: Inferior colliculus (IC) and auditory cortex (AC) responses, pre- and post-carboplatin

Robert Burkard^{1,2}, Kathleen Szalda¹

¹*Center for Hearing and Deafness, University at Buffalo, 3435 Main Street, Buffalo, NY, United States,* ²*Communicative Disorders and Sciences, University at Buffalo, 3435 Main Street, Buffalo, NY, United States*

We have previously shown that the auditory steady state response (ASSR), recorded from chinchilla IC, is larger to brief tonebursts (TB) than to two-tone (2-tone) stimuli with the same peak sound pressure level. We have also shown that pairing multiple stimuli (e.g., two TB or two 2-tone stimuli) reduces the amplitude of each component at moderate stimulus levels. Here, we extend these studies to the auditory cortex, pre- and post carboplatin.

Seven chinchillas had electrodes chronically implanted in the right IC and AC. Following recovery, they were placed in a passive restraint, with an earphone placed in the left ear canal. Both IC and AC were recorded from simultaneously. Stimuli were trains of one or two TBs presented at rates of 90 Hz (2 kHz) or 129 Hz (4 kHz). Alternatively, stimuli were one or two two-tone stimuli, with a difference tone frequency of 90 Hz (2000 Hz/2090 Hz) or 129 Hz (4000 Hz/4129 Hz). Following data acquisition, the animals were given 75 mg/kg carboplatin (IP), and ~4 weeks later, the animals were run on the same protocol, then sacrificed and hair cell counts made. Carboplatin produced substantial inner hair cell loss, and little or no outer hair cell loss. Precarboplatin, in the IC and AC, responses to TBs were larger than seen for 2-tone stimuli. The addition of a second stimulus typically reduced response amplitudes from IC and AC to both TBs and 2-tone stimuli. Post-carboplatin, response amplitudes typically decreased (re: precarboplatin amplitudes). The largest decrease in amplitude was typically for the single TB stimulus. In some instances, there was little effect of adding a second 2-tone stimulus on ASSR amplitude. This lack of

an effect of the addition of the second 2-tone stimulus was seen most clearly for the IC and AC responses for the 4 kHz stimuli.

Work supported by NIDCD DC03600

864 The Effects of a Second Two-Tone Stimulus on the Auditory Steady State Response (ASSR) from the Chinchilla Inferior Colliculus and Auditory Cortex:

Kathleen Szalda¹, Robert Burkard^{1,2}

¹Center for Hearing and Deafness, University at Buffalo, 3435 Main Street, Buffalo, NY, United States, ²Communicative Disorders and Sciences, University at Buffalo, 3435 Main Street, Buffalo, NY, United States

We examined the effects of a second two-tone stimulus on the ASSR, pre and post carboplatin. Tungsten electrodes were chronically implanted in the inferior colliculus (IC) and auditory cortex (AC) of seven adult chinchillas following anesthesia with ketamine/acepromazine. Chinchillas were put in a passive restraining device and placed in a sound-attenuating chamber. They were tested one week following surgery, subsequently given carboplatin (75 mg/kg), which causes selective IHC loss in chinchillas, and tested a second time approximately 4 weeks later. Stimuli consisted of either one or two two-tone stimuli which were presented to the left ear; recordings were made from the right IC and AC simultaneously. The stimuli through channel 1 remained constant and resulted in a difference tone (DT) of 90 Hz, while the stimuli through channel 2 varied and resulted in DTs of 50, 70, 129, 150, and 170 Hz. Each two-tone stimulus in channel 2, as well as the stimulus in channel 1, were presented alone. In addition, all of the stimuli in channel 2 were presented simultaneously with the stimuli in channel 1. The stimuli decreased from 80 to 30 dB pSPL in 10 dB steps. In most conditions, there was a decrease in response amplitude with the addition of a second two-tone stimulus in both the IC and AC, before and after the administration of carboplatin. The reduction in response amplitude was greater at the higher stimulus levels. Generally, there was a reduction in response amplitude in the IC following the administration of carboplatin when the two-tone stimuli were presented either alone or simultaneously. The AC response typically showed a decrease in response amplitude following the administration of carboplatin. Post-carboplatin, there was an increase in response amplitude, most notably for the single two-tone stimuli, for stimuli with DTs equal to or less than 70 Hz. This effect was most prominent at the higher stimulus levels.

Supported by NIH DC03600

865 Test-Retest Reliability of the P1-N1-P2 Acoustic Change Complex

Brett A. Martin^{1,2}, Wei Wei T. Lee², Mitchell Steinschneider³, Diane Kurtzberg³

¹School of Graduate Medical Education, Seton Hall University, 400 South Orange Avenue, South Orange, NJ, United States, ²Dept. of Otolaryngology, Albert Einstein College of Medicine, 1410 Pelham Parkway, Bronx, NY, United States, ³Depts. of Neurology and Neuroscience, Albert Einstein College of Medicine, 1410 Pelham Parkway, Bronx, NY, United States

The cortical auditory P1-N1-P2 complex is typically elicited by

stimulus onset. It can also be elicited by an acoustic change in an ongoing sound such as speech. This latter response is referred to as the acoustic change complex (ACC). The aims of this study were: 1) to determine the test-retest reliability of the ACC, and 2) to compare the test-retest reliability of the ACC to that of the mismatch negativity (MMN) and to the P1-N1-P2 evoked by stimulus onset.

Ten normal-hearing adults were enrolled in the study. Subjects were tested and retested in separate sessions. Stimuli for the ACC were the speech sound /ui/ and a tone complex consisting of pure tones sharing the same center frequency as the F0, F1, F2 and F3 of the speech sound. Stimuli for the MMN were /u/ and /i/ extracted from the sounds above. These stimuli were presented in an oddball paradigm with each sound presented as standards and deviants in separate runs. All stimuli were presented at 80 dB pSPL. Evoked potentials were recorded from 32 channels using surface electrodes.

Test-retest reliability was assessed in two ways. Waveform test-retest reliability was assessed using the intraclass correlation statistic (ρ), which takes into account latency and amplitude differences regardless of morphology. Second, test-retest reliability of peak amplitudes and latencies of each major component was assessed using t-tests.

Main findings of this study include the following: 1) The ACC shows excellent test-retest reliability for grand mean data and for data from individual subjects. 2) Test-retest reliability of the ACC to speech nearly matches that of the P1-N1-P2 elicited by stimulus onset. 3) The ACC is more reliable than the MMN. 4) The excellent test-retest reliability obtained for the ACC in individual subjects emphasizes that this evoked potential complex may serve as a useful index in the clinical evaluation of speech discrimination capacity.

[Work supported by DC05386 and DC00223]

866 Neural representation of amplified speech cues in persons with and without hearing loss

Kelly Tremblay, Pamela Souza, Laura Kalstein, Lendra Friesen, Curtis Billings

Dept. of Speech and Hearing Sciences, University of Washington, 1417 NE 42nd St., Seattle, WA, United States

The Acoustic Change Complex (ACC) cortical evoked potential is thought to reflect the neural detection of acoustic cues contained in speech. It is easy to record in clinical settings; therefore, there is interest in using the ACC to monitor changes in the neural representation of speech-sounds following amplification or auditory training. However, if the ACC is to be used to examine longitudinal changes in neural activity following rehabilitation, it is first critical to determine if: 1) the neural response patterns are stable from test to retest, and 2) different speech tokens evoke distinct neural patterns. This is especially important when recording the ACC in hearing aid users because acoustic stimuli are presented in sound field and then altered by the hearing aid. Therefore, we recorded the ACC response from seven normal-hearing and seven hearing-impaired adults wearing hearing aids in sound field. Stimuli were naturally produced 'see' and 'shee' tokens from the standardized UCLA version of the Nonsense Syllable Test (NST)

(Dubno and Schaefer, 1992). Each subject was fit monaurally with a behind the ear hearing aid set for linear (compression limiting) processing. The volume wheel was deactivated so that subjects could not adjust the amount of gain provided by the hearing aid. Using a repeated measures design, subjects were tested and then retested, in sound field, over an eight-day period.

Naturally produced speech syllables 'see' and 'shee' evoked distinct ACC patterns. Specifically, peak latencies signaling the onset of the vowel 'ee' were earlier for the 'shee', compared to the 'see' stimulus, consistent with the shorter fricative duration of the 'sh' than for the 's' sound. These patterns were reliably recorded in individuals and stable over time. Intraclass correlations comparing test and re-test waveforms ranged from .68 to .93. These data suggest that the ACC is a reliable measure for assessing transmission of speech cues through a hearing aid.

867 Effects of Contralateral Noise on the Auditory Middle Latency Response.

Vishakha Waman Rawool¹, Maria Virginia Brouse²

¹Communication Sciences and Disorders, Southwest Missouri State University, 901 S National Ave, Springfield, MO, United States, ²Audiology, Otolaryngology Physicians of Lancaster, 1918 Misty Dr, Mt Joy, Pa, United States

A few studies have reported the effects of contralateral noise on the auditory middle latency response (AMLR) of guinea pigs. The reported results are controversial, perhaps due to differences in state of arousal of guinea pigs. In the current study, effects of contralateral noise on the human AMLR were investigated. Thirty young women (19 to 29 years) participated in the study. They all had auditory sensitivity within normal limits and normal middle ear function. AMLRs were recorded by presenting rarefaction clicks (80 dB nHL) to the left ear without noise and with broadband noise (30, 40, 50 dB nHL) to the right ear. These four conditions were presented in random order. Neuro-electric activity was recorded by silver-silver chloride electrodes on ipsilateral and contralateral earlobes and vertex, with ground on the low forehead. Averaging occurred over a 100 ms time base. Two separate recordings (trial 1 and trial 2) of 256 averaged sweeps were obtained for each test condition. Participants were instructed to keep their eyes open and to focus on a picture in front of them. A break was provided after four recordings. All analyses were conducted on the Pa wave since Pa is considered the most consistent and reliable component of the AMLR. ANOVAs on the ipsilateral Pa amplitudes and latencies showed no effect of noise, but a significant trial effect was apparent. Specifically, a significant reduction in Pa amplitudes and increase in latencies were noted during the second trial of recordings when compared to the first trial of recordings in the same condition. These results suggest that contralateral noise has no effect on Pa amplitudes or latencies. The results also suggest that Pa amplitudes can decrease over time with the presentation of a repetitive stimulus, but the introduction of a novel stimulus such as noise in the opposite ear can avert this reduction. These results will be discussed with reference to the possible generators of the Pa component of the AMLR.

868 Correspondance of auditory evoked fields, psychoacoustic loudness, and simulated auditory-nerve activity produced by Schroeder tone complexes

Andre Rupp¹, Norman Sieroka¹, Torsten Dau²

¹Dept Neurology, University of Heidelberg, Sect Biomagnetism, INF 400, Heidelberg, Germany, ²Centre for Applied Hearing Research, Technical University of Denmark, Oersteds Plads, bldg. 352, Kgs. Lyngby, Denmark

Kohlrausch and Sander (1995) showed in experiments on psychophysical masking period patterns (MPP) that tone-complex maskers with negative Schroeder phase (m-) can produce higher detection thresholds for tones than the temporally inverted Schroeder positive (m+) maskers, due to the dispersive characteristics of the cochlear. The current experiments were conducted to investigate such dispersion effects and to assess the correspondence between neuromagnetic responses, psychoacoustical loudness, and (simulated) auditory-nerve (AN) activity produced by the same stimuli. MPPs were designed using a 5-ms tone pulse at 1100 Hz tone embedded in flat-spectrum maskers with a fundamental frequency of 100 Hz and harmonics between 200 and 2000 Hz. The phase choices of the maskers included (a) zero phase, (b) m+ phase, and (c) m- phase. The temporal position of the tone pulse was varied between five positions relative to the masker period (0, 2, 4, 6, and 8 ms). Middle latency auditory evoked fields (MAEF) were recorded in seven subjects using whole-head magnetoencephalography (MEG). The MAEF-magnitude showed a U-shaped pattern for both Schroeder phase maskers when plotted as a function of the delay of the tone pulse, with a minimum at 4 ms. However, in the m- conditions, all MAEF responses exhibited lower magnitudes than those obtained in the m+ condition. In contrast, the values for the zero-phase masker showed an inverse U-shaped pattern with the largest response at 4 ms. The obtained loudness scales, based on the Bradley-Terry-Luce method, and the simulated AN activity using a transmission-line filterbank model and Meddis' hair-cell model revealed similar qualitative patterns. Thus, the close correspondence between the neuromagnetic, psychoacoustical and AN-activity patterns suggest that MAEFs might serve as an objective tool to investigate peripheral dispersion effects in human listeners non-invasively.

869 Background noise activates attentional systems in an auditory oddball task: a PET and ERP study

Alan H. Lockwood^{1,2}, Mary Lou Coad³, David S. Wack⁴, Paul J. Galantowicz⁵, Robert F. Burkard⁶

¹Neurology and Nuclear Medicine, VA Western NY Healthcare System, Center for PET (115P), VAWNYHS, 3495 Bailey Ave, Buffalo, NY, United States, ²Neurology and Nuclear Medicine, University at Buffalo, 3495 Bailey Avenue, Buffalo, NY, United States, ³Nuclear Medicine, University at Buffalo, 3495 Bailey Avenue, Buffalo, NY, United States, ⁴Research, VA Western NY Healthcare System, 3495 Bailey Ave, Buffalo, NY, United States, ⁵Nuclear Medicine, VA Western NY Healthcare System, 3495 Bailey Ave, Buffalo, NY, United States, ⁶Communicative Disorders and Sciences, University at Buffalo, Parker Hall, 3435 Main St, Buffalo, NY, United States

Accurate perception of auditory stimuli becomes more difficult as

background noise increases. To investigate the mechanisms that underlie this phenomenon, we measured neural activity with 150-water PET scans and ERP recordings as 12 subjects (23.2 ± 4.1 years, SD, 9 M) with normal hearing performed an auditory odd-ball perception task amidst increasing levels of background noise. The frequent stimulus, .8 probability, was 950 Hz, .5 s duration, 80 dB SPL, and the rare stimulus, .2 probability, was 500 Hz, .5 s duration 80 dB SPL with an interstimulus interval that randomly ranged from 1.4 - 1.6 sec. Stimuli were delivered to the right ear. ERPs were computed from 64 channels of EEG. Four randomly ordered conditions were: one scan at rest, no auditory stimulation, no ERP; two scans of stimuli without background noise; two scans with stimuli plus 60 dBC background noise; and two scans with stimuli plus 80 dBC background noise. Statistical parametric analysis of the PET images in the noise versus rest comparisons showed increasing bilateral neural activity in auditory cortical sites ($L > R$) as the noise level increased. In the high noise condition, left-sided cortical activation extended into Broca's area but remained confined to primary and immediately adjacent auditory cortex on the right. In an attention-related site in the anterior cingulate, neural activity was increased in the high noise condition compared to the no noise condition. An analysis of the mean global field potentials associated with the N100 and P300 ERPs showed increased latencies and reduced voltages as noise levels increased. Extension of sites of neural activity anterior to left primary auditory cortex, most evident in the high noise condition, suggests these regions are activated by the cognitive demands of the P300 task. Increased task difficulty, caused by the addition of background noise, activates elements of the anterior attention system. Supported by a VA Merit Review Grant.

870 Noise Induces Inhibition of Speech Activation in fMRI Studies of Human Auditory Cortex in Normal Hearing Subjects

Jill B. Firszt¹, Wolfgang Gaggl¹, Christina L. Runge-Samuels¹, Phillip A. Wackym¹, John L. Ulmer², Robert W. Probst²

¹Otolaryngology and Communication Sciences, Medical College of Wisconsin, 9200 W. Wisconsin Avenue, Milwaukee, WI, United States, ²Radiology, Medical College of Wisconsin, 9200 W. Wisconsin Avenue, Milwaukee, WI, United States

In animal studies, measured responses for single auditory nerve fiber (Kiang, 1965) and cochlear nucleus units (Burkard & Palmer, 1997) have shown a decrease in response magnitude for click stimuli in the presence of broadband noise. In this study using speech stimuli, we examined the effects of noise on activation of the human auditory cortex. Speech stimulus /ba/ was presented at 80 dB HL monaurally to the right ear of adult subjects with normal hearing, and in the presence of speech spectrum noise at varied signal-to-noise ratios (e.g., +15, +10 and +5 dB). Functional magnetic resonance imaging (fMRI) was used to investigate hemispheric response activation. To reduce the impact of acoustic scanner noise, hemodynamic responses were measured with a clustered-volume acquisition sequence (Hall et al., 1999; Ulmer et al., 1998). The total number of activated voxels ($p < 0.01$) was calculated by hemisphere per experimental condition. Preliminary data suggest that, as expected, cortical activation for

speech in quiet was greater in the contralateral hemisphere. In the presence of noise, however, cortical activation was suppressed compared to that in quiet, and to a greater extent in the contralateral compared to ipsilateral hemisphere. Additionally, cortical activation in both contralateral and ipsilateral hemispheres was reduced with each subsequent increase in noise level. For the most challenging listening condition (SNR = +5), there was a reduction in asymmetry between hemispheres and a substantial decrease in overall activation compared to that observed for speech in quiet.

Supported by NIH/NIDCD K23DC05410

871 In-situ free field sound generation for fMRI of the auditory pathways

Joris J.J. Dirckx¹, Vincent Van Meir², Annemie Van Der Linden²

¹Biomedical Physics, University of Antwerp, Groenenborgerlaan 171, Antwerp, Belgium, ²Bio-imaging lab, University of Antwerp, Groenenborgerlaan 171, Antwerp, Belgium

Functional MRI of the auditory system brings basic insight in the complex pathways of auditory processing. On top of the usual challenges involved with fMRI, auditory studies face an additional problem: sound has to be conducted to the subject within the high static magnetic field of the MRI machine, without disturbing the imaging process. Systems using tubes for sound conduction are generally used, but inherently have reduced high frequency response. In studies using animal models an important additional problem occurs: it is virtually impossible to obtain a good fit between the ear canal and the sound conduction tube, which causes uncontrollable loss of sound pressure. Because in-situ measurement of the actual applied sound pressure in such systems is impossible, good calibration and reproducible frequency response is very difficult.

We present a system for free field sound generation inside the MRI magnet, based on dynamic speakers which use the MRI magnetic field to move the speaker coil, instead of the field of a ferro magnet. We explain how the magnet coil is set into motion in the linear field of the MRI magnet, instead of in the radial field which is normally present in a speaker. Instead of the normal piston like motion, a rocking motion of the speaker cone is to be expected, which will affect frequency response. Frequency response curves will be shown which demonstrate that the system performs particularly well in the high frequency region. The response curve is compared to tube systems. The only metal part in the speaker is the copper coil, with a weight of less than 50 mg. We present phantom measurements which demonstrate minimal imaging artifact. The system is demonstrated in an application example, where we use the system for fMRI studies of the auditory pathways in songbirds (starlings).

872 Functional Neuroimaging (PET) of Responses to Changes in Attack Time and Spectral Centroid

Arnaud Coez^{1,2}, Stephen McAdams^{3,4}, Bennett K. Smith³, Sandrine Vieillard³, Sophie Savel³, Monica Zilbovicius¹, Pascal Belin⁵, Séverine Samson⁶, Yves Samson⁷

¹ERM0205 INSERM-CEA, Service Hospitalier Frédéric Joliot, 4 place du Général Leclerc, Orsay, France, ²Laboratoire de, Correction Auditive, 20 rue Thérèse, Paris, France, ³PCM, IRCAM-CNRS, 1 place Igor Stravinsky, Paris, France, ⁴Département d'Etudes Cognitives, Ecole Normale Supérieure, 45 rue d'Ulm, Paris, France, ⁵Département de Psychologie, Université de Montréal, CP 6128 succ Centre-Ville, Montréal, PQ, Canada, ⁶UFR de Psychologie, Université de Lille III, Pont des Bois, BP 149, Villeneuve d'Ascq, France, ⁷Service des Urgences Cérébrovasculaires, Hôpital de la Salpêtrière, 91 bd de l'Hôpital, Paris, France

Cerebral responses to changes in acoustic parameters related to timbre were measured with PET. Listeners' sensitivity functions to changes in attack time and spectral centroid were determined psychophysically using constant stimuli and go/no-go paradigms. Individually determined differences corresponding to d' levels of 1.5, 2.5, 3.5 and 4.5 in a same/different paradigm were then presented in a go/no-go paradigm during brain imaging. Relative regional cerebral blood flow was determined using PET in two groups of eight listeners, one for each of the two timbre correlates. For each listener four baseline scans were performed with presentation of a standard stimulus. Eight scans were performed during two presentations of each of the four d' levels of stimulus change during which listeners were asked to mentally detect the deviant events. For attack time, rCBF increases relative to baseline were observed bilaterally in cerebellum, deep gray nuclei, inferior frontal gyrus, superior temporal gyrus and insula, in left pre-central cortex, and in right medial frontal gyrus and inferior parietal cortex. rCBF decreases for attack time were found in left frontal regions and in middle temporal gyrus bilaterally, in left posterior areas (BA7/19, BA20, BA37) and in right uncus and medial occipital gyrus. For spectral centroid, rCBF increases occurred in cerebellum, thalamus, lenticular nucleus, pre-central gyrus bilaterally, and in left superior frontal gyrus (BA6) and right frontal regions. rCBF decreases occurred in the posterior part of the brain in inferior and medial temporal gyri bilaterally, in left inferior temporal gyrus, occipital gyrus and parahippocampic gyrus, and in right precuneus and angular gyrus. For neither acoustic parameter were significant linear correlations found between d' and rCBF. The results are discussed in the context of similar studies on detection of level and duration changes.

873 Multi-channel recordings from combination-sensitive neurons in inferior colliculus of the mustached bat.

Kianoush Sheykholslami, Donald Gans, Jeff J Wenstrup
Neurobiology, NEOUCOM, 4209 state route 44 p.o. box 95, rootstown, oh, United States

We recorded single and multiple unit responses from the inferior colliculus (IC) of mustached bats using a 16-channel (Michigan) linear electrode array with 50 μ m spacing between recording sites.

The goals were to identify basic and complex response properties described in previous single unit studies of the IC, and to examine their spatial distribution. In "vertical" electrode penetrations (dorsal-to-ventral), all channels remained within the expanded 58-60 kHz representation of the IC. In "angled" penetrations (dorsolateral-to ventromedial) the active sites were distributed within both the 58-60 kHz and systematically higher frequency representations in the bat's audible range. Previous single unit recordings from these frequency representations showed combination sensitivity, in which the best frequency response was facilitated or inhibited by a second low-frequency tone (10-32 kHz) for particular temporal relationships. We assessed combination sensitivity by pairing high- and low-frequency tones at various delays. In all seven vertical penetrations, each of the 16 recording sites displayed combination-sensitive inhibition, in which best frequencies tuned to 58-60 kHz were inhibited by a simultaneous low-frequency tone. In four of six angled penetrations, we observed combination-sensitive inhibition in the more dorsal sites tuned to 58-60 kHz, but combination-sensitive facilitation occurred at non-zero delays at the more ventral sites tuned to higher frequencies. These facilitated, delay-tuned responses are thought to encode delays between a sonar call and returning echoes. Two other angled penetrations showed no facilitatory interactions tuned to these higher frequencies. These results show that the multi-channel array can reproduce many of the complex responses observed in single unit recordings. In addition, the multi-channel recordings suggest some structure to the arrangement of complex responses in the mustached bat's IC.

Supported by RO1 DC00937 from NIDCD.

874 The Representation of Categorically Perceived Vocalizations in Mouse Auditory Cortex

Robert C Liu¹, Jennifer F Linden², Christoph E Schreiner³

¹Sloan-Swartz Center, Physiology, Otolaryngology, UCSF, 513 Parnassus Avenue, San Francisco, CA, United States,

²Otolaryngology, UCSF, 513 Parnassus Avenue, San Francisco, CA, United States, ³Sloan-Swartz Center, Otolaryngology, UCSF, 513 Parnassus Avenue, San Francisco, CA, United States

Studies in mice suggest that they categorically perceive certain communication vocalizations, a behavior that enhances the value of the mouse as a model for auditory research. Specifically, isolated mouse pups emit ultrasound whistles that elicit searches and retrievals by mothers. Narrow bandwidth noise bursts in the ultrasound frequency range are effective models for these calls, evoking a similar preference level from mothers as natural vocalizations. However, when their bandwidth becomes too large (> 22.5 kHz), the noise bursts abruptly lose their favored status. Indeed, labeling and discrimination studies indicate that mothers categorically perceive these noise models as pup-like as a function of their bandwidth (Ehret and Haack, 1981). Although these behavioral experiments were carried out more than twenty years ago, the neural representation of this categorical auditory percept is still unknown.

To address this, we performed experiments on ketamine/medetomidine anesthetized mothers of the CBA/CaJ strain. Since histological studies hint that auditory cortex may reflect pup call recognition (Fichtel and Ehret, 1999), we focused on measuring

cortical activity driven by natural vocalizations and ultrasound noise models of different bandwidths. Although the responses of individual multiunit clusters seldom exhibit a clear bandwidth boundary at 22.5 kHz, pooled responses show greatest firing rate change with increasing bandwidth near 22-25 kHz. This representation might facilitate the formation of a categorical boundary.

875 Temporal Integration of Multisyllabic Sequences in the Frontal Auditory Field of the Mustached Bat, *Pteronotus parnellii*

Jagmeet S. Kanwal, Palle D. Prasada Rao, Zhicheng Lai, Matthew J. Clement

Physiology and Biophysics, Georgetown University, 3900 Reservoir Rd, NW, Washington, DC, United States

For auditory communication, temporal integration is an important neural mechanism for the representation and perception of complex, multisyllabic calls. To test for this function in a frontal auditory field (FAF), we recorded naturally emitted syllable sequences from a captive colony of free-flying mustached bats. Syllable sequences were digitized at a sampling rate of 250 kHz, recorded directly to a computer and prepared as stimuli. Using tungsten microelectrodes (~10 μm tip diameter), we recorded extracellular responses of single neurons ($n=33$), multiunit activity as well as evoked local field potentials (LFPs) from 27 sites in the FAF of 5 awake animals. Stimuli consisted of 3-4 second long multisyllabic sequences presented repeatedly, once every 5 seconds, at ~90 dB SPL. Syllables within sequences were presented as normal, in reversed order and as time-reversed. Of the 29 different syllables present within 4 separate sequences, at least 16 produced a distinct response at one or more recording sites. In 61% of the cases ($n=65$), the response latency, amplitude and/or shape of the averaged (over 50 trials) LFP elicited by a normal syllable was modified because of order-reversal; in 64% of the cases, it was modified because of time-reversal and in 41% of the cases, it was modified because of both order- and time-reversal of the syllable sequence. In nearly 30% of the cases, this affect was specific to the re-ordering of syllables in a sequence. Single unit responses frequently matched the LFP data, but were less robust. These data suggest that the response of FAF neurons to a particular syllable in a sequence can be influenced by the syllables preceding it. FAF neurons, however, did not show a nonspecific, end-of-sequence response, suggesting that in untrained bats, temporal integration of neural activity up to the level of the FAF is most likely limited to the subsecond range.

Supported by NIH/NIDCD research grant DC02054 to JK.

876 Spectral Modulation of Temporal Responses in Human and Monkey Primary Auditory Cortex: Relevance for Voice Onset Time (VOT) Encoding

Mitchell Steinschneider¹, Yonatan I Fishman¹, Igor O Volkov², Matthew A Howard, III²

¹Neurology, Albert Einstein College of Medicine, 1300 Morris Park Avenue, Bronx, NY, United States, ²Neurosurgery, University of Iowa College of Medicine, 200 Hawkins Dr, Iowa City, Iowa, United States

We have reported that population responses evoked by speech

sounds in Heschl's gyrus and monkey primary auditory cortex (A1) may facilitate categorical perception, as syllables with a short VOT and generally perceived as /da/ evoke a prominent response only to consonant release, while those with a longer VOT and identified as /ta/ elicit prominent responses to both consonant and voicing onsets. This scheme fails to directly account for VOT boundary shifts that occur with changes in consonant place of articulation (POA). We investigate this issue by examining responses evoked by syllables varying in both VOT and first formant (F1) frequency recorded directly from Heschl's gyrus in a patient undergoing surgical evaluation for medically intractable epilepsy (IRB and patient approved), and by evaluating activity in monkey A1 evoked by 2-tone complexes varying in their tone onset times.

Results in the human demonstrate that: 1) perceptual boundaries are associated with multiple physiological temporal response patterns; and 2) the strength of the response to voicing onset decreases with decreased F1 in a manner that parallels the subject's perceptual boundary shifts. Data in the monkey indicate that temporal response patterns are based on the relationship between the tone frequencies and the best frequency of the recording sites. Modeling A1 temporal response patterns indicate that as spectral disparity between the 2 tones increases, response strength to the second tone onset diminishes. These data offer an explanation for VOT boundary shifts with changes in consonant POA that is partly determined by basic physiological mechanisms of cortical sound encoding. Supported by DC00657 and DC00120.

877 What makes a 'complex sound' a speech sound, and what region of the brain makes the decision?

Roy D. Patterson¹, Stefan Uppenkamp², Ingrid Johnsrude³, Denis Norris³

¹Centre for the Neural Basis of Hearing, Physiology Department, Downing Street, Cambridge, United Kingdom, ²Medizinische Physik, Universität Oldenburg, 26111 Oldenburg, Oldenburg, Germany, ³Cognition and Brain Sciences Unit, Medical Research Council, 15 Chaucer Road, Cambridge, United Kingdom

In an effort to reveal where phonological processing of vowel sounds begins in the auditory system, we developed a set of 'damped' English vowels and a set of spectrally matched contrast stimuli that sound nothing like speech (musical rain). In an initial fMRI experiment, we showed that damped vowels and musical rain produced the same level of activation in auditory cortex [Heschl's gyrus (HG) and planum temporale (PT)], and that the first region that distinguished the speech sounds from the non-speech sounds was in the superior temporal sulcus (STS) below auditory cortex. The fine structure of damped vowels and musical rain differ along a number of dimensions, and so, in an effort to refine our understanding of the processing performed in our candidate 'phonological' region, we developed four more forms of synthetic speech (foreign vowels, inverted vowels, whispered vowels and sinusoidal vowels). They were all rated as less like speech than damped vowels and more like speech than musical rain. An fMRI experiment revealed: In the central section of HG, all of the six types of stimuli produced strong activation when contrasted with silence, but there was no differential activation for any one stimulus. In the STS and the middle temporal gyrus (MTG), the level of activation was strongly correlated with the speech-similarity rat-

ings except for the sinusoidal vowels which produced excess activation relative to their speech-similarity rating. Moreover, sinusoidal vowels produced much stronger activation than any of the other stimuli on the surface of the temporal lobe in the region just anterior to the lateral extension of HG. (Research supported by the UK Medical Research Council, G9901257)

878 Analysis of Vocalization Playback-Induced Immediate Early Gene Expression in Subdivisions of Marmoset Auditory Cortex Identified by Neurofilament Antibodies

Ashley L Pistorio¹, Stewart Hendry², Xiaoqin Wang¹

¹Department of Biomedical Engineering, Johns Hopkins School of Medicine, 720 Rutland Ave, 424 Ross Bldg, Baltimore, MD, United States, ²Department of Neuroscience, Johns Hopkins University, Zanvyl Krieger Mind/Brain Institute, 3400 N. Charles St, Krieger Hall Rm 338, Baltimore, MD, United States

Immediate early gene (IEG) localization is useful because it provides both physiological and anatomical markers in the same subject. In this study, we combined IEGs (*egr-1* and *c-fos*) with neurofilament-H (SMI-32 and NF-200) immunocytochemistry to identify cortical areas and specific cell types that are related to playback stimuli of marmoset vocalizations. These anatomical and histological analyses were further correlated with electrophysiological characterization of neurons in various auditory cortical areas, recorded in the same animals. The core (A1, R, and RT) and secondary (lateral and medial belt/parabelt) auditory areas could be consistently differentiated by the neurofilament-H stains, which also allow one to visualize lamina and cell types. In some animals, sections were double-labeled for neurofilament-H and for one IEG, enabling visualization of cell types expressing the IEG protein product and more precise distinction of any anatomical organization. In core areas, IEG expression occurred in sparse columnar patches, but additionally extended in a broad band spanning only through layers 2-3. Secondary areas, on the other hand, exhibited larger columnar patches of IEG expression, wider in both the rostral-caudal and the medial-lateral directions. *C-fos* appeared to be expressed in non-pyramidal cells, whereas *egr-1* was expressed in multiple cell types, including pyramidal cells. The combination of the techniques for studying IEG expression in response to well defined acoustic stimuli with anatomical analysis of cortical subdivisions and cell types should help pinpoint areas where more detailed electrophysiological recording or anatomical tracing experiments could be performed.

(Supported by NIDCD Grants DC03180, DC05808)

879 Discrimination of Natural Sounds in the Songbird Auditory Forebrain

Rajiv Narayan, Kamal Sen

Hearing Research Center, Biomedical Engineering, Boston University, 44 Cummington St., Boston, MA, United States

Although complex natural sounds such as human speech and birdsongs display dynamic patterns on multiple time-scales, conventional methods for characterizing neural discrimination typically neglect spike train dynamics. Here we use a computational model to investigate how the dynamic structure of spike trains contributes to the discrimination of natural sounds, and characterize changes

in discriminability as a function of time.

Our model is based on the spectral temporal receptive field (STRF), a quantitative description of the stimulus-response properties of auditory neurons. We use experimentally derived STRFs from field L (the avian analog of auditory cortex) to model neural spike trains in response to an ensemble of birdsongs. We then quantify the discriminability of spike trains elicited by different songs using the spike distance metric, a recently proposed theoretical measure that is sensitive to the dynamic structure in spike trains (M.C.W. van Rossum, *Neural Computation* vol. 13, 751-763, 2001).

Our results indicate a significant improvement in the discriminability of songs when the temporal variations of spike trains are taken into account. We also examine how discriminability evolves over time by quantifying the effect of increasing the duration of the spike train. Finally, we assess how changes in parameters of the model STRF affect the reliability and time-course of discrimination.

880 Seasonal variation of frequency and temporal response properties of single neurons in the inferior colliculus

Joziën Goense¹, Albert Feng²

¹Center for Biophysics and Computational Biology, University of Illinois Urbana Champaign, 405 N. Mathews Avenue, Urbana, IL, United States, ²Molecular and Integrative Physiology, University of Illinois Urbana Champaign, 405 N. Mathews Avenue, Urbana, IL, United States

Frogs rely on acoustic signaling to detect, discriminate, and localize mates. For seasonal breeders, reproduction occurs in the spring during which frogs exhibit overt acoustically guided behaviors; in response to the species mating trill males show evoked vocal responses or other territorial behaviors, and females show phonotactic responses. In winter, they hibernate and reside at the bottom of ponds showing no response to acoustic stimuli to which they respond in the spring. It is therefore possible that frog's auditory system displays a seasonal variation. This hypothesis was tested by evaluating the response characteristics of single neurons in the inferior colliculus of male leopard frogs to a synthetic mating call (a series of tone pulses at the unit's best frequency with a modulation rate of 20 Hz) in different times of the year. The stimulus was broadcasted from a loudspeaker in the free field. We also evaluated each unit's frequency selectivity. We found there was a seasonal shift in frequency tuning, with a dominance of low frequency (100-500 Hz) cells in the fourth quarter, and mid and high frequency cells (600-1800 Hz) in the first half of the year. The AM following response, as measured by the unit's synchronization coefficient, was also markedly different. In winter and early spring most cells showed weak following response, while in late spring and early summer the majority of the cells showed robust time-locked following responses (high synchronization coefficients). The seasonal differences in frequency and temporal processing indicate that auditory midbrain neurons in the leopard frog are likely to be subject to hormonal modulation. Supported by NIH-R01DC-00663.

881 The Social Communication Calls and Songs of Mexican Free-tailed Bats

Teh-Sheng Ma¹, Barbara French², Rachel Page³, George Pollak¹

¹Neurobiology, University of Texas at Austin, 1 University Station, C0920, Austin, TX, United States, ²BCI, Bat Conservation International, PO Box 162603, Austin, TX, United States, ³Integrative Biology, University of Texas at Austin, 1 University Station, C0920, Austin, TX, United States

While bats are best known for echolocation, they are also highly social animals that utilize a remarkably rich repertoire of signals for a variety of social interactions, including mother-infant interactions, courting, agonistic encounters, defense of territories and numerous other encounters of which we are only now becoming aware. Here we describe a sample of social communication calls emitted by Mexican free-tailed bats, each type recorded under specific behavior situations. The calls were recorded from a colony of approximately 80 bats that have been maintained by Barbara French for the past decade. Calls emitted under various behavioral conditions have unique spectro-temporal structures and different degrees of complexity. Some calls, such as the Directive Call emitted by a mother to her baby, consist of a single syllable that is repeated 2-5 times. Other calls are more complex. As one example, males emit the Herding Buzz when they bring a group of females together into a harem. The Herding Buzz is composed of a phrase repeated 2-4 times. Each phrase has 2 syllables, an initial syllable resembling a sinusoidally frequency and amplitude modulated tone, followed by 3-5 syllables composed of brief, downward FM sweeps. The most complex is the Territorial Call, which is a true song. A male guarding his harem emits this call. The song is emitted in response to the intrusion of another male attempting to enter the territory in which the harem resides. The call has two main phrases. The first phrase, or chirp, is composed of 5-7 syllables, and the call is initiated with 5-10 chirp repetitions. The chirps are followed by 4-6 repetitions of a trill. The combination of the 5-10 chirps and 4-6 trills, which continues approximately 100ms, is emitted while the bat is obviously agitated and appears as a stern warning to the intruder. If the intruding male does not depart immediately, a viscous fight ensues. We also show movies to illustrate the elegance of the Territorial Call and the behavioral context in which it is emitted.

This array of behavior associated communication calls establishes a foundation for exploring how mammalian bats with social hierarchy process these meaningful vocalization in their auditory system.

Supported by NIH grant DC 00268

882 Auditory function and hyperbilirubinemia in the developing neonate

Gerald R Popelka^{1,2}, Joseph W Martinosky³, Ralph E Walden³, Glenn R Gourley⁴

¹Scientific Research, Everest Biomedical Instruments, 16690 Swingley Ridge Rd, Chesterfield, MO, United States,

²Otolaryngology, Washington University, 660 South Euclid Ave, St. Louis, MO, United States, ³Engineering, Everest Biomedical Instruments, 16690 Swingley Ridge Rd, Chesterfield, MO, United States, ⁴Pediatric Gastroenterology, Oregon Health Sciences University, 707 SW Gaines Rd., Portland, OR, United States

Substantial levels of bilirubin are produced from catabolized red blood cells during the 14 day period after birth in the majority of neonates. Bilirubin can be toxic to the auditory neural pathways depending on the level of exposure. Our research focus is to understand the relation between bilirubin exposure and auditory neural effects. Accurate auditory neural measures in the developing neonate are difficult because they must be noninvasive and account for unrelated developmental factors. Previously we have shown that auditory brainstem responses can be measured accurately independent of maturational changes in the peripheral ear during the first 40 hours after birth. To extend these findings, distortion product otoacoustic emissions were measured in 50 neonates up to 14 days after birth. The measured otoacoustic emissions levels at 2, 3 and 4 kHz did not change during this period suggesting that outer hair cell maturation should not influence the neural measures during the period of maximum bilirubin exposure. Bilirubin exposures in the developing neonate also are difficult to measure because, ideally, noninvasive methods must be used as an alternative to blood samples to allow multiple measures. Production of carbon monoxide (CO) and bilirubin from catabolized red blood cells are stoichiometric. Because CO is excreted only in the lungs, the CO concentration in the breath stream is highly correlated with blood CO level. We developed a system to sample and analyze the neonatal breath stream noninvasively to accurately determine the concentration of end tidal CO that can be used as a measure of bilirubin production. Data show that CO measurement accuracy is highly dependent on the accuracy of determining breath waveform and breathing rate and the use of sensors that are not influenced by other exhaled gases such as hydrogen.

883 Neurotrophins in the Guinea Pig Auditory Brainstem Nuclei After Unilateral Cochlear Ablation

Sanoj K. Suneja, Leqin Yan, Steven J. Potashner
Neuroscience, Univ. Conn. Health Center, 263 Farmington Avenue, Farmington, CT, United States

Unilateral cochlear ablation (UCA) in young adult guinea pigs induced synaptic rearrangements, a growth of new synaptic contacts and altered transmitter release and postsynaptic receptor activities in brainstem auditory nuclei. Since neurotrophins can regulate plasticity in the adult brain, we determined if neurotrophin levels were altered after UCA. We used ELISA to measure NT-3 and BDNF levels in the subdivisions of the cochlear nucleus (CN), nuclei of the superior olivary complex (SOC) and the central nucleus of the inferior colliculus (ICc). Many of the sampled

nuclei exhibited decreased levels of NT-3 at 3 postablation days, elevated levels at 7 days and levels near the controls at 60 days. However, at 3 days, levels in the ipsilateral AVCN, contralateral MSO and MNTB, and the LSO did not change and were elevated in the contralateral AVCN and ICc. BDNF levels were elevated in the ipsilateral CN subdivisions at 3 and/or 60 postablation days, while contralaterally, a decline at 3 days returned to control levels by 60 days. In the MSO and ICc, BDNF levels declined at 3-7 days and recovered by 60 days. BDNF levels in the ipsilateral MNTB were elevated at 3 and 7 days and recovered to control levels by 60 days, while contralaterally levels declined at 7 days. These transient changes in BDNF and NT-3 levels, together with changes in expression of TrkB, the BDNF receptor (Suneja and Potashner, *Brain Res* 957: 366-368, 2002), suggest that neurotrophic support was altered after cochlear ablation. The findings suggest that changes in neurotrophin-dependent cellular signaling, especially during the first postablation week, probably governed many of the plasticities in the auditory pathways after UCA. Supported by DC00199.

884 Cochlear Ablation Results in Differentially Expressed Neurotransmitter Related Genes in the Auditory Brainstem

Avril Genene Holt¹, Mikiya Asako², Catherine A Lomax¹, Margaret I Lomax¹, Richard A Altschuler¹

¹Otolaryngology/KHRI, University of Michigan, 1301 East Ann Street, Ann Arbor, Michigan, United States, ²Otolaryngology, Kansai Medical University, 10-15 Fumizono-cho, Moriguchi-shi, Japan

The auditory system is uniquely ideal for studying plasticity due to our ability to remove function by deafening and to return function through the use of cochlear implants. In the present study we used Affymetrix Gene Chips to examine changes in gene expression at 3 and 21 days following deafening. Sprague Dawley rats were tested for normal hearing and used either as controls (n = 18) or bilaterally deafened (n = 36) by cochlear ablation. An ABR threshold shift of 80dB or greater was used as the criterion for inclusion in the study. Three or 21 days after deafening, total RNA was isolated and an analysis of gene expression was performed on RNA from six samples from each experimental group (n = 18 gene chips) using the Affymetrix Rat U34A chip. Data from Affymetrix chips were analyzed using the Bioconductor software package, normalized using quantile normalization and expression values calculated using a robust multichip average. All possible comparisons were tested using Significance Analysis of Microarrays software, which performs two-sample t-tests. Approximately 1,400 of the 8,000 genes on the chip showed differentially expressed genes at the 3 and 21 day time points. Differentially expressed genes fell into several categories including neurotransmitter and receptor related, dendritic spine and cytoskeletal related, synaptogenesis related, ion channel related, transcription regulator related, stress related and hormone related. Real time RT-PCR was used to confirm differential expression in 21 neurotransmitter related genes at the 3 and 21 day time points as well as an additional group 90 days following cochlear ablation. Increased expression was seen for several GABA, glycine and glutamate receptor subunits. GABA receptor beta 2 was most dramatic showing a 3 fold increase at three days increasing to 5 fold at 3 months. Indeed, very few of the

genes showing increases in expression by PCR returned to baseline by 3 months. Of the genes showing decreases in expression, tyrosine hydroxylase showed the largest decrease, dropping to less than 50% of normal by 3 days and remaining decreased at 3 weeks and 3 months.

885 Protein Kinases Regulate Glycine Receptor Activity in the Brainstem Auditory Nuclei After Unilateral Cochlear Ablation

Leqin Yan, Sanoj K. Suneja, **Steven J. Potashner**

Neuroscience, Univ. Conn. Health Center, 263 Farmington Avenue, Farmington, CT, United States

Unilateral cochlear ablation (UCA) in young adult guinea pigs altered glycine receptor activity in the ventral cochlear nucleus (VCN), the lateral (LSO) and medial (MSO) superior olive, and the inferior colliculus (IC) (Suneja et al., *Exptl Neurol* 154: 473-488, 1998). We determined if glycine receptor activity after UCA was regulated by protein kinase C (PKC), protein kinase A (PKA) and calcium/calmodulin-dependent protein kinase II (CaMKII). The specific binding of [³H]strychnine was measured in slices of the dorsal (DCN), posteroventral (PVCN) and anteroventral (AVCN) cochlear nucleus, the LSO, MSO and IC 145 days after UCA and in age-matched unlesioned controls. After UCA, decrements in specific binding in the ipsilateral AVCN, PVCN and LSO and bilaterally in the MSO were reversed by 3 μm PDBu, a PKC activator, but 50 nM Ro31-8220, a PKC inhibitor, had no effect in controls and after UCA. Similarly, 0.2 mM dibutyryl-cAMP, a PKA activator, reversed the UCA-induced decrements in specific binding in the ipsilateral VCN and bilaterally in the MSO, but 2 μm H-89, a PKA inhibitor, had no effect in controls and after UCA. In contrast, a CaMKII inhibitor, KN93 (4 μm), relieved or reversed UCA-induced decrements in specific binding in the ipsilateral AVCN, PVCN and LSO and bilaterally in the MSO and elevated specific binding in the IC. Thus, PKC, PKA and CaMKII can regulate glycine receptor activity after UCA. Also, PKC and PKA, if activated, can upregulate specific binding to reverse UCA-induced decrements in the VCN and the superior olive. Finally, after UCA, CaMKII negatively regulates receptor binding in the VCN, superior olive and IC. After UCA, the inactivity of PKC and PKA, together with the downregulatory action of CaMKII, may account for the postablation deficits in glycine receptor activity. Supported by DC00199.

886 Effects of Cochlear Ablation on Amino Acid Concentrations in Rat Cochlear Nucleus and Superior Olive

Donald A. Godfrey, Yong-ming Jin, Matthew A. Godfrey

Otolaryngology, Medical College of Ohio, 3065 Arlington Avenue, Toledo, Ohio, United States

Changes in central auditory chemistry following peripheral damage or disease may lead to distorted hearing and symptoms such as tinnitus and hyperacusis. We are studying effects of unilateral deafferentation, by cochlear ablation, on amino acids, which include major metabolites and neurotransmitters of the central auditory system. After ablation of the left cochlea, rats survived 2, 4, or 7 days or 1 or 2 months before euthanasia. Brains were quickly frozen and frozen sections cut and freeze dried. The

cochlear nucleus or superior olive portions of freeze-dried sections were cut into submicrogram samples for assay of amino acid concentrations by HPLC. Glutamate concentration was reduced in the lesioned-side caudal posteroventral cochlear nucleus, as compared to the control side, by 40%, 33%, 34%, and 27% at 2 and 7 days, 1 and 2 months, respectively. In the rostral anteroventral cochlear nucleus, glutamate concentration was reduced by 24% and 29% at 2 and 7 days on the lesioned side, but there was no significant difference between sides at 1 or 2 months of survival. In the deep layer of the dorsal cochlear nucleus, glutamate concentration was reduced by 24%, 38%, and 25% on the lesioned side at 2, 4, and 7 days, but there was no significant difference at 1 month. The most consistent change in the superior olive was for GABA concentration in the lateral superior olivary nucleus (LSO): no significant change on the lesioned side as compared to the control side at 2 days, but 42%, 48%, and 47% reduction at 7 days and 1 and 2 months survival, respectively. Loss of glutamate in cochlear nucleus regions should result from degeneration of the transected auditory nerve (Wenthold, 1978), whereas recovery at later times may represent plasticity in other neurons. Loss of GABA in the LSO may be secondary to loss of activity in its cochlear nucleus input or a retrograde effect following destruction of lateral olivocochlear terminals.

Supported by NIH grant DC03258

887 Choline Acetyltransferase in the Lateral Superior Olive and Ventral Nucleus of the Trapezoid Body of Cochlea-Ablated Rats

Yong-ming Jin, Donald A. Godfrey

Otolaryngology, Medical College of Ohio, 3065 Arlington Avenue, Toledo, Ohio, United States

The cholinergic olivocochlear bundle innervates the organ of Corti, where it functions to modulate cochlear mechanics. During development, motor neurons in the facial and hypoglossal nuclei have the same origin as cholinergic neurons in the superior olivary complex (SOC). Previous studies have reported decreased expression of protein and mRNA of choline acetyltransferase (ChAT), a marker of cholinergic neurons, after axotomy of facial and hypoglossal motor neurons. Cochlear ablation results in destruction of the distal parts of olivocochlear axons. We hypothesized that this axotomy would affect cholinergic neurons in the SOC similarly as axotomy affects facial and hypoglossal motor neurons. Using a radiometric assay combined with microdissection of freeze-dried sections, we measured ChAT activity in submicrogram samples of the lateral superior olive (LSO) and ventral nucleus of the trapezoid body (VNTB), the nuclear sources of the lateral and medial olivocochlear bundles, respectively. In normal rats, we documented a gradient of ChAT activity in the LSO, increasing from lateral to medial, but not in the VNTB. ChAT activity decreased, with also a decrease of the lateral-to-medial gradient, in the LSO ipsilateral to cochlear ablation, compared to the contralateral LSO, at 7 days, 1 month, and 2 months after surgery. No significant difference in ChAT activity was found in the VNTB at 7 days or 1 month after surgery, but there was a significant decrease at 2 months survival. Because the olivocochlear bundle is an important descending projection to the cochlea, the long term effects of cochlear ablation on the cholinergic influences to the cochlea and cochlear nucleus need further study.

Supported by NIH grant DC03258

888 Deafness related changes in glycine and GABA receptor subunit expression in the rat cochlear nucleus

Mikiya Asako^{1,2}, Avril Genene Holt², Cathy Ann Lomax², Jose Manuel Juiz³, Richard A Altschuler²

¹*Otolaryngology, Kansai Medical University, 10-15, Fumizono-cho, Moriguchi, Japan,* ²*Otolaryngology, University of Michigan/KHRI, 1301 E. Ann St., Ann Arbor, MI, United States,* ³*Catedratico de Histologia, Universidad de Catilla-La Mancha, 02071, Albacete, Spain*

GABA and glycine are major inhibitory neurotransmitters of mammalian central nervous system. We have previously used quantitative post embedding staining immunocytochemistry to show dramatic decreases in the number of glycine immunoreactive puncta on cell bodies in the cochlear nucleus (CN), 14 days following deafening (Asako et al, 2003). In the present study we used quantitative Real Time PCR to examine changes in the expression of glycine and GABA receptor (R) subunits in the cochlear nucleus 3, 21 and 90 days following cochlear ablation. Three different pools of RNA from the CN, each pool from the CN of four rats, were used for each experimental condition and age-matched normal hearing controls. For glycineR subunits, increases in expression were seen at 3 days following deafness in the alpha 1 and the alpha 3 subunits, the most dramatic change in the alpha 3 subunit. Expression decreased at 21 days following deafness, returning to baseline by 3 months. On the other hand, for the GABA-AR subunits, the largest increases in expression were seen 21 days following deafness, with smaller increases or no changes at 3 days. The most dramatic increases were for the alpha 1, alpha 2, and beta 3 subunits. Significant increases at 3 weeks were also seen in the beta 1, beta 3 and gamma 1 and 2L subunits. All receptor expressions returned to base line or showed decreases by 3 months after deafening.

889 Plastic Changes in Synaptic Vesicle Distribution in the Cochlear Nucleus Following Noise Exposure in Mice

Jennifer Bendiske, D. Kent Morest

Neuroscience, University of Connecticut Health Center, 263 Farmington Ave, Farmington, CT, United States

Our laboratory is studying the effects of acoustic trauma on synapses and neurotrophin expression in the cochlear nucleus (CN). Preliminary immunohistochemical analyses of CN sections of C57Bl/6J x CBA/J F1 control mice indicated that Trkc expression is limited to the cytoplasm of nerve cell bodies, while NT-3 appears to be localized to the neuropil and perisomatic sites. CN sections also were obtained from mice that survived for 1, 2, 4, or 8 weeks, following 6 hours of white noise exposure at frequencies >4 kHz at 110-dB SPL. Light microscopic evaluations of posteroventral CN (PVCN) sections, immunostained with antibodies against the synaptic vesicle protein SV-2, provided evidence that sound damage induces discrete changes in the mouse PVCN. SV-2 immunostained CN sections revealed a "band of denervation" in the PVCN, an anomaly that formed along the ventral border of the small cell shell in exposed, but not control mice. This band resulted

from a gradual loss in SV-2 immunoreactive material in perisomatic and neuropil locations that occurred over the 4 weeks following noise exposure, as compared to the staining intensity and pattern of control animals. Interestingly, PVCN sections of 8-week survival mice exhibited a different staining pattern. While SV-2 immunoreactivity in the neuropil continued to decline, there was an apparent recovery of SV-2 in perisomatic locations compared to unexposed mice. Because double-labeling studies demonstrated that NT-3 co-localized with SV-2, and therefore is present at synaptic endings, future studies will examine the effect of sound exposure on NT-3 expression. In sum, these data indicate that synaptic decline follows a single episode of acoustic trauma. Additionally, with time, there may be a recovery or new growth, involving re-organization of synaptic endings in particular CN locations. Supported by NIH grants F32 DC006120 and RO1 DC00127.

890 Spontaneous Single Unit Activity In The Dorsal Cochlear Nucleus Following Intense Sound Exposure

Paul G Finlayson, James Kaltenbach

Otolaryngology, Wayne State Univ., 550 E. Canfield, Detroit, MI, United States

Chronic hyperactivity, characterized by increases in multiunit spontaneous activity, can be induced in the DCN by previous exposure to intense sound. Thus far, little is known about the changes underlying this hyperactivity at the single unit level. In the present study, we examined the effects of intense tone exposure on single unit spontaneous discharges in the DCN of hamsters. Anesthetized (ketamine and xylazine) hamsters were either exposed to 127 dB SPL, 10 kHz continuous tone (exposed, n=5) using a headphone coupled to the left ear, or maintained in a sound proof booth (controls, n=5), for 4 hours. Recordings of units with CFs between 8 and 15 kHz were performed 28 days later in the left (ipsilateral) DCN, using glass micropipettes (8-14 Mohm). Three major differences in single unit activity after sound exposure were observed in preliminary data from 66 single units. First, single unit discharge rates in exposed animals were significantly higher ($P < 0.05$) than those in controls. Mean rates in exposed animals averaged 15.5 spikes/s while those in controls averaged 9.4 spikes/s. Second, there was a shift in the proportion of units exhibiting different spike waveforms. Units were classified according to their spike waveform into 4 groups: 1) broad W-shaped spikes, 2) broad M-shaped spikes, 3) short triphasic spikes, and 4) V-shaped spikes. There was a marked decrease in the proportion of neurons with short triphasic spikes and more cells with V- and broad M-shaped spikes in exposed animals. And third, exposed animals showed significant decreases in the duration of M- and W-shaped spike waveforms. These results suggest that following intense sound exposure, ionic conductances, which shape the spike waveform, are directly or indirectly altered. Changes in the extracellular spike waveform may, therefore, provide a means to examine underlying mechanisms of the hyperactivity in exposed animals. (Supported by NIDCD grant R01 DC03258)

891 The Modulation of Tyrosine Hydroxylase in the Lateral Olivocochlear Nucleus

Xianzhi Niu¹, Nenad Bogdanovic², Barbara Canlon¹

¹Physiology & Pharmacology, Karolinska Institutet, Karolinska Institutet, Stockholm, Sweden, ²Neurotec, Geriatric section, Karolinska Institutet, Huddinge University Hospital, Huddinge, Sweden

It has been previously shown that tyrosine hydroxylase (TH) immunoreactivity in the terminals of the lateral efferents under the inner hair cells of the cochlea is decreased by acoustic trauma. Sound preconditioning counter-acted this decrease and simultaneously protected against the trauma-induced hearing loss (Niu and Canlon, 2003). The purpose of the present study was to identify those neurons in the lateral olivocochlear system that is regulating the peripheral expression of tyrosine hydroxylase in the cochlea of guinea pigs, using a combination of techniques that included retrograde tracing with dextran, immunohistochemistry, and neuronal counting, the identification and distribution of tyrosine hydroxylase neurons in the lateral olivocochlear (LOC) system. Dextran labelled neurons were found predominantly in the ipsilateral LOC system including lateral superior olivary nucleus (LSO), and the surrounding periolivary regions (DPO, DLPO, LNTB). In the untreated control group 35% of the ipsilateral LOC neurons were immunostained with TH and 77% of the total population of TH neurons in the LOC system was double-stained (TH and Dextran). Acoustic trauma decreased the number of TH positive neurons in the LSO proper and the surrounding DLPO, and caused a reduction of fiber staining for TH immunolabeling in these regions. Changes were not noted in the LNTB or the DPO after acoustic trauma. On the other hand, sound conditioning protected against the decrease of TH immunolabelling by acoustic trauma and increased the fiber staining for TH. Sound conditioning did not alter the activity of the neurons in the DPO or the LNTB. These results provide evidence that TH positive neurons are identified in the LOC system in guinea pig and confirm a specific role for tyrosine hydroxylase in the LSO proper and DLPO of the LOC system. Protection against acoustic trauma by sound conditioning has a central component that is governed by the LSO and the surrounding DLPO region. Supported by RNID, The Swedish Research Council, Tysta Skolan and AMF.

892 Effects of Acute Noise Damage on Oxidative Metabolism in Chick Cochlear Nucleus

Christina L. Kaiser^{1,2}, Douglas A. Girod¹, Dianne Durham¹

¹Otolaryngology/Head and Neck Surgery, University of Kansas Medical Center, 3901 Rainbow Blvd, Kansas City, KS, United States, ²Anatomy and Cell Biology, University of Kansas Medical Center, 3901 Rainbow Blvd, Kansas City, KS, United States

Sound damage creates severe cochlear damage. Less is known about the effects of sound-induced cochlear hair cell loss on CNS auditory neurons. To investigate this issue, 10 week-old egg layer birds were placed in pairs into a sound attenuated chamber and exposed to a 1500 Hz pure tone, 120 dB SPL for 24 hours. Birds were perfused with formalin 24 hours later. Brains were removed and prepared for cryostat sectioning and histochemical analysis of cytochrome oxidase (CO) staining in n. magnocellularis (NM). Untreated age-matched controls were sacrificed for

comparison. Treated ears evaluated with SEM showed a crescent-shaped region devoid of hair cells extending between 25% and 54% of the basal to apical cochlear length. This cochlear region corresponds, by frequency, to an area 31% to 71% of the anterior to posterior (A/P) extent of NM. We measured optical density (OD) of cytoplasmic CO reaction product in individual NM neurons at 25% A/P (outside the affected area), as well as 50% and 60% A/P (within the affected area). OD measurements of a non-auditory area in each section were used to correct neuronal OD measurements and allow comparison between animals. When corrected averages of NM OD were evaluated, sound treated animals were not different from control animals. However, histograms made to assess the distribution of corrected individual NM OD values showed that differences between sound damaged animals and controls do exist. In controls, NM histograms displayed a normal distribution and small range of OD values. In treated birds, histograms from all NM locations showed that some OD values fell into a normal distribution. However, these neuronal distributions showed leptokurtosis, or a shift of some neuronal ODs to higher values. Although less robust than CO changes with cochlea removal or gentamicin treatment, these data suggest that sound-induced cochlear damage changes oxidative metabolism in some NM neurons throughout the nucleus.

Supported by R21 DC004982

893 Hyperactivity in the hamster dorsal cochlear nucleus: its relationship to tinnitus

Jinsheng Zhang¹, Henry E. Heffner², Gim Koay², James A. Kaltenbach¹

¹Otolaryngology-Head & Neck Surgery, Wayne State University, 4201 St. Antoine, Detroit, MI, United States, ²Psychology, University of Toledo, 2801 West Bancroft Street, Toledo, Ohio, United States

It has been demonstrated in animal studies that intense sound exposure induces elevation of spontaneous activity in the dorsal cochlear nucleus (DCN) and also causes tinnitus. This suggests that the induced hyperactivity in the DCN may represent a neural component that underlies tinnitus. The current study aimed to test this hypothesis. Twenty-eight adult male hamsters were divided into 4 groups according to exposure parameters or control treatment. Before exposure or control treatment, all animals were trained behaviorally for tinnitus testing using a two-choice sound localization test. Three groups of animals were then exposed under anesthesia at their left ears to a 10 kHz tone at 80, 110 and 125 dB SPL for 4 h, respectively, whereas 1 group of control animals were anesthetized but not sound exposed. Behavioral tests were performed during the week after sound exposure or control treatment to test for the presence of tinnitus. These tests were followed by measurements of thresholds of acoustically evoked auditory brainstem responses (ABR) to evaluate the degree of hearing loss. Spontaneous multiunit activity was then recorded on the DCN surface between 12 and 20 days postexposure. For each animal, we recorded 3 rows of 15 sites for a total of 45 sites, with spontaneous activity counted over 90 sec for each site. The behavioral results suggest that exposed animals developed tinnitus and that the severity of the tinnitus increased as a function of exposure intensity. Similarly, as the exposure intensity was increased, increases were observed both in spontaneous rates across the DCN and in the

degree of hearing loss as reflected by the ABR threshold shifts. Preliminary multivariate analysis indicated that the behavioral score for tinnitus was significantly correlated with spontaneous rate, and this correlation was dependent on the occurrence of hearing loss. The results suggest that hyperactivity in the DCN may be an important neural correlate of tinnitus but that hearing loss may be a necessary antecedent to this correlation. (Supported by the Tinnitus Research Consortium).

894 Effects of tinnitus-inducing factors, salicylate and quinine, on neuronal spontaneous activity and response to carbachol in the rat dorsal cochlear nucleus

Kejian Chen, Xiaodan Song, Donald A. Godfrey

Otolaryngology, Medical College of Ohio, 3065 Arlington Ave., Toledo, Ohio, United States

Understanding the underlying mechanisms of tinnitus is important for its treatment. Tinnitus can be caused by exposure to very loud sound or medicines such as salicylate or quinine. We previously found that, after intense sound exposure, there was increased bursting and decreased regular type of activity in the dorsal cochlear nucleus (DCN) of brain slices. Also after intense sound exposure, the bursting neurons became more sensitive to carbachol, an acetylcholine agonist. This study tested two other common tinnitus inducers, salicylate and quinine, to look for a common mechanism related to central tinnitus.

Young adult Sprague Dawley rats were treated with sodium salicylate (via drinking water, 8 mg/ml), and quinine (100 or 125 mg/kg, i.p.) for 2 days to 5 weeks. Age-matched controls received no treatment. Three types of spontaneous activity were recorded from the DCN of brain slices: regular, irregular, and bursting. After salicylate treatment, the overall neuronal densities (units/penetration) were similar to the controls, but the density of bursting activity increased by 11% ($p < 0.05$). The mean firing rate of bursting neurons of exposed rats was 12% higher than that of controls ($p < 0.005$). The mean firing rate of regular neurons of exposed rats was 7% higher than that of controls ($p = 0.05$). After 100 mg/kg quinine treatment, both the neuronal density and firing rate were similar to the controls. After 125 mg/kg quinine treatment, however, the neuronal density was 20% higher than controls ($p < 0.02$), and the mean firing rate of bursting neurons was 15% higher than controls. Limited data suggest that salicylate and quinine treatments slightly change the response of bursting neurons to carbachol.

In conclusion, changes of spontaneous activity in the DCN may reflect a common underlying mechanism of central tinnitus that may be triggered by a variety of factors.

(Supported by a grant from the American Tinnitus Association)

895 Comparison of the Ventral Cochlear Nuclei in Deaf Jerker and Hearing Mice

Xiaojie Cao, Matthew James McGinley, Donata Oertel

Physiology, University of Wisconsin, 1300 University Ave., Madison, Wisconsin, United States

To understand the consequences of hearing loss on the function of the cochlear nuclei, we have compared ventral cochlear nuclei

(VCN) in deaf *jerker* mice (-/-) with those in heterozygotes (-/+) and normal mice of the ICR strain (+/+). The intrinsic electrophysiological properties of octopus and T stellate cells were not detectably different in deaf and normal mice. Responses to pulses of current showed characteristic onset and tonic firing in octopus and T stellate cells respectively. Voltage-clamp recordings indicate that the amplitude of depolarization-activated potassium currents in octopus cells were similarly large in mutant and normal mice. As the frequency of spontaneous mEPSCs seemed to differ in mutants, we undertook a more detailed comparison of mEPSCs. These measurements show that mEPSCs occur significantly more frequently in deaf than hearing mice but that the amplitudes, 10-90% rise times, and decay time constants were not significantly different. In octopus cells from -/- mice, mEPSCs occurred at 82 ± 26 Hz (-/-) compared to 51 ± 24 Hz (-/+) and 47 ± 13 Hz (+/+). In T stellate cells they occurred at 8 ± 3 Hz (-/-) compared to 3 ± 1 Hz (-/+) and 2 ± 1 Hz (+/+).

The differences in the function of presynaptic terminals led us to examine the morphology of the cochlear nucleus in mutant mice. Extracellular injections of biocytin into the AVCN show that innervation of cochlear nuclei by auditory nerve fibers is similar in mutant and wild type animals. No changes in the auditory nerve fibers or the tonotopy of the nucleus were observed, though in homozygous mutant mice the shapes of end bulbs are more finger-like than ICR and heterozygote mice.

Supported by a grant from the NIH, DC00176

896 Single Dose Salicylate increases Fos-Immuno-reactivity at the Superior Olivary Complex

Jiunn Liang Wu¹, Tzai Wen Chiu², Paul W.F. Poon³

¹Otolaryngology, NCKU, University Road, Tainan, Taiwan, ²Basic Medical Institute, NCKU, University Road, Tainan, Taiwan,

³Physiology, NCKU, University Road, Tainan, Taiwan

Tinnitus is a phantom perception of sound in the absence of acoustic stimulation. Factors such as acoustic trauma and ototoxic drugs (e.g. salicylate, SA) are known to cause tinnitus in human. SA-induced tinnitus in animals is associated with over-activities at the central auditory pathways. The temporal pattern in which central auditory neurons may change their activity during the pathogenesis of SA-induced tinnitus remains unclear. In this study, we used Fos-immuno-histochemistry to map the over-active neurons at the auditory brainstem of animals following a single injection of SA and we compared results with those after repeated SA doses over a period of 5 days. Specifically we examined the Fos expression at the cochlear nucleus (CN), superior olivary complex (SOC), and inferior colliculus (IC).

Experimental rats (n=12) received single or multiple doses of SA (250 mg/kg, i.p.). Animals were all preconditioned inside a sound-treated room 8 hrs before sacrifice. For single injection experiments, animals were sacrificed 3 hrs after injection of SA. Animals receiving multiple doses of SA were sacrificed 30 hrs after the last injection. Standard ABC procedures were used for histological processing of frozen sections (40 μ m in thickness). Control animals received saline injections.

Immuno-histochemistry showed that following a single dose of SA injection, there was a significant increase ($p < 0.001$) in the

number of Fos-stains at the SOC. Such over-activity was not found in SOC after 5-daily injections of SA. In marked contrast, only a small number of IC neurons expressed Fos after single dose injection but there was a significant increase 30 hrs following 5-daily injections.

Our results of a transient increase of Fos-immuno-reactivity at SOC followed by a delayed increase at IC suggested that the pathogenesis of SA-induced tinnitus likely reflects long-term plastic changes. These plastic changes likely involve a temporal alteration in the neuronal activity of the auditory pathways, in particular the feed back control systems involving the SOC.

(Supported in part by National Science Council, Taiwan.)

897 Temporal Refinement Mediated by Suprathreshold Synapses in the Cochlear Nucleus

Matthew Alexander Xu-Friedman, Wade G. Regehr

Dept. Neurobiology, Harvard Medical School, 220 Longwood Ave, Boston, MA, United States

Precise action potential timing can enhance computational performance, and is important for sensory acuity and motor control. Synapses contribute to temporal precision by reducing variability in spike timing ("jitter"). Most computational models of jitter reduction have relied on convergence of many subthreshold inputs. However, the assumptions of these models do not apply to all systems. In the cochlear nucleus, many bushy cells (BCs) receive few (? 4) auditory nerve (AN) inputs, yet BCs fire with less jitter than AN fibers. It is unclear how temporal precision is improved by so few inputs. Here we examine how the AN to BC synapse reduces jitter using voltage-, current-, and dynamic-clamp recordings in mouse brain slices. We find that each AN input is suprathreshold, and these inputs interact in fundamentally different ways from subthreshold inputs. Therefore, the timing of the BC response is controlled by the earliest AN input, which leads to reduced jitter even with few inputs. This strategy improves precision equally well whether the jitter in the inputs is large or small. Thus this novel mechanism may be generally useful for improving temporal precision throughout the nervous system.

898 GABA_A Receptors Possibly Mediate the Inhibition of Depolarization-Induced Calcium Responses in Spherical Bushy Cells of the Gerbil

Ivan Milenkovic, Thomas Reinert, Marco Heinrich, Rudolf Rübsamen

Institute of Zoology, University of Leipzig, Liebig Str. 18, Leipzig, Germany

Spherical bushy cells (SBCs) in the anteroventral cochlear nucleus (AVCN) receive presumably glutamatergic input through large calyceal ending that has been thought to primarily determine SBC firing. Recently, the results from our group have shown that SBCs are also the target of acoustically driven inhibition. However, physiological mechanisms underlying the interaction between excitation and inhibition remain to be elucidated. Aiming to address this issue we explored the effects of glutamate and GABA on $[Ca^{2+}]_i$ in SBCs. Brainstem slices (200 μ m) containing AVCN were acquired

from P7-P11 gerbils and investigated using Fura-2 AM calcium imaging. SBCs were selected according to their localization at the rostral part of the AVCN and to their large soma size.

Depolarization induced by aCSF containing 20mM KCl, glutamate (500 μ M), nonNMDA iGluRs agonists (*S*-AMPA 25 μ M, kainate 50 μ M) and mGluR agonist (*1S,3R*-ACPD 200 μ M) evoked rapid and reliable changes in $[Ca^{2+}]_i$. AMPA- and kainate- but not ACPD-induced changes in $[Ca^{2+}]_i$ were blocked with CNQX (25 μ M), a nonNMDA iGluR antagonist.

Application of GABA (1mM) significantly increased $[Ca^{2+}]_i$ in 78.6% of investigated SBCs (n=229). Similar changes in $[Ca^{2+}]_i$ were obtained with muscimol, a GABA_A receptor agonist (100 μ M, n=79, 78.5%). On the other hand, application of baclofen (GABA_B receptor agonist, 10 μ M-100 μ M) showed no significant effect on $[Ca^{2+}]_i$. Both GABA- and muscimol-evoked calcium responses were blocked with GABA_A receptor antagonist, and they were not affected by inhibition of GABA_B receptors (gabazine 25 μ M and CGP 4638 50 μ M, respectively).

Our current results indicate that application of either GABA or muscimol prior to the aCSF containing 20mM KCl significantly inhibits the depolarization-induced (20mM KCl) calcium responses when compared to the control and washout stimulation. Our further experiments shall address the issue of GABA receptor-mediated inhibition of calcium signals induced by activation of different glutamate receptors.

899 **K_v1.1 Containing Channels Improve Action Potential Temporal Precision.**

Joshua X Gittelman¹, Bruce L Tempel^{1,2}

¹NB&B, U. Washington, PO 357923, Seattle, WA, United States,

²Otolaryngology-HNS, UW, PO 357923, Seattle, WA, United States

Action potential (AP) timing is critical for sound localization and noise filtration. Where measured, auditory neurons that fire with high temporal precision express a low threshold voltage gated potassium (K_v) current (I_{ki}), carried by channels containing K_v1.1 subunits, encoded by the *Kcna1* gene (Brew 2003). I_{ki} reduces the window for coincidence detection of multiple synaptic inputs, and in the medial nucleus of the trapezoid body (MNTB) is thought to prevent multiple APs in response to large, single synaptic events. Using whole cell patch clamp recordings from MNTB cells in mouse brain slices, we tested the role of K_v1.1 containing channels in the temporal precision of AP initiation by comparing control littermate (+/+) cells to: *Kcna1*^{-/-} cells (\approx 40% less I_{ki}); +/+ cells with 3nM dendrotoxin-K (DTX-K, selective for K_v1.1 subunits, \approx 40% less I_{ki}); and to +/+ with 100nM DTX-K (\approx 80% less I_{ki}). To measure AP latency and latency variability (jitter) we simulated excitatory post synaptic potentials by injecting 0.5ms duration square pulses in current clamp mode. We report AP latency as the time from pulse onset to AP peak, and jitter as the SD of AP latencies.

I_{ki} improved temporal precision in 2 ways.

First, the *Kcna1*^{-/-} and DTX-K treated cells showed significantly more jitter than +/+ cells in response to near-threshold current injection (I_{inj}, current to achieve 20-80% AP probability). The data is given as: average \pm SEM, n cells, p relative to +/+ cells using unpaired Student's t-test. In ms: +/+ 0.11 \pm .01, n = 13; -/- 0.16 \pm .02, n = 10, p < 0.05; 3nM 0.28 \pm .04, n = 13, p < 0.05; 100nM 4.2 \pm 1.2, n = 10, p < 0.01. The 3nM DTX-K treated cells permitted

more jitter than -/- cells (p < 0.05).

Second, +/+ cells had a significantly shorter temporal window for AP initiation compared to cells with reduced I_{ki}. The window for each cell was defined as the difference between the I_{inj} latency and the latency in response to a 2nA pulse. In ms: +/+ 0.71 \pm .04ms, n = 24; -/- 0.92 \pm .06ms, n = 11, p < 0.01; 3nM 0.98 \pm .07, n = 14, p < 0.01; 100nM 8.2 \pm 2, n = 11, p < 0.01. Here, -/- cells and 3nM DTX-K cells were not different.

We conclude K_v1.1-containing channels are critical for maintaining temporal precision during AP initiation in MNTB cells.

Supported by RO1 DC03805 and NIH T32 GM07108

900 **Neural Representation of Amplitude Modulated Sounds in the Cochlear Nucleus of Mice Lacking the Kv1.1 Potassium Channel**

Nicholas Schmuck¹, Paul Allen², James Ison², Joseph Walton^{3,4}

¹Otolaryngology, University of Rochester, 601 Elmwood Av., Rochester, NY, United States, ²Brain and Cognition, University of Rochester, Melieora Hall, Rochester, NY, United States, ³Otolaryngology, University of Rochester, 601 Elmwood Av., Rochester, NY, United States, ⁴Center for Navigation and Communication Sciences, University of Rochester, 601 elmwood av, rochester, ny, United States

Voltage-gated potassium channels play a key role in shaping the temporal response of cells in the auditory nervous system and the Kv1.1 channel is highly expressed in the auditory brainstem. In the present study we measured near-field potentials from the AVCN and PVCN to determine whether the lack of expression of the Kv1.1 subunit alters temporal coding to amplitude modulated (AM) noise. Initially, we recorded responses to 80 dB SPL, 12 kHz tone bursts, as a function of depth, using stereotaxic coordinates, in order to map out the amplitude by depth profile. Intensity functions were then obtained for frequencies from 3 to 48 kHz at the location of maximal response. Near-field potentials were elicited by AM noise carriers of 200 ms duration presented at 80, 60 and 40 dB SPL with modulation frequencies between 20 and 8000 Hz. We replicated each condition and responses were averaged over 100 presentations at a rate of 2 Hz. A custom LabView program computed power at the modulation frequency and higher harmonics, as well as an RMS measure of response strength, yielding two measures of the modulation transfer function (MTF) for 8 mice of each genotype (+/+ and -/-). There were no significant differences in thresholds between +/+ and -/- groups. In +/+ mice a prominent peak in the mean MTF was present at 400 Hz. Knockout mice (-/-) had significantly lower overall power for both MTF measures and the peak at 400 Hz was absent. In addition, the upper cutoff of the MTF in knockouts was typically lower indicating a reduction in AM encoding by the population of neurons contributing to the near-field response. Greater distortion, evidenced by the presence of harmonics, was correlated with modulation frequencies having decreased power in -/- mice. These results may relate to previous work showing that cells lacking the Kv1.1 channel fire multiple action potentials in vitro, which can disrupt temporal coding of AM sounds in vivo. Work supported by NIH-NIA AG000954.

901 The Potassium Channel KCNQ5 Is Present In Synaptic Endings Of The Auditory Brainstem

Elena Caminos¹, Carmen Vale¹, Juan Ramón Martínez¹, Rafael Luján¹, Álvaro Villarroel², José Manuel Juiz¹

¹*Ciencias Médicas, Universidad de Castilla-La Mancha, C/ Almansa s/n, Albacete, Spain, ²Instituto Cajal CSIC, Instituto Cajal CSIC, Av. Dr. Arce 37, Madrid, Spain*

KCNQ5 is the last cloned member of a family of voltage-dependent K⁺ channels (KCNQ2-5) which are responsible for the hyperpolarizing M-current and are associated with hereditary human diseases such as deafness or epilepsy. KCNQ5 seems to be present in the mammalian cochlea. However, it is not known whether it is expressed in central auditory neurons.

Here we describe the distribution of KCNQ5 in the rat central auditory system using a polyclonal antibody (aKN5 antiserum) raised against the C-terminal region of the protein. KCNQ5 immunoreactivity was particularly concentrated in nuclei of the caudal auditory brainstem, i.e., cochlear nuclei up to the nuclei of the lateral lemniscus (NLL). Labeling around cell bodies in a punctate pattern was found throughout the ventral cochlear nucleus and superior olivary complex. A similar pattern of immunostaining was seen in the NLL, although labeling was generally less intense. We observed virtually no labeling in the inferior colliculus, and medial geniculate body. Moderately stained neuronal and glial elements were found in the auditory cortex.

The distribution of KCNQ5-immunoreactivity in central auditory nuclei suggests that this potassium channel is present primarily in synaptic endings of the auditory brainstem, where it may contribute to spike-frequency adaptation, by virtue of its particular kinetic properties. Detailed analysis of KCNQ5 distribution in the central auditory pathway could open new perspectives for the understanding of regulation of auditory neuronal excitability and auditory system disorders.

Supported by CICYT-SAF00-0211; PAI-03-015 (Consejería de Ciencia y Tecnología; JCCM) and BFI2003-09147-C02-02 (MCYT).

902 Suprathreshold and subthreshold responses of DCN cartwheel cells

Mingjie Tong, Scott C. Molitor

Department of Bioengineering, University of Toledo, 2801 W. Bancroft St., Toledo, Ohio, United States

Cartwheel cells (CWCs) are a population of interneurons in the dorsal cochlear nucleus (DCN), part of the auditory brainstem complex that serves as the first obligatory synapse for auditory nerve fibers ascending from the cochlea. CWCs receive multimodal sensory input from a set of parallel fibers in the superficial DCN, and provide inhibition to pyramidal cells (PCs) that project to the inferior colliculus. Therefore, CWCs are poised to modulate the auditory output of the DCN in response to a variety of auditory and non-auditory stimuli.

In many *in vivo* and *in vitro* preparations, CWCs respond to suprathreshold stimuli with complex spikes, a rapid burst of fast Na⁺-mediated action potentials (APs) superimposed upon a slow underlying depolarization mediated by Ca²⁺. In contrast to other

bursting neurons, complex spikes in CWCs can be evoked by low-level stimuli, and do not require a hyperpolarized resting potential to precede the depolarizing stimulus. CWCs can also respond with simple spikes, and it is not known what determines whether these neurons will respond with simple or complex spikes. In whole-cell recordings from CWCs in a rat pup brainstem slice preparation, simple spikes evoke a characteristic after-depolarization (ADP) without any intervening hyperpolarization. ADPs are blocked by 500 μM Ni²⁺ and 100 μM Cd²⁺, and are therefore mediated by Ca²⁺ currents. It is likely that these ADPs are attenuated complex spikes that are not sufficient to evoke the repetitive fast Na⁺-mediated APs characteristic of complex spiking.

In addition to suprathreshold responses such as complex spikes, or simple spikes followed by ADPs, CWCs also exhibit active responses at membrane potentials below the threshold for evoking APs. In contrast to ADPs, these subthreshold depolarizations (SDPs) are not blocked by Ni²⁺ and Cd²⁺, but are partially blocked by TTX (500 nM – 1 μM) and are completely and reversibly blocked by Na⁺-free bathing media. Thus, these SDPs are evoked by a partial activation of Na⁺ currents insufficient to elicit a full Na⁺-mediated AP, or by a distinct subset of Na⁺ channels that have a lower activation threshold than those involved in AP generation. This subthreshold activation of Na⁺ channels may contribute to the ability of CWCs to respond to low-level stimuli with complex spikes.

903 Control of firing in cartwheel cells of the dorsal cochlear nucleus (DCN).

Laurence O. Trussell¹, Yuil Kim²

¹*Oregon Hearing Research Center, L-335A, Oregon Health and Science University, 3181 SW Sam Jackson Park Rd, Portland, OR, United States, ²Oregon Hearing Research Center, L335A, Oregon Health & Science University, 3181 SW Sam Jackson Park Rd, Portland, OR, United States*

Cartwheel cells are glycinergic interneurons which mediate feed-forward inhibitory transmission between parallel fibers and the fusiform (principal) cells of the DCN. It is well established that these cells fire spontaneously *in vivo* and *in vitro* with a mixture of simple (narrow) and complex (broad and multi-peaked) action potentials. We have set out to identify the ion channels that mediate this behavior, beginning here with a characterization of the ionic and pharmacological control of firing. Slices containing DCN were made from P17-24 mice and individual neurons recorded using patch pipettes. Neurons were identified by somatic morphology and by the presence of complex spikes, which are unique to cartwheel cells in the DCN. Several lines of evidence indicate that Ca²⁺ current, Ca²⁺-activated K⁺ channels, and incomplete inactivation of Na⁺ current are involved in shaping these action potentials.

Bath application of the Ca²⁺-channel blocker Cd²⁺ (200 μM) affected both spike shape and spiking pattern. The spiking pattern often developed into bursts of broadened simple spikes and a strongly hyperpolarized interburst interval. There was an increase in the width of simple spikes and the fast component of complex spikes. During wash-in of Cd²⁺, the slow depolarized part of complex spikes transiently widened but eventually narrowed, so that complex and simple spike were both transformed into similarly shaped spikes. Increasing the Ca²⁺-buffering capacity of the cell

interior by raising EGTA from 0.1 to 5 mM also broadened the slow, depolarized part of complex spikes. Application of 100 nM apamin, a selective blocker of the SK channel, lengthened complex spikes with no apparent effect on simple spikes. These data implicate Ca^{2+} -dependent channels in mediating spike repolarization; however, SK channels selectively limit complex spike duration. Bath application of 0.2 μM TTX blocked overshooting spikes, and led to a steady hyperpolarization, suggesting that a steady-state Na^+ current may contribute to the resting potential. Depolarizing current injection at this state evoked slow spikes which resembled the slow component of complex spikes. These spikes were abolished by 200 μM Cd^{2+} . Thus, Ca^{2+} , Na^+ , and K^+ currents converge to define the duration of both simple and complex spikes.

Supported by NIH NS28901

904 Reliability and Precision of Spike Timing in the Pyramidal Cells of the Dorsal Cochlear Nucleus

Sarah E. Street¹, Paul B. Manis²

¹Cell and Molecular Physiology, University of North Carolina at Chapel Hill, 103 Mason Farm Road CB#7545, Chapel Hill, NC, United States, ²Otolaryngology/Head and Neck Surgery, Univ. of North Carolina at Chapel Hill, 1123 Bioinformatics Bldg., 130 Mason Farm Rd. CB#7070, Chapel Hill, NC, United States

Pyramidal cells of the dorsal cochlear nucleus (DCN) receive input from many different sources, including the auditory nerve, the granule cell system, and inhibitory interneurons, and in many mammals give rise to an important pathway to higher auditory centers. Most studies of the DCN have focused on the representation of acoustic stimuli in terms of average peristimulus firing rate, and on response maps based on average rate. However, it has been suggested that neurons use precise spike timing to transmit information and that the pattern of synaptic input onto neurons specifically regulates the reliability and precision of the resulting spike trains (Mainen and Sejnowski, *Science* 268:1503, 1995). In the present study, we examined how fluctuations of input stimuli influenced the spike trains of DCN pyramidal cells. We recorded from pyramidal cells in rat brain slices, using whole cell current clamp. We injected low-pass filtered Gaussian noise into the cells to mimic time-varying synaptic inputs and recorded the resulting trains of action potentials. Increasing the amplitude of fluctuating inputs caused an increase in the reliability and timing precision of the spike trains. We also examined spike-triggered stimulus averages (reverse correlations) with noise that differed on each trial. These stimuli revealed that the cells preferentially spiked in response to a brief (< 5 msec) depolarizing current, and at higher firing rates the depolarizing current was preceded by a longer (10-20 msec) hyperpolarizing current. The shape of the pre-spike stimulus average depended on the frequency content of the stimulus. These results suggest that pyramidal cells are sensitive to the temporal patterns of their synaptic inputs, and can pass this information in a reliable fashion to higher auditory processing centers in the brain. Supported by NIDCD grant R01 DC00425 to PBM.

905 Hyperpolarization-Activated Cation Current, I_h , in Stellate Cells of the Ventral Cochlear Nucleus of Mice

Aldo Rogelis A. Rodrigues, Donata Oertel

Physiology, University of Wisconsin, 1300 University Ave., Madison, Wisconsin, United States

To understand what underlies the differences in the electrophysiological properties of neurons of the ventral cochlear nucleus (VCN), we have compared the hyperpolarization-activated current, I_h , in T and D stellate cells of the VCN with I_h in octopus cells of the posterior VCN (Bal and Oertel, 2000). We found that I_h differs among cell types in its voltage range of activation and in its kinetics but not in its reversal potential. T and D stellate cells were identified on the basis of criteria that were previously established (Oertel et al., 1990; Fujino and Oertel, 2001). I_h was blocked by 50.0 μM ZD7288 but was resistant to 2.0 mM 4-aminopyridine. In both T and D stellate cells, only 3 to 5% of g_h was activated at rest. The voltage for half-activation was -96.9 ± 1.6 mV ($n=8$) in T stellate cells, and -88.8 ± 0.5 mV in D stellate cells ($n=2$), compared with -65 mV in octopus cells. The activation of I_h was fitted with two exponentials whose time constants exhibited strong voltage dependence, both decreasing with hyperpolarization. The time constants were slower in T stellate than in D stellate neurons at all voltages tested. For example, the time constants to fit a voltage step from -62 to -107 mV were 776 ± 48 and 110 ± 12 ms in T stellate ($n=5$) and 280 ± 65 and 43 ± 13 ms in D stellate cells ($n=2$), compared with 84 and 16 ms in octopus cells. The reversal potentials of I_h were similar in T and D stellate and octopus cells, around -40 mV. Our results are based on patch-clamp experiments in 49 parasagittal slices from 17-20 day old mice at 33 °C.

This work was supported by a grant from the NIH DC 00176

906 GABA_B Receptor Activation Modulates GABA_A Receptor-mediated Inhibition in Chicken Nucleus Magnocellularis Neurons

Yong Lu, R. Michael Burger, Edwin W Rubel

Virginia Merrill Bloedel Hearing Research Center, Department of Otolaryngology-HNS, University of Washington, Box 357923, Seattle, WA, United States

Neurons of nucleus magnocellularis (NM), a division of avian cochlear nucleus, receive glutamatergic excitatory input solely from the eighth nerve and GABAergic inhibitory input mainly from the superior olivary nucleus. GABA activates both ligand-gated chloride channels (GABA_A receptors) and G-protein-coupled receptors (GABA_B receptors). The GABA_B-mediated inhibitory input to NM is robust because of its depolarizing feature and long-lasting kinetics. Interestingly, GABA_BRs are expressed at both the presynaptic terminals and postsynaptic NM neurons. We investigated modulation of GABA_A-mediated inhibition by GABA_BRs using whole-cell voltage clamp techniques. Both evoked inhibitory postsynaptic currents (eIPSCs) and miniature IPSCs (mIPSCs) recorded from NM neurons were blocked completely by bicuculline, a GABA_AR antagonist, and reversed at the predicted reversal potential. Bath-applied baclofen (0.1, 1, 10, and 100 μM), a GABA_BR agonist, produced dose-dependent suppression of

eIPSCs. This inhibition was largely blocked by CGP52432 (10 μ M), a potent and selective GABA_BR antagonist. Baclofen also appeared to reduce the frequency but not the amplitude of mIPSCs, suggesting a presynaptic mechanism for GABA_BR-mediated modulation on the inhibitory transmission. Moreover, blocking GABA_BRs by CGP52432 (10 μ M) increased the frequency of mIPSCs, indicating that a tonic GABA_BR-mediated suppression of the inhibitory input to NM neurons probably exists. The amplitude of mIPSCs was also increased by CGP52432, probably due to an increase in the frequency of synchronized spontaneous release of GABA. We propose that GABA_BRs function as autoreceptors on GABAergic terminals innervating NM neurons, regulating synaptic strength of GABA_BR-mediated depolarizing inhibition via a presynaptic mechanism. Supported by DC00466, DC00395, DC00018, and DC04661.

907 Gene Expression in the Anterior Ventral Cochlear Nucleus

David R. Friedland, Richard Raphael, Anne R. Hansen, Paul Popper, Joseph A. Cioffi

Otolaryngology and Communication Sciences, Medical College of Wisconsin, 9200 W Wisconsin Ave, Milwaukee, WI, United States

The anterior ventral cochlear nucleus (AVCN) serves as the principal relay station between the auditory nerve and higher brain stem centers. Bushy and multipolar neurons within this subdivision exhibit specialized electrophysiological properties important in processing acoustic stimuli. These cells have largely been characterized by anatomical and physiological features which have led to a confusing myriad of descriptions varying by protocol, species and investigator. As such, we have begun to focus on molecular biologic markers to identify the basic underlying properties of this nucleus and the fundamental differences between auditory brainstem neurons.

Cochlear nuclei were freshly dissected from Brown Norway rats and the AVCN separated. Serial analysis of gene expression (SAGE) was used to generate a quantitative library of tags reflecting gene transcription. Tags were matched to the NCBI rat SAGE database and evaluated using gene ontology (GO) terms.

Over 16,000 tags were analyzed, identifying approximately 2,000 known genes and several thousand partially characterized rat mRNAs. Our initial focus was on cell signaling. We identified 9 potassium channel subunits including Hcn2, Kcnb1, Kcnc1, Kcnc3, Kcnj14, Kcnj4, Kcnk6, Kcnn2, and Kv8.1. We further investigated the unique channel Kcnk6 and confirmed its expression by RT-PCR. We additionally identified multiple subunits of voltage-gated calcium, sodium, and chloride channels and 5 classes of gap junction channels. Multiple receptor subunits for GABA and glutamate/NMDA were also noted in abundance.

These results represent the early stages in characterizing the central auditory system in molecular biological terms. Identification of unique molecular markers can provide an objective means of classifying neurons and provide insight into their physiological and morphologic phenotypes.

Funded by the Robert J. Toohill Intramural Research Fund and the Triological Society Career Development Award.

908 Expression of Cannabinoid CB1 Receptor in the Avian Brainstem Auditory System

Todd L. Stincic, Richard L. Hyson

Psychology, Florida State University, Box 1270, Tallahassee, FL, United States

Neurotransmission within the chick auditory brainstem has been well characterized for both glutamate and GABA. However, little attention has been given to other receptor systems which may modulate glutamatergic and GABAergic transmission. One such system is the broadly expressed cannabinoid signaling system. The present report, examines the expression of the cannabinoid receptor 1 (CB1) subtype in the chick brain, focusing primarily on the brainstem auditory nuclei.

CB1 receptor expression was visualized using in situ hybridization. The brains of P10 chicks were fresh frozen and cryostat sectioned at 20 μ m. The sections were mounted onto slides and were fixed in 4% paraformaldehyde immediately before hybridization. A ³³P radiolabeled cDNA probe was synthesized from a 702 base pair cDNA fragment of the chicken CB1 receptor. The slides were then exposed to film to produce autoradiographs which were analyzed with the ImageJ program.

The pattern of labeling was generally consistent with reports of CB1 expression in other species. For example, CB1 mRNA was found throughout the brain in low levels, but was highly expressed in select areas such as the granule layer of the cerebellum. However, published literature has asserted that the brainstem is relatively devoid of CB1 expression. In contrast, we observe distinct labeling in the brainstem auditory nuclei: nucleus magnocellularis, nucleus laminaris, and nucleus angularis. Most remarkable was the dramatic labeling observed in the eighth nerve ganglion cells, which was equal to or greater than the level of labeling found in the cerebellum. Preliminary immunolabeling results using a CB1 receptor antibody are consistent with these in situ hybridization results. The robust labeling for CB1 receptor suggests the cannabinoids may play a significant role in the early processing of auditory and vestibular information.

909 Differential distribution of HCN1 and HCN2 in the rat auditory brainstem

Ursula Koch, Marianne Braun, Christoph Kapfer, Benedikt Grothe

Auditory Processing, Max-Planck Institute of Neurobiology, Am Klopferspitz 18A, Martinsried, Germany

The integration of synaptic inputs in neurons is largely determined by the composition and distribution of ion channels on the somata and dendrites. Auditory brainstem neurons that process sound with great temporal precision have ionic currents activated near the resting potential to shorten membrane time constants. One of these currents is the hyperpolarization-activated current (I_h). Molecular cloning of the channel underlying I_h revealed four different isoforms (HCN1-4) of which HCN1 and HCN2 are widely distributed in the brain. HCN1 activates several times faster upon hyperpolarisation, and its activation range is more depolarized compared to the HCN2 isoform. Furthermore, HCN2 is more sensitive to the modulation caused by the intracellular cAMP concentration.

We determined the distribution of HCN1 and HCN2 channels in the auditory brainstem and midbrain of P20-P30 rats, using standard immunohistochemical techniques.

HCN1 antibodies gave rise to punctuate staining on the somatic and dendritic membrane, whereas HCN2 labeling was only observed at the somata. Strong HCN1 staining was found on octopus cells and bushy cells of the ventral cochlear nucleus, principle neurons of the lateral and medial superior olive and neurons of the ventral nucleus of the lateral lemniscus. No HCN1 staining was observed in the dorsal cochlear nucleus and the medial nucleus of the trapezoid body (MNTB). In contrast, HCN2 staining was strongest in the MNTB and in the dorsal nucleus of the lateral lemniscus. Moderate HCN2 staining was also observed in unidentified large cells and bushy cells of the ventral cochlear nucleus. In the central nucleus of the inferior colliculus only a subpopulation of neurons showed HCN1 or HCN2 immunolabeling.

This differential distribution of HCN1 and HCN2 channels agrees with the physiologically observed Ih currents in corresponding neuronal populations and might represent the basis for functional heterogeneity and diverse sensitivity to neuromodulators.

910 Voltage Gated Channels Sharpen and Amplify EPSPs in Principal Neurons of the Medial Superior Olive

Paul J. Mathews¹, Nace L. Golding^{1,2}

¹*Institute for Neuroscience, University of Texas at Austin, 1 University Station, C0920, Austin, TX, United States,* ²*Section of Neurobiology, University of Texas at Austin, 1 University Station, C0920, Austin, TX, United States*

Principal neurons of the medial superior olive (MSO) encode sound localization cues by detecting the coincident arrival of their excitatory synaptic inputs. Dendritic and somatic patch-pipette recordings were used in gerbil brainstem slices to understand how voltage-gated channels shape the integration of these synaptic inputs. Simulated EPSC-shaped waveforms were injected during somatic whole-cell recordings. Voltage responses increased linearly with EPSC amplitude until ~10-15 mV below threshold, where responses began to exhibit amplification. This amplification was blocked in the presence of 1 μ M TTX, indicating that it was mediated by voltage-gated sodium channels (maximum increase 23.8 \pm 5.7% vs. TTX, n=4). Surprisingly, there was a TTX-sensitive amplitude-dependent decrease in response duration (maximum decrease 14.0 \pm 6.7 % vs. TTX, n=4) and an increase in the rate of repolarization (maximum slope increase 41.3 \pm 9.6% vs. TTX, n=4). This decrease in duration was not observed in the presence of the potassium channel blocker 4aminopyridine (5 mM), suggesting that voltage-gated potassium channels serve to maintain temporal fidelity in the face of sodium channel amplification.

To determine whether EPSP amplification occurs in the dendrites, we have begun to make simultaneous dendritic and somatic current-clamp recordings from MSO principal neurons. While the results are preliminary, synaptic amplification in the dendrites by voltage-gated channels was not apparent in response to dendritically injected EPSCs. However, simulated EPSPs decreased in duration and showed faster repolarization as they propagated from the dendrites to the soma, reflecting the activation of outward conductances.

Taken together, these results show that subthreshold synaptic integration in MSO principal neurons is shaped by voltage-gated sodium and potassium channels. The coordinated action of these channels provides synaptic amplification near the soma without loss of temporal fidelity.

911 An Organotypic Slice Co-culture of Postnatal Rat Brainstem and Mouse Embryonic Dorsal Root Ganglion Neurons

Charoensri Thonabulsombat^{1,2}, Saga Malin Johansson³, Petri N Olivius¹

¹*Center of Hearing and Communication Research, Karolinska Institutet, BLDG M1:00, KS, Stockholm, Sweden,* ²*Department of Anatomy, Institute of Science & Technology for Research & Development, Faculty of Science, Mahidol University, Bangkok, Thailand,* ³*Department of Neuroscience, Karolinska Institutet, Retziusvag 8 B2:414, Stockholm, Sweden*

The poor regeneration capability of the neural components of the mammalian inner ear has initiated different approaches to enhance the functionality after injury. An interesting alternative is to use a biological implant with the potential to establish synaptic contacts with the cochlear spiral ganglion neurons and with the perspective to develop into a functional auditory unit. In order to evaluate the essential factors for this the in vivo model may not be sufficient. Here we describe an in vitro model where neuronal components of the peripheral auditory neuronal system including the second order neuron have been removed to the petri dish. The factors essential for the survival of the implant could easily be modified in this system. In vitro models have frequently been employed to investigate and determine the factors of success for neuronal implantation. In order to visualize and study the biological properties of neurite outgrowth, we have developed this co-culture system as an in vitro brain stem slice preparation. Nervous tissue was implanted into the brainstem slices on the nerve by using Stoppini method and roller drum culture method. These in vitro methods allows to manipulate the system and find the appropriate survival factor(s) i.e neurotrophic factors, implant location etc. for long-time survival and auditory neural connections. Hence a slice culture preparation of the rat cochlear nucleus was utilized to investigate the characteristics and the neuronal outgrowth within and between the peripheral nervous system (PNS) and the central nervous system (CNS). These slice cultures from postnatal (P) day 12-14 rats were used as the host and co-cultures were made from transplantation with embryonic (E) dorsal root ganglion (DRG) neurons day 13-14 mouse on the nerve. The preliminary results showed survival of the slices co-cultured with DRGs for up to three weeks in both methods.

This study was performed to investigate the neuronal survival in the brainstem slice and the neurotrophic factors potentially needed for neurite outgrowth towards the cochlear nucleus. In the clinical situation hearing deficits due to the acoustic neuroma tumour may benefit from replacement of the vestibulocochlear nerve.

912 Response of single units in the mammalian cochlear nucleus to iterated rippled noise with negative gain

Jesko L Verhey¹, Veronika Neuert², Ian M Winter²

¹Physics, University of Oldenburg, Carl von Ossietzky Str 9-12, Oldenburg, Germany, ²Physiology, Cambridge University, Downing Street, Cambridge, United Kingdom

It is still unclear which unit types, if any, in the mammalian cochlear nucleus signal temporal pitch-related information to higher centres. Many studies have implicated either onset or chopper units, however, a recent study using iterated rippled noise (IRN) has shown primary-like units as being the best candidate. IRN can be generated by delaying a wideband noise and then either adding (IRN(+)) or subtracting (IRN(-)) it from the original noise. IRN(+) and IRN(-) have similar waveform envelopes but differ in spectrum and temporal fine structure. This results perceptually in different pitches for IRN(+) and IRN(-). IRN can thus reveal whether a unit responds to changes in temporal fine structure or responds to the waveform envelope. In the ventral cochlear nucleus VCN primary-like units are best able to signal the delay of IRN in terms of their temporal discharge patterns. The responses of non-PL units (mainly choppers) largely reflected the waveform envelope and not the temporal fine structure (Shofner, J. Neurophysiol. 1999). The inability to encode IRN(-) is a problem for the chopper theory of pitch encoding and so we have begun to explore the ability of all unit types in the cochlear nucleus to encode IRN(-). In this study we show that 11/18 units in the dorsal cochlear nucleus with best frequencies (BFs) below 0.5 kHz could show stimulus related responses to IRN(-) while all units with BFs greater than 0.5 kHz (n = 28) failed to show any pitch related activity. In the VCN 8/10 units with BFs below 1.1 kHz showed pitch-related activity to IRN(-) whereas all units with BFs greater than 1.1 kHz (n=16) failed to show any pitch related activity. Primary-like units can encode IRN(-) but our results suggest that, at least for transient-chopper and pause-build units there is a strong BF dependency. Crucially, however, we await further confirmation as to whether onset and sustained-chopper units with low-BFs can also encode IRN(-).

913 Acoustic Reflex Thresholds obtained with chirp stimuli compensating for cochlear dispersion

Matthias Müller-Wehlau¹, Manfred Mauermann¹, Torsten Dau², Birger Kollmeier¹

¹Medizinische Physik, Universität Oldenburg, Carl-von-Ossietzky Str. 9-11, Oldenburg, Germany, ²Centre for Applied Hearing Research, Acoustic Technology, Technical University of Denmark, Ørstedts Plads, Building 352, Lyngby, Denmark

Dau et al. (*J. Acoust. Soc. Am.*, 107, 1530-1540, 2000) demonstrated a significant gain of wave-V amplitude of auditory brainstem responses (ABR) by using a phase-optimized chirp stimulus. The chirp was designed such as to compensate for cochlear travel-time differences across frequency and theoretically produces a maximally synchronized neural excitation. Since the neural reflex arc comprises essential sources of ABR, the influence of neural synchrony on the acoustic reflex threshold (ART) was investigated

in the present study. The low-level reflex measurement paradigm suggested by Neumann et al. (*Audiol Neurootol* 1, 359-369, 1997) was used. The ART was measured for tone complexes (BMTC) consisting of a series of up-chirps that correspond to the chirps in the Dau et al. study. Corresponding measurements were also obtained with the temporally inversed complex (iBMTC) and a third tone complex with identical amplitude spectrum but random phases of the components (rTC). The experiments were conducted in 8 normal-hearing (NH) and 7 hearing-impaired (HI) subjects with a flat sensorineural hearing loss. For the NH listeners, the ART for the BMTC was about 20 dB lower than that for the iBMTC stimulus while, for the HI listeners, the difference was only about 7 dB. A dependence on the frequency spacing of the components within the tone complexes was found for the NH- but not for the HI-listeners. The NH showed lower ARTs for the rTC- than for the BMTC-stimuli while, for the HI, the ART was found to be between those for iBMTC and BMTC stimulation. For the rTC-stimulus, no dependence on the frequency spacing was found in both subject groups. The findings of the present study suggest that the ART is influenced by at least two different factors: (a) the amount of synchrony of neural activity across frequency, and (b) the nonlinear (and fast-acting) gain mechanism that is reduced in the case of a sensorineural hearing loss, as suggested by Kubli et al (*ARO Abstracts* 599, 2000).

914 Responses to Amplitude Modulated Tones of Neurons in the Ventral Nucleus of the Lateral Lemniscus of the Unanesthetized Rabbit.

Ranjan Batra

Anatomy, University of Mississippi Medical Center, 2500 North State Street, Jackson, MS, United States

Rapid variation in the amplitude of a sound is a common feature of the acoustic environment. Such variation can induce different percepts in listeners ranging from fluctuation to pitch, depending on the rate of variation. The ventral nucleus of the lateral lemniscus (VNLL) has been implicated in the processing of the temporal structure of sounds because it is hypertrophied in echolocating mammals. Here we report the responses of single neurons in the VNLL of a nonecholocating mammal, the rabbit, to sinusoidally amplitude modulated (SAM) tones.

Responses of individual neurons were characterized by their modulation transfer functions (MTFs): the variation in response as a function of modulation frequency. Modulation frequencies in the range 6 - 1600 Hz were used for testing. MTFs were based on both discharge rate (rMTFs) and on synchrony to the envelope (sMTFs). Two main types of rMTFs encountered were *bandpass* and *flat*, although a large proportion of neurons had MTFs with complex shapes that were not readily categorized.

Responses of neurons with bandpass and flat rMTFs differed in a number of respects. Most neurons with bandpass rMTFs had sMTFs that were flat; neurons with flat rMTFs typically had sMTFs that were lowpass. Neurons with bandpass rMTFs synchronized strongly to the modulation, with synchronization coefficients typically > 0.9. Neurons with flat rMTFs did not synchronize as strongly. Neurons with bandpass rMTFs responded to short tonebursts only near the onset, whereas neurons with flat

rMTFs responded throughout the burst.

The presence and characteristics of the neurons with bandpass rMTFs suggest that the VNLL plays a role in converting the temporal code for modulation frequency that is used in the auditory nerve into a rate-based code. However, the substantial proportion of neurons with complex MTFs indicates that the VNLL plays other roles in auditory processing as well.

Supported by NSF grant IBN-9807872.

915 Coding of the upper spectral edges of HRTF notches by DCN Type IVi neurons is predicted by second-order spectral weighting functions

Lina A. J. Reiss, Eric D. Young

Biomedical Engineering, Johns Hopkins Univ., 720 Rutland Ave, Baltimore, MD, United States

Recent psychophysical experiments using notch, band-pass, and hi-pass noise suggest that the upper spectral edges of HRTF mid-frequency notches are the relevant feature used by humans for vertical sound localization (Macpherson & Middlebrooks, 1999). In addition, ICC Type O neurons have been shown to give maximum excitatory responses to spectral edges, mostly the upper edge, aligned at BF (Davis & May, 2002). This suggests that vertical sound location might also be encoded in DCN Type IV neurons through excitatory responses to spectral edges, rather than inhibitory responses to spectral notches, as previously believed.

We recorded from DCN Type IV neurons in the decerebrate cat, and divided units into Type IVi, which had non-monotonic rate-level functions for broadband noise, and Type IV, which did not. For notch or band-pass noise presented at a range of center frequencies, 14/17 Type IVi neurons responded with excitatory peaks when the upper spectral edge was aligned with BF. The selectivity of this peak is sharper than the inhibitory response to the notch centered at BF. In contrast, only 1/7 Type IV neurons showed any selectivity in their response to spectral edges. We also computed linear and second order spectral weighting functions using responses to random spectrum stimuli (RSS). Linear weighting functions performed poorly in predicting edge sensitivity, but when second order weights were added, the predictions improved in 6/10 edge-sensitive neurons. These findings suggest that, like the other sound localization cues of ITD and ILD, HRTF cues are analyzed early in the auditory system, before integration in the inferior colliculus. The data also suggest that edge sensitivity is produced by non-linear spectral interactions in Type IVi units, which are often second order.

Supported by NIH grant DC00115.

916 DCN Unit Responses to Moving Spectral Notches in Broadband Noise

Michael J. Anderson, Eric D. Young

Biomedical Engineering, Johns Hopkins University, 720 Rutland Ave., 505 Traylor Building, Baltimore, Maryland, United States

Principal cells of the dorsal cochlear nucleus (the so-called type IV units) have a region of nonlinear integration to stimuli presented at high sound levels. The response to broadband stimuli is excitatory and the response to narrowband stimuli, centered at BF, is

inhibitory. However, responses to spectral notches, centered on BF, in broadband noise are also inhibitory. Based on the working model of type IV response generation, the nonlinearity is produced by two inhibitory interneurons: type II units, which are responsive to narrowband stimuli and the wide band inhibitor, which is responsive to broadband stimuli. To investigate the frequency of the inhibitory inputs to the type IV units and the behavior of type II units in the model, we used broadband noise stimuli containing 1kHz wide moving notches which increased and decreased in frequency. The moving notches were presented at three different starting frequencies relative to the BF of the unit, notch starting at BF, notch centered on BF, and notch ending at BF. The notch caused all DCN units to fire at lower average rates when it overlapped with the BF of the unit. The onset response nature of type II neurons caused them to have lower average response rates when the 1 kHz moving notch was located within 1kHz below BF compared with 1kHz above BF. The average response of type IV units were reduced when the moving notch overlapped with the BF of the unit compared with when the notch was away from BF. However, the 1 kHz moving notch seemed to have the same inhibitory effect on type IV units regardless of whether the notch was located within 1kHz below or 1kHz above BF. Support by NIH Grant DC0115.

917 Differential Timing of the Development of Inhibition Within the Superior Olivary Complex (SOC) Revealed by Optical Imaging

Geetha Srinivasan, Eckhard Friauf, Stefan Löhrike

Sinnes- und Entwicklungs-Neurobiologie, Abteilung für Tierphysiologie, Technische Universität Kaiserslautern, Postfach 3049, Kaiserslautern, Germany

Glycinergic inhibition plays important roles in neuronal information processing within the SOC, a mammalian auditory brainstem center. In the lateral superior olive (LSO), glycine-evoked responses are initially depolarizing and shift to hyperpolarizing at around postnatal day (P)7 (Kandler and Friauf, 1995). This shift is due to developmental changes in the intracellular chloride concentration (Ehrlich et al., 1999), regulated by the K⁺/Cl⁻ cotransporter KCC2 (Balakrishnan et al., 2003). So far, nothing is known about the development of glycine responses in other major SOC nuclei, namely the medial superior olive (MSO) and the superior paraolivary nucleus (SPN).

To study the development of glycine responses in the MSO and SPN, we employed an optical imaging method using the fast voltage-sensitive dye RH795. In acute brainstem slices of rats aged from embryonic day 19 to P9, contralateral inputs were stimulated by bipolar electrodes. The optical signals were detected by a 464-photodiode array (RedShirtImaging, USA). These measurements allow the simultaneous monitoring of electrical activity in several nuclei of the SOC as well as the detection of regional differences within a given nucleus.

In the MSO, we observed depolarizations until P7 and hyperpolarizations thereafter. No regional difference was found within the MSO. Concerning the SPN, the shift of glycine-evoked responses occurred several days earlier, i.e., around P0, also not showing any regional difference. To assess whether any regional differences occur within the LSO, we also tested this nucleus. We found that in

the lateral limb glycine-evoked depolarizations occurred until P7, as shown in our earlier studies. In contrast, in the medial limb they occurred only until P4, indicating that the shift in the LSO is in a tonotopic order. In summary, our results from optical imaging show a differential development of glycinergic inhibition within the SOC nuclei.

Support: Deutsche Forschungsgemeinschaft, Lo 718/1-3

918 Spatiotemporal dynamics of stimulus-driven neural activity along the tonotopic gradient of the hamster dorsal cochlear nucleus observed using real time optical imaging.

James A. Kaltenbach, Jinsheng Zhang, Jie Wang

Otolaryngology, wayne state university, 5E-UHC, Detroit, michigan, United States

The tonotopic organization of the mammalian dorsal cochlear nucleus (DCN) has been mapped electrophysiologically by recording the frequency tuning properties of neurons along a systematic set of coordinates that span the medial-lateral and rostrocaudal dimensions of this structure. Maps obtained in this manner display low characteristic frequencies (CFs) laterally and high CFs medially. However, the spatiotemporal dynamics of activity changes within the tonotopic framework have yet to be described for stimuli that vary over time. We have been experimenting with optical imaging as a means of studying these dynamics using the voltage sensitive dye, Di-2-ANEPEQ. After dye application, the DCN was examined with an ultra-fast, high resolution camera mounted onto an overhead microscope, and the surface of the DCN was imaged during presentation of static tones as well as dynamic stimuli consisting of frequency modulated tone sweeps. Static, pure tone stimulation produced increased fluorescent signal in discrete bands or patches on the DCN surface. The location of these signals varied in a frequency-dependent manner consistent with the known frequency representation of the DCN. Dynamic stimuli, consisting of low to high frequency tone sweeps also produced patches or narrow bands of signal. When the stimulus frequency was shifted from low to high, an increase in optical signal was observed to shift from lateral to more medial locations; when the stimulus frequency was swept from high to low, the optical signal shifted from medial to more lateral locations. However, in some animals, it appeared that the signal locations shifted in discontinuous steps or followed an irregular trajectory resembling a zig-zag pattern in response to tone sweeps. We are exploring the possibility that these irregularities reflect a finer grain of tonotopic organization than has been revealed in electrophysiologically defined maps. (This project was supported by NIH grant R21 DC006041)

919 The Dorsal Cochlear Nucleus Integrates Auditory and Somatosensory Information.

Susan E Shore, Jianzhong Lu

Otolaryngology, University of Michigan, 1301 E Ann St, Ann Arbor, MI, United States

Trigeminal projections to the granule cell domains of the ventral cochlear nucleus have characteristics associated with excitatory synapses (Shore et al., *J. Comp. Neurol.* 419:271-285; Haenggeli et al., *ARO # 966*, p244). Granule cells, in turn, can excite cartwheel and fusiform cells in the dorsal cochlear nucleus (DCN), or

indirectly inhibit fusiform cells via the inhibitory action of cartwheel cells. We investigated trigeminal system influences on these pathways by electrically stimulating the trigeminal ganglion while recording spontaneous and sound-driven activity from neurons in the DCN.

Guinea pigs were anesthetized, paralyzed with gallamine and artificially respired. A bipolar stimulating electrode was placed stereotaxically into the ipsilateral trigeminal ganglion. Electrical stimuli were applied as bipolar pulses, 200 μ sec per phase, at intervals of 200 ms, with amplitudes ranging from 10-100 μ A. Responses from DCN units were obtained using a 16-channel silicon electrode to enable simultaneous recordings from multiple neurons. Units were sorted using principal component analysis. Current pulses were presented alone, simultaneously with, or preceding 50 ms broadband noise (BBN) bursts. Units were classified using BBN and CF tonebursts.

DCN units showed excitatory and inhibitory responses to trigeminal ganglion stimulation. However, when paired with BBN stimulation, trigeminal stimulation usually inhibited the firing rate in response to BBN, reflecting multisensory integration. Pulses preceding the acoustic stimuli by as much as 80 ms were able to inhibit responses to BBN.

These results demonstrate that projections from the trigeminal system to the CN play a role in integration mechanisms involving different senses. This integration could be involved in plastic changes in the brain which may lead to perceptions of phantom sounds ("tinnitus") which can be modified by manipulations of somatic regions of the head and neck ("somatic tinnitus").

Supported by NIH grant 5 R01 DC004825-03 and Tinnitus Research Consortium.

920 Responses to contralateral sound of ventral cochlear nucleus neurons in guinea-pig

Christian Sumner, Susan E. Shore

Kresge Hearing Research Institute, University of Michigan, 1301 E. Ann Street, Ann Arbor, Michigan, United States

The cochlear nucleus (CN) responds to stimulation of the contralateral ear. This information is probably mediated by a direct commissural connection and descending connections from the superior olivary complex. In the dorsal division of the CN (DCN), responses are nearly all inhibitory, and different studies have suggested a variety of tuning characteristics. Contralateral responses have not been widely studied in the ventral division (VCN).

We have recorded the responses of VCN neurons to contralateral and binaural sound stimulation in anaesthetized guinea-pigs. Recordings were made using 16-channel silicon probes that allow collection of single and multi-unit responses from a number of neurons simultaneously.

VCN responses to contralateral sound are almost always inhibitory. Approximately 30% of VCN neurons show some reduction in firing rate in response to broadband noise (BBN). Rate-level functions are mostly monotonic and show good coding of interaural level differences, suggesting a potential role in localization. In response to contralateral amplitude modulated (AM) BBN, phase locking is inferior to ipsilateral stimulation, but can be weakly observed at modulation frequencies of several hundred Hertz. The response to contralateral pure tones is often weaker than for BBN,

suggesting broad tuning. However, when detectable, pure tone tuning varies, with some receptive fields as narrow as the ipsilateral excitatory tuning. Contralateral and ipsilateral best frequencies are usually close. These results are most consistent with direct commissural inputs from the opposite cochlear nucleus.

Supported by NIH grant 5 R01 DC004825-03 and Tinnitus Research Consortium

921 Duration Tuning in the Superior Paraolivary Nucleus of the Rat

Randy J. Kulesza, Jr., Albert S. Berrebi

Otolaryngology-H & N Surgery, West Virginia Univ. School of Medicine, Sensory Neurosci Res Center, Morgantown, WV, United States

The superior paraolivary nucleus (SPON) of the rat contains a homogenous population of multipolar GABAergic neurons that project to the ipsilateral inferior colliculus. We have previously shown that the SPON is a tonotopically organized structure whose cells respond transiently (usually with only 1 or 2 spikes) at the offset of best-frequency pure tone stimuli, and are capable of phase-locking to sinusoidally amplitude modulated BF tones. Interestingly, the firing rate of some SPON units changed as a function of stimulus duration. This suggested that the offset responses of SPON neurons might be involved in measuring stimulus duration, or may contribute to the formation of duration sensitivity in their target neurons in the inferior colliculus.

To dissect the SPON's role in tuning to sound duration, we used in vivo extracellular recording techniques to analyze single-unit responses to best-frequency pure tone stimuli (20 dB above threshold) of varying durations (1, 2, 5, 10, 25, 50, 100, 200, 400 and 800 msec). Preliminary results indicate that the majority of SPON neurons generate more spikes with increasing tone duration (ie., "long pass"), although most responses become saturated around 10 msec durations. However, a small population of SPON neurons displayed "band pass" duration functions. Units were considered band pass duration selective if their spike count at certain tone durations was at least 50% greater than the spike counts at both shorter and longer durations (Ehrlich et al, 1997). These findings suggest that duration tuned neurons may exist below the level of the inferior colliculus.

Supported by grant DC-06626 to ASB.

922 Persistent inhibition of high frequency neurons in the gerbil DNLL

Thomas Zahn, Ida Kollmar, Sylvie Baudoux, Michael Pecka, Benedikt Grothe

Auditory Processing, Max Planck Institute of Neurobiology, Am Klopferspitz 18a, Martinsried, Germany

Ipsilaterally inhibited and contralaterally excited (IE) cells in the dorsal nucleus of the lateral lemniscus (DNLL) exhibit a specific response feature when stimulated with interaural intensity differences (IID) favoring the ipsilateral ear ("positive" IIDs). Such stimuli will condition the cell's response to subsequent signals arriving within the next 10-30 ms, even if they are more intense at the contralateral, excitatory ear. This effect has yet only been described in bats (Burger et al. 2001).

We recorded the response from single neurons in the high frequency region of the gerbil DNLL (BF>2000Hz) to dichotic signals containing 3 sinusoidal pulses. While the first pulse was of binaural nature with positive IIDs, the 2 subsequent pulses contained only monaural pulses at the contralateral, excitatory ear.

Apparent persistent inhibition caused a gradual suppression of spike responses to the second (excitatory) pulse, not present during the identical third pulse. When varying the IID of the first pulse as well as the time gap between each pulse (Inter Pulse Intervall, IPI), the suppression increased with higher IIDs and decreased with higher IPIs.

Based on these recordings and the comparisons with a computational model, we suggest a strong hyperpolarization of DNLL cells by acoustical stimuli elicited by stimuli in the ipsilateral hemifield. This is assumed to last up to 30 ms after the end of the stimulus and may cause the suppression of responses to subsequent stimuli from the contralateral hemifield. The recorded effect is likely to contribute to the generation of the precedence effects at higher auditory centers.

923 A new visual dimension to auditory modelling using DSAM

Lowel Phillip O'Mard, Raymond Meddis

Psychology, CNBH, University of Essex, Wivenhoe Park, Colchester, United Kingdom

The design of auditory simulations has been made visually transparent and easy to follow using the new Simulation Design Interface (SDI), implemented for the Development System for Auditory Modelling (DSAM). This new facility can be used to modify and run auditory simulations using computer applications written using DSAM.

DSAM is a computing library designed as a standard platform for producing applications to create and evaluate auditory models. It brings together many published auditory models (produced by different research groups), analysis functions and general utility functions. All these features are available within a flexible, stable programming platform that has been extensively tested for robustness and accuracy.

The AMS computer application is written using the DSAM library and therefore inherits the interface and all the other features of DSAM. These include: applications portable to all computer systems; ready-compiled installations for major systems; comprehensive error handling; graphical displays (currently available for Unix and Windows) and flexible but simple simulation descriptions using DSAM "Simulation scripts".

AMS allows a variety of interface options. AMS accepts command-line options giving access to all parameters, so it can be employed to produce quite complex analysis runs using scripting tools. There is a graphical user interface (GUI) that allows the graphical design of simulations with comprehensive access to model and application parameters.

AMS is available as an "out of the box" Windows installation (98/NT/ME/2000 and XP) for PC's, Linux RPM's and can be installed on UNIX machines using its auto-configuration system. It is available for download from our WWW site, <http://www.essex.ac.uk/psychology/hearinglab/dsam>.

We use AMS to showcase the SDI with a model of a cochlear nucleus cell simulating binaural release from forward masking.

Acknowledgements

Funding from the BBSRC supports this project.

924 EarLab: A Virtual Laboratory for Auditory Research

David C. Mountain^{1,2}, David J Anderson¹, Glenn Bresnahan³, Socrates Deligeorges^{1,2}, Andrew W. Howitt^{1,2}, Lan Hu^{1,4}, Lee Lichtenstein^{1,4}, Viktor Vajda^{1,4}

¹Hearing Research Center, Boston University, 44 Cummington St., Boston, MA, United States, ²Biomedical Engineering, Boston University, 44 Cummington St., Boston, MA, United States,

³Scientific Computing and Visualization Group, Boston University, 111 Cummington St., Boston, MA, United States, ⁴Electrical and Computer Engineering, Boston University, 8 St. Mary's Street, Boston, MA, United States

The EarLab system is a virtual laboratory that is intended to allow scientists to perform experiments on large-scale distributed simulations of the mammalian auditory pathways. The EarLab simulations are based on interchangeable building blocks or modules each of which represents a different component of the auditory system or represents sound-source, data-acquisition and data-visualization subsystems. The modules are designed to run in a distributed heterogeneous computing environment and to be configured at run time. The physiological modules are designed to be species independent with species dependent parameters loaded from a parameter database. The current system includes modules that represent sound sources, propagation between the source and the tympanic membrane, and the subthalamic auditory pathways.

The overall simulation architecture is designed to be able to represent any physiological system or group of systems. The software is divided into five layers: the User Interface Layer, the Presentation Layer, the Control Layer, the Transport Layer and the Module Layer. The User Interface layer can be a standard Web browser or a dedicated desktop application. The Presentation Layer mediates between the User Interface and the Control Layer, passing user requests to the Control Layer and presenting Control Layer responses to those requests back to the user. The Control Layer manages the simulation environment while the Transport Layer mediates all data transfer between the Control Layer and the Module Layer and between elements of the Module Layer.

The Transport Layer is configured at the beginning of each run to reflect the desired connectivity between Modules. Once the simulation has been started, the Modules transfer data among themselves mediated by the Transport Layer, as well as communicating status information to the Control Layer, which may then be further summarized and presented to the User as information regarding overall progress in the current simulation.

This research is supported by NIDCD and NIMH, award DC04731

925 A Model for ITD sensitivity in the MSO: Interactions of excitatory and inhibitory synaptic inputs, channel dynamics, and cellular morphology

Yi Zhou¹, Laurel H. Carney², H. Steven Colburn¹

¹Biomedical Engineering, Boston University, 44 Cummington Street, Boston, MA, United States, ²Bioengineering & Neuroscience, Syracuse University, 621 Skytop Road, Syracuse, NY, United States

Recent physiological results from the gerbil MSO reveal that blocking glycinergic inhibition can shift the best ITD by as much as 0.2 ms (Brand et al., 2002, *Nature*, 417:543-7). The authors explained these results with a model that included a fast contralateral inhibitory input to the MSO that delays excitation from one side and therefore shifts the ITD at which bilateral excitatory inputs coincide. This mechanism requires a sub-millisecond duration inhibition, which has not been described in the auditory system. In an attempt to seek an alternative explanation for this result, we used a multi-compartment model to simulate a bipolar MSO cell with realistic parameters. The axon of the model cell was placed on the lateral dendrite, an interesting observation of MSO cells with unknown function (Smith, 1995, *J. Neurophysiol.* 73:1653-67). For this cell structure, contralateral excitatory inputs are attenuated more than ipsilateral inputs by the passive soma, en route to the axon, and the rate-ITD curve is thus skewed toward ipsilateral delays. Voltage-dependent ion channels on the soma, such as sodium currents, strengthen the contralateral excitation and move the centroid of the rate-ITD curve toward contralateral delays. Finally, inhibition on the soma counterbalances the active currents and shifts the ITD curve back toward ipsilateral delays. When the inhibitory currents are activated or blocked, the model cell successfully simulates the experimental results. The nonlinear interaction between synaptic inputs and the channel dynamics plays a key role in the ITD sensitivity of the model cell. These results suggest a mechanism for 'fine-tuning' the ITD sensitivity of MSO cells: the model cell's best ITD depends on a static ITD, determined by afferent delay lines, and is adjusted by inhibitory inputs. These modeling results also suggest a potential function for the asymmetrical axon placement on the MSO cell body. [Supported by NIH DC00100 & DC01641]

926 Spatial and Temporal Expression of Otolith Matrix Protein (OMP) mRNA in Zebrafish

Elena G Ignatova¹, Isolde Thalmann¹, David M Ornitz², Baogang Xu¹, Ruediger Thalmann¹

¹Otolaryngology, Washington University Medical School, 660 S. Euclid Avenue, Box 8115, St. Louis, MO, United States,

²Molecular Biology and Pharmacology, Washington University Medical School, 660 S. Euclid Avenue, Box 8103, St. Louis, MO, United States

The bony fish uses a single otolith in each macular end organ for vestibular mass load, as opposed to a large number of small otoconia serving the higher vertebrates. The otolith is composed of CaCO₃ in an aragonitic crystal lattice and contains a number of matrix proteins, the most prominent of which is a 54 kDa protein. The zebrafish is an ideally suited developmental model for several

reasons: The embryonic development takes place *ex utero*, allowing precise post-fertilization (pf) timing; the transparency of the embryo has the advantage for live observation of the otoliths, as well as visualization of stains; and numerous zebrafish mutants with impaired otolith formation are available. As a first step in the elucidation of the biochemical mechanisms leading to otolith formation and growth, we have selected to characterize the principal OMP. This protein has recently been cloned in the trout (Murayama et al., 2000). Using a zebrafish EST homologous to the trout sequence and performing a series of PCR, and 5' and 3' RACE reactions, we obtained the full length OMP-cDNA sequence. The deduced protein has a molecular mass of 40 kDa and shows homology to a C-terminal portion of human melanotransferrin. Twelve of 14 cysteine residues are conserved, suggesting similar arrangements of disulfide bridges. The OMP mRNA is first detected at 16 hpf, slightly preceding the otolith seeding event. In the early embryo the OMP mRNA is distributed diffusely throughout the otocyst. As the vestibular structures mature, the OMP mRNA localizes to the transitional epithelium and the phalangeal cells flanking the sensory epithelium. The sensory epithelium, *per se*, is free of OMP mRNA. At no time is OMP message detectable outside of the otocyst.

927 Isolation Of Messenger RNA From A Pure Population Of Supporting Cells From The Vestibular Sensory Epithelia Of The Rat

Ricardo Cristobal, Phillip A Wackym, Joseph Cioffi, Paul Popper

Department of Otolaryngology and Communication Sciences, Medical College of Wisconsin, 9200 W. Wisconsin Ave, Milwaukee, Wisconsin, United States

The cellular and molecular events leading to hair cell formation in the intact and regenerating inner ear of adult vertebrate species are currently under debate. Possible mechanisms include supporting cell mitosis, transdifferentiation of supporting cells or stem cells, hair cell repair, or a combination of these processes. The understanding of the process of regeneration has been hampered by the lack of supporting cell markers and the paucity of data on the patterns of gene expression in this cell population. The present study presents the first report of a technique to capture a pure population of supporting cells and isolate their mRNA, and provides evidence of mRNA integrity.

The vestibular sensory epithelia of adult rats were dissected out and immediately embedded in OCT and frozen at -80°C . Ten-micron sections were obtained in a cryostat. Sections were stained and dehydrated. Slides were placed in an Arcturus Pixcell II laser capture microscope system (Arcturus, Mountain View, CA). Individual supporting cells resting on the basal lamina of the sensory epithelia were identified and captured onto the film following the standard Arcturus protocol. The RNA was extracted using a PicoPure RNA Isolation Kit. The integrity of the RNA was confirmed with reverse transcriptase PCR using primers for rat beta-actin, a cytoskeletal protein expressed in supporting cells. The present study presents a powerful tool for the analysis of gene expression profiles in individual cell types within the sensory epithelia. This technique has significant potential for advancing our knowledge on the molecular makeup of hair cell precursors in the adult and regenerating inner ear sensory epithelia.

Supported by an intramural grant from the Toohill Research Fund of the Department of Otolaryngology and Communication Sciences, Medical College of Wisconsin, Milwaukee, Wisconsin and a grant from NIH/NIDCD RO1DC02971 (PAW).

928 Global Gene Expression Profiling of Neurofibromatosis Type 2 Vestibular Schwannomas

Joseph Cioffi, Richard Raphael, Christy Erbe, Paul Popper, Phillip Wackym

Otolaryngology and Communication Sciences, Medical College of Wisconsin, 9200 West Wisconsin Ave, Milwaukee, Wisconsin, United States

Neurofibromatosis type 2 (NF2) is an autosomal dominant genetic disorder characterized by the development of tumors in the central and peripheral nervous system. The hallmark of NF2 is bilateral vestibular schwannoma (VS) which occurs in greater than 90% of patients diagnosed with the disease. The most common method of treatment of VS is microsurgical removal which has inherent risks and substantial costs. Despite their common cellular origin, VS can exhibit vastly different macroscopic, microscopic, and growth characteristics. These phenotypic differences include solid, cystic, high vascularity, and low vascularity tumors. Our hypothesis is that the genesis, growth, and phenotypic characteristics of NF2-associated VS are determined by genetic alterations that vary in gene expression. We are currently using serial analysis of gene expression (SAGE) to generate global gene expression profiles of VS exhibiting marked phenotypic differences in vascularity, growth rates, and cellular character. Here we report the findings from one SAGE library constructed from a highly vascular, fast growing VS. We have sequenced 500 clones containing in excess of 16,000 tags. Preliminary analysis of this SAGE library has revealed the expression of many interesting genes including those involved in tumorigenesis, neural cell growth and differentiation, apoptosis, and angiogenesis. Osteonectin, a cellular marker associated with glioma invasiveness, was found to be very highly expressed. Furthermore, at least 14 proangiogenic factors and receptors were expressed in this highly vascular tumor. These include vascular endothelial growth factor/receptor, transforming growth factor- β /receptor, glial activating factor, neuropilin 1, hepatic growth factor, and fibroblast growth factor 2. Gene expression was confirmed by reverse transcription-polymerase chain reaction (RT-PCR) thus validating the SAGE results. In addition, we are using exon scanning to characterize NF2 gene mutations in these tumors. The identification of specific genes and molecular pathways controlling the growth and phenotypic characteristics of vestibular schwannomas may provide new insights into the management and treatment of NF2.

929 Vestibular abnormalities in insulin-like growth factor-1 mouse mutants

Jose A Morales-García¹, Patricia Vigil¹, Julio Contreras², Carlos Avendaño³, Isabel Varela-Nieto¹

¹Cellular Signaling, Instituto de Investigaciones Biomédicas A. Sols (CSIC-UAM), Arturo Duperier 4, Madrid, Spain, ²Department of Anatomy, Facultad de Veterinaria, Universidad Complutense, Avda Complutense, Madrid, Spain, ³Department of Morphology, Facultad de Medicina, Universidad Autónoma, Arturo Duperier 4, Madrid, Spain

Growth factors participate in the development of the otocyst into a mature inner ear and also in the maintenance and repair of the postnatal organ.

The insulin-like growth factor (IGF) system is formed by the ligands IGF-I, IGF-II and insulin, plus three receptors (IGF receptors types 1 and 2; IGF1R and IGF2R, and insulin receptor) and six binding proteins. IGF1R binds IGF-I with the highest affinity and specificity. IGF-I is a survival and differentiation factor for the developing and adult nervous system, where it is expressed. IGF-I is expressed during inner ear development in chicken and in the postnatal mouse cochlear ganglion. IGF-I regulates cochleovestibular ganglion neurogenesis in chicken embryos whereas IGF-I deficiency in the mouse severely affects postnatal survival, differentiation and maturation of the cochlear ganglion (Camarero et al., 2001; 2002 and 2003).

We have studied the vestibular phenotype of the *Igf-1^{-/-}* mouse. Our results indicate that at postnatal day (P5), the general vestibular structure is not altered in *Igf-1^{-/-}* mouse when compared to controls. At P20, immunohistochemistry analysis shows a more disorganized neurosensory epithelia and a delayed maturation in the vestibular ganglion. Finally, transmission electron microscopy studies show a decreased and altered myelination of the vestibular ganglion neurons and an increased number of cells with apoptotic profile.

Camarero, G.; Avendaño, C.; Fernández-Moreno, C.; Villar, M.A.; Contreras, J.; de Pablo, F.; G. Pichel, J.; Varela-Nieto, I. (2001). Delayed Inner Ear Maturation and Neuronal Loss in Postnatal *Igf-1*-Deficient Mice. *J. Neurosci.* 21 (19):7630-7641.

Camarero, G.; Villar, M.A.; Contreras, J.; Fernández-Moreno, C.; G. Pichel, J.; Avendaño, C.; Varela-Nieto, I. (2002). Cochlear abnormalities in insulin-like growth factor-1 mouse mutants. *Hearing Research* 170: 2-11.

Camarero, G.; Leon, Y.; Gorospe, I.; De Pablo, F.; Alsina, B.; Giraldez, F.; Varela-Nieto, I. (2003). Insulin-like growth factor-1 is required for survival of transit-amplifying neuroblasts and differentiation of otic neurons. *Dev. Biol.* (In press).

930 Postural Recovery During Vestibular Regeneration In Pigeons

Insook Lim¹, David Huss¹, J. David Dickman^{1,2}

¹Otolaryngology, Washington University, 660 S Euclid, B0x 8115, St. Louis, MO, United States, ²Anatomy and Neurobiology, Washington University, 660 S Euclid, B0x 8115, St. Louis, MO, United States

It has been known for some time that regeneration of vestibular receptors in birds occurs after ototoxic damage, with functional

recovery of the VOR and VCR noted (Carey et al., 1996; Goode et al., 1999). In the present study, we produced a complete lesion of all vestibular receptors cells and denervated the epithelium using an intralabyrinthine application of streptomycin (Frank et al. 1999). We then examined the recovery of vestibular related head posture and gait in pigeons during regeneration. Pigeons were operantly conditioned to navigate a 1.5 meter linear run for fluid reward and were filmed using quantitative videography. Variables for head posture included position, head bob, head turn, and head shakes. Gait variables included latency, number of lane changes, and number of steps. Normative behavior exhibited upright head control and stable posture with no evidence of head shakes or tremors. All birds had short latency maze runs of less than 8 seconds. Behavior immediately post streptomycin was characterized by severe postural instability, with devastatingly ataxia, stumbling, staggering, and an inability to maze run. Head posture was abnormal, including high frequency head shakes, side to side oscillations and low frequency tremors. As regeneration progressed, latencies to run the maze gradually decreased, with normal values being reached by 28 – 30 days post ototoxic insult. All head posture and gait variables returned to normal levels by 35 – 40 days regenerative recovery. Comparisons between behavioral recovery and hair cell density showed a correlative relationship, with head tremor mostly defined by loss of type I cells in the striola region.

Supported in part by funds from NIH DC003286 and NASA NCC2-1159.

931 Morphology and Afferent Innervation Patterns of Otolith Maculae following Regeneration from Ototoxic Damage

Zakir H Mridha, David Huss, David Dickman

Department of Otolaryngology, Washington University, 660 S Euclid Ave, Campus Box 8115, St. Louis, MO, United States

Common to all animals, pigeon vestibular afferents innervate two types of sensory cells: type I and type II hair cells, which are innervated by three classes of afferents including calyx, bouton and dimorphic afferents. It has been known for long time that aminoglycoside antibiotics are ototoxic and produce stereocilia loss, hair cell death and denervation. It is also now established that in time regeneration of vestibular hair cells and their reinnervation, occurs after the cessation of ototoxic treatment. The primary objective of the present study is to determine, whether similar or vastly different afferent innervation patterns develop in otolith organs of animals undergoing regeneration. Biotinylated Dextran Amine was injected into the vestibular nuclei of pigeons that had received complete loss of hair cells and denervated afferent via intralabyrinthine application of streptomycin 6-9 months earlier. In general the hair cell distributions of the regenerated utricular maculae as well as parent axon diameters were not different from normal units. In both normal and regenerated maculae calyx afferents contained more type I hair cells than dimorphs. But the average number of type I hair cells were significantly less in regenerated utricular and saccular afferent calyces than normal. Like normal utricular afferents regenerated calyx afferents had smallest fiber length among all three classes. For saccular dimorph afferents the total axonal length, number of boutons, number of type I hair cells were smaller than normals. In the utricular maculae, dimorph afferents had smaller calyceal terminals with fewer type I hair cells, but nearly normal numbers of bou-

ton terminals and branch fibers. Saccular bouton afferents in regenerated birds were smaller with less terminals and innervation areas than normals. Utricular bouton afferents appeared to have similar morphologies to normal birds.

This work was supported in part by NIDCD DC003286 and NCC2-1159

932 Comparative Cytoarchitectural Organization of Vertebrate Cristae Ampullares

Hussain Ali, Sapan S. Desai, Anna Lysakowski

Anatomy and Cell Biology, Univ. of Illinois at Chicago, 808 S. Wood St., Chicago, IL, United States

We examined the cellular organization of the crista sensory epithelium in skates, toadfish, grass frogs, bullfrog, chicken, finch, pigeon, squirrel monkey and mouse in order to better delineate the zonal boundaries between various regions. Sensory organs were sectioned transversely, longitudinally or horizontally at 4 μ m thickness, counterstained with Richardson's stain, and reconstructed using the NeuroLucida computer program.

Several principles appear to govern the organization of the crista sensory epithelium. Studies by other investigators have shown that fibers can vary in their fiber diameter, discharge pattern, and innervation patterns. These fibers can be divided into one or more central zones, and surrounding regions known as the peripheral zone. In non-mammalian cristae with an eminentium cruciatum, the crista is divided into two hemicristae each with a central zone located midway between the eminentium and the planum. In the turtle, chicken, pigeon, and finch, the central zone contains predominantly type I hair cells contacted by complex calyx terminals. These complex terminals contact up to 12 type I hair cells, the exact upper limit depending upon species. The organization of the central zone consists of a gradient pattern with the most complex terminals located innermost, surrounded by concentric areas of simpler and simpler calyces. The central zone is surrounded by a peripheral zone containing only type II hair cells.

The crista of toadfish contains proto-calyces, large afferent endings, contacting up to three hair cells. A circumscribed central zone found in each hemicrista of the sensory epithelium in skates, toadfish and frogs can be defined based on the thickest fibers, the location of the proto-calyces and wider hair cells. More precisely delineating the boundaries between various subzones of the crista will allow investigators to better elucidate physiological characteristics of each region.

Supported by R01 DC-02521 (AL) and F31 DC-05451 (SSD).

933 NOS Immunochemical Staining in Calyces in Chinchilla Vestibular Endorgans

Sapan S. Desai, Jasmeet Dhaliwal, Anna Lysakowski

Anatomy and Cell Biology, Univ. of Illinois at Chicago, 808 S. Wood St., Chicago, IL, United States

We have immunochemically localized nitric oxide synthase I (NOS-I) in the chinchilla vestibular sensory epithelium. NOS-I produces a gaseous neurotransmitter, nitric oxide. We have previously shown NOS-I to be present in calyces surrounding type I hair cells (Dhaliwal and Lysakowski, ARO Abst., 2000) and in a

subpopulation of brainstem efferent neurons and peripheral efferent boutons using NADPH diaphorase histochemistry (Lysakowski and Singer, JCN, 2000).

The localization of NOS-I and soluble guanylate cyclase (sGC), combined with calretinin as a marker for calyx afferents, was explored. Ten chinchillas were fixed with 4% paraformaldehyde, 1% picric acid, and 1% acrolein in phosphate buffer. Otolith organs were decalcified, all organs embedded in gelatin, and sectioned at 35 μ m. Sections were treated with 4% Triton for 1 hr, 1% NaBH₄ for 10 min, blocked in 0.5% fish gelatin and 1% BSA for 1 hr, incubated in primary antibody (1:200 sh anti-NOS, 1:200 gt anti-calretinin, and 1:200 rbt anti-sGC) for 72 hrs, then placed in secondary antibody (1:100 dky anti-sh IgG TRITC, 1:100 dky anti-gt IgG-FITC, and 1:100 dky anti-rbt IgG FITC) overnight. Sections were rinsed and examined in a confocal microscope. Some sections were used for EM immunogold experiments.

A subset of calyx endings containing NOS-IR were labeled with calretinin, indicating they belong to calyx afferents in the crista central zone and the macular striolar region. NOS-IR is restricted in peripheral dimorphic afferents to the synaptic zone of the calyx (below the level of the hair cell nuclei). NOS-I colocalizes in calyces with sGC, an enzyme that mediates the downstream effects of NO. We conclude that NO is produced in calyx terminals, where it may diffuse to affect surrounding afferent and efferent fibers. Precisely delineating the NO signal transduction cascade will help elucidate its neurochemical and physiological role in the vestibular system.

Supported by R01 DC-02521 (AL) and F31 DC-05451 (SSD).

934 Developmental Changes in the Distribution of Calretinin- and Peripherin-Positive Axons Projecting to the Mouse Utricle

Ben N. Bristow, Leslie Leonardo, Larry F. Hoffman

Surgery/Head & Neck, Geffen School of Medicine at UCLA, Box 951624, Los Angeles, California, United States

Vestibular primary afferent neurons exhibiting calyx and bouton dendritic morphologies have been found to exhibit unique molecular phenotypes represented by the exclusive expression of calretinin and peripherin, respectively, in the adult crista. Calretinin expression also appears to be confined to calyx afferents projecting to the adult utricular striola. In the present study, we implemented a double labeling immunocytochemistry protocol to study the distribution of peripherin-positive (PER+) fibers in the adult utricle (i.e. P28 days) in association with calretinin-positive (CAL+) fibers. Furthermore, we sought to determine the developmental appearance of these distinct molecular phenotypes. To achieve this goal the double-labeling protocol was also conducted in specimens at 1 (P1) and 7 (P7) days of age.

In the adult mouse utricle, CAL+ fibers and calyces were confined to the striolar region, similar to that previously reported. PER+ fibers were distributed throughout the sensory epithelium, including the juxtastricular and striolar regions. Double-labeled fibers were not found in the P28 specimens. At P7 CAL+ fibers exhibited a broader topographical distribution than that found at P28, and were not confined to the striolar region. The distribution of P7 PER+ fibers was topographically broad as observed in the adult. At this stage, some fibers were both CAL+ and PER+. This trend

of immaturity was even more pronounced in the P1 utricle, where CAL+ and PER+ fibers were both widely distributed, and double-labeled fibers were numerous. These data suggest that the development of molecular phenotypes for fibers projecting to the utricle parallels that previously reported for the crista. Peripherin is widely expressed in developing neurons of the peripheral vestibular system, as found for other developing peripheral neurons. These data further indicate that distinct molecular phenotypes of vestibular fiber subpopulations are not found until after P7.

Supported by DC005776 and the Stein/Opppenheimer Endowment Fund (LFH).

935 Receptive Fields of Angular Head Movement Kinematic State in Mammalian Semicircular Canal Afferent Neurons

Larry F. Hoffman¹, Michael G. Paulin²

¹*Surgery/Head & Neck, Geffen School of Medicine at UCLA, Box 951624, Los Angeles, California, United States,* ²*Department of Zoology, University of Otago, PO Box 56, Dunedin, New Zealand*

We are investigating the dynamic response diversity among mammalian semicircular canal afferent neurons using band-limited Gaussian stimuli and evaluating the resultant receptive fields (RFs) of head movement kinematic state. These represent the time domain analyses of the conditional probability of the afferent discharging when the head transcends a specific region of kinematic state space. This representation is compared to the traditional method of expressing vestibular afferent response dynamics as transfer functions in the frequency domain.

Spontaneous and rotation-evoked action potential trains were recorded from single semicircular canal afferent neurons in anesthetized adult male chinchillas. The peripheral vestibular receptor from which a given afferent projected was determined on the basis of its discharge modulation during clockwise and counterclockwise rotations. For each afferent, spontaneous discharge was recorded first, followed by responses to discrete frequency sinusoids (e.g. 0.025 - 1.6 Hz, 30 deg/sec peak velocity) and band-limited Gaussian rotations (0.05 - 2 Hz, 8 deg/sec rms).

We have found that mammalian semicircular canal afferents generate discrete RFs, as has been previously demonstrated for bullfrog afferents. The RFs corresponding to diverse afferents from the same vestibular receptor (e.g. the horizontal crista) are distributed throughout the space of head movements encoded by afferents from that receptor, with varying shapes (representing the covariance matrices) and loci of their centroids. These RFs reflect the diversity in afferent dynamics among afferents, and represent the distributed diversity in dynamics corresponding to their frequency domain transfer functions. RFs from afferents exhibiting more regular spontaneous discharge (i.e. CV < 0.05) tended to be centered along or close to the velocity axis, while those with more irregular spontaneous discharge tended to be centered closer to the acceleration axis.

Supported by NIH DC005059 (LFH)

936 Extracellular Recordings from Vestibular-Nerve Afferents in the Normal C57BL/6 Mouse

David M Lasker¹, Hong Ju Park^{1,2}, Lloyd B Minor¹

¹*Otolaryngology, Johns Hopkins University, 720 Rutland Ave Ross 710, Baltimore, Md, United States,* ²*Otolaryngology, Konkuk University, 1 Hwayang-dong Gwangjin-gu, Seoul, Korea, Republic of*

Extracellular recordings were made from 97 vestibular afferents from normal C57BL/6 mice. Animals were rotated about an earth vertical axis either on center or 50 cm offset from the center of rotation. Maximum sensitivity vectors were obtained for each canal unit by tilting the animal -20° , 0° and 20° in the interaural and naso-occipital planes and rotating the animal in each position at 0.7 Hz. Maximum sensitivity vectors were obtained for each otolith unit by tilting the animal $\pm 45^\circ$ in 15° increments in the same planes and rotating the animal at 0.7 Hz while offset 50 cm from the axis of rotation. Sinusoidal rotations 0.1 - 12 Hz, $2000^\circ/\text{s} \approx$ peak angular acceleration and 0.5 - 10 Hz, 0.45g peak tangential acceleration were delivered when the animal was placed in the center and offset 50 cm from the center, respectively.

The resting rate of regularly (CV < 0.1, n = 29) and irregularly (CV > 0.1, n = 55) discharging afferents was 41.5 ± 13.1 and 26.8 ± 12.6 sp/s. Vestibular time constants measured at 0.1 Hz were 3.3 ± 1.0 s for regular and 2.4 ± 0.7 for irregular canal afferents. Sensitivity and phase for regularly discharging canal afferents measured 0.14 ± 0.08 (sp/s)/($^\circ/\text{s}$) and a phase of -0.38 ± 9.43 (sp/s)/($^\circ/\text{s}$) re velocity at 0.5 Hz which increased by $20.0 \pm 30.8\%$ with a corresponding phase lead of $33.0 \pm 16.2^\circ$. Irregularly discharging canal afferents measured 0.22 ± 0.1 (sp/s)/($^\circ/\text{s}$) and a phase lead of $16.3 \pm 10.47^\circ$ re velocity at 0.5 Hz with an increase in sensitivity by $116 \pm 85\%$ at 12 Hz with a phase lead of $56.8 \pm 19.1^\circ$. Sensitivity and phase for regularly discharging otolith afferents measured 36.4 ± 23.2 sp/s/g and $1.0 \pm 5.9^\circ$ re acceleration at 0.5 Hz and declined to a sensitivity and corresponding phase lag of 13.8 ± 16.7 sp/s/g and $33.6 \pm 16.7^\circ$ at 10 Hz. Irregularly discharging otolith afferents measured 58.9 ± 19.2 sp/s/g and a phase lead of $19.2 \pm 22.0^\circ$ re acceleration at 0.5 Hz and declined slightly at 10 Hz with a sensitivity of 44.8 sp/s/g and a phase lead of $2.0 \pm 2.2^\circ$. (Supported by NIH R01 DC02390)

937 The Synaptic Ultrastructure of the Adult Mouse Utricular Macula

Maha Ahmad, Anna Lysakowski

Anatomy and Cell Biology, Univ. of Illinois at Chicago, 808 S. Wood St., Chicago, IL, United States

Synaptic ribbons provide innervation to the utricular macula by conveying head motion signals between hair cells and afferent terminals. Calyceal invaginations are hypothesized to play a role in synaptic transmission by facilitating vesicle recycling, and are only present between calyces and type I hair cells. We have shown that the number of calyceal invaginations are modified under conditions of controlled hypergravity (Ahmad and Lysakowski, ASGSB abst., 2002). Other studies have suggested a role for calyceal invaginations in ephaptic transmission between type I hair cells and calyx endings. (Goldberg, 1996). Previously, the synaptic

ultrastructure of the chinchilla crista ampullaris was examined (Lysakowski and Goldberg, 1997). The crista exhibited regional variations in the distribution of both synaptic ribbons and calyceal invaginations, which were found to be more numerous in the central zone compared to the peripheral zone. Type II hair cells possessed more afferent boutons peripherally than centrally.

The synaptic ultrastructure of the mouse utricular macula was studied in three disector samples. The disector method was used to estimate the number of synaptic ribbons and calyceal invaginations. The results are preliminary, based on 84.5 hair cell equivalents (52 in the invaginations data). The average number of synaptic ribbons was 10.5 ± 4.1 in type I hair cells and 12.9 ± 1 in type II hair cells. Some of the synaptic ribbons (20%) occur in clusters. A variety of shapes, ranging from spheroids to elongate and intermediate forms, was present also. The most widely expressed form of ribbons (45%) was spheroids. The average number of calyceal invaginations in type I hair cells was 30.4 ± 3.8 , with 25.2 ± 9 invaginations in type IC hair cells and 28.9 ± 4.7 in type IS hair cells. This number varied by region with more (52.6 ± 19.2) invaginations per type I hair cell in striola and fewer (30.6 ± 3.6) in extrastriola.

Supported by NASA NAG2-1589 and NIH R01 DC2521.

938 Organization of the utricular striola in *Trachemys scripta*: Stereocilia counts

William J. Moravec, Ellengene H. Peterson

Biological Sciences; Neuroscience Program, Ohio University, Irvine Hall, Athens, OH, United States

The striola is a ubiquitous feature of vertebrate otolith organs, but its function is poorly understood. We are addressing this issue by examining mechanically significant features of hair bundles in the utricle of a turtle, *T. scripta*. Previously we reported that the striola can be divided into two parallel zones that differ in stereocilia number and spacing (Peterson and Rowe, Soc. Neurosci. Abs, 2001). Zone 2 spans the line of polarity reversal. Zone 3 is more lateral, and its bundles have higher and more heterogeneous stereocilia counts than zone 2 bundles. Type I hair cells are restricted to zone 3, and indirect evidence suggested that type I and type II hair cells in zone 3 differ in stereocilia counts (Moravec et al., ARO, 2003). Here we present direct evidence that type I hair cells have significantly higher stereocilia counts than type II hair cells anywhere in the utricular macula. Our data are based on confocal scans of phalloidin-stained utricular wholemounts. We identified type I hair cells by labeling their postsynaptic calyces with biotinylated dextran amine applied to the utricular nerve.

Compared with hair cells in the adjacent extrastriola, striolar hair cells have significantly larger apical surfaces ($26.3 \pm 5.7 \mu\text{m}^2$), bundle areas ($10.6 \pm 2.9 \mu\text{m}^2$), and stereocilia counts (71.6 ± 20.8). Type II hair cells have similar stereocilia counts in striolar zones 2 and 3 (59.3 ± 9.5 ; range: 40 - 76), but type II bundle areas are larger in zone 2 than in zone 3 because inter-stereocilia spacing is greater (Peterson and Rowe, 2001). Type I hair cells have significantly higher stereocilia counts (90.7 ± 19.1 ; range: 60 - 130) than total striolar type II hair cells or type II hair cells in zone 3 alone (61.1 ± 8.5 ; range 47-72).

Our data indicate that the utricular striola is highly differentiated, with both regional and type-specific differences in mechanically

significant features of its hair bundles. Because stereocilia number affects hair bundle mechanics, type I hair cells represent a mechanically specialized subpopulation of striolar receptors.

939 Organization of the utricular striola in *Trachemys scripta*: Bundle heights

Jingbing Xue, Ellengene H. Peterson

Biological Sciences; Neuroscience Program, Ohio University, Irvine Hall, Athens, OH, United States

Theory and computational analyses suggest that the heights of kinocilia and stereocilia play significant roles in hair bundle mechanics. To understand how these bundle features vary with location and hair cell type we are using confocal microscopy of undehydrated slices from the utricle of a turtle, *T. scripta*. We double-stained slices with phalloidin and a monoclonal antibody to tubulin to visualize stereocilia and kinocilia, respectively, and we identified type I hair cells by labeling their postsynaptic calyces with biotinylated dextran amine applied to the utricular nerve. Here we report that striolar hair cells exhibit both location- and type-specific differences in bundle heights.

Within the striola, kinocilium heights increase systematically from the line of polarity reversal, laterally, to the medial extrastriola; they are significantly shorter in zone 2 than in zone 3 (see Moravec and Peterson, 2004, ARO for striolar zones). Kinocilia heights of type I and type II hair cells do not differ when location is held constant. Zone 2 hair cells are all type II; they have the longest stereocilia in the striola, and the ratio of kinocilium to stereocilia heights (KS-ratio) averages $1.4 (\pm 0.7)$. Zone 3 contains both type I and type II hair cells. For both hair cell types, maximum stereocilia heights decrease with distance from the reversal line, but the decrease is steeper for type II hair cells. As a result type I hair cells have significantly lower KS-ratios (1.7 ± 0.6) than adjacent type II hair cells (3.1 ± 1.5).

Differences in bundle heights and stereocilia counts (Moravec and Peterson, 2004) provide evidence that there are at least three mechanically distinct populations of striolar hair cells: type II cells in zone 2 and type I and type II hair cells in zone 3. The low KS-ratios and high stereocilia counts of type I hair cells suggest that they are stiffer than adjacent type II hair cells, and it raises questions about how each hair cell type responds when the overlying otoconial membranes move.

940 Functional study and electro-microscopic observation on the damage in guinea pigs vestibular organ caused by cobalt 60 irradiation

Jiadong Wang¹, Dalian Ding²

¹*Department of Otolaryngology-Head and Neck Surgery, Shanghai Renji Hospital, 145 Shandong Road, Shanghai, China, People's Republic of,* ²*Center for Hearing & Deafness, SUNY at Buffalo, 215 Parker hall, 3435 Main Street, Buffalo, NY, United States*

Cobalt 60 irradiation is commonly used in the treatment of cancer and can directly damage the surrounding tissue. To evaluate the acute destruction of cobalt 60 irradiation to vestibular organs, the temporal bone areas of guinea pigs were irradiated by cobalt 60 for

50 Gy. The nystagmus response evoked by ocular tracking, revolving stimulation and caloric stimulation were tested for 4 hours, 3 days and 5 days after cobalt 60 exposure. The pathological changes of the vestibular organs were also observed under scanning or transmission electron microscope. The duration of the nystagmus response was not changed with ocular tracking stimulation, but was significantly reduced with revolving and caloric stimulation 4 hours after cobalt 60 exposure, and getting worse following 3 to 5 days. The broken kinocilium and disheveled stereocilia were found 4 hours post-cobalt 60 exposure as evidence of early damage to vestibular hair cell surface. The intracellular damage consists of swollenness in the mitochondria and endoplasmic reticulum in the early stage followed by the burst of the endoplasmic reticulum. This indicates that the vestibular organs could be destroyed by the irradiation of cobalt 60.

941 Effects of thickness and curvature on Utricular Otolith Dynamics

John Wallace Grant, Julian Davis

Engr Sci & Mech Dept, VA Tech, ESM Dept, MC 0219, Blacksburg, VA, United States

Previous work has investigated the statics and dynamics of the utricular otolith organ using mathematical models (Grant et al, JVR 4:137, '94; Krondachuk, JVR 11:13, '01). These models treated the otolith as a flat organ, with uniformly thick layers. One model (Jager et al., HR 173:29, '02) included out of plane effects representing the human utricle. These interpretations of the utricular otolith are geometrically inaccurate for the real organ.

In the Red Eared Turtle the thickness of the Column Filament layer, Gel layer, and Otoconial layer change with location. In addition, the neuroepithelium is curved. In order to investigate how these changes affect the statics and dynamics of the utricle, four Finite Element models were constructed using ANSYS. These included: a flat organ with constant thicknesses, flat with varying thickness, curved with constant thickness, and curved with varying thickness. This last model represents the actual utricular otolith geometry. Results indicated that the curvature and variable thickness both contribute to the increasing the dynamic range of this sensory organ.

942 Distribution of Glutamate Transporters in the Anteroventral Cochlear Nucleus of Cats and Mice

Alison L. Wright¹, Jenna G. Los¹, Tan Pongstaphone¹, David K. Ryugo^{1,2}

¹Otolaryngology, Johns Hopkins University, Traylor 510, 720 Rutland Ave., Baltimore, MD, United States, ²Neuroscience, Johns Hopkins University, Traylor 510, 720 Rutland Ave., Baltimore, MD, United States

Glutamate is the putative neurotransmitter between auditory nerve endings and cochlear nucleus (CN) neurons. The endbulb of Held is a prominent synaptic ending with several specialized features. Of particular interest are intermembranous cisternae between endbulb and spherical bushy cell (SBC). These cisternae appear closely associated with synapses, and so were operationally considered "gutters" for excess glutamate. We investigated the distribution of a neuronal transporter, EAAC-1, and an astrocytic

transporter, GLT-1 (antibodies courtesy of Dr. Jeff Rothstein), using standard immunoperoxidase methods for light (LM) and electron (EM) microscopy. We sought to test whether the membranes forming cisternae contained transporters.

At the LM level, GLT-1 labeled neuropil and was especially dense around the somata of SBCs. The SBCs themselves were unlabeled. In contrast, EAAC-1 labeled the SBC somata. These observations were consistent for cats and mice.

At the EM level, GLT-1 was found in astrocytic processes surrounding axosomatic endings of the SBC. All SBC endings are encased in glial lamellae. The somata of SBCs and the endings of auditory nerve fibers were unstained. In contrast, EAAC-1 was found in the SBCs and the primary auditory endings; astrocytic processes were unstained. Interestingly, EAAC-1 was generally found on the somatic side of the cisternae.

Although these data are preliminary, it appears that at least 2 types of transporters function in the CN to recycle glutamate. We postulate that the GLT-1 transporters mediate recycling by astrocytes that extend processes throughout the CN neuropil. EAAC-1 transporters recycle the rest in SBCs, endbulbs, and intermembranous cisternae. These results also suggest a role for cisternae in synaptic transmission.

Supported by NIH grant RO1 DC00232

943 Distribution of Neurotransmitter Receptors in Type I and Type II Spiral Ganglion Neurons in vitro

Jacqueline Flores-Otero, Robin L. Davis

Cell Biology & Neuroscience, Rutgers University, 604 Allison Road, Piscataway, NJ, United States

Type I spiral ganglion neurons isolated from the cochlea of postnatal mice show region-specific variations in their firing properties and ion channel distribution (Adamson et al., JCN, 2002). Interestingly, type II neurons also show location-dependent characteristics, but in a manner quite distinct from the type I neurons (Reid & Davis, ARO, 2003). We have interpreted these findings to mean that spiral ganglion neurons show specializations tailored to the frequency of sound that they encode. A prediction of this hypothesis is that such specializations would carry through to the synapses made by or onto spiral ganglion neurons, and we have begun to investigate this issue by examining the distribution of AMPA glutamate receptor subunits in type I and type II spiral ganglion neurons isolated from the apex and base of the cochlea.

A triple immunocytochemical staining technique was utilized to visualize the distribution of GluR2/3 glutamate receptors within the population of type I and type II spiral ganglion neurons. We quantified GluR2/3 staining with luminance measurements and found that labeling of type II spiral ganglion neurons (37.2 ± 1.8 , $N=22$) was significantly higher than type I neurons (25.8 ± 1.8 , $N=64$; $P<0.01$). The type I/type II disparity was greatest in the apex, where GluR2/3 staining in type I neurons was surprisingly low (17.9 ± 0.5 , $N=40$) as compared to basal type I neurons (38.9 ± 3.4 , $N=24$; $P<0.01$).

These experiments yielded the expected result that the type II neurons, which form the greatest number of peripheral synapses, produced the greatest amount of AMPA receptor protein. What was

novel about our findings, however, was that AMPA receptors were also highly enriched in the basal type I spiral ganglion neurons, a result in accord with many of the voltage-gated ion channels that we have analyzed. Additional experiments are underway to evaluate the distribution of other glutamate receptor subunits. Supported by NIH R01 DC01856.

944 Differential Expression of Voltage-Gated Ion Channels in Apical and Basal Spiral Ganglion Neurons

Jennifer B. Ray, Lucy Y. Hsu, Robin L. Davis

Cell Biology & Neuroscience, Rutgers University, 604 Allison Road, Piscataway, NJ, United States

Previous work from our laboratory has shown that postnatal spiral ganglion neurons isolated from the apical and basal cochlea of CBA/CAJ mice exhibit distinct electrophysiological phenotypes. Neurons from the high frequency, basal region display rapid firing features such as short latencies, abbreviated action potential durations, and rapid accommodation. Neurons isolated from the low frequency, apical region show a predominance of slower firing characteristics. By using antibodies against specific ion channel subunits, we also showed that the density of certain voltage-gated ion channels correlated with these electrophysiological differences (Adamson et al., JCN 2002). For example, Kv3.1 subunits, which contribute to action potential repolarization were found to be enriched in the basal neurons. In order to elucidate mechanisms that regulate the firing features of spiral ganglion neurons, we are quantifying the expression of genes that code for voltage-gated ion channels.

Total RNA isolated from P7 apical and basal spiral ganglia was used for real-time qRT-PCR. Primers were tested and found to be specific for voltage-gated ion channels with known distributions in the spiral ganglion (Kv3.1, Kv4.2, Kv1.1, and Kv1.2). Neuron-specific enolase (NSE) and β -tubulin were used to estimate the relative contribution from the neuronal population. Multiple experiments were carried out to assess Kv3.1 gene expression levels (N=3). Consistent with our immunocytochemical analysis, greater Kv3.1 gene expression was observed in the basal spiral ganglion relative to the apical spiral ganglion when the levels were normalized to NSE ($P < 0.05$). Normalization to β -tubulin expression also showed a similar trend.

These data suggest that quantification of gene expression can be used to gain insights into the factors that produce the differential response properties of apical and basal spiral ganglion neurons. Supported by NIH R01 DC01856.

945 Regeneration of the human auditory nerve: *in vitro* demonstration of neural progenitor/stem cells in the adult human spiral ganglion

Helge Rask-Andersen¹, Shaden Khalifa¹, Marja Bostrom¹, Bengt Gerdin², Anders Kinnefors¹, Dan Lindholm³, Josef Miller⁴

¹Otolaryngology, Uppsala University Hospital, No, Uppsala, Sweden, ²Department of Surgical Sciences, Unit for Plastic Surgery and Burns, University Hospital, Uppsala, Sweden, ³Department of Neuroscience, Uppsala University, Artillerigatan, Uppsala, Sweden, ⁴Kresge Hearing Research Institute, University of Michigan, 1301 E. Ann St, Ann Arbor, MI, United States

Neural progenitor/stem cells (NSCs) in adult CNS tissue are capable of neuronal, astrocytic, and oligodendroglial differentiation and the expression of properties of mature CNS neurons. We demonstrate that multipotent (neuronal-oligodendroglial) precursors with stem cell features can be isolated from the adult human spiral ganglion in Rosenthals canal. The 1fl coiled ganglion was excised, neurospheres identified, expanded with EGF and FGF-2 as mitogens, and subcultured. Expanded neurospheres showed incorporation of bromodeoxyuridine (BrdU) and co-expression of the progenitor cell marker nestin. Cells cultured with glia cell line-derived neurotrophic factor (GDNF) and neurotrophins (BDNF and NT-3) differentiated into elongated neurites of approx. 2000 μ m. GFAP-positive cells also developed, believed to represent Schwann cells. These human cells first strongly expressed cell marker nestin and then neurofilament, during differentiation. Time-lapse video recordings of proliferating cells and clonal analysis suggested that the human auditory nerve has the capability for self-renewal and replacement. Human progenitor cells may provide a valuable resource for further exploration of auditory nerve including gene expression. The use of these cells may provide new strategies for repair and treatment of auditory neuronal damage.

This work was supported by UAW/GM funding and EU Project QLG3-2002-01563-BIOEAR

Correspondence should be addressed to H.Rask-Andersen e-mail: helge.rask.andersen@ent.uas.lul.se

946 "The Axon Analyzer" – A computerized technique for quantitative dimensional analysis of *in vitro* regenerating human auditory nerves

Henrik Bostrom¹, Josef Miller², Marja Bostrom¹, Helge Rask-Andersen¹

¹Otolaryngology, Uppsala University Hospital, No, Uppsala, Sweden, ²Kresge Hearing Research Institute, University of Michigan, 1301 E. Ann St, Ann Arbor, MI, United States

Neurite growth is a fundamental characteristic of neurons *in vitro*. The accurate and quantitative assessment of growth can provide basic information on the health and development of neurons and the extent to which these features are influenced by environmental factors. Moreover, a number of basic investigations to define and assess the mechanisms involved with neuron survival and death, and factors that may influence development and maturation,

depend on accurate evaluation of neurite growth. The purpose of this work was to develop a valid, reliable, objective and quantitative assessment of neurite growth. A computer-based image analysis system (Axon Analyzer) was developed. This is a Microsoft Windows® based digital image processing software for extracting and measuring neurite outgrowth images, including highly branched detailed neurites. The system removes background variations, is user-friendly, easy and efficient. The software contains several advanced image processing algorithms, specially designed for extracting and measuring neurite outgrowths.

The system was developed in cooperation with Centre for Image Analysis at Uppsala University. The Axon Analyzer provides a fast and reliable assessment of neurite length, branching and growth speed. Using both guinea pig and adult human spiral ganglion cells in culture, we have demonstrated systematic and significant effects on neurite growth with neurotrophic factors GDNF (glial cell-line derived neurotrophic factor), NT-3 (neurotrophin-3), BDNF (brain derived neurotrophic factor), and combinations of these factors. Greatest growth and branching was observed with GDNF; combinations of other factors were almost as effective, but not when presented alone. In human spiral ganglion cells, with neurotrophic factor support, neurite growth could be demonstrated from 36 hrs following seeding to 28 days in culture. We conclude that neurite measurements using Axon Analyzer provides a valuable tool for assessing neurotrophic activity of growth factors in human spiral ganglion cells grown in vitro.

This work was supported by UAW/GM funding and EU Project QLG3-2002-01563-BIOEAR

Correspondence should be addressed to H. Rask-Andersen e-mail: helge.rask.andersen@ent.uas.lul.se

947 Time Course of Neurotrophin Actions on the Electrophysiological Phenotype of Spiral Ganglion Neurons in vitro.

Zhiping Zhou, Robin L. Davis

Cell Biology & Neuroscience, Rutgers University, 604 Allison Road, Piscataway, NJ, United States

Spiral ganglion neurons are the neural link between hair cell receptors in the periphery and neurons in the CNS. We have shown that postnatal apical and basal spiral ganglion neurons in vitro show distinctive responses to depolarization. Neurons from the base of the cochlea fire action potentials with shorter latencies and durations with more rapid accommodation than apical neurons (Adamson et al., JCN 2002). Interestingly, these features are altered by prolonged exposure to brain-derived neurotrophic factor (BDNF) and neurotrophin-3 (NT-3). In particular, the latter causes basal neurons to lose their fast firing characteristics, resulting in action potentials with longer latencies, prolonged durations, and slower accommodation. BDNF has the opposite effect, causing apical neurons to adopt the characteristics of basal neurons (Adamson et al., J. Neurosci. 2002).

The goal of these experiments is to determine the time course of the NT-3 effect on spiral ganglion neurons to understand better its functional implications. Whole-cell current clamp recordings were made from mouse basal spiral ganglion neurons (P5-7) exposed to NT-3 for differing periods of time. We used accommodation as a measure of NT-3 effects, quantified as the maximum number of

action potentials fired during a 240ms depolarization (APmax). Neurons exposed to NT-3 for 4 days showed a significant increase in APmax when compared to control cultures (10.5 ± 2.5 vs. 1.0 ± 0.0 spikes, $N=4, 3$, respectively; $P<0.05$ one tailed t-test). Cultures exposed to NT-3 for 3 days showed the same trend: neurons in control dishes fired a maximum of 1 action potential ($N=4$), whereas those exposed to NT-3 for 3 days fired 1 – 16 times (4.9 ± 1.9 spikes, $N=7$; $P>0.08$).

These experiments establish that NT-3 alters the firing properties of basal spiral ganglion neurons faster than previously demonstrated. We are currently determining the minimum time required to produce this effect. Supported by NIH R01 DC01856

948 Glycine Receptor Expression Changes in Cultured Spiral Ganglion Neurons of Cochlea

Wei Sun, Ping Wang, Richard J. Salvi

Center for Hearing & Deafness, University at Buffalo, 3435 Main Street, Buffalo, NY, United States

The neurotransmitter receptors expressed on spiral ganglion neurons (SGN) are thought to be established early in development, but recent studies suggest that some neurons can switch from GABAergic to glycinergic phenotype. GABAergic receptors have been identified on immature and mature SGN, but glycinergic receptors have not been observed. Here we show that culturing SGN for several weeks in the absence of NT-3 and BDNF leads to the expression of functional glycinergic receptors. Dissociated SGN (P2 mice) were cultured for up to 28 days in the presence of NT-3 or BDNF and afterwards the whole cell patch clamp was used to identify glycinergic and GABAergic ion channels. When glycine (1 mM) was puffed onto SGNs that cultured for 1 week or more in neurotrophin-free medium, it induced a robust inward current in every cell (8/8); however, glycine-induced currents were absent from short term SGN (0/16) cultures. The glycine-induced current was totally blocked by applying strychnine (10 μ M). The amplitude and the polarity of glycine-induced currents varied with holding potential and chloride (Cl^-) concentration. The reversal potential shifted from 0 mV to -40 mV when the Cl^- concentration in the bath changed from 140 to 20 mM. This suggests the glycine-induced current was mainly carried by Cl^- . The proportion of SGNs expressing glycine-induced currents was suppressed by the addition of neurotrophic factors to the cultures. BDNF or NT-3 reduced the proportion of SGNs expressing glycinergic current to 38% versus 100% in neurotrophin-free cultures. Our results suggested that the absence of NT-3 and BDNF in long-term SGN cultures results in the upregulation of glycinergic receptors and down regulation of GABAergic receptors. This “GABA-to-glycine” receptor switch is reminiscent of that seen in developing neurons in the lateral superior olive.

Supported by NIH grant P01 DC03600-01A1

949 Whole-Cell Firing Properties of Mouse Vestibular Ganglion Neurons

Jeffrey R Holt, Jessica R. Risner

Neuroscience & Otolaryngology, University of Virginia, Lane Rd., MR4, Rm 5127, Charlottesville, VA, United States

We used the whole-cell, tight-seal technique in current-clamp

mode to examine the firing properties of mouse vestibular neurons *in vitro*. Vestibular ganglia excised from neonatal mice (P0-P5) were maintained in culture for one to three days. Immunocytochemistry with anti-neurofilament 200 revealed bipolar cells with an average diameter of $12.4 \pm 2.8 \mu\text{m}$ ($n = 101$). In the DIC microscope similar bipolar cells ($13.3 \pm 1.8 \mu\text{m}$ diameter, $n = 87$) were selected for electrophysiological characterization. Two populations emerged: low-threshold neurons which required $57 \pm 19 \text{ pA}$, ($n = 7$) to evoke action potentials (APs) and high-threshold neurons ($124 \pm 52 \text{ pA}$, $n = 26$). Low-threshold neurons always fired two or more APs and were tuned to frequencies between 1 and 49 Hz (median = 11 Hz). High-threshold neurons fired a single AP and were tuned to frequencies between 4 and 55 Hz (median = 22 Hz).

To better understand the firing properties, we characterized the voltage-dependent conductances under voltage-clamp mode. Depolarization evoked fast activating/fast inactivating inward currents that were blocked by $1 \mu\text{M}$ TTX, consistent with Na^+ currents in other neurons. Peak Na^+ currents ranged from -1.5 nA to -9.7 nA ($-5.2 \pm 2.1 \text{ nA}$, $n = 52$) with otherwise homogeneous properties.

Depolarization also evoked outward currents with amplitudes from 260 pA to over 12 nA at +76 mV (mean = 5.9 ± 2.3 , $n = 70$) that reversed at $-70 \pm 20 \text{ mV}$ ($n = 46$) consistent with the currents being carried by K^+ . Application of the K^+ channel antagonists, 4-AP or TEA, blocked part but not all of the outward current, suggesting the outward currents were comprised of several components. In 14 of 17 cells, 4-AP blocked a fast activating/fast inactivating current. In 17 of 19 cells TEA blocked a slowly activating current that did not inactivate. Interestingly, both 4-AP and TEA altered the firing properties such that high-threshold neurons fired APs in response to small current steps. We conclude that the firing properties of vestibular neurons are shaped by a heterogeneous population of K^+ channels.

Supported by NIDCD grant DC05439

950 Long term, interactive neuromonitoring of CAP, CM, and CBF during auditory nerve compression and manipulation.

Jorge Bohorquez¹, Krzysztof Morawski², Ozcan Ozdamar^{1,3}, Fred F. Telischi^{1,3}, Rafael E. Delgado^{1,4}, Erdem Yavuz¹

¹Biomedical Engineering, University of Miami, P.O.Box 248294, Coral Gables, Florida, United States, ²Otolaryngology, Silesian Medical Academy, Sklodowskiej 10, Zabrze, Poland,

³Otolaryngology, University of Miami, 1666 NW 10th Avenue, Suite 306, Miami, Florida, United States, ⁴Software Development, Intelligent Hearing Systems Inc., 7326 S.W. 48th street, Miami, Florida, United States

We developed a monitoring and analysis system for cochlear function, during surgery. The system allows real time assessment of the cochlear function during auditory nerve manipulation. A specially designed otic probe, placed into the round window (RW) niche, enables simultaneous acquisition of cochlear blood flow (CBF) and electrocochleogram (ECochG). Three different regions of cochlea have been simultaneously studied by using 70dB SPL, 5 ms tone-burst stimuli at frequencies of 4KHz, 8KHz and 12KHz. The neuromonitoring system performs an automatic analysis of

cochlear microphonics (CM) and compound action potentials (CAP) extraction and analysis for the three frequencies in real-time. The automatic measurement of the amplitudes of the first and second harmonics of CM is achieved using coherent filters. The CAP signal is processed with a zero phase shift spectral filter, tuned to enhance the action potential onset, which is sometimes embedded within the summing potential. An automatic peak detection and tracking algorithm is then applied to extract latency and amplitude of CAPs. We performed long-term cochlear function assessment during 20 experimental surgeries, in animal models. The dynamics of CM, CAP and CBF during nerve manipulation and compression have been studied. CBF and ECochG measurements at three frequencies, have been studied and correlated with the surgical maneuvers. The second harmonic of the CM has shown different response to surgical maneuvers compared to the first harmonic. The use of such long term real-time monitoring systems provides information on cochlear dynamics that cannot be easily observed in traditional recording paradigms.

951 Spontaneous activity of auditory-nerve fibers: an improved lifetime distribution model for interspike intervals

Heinrich Neubauer¹, Dexter Robert Francis Irvine², Mel Brown², Peter Heil¹

¹Auditory Learning and Speech, Leibniz Institute for Neurobiology, Brennekestrasse 6, Magdeburg, Germany,

²Psychology, Monash University, Wellington Road, Clayton, Australia

Mammalian AN fibers are spontaneously active, i.e. they discharge action potentials in the absence of experimenter-controlled or intentional auditory stimulation. Such stimulation alters a given fiber's spontaneous discharge behaviour in that it affects the timing of individual spikes and/or the mean spike rate. To thoroughly understand the effects of auditory stimulation on the spiking behaviour of AN fibers, it is thus desirable to characterize the baseline condition, i.e., the spontaneous activity, as accurately as possible. Most current attempts to describe and model this highly irregular and probabilistic spontaneous activity are based on Poisson distributions, but are not fully satisfactory.

We have recorded lengthy periods of spontaneous activity from AN fibers of 5 barbiturate-anesthetized cats, and examined cumulative interspike interval distributions, probability density functions, and hazard rates. In modeling those data we assume that the spiking probability is the result of the combination of two probabilities. One of those can be conceptualized as the probability of exocytosis from the inner hair cell at a given presynaptic site, and the other as the probability of spiking of the postsynaptic afferent fiber given an exocytotic event. We find that a 2-parameter lifetime distribution for the presynaptic component combined with a 2-parameter recovery process (absolute and relative refractory periods) yields excellent and satisfactory fits to all data sets and returns physiologically plausible and readily interpretable values of the 4 parameters. The model is superior to those currently in use.

Supported by grants of the Deutsche Forschungsgemeinschaft to P.H. (He1721/5-1 and 5-2).

952 Is There Really a Broad Distribution of Spontaneous Rates in the Auditory Nerve?: Due to Long-range Dependence, Two or Three Different Spontaneous Rates Can Account for Empirical Histograms

B. Scott Jackson¹, Laurel H. Carney²

¹*Institute for Sensory Research and Dept. of Bioengineering and Neuroscience, Syracuse University, 621 Skytop Road, Syracuse, NY, United States,* ²*Institute for Sensory Research and Dept. of Bioengineering and Neuroscience, Syracuse University, 621 Skytop Road, Syracuse, NY, United States*

Estimating the spontaneous firing rate (SR) of auditory nerve (AN) fibers by measuring the average rate in a long (e.g. 30-second) interval is common practice. These measurements are important since SR is apparently correlated with other properties, such as threshold to acoustic stimuli, shape of response functions for tonal stimuli, recovery from prior stimulation, and certain anatomical characteristics. Furthermore, histograms of SR estimates from large numbers of fibers suggest that these fibers can be divided into two (i.e. low and high) or three (i.e. low, medium, and high) classes.

Yet, even such “simple” statistical estimates as the average rate can behave surprisingly poorly for processes with long-range dependence (LRD), and the spontaneous activity of AN fibers is known to be LRD. In particular, LRD greatly increases the variability of mean spike rate estimates from single, long counting intervals. We investigated the implications of this LRD effect for our understanding of the SRs of AN fibers. The fractional-Gaussian-noise-driven Poisson process (fGnDP) is a good model of the LRD spike trains of AN fibers. Using rate estimates computed from this model, we were able to reproduce the general shape of published histograms of SR using only three fixed SR values. Moreover, by slightly modifying the inhomogeneous Poisson process in the fGnDP model, we were able to reproduce these histograms using only two fixed SR values.

These results suggest that AN fibers potentially have only two or three possible values for their long-term-average spontaneous firing rates. In other words, all “high-SR” neurons may actually have the same underlying SR. Furthermore, both “low-SR” and “medium-SR” neurons may have a single “true” SR value, or these two classes may each have a single “true” SR value. In addition, our modified inhomogeneous Poisson process may prove useful in other spike-train-modeling applications.

[Supported by NIH DC01641]

953 Conduction Velocity in the Feline Auditory Nerve

Barbara Robinson¹, Charles Miller^{1,2}, Paul Abbas^{1,2}, Kirill Nourski^{1,2}, Fuh-Cherng Jeng²

¹*Otolaryngology, University of Iowa, 200 Hawkins Drive, Iowa City, IA, United States,* ²*Speech Pathology & Audiology, University of Iowa, 250 Hawkins Drive, Iowa City, IA, United States*

Accurate estimates of action potential conduction velocity would contribute to the development of better computational models of auditory nerve fibers as well as to our understanding of basic phys-

iology. We have implemented a new experimental protocol using a custom designed, multi-shank, thin-film recording electrode, fabricated by The University of Michigan Center for Neural Communication Technology (CNCT), which enables us to record evoked potentials from multiple locations within the auditory nerve. Earlier estimates of auditory nerve conduction velocity were calculated using compound action potentials obtained from recording electrodes placed at various longitudinal positions on the surface of the nerve (Miller et al. 1998; Nguyen et al. 1999). The resulting 12 to 17 m/s conduction velocity estimates are consistent with predictions based on fiber diameter of myelinated central axons (Arnesen & Osen, 1978; Liberman & Oliver, 1984, Hursh, 1939; Burgess & Perl, 1973). Use of the thin-film array should provide a more accurate estimate of intraelectrode distance and a better representation of auditory nerve conduction velocity.

The dimensions of the recording array were chosen to take advantage of the length of the exposed auditory nerve. It is a two dimensional array of 16 electrodes arranged on 3 penetrating shanks which are separated by 500 μ m. Monopolar and bipolar stimulation is presented through an electrode array inserted into the scala tympani and responses are recorded serially from each intraneural electrode contact. Neural responses are evoked with single 40 μ s/phase biphasic pulses. Electric stimulation has the advantage of exciting all responding fibers with a higher synchrony than with acoustic stimulation. A sampling rate of 200 samples/s provided good temporal resolution. Initial measures of conduction velocity using the thin-film recording array are consistent with previous results obtained with extraneural electrodes.

Variation in nerve temperature has been shown to affect temporal measures in both human (Moller et al. 1994) and animal (Miyamoto et al. 1990; Nagy et al. 1978) models of peripheral nerve conduction. As it is likely that surgical exposure reduces the temperature of the nerve, we have begun to explore the effect of changes in nerve temperature. Preliminary results indicate that conduction velocity increases with increased temperature 2.27 m/s for each $^{\circ}$ C.

954 Reconstructing the Cochlear Vibration Pattern from Auditory Nerve Responses

Marcel van der Heijde¹, Philip X Joris

Lab. of Auditory Neurophysiology, K.U.Leuven, Campus GHB O&N, B-3000 Leuven, Belgium

Recently, we presented gain and phase characteristics of a single, intact, cochlea of a cat [van der Heijden & Joris, *J.Neurosci* 2003], derived from responses of the auditory nerve to irregularly spaced tone complexes. That approach, which overcomes limitations of pure-tone phase locking of the nerve, yielded transfer characteristics of a collection of fibers from a single cochlea of the cat covering a wide range of characteristic frequencies (CFs). The individual gain and phase curves covered almost all stimulus frequencies that excited the fibers.

We now present an across-CF analysis of these data that leads to a detailed reconstruction of the vibration pattern of the cochlea in response to tones of various frequencies. The reconstruction includes the variation of amplitude and phase with distance along the basilar membrane, “snapshots” of cochlear displacement, and estimates of wavelengths and phase velocities.

Overall, our high-CF reconstructions are consistent with current views on cochlear traveling waves. At low sound levels, excitation was confined to a narrow cochlear region containing only a few cycles of the wave. The wavelength of a single traveling wave decreases towards the apex showing that the wave slows down when approaching its best site. For the highest stimulus frequency considered in our snapshot analysis (14 kHz), our estimates of wavelength and phase velocity are 0.7 mm and 9.7 m/s, respectively.

A lack of low-CF data prevented the detailed reconstruction of apical vibration patterns. The group delays at low CFs, however, suggest deviations from the “ordinary” traveling wave at the apex.

Supported by the Fund for Scientific Research - Flanders (G.0083.02) and Research Fund K.U.Leuven (OT/10/42). MvdH was supported by a K.U.Leuven fellowship (F/00/92).

955 Level coding in the auditory nerve following noise-induced hearing loss

Michael G. Heinz, John B. Issa, Eric D. Young

Biomedical Engineering, Johns Hopkins Univ., 720 Rutland Ave., Baltimore, Maryland, United States

A number of perceptual phenomena related to normal and impaired level coding can be accounted for by the degree of basilar-membrane (BM) compression. However, the narrow dynamic ranges of auditory-nerve (AN) fibers complicate the representation of the BM I/O function in AN responses. For example, AN rate-level functions are not steeper than normal following noise-induced hearing loss (Heinz et al., ARO 2003), despite steeper estimated BM responses based on the same AN data. Because the AN serves as an information bottleneck, an improved understanding of the neural coding of level may clarify some of the limitations of current hearing aids.

The effects of impairment on level coding in the AN were examined by comparing the possible relation to perception of several response properties in normal-hearing cats and in cats with a noise-induced hearing loss. Response-level functions for several fixed stimuli (tones and broadband noise) were analyzed for AN-fiber populations from normal and impaired cats.

Estimated total AN discharge rate in impaired fibers grew at a normal rate with sound level up to 30-40 dB above threshold; above this level growth was only slightly steeper. Normal growth of total AN activity following impairment contrasts with impaired loudness growth, which is steeper than normal except within ~10 dB of threshold. Another psychophysical measure of level coding is the intensity JND, which can be predicted for tones based on AN discharge variability and the level dependencies in rate, synchrony, and phase responses (Colburn et al., JARO, 2003). Rate-level and phase-level slopes for tones were on average shallower than normal for impaired fibers. In contrast, AN discharge variability and phase-locking strength were unaffected by noise-induced hearing loss. Predictions of JNDs based on normal and impaired AN populations will evaluate the significance of these effects in accounting for JNDs in impaired listeners. [Supported by NIDCD]

956 What About the Consonants?

Eric Young¹, Michael Heinz¹, Sharba Bandyopadhyay¹, Teng Ji², Ian Bruce³

¹*Biomedical Engineering, Johns Hopkins Univ., 720 Rutland Ave., Baltimore, Maryland, United States,* ²*Medical School, Rush Medical College, 600 S. Paulina St., Chicago, Illinois, United States,* ³*Electrical and Computer Engineering, McMaster Univ., 1280 Main St. W., Hamilton, Ontario, Canada*

Studies of neural encoding of speech have usually focused on representation of formants. However, for many consonants the formant transitions are only a part of the signal and other sounds, associated with aspiration or frication, are also important. Also, real speech consists of a rapid sequence of sounds with different spectro-temporal characteristics. Here, responses of auditory nerve fibers, in both normal and acoustically-traumatized ears, were studied using the stimulus “Five women played basketball”, a natural utterance. For analysis, the stimulus was segmented into sections corresponding to phonemes or pairs of phonemes, with approximately constant spectral shape (50-70 ms in duration). The population response (rate versus BF) was computed for each segment, in BF bins representing equal steps along the basilar membrane. Similar phonemes cluster together in this analysis. Confusion matrices show accurate identification of the 19 segments in the sequence in normal ears. In impaired ears, the second formant representation was missing, resulting in moving together of the clusters and degraded identification performance. This way of quantifying performance degradation provides a direct way of evaluating hearing-aid algorithms. Supported by NIH grant DC00109.

957 Hearing in the amphibious mudskipper, *Periophthalmus barbarus*

Marcus A. Lindemann, David A. Mann

College of Marine Science, USF, 140 7th Ave South, St. Petersburg, FL, United States

Mudskippers (*Periophthalmus barbarus*) respire using either gill breathing or active gulping of air bubbles and subsequent storage in the buccopharyngeal cavity (BC). This adaptation allows them to survive out of water for extended periods. The effects of the air bubble on underwater hearing and the ability to hear in air were measured using the auditory brainstem response (ABR). The lowest hearing thresholds for mudskippers were in the frequency range between 100 Hz and 900 Hz. Thresholds were lower for submerged specimens when the BC was filled with air, with gains in sensitivity up to 26 dB. Laser vibrometer measurements showed the air bubble increased the velocity of the dorsocranial surface of submerged specimens. Mudskipper hearing thresholds in air were greater than 70 dB re 20 μ Pa, indicating poor sensitivity in air. Analysis of the saccular sensory epithelium by scanning electron microscopy (SEM) showed an enlargement of the surface area of the ventral group of sensory hair cells on the posterior end of the epithelium relative to other fishes. Because this epithelium lies directly above the BC, it is hypothesized that this variation is an adaptation related to sound stimulation via the air bubble in the BC.

958 Frequency tuning and directional preferences in lagenar nerve fibers of the goldfish, *Carassius auratus*

Michaela Meyer¹, Arthur N Popper², Richard R Fay³

¹Dept. of Biology, Univ. of Maryland, CP, Field house drive, College Park, MD, United States, ²Dept. of Biology, Univ. of Maryland, Field house drive, College Park, MD, United States, ³Parmly Hearing Inst. and Dept. of Psychology, Loyola Univ., 6525 North Sheridan Road, Chicago, IL, United States

Auditory portions of the teleost ear may include the utricle, saccule and lagena. While several studies investigated the encoding of stimuli by saccular nerve fibers, much less is known about encoding strategies in lagenar fibers. We investigated frequency tuning and directional preferences of lagenar nerve fibers of the right ear in response to oscillatory whole-body displacement. Recordings were made from single lagenar afferents during linear translatory motion along various axes in the horizontal and mid-sagittal planes.

Best frequency (BF) was determined for vertical motion. Most cells responded to frequencies between 100 and 200 Hz with 63% having their BF at 185 Hz and 20% at 141 Hz. The remaining units showed BFs of 100 Hz or lower (12.5%) and very few cells had their BFs at 244 Hz or higher (5%). Frequency responses varied considerably in bandwidth. A few frequency response functions had two peaks (e.g. at 84 Hz and 244 Hz). Most units had cosinusoidally shaped directional response profiles in the horizontal and mid-sagittal planes. In the mid-sagittal plane, 78% of all units had their best stimulus axis at angles between 60° to 120° elevation. Best azimuths ranged between -80° (to the left front) to 90° (to the right front) with 57% of the units responding best to angles between -30° and 0° (center). The directional preference of lagenar cells for stimulus angles in the vertical plane corresponds to the vertical orientation of the epithelium in the head. Hair cell orientations on the lagenar macula are distributed along a variety of different axes. This is consistent with the variations of directional preferences found in lagenar afferents. Due to its wider distribution of directional response preferences compared to the saccular fibers in both vertical and horizontal planes, the lagena nerve fibers seem to code more robustly for directional information as a population than the saccular fibers [this work was supported by the Parmly Hearing Institute].

959 Coding of Acoustic Particle Motion by Utricular Afferents in a Teleost Fish

Zhongmin Lu, Zemin Xu, William Buchser

Biology, University of Miami, 1301 Memorial Drive, Room 4, Coral Gables, FL, United States

The fish ear contains three otolith organs, the saccule, lagena, and utricle. In the sleeper goby (*Dormitator latifrons*), the three otolith organs vary greatly in size and orientation. Our previous studies have shown that the saccule plays a key role in directional hearing while the lagena contributes to elevational localization, particularly at high stimulus intensities where the response of the saccule becomes saturated. However, it is not known whether or not the utricle plays any role in sound localization in this species. Here we report response properties of single utricular afferents to linear

accelerations that simulate underwater acoustic particle motion. Like saccular and lagenar afferents, responses of most utricular afferents of the sleeper goby were phase-locked. For directional experiments, fish were linearly accelerated at 100 Hz along various axes in both the horizontal and mid-sagittal planes. For frequency experiments, they were stimulated along the longitudinal or side-to-side axis at eight frequencies from 50 to 400 Hz. Most utricular afferents had their characteristic frequencies in the range from 50 to 100 Hz (median = 80 Hz). Best sensitivity ranged from -70 to -35 dB re: 1 g (mean = -50 dB). Best response axes of utricular afferents distributed in a wide range of axes in the horizontal plane and clustered around the longitudinal axis of the fish in the mid-sagittal plane, which are consistent with the orientation of the utricle and morphological polarizations of hair cells in the utricle. Results of this study indicate that the utricle in the sleeper goby, probably as well as other fishes, plays a role in sound localization in the horizontal plane. (This work was supported by University of Miami start-up funds and NIH/NIDCD grants R29DC003275 and R01DC003275)

960 Frequency-dependence of auditory-nerve latency in the northern leopard frog, *Rana pipiens pipiens*

Leola W. Hau¹, Dwayne D. Simmons², Peter M. Narins¹

¹Physiological Science, University of California, Los Angeles, 621 Charles E. Young Drive South, Los Angeles, CA, United States,

²Otolaryngology and Central Institute for the Deaf, Washington University School of Medicine, 660 Euclid Avenue, St. Louis, MO, United States

In the northern leopard frog (*Rana pipiens pipiens*), there are two inner ear endorgans specialized for airborne sound reception: the amphibian papilla (AP) and the basilar papilla (BP). Both auditory organs are innervated by the posterior branch of the VIIIth cranial nerve. The AP contains sensitive auditory transducers with response characteristics approximating mammalian hair cells, and in one species [*E. coqui* (Hillery and Narins, 1987, *Hearing Res.* 25:233-48)], it exhibits characteristic frequency-dependent click latencies. Anatomically, it was found that the fibers innervating hair cells in the rostral (low-frequency) segment of the AP are have greater diameters than the fibers innervating hair cells from the caudal (mid-frequency) pole of the AP (Simmons *et al.*, unpublished data). This suggests that signals are transmitted faster from the rostral side than the caudal side, and therefore one might predict that the click latency would be shorter for low-frequency fibers than for mid-frequency fibers. However, our experimental findings of click latencies in northern leopard frogs contradict this prediction. The click latencies from the caudal fibers are shorter (2.5 ms; *n*=25) than the click latencies from the rostral (3.2 ms; *n*=19) and medial (3.0 ms; *n*=39) fibers of the AP, as well as the BP (2.8 ms; *n*=38) fibers. Thus we conclude that low-frequency cells must exhibit greater excitation and activation delays than high-frequency cells.

Supported by NIH grant DC-00222 to PMN.

961 The Influence of Maternal Thyroid Hormone on Auditory Function in *Tshr^{hyt}* Mutant Mice

JoAnn D. McGee^{1,2}, Jeremy R. Schue^{1,2}, Christopher A. Collura¹, Noelle Feldbauer¹, Elyssa Firas¹, Edward J. Walsh^{1,2}

¹Developmental Auditory Physiology Lab., Boys Town National Research Hospital, 555 North 30th St., Omaha, Nebraska, United States, ²Dept. of Biomedical Sciences, Creighton University School of Medicine, 2500 California St., Omaha, Nebraska, United States

Untreated congenital hypothyroidism leads to profound auditory disability in adult *Tshr^{hyt}* mutant mice, however, the influence of maternal thyroid hormone on the development of auditory function among affected individuals remains uncertain. This question was investigated by comparing auditory brainstem responses among three groups of animals: *Tshr^{hyt}* mutant animals born to hypothyroid dams (*Tshr_e*), *Tshr^{hyt}* mutant animals born to euthyroid dams (*Tshr_e*), and control littermates. As reported earlier, normal, euthyroid littermates acquire adult thresholds rapidly between the 12th and 15th postnatal days and *Tshr* mutants born to hypothyroid dams remain profoundly deaf as adults, even though thresholds improve slightly during roughly the first two months of life (Song *et al.*, ARO 24:99, 2001; ARO 25:167, 2002). Thresholds of *Tshr_e* mutant pups that were the focus of this investigation were intermediate, falling between values representing control and *Tshr_h* groups, regardless of age. Additionally, the development of thresholds followed an exponential trajectory, as was the case for normal animals, albeit along a significantly slower developmental track than that observed in control animals, and unlike *Tshr_h* mutants whose limited development tracked along a protracted, linear trajectory. Based on these results, it is clear that maternal hormone plays a significant role in cochlear development of *Tshr^{hyt}* mutant mice. Results of a parallel study focused on the anatomical characteristics of hypothyroid mice born to euthyroid dams (Walsh *et al.*, ARO 2004) suggest that histological features of the organ of Corti are qualitatively normal, and when combined with the results of a tuning curve analyses, these findings add additional weight to the notion that hypothyroid *Tshr^{hyt}* mice exhibit an enduring abnormality associated with active transduction mechanics. (Supported by NIH-NIDCD R01 DC04566).

962 The Organ of Corti and Efferent Olivocochlear Innervation in Congenitally Hypothyroid (*Tshr^{hyt}* Mutant) Mice

Edward J. Walsh¹, W. Bruce Warr², Jo Ellen Boche², JoAnn D. McGee¹

¹Developmental Auditory Physiology Lab., Boys Town National Research Hospital, 555 North 30th Street, Omaha, Nebraska, United States, ²Neuroanatomy Lab., Boys Town National Research Hospital, 555 North 30th Street, Omaha, Nebraska, United States

The *Tshr^{hyt}* mutant mouse expresses a point mutation in the gene that encodes the thyrotropin receptor rendering the receptor incapable of binding thyrotropin, a condition that leads to thyroid gland hypoplasia and profound congenital hypothyroidism and is

inherited as an autosomal recessive trait. We have previously shown that peripheral auditory function in adult *Tshr* mutant mice born to euthyroid dams is characteristically abnormal with animals exhibiting frequency-dependent threshold deficits ranging from approximately 20 to 40 dB relative to control littermates for low and high frequency stimuli, respectively (Sprenkle *et al.*, JARO 2:330-347, 2001). Furthermore, based on the observation that tip thresholds associated with auditory nerve tuning curves derived from ABR wave I are elevated while tail thresholds appear normal in mutant animals, we have suggested that active aspects of electromechanical transduction are impaired in *Tshr* mutant mice, while passive aspects of transduction appear normal. These findings further suggest that permanent cochlear abnormalities are limited to tissues associated with cochlear amplification. This issue was addressed by assessing the anatomical status of the organ of Corti in *Tshr* mutant mice in aldehyde fixed tissue stained for acetylcholinesterase (AChE). Unlike the condition of the end organ in goitrogen treated, profoundly hypothyroid rats, the organ of Corti in adult *Tshr* mutant mice appears anatomically normal from a qualitative perspective at the light level of microscopy; i.e., Kolliker's organ has differentiated, the tunnel of Corti appears normal, as does the tectorial membrane and efferent innervation based on AChE histochemistry in mutant animals. This finding is consistent with the notion that the permanent otological deficit associated with profound congenital hypothyroidism is best characterized as diminished cochlear amplification. (Supported by NIH-NIDCD R01 DC04566).

963 A gene knockout mouse model for Usher syndrome type IIa.

Gautam Bhattacharya¹, Daniel Meehan¹, Duane Delimont¹, Michael Ann Gratton², Yesha Lundburg¹, David Birch³, William Kimberling¹, Edward Walsh⁴, JoAnn McGee⁵, Dominic Cosgrove¹

¹National Usher Syndrome Center, Boystown National Research Hospital, 555 No 30th St, Omaha, Nebraska, United States, ²Otorhinolaryngology, University of Pennsylvania, 422 Curie Blvd, Philadelphia, Pennsylvania, United States, ³research, Retina foundation of the southwest, 9900 N. Central Expwy, Dallas, Texas, United States, ⁴research, Boystown National Research Hospital, 555 No 30th St, Omaha, Nebraska, United States, ⁵Research, Boystown National Research Hospital, 555 No 30th St, Omaha, Nebraska, United States

Usher syndrome type IIa is the most common (>50% of cases) of the 11 eleven different molecular subtypes associated with Usher syndrome, the predominant genetic cause of combined deafness and blindness in first-world countries. The gene was identified and its product characterized as a novel basement membrane protein abundant in both structural and vascular basement membranes of the cochlea and retina, but also found in many other non-pathologic organs. Biochemical characterization of the usherin protein identified a type IV collagen-binding domain, which may integrate the usherin protein into the basement membranes superstructure, as well as integrin binding domains, which may influence cell signaling pathways, impinging on cellular homeostatic mechanisms. A gene knockout mouse for one of the integrin binding partners was found to be associated with ultrastructural anomalies of the retinal pigment epithelial cell layer. A gene knockout mouse model

for Usher syndrome type IIa was developed and subjected to preliminary characterization. Auditory brainstem response measurements of C57 Bl/6 to 129 Sv/J F-2 generation intercross littermates indicated a wider variance for thresholds in usherin knockout mice compared to normal control littermates at 12 weeks of age, with no significant overall differences in thresholds. Preliminary electroretinographic analysis suggests a progressive visual loss. Ultrastructural analysis of the cochlea suggests an anomaly in the stria vascularis where marginal cells fail to properly form or maintain appropriate interdigitations with intermediate cells. Ultrastructural analysis of the retina was incomplete at the time this abstract was submitted. The mouse model should be a useful tool for defining the specific pathophysiology of Usher syndrome type IIa in the cochlea and the retina.

964 Targeted Expression of a Dominant Negative Kcnq4 Mutation in Mouse Inner Ear

Feng Feng¹, Kenneth A. Morris¹, Sonia S.M.S. Rocha-Sanchez¹, Judith A. Stribley², J. Michael Salbaum², Bernd Fritzschn¹, Kirk W. Beisel¹

¹Biomedical Sciences, Creighton University, 2500 California Plaza, Omaha, NE, United States, ²Genetics, Cell Biology, and Anatomy, University of Nebraska Medical Center, 985455 Nebraska Medical Center, Omaha, NE, United States

The pathogenic mechanism of DFNA2 [progressive high frequency hearing loss (PHFHL)] for the Kcnq4 auditory channelopathy is presently controversial. Based on Kcnq4 expression analyses by Jentsch and others, the pathogenic mechanisms were proposed to result from a disruption of K⁺ recirculation occurring at the level of OHCs and possibly a central auditory system dysfunction. Our in situ hybridization data (Beisel et al., 2000) suggest that dominant-negative (DN) Kcnq4 mutations directly result in a dysfunctional electrophysiology of basal turn/hook inner hair cells (IHCs) and spiral ganglion neurons that impairs their function as effective signal transducers. Kcnq4 channels in IHC were recently confirmed (Oliver et al., 2002). We used a transgenic mouse approach to test these hypotheses, where the Gly285Ser DN Kcnq4 mutation is selectively expressed in the pertinent neuronal and neurosensory cellular components of the central and peripheral auditory systems. Our initial transgenic construct incorporated the partial Myo7a promoter (Boeda et al., 2001), a floxed nuclear LacZ reporter, and a mouse site-directed mutagenized DN-Kcnq4 full length cDNA. This partial Myo7a promoter regulated a restricted expression of EGFP in the neurosensory cells of the vestibule and cochlea, specifically IHCs and some apical OHCs. Ten transgenic founder FVB mice were identified and the offspring examined for inner ear LacZ expression. Two lines examined to date exhibited strong expression of the reporter that was restricted to the cerebellum and the other restricted to spiral ganglion type II-like cells. We are presently establishing homozygous mouse lines. Matings with ROSA26 Cre recombinase mice should produce offspring with restricted DN-Kcnq4 expression in inner ear hair cells. Similar transgenic lines should provide supportive data for the role of the central and peripheral auditory systems and the associated cell types involved in the pathogenic mechanism of KCNQ4-mediated PHFHL.

965 Targeted deletion of Slc19a2, the high-affinity thiamine transporter, causes selective inner hair cell loss and an auditory neuropathy phenotype

M. C. Liberman¹, E. Tartaglioni², J. Fleming², E. Neufeld²

¹Eaton-Peabody Lab, Mass. Eye & Ear Infirmary, Charles St, Boston, MA, United States, ²Div. Hematology, Childrens Hospital, Longwood Ave, Boston, MA, United States

Thiamine-responsive megaloblastic anemia (TRMA) syndrome is a heritable disorder also characterized by diabetes and sensorineural hearing loss. The gene responsible (SLC19A2; Fleming et al. Nat Genet. 22:306, 1999) encodes a high-affinity thiamine transporter. To further study the disease, a mouse line was created with targeted disruption of the gene.

The targeting vector was electroporated into male 129 ES cells, injected into C57Bl/6 blastocysts. Chimeras were back-crossed to 129/SvEv females, thus male transgenic offspring were pure 129/SvEv. All animals were maintained on a normal diet (22 mg/kg thiamine) until ~45 days. Then, a subset of wildtype and homozygous mutants were put on a low-thiamine diet (2 mg/kg). After 12-38 days on diet, DPOAEs and tone-pip evoked ABRs were recorded, and cochleas were harvested.

Normal thresholds and morphology were seen in the -/- group on normal diet and in the +/- group on low-thiamine. In contrast, -/- animals on low-thiamine showed ABR threshold elevation of ~60 dB by 26 days on diet. Shifts in DPOAE thresholds were less severe, with maximum elevation of only ~20 dB. Inner hair cell loss was evident by 19 days on diet, first appearing in the apical turn. After 26 days, all -/- ears on low thiamine showed complete loss of inner hair cells in the apical 2/3 of the cochlea, yet minimal loss of outer hair cells (< 20%).

The functional phenotype of this thiamine transporter knockout could be described audiologically as "auditory neuropathy", i.e. depressed ABRs yet robust DPOAEs, although the primary pathology is in inner hair cells. It is not known if human TRMA shares these audiological or histopathological characteristics.

Supported by the NIDCD (DC00188 to MCL) and NIDDK (HL/DC66182 to EJM).

966 Hearing loss in an estrogen receptor beta knock out mouse

Hultcrantz Malou¹, Rusana Simonoska², Annika E Stenberg¹, Maoli Duan³, Eva Enmark⁴, Jan-Åke Gustavsson⁵

¹Otorhinolaryngology, KNV, Karolinska Hospital, Stockholm, Sweden, ²Otorhinolaryngology, KNV, Karolinska Hospital, Stockholm, Sweden, ³Center for Hearing and Communication, KNV, Forskningslab M, Karolinska Hospital, Stockholm, Sweden, ⁴Biosciences at Novum, Unit for receptor biology, Karolinska Institute, Huddinge, Sweden, ⁵CBT, Dep. of Biosciences at Novum, Unit for receptor biology, Karolinska Institute, Huddinge, Sweden

Background: Estrogen deficiency due to streak ovaries is the dominant problem in Turner's Syndrome (loss of one X chromosome, 45,X) affecting 1:2000 newborn girls. The phenotype will be a

female with short stature, infertility, and failure to spontaneously enter puberty. Ear and hearing problems are common among these patients and affect outer, middle and inner ear. Studies have shown that estrogen might have some impact on ear and hearing problems. Earlier, it has been shown that there are estrogen receptors in the inner ear in mice, rats and humans. Human fetuses with Turner's syndrome also have estrogen receptors. There are two estrogen receptors, the estrogen receptor alpha, ERalpha and the newly discovered estrogen receptor beta, ERbeta. From brain studies it is well known that estrogen offers neuroprotection and that loss of receptors might lead to neurodegeneration.

Aim: Hearing has been tested and morphology and immunology performed in order to follow the hearing loss over age in ERbeta knock out (BERKO) mice.

Methods: Ten mice homozygous for the ERbeta deletion, 10 heterozygous BERKO mice and 10 wild type mice have been tested according to auditory brainstem recordings (ABR). The mice were tested during anesthesia with a "tone pop" through the ear canal and potentials were recorded from scalp electrodes at the age of 3 months, 6 months and 1 year. Hearing thresholds were calculated.

Results: Loss of both genes for the ERbeta (homozygous) results in deafness at the age of 12 months as compared to normal hearing with age in the heterozygous and wild type mice. At this age the organ of Corti in the mid and apical turns of the cochlea has deteriorated.

Conclusion: An intact ERbeta appears essential for maintenance of hearing during ageing.

967 Rescue of Cochlear Dysfunction in the Piebald Lethal Mouse

Avner Ittah¹, Jie Ouyang², Anne Luebke³, Lidia Kos¹

¹Biological Sciences, Florida International University, Park Campus, Miami, FL, United States, ²Physiology & Biophysics, University of Miami School of Medicine, 1600 NW 10th Ave., Miami, FL, United States, ³Biomedical Engineering and Neurobiology and Anatomy, University of Rochester Medical Center, 601 Elmwood Ave., PO Box 603, Rochester, NY, United States

Waardenburg syndrome is a hereditary auditory pigmentary syndrome and Waardenburg syndrome type 4 is associated with Hirschsprung disease. A spontaneous mouse mutant - *piebald lethal*- exhibits striking similarities to the human condition, ie, hearing impairment, anomalies of pigmentation, and aganglionic megacolon. The mutation in the *piebald lethal* mouse has been found to be in the endothelin receptor-B gene (ENDRB). In order to try to rescue the pigmentation phenotype of the *piebald lethal* mouse, we introduced a transgene carrying EDNRB under the control of the dopachrome tautomerase promoter (Dct) that drives expression to melanocyte precursors as early as E10.5.

Piebald lethal mice carrying the transgene showed full coat color rescue. To clarify if a full rescue of pigmentation could also fully rescue the auditory impairment and inner ear pigmentation defects, we characterized the auditory phenotype in 10 week old control mice (n=6), 10 week old "rescued" *piebald lethal* mice (n=6), and 10 week old *piebald lethal* mice (n=3) by measuring 1) ABRs to tone pips at six log-spaced frequencies from 5.6-30 kHz, and 2) DPOAEs evoked by primaries at the same six frequency

values. The extent of pigmentation in the cochleae of these mice was also determined histologically.

Both the auditory thresholds and the DPOAE responses were restored to control levels in the "rescued" mice. In addition, the pigmentation defects in the inner ear were also "rescued" by the addition of a functional EDNRB. These findings suggest that the auditory dysfunction in the *piebald lethal* mutants can be fully "rescued" by the addition of a functional EDNRB.

968 Inner Ear Injury in Apolipoprotein E-deficient (Apo-EKO) mice

Yun-Kai Guo, Chunxiang Zhang, Mohammad Habiby Kermany, Xiaoping Du, Brandon Hill, Tai-June Yoo

Allergy/Immunology, University of Tennessee, 956 Court Ave., B318, Memphis, TN, United States

The purpose of study was to determine if hypercholesterolemia and atherosclerosis could attribute to hearing loss and further examine the relationship between the vascular dysfunction and hearing loss. We have used Apo E knockout homozygous mice (B6.129P2-ApoE tml/Unc) and wild type (C57BL/6J) mice (5-7 weeks old) and fed normal chow until the age of (10-12 weeks). At 10-12 weeks of age Apo-E k/o mice were given high fat, high cholesterol diet (TD88051) containing 1.25% (wt/wt) cholesterol, 0.5% (wt/wt) sodium cholate, 7.5% (wt/wt) cocoa butter, 7.5% (wt/wt) casin. ABR studies, plasma lipid analysis, vascular function studies, vascular histopathology and quantification of atherosclerotic lesions and inner ear histology were performed.

Results show (1) high fat diet increased plasma cholesterol LDL, VLDL, triglycerides, (2) atherosclerotic lesions were found in aortic sinus, ascending aorta (3) the relaxation responses in isolated aorta were decreased (4) auditory threshold were increased significantly at 8,16, and 32 kHz. (5) strong positive correlation between ABR thresholds and plasma cholesterol level (6) Apo-E k/o mice showed deformed organ of Corti, some loss of outer hair cells and inner hair cells, partial loss of spiral ganglion cells and markedly increased thickening of intima and narrower vascular lumen.

Conclusion: Apo-E k/o mice showed hearing loss, which is positively correlated with hypercholesterolemia and vascular dysfunction and those are damages in organ of Corti and vascular narrowing and spiral ganglion degeneration.

969 Modulation of Activity in Developing Spiral Ganglion Cells of the Rat Cochlea Slice

Anabella Gale¹, Elisabeth Glowatzki², Ian Russell¹

¹School of Life Sciences, University of Sussex, Falmer, Brighton, United Kingdom, ²University School of Medicine, Johns Hopkins, 521 Traylor Building, 720 Rutland Avenue, Baltimore, MD, United States

The spiral ganglion is comprised from the cell bodies of neurons forming the auditory nerve, and is innervated by hair cell ribbon synapses, where glutamate is thought to be the major transmitter. Spiral ganglion neurons are classified as type I, which are innervated by inner hair cells, and type II, which are innervated by outer hair cells. Although the electrophysiology of these cells has been studied in vitro (Santos-Sacchi, J Neurosci 13:3599-3611,1993;Lin, Hear Res 108:157-179,1997; Mo and Davis, J Neurophysiol 77(3):1294-1304, 1997), little is known about the

behaviour of the spiral ganglion neurons in an intact preparation. Whole cell recordings were made, using a perforated patch technique, from spiral ganglion neurons in the cochlear slice of postnatal rats (P0-P3) (Glowatzki et al., Neurosci. Abstr. 23:731,1999). Spontaneous events, i.e. action potentials and potentials of varying amplitude, most likely postsynaptic potentials, were recorded in current clamp. Activity was enhanced with cyclothiazide (a blocker of AMPA receptor desensitization), suggesting that this activity was due to transmitter release at the hair cell afferent synapse. Patterns of spontaneous and enhanced activity will be used as a basis for a comparison of firing patterns in type I and type II neurons.

Supported by the MRC and Wellcome Trust.

970 Aromatic compound hexachlorobenzene and salicylate affect hearing, noise sensitivity and spiral ganglion gene expression

Saïda Hadjab¹, Lukas Rüttiger¹, Philippe Siaud², Marlies Knipper¹

¹Molecular Neurobiology, THRC Tübingen Hearing Research Center, Elfriede-Authorn-Str.5, Tübingen, Germany, ²INSERM, Otolaryngology, Pierre Dramard Faculté de médecine Nord, Marseille, France

Hexachlorobenzene (HCB) is a persistent environmental pollutant that affects the sensory-motor coordination in children and cause autoimmune-like effects in humans and rats at high doses (100 to 1000 mg/kg b.w.). We tested the hearing function after application of low doses of HCB (16, 4, 0.16 mg/kg b.w.) for 4 weeks oral application (*per os*). We noticed a significant loss of CAP threshold (20 - 30 dB SPL).

Most interestingly a lower dose of HCB (0.16 mg/kg b.w.) which did not induce hearing loss was able to alter a noise-induced (105 dB SPL, 5 min, 8 kHz) transient threshold shift (TTS) to a more permanent threshold shift (PTS) of 20 to 30 dB SPL still observable 24 hours after noise exposure.

Long term (5 d) and short term (3 h) sodium salicylate treatments (300 mg/kg b.w.), in our hands, also induce threshold shifts of 25 dB SPL. In order to find out if the HCB and the sodium salicylate induced hearing impairment and noise sensitivity originates in the periphery (cochlea) or in central auditory regions, we compared the effect of both substances after systemic and local application.

Data which will be presented here show the differential effect of both substances on hair cell-/ spiral ganglion-genes expression and hair cell innervation, using these two different application methods.

Acknowledgements:

Supported by the European Commission, Marie Curie Training Site HEARING (QLG3-CT-2001-60009).

971 Rat hearing thresholds and distortion product functions suggest the integrity of outer hair cell function after salicylate

Lukas Rüttiger, Saïda Hadjab, Justin Tan, Claudia Braig, Dirk Watermann, Marlies Knipper

Molecular Neurobiology, THRC Tübingen Hearing Research Center, Elfriede-Authorn-Str. 5, Tübingen, Germany

Injection of sodium salicylate (salicylate, Aspirin®) is a reliable method to evoke phantom auditory experiences in rats and is used as an animal model for the examination of tinnitus. However, the mechanism of how salicylate affects the hearing function is still not well understood. In vitro studies reveal an effect of salicylate on the outer hair cell motor protein prestin. In vivo, salicylate injections led to an increased hearing threshold after 3 hours and most likely to a phantom auditory experience in behaving rats (Rüttiger et al. 2003, Hear. Res. 180, 39-50). From our experiments, the hearing loss was associated with no change in distortion product otoacoustic emissions (DPOAEs), suggesting that acute salicylate injections do not affect the prestin function after 3h. However, in vitro studies showed the prestin function to be reduced after salicylate application (Oliver et al. 2001, Science 292:2340-2343). Recently Peng et al (2003, Neurosci. Letters 343:21-24) suggested an increase of NMDA receptor sensitivity of spiral ganglia neurons after salicylate. Our own studies point to an effect of salicylate on the expression of activity dependent genes on spiral ganglia neurons (see poster Tan et al. Knipper, 2004), suggesting that the altered expression of activity dependent genes in the spiral ganglia neurons is one possible way how salicylate may affect hearing.

Acknowledgements:

Supported by DFG kni316/3-2, fortune 816-0-0 and SFB 430-B3 S. Hadjab was partially supported by the European Commission, Marie Curie Training Site HEARING (QLG3-CT-2001-60009).

972 Kappa opioid-receptor agonists depress compound action potential amplitude

Colleen G. Le Prell, Karin Halsey, David F. Dolan, Sanford C. Bledsoe, Jr.

Kresge Hearing Research Institute, Department of Otolaryngology, University of Michigan, 1301 East Ann Street, Ann Arbor, MI, United States

Disrupting lateral olivocochlear (LOC) innervation of the cochlea depresses compound action potential (CAP) amplitude, presumably as a consequence of reduced release of excitatory transmitter substances from the LOC neurons at their synapses with auditory nerve fibers (Le Prell et al., 2002; Le Prell and Bledsoe, 2003). LOC transmitters that may be excitatory include acetylcholine, calcitonin-gene related peptide, and dynorphin (for review, see Le Prell et al., 2001). Here we describe the effects on cochlear potentials of infusing the dynorphin kappa-receptor agonists U-50488 and U-62066 into the cochlea.

Guinea pigs were treated with intra-cochlear Ringer solution (control), followed by increasing concentrations of U-50488 or U-62066. In acute experiments, substances were allowed to diffuse across the round window membrane for 30 min, the middle ear was carefully dried, and evoked potentials were assessed and com-

pared to pre-treatment baseline values. In chronic experiments, Ringer solution (control) was infused via mini-pump, followed by mini-pump infusion of U-50488. Dynorphin agonists did not affect distortion product otoacoustic emission (DPOAE) input-output functions indicating no effect on outer hair cell function. In contrast, CAP amplitude was reduced in a dose-dependant and frequency-specific manner. That effects were greatest at the highest frequencies was not surprising based on the delivery of drugs to the basal turn of the cochlea. The effects of U-50488 were blocked by pre-treatment with the selective antagonist nor-binaltorphimine.

The reduction in CAP amplitude induced by kappa-receptor agonists applied to the cochlea contrasts with the enhancement of CAP amplitude, induced by intra-venous treatment with pentazocine, reported by Sahley and colleagues (1994, 1996). Auditory nerve recordings are needed to resolve this discrepancy and determine the actions of dynorphins in the cochlea.

Supported by NIH-NIDCD DC-00078 (SCB), DC-05188 (DFD), and DC-04194 (DFD).

973 Thapsigargin Suppresses Cochlear Potentials And DPOAEs And Is Toxic To Hair Cells

Richard P Bobbin, M Parker, L Wall

Otolaryngology; Kresge Hearing Research Laboratory, LSU Health Sciences Center, 533 Bolivar Street, 5th floor, New Orleans, LA, United States

Thapsigargin, a drug that inhibits sarco-endoplasmic reticulum Ca²⁺ ATPases (SERCAs), was infused into the perilymph compartment of the guinea pig cochlea for various periods of time and in increasing concentrations (0.1-10 μ M) while sound evoked cochlear potentials were monitored. With 10 min perfusions the largest effects were observed following 10 μ M thapsigargin and these effects became larger following post drug washes with artificial perilymph. Thapsigargin (10 μ M) significantly suppressed the compound action potential of the auditory nerve (CAP), cochlear microphonics (CM), and increased N1 latency at low (56 dB SPL) and high (92 dB SPL) intensity levels of sound, suppressed low intensity sound evoked summing potential (SP) and greatly increased the magnitude of the high intensity sound evoked SP. A 20 min perfusion of 10 μ M thapsigargin suppressed cubic distortion product otoacoustic emissions (DPOAEs; 2f₁-f₂ = 8 kHz, f₂=12 kHz) evoked by both high and low intensity primaries (45, 70 dB SPL). Thapsigargin (10 μ M; 30 min) increased the endocochlear potential slightly (5mV). In chronic animals that received thapsigargin (10 μ M; 60 min) and were allowed to recover for two weeks, many outer hair cells (OHCs) and some inner hair cells (IHCs), especially in the basal turns, were destroyed. These effects are consistent with the hypothesis that the inhibition of the SERCAs affects the function of the cochlear amplifier and OHCs to a greater degree than it affects other functions of the cochlea.

Supported by a grant from the National Institute of Deafness and Other Communication Disorders and by funds provided by the Marriott Foundation.

974 Onset and progression of physiological changes in carboplatin treated chinchillas

Mohamed El-Badry^{1,2}, Ann C. Eddins¹, Sandra L McFadden¹

¹Center for Hearing and Deafness, University at Buffalo, 215 Parker Hall, Buffalo, NY, United States, ²ENT Dept., El-Minia University Hospitals, Audiology Unit, El-Minia, Egypt

In chinchillas, carboplatin damages the central and peripheral processes of spiral ganglion neurons (SGNs) and their myelin sheath before it destroys SGNs and inner hair cells (IHCs). Neural damage starts almost immediately (within 1 h), whereas SGN and IHC loss begins approximately three days after injection. The purpose of this project was to study the physiological correlates of progressive morphological damage in the chinchilla cochlea. We recorded CM, DPOAE, SP, CAP, and IC-EVP in four chinchillas before carboplatin injection (75 mg/kg IP) and then at 1 h, 12 h, 1 day, 3 days, 5 days, 7 days and 14 days after injection. Cochleograms constructed 14 days after injection revealed IHC loss ranging from 65% to 95%, with minimal loss of OHCs. Amplitudes in response to 70, 75 and 80 dB SPL stimuli were averaged across animals and compared as a function of Time using repeated measures ANOVA. Amplitudes of the CM and DPOAE were significantly enhanced (by approximately 16% and 20%, respectively), beginning 1 h after injection. CAP and SP amplitudes were reduced by 10% or less until Day 3, when large (50% and 60%, respectively) and significant reductions occurred. Further significant declines in CAP and SP amplitudes (40% and 15%, respectively) occurred between Days 3 and 5, with no significant changes thereafter. The IC-EVP was least sensitive to morphological damage. IC-EVP amplitude decreased by 4% or less until Day 3, when a significant reduction (23%) occurred. IC-EVP amplitude decreased 17% more between Days 3 and 5, then recovered significantly (23%) between Days 7 and 14. The results of this study suggest that simple amplitude measures fail to detect significant peripheral pathology involving progressive loss of nerve fibers, myelin, SGNs and IHCs until some relatively high threshold level of damage has been exceeded. As with our companion study showing no physiological deficits in animals with significant neural pathology at 12 h, the results have important implications for interpreting electrophysiological test results.

Supported by NIH/NIDCD P01 DC03600 (SLM)

975 Morphological abnormalities 12 h after carboplatin are not reflected in various physiological measures

Mohamed El-Badry^{1,2}, Dalian Ding¹, Ann C. Eddins¹, Sandra L McFadden¹

¹Center for Hearing and Deafness, University at Buffalo, 215 Parker Hall, Buffalo, NY, United States, ²ENT Dept., El-Minia University Hospitals, Audiology Unit, El-Minia, Egypt

Carboplatin causes progressive morphological damage to the chinchilla cochlea, beginning with damage to the myelin of spiral ganglion neurons (SGNs) and their axons as early as 1-6 h post-injection, and progressing to inner hair cell (IHC) and SGN loss around 3 days post-injection. Our companion study of carboplatin-treated chinchillas showed only minor changes in several

measures of cochlear function prior to Day 3 post-injection. However, because those animals were tested over a 4 week period, it was not possible to correlate physiological measures with morphological damage in the same animals. In this study, the CM, SP, DPOAE, CAP, IC-EVP, and ABR were recorded before and 12 h after carboplatin injection (75 mg/kg IP) in 9 chinchillas. Variables analyzed were threshold, amplitude, and latency of the CAP and IC-EVP, and amplitude of the CM, SP, and DPOAE. For the ABR, the threshold, amplitude and latency of waves I, II, and III were analyzed; in addition, the effects of increasing click repetition rates from 10.1/s to 100.1/s were examined. Animals were sacrificed 12 h post-injection and cochleas were processed for light and electron microscopy (LM and EM). Averaged across animals, nearly no change was found in the threshold, amplitude or latency of any of the physiological measures, except a small enhancement in the DPOAE. LM examination revealed clear abnormalities in the SGNs and nerve fibers at the habenula perforatae. Quantitative analysis and EM examination of the SGNs and nerve fibers at the habenula are underway. Our results show that early morphologic abnormalities in the SGNs, nerve fibers and myelin are not detected by any of the physiological measures recorded in this study, suggesting a need for more sensitive measures of myelin and neural pathology.

Supported by NIH/NIDCD P01 DC03600 (SLM)

976 Progressive hearing loss in KCC3 knockout mice

Hannes Maier¹, Thomas Boettger², Marco B. Rust³, Christian A. Huebner³, Rudolf Leuwer¹, Thomas J. Jentsch³

¹ENT, University of Hamburg Medical School, Martinistr. 52, Hamburg, Germany, ²Center of Medical Basic Science, University of Halle-Wittenberg, Weinbergweg 22, Halle, Germany, ³Center of Molecular Neurobiology Hamburg, University of Hamburg Medical School, Falkenried 94, Hamburg, Germany

The K-Cl cotransporter KCC3, an isoform mutated in the human Anderman syndrome, is expressed in neurons, epithelia and other tissues. Beside an impaired cell volume regulation, motor abnormalities and a progressive neurodegeneration in the peripheral and central nervous system, *Kcc3*^{-/-} mice displayed a slowly progressive hearing loss.

KCC3 was present in the supporting cells of the inner and outer hair cells, where it was co-expressed with KCC4 (Boettger et al., 2002). In contrast to KCC4, KCC3 was prominently expressed in type I and III fibrocytes. KCC3 was undetectable in type II fibrocytes. Counterstaining with Kir4.1 and barttin revealed a lack of KCC3 expression in intermediate cells and marginal cells.

ABR responses to clicks in *Kcc3*^{-/-} mice showed a slowly decreasing hearing threshold over the first year of life. The time-course of *Kcc3*^{-/-} hearing loss was slower than in *Kcc4*^{-/-} mice. At three months of age, a degeneration of the organ of Corti was observed in only 2 out of 4 animals. In older animals (≥ 5 months), the organ of Corti was lost more frequently (12 out of 15 mice) and there was often a significant loss of type I and III fibrocytes. In contrast, type II fibrocytes were often preserved in KO animals that already displayed a severe loss of type I and type III fibrocytes. The temporal relationship between the degeneration of fibrocytes and hair

cells was variable. In most sections, OHCs and IHCs were either both present or both absent. However, there were a few examples where OHCs had degenerated while IHCs were still present.

The endocochlear potential and K⁺ concentration in the scala media showed no significant difference between WT and KO in young (<75 days) and old (>110 days) mice. The passive steady-state potential, measured after the elimination of active K⁺-secretion post mortem was not different between young WT and KO mice, but was significantly decreased in old animals (-22.4 ± 3.1 mV (WT) vs. -7.3 ± 2.5 mV (KO)).

977 Progressive Hearing Loss in *Claudin 11*-null mice

Alexander Gow¹, Caroline Davies², Cherie M Southwood³, Gregory Frolenkov⁴, Lily Ng⁵, Bechara Kachar⁶

¹Genetics, wayne state university, 3216 scott hall, 540 e canfield, detroit, mi, United States, ²NIDCD, NIH, 50 South Drive, Rm 4249, Bethesda, MD 20892-8027, md, United States, ³genetics, wayne state university, 3216 scott hall, 540 e canfield, detroit, mi, United States, ⁴NIDCD, NIH, 50 South Drive, Rm 4249, Bethesda, md, United States, ⁵human genetics, mount sinai school of medicine, 1425 madison ave, new york, ny, United States, ⁶NIDCD, NIH, 50 South Drive, Rm 4249, bethesda, md, United States

The importance of intercellular junctions to auditory function has been highlighted in recent years by the identification of multiple mutations in *CONNEXIN* and *CLAUDIN* genes in humans and mice that cause dominant and recessive forms of disease. Herein, we explore the pathophysiology of sensorineural hearing loss in *Claudin 11*-null mice. These mutants lack tight junction strands in the basal cell epithelium of the stria vascularis and adults exhibit profound hearing loss across the frequency spectrum as determined from auditory brainstem response (ABR) measurements. The absence of CNS pathology, hair cell loss in the organ of Corti, cell loss in the stria vascularis or other morphological changes in the cochlea suggest that the deafness phenotype of the null mice stems from the absence of basal cell tight junctions and is predicted from current mechanisms described in the literature. However, young *Claudin 11*-null mice exhibit normal ABR thresholds in the absence of compensation for Claudin 11 tight junctions. Moreover, endocochlear potentials only reach 30% of normal values. In this light, our data suggest important aspects of the conditions necessary for auditory function that are, hitherto, underappreciated.

978 Targeted deletion of glutamate receptor subunit $\delta 1$ causes high-frequency threshold elevation

S Maison*¹, J Gao*², S Jones³, X Wu², G Mittleman⁴, D Matthews⁴, MC Liberman¹, J Zuo²

¹Dpt Oto & Laryngo, Harvard Med School, 243 Charles St, Boston, MA, United States, ²Dpt Dev Neurobio, St Jude Children's Res Hosp, 332 N Lauderdale St, Memphis, TN, United States, ³Dpt Comm Disor, E. Carolina U., E. 5th St, Greenville, NC, United States, ⁴Dpt Psycho, U of Memphis, Psycho Bldg, Memphis, TN, United States

Glutamate receptors (GluRs) include classic NMDA, Kainate and AMPA type, as well as a novel type with two members: $\delta 1$ and $\delta 2$.

GluR δ 1 is expressed in the developing CNS and adult hippocampus. In the inner ear, it is expressed in inner hair cells (IHCs), vestibular hair cells and vestibular afferents (Safieddine and Wenthold, 1997). To study its role, we deleted the first three transmembrane domains of GluR δ 1 in mice, as confirmed by genomic Southern, PCR and Western analysis.

GluR δ 1 null mice had no developmental defects, except for smaller body size and no vestibular or hippocampal phenotype: in rotarod, VsEP (thresholds, peak latencies and amplitudes), or water-maze tests, there were no differences among wildtype, heterozygous and homozygous mutants. In contrast, ABR and DPOAE thresholds in null mice were elevated by 20 - 40 dB re wildtype, and suprathreshold responses were reduced, for frequencies \geq 16 kHz. Thresholds for heterozygotes were intermediate. The magnitude of efferent suppression evoked by shocks was unaffected. Mutant ears showed normal cochlear morphology, except for loss of type-IV spiral ligament fibrocytes in the basal turn. Efferent innervation density was unaffected in either IHC or OHC areas.

The pattern and degree of type-IV fibrocyte loss is similar to that seen after acoustic injury; however type-IV loss per se does not cause 40 dB threshold shift. The reduced DPOAEs and ABRs suggest OHC dysfunction or reduction in endolymphatic potential. Mechanisms underlying such changes are unclear, given selective expression of GluR δ 1 in IHCs. The lack of effect on the other tests suggests functional redundancy of GluR δ 1 in vestibular and hippocampal systems.

*Contributed equally

979 Localization of Free Cholesterol in the Cochlear Structure.

Angela-Maria Meyer zum Gottesbege¹, Heidi Felix², Thomas Massing¹, Günther Kappert³, Vera Balz¹

¹ORL, University of Düsseldorf, Moorenstr. 5, Düsseldorf, Germany, ²ORL, University of Zürich, Frauenklinik, Zürich, Switzerland, ³Inst. Clin. Chemistry and Lab. Medicine, University of Düsseldorf, Moorenstr. 5, Düsseldorf, Germany

Several studies suggest a contribution of hypercholesterolemia to the development of sensorineural hearing loss. Cholesterol is a prominent component of mammalian plasma membrane. Free cholesterol incorporates into the lateral wall of the outer hair cells (OHC) and influences its stiffness. Peroxisomes are ubiquitous cell organelles. They harbour enzymes catalyzing various oxidative and biosynthetic reactions including biosynthesis of cholesterol. Loss of function of the peroxisomal Mpv17 protein in mice causes focal segmental glomerulosclerosis and sensorineural deafness associated with increased cholesterol level in serum. In Mpv17^{-/-} mice the lateral wall of the degenerating OHCs appears floppy and wrinkly indicating alterations of their stiffness. A histochemical technique that allows to visualize free cholesterol in tissue was adapted for the inner ear. It takes advantage of the fact that in presence of cholesterol oxidase free cholesterol releases H₂O₂ with subsequent oxidization of 3,3-diaminobenzidine in presence of horse radish peroxidase. The reaction products are found mainly related to membranes and mitochondria especially in structures contributing to the ion transport, e.g. stria vascularis. In the organ of Corti an incorporation of free cholesterol into the lateral wall of

the OHCs leads to floppy and folded appearance similar to Mpv17^{-/-} mice at the beginning of the degeneration. They were differences in response between the cells and tissue compartments indicating that the cell types may differ in regulation of cholesterol content and its subcellular distribution. The distribution of free cholesterol was altered in Mpv17^{-/-} mice suggesting an important contribution of the peroxisomal Mpv17-protein in the biosynthesis of cholesterol.

980 Characterization of Vestibular Function in Ames Waltzer Mice

Kumar N Alagramam¹, John S Stahl², Sherri J Jones³, Karen S Pawlowski⁴, Charles G Wright⁴

¹Otolaryngology-HNS, University Hospitals of Cleveland, Case Western Reserve University, 11100 Euclid Avenue, Cleveland, OH, United States, ²Department of Neurology, University Hospitals of Cleveland, Case Western Reserve University, 11100 Euclid Avenue, Cleveland, OH, United States, ³Communication Sciences and Disorders, East Carolina University, Belk Annex, Greenville, NC, United States, ⁴Otolaryngology - HNS, University of Texas Southwestern Medical Center, 1966 Inwood Road, Dallas, TX, United States

Vestibular Evoked Potential (VsEP), angular Vestibulo-Ocular Reflex (aVOR) and optokinetic reflex (OPR) measurements were used to characterize vestibular function in Ames waltzer mice, a model for Usher syndrome 1F. Vestibular dysfunction in these mice was suspected since circling behavior in the mutants is obvious as early as 10 days after birth (P10). However, initial investigation of the vestibular anatomy of the Ames waltzer allele carrying a functional null mutation (Pcdh15 av-Tg) showed only a late onset (>P30) saccular degeneration. Therefore, a more thorough investigation into peripheral vestibular function was performed together with more detailed anatomic study of the peripheral vestibular apparatus. Scanning electron microscopy of sensory cells from the vestibular apparatus showed hair cell morphology of the mutants at P10 is similar to that of control littermates, suggesting that mutation in the protocadherin15 gene (Pcdh15) results in early functional abnormality in the hair cells. To investigate this possibility, peripheral vestibular function in the various alleles of Ames waltzer was evaluated using tests measuring VsEP, aVOR and OPR. Outcomes of tests for both the linear acceleration receptors and semicircular duct receptors demonstrated lack of function in all peripheral vestibular components. These results show that the compromised balance function mutation in the Ames waltzer mice is caused by lack of input from the vestibular receptors, and/or their associated nerves.

This work was supported by a grant from NIDCD to KNA.

981 Temporal Bone Histopathology associated with the Mitochondrial T7511C Mutation

Kotaro Ishikawa¹, Yuya Tamagawa¹, Katsumasa Takahashi², Yukiko Iino³, Keiko Kakizaki³, Yoshihiko Murakami³, Jun Kusakar⁴, Akira Hara⁵, Keiichi Ichimura¹
*1*Otolaryngology, Jichi Medical School, 3311-1 Yakushiji, Minami-kawachi, Japan, *2*Otolaryngology, Gunma University School of Medicine, 3-39-22 Showa-ku, Maebashi, Japan, *3*Otolaryngology, Teikyo University School of Medicine, 2-11-1 Kaga, Itabashi, Japan, *4*Otolaryngology, Institute of Clinical Medicine University of Tsukuba, 1-1-1 Tennodai, Tsukuba, Japan, *5*Otolaryngology, Institute of Clinical Medicine, University of Tsukuba, 1-1-1 Tennodai, Tsukuba, Japan

Recently we reported a T7511C mutation in the tRNA^{Ser(UCN)} gene in a Japanese family with nonsyndromic hearing loss (Ishikawa et al, 2002). To our knowledge, this family is the second one to have the T7511C mutation. Here we report histopathological findings of the temporal bone from one male patient in this family. He noticed hearing loss at 5 years old, and suffered from progressive sensorineural hearing loss. His audiogram showed symmetrical and down-sloping shape. The average pure-tone threshold was 62.5 dB in the right ear and 73.8 dB in the left one at the age of 44 years. He died at 60 years old. A temporal bone was harvested 5 hours postmortem, embedded in celloidin and sectioned for light microscopic study. Graphic reconstruction of the cochlea was performed using the method described by Schuknecht (1993). The most characteristic histopathological finding was severe loss of spiral ganglion cells in all turns of cochlea. The total spiral ganglion cell count was 5103, representing an 80% loss when compared with age-matched control samples and an 86% loss when compared with counts from normal newborns. Severe loss of neuronal filaments in Rosenthal's canal was observed in this patient. The organ of Corti showed scattered losses of inner and outer hair cells in the basal turn. Partial atrophy of the stria vascularis was observed in all turns of cochlea. The vestibular organ was normal. In conclusion, our results suggested that severe loss of spiral ganglion cells caused progressive sensorineural hearing loss associated with the T7511C mutation in the mitochondrial DNA.

982 Summating potential: Dependence on recording epoch and inner hair cell loss

Anthony T Cacace¹, Yuqing Guo², Robert Burkard²

*1*Neurology, Albany Medical College, The Neurosciences Institute, 47 New Scotland Avenue, Albany, New York, United States,

*2*Center for Hearing and Deafness, University at Buffalo, 215 Parker Hall, Buffalo, New York, United States

Summating potential (SP) produced by the inner ear has been described as a DC or very low frequency driven response to acoustic input. It is one of several components often quantified in electrocochleography measurements. SP is thought to be useful in differential diagnosis of otopathologic conditions, particularly in the incipient stages of endolymphatic hydrops. Moreover, there are basic science issues pertaining to SP detection especially with respect to the differential contributions from inner and outer hair cells. However, one recording parameter often overlooked is post-stimulus epoch time. Selection of epoch time is a signal processing issue pertinent to resolving low frequency waveforms. When elec-

trocochleography is recorded clinically, epoch times range from 5 ms to 50 ms (typically 5-10 ms). Whereas these particular parameters are appropriate for recording cochlear microphonic and compound action potential, they may not be optimal for recording SP.

In the present study, cochlear potentials were recorded from an implanted electrode placed at the round window of chinchilla and measurements were assessed pre and post carboplatin (75 mg/kg) treatment. Epoch times of 50 ms and 800 ms were used in response to suprathreshold (80 dB pSPL) unfiltered clicks, 1.0 kHz and 4.0 kHz tone bursts. Results showed that when tone bursts were 40 ms in duration, SP polarity was positive and amplitude was larger for 4.0 kHz vs. 1.0 kHz tone bursts; in some instances responses were larger in the 800 ms epoch time condition. Substantial reduction in SP amplitude was observed for both frequencies after carboplatin treatment.

In addition to post treatment reduction in SP amplitude, other complex changes occurred which will be discussed in the context of histopathologic findings.

(Work supported by NIDCD-DC03600)

983 Comparison of cochlear evoked potentials and distortion product otoacoustic emissions (DPOAE) for cochlea and VIII nerve function monitoring during cerebello-pontine angle surgery

Krzysztof Morawski¹, Fred F Telischi^{2,3}, Jorge Bohorquez³, Ozcan Ozdamar^{2,3}, Rafael Delgado^{3,4}, Erdem Yavuz³

*1*Otolaryngology Department, Silesian Medical Academy, Sklodowskiej 10, Zabrze, Poland, *2*Otolaryngology Department, University of Miami, 1666 NW 10th Avenue, Suite 306, Miami, FL, United States, *3*Department of Biomedical Engineering, University of Miami, 219 B Mc Arthur Annex, P.O. Box 248294, Coral Gables, FL, United States, *4*Software Development, Intelligent Hearing System Inc., 7356 SW 48th Street, Miami, FL, United States

We evaluated and compared the utility of DPOAE and cochlear evoked potentials for monitoring cochlear and eighth nerve functions during reversible cochlear ischemia.

Method: 15 albino rabbits were used. The round window (RW) visualization and the VIII nerve complex with internal auditory artery (IAA) approach via a sub-occipital posterior craniotomy were described in our earlier publication. In all cases cochlear blood flow (CBF) and evoked-potentials (i.e., cochlear microphonics [CM] and compound action potentials [CAP]) were measured using the otic probe placed into the RW niche. The first IAA compression inducing cochlear ischemia was maintained for 3-min while the second for 5-min. DPOAE-CBF data obtained in the first subgroup of animals and CM/CAP-CBF obtained in the second subgroup were recorded from the onset of ischemia through 20 min after reperfusion. Responses were obtained at 4, 8 and 12 kHz GMF for both techniques, respectively for 60 and 70 dB SPL.

Results: In all ears following IAA compression CBF was reduced to a background level. The DPOAE phase increase for all frequencies occurred within a few seconds while the DPOAE amplitudes decreased with slightly longer delay. CM/CAP amplitude decrease

was analogous to DPOAE pattern. After reperfusion, in both animal subgroups, DPOAE and CM recovered in the same way for both compressions stabilizing near the baseline. CM measured for the first 3 min compression for all frequencies was reduced 1-1.5 dB, while for the second 2.5-3 dB. DPOAE measured for 3 min compression was reduced only at 12 GMF kHz by 0.5-1 dB, while for 5 min compression this reduction was observed for 8 GMF kHz (2-2.5 dB) and 12 GMF kHz (7-9 dB). At all frequencies CAP began to recover within several minutes and showed changes in waveform morphology.

Conclusion: DPOAE effectively mirrored cochlear ischemia confirming earlier data. CM/CAP findings showed a more complex response reflecting the status of the cochlea and the VIII nerve, but the basal to apical susceptibility of the cochlea to ischemia was not as distinct as that revealed by DPOAE measurements.

984 The biological role of the medial olivocochlear efferent system in hearing

David W. Smith¹, E. Christopher Kirk², Emily Buss³

¹Hearing Research Laboratories, Div. of Otolaryngology-HNS, Duke University Medical Center, Box 3550, Durham, North Carolina, United States, ²Dept. of Anthropology, University of Texas at Austin, 1 University Station C3200, Austin, Texas, United States, ³Dept. of Otolaryngology-HNS, University of North Carolina at Chapel Hill, 130 Mason Farm Road, CB7070, 1115 Bioinformatics Bldg., Chapel Hill, North Carolina, United States

A better understanding of the biological role of the medial olivocochlear (MOC) efferent system in hearing (i.e., the functional role for which the system evolved) will significantly aid investigation of MOC effects in a range of physiological and perceptual phenomena. A more complete appreciation of the conditions under which MOC influences are biologically advantageous will serve to guide construction of optimal stimulus conditions for future research. This presentation reviews several studies that, we argue, shed light upon the MOC system's biological role. Two roles have most frequently been attributed to the action of MOC efferents: (1) Protecting the ear from acoustic trauma and (2) suppression of noise as a means of unmasking target signals. We have recently argued that the environmental conditions necessary to support evolution of the MOC system as a protective mechanism do not exist in nature (Kirk and Smith, *in press*). On the other hand, numerous physiological investigators have shown that the MOC system contributes to the suppression of background noise, serving to increase the neural representation (e.g., signal-to-noise ratio) of target signals. Recent work has shown that MOC activity produces a rapid adaptation of distortion product otoacoustic emissions, which provides an estimate of the time course of MOC effects on outer hair cell activity. We suggest that this finding also provides an MOC-based physiological explanation for some aspects of the psychophysical "overshoot" phenomenon. Support for this comes from Zeng et al. (2000, *Hear. Res.* 142, 102-112), who showed that overshoot is reduced or eliminated when the MOC tracts are cut in humans. Significantly, this result demonstrates that MOC effects on perception are substantial, up to 20 dB, and can be measured under ordinary listening conditions. The MOC time constant of 50-100 ms, differentially suppressing acoustic stimuli of greater than 50-100 ms, serves to accentuate the detection of transient signals. In the natural world, perhaps the most important transient sig-

nals are those used to locate sounds in 3-dimensional space. It is our contention that the biological role of the MOC system is fundamentally related to the critical process of *sound localization*, consistent with the binaural representation of the MOC.

985 Connexin Hemichannel Function in Cochlear Supporting Cells

Hong-Bo Zhao¹

¹Dept. of Surgery - Otolaryngology, University of Kentucky Medical Center, 800 Rose Street, Lexington, KY, United States

The fact that connexin mutations induce a high incidence of hearing loss indicates that cochlear gap junctional coupling plays an important role in hearing function. However, detail information about the function and performance of gap junctional coupling in the cochlea is little known. A gap junctional channel is docked by two hexad hemichannels. Its core function is to diffuse ions and metabolic molecules to mediate cell functions. In this experiment, the permeation of connexin hemichannels in native cochlear supporting cells was investigated to elucidate structure-function relationship of inner ear gap junctions. Cochlear supporting cells were freshly isolated from guinea pig inner ears and incubated with charge and size different fluorescent dyes, which include Alexa Fluo 350, EAM-1, Ethidium bromide, Lucifer yellow and propidium iodide. Supporting cells selectively permeated to these plasma membrane-impermeable fluorescent dyes in nominal Ca⁺⁺-free extracellular solution. In the same incubation, hair cells had no dye influx. Increase of Ca⁺⁺ and applications of gap junction blockers could block dye influx, indicating the dye influx indeed through connexin hemichannels. Thirty percentages of examined supporting cells exhibited only permeation to cationic dyes. Less than 5% of cells showed an anionic dye preference in their permeations. Different charge selective hemichannels distributed in cochlear supporting cells and docked forming charge selective, rectified integral gap junctional channels. The data indicates that cochlear connexin hemichannels have strong charge selectivity to selectively permeate endogenous materials to perform physiological functions in inner ears. It also visualized the configuration of cochlear gap junctional channels and further supports our previous reports that multiple connexins can assemble to form homomeric and heterotypic hybrid channels in the cochlea to induce directional, selective transjunctional passage.

Supported by DC04618

986 Residual Ca⁺⁺ Permeability in Gap Junctions (GJs) Comprised of Mutant Connexin26 Causing Human Deafness Suggests that Quantitative Alterations in GJ Permeability Could Cause Deafness.

Shoab Ahmad, Ben Gang Peng, Xi Lin

Gonda Dept. of Cell and Molecular Biology, House Ear Institute, 2100 West 3rd Street, Los Angeles, CA, United States

Mutations in the connexin26 (Cx26) gene are a major cause of nonsyndromic deafness in humans of many ethnic groups. However, little is known about how these mutations affect the ionic permeation through gap junctions (GJs). Here we quantitatively compared changes in the Ca⁺⁺ permeation among eight GJ mutants known to be associated with dominantly (R75W, W44C, delE42,

R184Q, D179N and C202F) or recessively (V84L and R143W) inherited hearing loss. The Ca⁺⁺ permeation of GJs comprised of EGFP-fused Cxs26 and/or 30, either homo- or hetero-merically assembled and reconstituted in communication-deficient HeLa cells by transient transfection, was investigated by the Ca⁺⁺ ratio imaging method. Visualization of the GFP fluorescence in transfected cells revealed that most of the mutants, except for D179N, formed GJs at the cell membranes where cells contact each other. Touching cells with patch-clamp style electrodes caused abrupt rises in intracellular Ca⁺⁺ concentrations. The Ca⁺⁺ readily diffused only to those neighboring cells that formed GJs with the cells being mechanically stimulated. Recording Fura-2 signals in these cells gave a quantitative description of the Ca⁺⁺ transfer between the cells. Results showed that most mutants completely disrupted the Ca⁺⁺ permeation through GJs comprised of Cxs 26 and/or 30. However, GJs comprised of Cx26 mutants W44C and R143W showed some residual Ca⁺⁺ permeation with much slower diffusion rate. The present study suggested that most mutations associated with hereditary sensorineural deafness resulted in a complete interruption of the Ca⁺⁺ permeation through either homo- or hetero-meric GJ channels comprised of Cxs26 and 30. However, residual Ca⁺⁺ permeation shown by Cx26 mutants W44C and R143W suggested that quantitative alterations, not necessarily a complete shut-off, of the ionic permeability through GJ channels could cause deafness as well.

987 ATP-sensitive potassium channels and regulation of gap junctional coupling in cochlear-Hensen cells

Alexander Bloedow^{1,2}, Anaclet Ngezahayo², Arneborg Ernst¹, Hans-Albert Kolb²

¹ENT-Department, Unfallkrankenhaus Berlin, Warenerstr.7, Berlin, Germany, ²Institute of Biophysics, University of Hanover, Herrenhäuserstr.2, Hanover, Germany

Using the double whole-patch clamp technique we show that intracellular ATP regulates gap junctional coupling of isolated Hensen cells of guinea pig in a dose dependent manner. Absence of ATP in the pipette filling solution caused progressive gap junctional uncoupling within 10-20 min. This run down could be suppressed by external presence of Ba²⁺, a nonselective blocker of inwardly rectifying K⁺-channels. The effect of ATP could be mimicked by replacement of ATP in the pipette filling solution by the non-hydrolysable analogue AMP-PNP. The results confirm that ATP hydrolysis is not required for the regulatory process. Since the cells were clamped at constant membrane potential and increases in intracellular calcium was made unlikely by high EGTA in the pipette solution a voltage and Ca²⁺ independent pathway between activity of ATP-dependent K⁺-channels and regulation of gap junctional permeability is proposed. It is suggested that activation of ATP-dependent K⁺-channels, a family of inward rectifiers, are linked to K⁺-efflux accompanied by closure of gap junctional channels of Hensen cells.

988 Expression of Kir4.1 potassium channels in the outer sulcus cells in the guinea pig cochlea

Toshihiko Chiba, Toshihiko Kikuchi, Ryuichi Yoshida, Toshimitsu Kobayashi

Otorhinolaryngology, Tohoku University Graduate School of medicine, 1-1, Seiryomachi, Aoba-ku, Sendai, Japan

Immunohistochemical localization of Kir4.1, an inward rectifying K⁺ channel, in the guinea pig cochlea was studied in the present study. Kir4.1-like immunoreactivity was found in the stria vascularis, the basolateral plasma membrane of the supporting cells in the organ of Corti and the satellite cells surrounding the spiral ganglion cells, as shown in the previous study (Hibino et al. *J Neurosci* 17, 4711-4721, 1997; Ando and Takeuchi. *Cell Tissue Res* 298, 179-183, 1999; Hibino et al. *Am J Physiol* 277, C638-644, 1999; Rosengurt et al. *Hear Res* 177, 71-80, 2003). The limited resolution provided by the light microscope made it difficult to assign the staining to any particular cell type in the stria vascularis.

In the present investigation, we found new additional information that intense Kir4.1-like immunoreactivity was also distributed in the root process of outer sulcus cells, which is the outermost member of the epithelia cell gap junction system. Immunostaining of outer sulcus cells for Kir4.1 showed a longitudinal gradient between cochlear turns. The outer sulcus cells in the basal turn showed more intense staining than in upper turns.

Activation of hair cells by mechanical stimuli induces the influx of K⁺ ions from the endolymph to sensory hair cells. The K⁺ ions are expelled basolaterally to the extracellular space of the organ of Corti, from which they enter the supporting cells. They move through the epithelial cell gap junction system (Kikuchi et al. *Med Electron Microsc* 33, 51-56, 2000) laterally to the lower part of the spiral ligament. The K⁺ ions are released into the extracellular space within the spiral ligament by root process of outer sulcus cells, and are taken up by the Na,K-ATPase and Na-K-Cl cotransporter in the type II fibrocytes.

Intense Kir4.1-like immunostaining in the basolateral plasma membranes of the cochlear supporting cells and the outer sulcus cells suggest that Kir4.1 in these sites may play important roles in the recycling system of the K⁺ ions in the cochlea.

This work was supported by Grant-in-Aid for Scientific Research No. 14571603 and No. 14370546 from the Ministry of Education, Culture, Sports, Science and Technology, Japan.

989 Cytologic specializations in upper versus lower strial levels mediate K⁺ transport and presumably function in the stria.

Samuel S Spicer, Bradley A Schulte

Pathology & Laboratory Medicine, Medical University of South Carolina, 171 Ashley Avenue, Charleston, SC, United States

Cytologic specializations in upper versus lower strial levels mediate K⁺ transport and presumably function in the stria.

Samuel S. Spicer, Bradley A. Schulte

Pathology & Laboratory Medicine, Medical University of South Carolina, Charleston, SC

Cytologic structures newly observed by ultrastructural

examination permit postulating ion transport pathways in the stria vascularis and speculating on their role in generating the high $[K^+]$ of endolymph and endocochlear potential (EP). In the postulated transport route, basal cells receive all of the K^+ recycled to the stria by three currently proposed pathways. Possessing characteristic, leaf-like horizontal processes that cover basal cells completely at gap junction-like contacts, intermediate cells (ICs) apparently resorb from basal cells all the recycled K^+ . Enlarged and foot-like processes, possessing many mitochondria and minirodlets and plasmalemmal Na,K-ATPase, expand the surface of marginal cells (MCs) in the basal strial level. These MC processes apparently function to draw part of the recycled K^+ from the most basally located ICs across a unique .120D space and are speculated thereby to generate the EP. The remainder of the recycled K^+ presumably flows through gap junctions from basal ICs and into distinctive ICs of mid to upper strial strata. Primary processes filled with one or two mitochondria, and ultrathin secondary processes protruding from or connecting primary processes, expand the MC surface in the apical strial region. These Na, K-ATPase rich processes are thought to resorb from dendrites and secondary processes of the upper level ICs the remaining recycled K^+ and direct it to overlying scala media, thereby generating the high $[K^+]$ in endolymph. This two tiered arrangement could provide a structural basis for the two principle functions of the stria vascularis.

990 Expression of gap junction protein connexin43 in the adult rat cochlea: Comparison with connexin26

Toshihiro Suzuki, Tatsuya Matsunami, Masakatsu Taki, Toshiaki Shibata, Hirofumi Sakaguchi, Satoshi Yamamoto, Yasuo Hisa

Otolaryngology, Kyoto Prefectural University of Medicine, Kawaramachi Hirokouji, Kamigyo-ku, Kyoto, Japan

To elucidate whether the two different gap junction proteins connexin43 (Cx43) and connexin26 (Cx26) are expressed and localized in a similar manner in the adult rat cochlea, we performed three-dimensional confocal microscopy using cryosections and surface preparations. In the cochlear lateral wall, Cx43-positive spots were localized mainly in the stria vascularis and only a few spots were present in the spiral ligament, whereas Cx26-positive spots were detected in both the stria vascularis and the spiral ligament. In the spiral limbus, Cx43 was widely distributed, whereas Cx26 was more concentrated on the side facing the scala vestibuli and in the basal portion. In the organ of Corti, although Cx43-positive spots were present between the supporting cells, they were fewer and much smaller than those of Cx26. These data demonstrated distinct differences between Cx43 and Cx26 in expression and localization in the cochlea. In addition, the area of overlap of zonula occludens-1 (ZO-1)-immunolabeling with Cx43-positive spots was small, whereas it was fairly large with Cx26-positive spots in the cochlear lateral wall, suggesting that the differences are not associated with the structural difference between carboxyl terminals, i.e., those of Cx43 possess sequences for binding to ZO-1 whereas those of Cx26 lack these binding sequences.

991 Expression of the CIC-K Chloride Channel in Rat Cochlea

Chunyan Qu¹, Wei Hu², Fenghe Liang¹, Zhijun Shen¹, Samuel S Spicer¹, Bradley A Schulte¹

¹Pathology & Laboratory Medicine, Medical University of South Carolina, 171 Ashley Avenue, Charleston, SC, United States,

²Department of Medicine, Medical University of South Carolina, 171 Ashley Avenue, Charleston, SC, United States

Expression of the CIC-K Chloride Channel in Rat Cochlea

Chunyan Qu, Wei Hu, Fenghe Liang, Zhijun Shen, Samuel S. Spicer, Bradley A. Schulte

Current models of the lateral K^+ recycling pathway in the mammalian cochlea incorporate three intracellular transport segments separated from one another by intercellular gaps. The first intercellular gap spans the space between outer hair cells and Dieters cells, the second is located between outer sulcus root cells and type II spiral ligament fibrocytes and the third constitutes the intrastrial space between intermediate and marginal cells in the stria vascularis. K^+ taken up by cells bordering these intercellular spaces via the activity of the K-Cl cotransporter, the Na-K-Cl cotransporter and Na,K-ATPase is accompanied by Cl⁻. The maintenance of cellular electrolyte balance and membrane potentials requires a mechanism for exit of this resorbed Cl⁻. One possible candidate for regulating this activity is CIC-K, a chloride channel previously thought to be kidney specific. Here we employed immunohistochemical, Western blot and RT-PCR analysis to evaluate the expression of both known isoforms of this channel (CIC-K1 and CIC-K2) in the organ of Corti, spiral ligament and stria vascularis of the adult rat cochlea. Selective strong immunostaining was observed in types II, IV, V and supralimbal fibrocytes, Dieters cells and spiral ganglion neurons using an antibody that recognizes both isoforms of CIC-K. Western blots from microdissected regions of rat cochlea revealed only two specific bands with molecular weights of 66~90 kDa and 98~110 kDa. The expression of the two isoforms in the different subfractions also was confirmed by RT-PCR employing isoform-specific primers. These results support a role for CIC-K as a mediator of Cl⁻ recycling in the cochlea and may help to explain the symptoms of Bartter's syndrome Type III, a mutation in the hCIC-KB gene (human analog of rCIC-K2) resulting in chronic renal failure without deafness. It is possible that the disrupted role of hCIC-KB in Bartter's syndrome may be compensated for by hCIC-KA (the human analog of rCIC-K1) thus explaining the continued maintenance of Cl⁻ homeostasis in the inner ear.

992 The Beta4 Subunit is a likely Candidate for Regulating the Inactivation of BK Channels in Spiral Ligament Fibrocytes

Fenghe Liang, Bradley A. Schulte, Zhijun Shen

Pathology & Lab Medicine, Medical University of South Carolina, 165 Ashley Avenue, Charleston, SC, United States

We have previously reported that a Ca²⁺- and voltage-dependent big conductance K channel (BK) is expressed in type I spiral ligament fibrocytes (SLFs) (Liang et al., Pflugers Arch. 445:683, 2003). Whole cell voltage and current clamp recordings have shown that the BK channel is the dominant membrane conduc-

tance in these cells implying an important role in controlling the membrane potential. The BK channel-mediated whole cell current displays a voltage-dependent incomplete inactivation (~90%). The I/V plots from a family of depolarization-activated whole cell currents showed a characteristic peak at a membrane potential of 60 mV under 10 μ M intracellular $[Ca^{2+}]$. The recovery time from inactivation was estimated to be ~ 6 ms. The inactivation of BK channels in neurons normally is modulated by BK channel β subunits.

We investigated the molecular mechanism underlying the inactivation of BK channels in type I SLFs by RT-PCR and the RACE (rapid amplification of cDNA ends) reaction. Sequence information for all four known rat BK β subunits ($\beta 1-4$) was obtained from Genbank but only the $\beta 4$ -specific primer produced a corresponding band from RNA isolated from gerbil type I SLFs. The PCR product was cloned into a pCR-2.1 vector for sequencing. New primers were designed for the RACE reaction based on the gerbil $\beta 4$ subunit sequence. The complete gerbil BK $\beta 4$ subunit was cloned and sequenced and found to be composed of 1028 base pairs and to have a 93% homology with its rat counterpart.

These data suggest strongly that the inactivation of whole cell membrane current in type I SLF is the result of an interaction between the BK channel's α and $\beta 4$ subunits. This modulation would provide the SLFs BK channels with a biophysical feature similar to that of BK channels in the nervous system and may play a crucial role in the control of membrane potential in type I SLF.

993 Na⁺/H⁺ Exchanger Isoform 1 is Not Essential for the Normal Function of the Murine Inner Ear

Daniel Choo, Jaye Ward, Alisa Reece, Hongwei Dou, John Greinwald

Otolaryngology, Center for Hearing and Deafness Research, 3333 Burnet Avenue, Cincinnati, Ohio, United States

Hongwei Dou¹, Jamie W. Meyer², Gary E. Shull², John H. Greinwald¹, Daniel Choo, M.D.^{1*}

¹Center for Hearing and Deafness Research

Department of Pediatric Otolaryngology

3333 Burnet Ave. Cincinnati, OH 45229

²Department of Molecular Genetics, Biochemistry and Microbiology

University of Cincinnati, College of Medicine

231 Bethesda Ave. Cincinnati, OH 45221

* Author to whom correspondence should be addressed:

Daniel Choo

Center for Hearing and Deafness Research

Department of Pediatric Otolaryngology

Cincinnati Children's Hospital Medical Center

3333 Burnet Avenue, Cincinnati, OH, USA. 45229-3039

(513) 636-4870, (513) 636-2886 (fax) Daniel.Choo@cchmc.org

Abstract: Changes of intracellular pH (pHi) in various cells of inner ear have been shown to result in their functional alteration possibly through effects on ion channel or cell volume regulations, transepithelial solute transport, or enzymatic activities. Several acid-base transporters involved in pHi regulation in the inner ear

have been identified, a major one being the electroneutral Na⁺-H⁺ exchanger. In this study, we investigated the expression pattern of Na⁺/H⁺ exchanger isoform 1 (NHE1) in the mouse inner ear by immunohistochemistry and examined morphological changes and functional consequences in the mouse inner ear with targeted disruption of gene encoding Nhe1. We found strong immunoreactive signals in the stria vascularis, inner and outer hair cells, interdental cells, cochlear and vestibular ganglion neurons, vestibular dark and transitional cells. NHE1 is also expressed at lower levels in the type II and type III fibrocytes of the spiral ligament, fibrocytes and sensory epithelium of the saccule, and in the apical membrane of scattered epithelial cells of the endolymphatic sac. Nhe1^{-/-} mice showed normal hearing sensitivity as demonstrated by auditory brainstem responses and comparable inner ear morphology to that of Nhe1^{+/+} mice.

The expression pattern of NHE1 suggests that it plays an important role in inner ear pH homeostasis. However, NHE1 activity is not essential for the normal function and the development of the mouse inner ear.

994 Comparative culture of inner ear and epidermal melanocytes

Marcos Sanchez-Hanke¹, Sabine Kief², Rudolf Leuwer¹, Ulrich Koch¹, Ingrid Moll², Johanna M. Brandner²

¹ENT-Department, University of Hamburg Medical School, Martinistr. 52, Hamburg, Germany, ²Dermatology, University of Hamburg Medical School, Martinistr. 52, Hamburg, Germany

Introduction: The presence of melanocytes in the membranous labyrinth was described to be important for the inner ear Ca²⁺ and K⁺ homeostasis. Other metabolic functions of these inner ear cells were not investigated so far. The aim of this study was to define the optimal conditions for the cultivation of these inner ear pigment cells and to compare their metabolic properties with a control group of cultivated epidermal melanocytes. Using immunohistochemical techniques, the different characteristics of both cell populations were investigated as well. **Material and Method:** Membranous labyrinth cells of freshly slaughtered sheep (n=19) were isolated. Fibroblasts and melanocytes were cultivated. Tyrosinase, Melan A, MEL 5 and HMB 45 antibodies were analyzed in the cultured cells. **Results:** In comparison to the dermal melanocytes the proliferation of the inner ear melanocytes was retarded. After 14 days, bipolar pigment cells began to proliferate exponentially for the first time, then spread and finally confluated in the surroundings of fibroblasts forming threedimensional clusters. Occasionally, the bipolar pigment cells differentiated into dendritic cells. This cell type contained more pigment than the bipolar cells because of its continuous proliferation of cytoplasmatic pigment granula. Immunohistochemical techniques proved the inner ear melanocytes to be tyrosinase positive, also Melan A and MEL 5 antibodies could be found. **Conclusion:** For the first time the authors succeeded in cultivation of inner ear pigment cells and proved them to be melanocytes by using immunohistochemistry. In comparison to epidermal melanocytes, the proliferation rate of these pigment cells is lower. Fibroblasts play an important role in the emigration and formation of pigment cell clusters and in the differentiation of bipolar melanocytes into dendritic cells.

995 Sphingosine-1-phosphat (S1P)-induced vasoconstrictions of the Spiral Modiolar Artery are mediated by activation of Rho kinase

Elias Q. Scherer^{1,2}, Elmar Oestreicher¹, Wolfgang Arnold¹, Ulrich Pohl², Steffen-Sebastian Bolz²

¹ENT-Department, Technische Universität München, Ismaninger Str. 22, Munich, Germany, ²Physiology Department, Ludwig-Maximilians-Universität, Schillerstr. 44, Munich, Germany

Increases in tone of the SMA may cause ischemia of the inner ear that can result in sudden hearing loss. Recently, the sphingolipid mediator S1P has been identified as an important endogenous mediator of microvascular tone. It is synthesized by sphingosine kinase (Sphk1) and can act as both, a second messenger and a high-affinity ligand for a group of membrane standing receptors (S1PR₁₋₃). We hypothesized that the Sphk1/S1P-pathway is an important modulator within the inner ear microcirculation. Since a physiological role of this pathway requires the presence of Sphk1 and candidate S1PRs, we studied the expression of these proteins within the SMA and whether exogenous S1P induced vasoconstrictions of the SMA via activation of Rho kinase.

SMA were isolated from the gerbil cochlea, cannulated with micromanipulator-mounted glass micropipettes on both ends and tied off using monofilament sutures. Transmural pressure was set to 45 mmHg. Vascular diameter and intracellular Ca²⁺ ([Ca²⁺]_i) were measured simultaneously using videotechnique and the Fura-2 method. RT-PCR was used to check for the expression of S1PR₁₋₃ and Sphk1.

RT-PCR of total RNA isolated from SMA revealed expression of S1PR₁₋₃ and Sphk1. S1P (n=7) induced dose-dependent, long-lasting vasoconstrictions with an EC₅₀ of 200 nM. Associated increases in [Ca²⁺]_i (n=7) were transient in nature despite continuous presence of S1P. Vasoconstrictions elicited by the highest dose of S1P (30 μM) were significantly reduced by the selective Rho kinase inhibitor Y27632 (0.5 μM, reduction by 63±16%, n=7). In contrast to S1P, the vasoconstrictor norepinephrine (30 μM, n=7) had no effect on vascular tone or [Ca²⁺]_i.

We conclude that S1P-induced vasoconstrictions of the SMA were partly mediated through activation of Rho kinase. Since all constituents of the Sphk1/S1P pathway, the Sphk1 and the S1PR₁₋₃, are present in the SMA, this pathway is a likely candidate to control SMA tone under physiological conditions.

996 Distinct channels responsible for acetylcholine-induced hyperpolarization and depolarization in guinea pig *in vitro* spiral modiolar artery

Zhi-Gen Jiang¹, Hui Zhao^{1,2}, Yu-Qin Yang¹

¹OHRC/Otolaryngology, Oregon Health & Science University, 3181 SW Sam Jackson Park Rd., Portland, OR, United States,

²Otolaryngology, Fudan University EENT hospital, Yueyang Rd., Shanghai, China, People's Republic of

Acetylcholine (ACh) exerts dual actions in the spiral modiolar artery (SMA): causing hyperpolarization and depolarization in low (~-40 mV) and high (~-75 mV) resting potential level, respec-

tively, of the recorded cells (Jiang et al. J. Physiol. 2001). ACh also produces vasodilation and constriction dual effects in various vessels including the SMA. We recently reported that the ACh-induced hyperpolarization and depolarization had qualitative (M₂) and quantitative (M₁ & M₃) differences in the sensitivity to muscarinic receptor subtype (M₁, M₂, M₃) antagonists (Zhao et al. 2003). Using isolated SMA preparations and intracellular recording methods, we examined ionic mechanisms underlying these opposite membrane effects. We found that: 1) ACh-hyperpolarization was associated with a decrease in input resistance, 2) the amplitude of ACh-hyperpolarization was enhanced by membrane depolarization and attenuated by hyperpolarization; 3) ACh-hyperpolarization, but not the depolarization, was blocked by 50 nM charybdotoxin, 10 μM nifedipine or 1 μM nimodipine, whereas the ACh-hyperpolarization was not blocked by 100 μM Cd²⁺ or Ni²⁺; 4) ACh-depolarization was associated with no significant input resistance changes, and the amplitude of ACh-depolarization was reduced by membrane depolarization (up to -10 mV); 5) Both ACh-hyperpolarization and depolarization were inhibited by 10 mM caffeine. We conclude that ACh-hyperpolarization is generated by opening of calcium-activated potassium channels (K_{Ca}); the responsible calcium influx is through a dihydropyridine-sensitive but not the L type of Ca²⁺-channel. The ACh-depolarization is probably due to activation of a non-specific cation channel. Both membrane effects involve intracellular calcium mobilization. Supported by grants of DRF, Oregon MRF and NIH NIDCD DC004716.

997 Functional basal NO production by multiple NOS isoforms in isolated guinea pig spiral modiolar artery

Yu-Qin Yang¹, Alfred L. Nuttall^{1,2}, Zhi-Gen Jiang¹

¹OHRC/Otolaryngology, Oregon Health & Science University, 3181 SW Sam Jackson Park Rd., Portland, OR, United States,

²Kresge Hearing Research Institute, University of Michigan, 1301 East Ann Street, Ann Arbor, MI, United States

Nitric oxide (NO) is a key messenger in vascular regulation including in control of cochlear circulation. Three NO synthase isoforms (nNOS, iNOS and eNOS) have been found to catalyze the NO production. We previously reported that NO-donor hyperpolarizes both endothelial and smooth muscle cells of *in vitro* spiral modiolar artery (SMA) via activation of ATP-sensitive K⁺-channel (K_{ATP}). Also, NO was detected in the SMA cells by NO-indicator dye in the *in vitro* basal condition. Using intracellular recording techniques, electrochemical NO-sensing measurement, and a vaso-diameter video tracking method, we investigated the basal release of NO from the *in vitro* SMA and its role in the vascular function. We found that 1) NO sensor in the close vicinity of the SMA detected a NO concentration of ~50 nM that was suppressed by NOS inhibitor L-NAME (300 μM) and enhanced by L-arginine (1-1000 μM); 2) iNOS-selective inhibitor 1400W (1 μM) caused a smaller inhibition (22% of L-NAME) while nNOS inhibitor 7-nitroindazole had little effect. 3) Both L-NAME, and 3 μM glipizide caused a depolarization in low resting potential cells whereas L-NAME, not glipizide, caused vaso-dilation;

4) NO-donor DPTA-NONOate (0.1 to 30 μM) applications produced about 8 to 245 nM of NO in the recording bath. This data indicates a NO concentration-hyperpolarization relation, with an

EC₅₀ of 22 nM. We conclude that a significant amount of NO is released from the *in vitro* SMA, which is above the EC₅₀ for activation of K_{ATP}, and thus contributes to the membrane polarization and vasotone relaxation. Endothelial NOS is primary responsible for the basal NO production but iNOS may also has minor contribution. Supported by grants of Deafness Research Foundation, Oregon Medical Research Foundation and NIH (NIDCD DC004716) (to Jiang), and by NIH (NIDCD DC00105) and VA RR&D (RCTR 597-0160) (to Nuttall).

998 Contribution of Stapedial Artery to Blood Flow in the Cochlea and its Surrounding Bone

Hiroshi Ymamoto¹, Mitsuo Tominaga¹, Michihiko Sone¹, Hiromi Ueda², Tsutomu Nakashima¹

¹Otorhinolaryngology, University of Nagoya, 65 Tsurumai-cho, Showa-ku, Nagoya, Japan, ²Otorhinolaryngology, Nagoya First Japan Red Cross Hospital, 35-3 Michisita-cho Nakamura-ku, Nagoya, Japan

This study was performed to elucidate the contribution of the stapedial artery (SA) which has been considered to be independent of the vertebralbasilar system to blood flow in the ear by observing ear blood flow in Sprague-Dawley rats. A laser-Doppler (LD) probe was positioned on the bony wall of the cochlear basal turn after removal of the middle ear mucosa. The LD output was measured while either or both the SA and the anterior inferior cerebellar artery (AICA) were occluded. Data were analyzed using Student's paired and unpaired t-tests. A difference was assumed to be statistically significant when the probability was $p < 0.05$. The distributions are reported as mean \pm SD.

The LD output decreased to $70.6 \pm 2.5\%$ of the baseline value following SA occlusion, and to $58.0 \pm 7.8\%$ following AICA occlusion in 12 animals. There were statistical differences in residual blood flow between the SA and AICA ($p < 0.01$). The rebound phenomenon of blood flow, which is a type of autoregulation, was only observed after releasing AICA occlusion. The rebound blood flow ($21.5 \pm 8.8\%$) related to autoregulation of the AICA was observed. After releasing the SA, the LD output returned to $100.4 \pm 2.1\%$, and no significant rebound phenomenon was observed. Simultaneous occlusion of the SA and AICA decreased the LD output to $27.0 \pm 5.5\%$ of the baseline value. From these findings, the role of the contribution of the SA and AICA to the LD output is discussed.

999 Interpretation of Distortion Changes during Endolymphatic Manipulations by an Analysis of Transducer Operating Point

Davud B. Sirjani, Alec N. Salt, Ruth M. Gill, Shane A. Hale

Otolaryngology, Washington University Medical School, 660 South Euclid, St. Louis, MO, United States

We investigated the relationship between distortion and operating point and utilized its co-dependence for the assessment of the functional state of the cochlea. Three interventions were used to disturb endolymph: 1) 200Hz tone exposure; 2) Artificial endolymph injection at 80, 200 or 400nl/min; 3) Injection of furosemide intravenously or intracochlearly. We measured the

effect of volume disturbance on: second harmonic distortion, summing potential, f2-f1 and 2f1-f2 emissions; thresholds at 2.8kHz and 8kHz; cochlear microphonic at 500Hz and 4kHz; and endocochlear potential. Operating point of the transducer was obtained from analysis of the cochlear microphonic waveform using the approach of Kirk and Patuzzi 1997 (Hear. Res. 112, 49). The operating point and second harmonic distortion showed a predictable pattern of change in all intervention groups. Threshold elevations were modest except in the groups receiving furosemide or artificial endolymph injections at a high rate. The f2-f1 emissions showed a greater sensitivity to the volume disturbance than did 2f1-f2. The 200Hz tone exposure, 200nl/min artificial endolymph injections and furosemide injection into scala tympani all showed an increase in operating point consistent with an induced acute state of endolymphatic hydrops. The direction of change in second harmonic distortion depended on the pre-treatment operating point value. Initial operating points ranged from +0.08 to -0.35 with the average starting operating point of -0.08. Typically, interventions showed a decrease in distortion if operating point moved towards zero and an increase in distortion if operating point moved away from zero. Distortion provides insight to the transducer operating point and perhaps the state of endolymph volume.

Supported by NIH/NIDCD grants RO1 DC01368 (AS) and T32 DC00022 (DS)

1000 Transducer Operating Point Shifts Account for Post-Onset Distortion Changes with Low Frequency Tones.

Colin S. Rodger, Alec N. Salt

Otolaryngology, Washington University Medical School, 660 South Euclid, St. Louis, MO, United States

Prior studies have shown that acoustic emissions show systematic changes with time as tonal stimuli are applied continuously. We have observed similar time-varying changes of second harmonic distortion in the cochlear microphonic response to a single tone. Averaged cochlear microphonic waveforms obtained from guinea pigs were analyzed spectrally and the transducer operating point was estimated using methods established by Kirk and Patuzzi, 1997 (Hear. Res. 112, 49). Measurements were performed repeatedly at 15 sec intervals during continuous tone delivery for 3 min and afterwards, with stimuli then only applied briefly as needed for data collection. A considerable variety of distortion changes with time was observed, with some animals showing sharp minima. The time courses were largely explained by operating point movements of the transducer. Operating point shifts were consistent across animals but their effects on distortion depended on the absolute value, which varied in different individuals. The relationship was studied as the 500 Hz tone level was systematically varied from 70 to 120 dB SPL. Below 80 dB operating point could not be reliably determined, although distortion changes comparable to those with higher levels were observed. With high level stimulation, larger operating point changes with more rapid time course were observed. The inclusion of a second tone for the measurement of acoustic emissions substantially changed the dependence of operating point and second harmonic on stimulus duration. Understanding the dynamic changes in transduction during tonal stimulation is essential for the interpretation of acoustic emission data. This is especially important for situations where operating

point is disturbed, such as with endolymph volume disturbances.

This study was supported by NIDCD grant RO1 DC01368.

1001 Medial-Efferent Stimulation Can Inhibit the Earliest Peak of Click Responses from Cat Single Auditory-Nerve Fibers

John J Guinan¹, Tai Lin², Holden Cheng³

¹Eaton Peabody Lab, Mass. Eye & Ear Infirmary, Harvard Medical School, 243 Charles St, Boston, MA, United States, ²Eaton Peabody Lab, Mass. Eye & Ear Infirmary, 243 Charles St, Boston, MA, United States, ³Speech and Hearing Science and Technology, Harvard-MIT Division of Health Sciences and Technology, 77 Mass. Ave, Cambridge, MA, United States

Despite the insights about cochlear mechanics that can be obtained from responses to clicks, medial efferent effects on click responses from single auditory-nerve fibers have not been previously studied. We recorded responses of cat single auditory-nerve fibers to randomized click level series with and without electrical stimulation of medial efferents.

For fibers of all CFs, efferent stimulation reduced responses to low-level clicks, as expected. For fibers with CFs <4 kHz, where separate response peaks can be seen, efferent stimulation reduced later response peaks more than middle peaks at all sound levels. When there was waxing and waning of response peaks, efferents preferentially reduced peaks after the first wane. Surprisingly, the earliest peak, which is seen only for moderate-to-high-level clicks, was sometimes reduced or abolished by efferent stimulation. Finally, efferent stimulation lowered the sound levels of peak "phase reversals," reminiscent of the efferent effect on high-level, tone-elicited phase reversals (Gifford & Guinan 1983, JASA 74:115).

Efferent inhibition of the earliest peak of auditory-nerve click responses indicates that this peak is not just a passive response. In contrast, the earliest peak of the basilar-membrane (BM) click response appears to be a passive mechanical response (Recio et al 1998, JASA 103:1972). Presuming that these differences are not due to species or CF differences, these observations imply that the inhibited part of the early peak of auditory-nerve click responses is due to a cochlear mechanical vibration mode that has a much greater influence on inner-hair-cell stereocilia than on BM motion. Since medial efferents inhibit this vibration mode, it appears to be due in some way to outer hair cell (OHC) motility. The presence of this OHC-generated vibration mode early in the response puts it at a time that could influence, shape, or be a first step in cochlear amplification.

(Supported by NIDCD RO1 DC00235)

1002 Impact of outer hair cell electromotility on organ of Corti vibration - results from an *in-situ* preparation

Manuela Nowotny, Hans-Peter Zenner, Anthony W. Gummer

Otolaryngology, University of Tuebingen, Elfriede-Aulhorn-Str. 5, Tuebingen, Germany

Stimulus modes of the stereocilia of inner hair cells (IHCs) were investigated by measuring the electrically-induced transverse

vibration patterns of the organ of Corti (OC) at different radial locations: i) on the reticular lamina (RL) and ii) on the upper and lower surfaces of the tectorial membrane (TM). Velocity was measured using a laser-interferometer (Polytec OFV 302), with a depth resolution of $\pm 1.8 \mu\text{m}$ from the focus plane (at -10 dB).

The results derive from an *in-situ* preparation of the first (N=19), second (N=25) and third (N=22) turns of the guinea-pig cochlea with CF of 0.9 - 30 kHz. The turn of interest was isolated by removal of the lateral part of all other turns. Reissner's membrane was left intact, allowing better preservation of the TM. For electrical stimulation, two platinum electrodes and one gold electrode were used; the latter also served as a mirror for illumination from the tympanic side of the organ. Stimulus frequency was 480 Hz to 74 kHz.

For frequencies up to at least 2 kHz, all three turns exhibited a phase lag of approximately 180° for the RL motion of the IHCs relative to outer hair cells (OHCs). For the second and first turns there was an additional phase lag of IHC re. OHC at CF, which amounted to 40° (CF: 5.5 kHz) and -180° (CF: 30 kHz), respectively. All four measurement points at the TM (lower and upper surfaces, over IHC and OHCs) vibrated almost in phase with the OHCs; the largest lag was about 50° at CF in the second turn. As a result, there was a phase lag of the RL of IHC relative to the lower surface of the overlying TM, which at CF amounted to 180° , 270° and 0° for the third, second and first turns, respectively. For frequencies up to at least 2 kHz, the difference was approximately 180° for all three turns. These results imply radial fluid motion in the subreticular space, except in the region of CF in the basal turn.

This work was supported by the Deutsche Forschungsgemeinschaft: SFB 430, Teilprojekt A4 and Gu 194/5-1,2.

1003 The Transverse Mechanical Impedance of the Organ of Corti

Marc P. Scherer¹, Anthony W. Gummer²

¹Otolaryngology, University Tuebingen, Elfriede-Aulhorn-Str. 5, Tuebingen, Germany, ²Otolaryngology, University Tuebingen, Elfriede-Aulhorn-Str. 5, Tuebingen, Germany

The point impedance of the organ of Corti in the transverse direction was measured in an attempt to understand how the electro-mechanical forces produced by the outer hair cells (OHC) are coupled into the traveling wave along the cochlear partition. The basilar membrane was mechanically clamped and the tectorial membrane removed, in an explant from turns one (N = 11), two (N = 17) and three (N = 7) of the adult guinea-pig cochlea. Impedance was derived from transverse velocity measurements (LDV OFV-302 and OFV-3000, Polytech) of a ferromagnetically coated atomic force cantilever placed on the reticular lamina (RL). The cantilever was stimulated magnetically to deliver a calibrated force to the RL over a frequency range of 480 Hz to 50 kHz. The impedance at all points along the cochlea was described by a generalized Voigt-Kelvin viscoelastic model, in which the stiffness was real-valued and independent of frequency, but the viscosity was complex-valued, with positive real part, which was dependent on frequency, and negative imaginary part, which was independent of frequency. Stiffness was 0.5 N/m, 0.4 N/m and 0.3 N/m at the tunnel of Corti in turns one to three, respectively. At high frequencies

- in the region of the best frequency for the longitudinal recording place -, the real part of the viscosity was independent of frequency. From the first to third turns, the real part of the viscosity ranged from 25 $\mu\text{N s/m}$ to 14 $\mu\text{N s/m}$ for the tunnel of Corti. These stiffness and viscosity parameters decreased monotonically in the radial direction; for example, in the first turn they were about a factor of five smaller at second row OHCs than at the tunnel. There was no evidence for an inertial component. In the absence of inertia, the mechanical load on the outer hair cells cause the electromotile displacement responses to be reduced by only ten fold over the entire range of auditory frequencies. Together with the absence of an inertial component in the transverse direction, this suggests that the electromechanical force produced by the OHCs is viscosity-coupled into the organ of Corti at high frequencies.

Supported by the Deutsche Forschungsgemeinschaft: SFB 430, Teilprojekt A4 and Gu 194/5-1,2.

1004 Electromechanical Force Generation across the Organ of Corti up to 50 kHz

Marc P. Scherer, Hans-Peter Zenner, Anthony W. Gummer
Otolaryngology, University Tuebingen, Elfriede-Aulhorn-Str. 5, Tuebingen, Germany

The mechanisms by which electromechanical force from the outer hair cells is coupled into the organ of Corti are still not understood. The electromechanically induced velocity, v , of the organ of Corti was measured *in vitro* at different radial positions on the reticular lamina of the adult guinea-pig cochlea. The velocity was measured with a laser Doppler vibrometer (LDV OFV-302 and OFV-3000, Polytech) and expressed relative to the electrical current density through the chamber. The LDV was sufficiently sensitive to permit measurements without introducing reflective materials onto the reticular lamina. The stimulus frequency was 0.5 to 76 kHz. The preparation consisted of half of a turn of the modiolar bone, the attached basilar membrane and the overlying organ of Corti. The tectorial membrane was removed and the tympanic side of the basilar membrane was clamped mechanically by placing it on a flat support. Preparations are from the first (N=11), second (N=17) and third (N=7) cochlear turns.

The mechanical impedance, Z , of the preparation at the position of the velocity measurement was derived from velocity measurements of a ferromagnetically coated atomic force cantilever placed at the reticular lamina. The cantilever was stimulated magnetically to deliver a calibrated force to the reticular lamina over the frequency range of 0.5-50 kHz. From Z and v , the mechanical force, F , acting on that point of the reticular lamina could be calculated according to $F = Z v$.

The magnitude of the force above the outer and inner hair cells remained constant up to 50 kHz, while its phase lagged 90° between 0.5-50 kHz. At other radial positions, the force exhibited more complicated frequency responses, which are likely caused by a complex and frequency dependent force transfer within the organ. Therefore, one prerequisite for optimal cochlear amplification, namely frequency independent coupling of the amplitude of the OHC force into the organ of Corti, is fulfilled over the entire frequency range, at least with respect to the current.

Supported by the Deutsche Forschungsgemeinschaft: SFB 430, Teilprojekt A4 and Gu 194/5-1,2.

1005 Distortion product otoacoustic emissions (DPOAEs) without prestin-mediated OHC motility

M. Charles Liberman¹, John J. Guinan², Jian Zuo³

¹*Eaton-Peabody Lab, Mass. Eye and Ear Infirmary, 243 Charles St, Boston, MA, United States*, ²*Eaton-Peabody Lab, Mass. Eye and Ear Infirmary, Charles St, Boston, MA, United States*, ³*Dept. Dev. Neurobio., St. Jude Childrens Res. Hosp., N. Lauderdale St, Memphis, TN, United States*

The distortion source for DPOAEs is thought to be forward transduction via OHC stereocilia, but the coupling of this distortion to cochlear vibration is poorly understood. Prestin is a key component of the cochlear amplifier, and its deletion removes reverse transduction via OHC somatic motility without affecting stereocilia function (Liberman et al. *Nature* 419;2002). Thus, prestin null mice can be used to probe mechanisms of DPOAE generation and coupling.

DPOAEs and cochlear microphonic (CM) were measured concurrently in prestin-null (-/-) mice and wildtype littermates. Tone-pip-evoked CAP threshold, re wildtype, was the loss-of-gain metric. In -/- animals, gain loss varied from 35 dB at 3.5 kHz to 55 dB at 16 - 32 kHz. CM in some -/- ears was within a few dB of wildtype, consistent with minimal effect of prestin deletion on forward transduction. CM distortion at 2f1-f2 was also strong: ~20 dB down from the primaries at high SPLs in both genotypes. DPOAEs at 2f1-f2 were absent at low SPL in all -/- mice. At high SPLs, some -/- ears retained a physiologically vulnerable 2f1-f2 DPOAE at a threshold elevation equal to the CAP-derived loss of gain.

Results are consistent with the low-level DPOAE distortion source being nonlinearities of OHC forward transduction, which are normally coupled to BM motion by receptor current activation of reverse transduction via the prestin motor. The maintenance of DPOAEs without prestin, when stimulus level is adjusted to compensate for the reduction of gain, suggests that 1) at high levels, DPOAE distortion arises from mechanical properties of OHC stereocilia, not the related current-gating nonlinearities, and 2) these mechanical nonlinearities are robustly coupled to cochlear motion to a degree that they can drive the middle ear.

Supported by grants from the NIDCD: DC00188 (MCL), DC00235 (JJG) and DC04761 (JZ)

1006 Cross-sectional Vibration of the Organ of Corti.

Anders Fridberger, Jacques Boutet de Monvel

Center for Hearing and Communication Research, Karolinska Institutet, Karolinska Sjukhuset M1:00, Stockholm, Sweden

A novel method for rapid confocal microscopy was used to simultaneously investigate the sound-evoked vibration of hair cells, supporting cells and the basilar membrane in the apical turn of an isolated temporal bone preparation. Images of the vibrating organ were analyzed using a wavelet-based method for optical flow estimation. During sound stimulation at frequencies appropriate for this cochlear region, structural relations within the organ were dynamically changing. Outer hair cells showed motion indicative of bending. The reticular lamina and the basilar membrane had different centers of rotation, leading to shearing motion within the

organ of Corti. These results refute classical models that presume rigid vibration with a single degree of freedom (see also Fridberger and Boutet de Monvel, *Nature Neuroscience* 6:446-448).

1007 Shear gain and tectorial membrane vibratory patterns at the basal and apical regions of the cochlea

Hongxue Cai, Brett Shoelson, Richard S Chadwick

NIDCD, NIH, 10 Center Dr. MSC1417, Bethesda, MD, United States

Knowledge of vibratory patterns in the cochlea is crucial to understanding the stimulation of mechano-sensory cells. Experiments to determine the motion of the cochlear partition and surrounding fluid are extremely challenging. As a result, the motion data are incomplete and often contradictory. The bending mechanism of hair bundles, thought to be related to the shear motion and endolymphatic flow between the tectorial membrane and reticular lamina, remains unclear. We therefore applied a hybrid analytical/finite-element approach to model both the basal and apical regions of the guinea pig cochlea, and solved the fluid-solid interaction eigenvalue problem for the axial wavenumber, fluid pressure, and vibratory relative motions of the cochlear partition as a function of frequency. A simple monophasic vibratory mode of the basilar membrane is found at both ends of the cochlea. However, this simple movement is accompanied with a complex, frequency-dependent relative deformation between the tectorial membrane and the reticular lamina. Deformations within the organ of Corti are also complex. When the basilar membrane oscillates, the tunnel of Corti rotates about the foot plate of the inner pillar cell, triggering a relatively large radial movement of the inner hair cell body. The reticular lamina is divided into two parts by the top of the tunnel of Corti; the left part moves essentially in the radial direction, while the right part contains both radial and transverse components. Our calculations of the cochlear shear gain as a function of frequency demonstrate, for the first time in a complex continuum model, that the motion of the tectorial membrane has a significant radial component that facilitates bending of outer hair cell stereocilia at appropriate frequencies at both the cochlear base and apex.

1008 Backward traveling waves in the cochlea? Comparing basilar membrane vibrations and otoacoustic emissions from individual guinea-pig ears.

Nigel P. Cooper¹, Christopher A. Shera²

¹*Mackay Institute of Communication and Neuroscience, School of Life Sciences, Keele University, Keele, United Kingdom,*

²*Eaton-Peabody Laboratory, Mass. Eye & Ear Infirmary, 243 Charles Street, Boston, MA, United States*

In order to distinguish between theories relating to the origin and existence of backward-traveling waves in the cochlea, basilar-membrane (BM) vibration patterns and stimulus-frequency and distortion-product otoacoustic emissions (SF and DP OAE) were recorded from individual, deeply-anesthetized guinea pigs. Methodological details are summarised elsewhere (Cooper, 1999; *J. Neurosci. Meth.* 88, 93-102; Shera and Guinan, 1999; *J. Acoust. Soc. Am.* 105, 782-798). Mechanical group delays associated with forward-traveling waves on the BM (at its characteristic-frequency

or CF) amounted to ~0.3 ms in the 20 - 30 kHz regions of the cochlea. Otoacoustic group delays measured at corresponding frequencies from SF and DP OAE's (at f_1 and $2f_2-f_1$, respectively, where $f_2=f_1+100$ Hz, with $L_1=40$ dB SPL and $L_2=55$ dB SPL) were approximately 0.6 ms. Thus, within the estimated uncertainty of the measurements, the OAE group delays were twice the CF mechanical group delays measured on the BM. These data are consistent with theories suggesting that SFOAEs and other reflection-source OAEs arise primarily via the coherent reflection of energy from regions of the BM where forward-traveling waves reach their peak amplitudes (e.g. Zweig and Shera, 1995; *J. Acoust. Soc. Am.* 98, 2018-2047). Analyses of BM responses to the two-tone stimuli used to evoke SF and DP OAEs revealed BM OAE-analogues that showed little accumulation of phase, relative to the f_1 primary, within ~0.25 octaves of CF. As f_1 and f_2 decreased further below CF, however, the BM OAE-analogues accumulated phase much more rapidly than the primary responses. These results are consistent with the existence of waves which travel backwards, along the BM, from more apical regions of the cochlea.

Supported by the Royal Society and by the NIDCD, National Institutes of Health.

1009 Harmonic Distortion from active forces within the organ of Corti

Wei Dong, Elizabeth S. Olson

Otolaryngology/Head & Neck Surgery, Columbia University, 630 W. 168th Street, New York, NY, United States

Harmonic distortion in scala tympani (s.t.) pressure has been reported by Elizabeth S Olson (2002), which showed the harmonic distortion was generated locally inside the cochlea. This report provides further evidence of harmonic distortion in intracochlear pressure in the basal turn of the gerbil cochlea and probes the non-linearity mechanism of truly active (i.e. physiologically normal) cochleae.

Pressure responses to single tones were recorded simultaneously both from the s.t. (at different positions to BM) and scala vestibuli (s.v., close to the stapes serving as cochlear inputs) using intracochlear sensors.

Compressive nonlinearity was observed in s.t. pressure measurements near the preparation's best frequency (BF) in the fundamental components in 'healthy' cochleae. S.T. pressure gain decreased 22 dB when the sound pressure level (SPL) decreased 50 dB at BF in one preparation. The phase accumulation of the fundamental component was up to more than two cycles when the s.t. sensor was positioned within 50 mm from basilar membrane. The absolute levels of harmonic distortion increased progressively with increasing of SPL. The 2nd and the 3rd harmonic distortion were firstly being detected at 50 / 60 dB SPL around BF. With the increase of the SPL, the harmonics distortion products developed a two-peak frequency distribution. One peak was located around the BF of the preparation; the other peak was located at about half (the 2nd) and 1/3 (the 3rd) of the BF. Harmonic distortion was physiologically vulnerable and rarely observed in s.v. pressure measurements. The observation was consistent with the motion study of harmonic distortion in the basal turn of the guinea-pig cochlea (Cooper, 1998, *J. Physiology*, 277-286).

Supported by the NIDCD

1010 Effect of multiple membranes on the heterodyne laser interferometer

Ombeline Louise de La Rochefoucauld, Shyam M. Khanna, Elizabeth S. Olson

Otolaryngology, Head and Neck Surgery, Columbia University, P&S 11-452, 630 West 168th street, New York, NY, United States

The Organ of Corti is composed of a complex structure with many reflecting surfaces, characterized by a wide range of reflectivity. Those membranes might move with different amplitudes and phases. Heterodyne interferometry is a useful tool to measure sub-microscopic motion of the Organ of Corti. The technique uses interference between two beams (object and reference). The velocity of the test object shifts the frequency of the object beam due to the Doppler effect. The heterodyne signal is decoded using a frequency demodulator. Here, we study the effect of competing signals at the input of the FM receiver, how light coming from out-of-focus structures can modify the output of the receiver and how the presence of multiple surfaces can affect the accuracy of the results.

For this study, first, two signals electronically generated (an FM wave and a pure sine wave) were summed at the input of the receiver. We studied the effect of the ratio of their amplitudes and also the relative phase between the two signals, as the two generators were not locked. Then, using the heterodyne interferometer, two optical signals were summed. The object was composed of two surfaces: the front one was semi transparent and vibrated upon sound stimulation and the back surface was fixed. A piezoelectric translator controlled the distance between the two surfaces ($\pm 50 \mu\text{m}$) and then changed the relative phase. The intensity of light coming from each surface depended on the optical sectioning of the interferometer. For both cases (electronics and optics), the theoretical expression of interference at the input of an FM receiver was used to explain experimental data. The change in the output depends on the relative phase between the two signals and the ratio of their amplitudes. Finally, we present how the confocal imaging system reduces the effect of competing signals.

1011 Propagation Direction of the Otoacoustic Emission along the Basilar Membrane

Tianying Ren

OHRC/Otolaryngology-Head and Neck Surgery, Oregon Health & Science University, 3181 SW Sam Jackson Park Road, NRC04, Portland, Oregon, United States

It has been widely believed that otoacoustic emissions are transmitted through the cochlear partition as a backward travelling wave propagating from apex to base. However, because of technical difficulties, the backward travelling wave has not been directly measured in the sensitive cochlea. Distortion product otoacoustic emissions were evoked in gerbils using two acoustic tones in this study, and the magnitude and phase of basilar membrane vibration at primary-tone and emission frequencies were measured as a function of the distance from the cochlear base using a scanning laser-interferometer microscope. Magnitude and phase spectra of basilar membrane and the stapes vibration were also obtained. Although a forward travelling wave from base to apex was observed at the emission frequency, there was no detectable backward travelling wave, and the stapes was observed to vibrate ear-

lier than the basilar membrane. The results contradict the current theory and suggest that the ear emits sound through the cochlear fluids as a compression wave rather than through the basilar membrane as a backward travelling wave.

Supported by NIH-NIDCD DC04554 and VA RR&D Center Grant, Portland VAMC.

1012 Longitudinal and Radial Pattern of Electrically Induced Basilar Membrane Motion in the Basal Turn in the Guinea Pig

Ning Hu¹, Alfred L. Nuttall^{1,2}, Tianying Ren¹

¹Otolaryngology and Head & Neck Surgery, OHRC, Oregon Health & Science University, 3181 SW Sam Jackson Park Rd, NRC04, Portland, Oregon, United States, ²Kresge Hearing Research Institute, The University of Michigan, 1301 East Ann St, Ann Arbor, Michigan, United States

Motion of the guinea pig basilar membrane (BM) evoked with intra-cochlear electric stimulation at frequencies higher than the characteristic frequency (CF) has been observed in our lab (Nuttall, 2003, Abstract of ARO meeting). This high frequency BM motion was considered as composed, in part, of local BM motion that originated from the somatic motility of outer hair cells (OHC) in response to the sinusoid electric stimulation (Nuttall, 2003, Abstract of ARO meeting). In the present experiment, we investigate what is the motion pattern of this high frequency BM motion in the longitudinal and radial directions. BM motion was measured using a laser interferometer. Three longitudinal BM locations were observed separately in the first turn and in the hook region, they were at 14.9 mm, 15.8 mm and 16.8 mm of distances from apex, corresponding to 17 kHz, 21.3 kHz and 28.0 kHz of CF (Greenwood, 1990, JASA, 87, 2592). At each longitudinal location, BM velocity was measured at different radial locations cross BM as well. It was found that the frequency of resonance of BM vibration (identified by a dip and phase reversal in magnitude and phase spectra at frequencies much higher than the CF) was different for the three radial locations of OHC, Hensen's cells and tunnel of Corti. In the longitudinal direction (at the location of the second row of OHC) the average value of the resonance at high frequencies was 49.8 kHz at 14.9 mm, 54.6 kHz at 15.8 mm and 73.2 kHz at 16.8 mm. Thus, the longitudinal distribution of high frequency resonance is correlated with the CF along BM. These results imply that the high frequency BM motion is related with mechanic properties of the cochlear partition including the OHCs themselves. Data also indicate higher vibration modes across the width of the organ of Corti.

Supported by: NIDCD DC00141, DC04554 and VA RR&D Center Grant

1013 Chlorpromazine Alters Cochlear Mechanics in the Sensitive Ear of Guinea Pigs

Jiefu Zheng¹, Alfred L. Nuttall^{1,2}

¹Oregon Hearing Research Center, Oregon Health & Science University, 3181 SW Sam Jackson Park Road, Portland, Oregon, United States, ²Kresge Hearing Research Institute, The University of Michigan, 1301 East Ann Street, Ann Arbor, Michigan, United States

Outer hair cell (OHC) electromotility is fundamental to the hear-

ing sensitivity of the mammalian cochlea. Chlorpromazine (CPZ), an antipsychotic drug that alters plasma membrane biomechanics, has been reported to alter isolated OHC membrane fluidity and electromotility (in the depolarizing direction). Meanwhile, low frequency cubic distortion product otoacoustic emissions (DPOAEs) were reported to increase by CPZ. This study aimed to investigate the effects of CPZ on basilar membrane (BM) velocity responses as well as on the DPOAEs in the sensitive cochlea. The BM velocity in response to pure tones (2 to 24 kHz) at the site corresponding to the best frequency (BF) of around 17 kHz was measured from a reflective bead on the BM in the OHC region using a laser interferometer. DPOAEs were evoked by a pair of pure tones ($f_2/f_1=1.2$, f_2 ranged 4 to 22 kHz) and were measured from the ear canal with an Etymotic microphone. CPZ in artificial perilymph (1 mM) was infused locally into the scala tympani of the basal cochlear turn. Approximately 10 to 20 dB loss in BM response sensitivity near the BF with a downward shift of the BF and broadened tuning was observed after CPZ perfusion. Loss of nonlinearity of BM input-output function was also observed. The magnitude of DPOAEs decreased in a manner that was comparable with the alteration of BM motion. The results indicate that the effects of CPZ on OHC plasma membrane biomechanics or motility result in a reduction of OHC mediated cochlear amplifier performance.

Supported by NIDCD R01 DC00141 and VA RR&D Center Grant

1014 Change of the Cochlear Microphonic with Pressure Applied to the Bony Shell of the Cochlea

Yuan Zou¹, Ning Hu¹, Tianying Ren¹, Alfred Nuttall^{1,2}

¹Otolaryngology and Head & Neck Surgery, OHRC, Oregon Health & Science University, 3181 SW Sam Jackson Park Rd, NRC04, Portland, Oregon, United States, ²Kresge Hearing Research Institute, The University of Michigan, 1301 East Ann St, Ann Arbor, Michigan, United States

The cochlear microphonic (CM) evoked by loud low frequency sound is thought to be generated by the outer hair cells (OHCs) near the recording electrode in response to displacement of the basilar membrane (BM). The shape of the CM waveform can be related to the displacement of stereocilia by a Boltzmann-type transfer function. In this experiment, we measured CM change caused by applying force on the otic capsule in guinea pigs. CM response to a 400Hz tone at 100dB SPL was recorded using a bipolar electrode in the first turn. Constant force (~0.14N) was applied to the bone shell over scala tympani at the 18kHz best frequency location using a blunt probe. This force caused a sudden reduction of CM amplitude, which then underwent a slow partial recovery toward the initial level and maintained constant. This time constant (TC) for recovery, fitted by the single exponential function, is about 10-30s. Removing the force caused a second reduction of the CM, followed by a total recovery with a much faster time course (TC~2-5s). Repeated application of force could lessen the degree of CM recovery and cause a 'tonotopic' sensitivity loss near 18kHz. Cochlear sensitivity and the cubic distortion product showed very similar reduction and recovery pattern as the CM. When the CM is reduced by force, the CM waveform became more asymmetric and distorted. In terms of offline analyzed parameters of the Boltzmann transfer function, the position of the stereocilia could be inferred to be shifted by the applied force.

Data indicate that the force on the otic capsule can distort cochlear shape and result in deflection of OHC stereocilia, causing CM to change. The sensitive cochlea appeared to have an 'adaptation-like' mechanism to restore sensitivity and optimal stereocilia position during the application of constant force.

Supported by: NIDCD DC00141 & DC04554

1015 Reverse Propagation of the Electrically Evoked Basilar Membrane Vibration in the Gerbil Cochlea

Tianying Ren, Jiefu Zheng, Ning Hu, Yuan Zou, Alfred L Nuttall

OHRC/Otolaryngology-Head & Neck Surgery, Oregon Health & Science University, 3181 SW Sam Jackson Park Road, NRC04, Portland, Oregon, United States

An electrical current passing through the cochlear partition can induce sound pressure change in the ear canal at the electrical-stimulus frequency, *i.e.*, the electrically evoked otoacoustic emission. It has been speculated that acoustic energy is generated at a site on the cochlear partition near the stimulating electrode, and propagates toward the cochlear base as a backward traveling wave. The aim of this study was to test the above hypothesis by measuring the wave propagation direction of electrically evoked basilar membrane (BM) vibration and the time relationship between BM and stapes vibration. A sinusoidal current was passed through the cochlear partition of the first turn in the gerbil, and the magnitude and phase of electrically evoked BM and stapes vibration, and sound in the ear canal were measured at the electrical-current frequency. Phase of BM vibration as a function of the distance from the cochlear base indicated a typical forward traveling wave at frequencies near characteristic frequencies of the measured location. Phase-spectrum difference between BM and stapes vibration showed a much shorter group delay than that for a traveling wave at frequencies above the CFs. The results suggest that the electrically evoked energy propagates toward the stapes through cochlear fluids as a compression wave rather than through the cochlear partition as a backward traveling wave.

Supported by NIH-NIDCD and VA RR&D.

1016 Bony Dehiscence of the Superior Semi-circular Canal: Cochleo-vestibular Pressure Loss Measurements

Euan Murugasu^{1,2}, Michael Murray¹, Joseph Roberson¹

¹Otology & Neurotology, California Ear Institute at Stanford, 801 Welch Road, Palo Alto, CA, United States, ²Mechanical Engineering, Stanford University, Durand 262, Stanford, CA, United States

BONY DEHISCENCE OF THE SUPERIOR SEMI-CIRCULAR CANAL: COCHLEO-VESTIBULAR PRESSURE LOSS MEASUREMENTS

Euan Murugasu, MD PhD ^{1,2}, Michael Murray, MD ¹, Joseph Roberson MD ¹

1. California Ear Institute at Stanford, Palo Alto, CA

2. Stanford University, Mechanics and Computation Division, Department of Mechanical Engineering, Palo Alto, CA

Superior Semicircular Canal Dehiscence can present as an apparent conductive hearing loss in patients. The third mobile window created by the bony dehiscence results in a dissipation of acoustic energy, and has been described a cause of “inner ear conductive hearing loss” [Minor et al, *Otology & Neurotology*, 2003]. Our aim is to determine the mean pressure loss associated with this bony dehiscence in a temporal bone model. Cochleo-vestibular pressure measurements in human temporal bones have been reported by Murugasu et al [3rd International Symposium on Middle Ear Mechanics in Research & Otology, 2003]. Presently, the ear canal pressure (P_c) and cochleo-vestibular pressure (P_v) were measured, in the 0.1 to 10 kHz range, in fresh cadaveric temporal bones using methods previously described [Puria, et al, 1997, *JASA*]. The following conditions were tested: 1. intact canal (normal ear) 2. bony dehiscence (diseased ear) 3. surgical correction with resurfacing (reconstructed ear). The pressure loss (L_{deh}) is defined as the ratio of P_v before and after creating the bony dehiscence in the superior semicircular canal. Preliminary results show that the dehiscence results in a significant loss of inner ear pressure, in the region of between 10 to 35 dB across the 0.1 to 10 kHz range. After surgical resurfacing, there is some recovery of the inner ear pressure. More data will be collected in future experiments, to confirm these preliminary results, and also to see if there is any correlation between size of the dehiscence and the associated pressure loss.

(Work supported in part by a grant from the NIDCD of NIH (DC03085) & by the Agency for Science, Technology & Research, Singapore)

1017 Mammalian Tectorial Membrane: Elasticity Follows Shape to Balance Protection, Efficiency During Shear

Brett D. Shoelson¹, Emiliios K. Dimitriadis², Hongxue Cai¹, Bechara Kachar³, Richard S. Chadwick¹

¹NIDCD, NIH, 10 Center Drive, 5D49, Bethesda, MD, United States, ²DBEPS, NIH, 13 South Drive, Bethesda, MD, United States, ³NIDCD, NIH, 50 Center Drive, Bethesda, MD, United States

The shearing motion of the tectorial membrane (TM) with respect to the reticular lamina subserves auditory function by bending the outer hair cell (OHC) bundles and inducing fluid flows that shear the inner hair bundles in response to sound energy. Recognizing the anisotropic nature of the membrane and the limitations inherent in stiffness measures, we examine the transverse shear modulus (an intrinsic material property) of the TM using atomic force microscopy to generate approximately 800 force-displacement curves. After discretizing the tissue samples into 3 longitudinal sections (base, middle, and apex) and 6 radial zones, we present a map of the elasticity of the tissue, and report a radial variation of the transverse shear modulus—namely, a softening in the region of the hair bundle articulations that suggests that the TM plays a role in protecting the fragile stereocilia of the OHCs. Further, we argue that this distribution of moduli varies inversely with the non-uniform thickness of the membrane, which balances the needs of protecting the fragile hair bundles and increasing the energy efficiency of the vibrational shearing.

1018 Modeling the Outer Hair Cell Nonlinearity in a Cochlea

Xiaoai Jiang, Karl Grosh

Mechanical Engineering, University of Michigan, 2350 Hayward Ave., Ann Arbor, MI, United States

The outer hair cell (OHC) is known to be the main source of nonlinear activity in the cochlea. In this work, we use a one dimensional model of the cochlea coupled to a nonlinear model of the mechanical-to-electric coupling of the OHC with the basilar membrane (BM). The nonlinearity arises from the voltage sensitivity of the stiffness of the OHC and the displacement dependence of the conductance of the stereocilia. We use a reciprocal nonlinear piezoelectric model of the OHC in combination with a linear relationship between stereocilia conductance and displacement (which results in a nonlinear circuit model). The resulting equations capture a cubic nonlinearity. The mechanical properties of the various components of the model are derived from physiological components of the cochlea. Simulations are shown for sinusoidal and multi-component forcing.

1019 An Energy-based Two State Boltzmann Model for Outer Hair Cells

Niranjan Deo, Karl Grosh

Mechanical Engineering, University of Michigan, 2350 Hayward, Ann Arbor, MI, United States

Outer Hair Cells (OHCs) in the mammalian cochlea exhibit remarkable electromotile properties. In vitro and in vivo experiments have shown that OHCs are capable of high frequency (up to 100kHz) voltage induced length and stiffness changes and exhibit strongly nonlinear piezoelectric behavior. In vivo experimental results on OHCs can be modeled using a two state Boltzmann model with elastic moduli dependant on the motor state (N. Deo, K. Grosh, 2003 ARO MWM). However the model is not reciprocal. We investigate the issue of reciprocity in the modified area motor model.

A one dimensional OHC model with stiffness dependent on motor state is constructed from an energy based approach and from micromechanical laws. Implications of the energy based approach on the micromechanical laws and of the micromechanics based approach on the energy barrier function of the motor are presented.

Work supported by grants from the NIH NIDCD (RO1 04084).

1020 A sandwich model of the cochlea with certain parameters matched to the gerbil

Shan Lu¹, David Mountain², John Spisak¹, **Allyn Hubbard**¹

¹College of Engineering, Boston University, 8 St. Mary's Street, Boston, MA, United States, ²College of Engineering, Boston University, 44 Cummings St., Boston, MA, United States

Although the outer hair cell (OHC) motility is believed to play a central role in the cochlear amplifier, the details of the amplification process are not well understood. We developed a one-dimensional, multi-compartment model of the cochlea that employs OHC force generation to create a slow-traveling pressure wave inside the organ of Corti, which is principally responsible for

enhanced (amplified) response of the basilar membrane (BM) [Hubbard A., Chen, F. and Mountain, D.C. (2002) in *Biophysics of the Cochlea: from Molecule to Model*. A.W. Gummer, E. Dalhoff, M. Nowotny, M. Scherer (Eds.). World Scientific, Singapore, 2002, pp. 351-358.] Using approximate physiological values for the parameters, this model has been shown to mimic physiological data reasonably well.

In an effort to improve model correspondence with gerbil data, we have revisited a number of key model parameters. We used measured scala and BM dimensions to obtain more accurate estimates of fluid mass and viscosity. We have also incorporated the geometry of the oval window and the helicotrema. In addition, to cover the possibility that our calculation of BM volume compliance based on point stiffness measurements may be slightly off, we have allowed the volume compliance used in the model to vary by as much as a factor of 2 in small increments. In addition, the quality factor (Q) of the model's BM is only an approximation, based on what has been observed for passive BM responses; and thus, that parameter was allowed to vary over a range from 2-10. Subsequently, many simulations of cochlear function were calculated, and a search over the data was done, according to a metric that minimizes error in comparison with BM velocity magnitude re. stapes data from the gerbil [Ren T. and Nuttall A. (2001) *Hearing Research* 151, pp. 48-60.]. We are able to find good approximations to the magnitude data using parameters within the range specified above.

NIH supported this work.

1021 A cochlear model designed to test the effect of modulating outer hair cell biophysical properties on basilar membrane mechanics

Chul-Hee Choi¹, Alexander A. Spector², John S. Oghalai¹

¹Dept. of Otolaryngology-HNS, Baylor College of Medicine, One Baylor Plaza, NA102, Houston, Texas, United States, ²Dept. of Biomedical Engineering, The Johns Hopkins University, 720 Rutland Ave., Baltimore, Maryland, United States

Although previous cochlear models have been developed considering outer hair cell (OHC) electromotility as the cochlear amplifier, most do not consider several unique biomechanical properties of the OHC. These include its orthotropic cytoskeleton, its intracellular turgor pressure, and the longitudinal and radial vectors related to force generation. This model was designed to incorporate these considerations. Basilar membrane (BM) velocity was calculated using a traditional one-dimensional transmission line model. Passive BM mechanics were modeled as mass, stiffness, and damping elements in series. To model electromotility, we first determined the OHC receptor potential using a second-order Boltzmann function. Force generation was derived using parameters for the elastic moduli of the orthotropic OHC lateral wall, active length and radius changes, and cell turgor pressure. These parameters were obtained from published *in vitro* data. Results from our active cochlear model showed that BM velocity increased up to 55 dB compared to a passive cochlear model. However, we are continuing to strive towards improving the sharpness of the tuning curve, as it is currently less than what has been measured *in vivo*. Future *in vivo* experiments are planned to test this cochlear model by modulating the biophysical properties of

OHCs while measuring BM velocity.

Supported by NIH grants: NIDCD DC02775, DC00354 (A.A.Spector) and DC05131 (J.S.Oghalai)

1022 Estimation of the amplitude and phase of the force generated by the outer hair cell motility using a finite-element model of the organ of Corti

Masayoshi Andoh, Hiroshi Wada

Bioengineering and Robotics, Tohoku University, Aoba-yama 01, Sendai, Japan

The outer hair cell (OHC) contracts and elongates in response to the depolarization and hyperpolarization of its membrane potential, respectively, and a force is generated in the organ of Corti (OC) by this OHC motility. Since this force magnifies the vibration of the OC, our auditory system is characterized by high sensitivity and sharp tuning. For investigation of the mechanism of cochlear amplification, knowledge of the dynamic characteristics of the force generated by the OHC motility in the OC is crucial. However, as the isolation process causes deterioration of the OHC and the mechanical constraints on the OHC are different from those *in vivo*, the exact magnitude of the force generated by the OHC motility *in vivo* has not yet been clarified. Regarding the phase of the force generated by the OHC motility relative to the deflection of the hair bundle, a phase delay of 90 deg. is commonly accepted in the high frequency range, this delay resulting from low-pass filtering at the membrane due to membrane resistance and membrane capacitance. It has also been proposed that the extracellular potential, which is a potential around the OHC caused by the electrical activities of other OHCs, modulates the membrane potential of the OHC, resulting in a further phase delay; this mechanism, however, has not yet been clarified. In this study, a finite-element model of the OC and two models of the lymph fluid surrounding the OC were constructed. Using these models, the magnitude and phase of the force generated by the OHC motility were obtained by comparing the numerically obtained gain of the BM vibration relative to that without the OHC motility with experimental data. Consequently, it was found that the phase delay of the force ranges from 45 deg. to 180 deg. and that the magnitude of the force is nearly 1.8 nN/nm. Moreover, it was suggested that the electric potential which drives the OHC is likely to be the extracellular potential rather than the receptor potential.

1023 A linear model of the cochlea with global mechanical-electrical-acoustic coupling

Sripriya Ramamoorthy¹, Karl Grosh²

¹Mechanical Engineering, University of Michigan, 2200 EECS, 2250 GGBrown, 2350 Hayward Street, Ann Arbor, MI, United States, ²Mechanical Engineering, University of Michigan, 3124 GG Brown, 2350 Hayward Street, Ann Arbor, MI, United States

A physiologically based three-dimensional linear finite element model is proposed and is used to predict the response of the cochlea to electrical and/or acoustic input. The components of the model include a micro-mechanical model for the cochlear structures, a two-duct acoustic model with structural-acoustic coupling at the Basilar membrane (BM). A novel component of the model is that the electrical potential is modeled by a global circuit as opposed to

the commonly used local radial circuit. The electrical-mechanical coupling is studied with particular emphasis on the high-frequency cut-off of OHC contribution to activity. The model predictions for cochlear microphonic and other cochlear potentials due to electrical and acoustic input are presented. The electrically evoked otoacoustic emissions (EEOAEs) are analysed. Qualitative comparison with published experimental data will be discussed.

This project is funded by NIH NIDCD R01 - 04084.

1024 Minimizing dispersive instability in time domain computation of steady state responses of cochlear models

Jack Xin

Mathematics, University of Texas at Austin, 1 University Station, Austin, Texas, United States

Dispersive instability is shown in time domain solutions of cochlear models. A derivation of optimal initial data is presented to minimize the effect of instability and reduce the computational time of steady states. A second order accurate implicit boundary integral method is introduced. Numerical solutions of two dimensional models show that the optimal initial data work successfully in time domain steady state computations for passive, active and nonlinear models.

1025 Distribution of Negatively Charged Phospholipids on Apical Hair Cell Membranes

Xiaorui Shi¹, Moritoshi Hirono¹, Peter G. Gillespie¹, Alfred L. Nuttall^{1,2}

¹Oregon Hearing Research Center, Oregon Health & Science University, NRC04 / Oregon Health Sciences University, 3181 SW Sam Jackson Pk. Rd., Portland, OR, United States, ²Kresge Hearing Research Institute, The University of Michigan, 1301 E. Ann St., 1301 E. Ann St., 1301 E. Ann St., Ann Arbor, MI, United States

Hair cell plasma membranes (PM) are polarized into discrete apical and basolateral domains, which are characterized by distinct physiological activities, protein complements, and lipid compositions. We have found an unusual distribution of phospholipids and phospholipid particles (PP) in the apical membranes of hair cells from the guinea pig organ of Corti and the bullfrog sacculle *in vitro*. We used scanning confocal microscopy with annexin V to label phosphatidylserine (PS) in live inner hair cells (IHCs) of wholemount organ of Corti and a monoclonal antibody to label phosphatidylinositol 4,5-bis phosphate (PIP₂) in vestibular hair cells (VHCs) of fixed sacculles. In most cells, negatively charged lipids are found on the intracellular PM leaflet and hence would not be accessible to our reagents. In live IHCs, we observed PS labeling only at the cell's apical pole. Labeled PP of various sizes were seen along a border of cuticular plate and were densely aggregated at the vestigial kinocilium location. Some PP moved during the observation period. Some cells had a relatively uniform distribution of PP along individual stereocilia, while in other cells they were distributed irregularly. Immunocytochemistry showed that the PP of IHCs and VHCs contained PM Ca²⁺-ATPase; Rab11 GTPase was detected in the apical cytoplasm of IHCs. In VHCs, with or without otolithic membranes, we detected PIP₂ in both PM

leaflets of hair cells. PP with PIP₂, reminiscent of particles associated with IHCs, often surrounded the hair bundle and were associated with the subotolithic filaments connecting the sacculle's apical surface to the otolithic membrane. We suggest that the PP derive from intracellular membrane and that the PP participate in membrane or cargo transport. The extracellular-leaflet expression of PS and PIP₂ may be a response to perilymph-like solutions, as we have not observed similar expression *in vivo*. Supported by NIH NIDCD DC 00105, 00141, 002368 and 004571.

1026 Development of "Giant Blebs" at the Apical Membrane of Inner Hair Cells *In Vitro*

Xiao-Rui Shi, Peter G. Gillespie, Alfred L. Nuttall

Oregon Hearing Research Center, Oregon Health & Sciences University, 3181 SW Sam Jackson Park Rd NRC04, Portland, OR, United States

Using differential interference contrast and fluorescence microscopy, we have observed that giant vesicles ("blebs") appeared adjacent to the apical membrane of inner hair cells (IHCs) of freshly isolated organ of Corti from adult guinea pigs. The tissues were incubated for up to 3 hrs in a chamber having constant perfusion of a perilymph-like solution. Generally, bleb formation had two phases. In the first phase, we observed apparent protrusions of the plasma membrane, which appeared as "bead-like" shaped particles at one edge of the cuticular plate. Some particles moved randomly. In the second phase, one or more of the protrusions increased in size over time while the total number of beadlike particles decreased, being apparently absorbed into the main bleb. After growing to a diameter of about 10 μm, a single giant bleb was seen attached to the cuticular plate or at the top of the stereocilia bundle. To understand the mechanism of this phenomenon, we used pharmacological reagents to (1) inhibit apoptosis, (2) disassemble microtubules, (3) reduce intracellular pressure, (4) block water channels, (5) deplete intracellular free calcium or ATP, or (6) inhibit endocytotic and intracellular protein transport. The results indicated that (1) the microtubule network is not required for this type of bleb formation, IHCs; (2) bleb formation is independent of the intracellular concentration of free calcium; (3) bleb formation was unaffected by reducing the IHC turgor pressure; and (4) blebs could not be inhibited by pro-caspase inhibition. In contrast, formation of the blebs can be prevented by depletion of intracellular ATP and their expansion could be slowed by inhibition of endocytotic and Golgi protein transport. We conclude that the blebs are not associated with apoptosis or cell mechanical effects but could result from disruption of apical membrane recycling caused by some factor of the *in vitro* incubation procedure. Supported by NIH NIDCD R01 DC 00105, DC 00141, DC 002368 and DC 004571.

1027 Calcium/calmodulin-dependent protein kinase IV is required for normal hearing

Donald Coling

Hearing Research Lab, University at Buffalo, 215 Parker Hall, Buffalo, NY, United States

We have previously reported the presence of calcium/calmodulin-dependent protein kinase activity and phosphoprotein substrates in the sensory epithelium of guinea pig (Coling and Schacht, 1991).

We showed that calcium-dependent radial contraction and circumferential elongation of guinea pig outer hair cells (ohc's, Dulon et al., 1990) is potently blocked by ML-9, an inhibitor of calmodulin-dependent protein phosphorylation (Coling et al., 1998). In subsequent experiments, we showed that electromotility of guinea pig ohc's could be modulated by agents that modulate protein phosphatase and calmodulin-dependent protein kinase activities and that antibodies against calmodulin-dependent protein kinase IV (camk4) selectively label ohc epitope(s) in the region of the electromotility motor and cortical cytoskeleton (Frolenkov et al., 2000). Here, we show that homozygous knockout mice lacking camk4 have normal hearing at post natal day 21, but exhibit an age-dependent hearing loss measured by click ABR. Heterozygous mice had a smaller but significant intermediate phenotype. Statistically significant threshold shifts were first detectable at 9 weeks after birth. By 16 weeks after birth, wild type controls had normal click thresholds of 7±3 dB SPL while heterozygote littermate's thresholds were 12±6 dB and homozygote littermate's thresholds were 62±32 dB (n=12,12 and 10 ears). Further experiments are underway to more rigorously test the hypotheses that camk4 is the effector kinase for calcium-dependent modulation of ohc electromotility, to determine whether camk4 is under the control of the medial olivary system of efferent innervation of ohc's and to establish the identity of camk4 phosphoprotein substrates.

1028 Post-embedding immunogold localization of calcium binding proteins in the rat cochlea

Shanthini Mahendrasingam¹, Robert Fettiplace², **Carole M Hackney**³

¹Life Sciences, Keele University, Keele, Stoke-on-Trent, United Kingdom, ²Physiology, University of Wisconsin-Madison, 1300 University Ave, Madison, Wisconsin, United States, ³Anatomy, University of Wisconsin-Madison, 1300 University Ave, Madison, Wisconsin, United States

Several calcium binding proteins, e.g. calbindin, calretinin and parvalbumin, have been proposed to function as calcium buffers in hair cells. Parvalbumin (PV) occurs in two forms: PV- α and PV- β (also known as oncomodulin). Recently, PV-3 (most similar to PV- β) has been identified in the bullfrog inner ear (Heller and Hudspeth, 2002: JARO 3, 488-498). Here we have used post-embedding immunogold labeling to determine their ultrastructural distribution in mammalian hair cells. Cochleas from young rats (up to 28 days old) were fixed in 4% paraformaldehyde and 0.1% glutaraldehyde in 0.1M sodium phosphate buffer (pH 7.4) for 2h. They were then embedded in LR-White resin. Ultrathin sections were cut from the apical turn onto nickel grids. The grids were incubated overnight at 4°C in polyclonal antibodies to calbindin (1:500, Chemicon), calretinin (1:500, Chemicon), PV- α (1:5000, SWant) and PV-3 (1: 5000, kindly provided by Dr. Heller) diluted in 1% bovine serum albumin (BSA) in 0.05M Tris buffered saline (TBS, pH 7.4), followed by goat anti-rabbit IgG-15 nm gold conjugate (1:20) in 1% BSA-TBS for 2 h at room temperature and examined using a JEOL 100-CX transmission electron microscope.

Immunogold labeling for calbindin and for both forms of parvalbumin, PV- α and PV-3 was found in both inner and outer hair cells with labeling occurring in the cytoplasm and the nuclei but not the

mitochondria. Labeling for calretinin was also present in both types of hair cell and showed a similar subcellular distribution to the calbindin and the parvalbumins. However, it was also found in supporting cells, particularly in the nuclei, suggesting it should not be regarded as a marker for hair cells. The concentration of each protein is now being estimated in hair cells from animals of different ages using the quantitative immunogold technique we developed for turtles (Hackney et al., 2003: J Neurosci 23, 4578-4589).

Supported by the Steenbock endowment and NIH RO1DC01362 (RF)

1029 *IN SILICO* MICROARRAY EXPRESSION ANALYSES AMONG SUBDISSECTED FRACTIONS OF THE ADULT MOUSE COCHLEA

Kenneth A. Morris¹, Einat Snir², Celine Pompeia³, Feng Feng¹, Irina V Koroleva², Bechara Kachar⁴, Piero Carninci⁵, Yoshihide Hayashizaki⁵, M. Bento Soares², Kirk W. Beisel¹

¹Biomedical Sciences, Creighton University, 2500 California Plaza, Omaha, NE, United States, ²Pediatrics-Genetics, Iowa University, 375 Newton Road - 4184 MERF, Iowa City, IA, United States, ³Section on Structural Cell Biology, NIH/NIDCD, Bldg 50/4249, Bethesda, MD, United States, ⁴Section on Structural Cell Biology, NIH/NIDCD, Bldg 50/4249, 50 South Drive, Bethesda, MD, United States, ⁵RIKEN Genomic Sciences Center, RIKEN Yokohama Institute, 1-7-22 Suehiro-cho Tsurumi-ku, Yokohama, Japan

The use of microarray technology to study the functional genomics of the inner ear has been limited by the lack of inner ear-pertinent microarrays and the difficulty in collecting sufficient amounts of total RNA for probe generation. We have developed a mouse inner ear-pertinent custom microarray chip (CMA-IE1) derived from the RIKEN subtracted inner ear set and the NIH organ of Corti library. We intend to use these methods to explore the functional genomics of pristine populations of inner ear-specific cell types, such as inner and outer hair cells, as well as for comparisons of normal versus dysfunctional cells and tissues. We are also working toward quantifying and increasing the sensitivity of the assays using novel techniques.

In order to test the validity of the chip and sensitivity of detection using amplified probe we compared the expression profiles among subdissected fraction of the cochlea (i.e., spiral ganglion (SG), organ of Corti (OC), and lateral wall (LW) and isolated hair cell populations. Total RNA samples were obtained from adult CF1 mice and two combined strategies were utilized to minimize the amount of total RNA required, which are to linearly amplify total RNA was using a T7-based protocol and to enhance the hybridization signal using a dendrimer-based strategy. Microarray experiments were performed using all possible combinations of the amplified RNA samples (e.g., OC vs. LW, OC vs. SG, and LW vs. SG). Approximately 20-25% of the genes on the array showed a positive signal above background. A number of differentially expressed genes were detected using modified t tests and other statistical methods. The percentage of differentially expressed genes varied depending on the comparison, confidence intervals, etc. Results were verified by (1) comparison to data present in the cur-

rent literature, (2) real-time quantitative PCR analysis, and (3) correlation to our knowledge of genes and gene families present in the various tissue types.

1030 Implantation of Neuroal Tissue into the Inner Ear – A Potential Clinical Implication for the Treatment of Inner Ear Disorders?

Petri Olivius¹, Zhengqing Hu², Christopher Regala², Leonid Alexandrov³, Elena Kozlova⁴, Mats Ulfendahl², Joe Miller⁵

¹*Clinical Neuroscience, Unit of Otorhinolaryngology, ENT department, Karolinska hospital, Stockholm, Sweden*, ²*Clinical Neuroscience, Unit of Otorhinolaryngology, Karolinska Institutet, Stockholm, Sweden*, ³*Russian Academy of Sciences, Institute of Higher Nervous Activity & Neurophysiology, Moscow, Russia, Russian Federation*, ⁴*Neuroscience, Neuroanatomy, Biomedical Center, Uppsala, Sweden*, ⁵*Ann Arbor, Kresge Hearing Research Institute, Michigan, Michigan, Mi, United States*

As the techniques and strategies of tissue engineering are increasing, allografting and xenografting in the human is receiving increased attention in many organ systems. In the dorsal root of the spinal cord it has been shown that implanted fetal dorsal root ganglion neurons (DRGs) can grow past the central-peripheral transitional zone and make functional contacts in the dorsal horn.

The poor regeneration capability of the sensory epithelium and neural components of the mammalian inner ear has initiated different approaches to enhance the functionality of these structures after injury. An interesting alternative is to use a biological implant with the potential to establish synaptic contacts with the cochlear spiral ganglion neurons and with the perspective to develop into a functional auditory unit.

We have in vivo implanted fetal DRG neurons and stem cells into the normal and deafened cochlea, adjacent to deafferented auditory spiral ganglion neurons. The DRG neurons were taken from transgenic animals expressing green fluorescence protein (GFP) or LacZ at embryonic days 13-14. The implants were transplanted into the scala tympani of adult rat inner ears. To enhance cell survival and possible neurite outgrowth, nerve growth factor (NGF) was perfused into the inner ear using a miniosmotic pump. The results show that transplanted DRG neurons survived for a postoperative survival time ranging from three to ten weeks, verified by GFP fluorescence, histochemical detection of LacZ and neuronal antibodies. The surviving DRG neurons were also observed within the Rosenthal's canal among the spiral ganglion neurons and their peripheral processes to the organ of Corti. NGF application stimulated extensive neurite outgrowth from the DRG neurons.

Our findings demonstrate the feasibility of using fetal sensory cells in a new strategy to repair or replace the auditory nerve. For example, in profoundly deaf patients, implanting neuronal tissue close to the auditory nerve could be used to regain auditory function.

1031 Embryonic neuronal co-grafts stimulate the neuronal integration of the embryonic stem cells into the adult mammalian auditory system

Zhengqing Hu¹, Daofeng Ni², Michael Andang³, Mats Ulfendahl¹

¹*Center for Hearing and Communication Research and Dept. of Clinical Neuroscience, Karolinska Institute, Karolinska Hospital Building M1:00, Stockholm, Sweden*, ²*Dept. of Otolaryngology, Peking Union Hospital, Chinese Academy of Medical Sciences, Peking Union Medical College Hospital, Beijing, China, People's Republic of*, ³*Department of Medical Biochemistry and Biophysics, Karolinska Institute, MBB, Solna, Karolinska Institute, Stockholm, Sweden*

To replace the damaged or absent cochlear sensory epithelium (organ of Corti) and its neural components, i.e. spiral ganglion neurons (SGN), cell replacement therapy strategies have been suggested. Embryonic stem cells (ESCs) offer an interesting alternative for the cell therapy. The embryonic microenvironment is considered to play important role in the stem cells differentiation. In order to provide an embryonic microenvironment and stimulate the neuronal differentiation of the ESCs in the inner ear embryonic dorsal root ganglion (DRG) were transplanted into the scala tympani of the adult guinea pig together with the implantation of ESCs expressing green fluorescent protein (GFP). Implanted ESCs survived in the scala tympani for a postoperative period of two and four weeks, as verified by the GFP fluorescence and immunohistochemical detection of a neuron marker, neural class III-tubulin (TUJ1) and glial cell marker, glial fibrillary acidic protein (GFAP). Transplanted ESCs were found close to the sensory epithelium as well as adjacent to the spiral ganglion and its peripheral dendritic processes. There is significant difference in the neuronal differentiation between the DRG co-graft and non-co-graft groups. In the DRG co-graft group large amount of ESCs were found to differentiate into neurons and generate axons towards the cochlear nerve fibers close to the organ of Corti. The axonal connections were also identified between the differentiated ESCs (TUJ1 positive) and the peripheral dendritic processes from SGNs. These results suggest not only the survival and neuronal integration of the ESCs in the adult inner ear but also the feasibility of a cell replacement strategy in the mature auditory system, thereby creating possibilities to replace the damaged cochlear sensory epithelium and its neural components in mammal.

1032 Regeneration of spiral ganglions by transplantation of embryonic stem cells of mice

Takayuki Nakagawa, Sakamoto Tatsunori, Endo Tsuyoshi, Tae-Soo Kim, Fukuichiro Iguchi, Shinji Takebayashi, Yasushi Naito, Juichi Ito

Otolaryngology, Head and Neck Surgery, Kyoto University, 54 Kawaharacho, Shogoin, Sakyo, Kyoto, Japan

Regeneration of spiral ganglions (SGs) is therefore an important issue as well as hair cell regeneration. Cell transplantation is becoming one of therapeutic strategies for neurodegenerative diseases. As a source for transplantation, cells with the ability for neu-

ral differentiation are required. PA6 cells (stromal cells derived from skull bone marrow) can induce highly efficient neural differentiation of embryonic stem (ES) cells when co-cultured with ES cells. This neural-inducing activity is named stromal-cell-derived inducing activity (SDIA). The aim of this study was thus to examine the possibility of SG regeneration by transplantation of ES cells treated with SDIA. Mouse ES cells treated with SDIA were injected into the modiolus of guinea pig cochleae deafened by pretreatment with kanamycin and ethacrynic acid. Sham-operated animals were received an injection of the medium containing no ES cells. Three weeks later, the electrically evoked auditory brainstem responses (eABRs) were recorded, and the temporal bones were collected and provided for histological analysis. Histological analysis revealed the survival of grafted ES cells in the modiolus. Immunohistochemical analyses revealed that about 90% of grafted cells differentiated into neural cells in the modiolus. In addition, expression of several neurotransmitters including tyrosine hydroxylase, GABA and glutamate was identified in grafted cells. The eABRs for sham-operated ears were not detected. In contrast, the eABRs for transplanted ears was detected, although their thresholds were higher than those of non-operated ears. These findings indicates the potential of transplantation of ES cells treated with SDIA for the restoration of SGs.

1033 Detection of Stem Cells Transplanted into the Cochlea by Fluorescent In Situ Hybridization

Mark Allen Parker^{1,2}, Brianna Gray¹, Adel Bakhtiarova¹, Evan Y. Snyder³, Luke Wall⁴, Richard P. Bobbin⁴, Douglas A. Cotanche^{1,2}

¹Otolaryngology, Children's Hospital, 300 Longwood Ave, FE9, Boston, MA, United States, ²Otology & Laryngology, Harvard Medical School, 300 Longwood Ave, FE9, Boston, MA, United States, ³Stem Cell & Regeneration Program, Burnham Institute, 10901 North Torrey Pines Road, La Jolla, CA, United States, ⁴Kresge Hearing Research Laboratory, LSU Health Sciences Center, 533 Bolivar Street, 5th Floor, New Orleans, LA, United States

In an effort to facilitate organ repair, we have injected neural stem cells into the sound damaged cochleas of guinea pigs. A significant problem in transplantation studies is the identification of the exogenous cells within the cochlea. The most commonly used methods of detection are to transplant cells that have been engineered to express either enhanced green fluorescent protein (EGFP) or beta-galactosidase (beta-Gal). However, there are limitations to these approaches. Here we show that there is a decrease in both EGFP fluorescence and beta-Gal enzymatic activity in neural stem cells after transplantation. Furthermore, the use of antibodies directed to the EGFP and beta-Gal constructs provides only limited detection of the transplanted cells. The most robust detection of exogenous stem cells was obtained by Fluorescence In Situ Hybridization (FISH) to the sex chromosomes of the transplanted XY cells which are distinguished from the endogenous XX cells of the host. We propose that FISH technique is a reliable and sensitive means of identification of the endogenous stem cells within the cochlea. Supported by a NOHR Hair Cell Regeneration Initiative Grant and NIH/NIDCD Grant #F32 DC005866.

1034 Replacement of Auditory Ganglion Neurons with Embryonic Stem Cell-Derived Sensory Neurons

Carleton Eduardo Corrales¹, Huawei Li¹, Jessica R Risner², Jeffrey R Holt², Stefan Heller¹

¹EPL - Dept. of Otolaryngology, Mass Eye & Ear Infirmary / Harvard Medical School, EPL - MEEI, 243 Charles Street, Boston, MA, United States, ²Depts. of Neuroscience and Otolaryngology, University of Virginia, Lane Rd. MR4, Charlottesville, VA, United States

Hair cell loss and degeneration of spiral ganglion neurons are significant problems for many patients suffering from hearing loss. We are focusing on replacing auditory ganglion neurons with a population of embryonic stem cell-derived neurons. We have developed a technique that allows us to select for a neural progenitor cell population that can be induced to differentiate into neurons that display immunological features of sensory neurons that are shared with auditory ganglion neurons. Furthermore, electrophysiological assays revealed that the differentiated cells have properties typical of auditory neurons including, expression of voltage-dependent Na⁺ and K⁺ currents and the ability to fire action potentials.

We hypothesize that these stem cell-derived sensory neurons, when transplanted into the damaged spiral ganglion, will integrate and grow neurites, and that through local environmental cues will be attracted to form synaptic contacts with hair cells. Our experimental setup is based on an organotypic culture system of the embryonic chicken basilar papilla. We applied β -Bungarotoxin (β -BT) in ovo at 3-day internals beginning on the 4th day of embryonic development which causes acoustico-vestibular ganglion cells to degenerate, while allowing all other inner ear cell types, including hair cells, to remain intact. We grafted murine embryonic stem cell-derived sensory neuron progenitors into β -BT denervated basilar papilla explants and maintained the organs in a 3-dimensional matrix culture system. Murine cells were traced using the transgenic marker gene lacZ. Our preliminary results suggest that the grafted neuronal progenitors survived in our 3-dimensional culture system and that, depending on the nature of the matrix, the differentiating neurons were able to send neurites towards the denervated organs' sensory epithelia.

1035 Cell Fusion in Xenotransplantation of Mouse Stem Cell-Derivatives into Chicken Hosts

Karen F Watters, Huawei Li, Carleton Eduardo Corrales, Stefan Heller

EPL - Dept. of Otolaryngology, Mass Eye & Ear Infirmary / Harvard Medical School, EPL - MEEI, 243 Charles Street, Boston, MA, United States

Transplantation of stem cell-derived progenitor cells to develop treatment strategies for hair cell or neuron degeneration in the inner ear is an exciting new avenue for regenerative medicine. It is desirable that grafted cells operate in a highly predictable fashion, which means that these cells should integrate at the desired place and fully differentiate into the desired cell type(s). One undesired fate of a grafted cell would be to simply fuse with cells of the host organism. We tested whether cell fusion occurs between adult

murine inner ear stem cell-derived progenitor cells and chicken embryonic inner ear host cells. Our experimental setup uses inner ear stem cells isolated from Math-1/nGFP mice that express enhanced green fluorescent protein under the control of an enhancer from the mouse *Atoh 1* gene, which encodes the transcription factor Math-1. We grafted mouse utricular stem cell-derived spheres into stage 15-17 chicken otic vesicles and we maintained the vesicles in vitro for four-seven days. Murine cells were identified with specific chromosomal probes; differentiating murine hair cells additionally displayed green fluorescent protein. Cells with these features were distinguishable from chicken hair cells that were specifically labeled with monoclonal antibodies to chicken hair cell antigen. To confirm hair cell identity, we additionally used antibodies to myosin VIIA and espin. Our early assessment of cell fusion corroborates the general view that fusion of stem cell-derived grafts with host cells is a rare event.

1036 Surgical techniques for cell transplantation into the mouse cochlea

Fukuichiro Iguchi¹, Takayuki Nakagawa¹, Ichiro Tateya², Tsuyoshi Endo¹, Tae-Soo Kim¹, Youyi Dong³, Tomoko Kita^{1,4}, Yasushi Naito¹, Juichi Ito¹

¹Department of Otolaryngology, Head and Neck Surgery, Kyoto University, 54 Kawahara-cho, Shogoin Sakyo-ku, Kyoto, Japan,

²Department of Surgery, Division of Otolaryngology Head and Neck Surgery, University of Wisconsin medical school, K4/789 Clinical Science Center, 600 Highland Avenue, Madison,

Wisconsin, United States, ³Department of Cell Physiology, Kagawa Medical University, 1750-1 Ikenobe, Miki-cho, Kida-Gun, Japan, ⁴Horizontal Medical Research Organization, Kyoto University, 54 Kawahara-cho, Shogoin Sakyo-ku, Kyoto, Japan

Recently, a number of studies on stem cells have been performed for regeneration of various organs including the inner ear. To utilize cell therapy for inner ear diseases, adequate donor cells and technique for transplantation into the inner ear are required. The aim of this study was to establish surgical procedures for cell transplantation into the mouse inner ear.

C57BL/6 mice were used as recipient animals. Fetal mouse neural stem cells expressing green fluorescence were used as donor cells. Two methods, an injection of transplants from the lateral semicircular canal (LSCC) and from the cochlear lateral wall (CLW) were examined. For the approach to the LSCC (LSCC method), small holes were made in LSCC and posterior semicircular canal. A glass needle was inserted into the LSCC. The cell suspension was injected using an infusion pump. Then, the holes in the semicircular canals were plugged with connective tissue and covered with an adhesive agent. As for the approach to the CLW (CLW method), the otic bulla was opened to expose the second turn of the cochlea. A small hole was then made to access to the scala media through the stria vascularis of the cochlear second turn. Two weeks after transplantation, the distribution of transplant-derived cells in the cochlea was examined. Effects on auditory function were assessed by measurements of auditory brain stem responses (ABR).

By LSCC method, transplant-derived cells mainly survived in the scala vestibuli and scala tympani. LSCC method caused elevation of ABR thresholds less than 10 dB SPL. On the other hand, CLW method resulted in considerable hearing loss, although transplant-derived cells settled in the scala media.

These findings demonstrate that LSCC method can be utilized for cell transplantation into the perilymph without apparent auditory disorder, and that CLW method enables delivery of cells in the endolymph despite of auditory dysfunction.

1037 Adult Stem Progenitor Cells in the Mouse and Guinea Pig Cochlea

Carrie R Fleming, Hong-Bo Zhao

Dept. of Surgery - Otolaryngology, University of Kentucky Medical Center, 800 Rose Street, Lexington, KY, United States

The mammalian cochlear sensory epithelium contains terminally differentiated hair cells and supporting cells and has no mitotic activity after birth. Hair cell degeneration can not be repaired and is a major cause of hearing loss. Recent stem cell research revealed that stem progenitor cells still exist in many adult tissues and can proliferate and differentiate both in vivo and in vitro under certain conditions. We have hypothesized that the adult mammalian cochlea may contain dormant stem progenitor cells, which can be stimulated to proliferate and differentiate in culture. In our previous studies, we have demonstrated that some cochlear cells derived from the organ of Corti of adult guinea pigs possess a stem cell phenotype – sphere colony with ability to differentiate and proliferate in culture. In this experiment, dissociated mouse cochlear cells were cultivated using the cell culture technique that we developed to culture guinea pig cochlear cells. Mouse cochlear cells could proliferate to form spherical colonies (cochleospheres) in culture, which could float in medium. Differentiation tests showed that these sphere-forming cells could differentiate into hair cell genotypes, neurons and other cell phenotypes. Single cell sub-cloning also showed that the sphere colony could be regenerated after the cochleosphere was dissociated. These data support our conception that stem progenitor cells exist in the mammalian cochlea and can proliferate and differentiate in culture.

Supported by UK Research Foundation.

1038 Analyses of otic inducing signals on ES cell differentiation

Tatsunori Sakamoto^{1,2}, Raj Ladher³, Yoshiki Sasai², Juichi Ito¹

¹Department of Otolaryngology, Kyoto University, 54, Shogoin-Kawahara-Cho, Sakyo-ku, Kyoto, Japan, ²Organogenesis and neurogenesis, RIKEN Center for Developmental Biology, 2-2-3, Minatojima Minami-Machi, Chuou-ku, Kobe, Japan, ³Lab for Sensory Development, RIKEN Center for Developmental Biology, 2-2-3, Minatojima Minami-Machi, Chuou-ku, Kobe, Japan

Increasing knowledge in developmental biology and progress in stem cell technology have prompted further investigation to restore hearing by hair cell regeneration. For this purpose, generation of suitable graft cells are indispensable. Embryonic stem cells (ES cells) are totipotent stem cells. Many attempts have been made to induce effective differentiation of ES cells into specific cell types including blood cells, islet cells of pancreas, neurons, glia, epidermal cells, neural crest derivatives and so on. Recently reported SDIA method (Kawasaki et al., Neuron, 2000) effectively induce neural differentiation from ES cells, and addition of BMP-4 brings them into epidermal fate, recapitulating in vivo role of BMP-4. Mizuseki et al. reported that addition of BMP-4 in later differenti-

ation days produced multiple types of neural crest cells including sensory neurons and smooth muscle cells. Inner ears are derived from otic placodes which first appear between neural tissue and epidermis, just lateral to neural crest. Thus, placodes are also expected to be induced together with neural crest cells from ES cells. Otic induction also require underlying mesoderm and adjacent neural tissue. Ladher et al. reported that otic induction by those tissue are mainly exerted by FGF19 and Wnt8c in chickens. In mice, Fgf3/Fgf10 double knockout mice fail to form proper otic anlage. In this report, the effects of those molecular players on ES cell differentiation are discussed.

1039 Manipulation of Human Embryonic Stem Cells and the generation of inner ear cell types.

Marcelo N. Rivolta, Duncan Liew, Matthew C. Holley, Paul Gokhale, Peter W Andrews

Biomedical Sciences, University of Sheffield, Western Bank, Sheffield, United Kingdom

A potential therapeutic approach to the loss of sensory cells in many forms of neurosensory deafness is to replace the lost cells by transplantation of exogenous, in vitro-maintained stem cells with the potential to generate the different inner ear cell types. Embryonic Stem (ES) cells are pluripotent cell lines derived from the inner cell mass of normal blastocysts and, in theory, an excellent source of mature ear cell types. Highly valuable information is being obtained from animal models (Li et al, ARO 2003 #806), but no data is yet available from a human system. Human data is particularly important because there are significant differences between the basic ES biology of human and mouse systems. For instance, the surface antigens SSEA-3 and SSEA-4 are expressed by human but not mouse ES cells, while SSEA-1 is expressed by mouse but not human ES cells. More important is the dependence of undifferentiated mouse ES cells on leukemia inhibitory factor (LIF). Human ES cells do not require LIF but need to grow on feeder layers. The first human ES cell (hES) lines were originally established by Thomson et al. (Science 282:1145-7, 1998). They can be grown over mouse embryonic fibroblasts (MEF) feeder layers to maintain their undifferentiated status, and then allowed to differentiate into derivatives of the three germ layers. We are exploring the potential of hES to produce otic phenotypes by manipulating their cultured environment. hES cells were maintained in an undifferentiated state by propagation in culture on a feeder layer of MEFs. To allow differentiation, hES colonies were disaggregated and allowed to form embryoid bodies (EBs) in suspension culture. EBs were then plated on gelatinized tissue culture plate for 2 weeks in the presence of either serum or different growth factors. In initial experiments we have detected the induction of markers such as PAX8 and pendrin in the differentiated cell population when compared to the undifferentiated one. These results are compatible with the generation of otic precursors from undifferentiated hES cells.

1040 Neural Differentiation and Lineage Specification from Adult Bone Marrow-Derived Stem Cells

Takako Kondo¹, Heather L Aloor¹, Raymond Romand², Eri Hashino¹

¹*Otolaryngology-HNS, Indiana University School of Medicine, 699 West Drive, RR132, Indianapolis, IN, United States*, ²*Institut de Biologie Moleculaire et Cellulaire, INSERM, BP 10142, Strasbourg, France*

Bone marrow stromal cells (MSCs), also called mesenchymal stem cells, are multi potent stem cells and normally give rise to mesenchymal derivatives such as chondrocytes, osteoblasts and adipocytes. MSCs were originally thought to be limited in their capacity for differentiation, but recent reports of their differentiation into muscle, glial and neural lineages has challenged this notion. To test the ability of MSCs to differentiate into inner ear sensory neurons, we applied neural induction signals in vitro to MSCs that were isolated from the femurs and tibias of adult mice. Within 48 hours after application of beta-mercaptoethanol and FGF2, over 70-80% of cultured MSCs exhibited dramatic changes in cell shape, from a flat mesenchymal cell shape to a round cell body. In addition, the number of BrdU-positive cells decreased dramatically after neural induction, suggesting that the majority of the stimulated MSCs were withdrawn from the cell cycle. These post-mitotic cells were positively labeled with several neuronal markers, including Islet1, Nse and Tau. Quantitative RT-PCR analysis substantiated these immunohistochemical data, by showing that SCG10, Tau and nse mRNA levels in MSC derived cells increased 5-, 8- and 10-fold, respectively, after neural induction. In contrast, mRNA expression of the majority of inner ear-specific transcription factors or vestibulocochlear neuron-specific genes remained undetectable or unchanged after neural induction. However, application of BDNF to stimulated MSCs substantially increased the expression levels of TrkB and Gbx2 mRNAs. These results suggest that lineage-specific neurons can be generated from adult MSCs and that secreted signaling proteins may play important roles in neuronal-lineage specification of marrow-derived stem cells. Further in vitro and in vivo characterization of MSCs would provide critical information for establishing an autologous stem cell therapy in the inner ear.

Supported by NIH R21DC005507

1041 Gene Expression Patterns and Distribution of Neurotrophic Factors in the Cochlea of Deafened Rats

Kirsten Wissel, Patrick Wefstaedt, Heike Rieger, Timo Stoeber

Dept. of Otolaryngology, Medical University of Hannover, Carl-Neuberg-Str. 1, Hannover, Germany

Hearing impairment is the most frequent disability of people in industrial countries and is often caused by destruction of the sensory cells within the cochlea. Furthermore loss of sensory cells lead to degeneration of the spiral ganglion cells (SGC). It has been shown that growth factors, especially members of the TGF- β superfamily, play key roles in protection of SGC and enhance the functional excitability of the auditory nerve fibers after drug- and

noise-induced trauma. The RNA expression of all glial cell line-derived neurotrophic factor (GDNF)-subfamily members and their corresponding receptors in cochlea-subfractions of rats was recently demonstrated suggesting potential functional importance of these neurotrophic factors (NTF) for protection of the sensory cells. The aim of the present study is to investigate which NTF and NTF-receptors are differentially expressed in the Modiolus (Mo) and colliculus inferior (IC) of deafened in comparison to non-treated rats. Adult rats (350 g) were deafened by local inner ear-injection of 10% neomycin and sacrificed after 26 days. RNA and cellular proteins were extracted from Mo and IC of normal and deafened rats. The tissue specific gene expression of GDNF, persephin, artemin and neurturin, their corresponding receptors GFRa1, GFRa2, GFRa3, GFRa4 and Ret, the brain-derived neurotrophic factor (BDNF) and its tyrosine kinase-receptor subtypes TrkA, TrkB and TrkC, as well the fibroblast growth factor 1 (FGF 1) were determined by semiquantitative RT-PCR. The corresponding protein expression in both tissue subfractions was verified by Western blotting. The results give a more close insight to expression patterns of NTF and their signal pathways in affected cochlea tissues and thus a better understanding in deafness induced changes in the inner ear.

1042 Overexpression of Fibroblast Growth Factor (FGF2) in the Adult Mouse Promotes Synaptic Survival in the Cochlear Nucleus (CN) Following Acoustic Overstimulation by Upregulating FGFR1 and NT3

Chrystal S. D'Sa¹, Julie S. Gross¹, Marja M. Hurley², D. Kent Morest¹

¹Dept. of Neuroscience, University of Connecticut Health Center, 263 Farmington Avenue, Farmington, CT, United States, ²Dept. of Medicine, University of Connecticut Health Center, 263 Farmington Avenue, Farmington, CT, United States

FGF2 has been implicated in synapse formation and innervation in the developing mouse CN. This role involves its interaction with BDNF and NT3. Our previous experiments on the effects of acoustic stimulation in mice where the FGF2 gene has been over-expressed showed a reduced amount of synaptic degeneration 7 days following noise damage compared to the levels seen in wild type mice exposed to noise. This led us to study the possible mechanism by which the excess of FGF2 in the overexpressor mice might promote the survival of synapses in the CN. In our present studies we observed the expression of FGFR1, the high affinity receptor of FGF2 and of NT3 in the FGF2 overexpressor mice, 3 days and 7 days following noise damage and compared the staining to the appropriate controls. In the overexpressor mouse before noise exposure, the levels of FGFR1 and NT3 in the CN were lower than in the wild type unexposed mouse. The expression of FGFR1 increased 3 days following noise exposure and was seen mainly in the processes of astrocytes and neurons. At 7 days following noise exposure, the expression shifted and was seen mainly in neuronal cell bodies. NT3 expression that appeared to be mainly in the neuronal processes increased 3 days following noise exposure and declined to control levels within 7 days. This shift in the level of expression of FGFR1 and NT3 was not seen in the corresponding wild type controls following noise damage. The present results indicate that the overexpressor mice up regulate FGFR1

and NT3 at the synapses 3 days after noise damage, followed by a shift in the FGFR1 expression to neurons. Interaction between the axonal endings and their surrounding glial processes may regulate FGFR1 as part of the mechanism by which FGF2 may protect synapses from acoustic overstimulation. Supported by NIH grants.

1043 Sensory Organ-specific Alternative Splicing of Clarin-1 mRNA in the Murine Cochlea and Retina.

Christy Rothermund, Randall Fields, Dominic Cosgrove
National Usher Syndrome Center, Boystown National Research Hospital, 555 No 30th St, Omaha, Nebraska, United States

Usher syndrome type 3 (USH3) is an autosomal recessive disorder associated with progressive hearing loss, vision loss due to retinitis pigmentosa (RP), and vestibular dysfunction. The USH3 transcript was recently identified as encoding a four-transmembrane protein and named clarin-1. The protein product is novel, with no previously ascribed functions. We developed antibodies against clarin-1, which localize the protein to the spiral limbus and the tension fibroblasts of the murine cochlea, and the retinal pigment epithelial cell layer of the murine retina. Cochlear localization appears to be primarily in acellular matrix-rich structures, while retinal localization appears closely associated with the retinal pigment epithelial cell layer. Earlier work from this laboratory suggested the existence of different isoforms of clarin-1 resulting from alternative splicing during mRNA processing. In this report, we extend these earlier findings. Expression of clarin-1 mRNA isoforms-specific mRNAs was examined in RNA preparations from newborn cochlea and retina. Multiple isoforms resulting from alternative splicing of primary clarin-1 RNA were observed, and some of these were distinct for the two sensory organs. Differential expression of isoforms-specific clarin-1 mRNA in cochlea versus retina suggests the existence of functionally distinct isoforms of the protein. Antibodies are currently under development aimed at testing this hypothesis.

1044 Isolation from cochlea of a novel human intronless gene with predominant fetal expression

Barbara Resendes¹, Sharon Kuo^{1,2}, Nancy Robertson¹, Anne Giersch^{1,3}, Dynio Dynio Honrubia^{3,4}, Osamu Osamu Ohara^{5,6}, Joe Adams^{7,8}, Cynthia Morton^{1,9}

¹Pathology, Brigham and Women's Hospital, HMS/NRB Rm 160, 77 Avenue Louise Pasteur, Boston, MA, United States, ²HST-SHBT, Harvard-MIT, E25-519, 77 Massachusetts Ave, Cambridge, MA, United States, ³Pathology, Harvard Medical School, 25 Shattuck Street, Boston, MA, United States, ⁴Department of Neonatal Care, Children's Hospital, 300 Longwood Avenue, Boston, MA, United States, ⁵Human Gene Research, Kazusa DNA Research Institute, 2-6-7 Kazusa-kamatari, Kisarazu, Japan, ⁶RIKEN Research Center for Allergy and Immunology, Laboratory of Immunogenomics, 1-7-22 Suehiro-cho, Tsurumi-ku, Yokohama, Japan, ⁷Dept. of Otolaryngology, Harvard Medical School, 243 Charles St., Boston, MA, United States, ⁸Eaton-Peabody Laboratory, 6Massachusetts Eye and Ear Infirmary, 243 Charles St., Boston, MA, United States, ⁹Departments of Obstetrics, Gynecology and Reproductive Biology, Brigham and Women's Hospital, 75 Fansics St., Boston, MA, United States

ABSTRACT

We have cloned a novel human gene, designated *PFET1* (predominantly fetal expressed T1 domain) (HUGO approved symbol *C13orf2*), by subtractive hybridization and differential screening of human fetal cochlear cDNA clones. Also, we have identified the mouse homolog, designated *Pfet1*. *PFET1/Pfet1* encode a single transcript of approximately 6 kb in human, and three transcripts of approximately 4, 4.5 and 6 kb in mouse with a 70% GC-rich open reading frame (ORF) consisting of 978 bp in human and 984 bp in mouse. Both genes have unusually long 3' untranslated (3' UTR) regions (4996 bp in human *PFET1*, 3700 bp in mouse *Pfet1*) containing 12 and five putative polyadenylation consensus sequences, respectively. Pfetin, the protein encoded by *PFET1/Pfet1*, is predicted to have 325 amino acids in human and 327 amino acids in mouse and to contain a voltage-gated potassium (K⁺) channel tetramerization (T1) domain. Otherwise, to date these genes have no significant homology to any known gene. *PFET1* maps to the long arm of human chromosome 13, in band q21 as shown by FISH analysis and STS mapping. *Pfet1* maps to mouse chromosome 14 near the markers D14Mit8, D14Mit93 and D14Mit145.1. The human 6 kb transcript is present in a variety of fetal organs, with highest expression levels in the cochlea and brain and in stark contrast, is detected only at extremely low levels in adult organs, such as brain and lung. Immunohistochemistry with a polyclonal antibody raised against a synthetic peptide to *PFET1* sequence (pfetin) reveals immunostaining in a variety of cell types in human, monkey, mouse, and guinea pig cochleas and the vestibular system, including type I vestibular hair cells.

1045 Promotor Analysis And Expression Of The Protocadherin 15 Gene In Mice.

Darrell Pitts¹, Nithin Adappa², Kumar Alagramam¹

¹Otolaryngology-HNS, University Hospitals of Cleveland, Case Western Reserve University, 11100 Euclid Avenue, Cleveland, OH, United States, ²Otolaryngology-HNS, Case Western Reserve School of Medicine, 11100 Euclid Avenue, Cleveland, OH, United States

Gene discovery in the mouse facilitated the identification of the human PCDH15 gene. Pcdh15 serves an important role in the auditory and vestibular development in mice. In humans, mutation in PCDH15 causes inner ear dysfunction and/or retinal degeneration. Understanding the biological function of Pcdh15 in the mouse will shed light on the molecular pathogenesis leading to sensory deficits in usher 1F patients. To understand the function of Pcdh15 in the development of the ear and the eye, it is important to understand how the expression of Pcdh15 is regulated in these organs. Vital to this effort is the need to identify DNA sequence that controls the temporal and spatial expression of Pcdh15. The elements (core promoter, enhancer, etc) that control Pcdh15 expression remain to be identified. Another potential source of regulation is alternative splicing, a process that could produce organ specific transcripts. Mutations in alternatively spliced products has been associated with different disease states in humans, such as syndromic versus nonsyndromic. RT-PCR analysis suggests that Pcdh15 is regulated at the level of transcription. Pcdh15 is expressed in the mouse brain, ear, and eye while absent in the liver, lung, and kidney. RT-PCR analysis demonstrated that Pcdh15 is expressed as early as P0 and is persistent at P70 in the mouse retina. Also shown is that Pcdh15 is expressed in otocyst at E12.5,

suggesting that Pcdh15 may play a role in early stages of inner ear development. Alternative splicing was also found in the transcripts of Pcdh15. Exon 4 was found to be absent in one transcript and exons 2 and 4 were found to be missing in another. Another splice variant was demonstrated in exon 34 where a 30bp deletion was found at near the 5' end of the exon. To test for promoter regulatory elements, in silico analysis was performed on the 5' upstream region of and including exon 1. Three areas were predicted to contain promoter elements in a 10kb region including exon 1: one area was predicted within exon 1, a second 4kb upstream of exon 1, and a third predicted 8.9kb upstream of exon 1. Fragments of the 10kb region and several smaller fragments within the 10kb region were generated by long-range PCR and cloned into the pBlue vector upstream of a lacZ reporter gene. These constructs are currently being tested in mouse 3T3-L1 fibroblast cells. Data obtained thus far suggest that the regulation of Pcdh15 expression is complex and more data is required before we can correlate expression and function of this gene. Additional experiments are underway and data obtained from these work will be presented at the meeting. Work supported by NIH-NIDCD grant to KNA.

1046 Comparative analysis of mouse and human prestin promoter fragments.

Thomas Weber¹, Juergen-Theodor Fraenzer¹, Jian Zuo², Marlies Knipper¹

¹Molecular Neurobiology, Tuebingen Hearing Research Center, Elfriede-Aulhornstr.5, Tuebingen, Germany, ²Department of Developmental Neurobiology, St. Jude Children's Research Hospital, 332 N. Lauderdale St., Memphis, TN, United States

The expression of the motor protein prestin (SLC26A5) is restricted to the outer hair cells of the Organ of Corti. Expression of prestin has not been observed in other structures and tissues within the cochlea including the non-motile inner hair cells indicating a very strict regulation of the gene. Our aim is to find the genomic regions that form the prestin promoter and to learn more about the regulation of the gene. We have recently demonstrated that a minimal promoter containing the start site of transcription resides within the untranslated exon I of the human prestin gene (Weber et al., Assoc Res Otolaryngol. 26, abstract 513). Promoter activity has also been reported for a 9-kb genomic fragment including exon III and part of intron III of the mouse prestin gene (Mingyuan Li et al. Assoc Res Otolaryngol. 26, abstract 605). In this study we cloned several genomic fragments of the prestin upstream-region from both the human and mouse prestin gene. We compared these fragments for their respective promoter strength using luciferase reporter gene assays, and analysed putative cis-elements for their interaction with HeLa-scribe nuclear extract using electrophoretic mobility shift assays (EMSA).

This work was supported by a grant from the Federal Ministry of Education and Research (Fö. 01KS9602) and the Interdisciplinary Center of Clinical Research Tübingen (IZKF).

1047 Expression of 72 kDa and 92 kDa type IV collagenases (gelatinase A/ MMP-2 and gelatinase B/ MMP-9) in mouse stria: implications for Alport inner ear pathogenesis

Velidi H. Rao¹, Daniel T Meehan¹, Dominic E. Cosgrove¹, Michael Anne Gratton²

¹Division for Therapeutic Strategy Development, Boys Town National Research Hospital, 555 N. 30th St, Omaha, NE, United States, ²Otorhinolaryngology-HNS, University of Pennsylvania, 3400 Spruce St, Philadelphia, PA, United States

Alport syndrome is a group of genetic disorders from mutations in $\alpha 3(\text{IV})$, $\alpha 4(\text{IV})$ or $\alpha 5(\text{IV})$ collagen. This disease is characterized by a progressive glomerulonephritis, usually a high frequency sensorineural hearing loss, and ocular abnormalities. The mouse model of Alport syndrome has all the hallmarks of human disease. Defects in the collagen IV gene in the Alport mouse result in thickened stria capillary basement membranes.

Basement membrane thickening can result from modulation of synthesis and/or degradation of matrix proteins by matrix metalloproteinases (MMPs). The MMPs constitute a family of structurally and functionally related endopeptidases, which collectively degrade components of extracellular matrix. They are implicated in connective tissue remodeling processes associated with embryonic development, pregnancy, growth, and wound repair. We have previously demonstrated that the thickened stria capillary basement membrane in Alport syndrome contain elevated levels of collagen IV and entactin. Thus, in this study we examined stria samples from 9 week-old normal and Alport mice for MMP-2 and MMP-9. Gelatin zymography and real-time PCR were employed to investigate the expression of type IV collagenase (MMP-2 and MMP-9) activity and mRNA, respectively.

Gelatin zymography of Alport stria showed lytic bands at Mr 92000 (MMP-9) and 72000 (MMP-2). In contrast, control stria contained only MMP-2. EDTA, a well-known inhibitor of the MMPs, inhibited these enzyme activities. We confirmed these results by real-time PCR for MMP-2 and MMP-9 using specific probes and primers. The results from our study identify for the first time that MMP-2 and MMP-9 are significantly elevated at the protein and mRNA levels in isolated stria from Alport mice. These findings suggest that altered matrix metabolism may play an important role in basement membrane accumulation in stria capillaries in the Alport mouse.

1048 Construction, Characterization, and Interrogation of a Microarray Specific to Healing Fetal Wounds

Sandeep Kathju, Duane Oswald, Mandal Singh, Geza Erdos, J. Christopher Post, Garth D. Ehrlich

Center for Genomic Sciences, Allegheny General Hospital, 320 E North Ave., Pittsburgh, PA, United States

Adult mammalian tissues heal injury with scar formation. Although useful in sealing an injured area, scar can itself be a source of significant morbidity, interfering with respiration, hearing, speech, restricting movement, etc. In contrast, mammalian fetal tissue can heal without scar. We have undertaken to

construct, characterize, and screen a microarray from a complementary DNA (cDNA) library specifically encompassing the expressome of a healing fetal wound.

Incisional wounds were made on New Zealand white fetal rabbits at gestational age 20 days. Twelve hours post-injury the wounds were excised and total RNA was isolated. An amplified cDNA library of some 7200 clones was constructed; this library was then normalized to remove over-represented sequences, yielding some 6200+ clones. These cloned cDNA inserts were then gridded as a microarray on glass slides and hybridized to cDNA probes from multiple tissue types.

A preliminary analysis of the library by randomly sequencing 148 gridded subclones (amounting to approximately 2% of the library) reveals that over 60% of the cloned inserts correspond to unique messages; some 25% identify as expressed sequence tags of unknown function or have no clear match in the GenBank database, potentially representing novel gene products. Interrogation of our microarrays with fetal control (unwounded), adult control (unwounded), and fetal liver tissues demonstrates substantially different patterns of gene expression among these disparate tissue types compared to the fetal wound tissue whence the microarray derives. Multiple differentially expressed gene products have been identified.

We have built and successfully utilized a microarray specific to healing fetal wounds to elucidate differential gene expression during scarless fetal wound healing. Use of this technological approach allows simultaneous assay of a large number of physiologically relevant genes without need for a priori sequence knowledge.

1049 Developmental Expression Profile changes of the Organ of Corti from Deaf Mouse Mutants

Jiewu Yang¹, Rachel Hardisty¹, Anabl Varela¹, Nick Parkinson¹, John William¹, Clare Pritchard², Peter Underhill², Helen Hilton², Joanna Madge¹, Sue Morse¹, Philomena Mburu¹, Alisoun H. Carey³, Helene Jones³, Bento Soares⁴, Steve D.M. Brown¹

¹MGC and MGU, MRC Harwell, Harwell, Didcot, United Kingdom,

²Microarray group, MRC Harwell, Harwell, Didcot, United Kingdom,

³Oxagen Ltd, Oxagen Ltd, 91 Milton park, Abingdon, United Kingdom, ⁴Pediatrics-Genetics, University of Iowa, 4184 Newton Rd, Iowa city, Iowa, United States

We have used cDNA microarrays to explore gene expression profile changes accompanying the development of the sensory neuroepithelium, the organ of Corti (OC), in the inner ear of deaf mouse mutations at P1 and P3, which is one of the crucial periods for sensory hair cell differentiation. Of 6700 random genes arrayed from a normalised newborn mouse inner ear (NMIE) cDNA library, we found the expression level of 364 genes increased 2 fold or more and 90 genes decreased at least 2 fold during normal OC development from P1 to P3. In comparison, the OC of the whirler mice, a mutant that shows abnormal elongation and development of stereocilia, shows 184 genes increased and 219 decreased between P1 and P3.

The developmental expression pattern of several clusters of genes in the mutant OC does not follow that of wild type (wt). 29 genes,

whose expression level increased significantly between P1 and P3 in wt OC, decreased dramatically in the mutant OC over the same period. 17 genes which did not show a significant increase in wt OC, decreased significantly in mutant OC from P1 to P3. There are 15 genes whose expression increased significantly in mutant OC, but were unchanged in the wt OC. We have also found a group of 10 genes whose expression decreased significantly during wt OC development, but did not change significantly in mutant OC development. These genes represent molecules with potential involvement in stereocilia development that will be investigated further.

1050 Generating a Cre Expressing Line in Hair Cells with a Modified Prestin BAC

Yong Tian, Jian Zuo

Dept. Developmental Neurobiology, St Jude Children's Research Hospital, 332 N Lauderdale, Memphis, TN, United States

Hair-cell specific gene targeting is necessary for the determination of the function of many genes in hair cells of the inner ear. The Cre/loxP system has been used successfully for cell-type specific gene targeting in other tissues including the nervous system. In this study, we hope to create mouse lines in which Cre activity is specifically expressed in hair cells of the inner ear.

We modified the prestin BAC by inserting IRES-Cre after the stop codon of prestin. We injected the modified BAC into the pronuclei of FVB/NJ and screened the pups with primers covering Cre and BAC vector. One founder was obtained and subsequently crossed with a reporter line ROSA26. Pups were then screened with Cre and LacZ using PCR. PCR flanking the two LoxP sites upstream of the LacZ reporter showed that Cre activity was only detected in testis and cochlea starting at approximately P7, similar to the expression of prestin in vivo. Characterization using β -gal immunohistochemistry shows Cre activity is mainly located in the inner and outer hair cells and a subset of spiral ganglia, but not in vestibular hair cells. This Cre line provides a valuable tool for analysis of gene functions in hair cells.

This work is supported in part by NIH grants to J.Z. (DC04761, DC05168), NIH Cancer Center Support CORE grant CA21765, and the American Lebanese Syrian Associated Charities (ALSAC).

1051 Towards Macaque Models For Connexin 26 Hearing Loss and Usher Syndrome

Dana J Orten¹, Amy M Hemje¹, Vanessa A Vogltanz¹, Carol A Carney¹, Martha Neuringer², Leslie A Lyons³, Stacy E Waltz⁴, Joseph W Kemnitz⁵, William J Kimberling¹

¹Genetics, Boystown National Research Hospital, 555 N. 30th St., Omaha, NE, United States, ²Medicine & Ophthalmology, Oregon National Primate Research Center, 505 NW 185th Avenue, Beaverton, OR, United States, ³Population Health & Reproduction, California National Primate Research Center, 1114 Tupper Hall, Davis, CA, United States, ⁴Clinical Pathology Laboratory, Wisconsin National Primate Research Center, 1220 Capitol Court, Madison, WI, United States, ⁵Physiology, Wisconsin National Primate Research Center, 1220 Capitol Court, Madison, WI, United States

Mutations in connexin 26 (GJB2) cause 10-20% of childhood

hearing loss in Americans and Europeans. Usher syndrome, a recessive disorder characterized by retinitis pigmentosa and sensorineural hearing loss, is the leading cause of combined hearing and vision loss in the industrialized world, affecting 25,000-30,000 people in the United States. Our objective is to create macaque models of the most prevalent Usher Syndrome (USH2A) and recessive hearing loss (GJB2) genes, by screening outbred primates. Based on the carrier rate for the average recessive gene, we predict that screening >500 macaques has a >95% probability of detecting a pathologic mutation. Samples from 595 unrelated macaques were obtained from three National Primate Research Centers. Three common variants and >17 rare variants were detected in the *Macaca mulatta* GJB2 gene by DHPLC and sequencing. None of the variants were predicted to alter the protein, and none occurred in the region containing the common human mutations. We found >15 common variants in 30-50% of the macaque USH2A coding sequence. More than 80 rare variants were found, 30 of which altered amino acids. Pathology of putative mutations was evaluated based on frequency and predicted alteration of splicing or protein structure. An alu insertion in IVS7 was predicted to be nonpathologic based on allele frequency (1.4%). Pathologic missense mutation candidates include alterations in partially conserved residues in the signal peptide, amino terminal region, laminin type VI and laminin EGF domains. The best candidate creates a strong splice donor site in exon 8, predicted to lead to a frameshift and stop codon. We plan to test USH2A mRNA from salivary gland biopsies to determine if aberrantly spliced RNA is produced. A macaque model will provide insights into pathologic mechanisms and treatment strategies that could reduce or prevent inherited deafness and blindness. Support: NIH-NEI R03 EY013991-02, NIH-NIDCD R21DC05472-02, DRF

1052 Audiologic findings and GJB2/GJB6 mutations in infants/toddlers identified with hearing loss

Yvonne S. Sininger¹, Ariadna Martinez², Michelle Fox³, Barbara Crandall⁴, Nina Shapiro⁵, Milhan Telatar⁶, Wayne Grody⁷, Lisa Schimmenti⁸, Christina Palmer²

¹Head & Neck Surgery, University of California Los Angeles, 62-132 CHS Box 951624, Los Angeles, CA, United States,

²Psychiatry, UCLA, 760 Weswood Plaza, Los Angeles, CA, United States, ³Pediatrics, UCLA, 760 Weswood Plaza, Los Angeles, CA, United States, ⁴Psychiatry & Pediatrics, UCLA, 760 Weswood Plaza, Los Angeles, CA, United States, ⁵Head & Neck Surgery, UCLA, 62-132 CHS Box 951624, Los Angeles, CA, United States, ⁶Pathology, UCLA, 760 Weswood Plaza, Los Angeles, CA, United States, ⁷Pathology, Pediatrics, Human Genetics, UCLA, 760 Weswood Plaza, Los Angeles, CA, United States, ⁸Human Genetics, University of Minnesota, 760 Weswood Plaza, Los Angeles, CA, United States

Considerable discussion has centered upon including GJB2/GJB6 testing within the early hearing detection and intervention (EHDI) process. Before genetic testing is applied universally within the EHDI process, it is important to understand the impact of such testing and counseling. Data presented are the audiologic and genetic findings of a prospective study whose aims include assessment of the logistics, and potential advantages and disadvantages to families of including genetic testing in the EHDI process.

Subjects for the study are children with sensorineural hearing loss who are under 2 years of age with no other known medical complications. Following informed consent through parental genetic counseling, genomic DNA from participating children is subject to mutation analysis (*GJB2*: 35delG, 235delC, 167delT; *GJB6*: 342 kb deletion) followed by *GJB2* sequencing as needed. All children are evaluated by a clinical geneticist, and medical and audiology records are obtained for up to 4 years. To date, 11 ethnically diverse families (Caucasian, Hispanic, Asian), with no other family history of congenital hearing loss, have enrolled and data is available on 10 children, 6 males and 4 females. Five of the 10 babies were found to have two *GJB2* mutations (35delG/35delG [n=2], 35delG/311del14 [n=1], 235delC/235delC [n=1]), in four children no mutation was found and in one the data was inconclusive because it was not possible to amplify *GJB2* exon 1. *GJB6* deletion was not present in any of the children. Subjects were evaluated by frequency specific ABR or visual reinforcement audiometry when age-appropriate. Audiometric data revealed moderate to profound, sensorineural, bilateral hearing losses that were generally symmetrical in all but one. In that child, negative for connexin mutation, an average 25 dB asymmetry was found. The average degree of hearing loss more severe in the infants who were positive for two *GJB2* mutations by 14.6 dB in the left and 10.9 dB in the right ear but differences do not reach statistical significance.

1053 Naked DNA Encoding INF-gama Enhances Tubulin Induced Hearing Loss in Guinea Pigs

Tai-June Yoo, Xiaoping Du, Hideo Matsuno, Siva Kanangat, Usha Nair, Weihau Cheng, Brandon D Hill, Mohammad Habiby Kermany, Tai June Yoo

Allergy/Immunology, University of Tennessee, 956 Court Ave., B318, Memphis, TN, United States

The purpose of this study is to delineate the immune injury mechanisms that involved in the autoimmune inner ear disease by introducing plasmid DNA encoding of TH1 cytokines (INF-g) into the inner ear. b-tubulin is a microtubular protein which we found as an important autoantigenic in Meniere's Disease as well as other autoimmune hearing loss. Hearing loss was induced in mice and guinea pigs when they are immunized with the tubulin molecules. Autoimmune hearing loss could be the results of TH1 cytokine responses from autoimmune injury. To test the hypothesis, guinea pigs were immunized with 200mg of tubulin in CFA and boosted once more. Two weeks later, we introduced 100ug (5ul) of naked DNA encoding INF-g was injected into the left side inner ear through round window. Same volume of 0.1M PBS was injected into right side as control. ABR was recorded before and after the injection. 15 weeks after the injection, the animals were sacrificed and temporal bones were examined with H-E and INF-g immunocytochemical staining. The ears injected with the plasmid DNA-INF-g had an enhanced hearing loss (30 dB), and degeneration of the spiral ganglion was found in these ears. However, the injection of the naked DNA encoding INF-g did not change the expression of the INF-g in the inner ears. These results suggest that autoimmune hearing loss could be the result of TH1 responses to inner ear autoantigens. (This study is supported by NIH grant)

1054 Immunostaining with Fluorescent Antibodies as an Adjunct to the Diagnosis of Usher Syndrome

Edward S Cohn¹, Gautam Bhattacharya,² Dana J Orten², William J Kimberling², Dominick E. Cosgrove²

¹*Otolaryngology and Genetics, Boys Town National Research Hospital, 555 North 30th St, Omaha, Nebraska, United States,*

²*Genetics, Boys Town National Research Hospital, 555 North 30th St, Omaha, Nebraska, United States*

Mutations in the MYO7A gene are responsible for about 60% of all Usher I cases. Currently, confirmation of a MYO7a diagnosis depends upon the observation of a mutation in that gene, an expensive and time-consuming procedure. An alternative, non-DNA based method of subtype diagnosis would be welcome. Wolfrum et al. (1998) noted the presence of the myosin VIIa protein in cells from respiratory mucosa. This observation suggested the possibility that ciliated nasal mucosa could be tested using antibody against myosin VIIa for the presence or absence of that protein. The absence of myosin VIIa would establish that the patient has a mutation in the MYO7A gene that interferes with the production of the protein. Ciliated nasal epithelium was obtained from 4 subjects having Usher Ib with a variety of mutant genotypes, 1 Usher I in a family where a mutation in *myo7a* has not been observed, and 10 unaffected control subjects.

Three Usher Ib subjects from two families with missense mutations were observed to stain for myosin VIIA in nasal epithelia cells, whereas, 1 Usher Ib subject with two null mutations, and 1 Usher I unclassified subject, had no myosin VIIA detected. This preliminary study is a strong indication certain Usher Ib cases may be diagnosed using nasal cytology and immunostaining techniques that detect myosin VIIA. The procedure is likely to be valid only when the mutation disrupts protein production. Immunostaining of easily collected nasal epithelial cells could be employed in a 1st stage diagnostic strategy; cases lacking myosin VIIa can then be rigorously screened for the causative mutation without concern that the defect may be in one of the other Usher genes.

1055 Temporal bone anomalies associated with congenital heart disease

Kazuyasu Baba^{1,2}, Sebahattin Cureoglu^{1,3}, Patricia A Schachern¹, Takeshi Kusunoki^{1,4}, Andre LL Sampaio¹, Michael M Paparella⁵, Toshio Yamashita²

¹*Otolaryngology, University of Minnesota, 420 Delaware Street, Minneapolis, MN, United States,* ²*Otolaryngology, Kansai Medical University, Fumizono-cho 10-15, Moriguchi, Japan,*

³*Otolaryngology, International Hearing Foundation, 701 25th Ave.S. Suite 200, Minneapolis, MN, United States,*

⁴*Otolaryngology, Kinki University, School of Medicine, Onohigashi377-2, Osakasayama, Japan,* ⁵*Otolaryngology, Minnesota Ear Head and Neck Clinic, 701 25th Ave.S. Suite 200, Minneapolis, MN, United States*

Congenital heart disease most commonly occurs between the 4th to 8th weeks of intra-uterine development. It is at the same period of time that the cochlea, semicircular canal, and ossicular chain begin to develop. It is well known that temporal bone anomalies often occurred with other anomalies. We studied 149 temporal

bones from 78 patients with congenital heart disease. Ages ranged from stillborn to 35 years (mean 4.4). Heart anomalies included: 1) 27 cases with ventricular septal defect (VSD); 2) 11 cases with atrial septal defect (ASD); 3) 15 cases with transposition of great vessels (TGA); 4) 25 cases with valve problems; 5) 13 cases with patent foramen ovale (PFO); and 6) 20 cases with patent ductus arteriosus (PDA). We observed the following temporal bone anomalies: 1) ear canal stenosis- 30/142 ears (21.1 %); 2) agenesis of the oval window -8/139 ears (5.8 %); 3) agenesis of round window- 2/132 ears (1.5 %); 4) dehiscent facial nerve- 76/141 ears (54 %); 5) deformity of malleus - 4/138 ears (3 %); 6) deformity of incus- 7/136 ears (5.2%); 7) deformity of stapes - 14/135 ears (10.4 %); 8) persistence of stapedia artery- 6/138 ears (4.4 %); 9) dehiscent carotid artery- 3/137 ear (2.2 %); 10) hair cell loss- 24/114 ears (14.92 %); 11) ganglion cell decrease- 8/118 ears (15 %); and 12) strial concretion- 26/144 (18 %). We correlated the incidence of temporal bone anomalies with heart anomalies. Ear canal stenosis was most common in patients with PFO (38 %). Wide angle of facial nerve genu was most common in patients with ASD (60 %). Dehiscent facial nerve was observed more commonly in patients with PFO and ASD (70 % and 73 %). Strial concretion was found more commonly in patients with PFO and PDA (39 % and 32 %). Our results indicated that temporal bone anomalies have been observed commonly in patients with congenital heart disease. Physicians should be aware of the presence of otologic anomalies in the patients with heart anomalies.

1056 Autosomal Dominant Progressive Distal Auditory Neuropathy: Phenotype, Physiology, and Psychophysics

Arnold Starr¹, Fan-Gang Zeng², Henry Michalewski³, Ying Kong², Paula Beale³, Bronya Keats⁴, Brandon Isaacson⁵, Marci Lesperance⁵

¹Neurology, University of California, 154 Med Surge I, Irvine, California, United States, ²Otolaryngology - Head and Neck Surgery, University of California, 364 Med Surge II, Irvine, California, United States, ³Neurology, University of California, 150 Med Surge I, Irvine, California, United States, ⁴Genetics, Louisiana State University, 533 Bolivar Street, New Orleans, Louisiana, United States, ⁵Otolaryngology, University of Michigan, 1500 E. Medical Center Drive, Ann Arbor, Michigan, United States

We have studied 77 members from a large kindred with a hearing disorder inherited in an autosomal dominant pattern. The initial phenotypic features of the hearing loss were compatible with an auditory neuropathy (AN) showing absent or markedly abnormal auditory brainstem responses (ABRs) and normal otoacoustic emissions (OAEs). Speech comprehension was markedly affected. The hearing loss progressed over 10 to 20 years to involve outer hair cells as well producing a picture of sensorineural hearing loss (absent ABRs and OAEs). Affected family members did not have evidence of a peripheral neuropathy. There was evidence that the auditory nerve, late in the course of the illness, atrophies. We made objective measures of the changing phenotypes using audiological, physiological, and psychoacoustic measures. There was a marked improvement of auditory functions after cochlear implantation with return of evoked brainstem potentials, psychophysical measures, and speech comprehension. The findings suggest that the site

of lesion is distal along the auditory nerve affecting one or all of the components in the auditory periphery including terminal dendrites, hair cells, or their synapses, sparing auditory ganglion cells and their axons. We have suggested the term distal auditory neuropathy (Type II AN) is appropriate to contrast with prior reports of primary degeneration of auditory nerve sparing hair cells (Type I AN). The responsible gene has been mapped to the AUNA1 locus (see companion abstract).

1057 Autosomal Dominant Progressive Auditory Neuropathy: Phenotype, Physiology, and Psychophysics

Arnold Starr¹, Brandon Isaacson², Paula Beale³, Y. Y. Kong¹, Henry Michalewski¹, Fan Zeng¹, Marci Lesperance², Bronya Keats⁴

¹Neurology, UC - Irvine, Department of Neurology, Irvine, CA, United States, ²Otolaryngology, University of Michigan, Medical Center Drive, Ann Arbor, MI, United States, ³Audiology, OSU, 12th Ave, Columbus, Ohio, United States, ⁴Genetics, LSU Health Sciences Center, 533 Bolivar Street, New Orleans, LA, United States

We have studied 77 members from a large kindred with a hearing disorder inherited in an autosomal dominant pattern. The initial phenotypic features of the hearing loss were compatible with an auditory neuropathy (AN) showing absent or markedly abnormal ABRs and normal otoacoustic emissions (OAEs). Speech comprehension was markedly affected. The hearing loss progressed over 10 to 20 years to involve outer hair cells as well as producing a picture of sensorineural hearing loss (absent ABRs and OAEs). Affected family did not have evidence of a peripheral neuropathy. There was evidence that the auditory nerve, late in the course of the illness, atrophies. We made objective measures of the changing phenotypes using audiological, physiological, and psychoacoustic measures. There was a marked improvement of auditory functions after cochlear implantation with return of evoked brainstem potentials, psychophysical measures, and speech comprehension. The findings suggest that the site of lesion is distal along the auditory nerve affecting one or all of the components in the auditory periphery including terminal dendrites, hair cells, or their synapses, sparing auditory ganglion cells and their axons. We suggest that the term distal auditory neuropathy (Type II AN) is appropriate to contrast with prior reports of primary degeneration of auditory nerve sparing hair cells (Type I AN).

1058 An Estimate of Heritability of Auditory Processing Skills

Robert J Morrell¹, Carmen C Brewer², Christopher K Zalewski², Mary Ann Mastroianni², Dennis Drayna¹, Kimberly S Laws³, Allyson Segar³, Thomas B Friedman¹

¹Laboratory of Molecular Genetics, NIDCD/NIH, 5 Research Court, Rockville, MD, United States, ²Hearing Section, NIDCD/NIH, 9000 Rockville Pike Bldg 10/5C306, Bethesda, MD, United States, ³Hearing and Speech Sciences, University of Maryland, LeFrak Hall, College Park, MD, United States

It is well known that variation in auditory processing abilities exists in the general population, but it is not well understood to what extent, if any, these abilities are hereditary. Twins offer a

unique opportunity to evaluate genetic contribution to auditory processing skills. Five tests of auditory processing were administered to twins attending the 2002 and 2003 Annual Twins Festival in Twinsburg, Ohio. This was conducted as a pilot study to gain experience administering a central auditory processing research protocol outside of a controlled clinical setting. The five tests administered were the Filtered Words (FW), Auditory Figure-Ground (AFG) and Competing Words (CW) subtests of theSCAN-A (Keith 1995), a dichotic consonant vowel (CV) test, and the Click Order Lateralization Test (COLT) developed by F. Musiek. Testing was conducted in a trailer. Sound attenuating earmuffs in combination with insert earphones were used to reduce ambient noise. Normal pure-tone hearing sensitivity for 500-4000 Hz and normal tympanometry were confirmed for each participant prior to administration of the auditory processing tests. By comparing scores between monozygotic (MZ) and dizygotic (DZ) twin pairs, an estimate of the heritability of auditory processing skills was made. The CW subtest of the SCAN-A gave the strongest evidence for heritability. MZ concordance was > 0.8 while DZ concordance was ~ 0.55 . These rates are not significantly different, mostly due to the small sample size for the DZ group (54 MZ pairs; 11 DZ pairs; $p = 0.099$). At the present time we estimate the fraction of the variability on CW test performance that can be attributed to hereditary factors (h^2) to be approximately 57%. The other tests of auditory processing skills showed little differences in concordance rates between MZ and DZ twins and thus provided no evidence for significant contribution of hereditary factors in test performance levels.

1059 Patient's and Family's Understanding of Genetic Test Results for Hearing Loss: Ignorance is Bliss?

Heidi L Rehm^{1,2}, Janet N Horgan³, Margaret A Kenna^{4,5}

¹Pathology, Harvard Medical School, 65 Landsdowne St, Cambridge, MA, United States, ²Center for Genetics and Genomics, Brigham & Women's Hospital, 65 Landsdowne St, Cambridge, MA, United States, ³ALM, Harvard University, 51 Brattle St, Cambridge, MA, United States, ⁴Otology and Laryngology, Harvard Medical School, 300 Longwood Ave, Boston, MA, United States, ⁵Otolaryngology and Communication Disorders, Children's Hospital, 300 Longwood Ave, Boston, MA, United States

Genetic testing is common in the workup of a patient with hearing loss (HL). It is unclear how well the results are understood by the patient or family receiving them.

We performed a pilot study to determine the use and effectiveness of genetic counseling for HL. We sent a survey to parents of 80 children with HL who had genetic testing. 32 questions addressed: 1) Why did your child have a genetic test and what do you remember about the results? 2) Did you have counseling and who provided it? 3) What sources of information did you use to understand the testing? The survey also asked 5 "quiz" questions to address respondent knowledge of genetic testing, including recurrence risk, source of mutations, and significance of a negative test.

31 patients responded. There was little difference between the score of respondents whose child had a genetic cause of HL and those whose child did not (57% vs. 45% correct). Those who saw a genetic professional (genetic counselor or geneticist) did score

much better (70% correct) than those who did not (38% correct). 44% did not know what genetic tests their child had and 7% did not know if a genetic cause was found. 38% who had connexin 26 testing did not know if any mutations were found. Despite the poor performance on quiz questions (average 49% correct) and the lack of knowledge about their testing, 80% of respondents reported being satisfied with their understanding of genetic testing and 86% did not plan to pursue counseling in the near future.

These results suggest that parents are not only uneducated about the implications of genetic testing, but are unaware of their ignorance and thus not likely to pursue resources which may help them improve their understanding. It is imperative that the physician giving the genetic test results provide better information about the benefits of genetic counseling. Clear written information about the results and their implications should be provided in case patients never pursue counseling.

¹ Haacke, W. Ueber Wesen, Ursachen und Vererbung von Albinismus und Scheckung und ueber deren Bedeutung fuer vererbungstheoretische und entwicklungsmechanische Fragen. Biologisches Centralblatt, Bd. 15: 44-78. 1895.

² Rawitz, B. "Das Gehoerorgan der japanischen Tanzmaeuse. Archiv fuer Anatomie und Physiologie, Physiologische Abtheilung, 1899: 236-243.

Author Index

(Indexed by abstract number)

- Aalto, Heikki, 69
Abbas, Paul, 255, 953
Abdala, Carolina, 107
Abraham, David, 454
Abrashkin, Karen, 741
Acuna, Dora, 277, 738
Adams, Joe, 531, 1044
Adappa, Nithin, 1045
Adato, Avital, 250
Agrawal, Smita S., 168
Aguñaga, Salvador, 443
Ahlstrom, Jayne B., 117
Ahmad, Maha, 937
Ahmad, Nadir, 655
Ahmad, Shoab, 763, 986
Ahmed, Azad, 294
Ahmed, Zubair M., 204, 205, 252
Ahn, Joong Ho, 388
Ahn, Kyung, 759
Ahsan, Syed, 529
Ahuja, Tarun K., 596
Ajalli, Rahim, 751
Akil, Omar, 716, 721
Akita, Jiro, 235
Al-Mahaidi, Senan, 624
Alagramam, Kumar N., 226, 980, 1045
Alais, David, 621
Alam, Shaheen Ara, 178
Albrecht, Beatrice, 201
Aletsee, Christoph, 267, 719, 726
Alexandrov, Leonid, 1030
Ali, Hussain, 932
Allen, Paul, 331, 650, 659, 900
Allen, Susan J., 488
Allum, John H. J., 75, 76
Alonso, Maria Teresa, 776
Alonso, Ophelia F., 30
Aloor, Heather L., 214, 1040
Alper, Seth, 203
Altrock, Wilko, 708
Altschuler, Richard, 522, 562, 884, 888
Altshuler, Richard, 268
Alvarez, Yolanda, 776
Alves-Pinto, Ana, 129
Amadio, Marialaura, 275
Amalfitano, Andrea, 506
Amalfitano, Andreas, 505
Amitay, Sygal, 813, 814
Anand, Payal, 353
Andang, Michael, 1031
Anderson, David J., 158, 323, 924
Anderson, John H., 82
Anderson, Julia, 702
Anderson, Lee Ching Wu, 639
Anderson, Lucy Anne, 320, 333
Anderson, Michael J., 916
Andoh, Masayoshi, 1022
Andrews, Peter W., 1039
Angelaki, Dora E., 271
Anne, Samantha, 712
Antonelli, Patrick J., 20, 33, 35
Anvari, Bahman, 438, 439, 802
Apoux, Frederic, 119
Arai, Shoji, 27
Arcaroli, Jennifer, 259
Arendt, Heather, 373
Arezzo, Joseph, 582
Arne, Scholtz, 562
Arnold, Wolfgang, 396, 995
Arosarena, Oneida Albania, 758
Asako, Mikiya, 884, 888
Atzori, Marco, 584
Auer, Manfred, 792
Austin, Darrell A., 290
Avenidaño, Carlos, 929
Avraham, Karen B., 206, 233, 487
Ayliffe, H. E. Ted, 801
Azuma, Hiroshi, 196
Azuma, Miki, 73
Baba, Kazuyasu, 1055
Backus, Bradford C., 535
Bacon, Sid P., 119
Badri, Rohima, 548
Bai, Jun-Ping, 436, 800
Baird, Richard A., 395
Bajaj, Chandrajit, 792
Bajaj, Harjeet S., 337
Bak, Marek, 114
Baker, Kim, 529, 743
Bakhtiarova, Adel, 1033
Balaban, Carey D., 197, 295, 375, 376, 377, 408, 409
Balkany, Thomas, 30, 188, 232, 236, 529, 563, 568
Baloh, Robert, 635
Balz, Vera, 979
Bamiou, Doris Eva, 55, 580
Bandyopadhyay, Sharba, 956
Banks, Juliane M., 295, 296, 297
Banks, Matthew, 589, 590
Barald, Kate F., 488, 746
Barber, Brent, 760
Barbieri, Marco, 172
Barco, Amy L., 262, 569
Barsz, Kathy, 331
Bartles, James R., 517, 793
Bashiardes, Stavros, 755, 787
Basinger, David, 122
Bassim, Marc K., 256, 604
Basta, Dietmar, 23, 340
Batra, Ranjan, 914
Batta, Tamás József, 446
Baudoux, Sylvie, 364, 922
Bauer, Eric, 165
Bauer, Karl, 723
Baumann, Uwe, 257, 827
Beale, Paula, 1056, 1057
Bean, N. Jay, 305
Bedenbaugh, Purvis, 807
Bee, Mark A., 314
Behne, Nicole, 861
Beisel, Kirk W., 462, 477, 694, 964, 1029
Beitel, Ralph E., 565, 845
Belagaje, Sudhir R., 92
Belin, Pascal, 872
Belyantseva, Inna A., 204, 205, 252, 791
Ben-Yosef, Tamar, 252
Bendig, Garnet, 309
Bendiske, Jennifer, 889
Benson, Christina, 577
Benson, Thane E., 361
Berg, Bruce G., 512
Berggren, Diana, 752
Bergles, Dwight E., 709
Bergson, Eric, 213
Berrebi, Albert S., 731, 735, 736, 921
Bershadsky, Alexander, 246
Betha, John R., 764
Beule, Achim G., 75
Beyer, Lisa, 518
Bhagat, Shaum P., 97
Bhattacharya, Gautam, 963, 1054
Bian, Lin, 106
Bian, Zhao, 685
Bianchi, Lynne M., 488
Bibas, A., 822
Biebel, Ulrich W., 342
Bielefeld, Eric C., 386, 686
Billig, Isabelle, 375
Billings, Curtis, 866
Billings, Peter B., 174, 391
Birch, David, 963
Bishop, Deborah C., 324
Biswas, Ankoor Neil, 512
Bitsche, Mario, 562
Bizley, Jennifer K., 573
Black, F. Owen, 64, 71, 669
Blair, Andrew, 425
Blakley, Brian W., 1, 48
Blanco, José L., 547
Blanton, Susan, 236
Bledsoe, Jr., Sanford C., 972
Bloch, Robert J., 418
Blödown, Alexander, 23, 987
Boasen, Jared F., 184
Bobbins, Richard P., 973, 1033
Boche, Jo Ellen, 360, 419, 962
Bodmer, Daniel, 528, 719
Bodmer, Morana, 528
Boerner, Susan, 470
Boettger, Thomas, 976
Bogdanovic, Nenad, 370, 891
Boger, Erich T., 791
Bogerts, Bernhard, 862
Bohne, Barbara A., 393, 394
Bohorquez, Jorge, 950, 983
Bok, Jinwoong, 775
Bolz, Steffen-Sebastian, 995
Bonham, Ben H., 564, 847
Bonny, Christophe, 673
Bostrom, Henrik, 946
Bostrom, Marja, 945, 946
Botta, Laura, 275
Bourdette, Dennis, 60
Bowden, Michele, 329
Bowen-Pope, Daniel, 672
Boyle, Richard, 16
Boëda, Batiste, 250
Braid, Louis D., 578
Braig, Claudia, 724, 971
Brand, Antje, 608
Brandner, Johanna M., 994
Brandt, Andreas, 708
Braun, Allen R., 95
Braun, Katharina, 339
Braun, Marianne, 909
Braun, Susanne, 339, 854
Breakefield, Xandra, 505, 507
Brechmann, André, 861, 862
Bredberg, Göran, 846
Brescia, Aaron Isaac, 645
Bresnahan, Glenn, 924
Breuninger, Christian, 820
Brewer, Carmen C., 1058
Bricker, Kathy, 568
Brigande, John V., 482
Brimjoin, Wm. Owen, 859, 860
Brinsko, Kelly M., 497
Bristow, Ben N., 934
Brochard-Wyart, Françoise, 249
Brodie, Hilary A., 29, 177
Broide, David, 286
Brooker, Debra, 225
Brooks, Andrew, 660, 661
Broers, Dominik, 267, 528, 719, 726
Brosch, Michael, 581
Brough, Douglas, 743, 747
Brouse, Maria Virginia, 867
Brown, Carolyn J., 53
Brown, John A., 356
Brown, M. Christian, 354, 361, 362
Brown, Martin, 580
Brown, Mel, 951
Brown, Nadine, 524
Brown, Steve D. M., 494, 1049
Brown, Steve M., 225
Brownell, William, 437, 438, 439, 440, 441, 801, 802, 803
Brownstein, Zippora, 233
Bruce, Ian C., 337, 956
Brugge, John F., 574
Brungart, Douglas S., 118
Bryant, Jane Elizabeth, 672
Buchman, Craig Alan, 287, 289
Buchser, William, 959
Buck, Linda, 9
Burger, Michael R., 165, 906
Burgess, Barbara J., 415
Burgio, Don L., 48
Burkard, Robert, 330, 347, 350, 495, 863, 864, 869, 982
Burns, Edward M., 540
Burr, David, 621
Burrows, Amy, 291
Burton, Miriam, 395
Buss, Emily, 984
Butts, Stacy, 568
Butts, Sydney C., 215
Buus, Søren, 124
Cacace, Anthony T., 982
Cai, Hongxue, 1007, 1017
Calvez, Sophie Le, 421
Cameron, Peter, 274
Caminos, Elena, 734, 901
Campbell, Robert A. A., 169
Canlon, Barbara, 370, 422, 681, 685, 752, 891
Cannuscio, Joseph F., 643
Cant, Nell, 577, 769
Cantos, Raquel, 471
Cao, Xiaojie, 895
Caputo, Christine, 745
Carey, Alisoun H., 1049
Carey, John P., 637, 638, 639
Carey, Thomas E., 175, 176
Carliile, Simon, 620, 624
Carlyon, Robert P., 261, 848
Carney, Carol A., 1051
Carney, Laurel H., 840, 842, 925, 952
Carninci, Piero, 1029
Carrasco, Rafael A., 137
Carter, M., 170
Caspary, Donald M., 648, 649
Cass, Stephen P., 6
Cass, Stephen, 373
Casseday, J. H., 157, 170
Cederroth, Christopher Robin, 673
Cera, Amanda J., 539
Cervera-Paz, Francisco Javier, 426
Chadwick, Richard S., 1007, 1017
Chair, Leila, 368
Chait, Maria, 150
Chakradeo, Vinaya, 824
Champlin, Craig A., 97
Chang, Sun O., 50, 72, 224
Chang, Weise, 227
Changyaleket, Benjarat, 517
Chase, Steven M., 603
Chau, Felix Y., 85
Chavez, Eduardo, 729
Cheatham, Mary Ann, 799
Chen, Arthur F., 231
Chen, Bing-Zhong, 572

- Chen, Guang-Di, 389
 Chen, Haiming, 85
 Chen, Hongbin, 553
 Chen, Kejian, 341, 645, 894
 Chen, Ping, 478, 484, 782
 Chen, Ye Ting H., 136
 Chen, Zheng Yi, 764
 Chen, Zheng-Yi, 232, 485, 784, 786
 Cheng, Holden, 1001
 Cheng, Ning, 709
 Cheng, Weihau, 1053
 Chennupati, S. Kiran, 437
 Cherian, Neil, 78, 378
 Chertoff, Mark, 106, 109
 Chestovich, Paul J., 214
 Cheung, Bruce, 463
 Chiba, Toshihiko, 420, 693, 988
 Chiu, Tzai Wen, 740, 896
 Cho, Baek-Hwan, 120
 Cho, Kyoun In, 500
 Cho, Won J., 712
 Cho, Yang-Sun, 677, 828
 Choi, Byung Yoon, 72
 Choi, Chul-Hee, 1021
 Choi, Jae Yeon, 828
 Chole, Richard A., 283, 284, 299
 Choo, Daniel, 203, 221, 223, 993
 Choung, Yun-Hoon, 282
 Christ, Stephanie, 723
 Christensen-Dalsgaard, Jakob, 163, 601
 Christova, Peka, 82
 Chung, Jong Woo, 388
 Chung, Won-Ho, 500, 677, 828
 Church, M. W., 48, 56
 Cioffi, George, 71
 Cioffi, Joseph, 907, 927, 928
 Clement, Matthew J., 304, 875
 Clifford, Sarah, 801
 Coad, Mary Lou, 869
 Coale, Kathleen D., 63
 Coburn, Michael, 858
 Coez, Arnaud, 872
 Coffey, Charles S., 256, 604
 Coffin, Allison B., 208
 Coghill, Emma Louise, 494
 Cohen, Helen S., 62, 67
 Cohen, Mazal, 55, 57
 Cohen, Oren, 606
 Cohen-Salmon, Marine, 761
 Cohn, Edward S., 1054
 Colburn, H. Steven, 130, 146, 258, 925
 Coleman, John K., 184, 525, 688
 Coleman, John, 348
 Colesa, Deborah J., 560, 566
 Coling, Donald, 1027
 Collazo, Andres, 782
 Collins, Wesley Logan, 758
 Collura, Christopher A., 961
 Cone-Wesson, Barbara K., 579
 Connell, Sarah S., 177
 Contreras, Julio, 929
 Cooke, James E., 327
 Coomes, Diana L., 357, 358
 Cooper, Nigel P., 1008
 Copeland, Neal G., 780
 Corey, David, 784
 Corfas, Gabriel, 679
 Corliss, Deborah, 702
 Cormier, Marie-Andrée, 670
 Corrales, Carleton Eduardo, 785, 1034, 1035
 Corwin, Jeffrey, 753, 784, 789
 Cosgrove, Dominic E., 963, 1043, 1047, 1054
 Costello, Michael, 184, 525
 Cotanche, Douglas, 404, 405, 702, 1033
 Coticchia, James, 32
 Cotter, Lucy, 373
 Covey, Ellen, 157, 170, 335
 Cowan, Justin, 58
 Crandall, Barbara, 1052
 Crawford, Andrew, 796
 Crenshaw, III, E Bryan, 759
 Cristobal, Ricardo, 927
 Crocker, William, 256, 604
 Crook, John M., 591
 Cross, Sally, 494
 Crum, Poppy A. C., 837
 Cuajungco, Math, 458
 Cueille, Nathalie, 673, 781
 Cullen, Robert D., 256
 Cuneyt, Alper M., 296, 297
 Cunningham, Dale, 413
 Cunningham, Lisa L., 187, 412, 413
 Curcic, Branislava, 211
 Cureoglu, Sebahattin, 38, 209, 636, 1055
 Cushing, Ross, 308
 Cynx, Jeffrey, 305
 Cyr, Janet L., 207
 D'Angelo, William, 595
 D'Azzo, Sandra, 767
 D'Haese, Patrick S. C., 262, 569
 D'Sa, Chrystal S., 1042
 D'Souza, Mary, 660, 661
 Dabdoub, Alain, 519
 Dallos, Peter, 443, 799
 Daneman, Meredyth, 665
 Daniel, Sam, 40
 Daruwalla, Zeeba, 488
 Dau, Torsten, 805, 868, 913
 Davidson, Beverly, 505, 509
 Davies, Caroline, 794, 977
 Davies, Dawn, 217, 753
 Davis, Adrian C., 58
 Davis, James Gordon, 720
 Davis, Julian, 941
 Davis, Kevin A., 141
 Davis, Robin L., 943, 944, 947
 Dazert, Stefan, 267, 719, 726
 de Boer, Egbert, 543, 544
 De Groot, John C. M. J., 678
 de La Rochefoucauld, Ombeline L., 1010
 de Monvel, Jacques Boutet, 1006
 de Ribaupierre, Francois, 673, 781
 Deak, Levente, 443
 Deal, Kelly M., 39, 113
 Deeks, John M., 261
 Deeks, John, 848
 Deingruber, Kerstin, 396
 del Castillo, Franscisco, 761
 Delgado, Rafael E., 355, 950, 983
 Delgutte, Bertrand, 146, 154
 Deliano, Matthias, 159
 Deligeorges, Socrates, 857, 924
 Delimont, Duane, 963
 Delprat, Benjamin, 765
 Demany, Laurent, 836
 Deng, Xiaohong, 414
 Denney, Keith, 228
 Dent, Michael L., 614, 774
 Deo, Niranjana, 1019
 Depireux, Didier A., 152, 572
 Desai, Anurdha, 25
 Desai, Sapan S., 932, 933
 Deutscher, Anke, 855
 Devore, Sasha, 617
 DeWeese, Michael, 585, 587
 Dhaliwal, Jasmeet, 933
 Diaz, Rodney C., 698
 Dickman, David, 931
 Dickman, J. David, 14, 15, 271, 930
 Dierking, Darcia M., 99, 100
 Dietrich, Dalton W., 30
 Dimitriadis, Emiliios K., 1017
 Ding, Dalian, 186, 416, 495, 662, 674, 940, 975
 Dionne-Fournelle, Odrée, 670
 Dirckx, Joris J. J., 279, 871
 Discolo, Christopher, 392
 Divenyi, Pierre L., 664, 806
 Dixon, Julian, 287, 289
 Dobbins, Heather D., 572
 Doetzlhofer, Angelika, 788
 Doi, Katsumi, 219
 Dolan, David F., 111, 112, 349, 534, 741, 972
 Dolle, Pascal, 480
 Donahue, Amy, 243
 Donfack, Joseph, 294
 Dong, Luhua, 41
 Dong, Wei, 824, 1009
 Dong, Youyi, 479, 1036
 Dong-Hoon, Shin, 181
 Dooling, Robert J., 166, 306, 307, 732
 Dootz, Gary, 656
 Dorman, Michael, 844
 Dormer, Kenneth John, 826
 Dosch, Hans Günter, 550
 Doshier, Barbara, 811
 Dou, Hongwei, 203, 223, 993
 Doucet, John, 360, 513
 Doyle, Karen J., 276, 698
 Doyle, William J., 295, 296, 297
 Drayna, Dennis, 1058
 Drescher, Dennis G., 457, 711, 712, 713
 Drescher, Marian J., 711, 712, 713, 714
 Drga, Vit, 128
 Drottat, Marie, 190
 du Lac, Sascha, 272
 Du, Baodong, 186
 Du, Guo-Guang, 443
 Du, Li Lin, 232, 236
 Du, Xiaoping, 504, 968, 1053
 Duan, Maoli, 966
 Dubno, Judy R., 117
 Duncan, Luke, 404, 405
 Duncan, Robert Keith, 460
 Dunckley, Kathleen T., 113
 Durham, Dianne, 109, 338, 644, 892
 Dutton, Jeffrey A., 363
 Duzhyy, Dmytro, 461
 Dziejewit, J. Andrew, 706
 Eatock, Ruth Anne, 455, 803
 Ebert, Charles S., 604
 Ebert, Jr., Charles Stephen, 256
 Ebmeyer, Joerg, 286
 Ebmeyer, Jörg, 290
 Ebmeyer, Umay, 286
 Ehteler, Stephen, 720
 Eddins, Ann C., 974, 975
 Eddins, David A., 613, 835
 Edelyi, F., 589
 Edge, Roxanne, 799
 Edmond, John, 738
 Edwards, Bruce M., 54
 Eggermont, Jos Jan, 140, 328
 Ehrlich, Garth D., 294, 1048
 Eiber, Albrecht, 820
 Ekborn, Andreas, 681
 El-Amroui, Aziz, 250, 765
 El-Badry, Mohamed, 974, 975
 Eldis, F. E., 56
 Elgoyhen, Ana B., 717
 Elhilali, Mounya, 135
 Elkon, Rani, 487
 Elliott, Taffeta Marie, 163
 Enas, Lija M., 497
 Endo, Tsuyoshi, 191, 216, 411, 479, 675, 1036
 Engel, Jutta, 456, 724
 Enmark, Eva, 966
 Erbe, Christy, 928
 Erdos, Geza, 294, 1048
 Ermilov, Sergey, 438, 439, 802
 Ernst, Arne, 23, 340, 987
 Escabi, Monty A., 326
 Escabi, Monty Armando, 153
 Escaño, Michael Francis Teraoka, 470
 Eshraghi, Adrien A., 30, 529, 563
 Espasandin, Maria, 580
 Esteban-Cruciani, Nora, 526
 EunJoo, Kang, 90, 93
 Everett, Lorraine A., 201
 Ewert, Stephan D., 805
 Ewert, Stephan, 836
 Eybalin, Michel, 708, 781
 Fabry, David A., 61
 Faddis, Brian T., 299, 300
 Fainberg, Jolie, 844
 Fairfield, Damon A., 522
 Fakler, Bernd, 459, 718
 Falk, Stephanie E., 256, 605
 Falkner, Annegret, 228
 Fantini, Deborah Ann, 126, 839
 Farahbakhsh, Nasser A., 804
 Farrell, Brenda, 440
 Farris, H. E., 795
 Fathman, C. Garrison, 504
 Faulkner, Andrew, 91, 849, 850
 Faulkner, Kathleen F., 498
 Faulstich, Bernd Michael, 272
 Fauser, Claudius, 339
 Fausti, Stephen, 39, 49, 60, 113
 Fay, Richard R., 161, 313, 958
 Fayad, Jose, 824
 Fechter, Laurence D., 387
 Feeney, M. Patrick, 829
 Feiveson, Alan H., 669
 Fekete, Donna M., 482, 483
 Feuldbauer, Noelle, 961
 Feliksiak, Anna, 609
 Felix, Heidi, 979
 Felix, II, Richard A., 344
 Feng, Albert, 336, 880
 Feng, Bin, 823
 Feng, Feng, 694, 964, 1029
 Feng, Weihong, 276, 462, 463, 697, 698
 Ferrary, Evelyne, 280, 281
 Ferrándiz, Noelia Sánchez, 43, 45
 Feth, Larry, 553
 Fettiplace, Robert, 796, 1028
 Fields, Randall, 1043
 Filipovic, Blagoje, 52, 595
 Finlayson, Paul G., 890
 Finley, Charles C., 256
 Finley, Clay, 197, 348
 Firbas, Elyssa, 961
 Firestein, Gary S., 391
 Firszt, Jill B., 86, 89, 870
 Fischer, Christopher, 445
 Fishman, Yonatan I., 582, 876
 Fiszer, Marta, 114
 Fitzgibbons, Peter J., 116
 Fitzpatrick, Douglas C., 256, 604, 605
 Fleming, Carrie R., 1037
 Fleming, J., 965
 Flora, Adriano, 477
 Florentine, Mary, 124
 Flores-Hernandez, Jorge, 584
 Flores-Otero, Jacqueline, 943
 Floyd, Robert A., 2
 Folbe, Adam J., 711
 Foldes, Stephen, 253

- Forte, Vito, 40
 Fox, Michelle, 1052
 Fraenzer, Juergen-Theodor, 723, 1046
 Francis, Howard W., 424
 Frank, Michael, 635
 Franklin, Samuel R., 371
 Fransson, Anette Elisabeth, 846
 Freeman, Nancy, 243
 French, Barbara, 881
 French, Christopher C., 317
 Frenz, Dorothy, 213, 215, 682, 752
 Freyman, Richard L., 87
 Friauf, Eckhard, 917
 Fridberger, Anders, 421, 1006
 Friedland, David R., 907
 Friedman, Rick A., 502
 Friedman, Sarah, 116
 Friedman, Thomas, 204, 205, 252, 487, 791, 1058
 Friedrich, Jr., Victor L., 17, 631
 Friesen, Lendra, 866
 Frisina, D. Robert, 660, 661, 666, 667, 668
 Frisina, Robert D., 645, 647, 651, 652, 653, 654, 660, 661, 666, 668
 Frisina, Susan T., 666, 667, 668
 Fritz, Jonathan, 135
 Fritzsich, Bernd, 316, 477, 779, 964
 Frolenkov, Gregory, 444, 977
 Frydman, Moshe, 233
 Fuchs, Elaine, 247
 Fuchs, Paul A., 460, 709, 715, 716, 717
 Fujii, Masato, 397, 429
 Fujino, Kiyohiro, 675
 Fujioka, Masato, 756
 Fukumoto, Kanehisa, 790
 Fukushima, Hisaki, 38
 Fukushima, Naomi, 38
 Funnell, W. Robert J., 815
 Furman, Joseph M., 65, 376, 642
 Furness, David N., 530, 703
 Furst, Miriam, 606
 Furukawa, Masayuki, 286, 290
 Furukawa, Shigeto, 610, 612
 Fushiki, Shinji, 218
 Fuzessery, Zoltan M., 858
 Füllgrabe, Christian, 836
 Gabor, Szabo, 589
 Gabriele, Mark L., 317
 Gaggl, Wolfgang, 86, 89, 870
 Gagnon, Patricia M., 496, 498
 Galantowicz, Paul J., 869
 Gale, Anabella, 969
 Gallego, Mireille, 671
 Gallun, Frederick J., 551
 Gan, Lin, 484
 Gan, Rong Zhu, 823
 Gandour, Jackson, 352
 Gans, Donald, 334, 873
 Gantz, Jay, 84
 Gao, J., 978
 Gao, Jiangang, 492, 799
 Garcia, Jasmine L., 455
 Gargano, Frank, 78
 Ge, Xianxi, 184, 525
 Gearhart, Caroline, 387
 Geálér, Hyun-Soon, 723
 Gerdin, Bengt, 945
 Germiller, John A., 746
 Gianna-Poulin, Claire, 71
 Giaume, Christian, 374
 Gibbons, Joanna, 137
 Gideon, Rechavi, 487
 Giersch, Anne B. S., 521, 1044
 Gill, Ruth M., 999
 Gillespie, Deda C., 733
 Gillespie, Peter G., 1025, 1026
 Gilley, Phillip M., 844
 Girod, Douglas, 109, 892
 Gittelman, Joshua X., 899
 Glassinger, Emily, 451
 Glattfelder, Jerry, 527
 Gleich, Otto, 310
 Glowatzki, Elisabeth, 709, 969
 Glueckert, Rudolf, 428
 Godfrey, Donald A., 341, 645, 886, 887, 894
 Godfrey, Matthew A., 341, 886
 Goense, Jozien, 336, 880
 Gokhale, Paul, 1039
 Goldberg, Jay M., 627, 628, 629
 Golding, Nace L., 910
 Goldowitz, Daniel, 493
 Golub, Lorne M., 28
 Gomez, Christopher M., 82
 Gonzalez, Secudino
 Fernández, 43, 45
 Goode, Richard L., 816, 832
 Goodman, Shawn S., 532
 Goodyear, Richard, 250, 490, 672
 Gopal, Kamakshi V., 59
 Gordon, Jane S., 39
 Gordon-Salant, Sandra, 116
 Gorelik, Julia, 444
 Gorga, Michael P., 99, 100
 Goswami, J., 795
 Gotoh, Satoru, 762
 Gottfried, Irit, 206
 Gottshall, Kim R., 62, 197, 348
 Gourley, Glenn R., 882
 Gow, Alexander, 977
 Grabul, Daniela S., 311
 Grant, John Wallace, 941
 Grant, Laura, 534
 Grati, M'Hamed, 212
 Gratton, Michael Anne, 173, 382, 383, 643, 697, 698, 963, 1047
 Gray, Brianna, 1033
 Gray, Lincoln C., 315
 Grayeli, Alexis Bozorg, 280, 281
 Green, Eric D., 201
 Green, Gary, 841, 853
 Green, Steven H., 178, 266
 Green, Tim, 849
 Greinwald, John Herman, 234
 Greinwald, John, 203, 223, 993
 Greinwald, Jr., John H., 221
 Griffith, Andrew J., 444, 766
 Griffiths, Timothy D., 555
 Grimes, Janelle L., 735
 Grody, Wayne, 1052
 Groh, Daniel, 47
 Grosh, Karl, 111, 112, 543, 544, 1018, 1019, 1023
 Gross, Julia, 363
 Gross, Julie, 1042
 Grothe, Benedikt, 171, 364, 372, 608, 909, 922
 Groves, Andy, 468, 788
 Grunwald, Jan-Eric, 303
 Gruss, Michael, 339
 Gu, Rende, 527, 745
 Guan, Min Xin, 237, 238, 239, 520
 Guimaraes, Patricia, 667
 Guinan, John J., 74, 535, 1001, 1005
 Guinan, Jr., John J., 538
 Guitton, Matthieu, 671
 Gummer, Anthony W., 448, 449, 1002, 1003, 1004
 Gundelfinger, Eckart, 708
 Guo, Jizhou, 301
 Guo, Yingshi, 234
 Guo, Yun-Kai, 493, 504, 767, 968
 Guo, Yuqing, 330, 347, 495, 982
 Gupta, Anil K., 48
 Gurrola, II, Jose G., 32
 Gurrung, Bina, 316
 Gustavsson, Jan-Åke, 966
 Guthrie, O'Neil W., 408
 Gutierrez, Gabriel, 784
 Guzman, Jose, 188, 529
 Gygi, Brian, 664, 806
 Gómez-Casati, Marja E., 717
 Géléoc, Gwenaëlle S. G., 454, 722, 797
 Ha, Oh Seung, 725
 Hachmeister, Jorge E., 441
 Hackney, Carole M., 1028
 Hadjab, Saida, 523, 970, 971
 Hafter, Ervin R., 837
 Haga, Nobuhiko, 235
 Hagemann, Regina, 115
 Hahn, Hartmut, 193
 Hale, Shane A., 195, 999
 Hall, Ameer J., 611
 Hallworth, Richard, 417, 418
 Halsey, Karin, 111, 112, 534, 972
 Halsey, Karin, 741
 Hamajima, Yuki, 292, 473, 474
 Hamaker, Sara, 521
 Hamann, Ingo, 310
 Hammershoi, Dorte, 104
 Hamoudi, Rifat, 230
 Han, Dongyi, 432
 Han, Sam, 783
 Han, Weiju, 379
 Haneda, Eri, 94
 Hansen, Anne R., 907
 Hansen, Stefan, 726
 Hara, Akira, 381, 384, 398, 399, 981
 Hara, Hirotaka, 626
 Harada, Narinobu, 27, 465, 467
 Harada, Tamotsu, 38, 219
 Harasztosi, Csaba, 448
 Hardelein, Jean-Pierre, 761
 Harding, Gary W., 393, 394
 Hardisty, Rachel, 1049
 Hari, Riitta, 145
 Harper, Elizabeth, 184, 688
 Harrington, Ian A., 147, 148
 Harris, Belinda S., 503
 Harris, Jeffrey P., 391
 Harris, Julie A., 369
 Harris, Kelly Carney, 687
 Hart, Alan, 494
 Hartmann, Rainer, 254, 345
 Hartung, Klaus, 52
 Haruta, Atsushi, 545
 Harvey, Charla, 175
 Harvey, Margaret, 461
 Hashimoto, Shigehisa, 391
 Hashino, Eri, 214, 480, 1040
 Hastings, Mardi C., 833
 Hata, Masaki, 790
 Hatfield, James S., 711, 712, 713
 Hattori, Taku, 22
 Hau, Leola W., 960
 Haubenreich, Kristen, 111, 112
 Haussinger, Deiter, 662
 Hawkey, David J. C., 813, 814
 Hawkins, David, 755, 787
 Hawkins, Joseph E., 663
 Hayashizaki, Yoshihide, 1029
 Hayes, Jay D., 294
 He, David Z. Z., 464, 798
 He, David Z.Z., 210
 He, Jiae, 30
 He, Jiao, 529, 563
 He, Xiaofan, 31
 Hebda, Patricia A., 297
 Hedrick, Michelle, 189
 Heffner, Henry E., 147, 893
 Hegeman, Judith, 76
 Heil, Peter, 951
 Heinrich, Marco, 898
 Heinz, Michael G., 955, 956
 Helfer, Karen S., 87
 Helfert, Robert H., 646
 Heller, Stefan, 458, 748, 785, 1034, 1035
 Helt, Wendy J., 39
 Hemje, Amy M., 1051
 Henderson, Donald, 185, 385, 386, 686, 687
 Henderson, Scott C., 631
 Hendriksen, Ferry, 678
 Hendry, Stewart, 878
 Henkel, Craig K., 371
 Henkemeyer, Mark, 719
 Henry, James A., 39
 Herrmann, Barbara S., 74
 Hertzano, Ronna, 206, 487
 Hickman, Elizabeth D., 666
 Hiel, Hakim, 709, 715, 716
 Higashiyama, Kasumi, 196
 Highstein, Stephen M., 16, 273, 631
 Hill, Brandon, 172, 504, 968, 1053
 Hilton, Helen, 1049
 Hind, Sally E., 58
 Hinds, Philip, 784
 Hirono, Moritoshi, 1025
 Hirose, Keiko, 390, 392
 Hirsch, June C., 374
 Hirt, Bernhard, 724
 Hirvonen, Meeli, 69
 Hirvonen, Timo P., 69, 639
 Hiryu, Shizuko, 625
 Hisa, Yasuo, 218, 990
 Ho, Kim Young, 489
 Ho, Lee Jun, 725
 Ho, Steven, 559
 Hoahino, Tomohuhi, 384
 Hodges, Annelle, 568
 Hoedl, Walter, 311
 Hoffer, Michael E., 62, 197, 348
 Hoffman, Larry F., 934, 935
 Hoidis, Silivi, 423
 Holley, Matthew C., 1039
 Holley, Matthew, 786
 Holmer, Nicole M., 831
 Holmes, Michael G., 321
 Holstein, Gay R., 17, 273, 631
 Holt, Avril Genene, 884, 888
 Holt, Jeffrey, 454, 505, 722, 797, 949, 1034
 Holt, Joseph Christopher, 627, 628, 629
 Holt, Lori L., 808
 Homer, Louis, 669
 Honegger, Flurin, 76
 Hong, Sung Hwa, 120, 500, 677, 828
 Honjo, Tasuku, 744
 Honrubia, Dynio Dynio, 1044
 Hooper, Rebecca A., 395
 Hoover, Brenda M., 99, 100
 Hoppenbrouwers, Mieke, 77
 Horak, Fay, 83
 Hordichok, Andrew J., 400, 401
 Horgan, Janet N., 1059
 Horii, Arata, 219
 Horiike, Osamu, 183
 Horwitz, Amy R., 117
 Horwitz, Barry, 552
 Hoshino, Tomofumi, 381
 Hossain, Waheeda Amin, 692
 Hou, Qiulai, 41
 Houya, Noriyuki, 397
 Howard, III, Matthew A., 876

- Howard, Matthew A., 574
 Howell, David M., 736
 Howitt, Andrew W., 924
 Hradek, Gary T., 368
 Hromadka, Tomas, 585
 Hsu, Chi, 747
 Hsu, Kenneth, 393
 Hsu, Lucy Y., 944
 Hu, Bohua, 185, 385, 687
 Hu, Fen Ze, 294
 Hu, Lan, 924
 Hu, Ning, 1012, 1014, 1015
 Hu, Wei, 991
 Hu, Wen Hui, 764
 Hu, Zhengqing, 1030, 1031
 Huang, M., 786
 Huang, MingQian, 485, 784
 Huang, Xinyan, 179
 Huang, Yuyou, 31
 Hubbard, Allyn, 1020
 Huber, Alexander M., 816, 820
 Hubka, Peter, 345
 Hudspeth, A. J., 792
 Huebner, Christian A., 976
 Hughes, Larry F., 646, 648, 649
 Hullar, Timothy E., 633
 Hultcrantz, Malou, 279
 Humphrey, Kurt D., 241
 Hundal, Harkawal S., 598
 Hunter, A Jackie, 225
 Hurley, Laura M., 599
 Hurley, Marja M., 1042
 Hurst, Sawan, 760
 Husain, Fatima Tazeena, 552
 Huss, David, 14, 15, 930, 931
 Hutson, Ken, 577
 Hutter, Michele M., 60
 Huynh, Kristin, 799
 Hwang, Chan-Ho, 224
 Hyson, Richard L., 908
 Hyun, Jung Hak, 489
 Hébert, Sylvie, 670
 Höhne, Karl-Heinz, 24
 Hübner, Mathias, 618
 Ichimura, Keiichi, 751, 981
 Ide, Charles F., 356
 Idrizbegovic, Esma, 370
 Ifediba, Marytheresa A., 632, 633
 Iglesia, Francisco Vazquez de la, 45
 Iglesia, Francisco V zquez de la, 43
 Ignatova, Elena G., 926
 Iguchi, Fukuichiro, 191, 216, 411, 479, 675, 1032, 1036
 Iida, Koji, 447
 Iino, Yukiko, 430, 981
 Ikeda, Hiromi, 27
 Ikeda, Katsuhisa, 762
 Ikegawa, Shirou, 235
 Ilie, Sorin L., 29
 Im, Gi Jung, 285
 Imaizumi, Kazuo, 575
 Imauchi, Yutaka, 280, 281
 Imbrogini, Valentina, 731
 Imig, Thomas J., 338
 Ino, Chiyonori, 44
 Inoue, Taku, 398
 Inoue, Yasuhiro, 756
 Irons-Brown, Shunda R., 706
 Irvine, Dexter Robert Francis, 951
 Isaacson, Brandon, 242, 1056, 1057
 Ishibashi, Toshio, 222
 Ishikawa, Kotaro, 981
 Ishimoto, Shin-ichi, 691
 Ishiyama, Akira, 277, 635
 Ishiyama, Gail, 635
 Ison, James, 331, 650, 659, 900
 Issa, John B., 955
 Itani, Jameel, 187, 413
 Ito, Juichi, 191, 216, 411, 479, 675, 744, 790, 1032, 1036
 Ito, Jyuichi, 1038
 Ittah, Avner, 967
 Itza, Erin M., 201
 Iwai, Koji, 479, 675
 Iwasa, Kuni H., 452
 Iyer, Nandini, 336
 Izumikawa, Masahiko, 465, 741, 742
 Jabba, Sairam V., 201
 Jackson, B. Scott, 952
 Jackson, Ian, 494
 Jackson, Ronald L., 184, 525, 686, 688
 Jacqueline, Hakes J., 134
 Jacques, Bonnie E., 475
 Jaehyup, Kim, 181
 Jain, Roshini, 137, 323
 Jamora, Colin, 247
 Jaquish, Dawn V., 25
 Jasko, Jeffrey G., 66
 Jastreboff, Margaret M., 34
 Jastreboff, Pawel J., 34
 Jeffcoat, Ben, 641
 Jelaso, Anna M., 356
 Jeng, Fuh-cherng, 255, 953
 Jenkins, Nancy A., 780
 Jennings, Amanda R., 555
 Jennings, J. Richard, 65, 642
 Jensen-Smith, Heather C., 418
 Jentsch, Thomas J., 976
 Jeong, Lee Hyo, 725
 Jeronimidis, G., 822
 Jesteadt, Walt, 536
 Ji, Teng, 956
 Ji, Weiqing, 132
 Ji, Yadong, 572
 Jia, Shuping, 210, 464, 798
 Jian, Brian, 373
 Jiang, D., 822
 Jiang, Haiyan, 495, 662, 674
 Jiang, Hong Yan, 524
 Jiang, Hongyan, 406, 656
 Jiang, Xiaoi, 1018
 Jiang, Zhi-Gen, 996, 997
 Jin, Yong-ming, 886, 887
 Jin, Zhe, 695
 Jin, Zhen-Hua, 420, 762
 Johansson, Peter, 685
 Johansson, Saga Malin, 911
 John, Earnest O., 298, 445
 Johnson, Jane E., 484, 782
 Johnson, Kaalan E., 298, 445
 Johnson, Ken R., 503
 Johnson, Kenneth R., 501
 Johnson, Krista L., 351
 Johnson, Sam, 853
 Johnson, Steve N., 395
 Johnson, Tiffany A., 53, 99
 Johnsrude, Ingrid, 877
 Johnstone, Patti M., 259, 570
 Jones, Gavin E., 184
 Jones, Helene, 1049
 Jones, Jennifer Michelle, 472
 Jones, Linda G., 737
 Jones, S., 978
 Jones, Sherri J., 980
 Jordan, James Randy, 641
 Joris, Philip X., 142, 954
 Joshi, Dipa, 655
 Juhn, Steven K., 220
 Juiz, Jose Manuel, 343, 734, 888
 Juiz, José Manuel, 901
 Jung, Hak Hyun, 285
 Jung, Jae, 283
 Jung, Timothy T. K., 298, 445
 Järlebark, Leif E., 695
 K.Brunso-Bechtold, Judy, 371
 Kabara, Lisa, 534, 741
 Kachar, Bechara, 793, 794, 977, 1017, 1029
 Kachroo, Puja, 824
 Kaga, Kimitaka, 222, 680
 Kaiser, Adam R., 88
 Kaiser, Christina L., 892
 Kaiser, Thomas, 561
 Kakimoto, Shingo, 27
 Kakizaki, Keiko, 981
 Kalinec, Federico, 433, 526
 Kalinec, Gilda, 526
 Kallman, Jeremy C., 240
 Kalluri, Radha, 537
 Kalstein, Laura, 866
 Kaltenbach, James A., 893, 918
 Kaltenbach, James, 890
 Kamiya, Kazusaku, 397
 Kanangat, Siva, 172, 1053
 Kanazawa, Takeharu, 176
 Kandler, Karl, 733
 Kaneko, Ken-ichi, 145
 Kaneko, Toshihiko, 448, 465
 Kang, Huny, 388
 Kang, Robert, 213
 Kang, Sung Ook, 282
 Kanwal, Jagmeet S., 139, 304, 583, 875
 Kanzaki, Sho, 756
 Kapfer, Christoph, 372, 909
 Kappert, Günther, 979
 Karet, Fiona, 203
 Karimi, Kambiz, 784
 Kariya, Shin, 636
 Kashino, Makio, 610
 Kashio, Akinori, 690
 Katbamna, Bharti, 356
 Kathju, Sandeep, 1048
 Katori, Yukio, 762
 Katsura, Koji, 625
 Katz, Eleonora, 717
 Kaufman, Galen D., 270
 Kaura, Samantha, 298
 Kawakyu, Kosuke, 616
 Kawamoto, Kohei, 741, 742
 Kawano, Hirokazu, 545
 Kazzi, N. J., 56
 Ke, Xiaomei, 236
 Keasler, Jodi, 390, 392
 Keats, Bronya, 242, 1056, 1057
 Keefe, Douglas H., 108, 532
 Keefe, Douglas, 536
 Keefe, Randy M., 294
 Keithley, Elizabeth M., 174, 391, 502
 Keller, Clifford H., 602
 Kelley, Darcy B., 163
 Kelley, Matthew W., 472, 475, 487, 519, 749, 780
 Kelley, Matthew, 208, 476, 481, 505
 Kelly, Jack B., 144, 327, 592, 600
 Kemnitz, Joseph W., 1051
 Kempe, Steven G., 363
 Kempton, Beth, 36, 37
 Kenna, Margaret A., 1059
 Kennedy, Helen, 796
 Kenyon, Judy, 429
 Kermany, Mohammad
 Habiby, 172, 493, 504, 968, 1053
 Kerschner, Joseph Edward, 291
 Ketels, Kathleen V., 730
 Ketten, Darlene R., 833
 Khalifa, Shaden, 945
 Khan, Khalid M., 711, 713
 Khanna, Shyam M., 1010
 Khimich, Darina, 708
 Kidd, Jr., Gerald, 551
 Kief, Sabine, 994
 Kieft, Michael, 809, 893
 Kiemele, Kevin L., 240
 Kiernan, Amy, 503
 Kikuchi, Shojiro, 790
 Kikuchi, Toshihiko, 420, 693, 762, 988
 Kil, Jonathan, 527, 745
 Kildebeck, Eric J., 136
 Kileny, Paul R., 54
 Kilgard, Michael P., 136, 137
 Killian, Peter, 197, 348
 Kim, Chong Sun, 72
 Kim, Chong-Sun, 50, 224
 Kim, In Young, 677
 Kim, In-Young, 120
 Kim, Jeong Lim, 285
 Kim, Myung Soon, 500, 677
 Kim, Sum I., 120
 Kim, Sun I., 828
 Kim, SungHee, 654, 666, 667, 668
 Kim, Tae-Soo, 191, 216, 411, 479, 675, 790, 1032, 1036
 Kim, Theresa, 242
 Kim, Youngki, 292
 Kim, Yuil, 903
 Kimball, Jeremiah, 141
 Kimball, Kay T., 67
 Kimberling, William J., 241, 963, 1051, 1054
 Kimitaka, Kaga, 751
 Kimura, Yurika, 430
 Kindler, Christoph H., 231
 King, Andrew J., 169, 573
 King, Curtis, 273
 King, John, 568
 King, Mary-Claire, 206
 Kinnefors, Anders, 945
 Kirk, E. Christopher, 984
 Kirkegaard, Mette, 683
 Kirl, Karen Iler, 92
 Kita, Tomko, 216
 Kita, Tomoko, 191, 411, 675, 1036
 Kitahara, Tadashi, 295, 409
 Kitajiri, Shin-ichiro, 675, 790
 Kitamura, Ken, 430, 431
 Kittel, Malte Christian, 310
 Klein, David, 152
 Klink, Karin B., 309
 Klinke, Rainer, 254, 345
 Klis, Sjaak F. L., 676
 Kluender, Keith R., 809
 Kluk, Karolina, 549
 Klump, Georg M., 309, 312, 314
 Klump, Georg, 310
 Klöcker, Nikolaj, 718
 Knierim, James J., 18
 Knipper, Marlies, 523, 699, 718, 723, 724, 970, 971, 1046
 Knirsch, Martina, 456
 Ko, Jennifer, 337
 Koay, Gim, 893
 Kobayashi, Toshimitsu, 420, 693, 988
 Kobiellak, Agnes, 247
 Kobiellak, Kris, 247
 Koch, Ulrich, 994
 Koch, Ursula, 372, 909
 Koda, Hiroko, 430
 Kodama, Atsuko, 247
 Kodama, Takao, 545
 Koehn, Fred J., 25
 Koepl, Christine, 164, 541
 Koh, Christine K., 578
 Kohrman, David C., 518
 Koizuka, Izumi, 73
 Kojima, Ken, 216, 411, 675
 Kolb, Hans-Albert, 987
 Kollmar, Ida, 171, 922
 Kollmeier, Birger, 98, 913
 Komatsubara, Sachiko, 545
 Kommareddi, Pavan K., 175, 176
 Komune, Shizuo, 545, 825
 Kondo, Kenji, 691, 757
 Kondo, Takako, 214, 480, 1040
 Kong, Y. Y., 1057
 Kong, Ying, 1056
 Kong, Ying-Yee, 811

- Konrad-Martin, Dawn, 39, 108, 113
Koo, Ja Won, 72, 377
Kopco, Norbert, 615
Kopke, Richard D., 184, 525, 686, 688
Korchev, Yuri E., 444
Koroleva, Irina V., 1029
Korsak, Rosa A., 738
Kos, Lidia, 967
Koster, Bram, 792
Kotak, Vibhakar C., 346
Koterski, Sandra, 727
Kotylo, Piotr, 114
Kozlova, Elena, 1030
Kozma, Kelley, 175
Kral, Andrej, 254, 345
Kraus, Nina, 121, 351
Kretzmer, Erika, 843
Krips, Ram, 606
Krishnan, Ananthanarayan, 352, 353
Kros, Corne J., 444
Kros, Corné, 672
Krupin, Alison, 481
Kubo, Nobuo, 27
Kubo, Takeshi, 219
Kucinski, Thomas, 26
Kudo, Takayuki, 762
Kujawa, Sharon G., 74, 497
Kulesza, Jr., Randy J., 921
Kumagai, Izumi, 447
Kumanomido, Hiroshi, 429
Kumar, Gagan, 557, 558
Kume, Akihiro, 751
Kunaratnam, Nanthini, 55
Kuo, Sharon, 1044
Kuo, Yu-ching, 850
Kurian, Rachel, 383
Kurt, Simone, 591
Kurtzberg, Diane, 865
Kusakari, Jun, 381, 981
Kusunoki, Takeshi, 636, 1055
Kutz, Jr., J. Walter, 437
Kuwabara, Nobuyuki, 359
Kuwada, Shigeyuki, 52, 595
Kuzdak, Nancy E., 184
Kwan, Tao, 490
Kwon, Bomjun, 84
Kwon, See Youn, 500
Köpschall, Iris, 523, 723
Kühn-Inacker, Heike, 569
Ladher, Raj K., 470, 1038
Ladrech, Sabine, 671
Laflen, J. Brandon, 253
LaGasse, James, 527, 745
Lagziel, Ayala, 204, 252
Lai, Zhicheng, 875
Laine, Pascale, 280, 281
Lake, Jennifer, 570
Lalwani, Anil K., 231, 505
Lamm, Kerstin, 396
Lan, Yinyin, 31
Lane, Courtney C., 146
Lang, Hainan, 189, 658
Langemann, Ulrike, 312, 314
Langer, Patricia, 724
Langner, Gerald, 325, 854
Larue, David T., 598
Las, Liora, 151
Lasker, David M., 936
Lassonde, Maryse, 145
Lauder, Jean M., 728
Lauer, Amanda M., 307
Laurell, Goran, 681
Lawoko-Kerali, Grace, 786
Laws, Kimberly S., 1058
Lawton, D M., 703
Lawton, D. Maxwell, 530
Le Prell, Colleen G., 972
Leake, Patricia A., 368, 565
Lee, Daniel J., 354
Lee, F. A., 346
Lee, Fan, 253
Lee, Gi Soo, 783
Lee, Hsi-Ming, 28
Lee, Hyo Jeong, 90, 93
Lee, James C., 33
Lee, James, 35
Lee, Ji Eun, 411
Lee, Jun Ho, 201
Lee, Jungmee, 102, 103
Lee, Sang Min, 120, 828
Lee, Te-Chung, 186
Lee, Wei Wei T., 865
Lee, Yun Woo, 220
Lee, Yun-Shain, 478, 788
Legan, Kevin, 490, 672
Legrain, Pierre, 765
Lehar, Mohamed, 639
Leibold, Lori J., 810
Leigh-Paffenroth, Elizabeth, 113
Leight, William D., 289
Leight, William Derek, 287
Lenarz, Minoo, 160
Lenarz, Thomas, 160, 561
Lenhardt, Martin Louis, 51
Lenoir, Marc, 413, 671, 781
Leonard, Gerald, 52
Leonardo, Leslie, 934
Leong, Francis, 655
Leow, Mei-Chern, 261
Lepore, Franco, 145
Lesniak, Wojciech, 407
Lesperance, Marci, 242, 1056, 1057
Lett, Jaclynn M., 496
Leung, Johann, 620, 624
Leuwer, Rudolf, 24, 26, 115, 122, 827, 976, 994
Levine, Stephen Robert, 819
Lewandoski, Mark, 475
Lewcock, Joseph W., 11
Lewelling, Kevin, 826
Lewis, M. Samantha, 60
Li, Chaoying, 486
Li, Fang, 764
Li, Geming, 213, 682
Li, Ha-sheng, 409
Li, Hongzhe, 332
Li, Huawei, 458, 785, 1034, 1035
Li, Jiang, 231
Li, Jianxiong, 696, 710
Li, Liang, 665
Li, Rong-Hua, 239
Li, Xiankui, 782
Li, Xiao-Ming, 238
Li, Xiaorong, 641
Li, Xingqi, 710
Li-Korotky, Ha-Sheng, 295, 296, 297
Liang, Fenghe, 701, 991, 992
Liang, Guihua, 695
Liang, Jianning, 230
Liao, Lingya, 704
Lieberman, M. C., 965
Lieberman, M. Charles, 190, 415, 497, 679, 978, 1005
Lichtenhan, Jeffery, 109
Lichtenstein, Lee, 924
Liew, Duncan, 1039
Lig, Liang Kong, 625
Lilly, David J., 60, 113
Lim, David J., 293
Lim, Dukhwan, 50
Lim, Hubert H., 158
Lim, Insook, 930
Limb, Charles J., 95
Lin, Jizhen, 220, 292, 473, 474
Lin, Tai, 1001
Lin, Xi, 763, 782, 986
Lin, Zhengshi, 223, 471
Lindemann, Marcus A., 957
Linden, Jennifer F., 138, 874
Lindholm, Dan, 945
Lindvall-Weinreich, Charlotta, 519
Ling, Jie, 203
Ling, Lynne, 649
Linthicum, Fred Hamilton, 426
Lister, Jennifer J., 546
Litovsky, Ruth L., 619
Litovsky, Ruth Y., 168, 259, 570
Litvak, Leonid, 851
Liu, Dong, 469
Liu, Feng, 478
Liu, Hong, 785
Liu, Jeremy, 553
Liu, Jianzhong, 184, 525, 686, 688
Liu, Jun, 710
Liu, Robert C., 874
Liu, Wei, 213, 215, 682, 752
Liu, Xue Zhong, 232, 236, 764
Liu, Yuhe, 751
Lo, Chia-Yee, 295, 296, 297
Lobarinas, Edward, 308
Lockwood, Alan H., 869
Loftus, William C., 324
Lohr, Bernard, 166
Loizou, Philip, 263
Lomakin, Oleg, 141
Lomax, Cathy Ann, 884, 888
Lomax, Margaret I., 522
Lomber, Stephen G., 149, 611
Lombes, Marc, 280
Long, Christopher J., 261
Long, Christopher Joseph, 848
Long, Glenis R., 102, 103
Long, Julie A., 199
Lonsbury-Martini, B. L., 110
Loomis, Patricia A., 517
Lopez, Ivan, 277, 635, 738
Lopez-Poveda, Enrique A., 129, 547
Lorenzi, Christian, 836
Lormore, Kelly, 92
Los, Jenna G., 942
Lotto, Andrew J., 808
Louage, Dries H., 142
Loughlin, Patrick J., 66
Loughlin, Patrick, 81
Lovett, Michael, 755, 787
Lozito, Thomas, 552
Lu, Jianzhong, 919
Lu, Shan, 1020
Lu, Yong, 906
Lu, Zhi, 141
Lu, Zhong-Lin, 811
Lu, Zhongmin, 162, 959
Ludueña, Richard F., 417
Ludwig, Jost, 718
Luebke, Anne, 505, 967
Luethke, Lynn, 243
Luijendijk, Mirjam W.J., 241
Luján, Rafael, 901
Lundburg, Yesha, 963
Lupien, Sonia J., 670
Lurie, Diana I., 737, 749
Lustig, Lawrence R., 716, 721
Lutman, Mark E., 556
Luxon, Linda M., 55, 580
Lyall, Kristen, 521
Lynch, Eric Daniel, 527, 745
Lynch-Erhardt, Martha, 660, 661
Lyons, Leslie A., 1051
Lysakowski, Anna, 14, 15, 274, 932, 933, 937
Löhrke, Stefan, 917
Ma, Chun-Lei, 592, 600
Ma, Ellen, 107
Ma, Teh-Sheng, 881
Ma, Xiaofeng, 133
MacDonald, Glen, 412
Machens, Christian, 588
Macklin, Christopher, 488
Macpherson, Ewan A., 148, 622, 623
Madge, Joanna, 1049
Maganti, Rajanikanth J., 201
Magnusson, Anna K., 372
Mahboobin, Arash, 81
Mahendrasingam, Shanthini, 1028
Maier, Hannes, 26, 115, 122, 421, 827, 976
Maison, S., 978
Maki, Katuhiro, 610, 612
Makishima, Tomoko, 766
Makmura, Linna, 502
Malhotra, Shveta, 149, 611
Malmierca, Manuel S., 318, 324, 335
Malou, Hultcrantz, 966
Mangiardi, Dom, 405
Mangiardi, Dominic A., 404
Mani, Arunvijay, 263
Manis, Paul B., 367, 904
Manley, Geoffrey A., 541
Mann, David A., 957
Mann, Linda, 767
Mann, Sabine, 458
Manning, Brian P., 700
Manrique, Manuel Jesus, 426
Mansell, Siobhan, 225
Mansour, Suzanne L., 486
Mansour, Suzi, 777
Mantela, Johanna, 778
Mao, Huajie, 41
Mapes, Frances M., 666
Mapes, Francis, 667, 668
Marcus, Daniel C., 198, 199, 200, 201
Marcus, Dawn A., 65
Margolin, Gregory, 279
Margolskee, Robert F., 10
Marietta, Chandler, 668
Marshall, Allen F., 256, 605
Martin, Brett A., 865
Martin, Eduardo, 68
Martin, G. K., 110
Martin, Kathryn, 844
Martin, William Hal, 542
Martinelli, Georgio, 273
Martinelli, Giorgio P., 17, 631
Martinez, Ariadna, 1052
Martinez-Galan, Juan Ramon, 734
Martinosky, Joseph W., 882
Martinez, Juan Ramon, 901
Maruyama, Jun, 846
Marvit, Peter, 572
Mason, Christine R., 551
Massing, Thomas, 979
Mastroianni, Mary Ann, 1058
Matei, Veronica Ana, 477
Mathers, Peter H., 731, 735, 736
Mathews, Paul J., 910
Matsubara, Atsushi, 398, 399
Matsumoto, Nozomu, 433
Matsunaga, Tatsuo, 397, 429
Matsunami, Tatsuya, 990
Matsuno, Hideo, 1053
Matsushita, Soichiro, 80
Matthews, D., 978
Mattox, Douglas E., 34
Mattson, Mark P., 265
Mauermann, Manfred, 98, 827, 913
Maves, Lisa, 469
Maxeiner, Stephan, 761
Mazelova, Jana, 47
Mburu, Philomena, 1049
McAdams, Stephen, 872
McCandless, Cyrus H., 377
McCormack, Joe, 124
McDermott, Daniel, 49
McFadden, Sandra L., 975
McFadden, Sandra L., 674, 974
McGee, JoAnn D., 961, 962
McGee, JoAnn, 244, 723, 963
McGinley, Matthew James, 895
McKenzie, Erynn Elizabeth, 481

- McMenamy, Alyssa, 137
 McMullen, Nathaniel T., 321
 McNaughton, Bruce L., 18
 Meddis, Ray, 547, 841
 Meddis, Raymond, 923
 Medvedev, Andrei V., 583
 Meehan, Daniel T., 1047
 Meehan, Daniel, 963
 Meenderink, Sebastiaan W. F., 101
 Mehta, Ajay J., 20
 Melcher, Jennifer, 155
 Melikyan, Armenuhi, 581
 Meltser, Inna, 685
 Mensinger, A. F., 16
 Mercado, III, Eduardo, 138
 Merchan, Miguel A., 318
 Merchant, Saumil N., 821
 Merriam, Elliott B., 590
 Merrill, Bradley J., 247
 Merzenich, Michael M., 138
 Metter, E. Jeffrey, 669
 Metzner, Walter, 302
 Meuer, Katrin, 325
 Meyer zum Gottesbege, Angela-Maria, 979
 Meyer, Michaela, 958
 Meyer, Ted A., 85
 Meyers, Jason R., 789
 Meziane, Hamid, 494
 Mhatre, Anand N., 231
 Micco, Alan, 557, 558
 Michaelis, Christiane Elisabeth, 396
 Michaels, Leslie, 230
 Michalewski, Henry, 1056, 1057
 Michel, Vincent, 761
 Micheyl, Christophe, 155
 Michna, Marcus, 456
 Middlebrooks, John C., 148, 622, 623, 847
 Migliaccio, Americo A., 637
 Mikhael, Chadia S., 815
 Miko, Ilona J., 594
 Milenkovic, Ivan, 898
 Miller, Charles A., 255
 Miller, Charles, 953
 Miller, David B., 315
 Miller, Joe, 1030
 Miller, Josef M., 268
 Miller, Josef, 524, 562, 689, 846, 945, 946
 Miller, Kimberly, 157
 Miller, Lee M., 326
 Millman, Rebecca Elizabeth, 841
 Milo, Marta, 786
 Minami, Shujiro, 689
 Minoda, Ryosei, 180, 741, 742
 Minor, Lloyd B., 637, 638, 639, 936
 Minowa, Osamu, 762
 Mishra, Lakshmi, 851
 Mistretta, Charlotte M., 12
 Mistry, Shilpa T., 136
 Mitchem, Kristina, 518
 Mittleman, G., 978
 Miyazawa, Toru, 42, 44
 Mizukami, Hiroaki, 751
 Mlynski, Robert, 726
 Modi, Dimple, 274
 Moita, Marta, 156
 Molitor, Scott C., 902
 Moll, Ingrid, 994
 Mombaerts, Peter, 13
 Montcouquiol, Mireille E., 780
 Montcouquiol, Mireille, 472, 476, 487
 Montey, Karen, 843
 Moon, Sung-Kyun, 282
 Moore, Brian C. J., 549, 836
 Moore, Brian, 125
 Moore, David R., 343
 Moore, David R., 58, 169, 813, 814
 Moore, Jordan, 335
 Moore, Robert J., 62
 Moorehead, Morrill T., 298
 Mora, Renzo, 172
 Moradzadeh, Arash, 391
 Morales-Garcja, Jose A., 929
 Moravec, William J., 938
 Morawski, Krzysztof, 950, 983
 Morell, Robert J., 204
 Morell, Robert, 252
 Morest, D. Kent, 692, 739, 889, 1042
 Morest, Kent D., 363
 Moriyama, Hiroshi, 693
 Moroy, Tarik, 487
 Morrell, Robert J., 1058
 Morris, K., 462
 Morris, Kenneth A., 694, 964, 1029
 Morse, Sue, 1049
 Morton, Cynthia C., 521, 766
 Morton, Cynthia, 1044
 Moser, Tobias, 708
 Mou, Cai Hong, 529
 Moucha, Raluca, 137
 Mountain, David C., 404, 857, 924
 Mountain, David, 1020
 Mouton, Peter R., 424
 Moy, Patricia L., 258
 Mridha, Zakir H., 931
 Mu, Karen J., 697
 Mueller, Anne, 115
 Mueller, Ulrich, 251
 Muenkner, Stefan, 456
 Muenscher, Adrian, 827
 Mugnaini, Enrico, 517
 Mullen, Lina M., 267, 729
 Mullinex, April H., 338
 Murakami, Yoshihiko, 981
 Muramatsu, Shinichi, 751
 Murashita, Hidekazu, 381, 384
 Murata, Junko, 219
 Murayama, Ayako, 219
 Murdock, David R., 439
 Murdock, David, 802
 Murray, Michael, 1016
 Murugasu, Euan, 1016
 Musacchia, Gabriella A. E., 121
 Musiek, Frank E., 580
 Mustain, William, 640
 Mutai, Hideki, 748, 785
 Muzyczka, Nicholas, 505, 508
 Myers, Steven F., 714
 Myrdal, Sigrid E., 401, 402, 403
 Möller, Claes, 241
 Müller, Marcus, 423, 699
 Müller, Markus, 724
 Müller-Wehlau, Matthias, 827, 913
 Nadol, Jr., Joseph B., 415
 Naganawa, Shinji, 22
 Nair, Thankam S., 175, 176
 Nair, Usha, 172, 1053
 Naito, Yasushi, 191, 216, 479, 675, 1032, 1036
 Nakagawa, Susumu, 397
 Nakagawa, Takayuki, 191, 216, 411, 479, 675, 790, 1032, 1036
 Nakaizumi, Toshihiko, 180, 560
 Nakajima, Hideko Heidi, 821
 Nakamori, Akiko, 398, 399
 Nakamura, Akihiko, 27
 Nakashima, Tsutomu, 22, 202, 998
 Nakayama, Atsuo, 202
 Nakmal, Don, 823
 Namba, Atsushi, 235
 Nance, Walter E., 236
 Narayan, Rajiv, 879
 Narins, Peter M., 101, 311, 804, 960
 Nassiri, Reza, 153
 Nathans, Jeremy, 519
 Navaratnam, Dhasakumar, 436, 453, 800
 Nchols, David H., 477
 Needham, A. J., 822
 Neely, Stephen T., 99, 100
 Nehme, Omar, 30
 Nelken, Israel, 151
 Nelson, Paul C., 840
 Nesse, William, 273
 Neubauer, Heinrich, 951
 Neuburger, Heidi, 94
 Neuert, Veronika, 912
 Neufeld, E., 965
 Neuman, Arlene, 260
 Neuringer, Martha, 1051
 Newman, Scott R., 653
 Ng, Lily, 977
 Ngezahayo, Anaclet, 987
 Ni, Daofeng, 1031
 Nickel, Regina, 164
 Nicol, Trent G., 351
 Nicol, Trent, 121
 Nicolson, Teresa, 229
 Nicotera, Thomas M., 385
 Nicotera, Thomas, 687
 Nie, Liping, 462, 463, 694, 697, 698
 Niimi, Seiji, 429
 Nijhuis, Lars, 76
 Niparko, John K., 95
 Nishimura, Gen, 235
 Nishizaki, Kazunori, 636
 Niu, Haoru, 502
 Niu, Xianzhi, 891
 Nixdorf-Bergweiler, Barbara E., 325
 Nobbe, Andrea, 257
 Noben-Trauth, Konrad, 501
 Noda, Tetsuo, 762
 Nodal, Fernando R., 573
 Noguchi, Yoshihiro, 431
 Nomoto, Tatsuya, 751
 Nopp, Peter, 262, 569
 Norena, Arnaud Jean, 140
 Norena, Arnaud, 328
 Norris, Denis, 877
 Northrop, Clarinda Carrington, 819
 Nourski, Kirill V., 255, 953
 Nouvian, Regis, 708
 Novak, Edward, 495
 Nowotny, Manuela, 1002
 Nuttall, Alfred L., 543, 544, 657, 997, 1012, 1013, 1014, 1015, 1025, 1026
 Nyengaard, Jens R., 427, 683
 O'Connor, A. Fitzgerald, 822
 O'Donovan, Anne B., 521
 O'Mard, Lowel Phillip, 923
 O'Neill, William E., 859, 860
 O, Chang Sun, 725
 Oas, John G., 78, 378
 Oba, Toshihiko, 80
 Oddsson, Lars, 79
 Odeh, Hana, 518
 Oertel, Donata, 768, 895, 905
 Oestreicher, Elmar, 339, 995
 Ogawa, Kaoru, 80, 756
 Oghalai, John S., 441, 499, 1021
 Oh, Seung-Ha, 72, 90, 93, 181, 224
 Ohara, Osamu Osamu, 1044
 Ohashi, Mitsuru, 825
 Ohl, Frank W., 159, 576
 Ohlemiller, Kevin K., 496, 498
 Ohyama, Taka, 468
 Okada, Takashi, 751
 Okamoto, Yasuhide, 397
 Okano, Hideyuki, 218, 219, 756
 Oktay, Mehmet Faruk, 636
 Okuda, Takeshi, 182, 626, 630, 684
 Oliver, Dominik, 459, 718
 Oliver, Doug, 771
 Oliver, Douglas L., 143, 318, 319, 324, 597
 Oliver, Douglas, 595
 Olivius, Petri N., 911
 Olivius, Petri, 279, 1030
 Olsen, Sarah E., 831
 Olsheski, Christopher, 373
 Olson, Elizabeth S., 1009, 1010
 Olson, Elizabeth Sue, 824
 Omelchenko, Irina, 657
 Ondrey, Frank G., 292, 473
 Onoda, Norihiko, 42
 Onori, Kimberly Ann, 272
 Orduna, Itzel, 138
 Orem, Alexander R., 442, 443
 Ornitz, David M., 778, 926
 Ortega, Alberto, 453
 Orten, Dana J., 1051, 1054
 Ortigoza, Eric B., 95
 Ortmann, Amanda J., 498
 Oshurkova, Elena, 581
 Osmanski, Michael S., 306
 Ostapoff, Michael E., 363
 Oswald, Duane, 1048
 Otazu, Gonzalo, 571
 Otsuki, Junichi, 80
 Otsuki, Kazuoki, 80
 Ouyang, Jie, 967
 Ouyang, Xiao Mei, 232, 764
 Ouyang, Xiaomei, 236
 Overstreet, Edward Holman, 92
 Owens, Kelly N., 187, 412, 413
 Oxenham, Andrew J., 128, 155
 Ozawa, Hiroyuki, 397
 Ozawa, Keiya, 751
 Ozdamar, Ozcan, 355, 950, 983
 Ozeki, Masashi, 473, 474
 Ozeki, Masashi, 220
 Paasche, Gerrit, 561
 Page, Rachel, 881
 Pak, Kwang, 267, 286, 290, 719, 729
 Palmer, Alan R., 320
 Palmer, Alan Richard, 333
 Palmer, Christina, 1052
 Paloski, William H., 669
 Pan, Ling, 484
 Pandya, Arty, 236
 Pandya, Pritesh K., 137
 Pang, Jiaqing, 760
 Panyi, György, 446
 Paparella, Michael M., 38, 636, 1055
 Paparella, Michael, 209
 Parameshwaran-Iyer, Suchitra, 715, 716
 Park, Hong Joon, 500
 Park, Hong Ju, 936
 Park, Keehyun, 282
 Park, Seong Kook, 298, 445
 Park, Sook Kyung, 500, 677
 Park, Thomas, 608
 Park, Yong-Ho, 224
 Parker, M., 973
 Parker, Mark Allen, 702, 1033
 Parkinson, Aaron, 259, 570
 Parkinson, Nicholas, 225
 Parkinson, Nick, 1049
 Parrish, Sarah K., 36, 37
 Parsons, Thomas D., 706, 707
 Pascale, Alessia, 275
 Pashia, Mary, 283
 Patel, Nimisha, 655
 Patrick, Jim, 160
 Patterson, D. Michael, 173
 Patterson, Roy D., 877
 Pauley, Sarah, 779

- Paulin, Michael G., 935
Pauwels, Griet, 77
Pawlowski, Karen S., 226, 980
Payne, Lisa, 34
Peake, William T., 821
Pecka, Michael, 922
Pecoraro, Vincent, 407
Peng, Ben Gang, 986
Peng, Ben-Gang, 763
Percaccio, Cherie R., 136
Pereira, Fred A., 499
Perez, Nicolas, 68
Perez-Gonzalez, David, 335
Perfettini, Isabelle, 765
Perin, Paola, 275
Pershouse, Mark, 737
Peterka, Robert, 83
Peters, B. Robert, 570
Petersik, Andreas, 24
Peterson, Ellengene H., 938, 939
Petit, Christine, 250, 761, 765
Peusner, Kenna D., 374
Pfaller, Kristian, 428
Pfungst, Bryan E., 560, 566, 567
Pfister, Markus H. F., 699, 724
Pflesser, Bernhard, 24
Pham, Viet, 425
Phillips, David S., 39
Phillips, Kelli R., 207
Picaud, Serge, 494
Pickles, Raymond, 287, 289
Pierce, Carol, 527
Pilipenko, Valentina V., 221, 234
Pillers, De-Ann M., 760
Pineda, Juan Carlos, 584
Pingle, Sandeep, 410
Pirvola, Ulla, 778
Pistorio, Ashley L., 878
Pitts, Darrell, 1045
Plack, Christopher J., 126, 128, 547, 839
Plomann, Markus, 458
Plontke, Stefan K. R., 192, 193
Plotz, Karsten, 827
Poe, Gina R., 18
Poepfel, David, 150
Pohl, Ulrich, 995
Poissant, Sarah F., 87
Polak, Marek, 30, 563, 568
Pollak, George, 322, 593, 881
Pompeia, Celine, 1029
Pondugula, Satyanarayana R., 198, 199, 200
Pongstaphone, Tan, 942
Pongstaporn, Tan, 365
Poon, Paul W. F., 740, 896
Popel, Aleksander S., 803
Popelar, Jiri, 47, 586
Popelka, Gerald R., 882
Popper, Arthur N., 208, 414, 833, 958
Popper, Paul, 634, 907, 927, 928
Porter, C. A., 110
Portfors, Christine Verdie, 344
Portfors, Christine, 772
Post, J. Christopher, 294, 1048
Poston, Amanda N., 287, 289
Potashner, Steven J., 883, 885
Potyagaylo, Valeria, 637, 638
Poulsen, David J., 749
Pouyatos, Benoit, 387
Praetorius, Mark, 743, 747
Price, Steve, 14
Price, Steven D., 15, 274
Prieve, Beth A., 515, 516, 830
Prigioni, Ivo, 466
Pritchard, Clare, 1049
Pritschow, Bernd W., 449
Probst, Rudolf, 609
Probst, Rudolph R., 75
Prosen, Cynthia A., 380
Prost, Robert W., 870
Pruette, Autumn L., 136
Puckett, Amanda, 137
Puel, Jean Luc, 673
Pujol, Remy, 187, 413
Puria, Sunil, 818
Qi, James G., 665
Qi, Li, 815
Qian, Feng, 439, 802
Qian, Jinyu, 613
Qu, Chunyan, 991
Quade, Bradley J., 521
Quirk, Wayne, 655
Rabbitt, Richard D., 273, 631, 632, 633, 801
Rachel, Rivka A., 780
Rafano, C. M., 170
Raggio, Marcia W., 565, 845
Rahman, Aniusur Palash, 279
Raible, David W., 187, 412, 413
Rajguru, Suhrud M., 632, 633
Rama, Julio, 68
Ramakrishna, Rohan, 383
Ramakrishnan, Neelivath A., 457, 711, 713, 714
Ramamoorthy, Sripriya, 1023
Ramkumar, Vickram, 410
Randell, Scott H., 289
Rao, Palle D. Prasada, 139, 875
Rao, Velidi H., 1047
Raphael, Richard, 907, 928
Raphael, Robert M., 401, 451
Raphael, Yehoash, 180, 181, 518, 560, 741, 742
Rasband, Matthew N, 692
Rash, Sean, 760
Rashi-Elkeles, Sharon, 487
Rask-Andersen, Helge, 194, 428, 945, 946
Ratan, Rajiv, 190
Ratnam, Rama, 336
Ratner, Nancy, 276
Rauch, Steven D., 74
Raveendran, Nithyanandhini, 198, 199
Ravicz, Michael E., 816, 817
Rawool, Vishakha Waman, 867
Ray, Jennifer B., 944
Raynov, Alexander Markov, 282
Read, Heather L., 153, 326
Rebscher, Steve J., 564
Redfern, Mark S., 65, 66, 642
Redfern, Mark, 81
Reece, Alisa, 221, 223, 993
Reed, Randall R., 11
Rees, Adrian, 770, 841, 853
Regala, Christopher, 1030
Regehr, Wade G., 897
Rehm, Heidi L., 1059
Reinert, Thomas, 898
Reisinger, Ellen, 718
Reiss, Lina A. J., 915
Remtulla, Rahim A., 33, 35
Ren, Tianying, 543, 1011, 1012, 1014, 1015
Rennie, Katherine J., 278
Resendes, Barbara, 1044
Reuter, Guenter, 160
Reuter, Karen, 104
Rhodes, Charlotte Rebecca, 225
Riazuddin, Saima, 205, 252
Ricci, A. J., 795
Ricci, Anthony J., 278, 703
Rich, Kathryn A., 288, 293
Richards, Ayo-Lynn, 488
Richardson, Dustin, 858
Richardson, Guy P., 444
Richardson, Guy, 250, 490, 672
Richter, Claus-Peter, 557, 558, 559, 727
Rieger, Heike, 1041
Rinchik, Evgeni M., 493
Rinzel, John, 346
Riquelme, Raquel, 52, 595
Riquimaroux, Hiroshi, 610, 625
Risner, Jessica R., 797, 949, 1034
Ritter, Steffen, 550
Rivas, Alejandro, 424
Rivoli, Peter J., 650, 659
Rivolta, Marcelo N., 786, 1039
Roberson, David W., 190
Roberson, Joseph, 1016
Robert, Mark E., 852
Roberts, Rachel M., 105
Roberts, Richard A., 546
Roberts, William M., 704, 705
Robertson, Nahid G., 766
Robertson, Nancy, 1044
Robinson, Barbara K., 255
Robinson, Barbara, 953
Robinson, D. O., 56
Rocha-Sanchez, S.M.S., Sonia, 964
Rodger, Colin S., 1000
Rodrigues, Aldo Rogelis A., 905
Rodriguez, Clara I., 766
Rogers, Alyssia, 380
Rohbock, Karin, 523, 723
Romand, Raymond, 480, 494, 1040
Rosen, Stuart, 55, 57, 849, 850
Rosowski, John J., 816, 817, 821
Rosowski, John, 511
Rossman, Ian Jay, 305
Rotenberg, Brian, 40
Roth, Heidi, 807
Roth, Vincent, 781
Rothermund, Christy, 1043
Rowan, Daniel, 556
Rowland, Kevin C., 607
Royaux, Ines E., 201
Rubel, Edwin W., 165, 187, 369, 412, 413, 906
Ruben, Robert, 491
Rubinstein, Jay T., 85
Ruckenstein, Michael J., 173
Rudolf, Glueckert, 562
Ruggero, Mario, 539
Ruiz, Jose W., 188
Runge-Samuelsen, Christina L., 86, 89, 870
Rupert, Angus H., 64
Rupp, Andre, 868
Rupp, André, 550
Russell, Ian, 969
Russo, Giancarlo, 466
Rust, Marco B., 976
Ruth, Peter, 699, 724
Rutherford, Mark, 705
Ruttley, Tara, 270
Ryals, Brenda M., 732
Ryan, Allen F., 174, 267, 286, 290, 719, 726, 729
Rybak, Leonard P., 179, 410
Rybak, Leonard, 4
Rybalchenko, Volodymyr, 434, 436
Ryoo, Zae Young, 500
Ryugo, David K., 365, 424, 843, 942
Rzadzinska, Agnieszka K., 793, 794
Rübsamen, Rudolf, 898
Rüsch, Alfons, 724
Rüttiger, Lukas, 523, 699, 724, 970, 971
Sabin, Andrew T., 622, 623
Saccone, Nancy, 755
Sadrazodi, Kamran, 714
Saeed, Abdelwahab, 504
Sage, Cyrille, 485, 784
Sahani, Maneesh, 138
Saido, Takaomi, 671
Saint Marie, Richard L., 143, 318, 319
Sakaguchi, Hirofumi, 218, 990
Sakamoto, Tatsunori, 1038
Salbaum, J. Michael, 964
Salt, Alec N., 192, 193, 194, 195, 999, 1000
Salvi, Richard J., 186, 308, 416, 662, 674, 948
Samadi, Daniel, 759
Samaranayake, Haresha, 453, 800
Sampaio, Andre L. L., 636, 1055
Sams, Mikko, 121
Samson, Séverine, 872
Sanchez-Hanke, Marcos, 994
Sanes, Dan H, 343
Sanes, Dan H., 346, 594
Sanford, Chris A., 829
Sani, Sanaz Zhalehdoust, 617
Sanneman, Joel, 198, 199, 200
Sanovich, Elena, 732
Sanpetrino, Nicole M., 123, 127
Sans, Nathalie A., 780
Santi, Peter, 244, 425
Santina, Charles C. Della, 637, 638
Santos, Felipe, 412
Santos, Teresa P. G., 362
Santos-Sacchi, Joseph, 434, 435, 436, 453, 800
Sanuki, Tetsuji, 299, 300
Saoji, Aniket, 835
Sarampalis, Anastasios, 839
Sarko, Diana, 807
Sasai, Yoshiki, 1038
Sasaki, Akira, 398, 399
Sasaki, Hiroyuki, 790
Sasaki, Toru, 222
Sato, Eisuke, 202
Satoh, Takunori, 483
Saunders, James C., 383, 643, 759
Sausbier, Matthias, 699, 724
Savel, Sophie, 872
Schachern, Patricia A., 38, 636, 1055
Schachern, Patricia, 209
Schacht, Jochen, 406, 407, 524, 656, 663, 689
Schairer, Kim S., 536
Scheich, Henning, 159, 576, 581, 591, 855, 856, 861, 862
Scheler, Renate, 396
Scherer, Elias Q., 995
Scherer, Marc P., 1003, 1004
Schimmang, Thomas, 776
Schimmenti, Lisa, 1052
Schlegel, Todd T., 64
Schleich, Peter, 569
Schlantz, Eileen P., 473
Schmiedt, Richard A., 189, 658
Schmitt, Nicole, 393
Schmuck, Nicholas, 900
Schnee, Michael E., 703
Schneider, Bruce A., 665
Schneider, Mark E., 794

- Schneider, Mark Edward, 793
 Schofield, Brett R., 357, 358, 359
 Schor, Robert, 376
 Schraufnagel, Annabelle, 425
 Schreiner, Christoph E., 326, 565, 575, 845, 874
 Schrott-Fischer, Annelies, 428, 562
 Schrottge, Ines, 856
 Schuchmann, Maike, 618
 Schue, Jeremy R., 961
 Schulte, Bradley A., 189, 658, 701, 989, 991, 992
 Schultz, Julie M., 204
 Schultz, Julie, 252
 Schulze, Holger, 591, 855, 856
 Schumann, Timothy, 376
 Schwanke, Corbin, 737
 Schörnich, Sven, 303
 Scott, Daryl, 486
 Seedorf, Hartwig, 26
 Seeney, Charles S., 826
 Segar, Allyson, 1058
 Segil, Neil, 478, 484, 782, 788
 Seidman, Jake E., 655
 Seidman, Michael D., 655
 Seifert, Ron, 672
 Sekerkova, Gabriela, 517
 Seki, Satoshi, 21
 Selezneva, Elena, 581
 Sen, Kamal, 879
 Sendtner, Michael, 726
 Sepmeijer, Jan Willem, 676
 Sequeira, Damien, 820
 Serrador, Jorge M., 64
 Seshagiri, Chandran, 154
 Severinsen, Stig Åvall, 427
 Sewell, William F., 700
 Sha, Su-Hua, 406, 656
 Shackleton, Trevor M., 333
 Shafiro, Valeriy, 96
 Shah, Gaurav D., 578
 Shaikh, Aasef G., 271
 Shamma, Shihab, 135, 152
 Shang, Jialin, 783
 Shannon, Robert, 269
 Shao, Mei, 374
 Shapiro, Nina, 1052
 Sharma, Anu, 844
 Sheehy, Conor, 360
 Sheft, Stanley, 834, 836
 Shen, Jing, 465, 467
 Shen, Yan, 432
 Shen, Zhijun, 701, 991, 992
 Shera, Christopher A., 450, 537, 538, 1008
 Sheykholeslami, Kianoush, 334, 751, 873
 Shi, Xiao-Rui, 1026
 Shi, Xiaorui, 1025
 Shi, Yongbing, 542
 Shibata, Toshiaki, 990
 Shiga, Atsushi, 411
 Shim, Hee-Yeon, 828
 Shimazaki, Kuniko, 751
 Shimogori, Hiroaki, 182, 183, 626, 630, 684
 Shin, Jung-Eun, 388
 Shinkawa, Hideichi, 235, 398, 399
 Shinn-Cunningham, Barbara Gail, 615, 616, 617
 Shinoda, Hideo, 21
 Shoelson, Brett D., 1007, 1017
 Shope, Cynthia, 440
 Shore, Susan E., 323, 919, 920
 Shore, Susan, 366
 Shub, Daniel E., 130
 Si, Fan, 29
 Siaud, Philippe, 970
 Siebeneich, Wolfgang, 634
 Siedow, Norbert, 192
 Siegel, Jonathan, 514, 539, 548
 Sienknecht, Ulrike J., 541
 Sienko, Kathleen, 79
 Sieroka, Norman, 868
 Silveira, M. Beatriz, 74
 Sim, Jae Hoon, 818
 Simmons, Dwayne D., 395, 721, 960
 Simmons, Jeffrey L., 108
 Simon, Jonathan Z., 150
 Simon, Jonathan, 152
 Simon, Rosie, 568
 Simonis, Claudia, 854
 Simonoska, Rusana, 966
 Simpson, Brian D., 118
 Simpson, Ivra, 640
 Sinex, Donal G., 321
 Sinex, Donal, 332
 Singh, Mandal, 1048
 Sininger, Yvonne S., 1052
 Sirjani, David B., 999
 Sivakumaran, Theru A., 242
 Sivaramkrishnan, Shobhana, 595, 597
 Skaggs, John D., 604, 605
 Skaggs, John, 256
 Sklare, Daniel, 243
 Sliwinska-Kowalska, Mariola, 114
 Smallwood, Phil, 519
 Smedstad, Hanna B., 602
 Smiley, Elizabeth C., 746
 Smith, Bennett K., 872
 Smith, David W., 984
 Smith, Matthew, 91
 Smith, Michael E., 833
 Smith, Richard J. H., 231
 Smith, Robert L., 123
 Smith, Shelley, 429
 Smittkamp, Susan Elizabeth, 644
 Smittkamp, Susan, 109
 Smolders, Jean W. Th., 342, 423
 Smoorenburg, Guido F., 676, 678
 Smoot, Jaime E., 317
 Smotherman, Michael, 302
 Smouha, Eric E., 28
 Smurzynski, Jacek, 609
 Snir, Einat, 1029
 Snyder, Evan Y., 702, 1033
 Snyder, Russell L., 368, 564, 565, 847
 Snyder, William N., 173
 Soares, Bento, 1049
 Soares, M. Bento, 1029
 Sobe, Tama, 206
 Soellner, Christian, 229
 Sokolowski, Bernd, 461
 Soleimani, Manoocher, 203
 Soma, Kiran K., 311
 Sone, Michihiko, 22, 202, 998
 Song, Chang-Woo, 224
 Song, Lei, 435, 436
 Song, Xiaodan, 894
 Soo, Lee Dong, 90, 93
 Sorsa, Timo, 28
 Soucek, Sava, 230
 Southwood, Cherie M., 977
 Souza, Pamela, 866
 Sparto, Patrick J., 65, 66, 81
 Specht, Hans-Joachim, 550
 Speck, Judy, 754
 Spector, Alexander A., 803, 1021
 Spencer, Nathan, 401
 Spicer, Samuel S., 989, 991
 Spirou, George A., 607, 731, 735, 736
 Spisak, John, 1020
 Spurr, Nigel, 225
 Srinivasan, Geetha, 917
 Staecker, Hinrich, 505, 529, 743, 747
 Stagner, B. B., 110
 Stahl, John S., 980
 Stallings, Valerie, 71
 Starr, Arnold, 242, 1056, 1057
 Statler, Kennyn, 83
 Stauffer, Eric A., 722
 Stecker, G. Christopher, 148
 Steel, Karen P., 225
 Steele, Charles R., 818
 Steinhoff, Hans-Joachim, 396
 Steinschneider, Mitchell, 574, 582, 865, 876
 Stenberg, Annika E., 966
 Sterbing-D'Angelo, Susanne, 595
 Sterkers, Olivier, 280, 281
 Sterns, Anita R., 515, 516
 Stevens, Gary R., 20
 Stevens, John, 580
 Stewart, Christopher C., 812
 Stewart, Colin L., 766
 Steyger, Peter S., 400, 401, 402, 403
 Stickney, Ginger S., 554
 Stierna, Pontus, 685
 Stincic, Todd L., 908
 Stoever, Timo, 561, 1041
 Stone, Ida M., 749
 Stone, Jennifer, 228, 783
 Street, Sarah E., 904
 Street, Valerie Ann, 240
 Stribley, Judith A., 964
 Strutz, Jürgen, 310
 Su, Gina, 566
 Suarez, Hamlet, 70
 Subramani, Munirathinam, 363, 739
 Sudhoff, Holger, 230
 Suga, Nobuo, 131
 Suga, Nubuo, 132, 133
 Sugahara, Kazuma, 182, 626, 630, 684
 Sugai, Susumu, 44
 Sugai, Tokio, 42
 Sukanuma, Tatsuo, 825
 Sugawara, Mitsuru, 679
 Sumner, Christian, 920
 Sun, Jian-Jun, 763
 Sun, Kim Chong, 90, 93, 181, 725
 Sun, Qing, 710
 Sun, Wei, 308, 696, 948
 Sun, Xiao-Ming, 533
 Suneja, Sanoj K., 883, 885
 Sung, Young Ju, 500
 Suta, Daniel, 586
 Suzuki, Kazuteru, 73
 Suzuki, Mitsuya, 680, 690, 691, 757
 Suzuki, Ryuji, 354
 Suzuki, Toshihiro, 218, 990
 Svirskis, Gytis, 346
 Svirsky, Mario A., 88, 94, 253
 Swank, Richard, 495
 Swarts, J. Douglas, 296, 297
 Syka, Josef, 47, 586
 Szalda, Kathleen, 350, 495, 863, 864
 Sziklai, István, 446
 Szymczak, Wieslaw, 114
 Sørensen, Mads Solvsten, 427
 Tabata, Yasushi, 191
 Tabuchi, Keiji, 381, 384, 398, 399
 Taggart, Thomas, 429
 Tahera, Yeasmin, 685
 Tai, Lung-Hao, 156
 Taiji, Hidenobu, 397
 Takahashi, Katsumasa, 430, 981
 Takahashi, Sugata, 21
 Takahashi, Terry, 602, 773
 Takebayashi, Shinji, 216, 479, 675, 1032
 Takeda, Taizo, 196
 Takeichi, Masatoshi, 248
 Takemoto, Tsuyoshi, 183, 626, 630, 684
 Takeuchi, Koichi, 751
 Takeuchi, Shunji, 196
 Taki, Masakatsu, 990
 Talaska, Andra, 406
 Talavage, Thomas M., 94, 253
 Talkowski, Michael E., 642
 Talmadge, Carrick L., 102, 103, 538
 Tamagawa, Yuya, 981
 Tamura, Tetsuya, 191, 411, 675
 Tan, Justin, 523, 971
 Tan, Zulin, 710
 Tanaka, Koichi, 420
 Tanaka, Kuniyoshi, 183, 630, 684
 Tang, Yong, 635
 Tanigaki, Kenji, 744
 Tartaglini, E., 965
 Tateya, Ichiro, 1036
 Tatsunori, Sakamoto, 1032
 Tayeh, Nadia, 566
 Taylor, Megan E., 317
 Teissier, Natacha, 52
 Telatar, Milhan, 1052
 Telischi, Fred F., 30, 355, 950, 983
 Temchin, Andre N., 539
 Tempel, Bruce L., 497, 899
 Thalmann, Isolde, 926
 Thalmann, Ruediger, 926
 Thaung, Caroline, 494
 Theis, Martin, 761
 Thiers, Fabio A., 415
 Thompson, Ann M., 728
 Thompson, Jesse M., 607
 Thonabulsombat, Charoensri, 911
 Thurm, Henrike, 459
 Tian, Yong, 1050
 Tiede, Ulf, 24
 Tillein, Jochen, 254
 Tinling, Steven P., 29, 177, 284
 Todd, N. Wendell, 844
 Todt, Ingo, 23, 340
 Toji, Masao, 80
 Tollin, Daniel J., 167, 614, 774
 Tolsdorff, Boris, 827
 Szymczak, Wieslaw, 162
 Tomimaga, Mitsuo, 998
 Tomita, Masahiko, 328
 Tomo, Igor, 421
 Tomoda, Koichi, 42, 44
 Tong, Mingjie, 902
 Tong, Song, 207
 Tramo, Mark Jude, 578
 Tran, Huy, 527
 Trask, Barbara J., 7
 Tremblay, Kelly, 866
 Trune, Dennis R., 36, 37, 786
 Trussell, Laurence O., 903
 Tsai, Hsun, 225
 Tsuchiya, Katsuyuki, 292, 473
 Tsuji, Masayuki, 744
 Tsukita, Sachiko, 790
 Tsumoto, Kouhei, 447
 Tsuprun, Vladimir, 209
 Tsuyoshi, Endo, 1032
 Tubis, Arnold, 538
 Turner, Jeremy G., 648
 Tuttle, David, 651
 Uchida, Hikaru, 44
 Ueda, Hiromi, 998
 Ulanovsky, Nachum, 151
 Ulfendahl, Mats, 421, 695, 846, 1030, 1031
 Ulloa, Antonio, 552
 Ulmer, John L., 870
 Underhill, Peter, 1049
 Uppenkamp, Stefan, 877

- Urrutia, Rafael Garcja-Tapia, 43, 45
 Urrutia, Raul, 526
 Ursitti, Jeanine A., 418
 Usami, Shin-ichi, 235, 429
 Ushio, Munetaka, 680
 Vaezi, Alec, 247
 Vajda, Viktor, 924
 Vakkalanka, Sarah, 557
 Vale, Carmen, 343, 734, 901
 Valli, Paolo, 275
 van de Heyning, Paul H., 77
 Van de Sande, Bram, 142
 Van De Water, Thomas R., 30, 188, 529, 563, 752
 van den Honert, Chris, 84
 van der Heijden, Marcel, 142, 954
 Van Der Linden, Annemie, 871
 van Dijk, Pim, 101
 Van Meir, Vincent, 871
 van Netten, Sietse, 211
 Van Ruijven, Marjolein W. M., 678
 van Wieringen, Astrid, 848
 Van Winkle, Rebecca, 418
 Vander Werff, Kathy R., 516, 830
 Vanniasegaram, lyngaram, 57
 Varela, Anabl, 1049
 Varela-Nieto, Isabel, 929
 Varghese, George I., 652
 Vaughan, Nancy, 49
 Vazquez, Ana E., 382, 462, 463, 697
 Velenovsky, David S., 321
 Vendrell, Victor, 776
 Vent, Julia, 417
 Verbny, Yakov, 589
 Verhey, Jesko L., 912
 Vetter, Douglas E., 746
 Viberg, Agneta, 370, 422, 681, 752
 Vieillard, Sandrine, 872
 Viemeister, Neal Frank, 838
 Vigil, Patricia, 929
 Villarroel, Álvaro, 901
 Visser-Dumont, Leslie, 107
 Vogltanz, Vanessa A., 1051
 Voie, Arne, 425
 Volkenstein, Stefan, 726
 Volkman, Niels, 792
 Volkov, Igor O., 574, 876
 Vollmer, Maïke, 254, 565, 845
 von Huenerbein, Karen, 423
 Wack, David S., 869
 Wackym, Phillip, 86, 89, 634, 870, 927, 928
 Wada, Hiroshi, 447, 1022
 Wada, Yuki, 545
 Wagner, Eva, 124
 Wagner, Hans-Joachim, 414
 Wake, Gordon, 853
 Walden, Ralph E., 882
 Waldmann, Bernd, 122
 Wall, Conrad, 79
 Wall, III, Conrad, 74
 Wall, L., 973
 Wall, Luke, 1033
 Wall, Susan M., 201
 Wallace, Mark N., 320, 333
 Wallhäuser-Franke, Elisabeth, 325
 Walsh, Edward, 244, 723, 961, 962, 963
 Walsh, Vanessa, 206
 Walton, Joseph, 331, 900
 Walton, Peggy L., 161
 Waltz, Stacy E., 1051
 Wang, Da Neng, 792
 Wang, Eric, 283
 Wang, Jiadong, 940
 Wang, Jian, 329
 Wang, Jianjun, 41
 Wang, Jie, 655, 918
 Wang, Kai, 329
 Wang, Ping, 186, 948
 Wang, Qiuju, 432
 Wang, Vincent, 477
 Wang, Xiaobo, 174, 502
 Wang, Xiaofen, 486
 Wang, Xiaoqin, 878
 Wang, Yanshu, 519
 Wang, Yong, 367
 Wang, Zhaohui, 203
 Wangemann, Philine, 201
 Warchol, Mark E., 754, 755, 787
 Ward, Jaye, 223, 993
 Ward-Bailey, Patricia, 503
 Warr, W. Bruce, 360, 419, 962
 Warskulat, Ulrich, 662
 Washuta, Natalie, 568
 Wasserman, Stephen, 286
 Watanabe, Shoji, 73
 Watanabe, Yoshiaki, 625
 Waterman, Marjorie S., 651
 Watermann, Dirk, 971
 Watters, Karen F., 1035
 Webber, Douglas S., 738
 Weber, Thomas, 723, 1046
 Webster, Nicholas J. G., 290
 Webster, Paul, 288, 293
 Webster, Simon, 288
 Wefstaedt, Patrick, 1041
 Wegener, Raimund, 192
 Wehr, Michael, 588
 Wei, Ling, 189
 Weinberger, Norman M., 554
 Weleber, Richard, 760
 Weng, Tianxiang, 270
 Wenstrup, Jeffrey James, 334, 873
 Wenthold, Robert J., 212, 780
 Wenzel, Gentiana I., 499
 Wenzel, Sören, 26
 Werner, Lynne A., 810, 831
 Werner, Mimmi, 752
 Wester, Derin Charles, 197, 348
 Westerfield, Monte, 469
 Weston, Michael D., 241
 Wetzel, Wolfram, 576
 White, Judith, 63
 White, Patricia M., 788
 Whitlon, Donna, 517, 730
 Whitmal, III, Nathaniel A., 87
 Whitworth, Craig A., 179, 410
 Wiegrebe, Lutz, 303, 618
 Wilcox, Edward, 205, 252
 Wilkinson, Katherine, 373
 Willecke, Klaus, 761
 William, John, 1049
 Williams, Bart O., 519
 Williams, John, 519
 Williamson, Kate, 404, 405
 Wilson, E. Courtenay, 155
 Wilson, Teresa S., 646
 Windham, Byron Pearson, 641
 Winer, Jeffery A., 326, 598
 Winter, Harald, 723, 724
 Winter, Ian M., 912
 Wissel, Kirsten, 1041
 Withnell, Robert H., 105
 Wittig, John H., 707
 Wojtczak, Magdalena, 838
 Wolters, Francisca L. C., 676
 Won, Jong Ho, 120
 Woo, Ji Hwan, 500
 Woo, Jihwan, 120, 677
 Wood, Mark, 823
 Wood, Scott J., 64
 Wood, William, 46
 Woods, Chad, 476, 519
 Woods, Charles I., 515, 516
 Woodward, William, 760
 Woolf, Nigel Keith, 25
 Woollorton, Julian R., 455
 Wouters, Jan, 848
 Wright, Alison L., 942
 Wright, Beverly A., 351, 812
 Wright, Charles G., 226, 980
 Wright, Tracy, 777
 Wrisley, Diane, 83
 Wu, Doris K., 227, 471, 775
 Wu, Jiunn Liang, 896
 Wu, Shu Hui, 592, 596, 600
 Wu, Siva, 288, 293
 Wu, Tao, 201
 Wu, X., 978
 Wu, Xudong, 767
 Wunderlich, Julia L., 579
 Wuyts, Floris L., 77
 Xie, Ruli, 322, 593
 Xin, Jack, 1024
 Xu, Baogang, 926
 Xu, Li, 567
 Xu, Qiang, 519
 Xu, Yisheng, 352
 Xu, Youguo, 640
 Xu, Zemin, 959
 Xu-Friedman, Matthew Alexander, 897
 Xuan, Weijun, 31
 Xue, Jin-Tang, 627, 628, 629
 Xue, Jingbing, 939
 Yamamoto, Norio, 216, 479, 744
 Yamamoto, Satoshi, 990
 Yamashita, Daisuke, 524, 689
 Yamashita, Hiroshi, 182, 183, 626, 630, 684
 Yamashita, Toshio, 27, 465, 467, 1055
 Yamasoba, Tastuya, 691
 Yamasoba, Tatsuya, 680, 690, 757
 Yamoah, Ebenezer, 276, 462, 463, 694, 697, 698
 Yan, Denise, 232, 236, 764
 Yan, Jun, 134
 Yan, Leqin, 883, 884, 885
 Yan, Yi-Lin, 469
 Yang, Chris, 291
 Yang, Jiewu, 1049
 Yang, Wei-Ping, 185, 385
 Yang, Weiyang, 432
 Yang, Yu-Qin, 996, 997
 Yang, Yue, 143
 Yaoi, Takeshi, 218
 Yarbrough, Wendell G., 46
 Yarlagadda, Sushma, 175
 Yashima, Takatoshi, 431
 Yates, Bill, 373
 Yavuz, Erdem, 355, 950, 983
 Ye, Xuehua, 41
 Yin, Tom C. T., 614, 774
 Ylikoski, Jukka, 778
 Ymamoto, Hiroshi, 998
 Yong-Ho, Park, 181
 Yoo, T. J., 493
 Yoo, Tai-June, 172, 504, 968, 1053, 1053
 Yoshida, Ryuichi, 420, 693, 988
 Yoshino, Takahiko, 202
 Yost, C. Spencer, 231
 Yost, William A., 834
 Young, Eric, 603, 915, 916, 955, 956
 Young, Lawrence R., 19
 Yu, Gong Qiang, 168, 570, 619
 YU, Heping, 503
 Yu, Sam-Mi, 500
 Yu, Zi Long, 750
 Zador, Anthony, 156, 571, 585, 587, 588
 Zahn, Thomas, 922
 Zalewski, Christopher K., 1058
 Zamysłowska-Szmytke, Ewa, 114
 Zanation, Adam M., 46
 Zaya, Ninef E., 646
 Zdanski, Carlton J., 256
 Zecker, Steven, 351
 Zeddies, David G., 313
 Zelarayan, Laura, 776
 Zeng, Fan, 1057
 Zeng, Fan-Gang, 512, 553, 554, 811, 1056
 Zenner, Hans-Peter, 192, 193, 1002, 1004
 Zerbi, Marian, 262
 Zettel, Martha L., 647, 660, 661
 Zhan, Xiping, 365
 Zhang, Chunxiang, 968
 Zhang, Duan-Sun, 784
 Zhang, Fawen, 533
 Zhang, Huiming, 144
 Zhang, Jinsheng, 893, 918
 Zhang, Liqun, 287, 289
 Zhang, Mei, 33, 35, 416
 Zhang, Wei, 349
 Zhang, Xuedong, 842
 Zhang, Yi, 462
 Zhang, Yongkui, 131
 Zhang, Yunfeng, 134
 Zhang, Yuxuan, 812
 Zhao, Hong-Bo, 985, 1037
 Zhao, Hui, 237, 996
 Zhao, Lidong, 710
 Zhao, Shouqin, 301, 832
 Zheng, Jiefu, 543, 686, 1013, 1015
 Zheng, Jing, 442, 443
 Zheng, Lili, 517
 Zheng, Qing Yin, 501, 503
 Zhou, Daohong, 658
 Zhou, Guangwei, 74
 Zhou, Jianxun, 366, 377
 Zhou, Wu, 640, 641
 Zhou, Yi, 925
 Zhou, Zhiping, 947
 Zhu, Hong, 641
 Zhu, Xiaoxia, 651, 652, 653, 654, 660, 661
 Zhuang, Lei, 283
 Ziese, Ulrike, 792
 Zilbovicius, Monica, 872
 Zimmermann, Ulrike, 523, 718, 723, 724
 Zine, Azel, 673, 781
 Zoghbi, Huda, 477
 Zokoll, Melanie A., 312
 Zou, Yuan, 1014, 1015
 Zucker, Stanley, 28
 Zuo, J., 978
 Zuo, Jian, 492, 493, 767, 799, 1005, 1046, 1050
 Zwislocki, Jozef J., 123, 127
 Zwolan, Teresa, 92
 Zwolan, Terry A., 54

Association For Research In Otolaryngology

19 Mantua Road

Mt. Royal, NJ 08061

Phone: (856) 423-0041

FAX: (856) 423-3420

E-Mail: headquarters@aro.org

Website: <http://www.aro.org>